

# **Trajectory Prediction Accuracy and Error Sources for Regional Jet Descents**

## **Part I—Results of a 2010 Flight Trial at Denver International Airport Using a Global 5000 Test Aircraft**

*Jeff Henderson  
Engility Corporation, Billerica, Massachusetts*

*Steven M. Green  
Ames Research Center, Moffett Field, California*

*Minghong G. Wu  
UARC, University of California, Santa Cruz  
Ames Research Center, Moffett Field, California*

## NASA STI Program ... in Profile

Since its founding, NASA has been dedicated to the advancement of aeronautics and space science. The NASA scientific and technical information (STI) program plays a key part in helping NASA maintain this important role.

The NASA STI program operates under the auspices of the Agency Chief Information Officer. It collects, organizes, provides for archiving, and disseminates NASA's STI. The NASA STI program provides access to the NTRS Registered and its public interface, the NASA Technical Reports Server, thus providing one of the largest collections of aeronautical and space science STI in the world. Results are published in both non-NASA channels and by NASA in the NASA STI Report Series, which includes the following report types:

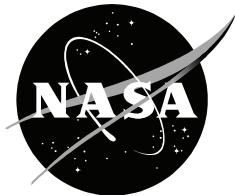
- **TECHNICAL PUBLICATION.** Reports of completed research or a major significant phase of research that present the results of NASA Programs and include extensive data or theoretical analysis. Includes compilations of significant scientific and technical data and information deemed to be of continuing reference value. NASA counterpart of peer-reviewed formal professional papers but has less stringent limitations on manuscript length and extent of graphic presentations.
- **TECHNICAL MEMORANDUM.** Scientific and technical findings that are preliminary or of specialized interest, e.g., quick release reports, working papers, and bibliographies that contain minimal annotation. Does not contain extensive analysis.
- **CONTRACTOR REPORT.** Scientific and technical findings by NASA-sponsored contractors and grantees.

- **CONFERENCE PUBLICATION.** Collected papers from scientific and technical conferences, symposia, seminars, or other meetings sponsored or co-sponsored by NASA.
- **SPECIAL PUBLICATION.** Scientific, technical, or historical information from NASA programs, projects, and missions, often concerned with subjects having substantial public interest.
- **TECHNICAL TRANSLATION.** English-language translations of foreign scientific and technical material pertinent to NASA's mission.

Specialized services also include organizing and publishing research results, distributing specialized research announcements and feeds, providing information desk and personal search support, and enabling data exchange services.

For more information about the NASA STI program, see the following:

- Access the NASA STI program home page at <http://www.sti.nasa.gov>
- E-mail your question to [help@sti.nasa.gov](mailto:help@sti.nasa.gov)
- Phone the NASA STI Information Desk at 757-864-9658
- Write to:  
NASA STI Information Desk  
Mail Stop 148  
NASA Langley Research Center  
Hampton, VA 23681-2199



# **Trajectory Prediction Accuracy and Error Sources for Regional Jet Descents**

## **Part I—Results of a 2010 Flight Trial at Denver International Airport Using a Global 5000 Test Aircraft**

*Jeff Henderson  
Engility Corporation, Billerica, Massachusetts*

*Steven M. Green  
Ames Research Center, Moffett Field, California*

*Minghong G. Wu  
UARC, University of California, Santa Cruz  
Ames Research Center, Moffett Field, California*

National Aeronautics and  
Space Administration

*Ames Research Center  
Moffett Field, CA 94035-1000*

---

**October 2014**

## Acknowledgments

The authors thank Robert A. Vivona of Engility Corporation for contributing feedback and Karen Cate of NASA Ames for reviewing the manuscript. The authors also thank Sharon Woods and Brendan LeFebvre of Engility and Amir Farrahi of University of California, Santa Cruz, for assistance developing the MATLAB analysis tools for trajectory comparison. This work was supported by NASA Ames Research Center under contract NNA12A09C.

The use of trademarks or names of manufacturers in this report is for accurate reporting and does not constitute an official endorsement, either expressed or implied, of such products or manufacturers by the National Aeronautics and Space Administration.

Available from:

NASA Center for AeroSpace Information  
7115 Standard Drive  
Hanover, MD 21076-1320  
443-757-5802

National Technical Information Service  
5301 Shawnee Road  
Alexandria, VA 22312  
703-605-6000

This report is also available in electronic form at

<http://ntrs.nasa.gov>

## Table of Contents

Nomenclature .....	v
Summary .....	1
1. Introduction .....	1
2. Flight Trial.....	2
2.1. Test Matrix .....	3
2.2. Arrival Routing.....	4
2.3. VNAV.....	4
2.4. Data Collection .....	4
3. Trajectory Prediction .....	5
4. Trajectory Prediction Accuracy .....	6
5. Description of Error Sources .....	7
5.1. Tracker Jumps.....	7
5.2. Wind .....	8
5.3. CAS Deceleration .....	9
5.4. Speed Conformance.....	11
5.5. Target Mach .....	12
5.6. Atmosphere/Altitude.....	13
5.7. Path Distance .....	14
6. Method to Quantify Magnitude of Error Sources.....	16
6.1. Tracker Jumps.....	16
6.2. Wind .....	18
6.3. CAS Deceleration .....	18
6.4. Speed Conformance.....	19
6.5. Target Mach.....	20
6.6. Atmosphere/Altitude.....	20
6.7. Path Distance .....	20
7. Results .....	20
7.1. Magnitude of Error Sources.....	20
7.2. Percentage Contribution to Total Variance .....	22
7.3. Comparison to 1994 Flight Test Using NASA's Boeing 737 Test Aircraft .....	25
7.4. Comparison to 2009 3D PAM Flight Trial Using Revenue Flights .....	27
7.5. Error Mitigation.....	27
8. Conclusions .....	28
9. References .....	29
Appendix A: Run-by-Run Magnitude of Tracker Jump Error Source.....	31
Appendix B: Run-by-Run Ranked Effect of Error Sources.....	33
B.1. Tracker Jumps .....	33
B.2. Wind.....	35
B.3. CAS Deceleration .....	37
B.4. Speed Conformance.....	39
B.5. Target Mach .....	41
B.6. Atmosphere/Altitude.....	43
B.7. Path Distance .....	45
B.8. Residual.....	47

## Table of Contents (cont.)

Appendix C: Run-by-Run Results for Direct Runs .....	49
C.1. Incremental Error Source Effect on Time Error .....	49
C.2. Run 1 .....	51
C.3. Run 2 .....	65
C.4. Run 3 .....	79
C.5. Run 4 .....	93
C.6. Run 7 .....	107
C.7. Run 10 .....	121
C.8. Run 12 .....	135
C.9. Run 14 .....	149
C.10. Run 18 .....	163
C.11. Run 19 .....	177
C.12. Run 21 .....	191
C.13. Run 22 .....	205
C.14. Run 23 .....	219
C.15. Run 24 .....	233
C.16. Run 25 .....	247
C.17. Run 26 .....	261
C.18. Run 28 .....	275
C.19. Run 29 .....	289
C.20. Run 30 .....	303
C.21. Run 31 .....	317
C.22. Run 32 .....	331
C.23. Run 34 .....	345
C.24. Run 35 .....	359
C.25. Run 36 .....	373
C.26. Run 37 .....	387
C.27. Run 38 .....	401
C.28. Run 39 .....	415
C.29. Run 41 .....	429
C.30. Run 42 .....	443
C.31. Run 43 .....	457
C.32. Run 44 .....	471
Appendix D: Run-by-Run Results for Path-Stretch Runs .....	485
D.1. Run 6 .....	486
D.2. Run 8 .....	500
D.3. Run 13 .....	514
D.4. Run 15 .....	528
D.5. Run 17 .....	542
D.6. Run 20 .....	556
D.7. Run 27 .....	570
D.8. Run 33 .....	584
D.9. Run 40 .....	598
Appendix E: Mean and Standard Deviation of Error Source Effect at Five Locations from Top of Descent to Meter Fix.....	613

## Nomenclature

$f_{0,i}$	= Compressibility factor at sea level at radar track index $i$
$f_i$	= Compressibility factor at altitude aircraft is flying at radar track index $i$
$g$	= Standard gravity
$i$	= Radar track index
$K$	= Error source index
$p_0$	= International Standard Atmosphere pressure at sea level
$p_i$	= Static pressure at radar track index $i$
$P_K$	= Percentage of total arrival-time error variance at meter fix due to error source $K$
$q_{c,i}$	= Impact pressure at radar track index $i$
$R$	= Gas constant for air
$r$	= Turn radius
$s_i^K$	= Along path distance from initial condition to radar track index $i$ . If $K = G$ , then this is flown data collected on board aircraft, otherwise it is based on CTAS prediction.
$t_i^{flown}$	= Flown time at radar track index $i$ using data collected on board aircraft
$t_i^{pred}$	= CTAS predicted time at radar track index $i$
$\Delta t_i^0$	= Uncorrected time error (flown minus predicted) at radar track index $i$
$\Delta t_i^K$	= Time error corrected for error source $K$ at radar track index $i$
$T_i$	= Temperature at radar track index $i$
$v$	= Ground speed
$\overline{V_{CAS,i}}$	= Calibrated airspeed (CAS) at radar track index $i$
$\overline{V_{Mach,i}}$	= Mach at radar track index $i$
$\overline{V_{TAS,i}}$	= True airspeed (TAS) at radar track index $i$
$\overline{V_{TAS2,i}}$	= Ratio of TAS to Mach. Used as a factor to convert flown Mach to TAS while considering predicted atmospheric and altitude effects.
$\overline{V_{Mach2,i}}$	
$\overline{\overline{V_{TAS2,i}}}$	= Ratio of true airspeed to CAS. Used as a factor to convert flown CAS to TAS while considering predicted atmospheric and altitude effects.
$\overline{V_{CAS2,i}}$	
$\varepsilon_j^A$	= Magnitude of tracker jump error source A at radar track index $j$
$\gamma$	= Specific heat for air
$\rho_0$	= Air density at sea level
$\rho_i$	= Air density at aircraft altitude
$\sigma_{K,j}^2$	= Covariance between error sources $K$ and $j$
$\sigma^2$	= Total arrival-time error variance at meter fix
$\theta$	= Bank angle



## Summary

The Efficient Descent Advisor (EDA) controller automation tool generates trajectory-based speed, path, and altitude-profile advisories to facilitate efficient, continuous descents into congested terminal airspace. While prior field trials have assessed the trajectory prediction accuracy for large jet (i.e., Boeing and Airbus) types, smaller (i.e., regional and business) jet types present unique challenges involving different descent procedures and Flight Management System (FMS) capabilities. A small-jet field trial was conducted at Denver in the fall of 2010 with the objective of measuring trajectory prediction accuracy and quantifying the primary sources of error. This paper uses data collected on board a Bombardier Global 5000 test aircraft to quantify the size and sources of trajectory prediction error. Error sources were quantified for 44 runs by incrementally replacing predicted data with data collected on board the aircraft and measuring the effect on time error. Results for en route descents, from prior to top of descent to the meter fix 60 to 120 nmi downstream, indicate that the aircraft arrived an average of 15 seconds earlier than predicted, with a standard deviation of 10 seconds. Target Mach and calibrated airspeed (CAS) deceleration were found to be the two largest error sources. If CAS deceleration error was reduced using a typical, more predictable level flight deceleration, then the arrival-time prediction error in 2010 would be on par with a 2009 flight trial of Airbus and Boeing revenue flights. Four of the error sources—tracker jumps, CAS deceleration, target Mach, and path distance—lend themselves to significant reductions with modest changes to air traffic control automation and/or procedures. Wind error and its impact on arrival-time error was significantly reduced in 2010 compared to a 1994 flight test using NASA's Boeing 737 test aircraft.

### 1. Introduction

Arrival congestion often inhibits efficient, continuous descent operations at many airports. Current air traffic control (ATC) techniques, without the aid of trajectory-based automation advisories, lead to many corrective changes in speed, path, and altitude profiles when controllers attempt to meter arrivals and maintain separation. The Efficient Descent Advisor (EDA)<sup>1-4</sup> is an automation tool that supports controllers with clearance advisories prior to top of descent that are designed to achieve precise meter-fix scheduled times of arrival while enabling continuous descents. Three-Dimensional Path Arrival Management (3D PAM)<sup>3,5-7</sup> is a concept for operational deployment of EDA that leverages EDA automation and the onboard vertical navigation (VNAV) capabilities of Flight Management Systems (FMS). What distinguishes 3D PAM from other EDA operational deployment concepts is that 3D PAM does not require an air/ground data-link communications capability. The 3D PAM clearance is designed so that the controller does not need to vector or assign temporary altitudes until the aircraft crosses the meter fix. The ability to fly more efficient speed and altitude profiles reduces fuel burn and emissions and maximizes utilization of the FMS. System benefits include increased flight path predictability and increased arrival-time delivery accuracy at the meter fix.

The 3D PAM descent procedures were validated in a field test involving United and Continental Airlines flights arriving at Denver International Airport in the fall of 2009.<sup>3</sup> The mean absolute value of the arrival-time error at the meter fix was estimated to be about 12 seconds with wind modeling noted as the main error source. While this and previous field trials focused on large (i.e., Boeing and Airbus) transport types, little attention has been paid to smaller (i.e., regional and business) jet types. Aside from the obvious differences in aircraft performance, the FMS capabilities and descent procedures involve significant differences critical to the accurate prediction of descent trajectories. The larger types, employing full performance-based VNAV capabilities for planning and executing continuous idle/near-idle descents, typically execute a relatively predictable profile that varies primarily with wind and descent speed. In comparison, the smaller jets employ a simpler FMS with "kinematic" VNAV guidance typically

based on a fixed (inertial) flight-path angle. Moreover, the choice of descent angle is up to the pilot, and there exists little standardization in the selection of descent path or pilot procedure.

To address this gap, a flight trial of 3D PAM small-jet descents was conducted in collaboration with the FAA and Boeing at Denver in the fall of 2010 using a Bombardier Global 5000 flight test aircraft provided by the FAA. The purpose of this test was threefold: (1) to develop and evaluate procedures in preparation for trials involving revenue flights with a regional carrier; (2) to assess the trajectory prediction accuracy under more controlled conditions; and (3) to collect the airborne data necessary to analyze the source and magnitude of prediction errors. A related field trial involving SkyWest Canadair Regional Jet revenue flights is addressed in Part II of this paper.<sup>8</sup> A prior EDA flight trial<sup>9-10</sup> conducted at Denver in 1994 using a NASA B737 test aircraft with a performance-based FMS VNAV capability found that the dominant error source was the predicted winds aloft.<sup>11</sup>

The focus of this paper is quantifying the Center-TRACON Automation System (CTAS)<sup>12-14</sup> trajectory prediction accuracy for small-jet descents and to identify and measure the trajectory prediction error sources. This work expands on an earlier paper<sup>15</sup> by elaborating on the error source quantification methodology and run-by-run results that quantify the impact of the error sources on the 44 runs. Trajectory prediction accuracy is useful for determining the operational viability of the 3D PAM concept in terms of meeting required times of arrival, conflict detection and resolution, and total prediction accuracy, such as accuracy of the vertical profile prior to the meter fix. If the trajectory predictions are too inaccurate, then controllers will need to issue additional tactical clearances for separation and conformance to the scheduled time of arrival. Insight into the trajectory prediction error sources could be used to develop techniques to compensate for these errors or, if necessary, to create larger uncertainty buffers used in automation tools.

To measure the trajectory prediction accuracy, the CTAS trajectory synthesizer component is used to generate predictions that are compared to the flown trajectories in the trials. The primary consideration is the predicted time error. Other trajectory prediction accuracy metrics, such as predicted top of descent, bottom of descent, flight path angle, and altitude relative to the flown trajectory are used to describe differences between the predicted and flown trajectories. Seven error sources are identified and quantified based on analysis of radar track data along with air data computer (ADC) and global positioning system (GPS) data collected during the flight trial. The contribution of each error source to the time error is quantified along the predicted trajectory from top of descent to the meter fix and aggregated over all the runs.

The paper is organized as follows. Section 2 describes the Global 5000 3D PAM flight trial at Denver. Section 3 describes how CTAS was used to predict trajectories. The quantification of arrival path trajectory prediction accuracy is presented in Section 4. Section 5 describes seven arrival path trajectory prediction error sources. Section 6 describes the method to quantify each of these seven error sources by incrementally replacing predicted data with data sensed on board the aircraft. This method was applied in Section 7 to quantify the relative magnitude of the seven error sources in terms of their contribution to time error along the descent prediction. These results are compared to a 1994 NASA B737 trial. Conclusions are then presented in Section 8. The Appendices provide run-by-run details including a ranking of which runs were most impacted by specific error sources and plots of the effects of each error source on each run.

## 2. Flight Trial

Data for the Global 5000 flight trial were collected between September 27, 2010, and October 8, 2010. This section describes the flight trial procedure, including the test matrix, arrival routing, VNAV procedures, and data collection.

## 2.1. Test Matrix

A desired test matrix of 45 descent runs was comprised of a primary matrix, involving 36 straight-path descents using speed control, and 9 runs with path stretch and speed control. These descent runs are respectively referred to as “direct” and “path stretch” through this paper. The Global 5000 aircraft was able to complete 35 of the 36 direct runs and all 9 path-stretch runs. One of the runs was scratched, and the desired test matrix was not completed, due to conflicting priorities with other flight trial objectives. A summary of the 44 flown runs is shown in Table 1.

Each descent run involved a fixed flight path angle (FPA) descent with a vertical profile anchored at the meter-fix crossing restriction and extending back upstream to define the top of descent. For the purpose of this test, the flight crew had the option of selecting one of two predefined FPAs depending on the cruise Mach and descent calibrated airspeed (CAS) combinations shown in Table 1. These two FPAs were defined to be consistent with typical descents performed by the FAA pilots in the Global 5000 aircraft. The choice allowed the pilot to pick the angle best suited for the relative winds aloft during that particular run. While the methodology for selecting the FPA would be ambiguous in current-day operations, it is assumed here that the selection is procedurally defined to ensure that ATC and the supporting automation have accurate knowledge of the planned FPA.<sup>16,17</sup> The right-hand columns of Table 1 show the number of flown runs for each FPA for direct and path-stretch runs, which differs from the desired test matrix.

The goal of the primary matrix was to obtain an even sampling of nine direct runs, each across the four main arrival gates of the Denver TRACON, to obtain a balance of headwind and tailwind cases. The four meter fixes (LANDR, RAMMS, QUAIL, and LARKS) correspond to the four arrival gates shown in the left-hand column of Table 1. The nine runs were comprised of three descent speed profiles, spanning the speed envelope (250, 280, and 300 knots CAS), repeated three times each. The total, which was planned to equal three, was obtained by totaling the runs for each FPA. LANDR is missing one 250-knot descent, and there was one extra 280-knot descent into LARKS instead of a 250-knot descent. This was caused by a late clearance during run 10 where the pilot declared unable to descend at -2.0 degrees at 250 knots, which resulted in a revised clearance of -2.5 degrees at 280 knots. Of the nine path-stretch test matrix runs planned, three runs for each descent CAS irrespective of meter fix, only two were collected at 250 knots, three at 280 knots, and four at 300 knots.

**Table 1. Descent runs by meter fix, CAS, and FPA.**

Arrival Gate	Meter Fix	Available Combinations of Mach, CAS, and FPA			No. of Runs Flown for Each FPA						
		Cruise Mach	Descent CAS (knots)	Available FPAs	Direct			Path Stretch			
					-2.0	-2.5	-3.0	Total	-2.0	-2.5	-3.0
Northeast	LANDR	0.74	250	-2.0, -2.5	2			2	1	1	
		0.76	280	-2.5, -3.0				3	3		
		0.78	300	-2.5, -3.0		1	2	3			2
Northwest	RAMMS	0.74	250	-2.0, -2.5	2	1		3			
		0.76	280	-2.5, -3.0		2	1	3		1	1
		0.78	300	-2.5, -3.0		2	1	3			1
Southeast	QUAIL	0.74	250	-2.0, -2.5		3		3			
		0.76	280	-2.5, -3.0		2	1	3			1
		0.78	300	-2.5, -3.0		1	2	3			
Southwest	LARKS	0.74	250	-2.0, -2.5	1	1		2			
		0.76	280	-2.5, -3.0		3	1	4			
		0.78	300	-2.5, -3.0		1	2	3			1

## 2.2. Arrival Routing

The arrival routes for each of the four arrival gates are shown in Figure 1. Each arrival, both direct (solid black line) and path stretch (dashed black line), began at a cruising altitude of 30,000 to 36,000 feet approximately 95 to 120 nmi from the meter fix. The flight crew then descended the aircraft to the meter-fix crossing altitude of 19,000 feet with a deceleration initiated during descent in time to meet the meter-fix crossing speed restriction of 250 knots. Once past the meter fix, ATC vectored the aircraft to the starting point for the next run (grey line) while the aircraft climbed back to the desired initial altitude for that run. For example, the direct-path arrival route for the northeast arrival gate was initiated at SNY050040 (a position 40 nmi from the Sidney (SNY) VORTAC along the 050° radial), and flown direct to LANDR. The corresponding path-stretch route was also initiated at SNY050040 and flown direct SNY140035, direct LANDR. Repositioning the aircraft for another run from the northwest involved vectors to YOKES, then direct COPLA, direct HANKI, direct SNY030045, and direct SNY050040.

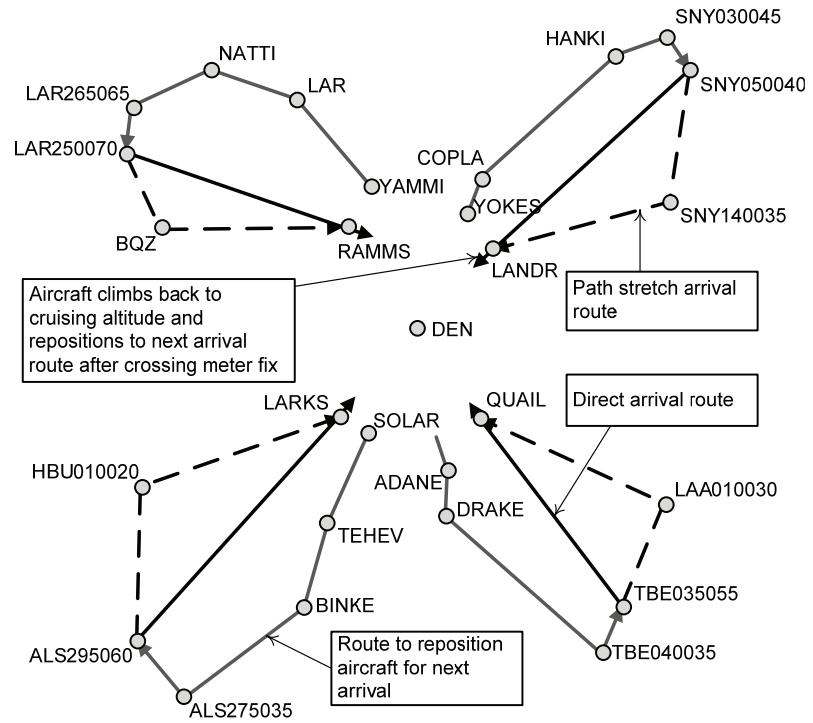


**Figure 1. Arrival routes for each of the four Denver arrival gates.**

## 2.3. VNAV

During the flight trial, VNAV capability was used for vertical guidance only and was not coupled to the autopilot and autothrottle. VNAV was set up in this way on the Global 5000 to be consistent with the capabilities of the FMS aboard Canadair Regional Jet (CRJ) models 200, 700, and 900. These CRJ models were used for 3D PAM flight trials involving SkyWest airlines that followed the Bombardier Global 5000 runs and are the subject of Part II of this paper.<sup>8</sup>

## 2.4. Data Collection

The following subset of ADC and GPS data were automatically recorded during the flight test and used to identify and quantify the error sources. Time, latitude, longitude, pressure altitude (ADC), and ground-referenced altitude (GPS) were recorded to establish aircraft position. The current aircraft speed was recorded including indicated airspeed (IAS), true airspeed (TAS), Mach, and ground speed. The Mach and CAS being targeted were recorded to establish the target speed. The atmospheric conditions recorded and used in this analysis included wind speed, wind direction, temperature, and air density.

Details of the clearance and other comments were manually recorded on board and on the ground. Denver Air Route Traffic Control Center (ARTCC) radar track data was recorded at the 12-second radar sweep update rate. Atmospheric information from the National Oceanic and Atmospheric Administration's (NOAA's) Rapid Update Cycle (RUC) data was recorded and archived for post-

analysis. The EDA clearances, rather than the trajectory predictions, were recorded during the flight test to facilitate the generation of the CTAS-predicted trajectories during post-processing.

### 3. Trajectory Prediction

The trajectory predictor used for this study was the trajectory synthesizer (TS) component of the CTAS12-1414 software version. It generated a four-dimensional (4D) trajectory prediction (three spatial dimensions and time) based on the radar track position and ground speed at each run's initial condition. This initial position was typically 60 to 85 nmi from the meter fix for the direct runs, and 100 to 120 nmi from the meter fix for path-stretch runs. The initial condition for direct runs was selected to be a point at which the aircraft had repositioned itself on the direct route with its course stabilized for 4 to 8 nmi. The initial condition for path-stretch runs was selected at a point about 5 to 8 nmi before the aircraft started its path-stretch turn. For the path-stretch runs, the initial condition was selected at points outside any turn to avoid ground speed bias in the track data during turns.

Because CTAS requires special processing to parse a flight plan that contains more than one arrival or departure route, the flight plans issued for the Global 5000 test flight—which included repeated arrival and departure routes—could not be readily parsed by CTAS in real time. Accordingly, the trajectory predictions were computed off-line after the field trial had ended, using the atmospheric conditions, EDA clearances, and meter-fix crossing restrictions that would have been known to the ground automation system at the start of each run. Each trajectory prediction was run once and not updated during the descent to the meter fix.

The horizontal path for each descent trajectory was modeled as a sequence of straight-line and turn segments around waypoints. For the turns, the TS used a default bank angle ( $\theta$ ) of 20.8 degrees, standard gravity ( $g$ ), and an estimated average ground speed ( $v$ ) at the location of the turn to compute the turn radius ( $r$ ) according to equation (1). The default bank angle ( $\theta$ ) was used by the TS for the trajectories of all flights in the Center.

$$r = v^2 / (g \tan \theta) \quad (1)$$

Figure 2 shows segments of the vertical profile modeled by TS for the Global 5000 runs. Segment 1 turned out to be unnecessary because, prior to issuing the clearances, controllers ascertained the aircraft's current Mach number and instructed pilots to maintain that Mach number as the target cruise Mach number. Descent segments 3, 4, and 5 maintained a constant FPA in accordance with the issued clearance. Segment 5 had non-zero duration of time only if the descent CAS was greater than the meter-fix crossing restriction speed. Among the 44 runs analyzed, 22 required a CAS deceleration segment.

The cruise Mach segment (segment 2) was constructed by TS using a cruise Mach number computed from CTAS-estimated ground speed at the initial condition. Due to tracker jumps and weather/wind forecast errors, this estimated cruise Mach number differed from the flown target cruise Mach number.

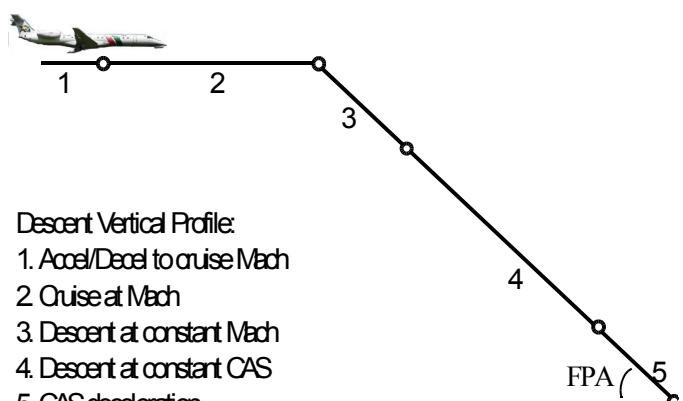


**Figure 2. Descent vertical profile modeled for the Global 5000 runs.**

The CAS deceleration segment (segment 5) at the end of the trajectory was modeled as follows. The TS first attempted a constant FPA, idle thrust descent for the 22 runs with descent CAS higher than the meter-fix crossing speed restriction. For some runs, the trajectory generation failed as the idle thrust descent could not slow down the aircraft to meet the meter-fix crossing speed restriction. Technically, the equations of motion were integrated backward from the meter fix up the descent segment. A trajectory would fail if the descent segment did not have enough length to allow the airspeed to capture the descent CAS during the descent. In these cases, the effect of deployed speed brake was modeled. The TS modeled the speed brake drag by a fixed “dirty” drag coefficient (arising from the aircraft’s change from its clean configuration), and a percentage of speed brake usage. Due to the lack of a standard procedure, it was assumed that pilots would use the minimum speed brake needed to capture the target speed. This modeling choice is discussed in Section 7, Results. The speed brake drag coefficient was increased incrementally by 10 percent until a valid trajectory was generated. Among the 22 runs that required a deceleration segment, 10 of them (runs 1, 5, 6, 7, 16, 18, 20, 24, 27, and 40) required 10 percent of full speed brake deployment. Run 13, in particular, required 20 percent of full speed brake deployment. The other 11 runs did not require speed brake usage.

#### 4. Trajectory Prediction Accuracy

The accuracy of the CTAS trajectory predictor was measured by comparing the recorded radar tracks from the 3D PAM flight trials with the corresponding trajectories predicted by CTAS. This comparison was based on the spatial location (latitude/longitude) on the predicted trajectory closest to each radar track position. This technique<sup>18</sup> is referred to as “closest segment spatial error” or spatial correlation.

The distribution of time error at the meter fix across all runs is presented in Figure 3. Aircraft generally arrived at the fix earlier than predicted as indicated by the negative values along the x-axis in Figure 3. The trajectory prediction error sources described in Section 5 and quantified in Section 7 are used to explain this time error.

The mean ( $-15.4$  sec) and standard deviation ( $9.9$  sec) of the time error at the meter fix for direct runs are shown in the left columns in Table 2, along with other summary statistics. Runs with path stretches shown in the right columns in Table 2 show a significantly larger mean error ( $-27.0$  sec) and standard deviation ( $25.8$  sec) than direct runs.

The top of descent (ii) and bottom of descent (iii) were both  $0.3$  nmi closer to the meter fix than predicted for direct runs. For path-stretch runs, the top of descent and bottom of descent were  $0.5$  nmi and  $0.7$  nmi respectively, closer to the meter fix. The relatively small FPA (iv) error for both direct ( $-0.01$  deg) and path-stretch ( $-0.03$  deg) runs indicates that the aircraft flew a slightly steeper descent than predicted. The maximum cross-track error (v) is the average of the maximum cross-track error for each of the direct ( $0.4$ -nmi cross-track error) and path-stretch ( $2.2$ -nmi cross-track error) runs. The altitude error (vi) ranged

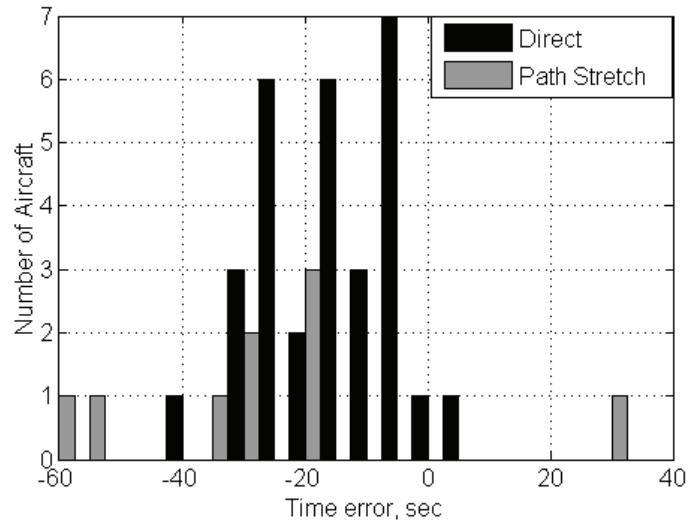


Figure 3. Distribution of time error (flown trajectory minus predicted trajectory) at meter fix. A negative value indicates that the aircraft arrived earlier than predicted.

from 30 to 100 feet lower than predicted during direct descents and 100 to 175 feet lower than predicted during path-stretch descents.

## 5. Description of Error Sources

Seven principal sources of error were identified: tracker jumps, wind, CAS deceleration, speed conformance, target mach, atmosphere/altitude, and path distance. These are annotated as sources A through G in Figure 4. The white circles along the vertical profile in Figure 4 correspond to nine reference locations along the predicted trajectory where results were aggregated across all runs. While the bottom of descent should coincide with the meter-fix location, they are analyzed separately because of the differences in the actual bottom-of-descent flown (quantified as the bottom-of-descent location metric in Table 2). Section 6 describes the method to quantify error source magnitudes.

### 5.1. Tracker Jumps

Tracker jumps, due to truncation of the time component (i.e., dropping significant digits) of the En Route Host radar tracker resulting from legacy technical limitations, introduce noise into the time error data. The dashed line in Figure 5 shows an example of tracker jumps from the second run. The x-axis is the distance along the predicted path starting at the initial condition and ending at the meter fix. The y-axis is the flown time minus the predicted time at the specified distance from the initial condition. The uncorrected curve (dashed line) shows “jumps” of approximately 6 seconds in the time difference between successive values while the corrected curve (solid line) somewhat mitigates this effect. The magnitude of the jumps is included in Appendix A based on the method described in Section 6.

The tracker jump error was aggregated across all runs at the nine locations shown along the x-axis of the Figure 6 box plot. The top and bottom whiskers are the minimum and maximum values of the tracker jump error effect. The top and bottom of the box are the first and third quartiles, and the line in the box is the median. The median line is not shown at some of the locations because 0-second error magnitudes occur about a third of the time, causing the median to equal the

**Table 2. Summary of trajectory prediction errors.  $\mu$  = mean error and  $\sigma$  = standard deviation of error.**

Error Description, units	Direct		Path Stretch	
	$\mu$	$\sigma$	$\mu$	$\sigma$
i) Time error at meter fix, sec	-15.6	9.9	-27.0	25.8
ii) Top-of-descent location, nmi	0.3	0.8	0.5	1.0
iii) Bottom-of-descent location, nmi	0.3	0.4	0.7	0.6
iv) Flight path angle error, deg	-0.01	0.04	-0.03	0.07
v) Maximum cross-track error, nmi	0.4	0.2	2.2	0.8
vi) Altitude error				
Top of descent, ft	-116	74	-143	124
Initial condition – 2,000 ft, ft	-63	145	-98	274
Initial condition – 4,000 ft, ft	-34	94	-143	168
Initial condition – 6,000 ft, ft	-34	92	-152	125
Fix altitude + 4,000 ft, ft	-67	121	-158	153
Fix altitude + 2,000 ft, ft	-69	93	-174	185
Bottom of descent, ft	35	115	12	23
Meter fix, ft	35	115	12	23

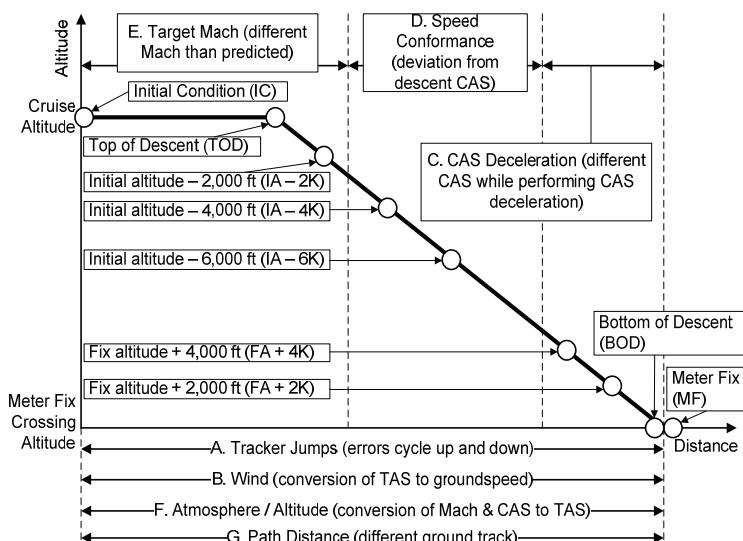


**Figure 4. Seven error sources plotted on the vertical profile from the initial condition at cruise altitude to the meter-fix crossing altitude. Also shown are nine reference locations along the predicted trajectory (initial condition (IC) to meter fix (MF)).**

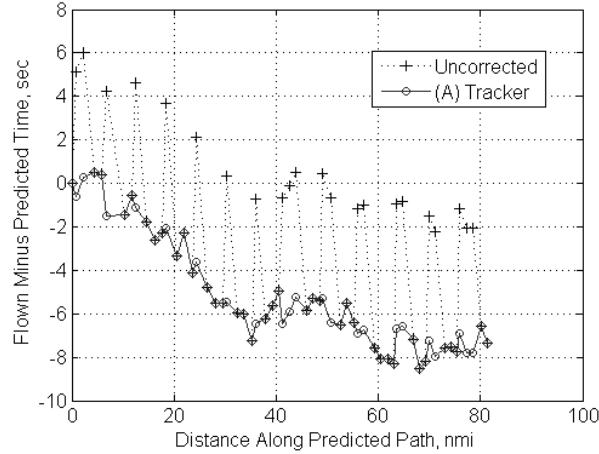


**Figure 5. Example time error from run 2. Solid line has been corrected for tracker jumps while dashed line is uncorrected.**

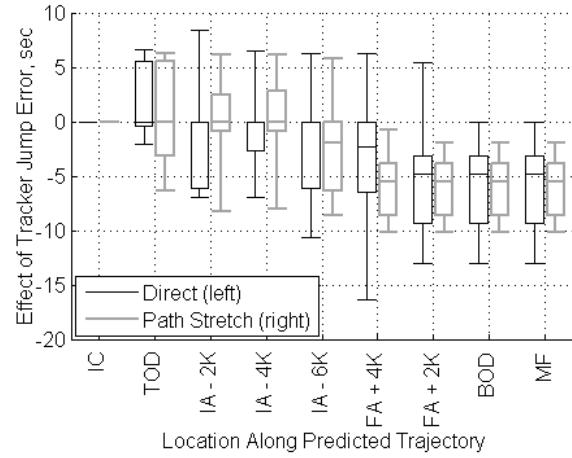


**Figure 6. Tracker jump error at locations along predicted trajectory.**

third quartile. The error due to tracker jumps does not significantly grow in magnitude along the trajectory, which is the case for the other six error sources discussed next.

## 5.2. Wind

There are two sources of error with respect to the atmospheric model used in the trajectory predictor. One is the difference between winds estimated in the NOAA RUC model and the winds observed by aircraft sensors. Section 5.6 describes the second atmospheric model error source, which is the difference between the temperature and pressure estimated by the models, and the values sensed by the aircraft. Figure 7 shows an example where the aircraft flew into less of a headwind than expected (negative values along y-axis indicate headwind). The difference between the RUC model-predicted winds and winds recorded by the ADC is used to generate the effect of corrected winds on ground speed in Figure 8. There is a small wind error (< 5 knots) up to about 40 nmi along the predicted path (about 20 nmi after the top of descent). The wind error then grows to a maximum of about 17 knots overpredicted headwind (i.e., RUC model predicted a stronger headwind than occurred) at about 55 nmi along the predicted path. This difference in predicted vs. actual winds results in about a 6-second time difference at the meter fix as shown in the Figure 9 time error plot.

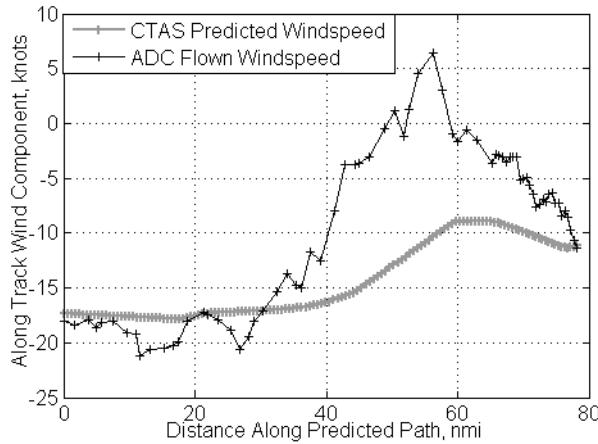


**Figure 7. Example along track component of wind speed for run 34 showing less of a headwind than was predicted.**

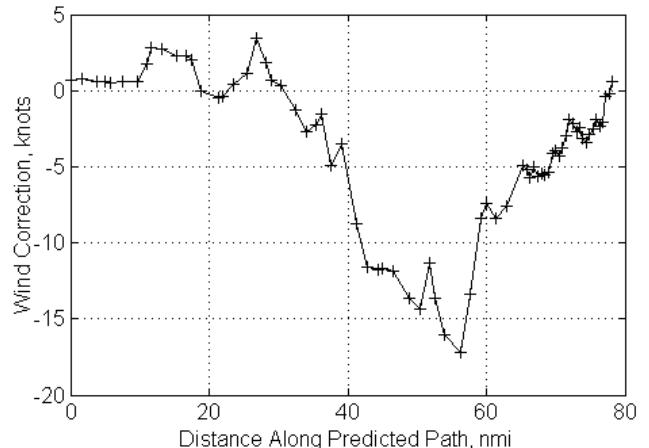


**Figure 8. Example showing effect of corrected winds on ground speed for run 34.**

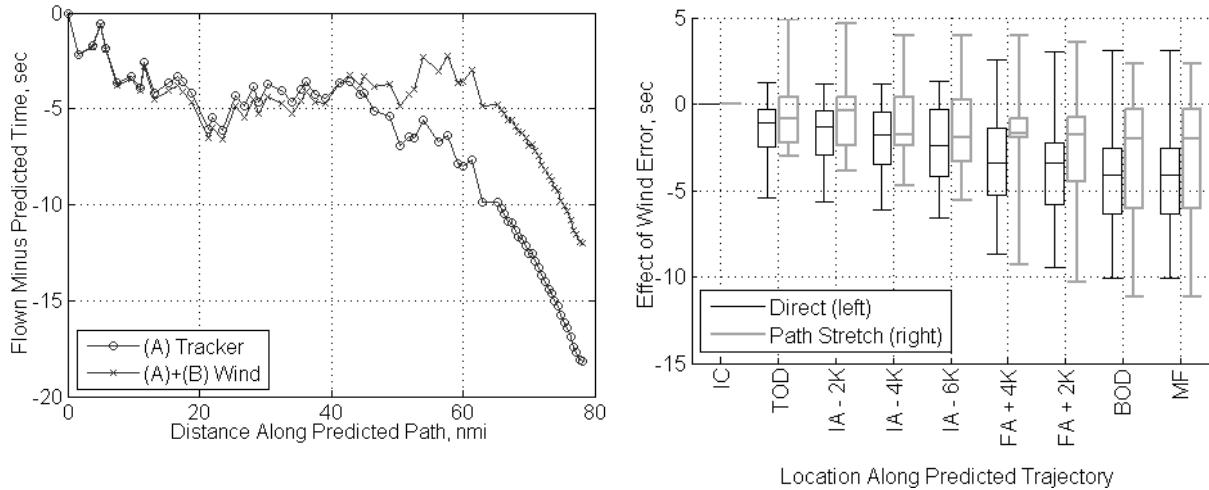


**Figure 9. Example effect of wind on time error for run 34. Both curves corrected for tracker jumps. ‘x’ marker curve has wind error removed.**

**Figure 10. Wind error at locations along predicted trajectory.**

The wind error, which is the difference between the uncorrected and corrected trajectory times, was aggregated to generate the wind error box plot shown in Figure 10. Figure 10 shows that there was more of a tailwind (median is negative) than predicted, which caused the aircraft to arrive at the fix earlier than predicted. The wind errors are also cumulative and increase in magnitude from the top of descent to the meter fix.

### 5.3. CAS Deceleration

All aircraft were required to cross their assigned meter fix at or below a defined CAS. However, there may be differences in how a pilot reduces CAS to meet the meter-fix crossing airspeed. Generally, the Global 5000 flight crew did not level the aircraft off at the meter-fix altitude and reduce CAS in a level segment. In order to be consistent with this behavior, the CTAS trajectory synthesizer did not model a level segment at the meter-fix altitude. However, the level-off segment was an error source for a few of the runs where the aircraft reached its bottom of descent before crossing the meter fix.

The start of the CAS deceleration segment is defined as the location where the aircraft is predicted to start reducing airspeed below the issued descent CAS. For example, in Figure 11 the constant CAS of 300 knots was predicted to occur at approximately 53 to 60 nmi from the initial condition. The aircraft was predicted to begin decelerating from 300- to 250-knots CAS starting at approximately 60 nmi from the initial condition. In this case, the aircraft actually maintained the descent CAS of 300 knots until approximately 70 nmi from the initial condition. At about 75 nmi along the predicted path, the aircraft TAS is about 30 knots higher than was predicted in the “Effect of CAS deceleration” plot in Figure 12. This difference would cause the aircraft to arrive at the meter fix 13 seconds earlier than predicted in the absence of other error sources as shown in the time error plot in Figure 13.

The CAS deceleration error was aggregated to generate the box plot shown in Figure 14. The deceleration error is negligible near the top of descent because only a few runs were predicted to begin the CAS deceleration segment within 6,000 feet of the initial altitude (IA-6K). The CAS deceleration error begins to grow significantly near the bottom of descent because this error source is only quantified in locations where the aircraft is predicted to be reducing CAS.

On average, the CAS deceleration errors are negative, indicating a similar behavior to that shown in Figure 11. The behavior in Figure 11, and for the majority of the cases, has the predicted CAS deceleration starting to occur earlier than the flown trajectory and at a slower rate of deceleration. A faster flown deceleration rate allowed the aircraft to be closer to the meter fix before starting to decelerate. These results suggest that the pilots may have used speed brake more heavily than modeled by the CTAS trajectory predictor. Alternatively, at idle thrust the aircraft may have reduced CAS faster than CTAS predicted due to inaccurate performance parameters for the Global 5000 test aircraft.

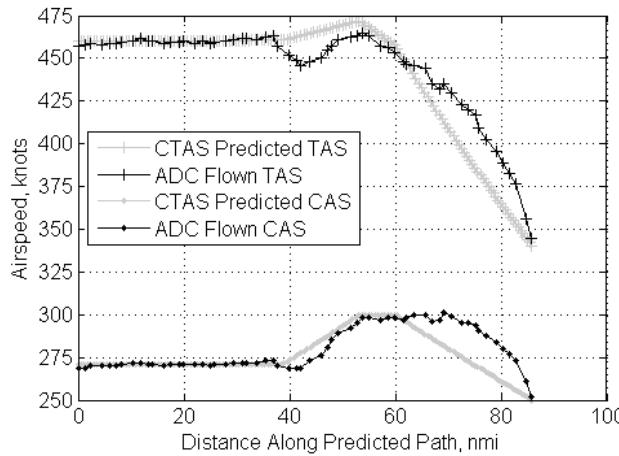


**Figure 11.** Example flown (ADC) and predicted (CTAS) TAS (top two curves) and CAS (bottom curves) for run 3 showing that the aircraft reduced CAS to 250 knots later than predicted.

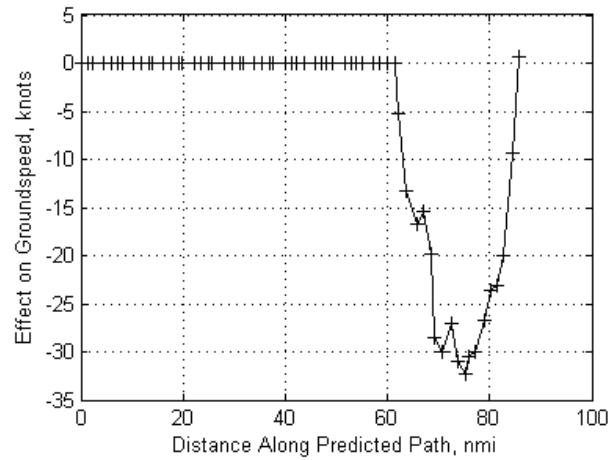


**Figure 12.** Example showing effect of CAS deceleration on ground speed for run 3.

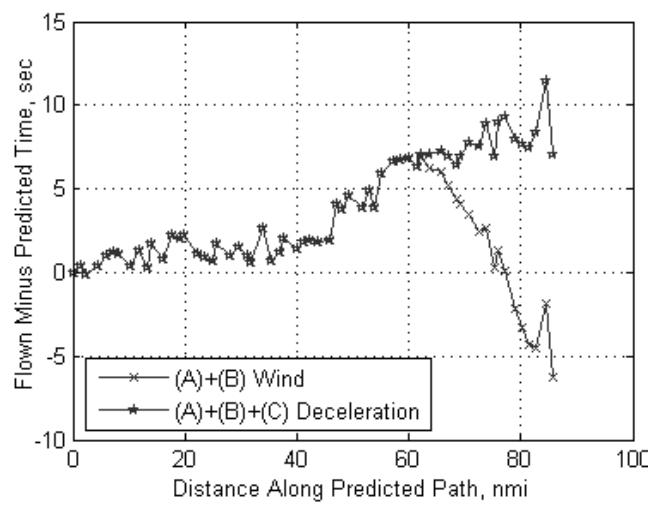


**Figure 13.** Example effect of CAS deceleration on time error for run 3. Both curves have been corrected for tracker jumps and wind. Curve with star marker has also been corrected for deceleration.

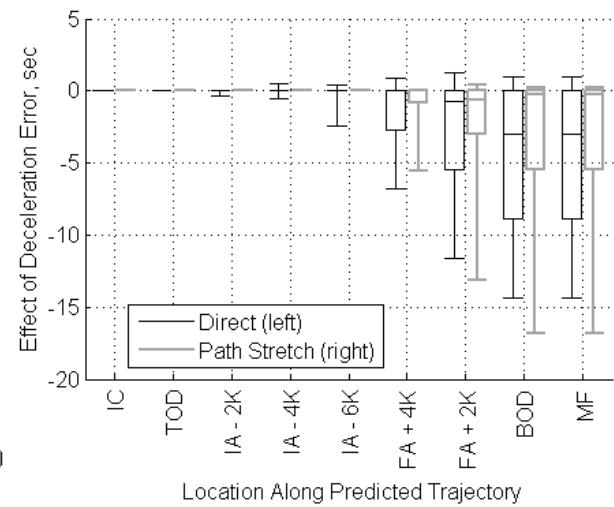


**Figure 14.** CAS deceleration error at locations along predicted trajectory.

#### 5.4. Speed Conformance

A speed conformance error occurs when an aircraft deviates from its target CAS. For example, if an aircraft is targeting a descent CAS of 250 knots but is flying 260 knots, then there is a speed conformance error of 10 knots. This is the case for the example shown in Figure 15, which is corrected starting at about 20 nmi from the initial condition (about 60 nmi from meter fix). The effect of corrected speed conformance on ground speed is shown in Figure 16. As the descent proceeds, the impact of speed conformance grows to about 3 seconds when the aircraft is about 45 nmi from the initial condition. In the end, however, speed conformance does not significantly impact time error at the meter fix in this case, as shown in Figure 17.

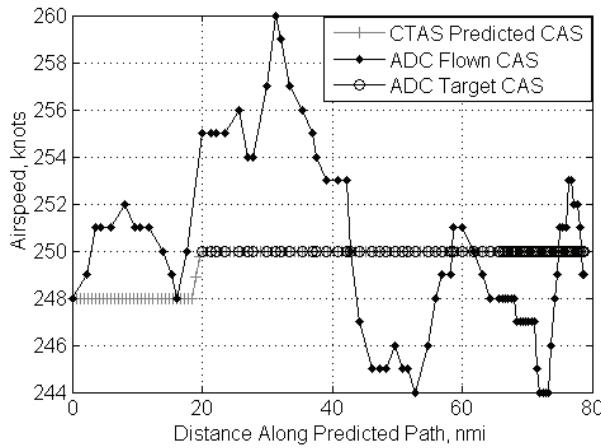


**Figure 15.** Example flown (ADC) and predicted (CTAS) CAS for run 43 showing deviation from 250-knot target CAS during descent.

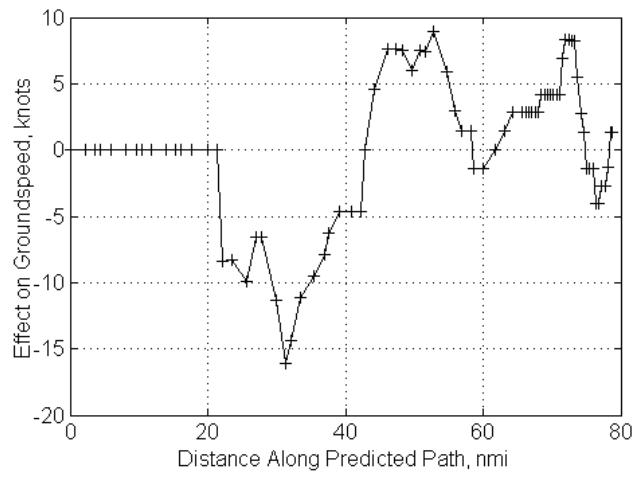


**Figure 16.** Example showing effect of corrected speed conformance on ground speed for run 43.

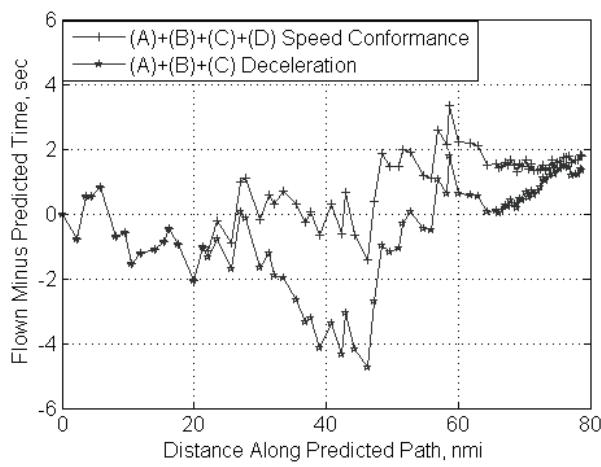


**Figure 17.** Example effect of speed conformance on time error for run 43. Both curves have been corrected for tracker jumps, wind, and deceleration. Curve with '+' marker has also been corrected for speed conformance.

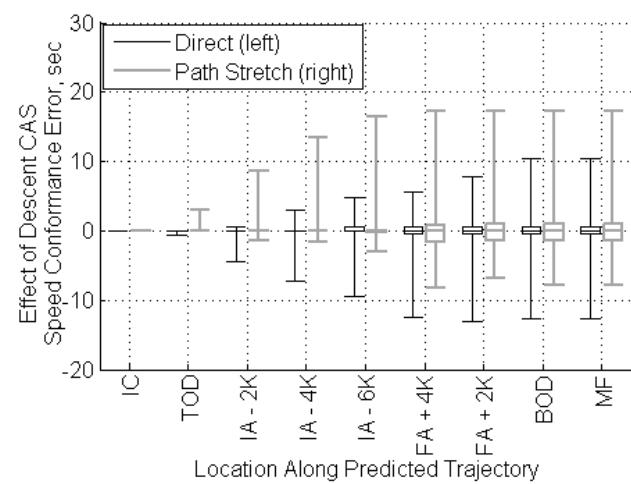


**Figure 18.** Speed conformance error at locations along predicted trajectory.

The speed conformance effect on ground speed is quantified along the predicted constant-CAS segment between the predicted Mach-to-CAS transition location and the location where the aircraft is predicted to start to decelerate to meet the meter-fix speed restriction. The start of the constant-CAS segment was identified by two conditions: (1) the altitude is below the initial altitude, and (2) the Mach is below the initial Mach for the en route segment. The last data point of the segment is when the aircraft is predicted to start decelerating, and the CAS drops below the descent CAS.

The speed conformance error was aggregated in order to generate the box plot shown in Figure 18. Figure 18 shows that the effect of speed conformance grows between the top of descent and bottom of descent, which in this study is expected because error source quantification is cumulative from the initial condition to the meter fix.

### 5.5. Target Mach

The aircraft may have been targeting a different Mach than was predicted by the CTAS trajectory synthesizer. Run 36 shown in Figure 19 is an example of target Mach error where the aircraft is flying a faster Mach than predicted prior to the transition from constant Mach to constant CAS, located about 45 nmi downstream of the initial condition (about 35 nmi from the meter fix). The predicted Mach is low due to the low ground speed estimated by the radar tracker after the aircraft turns onto the arrival route to begin its run. The flown target Mach of 0.76 (black ‘o’ marker), flown Mach between 0.73 and 0.76 (black filled marker), and predicted Mach of 0.72 (grey ‘+’ marker) are all shown in Figure 19. This Mach difference is converted into an effect on ground speed as shown in Figure 20. Removing this error source in Figure 21 shows that the faster Mach causes the aircraft to arrive at the meter fix about 15 seconds earlier than predicted.

The target Mach error was aggregated in order to generate the box plot shown in Figure 22. Figure 22 shows that, on average, the aircraft flew a faster Mach than was predicted (negative values). Also, as expected, the target Mach error primarily occurred prior to top of descent because during descent the aircraft transitions to constant CAS. The target Mach error was higher for path-stretch runs than direct runs because the initial condition for path-stretch runs is closer to the turn from the repositioning route to the arrival route (i.e., further from the meter fix), which causes the path-stretch runs to be impacted more by the ground speed estimated by the radar tracker than the direct runs.

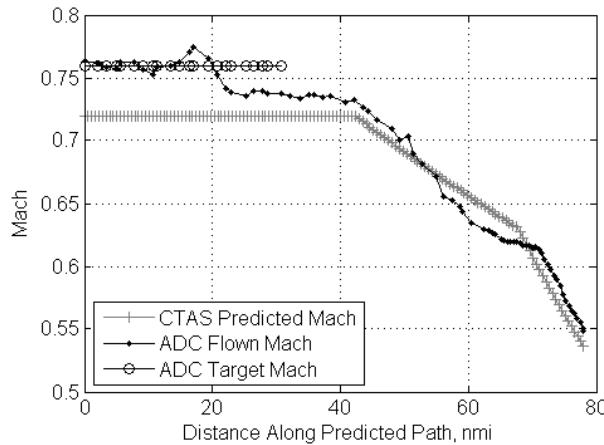


**Figure 19. Example flown (ADC) and predicted (CTAS) Mach for run 36 showing deviation from the 0.72 target Mach prior to the constant-Mach to constant-CAS transition.**

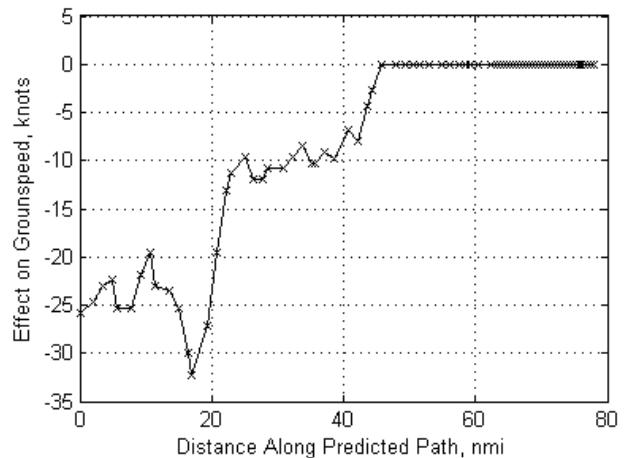


**Figure 20. Example showing effect of corrected target Mach on ground speed for run 36.**

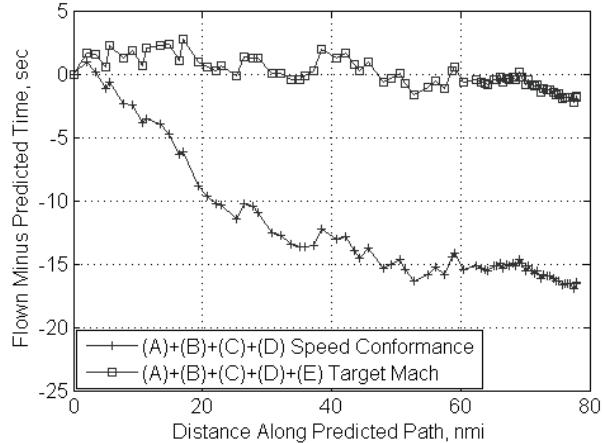


**Figure 21. Example effect of a different Mach than predicted on time error for run 36. Both curves have been corrected for tracker jumps, wind, deceleration, and speed conformance. Curve with square marker has also been corrected for target Mach.**

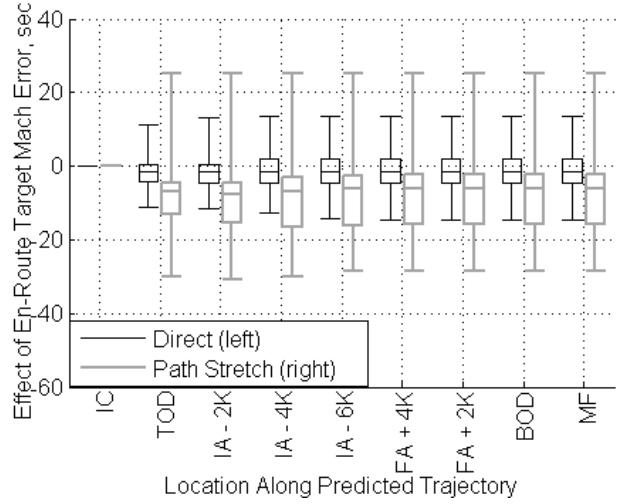


**Figure 22. Target Mach error at locations along predicted trajectory.**

## 5.6. Atmosphere/Altitude

Atmospheric conditions including temperature and air density are used to convert the targeted airspeed to TAS which, taking into account winds, is then converted to ground speed. This error source focused on the predicted vs. flown atmospheric conditions, which introduce errors in the conversion of Mach and CAS to TAS. In the case of Mach, TAS is the product of Mach, speed of sound at sea level (a constant), and the square root of the ratio of static air temperature in which the aircraft is flying (recorded by ADC) to the temperature at sea level (a constant). In the case of CAS, TAS is a product of CAS and the square root of the ratio of air density at sea level (a constant) to the air density in which the aircraft is flying (recorded by ADC). Flying higher or lower than predicted similarly changes the TAS through changes in air temperature and density, and was also captured by this error source. The altitude/atmosphere errors were quantified as a CAS-to-TAS and Mach-to-TAS conversion error as described in Section 6. A comparison between predicted and flown altitude, air temperature, and air density is included in Appendices C and D even though these were not used directly to quantify the magnitude of the atmosphere/altitude error source.

For example, Figure 23 shows a case where the aircraft was up to 175 feet lower than predicted from the top of descent at about 20 nmi from the initial condition to about 15 nmi from the meter fix. This caused the aircraft to be flying about 1 to 1.5 knots faster than predicted, which is corrected according to the “effect of atmosphere/altitude on ground speed” plot in Figure 24. Figure 25 shows that the atmosphere and altitude error source increased the arrival-time error from about 1 second to about 2 seconds.

The box plot aggregating the atmosphere and altitude errors in Figure 26 shows that the error primarily impacts the descent portion, which is expected because this is the location most likely to have a difference between predicted and flown altitudes. The negative medians in the box plot indicate that, on average, the aircraft flew a lower altitude than predicted, which increased ground speed and caused the aircraft to arrive at the meter fix earlier than predicted.

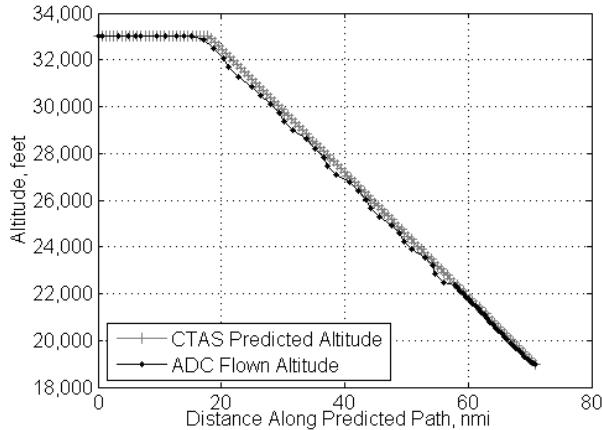


**Figure 23. Example showing predicted and flown altitude for run 14.**

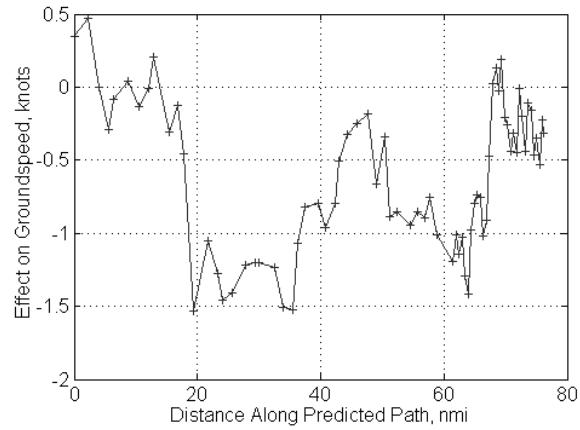


**Figure 24. Example showing effect of corrected atmosphere/altitude on ground speed for run 14.**

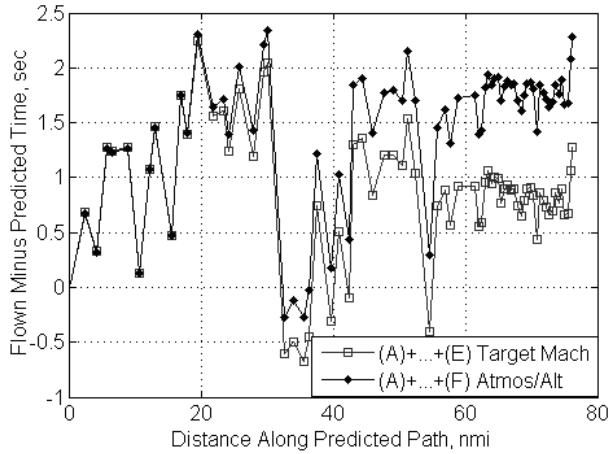


**Figure 25. Effect of atmosphere and altitude on time error for run 14. Curve with diamond marker has been corrected for atmosphere and altitude.**

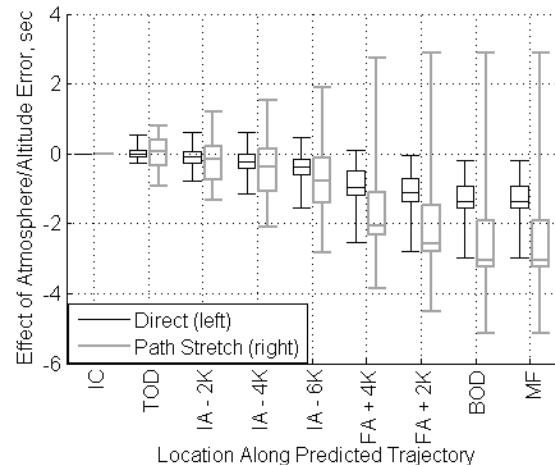


**Figure 26. Atmosphere and altitude error at locations along predicted trajectory.**

## 5.7. Path Distance

Aircraft deviated from their predicted lateral path causing variance in the distance from the initial condition to the meter fix. For direct runs, any variance from the predicted lateral path would result in a longer flown path distance than predicted. However, all of the path-stretch runs flew a shorter path through the turn than predicted. The lateral profile in Figure 27 is an example of using a shorter path midway through a southeast-bound descent that starts in the upper right corner of the plot. At the middle of the curve, the aircraft is about 1.8 nmi away from the predicted lateral path (i.e., cross-track error of 1.8 nmi). This path is about 1.2 nmi shorter than predicted and is applied as a change in path distance shown in Figure 28 rather than the ground speed change applied in the previous error sources excluding tracker jumps. The shorter path distance contributes about 9 seconds to the aircraft being early to the meter fix as shown in the time error plot in Figure 29. As expected, the shorter path distance in the path-stretch runs

caused the aircraft to arrive earlier than predicted, as shown in the box plot that aggregates the path distance in Figure 30. The path stretch occurs at or near the top of descent, which is why the effect of path distance is primarily before the top of descent as shown in Figure 30. The longer path distance in the direct runs caused the aircraft to arrive later than predicted as indicated by the positive errors in Figure 30.

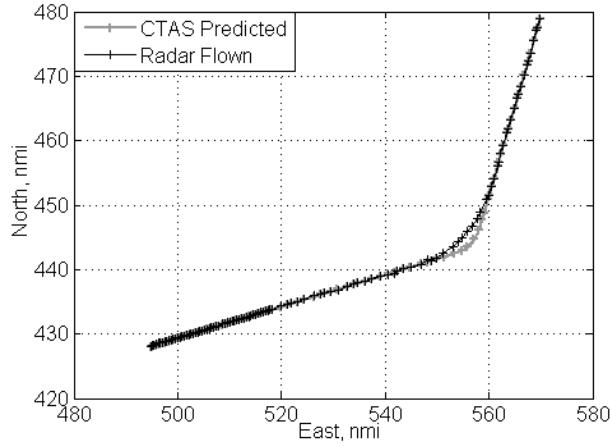


**Figure 27. Example showing predicted and flown lateral path for run 33.**

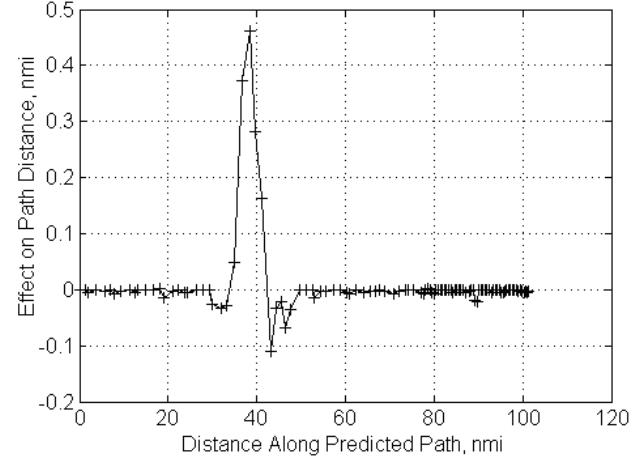


**Figure 28. Example showing effect of removing path distance error source for run 33,**

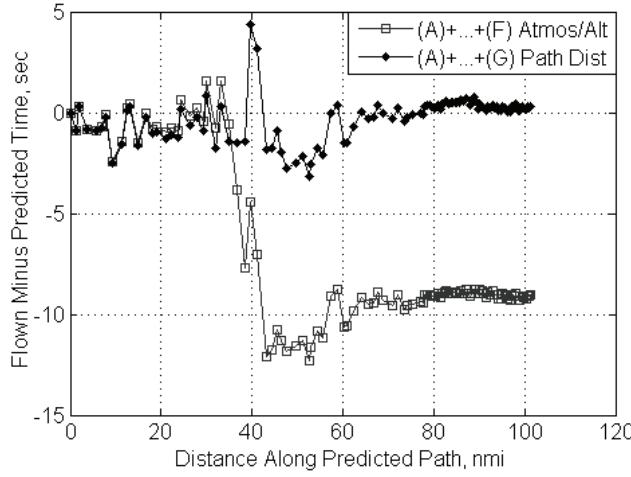


**Figure 29. Example effect of path distance on time error for run 33. Curve with diamond marker has been corrected for path distance.**

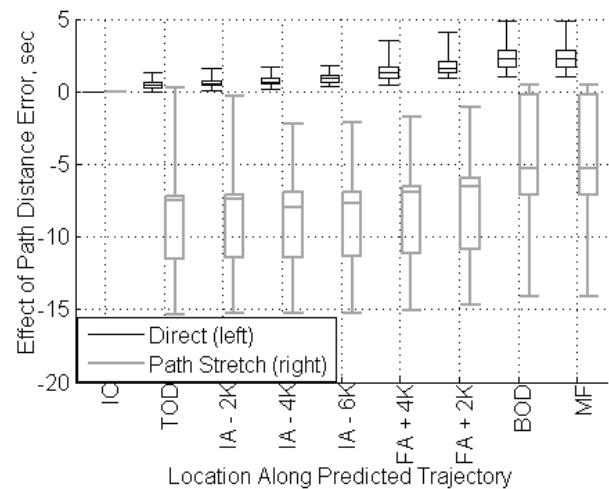


**Figure 30. Path distance error at locations along predicted trajectory.**

## 6. Method to Quantify Magnitude of Error Sources

Error sources are quantified incrementally (i.e., quantify wind and tracker jumps after correcting for tracker jumps only) to isolate the contribution of each error source to the overall trajectory time error. For example, comparing a trajectory that has wind and tracker jump error sources removed against a trajectory that has just the tracker jump error source removed will estimate the impact of wind errors. Any interactions between error sources will affect the error source magnitudes. Larger interactions between error sources are expected to cause the order that error sources are quantified to become more significant. However, the interactions are relatively small in magnitude as shown by the normalized correlation coefficients in Section 7, so the focus will be on first-order analysis of error sources.

The order in which the error sources were quantified was based on an initial estimate of the magnitude of the errors and potential interactions between error sources. The tracker jump quantification method was applied first to remove noise so that trends due to the other error sources could be examined. Wind was quantified next because it was found to be the largest error source from an earlier flight trial of large jets.<sup>11</sup> CAS deceleration, speed conformance, and target Mach error sources were modeled (at different locations along the cruise and descent) to interact with wind and atmosphere/altitude, therefore the error source quantification method was not impacted by the order of these three error sources. Atmosphere/altitude and path distance had the smallest error magnitudes as described in Section 7 and were quantified last. The impact of error source quantification order was estimated by shifting the wind and atmosphere/altitude error source before and after each of the other error sources. Shifting the quantification of the wind error source, which has a relatively large impact compared to the other error sources, was found to impact the mean time error attributed to the other error sources by 2.4 percent or less, and the standard deviation of the time error attributed to the other error sources by 3.0 percent or less. Similarly shifting the atmosphere/altitude error source impacted the mean time error attributed to the other error sources by 1.2 percent or less, and the standard deviation of the time error attributed to the other error sources by 1.3 percent or less.

Removing the tracker jump error source directly alters the time error. The other error sources, except path distance, are removed by replacing predicted components of the ground speed (wind, TAS, CAS, Mach, temperature, air density) with the observed values recorded by the air data computer. The time error is then derived from the updated CTAS-predicted time component along the trajectory. The path distance error source is removed by replacing predicted distance with the flown distance.

### 6.1. Tracker Jumps

Tracker jump errors are quantified along two segments: (1) the en route radar segment, and (2) at the transition between the en route radar and terminal radar. An example of these two locations is shown in Figure 31 for run 4. The en route radar segment shown on the

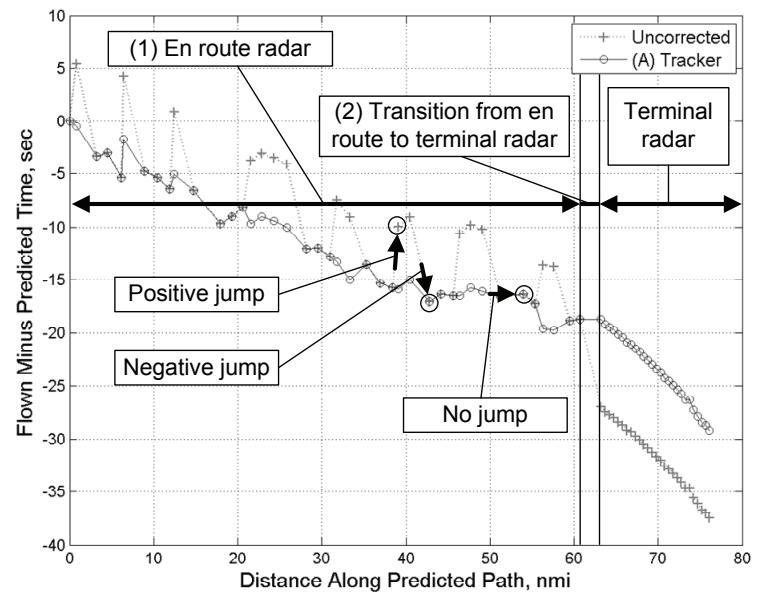


**Figure 31. Example transition from en route to terminal radar during run 4. Also shown are examples of a negative jump, no jump, and a positive jump.**

left contains negative jumps, no jumps, and positive jumps between successive radar tracks. The transition between the en route and terminal radar may also contain a jump. The transition is shown between two vertical lines where the left vertical line is aligned with the last en route radar track, and the right vertical line is aligned with the first terminal radar track. There were no jumps observed within the terminal radar segment.

The magnitudes of the jumps in the en route radar segment are quantified as follows. The y-axis of Figure 31 is the time error, which is not expected to change significantly between radar locations. If the change, either positive or negative, is too high, then it is marked for correction. Radar tracks with jumps were corrected rather than omitted because there could be several track updates in a row with jumps, and locations, such as the location of top of descent, needed to be identified. The correction is used as the magnitude of the error source. Positive (3.30 sec) and negative (-3.35 sec) thresholds that define “too high” were selected by examining histograms of the change in time error as shown in Figure 32 for all runs. The average of the data points outside the threshold is used to estimate the magnitude of the error for negative jumps (e.g., -7.2 sec for run 4) and positive jumps (e.g., 5.9 sec for run 4). The negative of this error is applied to each jump as a correction. If this correction does not sum to zero, then it is subsequently adjusted by increasing the magnitude of the smaller error, either positive or negative jump, as a correction. A summary of the magnitudes of the tracker jump error source for all runs is included in Appendix A.

Equations (2) to (8) describe the quantification of the tracker jump error source and the other error sources. Equation (2) is the initial time error that has not been corrected for any error sources. This initial time error ( $\Delta t_i^0$ ) is the data series labeled “Uncorrected” in Figure 31 and is the flown time at radar track  $i$  ( $t_i^{flown}$ ) minus the CTAS-predicted time at radar track  $i$  ( $t_i^{pred}$ ). The errors are then subtracted out for each error source  $K = A$  to  $G$  according to Equation (2) to provide a revised time estimate ( $\Delta t_i^K$ ) that is labeled “(A) Tracker” in Figure 31 for  $K = A$ . The magnitude of the tracker jump error source is the second term on the right-hand side of Equation (3). This second term is the summation of all tracker jump errors up to and including the current radar track  $i$  using the magnitudes ( $e_j^A$ ) specified in Appendix A.

The third term in Equation (3), which is surrounded by square brackets, is the magnitude of the error source for error sources  $K = B$  to  $G$  and is used to iteratively subtract out the effects of each error source. The first term in the square brackets is an estimate of the time between radar track locations, calculated as path distance ( $s_i^{K-1} - s_{i-1}^{K-1}$ ) divided by true airspeed ( $\overline{V_{TAS,i}^{K-1}}$ ) plus the wind vector ( $\overline{V_{W,i}^{K-1}}$ ), using a combination of CTAS-predicted and aircraft data according to Table 3. The second term in the square brackets substitutes aircraft data to mitigate the effects of error source  $K$ . This substitution of aircraft data for CTAS-predicted data is described in Table 3 and Sections 6.2 to 6.7. Equations (4) to (7) are used to convert CAS to TAS<sup>19</sup> and are discussed in Sections 6.3 and 6.4. Equation (8) is similarly used to convert Mach to TAS<sup>19</sup> and is discussed in Section 6.5.

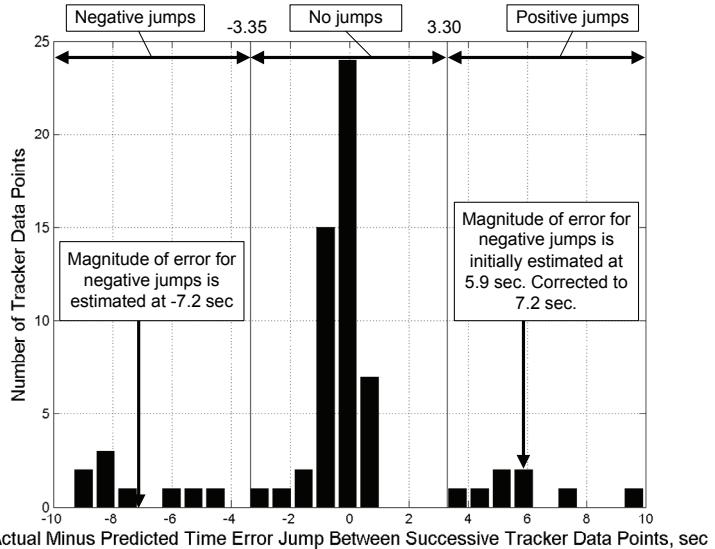


Figure 32. Classification of difference between successive radar tracker data points into negative jumps, no jumps, and positive jumps for run 4. The x-axis of this figure is the difference between the y-axis of successive data points shown in Figure 31.

$$\Delta t_i^0 = t_i^{f\text{low}n} - t_i^{pred} \quad (2)$$

$$\Delta t_i^K = \Delta t_i^{K-1} - \sum_{j=1}^i \varepsilon_j^A - \left[ \frac{s_i^{K-1} - s_{i-1}^{K-1}}{\left| \overrightarrow{V_{TAS,i}^{K-1}} + \overrightarrow{V_{W,i}^{K-1}} \right|} - \frac{s_i^K - s_{i-1}^K}{\left| \overrightarrow{V_{TAS,i}^K} + \overrightarrow{V_{W,i}^K} \right|} \right] \quad (3)$$

$$\overrightarrow{V_{TAS,i}} = \overrightarrow{V_{CAS,i}} \frac{\overrightarrow{V_{TAS2,i}}}{\overrightarrow{V_{CAS2,i}}} = \overrightarrow{V_{CAS,i}} \frac{f_i}{f_{0,i}} \sqrt{\frac{\rho_0}{\rho_i}} \quad (4)$$

$$f_i = \sqrt{\frac{\gamma}{\gamma-1} \frac{p_i}{q_{c,i}} \left[ \left( \frac{q_{c,i}}{p_i} + 1 \right)^{\gamma-1/\gamma} - 1 \right]} \quad (5)$$

$$f_{0,i} = \sqrt{\frac{\gamma}{\gamma-1} \frac{p_0}{q_{c,i}} \left[ \left( \frac{q_{c,i}}{p_0} + 1 \right)^{\gamma-1/\gamma} - 1 \right]} \quad (6)$$

$$\rho_i = \frac{p_i}{RT_i} \quad (7)$$

$$\overrightarrow{V_{TAS,i}} = \overrightarrow{V_{Mach,i}} \frac{\overrightarrow{V_{TAS2,i}}}{\overrightarrow{V_{Mach2,i}}} = \overrightarrow{V_{Mach,i}} \sqrt{\gamma RT_i} \quad (8)$$

## 6.2. Wind

The wind error is quantified by replacing the CTAS-predicted winds with the winds recorded on board the aircraft. This is specified as flown in the ( $\overrightarrow{V_{W,i}^K}$ ) row of the Wind column in Table 3.

## 6.3. CAS Deceleration

The CAS deceleration error source is quantified by replacing the CTAS-predicted CAS with the CAS recorded on board the aircraft ( $\overrightarrow{V_{CAS,i}^K}$ ) along the segment where CTAS is predicting the aircraft to decelerate to the meter-fix crossing speed restriction. This replacement has no effect on the constant-Mach and constant-CAS segments. Flown CAS is multiplied by the ratio of predicted true airspeed ( $\overrightarrow{V_{TAS2,i}^K}$ ) to predicted CAS ( $\overrightarrow{V_{CAS2,i}^K}$ ) according to Equation (3) to derive true airspeed. The ratio accounts for compressibility and air density effects, and will be replaced by flown data when the atmosphere and altitude error source is quantified according to Section 6.6. The ratio could be replaced in the model to convert CAS to TAS as shown in Equations (4) to (6) in order to identify which condition—static pressure ( $p_i$ ), impact pressure ( $q_{c,i}$ ), or temperature ( $T_i$ )—has the greatest effect on the atmosphere/altitude error source. However, using Equations (4) to (6) to convert CAS to TAS using flown CAS, static pressure, impact pressure, and temperature was found to produce a TAS value that deviated from flown TAS by as much as 3 knots, which is similar to introducing a conversion error source. Plots of this deviation are included for each direct run in Appendix C and for each path-stretch run in Appendix D. For this reason, the “TAS divided by CAS” ratio was used throughout to mitigate this effect.

Other terms introduced in Equations (3) to (6) include the ratio of specific heats for air ( $\gamma$ ), air density at sea level ( $\rho_0$ ), air density at aircraft altitude ( $\rho_i$ ) calculated according to Equation (6), gas constant for air ( $R$ ), atmospheric pressure at sea level ( $p_0$ ), and compressibility factors ( $f_i, f_{0,i}$ ) calculated according to Equations (4) and (5).

#### 6.4. Speed Conformance

The speed conformance error source is quantified similar to the CAS deceleration error source by replacing CTAS-predicted CAS with CAS recorded onboard the aircraft. However, the speed conformance error source applies along the constant-CAS descent segment. The CAS deceleration and speed conformance columns in Table 3 are the same, but the changes are applied at different locations. The target Mach error source is similarly only applied from the initial condition up to the location of the transition from constant Mach to constant CAS.

**Table 3. Substitution of aircraft data (flown) for CTAS-predicted data (pred) to quantify magnitude of error sources using Equations (3) through (8).**

Term in Equations (3) to (8)	Error Source						
	Tracker Jumps	Wind	CAS Deceleration	Speed Conformance	Target Mach	Atmosphere/Altitude	Path Distance
$K$	A	B	C	D	E	F	G
$K-1$	0	A	B	C	D	E	F
$\overrightarrow{V_{W,t}^{K-1}}$	pred	pred	flown	flown	flown	flown	flown
$\overrightarrow{V_{W,t}^K}$	pred	flown	flown	flown	flown	flown	flown
$\overrightarrow{V_{TAS,t}^{K-1}}$	pred	pred	pred	pred	N/A	N/A	flown
$\overrightarrow{V_{TAS,t}^K}$	pred	pred	N/A	N/A	N/A	flown	flown
$\overrightarrow{V_{CAS,t}^{K-1}}$	N/A	N/A	N/A	N/A	N/A	flown	N/A
$\overrightarrow{V_{CAS,t}^K}$	N/A	N/A	flown	flown	N/A	N/A	N/A
$\overrightarrow{\frac{V_{TAS2,t}^{K-1}}{V_{CAS2,t}^{K-1}}}$	N/A	N/A	N/A	N/A	N/A	pred	N/A
$\overrightarrow{\frac{V_{TAS2,t}^K}{V_{CAS2,t}^K}}$	N/A	N/A	pred	pred	N/A	N/A	N/A
$\overrightarrow{V_{Mach,t}^{K-1}}$	N/A	N/A	N/A	N/A	N/A	flown	N/A
$\overrightarrow{V_{Mach,t}^K}$	N/A	N/A	N/A	N/A	flown	N/A	N/A
$\overrightarrow{\frac{V_{TAS2,t}^{K-1}}{V_{Mach2,t}^{K-1}}}$	N/A	N/A	N/A	N/A	N/A	pred	N/A
$\overrightarrow{\frac{V_{TAS2,t}^K}{V_{Mach2,t}^K}}$	N/A	N/A	N/A	N/A	pred	N/A	N/A
$s_i^{K-1} - s_{i-1}^{K-1}$	pred	pred	pred	pred	pred	pred	pred
$s_i^K - s_{i-1}^K$	pred	pred	pred	pred	pred	pred	flown

## 6.5. Target Mach

The target Mach error source is quantified by replacing the CTAS-predicted Mach with Mach recorded on board the aircraft ( $\overline{V_{Mach,i}^K}$ ) from the initial condition to the location of the transition from constant Mach to constant CAS. Flown Mach is multiplied by the ratio of predicted true airspeed ( $\overline{V_{TAS2,l}^K}$ ) to predicted Mach ( $\overline{V_{Mach2,l}^K}$ ) according to Equation (7) to derive true airspeed. The ratio accounts for temperature and other atmospheric effects, and is replaced by flown data when the atmosphere and altitude error source is quantified next in Section 6.6. Similar to CAS, a model for converting Mach to TAS could be substituted for the ratio, but an error source may be introduced, and significant additional insights would not be expected due to the relatively small residual and atmosphere/altitude error source as compared to the magnitude of the other error sources.

## 6.6. Atmosphere/Altitude

The atmosphere/altitude error source focused on the predicted vs. flown atmospheric conditions, which introduce errors in the conversion of Mach (constant-Mach segment) and CAS (constant-CAS and deceleration segments) to true airspeed. Flying higher or lower than predicted similarly changes the true airspeed and was also captured by this error source. This error source was quantified by replacing true airspeed calculated according to Equations (3) and (7) with true airspeed recorded on board the aircraft ( $\overline{V_{TAS,i}^K}$ ).

Appendices C and D provide comparisons of CTAS-predicted to flown static pressure, impact pressure, and temperature, even though these components were not each converted to an impact on time error.

## 6.7. Path Distance

Path distance is quantified by replacing the CTAS-predicted path distance between successive locations with the flown distance between successive locations ( $s_i^K - s_{i-1}^K$ ). The only predicted data in Equation (2) when quantifying path distance ( $K = G$ ) is  $s_i^{K-1} - s_{i-1}^{K-1}$ .

# 7. Results

This section presents the combined impact of the seven trajectory prediction error sources at locations along the predicted trajectory. Also, the percentage contribution of the error sources to the total time-error variance at the meter fix is shown. A comparison to the results of a 1994 flight test using NASA's Boeing 737 test aircraft is presented last.

Four of the direct runs (runs 5, 9, 11, and 16) contained anomalies that are not expected to be consistent with future EDA operations (e.g., pilot changing target descent CAS midway through descent) and were therefore excluded from the analysis. Details of these runs are provided in Appendix C. Excluding these runs had less than a 4-percent impact on the means and standard deviations presented in this section.

## 7.1. Magnitude of Error Sources

The magnitude of the error sources is shown at the top of descent (Fig. 33) and meter fix (Fig. 34). In both of the figures the seven error sources—from tracker jumps (error source A) to path distance (error source G)—are presented along the x-axis. Also presented on the x-axis are the combined effect of these seven error sources (total error) and the residual error after correcting for these seven error sources. Figure 33 shows the contribution of each error source to time errors that accumulate from the initial condition to the top of descent. Comparing Figure 34 to Figure 33 shows the contribution of each error source that accumulates during descent from the top of descent to the meter fix.

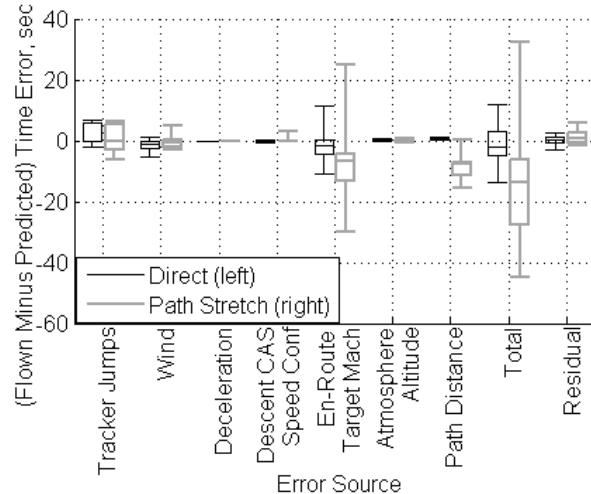


**Figure 33. Relative magnitude of the error sources and residual error at top of descent.**

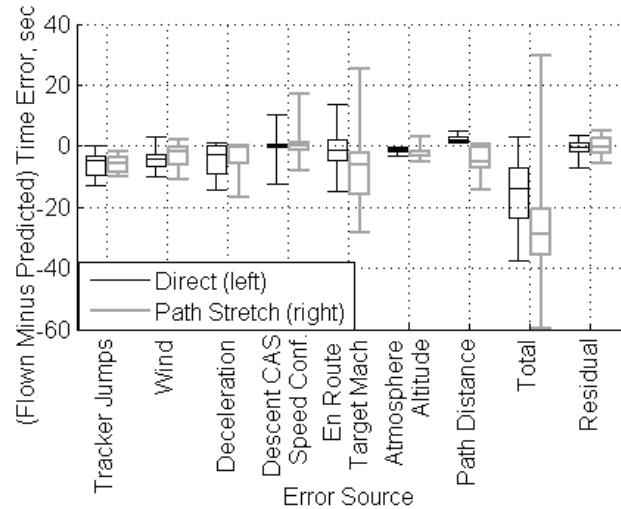


**Figure 34. Relative magnitude of the error sources and residual error at meter fix.**

For direct runs, the target Mach error source is the most dominant error source at the top of descent ( $\mu = -1.7$  sec,  $\sigma = 4.3$  sec at TOD) and remains, relatively, the most significant error source throughout the descent ( $\mu = -1.1$  sec,  $\sigma = 5.7$  sec at MF) as measured by the standard deviation of the error sources. The focus is more on the standard deviation of the error rather than the mean of the error because the mean and median effects of the error sources are generally close to zero, but there can be a large spread in the data. The deceleration error source becomes significant ( $\mu = -5.0$  sec,  $\sigma = 5.2$  sec at MF), and approximately the same magnitude of effect as target Mach near the meter fix. The wind, speed conformance, altitude/atmosphere, and path distance error sources are the smallest in magnitude relative to the other error sources at the meter fix.

For path-stretch runs, the target Mach error source has the largest effect on time error throughout the descent. As expected, the path stretch results in higher contributions of path distance to total error for the path-stretch runs ( $\mu = -5.2$  sec,  $\sigma = 5.0$  sec at MF) as compared to the direct runs ( $\mu = 2.3$  sec,  $\sigma = 0.9$  sec at MF). The other error sources have a similar and less significant effect on the total error than target Mach and path distance.

A summary of the mean and standard deviation of the effect of the error sources at the meter fix is included in Table 4. The mean and standard deviation at five locations from the top of descent to the meter fix is included in Appendix E. For example, the row for target Mach shows a -1.1-second and 5.7-second mean and standard deviation, respectively, for direct descents, and a -7.5-second and 15.9-second mean and standard deviation, respectively, for path-stretch descents. The difference between the direct and path-stretch runs may be attributed to the path-stretch routing, which was in close proximity of a turn. Mean and standard deviation at six locations along the predicted trajectory are included in Appendix B for completeness.

**Table 4. Mean ( $\mu$ ) and standard deviation ( $\sigma$ ) at the meter fix for 2010 Global 5000 error sources and equivalent 1994 Boeing 737 test aircraft error sources. Mean and standard deviation are in units of seconds.**

Error Source	2010 Global 5000 Flight Trial				1994 B737 Test Aircraft Flight Trial		
	Direct		Path Stretch		Equivalent Error Source	Turn <sup>a</sup>	
	$\mu$	$\sigma$	$\mu$	$\sigma$		$\mu$	$\sigma$
A. Tracker Jumps	-6.1	3.7	-6.0	2.9	<i>Corrected before error analysis</i>		
B. Wind	-4.0	3.4	-3.1	4.5	Wind	-5.0	11.0
C. CAS Deceleration	-5.0	5.2	-3.5	5.6	<i>See airspeed conformance below</i>		
D. Speed Conformance	0.1	3.4	1.0	6.7			
C+D. Decel + Speed Conf	-4.9	6.1	-2.5	3.1	Airspeed conformance	-1.0	2.4
E. Target Mach	-1.1	5.7	-7.5	15.9	Initial ground speed	-1.6	1.5
F. Atmosphere/Altitude	-1.3	0.6	-2.3	2.3	Temperature	1.3	1.1
					Altitude	1.6	2.4
G. Path Distance	2.3	0.9	-5.2	5.0	Turn overshoot	-0.3	0.7
Total	-15.6	9.9	-27.0	25.8	Total <sup>b</sup>	-4.6	13.9
Residual	-0.6	2.5	-0.4	3.4	Residual	2.6	1.6

<sup>a</sup> The turn in 1994 was similar to the path-stretch runs in 2010 in that the waypoint defining the turn was programmed into the FMS prior to descent.

<sup>b</sup> Excludes experimental error source.

## 7.2. Percentage Contribution to Total Variance

The contributions of each error source to the mean total error at the meter fix are a straightforward summation of the mean errors. However, the percentage contribution of each error source to the variance ( $\sigma^2$ ) of the time error at the meter fix requires estimating and applying a variance-covariance matrix shown in rows labeled “cov” in Tables 5 and 6 for direct and path-stretch runs, respectively.

The diagonal of the variance-covariance matrix is the variance for each of the error sources. For example, the variance of the tracker jump error source at the meter fix ( $\sigma_{A,A}^2 = 13.5 \text{ sec}^2$ ) shown in the upper left in Table 5 is the square of the standard deviation at the meter fix ( $\sigma_{A,A} = 3.7 \text{ sec}$ ) shown in Table 4. The covariance values off the diagonal can be either positive or negative. Positive covariance indicates a relationship where higher values of one error source are associated with higher values of another error source. For example, for the covariance in Table 5 for direct runs, the covariance between wind and speed conformance ( $\sigma_{B,D}^2 = 2.42 \text{ sec}^2$ ) is positive indicating that higher time errors caused by wind are associated with higher time errors caused by speed conformance.

Negative covariance indicates a relationship where higher values of one error source are associated with lower values of another compensating error source. For example, for the covariance in Table 6 for path-stretch runs, the covariance between deceleration and speed conformance ( $\sigma_{C,D}^2 = -32.79 \text{ sec}^2$ ) is negative indicating that higher speed conformance errors are associated with lower deceleration errors. A normalized correlation coefficient that ranges from -1 to 1 is also given in Tables 5 and 6 to show the strength of a linear relationship between the error sources. The largest correlation coefficient was between the target Mach and the atmosphere/altitude (0.70), because the target Mach error results from temperature and pressure forecast errors.

**Table 5. Variance-Covariance (cov) and correlation (corr) matrix among error sources for direct-run arrival-time errors to the meter fix. Covariance is in units of sec<sup>2</sup>, and correlation is dimensionless. Values in the table are symmetric about the diagonal cells.**

	Covariance (cov) Correlation (corr)	A. Tracker Jumps	B. Wind	C. CAS Deceleration	D. Speed Conformance	E. Target Mach	F. Atmosphere/Altitude	G. Path Distance	Residual
A. Tracker Jumps	cov	13.49	-3.02	-1.26	-1.77	1.58	0.67	-0.88	0.02
	corr	1.00	-0.24	-0.07	-0.14	0.07	0.29	-0.27	0.00
B. Wind	cov	-3.02	11.52	3.49	2.42	-4.47	-0.28	1.26	-1.40
	corr	-0.24	1.00	0.20	0.21	-0.23	-0.13	0.42	-0.17
C. CAS Deceleration	cov	-1.26	3.49	27.26	-0.45	-6.25	-1.00	1.68	-0.35
	corr	-0.07	0.20	1.00	-0.03	-0.21	-0.30	0.37	-0.03
D. Speed Conformance	cov	-1.77	2.42	-0.45	11.30	0.74	-0.02	0.69	0.75
	corr	-0.14	0.21	-0.03	1.00	0.04	-0.01	0.23	0.09
E. Target Mach	cov	1.58	-4.47	-6.25	0.74	32.99	2.54	-0.45	3.19
	corr	0.07	-0.23	-0.21	0.04	1.00	0.70	-0.09	0.22
F. Atmosphere/Altitude	cov	0.67	-0.28	-1.00	-0.02	2.54	0.40	-0.05	0.08
	corr	0.29	-0.13	-0.30	-0.01	0.70	1.00	-0.10	0.05
G. Path Distance	cov	-0.88	1.26	1.68	0.69	-0.45	-0.05	0.78	-0.64
	corr	-0.27	0.42	0.37	0.23	-0.09	-0.10	1.00	-0.29
Residual	cov	0.02	-1.40	-0.35	0.75	3.19	0.08	-0.64	6.18
	corr	0.00	-0.17	-0.03	0.09	0.22	0.05	-0.29	1.00
Sum of covariance		8.83	9.52	23.12	13.66	29.87	2.34	2.39	7.83
Total variance (%)		9.1	9.8	23.7	14.0	30.6	2.4	2.4	8.0

The total variance is the sum of all elements in the variance-covariance matrices in Tables 5 and 6 for direct ( $\sigma^2 = 9.88^2 = 97.54 \text{ sec}^2$ ) and path-stretch ( $\sigma^2 = 25.78^2 = 664.73 \text{ sec}^2$ ) runs, respectively. It is not possible to completely decouple the contribution of each error source to the total variance due to covariance between the error sources. However, the percentage of the total variance ( $P_K$ ) due to error source  $K$  is approximated in Equation 9 by dividing covariance equally between the two error sources. Because the variance-covariance matrix is symmetrical and covariance appears twice, the percentage ( $P_K$ ) is calculated by summing the variance ( $\sigma_{K,K}^2$ ) and covariance ( $\sigma_{K,j}^2$ , where  $j$  does not equal  $K$ ) in the  $K^{th}$  column and then dividing by the total variance ( $\sigma^2$ ). The right-hand side numerator (sum of covariance) and the percentage (percent of total variance) in Equation 9 are calculated and shown in the last two rows in Tables 5 and 6.

$$P_K = \frac{\sum_{j=A}^G \sigma_{K,j}^2}{\sigma^2} \quad (9)$$

The target Mach error source (30.6 percent for direct and 60.2 percent for path stretch) had the highest contribution to the total time error variance at the meter fix. The target Mach error source for direct runs also had significant positive covariance with the other error sources, which resulted in a higher contribution to the total time error variance than would have occurred in the absence of other error sources. Deceleration (23.7 percent for direct and -17.5 percent for path stretch) and speed conformance (14.0 percent for direct and 16.8 percent for path stretch) are other error sources with a relatively large contribution to the total time error variance. The negative contribution of CAS deceleration (-17.5 percent), which is caused by negative covariance with other error sources that is larger in magnitude than the CAS deceleration positive variance, to the total time error variance indicates that CAS deceleration compensates for other error sources during path-stretch runs.

The results in Tables 5 and 6 are based on the error source quantification order described previously in Section 6. Changing this order impacts the percentage of the total variance attributed primarily to the wind error source. The wind error source is reduced from 9.8 percent to 9.3 percent for direct runs and increased from 1.2 percent to 1.8 percent for path-stretch runs if the wind error source is quantified after the target Mach error source.

**Table 6. Variance-Covariance (cov) and correlation (corr) matrix among error sources for path-stretch run arrival-time errors to the meter fix. Covariance is in units of sec<sup>2</sup>, and correlation is dimensionless.**

	Covariance (cov) Correlation (corr)	A. Tracker Jumps	B. Wind	C. CAS Deceleration	D. Speed Conformance	E. Target Mach	F. Atmosphere/Altitude	G. Path Distance	Residual
A. Tracker Jumps	cov	8.57	-4.06	-1.76	-2.40	23.02	2.14	5.44	7.68
	corr	1.00	-0.30	-0.11	-0.12	0.49	0.32	0.37	0.77
B. Wind	cov	-4.06	20.68	-13.30	16.07	-6.81	1.01	-4.46	-1.30
	corr	-0.30	1.00	-0.53	0.53	-0.09	0.10	-0.20	-0.08
C. CAS Deceleration	cov	-1.76	-13.30	30.99	-32.79	-63.80	-10.38	-15.35	-10.01
	corr	-0.11	-0.53	1.00	-0.88	-0.72	-0.82	-0.55	-0.53
D. Speed Conformance	cov	-2.40	16.07	-32.79	44.48	57.71	10.74	10.31	7.36
	corr	-0.12	0.53	-0.88	1.00	0.54	0.71	0.31	0.32
E. Target Mach	cov	23.02	-6.81	-63.80	57.71	253.96	33.49	59.00	43.69
	corr	0.49	-0.09	-0.72	0.54	1.00	0.92	0.74	0.80
F. Atmosphere/Altitude	cov	2.14	1.01	-10.38	10.74	33.49	5.17	6.72	4.97
	corr	0.32	0.10	-0.82	0.71	0.92	1.00	0.59	0.64
G. Path Distance	cov	5.44	-4.46	-15.35	10.31	59.00	6.72	24.89	9.26
	corr	0.37	-0.20	-0.55	0.31	0.74	0.59	1.00	0.54
Residual	cov	7.68	-1.30	-10.01	7.36	43.69	4.97	9.26	11.65
	corr	0.77	-0.08	-0.53	0.32	0.80	0.64	0.54	1.00
Sum of covariance		38.63	7.83	-116.40	111.48	400.26	53.86	95.81	73.30
Total variance (%)		5.8	1.2	-17.5	16.8	60.2	8.1	14.4	11.0

### 7.3. Comparison to 1994 Flight Test Using NASA's Boeing 737 Test Aircraft

An analysis on trajectory error sources was performed for a NASA B737 test aircraft using results from a 1994 EDA field trial.<sup>11</sup> Those results were compared to the results from the 2010 flight trial using Global 5000 aircraft. The earlier study considered 4 levels of cockpit automation during 25 arrival runs to Denver. The comparison presented here will focus on six of the 1994 runs that used a conventional FMS with lateral navigation (LNAV) and VNAV. Seven error sources were identified in the earlier field trial: (1) experimental error, (2) temperature, (3) airspeed conformance, (4) altitude, (5) initial ground speed, (6) turn overshoot, and (7) wind. The mean and standard deviation of these error sources are shown in Table 4.

The total error was lower in 1994 ( $\mu = -4.6$  sec,  $\sigma = 13.9$  sec) than the error in 2010 for direct ( $\mu = -15.6$  sec,  $\sigma = 9.9$  sec) and path-stretch ( $\mu = -27.0$  sec,  $\sigma = 25.8$  sec) runs. However, the experimental setup in 1994 was different than 2010, complicating the comparison. There was a position bias in the radar tracker in 1994 that led to the error source analysis being partly based on GPS position data recorded on board the B737 rather than using the radar tracker position (radar tracker speed was still used for the initial condition). Therefore, the tracker jump error source in 2010 has no equivalent in 1994. The 1994 initial condition was based on both cruise and descent speeds issued by controllers, which reduce the error in estimated Mach at the initial condition. In 2010, only the issued descent speed was used in generating CTAS predictions, and the target Mach was estimated by the radar tracker ground speed, rather than by the Mach issued by ATC, which increases this error source relative to 1994. Lastly, the 1994 flight trial used a calibrated B737 model in CTAS that would better predict turns than the 2010 Global 5000 turn model.

For these reasons a comparison of the total error between 1994 and 2010 was made based on the mean of the following error sources: wind, CAS deceleration, airspeed conformance, atmosphere, altitude, and temperature. When comparing this error source subset, the total mean error is higher in 2010 for both direct ( $\mu = -10.2$  sec) and path-stretch ( $\mu = -7.9$  sec) runs than was observed in 1994 ( $\mu = -3.4$  sec). This higher error is primarily due to higher CAS deceleration errors in 2010. A discussion of the seven 1994 error sources is included next with their closest equivalent error source identified in 2010.

Experimental errors were caused by CTAS computational and data errors that were corrected after the 1994 flight trial. These errors did not exist in the results from the Global 5000 runs. Temperature and altitude were combined into a single error source with a resulting mean and standard deviation of less than 3 seconds for both direct and path-stretch runs. The 1994 results were similar, with temperature having a negligible effect and altitude have a small effect.

The 1994 airspeed conformance error contributed 1 second to the arrival time error ( $\mu = 1.0$  sec,  $\sigma = 2.4$  sec). The 2010 Global 5000 runs had higher standard deviation of the errors associated with speed conformance for both the direct ( $\mu = 0.1$  sec,  $\sigma = 3.4$  sec) and path-stretch ( $\mu = 1.0$  sec,  $\sigma = 6.7$  sec) runs. CAS deceleration was quantified separately from speed conformance for the 2010 Global 5000 runs but not for the 1994 results. Speed conformance and CAS deceleration can be combined using variance and covariance to derive a standard deviation of 6.1 seconds for direct cases and 3.1 seconds for path-stretch cases. Both are larger than the 1994 airspeed conformance standard deviation of about 2 seconds. The different airspeed conformance and deceleration errors between 1994 and 2010 are potentially due to different aircraft and different flight crews. The different errors due to airspeed conformance could also be attributed to VNAV being guidance-only and not coupled to the autopilot or autothrottle. The 1994 test non-FMS runs exhibited a 4-second standard deviation of airspeed conformance error, which is higher than the approximately 2-second standard deviation exhibited by the test aircraft that used the FMS with

LNAV and VNAV capabilities. For this reason, the 2010 airspeed conformance standard deviation of 3.4 seconds is consistent with expectations that it would fall between the standard deviation for non-FMS runs and runs with LNAV and VNAV.

The different errors due to deceleration, in addition to different aircraft types and flight crew, could be caused by the procedure to meet the meter-fix crossing speed. In 1994, the aircraft CAS was reduced by maintaining idle thrust at bottom of descent, pitching the aircraft to a level segment, and then using the level segment to reduce speed to meet the meter-fix crossing speed. In 2010, the descent CAS was diminished by reducing throttle to at or near idle, using pitch to maintain the vertical profile, and using speed brakes as needed to meet the meter-fix crossing speed restriction. It is easier to predict a reduction in CAS during a level segment than in descent, because the level segment deceleration procedure is more standardized.

The target Mach error source has roughly the same cause as the initial ground speed used in the error source analysis of the 1994 field trial. However, the 2010 Global 5000 runs had much higher errors attributed to the target Mach for direct ( $\mu = -1.1$  sec,  $\sigma = 5.7$  sec) and path-stretch ( $\mu = -7.5$  sec,  $\sigma = 15.9$  sec) runs as compared to the error source analysis of initial ground speed ( $\mu = -1.6$  sec,  $\sigma = 1.5$  sec) from the 1994 trial. The higher target Mach error in 2010 is attributed in large part to the aircraft turning onto the arrival route closer (about 90 to 120 nmi from meter fix) to the meter fix than in 1994 (about 130 nmi from meter fix). This turn causes a transient error in the radar track ground speed estimate, often lower than the aircraft's actual ground speed, at the initial condition, which occurs after the turn has completed. A lower ground speed, from which Mach is determined by subtracting out winds and converting TAS to Mach using atmospheric conditions, results in a lower Mach than was recorded on the aircraft.

The turn overshoot ( $\mu = 0.3$  sec,  $\sigma = 0.7$  sec) is roughly equivalent to the path-distance ( $\mu = -5.2$  sec,  $\sigma = 5.0$  sec) error source. However, in the 2010 Global 5000 path-stretch runs, the aircraft consistently undershot the turn, causing the aircraft to arrive earlier than predicted at the meter fix and resulting in a larger standard deviation than was observed in 1994. Potential reasons for the difference are as follows. The turn radius of an aircraft is defined by ground speed and bank angle. A higher ground speed requires a longer turn radius at the same bank angle. The flown ground speed is higher than predicted (discussed in the previous paragraph), which is consistent with a larger flown turn radius as compared to the CTAS-predicted turn radius. Another possibility is that the bank angle used by CTAS in 1994 was more appropriate for a Boeing 737 than the bank angle used by CTAS in 2010 for a Global 5000 aircraft. The default bank angle of 20.8 degrees used in CTAS according to Equation (1) in Section 3 to model the Global 5000 aircraft could have been an underestimate, because a larger bank angle would result in a shorter turn radius that would more closely match the Global 5000 turns.

Winds aloft prediction had a larger effect on the standard deviation of meter-fix arrival time error in 1994 ( $\mu = -5$  sec,  $\sigma = 11$  sec) than in 2010 for both the direct ( $\mu = -4.0$  sec,  $\sigma = 3.4$  sec) and path-stretch ( $\mu = -3.1$  sec,  $\sigma = 4.5$  sec) cases. The predicted wind speed error often exceeded 20 knots, and exceeded 60 knots in some cases, in 1994. By comparison, only 4 of the 44 runs had wind speed errors that exceeded 15 knots, and none of the runs experienced a wind speed error of more than 20 knots at any location along the trajectory. These lower wind speed errors were a result of better winds-aloft predictions in 2010, which are more appropriate for trajectory prediction than the wind models used in 1994. For example, CTAS wind updates in 2010 occurred at a 1-hour interval, which is more frequent than the 3-hour interval used in 1994. Besides the reduction of the RUC wind forecast interval from 3 hours (available in 1994) to 1 hour (available in 2010), improvements in the state of the art have reduced wind forecast errors substantially.<sup>20</sup>

#### **7.4. Comparison to 2009 3D PAM Flight Trial Using Revenue Flights**

A 3D PAM field trial was conducted at Denver in September 2009 using Boeing 737, Boeing 757, and Airbus 319/320 aircraft during revenue flights.<sup>3</sup> Analysis was performed on 270 flight-issued cruise and descent speeds that were uninterrupted during descent. The top-of-descent (TOD) error and meter-fix arrival-time error were calculated differently for the 2009 flight trial than for the 2010 flight trial, however an approximate comparison is presented next. The direct runs were used for comparison because they were less influenced by the turn near the initial condition. This turn would generally not exist in the revenue flights.

The TOD prediction error in 2009 was reported as a mean absolute value of 5.4 nmi; 47 percent of the flights had errors of less than 5 nmi. The TOD prediction error in 2010 was an order of magnitude smaller at 0.7-nmi mean absolute value; 100 percent of the runs had errors of less than 5 nmi.

The arrival-time error in 2009 was reported as 11.5 seconds mean absolute value; 80 percent of the flights had errors of less than 20 seconds. The error in 2010 was 15.6 seconds mean absolute value; 67 percent of the runs had errors of less than 20 seconds. However, if the deceleration error source was removed, as would be expected if the Global 5000 decelerated in a more predictable level segment, the error would be reduced to 11.2 seconds mean absolute value with 83 percent of the runs having an arrival-time error less than 20 seconds. The Global 5000 results in 2010 are similar to the Boeing and Airbus results of 2009 in the absence of a Global 5000 deceleration prediction error. To definitively confirm this result, the Global 5000 runs would need to be repeated using the different deceleration procedure.

#### **7.5. Error Mitigation**

Several of the error sources identified in 2010 lend themselves to significant reduction with modest to no changes to ATC automation and/or procedures. The tracker jump error source may require no additional mitigation strategy because the FAA En Route Automation Modernization (ERAM) was deployed after the 2010 flight trial. ERAM replaces the En Route Host tracker with a more modern algorithm that is expected to greatly reduce, if not eliminate, the radar track jumps.

The CAS deceleration error source could be reduced by using a level segment CAS deceleration similar to the procedure used by large jets. During a level segment CAS deceleration, the aircraft levels at the meter-fix crossing altitude prior to the fix and maintains the altitude at idle thrust to reduce CAS. This level segment CAS deceleration is expected to be more predictable than CAS deceleration during descent.

There are multiple changes that could reduce the magnitude of the target Mach error source. The ERAM radar tracker is expected to more accurately estimate ground speed during turns and, therefore, reduce the magnitude of the target Mach error source. The impact of the turn could also be mitigated by limiting trajectory prediction updates to more steady state conditions, which is more closely aligned with 3D PAM validation tests. Another target Mach mitigation strategy could be to use both the issued cruise airspeed and descent speed for trajectory predictions. This flight trial was based on passively estimating airspeed at the initial condition using radar track ground speed, which is converted to airspeed by considering winds and atmosphere. This more closely represents the conditions of an en route conflict probe. However, it would be more consistent with existing 3D PAM validation testing to have ATC issue cruise airspeed and use the airspeed for the trajectory prediction.

The path distance error source is influenced by the turn modeling in CTAS. Path distance errors could be reduced by calibrating an aircraft model that is used in CTAS to better predict aircraft behavior during turns.

## 8. Conclusions

This paper estimated the trajectory prediction accuracy and error sources of 3D PAM descents based on a field trial at Denver International Airport using the Global 5000 aircraft. The predicted trajectory used the CTAS trajectory synthesizer and data known on the ground prior to the aircraft descending approximately 60 to 120 nmi from the meter fix. The flown trajectory and other data, including atmospheric and wind conditions, were obtained from an onboard air data computer. The Global 5000 aircraft arrived to the meter fix about 15 and 27 seconds earlier than predicted on average for direct and path-stretch runs, respectively. About a 10-second (direct) and 26-second (path-stretch) standard deviation of the error associated with the early arrival of the Global 5000 aircraft was observed.

Seven error sources were identified including (a) tracker jumps, (b) wind, (c) deceleration to meter-fix crossing speed, (d) speed conformance during descent, (e) targeted Mach prior to descent, (f) atmosphere and altitude, and (g) path distance. Targeted Mach had the largest effect on arrival-time error variance, representing about 31 percent (direct) and 60 percent (path stretch) of the total arrival-time error variance. The target Mach error was due to radar track ground speed errors associated with maneuvers to reposition the aircraft to initiate each run. Speed conformance—representing 14 percent (direct) and 17 percent (path stretch)—as well as CAS deceleration—representing 24 percent (direct) and -18 percent (path stretch)—are the next highest components of total variance. A negative value for CAS deceleration during path-stretch runs indicates that CAS deceleration compensates for other error sources. Four of the error sources—tracker jumps, CAS deceleration, target Mach, and path distance—lend themselves to significant reduction with modest to no changes to ATC automation and/or procedures. These changes could significantly reduce trajectory prediction error.

The TOD prediction error in 2010 was an order of magnitude smaller than in 2009. While the mean arrival-time error was about 30 percent higher in 2010 compared to 2009, if the deceleration error source was removed as it would be if the Global 5000 decelerated in a level segment, then the results would be on par. When comparing the 2010 results to the 1994 results, the largest difference not due to experimental design and artifact was the impact of the wind-prediction error. The reduction from 11-second standard deviation in 1994 to a less than 5-second standard deviation in 2010 was, in large part, due to better winds-aloft prediction.

## 9. References

- <sup>1</sup>Coppenbarger, R.; Hayashi, M.; Nagle, G.; Sweet, D.; and Salcido, R.: The Efficient Descent Advisor: Technology Validation and Transition. *12th AIAA Aviation Technology, Integration, and Operations (ATIO) Conference*, Indianapolis, IN, Sept. 17–19, 2012.
- <sup>2</sup>Coppenbarger, R.A.; Lanier, R.; Sweet, D.; and Dorsky, S.: Design and Development of the En Route Descent Advisor (EDA) for Conflict-Free Arrival Metering. *AIAA Guidance, Navigation, and Control (GNC) Conference*, Providence, RI, Aug. 2004.
- <sup>3</sup>Coppenbarger, R.; Dyer, G.; Hayashi, M.; Lanier, R.; Stell, L.; and Sweet, D.: Development and Testing of Automation for Efficient Arrivals in Constrained Airspace. *27th International Congress of the Aeronautical Sciences (ICAS)*, Nice, France, 2010.
- <sup>4</sup>Green, S.M., and Vivona, R.A.: En Route Descent Advisor Concept for Arrival Metering. *AIAA Guidance, Navigation, and Control (GNC) Conference*, Montreal, Canada, Aug. 6–9, 2001.
- <sup>5</sup>Haraldsdottir, A.; Scharl, J.; Berge, M.E.; Schoemig, E.G.; and Coats, M.L.: Arrival Management With Required Navigation Performance and 3D Paths. *7th USA/Europe Air Traffic Management Research and Development Seminar*, Barcelona, Spain, 2007.
- <sup>6</sup>Schoemig, E.G.; Armbruster, J.; Boyle, D.E.; and Haraldsdottir, A.: 3D Path Concept and Flight Management System (FMS) Trades. *25th Digital Avionics System Conference*, Portland, OR, Oct. 2006.
- <sup>7</sup>Nagle, G.; Sweet, D.; Carr, G.; Felipe, V.; Trapani, A.; Coppenbarger, R.; and Hayashi, M.: Human-in-the-Loop Simulation of Three-Dimensional Path Arrival Management With Trajectory Error. *11th AIAA Aviation Technology, Integration, and Operations (ATIO) Conference*, Virginia Beach, VA, Sept. 20–22, 2011.
- <sup>8</sup>Henderson, J.; Green, S.M.; and Wu, M.G.: Trajectory Prediction Accuracy and Error Sources for Regional Jet Descents: Part II—Results of a 2010 Flight Trial at Denver International Airport Using SkyWest Revenue Flights. NASA TM-2014-218342, Oct. 2014.
- <sup>9</sup>Green, S., and Vivona, R.: Field Evaluation of Descent Advisor Trajectory Prediction Accuracy. *AIAA Guidance, Navigation, and Control Conference*, San Diego, CA, July 1996.
- <sup>10</sup>Green, S.M.; Vivona, R.A.; Grace, M.P.; and Fang, T.-C.: Field Evaluation of Descent Advisor Trajectory Prediction Accuracy for En-route Clearance Advisories. *AIAA Guidance, Navigation, and Control (GNC) Conference*, 1998.
- <sup>11</sup>Green, S.; Grace, M.P.; and Williams, D.H.: Flight Test Results: CTAS and FMS Cruise/Descent Trajectory Prediction Accuracy. *3rd USA/Europe Air Traffic Management Research and Development Seminar*, Napoli, Italy, June 3–6, 2000.
- <sup>12</sup>Slattery, R., and Zhao, Y.: En-route Descent Trajectory Synthesis for Air Traffic Control Automation. *Proceedings of the American Control Conference*, vol. 5, June 1995, pp. 3430–3434.
- <sup>13</sup>Slattery, R., and Zhao, Y.: Trajectory Synthesis for Air Traffic Automation. *Journal of Guidance, Control, and Dynamics*, vol. 20, no. 2, Mar. 1997, pp. 232–238.
- <sup>14</sup>Lee, A.G.; Bouyssounouse, X.; and Murphy, J.R.: The Trajectory Synthesizer Generalized Profile Interface. *10th AIAA Aviation Technology, Integration and Operations (ATIO) Conference*, Fort Worth, Texas, Sept. 13–15, 2010.
- <sup>15</sup>Henderson, J.; Vivona, R.; and Green, S.: Trajectory Prediction Accuracy and Error Sources for Regional Jet Descents. *AIAA Guidance, Navigation, and Control (GNC) Conference*, Boston, MA, Aug. 19–22, 2013.

<sup>16</sup>Wu, M.G., and Green, S.M.: Strategies for Choosing Descent Flight-Path Angles for Small Jets. *AIAA Guidance, Navigation, and Control Conference*, Minneapolis, MN, Aug. 13–16, 2012.

<sup>17</sup>Wu, M.G., and Green, S.M.: Choosing Descent Flight-Path Angles for Small Jets: Adaptation to the JFK Airport. *AIAA Aviation Technology, Integration, and Operations (ATIO) Conference*, Los Angeles, CA, Aug. 12–14, 2013.

<sup>18</sup>Ryan, H.F.; Paglione, M.M.; and Green, S.M.: Review of Trajectory Accuracy Methodology and Comparison of Error Measurement Metrics. *AIAA Guidance, Navigation, and Control (GNC) Conference*, Providence, RI, Aug. 2004.

<sup>19</sup>Gracey, W.: Measurement of Aircraft Speed and Altitude. NASA Reference Publication 1046, 1980.

<sup>20</sup>Cole, R.E.; Green, S.; Jardin, M.; Schwartz, B.E.; and Benjamin, S.G.: Wind Prediction Accuracy for Air Traffic Management Decision Support Tools. *3rd USA/Europe Air Traffic Management Research and Development Seminar*, Napoli, Italy, June 3–6, 2000.

## Appendix A: Run-by-Run Magnitude of Tracker Jump Error Source

This appendix provides a summary of the magnitude of errors in the en route radar segment, as well as the magnitude of the transition from en route to terminal radar (see Table 7). The left four columns provide the run number, negative jump error magnitude, positive jump error magnitude, and magnitude of the error when transitioning from the en route radar to the terminal radar for the non-path-stretch runs. The error magnitude  $\varepsilon_j^A$  is used in Equation (2) described in Section 6.1 to quantify the magnitude of the track jump error source. The right four columns show the same information including path-stretch runs shown as the last nine rows after the shaded row. Tracker jump errors are cumulative so that the error applies at the radar track where the jump occurs and all subsequent tracks. The terminal radar track is considered to be in error, even though it may be more accurate than the en route radar, in this analysis when it does not match the en route radar at the transition because the en route controller only has access to the en route radar and controls the aircraft based on the radar tracks returned from the en route radar. If possible, future analysis of this type should exclusively use en route radar tracks.

**Table 7. Magnitude of track jumps in en route radar segment and at transition from en route to terminal radar.**

Non-Path-Stretch Run	Negative Jump Error Magnitude (sec)	Positive Jump Error Magnitude (sec)	Transition Error Magnitude (sec)	Non-Path-Stretch Run	Negative Jump Error Magnitude (sec)	Positive Jump Error Magnitude (sec)	Transition Error Magnitude (sec)
1	-6.9	6.9	-2.8	32	-7.4	7.4	-6.8
2	-6.0	6.0	0.0	34	-6.6	6.6	-4.6
3	-6.1	6.1	0.0	35	-7.7	7.0	-1.8
4	-7.3	7.3	-8.3	36	-7.0	7.0	-3.2
5	-6.5	6.5	-4.8	37	-6.5	6.5	-3.2
7	-6.5	6.5	-6.5	38	-6.3	6.3	-1.8
9	-6.0	6.0	-3.5	39	-6.3	6.3	-4.0
10	-5.8	5.8	-3.0	41	-6.9	6.9	-3.8
11	-6.8	6.8	-2.7	42	-6.2	6.2	-3.3
12	-6.5	6.5	-3.3	43	-6.4	6.4	-2.7
14	-6.4	6.4	-3.0	44	-5.9	5.9	-4.2
16	-6.1	6.1	-4.9				
18	-6.0	7.0	-4.6	Path-Stretch Run	Negative Jump Error Magnitude (sec)	Positive Jump Error Magnitude (sec)	Transition Error Magnitude (sec)
19	-6.5	6.5	-1.7				
21	-5.4	5.4	-4.1				
22	-6.2	6.2	-4.6	6	-5.9	5.5	-5.7
23	-8.0	8.0	-3.7	8	-5.8	6.8	-5.5
24	-6.8	6.8	-4.8	13	-5.5	6.4	-3.8
25	-6.4	6.4	-5.3	15	-5.5	7.3	-2.7
26	-6.0	6.0	-3.2	17	-6.0	6.4	-3.8
28	-7.0	7.0	-2.3	20	-5.6	6.2	-2.4
29	-6.2	6.2	-4.8	27	-6.5	6.3	-3.8
30	-6.9	6.9	-3.1	33	-6.5	6.2	-4.6
31	-6.4	6.4	-2.8	40	-6.0	6.5	-2.0



## Appendix B: Run-by-Run Ranked Effect of Error Sources

This appendix provides a ranking of the impact of each error source on (1) the maximum time error along the trajectory, and (2) the time error at the meter fix. The top-ranked run is the run that has the largest absolute value impact from a specific error source. See Tables 8 through 23.

### B.1. Tracker Jumps

**Table 8. Ranked effect of tracker jump error source at maximum tracker jump error location and at meter fix for direct runs. Ranking is based on absolute value of tracker jump error source effect.**

Ranking Based on Maximum Error Source Effect Along Trajectory				Ranking at Meter Fix		
Run	Max Effect (sec)	Absolute Value of Max Effect (sec)	Distance From Initial Condition (nmi)	Run	Max Effect (sec)	Absolute Value of Max Effect (sec)
18	-16.3	16.3	45.4	7	-13.1	13.1
7	-13.1	13.1	72.3	34	-11.2	11.2
34	-11.2	11.2	65.2	18	-11.0	11.0
29	-10.9	10.9	70.4	29	-10.9	10.9
22	-10.8	10.8	53.5	22	-10.8	10.8
24	-10.5	10.5	52.2	36	-10.1	10.1
23	-10.2	10.2	42.0	12	-9.8	9.8
36	-10.1	10.1	63.2	14	-9.5	9.5
12	-9.8	9.8	60.8	31	-9.2	9.2
14	-9.5	9.5	61.4	43	-9.1	9.1
31	-9.2	9.2	65.5	4	-8.3	8.3
42	-9.1	9.1	41.3	19	-8.2	8.2
43	-9.1	9.1	65.7	38	-8.0	8.0
28	-8.9	8.9	44.3	35	-7.4	7.4
4	-8.3	8.3	63.2	32	-6.8	6.8
19	-8.2	8.2	65.8	25	-5.3	5.3
38	-8.0	8.0	51.6	16	-4.9	4.9
35	-7.4	7.4	63.8	5	-4.8	4.8
32	-6.8	6.8	57.8	24	-4.8	4.8
5	6.3	6.3	3.7	44	-4.2	4.2
37	6.2	6.2	3.9	21	-4.1	4.1
26	6.0	6.0	4.1	39	-4.0	4.0
44	5.9	5.9	2.4	41	-3.8	3.8
9	5.8	5.8	2.2	23	-3.7	3.7
16	5.8	5.8	2.2	9	-3.5	3.5
39	5.8	5.8	2.3	42	-3.3	3.3
2	5.7	5.7	0.8	37	-3.2	3.2
3	5.7	5.7	2.3	26	-3.2	3.2

**Table 8. Continued.**

Ranking Based on Maximum Error Source Effect Along Trajectory				Ranking at Meter Fix		
Run	Max Effect (sec)	Absolute Value of Max Effect (sec)	Distance From Initial Condition (nmi)	Run	Max Effect (sec)	Absolute Value of Max Effect (sec)
11	5.7	5.7	0.6	30	-3.1	3.1
11	5.7	5.7	0.6	30	-3.1	3.1
25	5.5	5.5	2.3	10	-3.0	3.0
41	5.5	5.5	0.8	1	-2.8	2.8
30	5.5	5.5	23.4	11	-2.7	2.7
10	5.5	5.5	2.3	28	-2.3	2.3
1	5.5	5.5	1.0	2	0.0	0.0
21	5.4	5.4	5.1	3	0.0	0.0

**Table 9. Ranked effect of tracker jump error source at maximum tracker jump error location and at meter fix for path-stretch runs. Ranking is based on absolute value of tracker jump error source effect.**

Ranking Based on Maximum Error Source Effect Along Trajectory				Ranking at Meter Fix		
Run	Max Effect (sec)	Absolute Value of Max Effect (sec)	Distance From Initial Condition (nmi)	Run	Max Effect (sec)	Absolute Value of Max Effect (sec)
15	-10.7	10.7	35.9	13	-10.2	10.2
13	-10.2	10.2	96.2	15	-10.0	10.0
20	-8.6	8.6	74.4	20	-8.6	8.6
17	8.1	8.1	32.0	6	-5.7	5.7
27	6.3	6.3	3.6	8	-5.5	5.5
33	6.2	6.2	2.0	33	-4.6	4.6
40	6.0	6.0	1.8	27	-3.8	3.8
8	5.8	5.8	0.8	17	-3.8	3.8
6	-5.7	5.7	83.4	40	-2.0	2.0

## B.2. Wind

**Table 10. Ranked effect of wind error source at maximum wind error location and at meter fix for direct runs. Ranking is based on absolute value of wind error source effect.**

Ranking Based on Maximum Error Source Effect Along Trajectory				Ranking at Meter Fix		
Run	Max Effect (sec)	Absolute Value of Max Effect (sec)	Distance From Initial Condition (nmi)	Run	Max Effect (sec)	Absolute Value of Max Effect (sec)
44	-10.0	10.0	69.1	44	-10.0	10.0
37	-9.8	9.8	73.7	37	-9.8	9.8
1	-8.5	8.5	72.2	3	-8.4	8.4
3	-8.4	8.4	84.6	2	-8.1	8.1
2	-8.1	8.1	80.1	1	-7.9	7.9
43	-7.6	7.6	78.5	43	-7.6	7.6
7	-6.9	6.9	84.5	7	-6.9	6.9
42	-6.5	6.5	64.3	42	-6.5	6.5
34	-6.2	6.2	77.7	34	-6.2	6.2
25	-5.8	5.8	62.2	12	-5.3	5.3
12	-5.3	5.3	73.9	21	-5.2	5.2
21	-5.2	5.2	73.0	18	-5.1	5.1
18	-5.1	5.1	69.1	30	-4.9	4.9
30	-4.9	4.9	75.8	29	-4.9	4.9
29	-4.9	4.9	83.1	9	-4.8	4.8
9	-4.8	4.8	79.2	11	-4.5	4.5
11	-4.5	4.5	72.7	25	-4.1	4.1
32	-4.0	4.0	70.5	32	-4.0	4.0
4	-3.8	3.8	68.3	41	-3.5	3.5
22	-3.7	3.7	38.3	19	-3.5	3.5
26	-3.7	3.7	58.5	26	-3.4	3.4
41	-3.5	3.5	79.5	36	3.2	3.2
19	-3.5	3.5	78.2	22	-3.2	3.2
36	3.2	3.2	77.9	31	3.2	3.2
35	-3.2	3.2	72.0	4	-3.1	3.1
31	3.2	3.2	78.4	35	-3.0	3.0
10	-3.1	3.1	66.0	10	-2.8	2.8
24	-2.4	2.4	65.8	24	-2.3	2.3
38	1.7	1.7	65.8	38	1.6	1.6
14	-1.6	1.6	39.6	39	-0.9	0.9
39	-1.3	1.3	29.0	28	-0.6	0.6
28	1.1	1.1	26.7	14	-0.6	0.6
5	1.0	1.0	40.8	23	-0.4	0.4
16	0.9	0.9	34.7	5	-0.3	0.3
23	-0.8	0.8	45.6	16	-0.2	0.2

**Table 11. Ranked effect of wind error source at maximum wind error location and at meter fix for path-stretch runs. Ranking is based on absolute value of wind error source effect.**

Ranking Based on Maximum Error Source Effect Along Trajectory				Ranking at Meter Fix		
Run	Max Effect (sec)	Absolute Value of Max Effect (sec)	Distance From Initial Condition (nmi)	Run	Max Effect (sec)	Absolute Value of Max Effect (sec)
33	-11.4	11.4	101.1	33	-11.4	11.4
8	-8.5	8.5	103.6	8	-8.5	8.5
17	-6.3	6.3	100.1	17	-6.3	6.3
15	4.5	4.5	79.4	13	-2.2	2.2
40	-3.9	3.9	35.7	6	2.1	2.1
6	3.0	3.0	32.1	20	-1.9	1.9
13	-2.6	2.6	106.3	27	-1.8	1.8
20	-2.3	2.3	56.1	15	1.8	1.8
27	2.1	2.1	35.8	40	-0.2	0.2

### B.3. CAS Deceleration

**Table 12. Ranked effect of CAS deceleration error source at maximum CAS deceleration error location and at meter fix for direct runs. Ranking is based on absolute value of CAS deceleration error source effect.**

Ranking Based on Maximum Error Source Effect Along Trajectory				Ranking at Meter Fix		
Run	Max Effect (sec)	Absolute Value of Max Effect (sec)	Distance From Initial Condition (nmi)	Run	Max Effect (sec)	Absolute Value of Max Effect (sec)
16	-19.0	19.0	66.4	16	-19.0	19.0
4	-14.4	14.4	75.7	4	-14.4	14.4
7	-14.1	14.1	84.5	7	-14.1	14.1
22	-13.8	13.8	65.9	22	-13.8	13.8
3	-13.3	13.3	84.6	3	-13.3	13.3
1	-12.6	12.6	82.2	1	-12.6	12.6
42	-10.7	10.7	65.1	42	-10.7	10.7
18	-10.4	10.4	69.1	18	-10.4	10.4
35	-9.8	9.8	76.0	35	-9.8	9.8
23	-7.9	7.9	58.4	23	-7.9	7.9
39	-7.8	7.8	78.0	39	-7.8	7.8
24	-7.6	7.6	67.7	24	-7.6	7.6
9	-7.2	7.2	79.2	9	-7.2	7.2
10	-6.7	6.7	72.5	10	-6.7	6.7
28	-6.5	6.5	58.0	28	-6.4	6.4
19	-5.9	5.9	78.2	19	-5.9	5.9
5	-4.8	4.8	71.5	5	-4.8	4.8
44	-3.2	3.2	69.1	44	-3.2	3.2
34	-3.0	3.0	77.7	34	-3.0	3.0
37	-2.7	2.7	73.2	37	-2.7	2.7
26	-2.6	2.6	77.4	26	-2.6	2.6
41	-2.4	2.4	80.0	41	-2.4	2.4
30	1.7	1.7	66.3	36	1.0	1.0
36	-1.2	1.2	54.9	21	-0.9	0.9
21	-0.9	0.9	74.3	30	0.7	0.7
11	0.0	0.0	0.0	11	0.0	0.0
12	0.0	0.0	0.0	12	0.0	0.0
2	0.0	0.0	0.0	2	0.0	0.0
14	0.0	0.0	0.0	14	0.0	0.0
25	0.0	0.0	0.0	25	0.0	0.0
29	0.0	0.0	0.0	29	0.0	0.0
31	0.0	0.0	0.0	31	0.0	0.0
32	0.0	0.0	0.0	32	0.0	0.0
38	0.0	0.0	0.0	38	0.0	0.0
43	0.0	0.0	0.0	43	0.0	0.0

**Table 13. Ranked effect of CAS deceleration error source at maximum CAS deceleration error location and at meter fix for path-stretch runs. Ranking is based on absolute value of CAS deceleration error source effect.**

Ranking Based on Maximum Error Source Effect Along Trajectory				Ranking at Meter Fix		
Run	Max Effect (sec)	Absolute Value of Max Effect (sec)	Distance From Initial Condition (nmi)	Run	Max Effect (sec)	Absolute Value of Max Effect (sec)
6	-17.0	17.0	96.3	6	-16.8	16.8
20	-6.0	6.0	105.2	20	-5.9	5.9
27	-5.8	5.8	98.8	27	-5.5	5.5
40	-3.2	3.2	106.2	40	-3.2	3.2
15	-0.8	0.8	114.4	15	-0.3	0.3
13	0.4	0.4	104.2	8	0.2	0.2
8	0.4	0.4	97.4	13	0.1	0.1
17	0.0	0.0	0.0	17	0.0	0.0
33	0.0	0.0	0.0	33	0.0	0.0

#### B.4. Speed Conformance

**Table 14. Ranked effect of speed conformance error source at maximum speed conformance error location and at meter fix for direct runs. Ranking is based on absolute value of speed conformance error source effect.**

Ranking Based on Maximum Error Source Effect Along Trajectory				Ranking at Meter Fix		
Run	Max Effect (sec)	Absolute Value of Max Effect (sec)	Distance From Initial Condition (nmi)	Run	Max Effect (sec)	Absolute Value of Max Effect (sec)
32	-13.1	13.1	62.1	32	-12.6	12.6
11	-12.8	12.8	36.5	11	-11.8	11.8
31	10.4	10.4	78.4	31	10.4	10.4
29	5.0	5.0	83.1	29	5.0	5.0
38	4.7	4.7	28.9	21	-4.4	4.4
21	-4.4	4.4	60.5	37	2.9	2.9
43	-3.7	3.7	42.3	38	2.7	2.7
37	2.9	2.9	63.3	7	2.0	2.0
14	-2.6	2.6	30.1	26	1.5	1.5
7	2.1	2.1	59.2	9	1.5	1.5
2	-2.0	2.0	33.7	14	-1.4	1.4
26	1.6	1.6	60.2	34	-1.2	1.2
9	1.5	1.5	58.8	16	0.9	0.9
41	-1.3	1.3	57.7	39	0.6	0.6
34	-1.2	1.2	65.2	35	-0.6	0.6
16	1.1	1.1	40.8	36	-0.6	0.6
12	-0.9	0.9	55.1	25	0.5	0.5
25	0.7	0.7	37.9	44	-0.5	0.5
10	-0.7	0.7	41.9	3	0.5	0.5
39	0.6	0.6	37.4	28	0.5	0.5
35	-0.6	0.6	53.6	43	-0.4	0.4
36	-0.6	0.6	45.7	1	-0.4	0.4
44	-0.5	0.5	58.1	10	-0.4	0.4
3	0.5	0.5	60.0	2	-0.4	0.4
28	0.5	0.5	21.1	12	-0.4	0.4
5	0.4	0.4	60.1	5	0.4	0.4
1	-0.4	0.4	60.9	23	-0.2	0.2
23	-0.2	0.2	35.4	18	0.2	0.2
18	0.2	0.2	39.2	41	-0.2	0.2
42	-0.2	0.2	27.8	42	-0.2	0.2
30	-0.2	0.2	39.8	30	-0.2	0.2
19	-0.1	0.1	39.0	19	-0.1	0.1
4	-0.1	0.1	46.4	4	-0.1	0.1
22	0.0	0.0	38.3	22	0.0	0.0
24	0.0	0.0	44.2	24	0.0	0.0

**Table 15. Ranked effect of speed conformance error source at maximum speed conformance error location and at meter fix for path-stretch runs. Ranking is based on absolute value of speed conformance error source effect.**

Ranking Based on Maximum Error Source Effect Along Trajectory				Ranking at Meter Fix		
Run	Max Effect (sec)	Absolute Value of Max Effect (sec)	Distance From Initial Condition (nmi)	Run	Max Effect (sec)	Absolute Value of Max Effect (sec)
6	17.2	17.2	74.0	6	17.2	17.2
17	-8.6	8.6	75.7	17	-7.9	7.9
8	-2.7	2.7	84.9	8	-1.5	1.5
27	2.6	2.6	76.6	33	-1.4	1.4
33	-2.0	2.0	74.1	13	1.3	1.3
13	1.3	1.3	101.4	27	0.9	0.9
15	0.4	0.4	108.7	15	0.4	0.4
20	-0.2	0.2	85.1	20	-0.2	0.2
40	0.0	0.0	78.1	40	0.0	0.0

## B.5. Target Mach

**Table 16. Ranked effect of target Mach error source at maximum target Mach error location and at meter fix for direct runs. Ranking is based on absolute value of target Mach error source effect.**

Ranking Based on Maximum Error Source Effect Along Trajectory				Ranking at Meter Fix		
Run	Max Effect (sec)	Absolute Value of Max Effect (sec)	Distance From Initial Condition (nmi)	Run	Max Effect (sec)	Absolute Value of Max Effect (sec)
36	-14.7	14.7	44.3	36	-14.7	14.7
7	13.4	13.4	44.8	7	13.4	13.4
4	-11.7	11.7	42.8	4	-11.6	11.6
5	-10.4	10.4	35.6	5	-10.1	10.1
9	-10.2	10.2	39.6	24	-8.2	8.2
24	-8.3	8.3	41.3	9	-7.9	7.9
44	-7.5	7.5	31.2	44	-7.4	7.4
21	7.2	7.2	34.2	21	7.2	7.2
30	-6.6	6.6	23.4	10	6.4	6.4
10	6.4	6.4	20.2	30	-6.0	6.0
25	-5.9	5.9	21.9	25	-5.9	5.9
1	-5.8	5.8	47.0	37	5.6	5.6
12	-5.6	5.6	14.7	1	-5.5	5.5
37	5.6	5.6	21.9	39	5.4	5.4
39	5.4	5.4	35.9	12	-5.2	5.2
31	-4.4	4.4	20.6	31	-4.1	4.1
34	-4.2	4.2	18.9	3	3.8	3.8
35	-3.9	3.9	20.0	18	3.6	3.6
3	3.8	3.8	52.9	16	3.1	3.1
41	-3.7	3.7	29.5	34	-3.0	3.0
18	3.6	3.6	38.5	11	-3.0	3.0
19	-3.2	3.2	25.4	14	-2.6	2.6
16	3.1	3.1	33.2	35	-2.5	2.5
11	-3.0	3.0	15.2	19	-2.3	2.3
14	-2.6	2.6	19.3	26	2.1	2.1
22	-2.3	2.3	31.2	28	2.0	2.0
26	2.1	2.1	33.3	22	-1.7	1.7
28	2.0	2.0	19.9	2	-1.6	1.6
2	-1.6	1.6	24.3	38	1.5	1.5
38	1.5	1.5	11.0	23	-1.4	1.4
23	-1.4	1.4	21.0	41	-1.4	1.4
43	-1.2	1.2	21.3	43	-1.2	1.2
29	1.1	1.1	12.0	29	1.0	1.0
32	-0.7	0.7	17.1	32	-0.7	0.7
42	0.3	0.3	15.0	42	0.0	0.0

**Table 17. Ranked effect of target Mach error source at maximum target Mach error location and at meter fix for path-stretch runs. Ranking is based on absolute value of target Mach error source effect.**

Ranking Based on Maximum Error Source Effect Along Trajectory				Ranking at Meter Fix		
Run	Max Effect (sec)	Absolute Value of Max Effect (sec)	Distance From Initial Condition (nmi)	Run	Max Effect (sec)	Absolute Value of Max Effect (sec)
15	-30.8	30.8	86.4	15	-28.4	28.4
13	-28.3	28.3	81.2	13	-25.3	25.3
6	25.1	25.1	49.8	6	25.1	25.1
40	-16.5	16.5	69.4	40	-15.6	15.6
20	-14.8	14.8	71.4	20	-13.0	13.0
27	-7.7	7.7	57.5	33	-6.0	6.0
33	-6.5	6.5	41.1	8	-2.6	2.6
8	-4.9	4.9	49.9	27	-2.1	2.1
17	0.7	0.7	25.5	17	0.7	0.7

## B.6. Atmosphere/Altitude

**Table 18. Ranked effect of atmosphere/altitude error source at maximum atmosphere/altitude error location and at meter fix for direct runs. Ranking is based on absolute value of atmosphere/altitude error source effect.**

Ranking Based on Maximum Error Source Effect Along Trajectory				Ranking at Meter Fix		
Run	Max Effect (sec)	Absolute Value of Max Effect (sec)	Distance From Initial Condition (nmi)	Run	Max Effect (sec)	Absolute Value of Max Effect (sec)
36	-1.7	1.7	44.3	36	-1.7	1.7
19	-0.7	0.7	37.5	19	-0.7	0.7
4	-0.7	0.7	45.7	4	-0.7	0.7
41	-0.7	0.7	45.2	41	-0.7	0.7
9	-0.7	0.7	47.0	9	-0.7	0.7
35	-0.6	0.6	42.5	35	-0.6	0.6
24	-0.6	0.6	43.7	24	-0.6	0.6
34	-0.6	0.6	45.0	34	-0.6	0.6
42	0.6	0.6	26.4	42	0.6	0.6
30	-0.4	0.4	39.0	30	-0.4	0.4
44	0.4	0.4	21.0	1	-0.4	0.4
1	-0.4	0.4	55.2	31	-0.4	0.4
31	-0.4	0.4	24.0	43	0.3	0.3
11	-0.3	0.3	15.2	11	-0.3	0.3
43	0.3	0.3	20.0	22	-0.3	0.3
22	-0.3	0.3	36.9	38	-0.3	0.3
38	-0.3	0.3	11.0	21	-0.2	0.2
5	-0.2	0.2	42.4	5	-0.2	0.2
16	0.2	0.2	19.1	16	0.2	0.2
21	-0.2	0.2	24.8	44	0.2	0.2
3	0.2	0.2	36.9	12	-0.2	0.2
18	0.2	0.2	16.7	26	0.1	0.1
12	-0.2	0.2	16.7	10	0.1	0.1
26	0.2	0.2	15.2	3	-0.1	0.1
10	0.1	0.1	20.2	18	-0.1	0.1
39	0.1	0.1	25.0	29	0.1	0.1
29	0.1	0.1	12.0	14	-0.1	0.1
23	0.1	0.1	15.7	39	0.1	0.1
14	-0.1	0.1	19.3	37	-0.1	0.1
25	0.1	0.1	14.2	23	0.0	0.0
7	-0.1	0.1	36.4	2	0.0	0.0
37	-0.1	0.1	21.9	25	0.0	0.0
28	0.0	0.0	14.1	32	0.0	0.0
2	0.0	0.0	24.3	7	0.0	0.0
32	0.0	0.0	17.1	28	0.0	0.0

**Table 19. Ranked effect of atmosphere/altitude error source at maximum atmosphere/altitude error location and at meter fix for path-stretch runs. Ranking is based on absolute value of atmosphere/altitude error source effect.**

Ranking Based on Maximum Error Source Effect Along Trajectory				Ranking at Meter Fix		
Run	Max Effect (sec)	Absolute Value of Max Effect (sec)	Distance From Initial Condition (nmi)	Run	Max Effect (sec)	Absolute Value of Max Effect (sec)
15	-2.5	2.5	94.5	15	-2.5	2.5
13	-1.8	1.8	92.1	13	-1.8	1.8
40	-1.5	1.5	77.6	40	-1.5	1.5
20	-1.5	1.5	83.4	20	-1.5	1.5
8	-0.8	0.8	63.8	8	-0.8	0.8
6	0.7	0.7	49.8	6	0.7	0.7
27	0.6	0.6	46.6	17	0.4	0.4
17	0.4	0.4	25.5	33	-0.1	0.1
33	-0.1	0.1	46.4	27	0.0	0.0

## B.7. Path Distance

**Table 20. Ranked effect of path distance error source at maximum path distance error location and at meter fix for direct runs. Ranking is based on absolute value of path distance error source effect.**

Ranking Based on Maximum Error Source Effect Along Trajectory				Ranking at Meter Fix		
Run	Max Effect (sec)	Absolute Value of Max Effect (sec)	Distance From Initial Condition (nmi)	Run	Max Effect (sec)	Absolute Value of Max Effect (sec)
38	4.9	4.9	81.3	38	4.9	4.9
18	3.8	3.8	69.2	18	3.8	3.8
36	3.8	3.8	78.0	36	3.8	3.8
34	3.3	3.3	78.1	34	3.3	3.3
42	3.2	3.2	65.1	42	3.2	3.2
31	3.1	3.1	78.4	31	3.1	3.1
5	3.0	3.0	72.0	5	3.0	3.0
39	2.9	2.9	78.2	39	2.9	2.9
28	2.9	2.9	59.5	28	2.9	2.9
41	2.8	2.8	80.6	41	2.8	2.8
11	2.7	2.7	72.7	11	2.7	2.7
43	2.6	2.6	78.5	43	2.6	2.6
2	2.6	2.6	81.3	2	2.6	2.6
30	2.6	2.6	75.9	30	2.6	2.6
14	2.5	2.5	76.1	14	2.5	2.5
9	2.4	2.4	77.9	9	2.4	2.4
24	2.4	2.4	68.0	24	2.4	2.4
21	2.4	2.4	75.3	21	2.4	2.4
12	2.3	2.3	74.2	12	2.3	2.3
37	2.1	2.1	74.0	37	2.1	2.1
25	1.9	1.9	70.9	25	1.9	1.9
29	1.9	1.9	83.5	29	1.9	1.9
44	1.8	1.8	69.1	44	1.8	1.8
19	1.8	1.8	78.3	19	1.8	1.8
23	1.7	1.7	58.4	23	1.7	1.7
22	1.7	1.7	65.4	22	1.7	1.7
10	1.7	1.7	72.8	10	1.7	1.7
7	1.5	1.5	84.9	7	1.5	1.5
35	1.5	1.5	76.1	35	1.5	1.5
4	1.4	1.4	75.7	4	1.4	1.4
1	1.4	1.4	82.4	1	1.4	1.4
32	1.3	1.3	70.8	32	1.3	1.3
16	1.2	1.2	66.6	16	1.2	1.2
3	1.1	1.1	85.8	3	1.1	1.1
26	1.1	1.1	76.4	26	1.1	1.1

**Table 21. Ranked effect of path distance error source at maximum path distance error location and at meter fix for path-stretch runs. Ranking is based on absolute value of path distance error source effect.**

Ranking Based on Maximum Error Source Effect Along Trajectory				Ranking at Meter Fix		
Run	Max Effect (sec)	Absolute Value of Max Effect (sec)	Distance From Initial Condition (nmi)	Run	Max Effect (sec)	Absolute Value of Max Effect (sec)
15	-18.0	18.0	41.1	15	-14.1	14.1
40	-13.4	13.4	35.7	13	-10.2	10.2
13	-12.9	12.9	36.9	33	-7.1	7.1
33	-10.3	10.3	41.1	40	-6.5	6.5
17	-9.3	9.3	39.8	17	-5.3	5.3
20	-8.7	8.7	36.9	27	-3.8	3.8
27	-8.4	8.4	40.8	6	0.4	0.4
8	-7.9	7.9	34.2	8	0.4	0.4
6	-4.0	4.0	38.7	20	-0.2	0.2

## B.8. Residual

**Table 22. Ranked effect of error source residual at maximum residual location and at meter fix for direct runs. Ranking is based on absolute value of residual.**

Ranking Based on Maximum Error Source Effect Along Trajectory				Ranking at Meter Fix		
Run	Max Residual (sec)	Absolute Value of Residual (sec)	Distance From Initial Condition (nmi)	Run	Max Residual (sec)	Absolute Value of Residual (sec)
31	-9.2	9.2	31.6	34	-7.5	7.5
34	-7.5	7.5	78.1	19	-4.2	4.2
3	6.2	6.2	84.6	18	-4.0	4.0
18	5.8	5.8	40.6	36	-3.8	3.8
7	5.0	5.0	72.8	7	3.5	3.5
22	4.5	4.5	40.4	5	-3.4	3.4
19	-4.2	4.2	78.3	41	-3.0	3.0
16	4.1	4.1	59.4	44	-3.0	3.0
21	-4.0	4.0	23.9	42	-2.7	2.7
36	-3.9	3.9	77.5	16	2.6	2.6
32	-3.5	3.5	36.7	38	-2.6	2.6
23	-3.5	3.5	42.0	30	-2.6	2.6
1	-3.5	3.5	79.4	29	-2.5	2.5
5	-3.4	3.4	72.0	24	-2.4	2.4
29	-3.4	3.4	33.8	35	-2.4	2.4
39	-3.4	3.4	33.7	25	2.0	2.0
4	-3.4	3.4	6.2	28	-1.9	1.9
10	-3.2	3.2	57.2	26	-1.8	1.8
37	-3.1	3.1	9.4	3	1.7	1.7
38	-3.0	3.0	71.6	32	-1.7	1.7
41	-3.0	3.0	80.6	9	-1.7	1.7
44	-3.0	3.0	69.1	37	-1.4	1.4
25	2.8	2.8	52.0	11	-1.4	1.4
43	2.8	2.8	58.7	21	1.3	1.3
42	-2.7	2.7	65.1	14	-1.2	1.2
30	-2.7	2.7	75.8	10	-1.2	1.2
35	-2.2	2.5	35.5	1	-1.1	1.1
26	-2.5	2.5	53.2	23	-1.1	1.1
24	-2.4	2.4	68.0	12	-1.1	1.1
12	-2.4	2.4	49.3	4	-0.8	0.8
9	2.1	2.1	58.8	39	-0.7	0.7
11	2.1	2.1	2.0	43	0.2	0.2
2	2.0	2.0	64.8	31	0.1	0.1
28	-1.9	1.9	59.5	2	0.1	0.1
14	-1.8	1.8	54.5	22	0.0	0.0

**Table 23. Ranked effect of error source residual at maximum residual location and at meter fix for path-stretch runs. Ranking is based on absolute value of residual.**

Ranking Based on Maximum Error Source Effect Along Trajectory				Ranking at Meter Fix		
Run	Max Effect (sec)	Absolute Value of Max Effect (sec)	Distance From Initial Condition (nmi)	Run	Max Effect (sec)	Absolute Value of Max Effect (sec)
20	10.2	10.2	33.0	13	-7.0	7.0
40	8.6	8.6	67.0	6	6.6	6.6
15	8.0	8.0	38.9	15	-6.5	6.5
6	-7.5	7.5	54.8	20	-4.3	4.3
13	-7.0	7.0	110.5	8	-2.4	2.4
33	4.3	4.3	39.6	27	-2.2	2.2
17	4.2	4.2	38.2	33	-1.6	1.6
8	-3.0	3.0	67.0	40	0.4	0.4
27	-2.4	2.4	100.0	17	0.3	0.3

## Appendix C: Run-by-Run Results for Direct Runs

This appendix includes plots for direct runs without path-stretch clearances. A description of the plots as they relate to the error sources is presented first, followed by the plots for each run.

### C.1. Incremental Error Source Effect on Time Error

The first plot presented for each run (e.g., Fig. 35) shows the incremental effect that removing each error source has on the flown minus predicted time error. The data series labeled “Uncorrected” represents the flown minus predicted time without removing any error sources. The data series labeled “(A) Tracker” is the time error after the tracker jump error source has been removed. Also removing the wind error source results in the data series labeled “(A)+(B) Wind.” This incremental removal of error sources continues until all identified error sources have been removed in the data series labeled “(A)+…+(G) Dist.”

#### C.1.A. Tracker Jumps

The first plot (e.g., Fig. 36) in the tracker jumps error source subsection isolates the effect of the tracker jump error source on the time error for each run similar to the previous plot. This plot is included because the previous data plot contains seven data series, and distinguishing between them may be difficult.

The second plot (e.g., Fig. 37) shows the magnitude of the tracker jump error source. Subtracting the data series in this plot from the “Uncorrected” data series in the previous plot results in the “(A) Tracker” data series.

#### C.1.B. Wind

The first plot (e.g., Fig. 38) in the wind error source subsection isolates the effect of the wind error source on the time error for each run.

The second plot (e.g., Fig. 39) in the wind error source subsection shows the predicted and flown wind effect on ground speed. The y-axis is the magnitude when subtracting the TAS vector from the ground speed vector. Subtracting the “ADC Flown Wind Speed” data series from the “CTAS Predicted Wind Speed” in this plot results in the change in ground speed after removing this error source. This change in ground speed is shown as the “(B) Wind” data series in the next plot (e.g., Fig. 40). This plot, which does not incrementally add the error source effects, shows the change in predicted ground speed by removing the five error sources listed. Two error sources, tracker jumps and path distance, are not converted to a ground speed effect.

#### C.1.C. CAS Deceleration

The first plot (e.g., Fig. 41) in the CAS deceleration error source subsection isolates the effect of the CAS deceleration error source on the time error for each run.

The second plot (e.g., Fig. 42) in the CAS deceleration error source subsection shows the flown and predicted CAS. The CAS value that is being targeted is shown in this plot with circle markers. The difference between flown and predicted CAS for this error source is only applied after the aircraft is predicted to start decelerating to the meter-fix crossing speed restriction. This occurs at approximately 60 nmi along the predicted path in Fig. 42. The difference between flown and predicted CAS during the constant CAS segment, which is the horizontal segment at 300 knots CAS, is applied during the quantification of the speed conformance error source. The difference between flown and predicted CAS before the constant CAS segment was not used in this analysis.

The third plot (e.g., Fig. 43) in the CAS deceleration error source subsection shows the flown and predicted TAS/CAS ratio that was used to convert flown CAS to TAS as described in Subsection 6.3 of Section 6.

The fourth plot (e.g., Fig. 44) in the CAS deceleration error source subsection shows the flown and predicted TAS. This plot was not used in the error source analysis but is included for completeness.

The fifth plot (e.g., Fig. 45) in the CAS deceleration error source subsection shows deviation from flown TAS if a TAS was derived from CAS and Mach using atmospheric temperature and pressure according to Equations (3) to (7) in Section 6.1.

#### C.1.D. Speed Conformance

The first plot (e.g., Fig. 46) in the speed conformance error source subsection isolates the effect of the speed conformance error source on the time error for each run.

The location where the speed conformance error source applies can be determined by locating the constant CAS segment in the flown vs. predicted CAS plot described earlier (e.g., Fig. 42). Throttle may have been adjusted to maintain constant CAS during this segment. Though not used in quantifying this error source, the engine N1, N2 (e.g., Fig. 47) and EPR (e.g., Fig. 48) are included to show if thrust may have been changed during descent.

#### C.1.E. Target Mach

The first plot (e.g., Fig. 49) in the target Mach error source subsection isolates the effect of the target Mach error source on the time error for each run.

The second plot (e.g., Fig. 50) in the target Mach error source subsection shows the flown and predicted Mach. The difference between the flown and predicted Mach at the initial condition at zero along the x-axis is of interest because predicted Mach is not changed during the constant Mach segment; the difference is considered along the constant Mach segment that occurs from zero to about 52 nmi along the x-axis in Figure 50.

The third plot (e.g., Fig. 51) in the target Mach error source subsection shows the flown and predicted TAS/Mach ratio that was used to convert flown Mach to TAS as described in Subsection 6.5 of Section 6.

#### C.1.F. Atmosphere/Altitude

The first plot (e.g., Fig. 52) in the atmosphere/altitude error source subsection isolates the effect of the atmosphere/altitude error source on the time error for each run.

The second plot (e.g., Fig. 53) in the atmosphere/altitude error source subsection shows the flown (radar and aircraft ADC) and predicted (CTAS) vertical profile. The radar altitude minus the CTAS predicted altitude is shown in the next plot (e.g., Fig. 54).

The fourth (e.g., Fig. 55), fifth (e.g., Fig. 56) and sixth (e.g., Fig. 57) plots in the atmosphere/altitude error source subsection compare flown (ADC) and predicted (CTAS) static air temperature, impact pressure, and static pressure, respectively.

#### C.1.G. Path Distance

The first plot (e.g., Fig. 58) in the path distance error source subsection isolates the effect of the path distance error source on the time error for each run.

The second plot (e.g., Fig. 59) in the path distance error source subsection shows the flown minus predicted path length. This is followed by a ground track profile (e.g., Fig. 60) and cross-track error (e.g., Fig. 61).

## C.2. Run 1

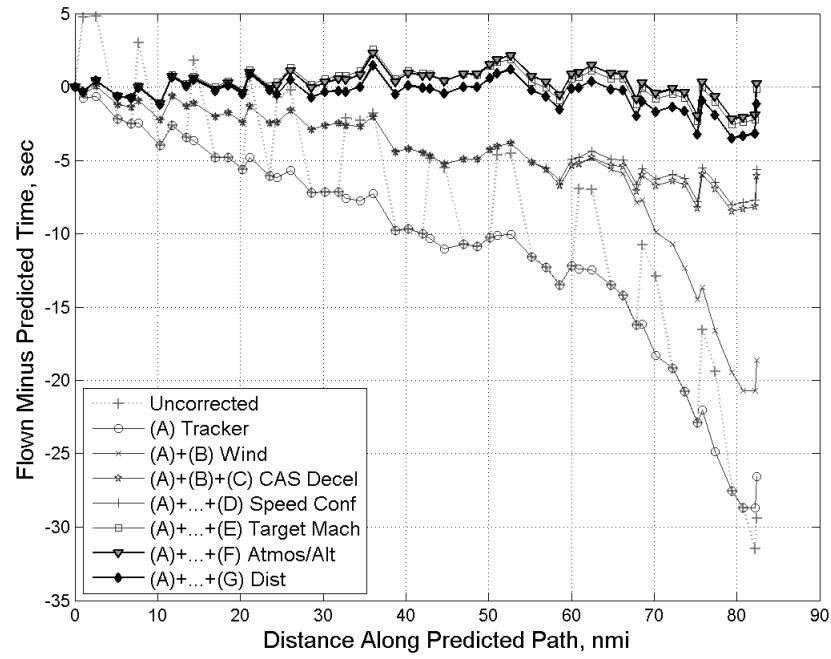


**Figure 35: Time error for run 1 showing incremental effect of removing each error source.**

### C.2.A. Tracker Jumps

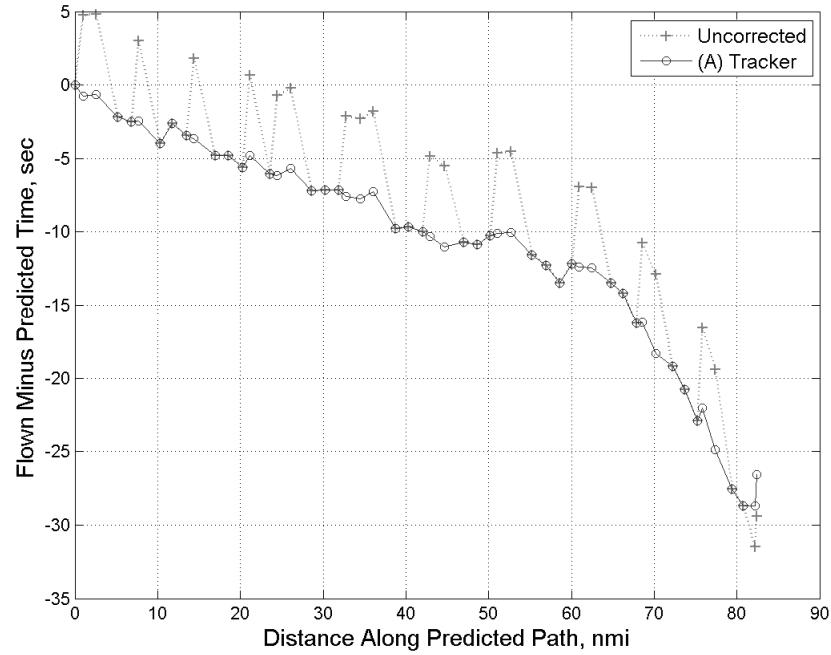


**Figure 36: Time error for run 1 before (Uncorrected) and after ((A) Tracker) removing tracker jump error source.**

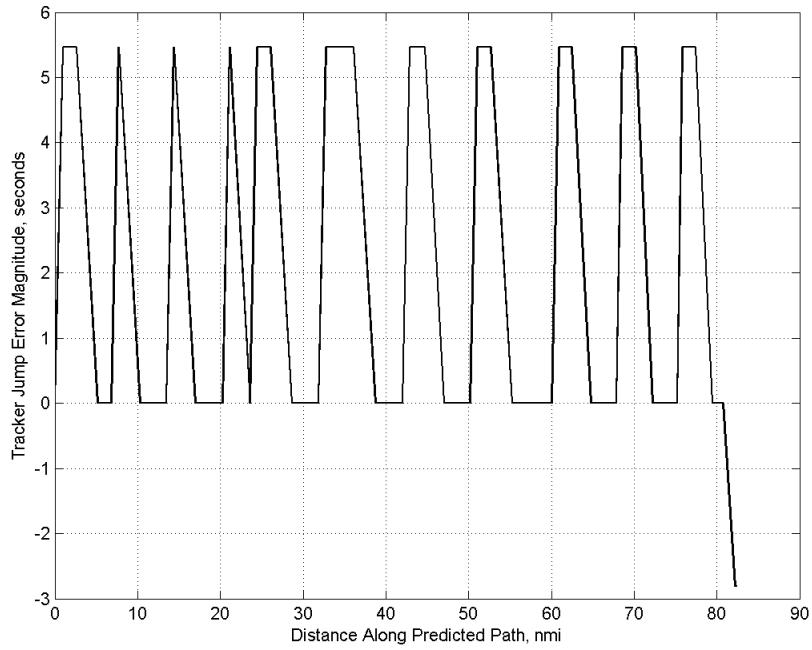


**Figure 37: Effect of tracker jump error source on time error for run 1.**

### C.2.B. Wind

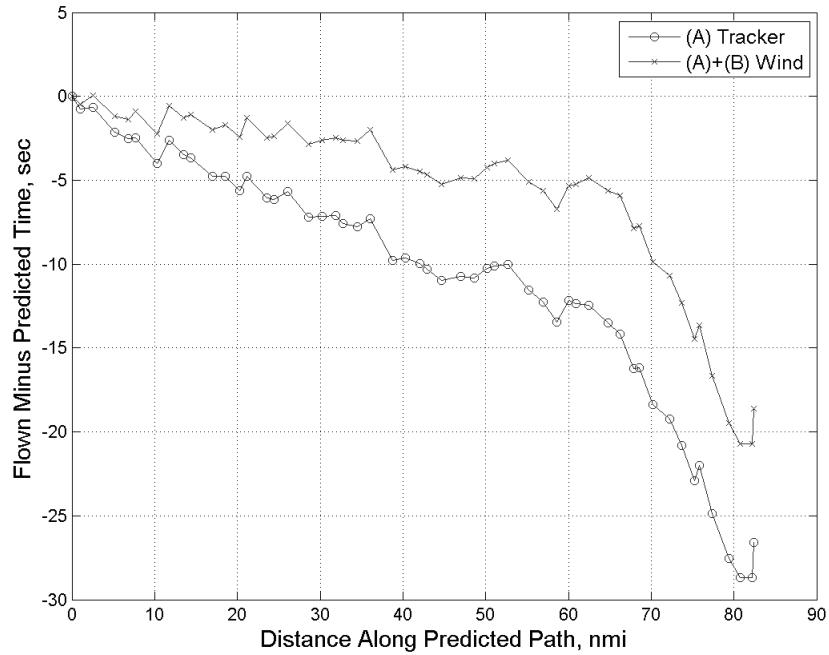


**Figure 38: Time error for run 1 before ((A) Tracker) and after ((A)+(B) Wind) removing wind error source.**

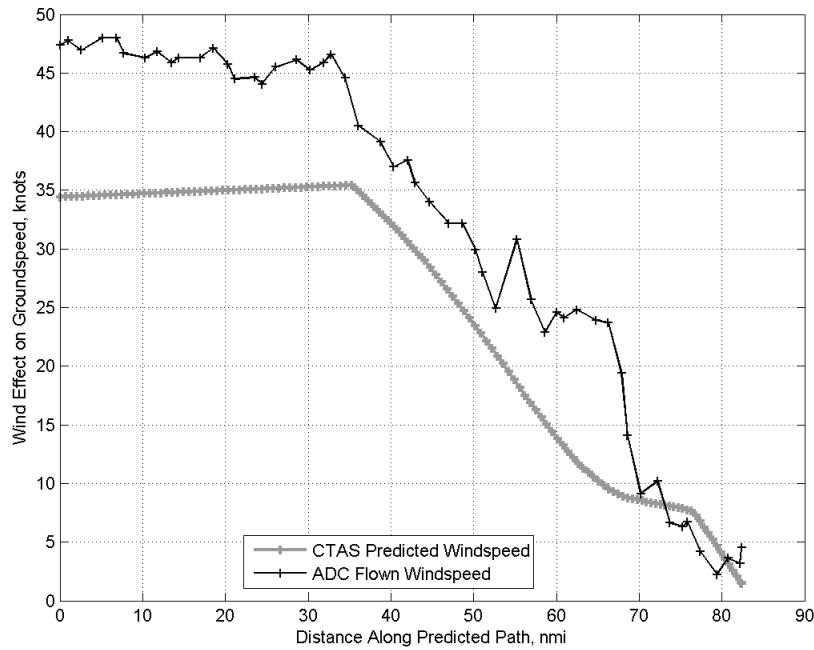


**Figure 39: CTAS predicted and ADC flown wind effect on ground speed for run 1. Negative values indicate a headwind.**

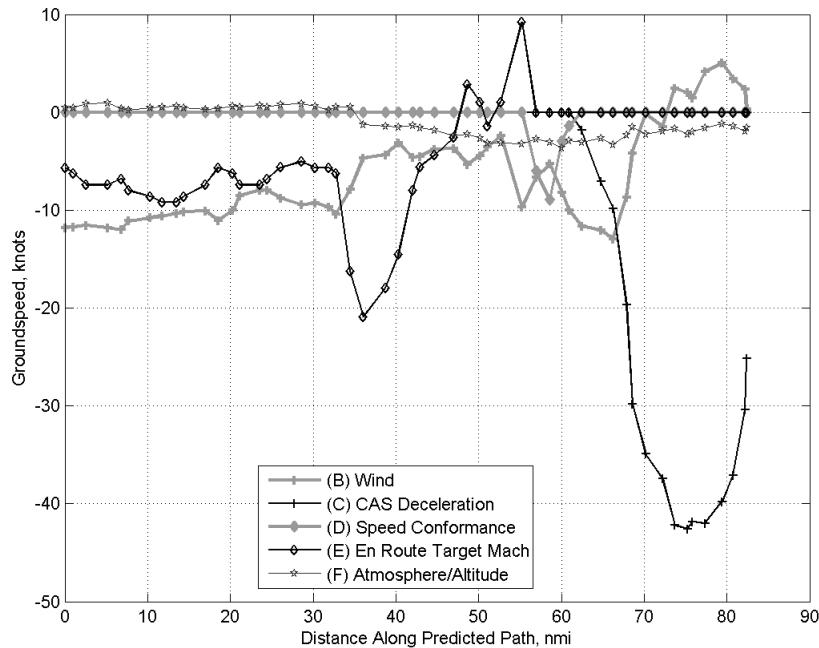


**Figure 40: Error sources (flown minus predicted) converted to a ground speed effect for run 1. Positive values indicate the flown ground speed was faster than the CTAS prediction.**

### C.2.C. CAS Deceleration

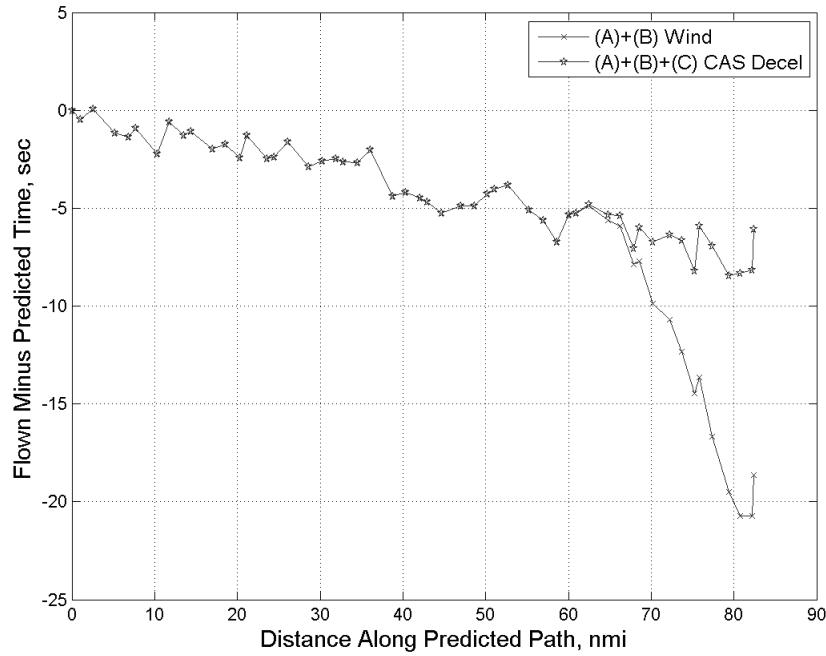


**Figure 41:** Time error for run 1 before ((A)+(B) Wind) and after ((A)+(B)+(C) CAS Decel) removing CAS deceleration error source.

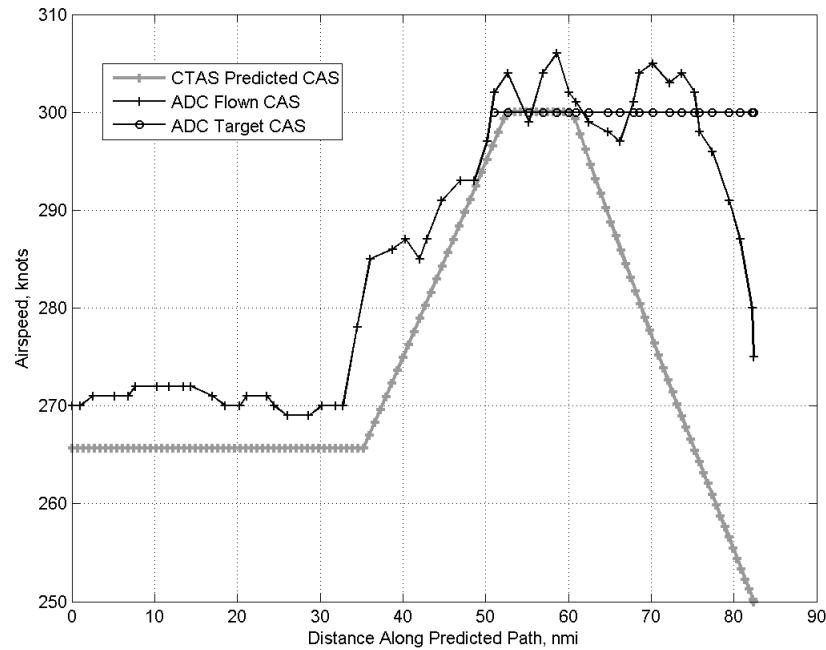


**Figure 42:** CTAS predicted and ADC flown CAS for run 1. CAS that is being targeted is shown with circle markers.

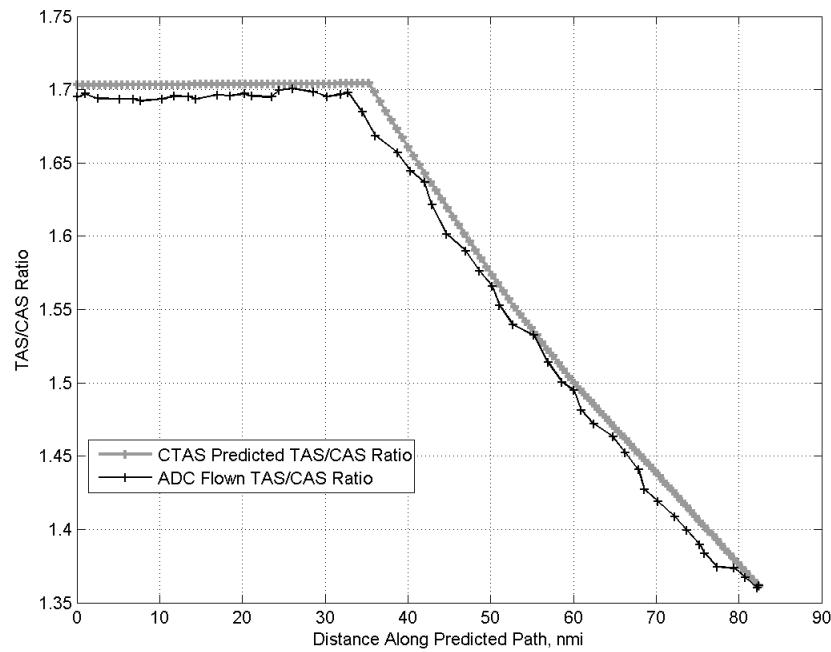


**Figure 43: CTAS predicted and ADC flown TAS/CAS ratio for run 1.**

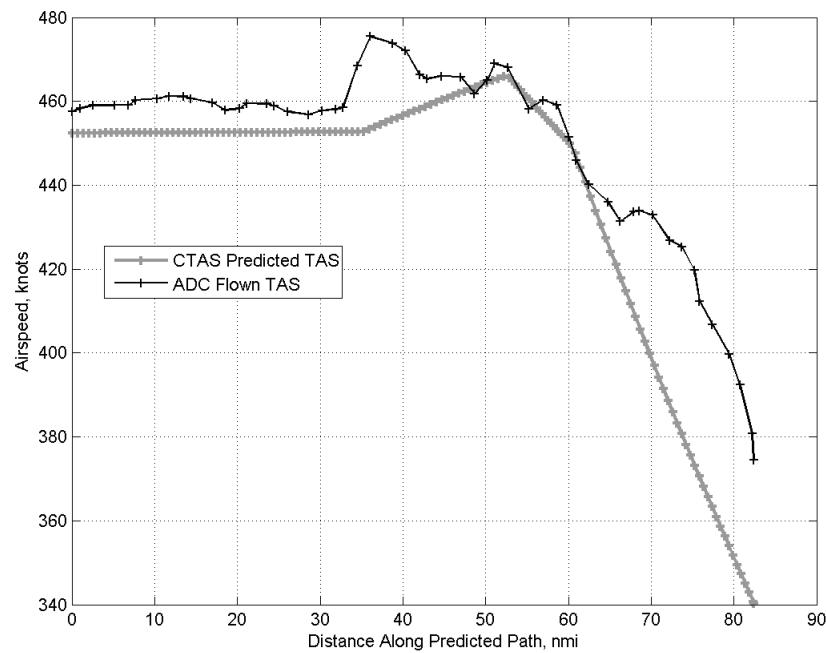


**Figure 44: CTAS predicted and ADC flown TAS for run 1.**

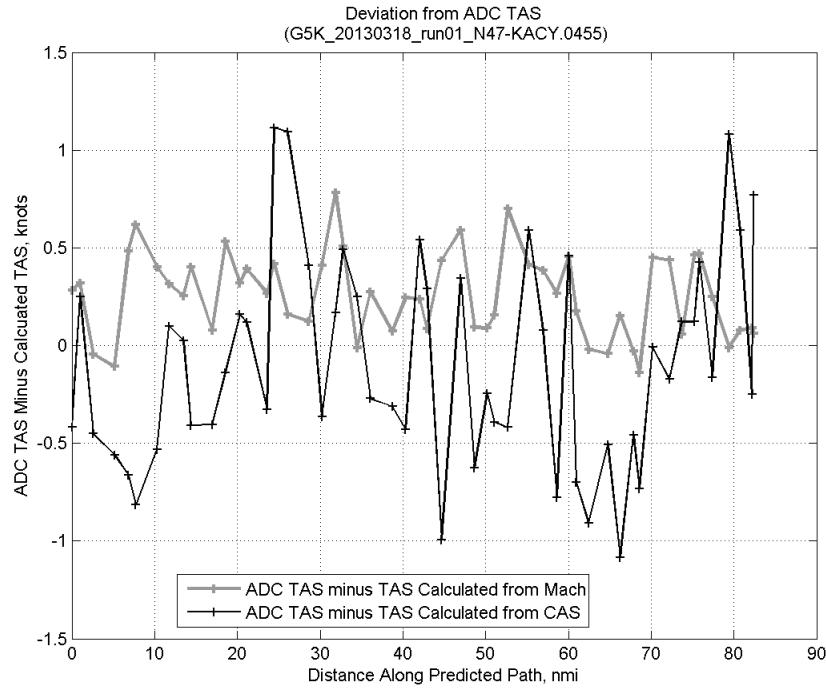


**Figure 45:** Deviation from ADC flown TAS if calculating TAS using ADC flown CAS, Mach, atmospheric temperature, and atmospheric pressure for run 1.

#### C.2.D. Speed Conformance

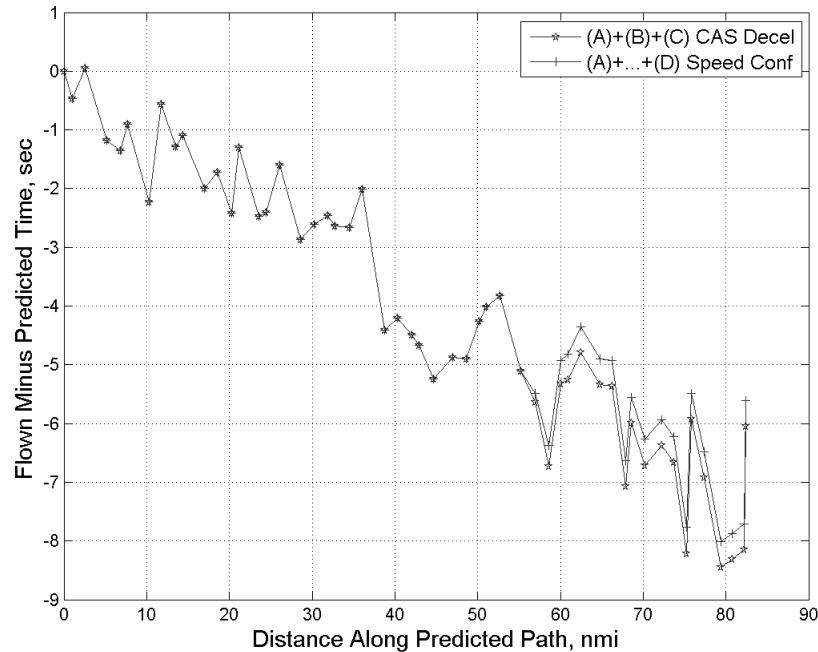


**Figure 46:** Time error for run 1 before ((A)+(B)+(C) CAS Decel) and after ((A)+...+(D) Speed Conf) removing speed conformance error source.

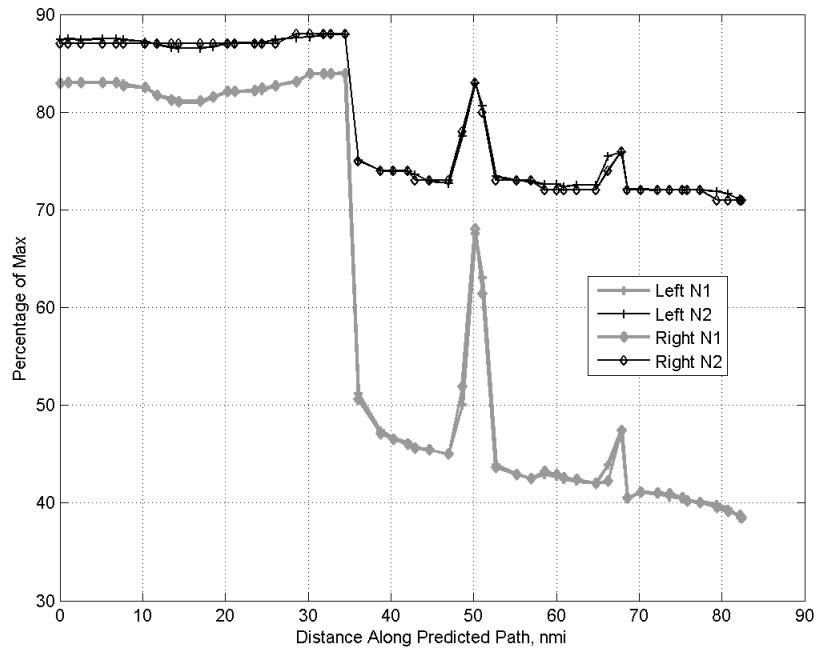


**Figure 47: Flown engine N1 and N2 for run 1.**

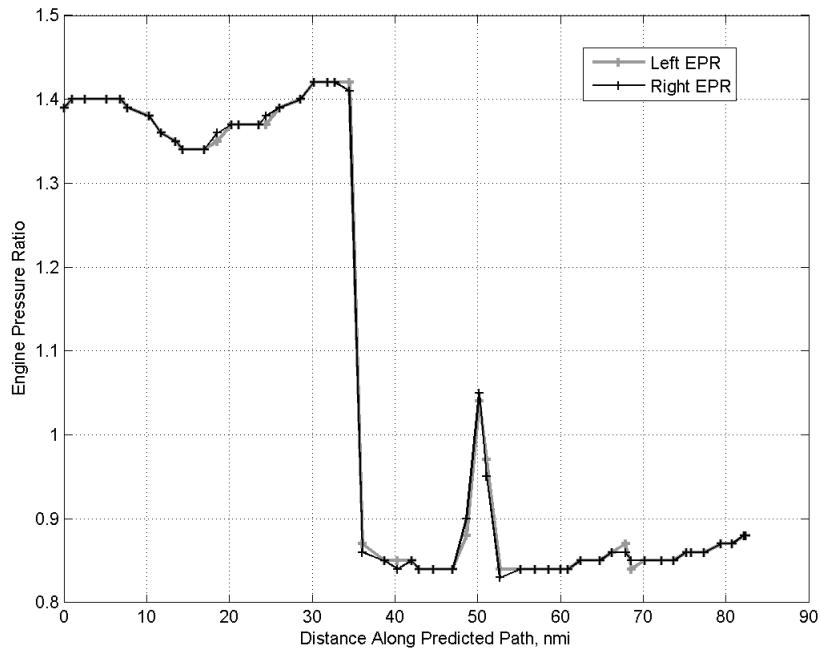


**Figure 48: Flown engine EPR for run 1.**

### C.2.E. Target Mach

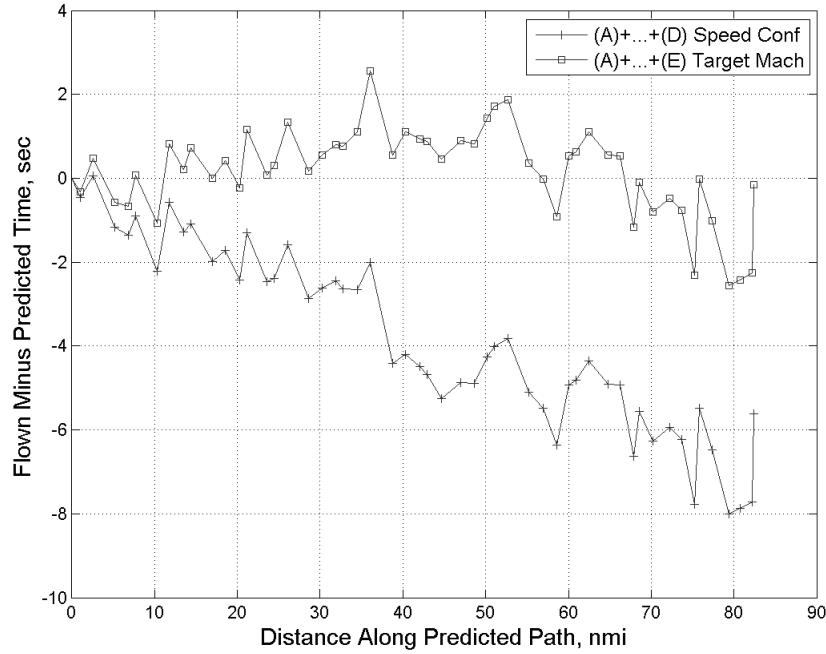


**Figure 49:** Time error for run 1 before ((A)+...+(D) Speed Conf) and after ((A)+...+(E) Target Mach) removing target Mach error source.

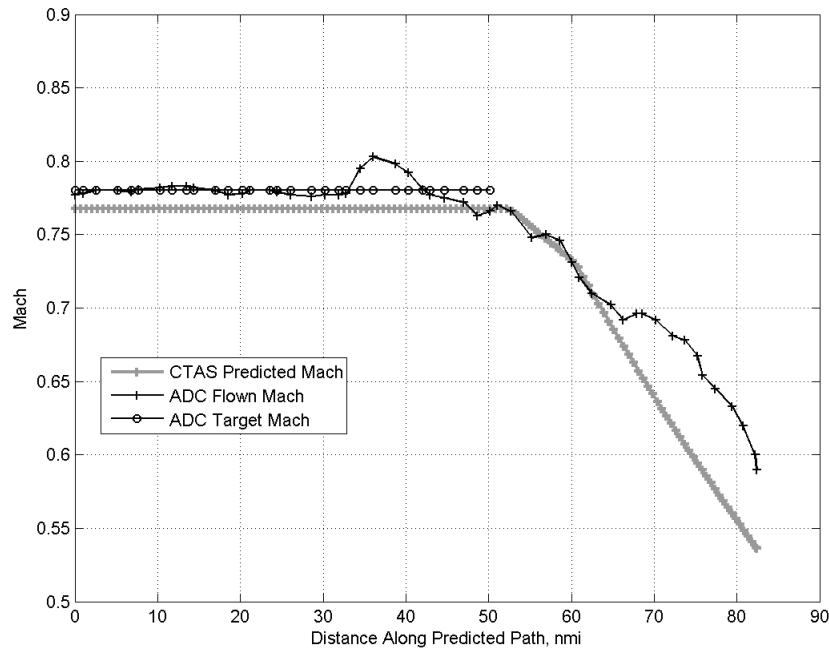


**Figure 50:** CTAS predicted and ADC flown Mach for run 1. Mach being targeted (ADC) shown with circle markers.

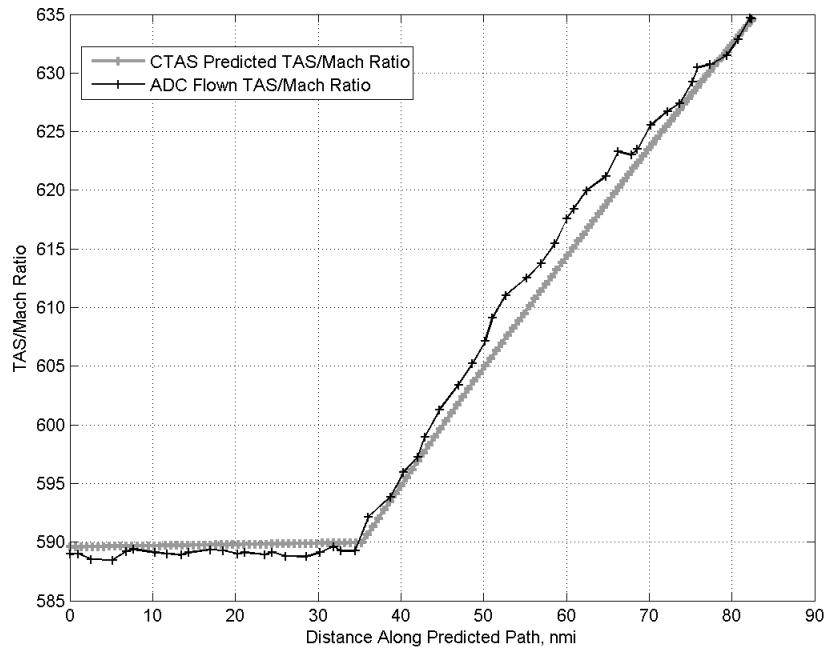


**Figure 51: CTAS predicted and ADC flown TAS/Mach ratio for run 1.**

#### C.2.F. Atmosphere/Altitude

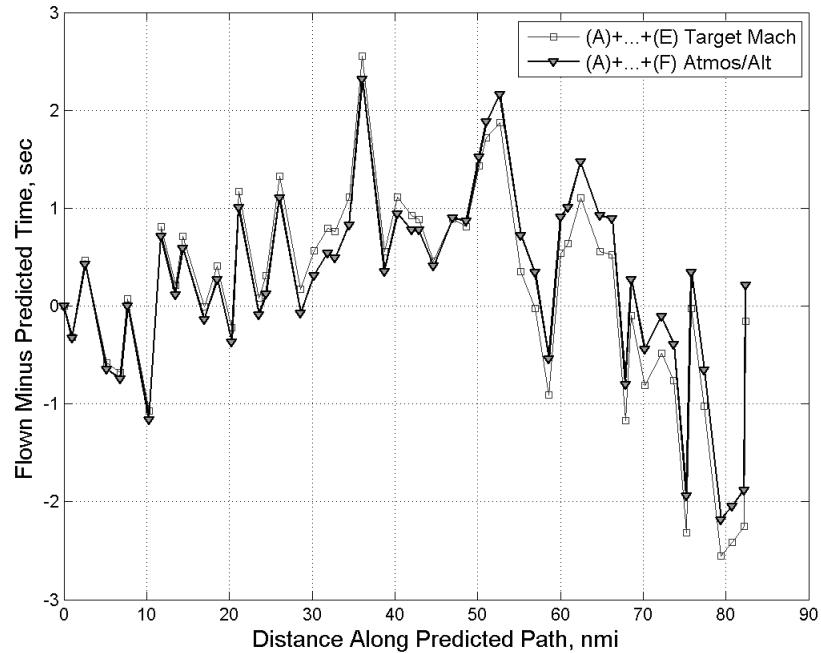


**Figure 52: Time error for run 1 before ((A)+...+(E) Target Mach) and after ((A)+...+(F) Atmos/Alt) removing atmosphere/altitude error source.**

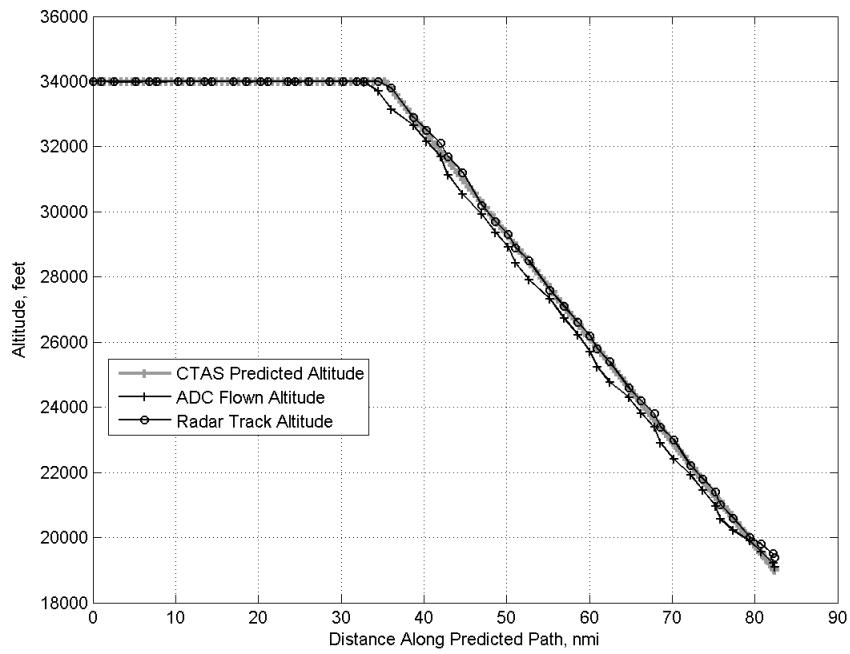


**Figure 53: Flown (ADC) and predicted (CTAS) vertical profile for run 1.**

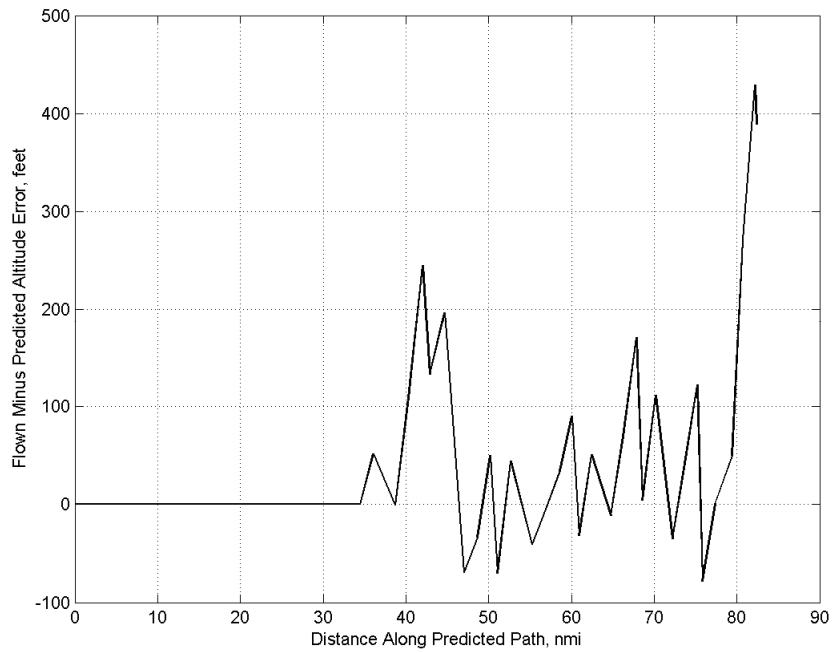


**Figure 54: Vertical error (flown minus predicted altitude) for run 1. Positive values indicate aircraft flew higher than predicted by CTAS.**

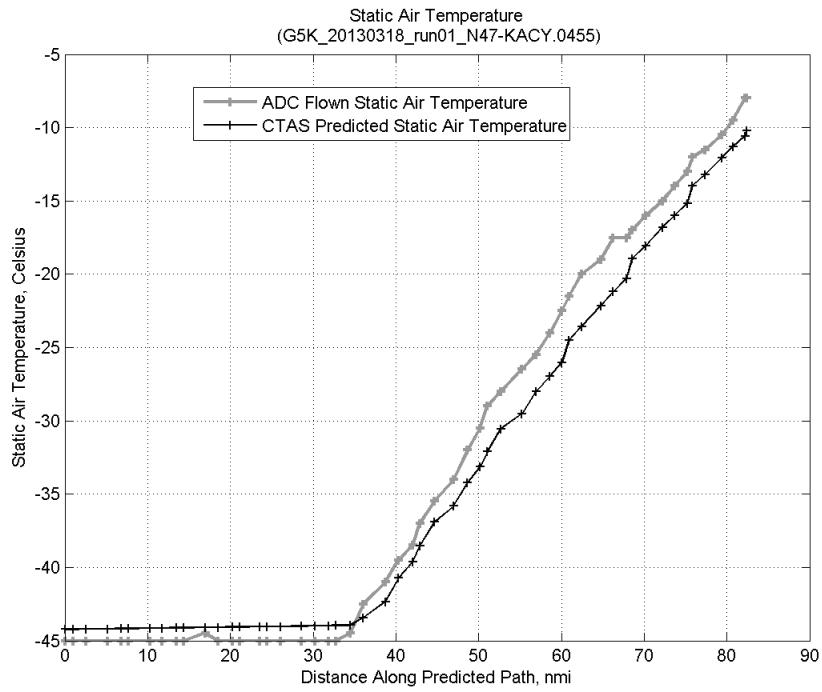


**Figure 55: Flown (ADC) and predicted (CTAS) static air temperature for run 1.**

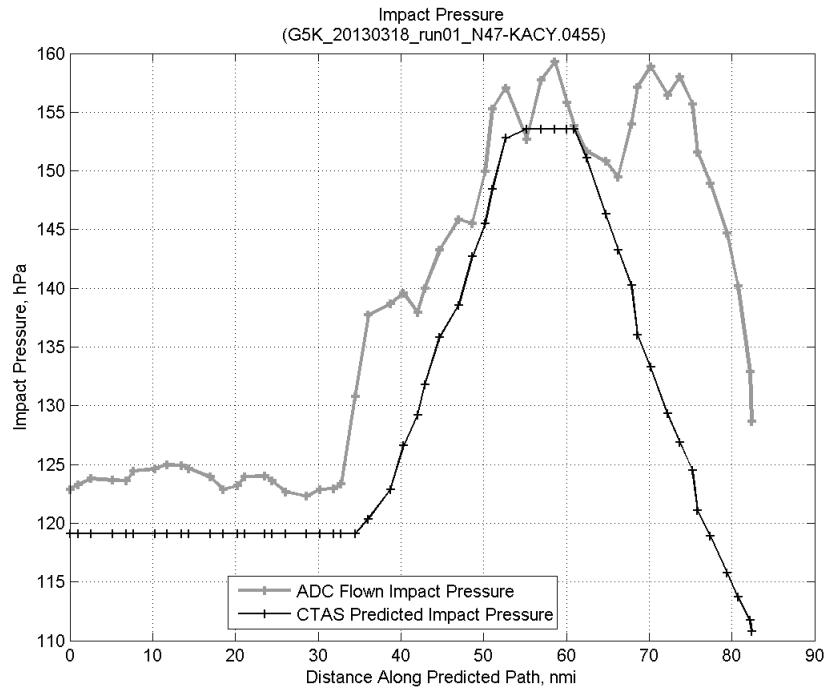


**Figure 56: Flown (ADC) and predicted (CTAS) impact pressure for run 1.**

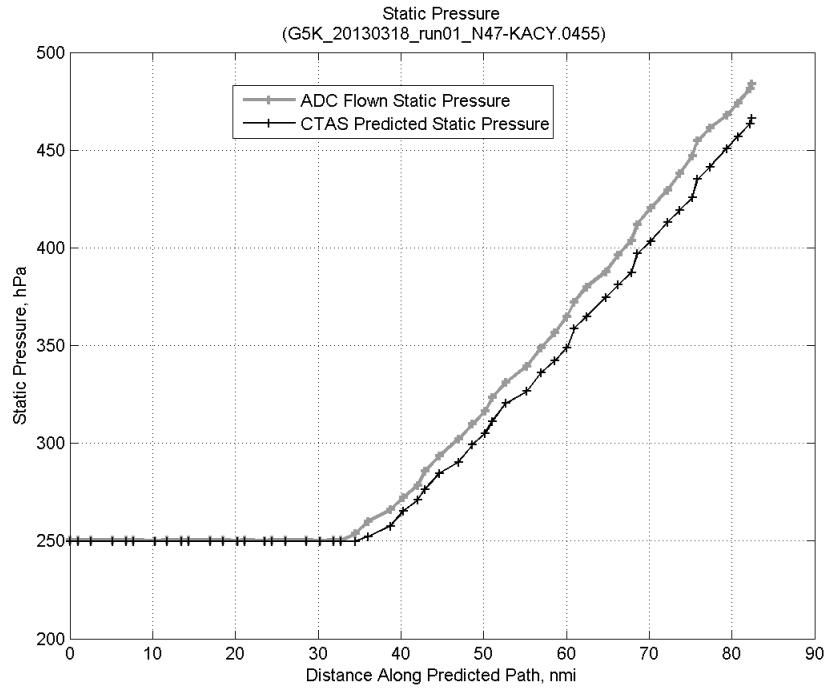


**Figure 57: Flown (ADC) and predicted (CTAS) static pressure for run 1.**

### C.2.G. Path Distance

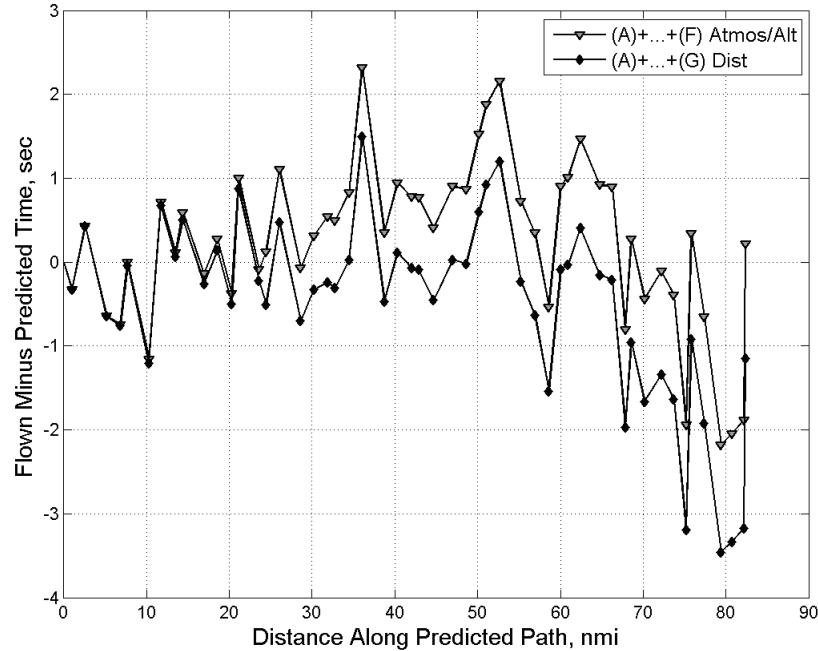


**Figure 58: Time error for run 1 before ((A)+...+(F) Atmos/Alt) and after ((A)+...+(G) Dist) removing path distance error source.**

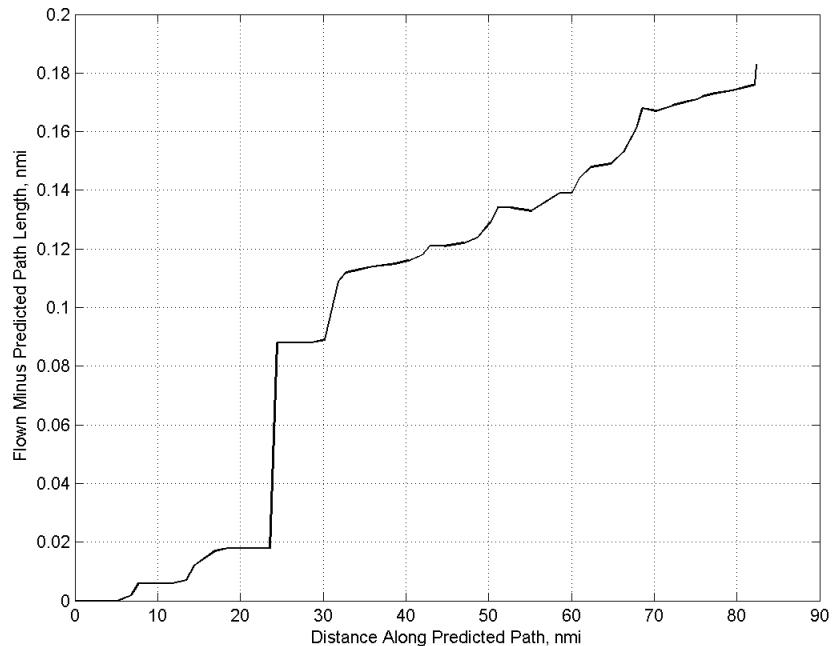


**Figure 59:** ADC flown minus CTAS predicted path length for run 1. Positive values indicate aircraft followed a longer path than predicted by CTAS.

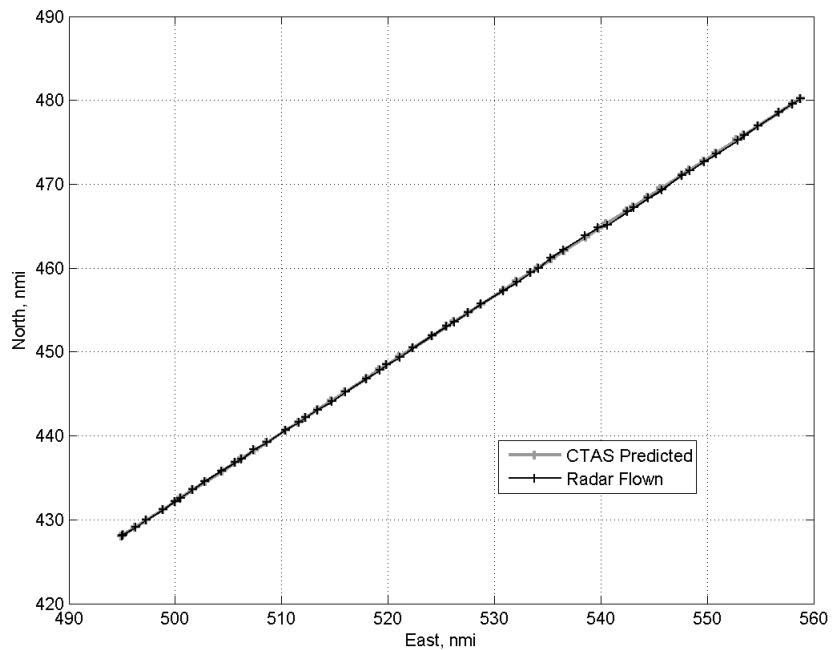


**Figure 60:** CTAS predicted and radar flown ground track profile for run 1.

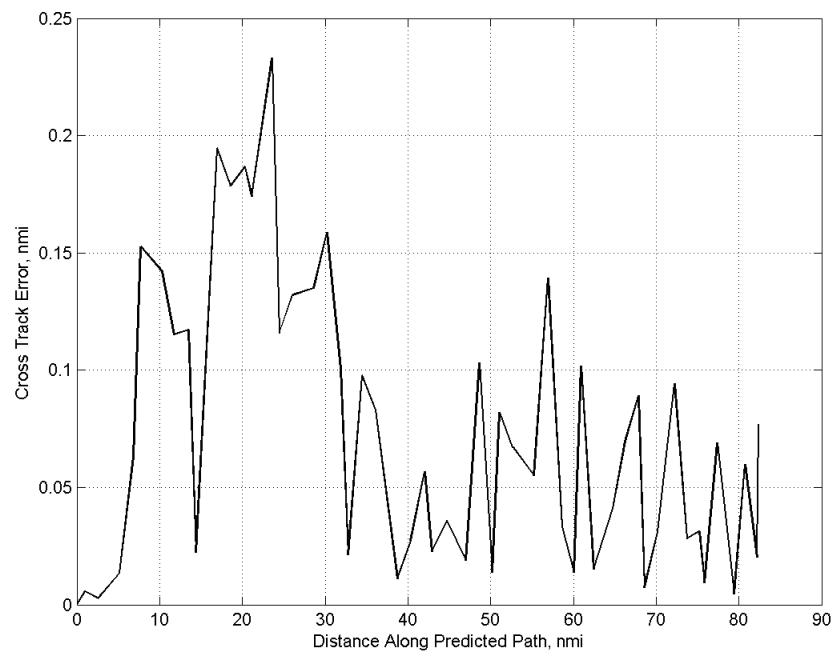


**Figure 61: Ground (cross) track error for run 1.**

### C.3. Run 2

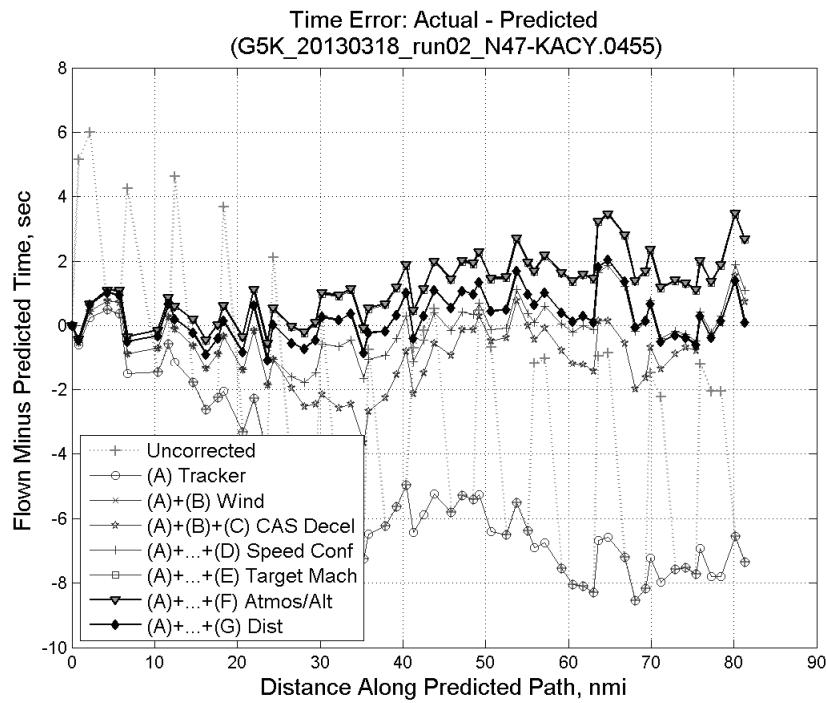


**Figure 62: Time error for run 2 showing incremental effect of removing each error source.**

#### C.3.A. Tracker Jumps

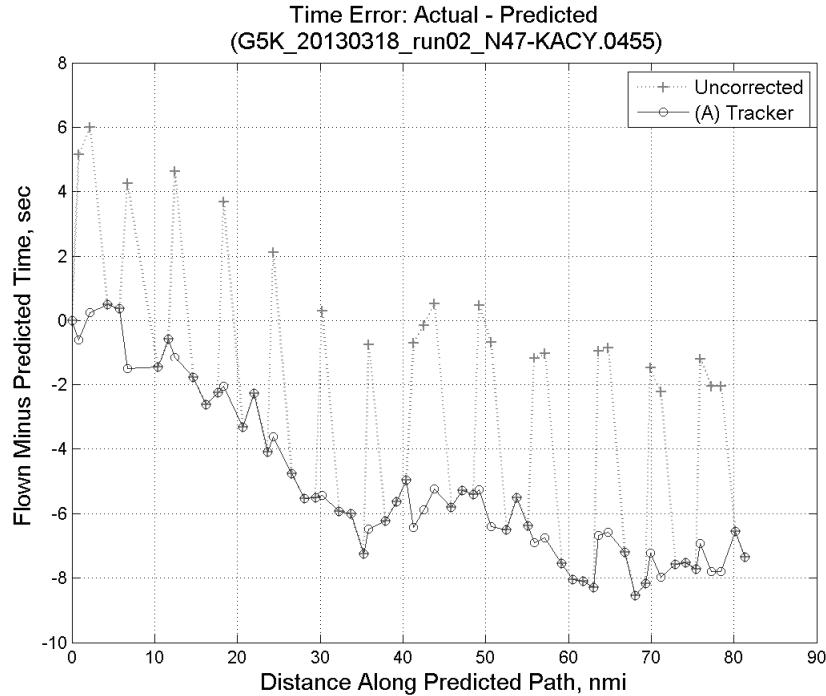


**Figure 63: Time error for run 2 before (Uncorrected) and after ((A) Tracker) removing tracker jump error source.**

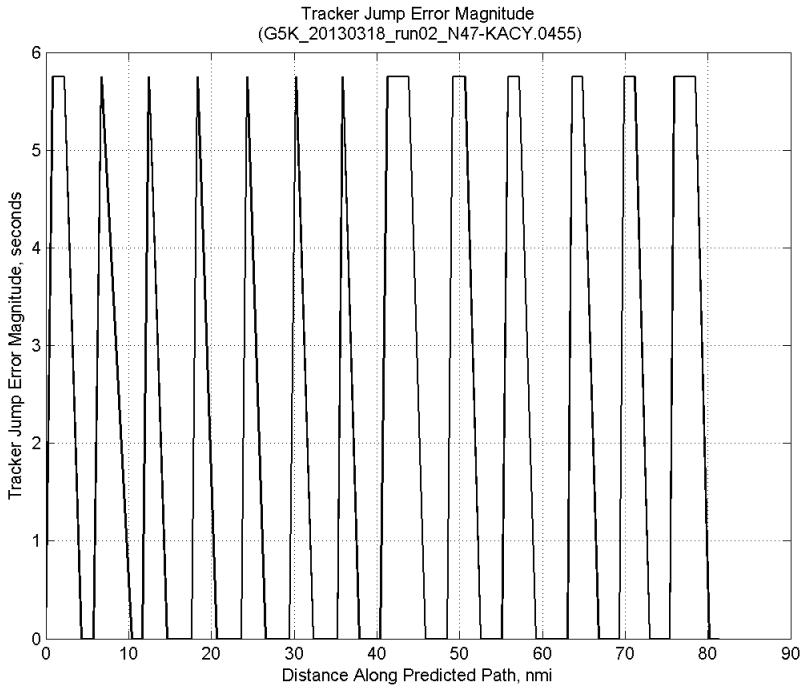


**Figure 64: Effect of tracker jump error source on time error for run 2.**

### C.3.B. Wind

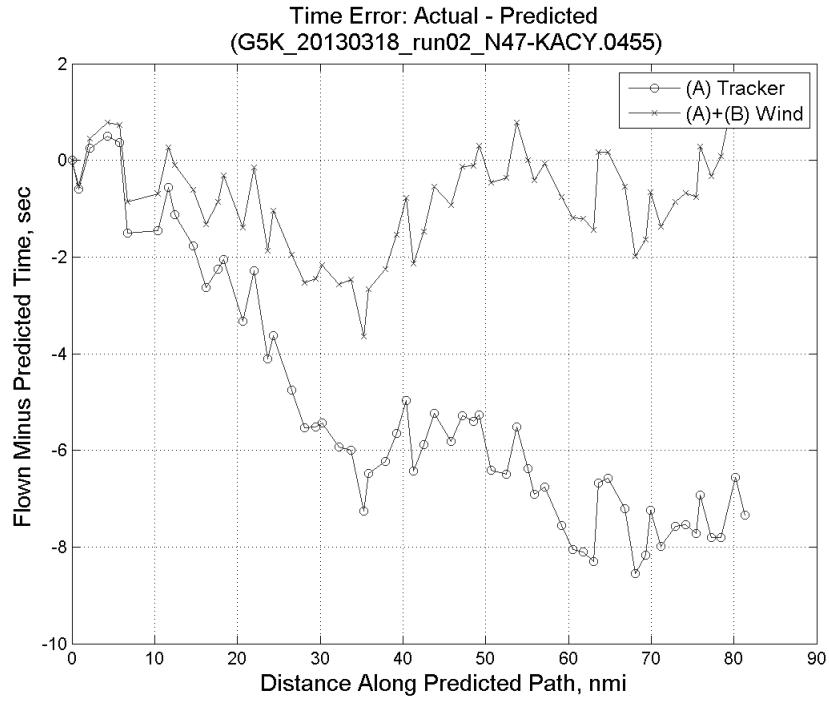


**Figure 65: Time error for run 2 before ((A) Tracker) and after ((A)+(B) Wind) removing wind error source.**

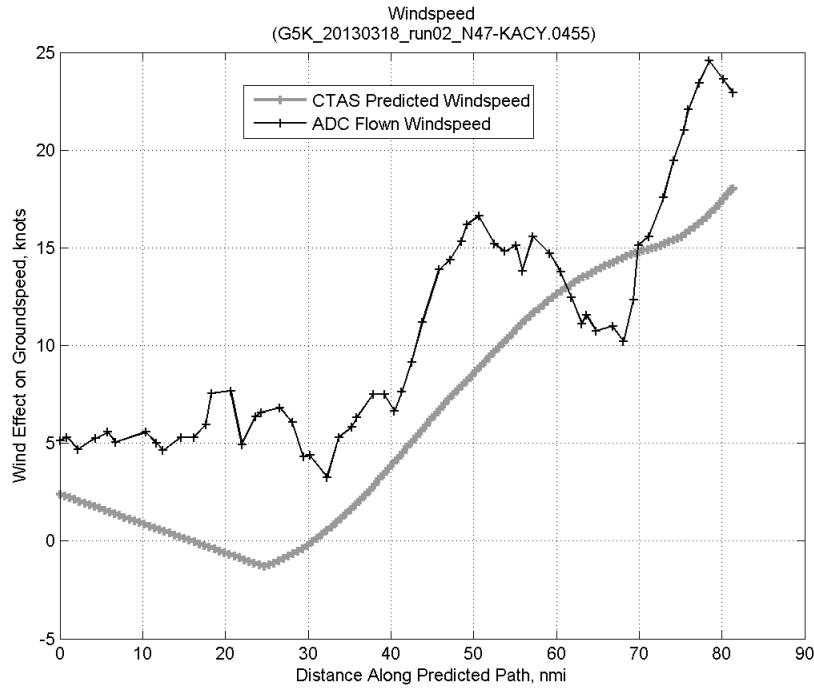


**Figure 66: CTAS predicted and ADC flown wind effect on ground speed for run 2. Negative values indicate a headwind.**

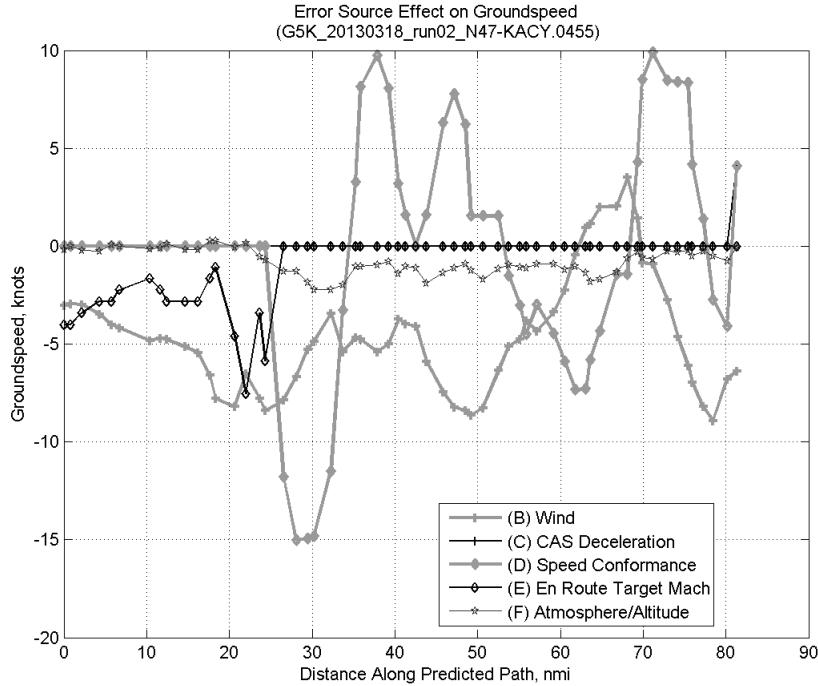


**Figure 67: Error sources (flown minus predicted) converted to a ground speed effect for run 2. Positive values indicate the flown ground speed was faster than the CTAS prediction.**

### C.3.C. CAS Deceleration

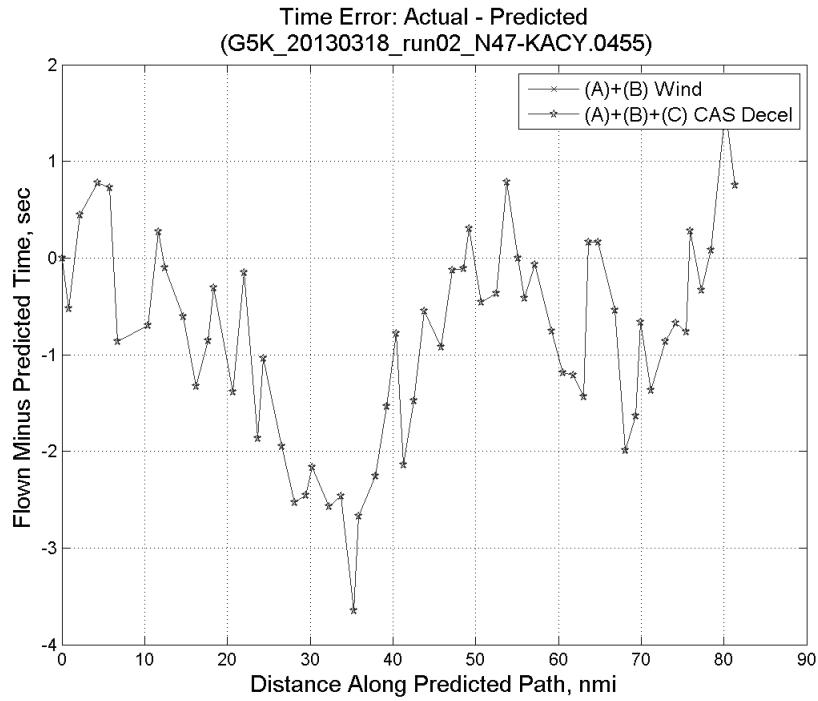


**Figure 68:** Time error for run 2 before ((A)+(B) Wind) and after ((A)+(B)+(C) CAS Decel) removing CAS deceleration error source.

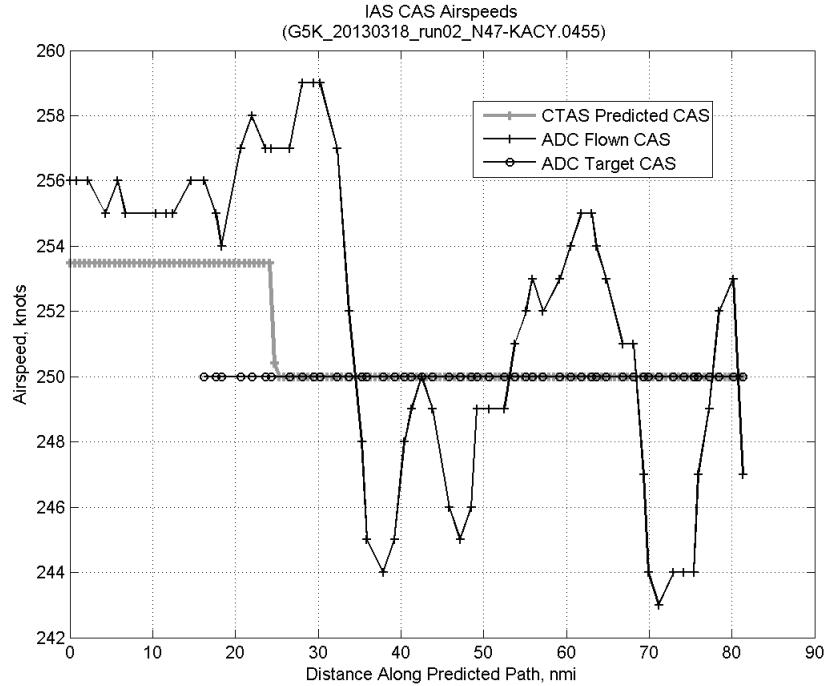


**Figure 69:** CTAS predicted and ADC flown CAS for run 2. CAS that is being targeted is shown with circle markers.

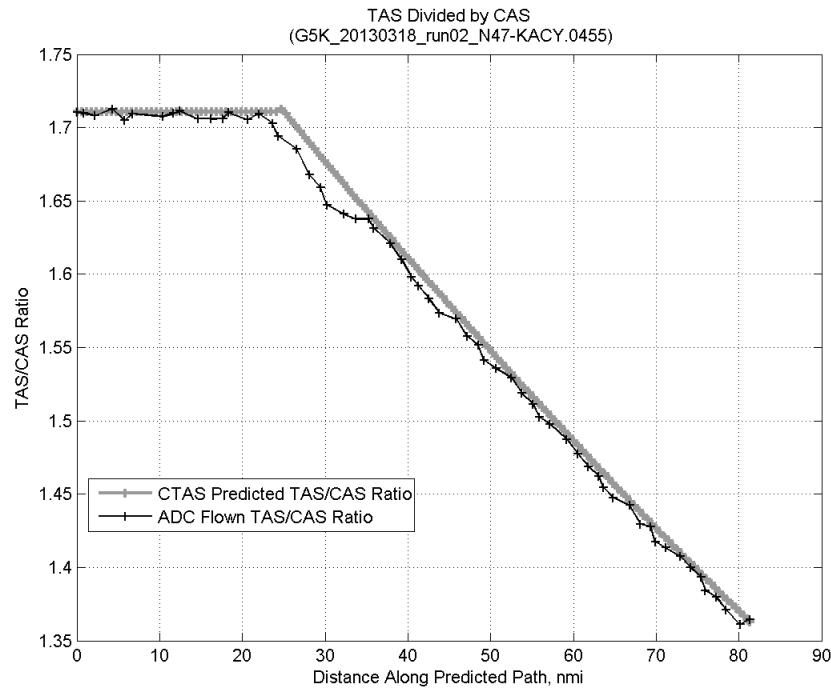


**Figure 70: CTAS predicted and ADC flown TAS/CAS ratio for run 2.**

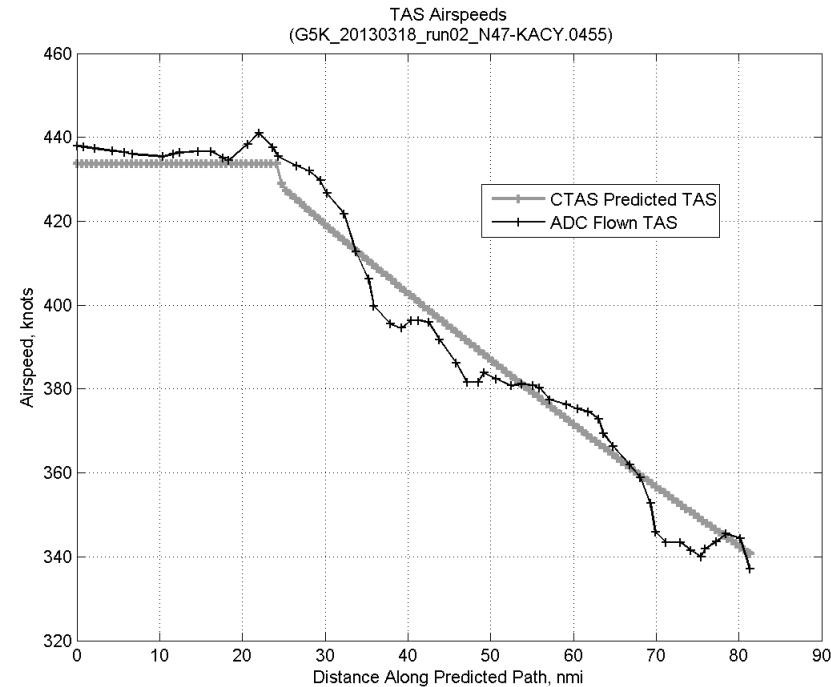


**Figure 71: CTAS predicted and ADC flown TAS for run 2.**

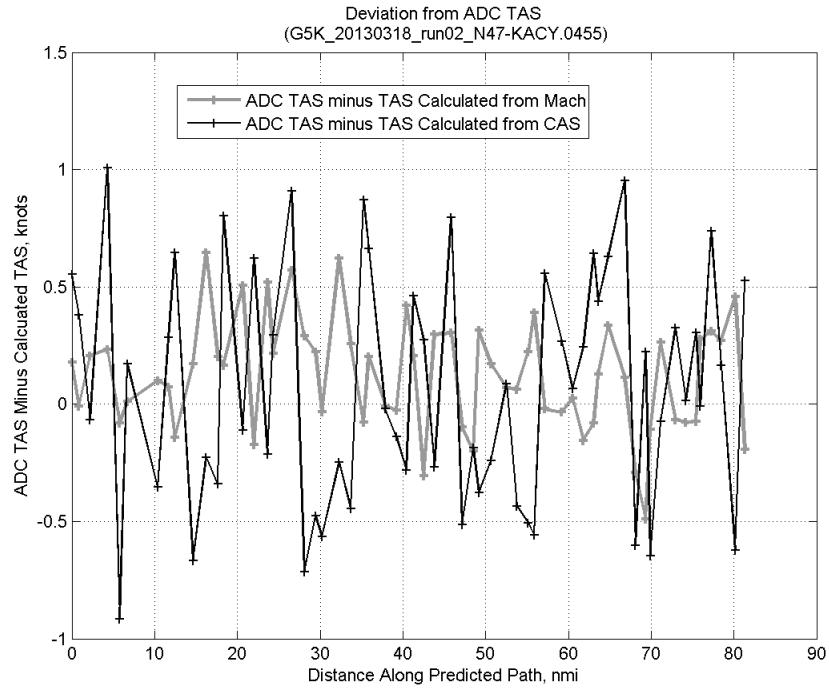


**Figure 72: Deviation from ADC flown TAS if calculating TAS using ADC flown CAS, Mach, atmospheric temperature, and atmospheric pressure for run 2.**

### C.3.D. Speed Conformance

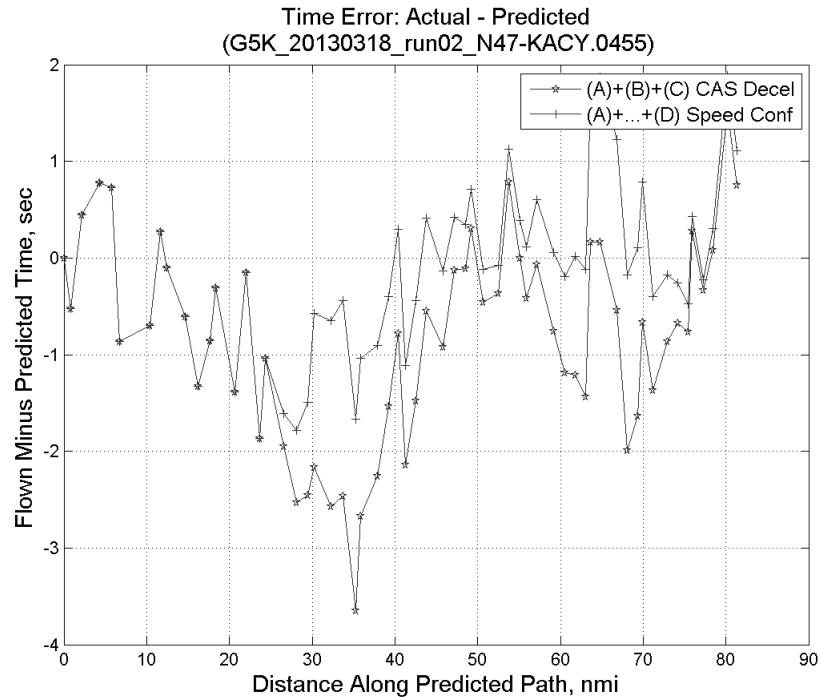


**Figure 73: Time error for run 2 before ((A)+(B)+(C) CAS Decel) and after ((A)+...+(D) Speed Conf) removing speed conformance error source.**

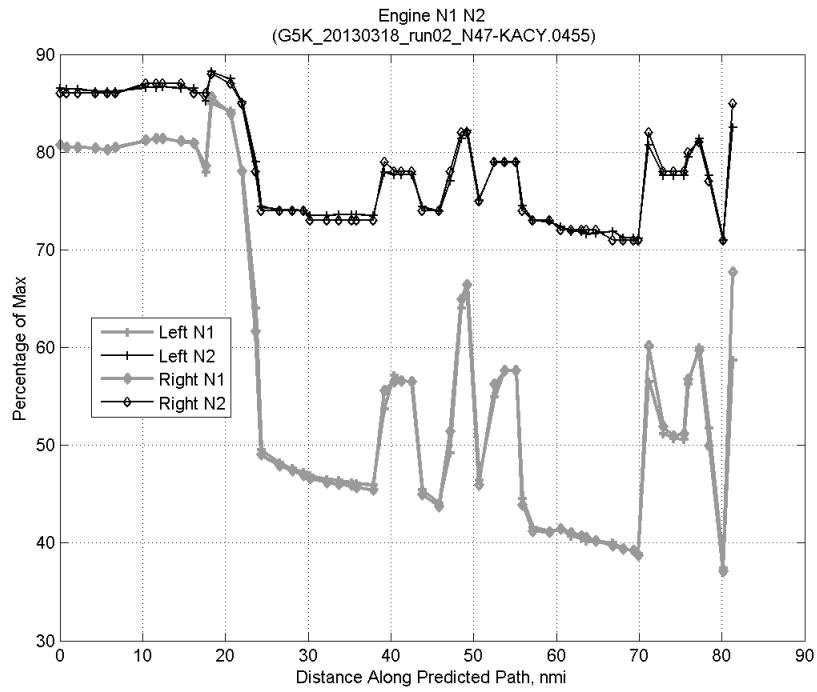


**Figure 74: Flown engine N1 and N2 for run 2.**

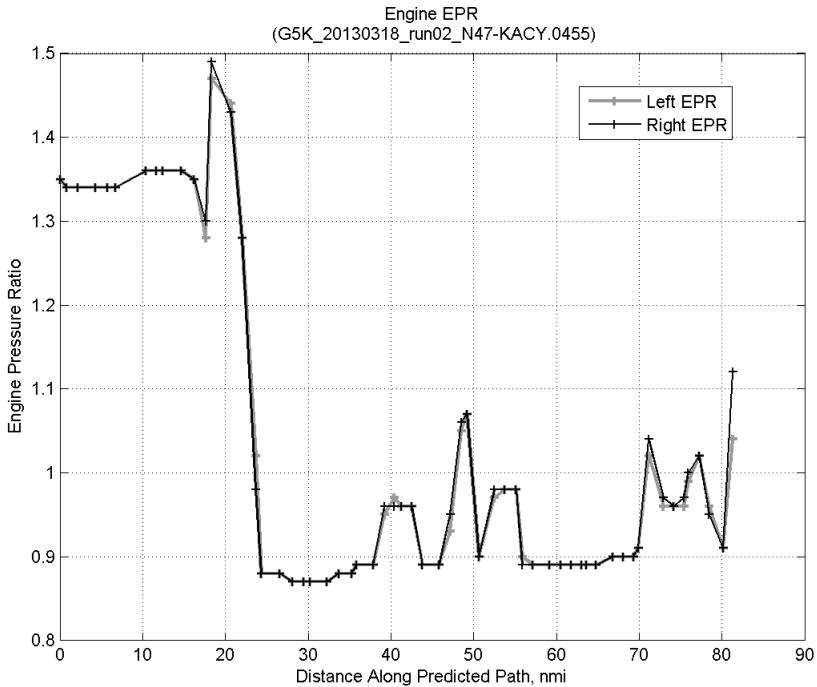


**Figure 75: Flown engine EPR for run 2.**

### C.3.E. Target Mach

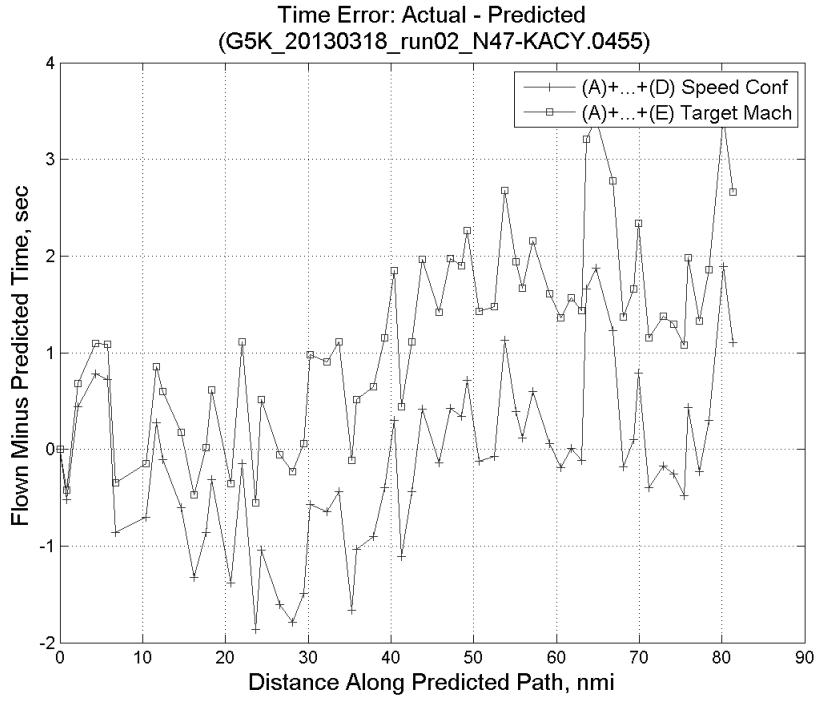


**Figure 76:** Time error for run 2 before ((A)+...+(D) Speed Conf) and after ((A)+...+(E) Target Mach) removing target Mach error source.

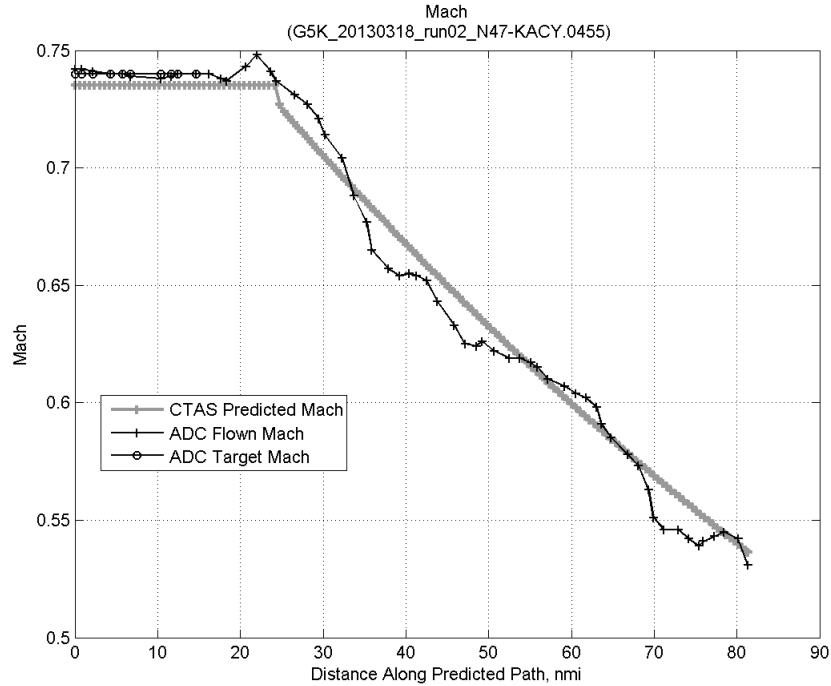


**Figure 77:** CTAS predicted and ADC flown Mach for run 2. Mach being targeted (ADC) shown with circle markers.

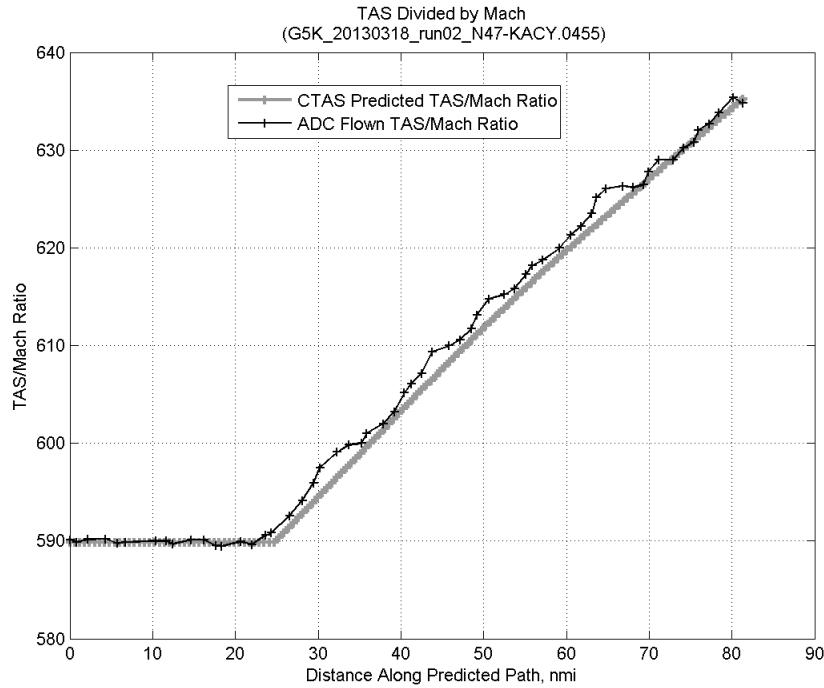


**Figure 78: CTAS predicted and ADC flown TAS/Mach ratio for run 2.**

### C.3.F. Atmosphere/Altitude

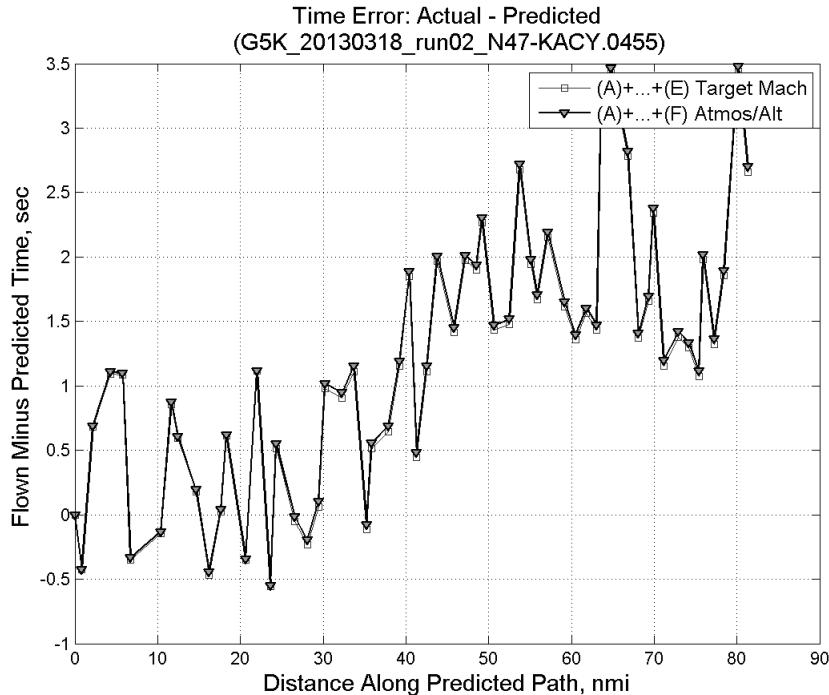


**Figure 79: Time error for run 2 before ((A)+...+(E) Target Mach) and after ((A)+...+(F) Atmos/Alt) removing atmosphere/altitude error source.**

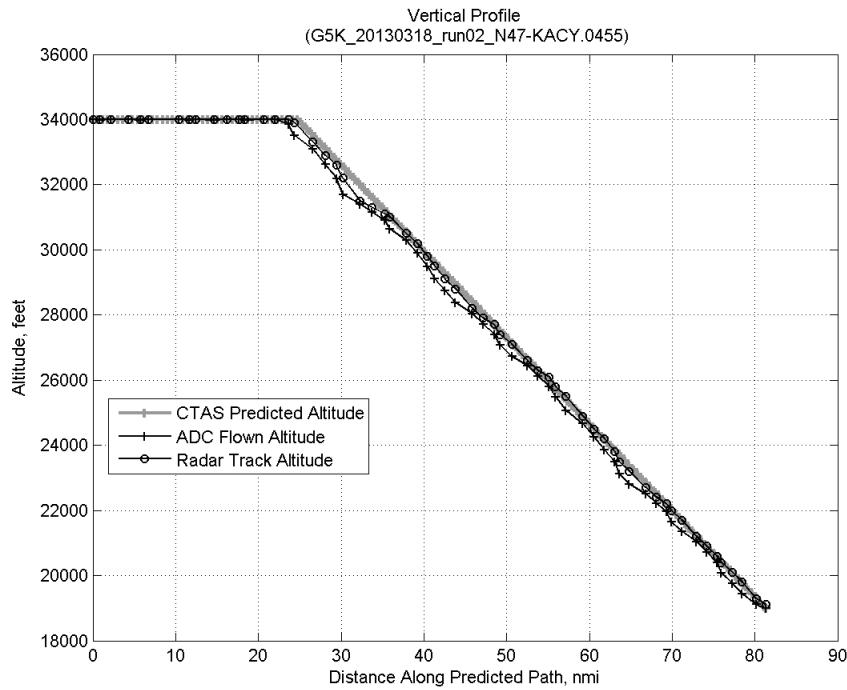


**Figure 80: Flown (ADC) and predicted (CTAS) vertical profile for run 2.**

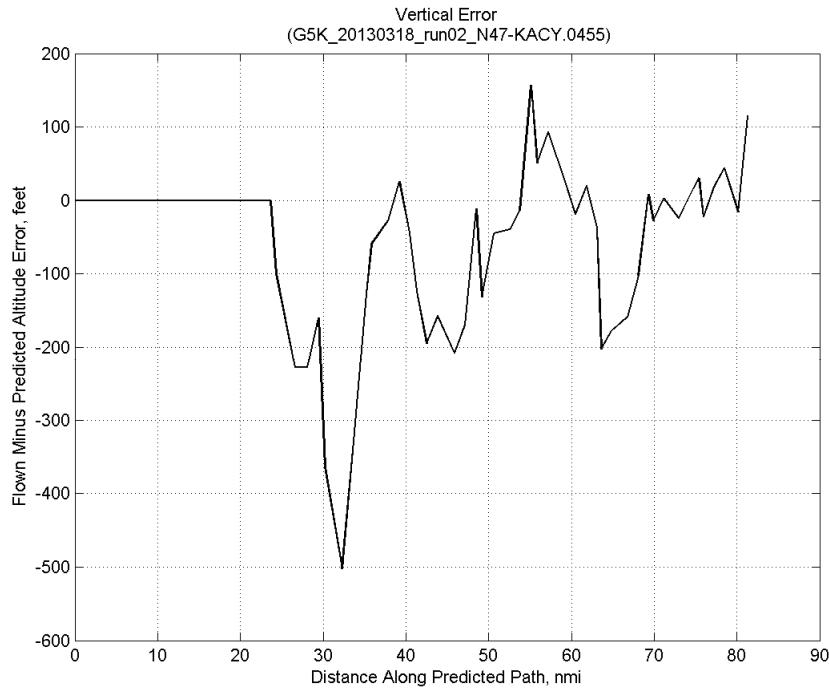


**Figure 81: Vertical error (flown minus predicted altitude) for run 2. Positive values indicate aircraft flew higher than predicted by CTAS.**

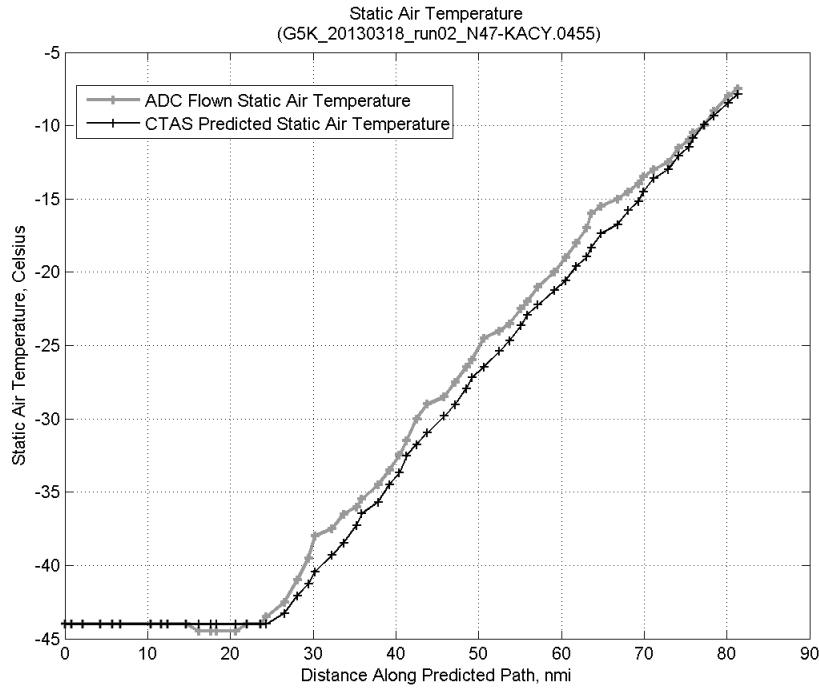


**Figure 82: Flown (ADC) and predicted (CTAS) static air temperature for run 2.**

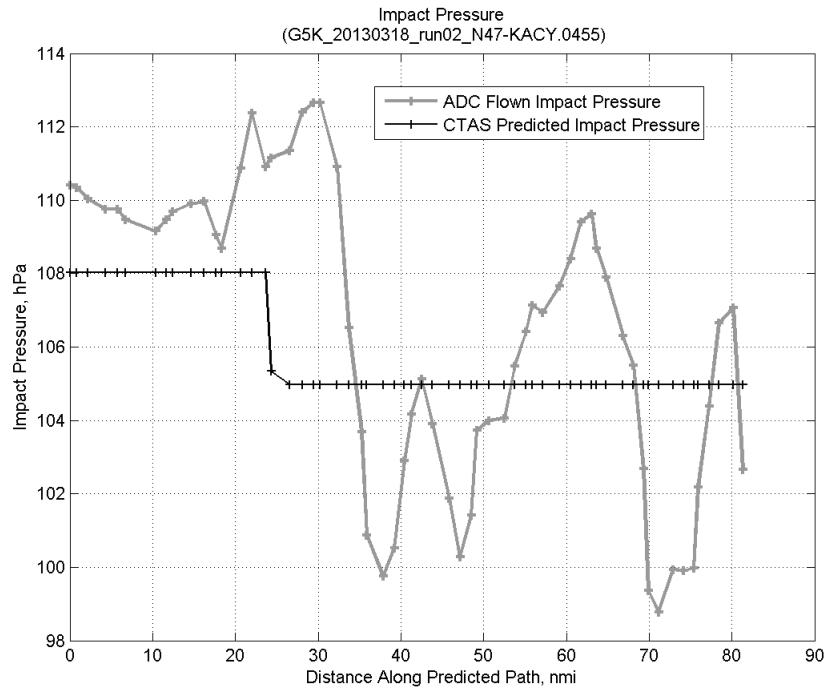


**Figure 83: Flown (ADC) and predicted (CTAS) impact pressure for run 2.**

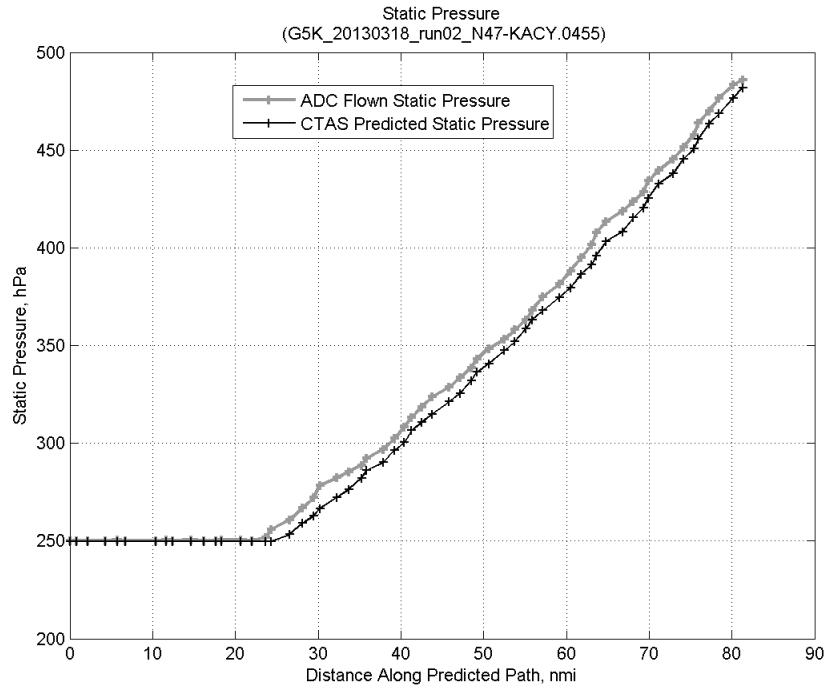


**Figure 84: Flown (ADC) and predicted (CTAS) static pressure for run 2.**

### C.3.G. Path Distance

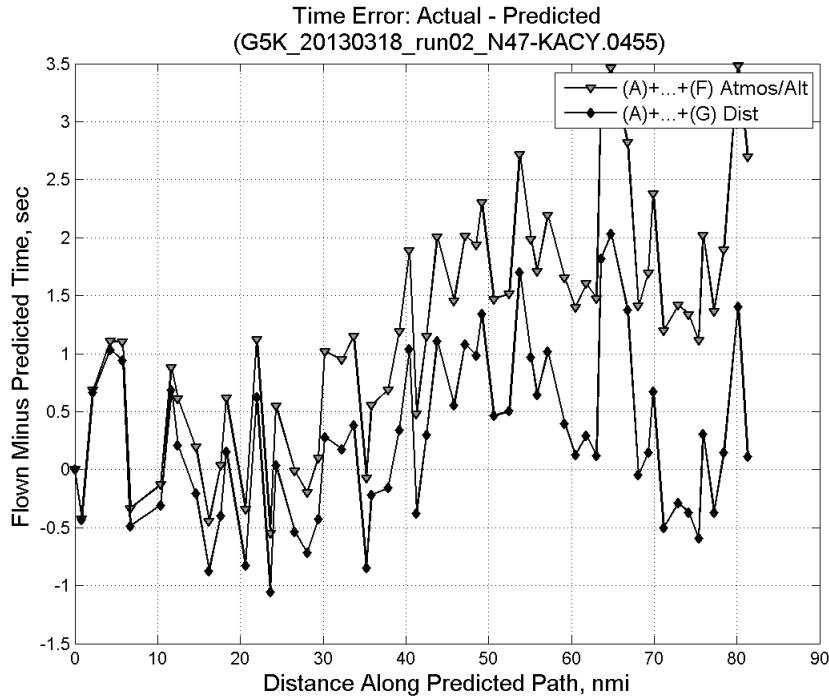


**Figure 85: Time error for run 2 before ((A)+...+(F) Atmos/Alt) and after ((A)+...+(G) Dist) removing path distance error source.**

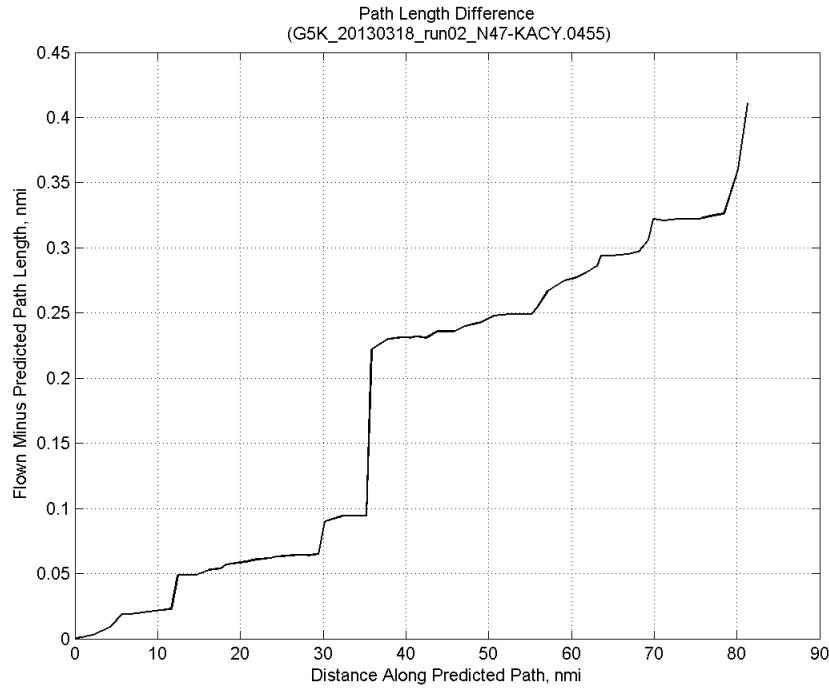


**Figure 86: ADC flown minus CTAS predicted path length for run 2. Positive values indicate aircraft followed a longer path than predicted by CTAS.**

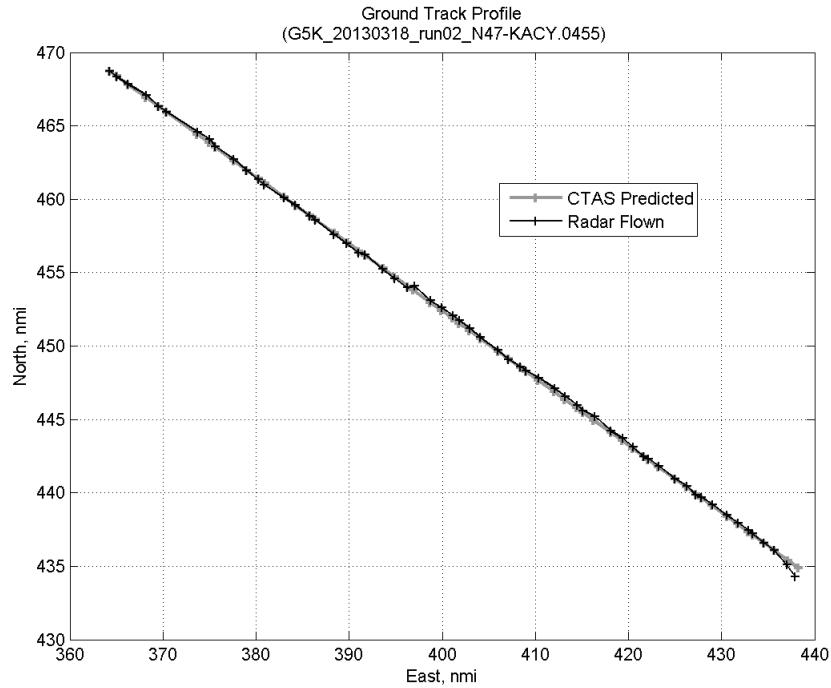


**Figure 87: CTAS predicted and radar flown ground track profile for run 2.**

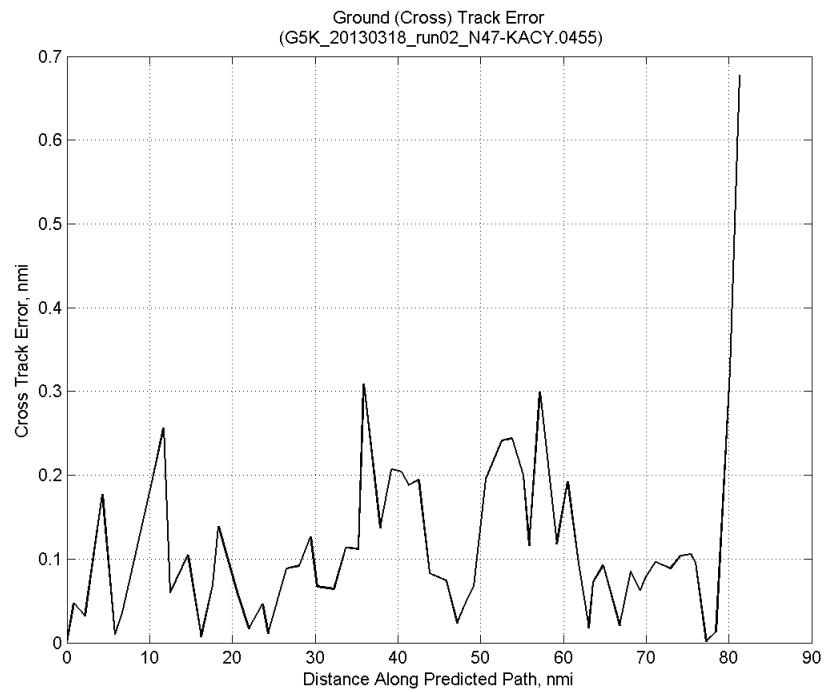


**Figure 88: Ground (cross) track error for run 2.**

#### C.4. Run 3

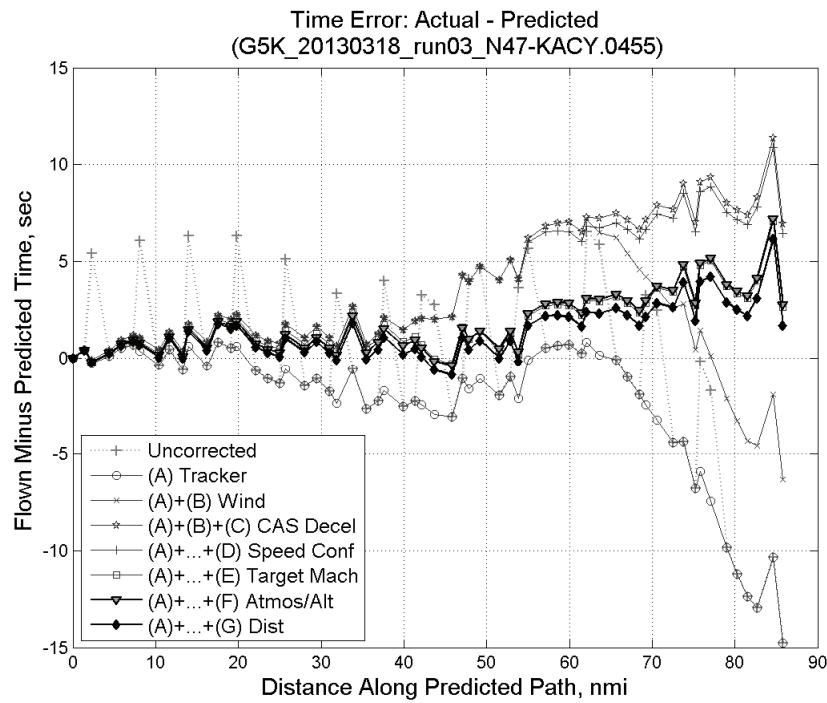


**Figure 89: Time error for run 3 showing incremental effect of removing each error source.**

#### C.4.A. Tracker Jumps

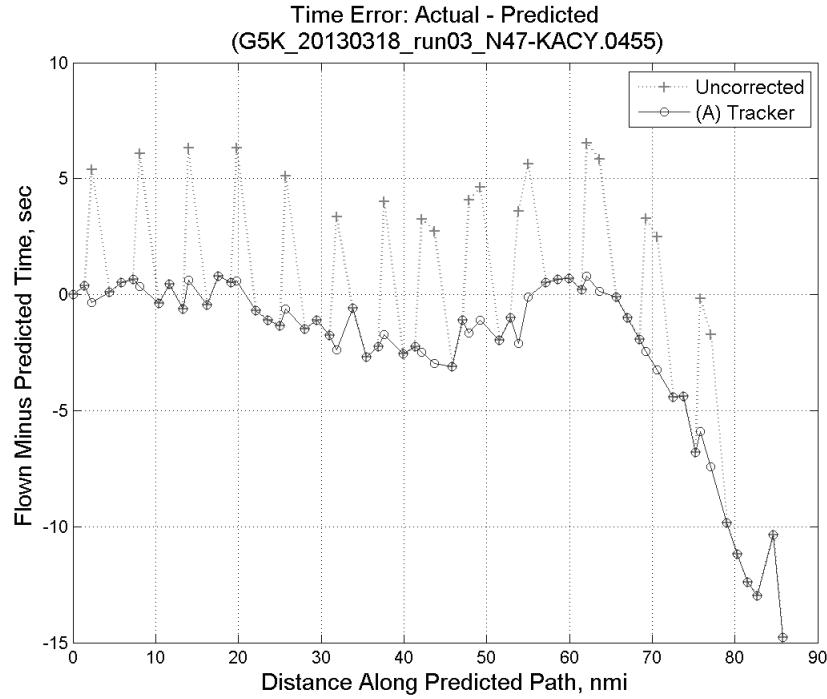


**Figure 90: Time error for run 3 before (Uncorrected) and after ((A) Tracker) removing tracker jump error source.**

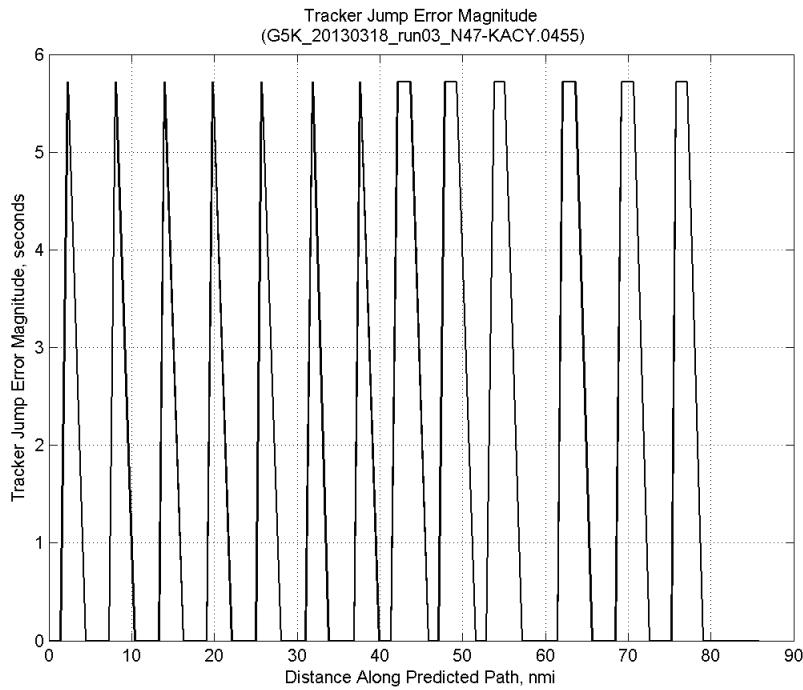


**Figure 91: Effect of tracker jump error source on time error for run 3.**

#### C.4.B. Wind

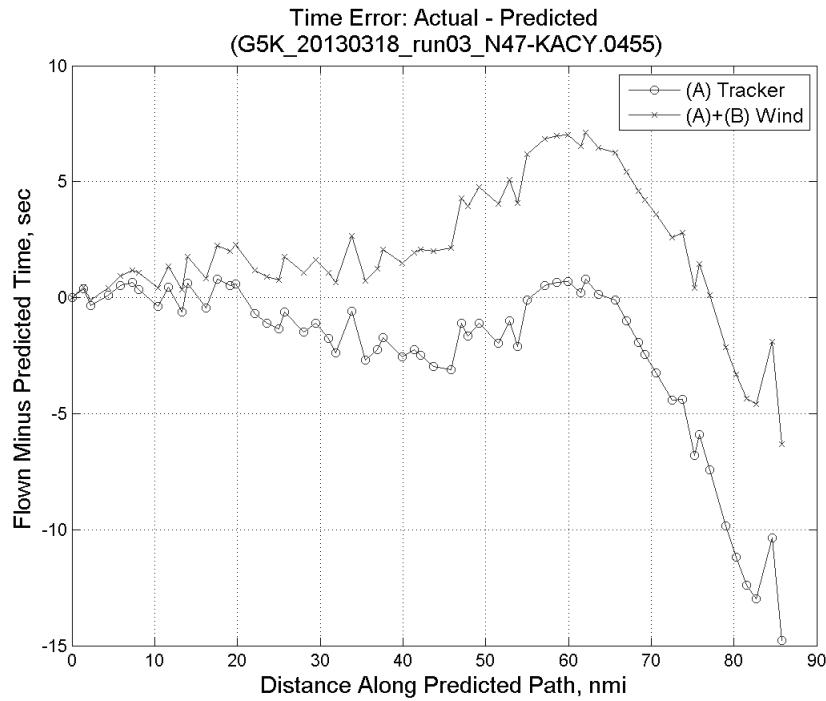


**Figure 92: Time error for run 3 before ((A) Tracker) and after ((A)+(B) Wind) removing wind error source.**

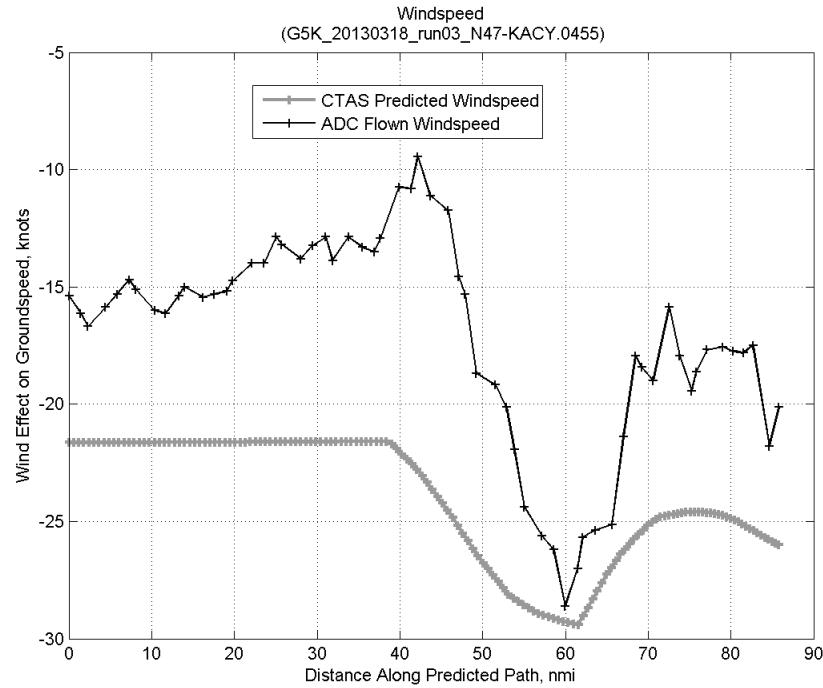


**Figure 93: CTAS predicted and ADC flown wind effect on ground speed for run 3. Negative values indicate a headwind.**

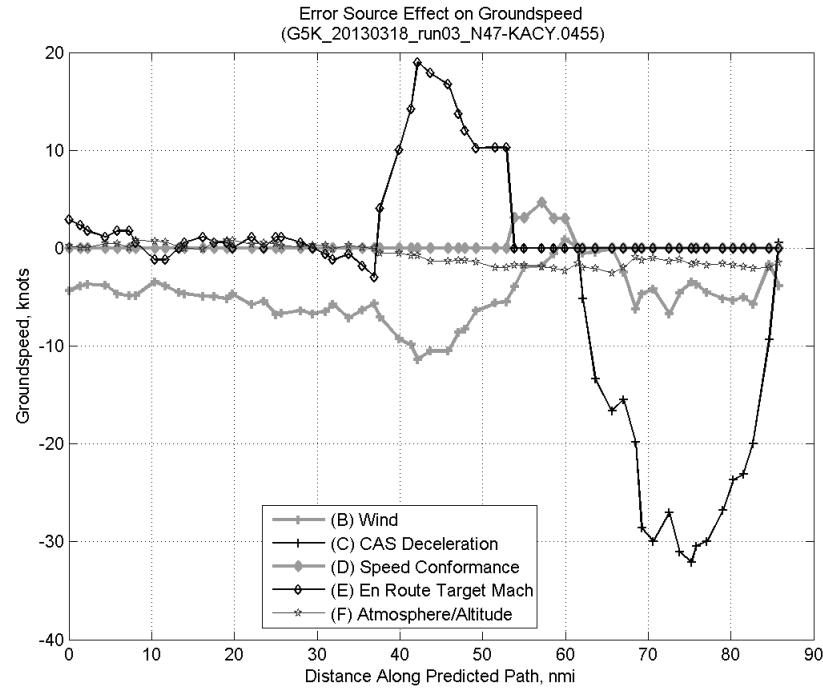


**Figure 94: Error sources (flown minus predicted) converted to a ground speed effect for run 3. Positive values indicate the flown ground speed was faster than the CTAS prediction.**

### C.4.C. CAS Deceleration

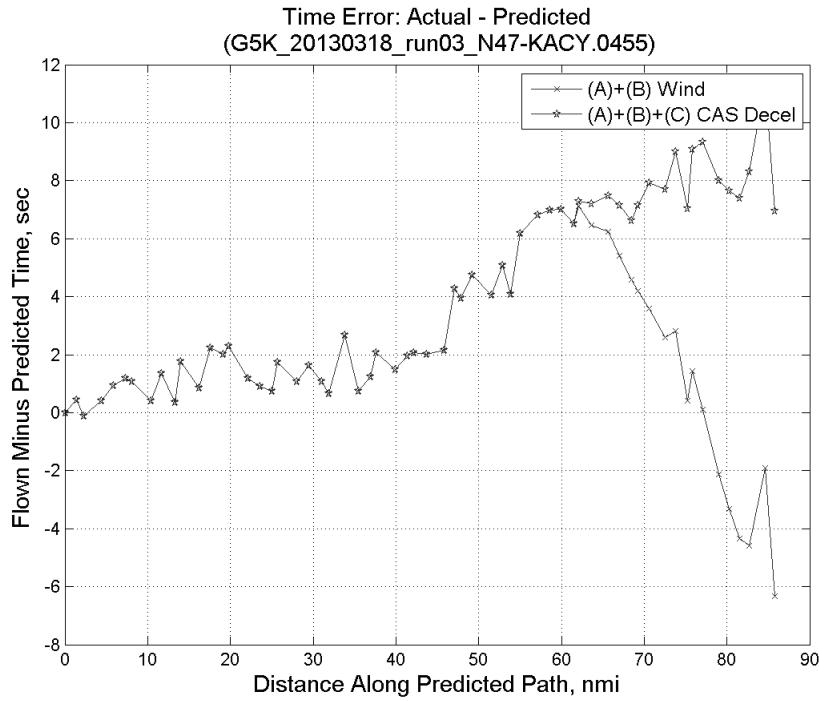


**Figure 95:** Time error for run 3 before ((A)+(B) Wind) and after ((A)+(B)+(C) CAS Decel) removing CAS deceleration error source.

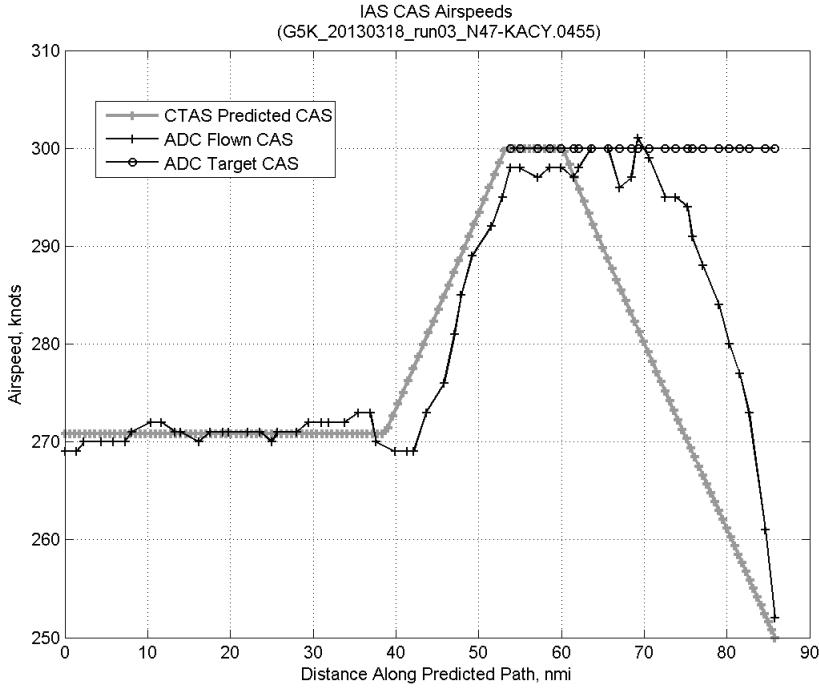


**Figure 96:** CTAS predicted and ADC flown CAS for run 3. CAS that is being targeted is shown with circle markers.

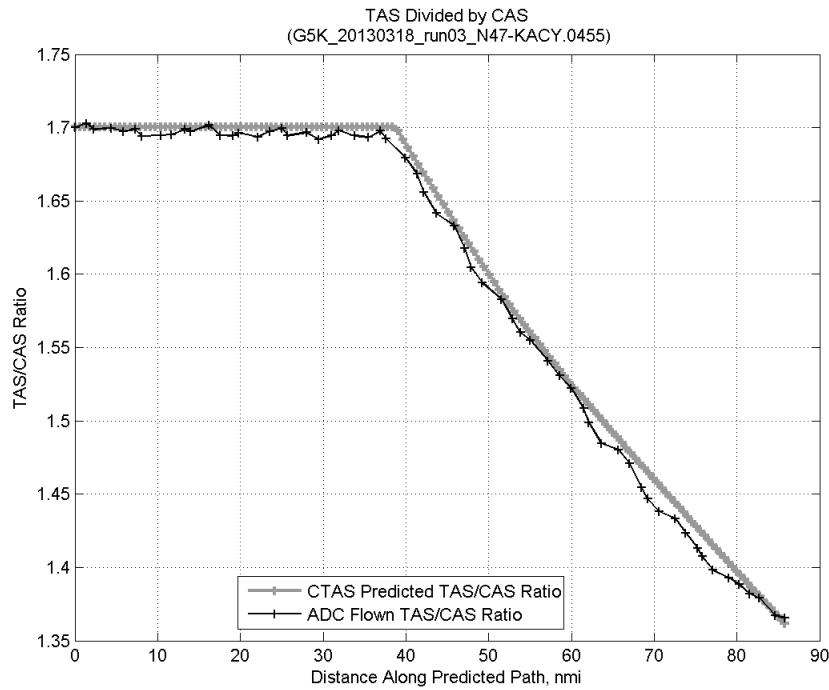


**Figure 97: CTAS predicted and ADC flown TAS/CAS ratio for run 3.**

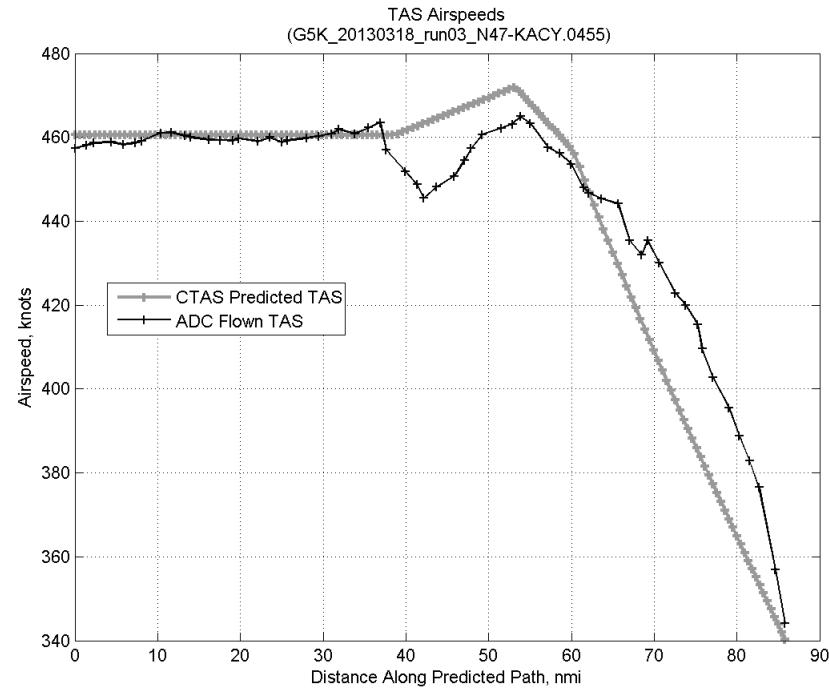


**Figure 98: CTAS predicted and ADC flown TAS for run 3.**

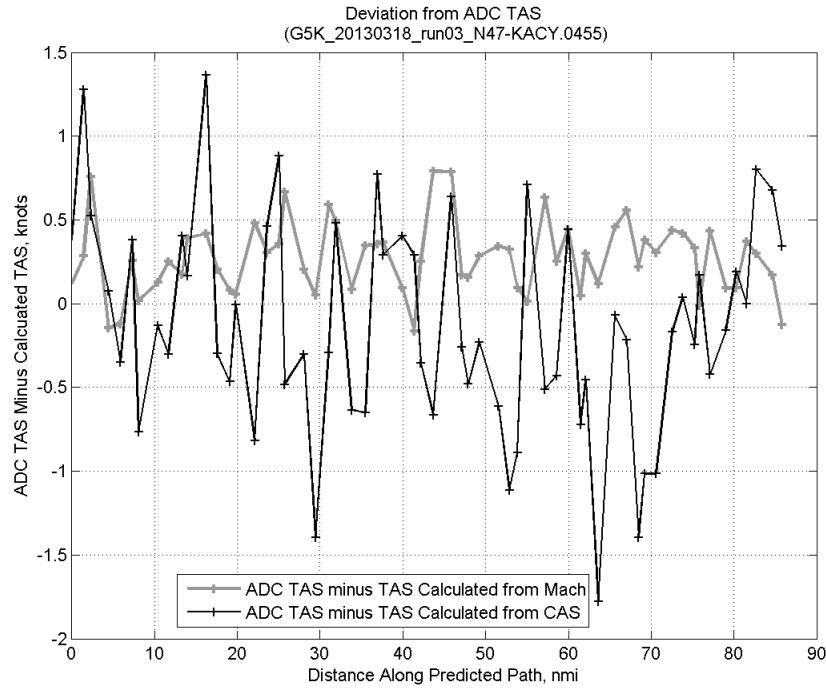


**Figure 99:** Deviation from ADC flown TAS if calculating TAS using ADC flown CAS, Mach, atmospheric temperature, and atmospheric pressure for run 3.

#### C.4.D. Speed Conformance

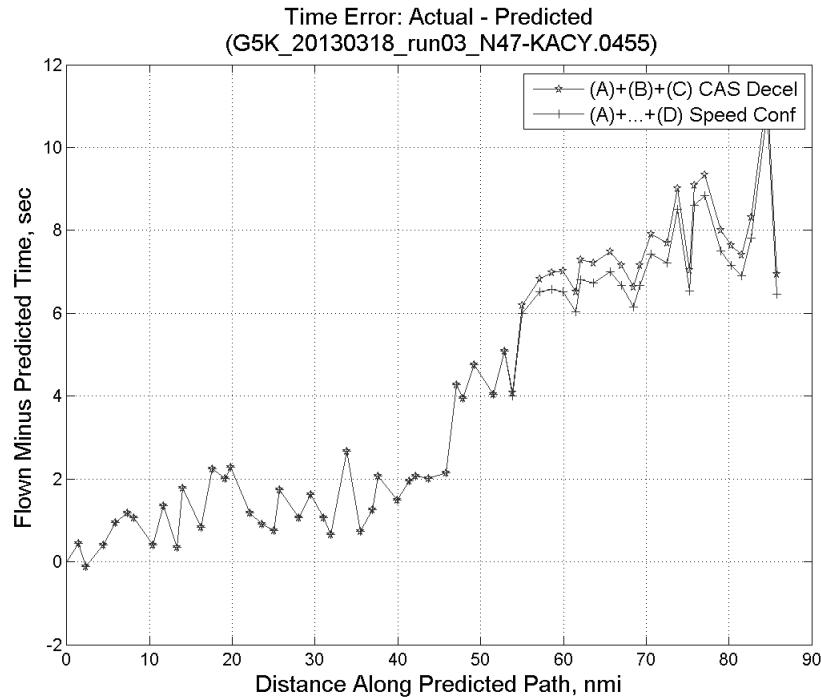


**Figure 100:** Time error for run 3 before ((A)+(B)+(C) CAS Decel) and after ((A)+...+(D) Speed Conf) removing speed conformance error source.

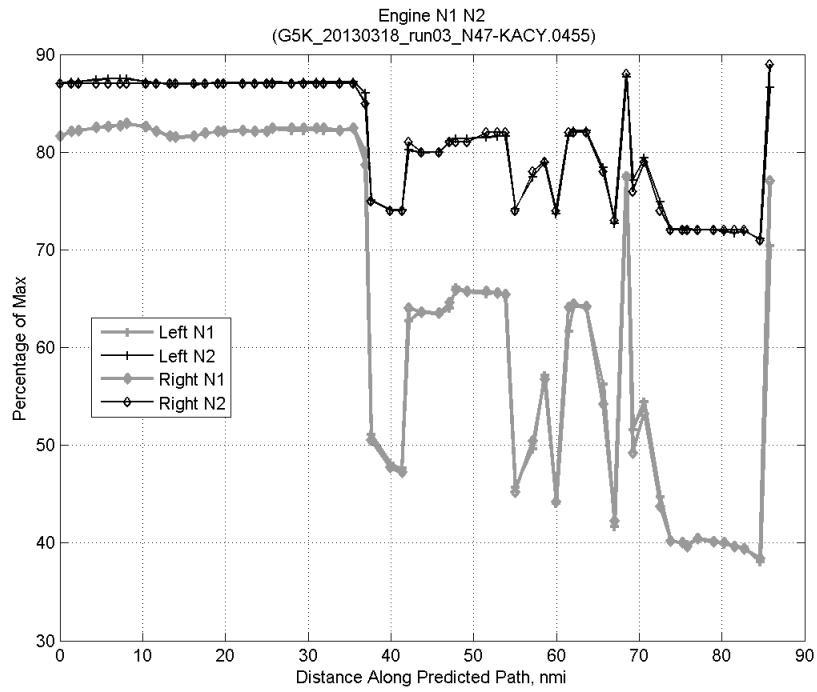


**Figure 101: Flown engine N1 and N2 for run 3.**

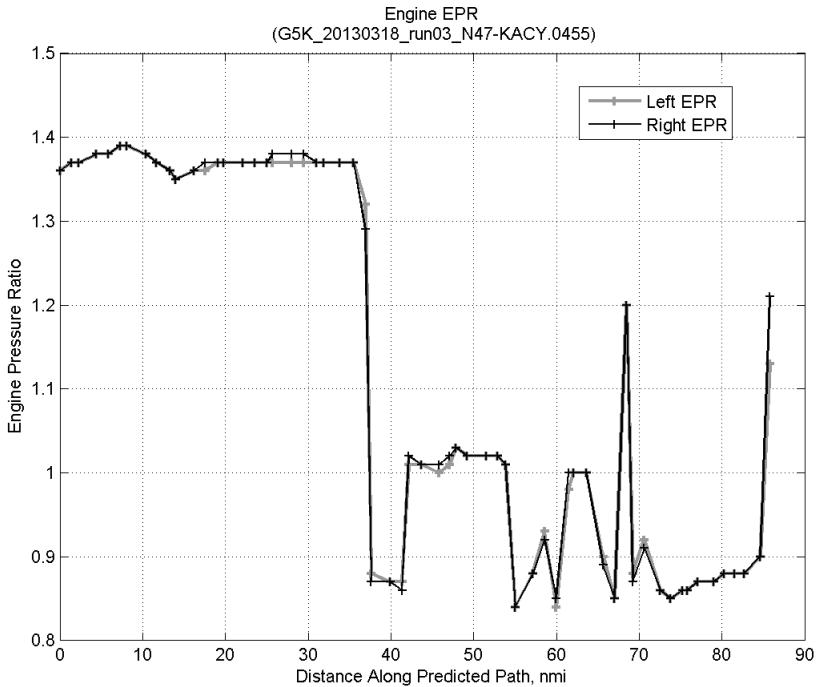


**Figure 102: Flown engine EPR for run 3.**

#### C.4.E. Target Mach

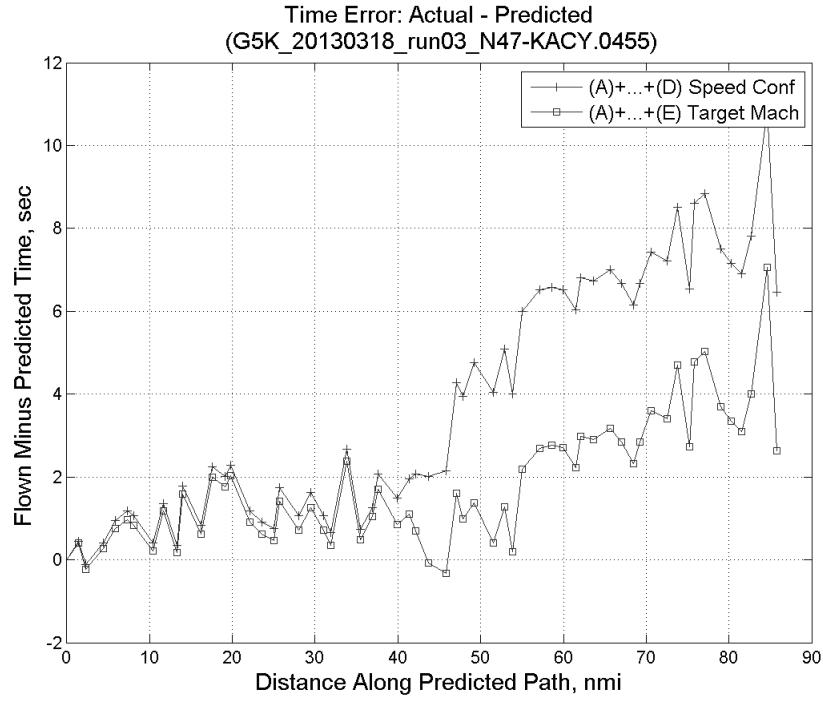


**Figure 103:** Time error for run 3 before ((A)+...+(D) Speed Conf) and after ((A)+...+(E) Target Mach) removing target Mach error source.

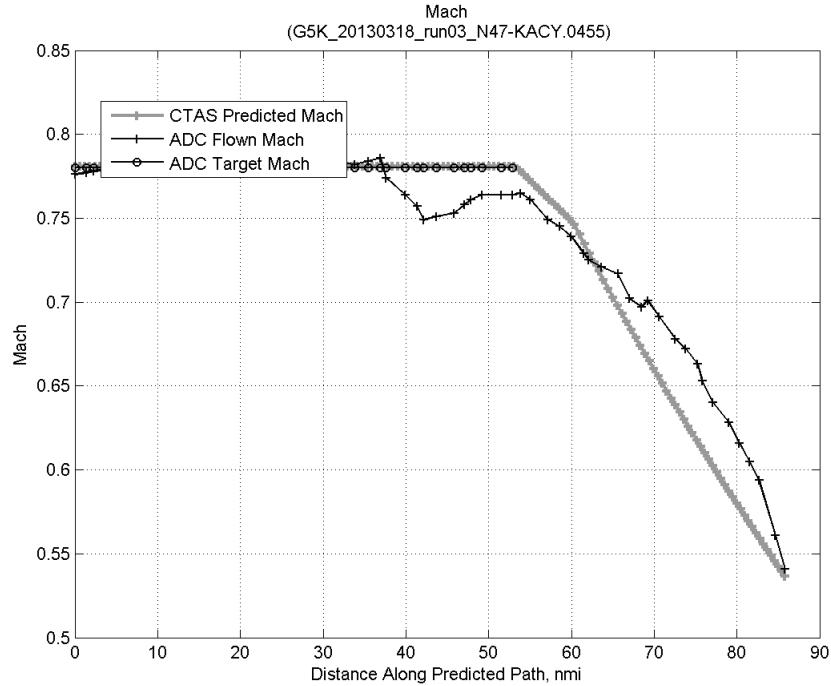


**Figure 104:** CTAS predicted and ADC flown Mach for run 3. Mach being targeted (ADC) shown with circle markers.

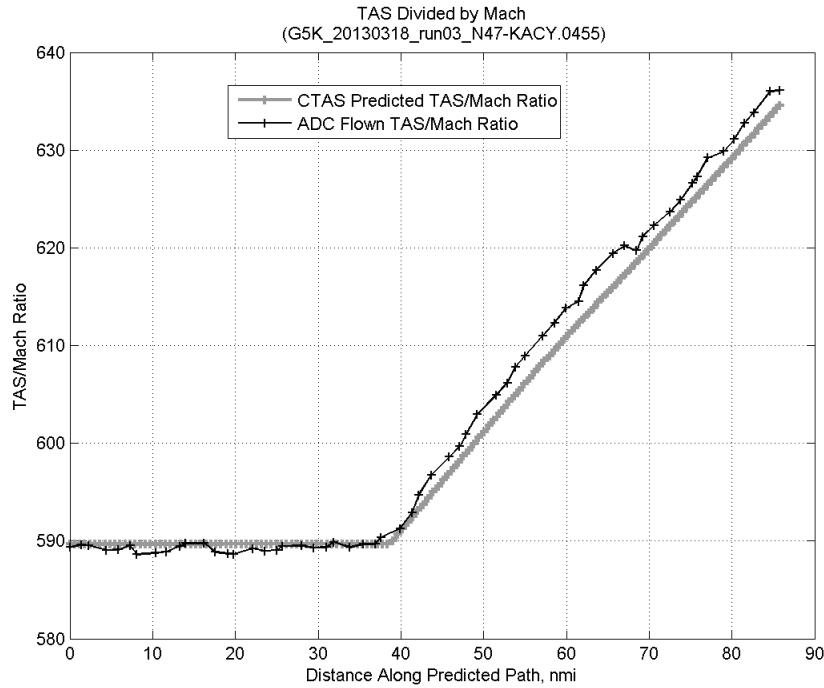


**Figure 105: CTAS predicted and ADC flown TAS/Mach ratio for run 3.**

#### C.4.F. Atmosphere/Altitude

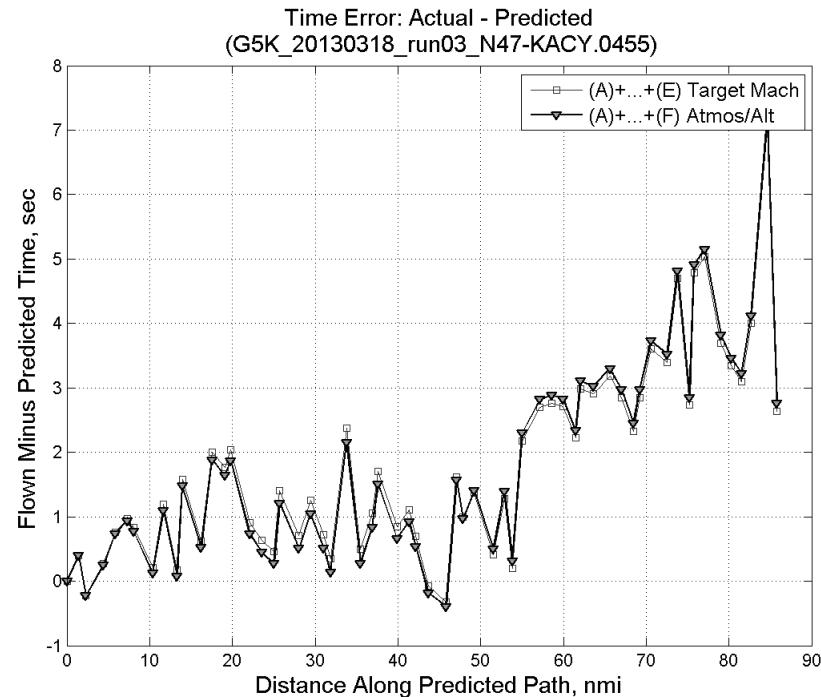


**Figure 106: Time error for run 3 before ((A)+...+(E) Target Mach) and after ((A)+...+(F) Atmos/Alt) removing atmosphere/altitude error source.**

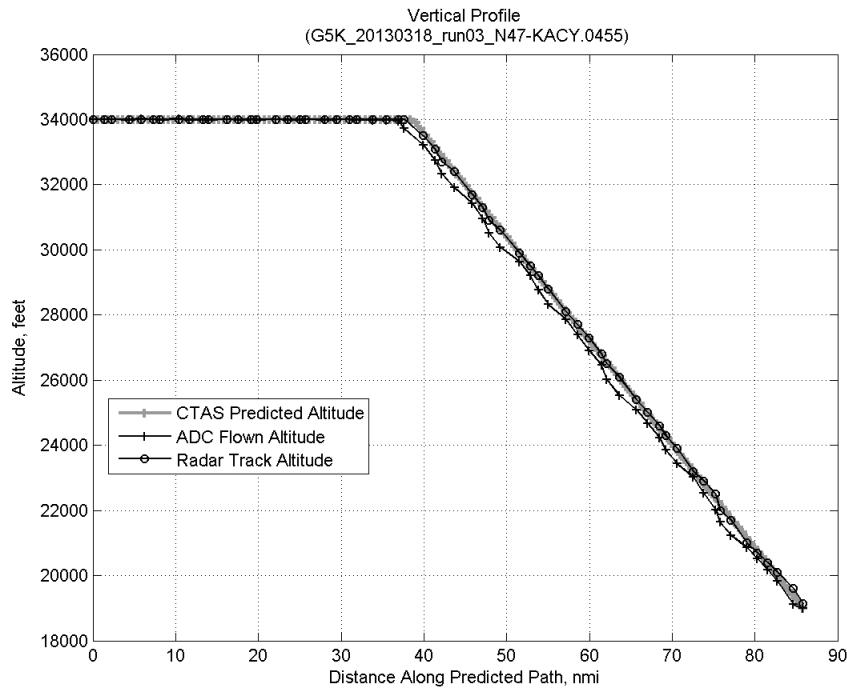


**Figure 107: Flown (ADC) and predicted (CTAS) vertical profile for run 3.**

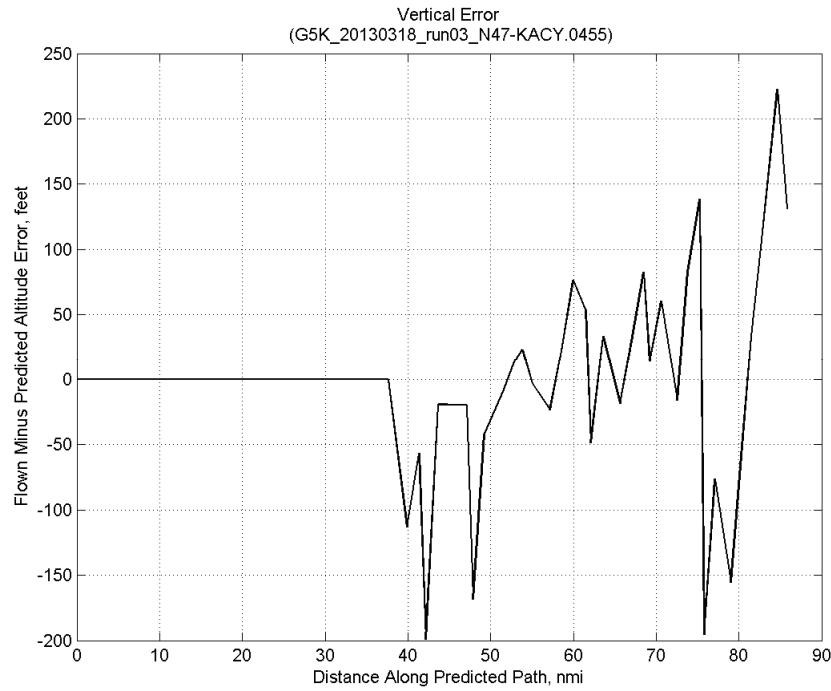


**Figure 108: Vertical error (flown minus predicted altitude) for run 3. Positive values indicate aircraft flew higher than predicted by CTAS.**

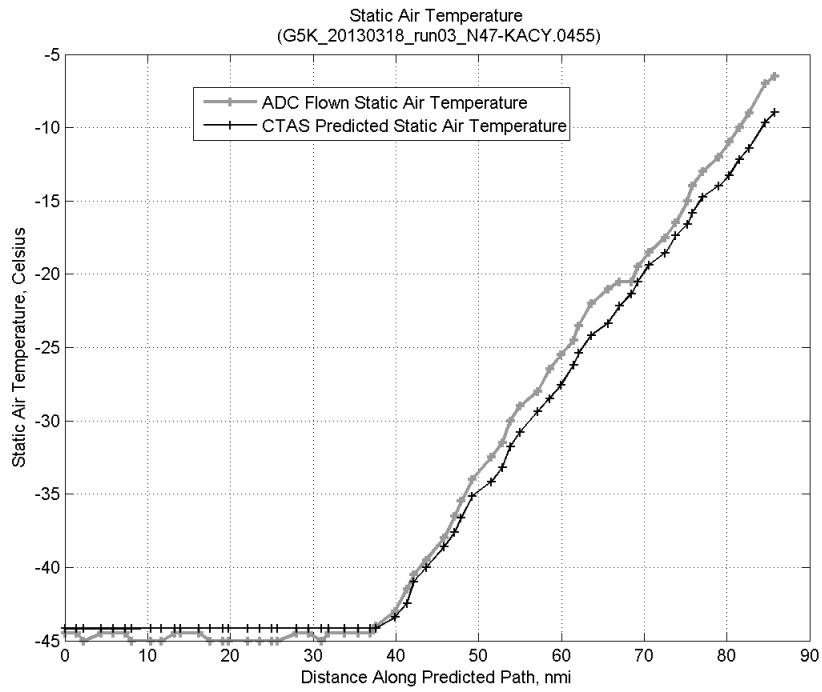


**Figure 109: Flown (ADC) and predicted (CTAS) static air temperature for run 3.**

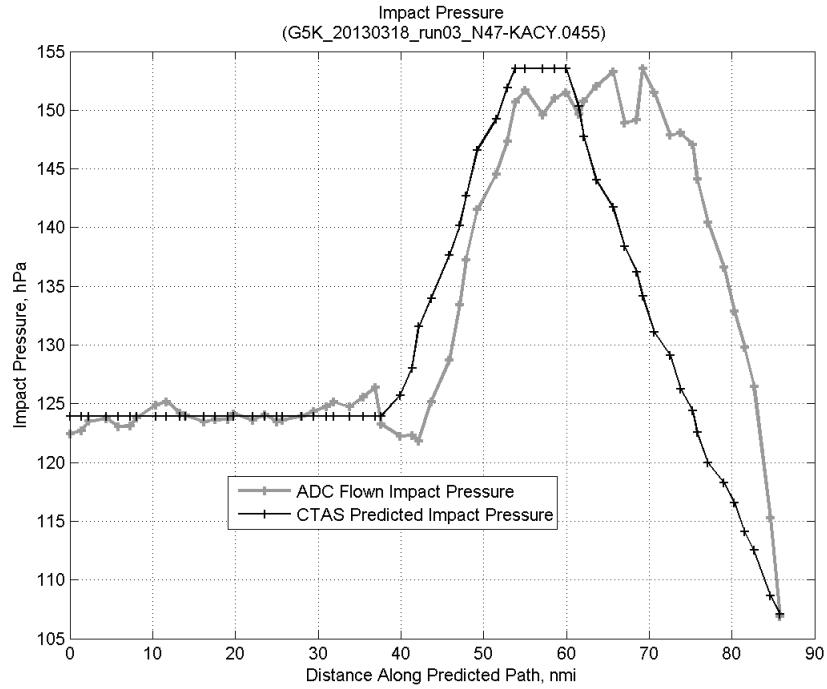


**Figure 110: Flown (ADC) and predicted (CTAS) impact pressure for run 3.**

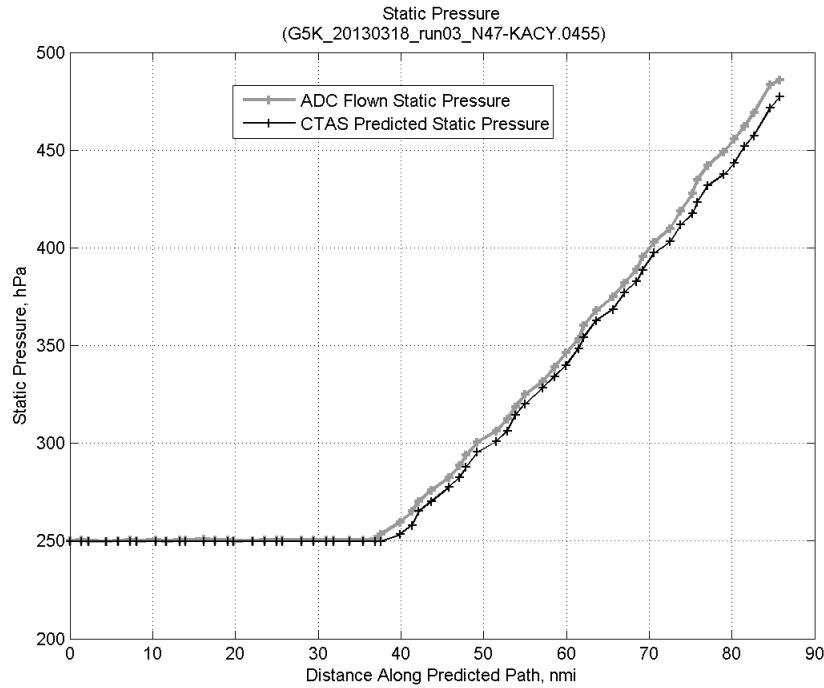


**Figure 111: Flown (ADC) and predicted (CTAS) static pressure for run 3.**

#### C.4.G. Path Distance

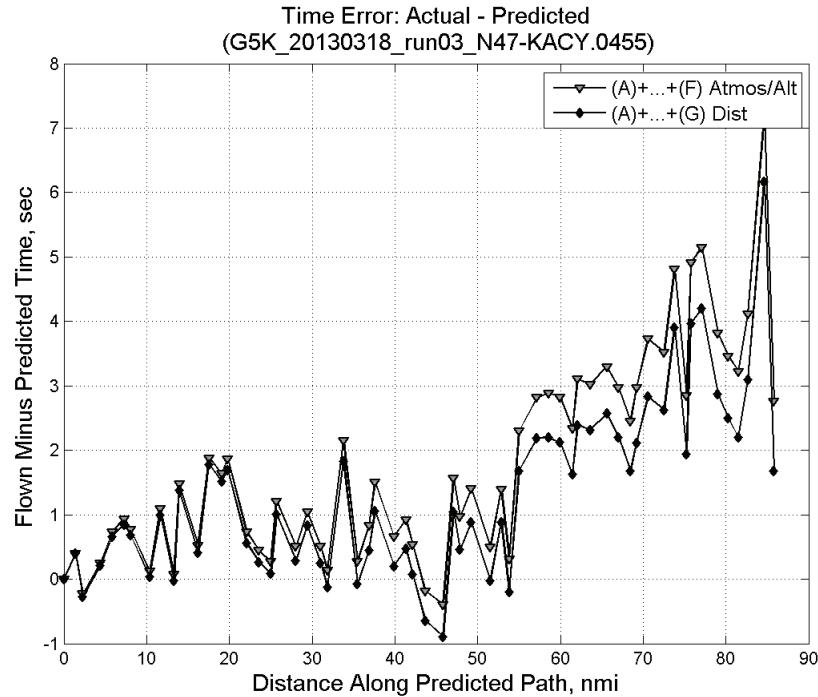


**Figure 112: Time error for run 3 before ((A)+...+(F) Atmos/Alt) and after ((A)+...+(G) Dist) removing path distance error source.**

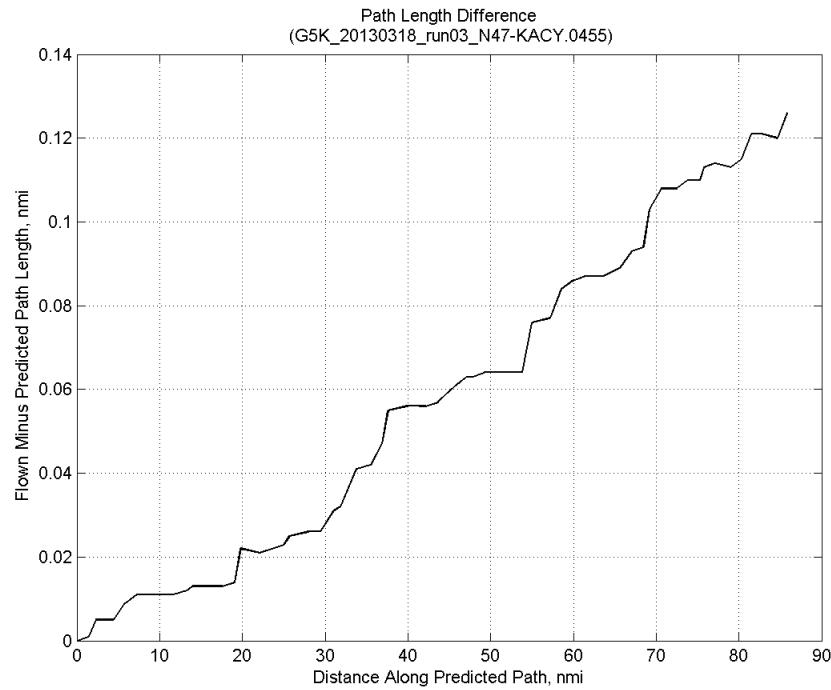


**Figure 113: ADC flown minus CTAS predicted path length for run 3. Positive values indicate aircraft followed a longer path than predicted by CTAS.**

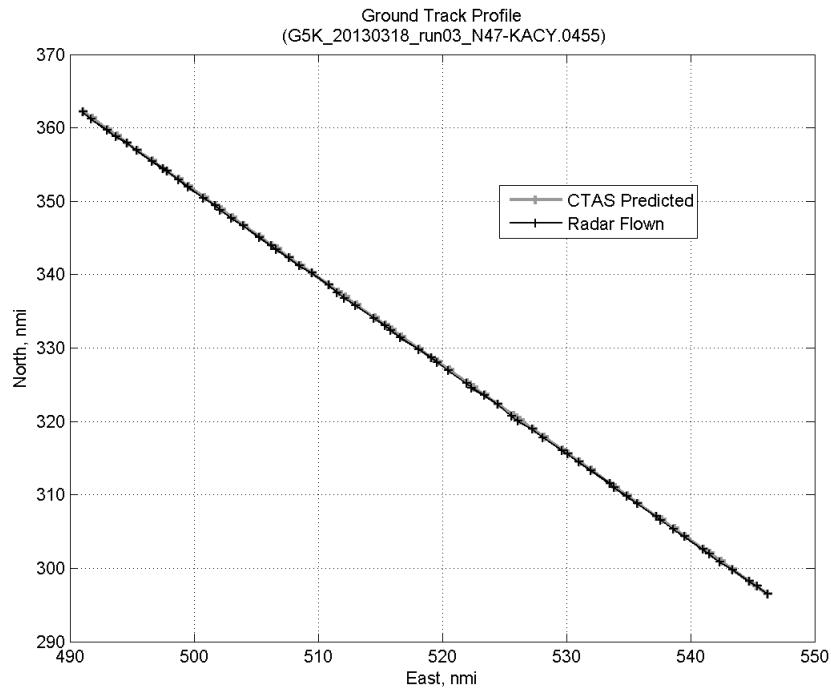


**Figure 114: CTAS predicted and radar flown ground track profile for run 3.**

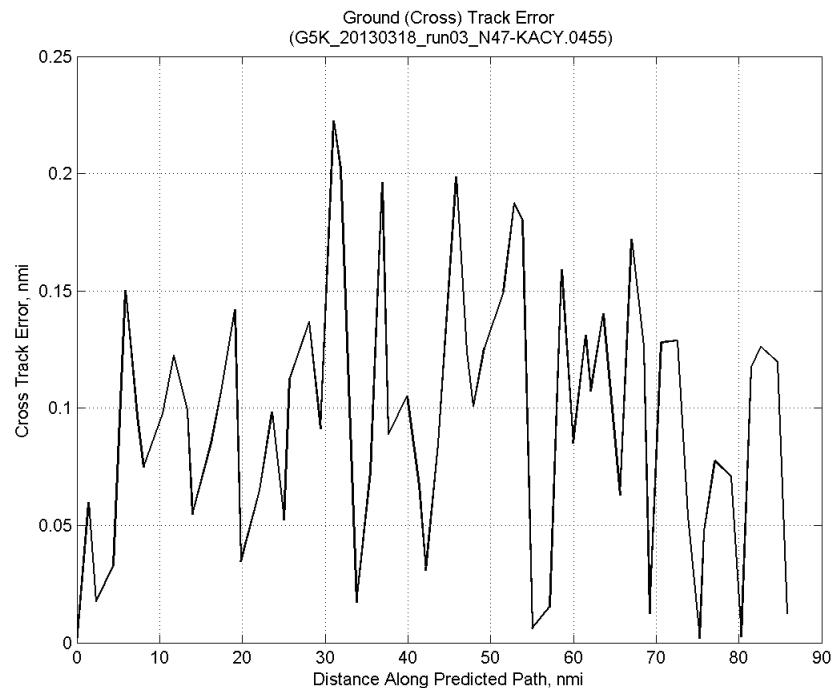


**Figure 115: Ground (cross) track error for run 3.**

### C.5. Run 4

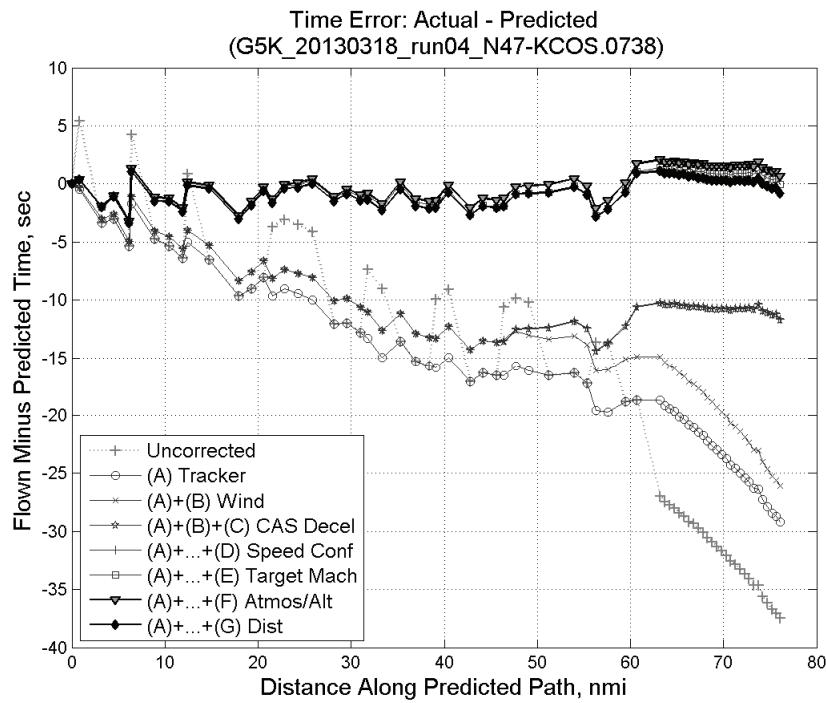


**Figure 116: Time error for run 4 showing incremental effect of removing each error source.**

#### C.5.A. Tracker Jumps

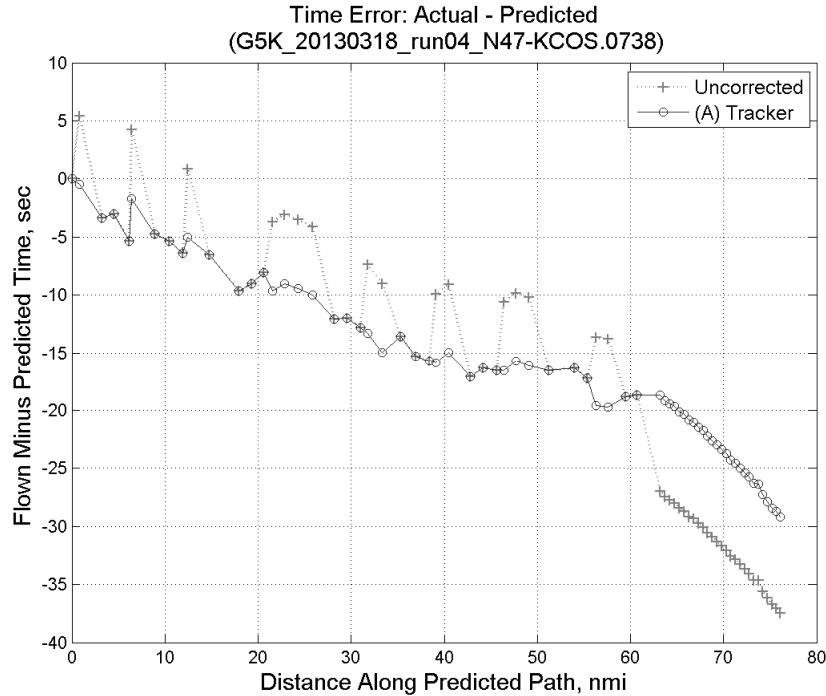


**Figure 117: Time error for run 4 before (Uncorrected) and after ((A) Tracker) removing tracker jump error source.**

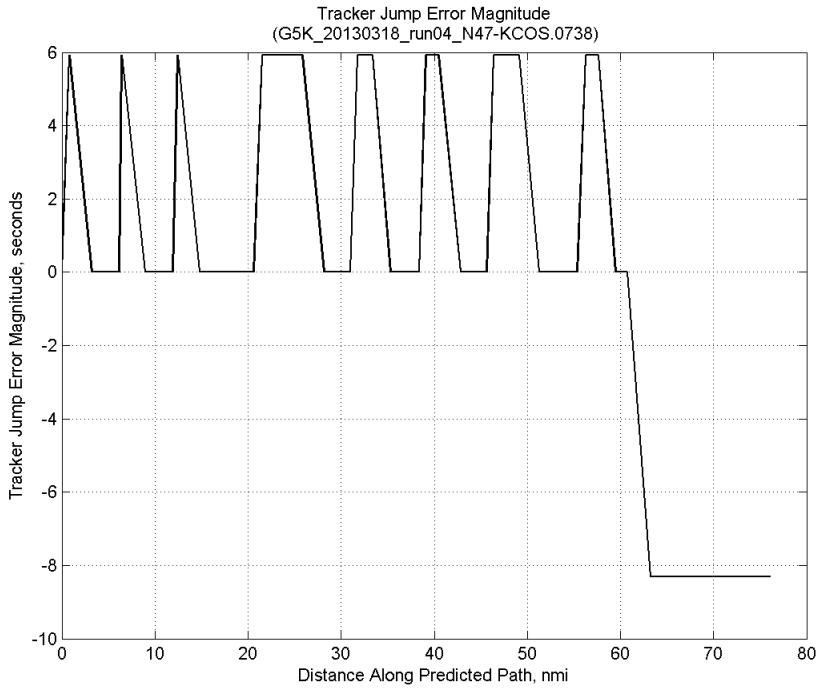


**Figure 118: Effect of tracker jump error source on time error for run 4.**

### C.5.B. Wind

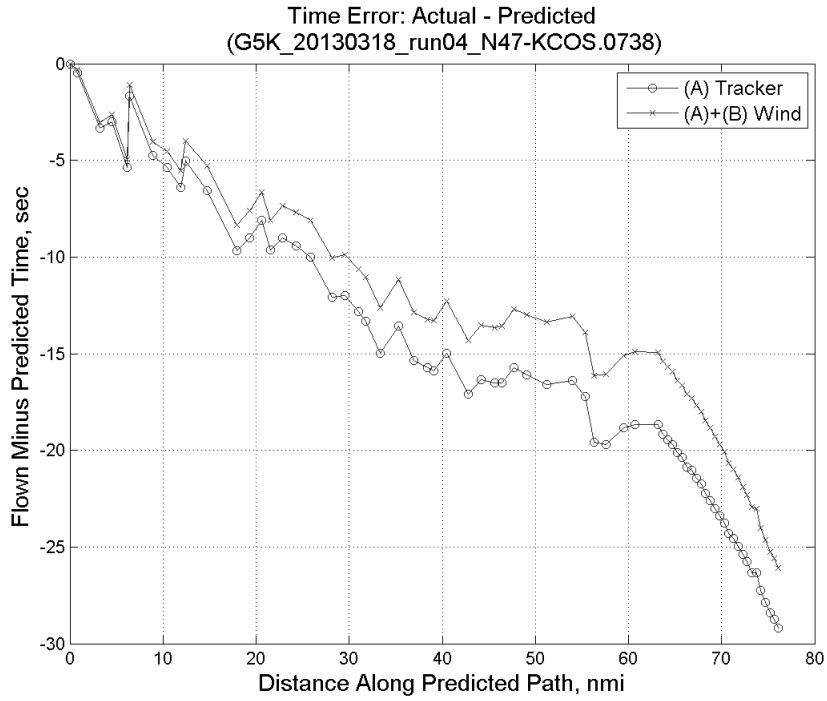


**Figure 119: Time error for run 4 before ((A) Tracker) and after ((A)+(B) Wind) removing wind error source.**

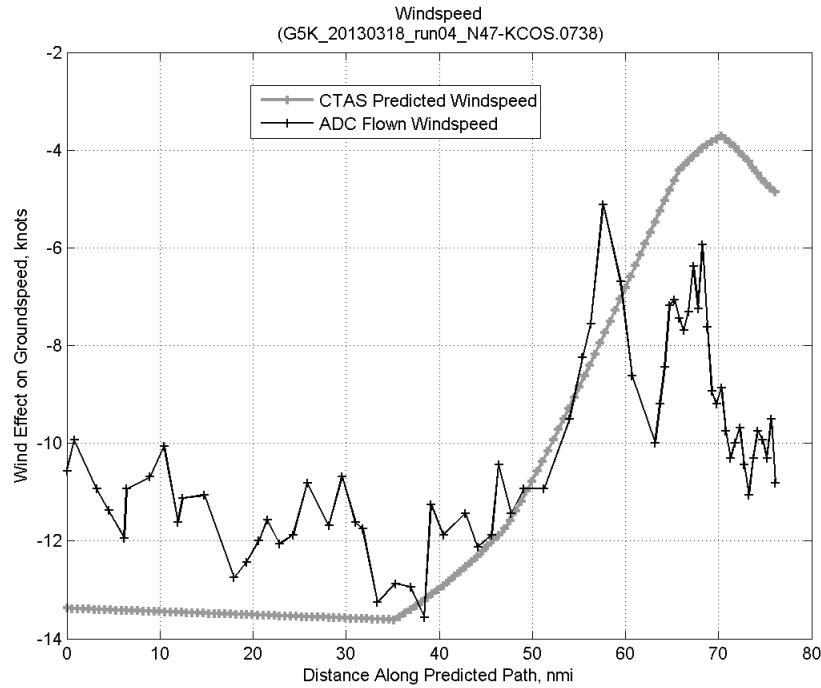


**Figure 120: CTAS predicted and ADC flown wind effect on ground speed for run 4. Negative values indicate a headwind.**

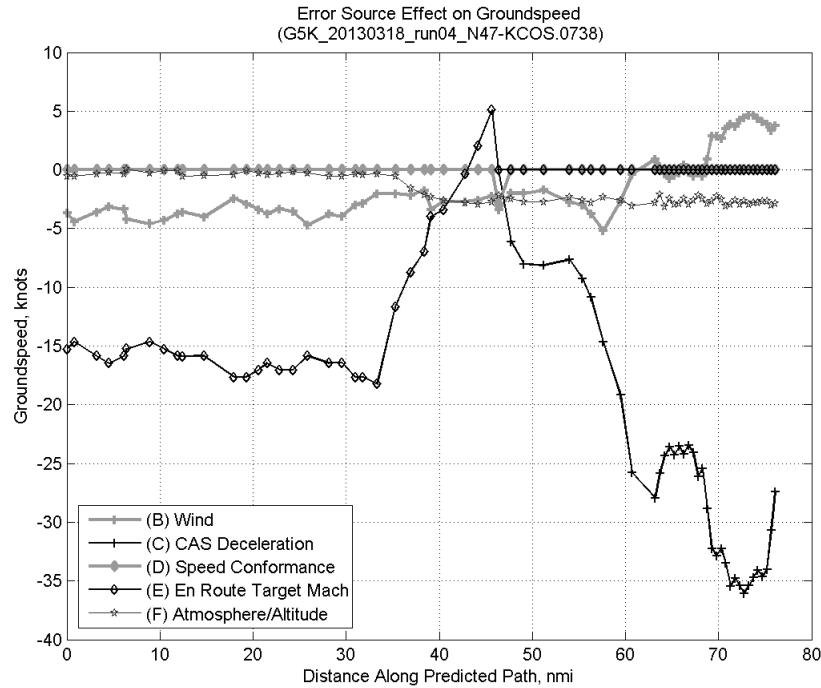


**Figure 121: Error sources (flown minus predicted) converted to a ground speed effect for run 4. Positive values indicate the flown ground speed was faster than the CTAS prediction.**

### C.5.C. CAS Deceleration

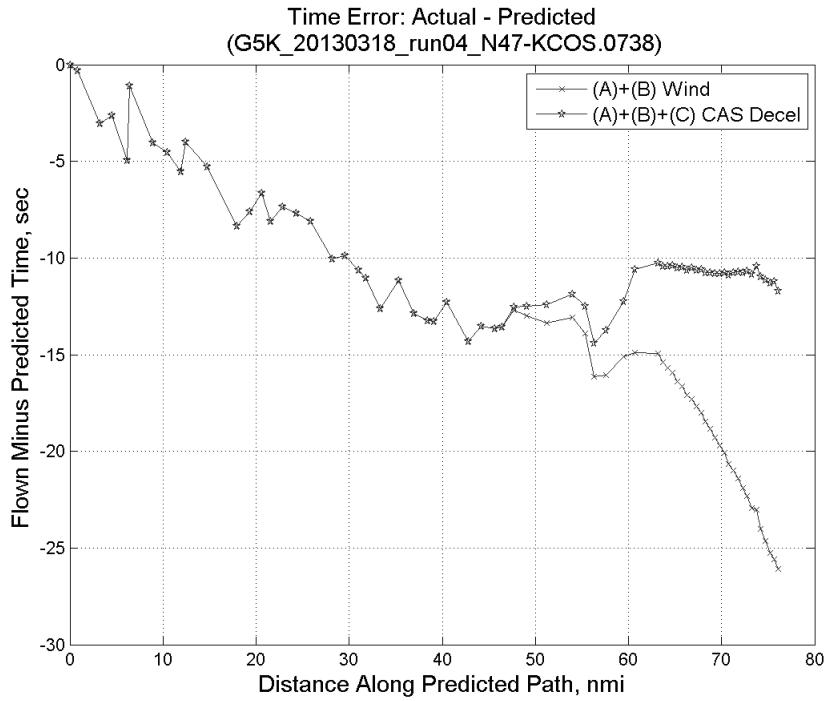


**Figure 122: Time error for run 4 before ((A)+(B) Wind) and after ((A)+(B)+(C) CAS Decel) removing CAS deceleration error source.**

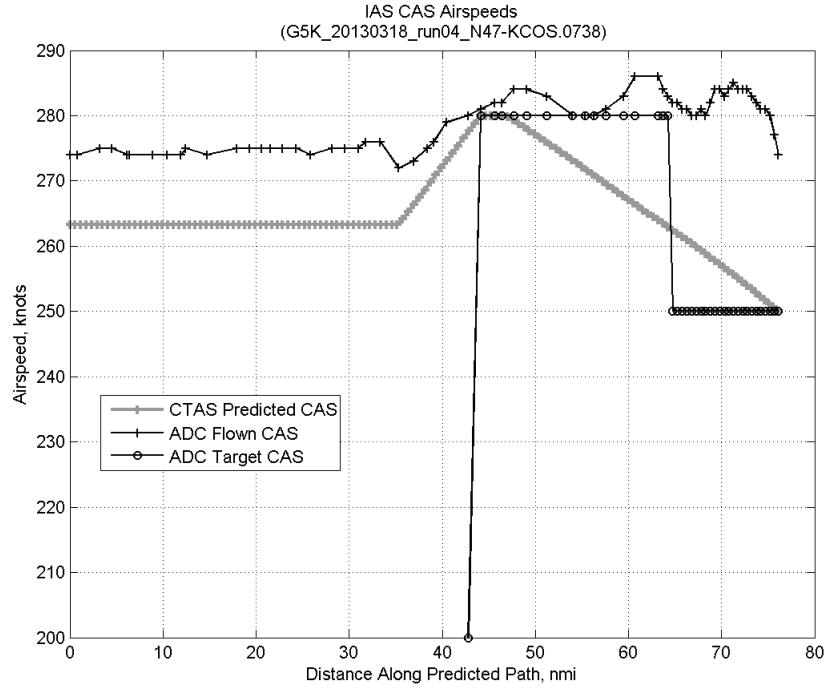


**Figure 123: CTAS predicted and ADC flown CAS for run 4. CAS that is being targeted is shown with circle markers.**

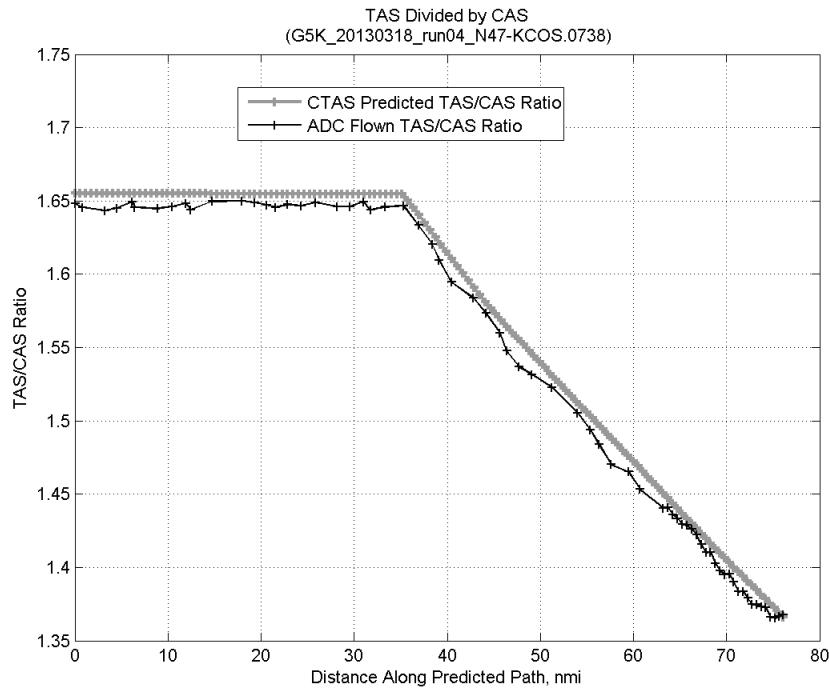


**Figure 124: CTAS predicted and ADC flown TAS/CAS ratio for run 4.**

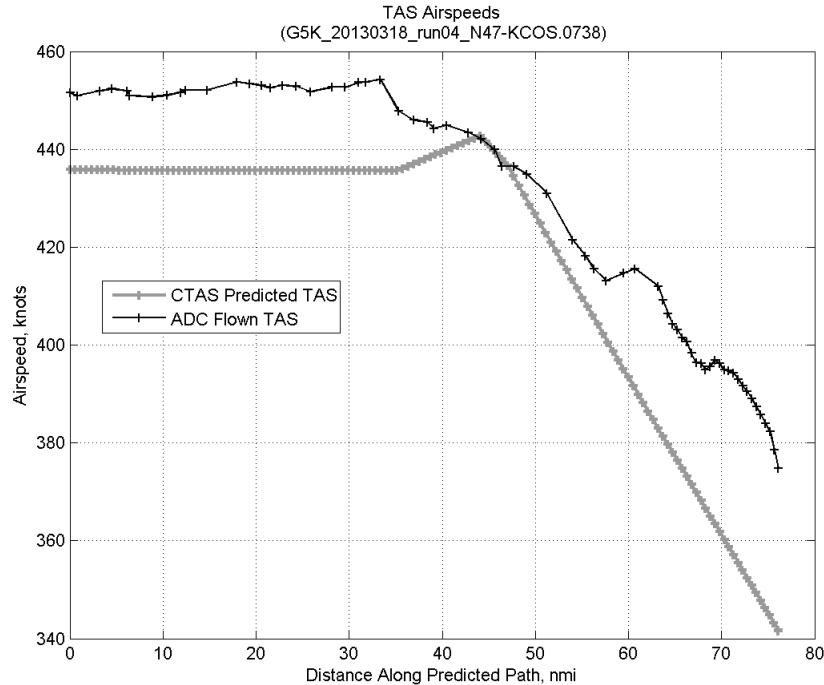


**Figure 125: CTAS predicted and ADC flown TAS for run 4.**

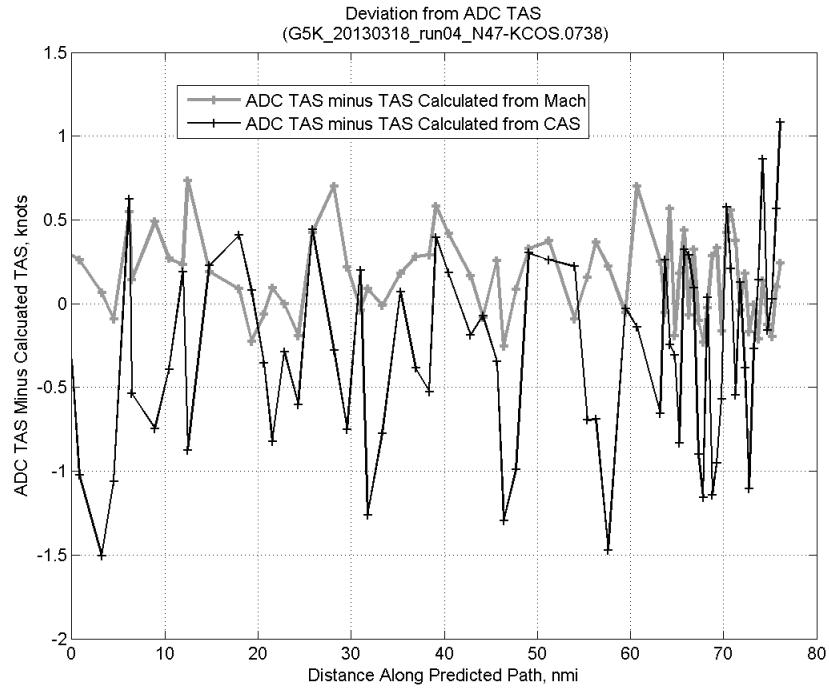


**Figure 126: Deviation from ADC flown TAS if calculating TAS using ADC flown CAS, Mach, atmospheric temperature, and atmospheric pressure for run 4.**

#### C.5.D. Speed Conformance

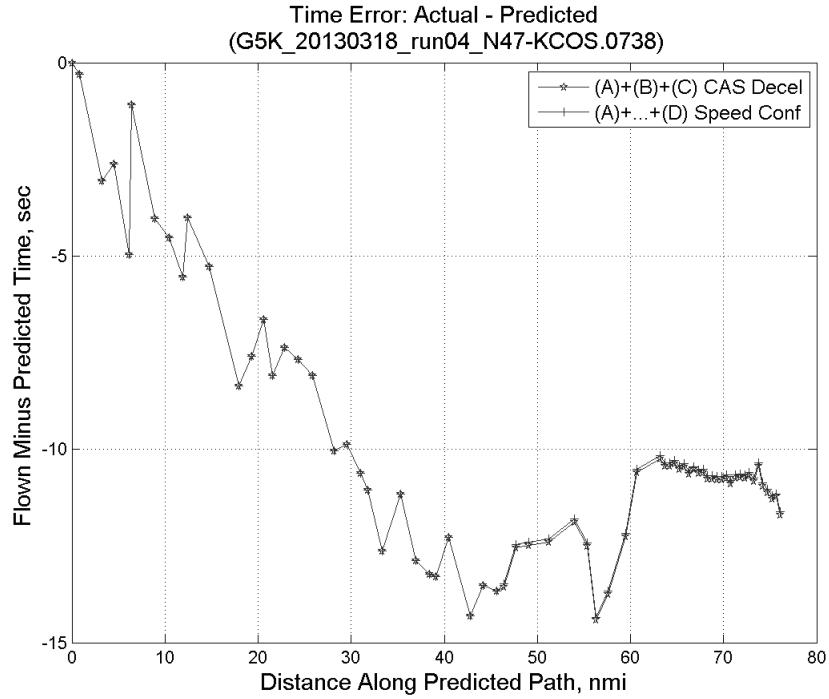


**Figure 127: Time error for run 4 before ((A)+(B)+(C) CAS Decel) and after ((A)+...+(D) Speed Conf) removing speed conformance error source.**

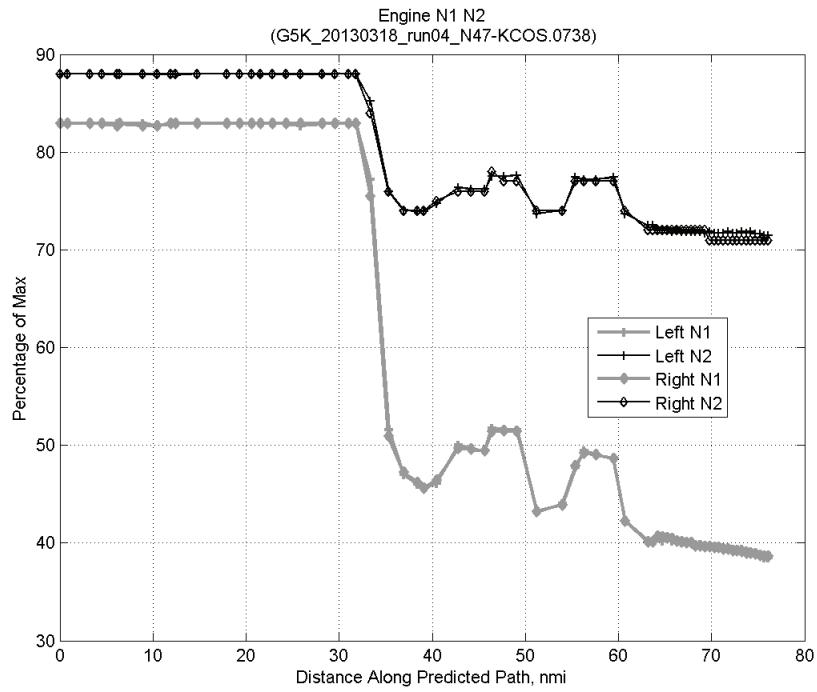


**Figure 128: Flown engine N1 and N2 for run 4.**

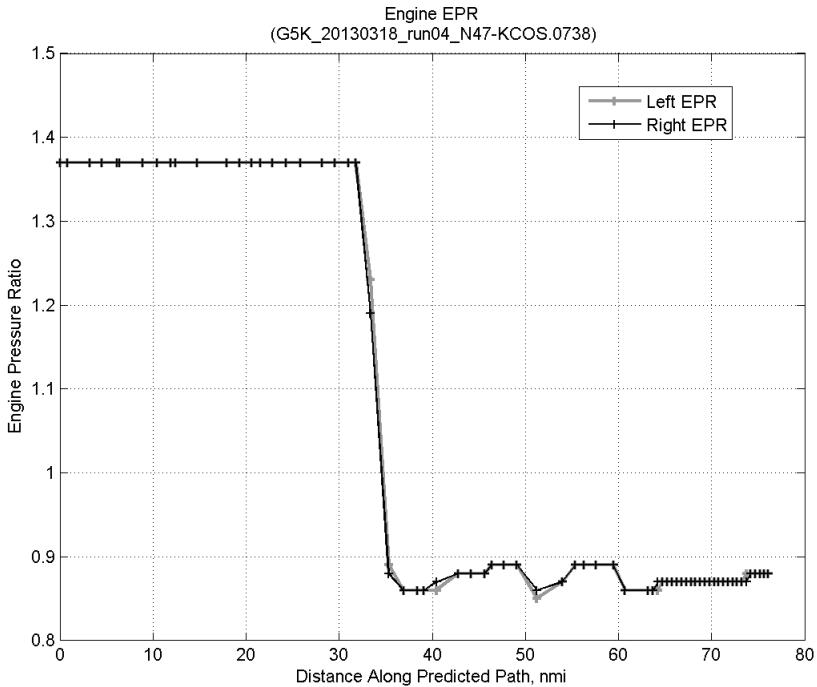


**Figure 129: Flown engine EPR for run 4.**

### C.5.E. Target Mach

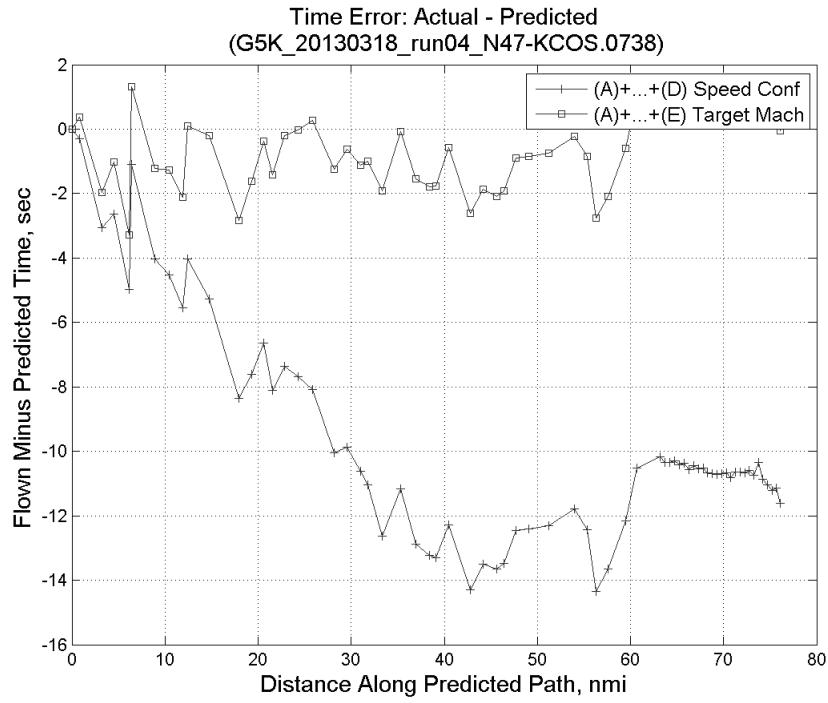


**Figure 130: Time error for run 4 before ((A)+...+(D) Speed Conf) and after ((A)+...+(E) Target Mach) removing target Mach error source.**

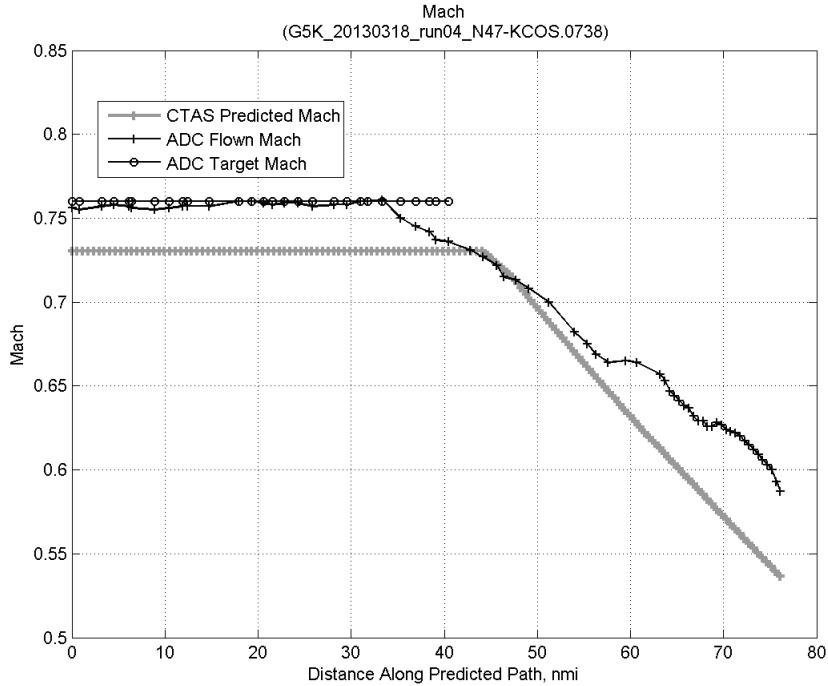


**Figure 131: CTAS predicted and ADC flown Mach for run 4. Mach being targeted (ADC) shown with circle markers.**

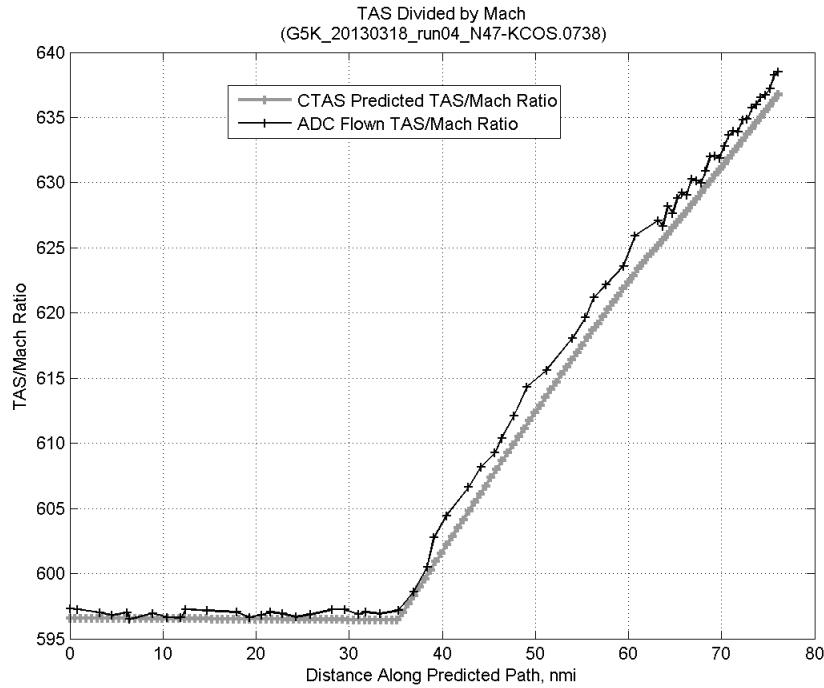


**Figure 132: CTAS predicted and ADC flown TAS/Mach ratio for run 4.**

#### C.5.F. Atmosphere/Altitude

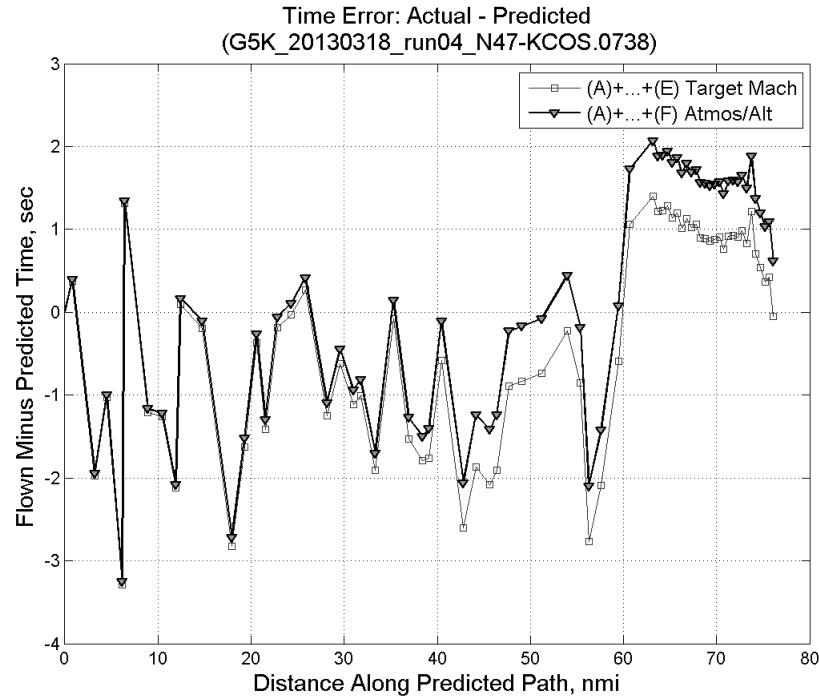


**Figure 133: Time error for run 4 before ((A)+...+(E) Target Mach) and after ((A)+...+(F) Atmos/Alt) removing atmosphere/altitude error source.**

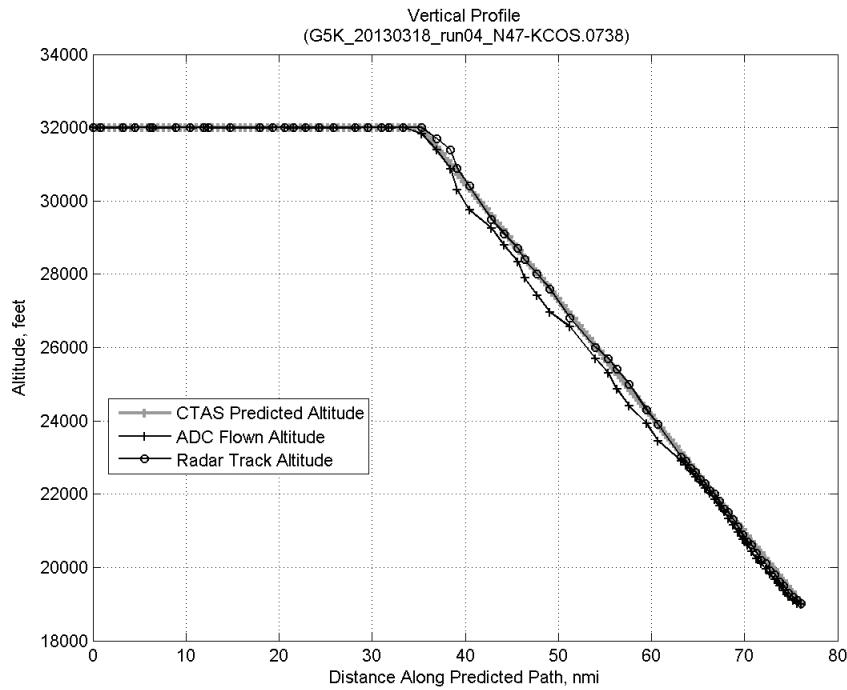


**Figure 134: Flown (ADC) and predicted (CTAS) vertical profile for run 4.**

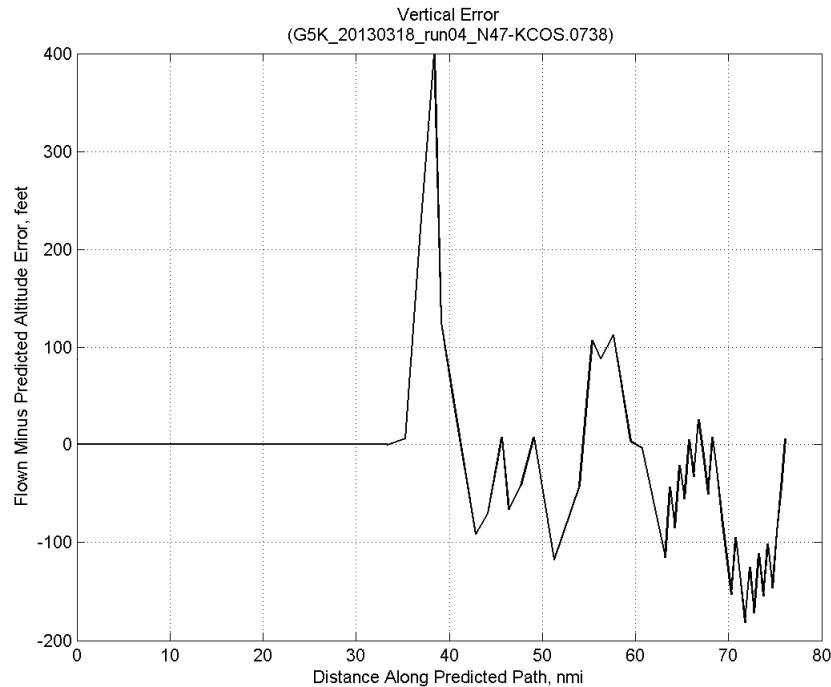


**Figure 135: Vertical error (flown minus predicted altitude) for run 4. Positive values indicate aircraft flew higher than predicted by CTAS.**

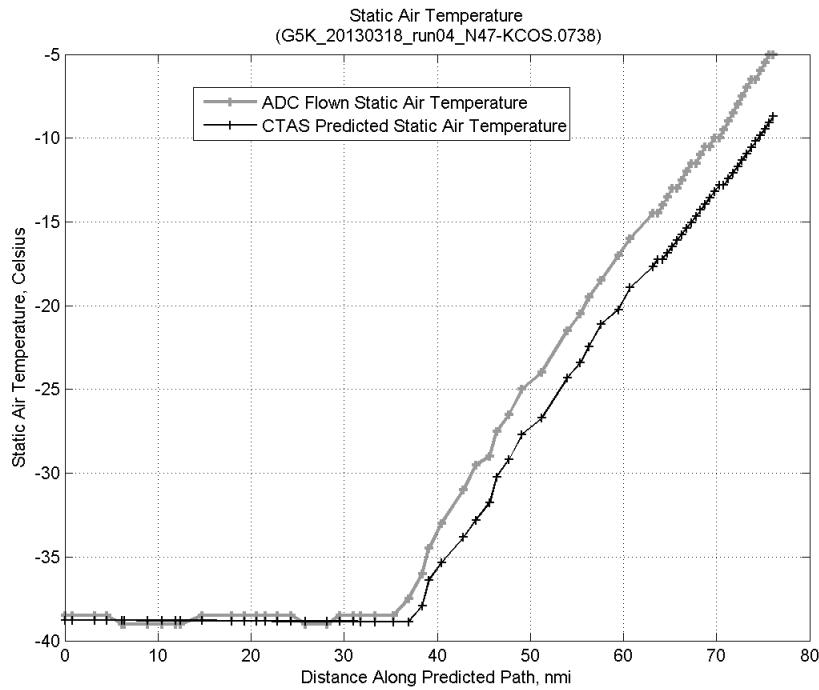


**Figure 136: Flown (ADC) and predicted (CTAS) static air temperature for run 4.**

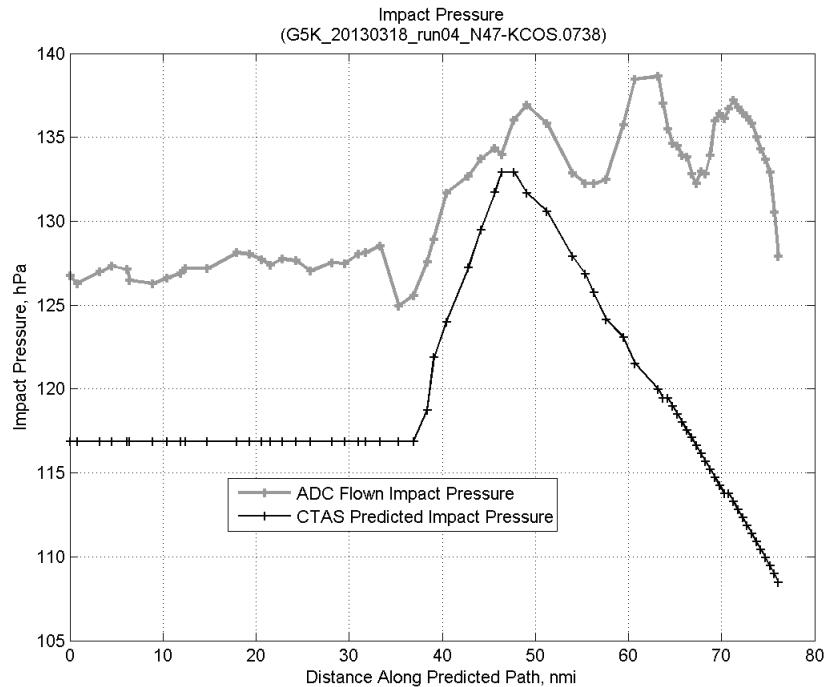


**Figure 137: Flown (ADC) and predicted (CTAS) impact pressure for run 4.**

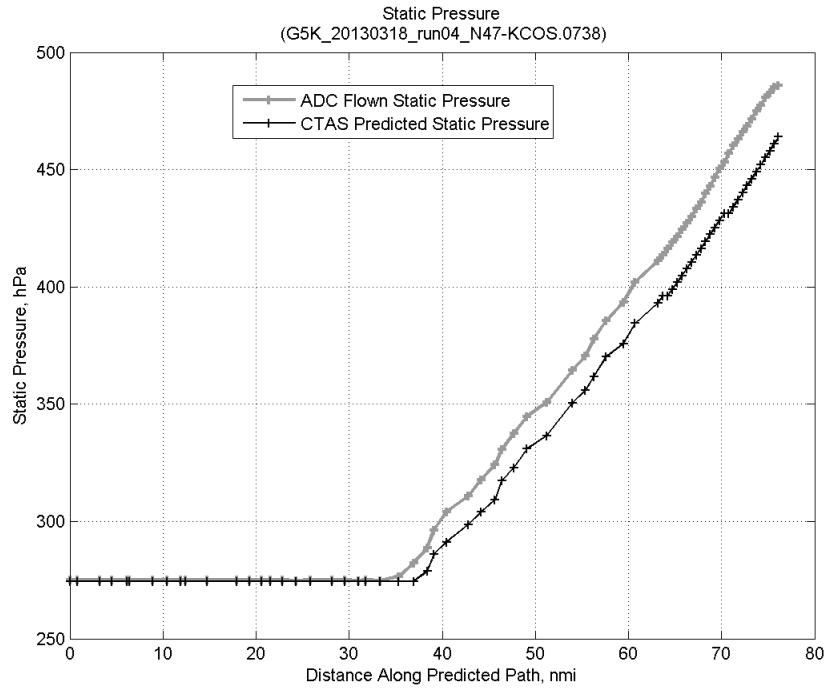


**Figure 138: Flown (ADC) and predicted (CTAS) static pressure for run 4.**

### C.5.G. Path Distance

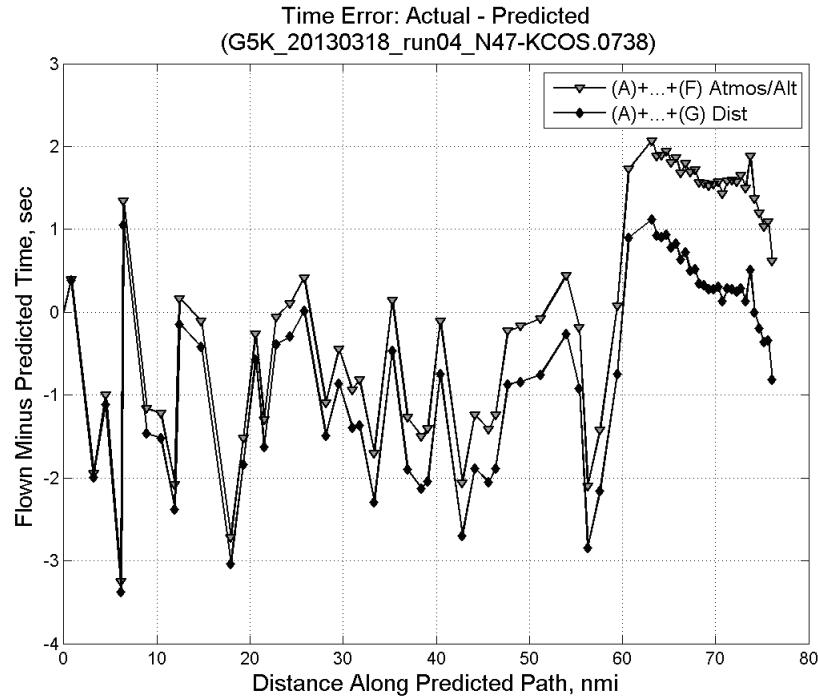


**Figure 139: Time error for run 4 before ((A)+...+(F) Atmos/Alt) and after ((A)+...+(G) Dist) removing path distance error source.**

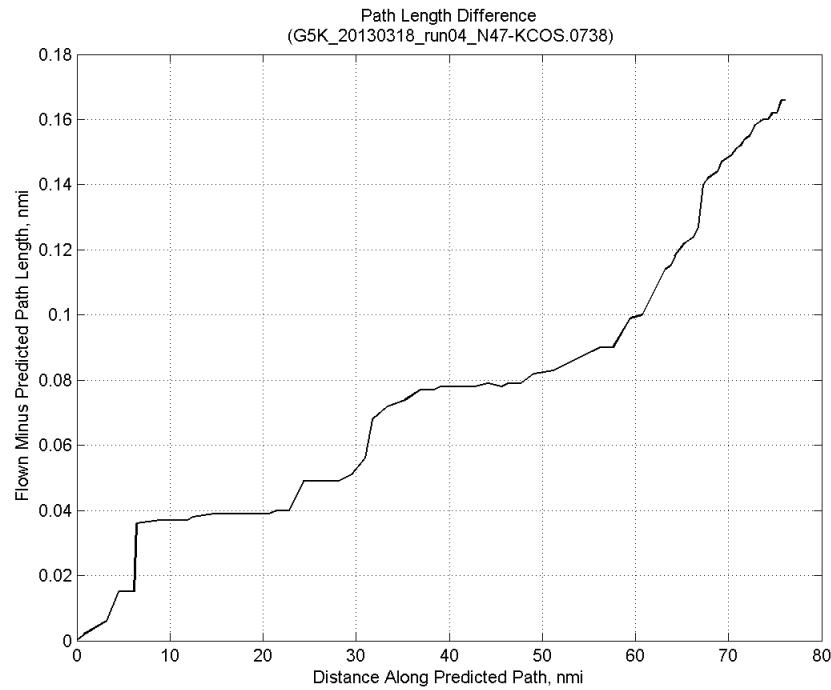


**Figure 140: ADC flown minus CTAS predicted path length for run 4. Positive values indicate aircraft followed a longer path than predicted by CTAS.**

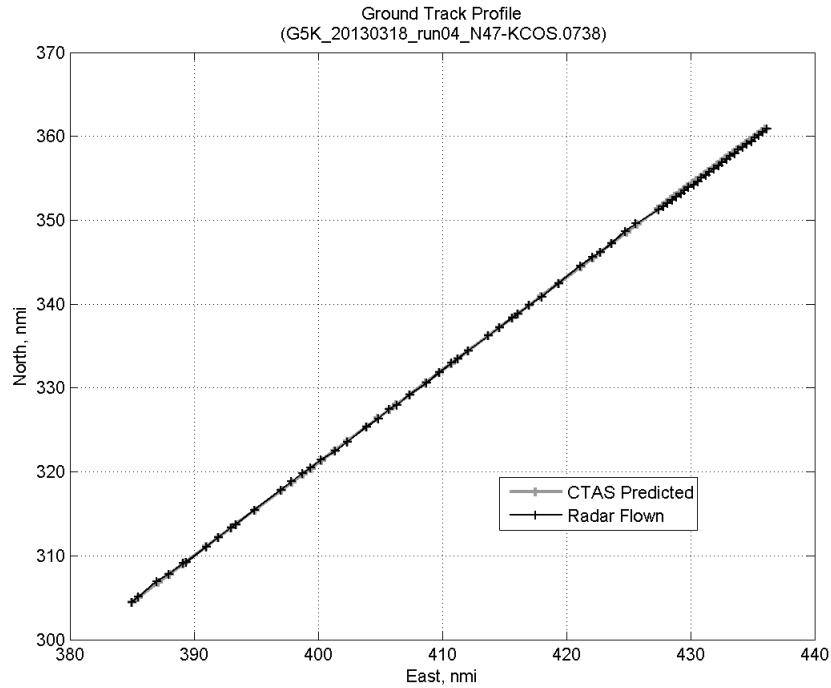


**Figure 141: CTAS predicted and radar flown ground track profile for run 4.**

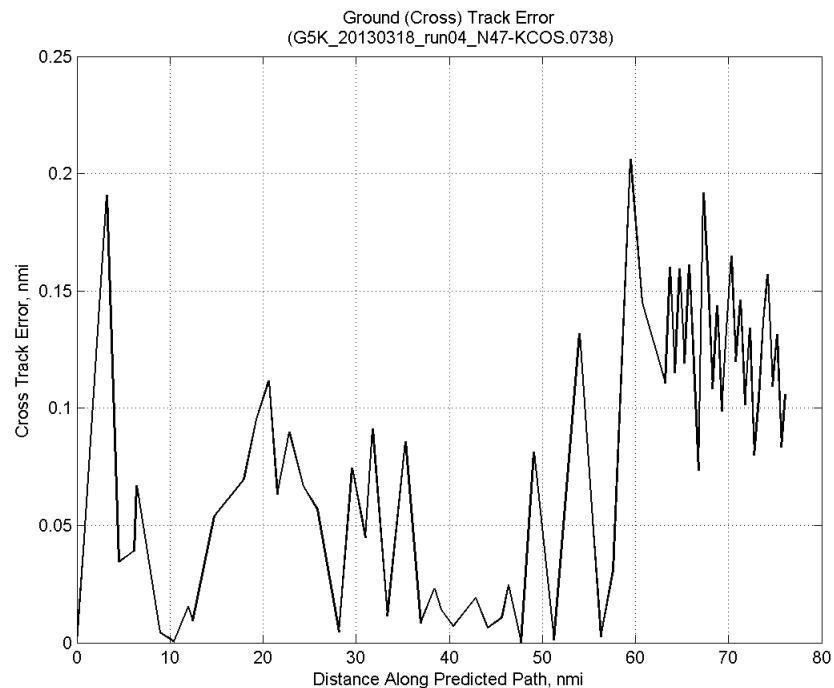


**Figure 142: Ground (cross) track error for run 4.**

## C.6. Run 7

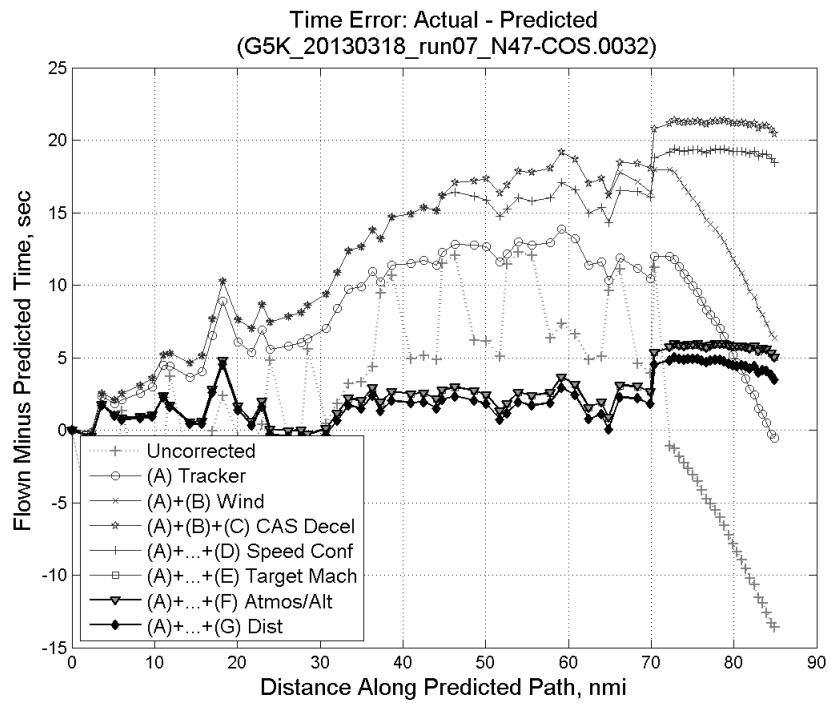


**Figure 143:** Time error for run 7 showing incremental effect of removing each error source.

### C.6.A. Tracker Jumps

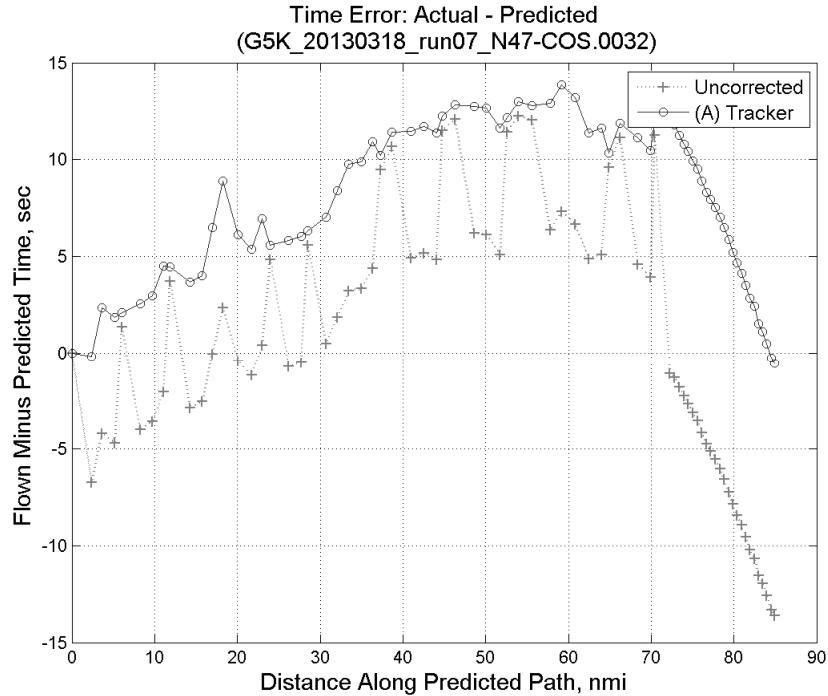


**Figure 144:** Time error for run 7 before (Uncorrected) and after ((A) Tracker) removing tracker jump error source.

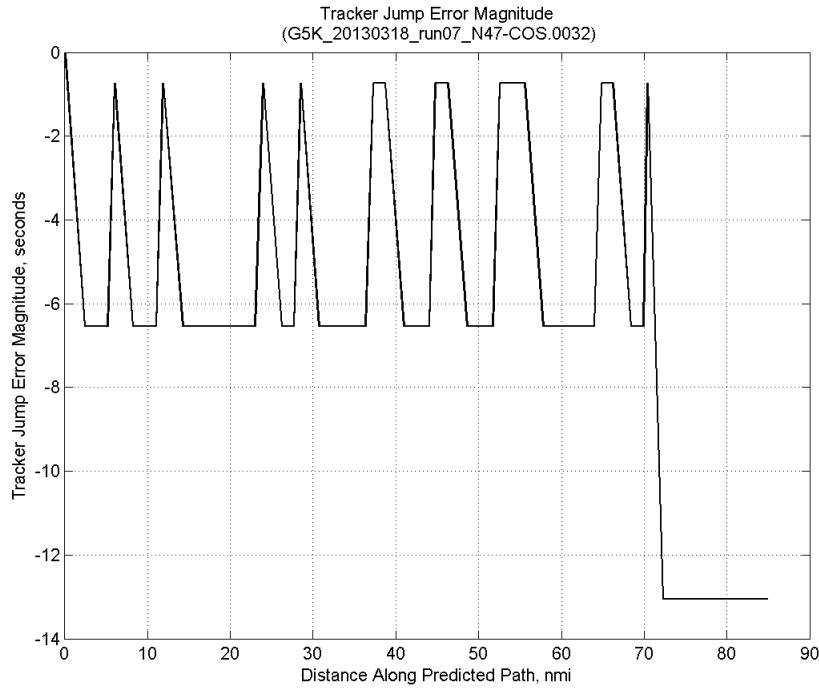


**Figure 145: Effect of tracker jump error source on time error for run 7.**

### C.6.B. Wind

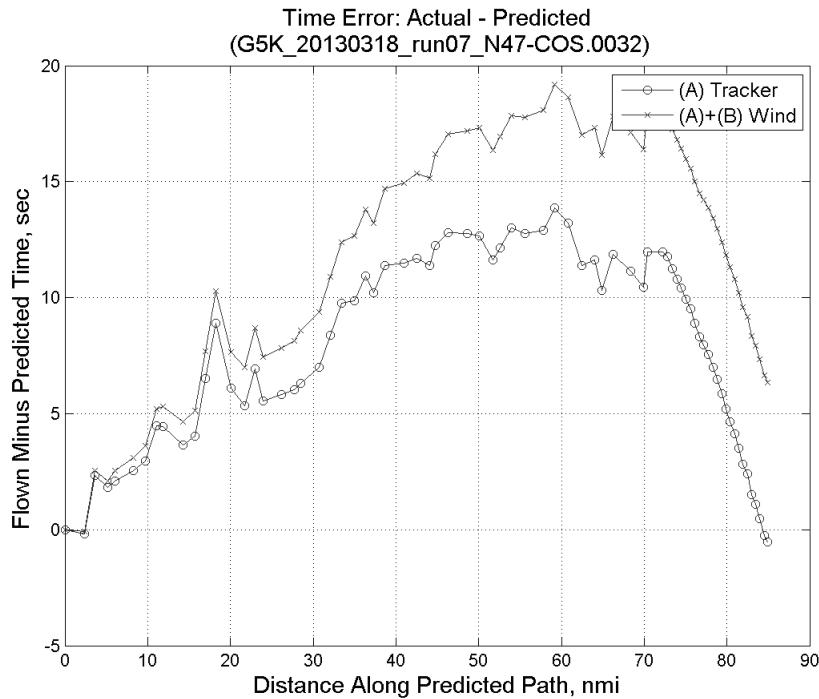


**Figure 146: Time error for run 7 before ((A) Tracker) and after ((A)+(B) Wind) removing wind error source.**

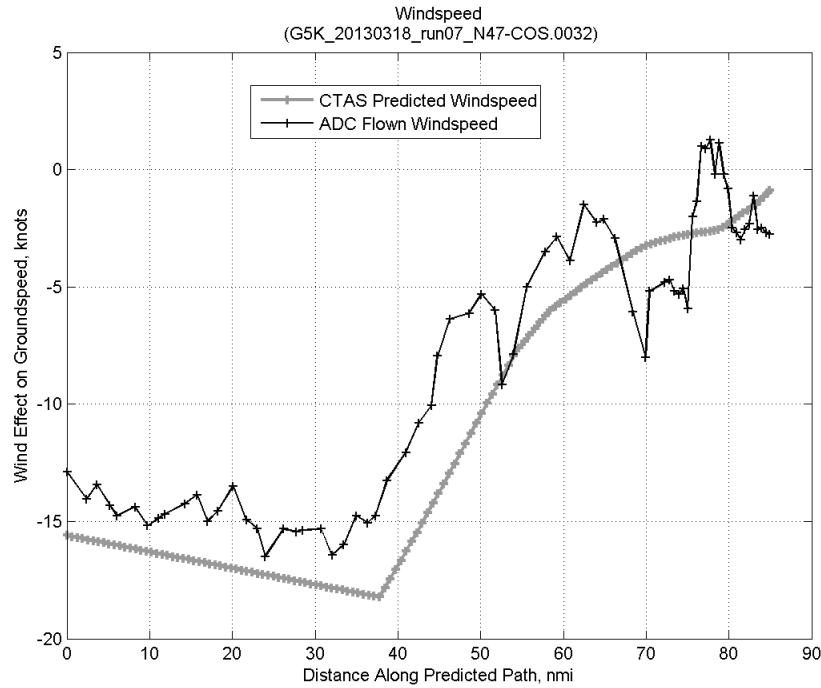


**Figure 147: CTAS predicted and ADC flown wind effect on ground speed for run 7. Negative values indicate a headwind.**

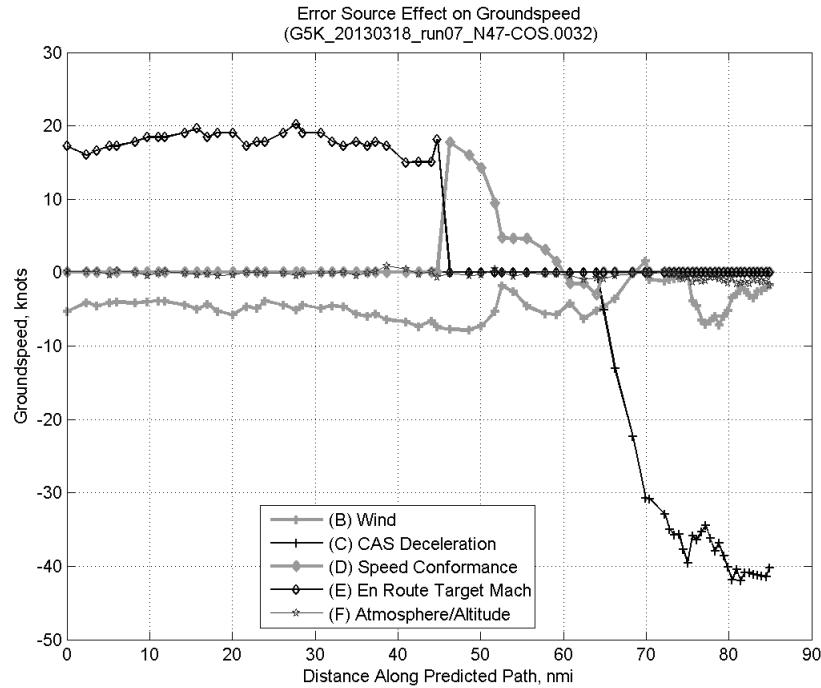


**Figure 148: Error sources (flown minus predicted) converted to a ground speed effect for run 7. Positive values indicate the flown ground speed was faster than the CTAS prediction.**

### C.6.C. CAS Deceleration

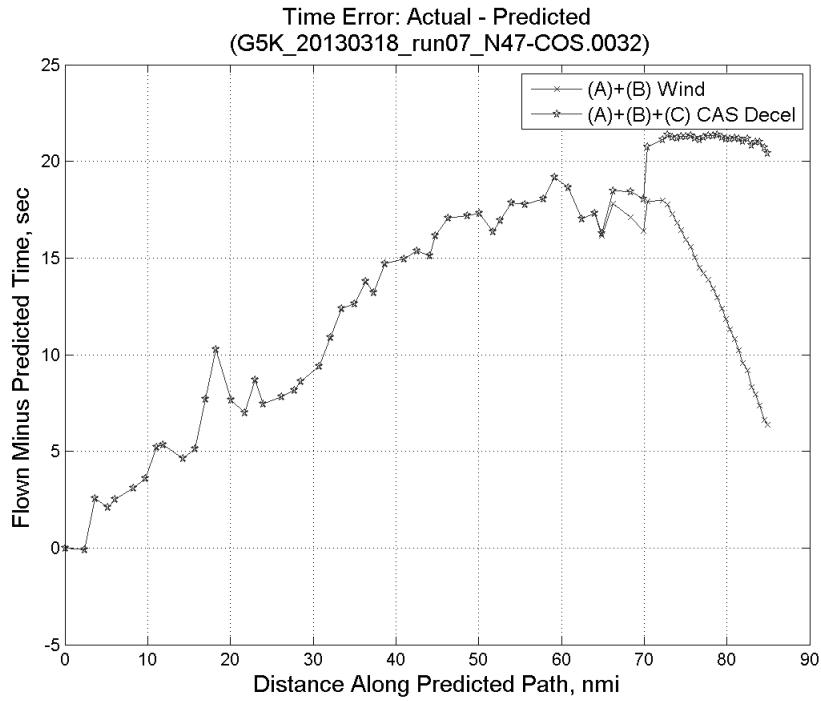


**Figure 149:** Time error for run 7 before ((A)+(B) Wind) and after ((A)+(B)+(C) CAS Decel) removing CAS deceleration error source.

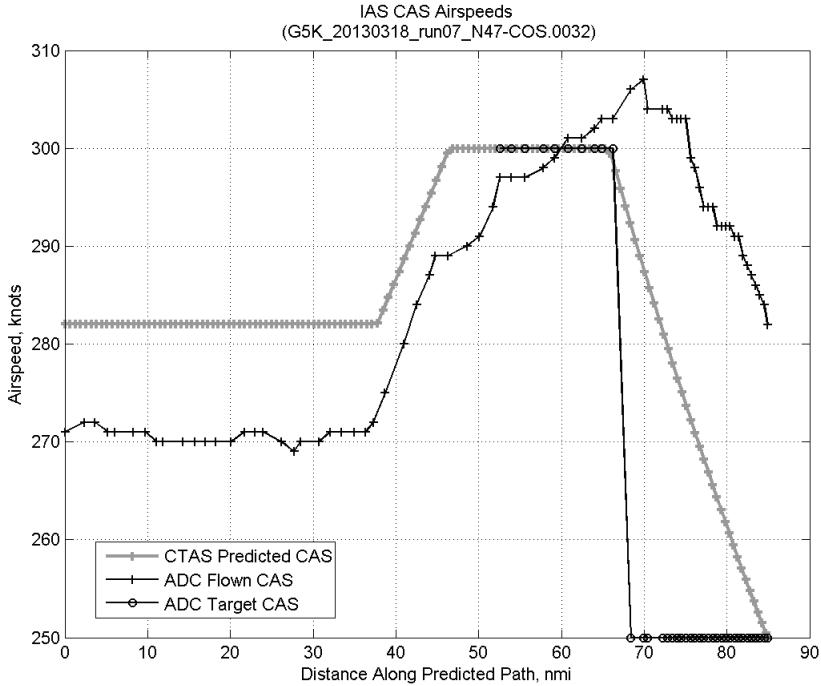


**Figure 150:** CTAS predicted and ADC flown CAS for run 7. CAS that is being targeted is shown with circle markers.

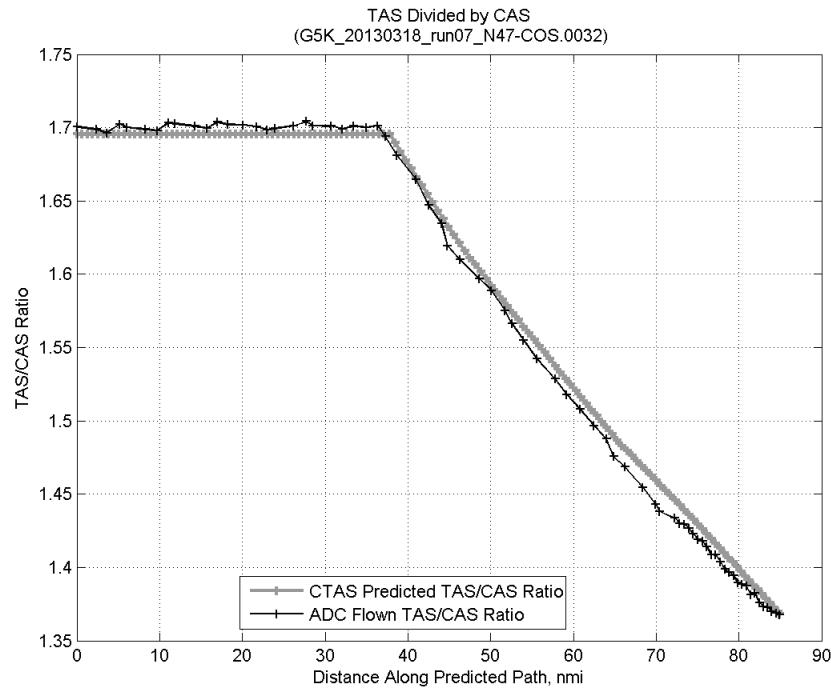


**Figure 151:** CTAS predicted and ADC flown TAS/CAS ratio for run 7.

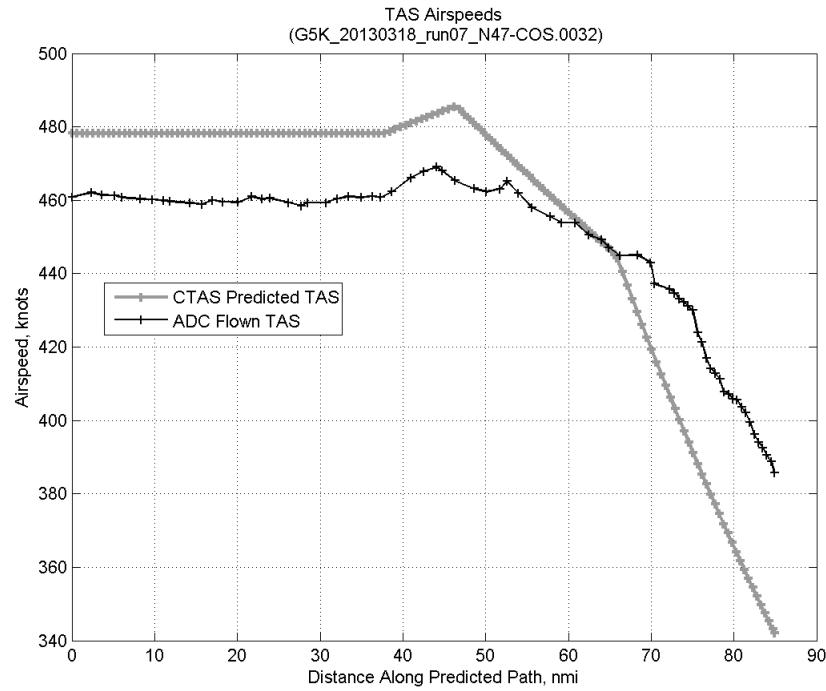


**Figure 152:** CTAS predicted and ADC flown TAS for run 7.

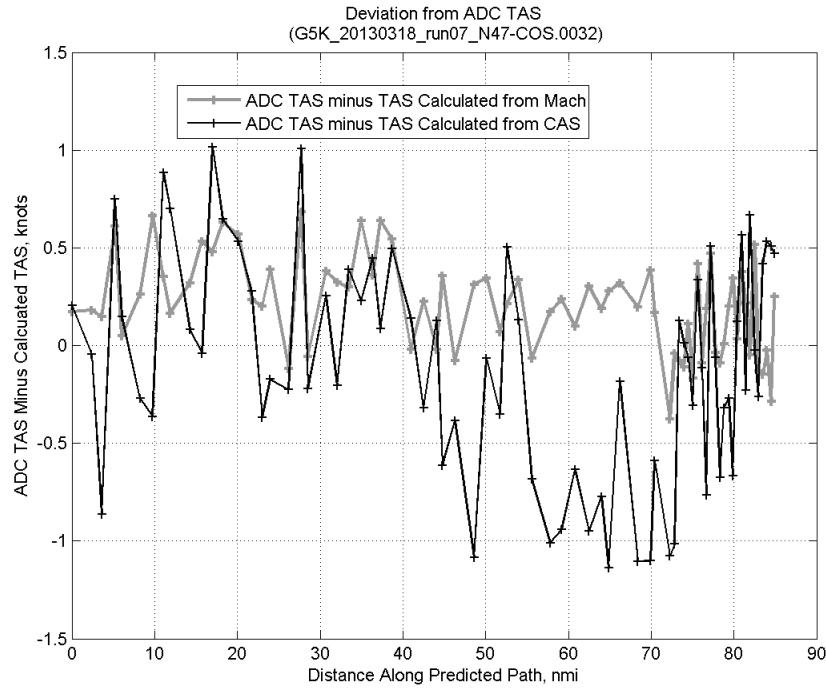


**Figure 153:** Deviation from ADC flown TAS if calculating TAS using ADC flown CAS, Mach, atmospheric temperature, and atmospheric pressure for run 7.

#### C.6.D. Speed Conformance

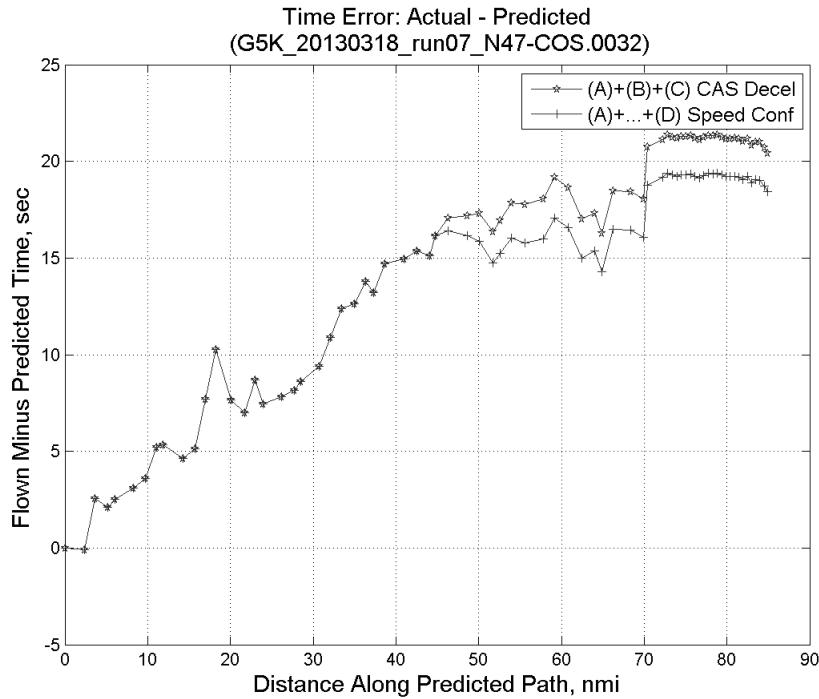


**Figure 154:** Time error for run 7 before ((A)+(B)+(C) CAS Decel) and after ((A)+...+(D) Speed Conf) removing speed conformance error source.

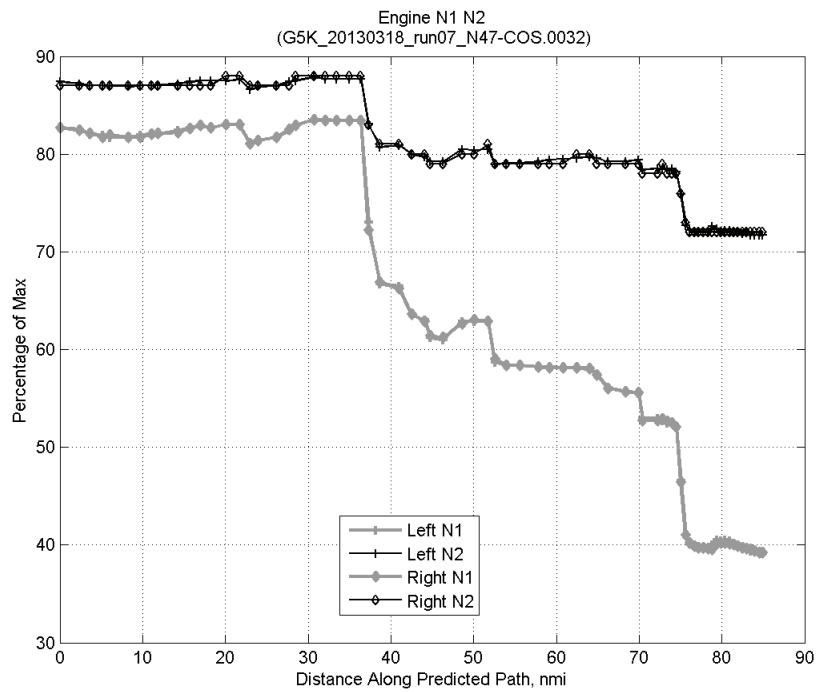


**Figure 155: Flown engine N1 and N2 for run 7.**

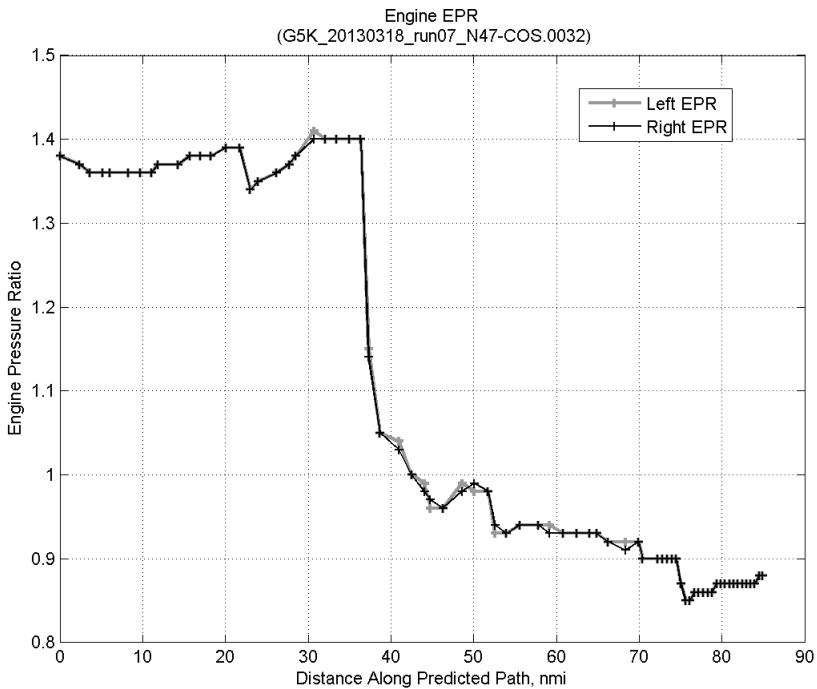


**Figure 156: Flown engine EPR for run 7.**

### C.6.E. Target Mach

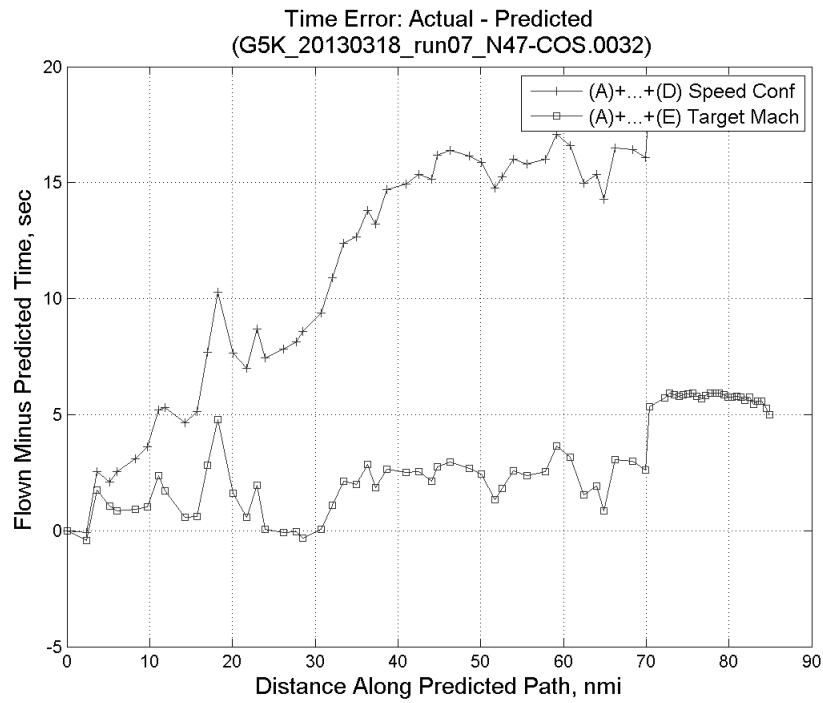


**Figure 157: Time error for run 7 before ((A)+...+(D) Speed Conf) and after ((A)+...+(E) Target Mach) removing target Mach error source.**

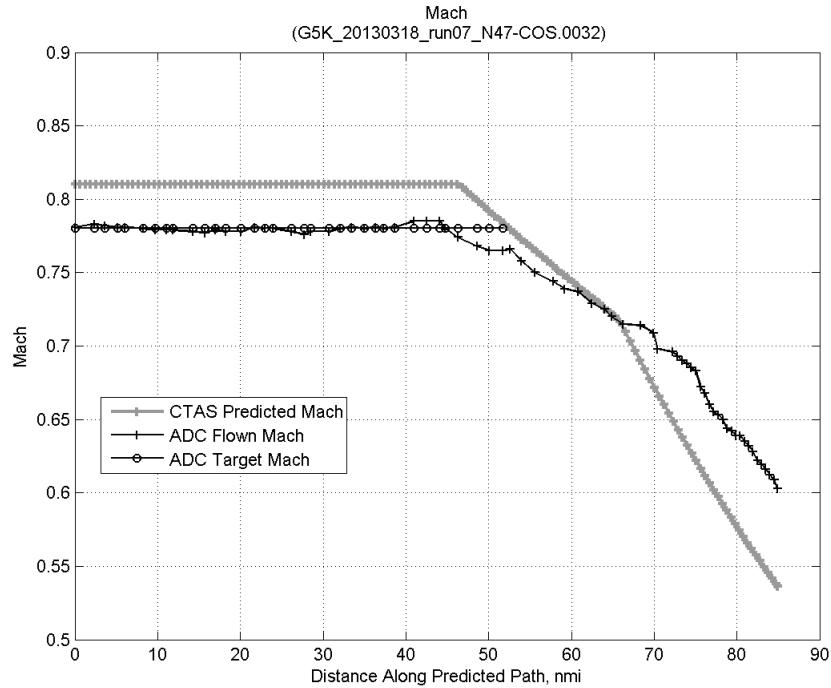


**Figure 158: CTAS predicted and ADC flown Mach for run 7. Mach being targeted (ADC) shown with circle markers.**

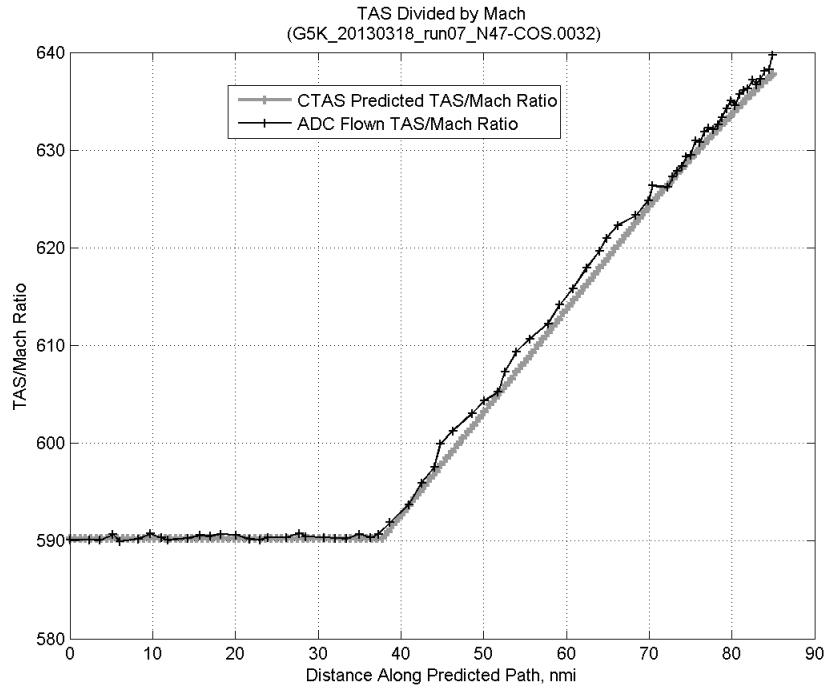


**Figure 159: CTAS predicted and ADC flown TAS/Mach ratio for run 7.**

#### C.6.F. Atmosphere/Altitude

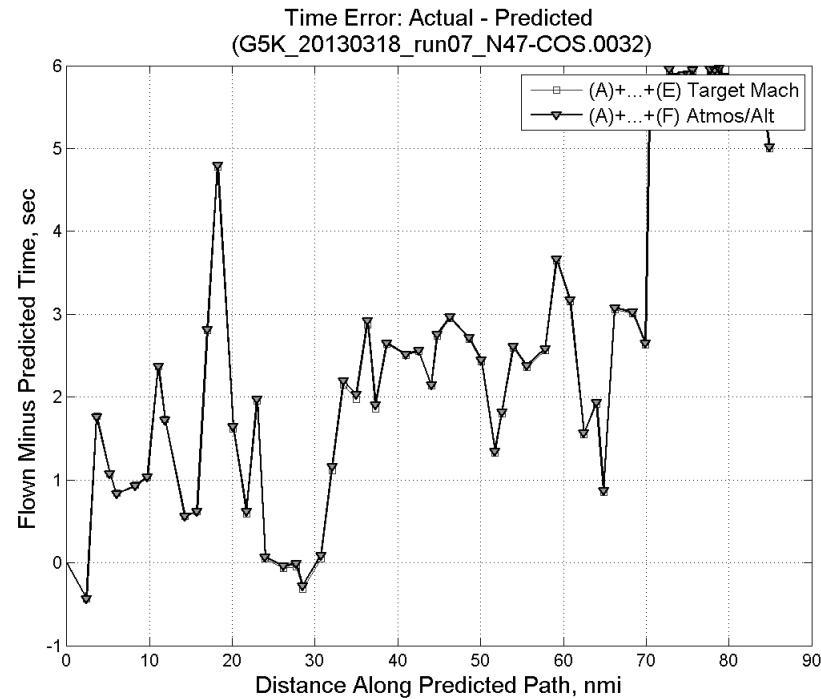


**Figure 160: Time error for run 7 before ((A)+...+(E) Target Mach) and after ((A)+...+(F) Atmos/Alt) removing atmosphere/altitude error source.**

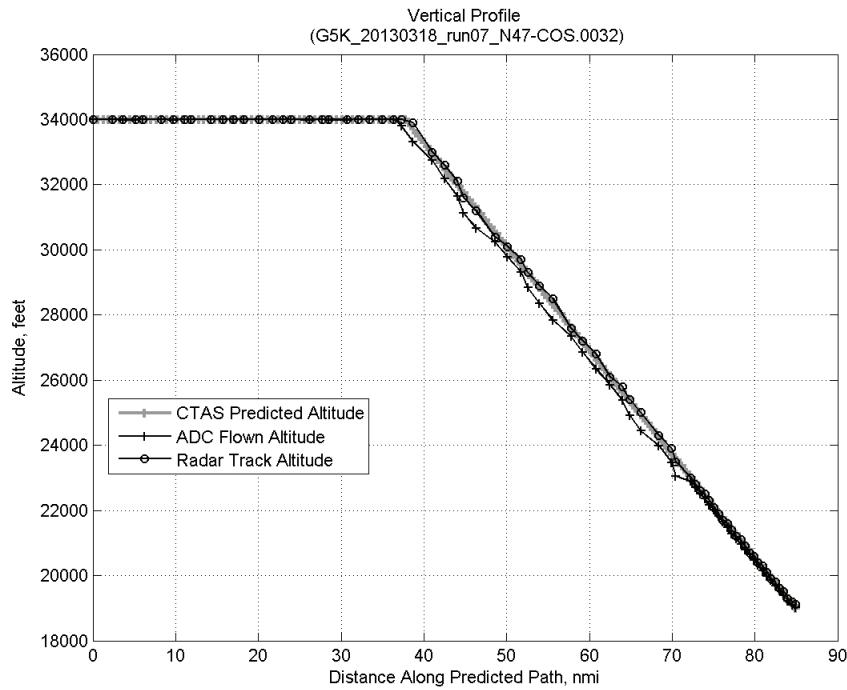


**Figure 161: Flown (ADC) and predicted (CTAS) vertical profile for run 7.**

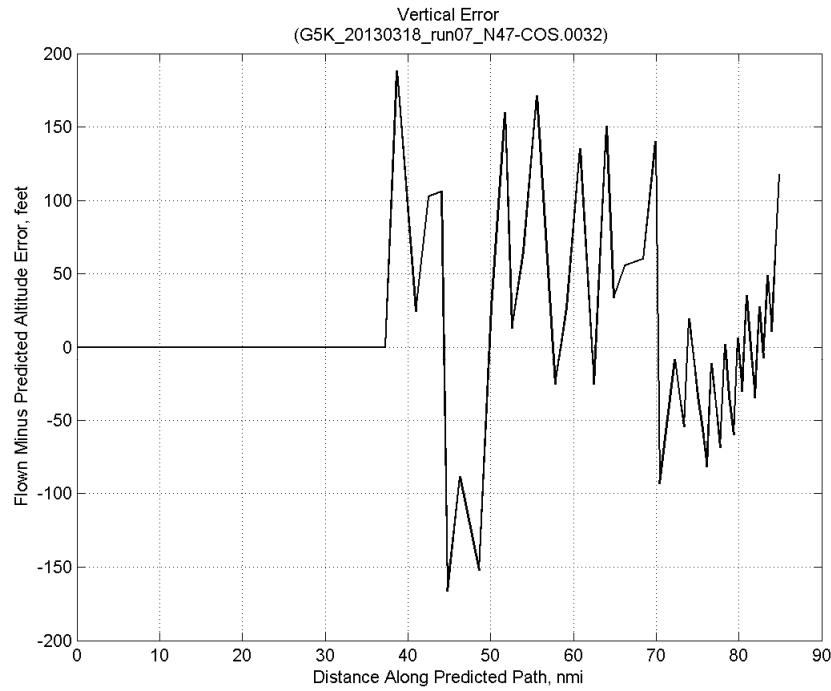


**Figure 162: Vertical error (flown minus predicted altitude) for run 7. Positive values indicate aircraft flew higher than predicted by CTAS.**

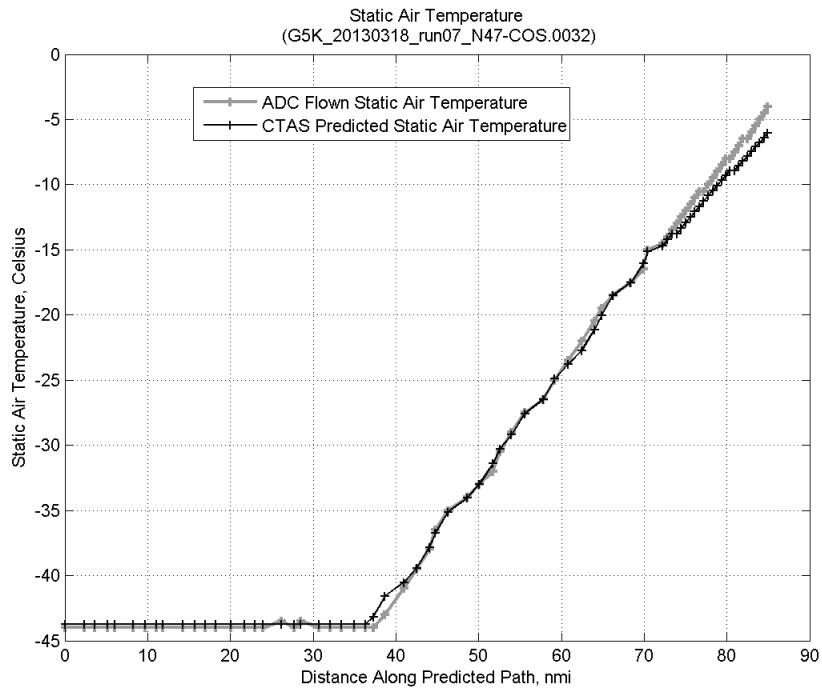


**Figure 163: Flown (ADC) and predicted (CTAS) static air temperature for run 7.**

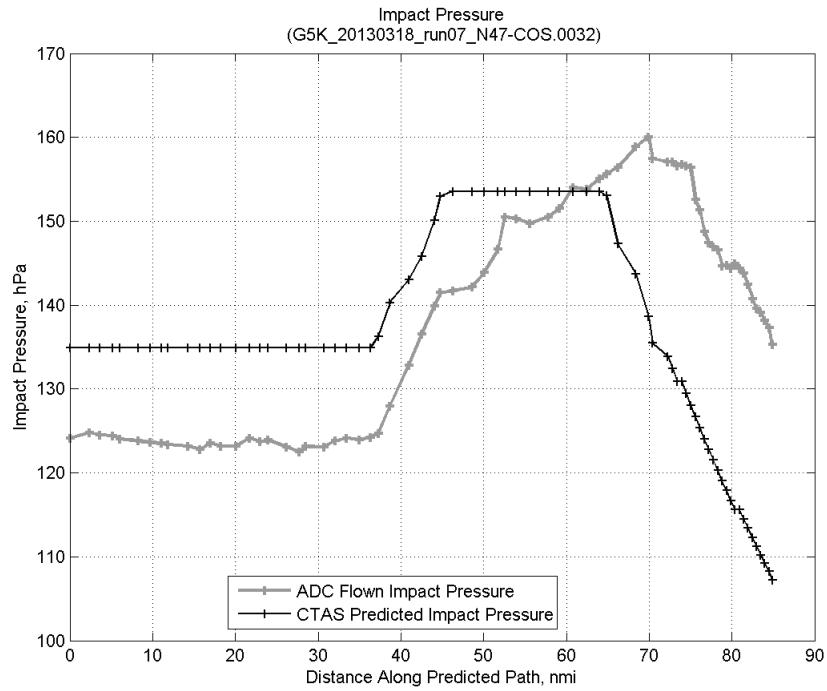


**Figure 164: Flown (ADC) and predicted (CTAS) impact pressure for run 7.**

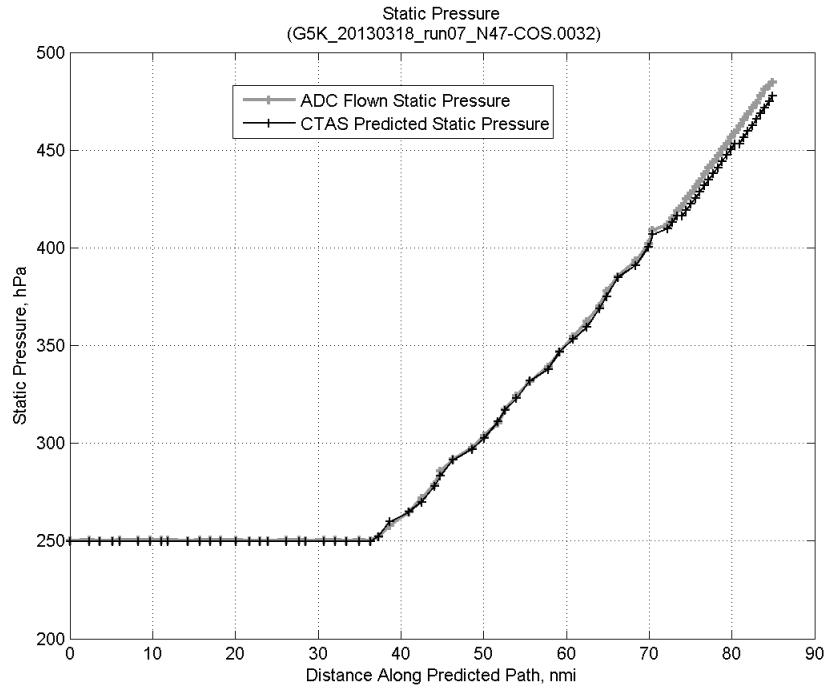


**Figure 165: Flown (ADC) and predicted (CTAS) static pressure for run 7.**

#### C.6.G. Path Distance

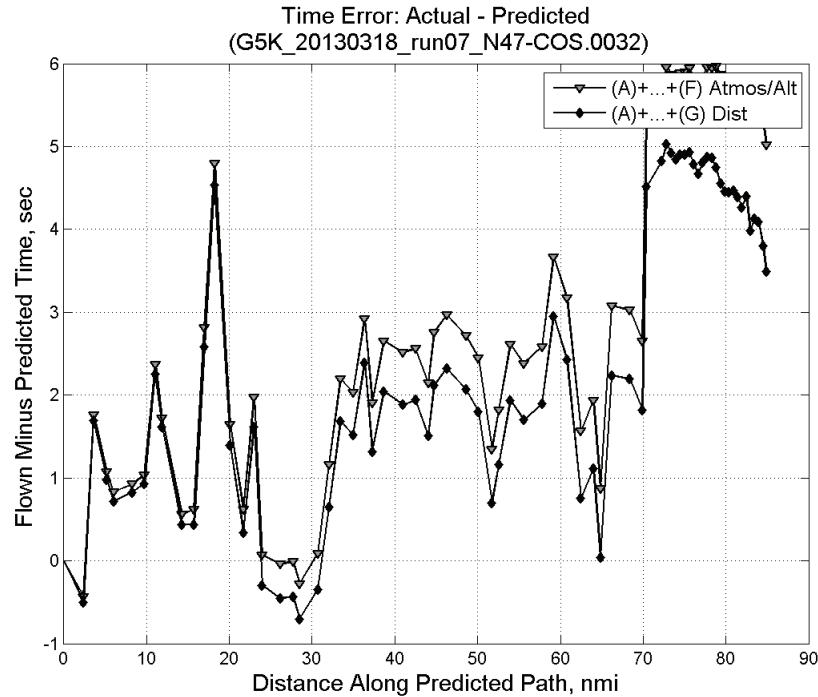


**Figure 166: Time error for run 7 before ((A)+...+(F) Atmos/Alt) and after ((A)+...+(G) Dist) removing path distance error source.**

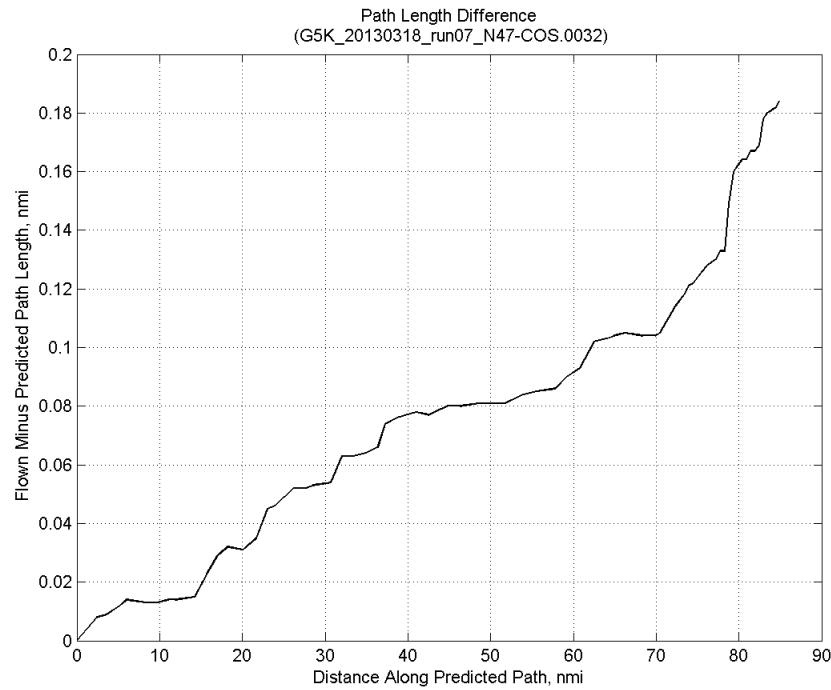


**Figure 167: ADC flown minus CTAS predicted path length for run 7. Positive values indicate aircraft followed a longer path than predicted by CTAS.**

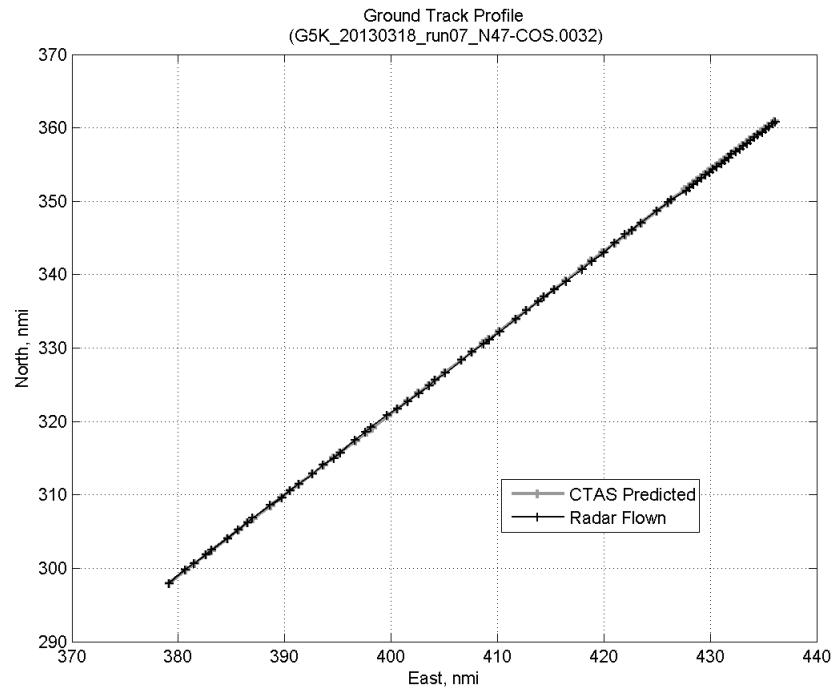


**Figure 168: CTAS predicted and radar flown ground track profile for run 7.**

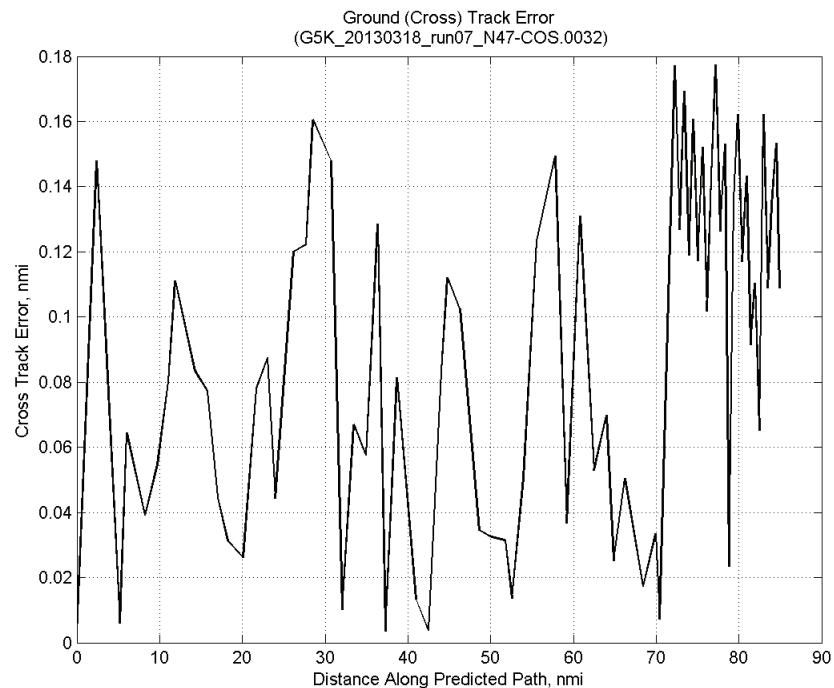


**Figure 169: Ground (cross) track error for run 7.**

### C.7. Run 10

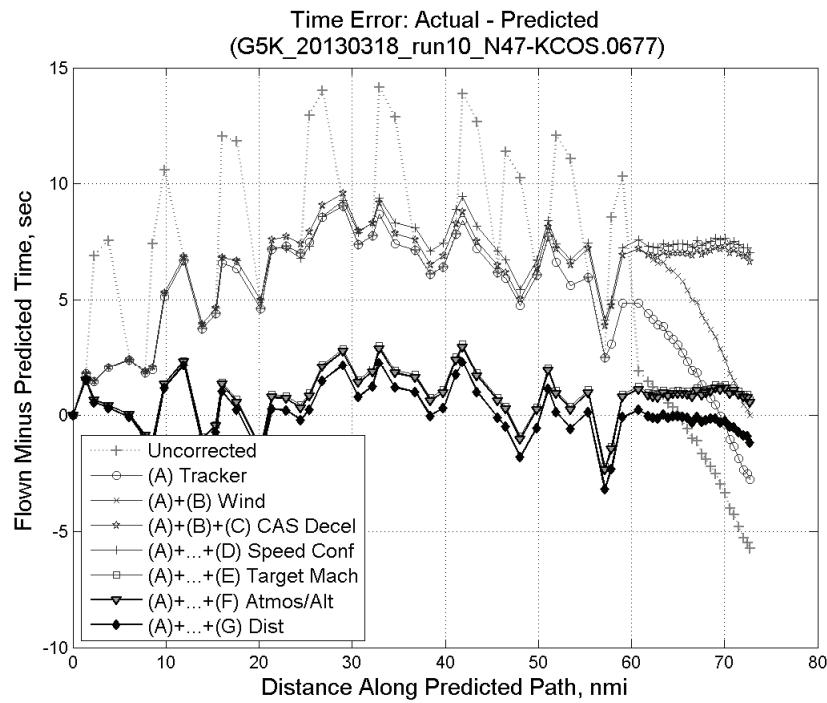


**Figure 170: Time error for run 10 showing incremental effect of removing each error source.**

#### C.7.A. Tracker Jumps

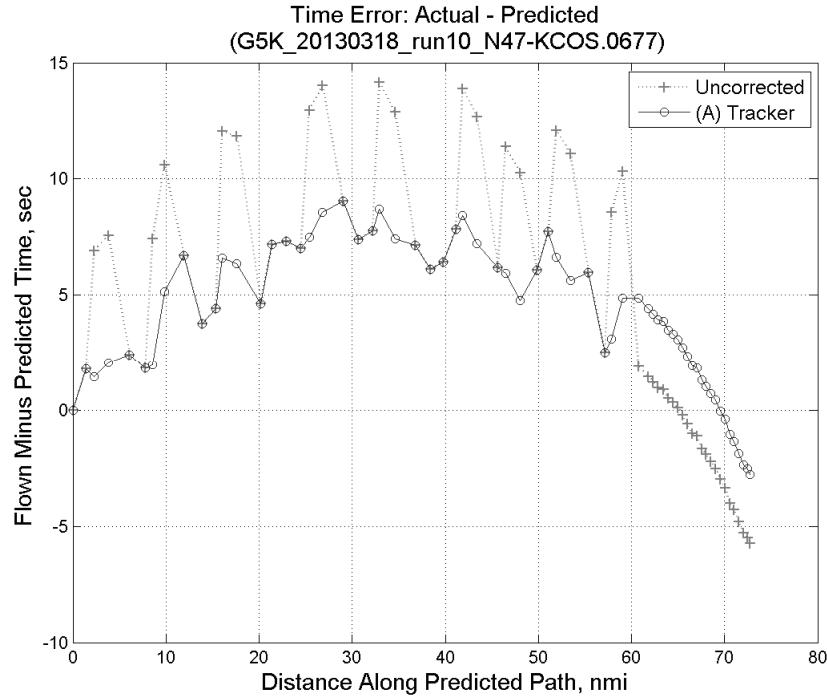


**Figure 171: Time error for run 10 before (Uncorrected) and after ((A) Tracker) removing tracker jump error source.**

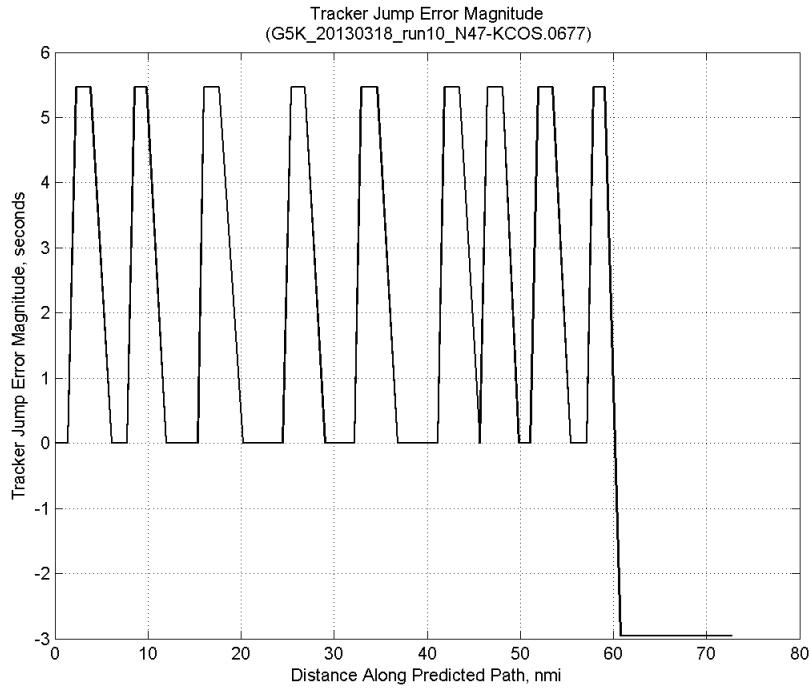


**Figure 172: Effect of tracker jump error source on time error for run 10.**

### C.7.B. Wind

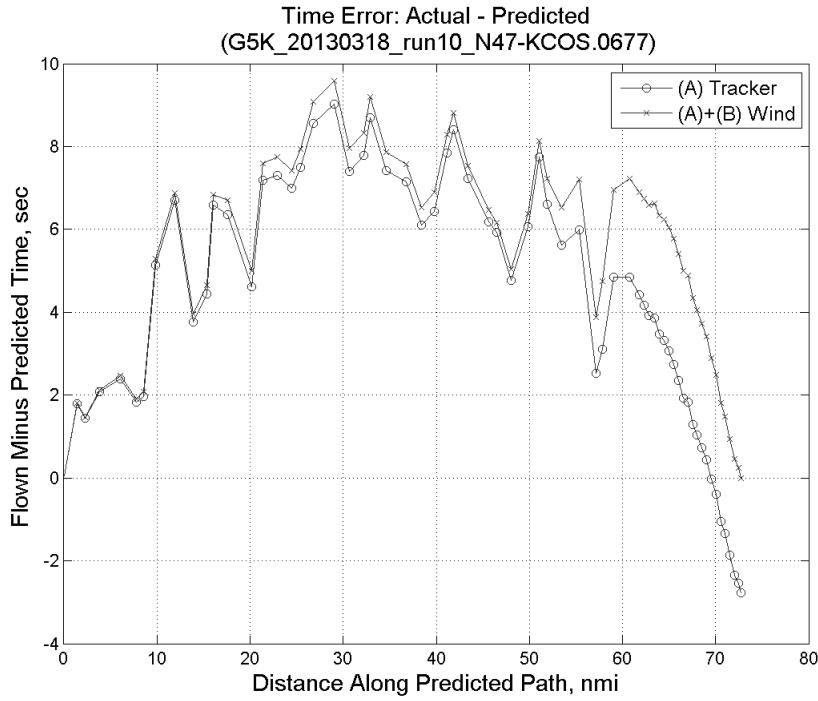


**Figure 173: Time error for run 10 before ((A) Tracker) and after ((A)+(B) Wind) removing wind error source.**

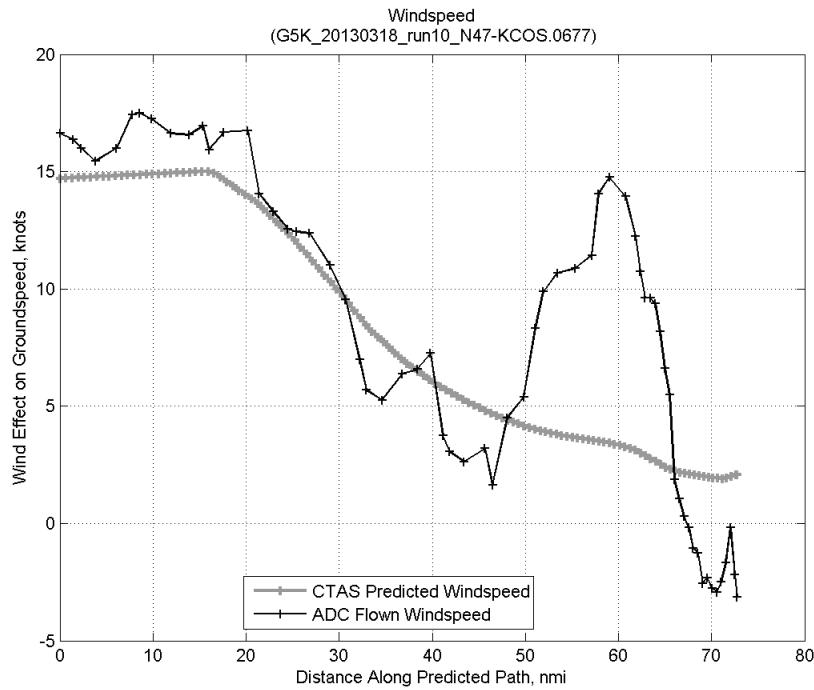


**Figure 174: CTAS predicted and ADC flown wind effect on ground speed for run 10. Negative values indicate a headwind.**

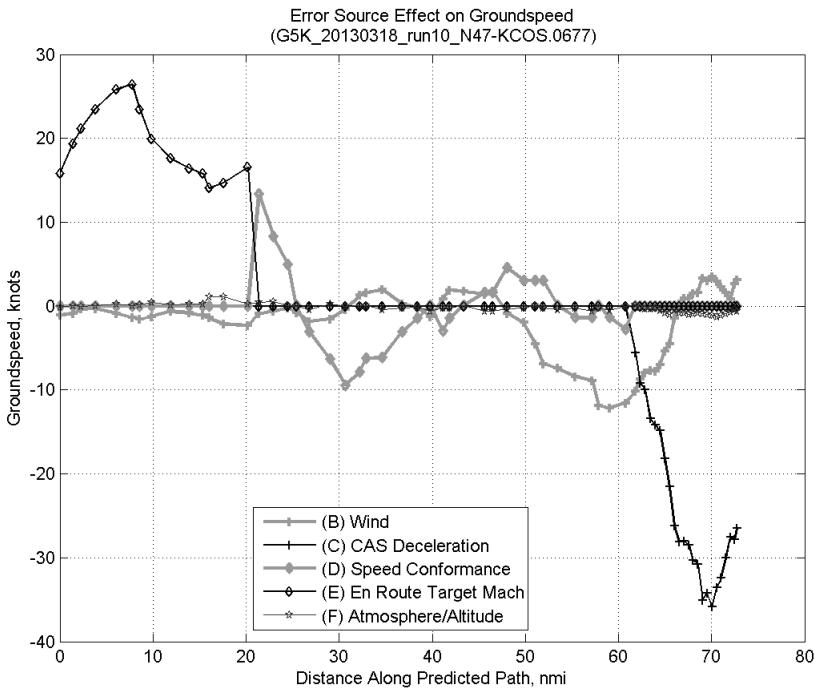


**Figure 175: Error sources (flown minus predicted) converted to a ground speed effect for run 10. Positive values indicate the flown ground speed was faster than the CTAS prediction.**

### C.7.C. CAS Deceleration

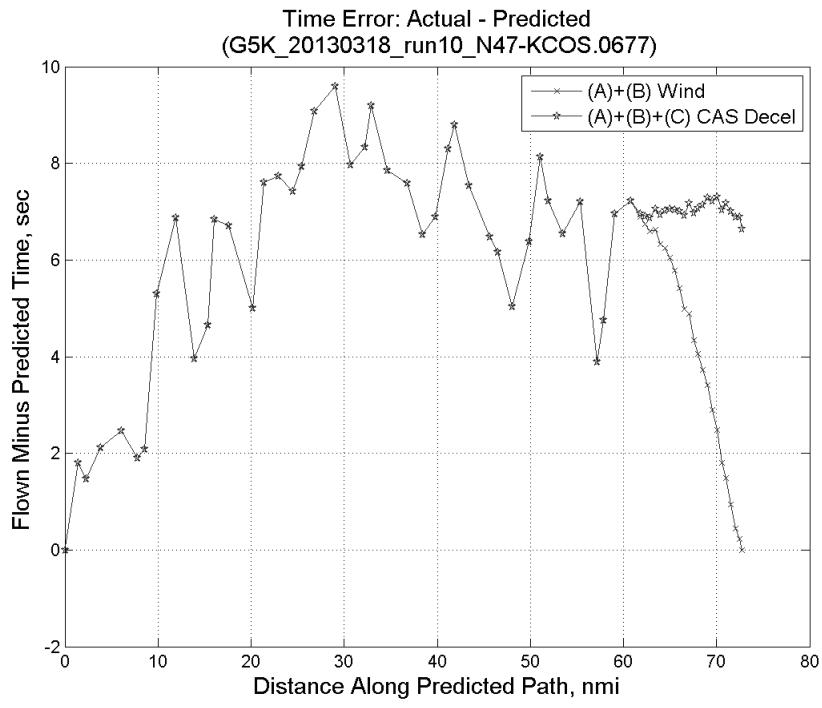


**Figure 176:** Time error for run 10 before ((A)+(B) Wind) and after ((A)+(B)+(C) CAS Decel) removing CAS deceleration error source.

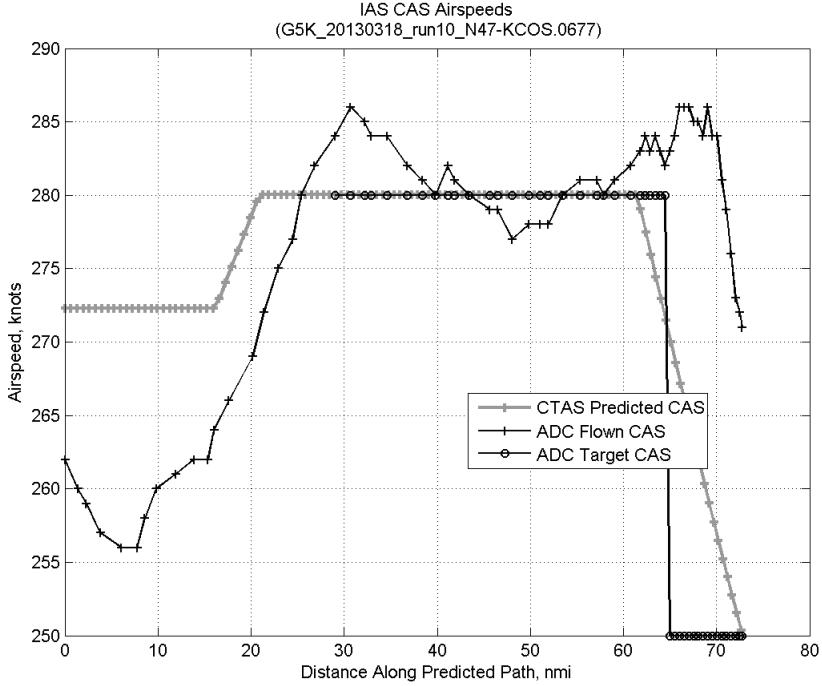


**Figure 177:** CTAS predicted and ADC flown CAS for run 10. CAS that is being targeted is shown with circle markers.

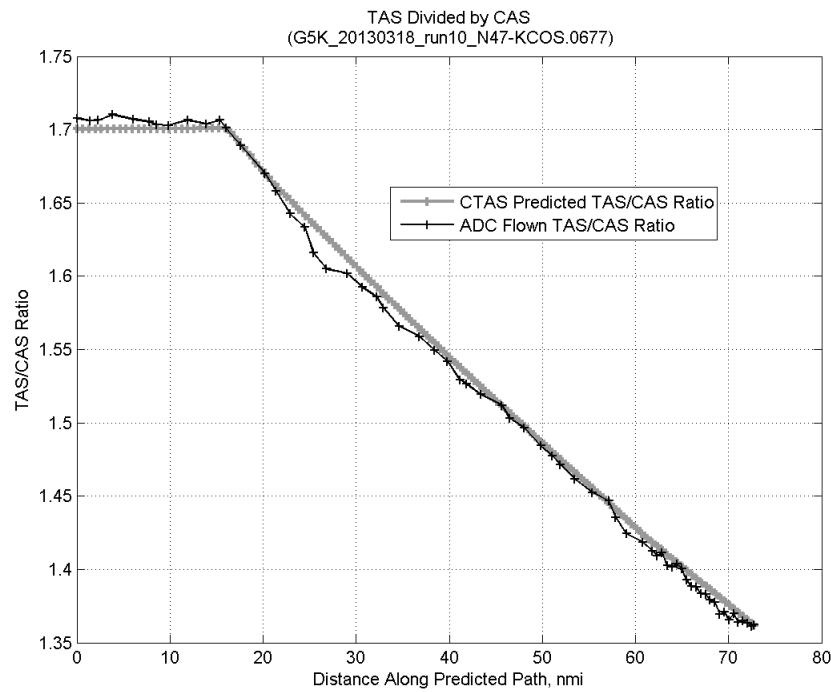


**Figure 178: CTAS predicted and ADC flown TAS/CAS ratio for run 10.**

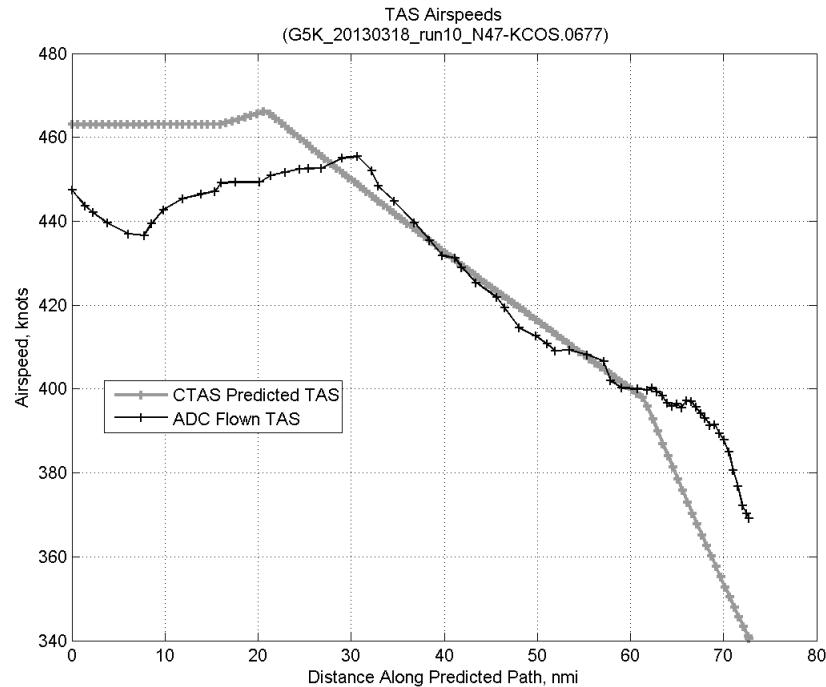


**Figure 179: CTAS predicted and ADC flown TAS for run 10.**

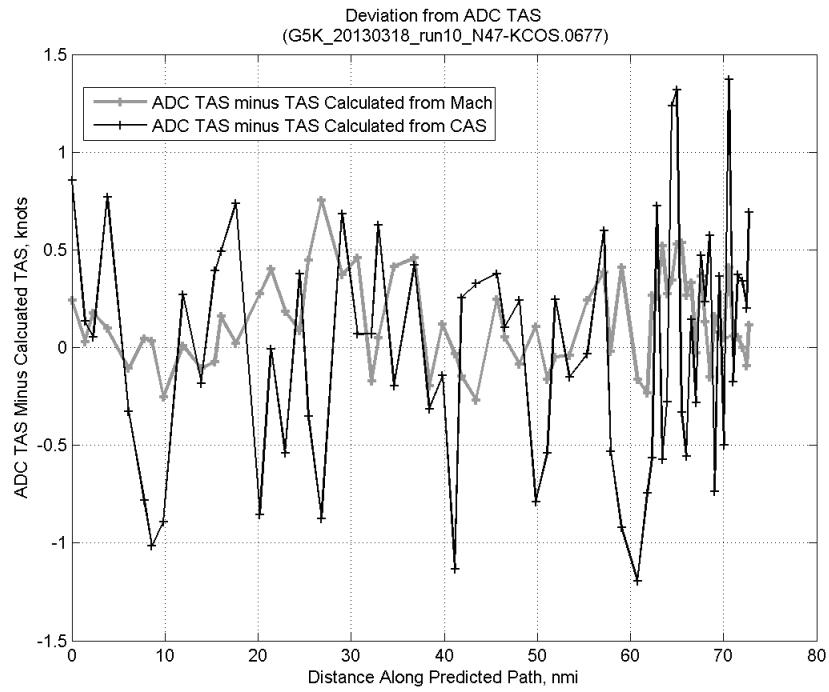


**Figure 180: Deviation from ADC flown TAS if calculating TAS using ADC flown CAS, Mach, atmospheric temperature, and atmospheric pressure for run 10.**

#### C.7.D. Speed Conformance

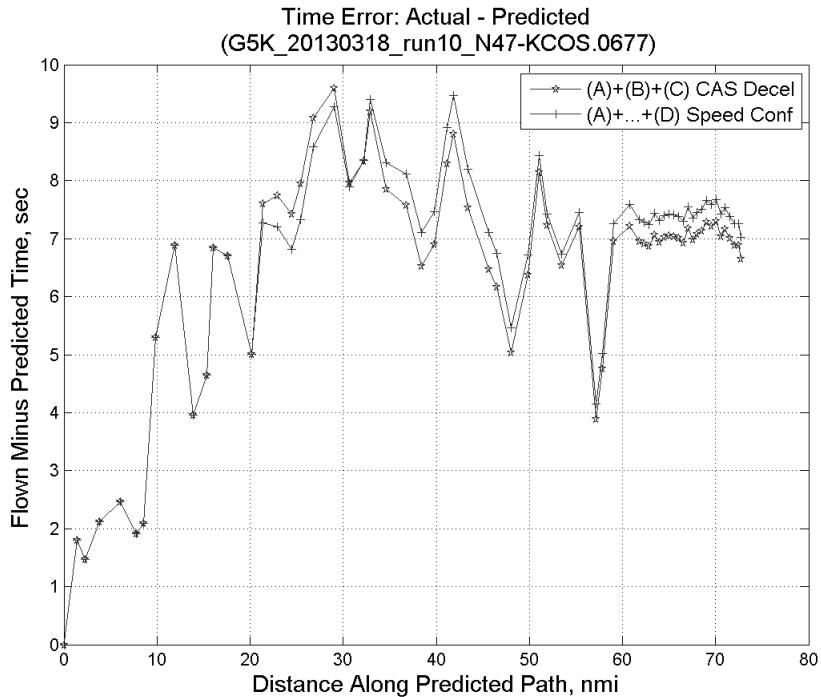


**Figure 181: Time error for run 10 before ((A)+(B)+(C) CAS Decel) and after ((A)+...+(D) Speed Conf) removing speed conformance error source.**

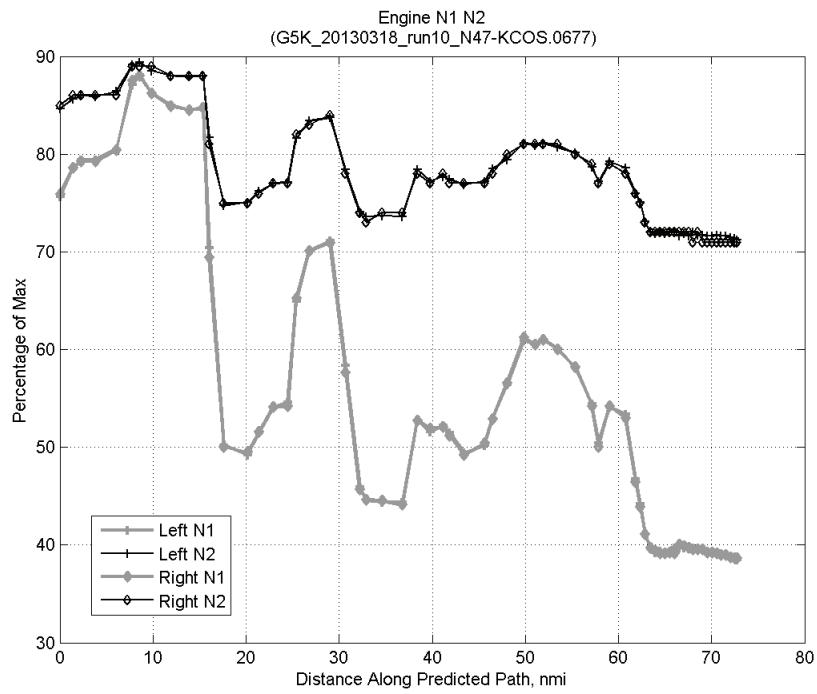


**Figure 182: Flown engine N1 and N2 for run 10.**

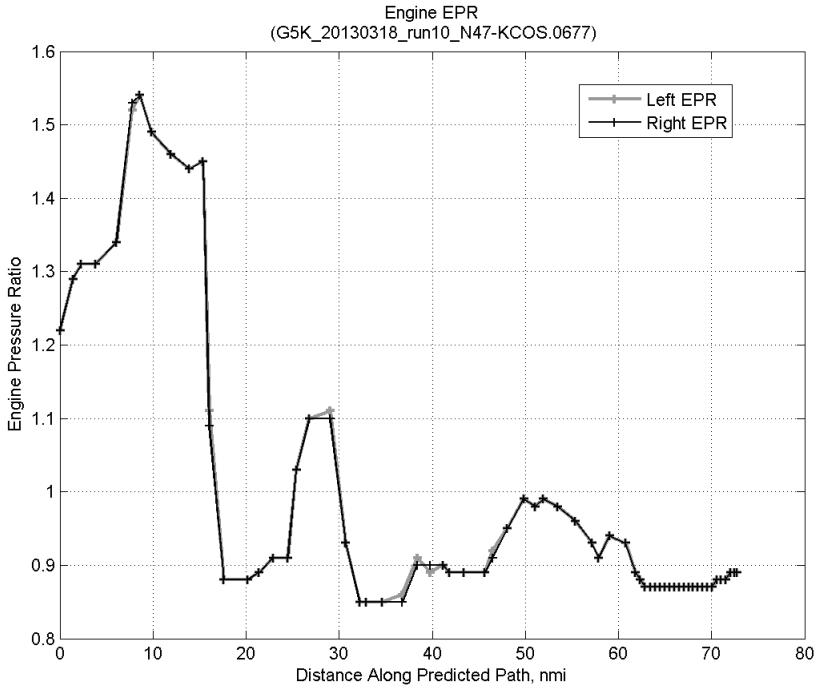


**Figure 183: Flown engine EPR for run 10.**

### C.7.E. Target Mach

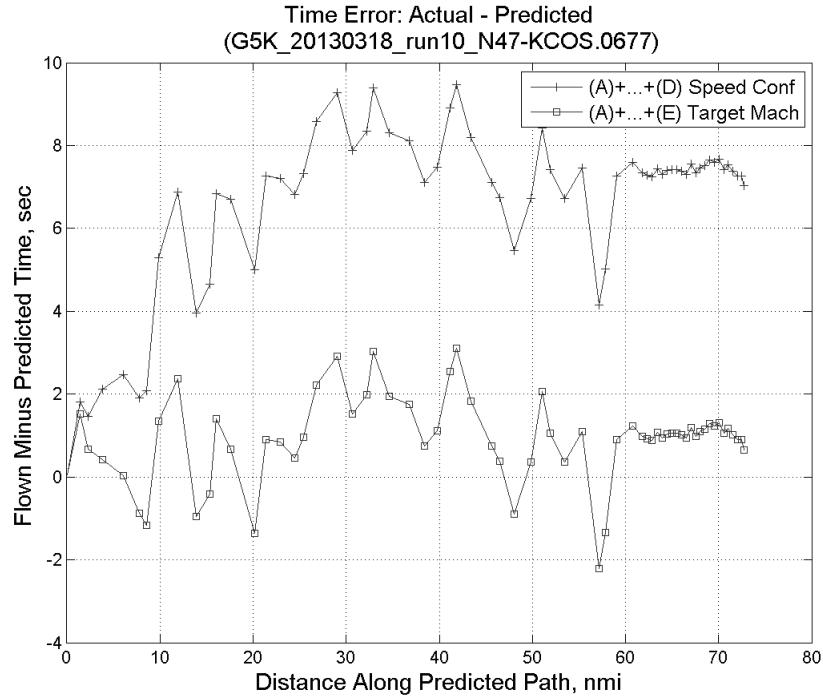


**Figure 184:** Time error for run 10 before ((A)+...+(D) Speed Conf) and after ((A)+...+(E) Target Mach) removing target Mach error source.

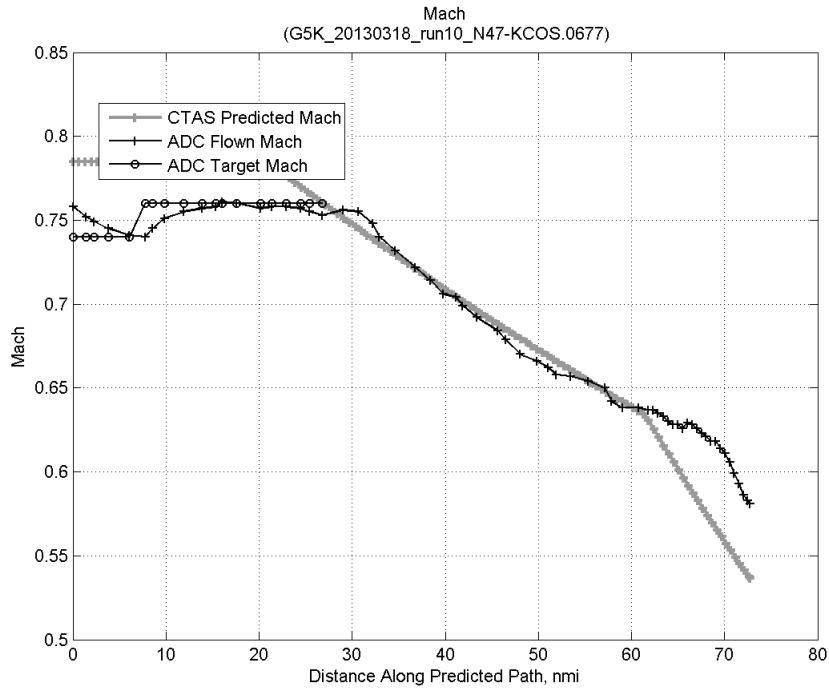


**Figure 185:** CTAS predicted and ADC flown Mach for run 10. Mach being targeted (ADC) shown with circle markers.

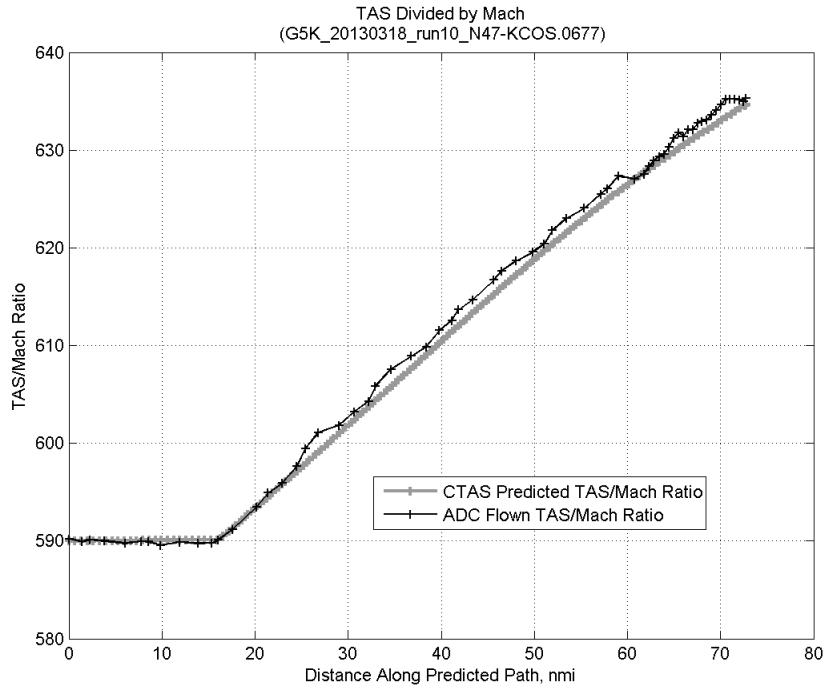


**Figure 186: CTAS predicted and ADC flown TAS/Mach ratio for run 10.**

#### C.7.F. Atmosphere/Altitude

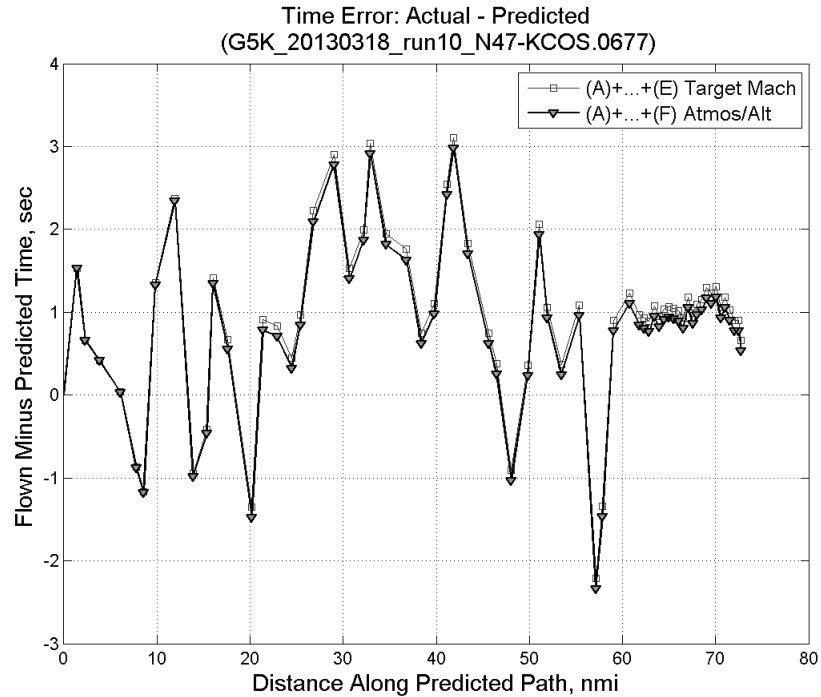


**Figure 187: Time error for run 10 before ((A)+...+(E) Target Mach) and after ((A)+...+(F) Atmos/Alt) removing atmosphere/altitude error source.**

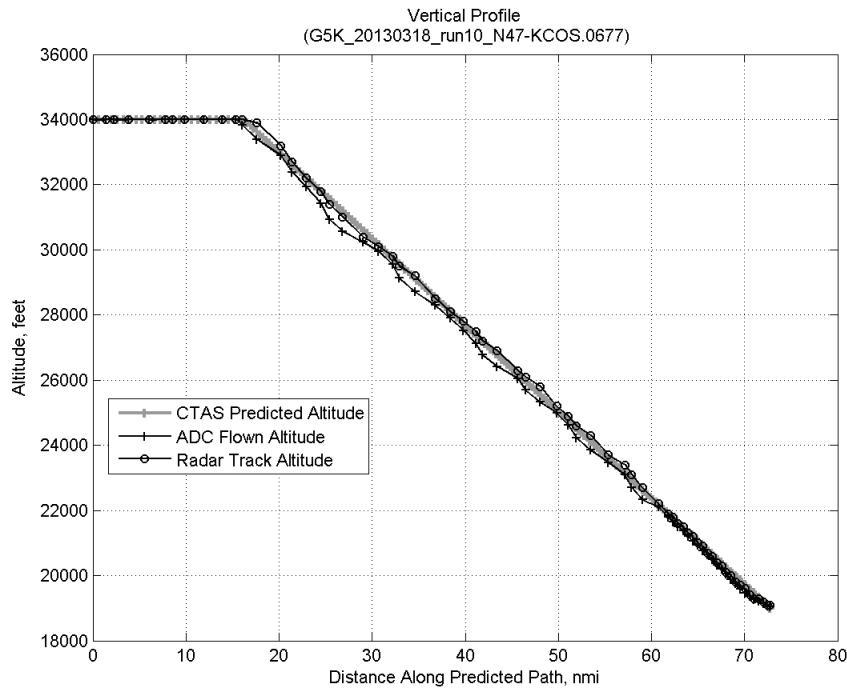


**Figure 188: Flown (ADC) and predicted (CTAS) vertical profile for run 10.**

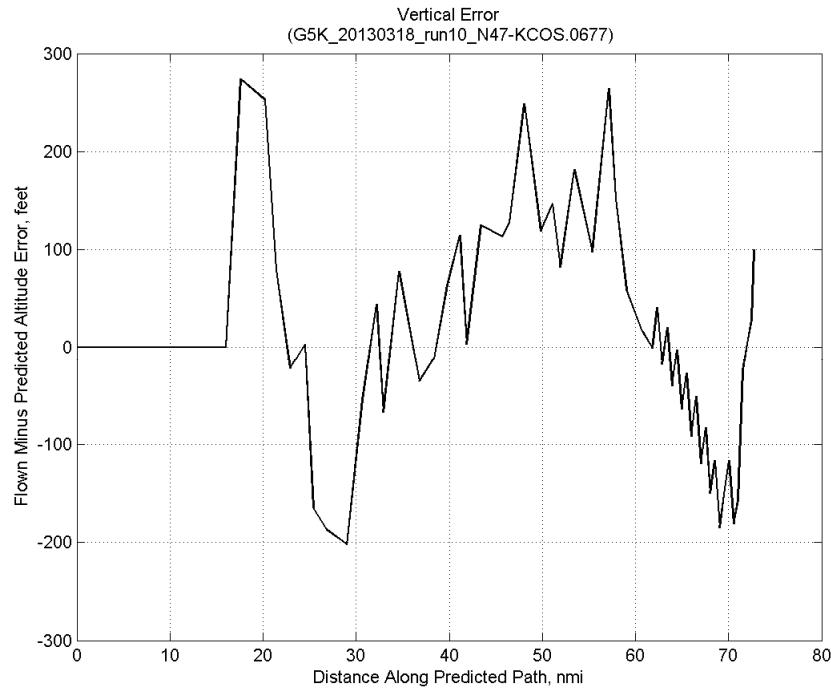


**Figure 189: Vertical error (flown minus predicted altitude) for run 10. Positive values indicate aircraft flew higher than predicted by CTAS.**

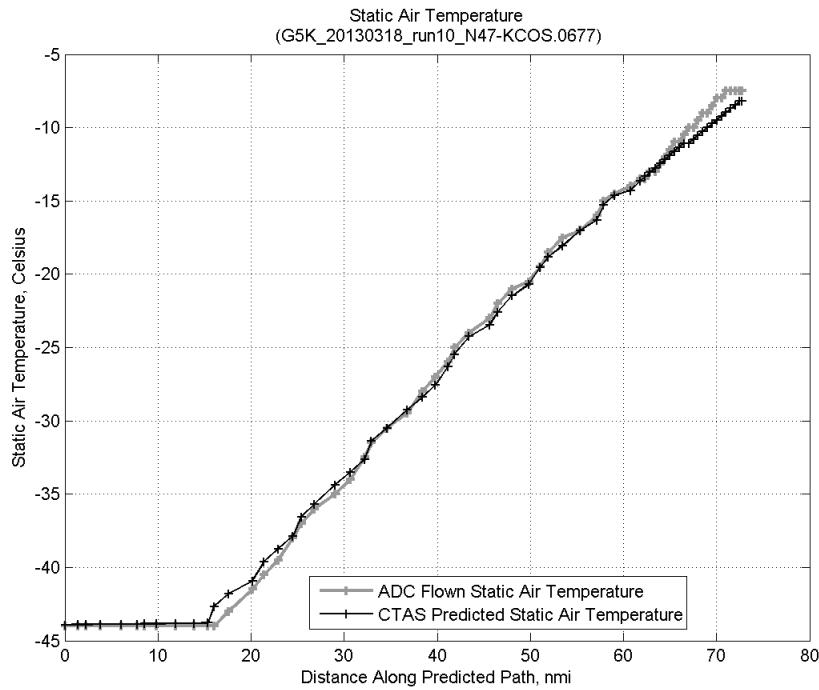


**Figure 190: Flown (ADC) and predicted (CTAS) static air temperature for run 10.**

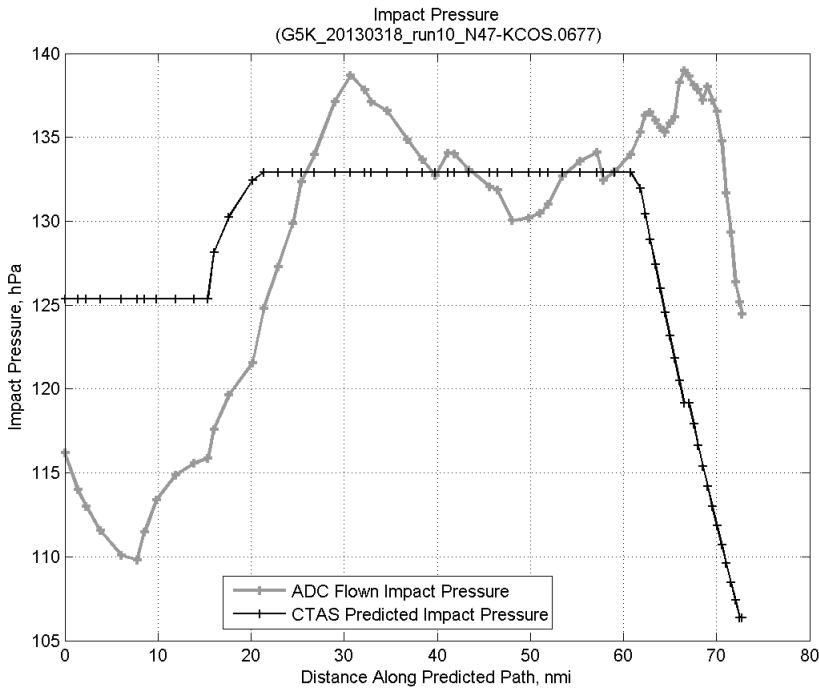


**Figure 191: Flown (ADC) and predicted (CTAS) impact pressure for run 10.**

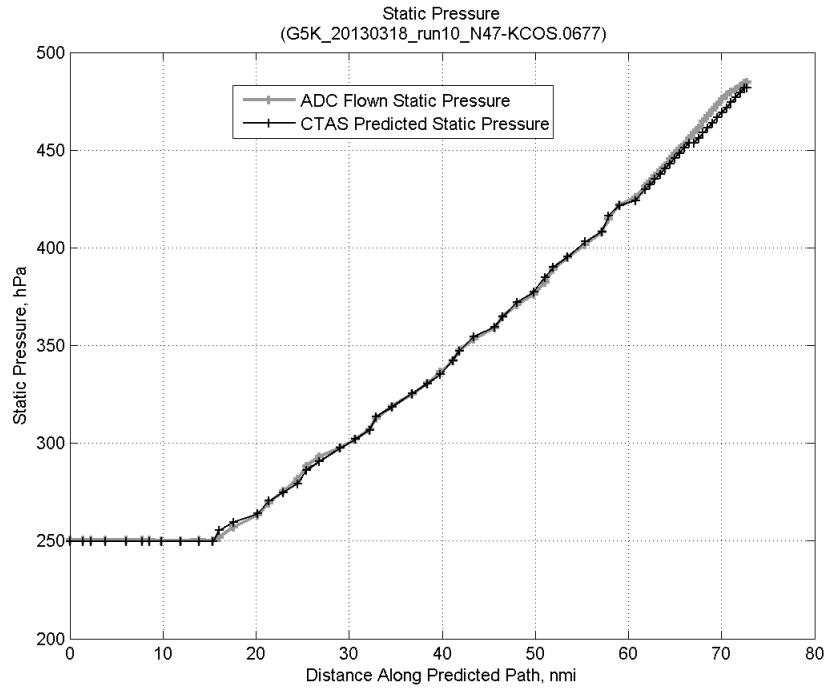


**Figure 192: Flown (ADC) and predicted (CTAS) static pressure for run 10.**

#### C.7.G. Path Distance

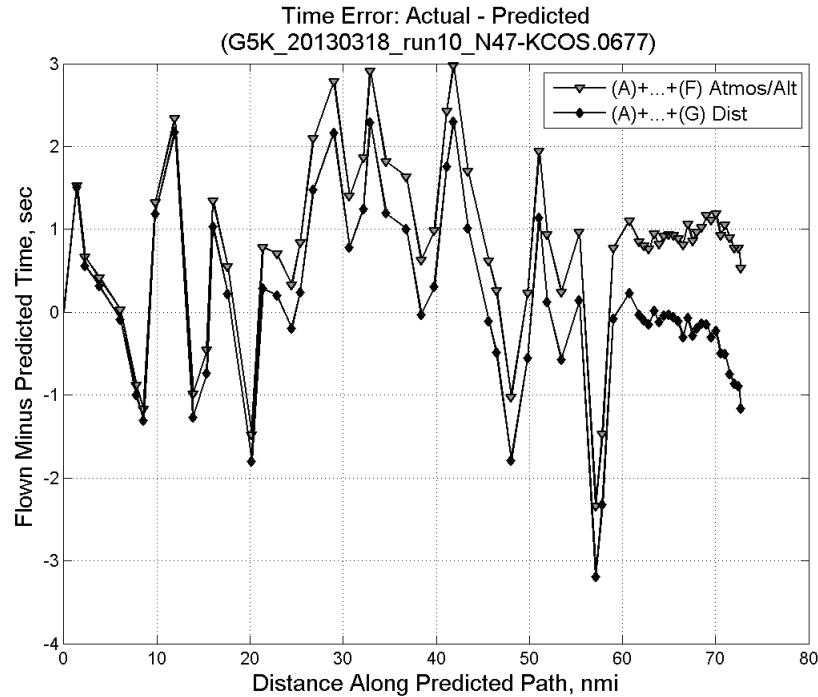


**Figure 193: Time error for run 10 before ((A)+...+(F) Atmos/Alt) and after ((A)+...+(G) Dist) removing path distance error source.**

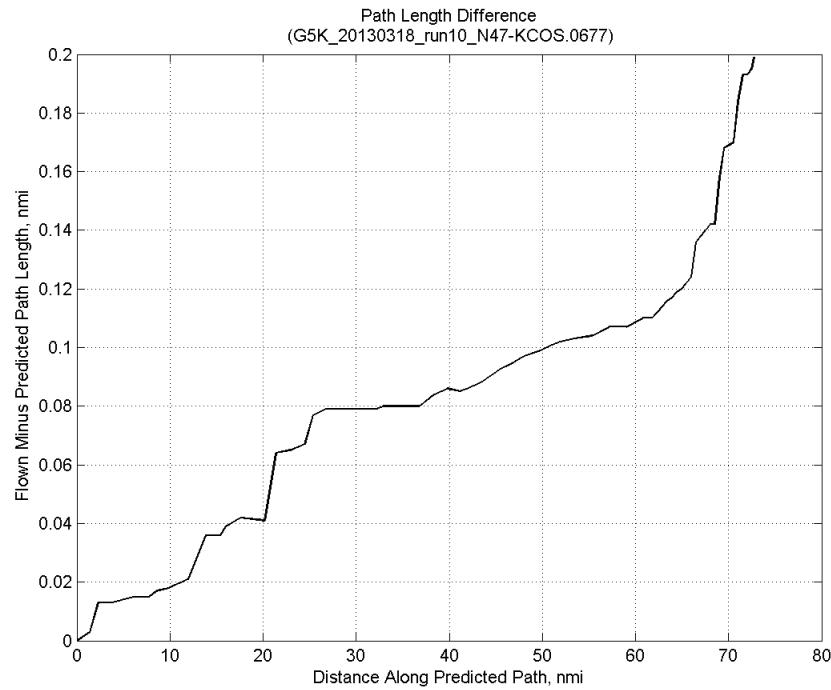


**Figure 194: ADC flown minus CTAS predicted path length for run 10. Positive values indicate aircraft followed a longer path than predicted by CTAS.**

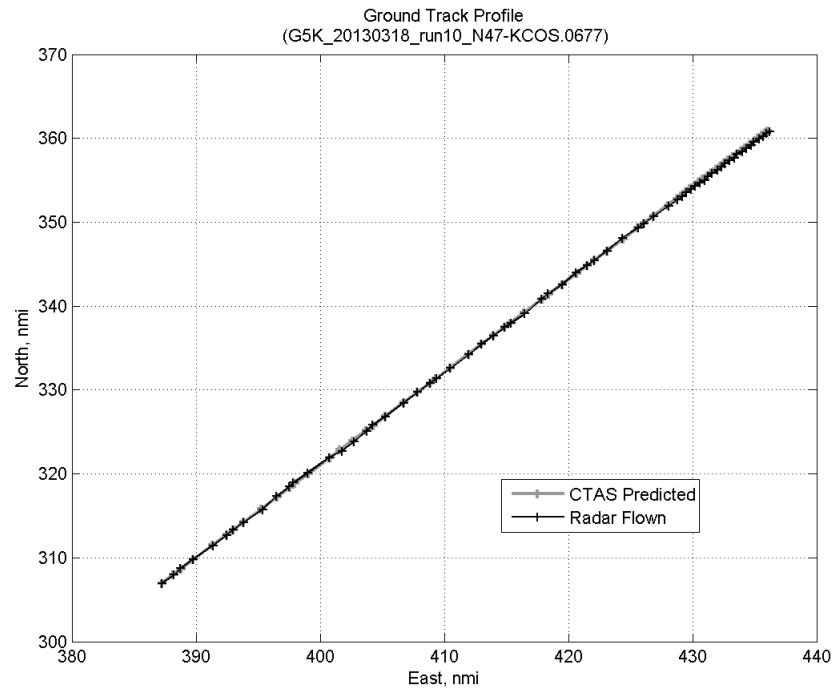


**Figure 195: CTAS predicted and radar flown ground track profile for run 10.**

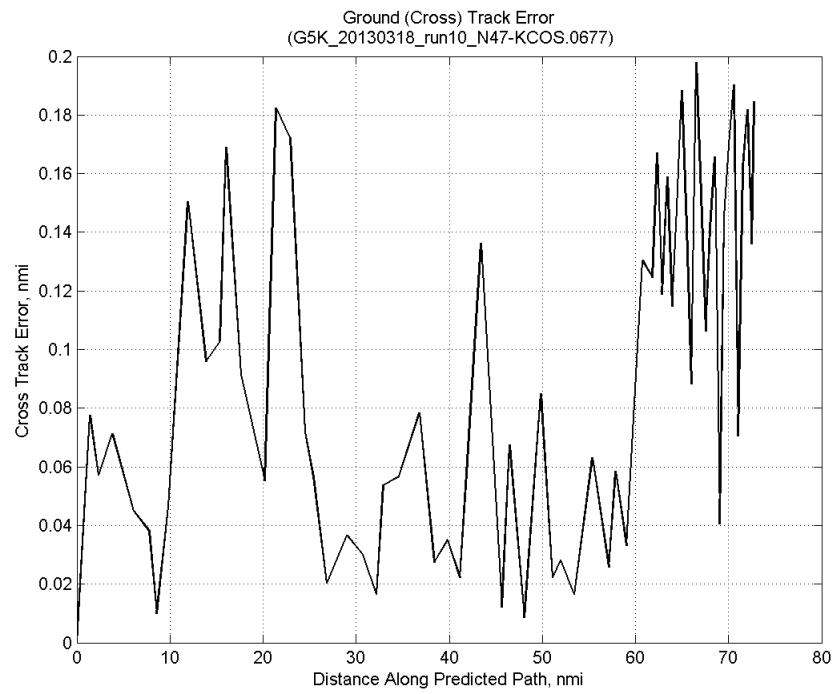


**Figure 196: Ground (cross) track error for run 10.**

## C.8. Run 12

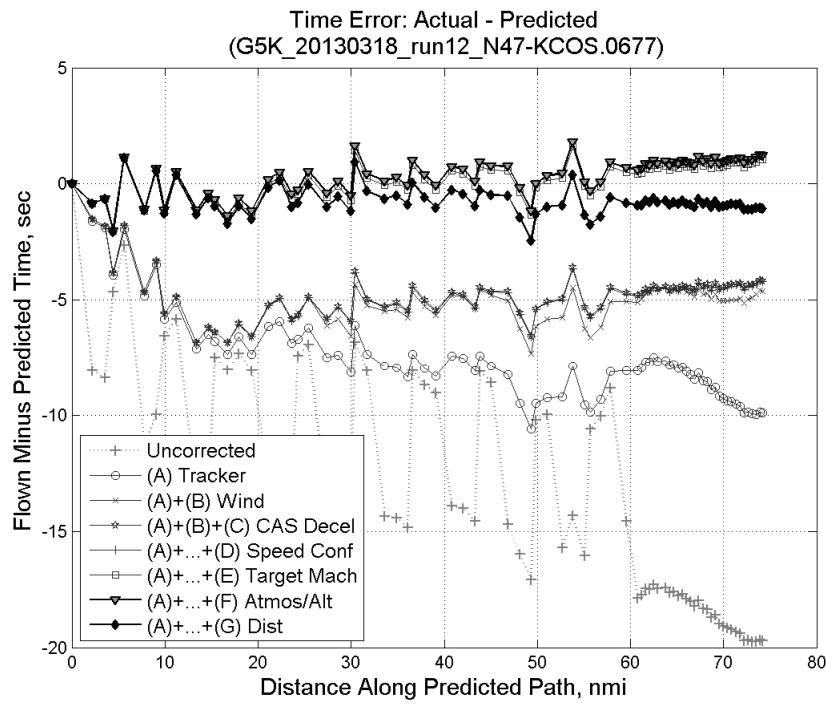


**Figure 197: Time error for run 12 showing incremental effect of removing each error source.**

### C.8.A. Tracker Jumps

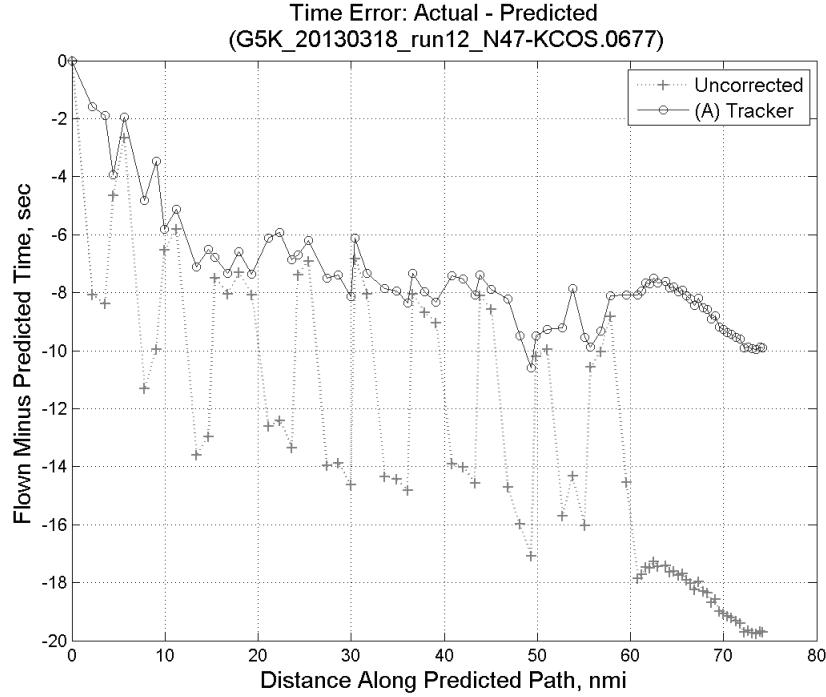


**Figure 198: Time error for run 12 before (Uncorrected) and after ((A) Tracker) removing tracker jump error source.**

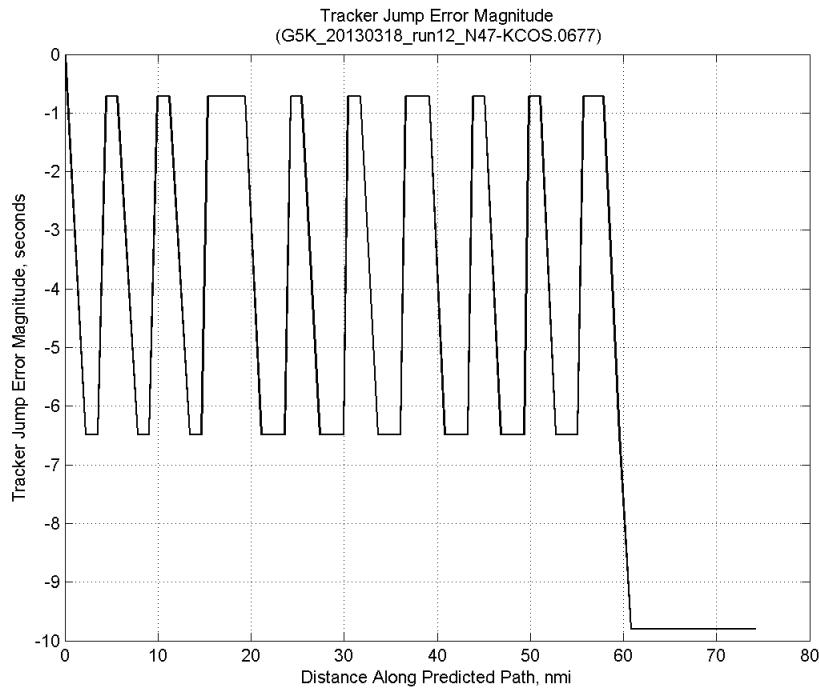


**Figure 199: Effect of tracker jump error source on time error for run 12.**

### C.8.B. Wind

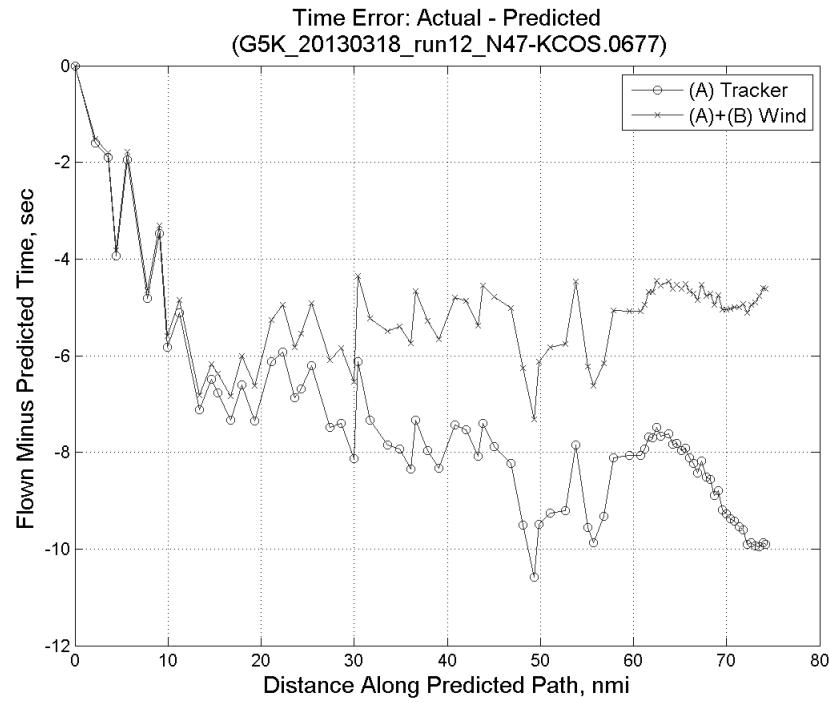


**Figure 200: Time error for run 12 before ((A) Tracker) and after ((A)+(B) Wind) removing wind error source.**

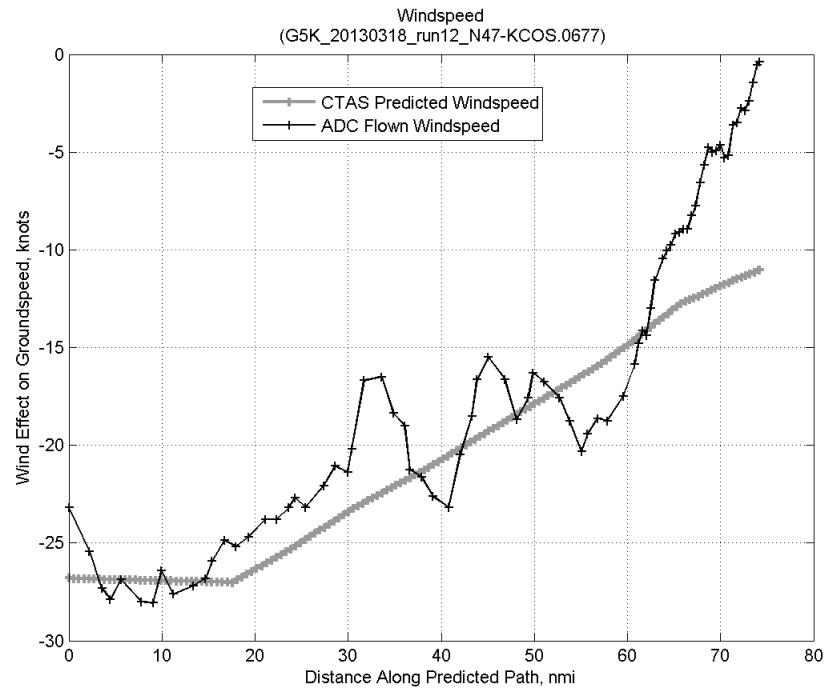


**Figure 201: CTAS predicted and ADC flown wind effect on ground speed for run 12. Negative values indicate a headwind.**

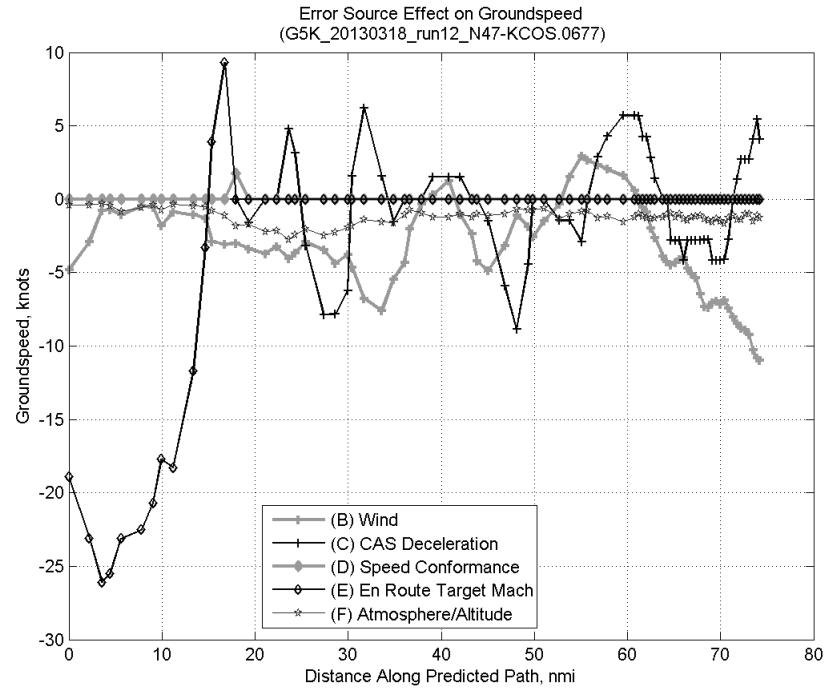


**Figure 202: Error sources (flown minus predicted) converted to a ground speed effect for run 12. Positive values indicate the flown ground speed was faster than the CTAS prediction.**

### C.8.C. CAS Deceleration

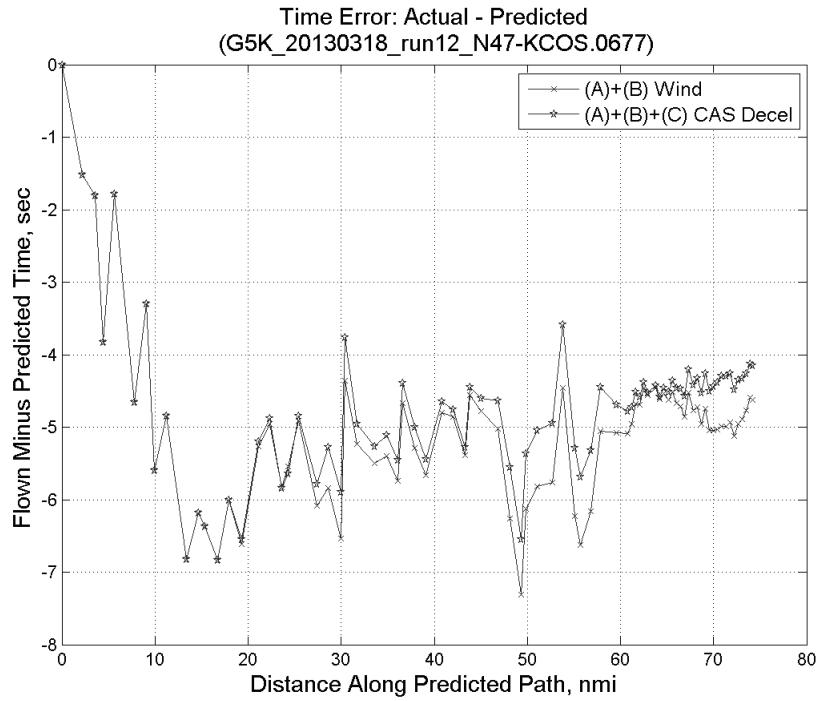


**Figure 203: Time error for run 12 before ((A)+(B) Wind) and after ((A)+(B)+(C) CAS Decel) removing CAS deceleration error source.**

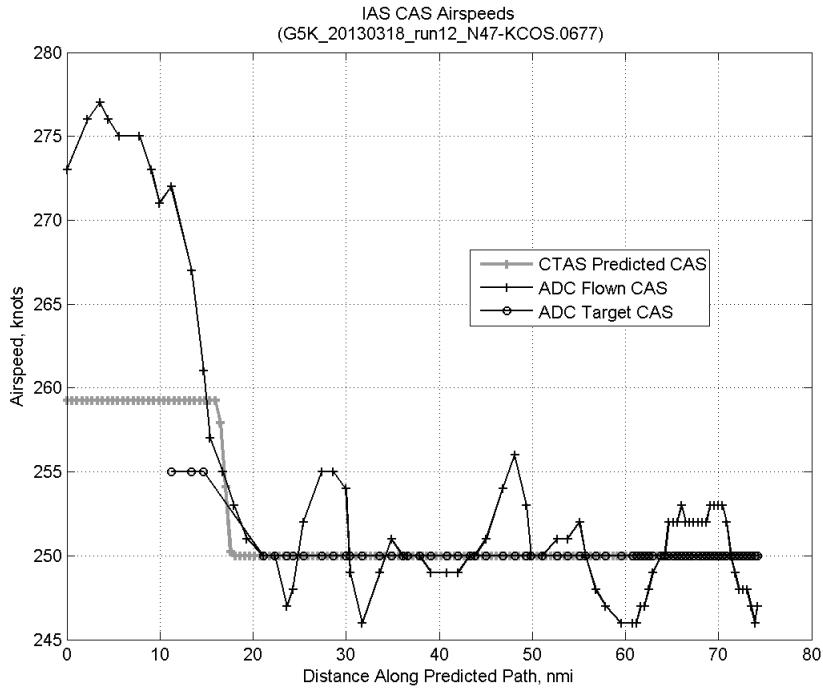


**Figure 204: CTAS predicted and ADC flown CAS for run 12. CAS that is being targeted is shown with circle markers.**

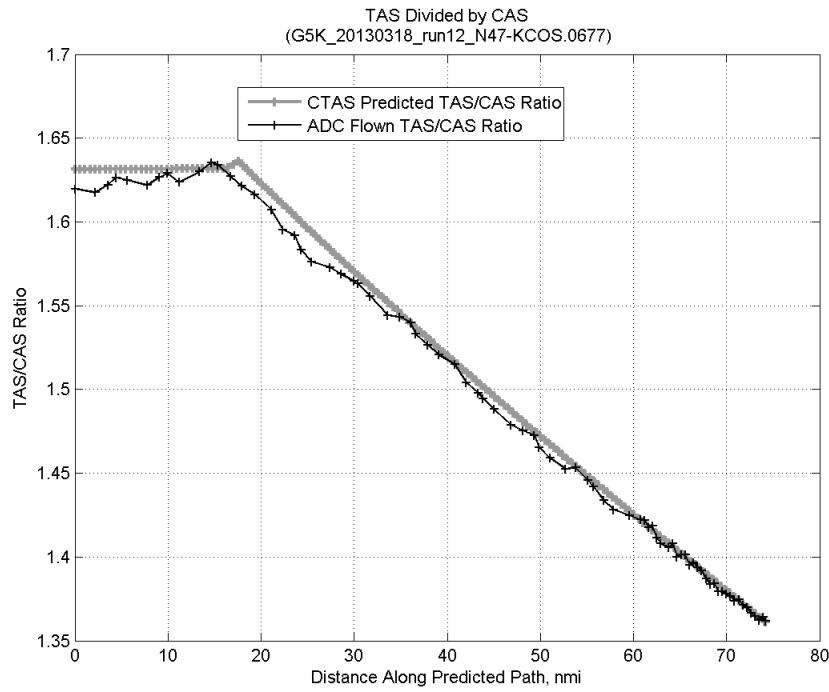


**Figure 205: CTAS predicted and ADC flown TAS/CAS ratio for run 12.**

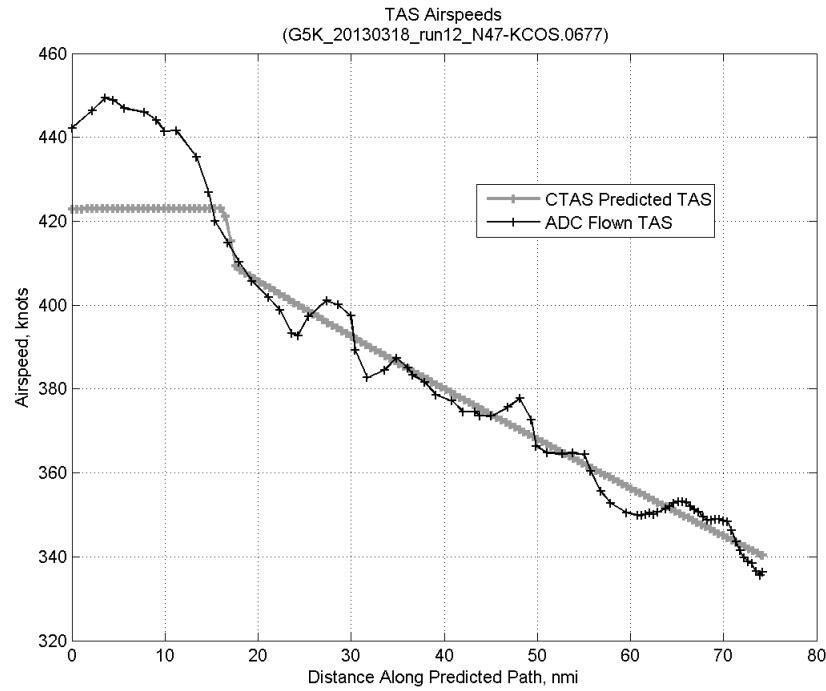


**Figure 206: CTAS predicted and ADC flown TAS for run 12.**

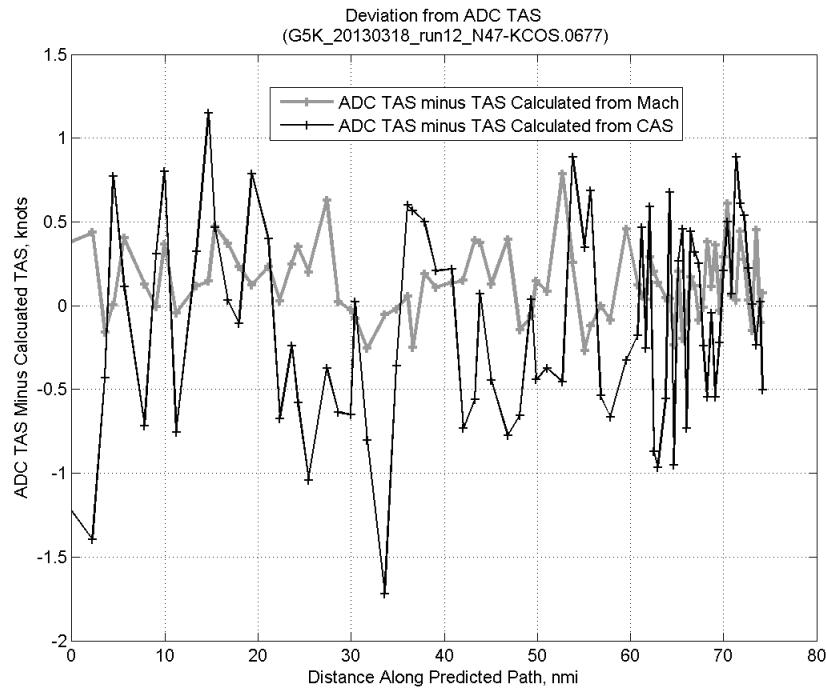


**Figure 207: Deviation from ADC flown TAS if calculating TAS using ADC flown CAS, Mach, atmospheric temperature, and atmospheric pressure for run 12.**

#### C.8.D. Speed Conformance

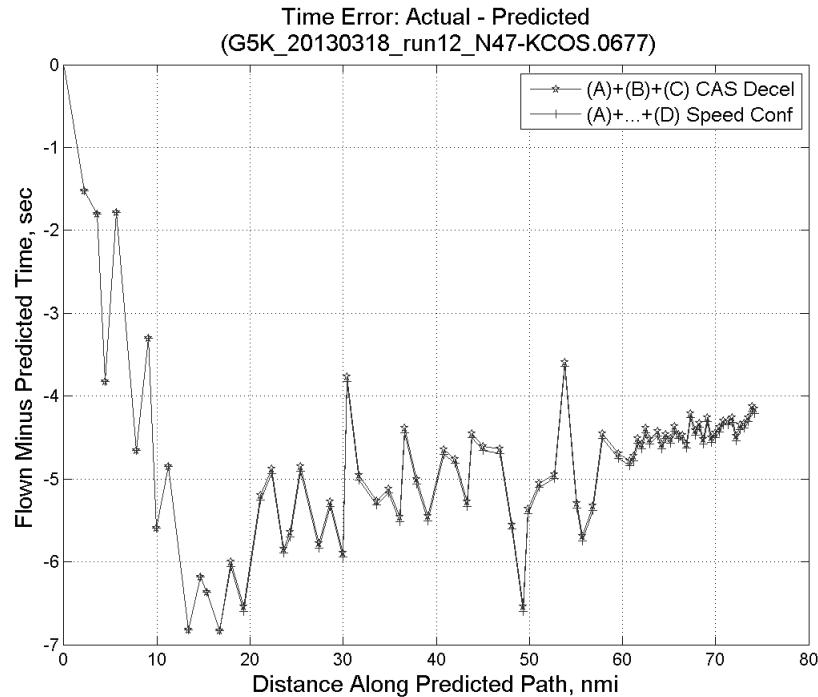


**Figure 208: Time error for run 12 before ((A)+(B)+(C) CAS Decel) and after ((A)+...+(D) Speed Conf) removing speed conformance error source.**

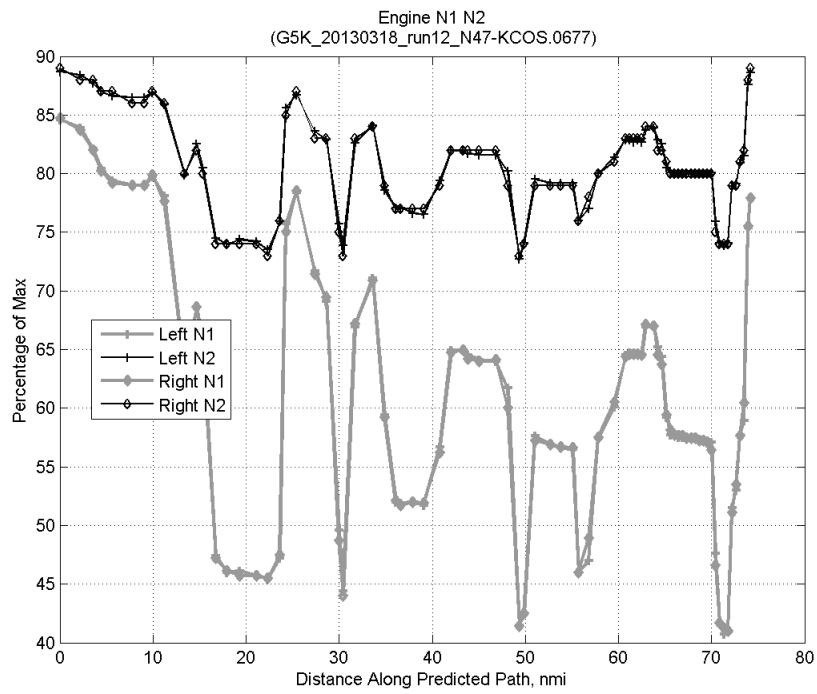


**Figure 209: Flown engine N1 and N2 for run 12.**

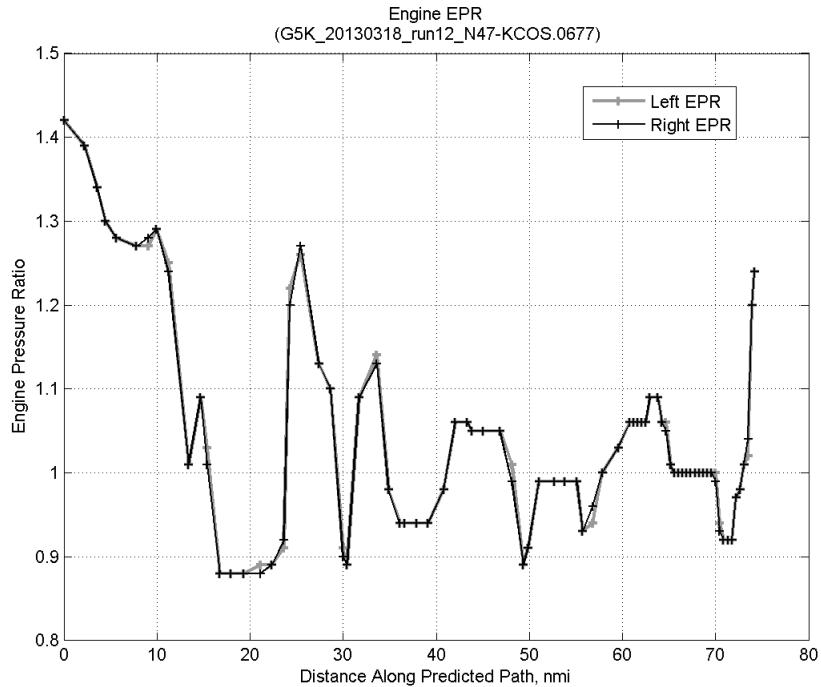


**Figure 210: Flown engine EPR for run 12.**

### C.8.E. Target Mach

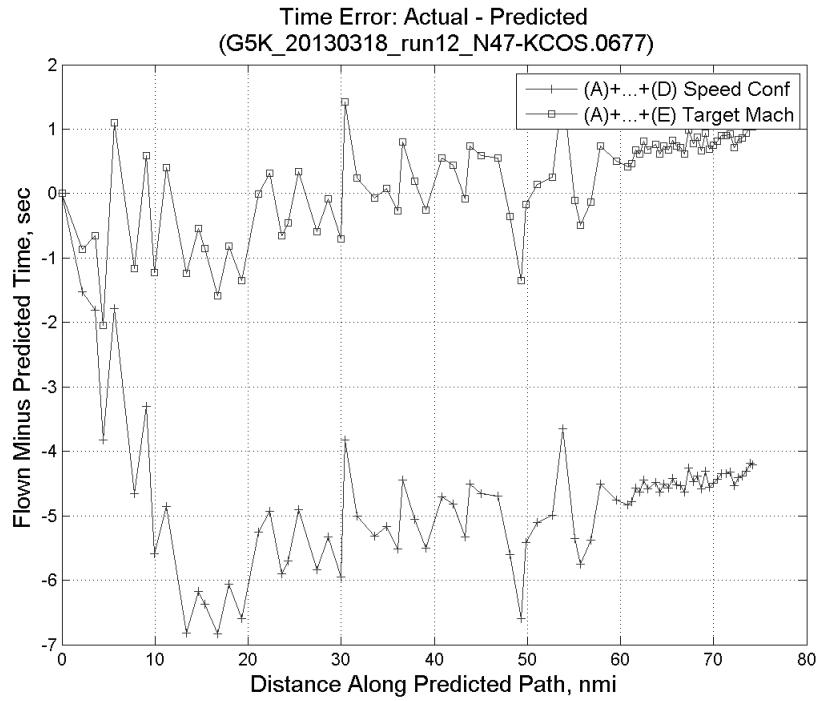


**Figure 211:** Time error for run 12 before ((A)+...+(D) Speed Conf) and after ((A)+...+(E) Target Mach) removing target Mach error source.

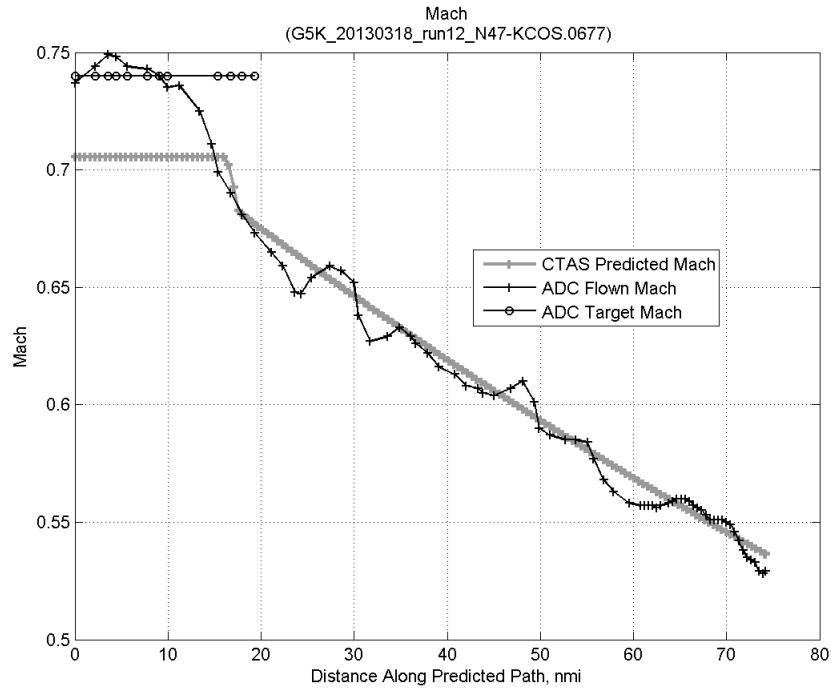


**Figure 212:** CTAS predicted and ADC flown Mach for run 12. Mach being targeted (ADC) shown with circle markers.

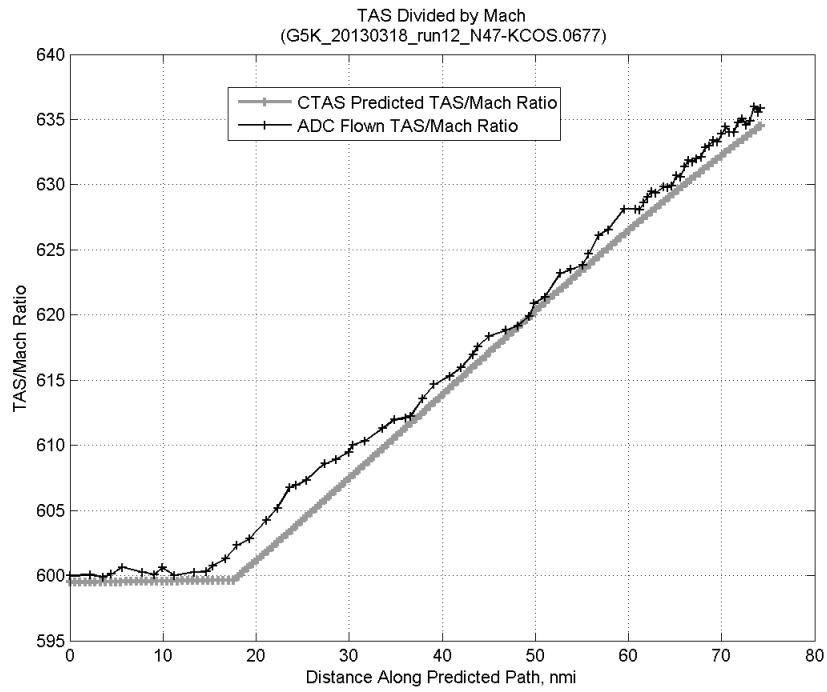


**Figure 213:** CTAS predicted and ADC flown TAS/Mach ratio for run 12.

#### C.8.F. Atmosphere/Altitude

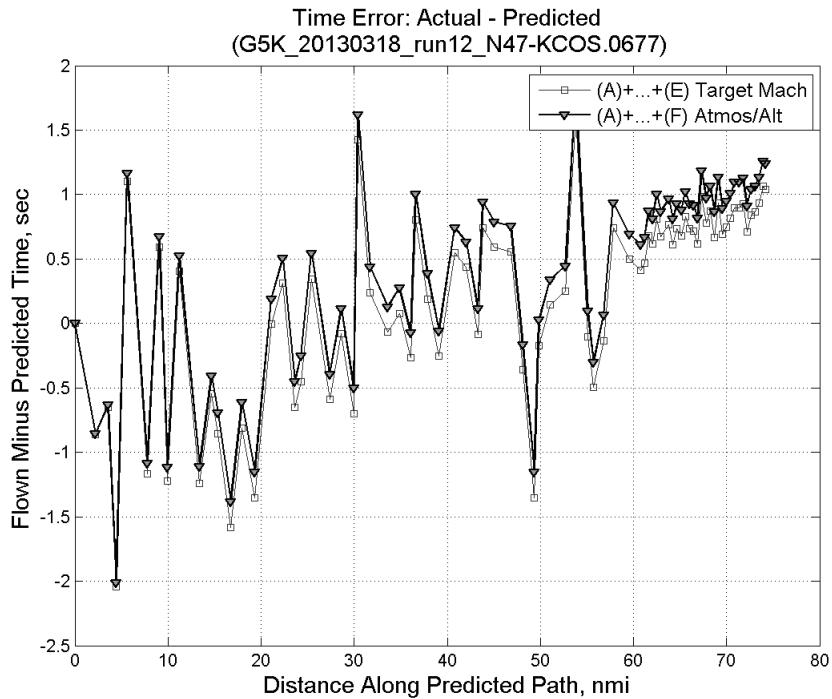


**Figure 214:** Time error for run 12 before ((A)+...+(E) Target Mach) and after ((A)+...+(F) Atmos/Alt) removing atmosphere/altitude error source.

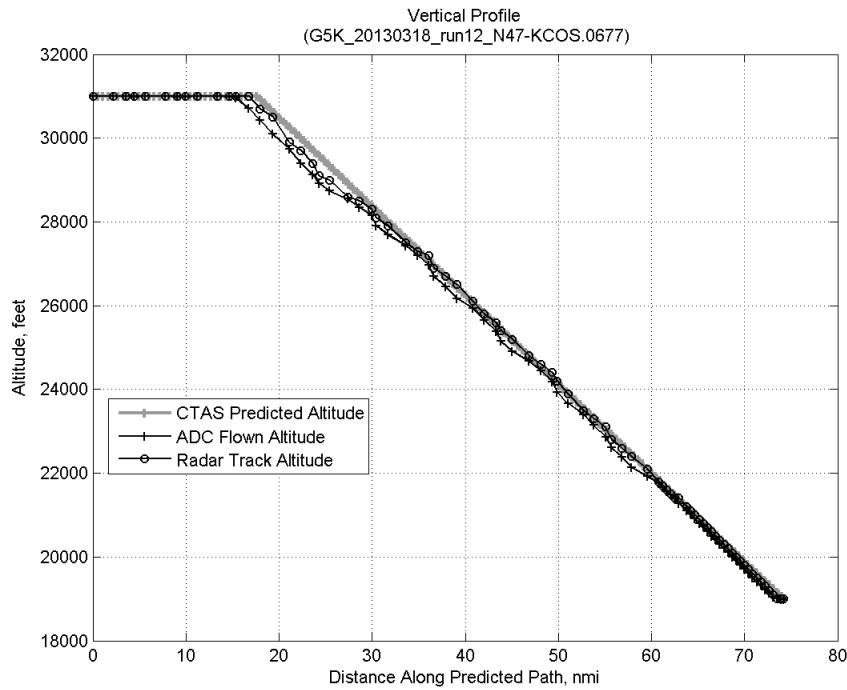


**Figure 215: Flown (ADC) and predicted (CTAS) vertical profile for run 12.**

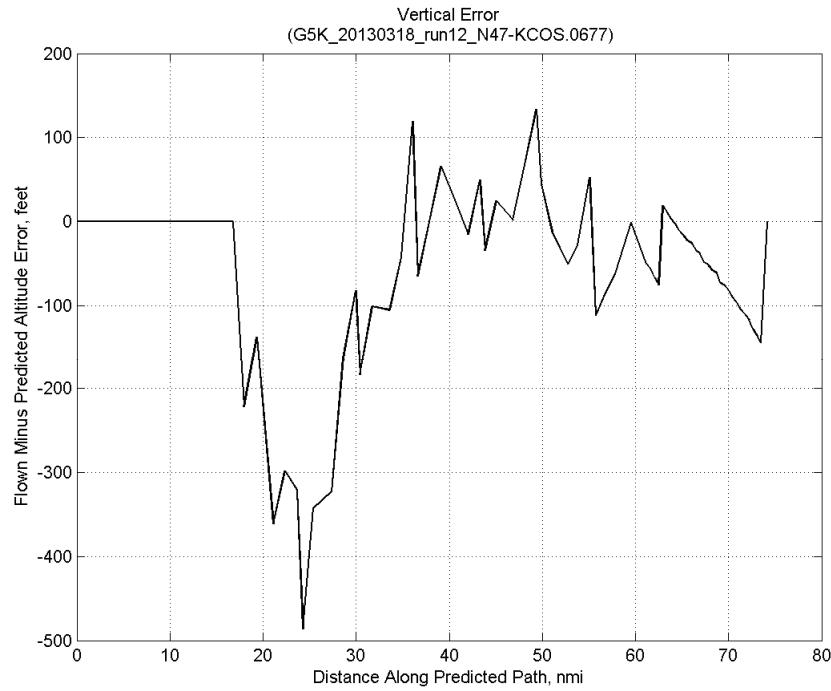


**Figure 216: Vertical error (flown minus predicted altitude) for run 12. Positive values indicate aircraft flew higher than predicted by CTAS.**

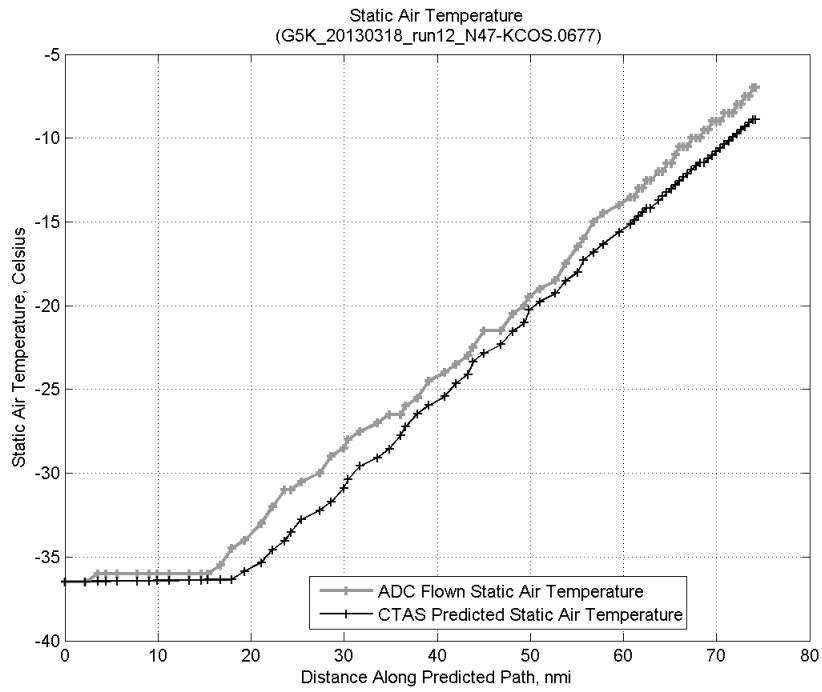


**Figure 217: Flown (ADC) and predicted (CTAS) static air temperature for run 12.**

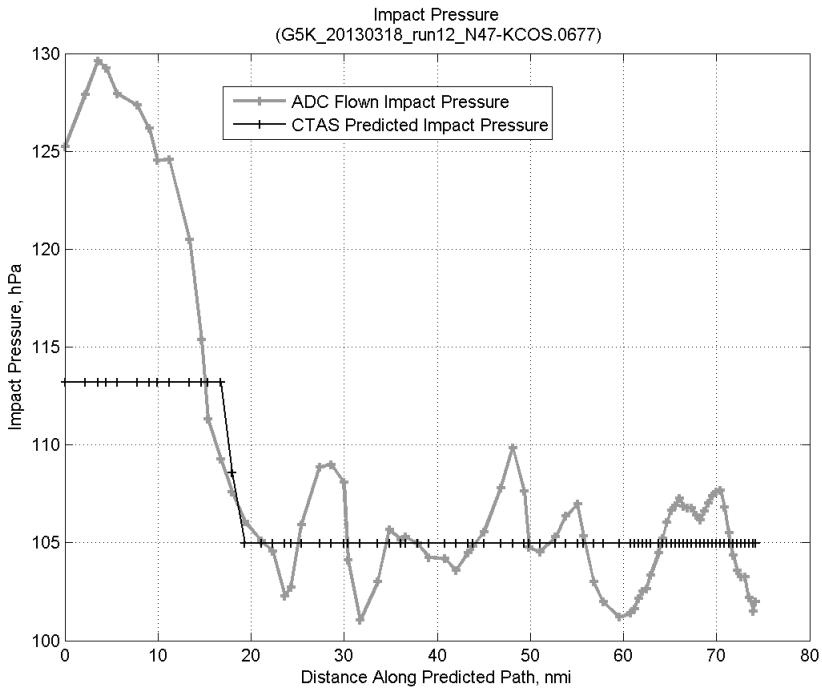


**Figure 218: Flown (ADC) and predicted (CTAS) impact pressure for run 12.**

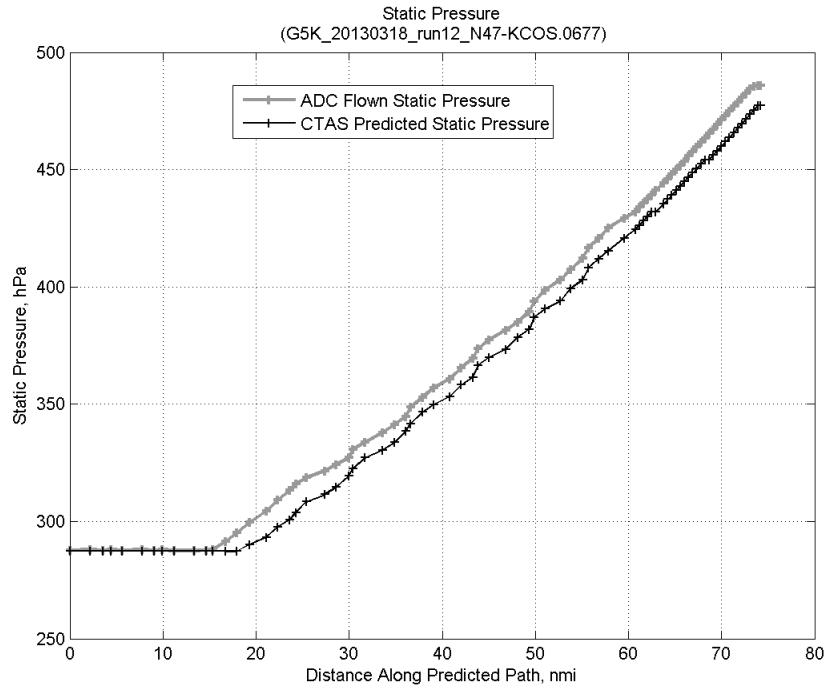


**Figure 219: Flown (ADC) and predicted (CTAS) static pressure for run 12.**

#### C.8.G. Path Distance

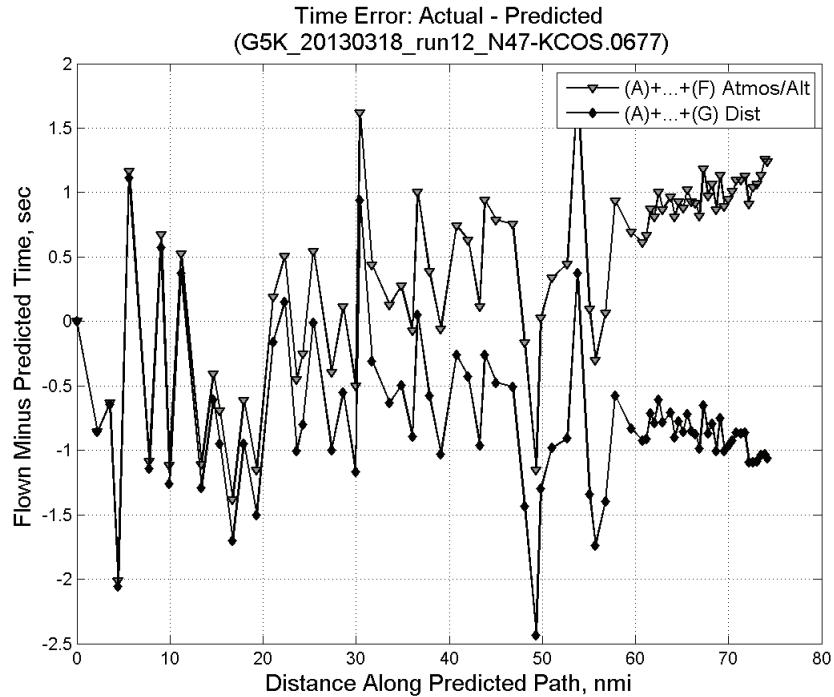


**Figure 220: Time error for run 12 before ((A)+...+(F) Atmos/Alt) and after ((A)+...+(G) Dist) removing path distance error source.**

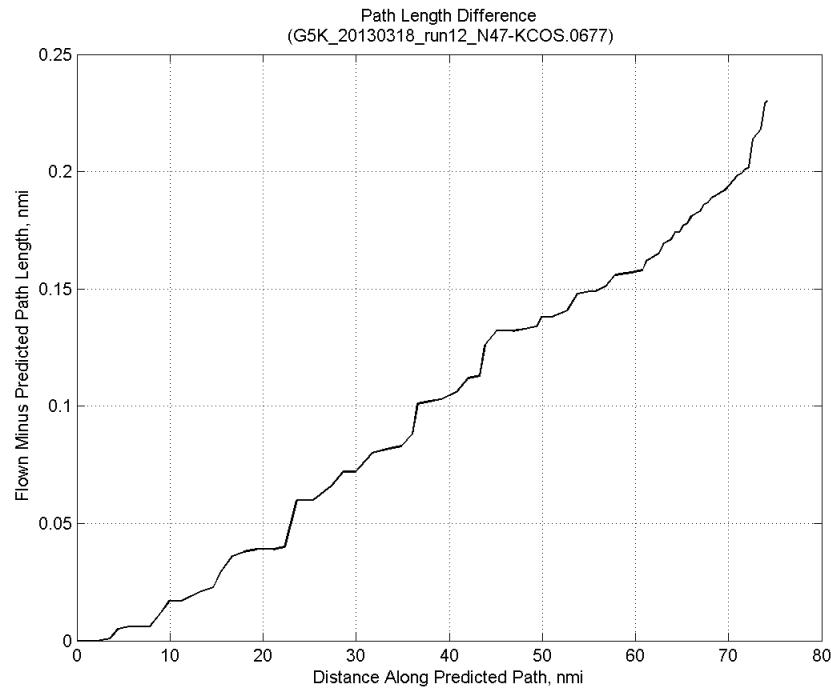


**Figure 221: ADC flown minus CTAS predicted path length for run 12. Positive values indicate aircraft followed a longer path than predicted by CTAS.**

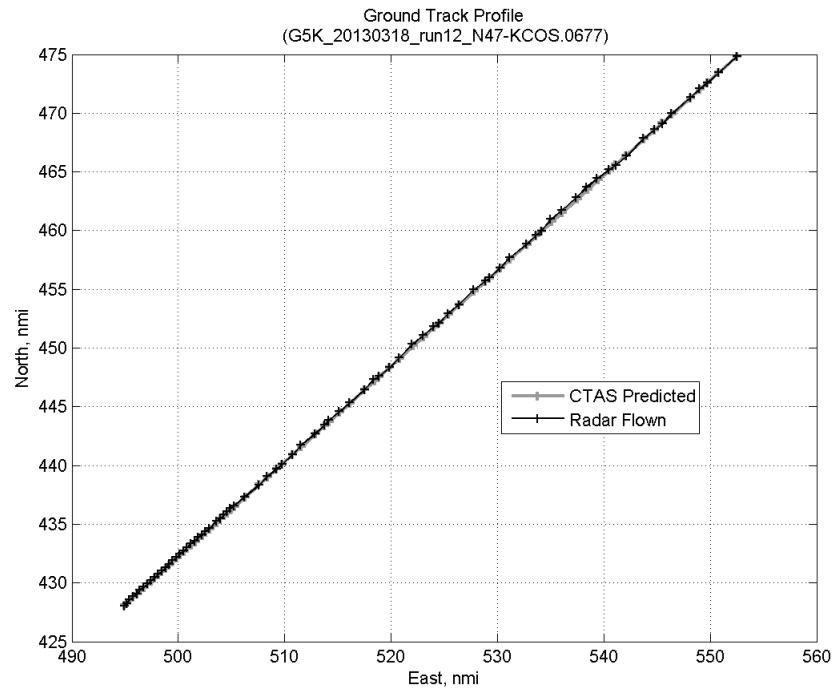


**Figure 222: CTAS predicted and radar flown ground track profile for run 12.**

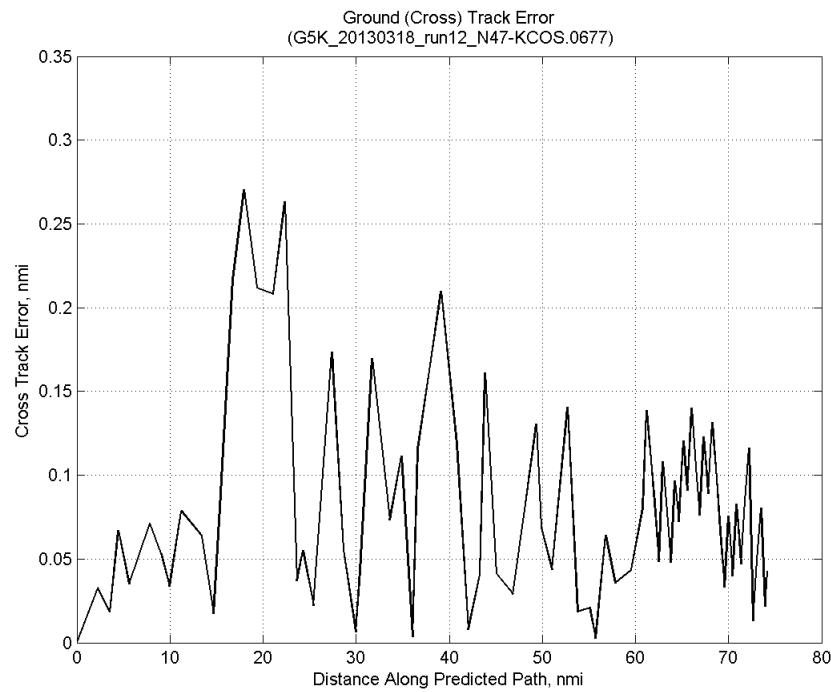


**Figure 223: Ground (cross) track error for run 12.**

### C.9. Run 14

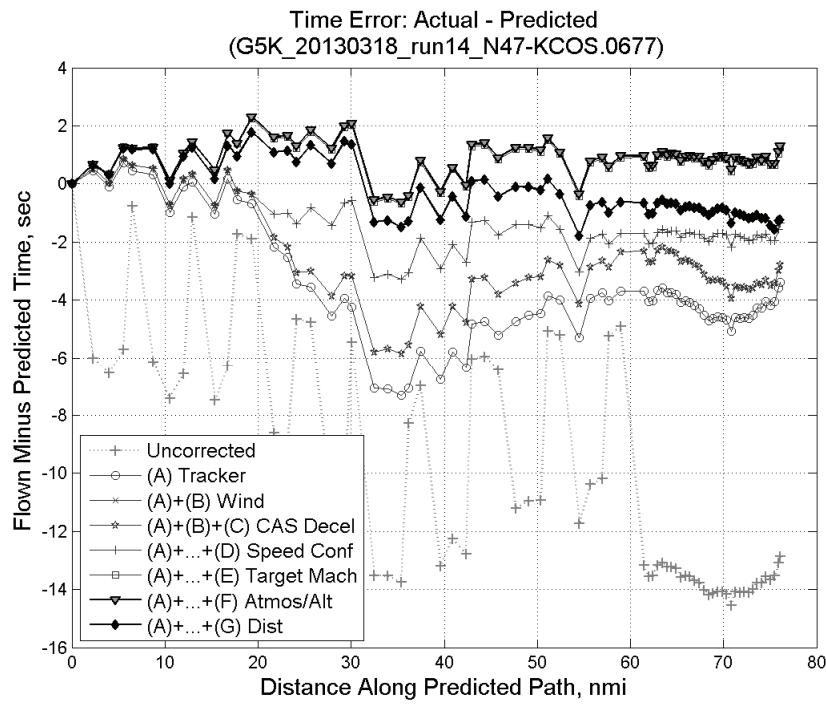


**Figure 224: Time error for run 14 showing incremental effect of removing each error source.**

#### C.9.A. Tracker Jumps

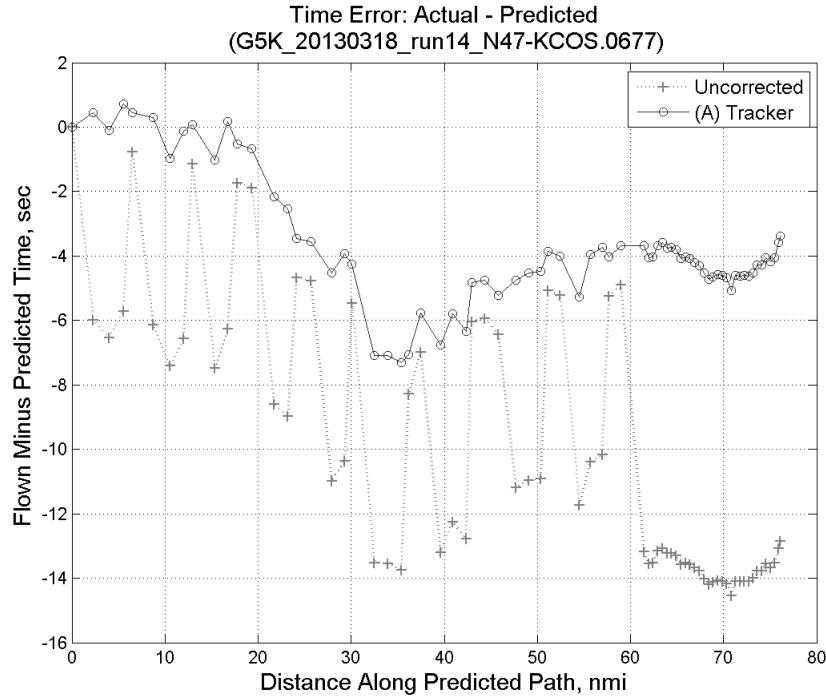


**Figure 225: Time error for run 14 before (Uncorrected) and after ((A) Tracker) removing tracker jump error source.**

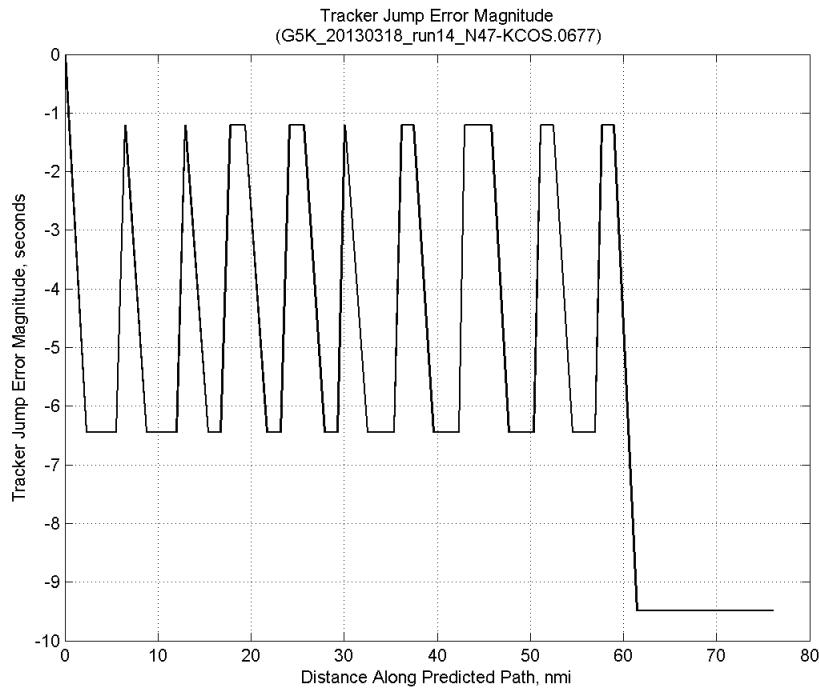


**Figure 226: Effect of tracker jump error source on time error for run 14.**

### C.9.B. Wind

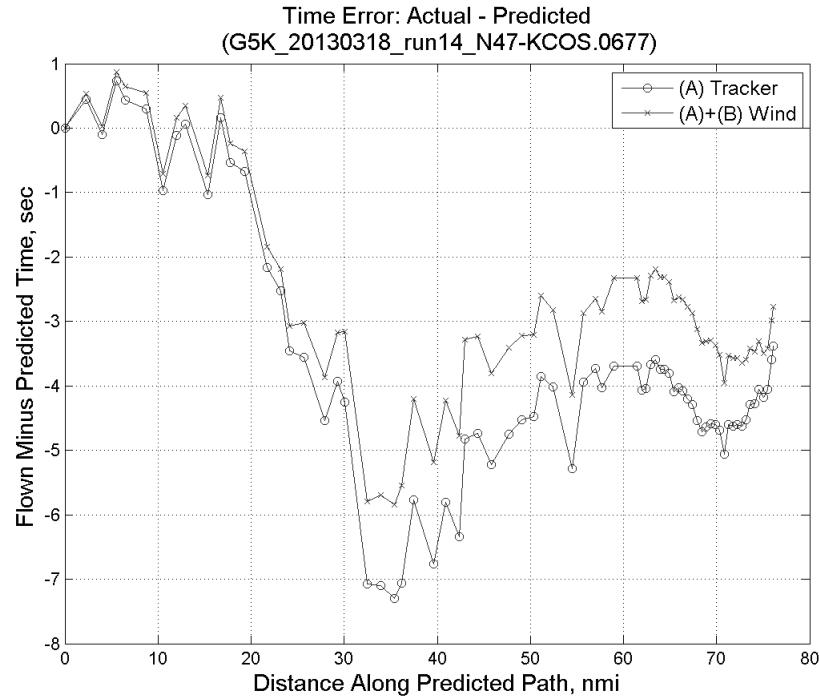


**Figure 227: Time error for run 14 before ((A) Tracker) and after ((A)+(B) Wind) removing wind error source.**

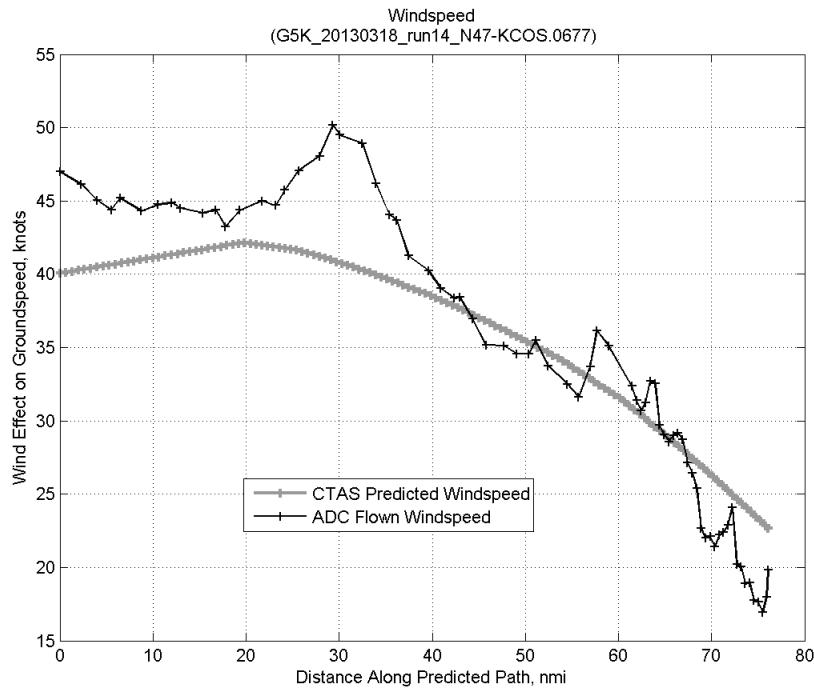


**Figure 228: CTAS predicted and ADC flown wind effect on ground speed for run 14. Negative values indicate a headwind.**

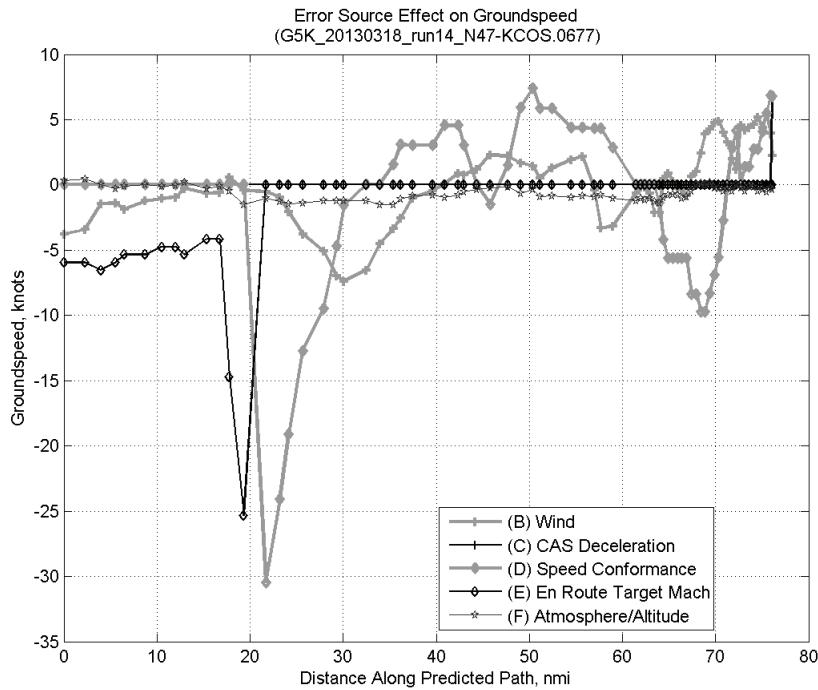


**Figure 229: Error sources (flown minus predicted) converted to a ground speed effect for run 14. Positive values indicate the flown ground speed was faster than the CTAS prediction.**

### C.9.C. CAS Deceleration

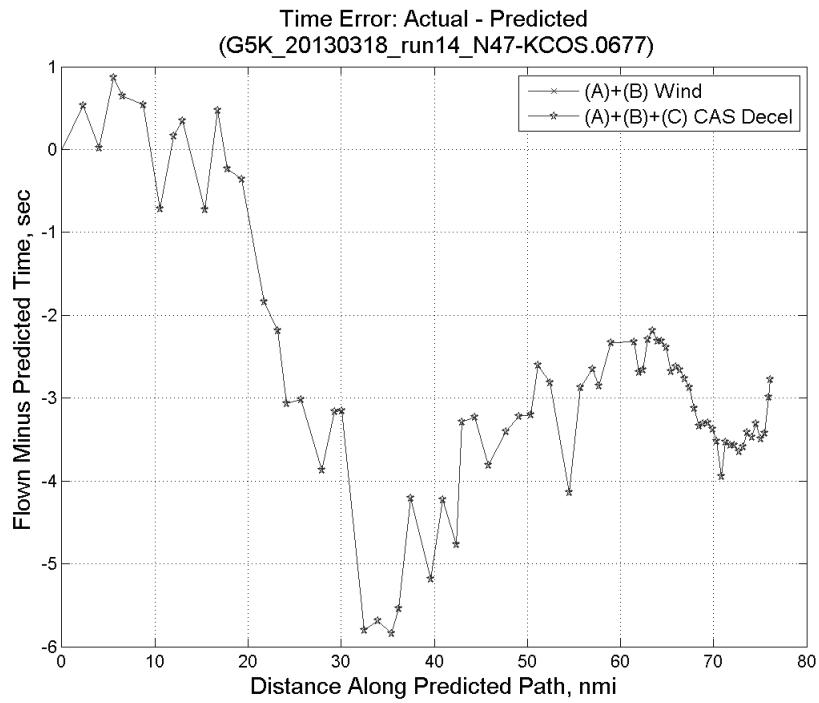


**Figure 230:** Time error for run 14 before ((A)+(B) Wind) and after ((A)+(B)+(C) CAS Decel) removing CAS deceleration error source.

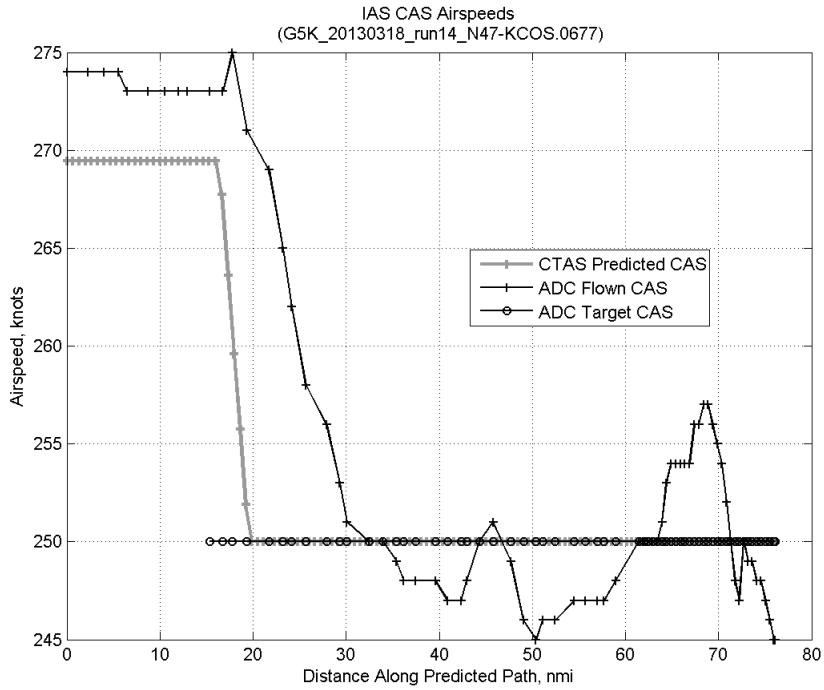


**Figure 231:** CTAS predicted and ADC flown CAS for run 14. CAS that is being targeted is shown with circle markers.

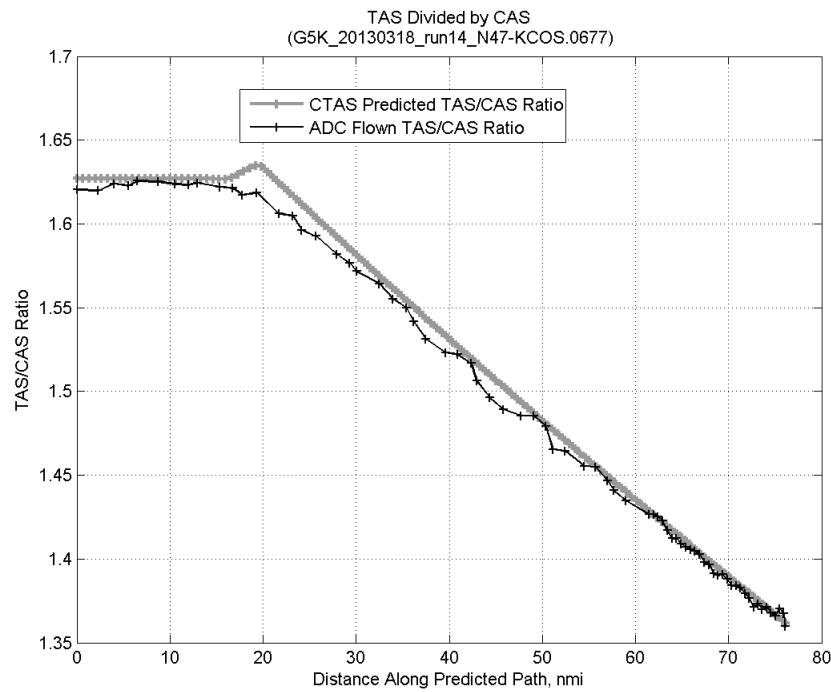


**Figure 232: CTAS predicted and ADC flown TAS/CAS ratio for run 14.**

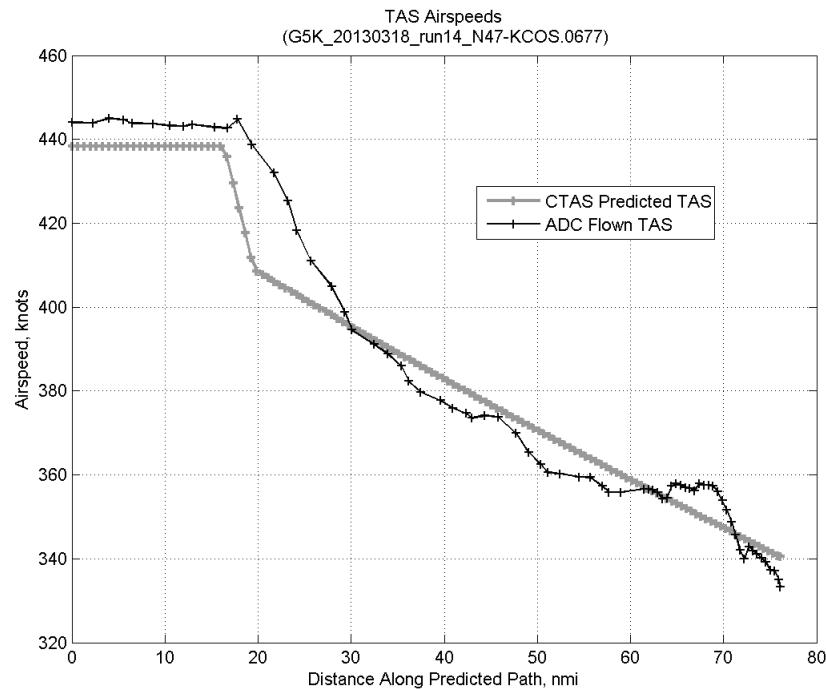


**Figure 233: CTAS predicted and ADC flown TAS for run 14.**

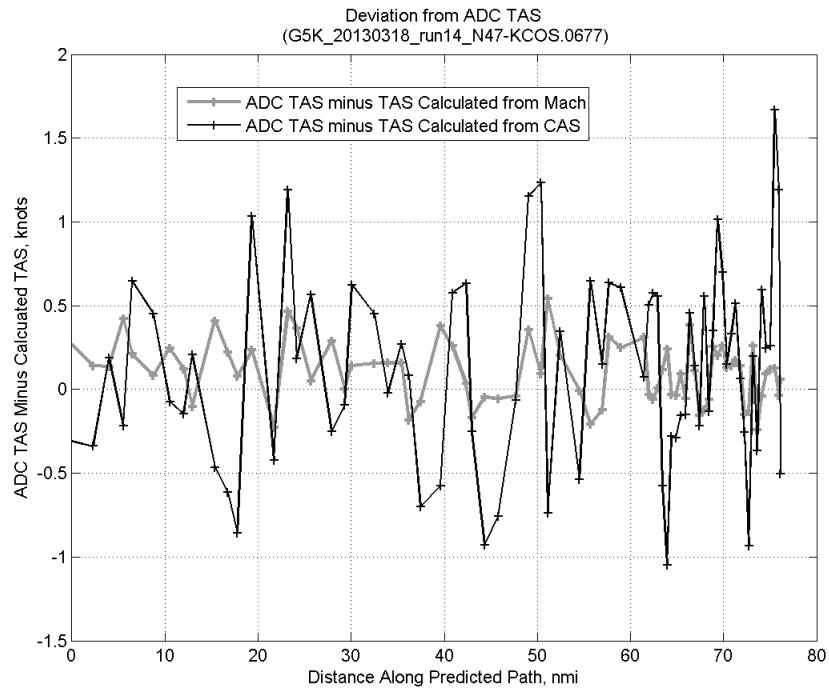


**Figure 234: Deviation from ADC flown TAS if calculating TAS using ADC flown CAS, Mach, atmospheric temperature, and atmospheric pressure for run 14.**

#### C.9.D. Speed Conformance

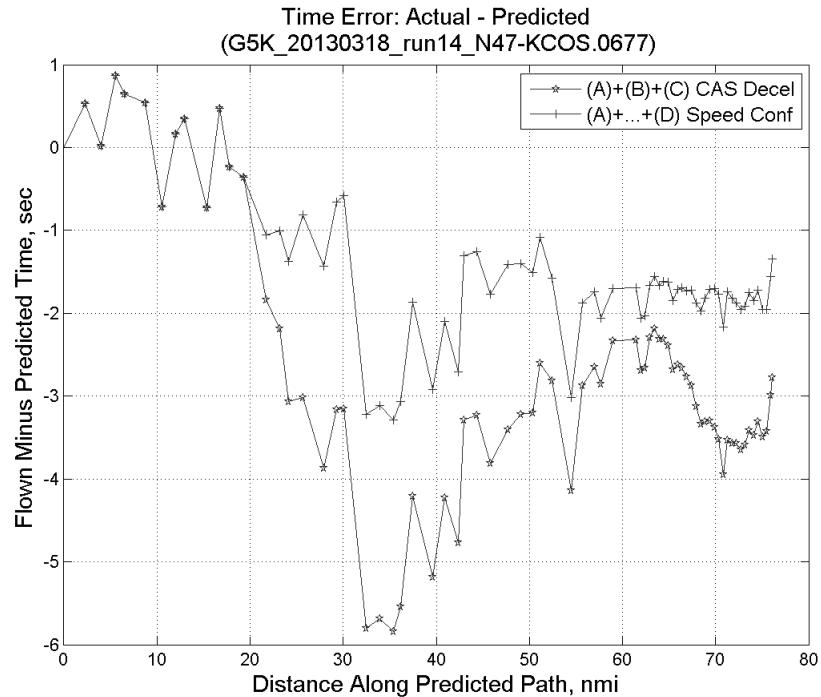


**Figure 235: Time error for run 14 before ((A)+(B)+(C) CAS Decel) and after ((A)+...+(D) Speed Conf) removing speed conformance error source.**

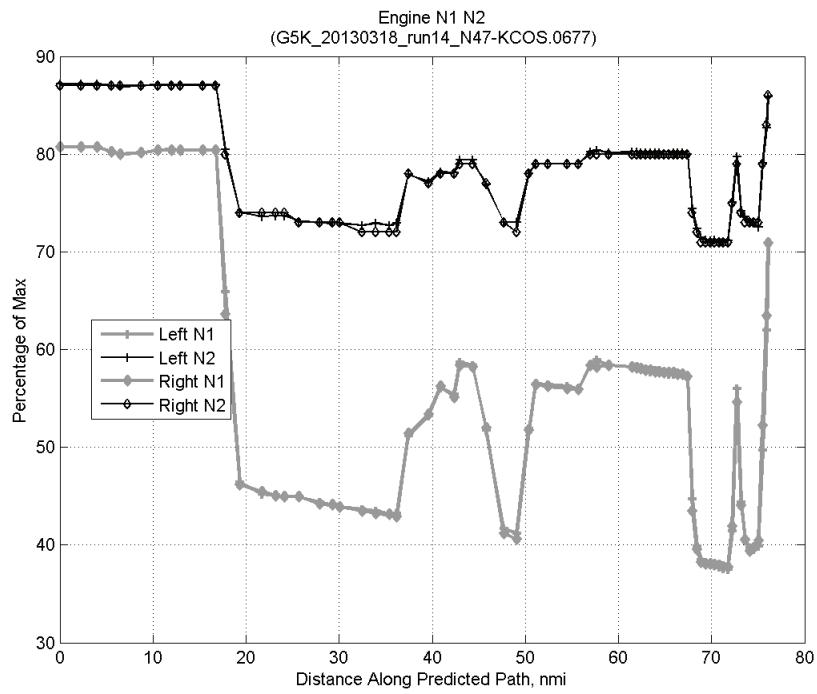


**Figure 236: Flown engine N1 and N2 for run 14.**

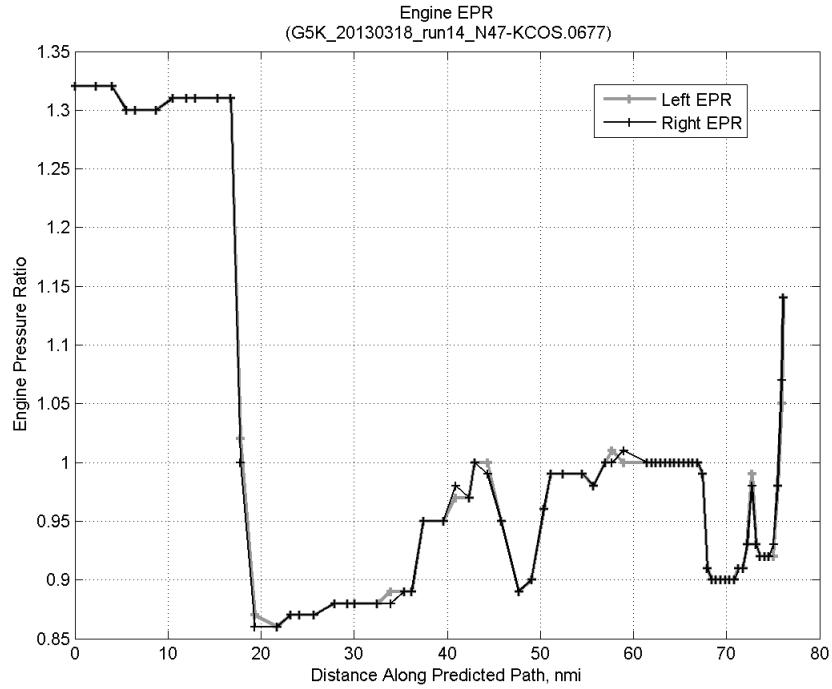


**Figure 237: Flown engine EPR for run 14.**

### C.9.E. Target Mach

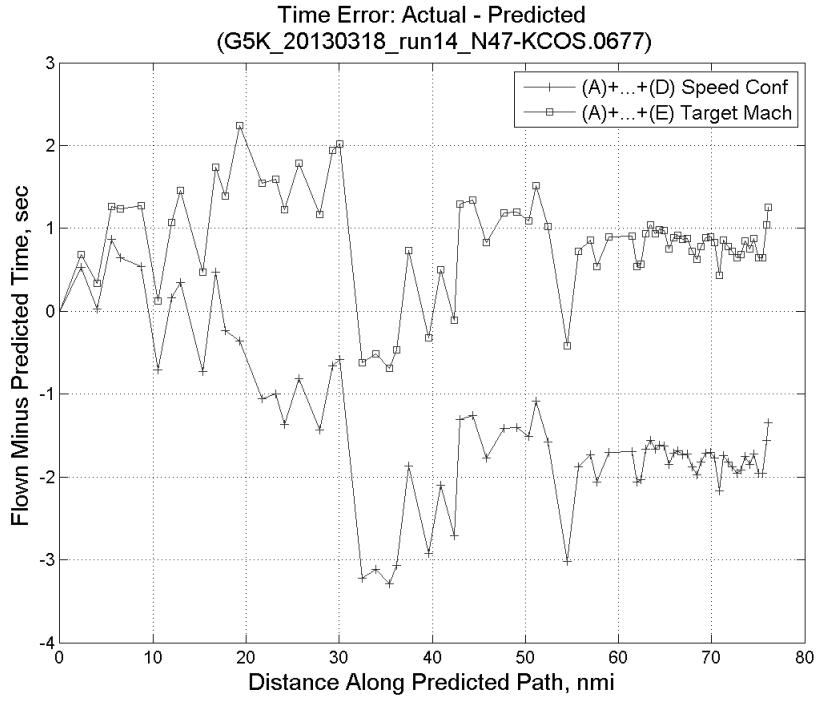


**Figure 238:** Time error for run 14 before ((A)+...+(D) Speed Conf) and after ((A)+...+(E) Target Mach) removing target Mach error source.

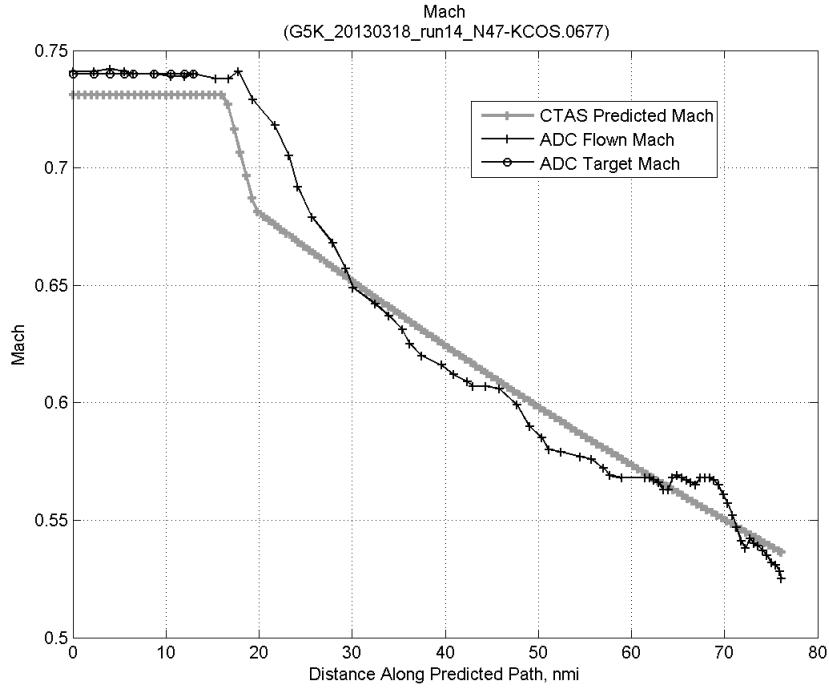


**Figure 239:** CTAS predicted and ADC flown Mach for run 14. Mach being targeted (ADC) shown with circle markers.

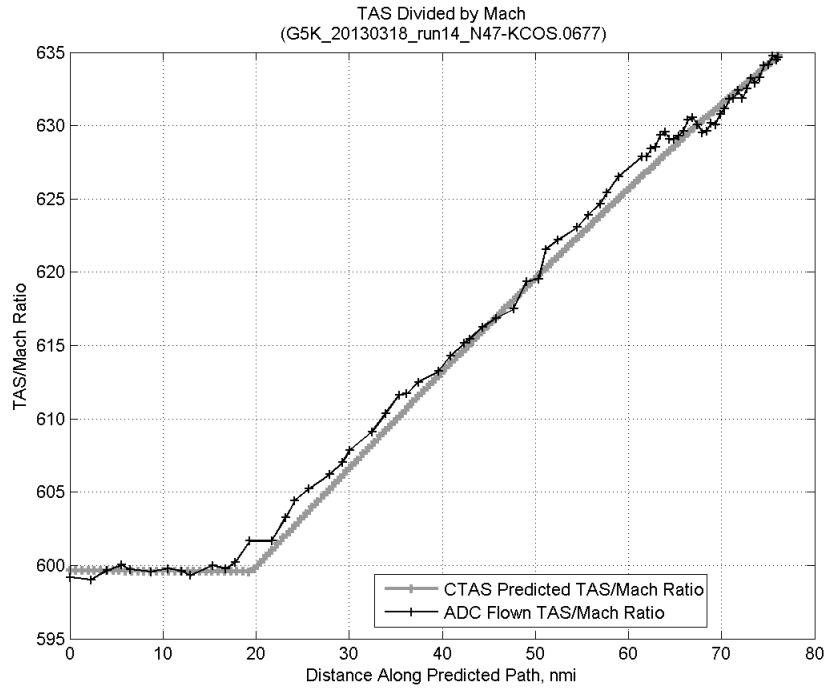


**Figure 240: CTAS predicted and ADC flown TAS/Mach ratio for run 14.**

#### C.9.F. Atmosphere/Altitude

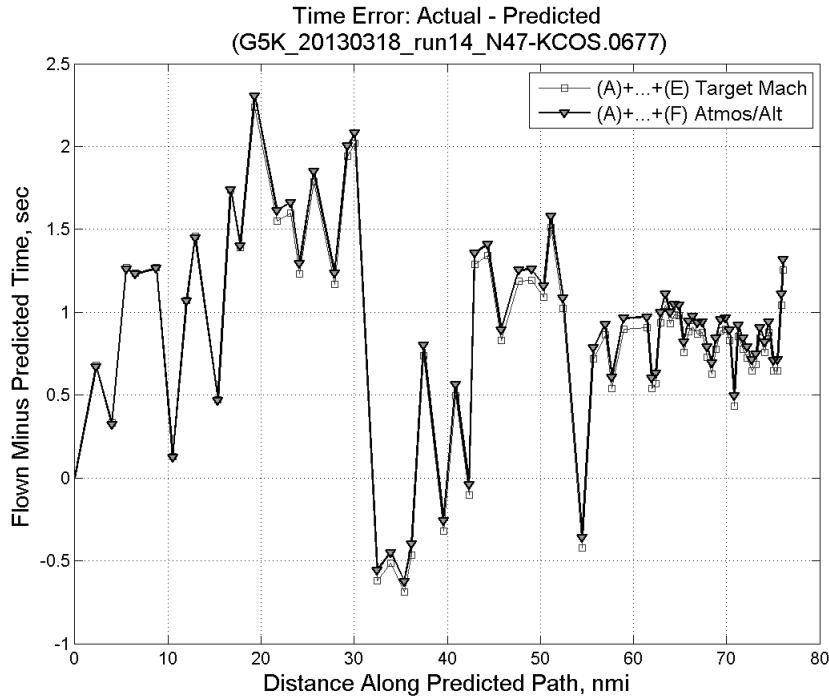


**Figure 241: Time error for run 14 before ((A)+...+(E) Target Mach) and after ((A)+...+(F) Atmos/Alt) removing atmosphere/altitude error source.**

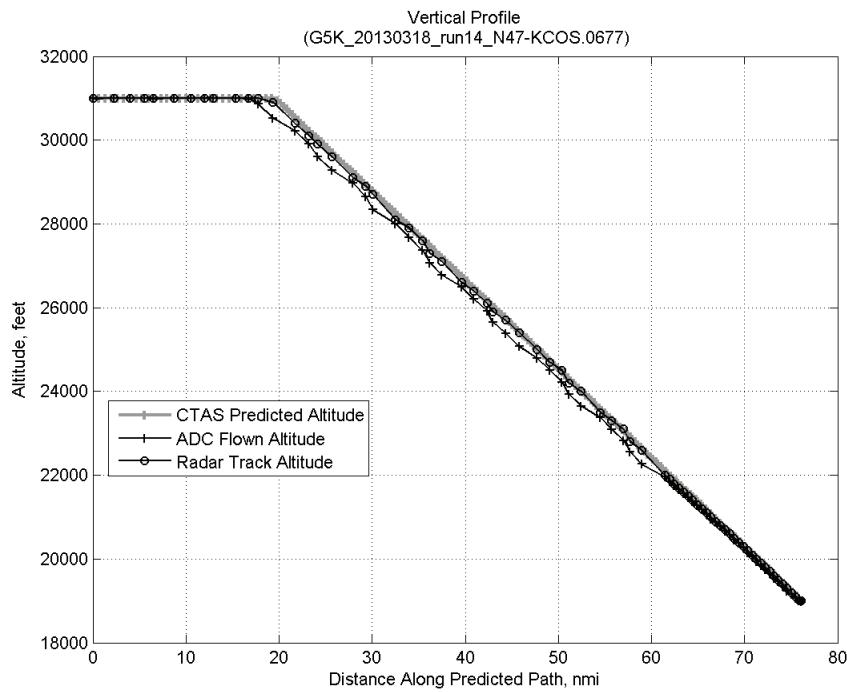


**Figure 242: Flown (ADC) and predicted (CTAS) vertical profile for run 14.**

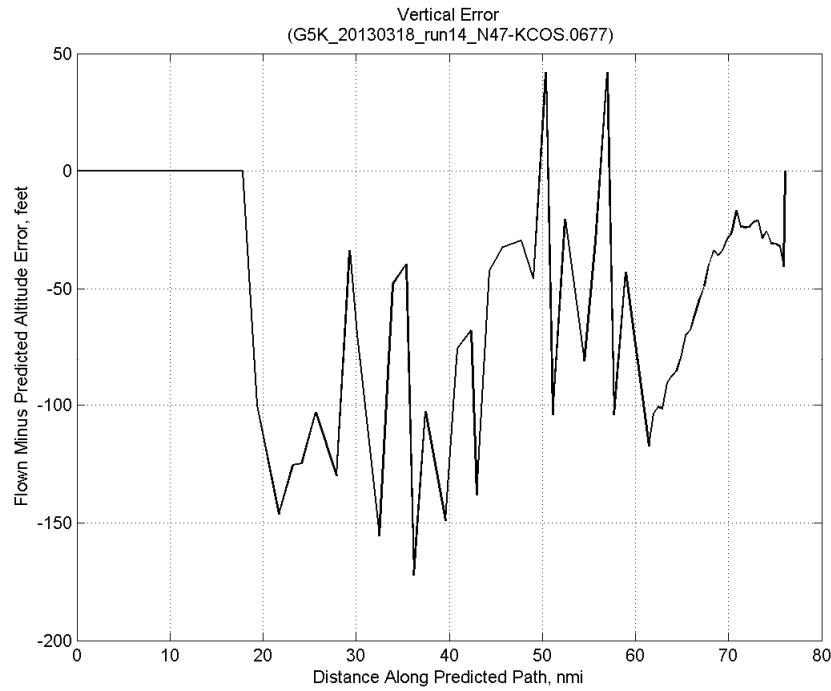


**Figure 243: Vertical error (flown minus predicted altitude) for run 14. Positive values indicate aircraft flew higher than predicted by CTAS.**

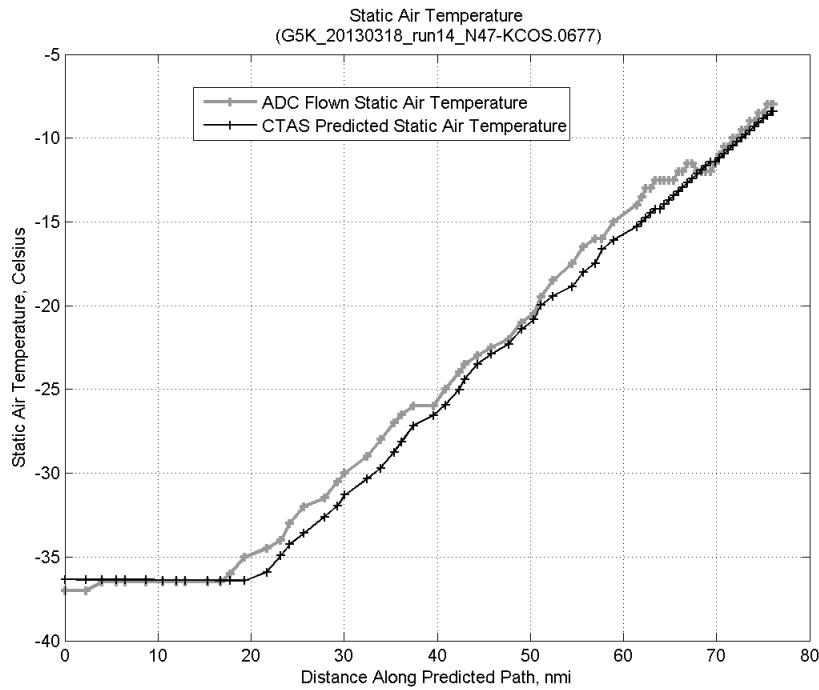


**Figure 244: Flown (ADC) and predicted (CTAS) static air temperature for run 14.**

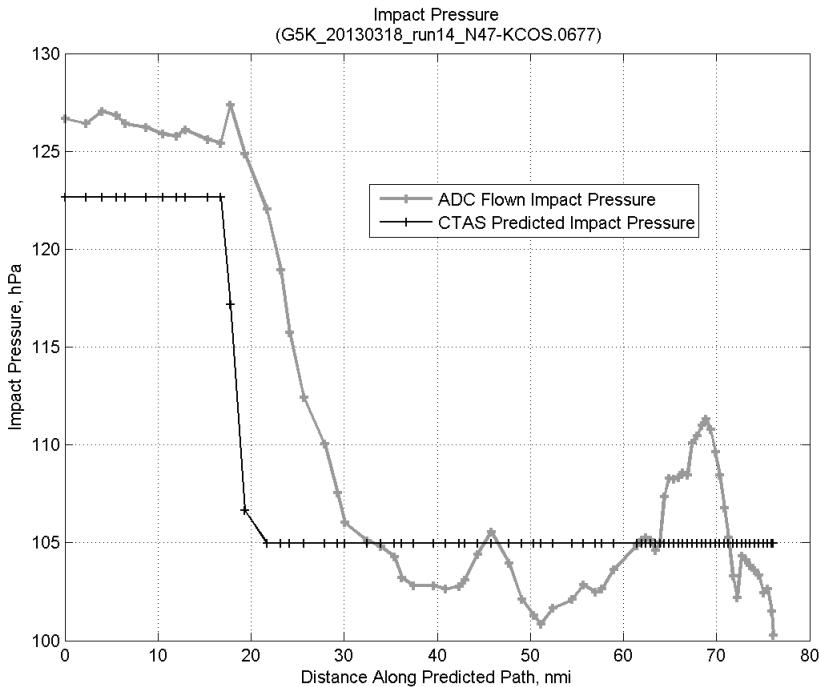


**Figure 245: Flown (ADC) and predicted (CTAS) impact pressure for run 14.**

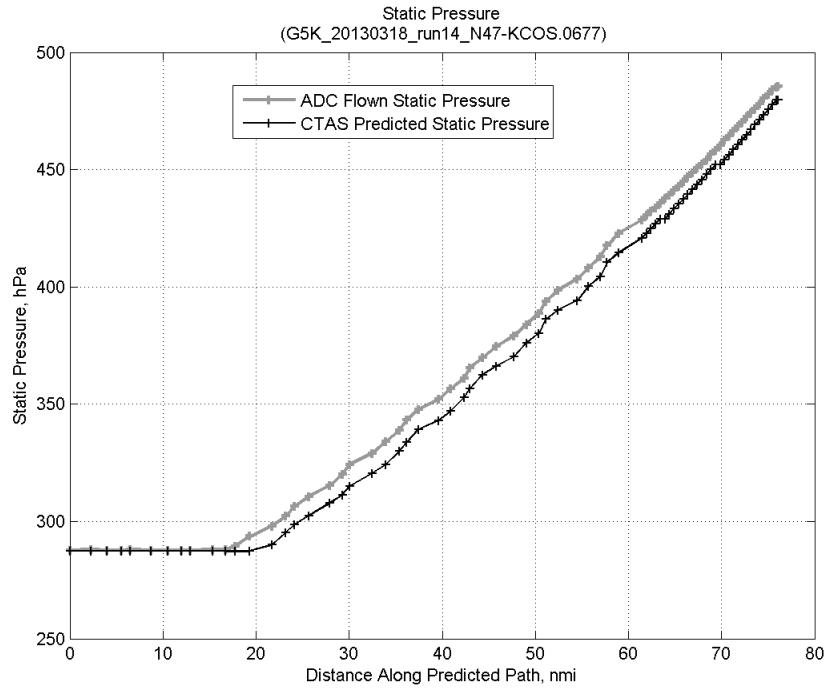


**Figure 246: Flown (ADC) and predicted (CTAS) static pressure for run 14.**

#### C.9.G. Path Distance

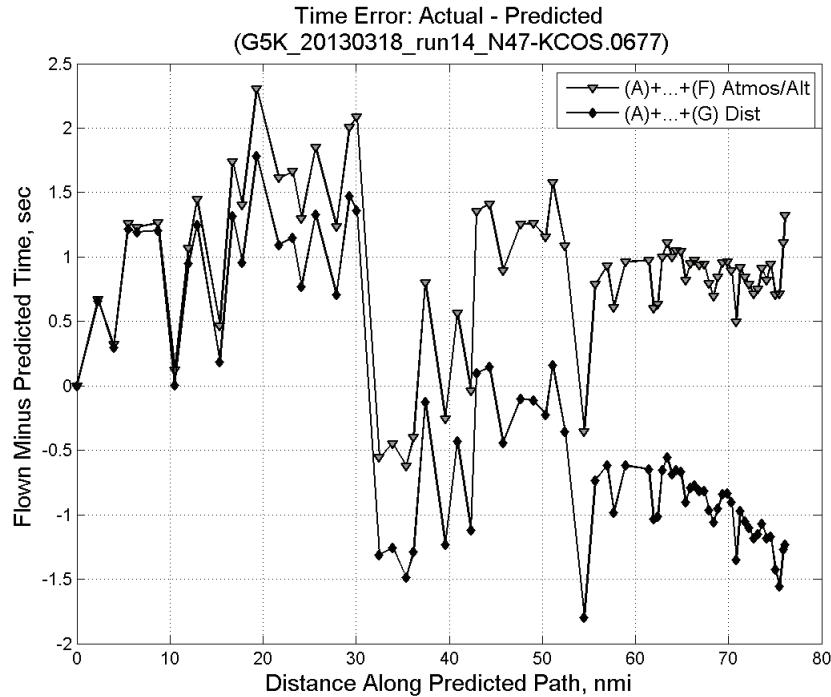


**Figure 247: Time error for run 14 before ((A)+...+(F) Atmos/Alt) and after ((A)+...+(G) Dist) removing path distance error source.**

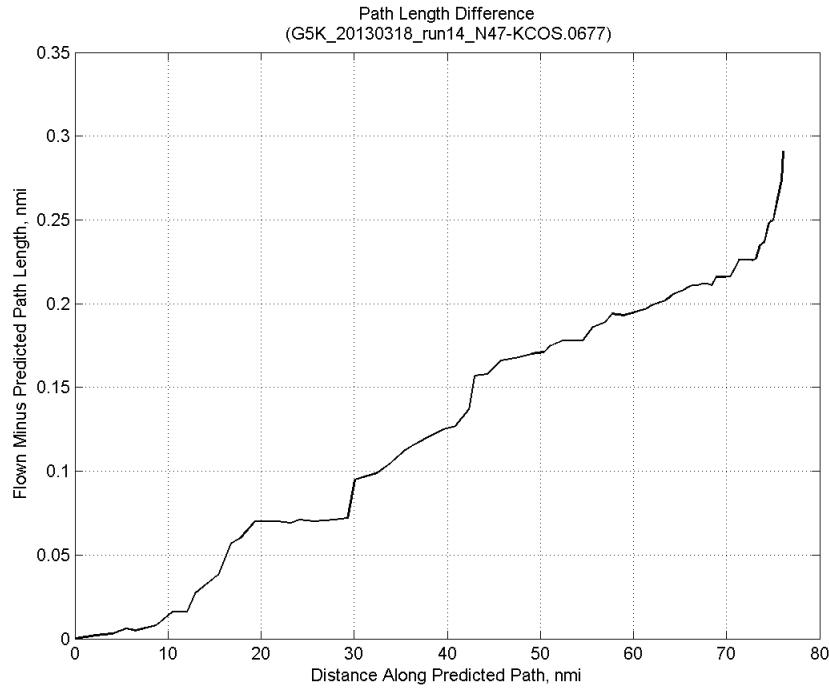


**Figure 248: ADC flown minus CTAS predicted path length for run 14. Positive values indicate aircraft followed a longer path than predicted by CTAS.**

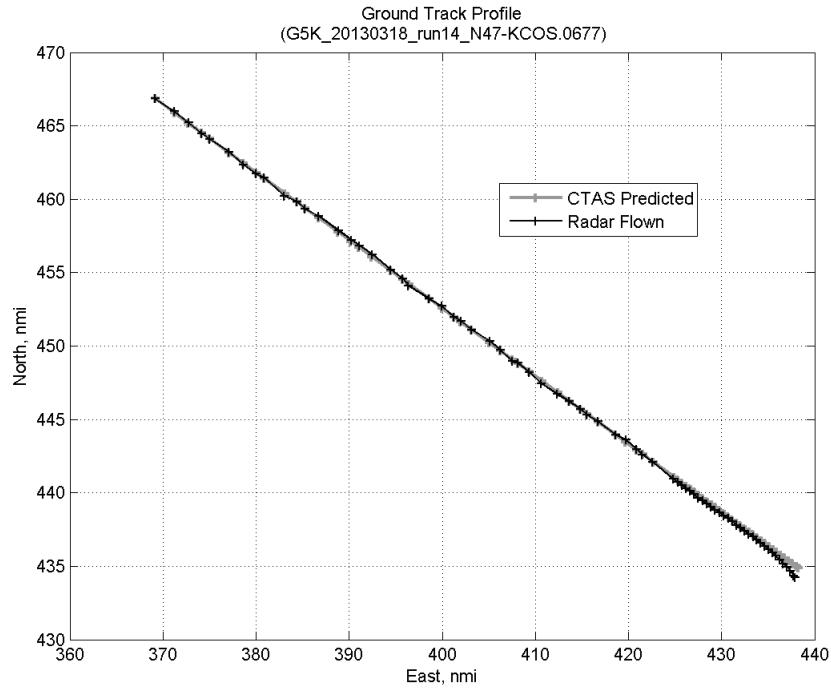


**Figure 249: CTAS predicted and radar flown ground track profile for run 14.**

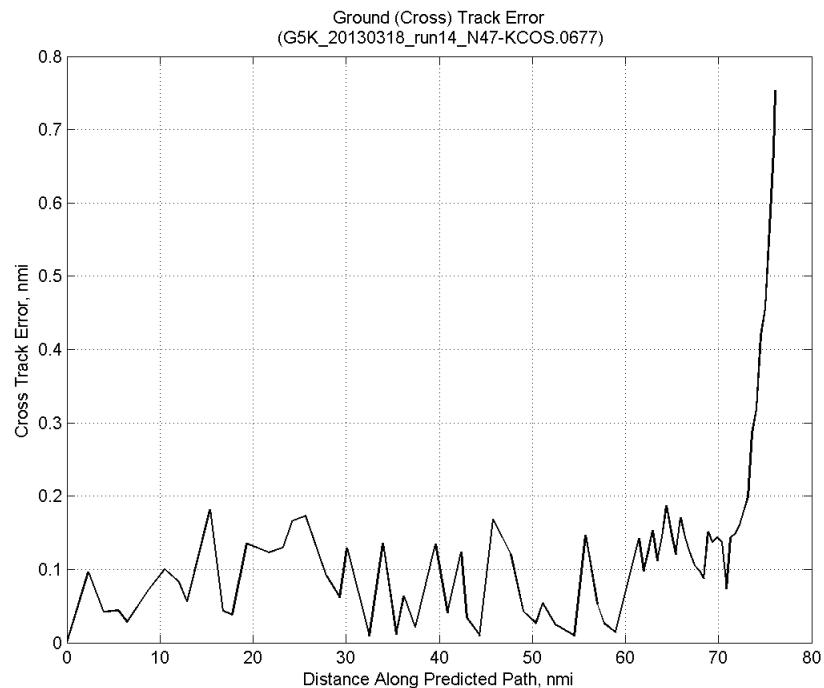


**Figure 250: Ground (cross) track error for run 14.**

### C.10. Run 18

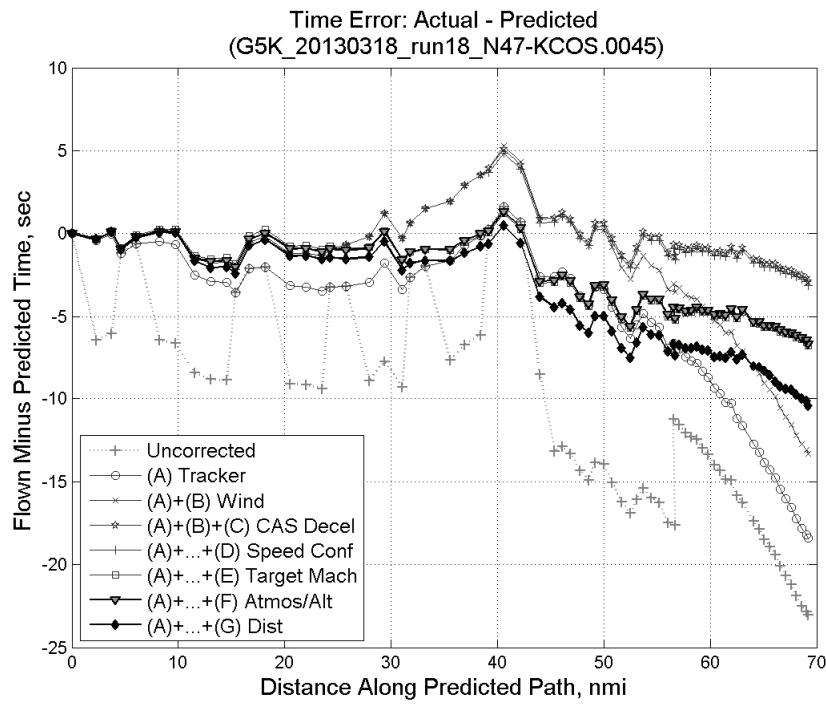


**Figure 251: Time error for run 18 showing incremental effect of removing each error source.**

#### C.10.A. Tracker Jumps

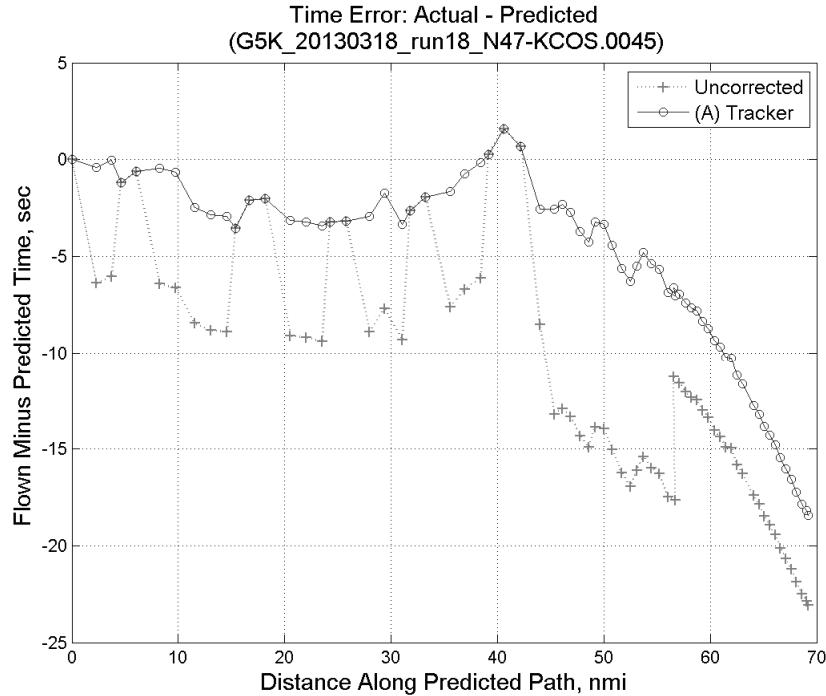


**Figure 252: Time error for run 18 before (Uncorrected) and after ((A) Tracker) removing tracker jump error source.**

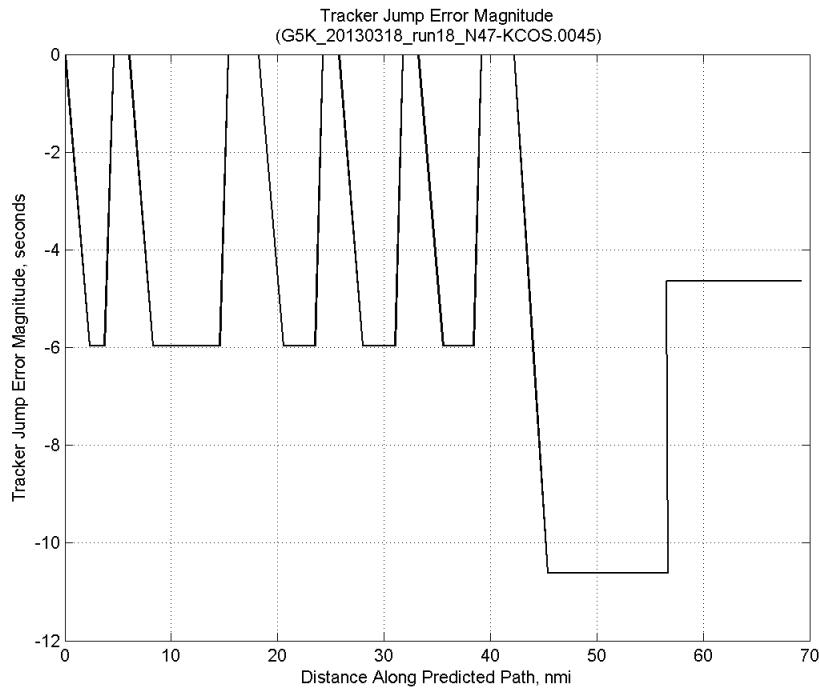


**Figure 253: Effect of tracker jump error source on time error for run 18.**

### C.10.B. Wind

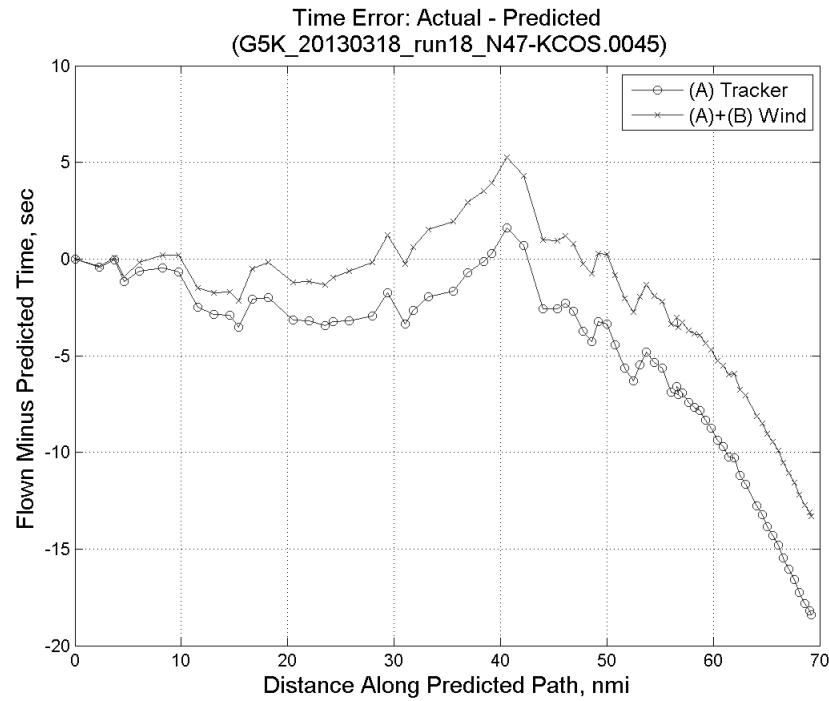


**Figure 254: Time error for run 18 before ((A) Tracker) and after ((A)+(B) Wind) removing wind error source.**

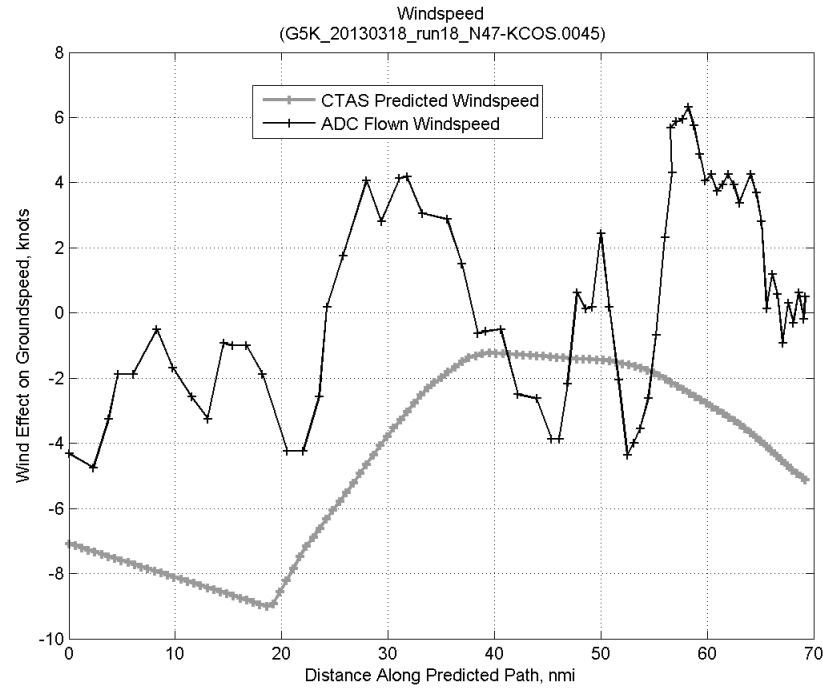


**Figure 255: CTAS predicted and ADC flown wind effect on ground speed for run 18. Negative values indicate a headwind.**

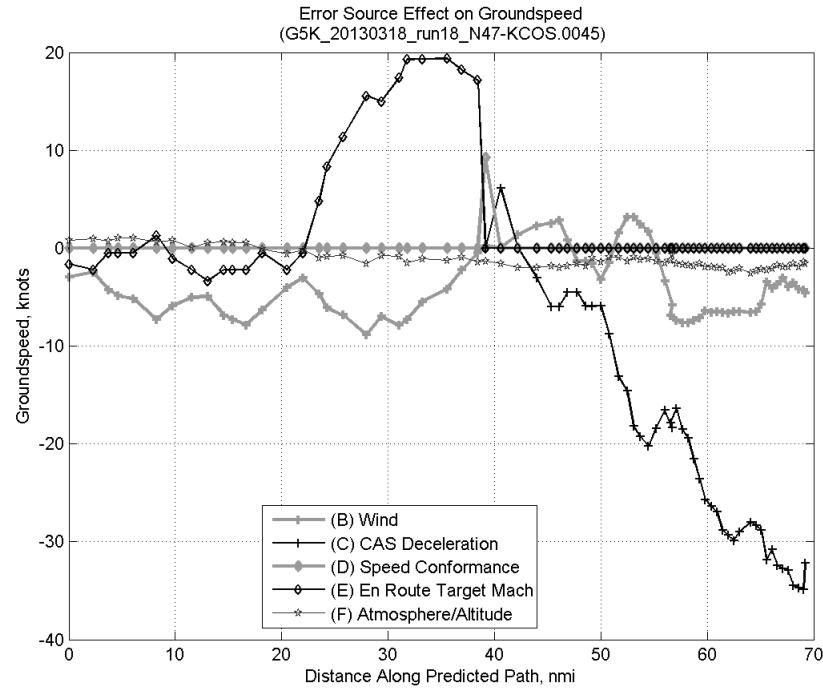


**Figure 256: Error sources (flown minus predicted) converted to a ground speed effect for run 18. Positive values indicate the flown ground speed was faster than the CTAS prediction.**

### C.10.C. CAS Deceleration

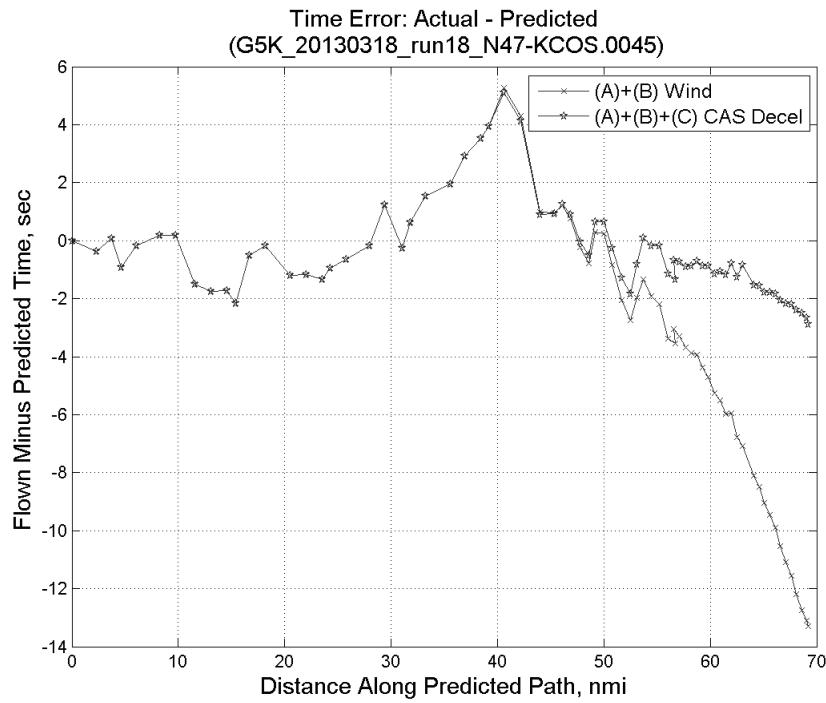


**Figure 257: Time error for run 18 before ((A)+(B) Wind) and after ((A)+(B)+(C) CAS Decel) removing CAS deceleration error source.**

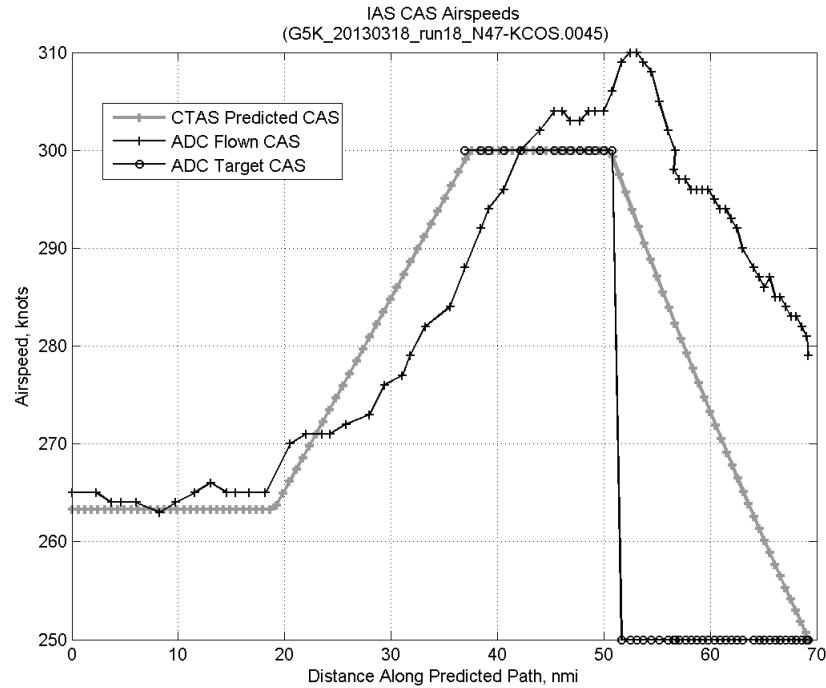


**Figure 258: CTAS predicted and ADC flown CAS for run 18. CAS that is being targeted is shown with circle markers.**

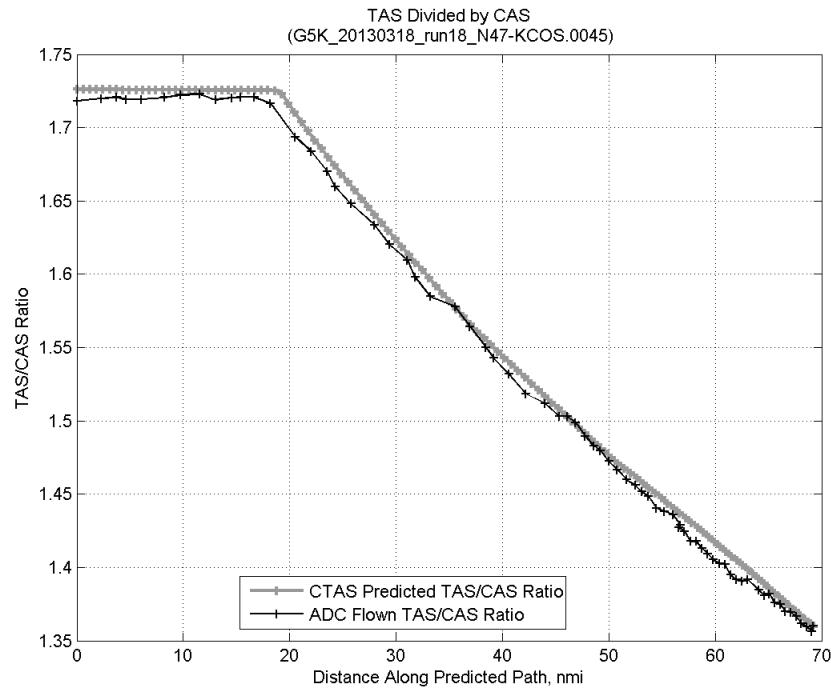


**Figure 259: CTAS predicted and ADC flown TAS/CAS ratio for run 18.**

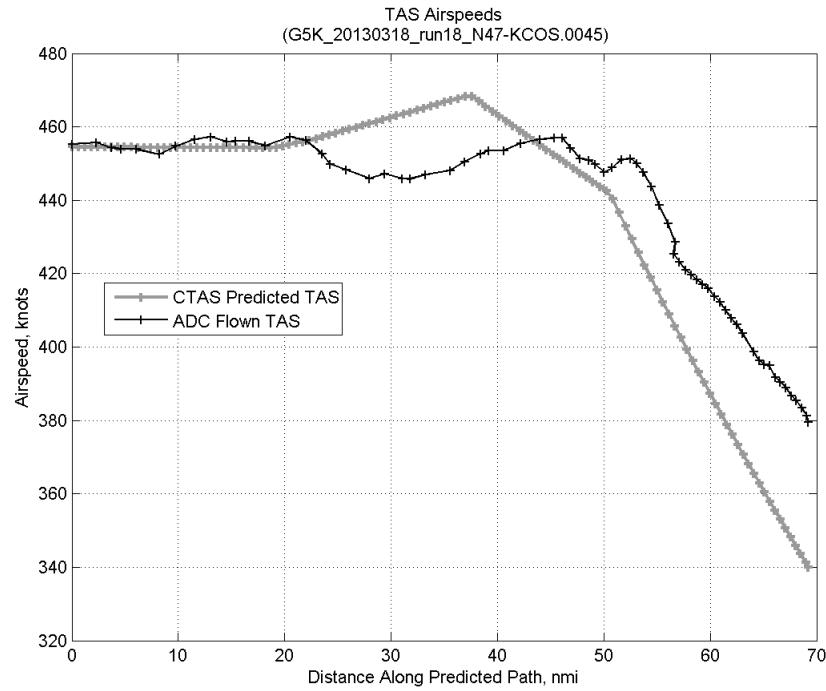


**Figure 260: CTAS predicted and ADC flown TAS for run 18.**

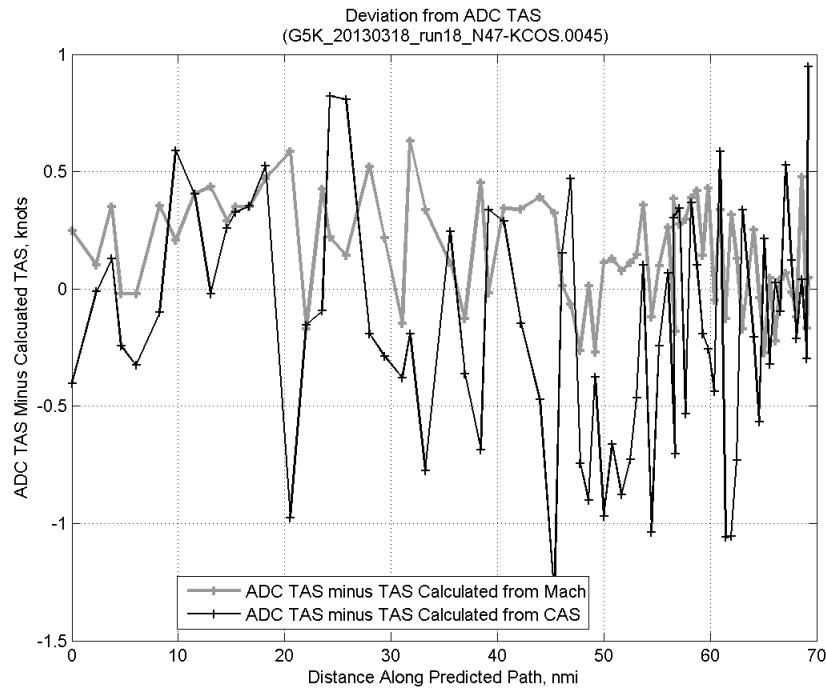


**Figure 261:** Deviation from ADC flown TAS if calculating TAS using ADC flown CAS, Mach, atmospheric temperature, and atmospheric pressure for run 18.

#### C.10.D. Speed Conformance

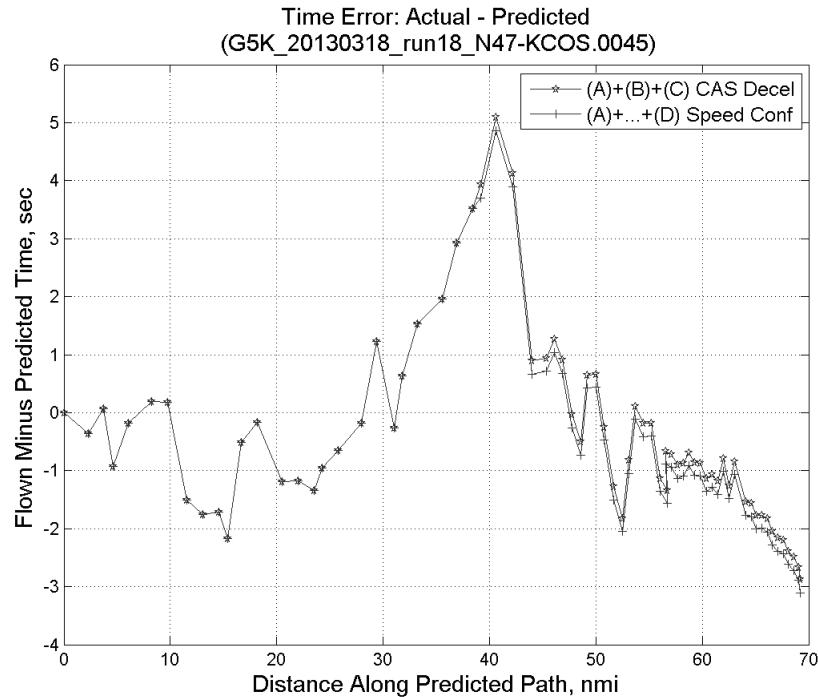


**Figure 262:** Time error for run 18 before ((A)+(B)+(C) CAS Decel) and after ((A)+...+(D) Speed Conf) removing speed conformance error source.

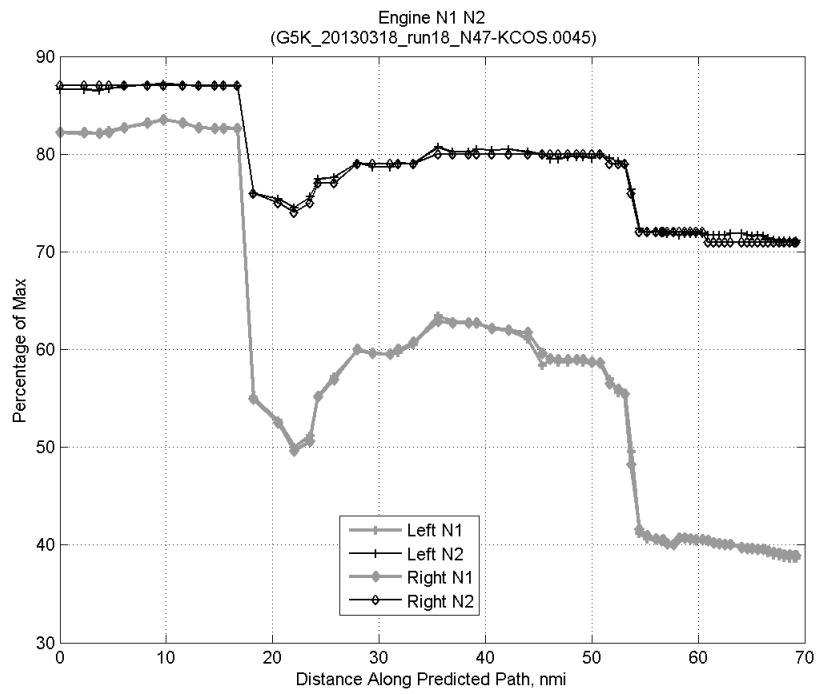


**Figure 263: Flown engine N1 and N2 for run 18.**

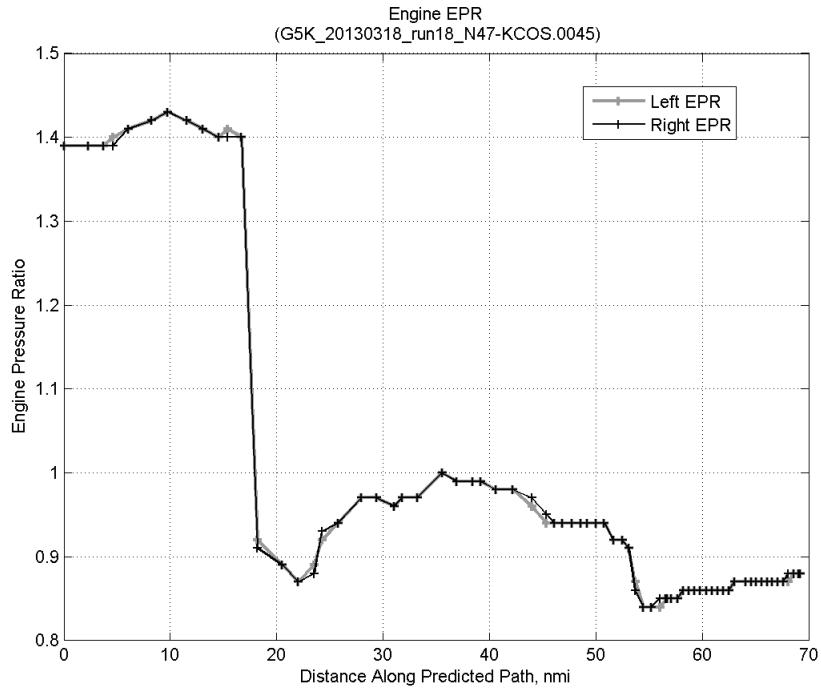


**Figure 264: Flown engine EPR for run 18.**

### C.10.E. Target Mach

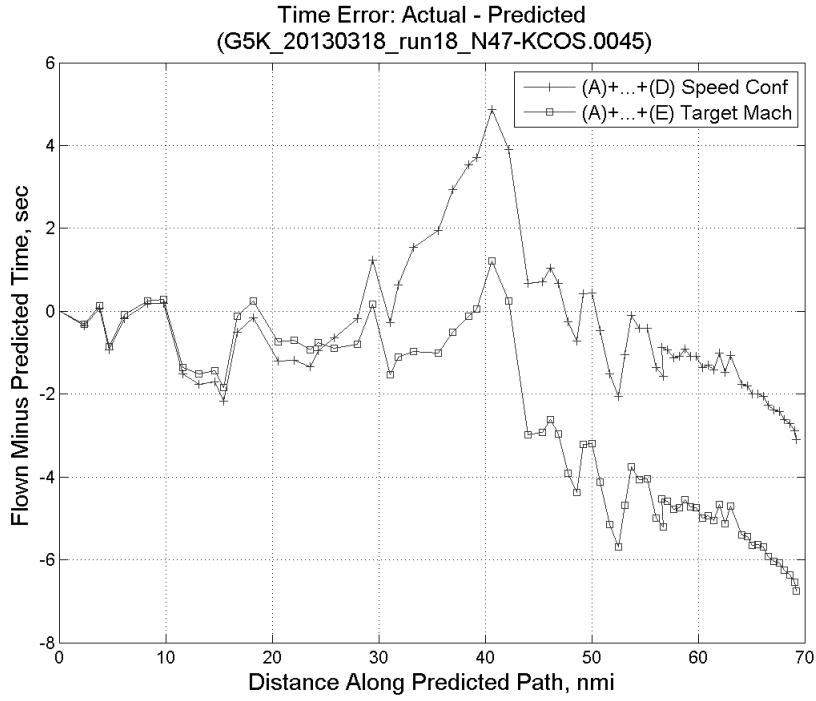


**Figure 265:** Time error for run 18 before ((A)+...+(D) Speed Conf) and after ((A)+...+(E) Target Mach) removing target Mach error source.

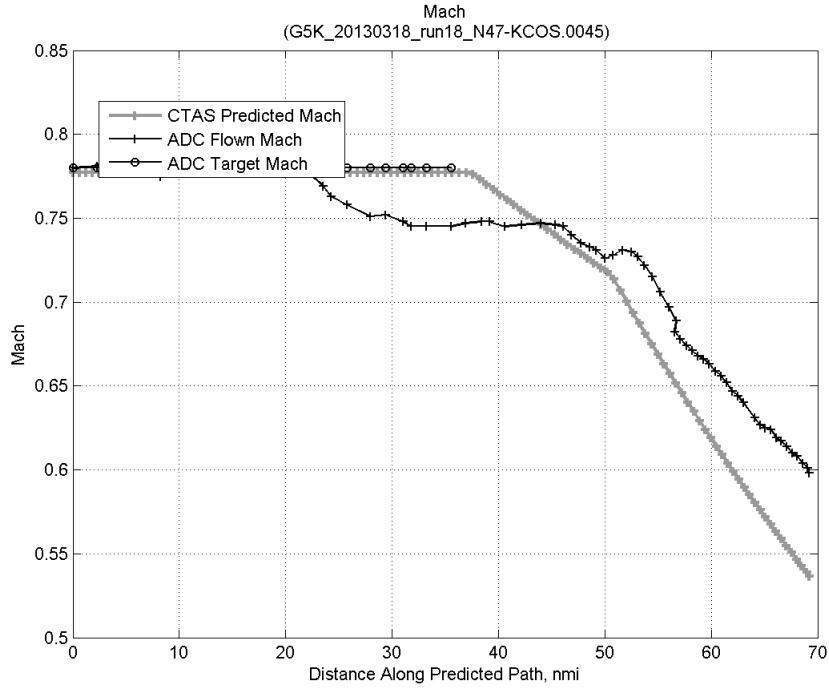


**Figure 266:** CTAS predicted and ADC flown Mach for run 18. Mach being targeted (ADC) shown with circle markers.

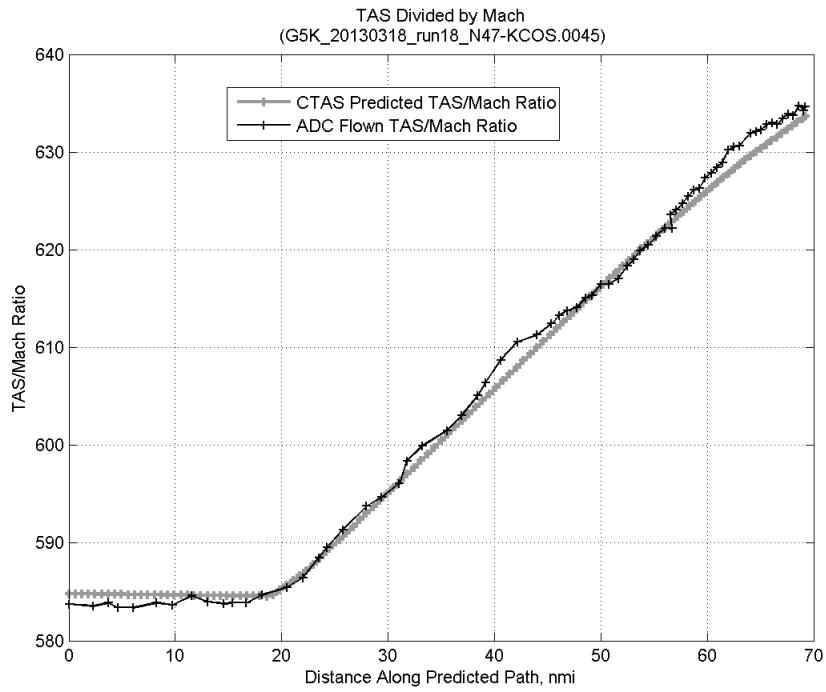


**Figure 267: CTAS predicted and ADC flown TAS/Mach ratio for run 18.**

#### C.10.F. Atmosphere/Altitude

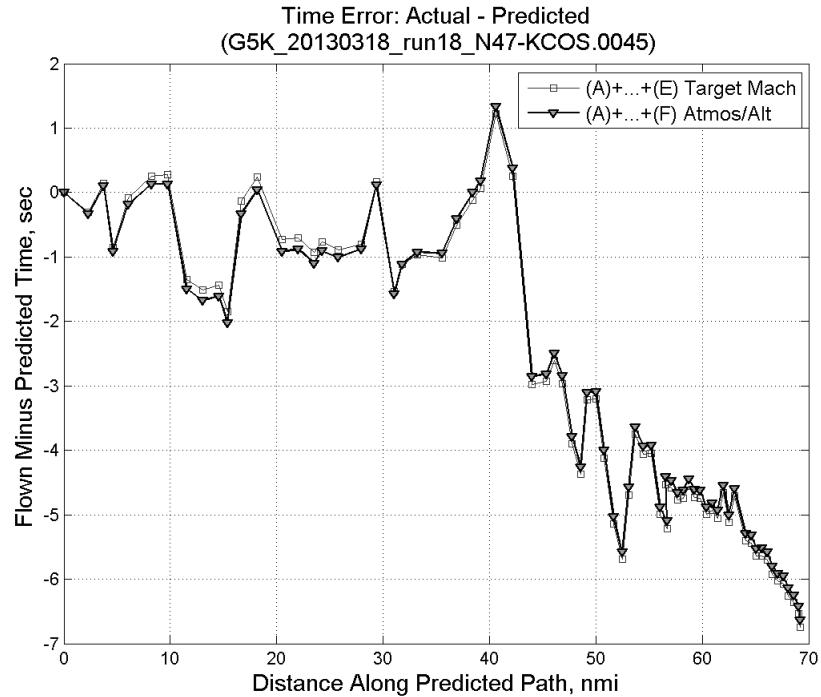


**Figure 268: Time error for run 18 before ((A)+...+(E) Target Mach) and after ((A)+...+(F) Atmos/Alt) removing atmosphere/altitude error source.**

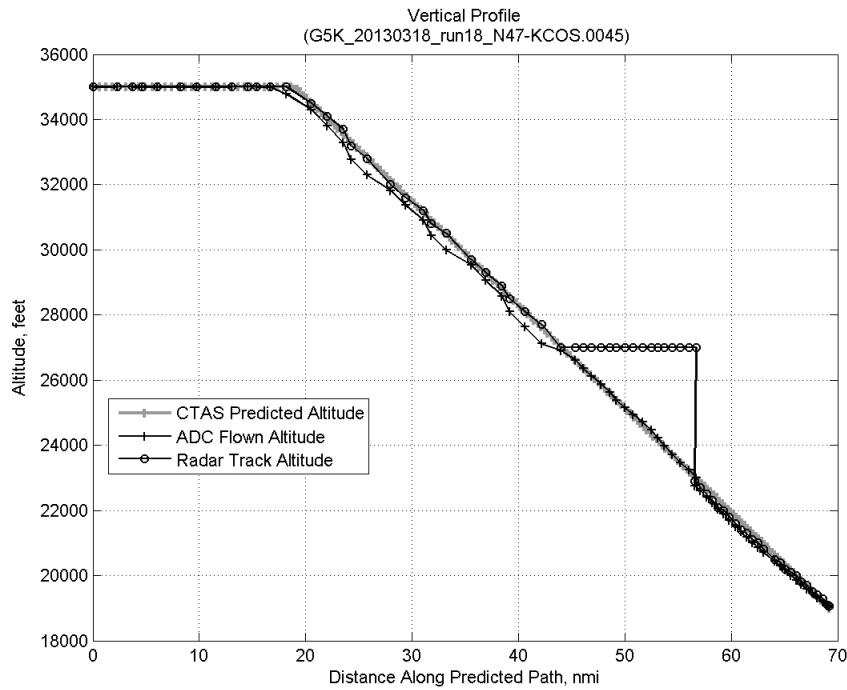


**Figure 269: Flown (ADC) and predicted (CTAS) vertical profile for run 18.**

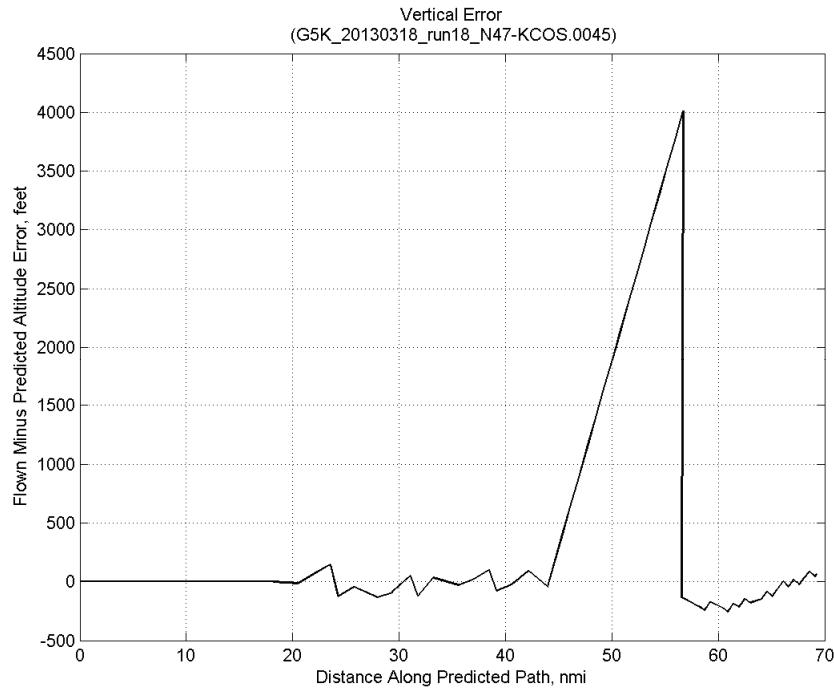


**Figure 270: Vertical error (flown minus predicted altitude) for run 18. Positive values indicate aircraft flew higher than predicted by CTAS.**

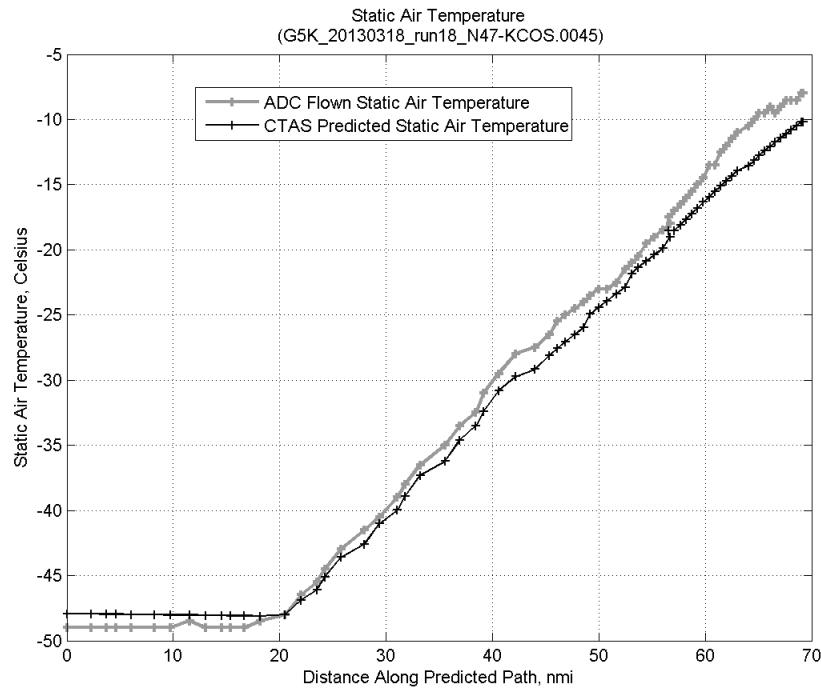


**Figure 271: Flown (ADC) and predicted (CTAS) static air temperature for run 18.**

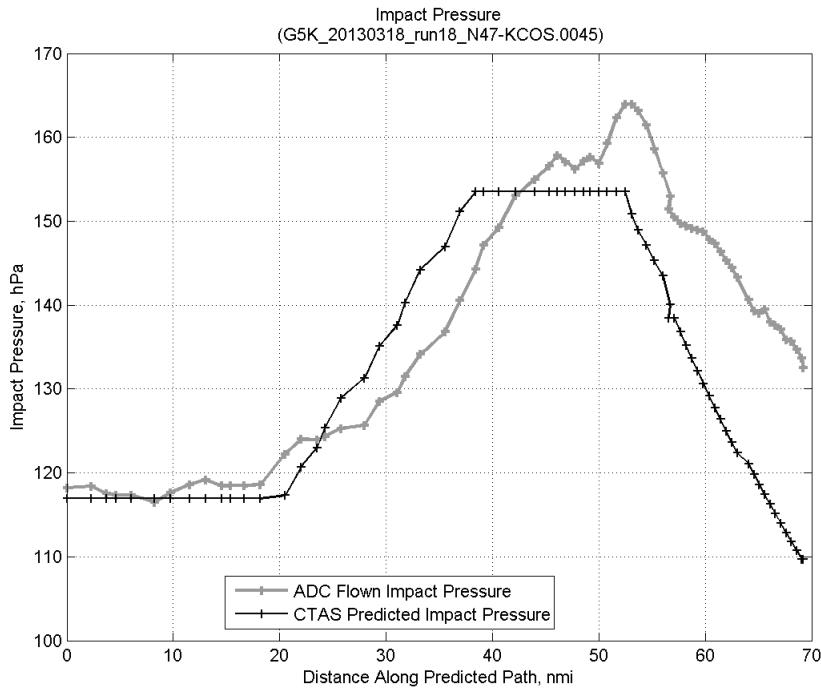


**Figure 272: Flown (ADC) and predicted (CTAS) impact pressure for run 18.**

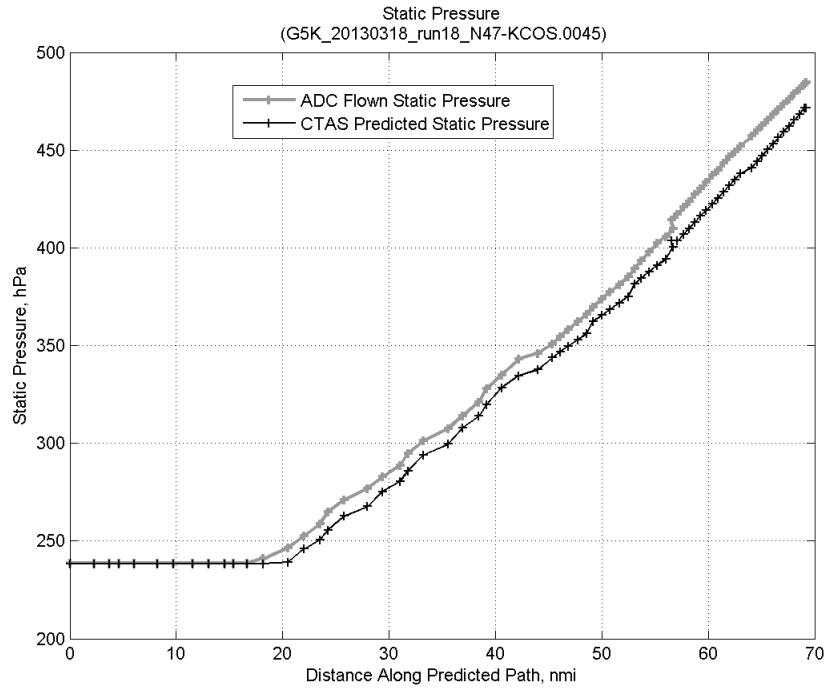


**Figure 273: Flown (ADC) and predicted (CTAS) static pressure for run 18.**

#### C.10.G. Path Distance

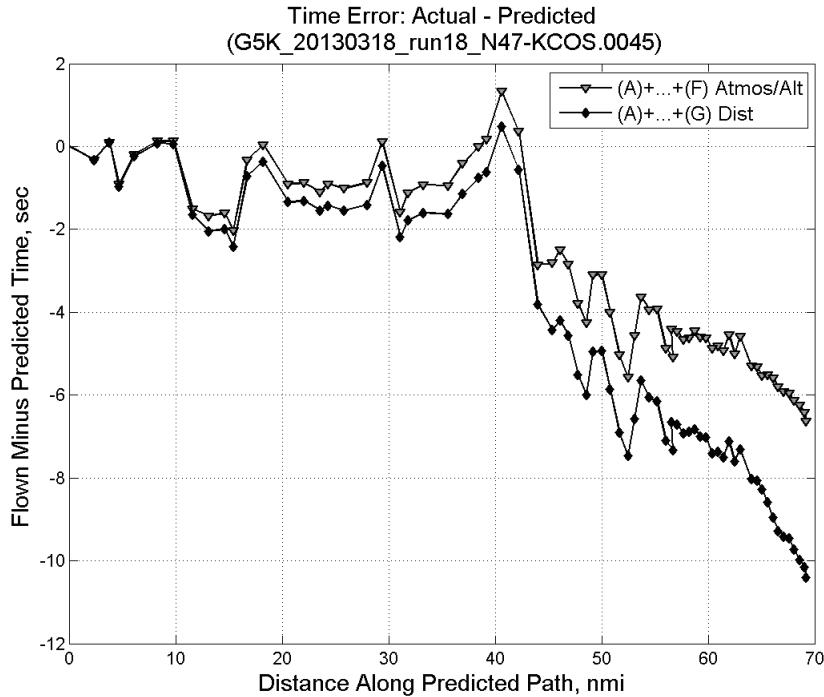


**Figure 274: Time error for run 18 before ((A)+...+(F) Atmos/Alt) and after ((A)+...+(G) Dist) removing path distance error source.**

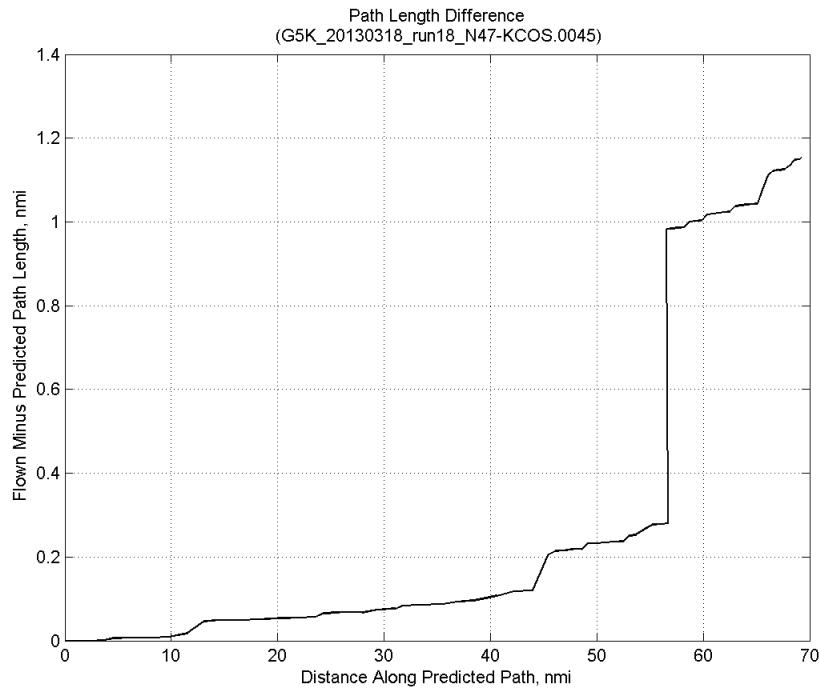


**Figure 275: ADC flown minus CTAS predicted path length for run 18. Positive values indicate aircraft followed a longer path than predicted by CTAS.**

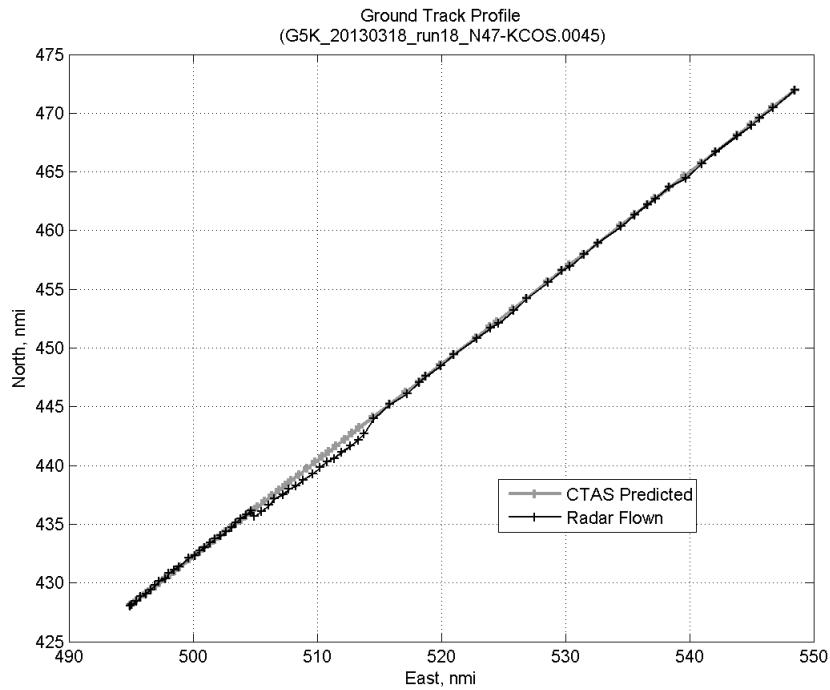


**Figure 276: CTAS predicted and radar flown ground track profile for run 18.**

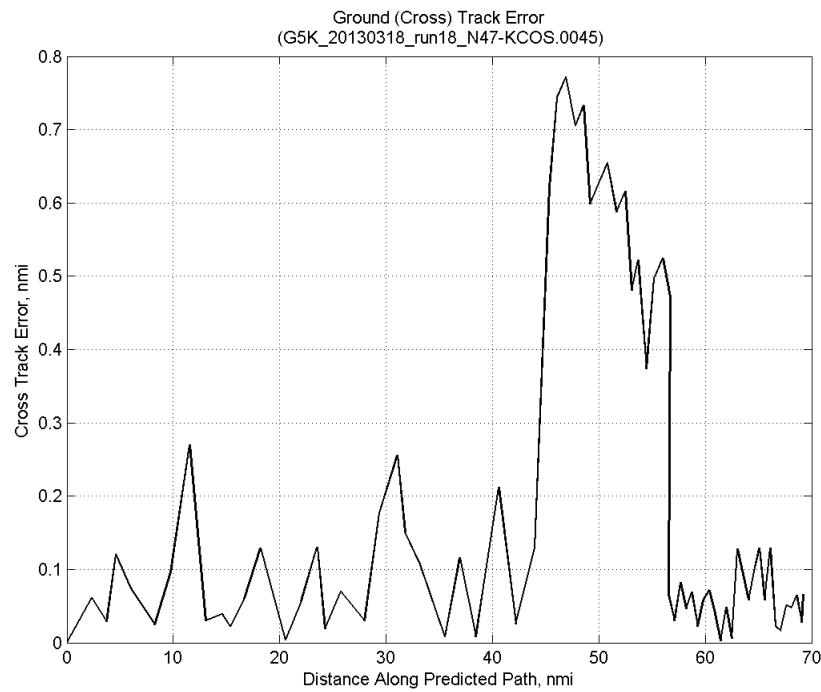


**Figure 277: Ground (cross) track error for run 18.**

### C.11. Run 19

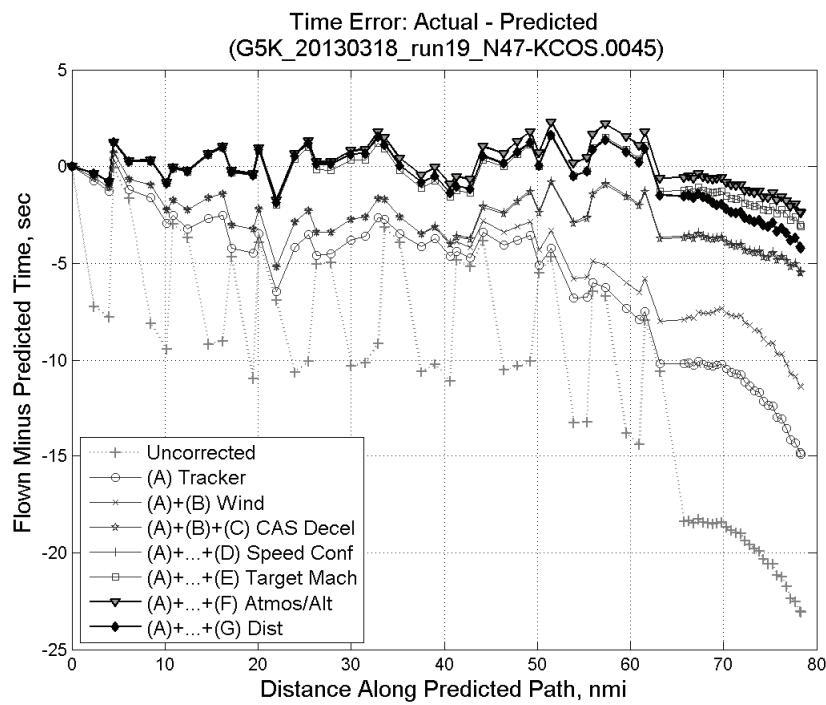


**Figure 278: Time error for run 19 showing incremental effect of removing each error source.**

#### C.11.A. Tracker Jumps

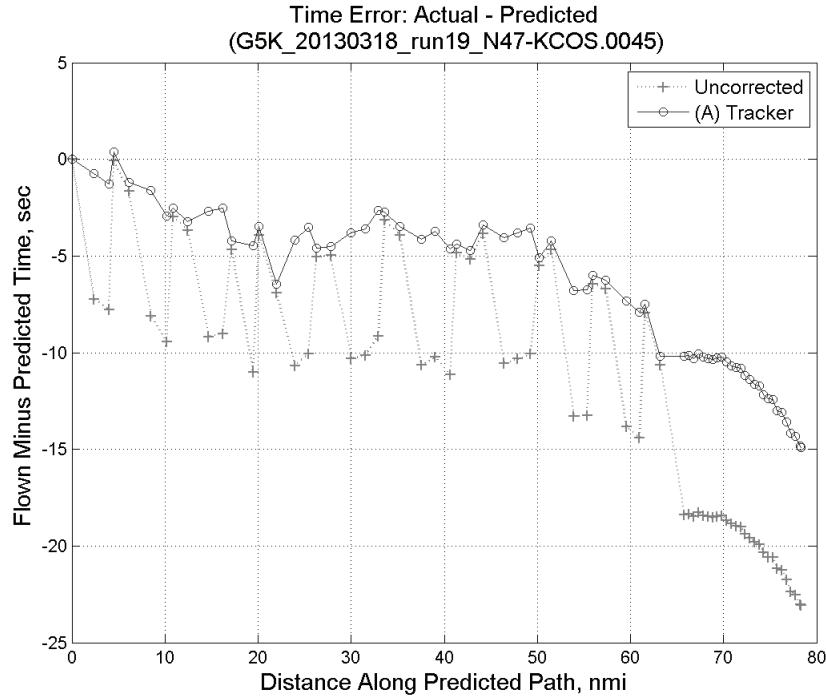


**Figure 279: Time error for run 19 before (Uncorrected) and after ((A) Tracker) removing tracker jump error source.**

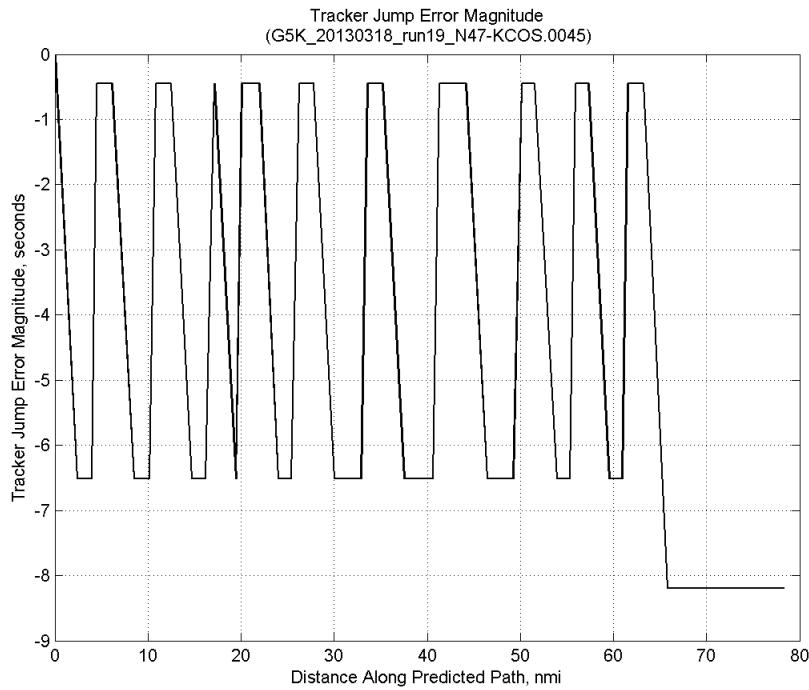


**Figure 280: Effect of tracker jump error source on time error for run 19.**

### C.11.B. Wind

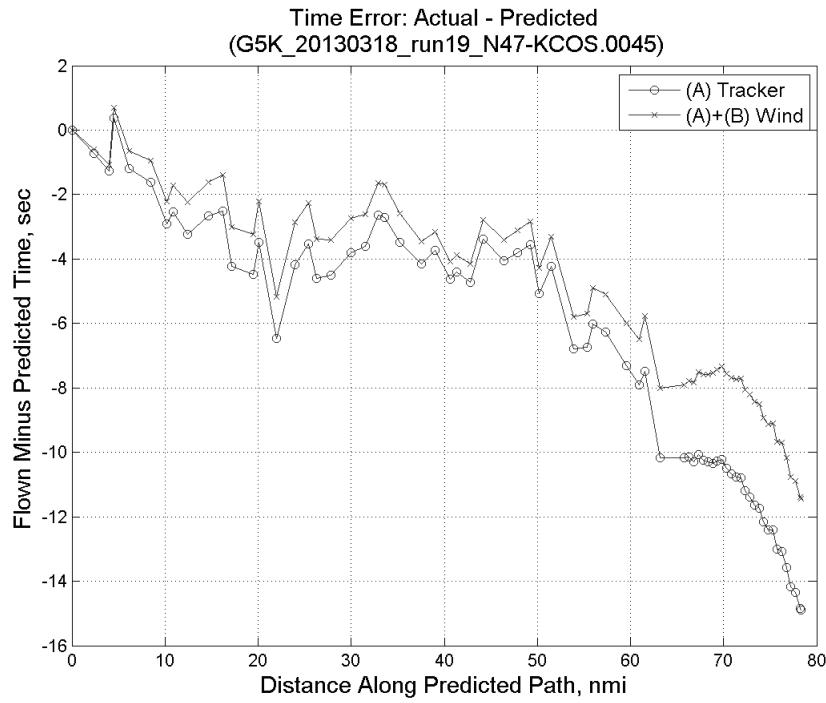


**Figure 281: Time error for run 19 before ((A) Tracker) and after ((A)+(B) Wind) removing wind error source.**

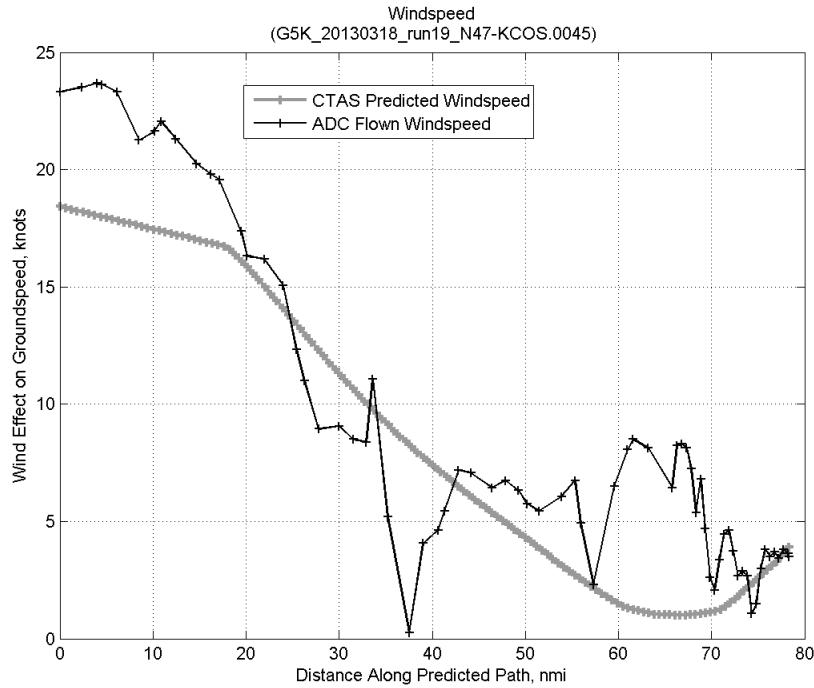


**Figure 282: CTAS predicted and ADC flown wind effect on ground speed for run 19. Negative values indicate a headwind.**

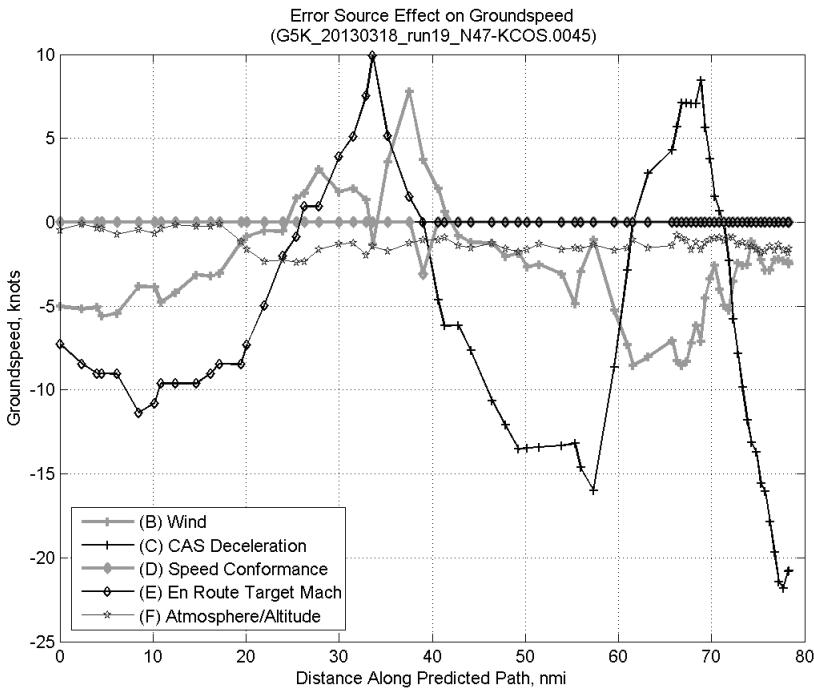


**Figure 283: Error sources (flown minus predicted) converted to a ground speed effect for run 19. Positive values indicate the flown ground speed was faster than the CTAS prediction.**

### C.11.C. CAS Deceleration

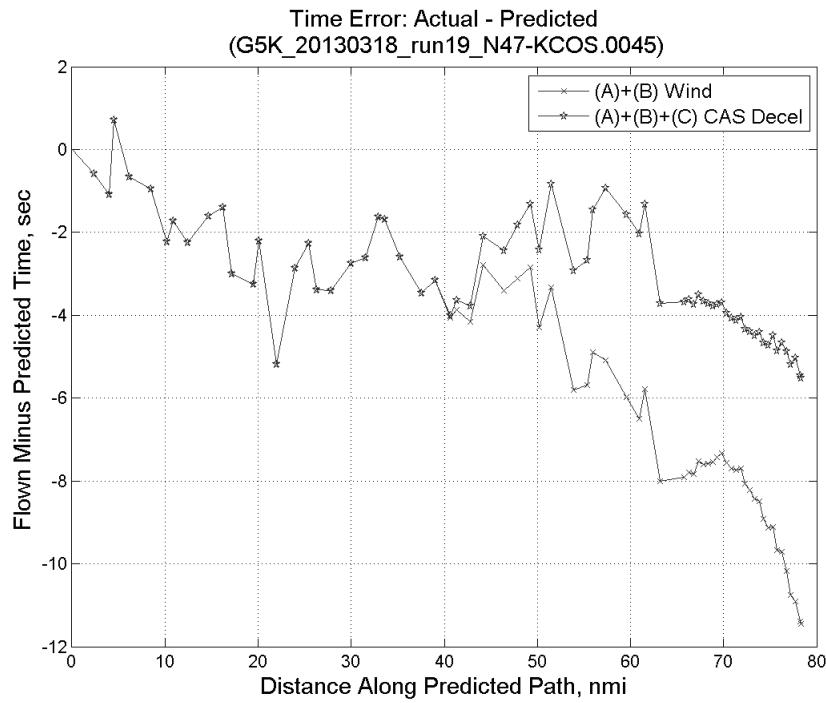


**Figure 284:** Time error for run 19 before ((A)+(B) Wind) and after ((A)+(B)+(C) CAS Decel) removing CAS deceleration error source.

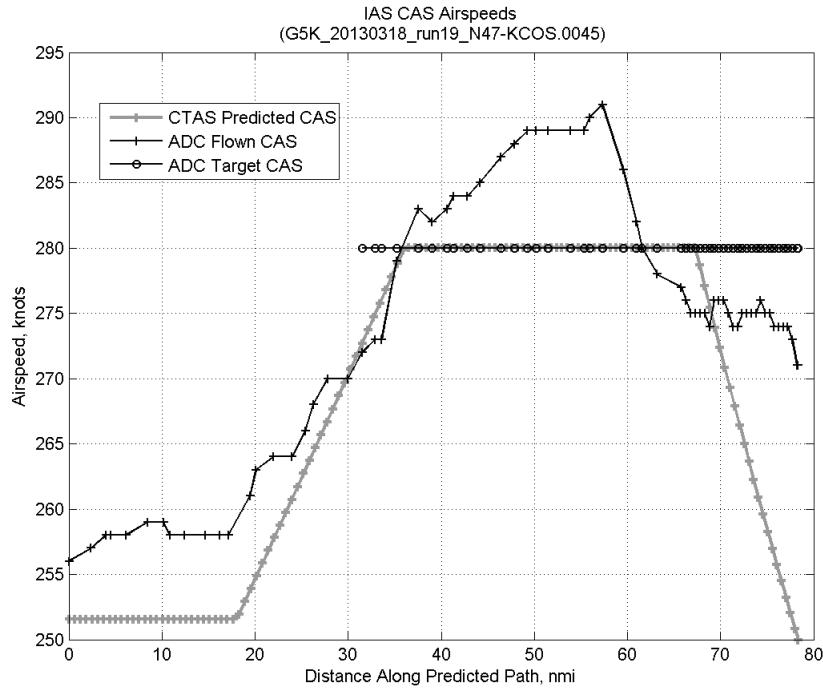


**Figure 285:** CTAS predicted and ADC flown CAS for run 19. CAS that is being targeted is shown with circle markers.

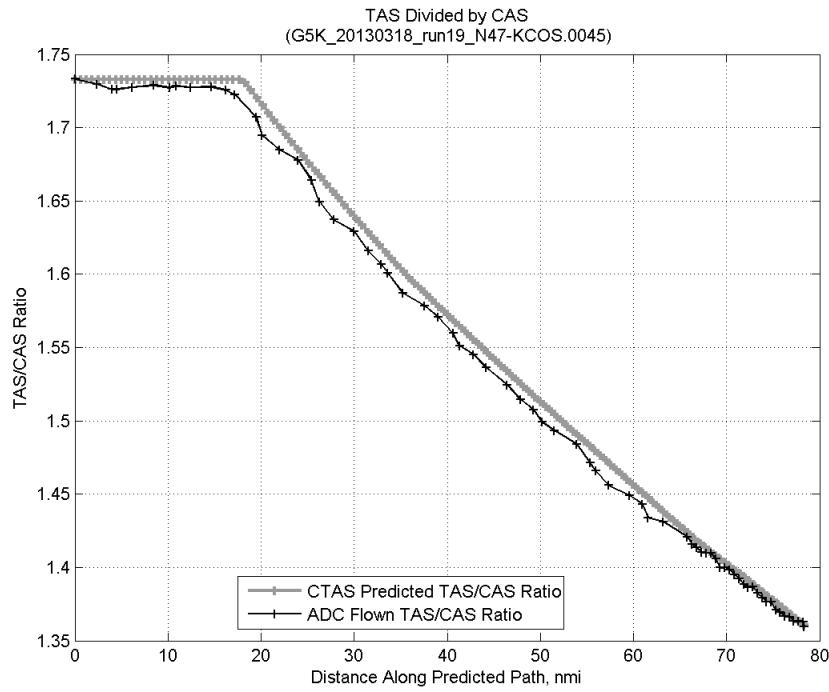


**Figure 286: CTAS predicted and ADC flown TAS/CAS ratio for run 19.**

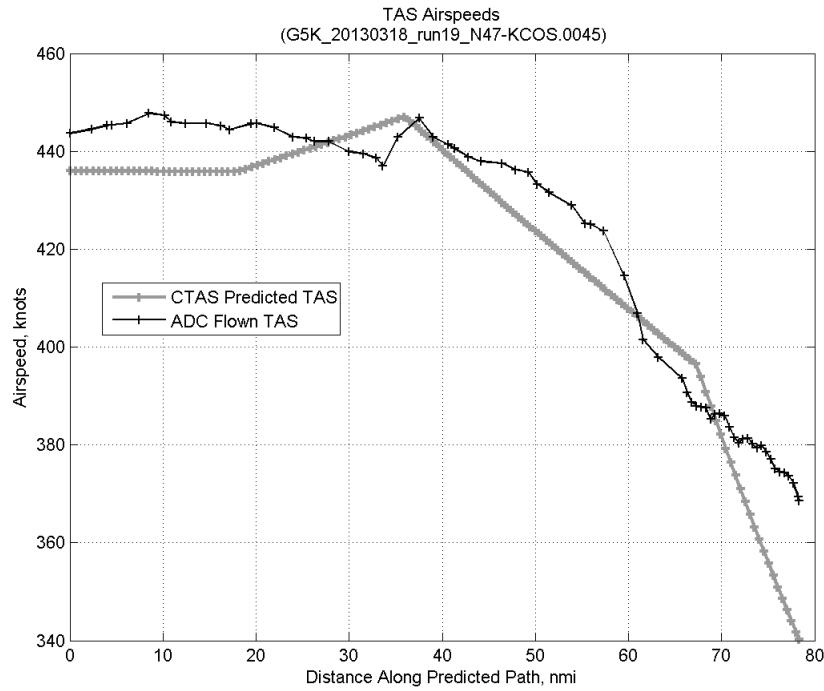


**Figure 287: CTAS predicted and ADC flown TAS for run 19.**

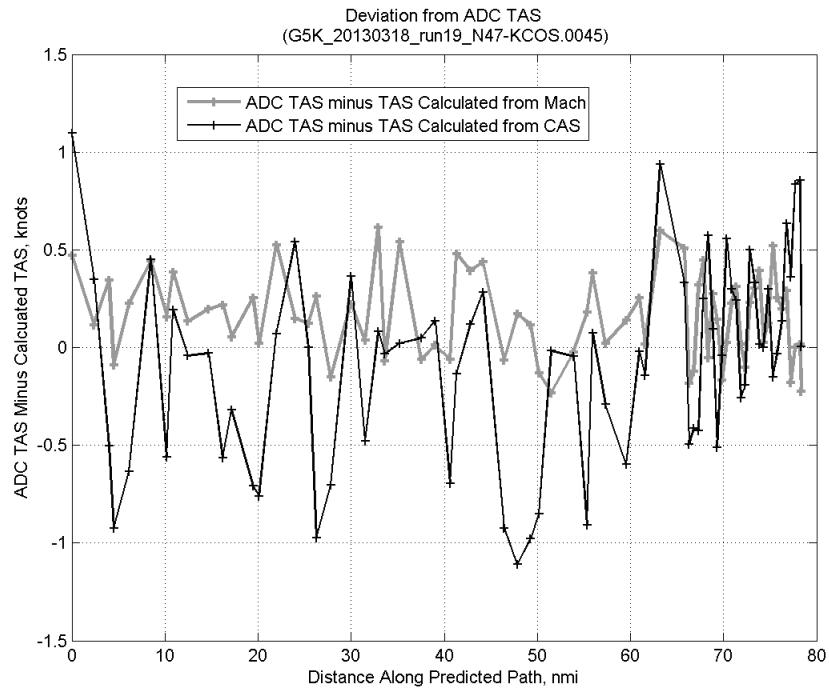


**Figure 288:** Deviation from ADC flown TAS if calculating TAS using ADC flown CAS, Mach, atmospheric temperature, and atmospheric pressure for run 19.

#### C.11.D. Speed Conformance

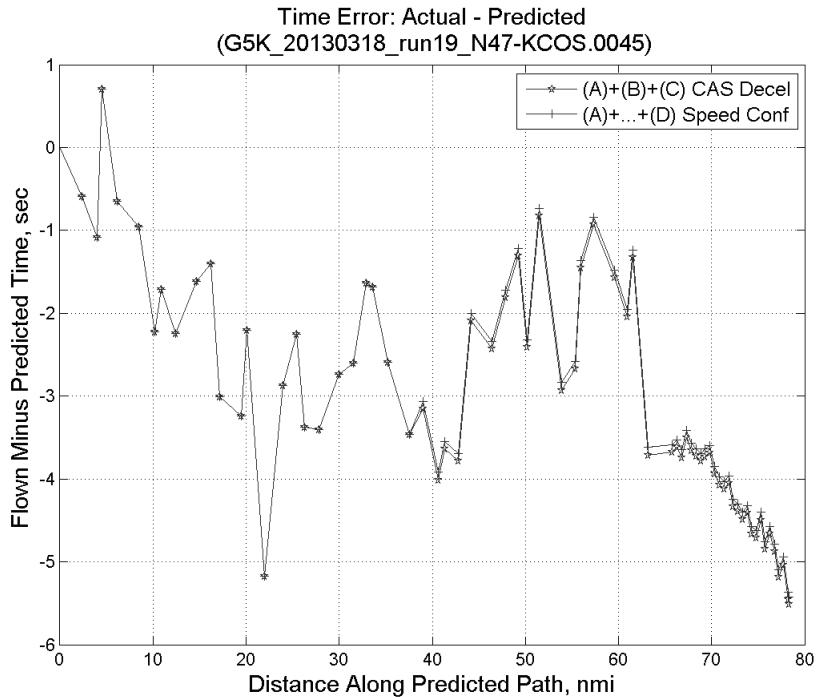


**Figure 289:** Time error for run 19 before  $((A)+(B)+(C) \text{ CAS Decel})$  and after  $((A)+\dots+(D) \text{ Speed Conf})$  removing speed conformance error source.

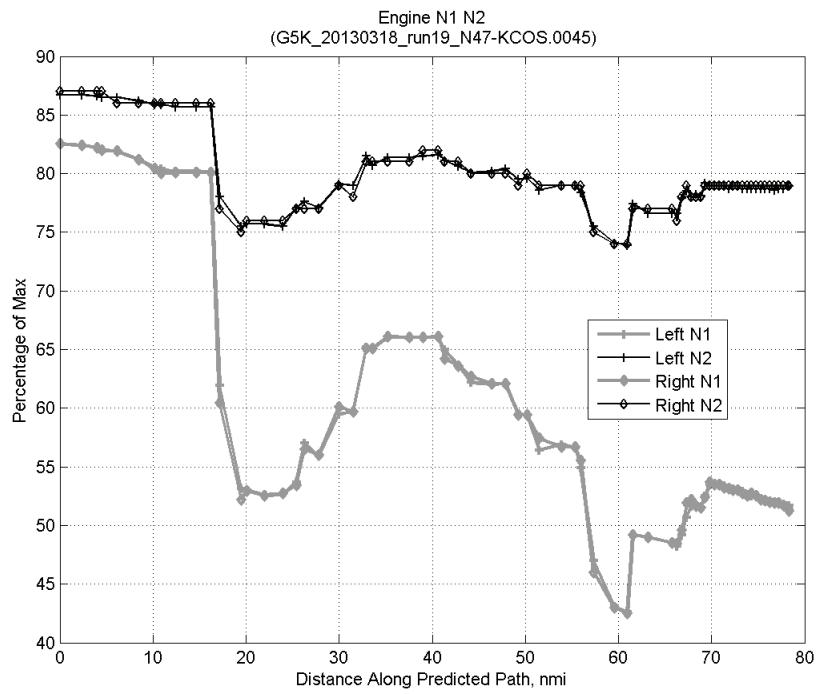


**Figure 290: Flown engine N1 and N2 for run 19.**

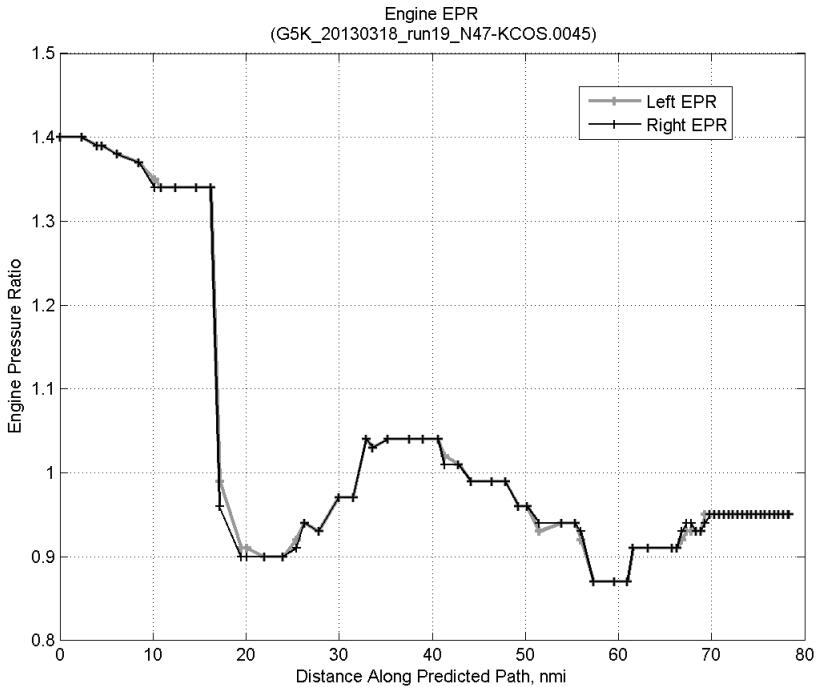


**Figure 291: Flown engine EPR for run 19.**

### C.11.E. Target Mach

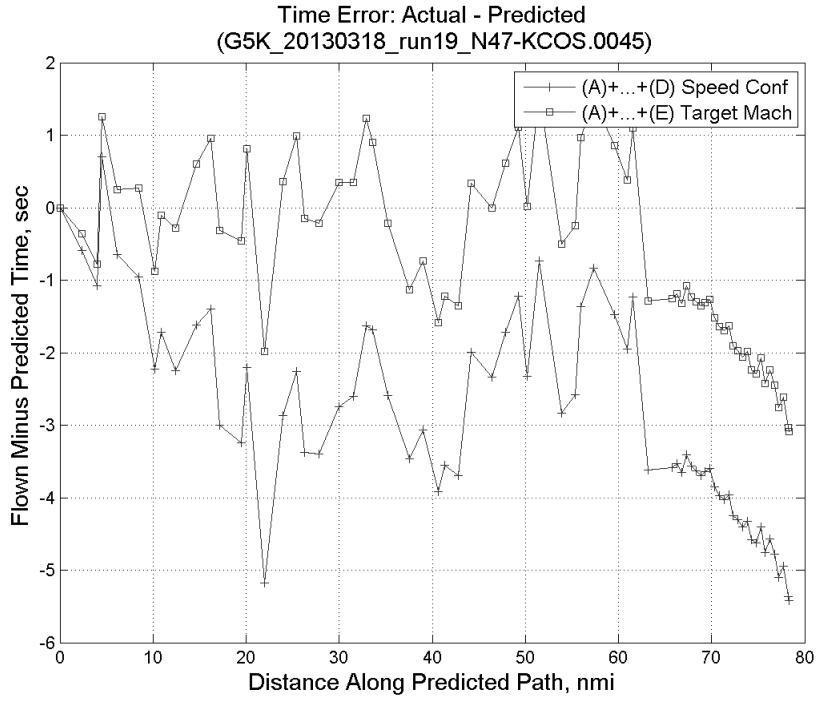


**Figure 292:** Time error for run 19 before ((A)+...+(D) Speed Conf) and after ((A)+...+(E) Target Mach) removing target Mach error source.

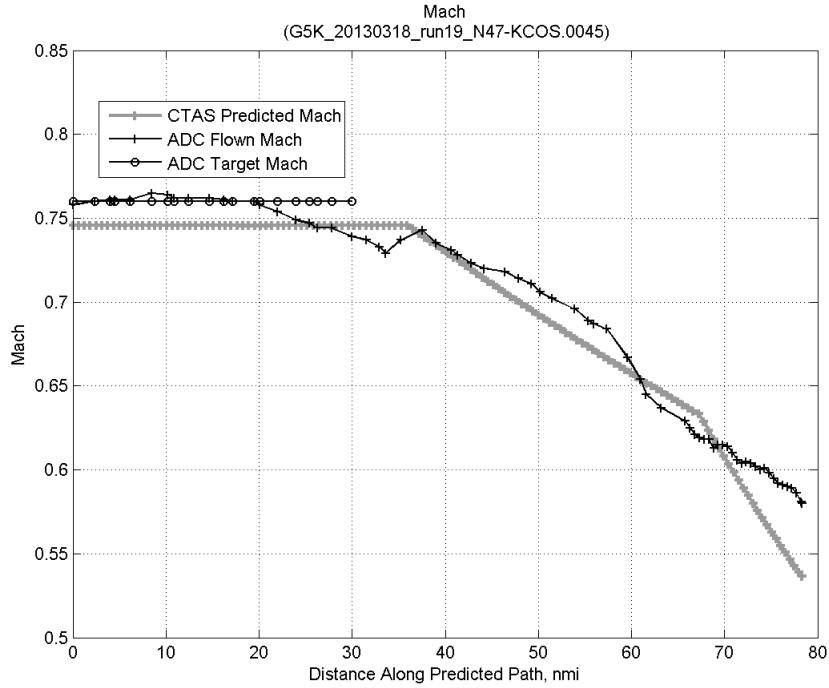


**Figure 293:** CTAS predicted and ADC flown Mach for run 19. Mach being targeted (ADC) shown with circle markers.

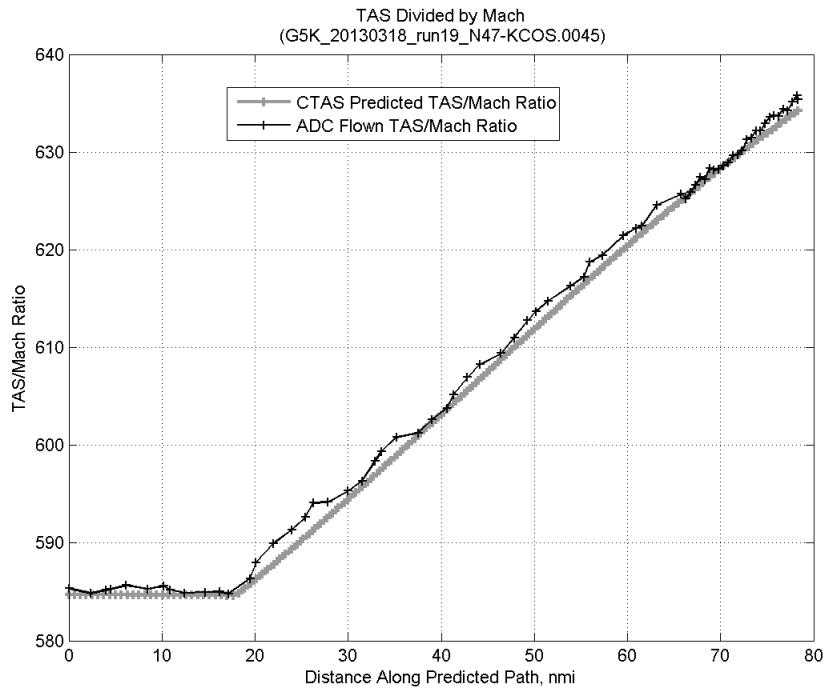


**Figure 294: CTAS predicted and ADC flown TAS/Mach ratio for run 19.**

#### C.11.F. Atmosphere/Altitude

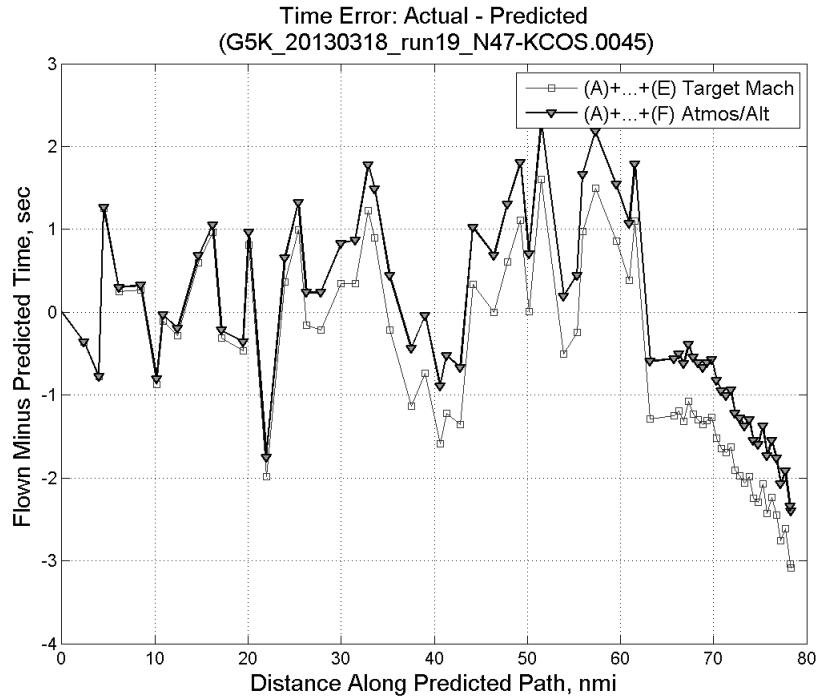


**Figure 295: Time error for run 19 before ((A)+...+(E) Target Mach) and after ((A)+...+(F) Atmos/Alt) removing atmosphere/altitude error source.**

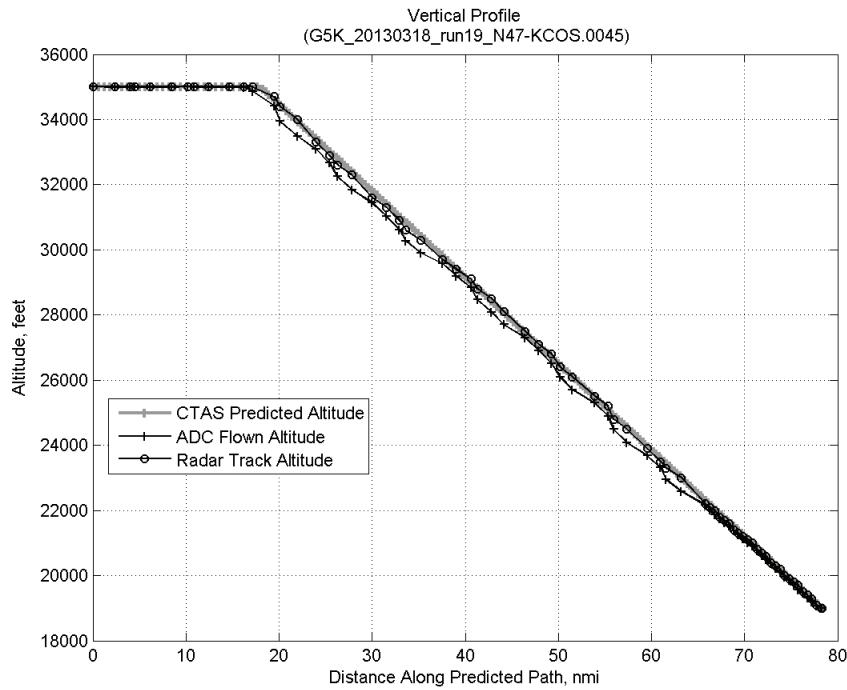


**Figure 296: Flown (ADC) and predicted (CTAS) vertical profile for run 19.**

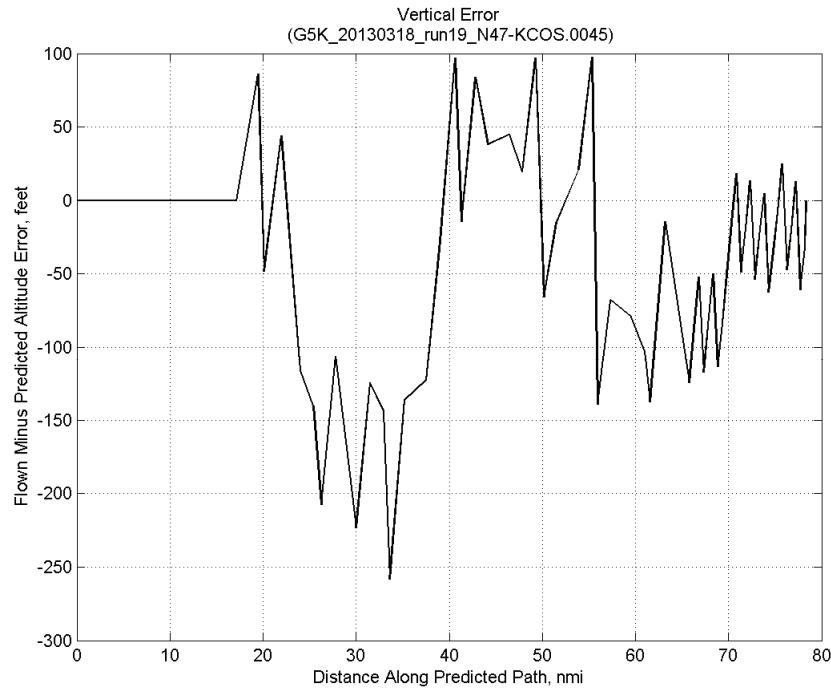


**Figure 297: Vertical error (flown minus predicted altitude) for run 19. Positive values indicate aircraft flew higher than predicted by CTAS.**

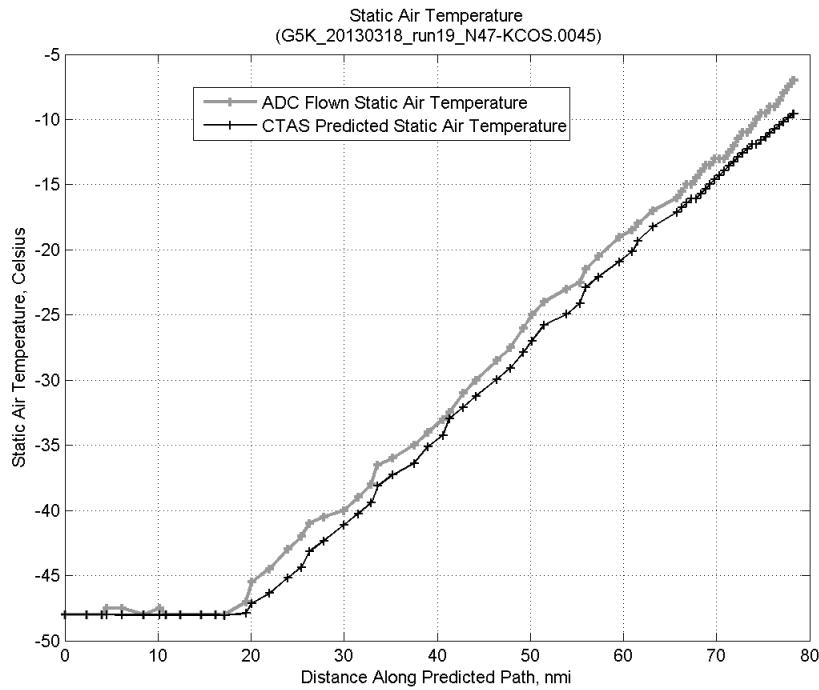


**Figure 298: Flown (ADC) and predicted (CTAS) static air temperature for run 19.**

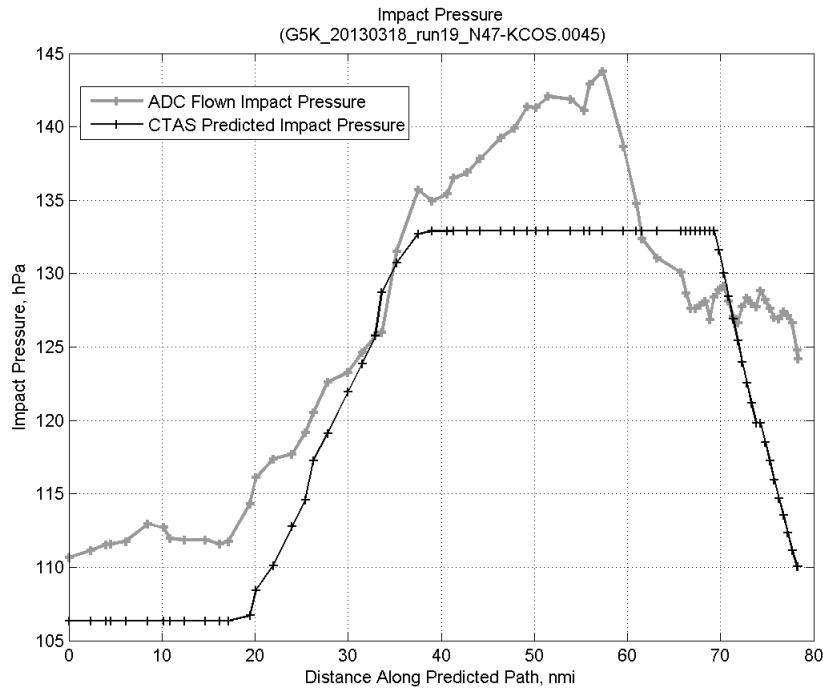


**Figure 299: Flown (ADC) and predicted (CTAS) impact pressure for run 19.**

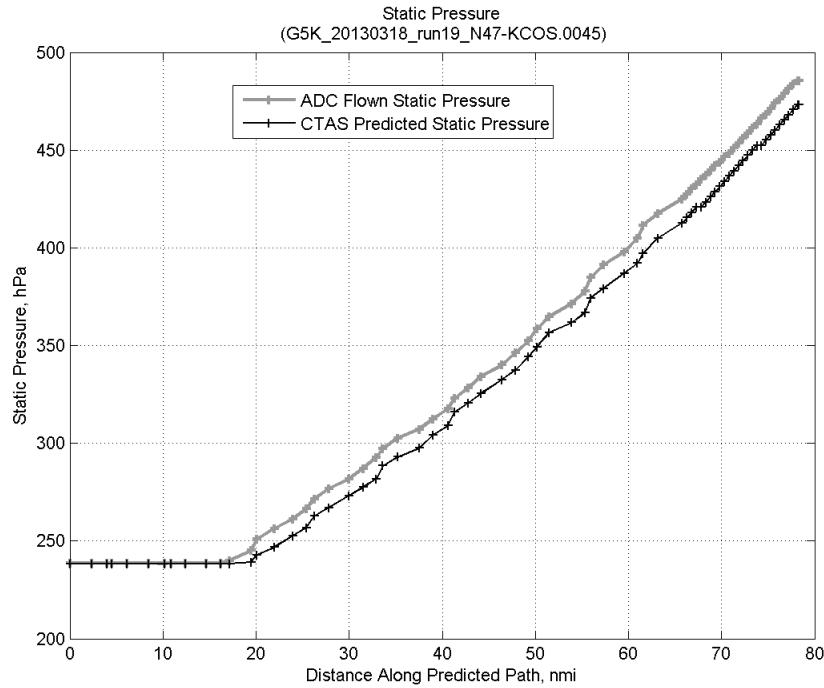


**Figure 300: Flown (ADC) and predicted (CTAS) static pressure for run 19.**

#### C.11.G. Path Distance

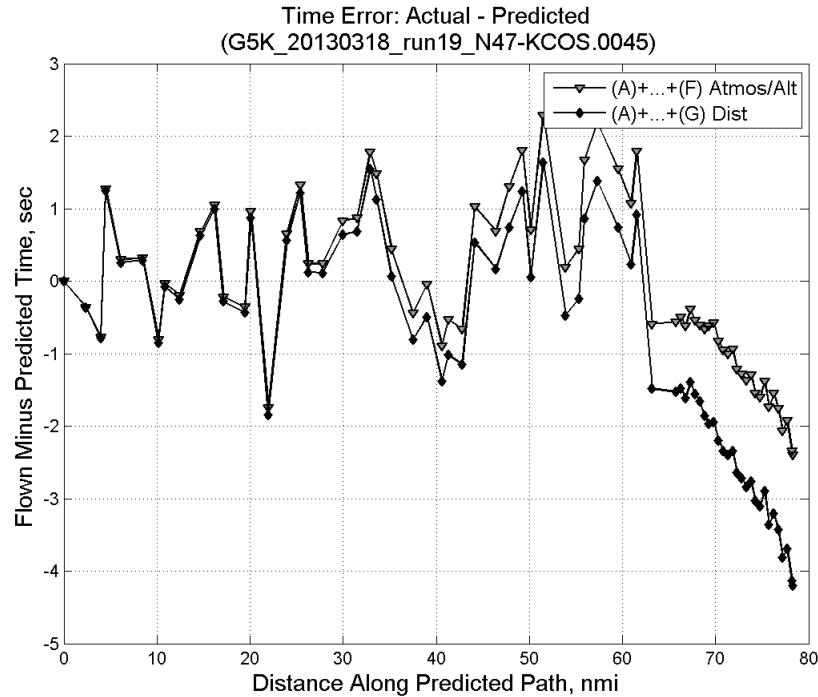


**Figure 301: Time error for run 19 before ((A)+...+(F) Atmos/Alt) and after ((A)+...+(G) Dist) removing path distance error source.**

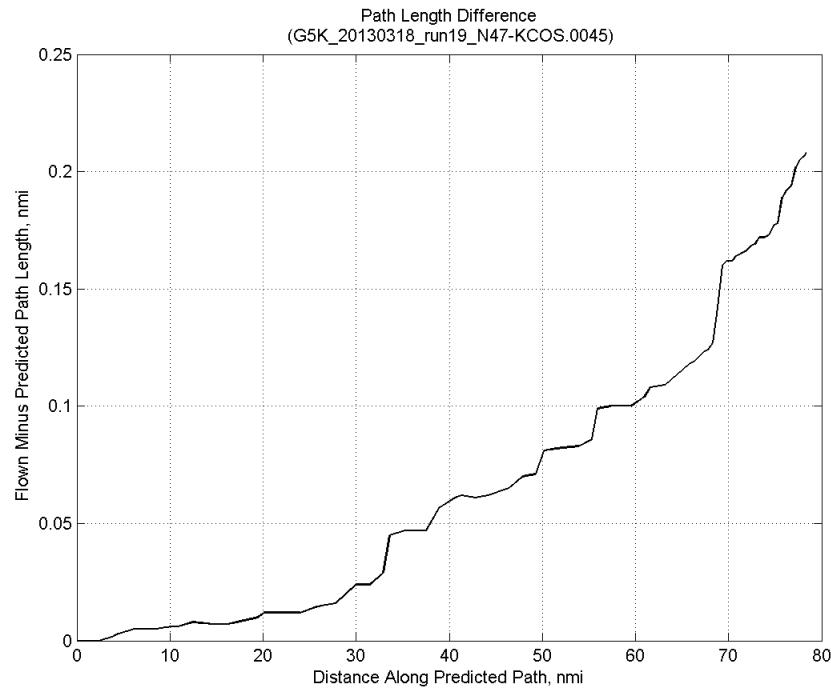


**Figure 302: ADC flown minus CTAS predicted path length for run 19. Positive values indicate aircraft followed a longer path than predicted by CTAS.**

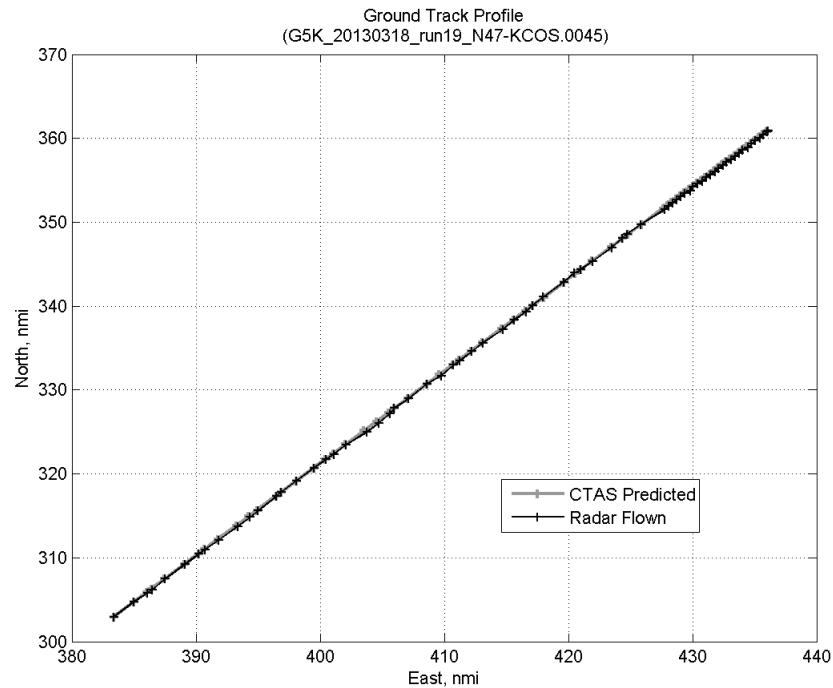


**Figure 303: CTAS predicted and radar flown ground track profile for run 19.**

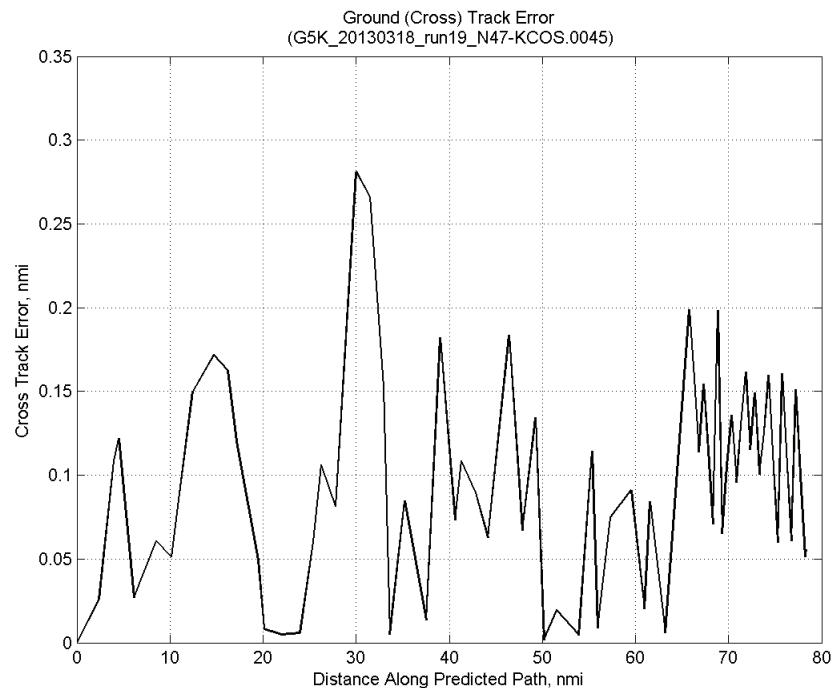


**Figure 304: Ground (cross) track error for run 19.**

## C.12. Run 21

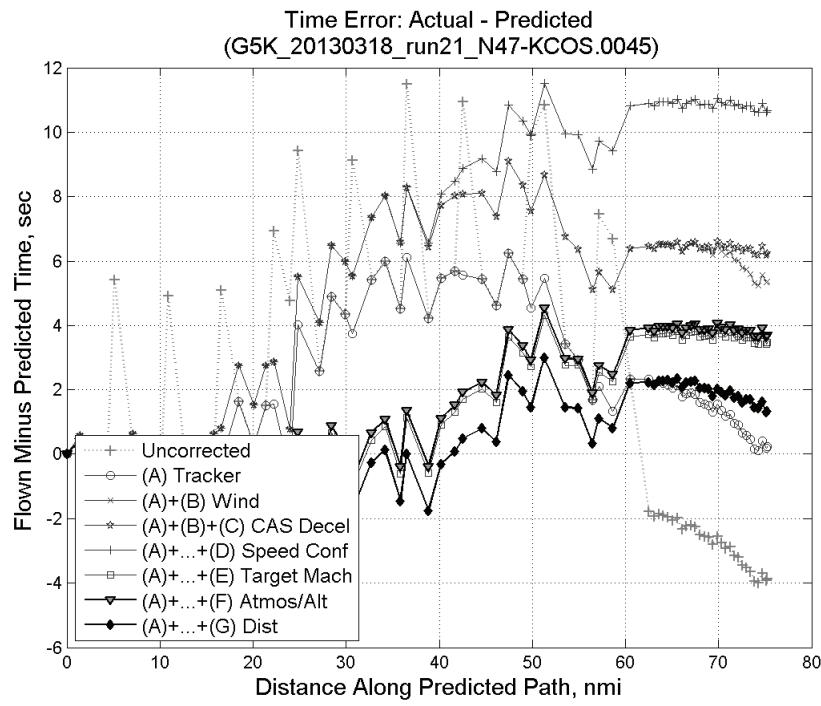


**Figure 305: Time error for run 21 showing incremental effect of removing each error source.**

### C.12.A. Tracker Jumps

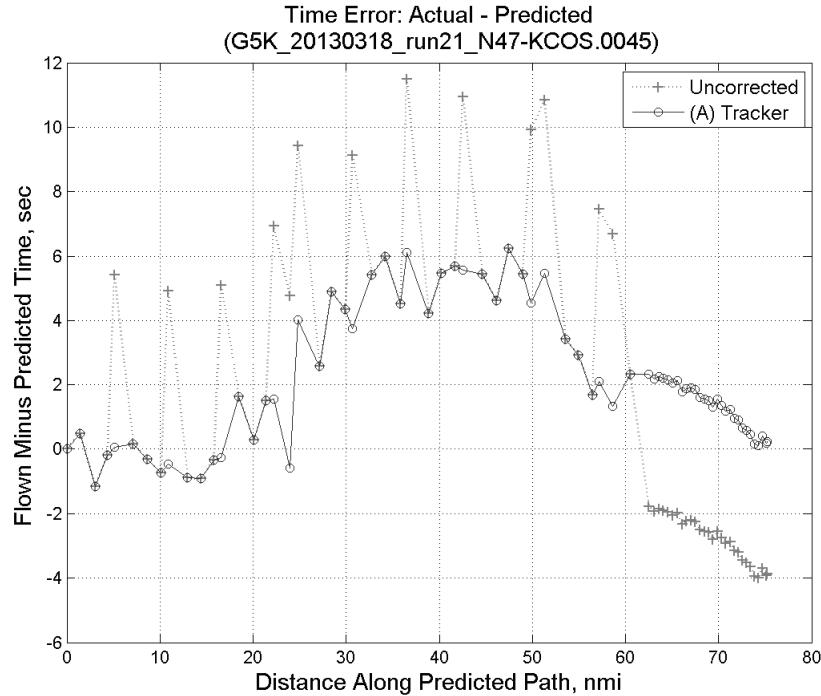


**Figure 306: Time error for run 21 before (Uncorrected) and after ((A) Tracker) removing tracker jump error source.**

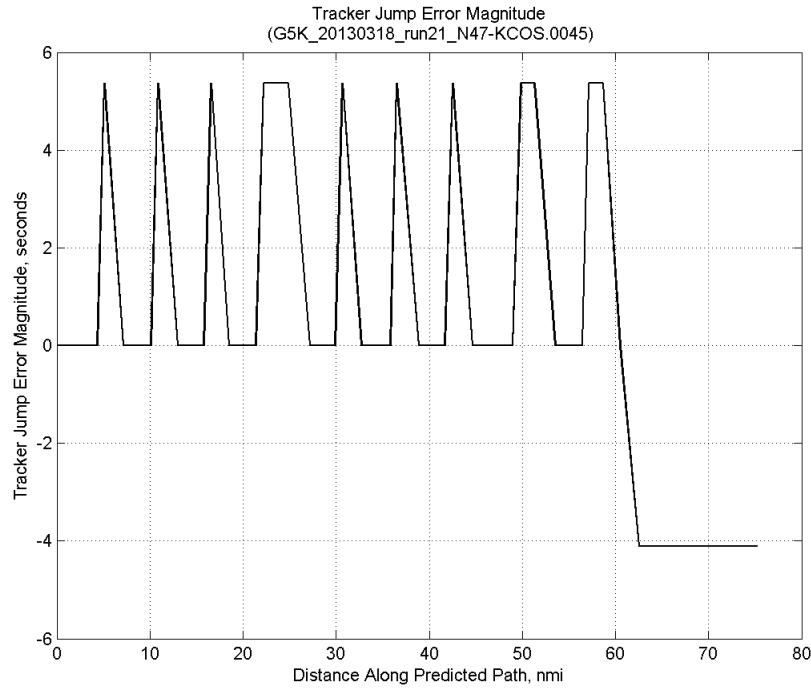


**Figure 307: Effect of tracker jump error source on time error for run 21.**

### C.12.B. Wind

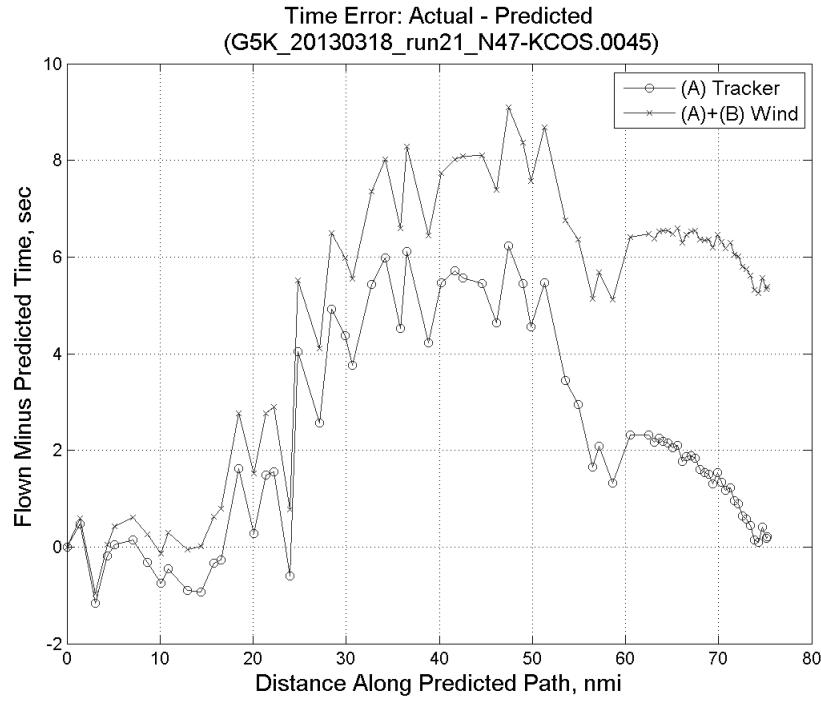


**Figure 308: Time error for run 21 before ((A) Tracker) and after ((A)+(B) Wind) removing wind error source.**

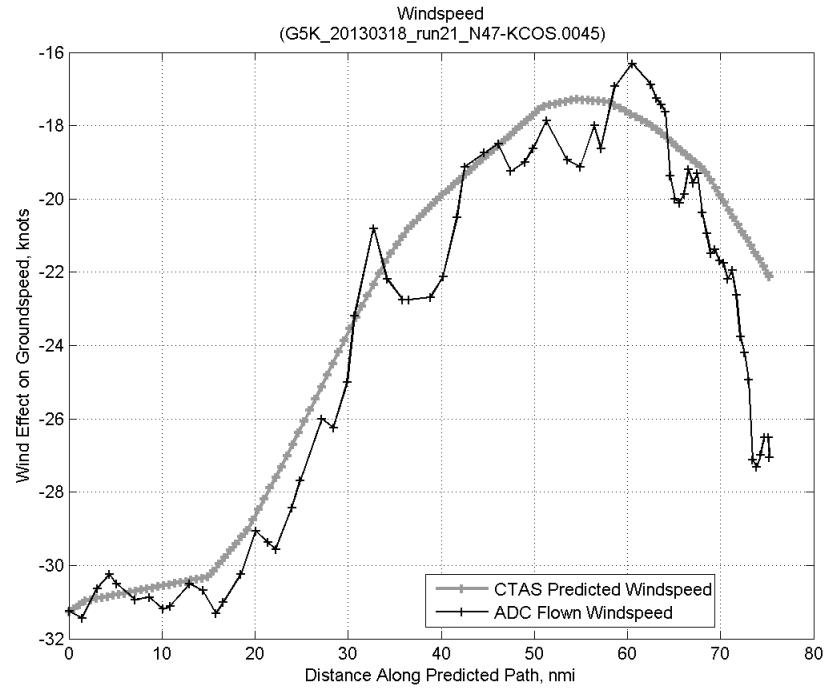


**Figure 309: CTAS predicted and ADC flown wind effect on ground speed for run 21. Negative values indicate a headwind.**

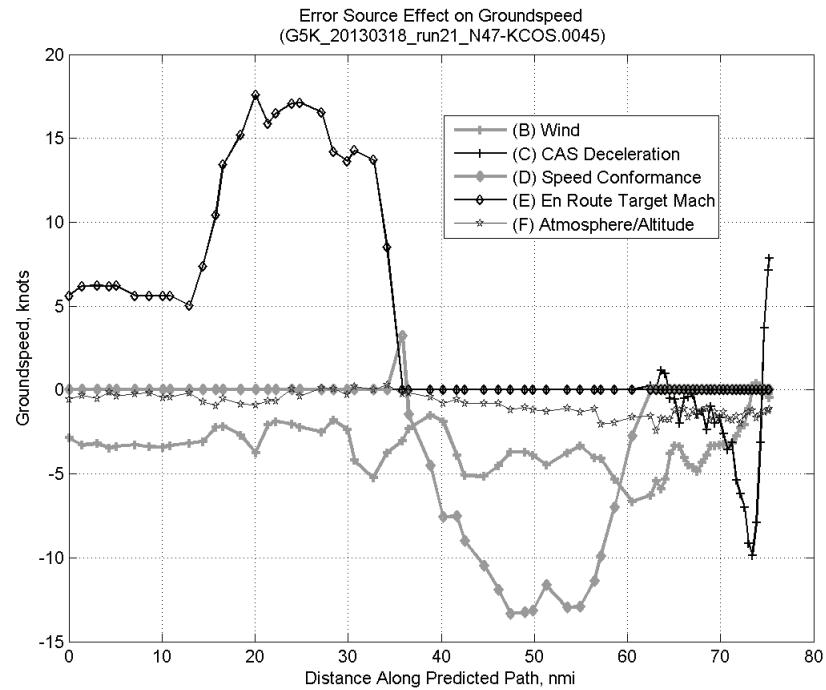


**Figure 310: Error sources (flown minus predicted) converted to a ground speed effect for run 21. Positive values indicate the flown ground speed was faster than the CTAS prediction.**

### C.12.C. CAS Deceleration

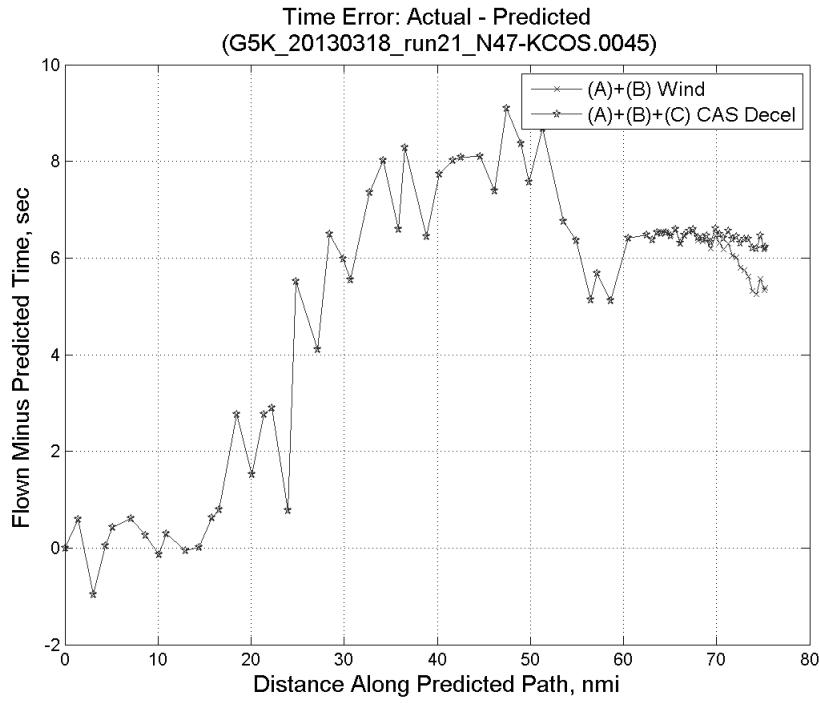


**Figure 311:** Time error for run 21 before ((A)+(B) Wind) and after ((A)+(B)+(C) CAS Decel) removing CAS deceleration error source.

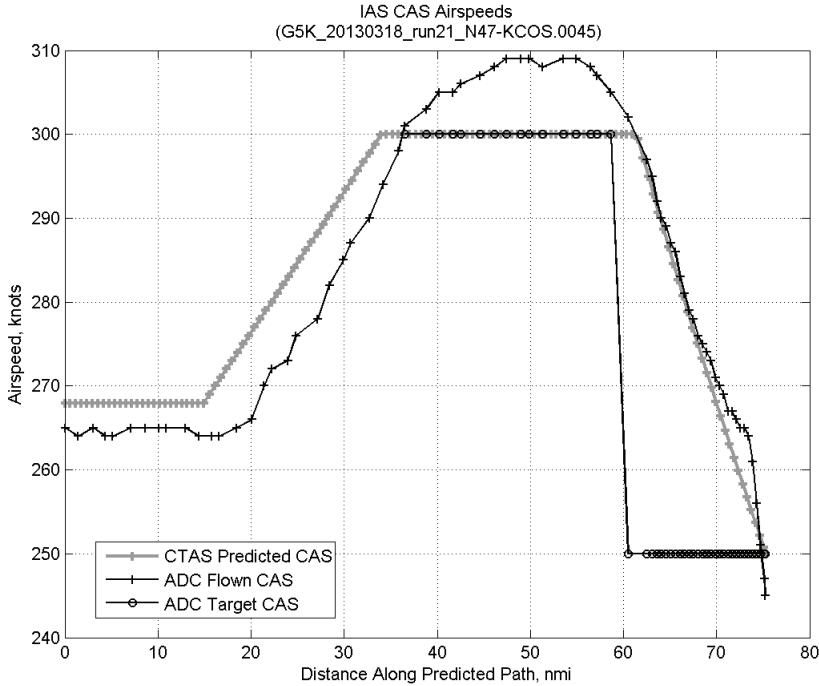


**Figure 312:** CTAS predicted and ADC flown CAS for run 21. CAS that is being targeted is shown with circle markers.

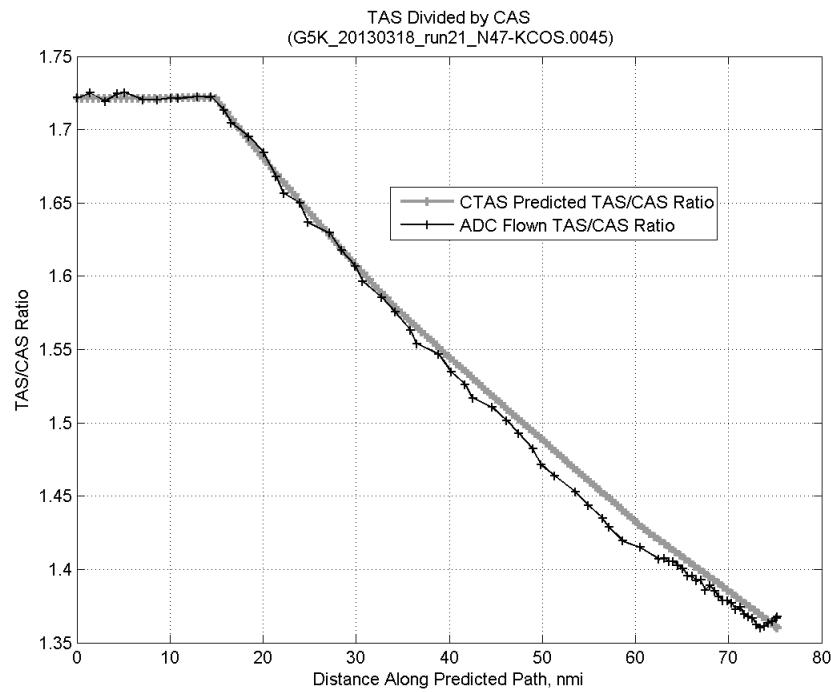


**Figure 313: CTAS predicted and ADC flown TAS/CAS ratio for run 21.**

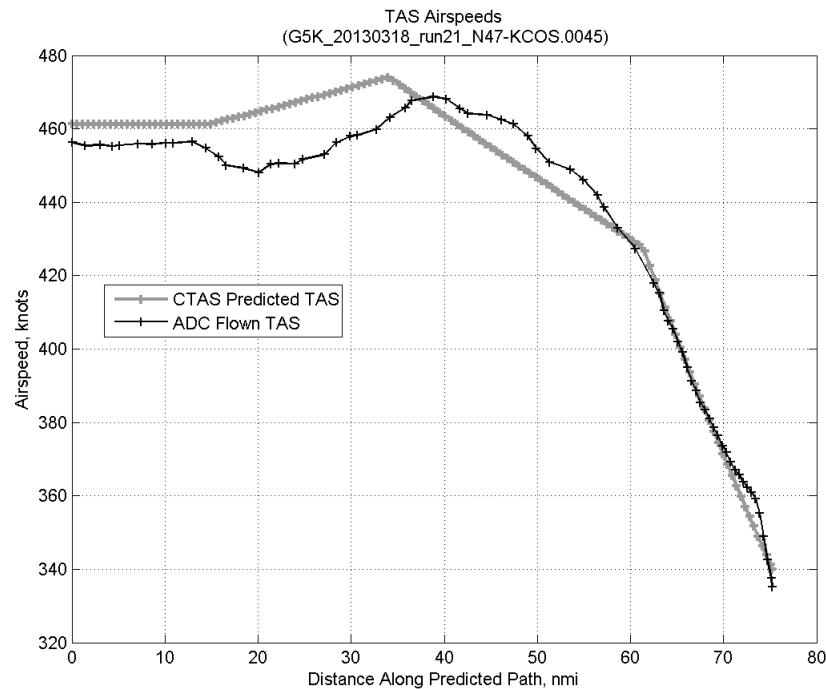


**Figure 314: CTAS predicted and ADC flown TAS for run 21.**

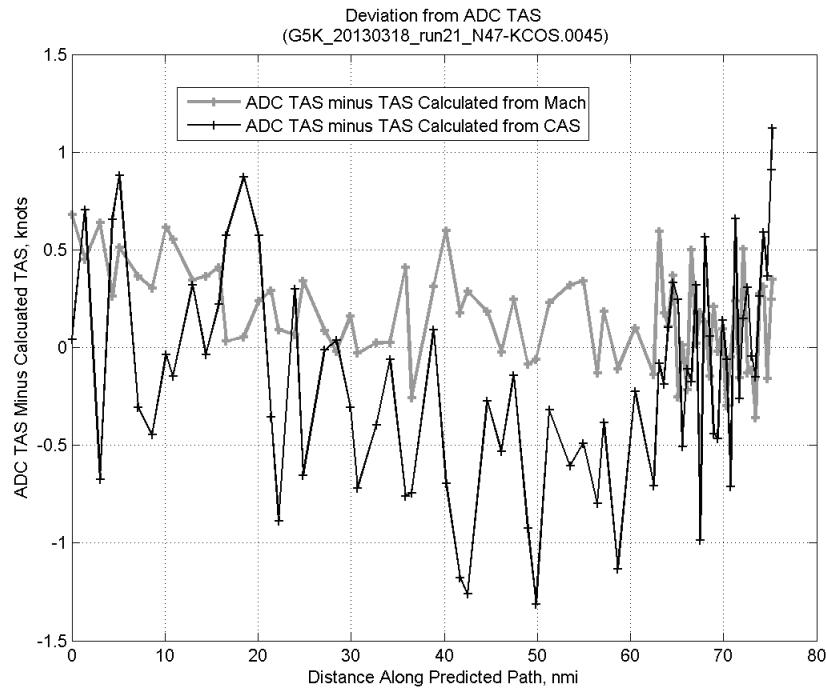


**Figure 315:** Deviation from ADC flown TAS if calculating TAS using ADC flown CAS, Mach, atmospheric temperature, and atmospheric pressure for run 21.

#### C.12.D. Speed Conformance

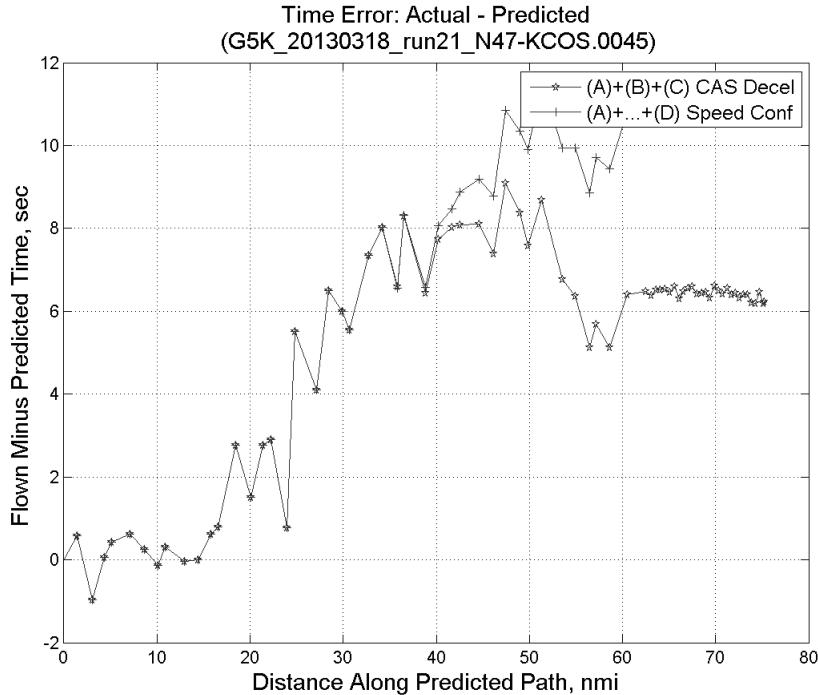


**Figure 316:** Time error for run 21 before  $((A)+(B)+(C) \text{ CAS Decel})$  and after  $((A)+\dots+(D) \text{ Speed Conf})$  removing speed conformance error source.

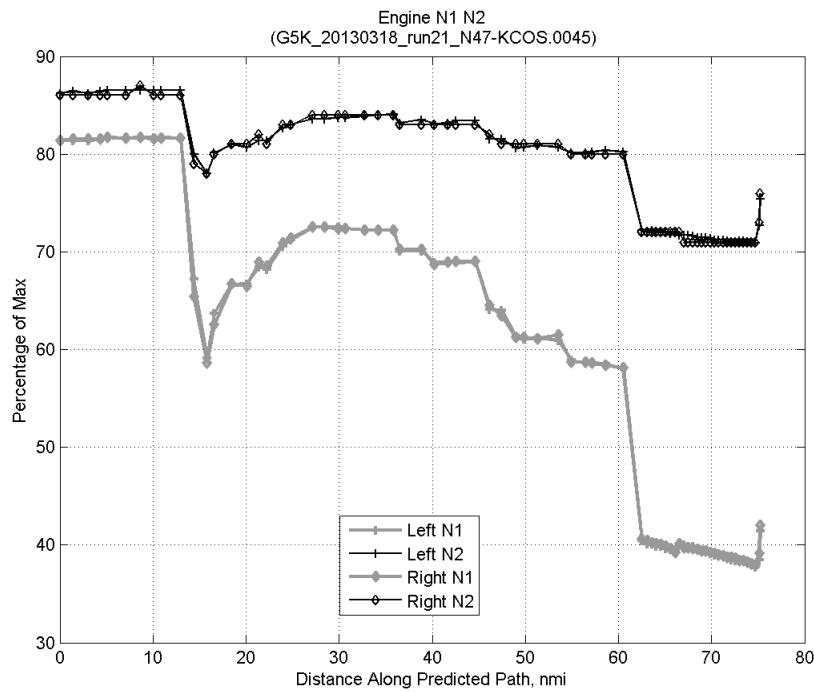


**Figure 317: Flown engine N1 and N2 for run 21.**

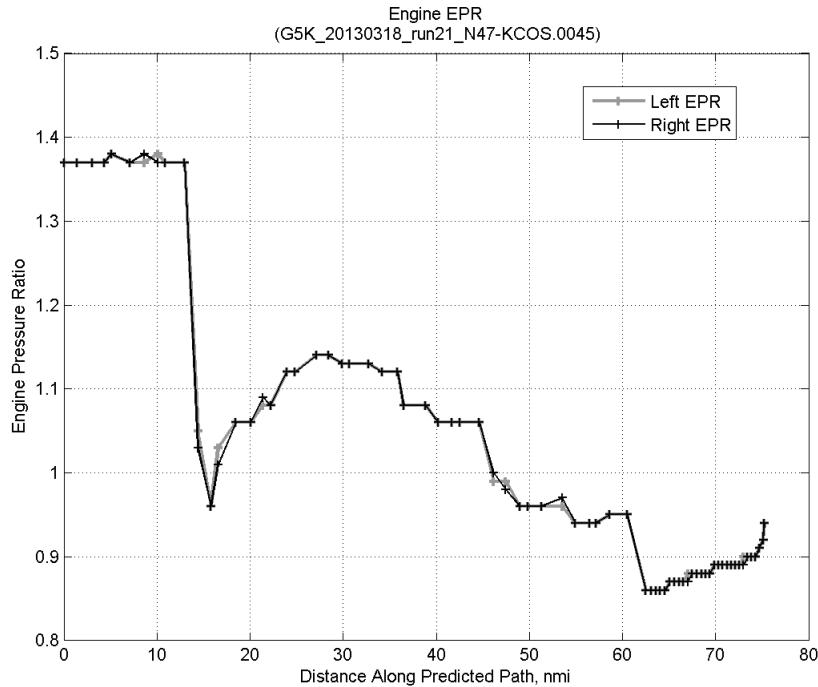


**Figure 318: Flown engine EPR for run 21.**

### C.12.E. Target Mach

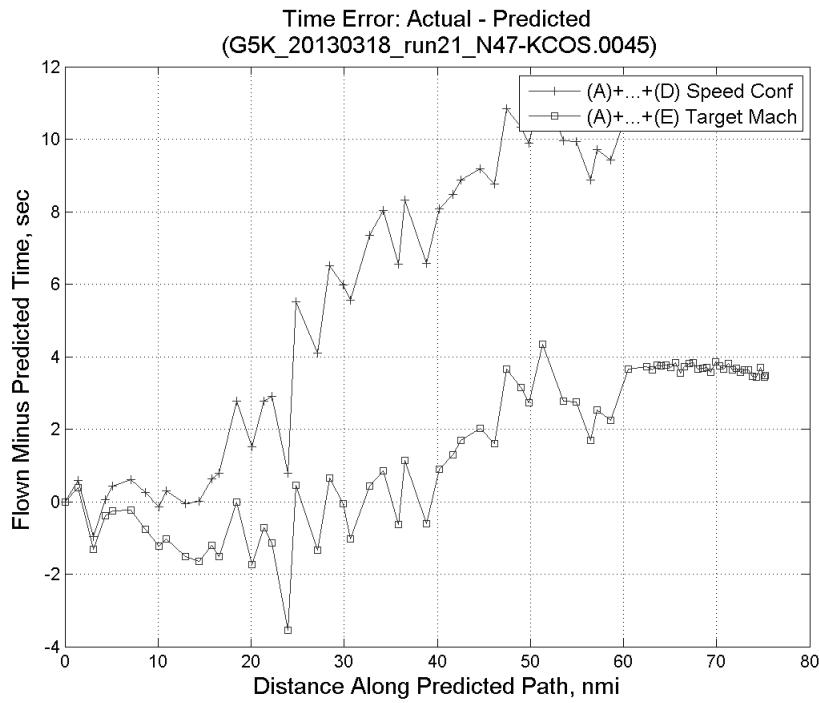


**Figure 319:** Time error for run 21 before ((A)+...+(D) Speed Conf) and after ((A)+...+(E) Target Mach) removing target Mach error source.

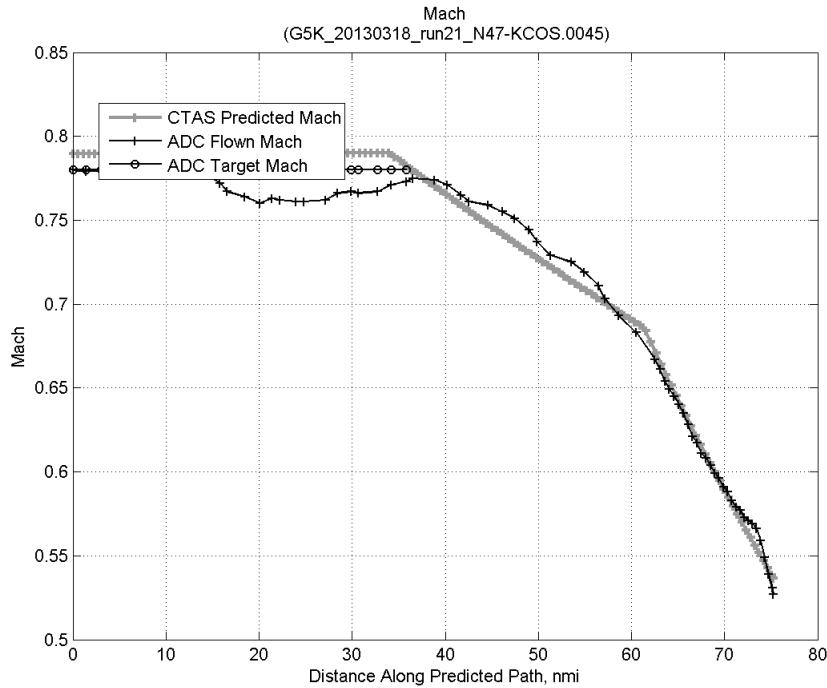


**Figure 320:** CTAS predicted and ADC flown Mach for run 21. Mach being targeted (ADC) shown with circle markers.

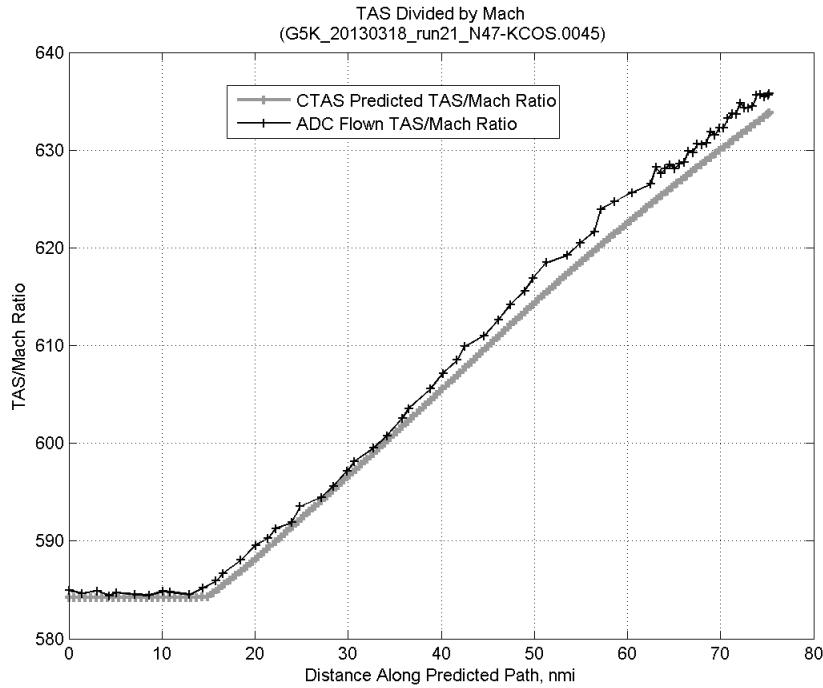


**Figure 321: CTAS predicted and ADC flown TAS/Mach ratio for run 21.**

#### C.12.F. Atmosphere/Altitude

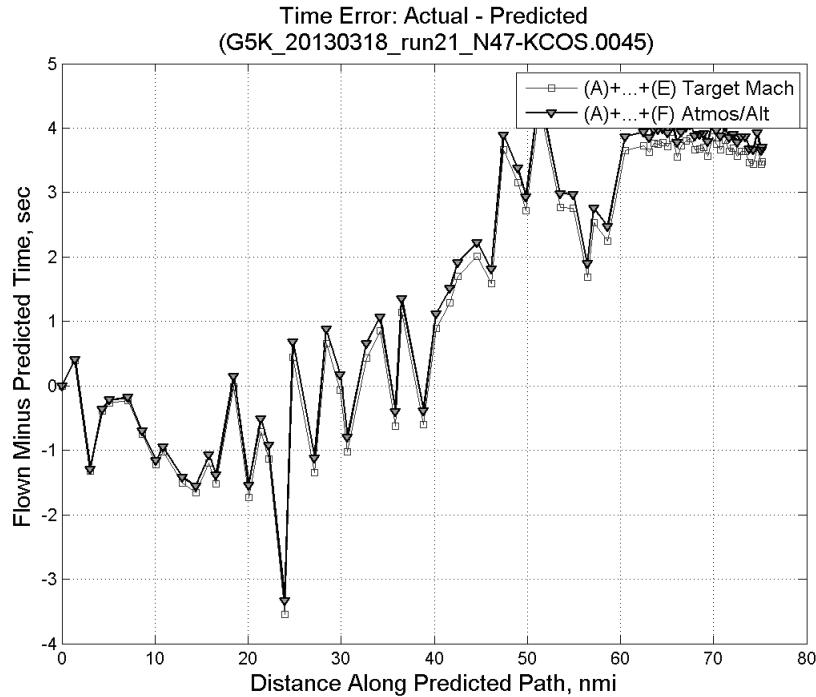


**Figure 322: Time error for run 21 before ((A)+...+(E) Target Mach) and after ((A)+...+(F) Atmos/Alt) removing atmosphere/altitude error source.**

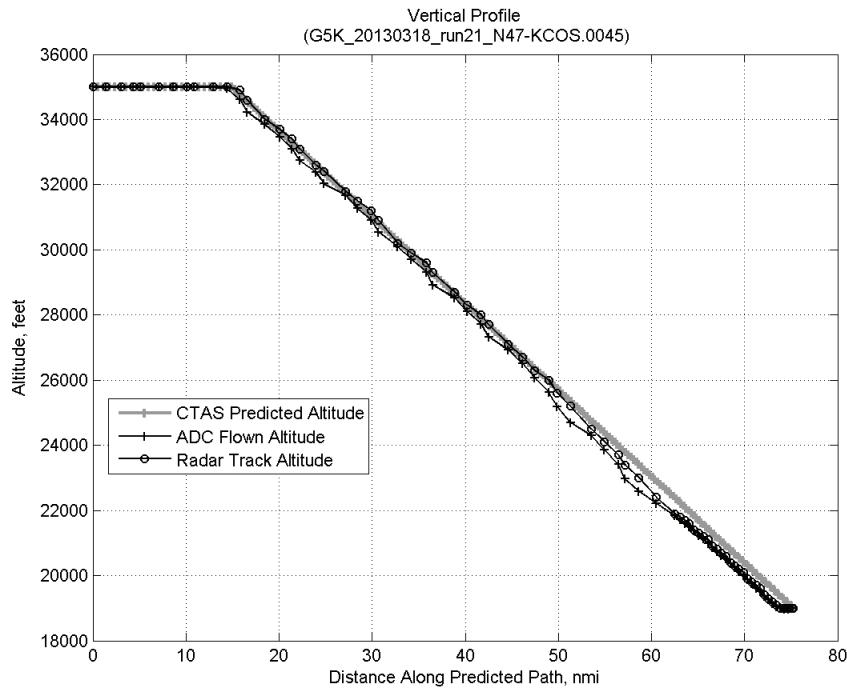


**Figure 323: Flown (ADC) and predicted (CTAS) vertical profile for run 21.**

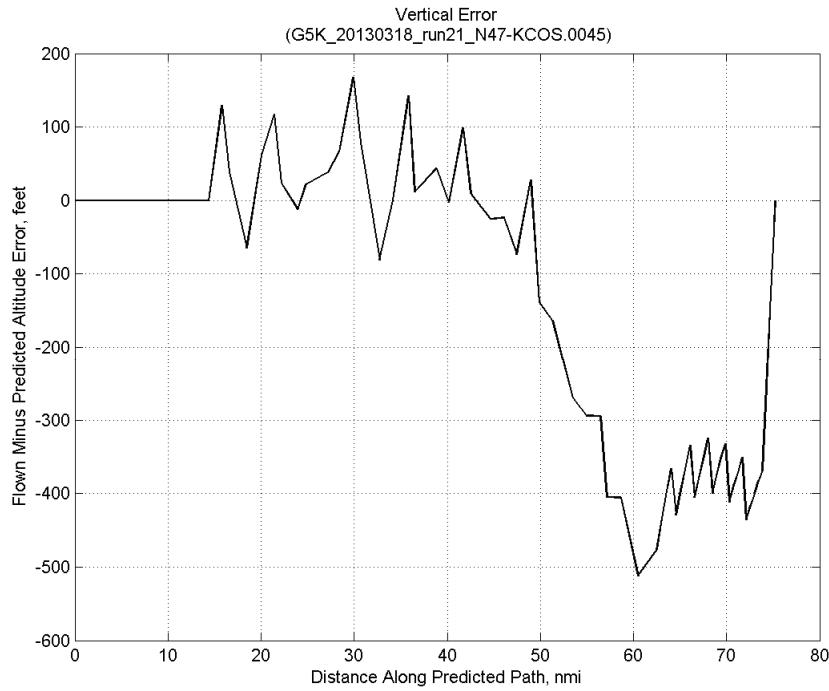


**Figure 324: Vertical error (flown minus predicted altitude) for run 21. Positive values indicate aircraft flew higher than predicted by CTAS.**

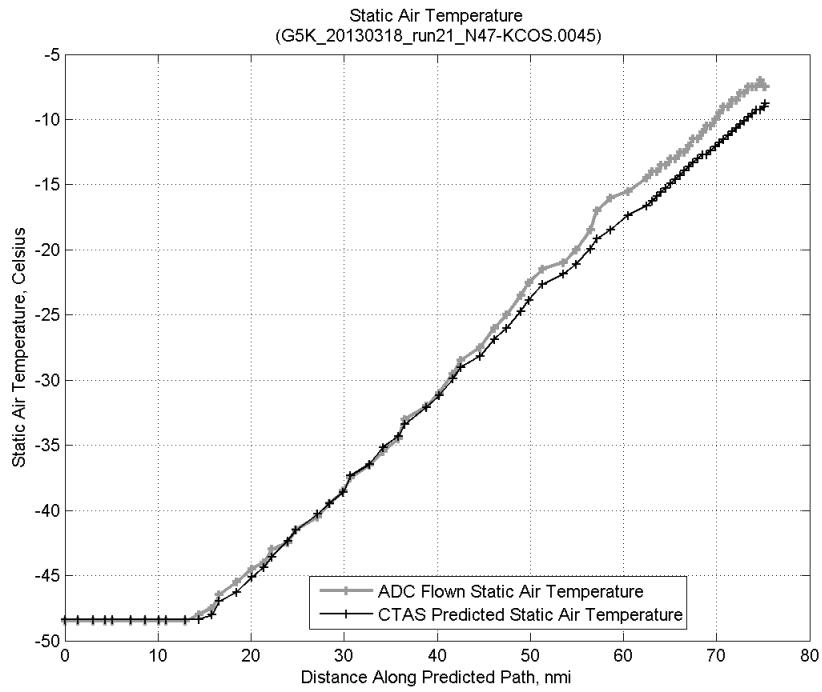


**Figure 325:** Flown (ADC) and predicted (CTAS) static air temperature for run 21.

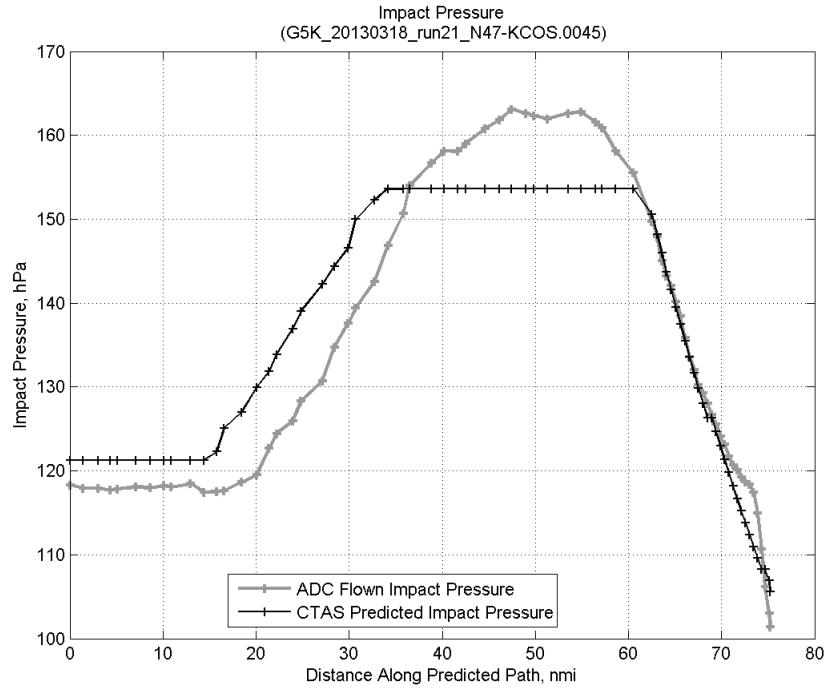


**Figure 326:** Flown (ADC) and predicted (CTAS) impact pressure for run 21.

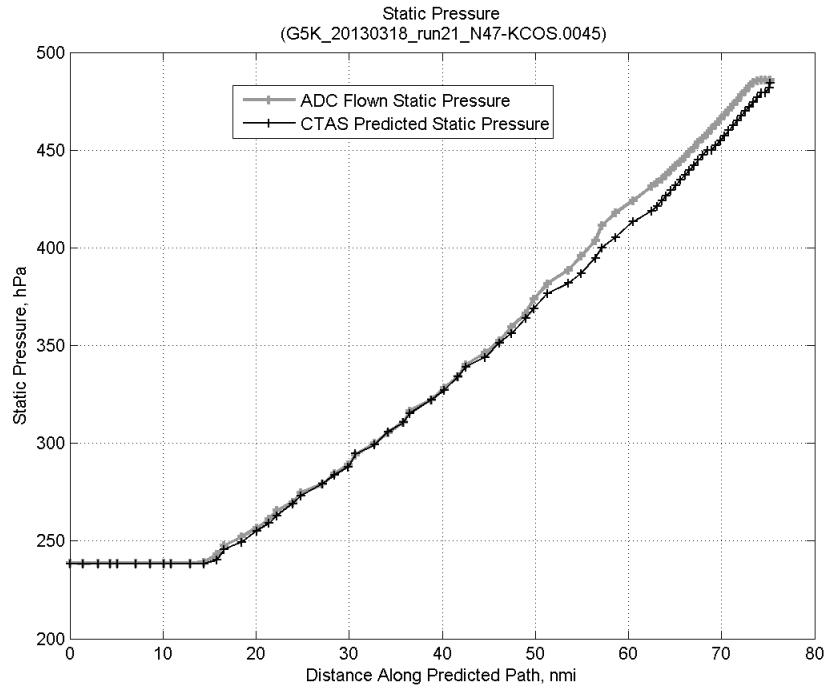


**Figure 327: Flown (ADC) and predicted (CTAS) static pressure for run 21.**

#### C.12.G. Path Distance

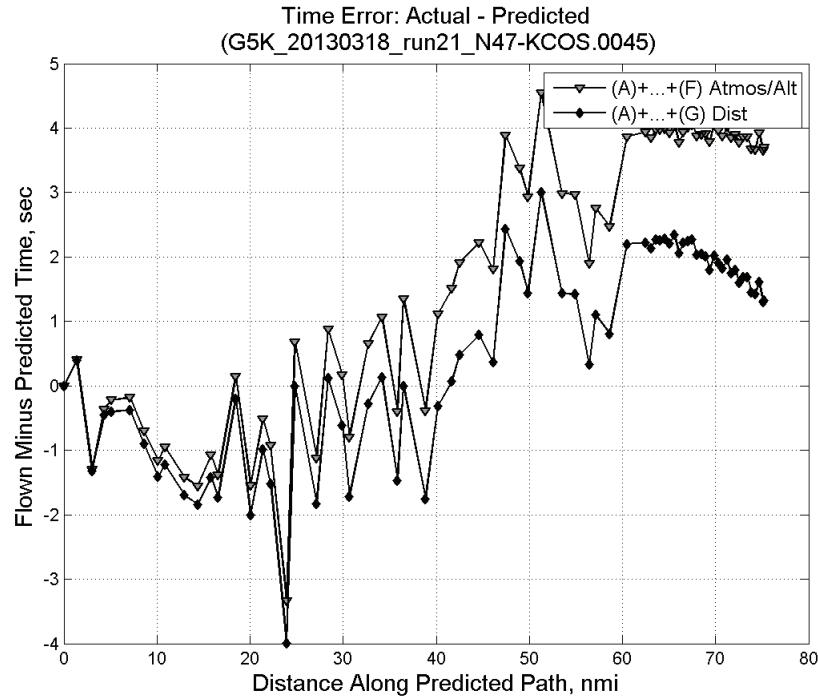


**Figure 328: Time error for run 21 before ((A)+...+(F) Atmos/Alt) and after ((A)+...+(G) Dist) removing path distance error source.**

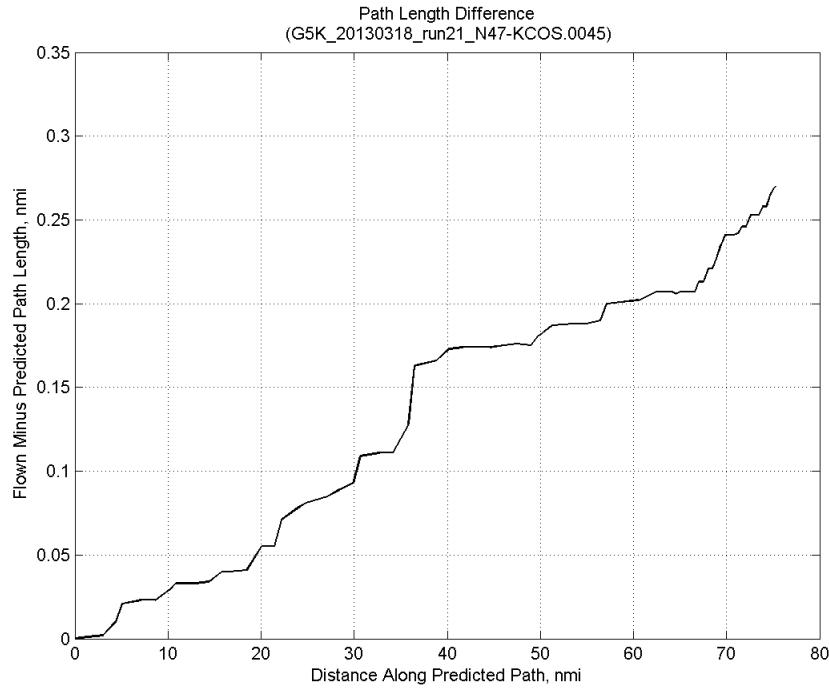


**Figure 329: ADC flown minus CTAS predicted path length for run 21. Positive values indicate aircraft followed a longer path than predicted by CTAS.**

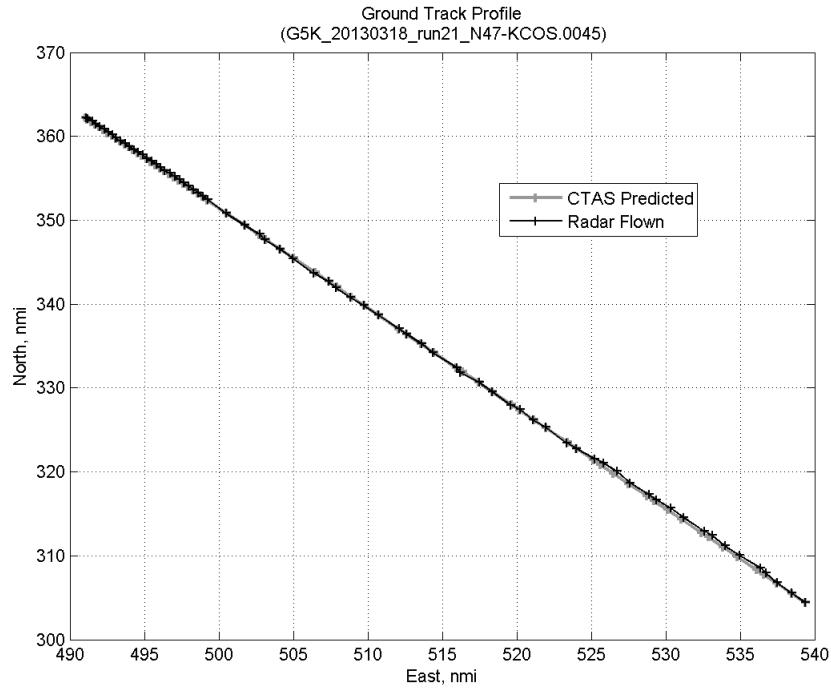


**Figure 330: CTAS predicted and radar flown ground track profile for run 21.**

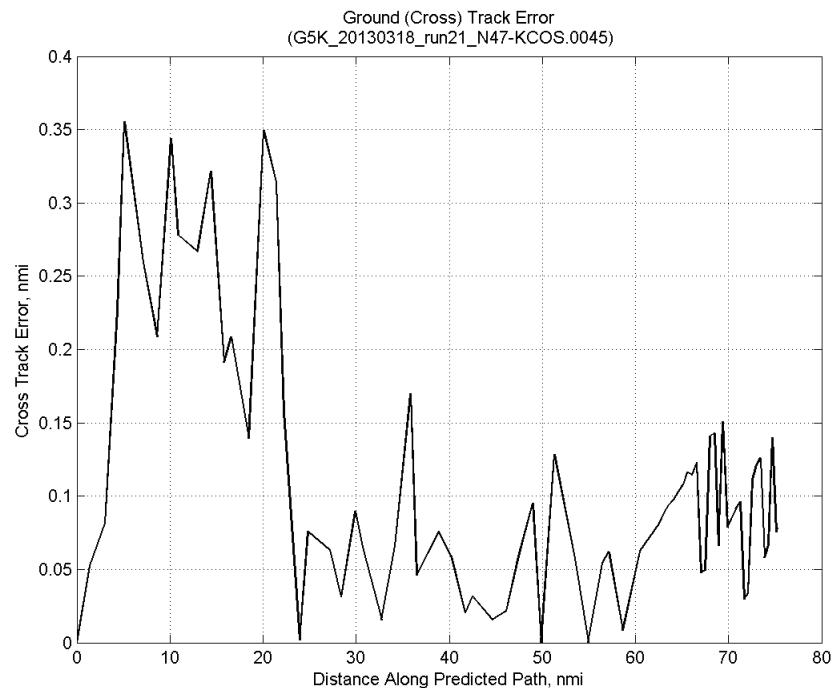


**Figure 331: Ground (cross) track error for run 21.**

### C.13. Run 22

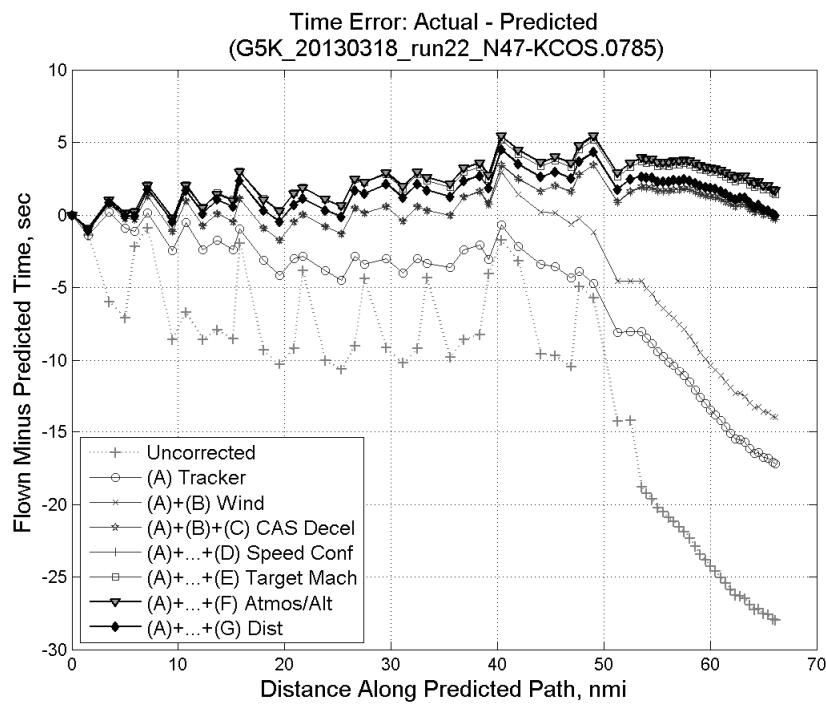


**Figure 332: Time error for run 22 showing incremental effect of removing each error source.**

#### C.13.A. Tracker Jumps

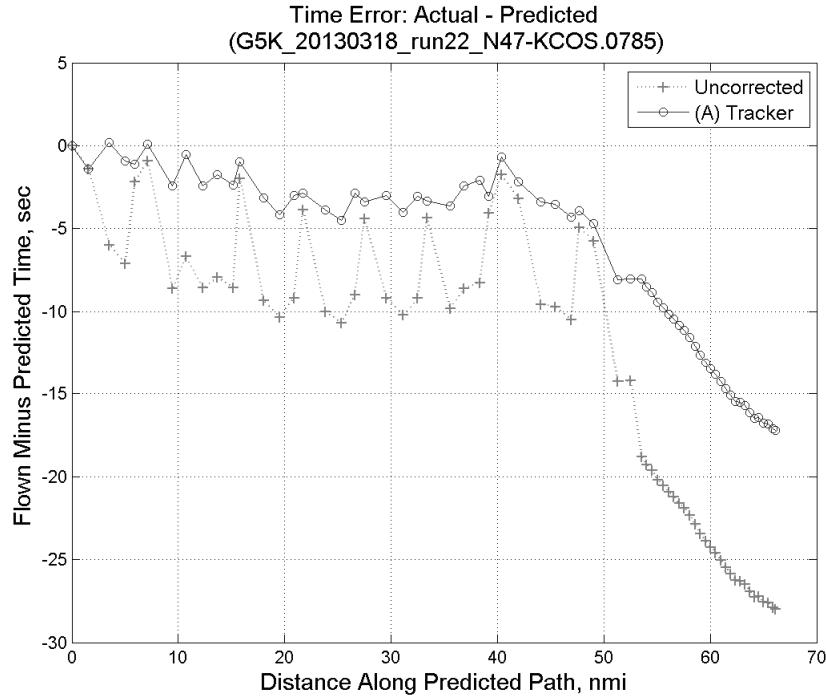


**Figure 333: Time error for run 22 before (Uncorrected) and after ((A) Tracker) removing tracker jump error source.**

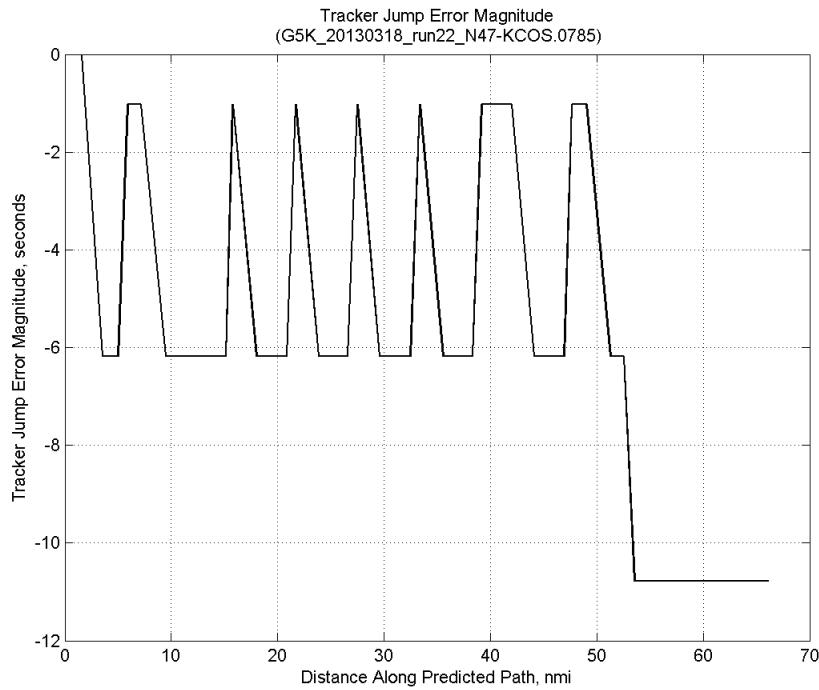


**Figure 334: Effect of tracker jump error source on time error for run 22.**

### C.13.B. Wind

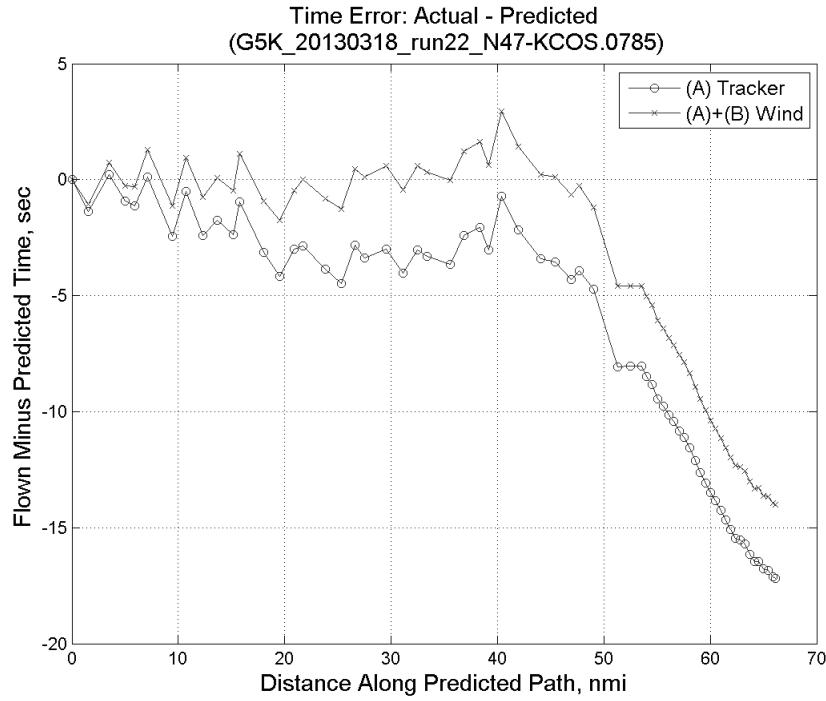


**Figure 335: Time error for run 22 before ((A) Tracker) and after ((A)+(B) Wind) removing wind error source.**

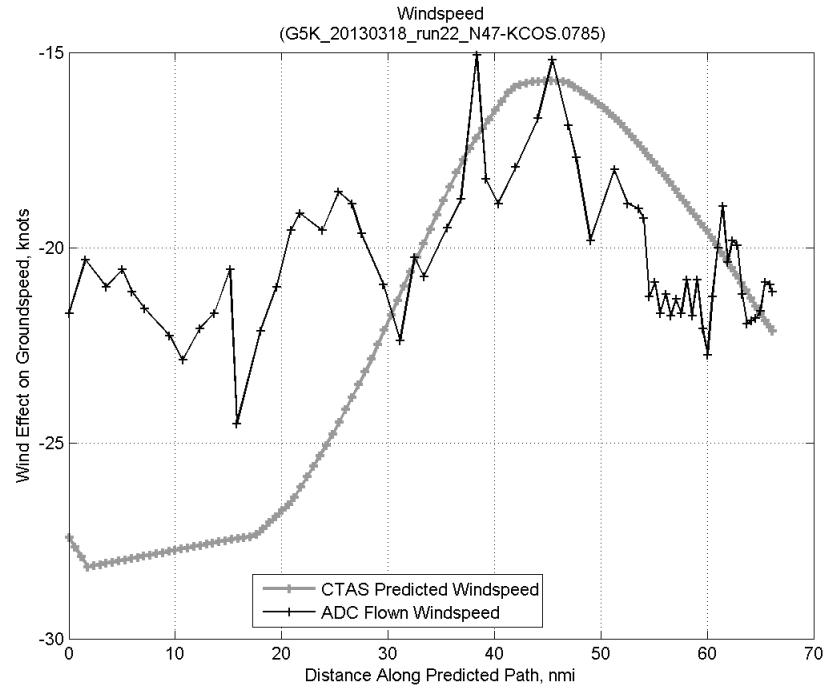


**Figure 336: CTAS predicted and ADC flown wind effect on ground speed for run 22. Negative values indicate a headwind.**

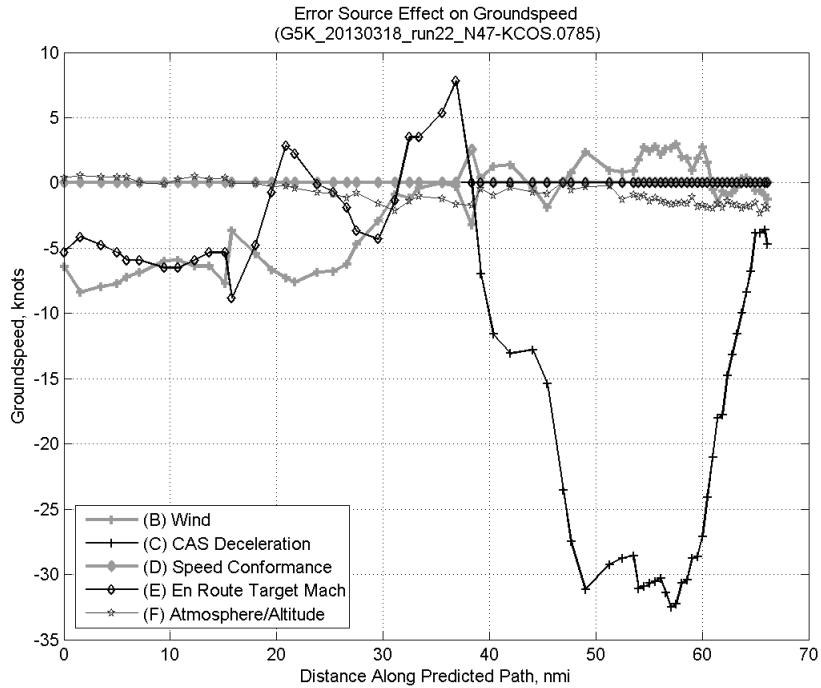


**Figure 337: Error sources (flown minus predicted) converted to a ground speed effect for run 22. Positive values indicate the flown ground speed was faster than the CTAS prediction.**

### C.13.C. CAS Deceleration

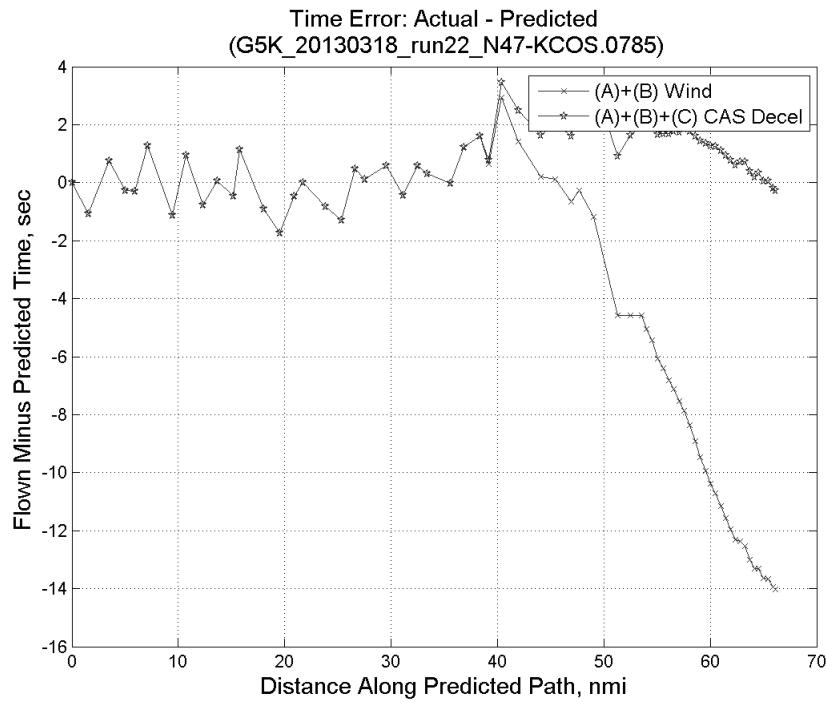


**Figure 338:** Time error for run 22 before ((A)+(B) Wind) and after ((A)+(B)+(C) CAS Decel) removing CAS deceleration error source.

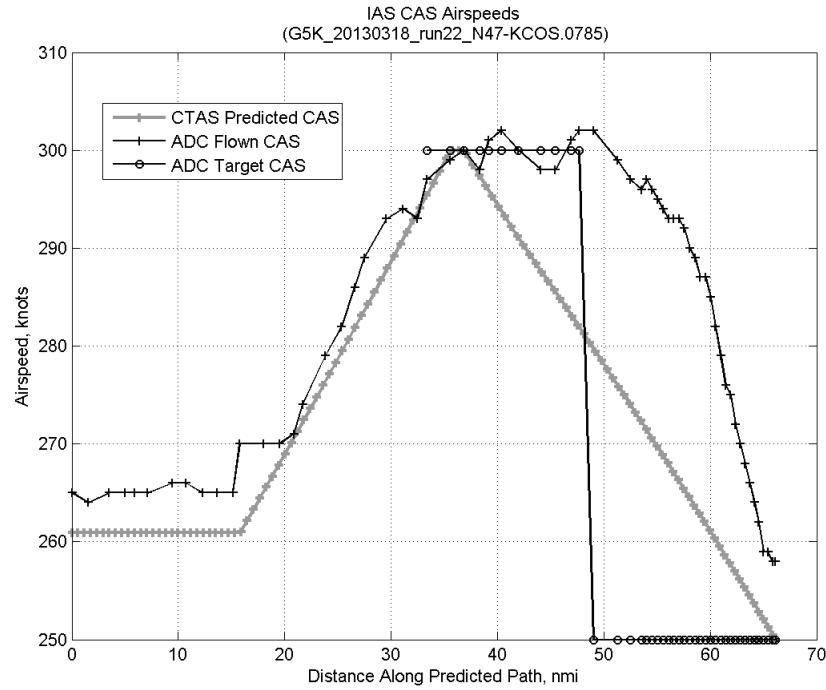


**Figure 339:** CTAS predicted and ADC flown CAS for run 22. CAS that is being targeted is shown with circle markers.

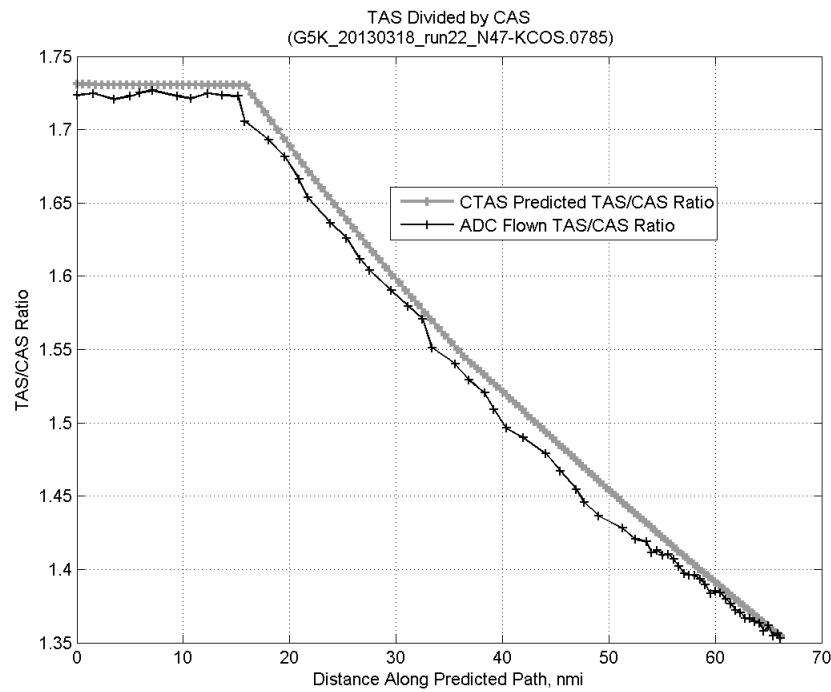


**Figure 340: CTAS predicted and ADC flown TAS/CAS ratio for run 22.**

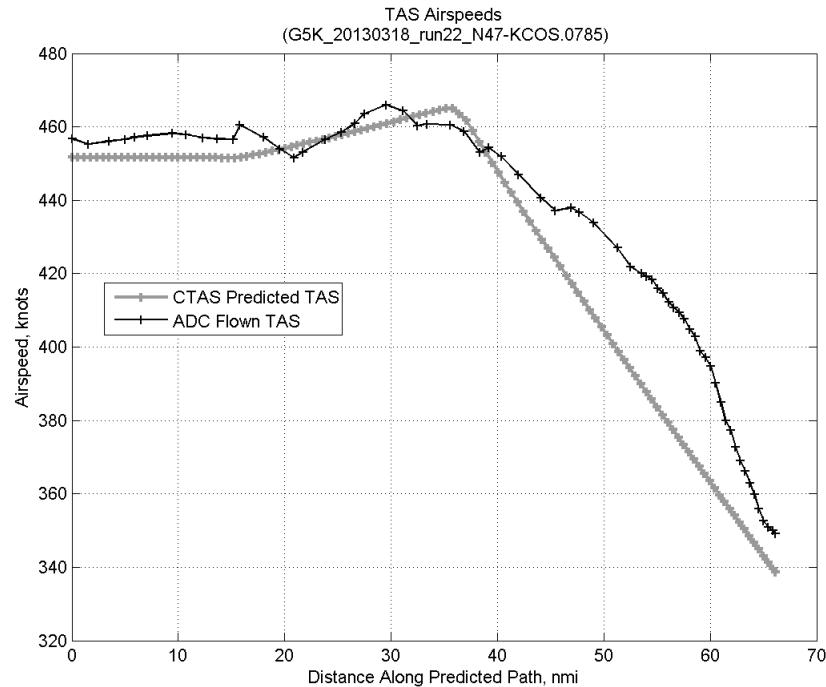


**Figure 341: CTAS predicted and ADC flown TAS for run 22.**

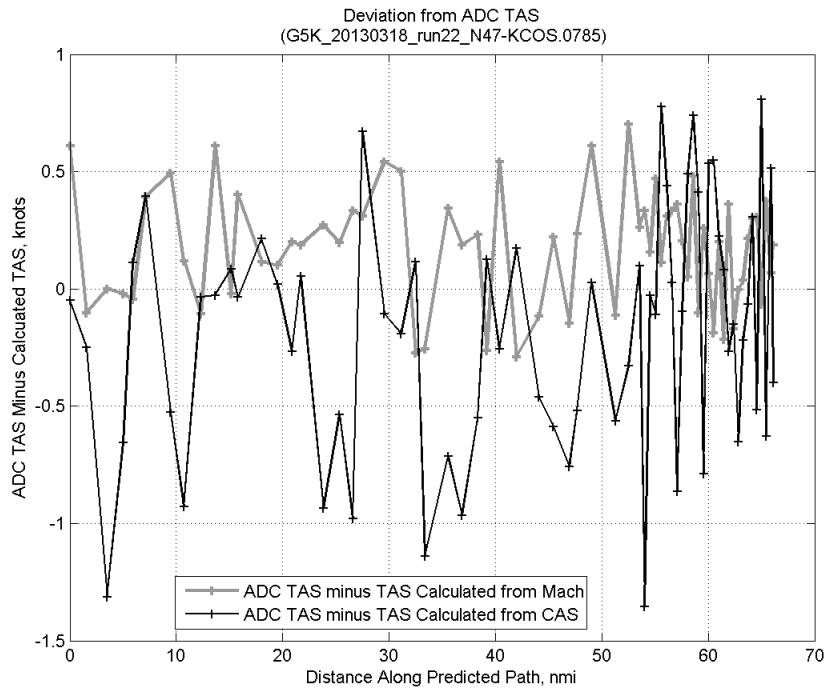


**Figure 342: Deviation from ADC flown TAS if calculating TAS using ADC flown CAS, Mach, atmospheric temperature, and atmospheric pressure for run 22.**

#### C.13.D. Speed Conformance

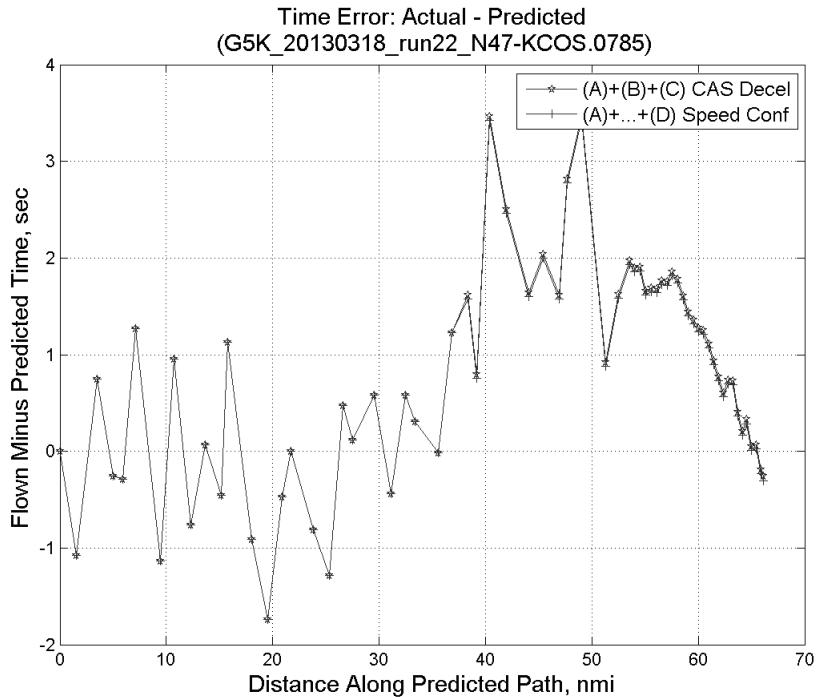


**Figure 343: Time error for run 22 before ((A)+(B)+(C) CAS Decel) and after ((A)+...+(D) Speed Conf) removing speed conformance error source.**

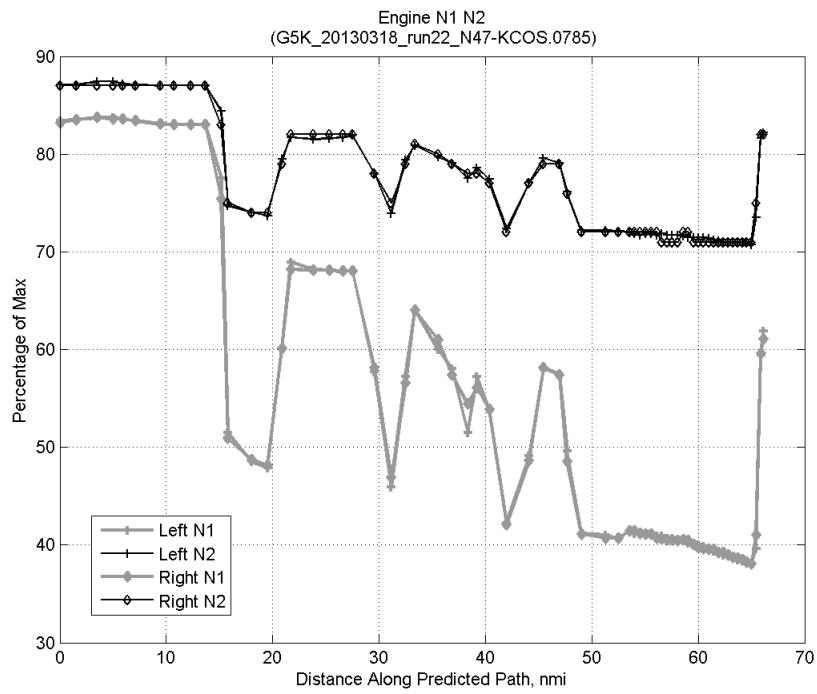


**Figure 344: Flown engine N1 and N2 for run 22.**

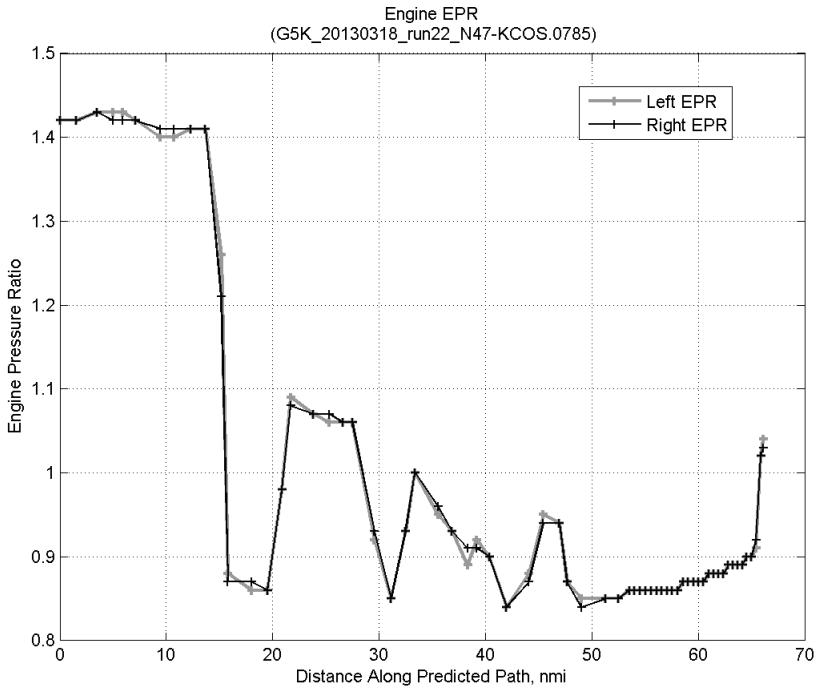


**Figure 345: Flown engine EPR for run 22.**

### C.13.E. Target Mach

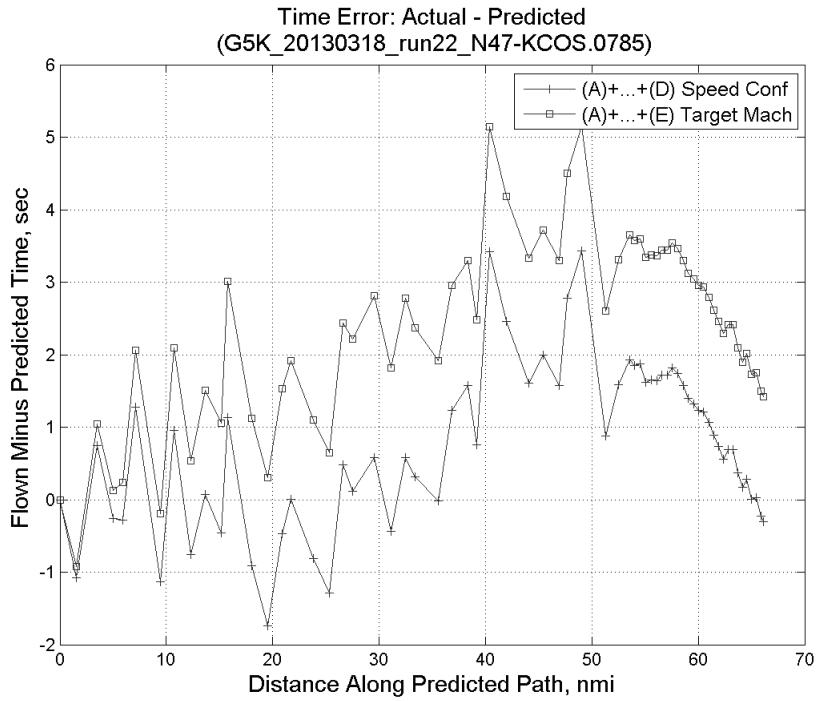


**Figure 346:** Time error for run 22 before ((A)+...+(D) Speed Conf) and after ((A)+...+(E) Target Mach) removing target Mach error source.

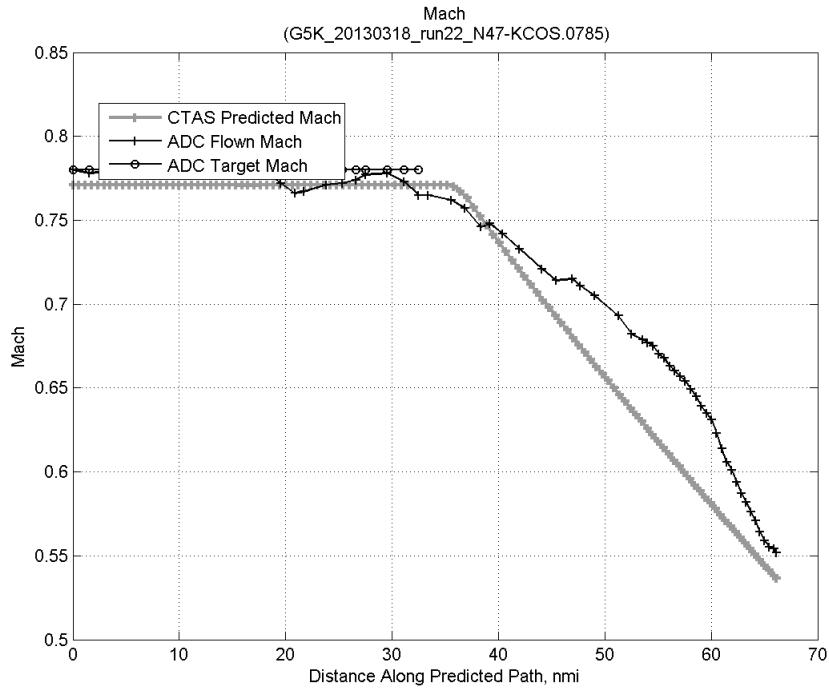


**Figure 347:** CTAS predicted and ADC flown Mach for run 22. Mach being targeted (ADC) shown with circle markers.

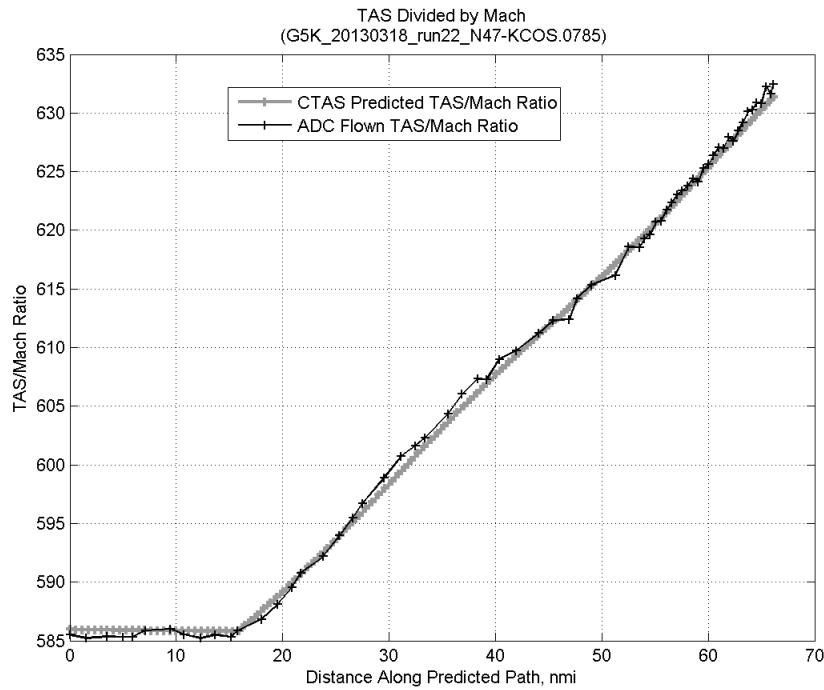


**Figure 348: CTAS predicted and ADC flown TAS/Mach ratio for run 22.**

#### C.13.F. Atmosphere/Altitude

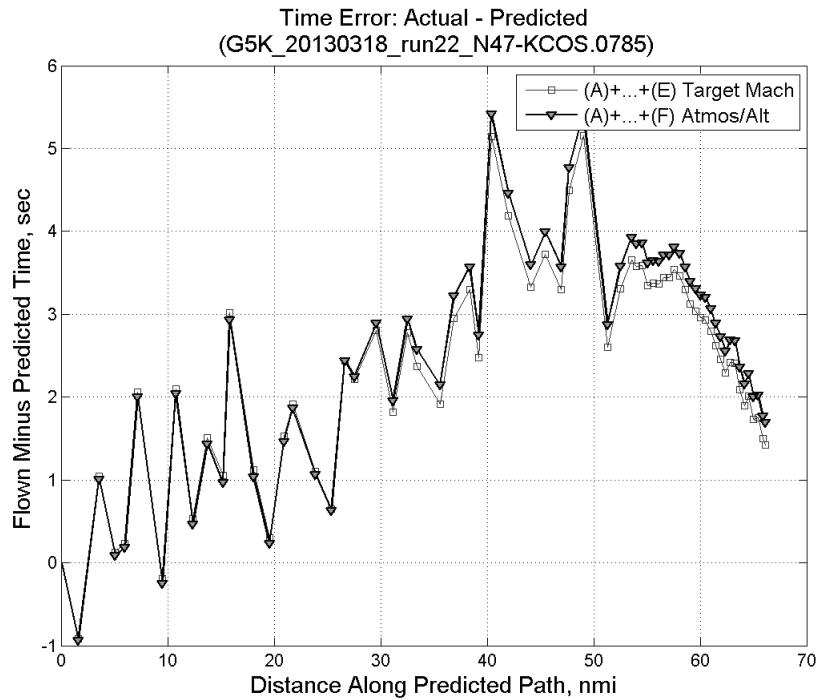


**Figure 349: Time error for run 22 before ((A)+...+(E) Target Mach) and after ((A)+...+(F) Atmos/Alt) removing atmosphere/altitude error source.**

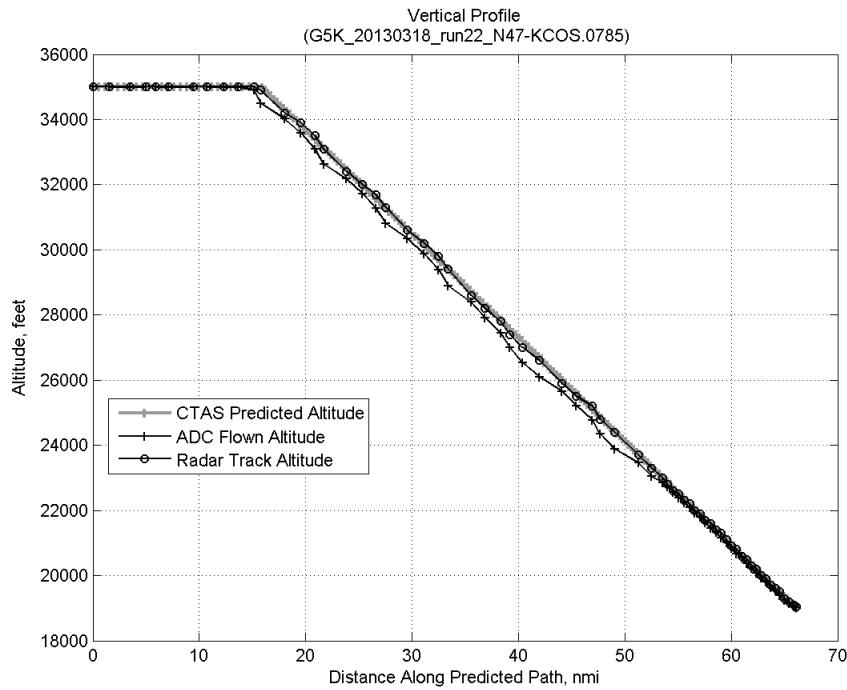


**Figure 350: Flown (ADC) and predicted (CTAS) vertical profile for run 22.**

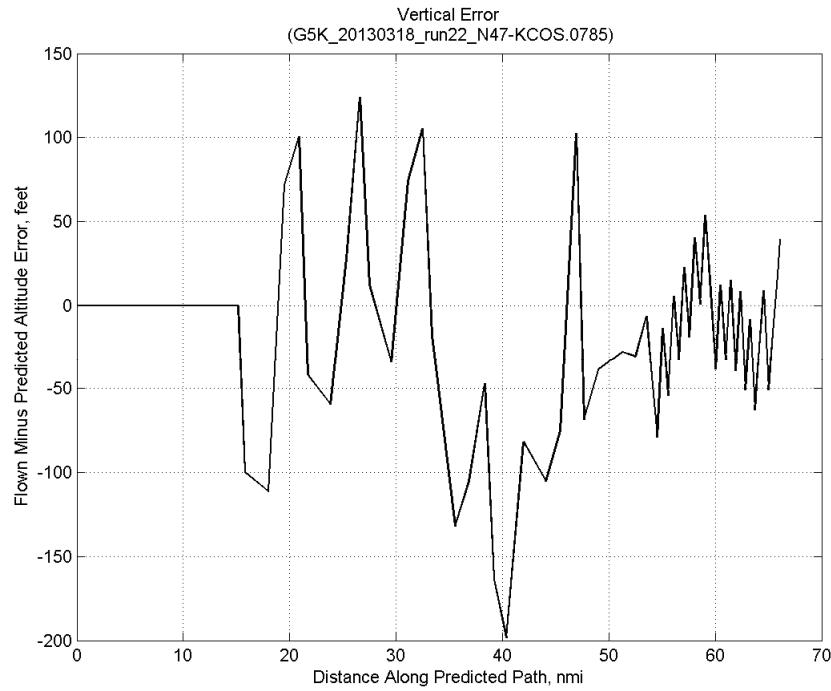


**Figure 351: Vertical error (flown minus predicted altitude) for run 22. Positive values indicate aircraft flew higher than predicted by CTAS.**

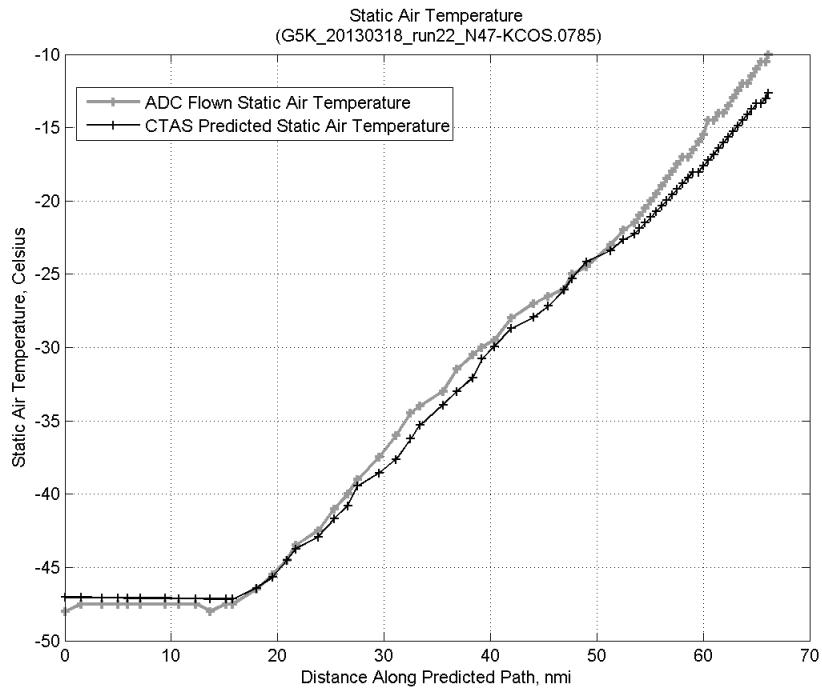


**Figure 352: Flown (ADC) and predicted (CTAS) static air temperature for run 22.**

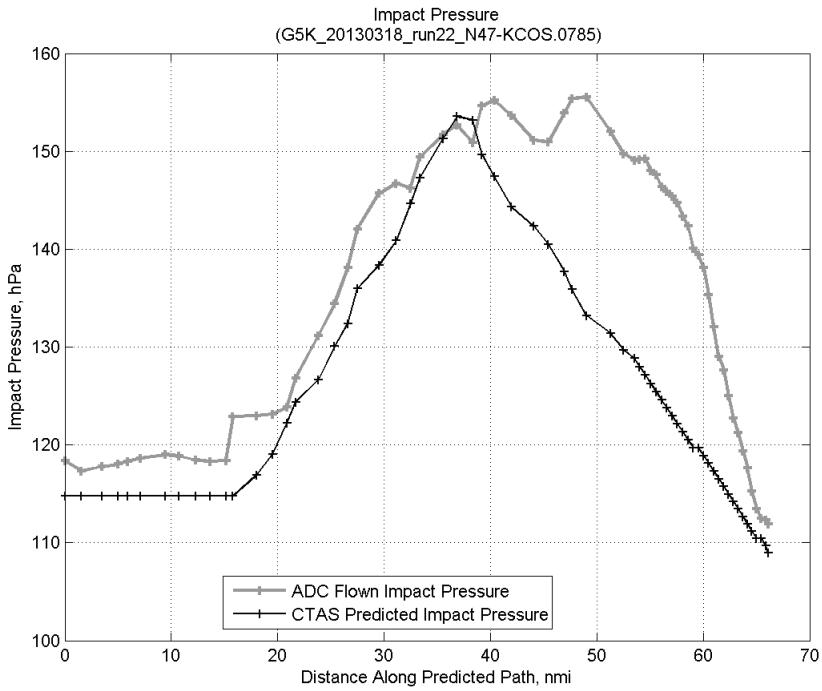


**Figure 353: Flown (ADC) and predicted (CTAS) impact pressure for run 22.**

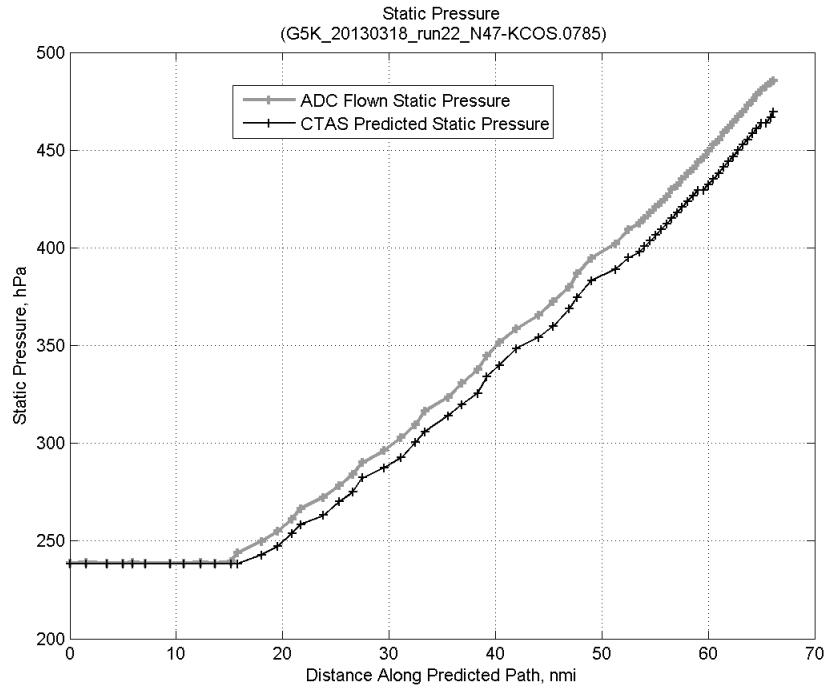


**Figure 354: Flown (ADC) and predicted (CTAS) static pressure for run 22.**

### C.13.G. Path Distance

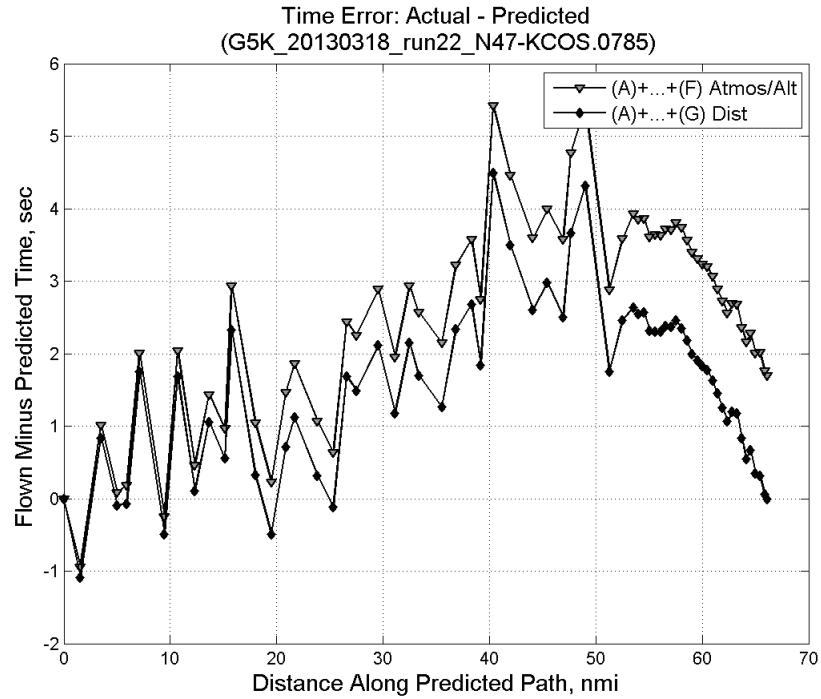


**Figure 355: Time error for run 22 before ((A)+...+(F) Atmos/Alt) and after ((A)+...+(G) Dist) removing path distance error source.**

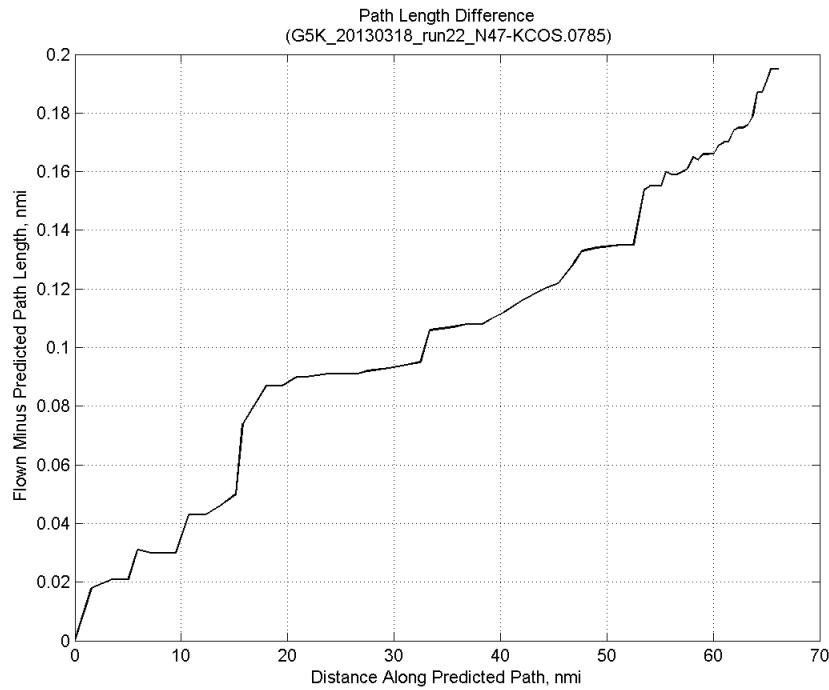


**Figure 356: ADC flown minus CTAS predicted path length for run 22. Positive values indicate aircraft followed a longer path than predicted by CTAS.**

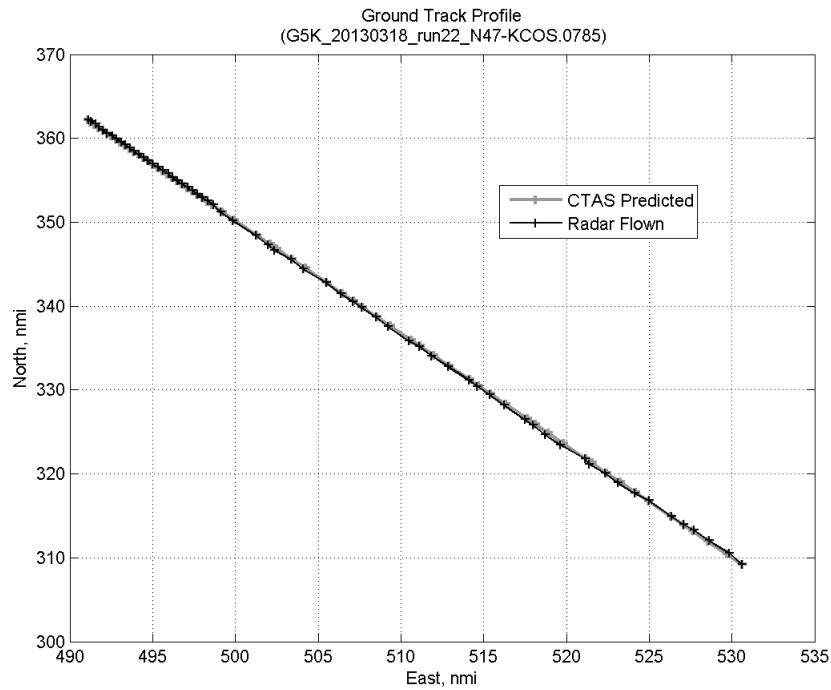


**Figure 357: CTAS predicted and radar flown ground track profile for run 22.**

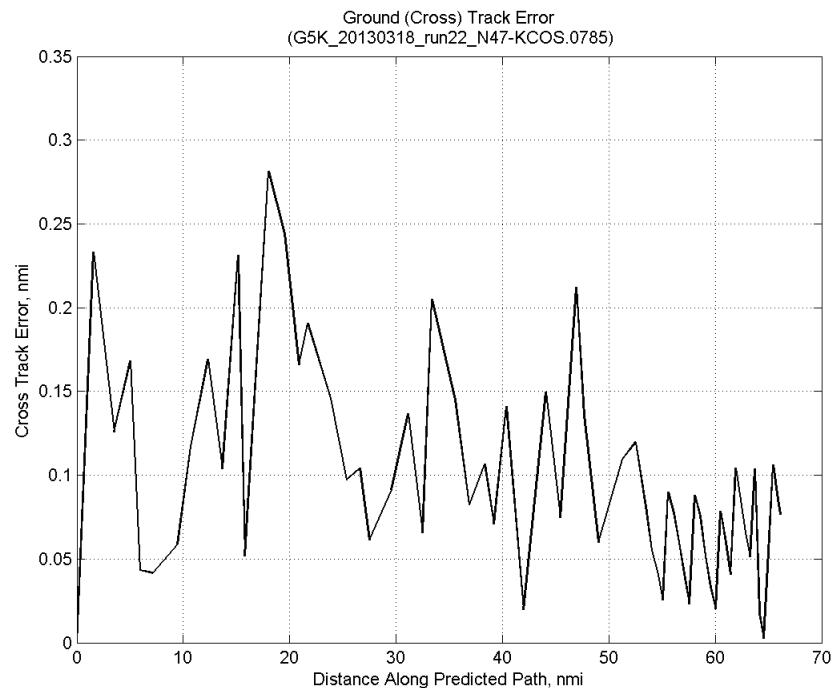


**Figure 358: Ground (cross) track error for run 22.**

### C.14. Run 23

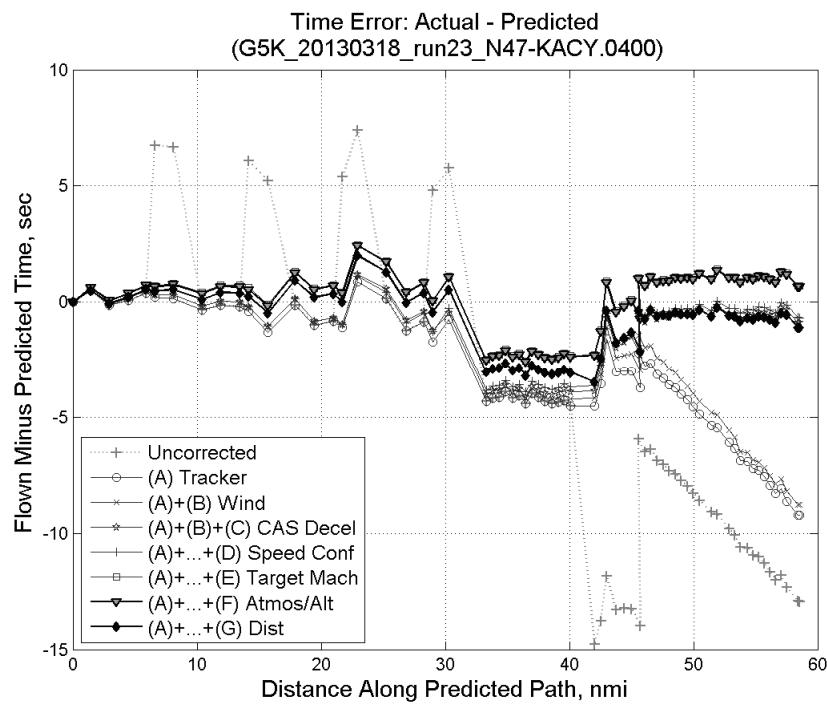


**Figure 359: Time error for run 23 showing incremental effect of removing each error source.**

#### C.14.A. Tracker Jumps

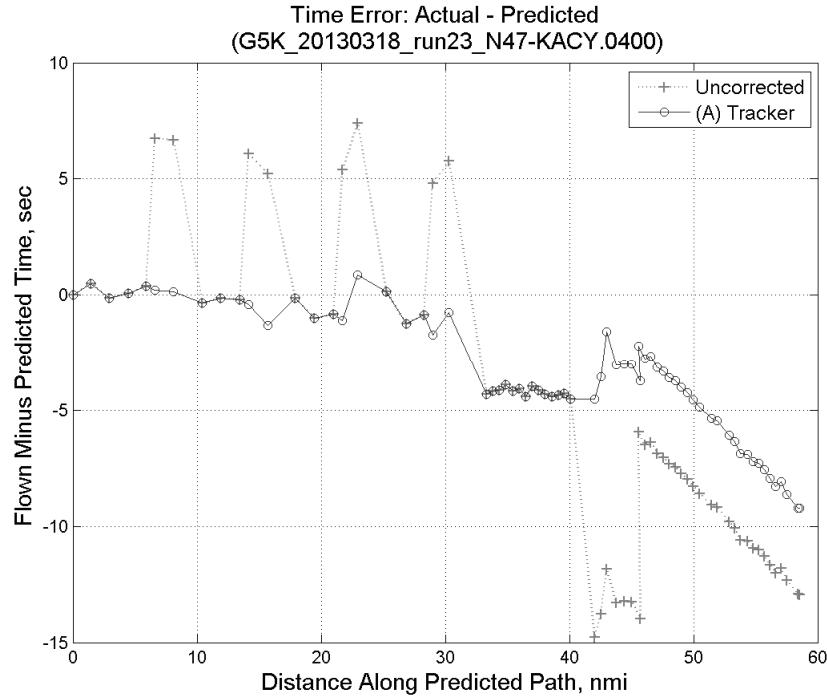


**Figure 360: Time error for run 23 before (Uncorrected) and after ((A) Tracker) removing tracker jump error source.**

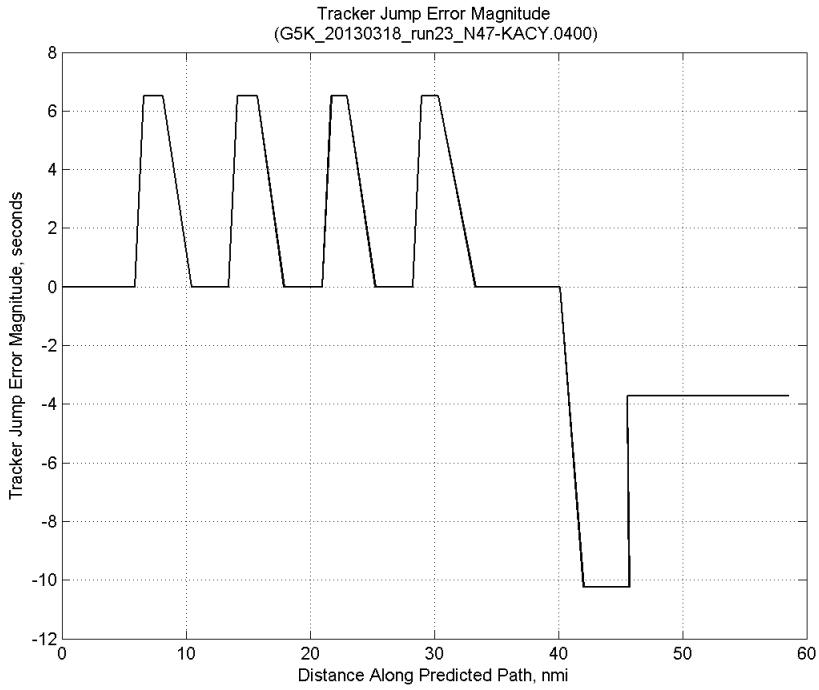


**Figure 361: Effect of tracker jump error source on time error for run 23.**

#### C.14.B. Wind

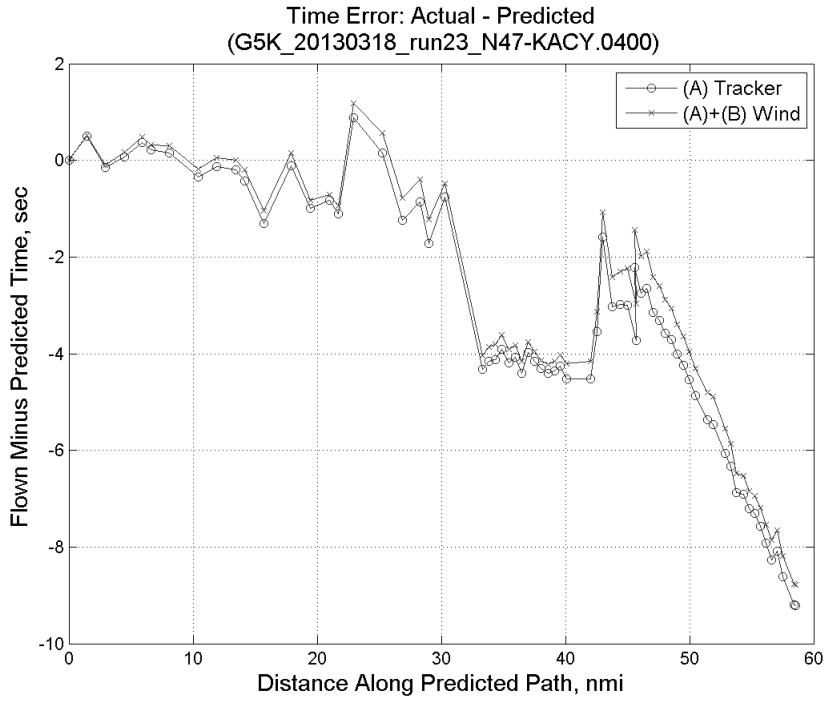


**Figure 362: Time error for run 23 before ((A) Tracker) and after ((A)+(B) Wind) removing wind error source.**

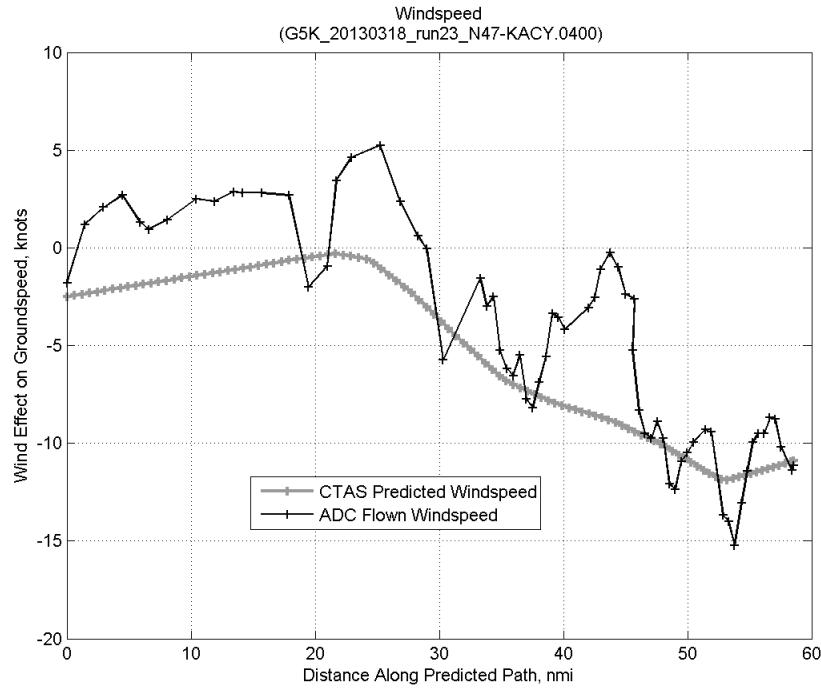


**Figure 363: CTAS predicted and ADC flown wind effect on ground speed for run 23. Negative values indicate a headwind.**

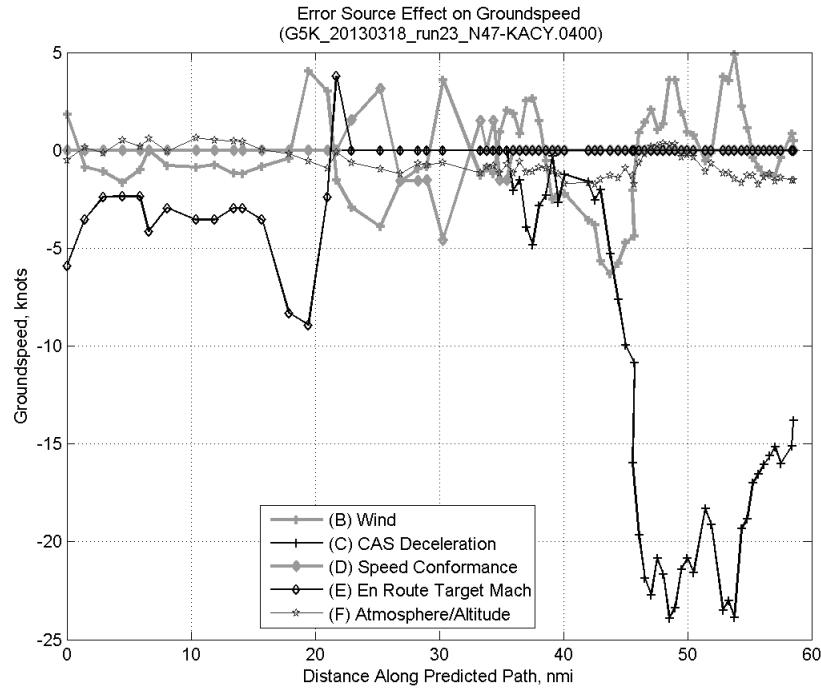


**Figure 364: Error sources (flown minus predicted) converted to a ground speed effect for run 23. Positive values indicate the flown ground speed was faster than the CTAS prediction.**

### C.14.C. CAS Deceleration

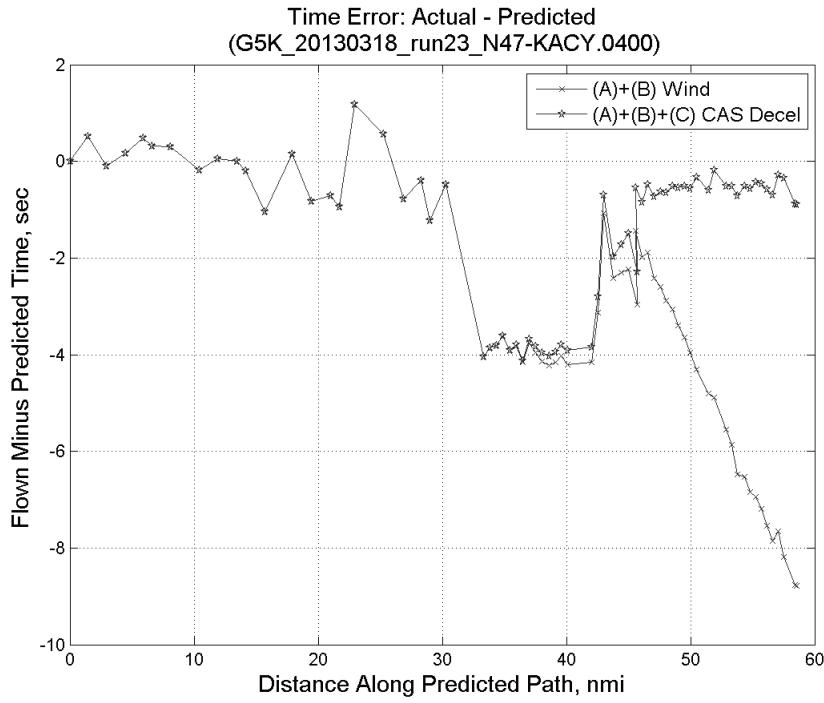


**Figure 365:** Time error for run 23 before ((A)+(B) Wind) and after ((A)+(B)+(C) CAS Decel) removing CAS deceleration error source.

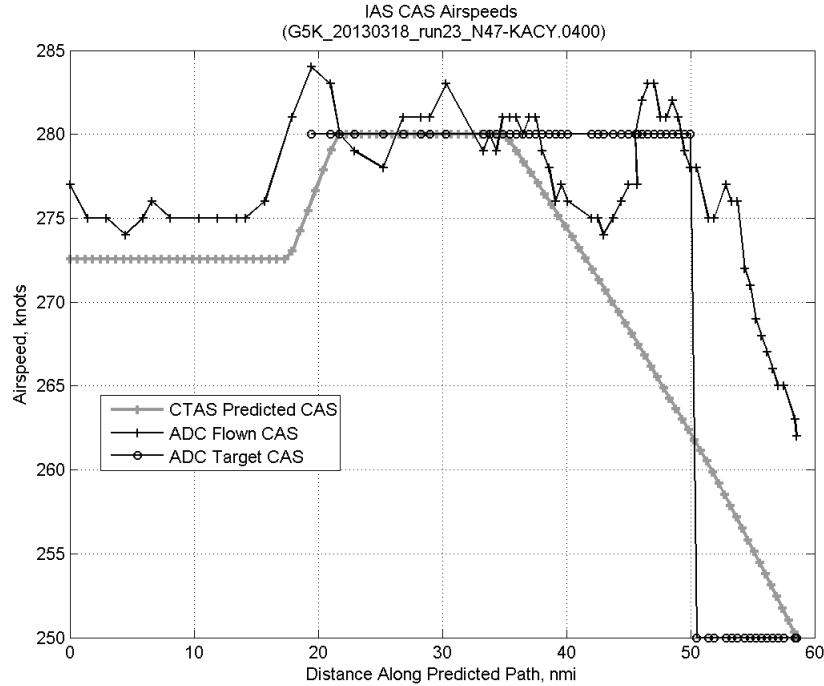


**Figure 366:** CTAS predicted and ADC flown CAS for run 23. CAS that is being targeted is shown with circle markers.

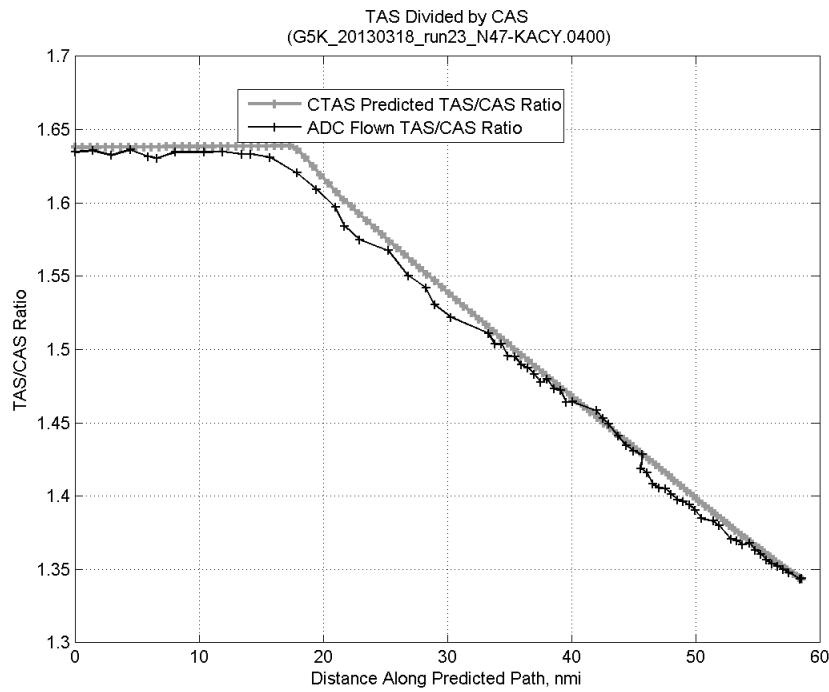


**Figure 367: CTAS predicted and ADC flown TAS/CAS ratio for run 23.**

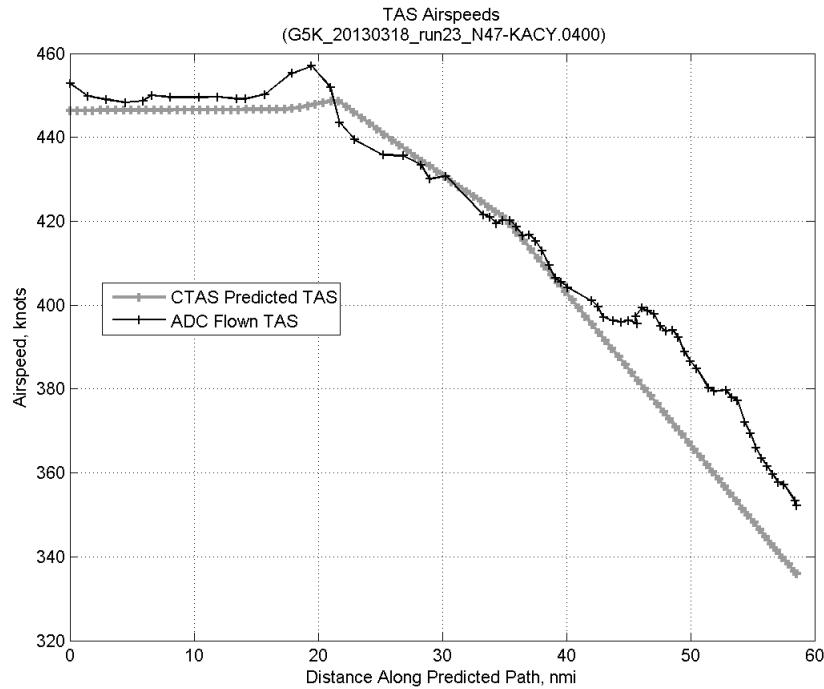


**Figure 368: CTAS predicted and ADC flown TAS for run 23.**

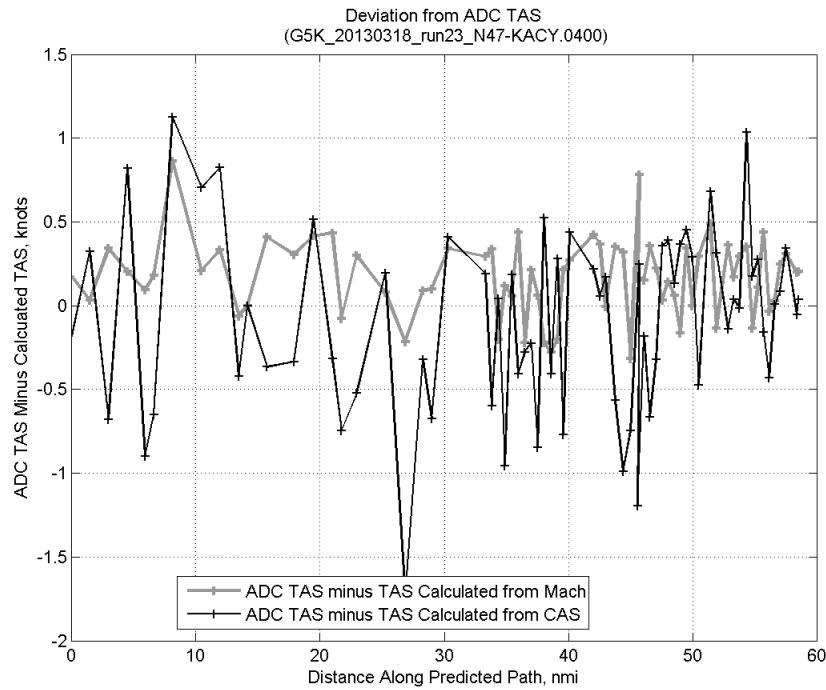


**Figure 369:** Deviation from ADC flown TAS if calculating TAS using ADC flown CAS, Mach, atmospheric temperature, and atmospheric pressure for run 23.

#### C.14.D. Speed Conformance

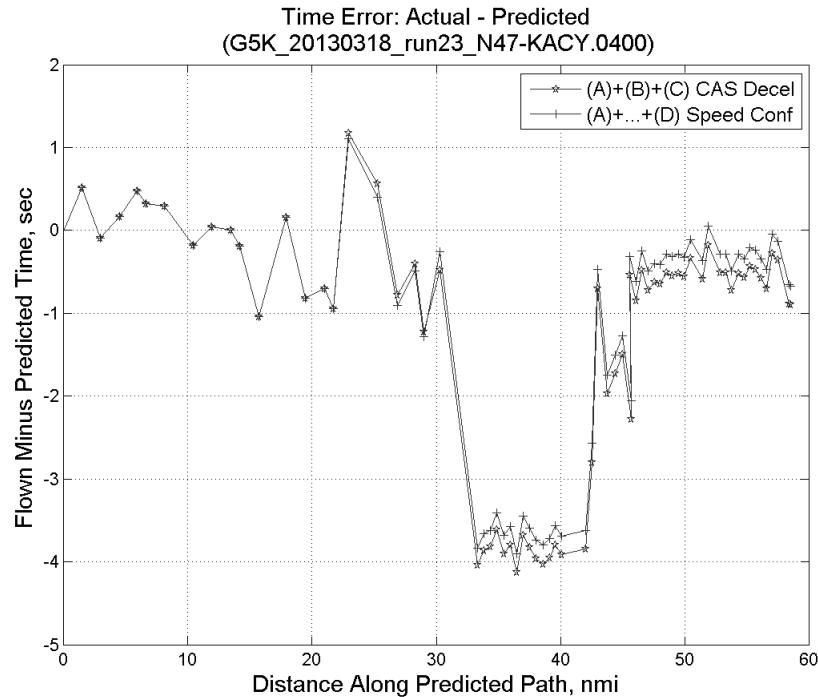


**Figure 370:** Time error for run 23 before ((A)+(B)+(C) CAS Decel) and after ((A)+...+(D) Speed Conf) removing speed conformance error source.

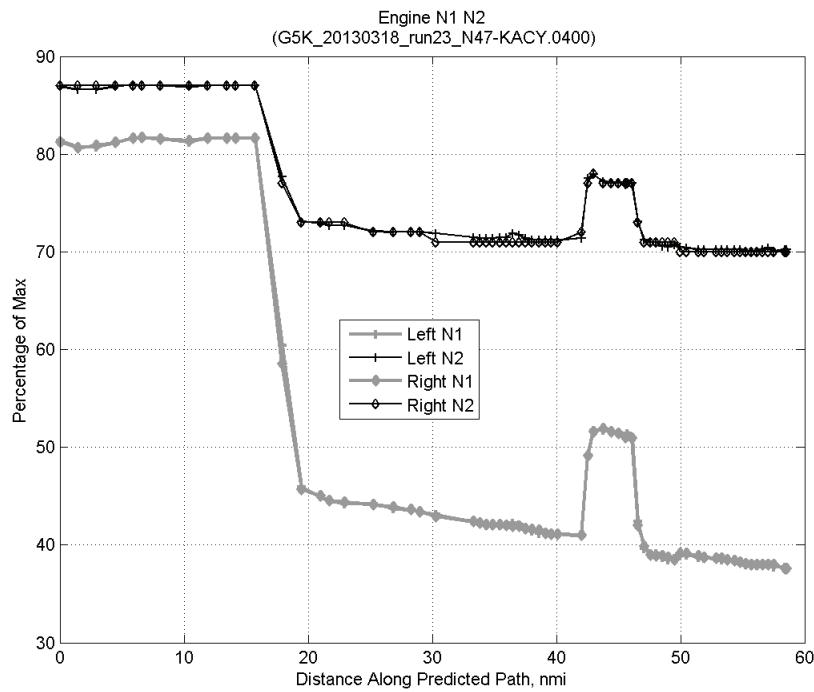


**Figure 371: Flown engine N1 and N2 for run 23.**

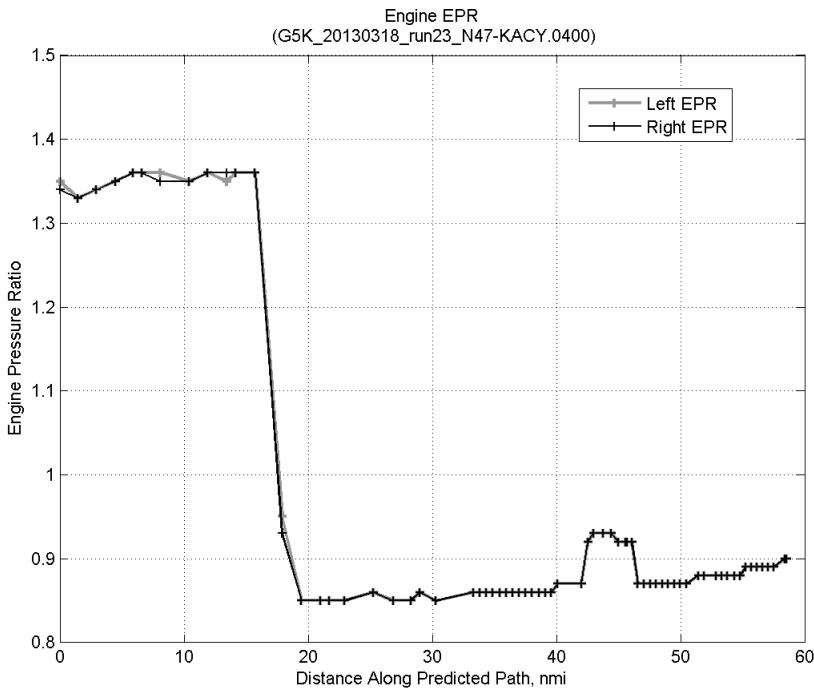


**Figure 372: Flown engine EPR for run 23.**

### C.14.E. Target Mach

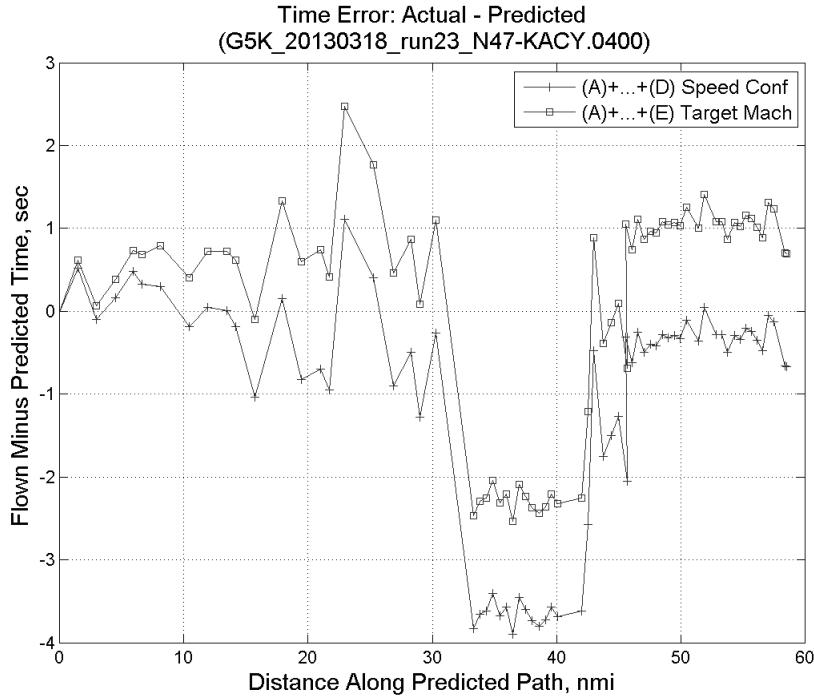


**Figure 373:** Time error for run 23 before ((A)+...+(D) Speed Conf) and after ((A)+...+(E) Target Mach) removing target Mach error source.

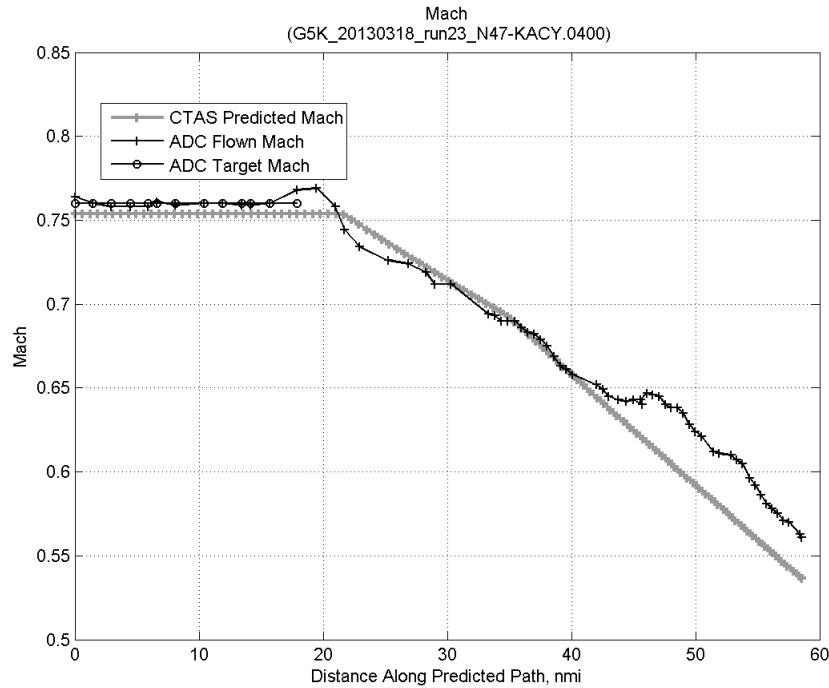


**Figure 374:** CTAS predicted and ADC flown Mach for run 23. Mach being targeted (ADC) shown with circle markers.

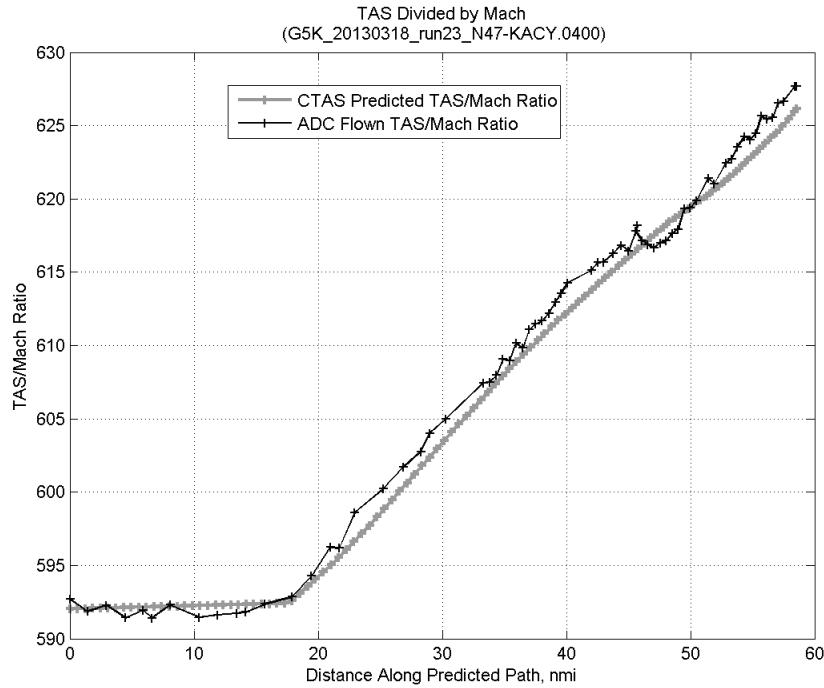


**Figure 375:** CTAS predicted and ADC flown TAS/Mach ratio for run 23.

#### C.14.F. Atmosphere/Altitude

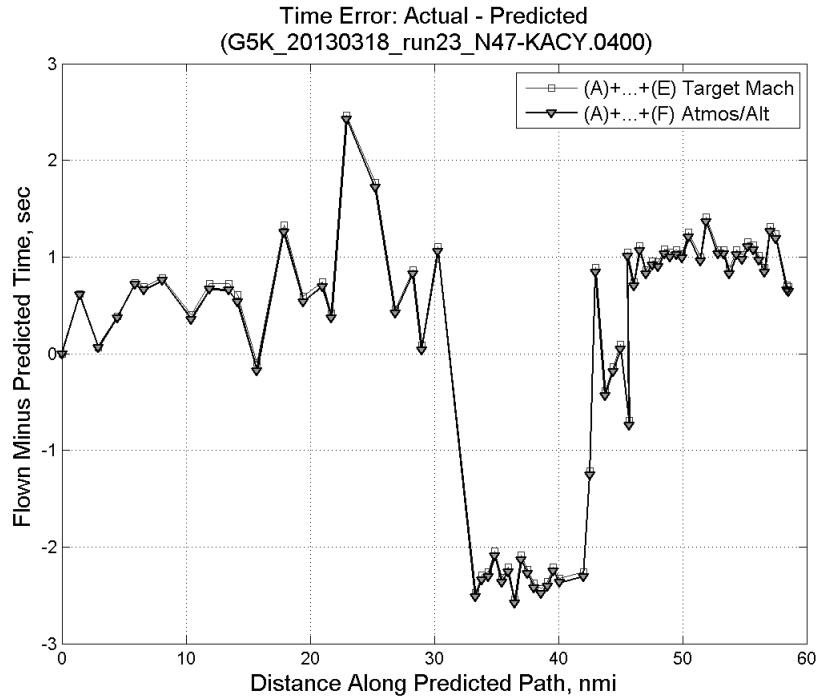


**Figure 376:** Time error for run 23 before ((A)+...+(E) Target Mach) and after ((A)+...+(F) Atmos/Alt) removing atmosphere/altitude error source.

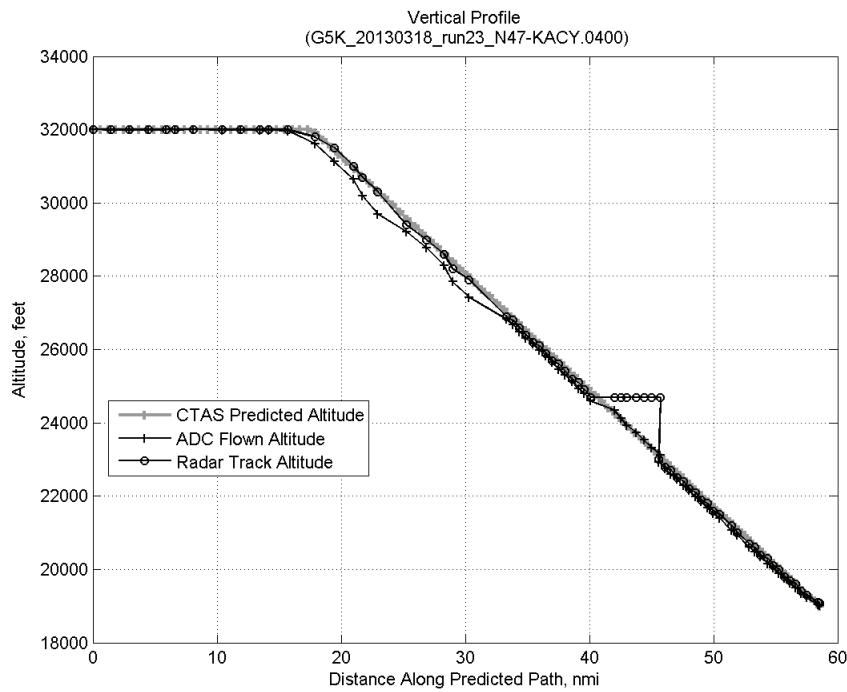


**Figure 377: Flown (ADC) and predicted (CTAS) vertical profile for run 23.**

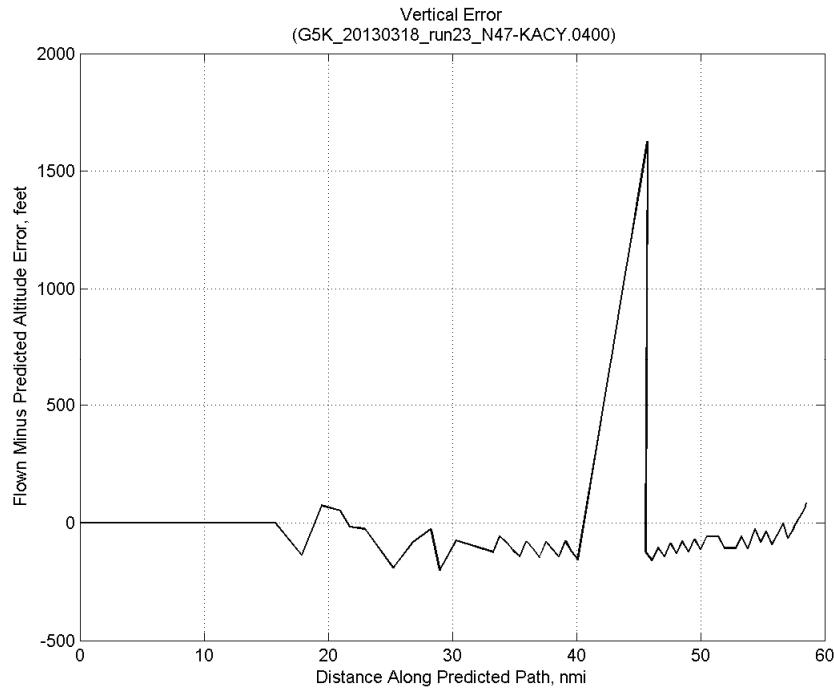


**Figure 378: Vertical error (flown minus predicted altitude) for run 23. Positive values indicate aircraft flew higher than predicted by CTAS.**

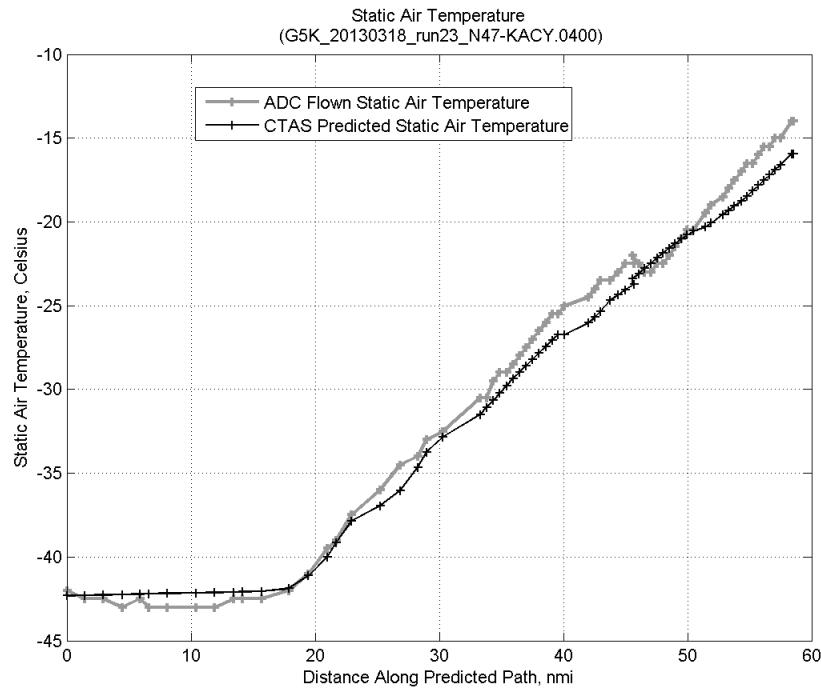


**Figure 379: Flown (ADC) and predicted (CTAS) static air temperature for run 23.**

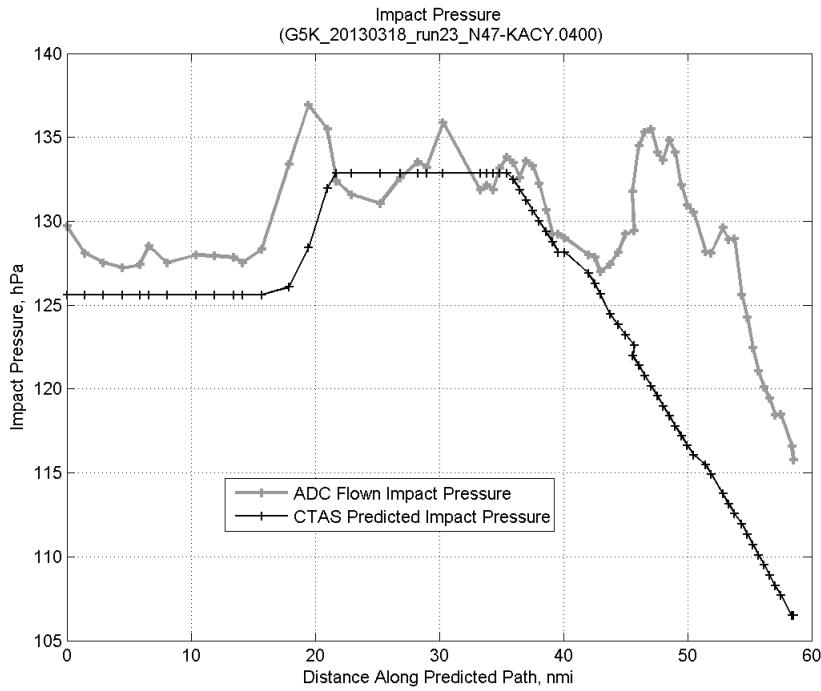


**Figure 380: Flown (ADC) and predicted (CTAS) impact pressure for run 23.**

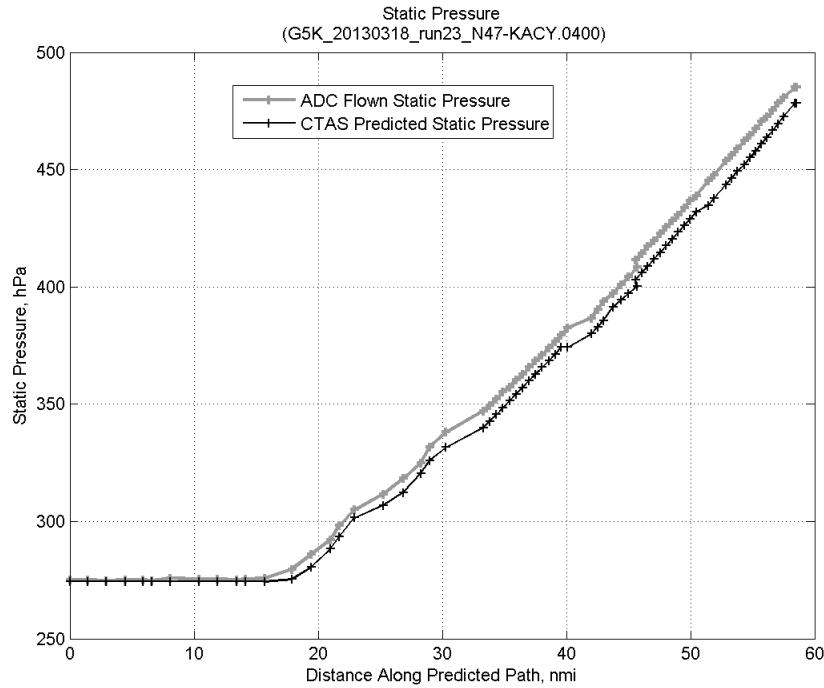


**Figure 381: Flown (ADC) and predicted (CTAS) static pressure for run 23.**

#### C.14.G. Path Distance

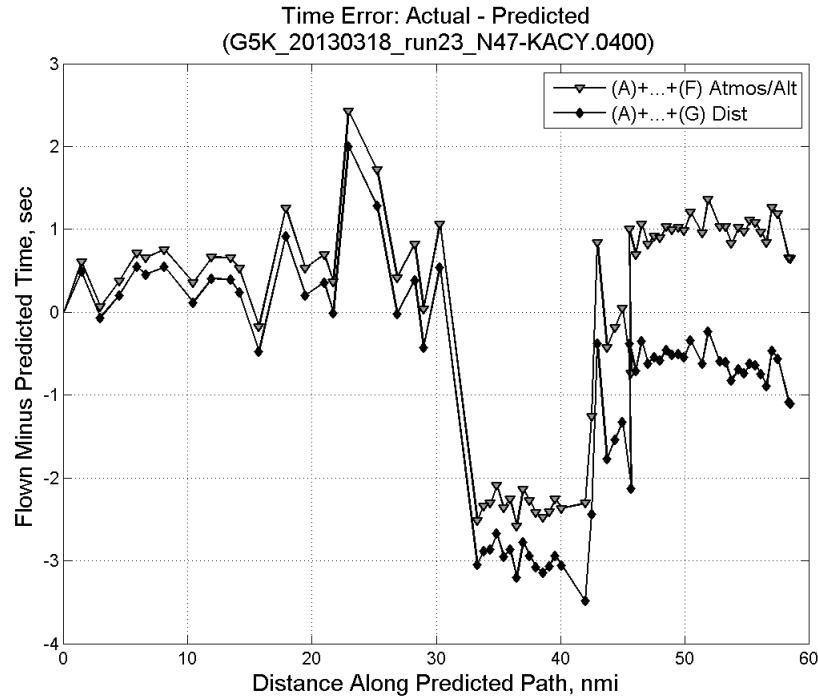


**Figure 382: Time error for run 23 before ((A)+...+(F) Atmos/Alt) and after ((A)+...+(G) Dist) removing path distance error source.**

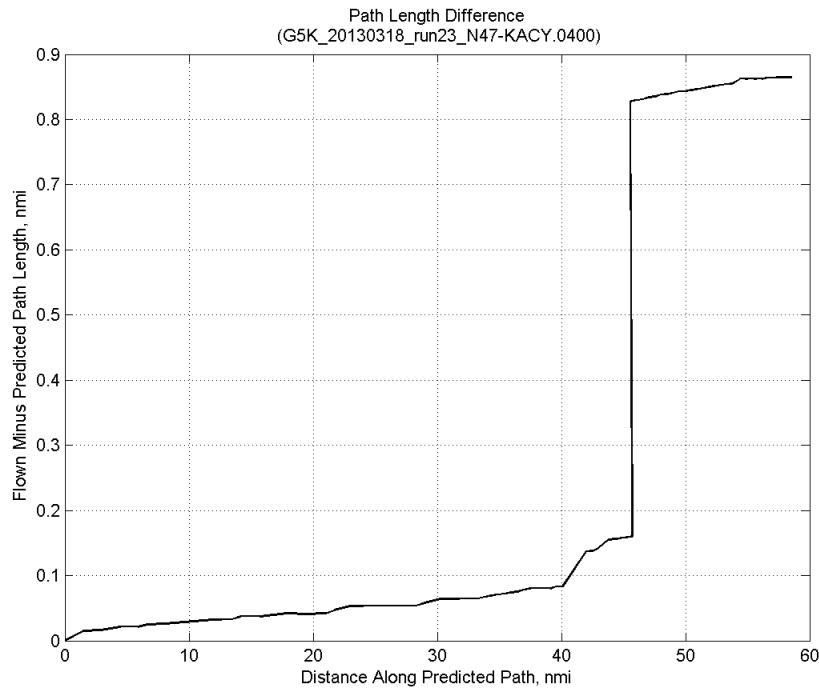


**Figure 383: ADC flown minus CTAS predicted path length for run 23. Positive values indicate aircraft followed a longer path than predicted by CTAS.**

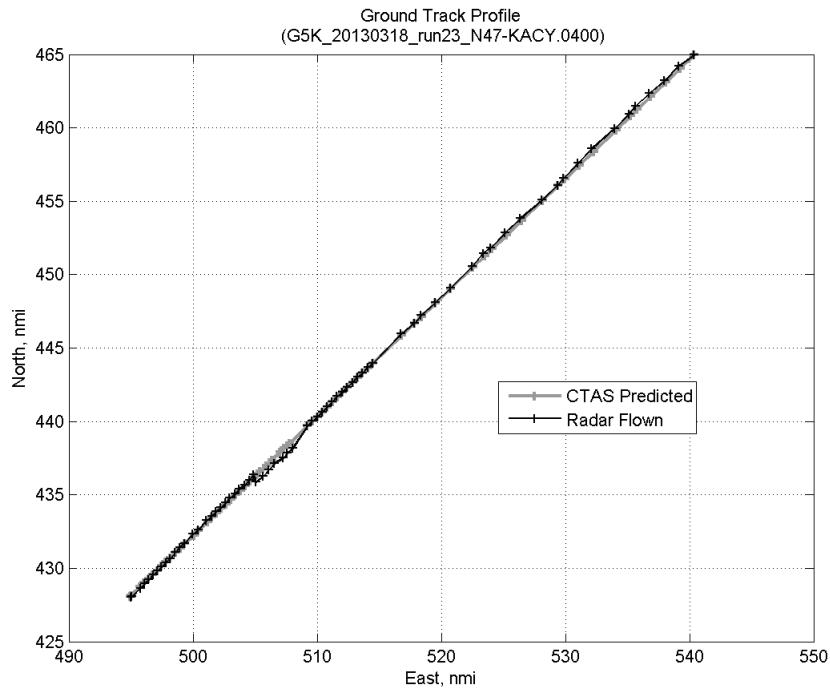


**Figure 384: CTAS predicted and radar flown ground track profile for run 23.**

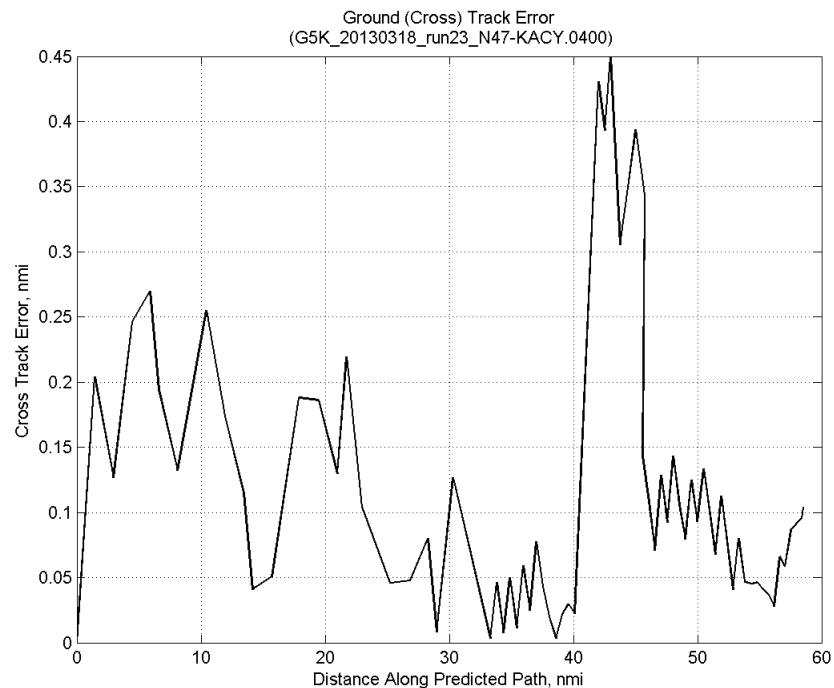


**Figure 385: Ground (cross) track error for run 23.**

### C.15. Run 24

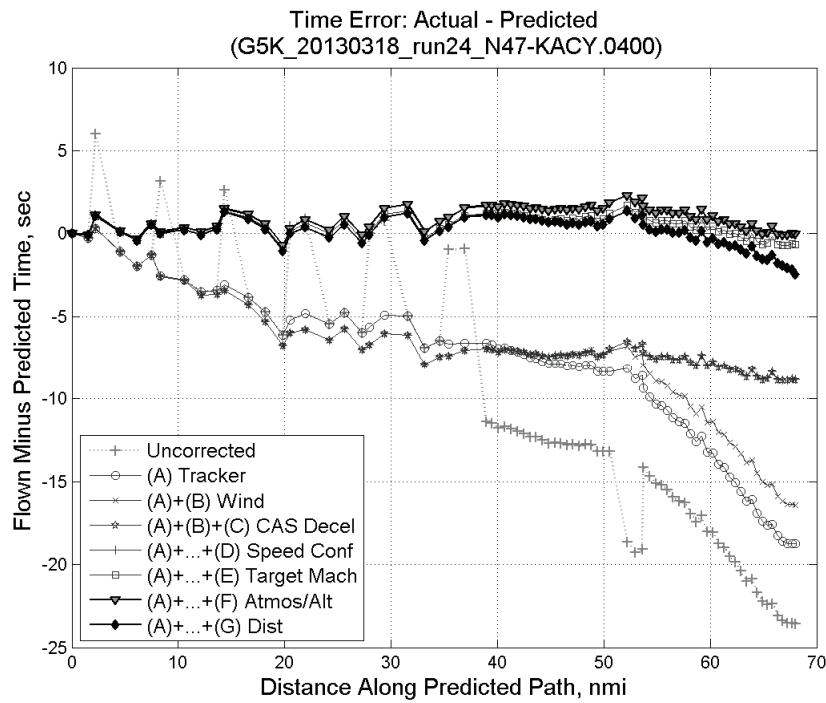


**Figure 386: Time error for run 24 showing incremental effect of removing each error source.**

#### C.15.A. Tracker Jumps

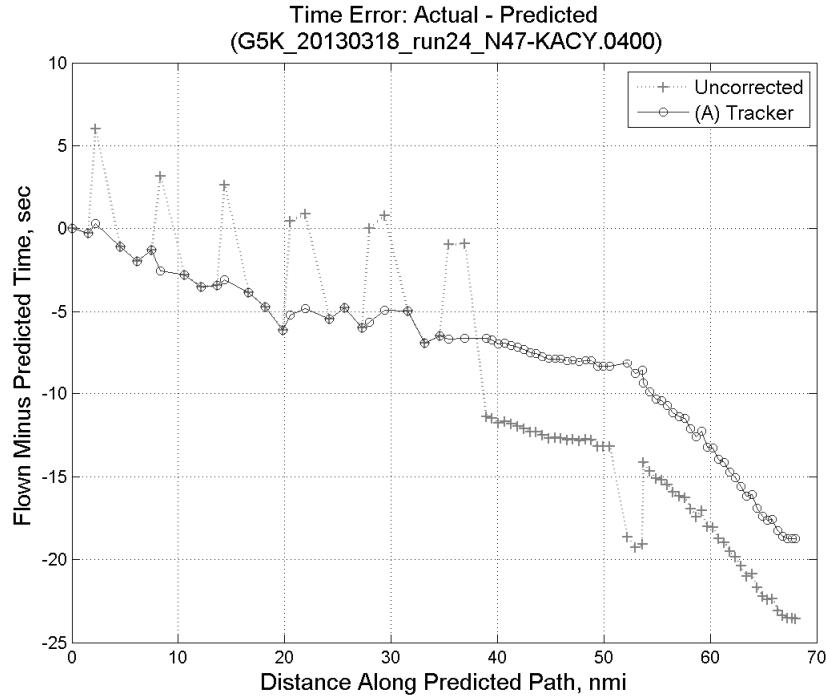


**Figure 387: Time error for run 24 before (Uncorrected) and after ((A) Tracker) removing tracker jump error source.**

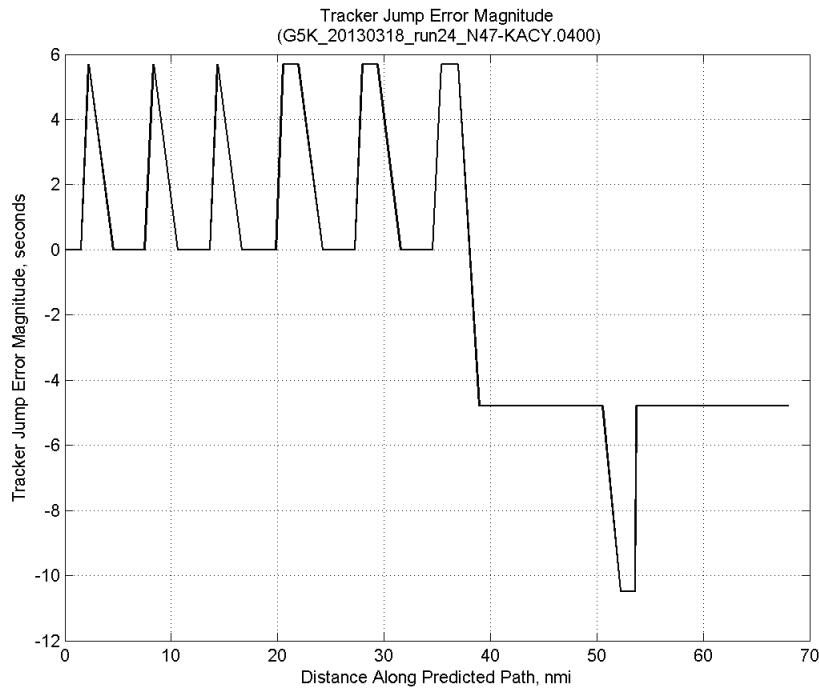


**Figure 388: Effect of tracker jump error source on time error for run 24.**

### C.15.B. Wind

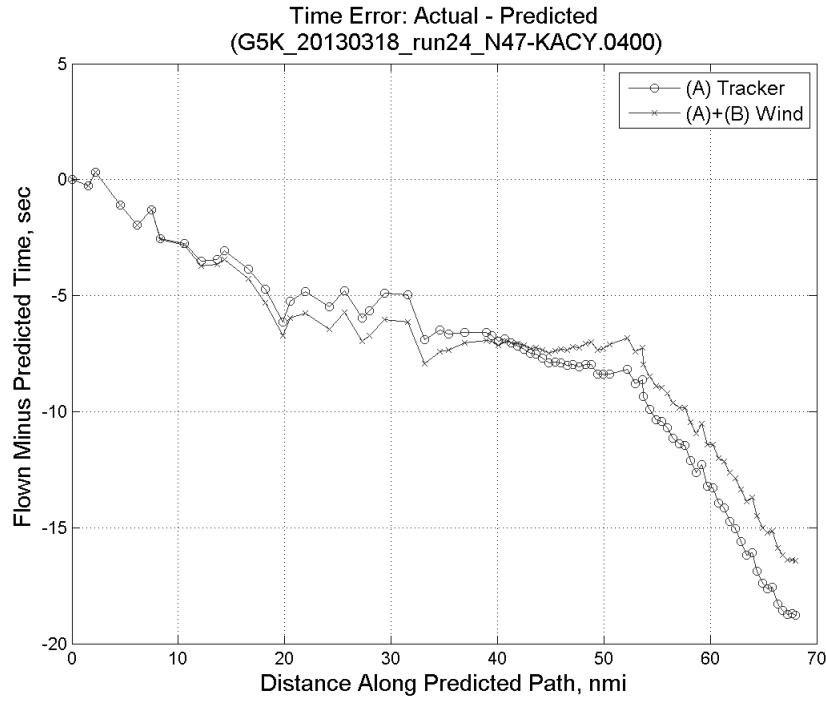


**Figure 389: Time error for run 24 before ((A) Tracker) and after ((A)+(B) Wind) removing wind error source.**

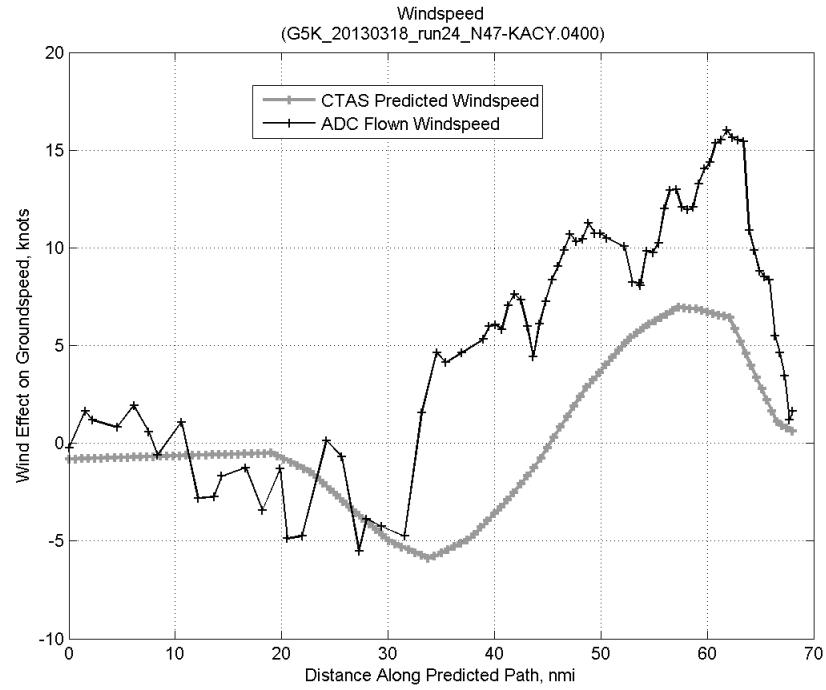


**Figure 390: CTAS predicted and ADC flown wind effect on ground speed for run 24. Negative values indicate a headwind.**

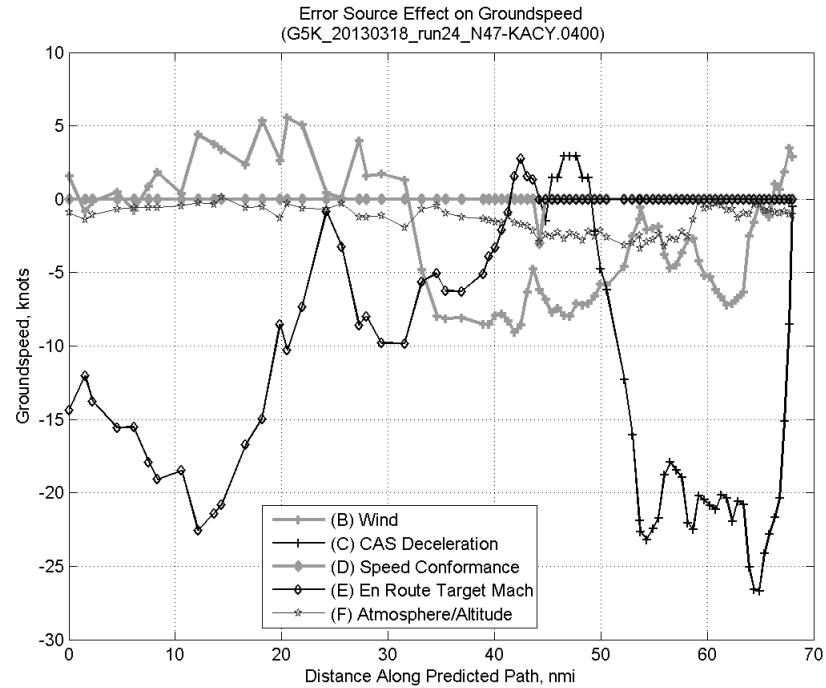


**Figure 391: Error sources (flown minus predicted) converted to a ground speed effect for run 24. Positive values indicate the flown ground speed was faster than the CTAS prediction.**

### C.15.C. CAS Deceleration

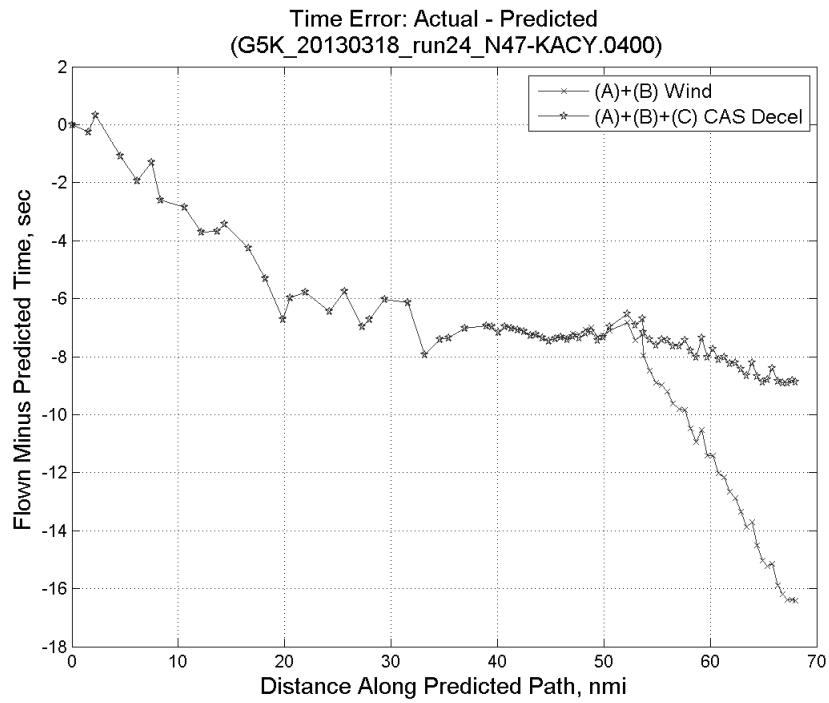


**Figure 392:** Time error for run 24 before ((A)+(B) Wind) and after ((A)+(B)+(C) CAS Decel) removing CAS deceleration error source.

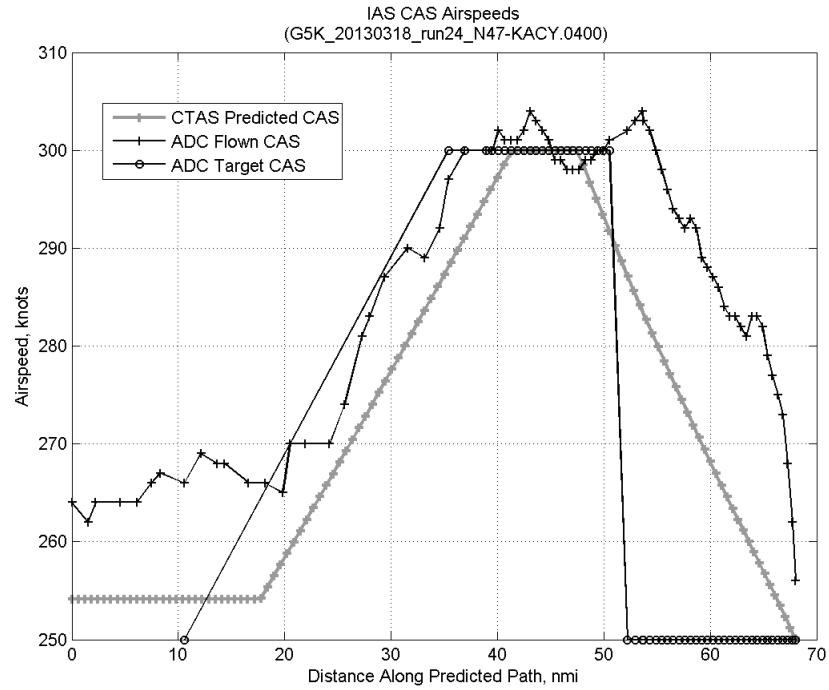


**Figure 393:** CTAS predicted and ADC flown CAS for run 24. CAS that is being targeted is shown with circle markers.

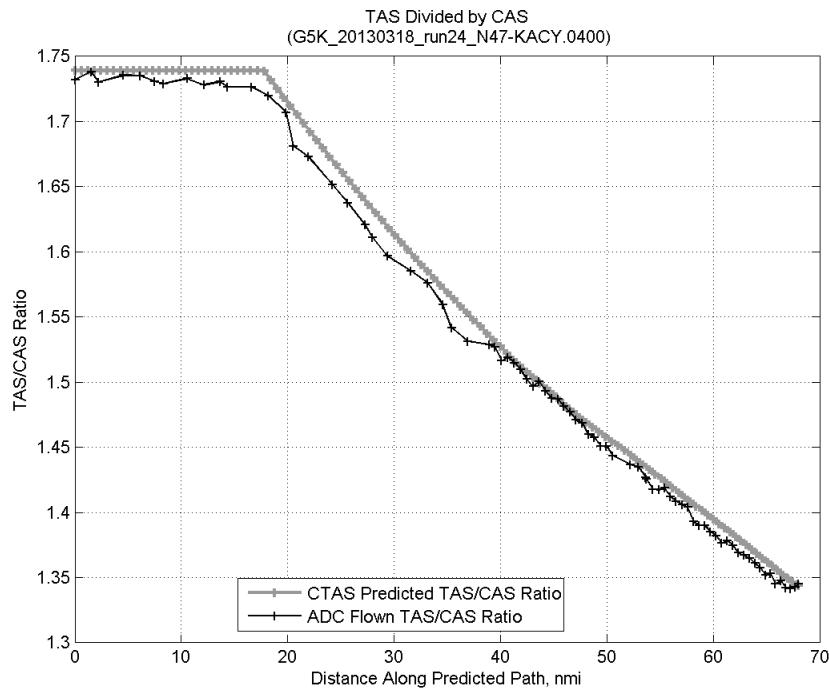


**Figure 394: CTAS predicted and ADC flown TAS/CAS ratio for run 24.**

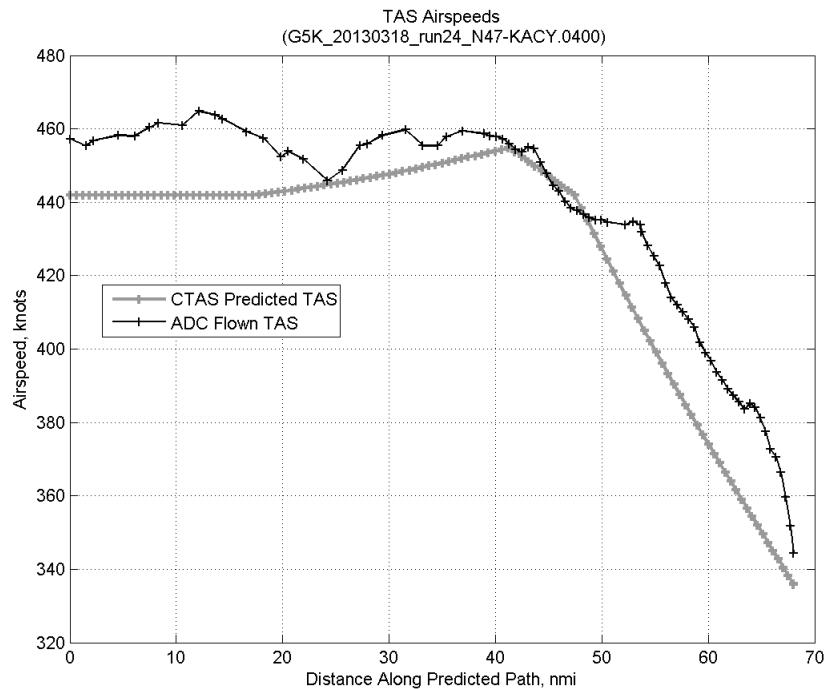


**Figure 395: CTAS predicted and ADC flown TAS for run 24.**

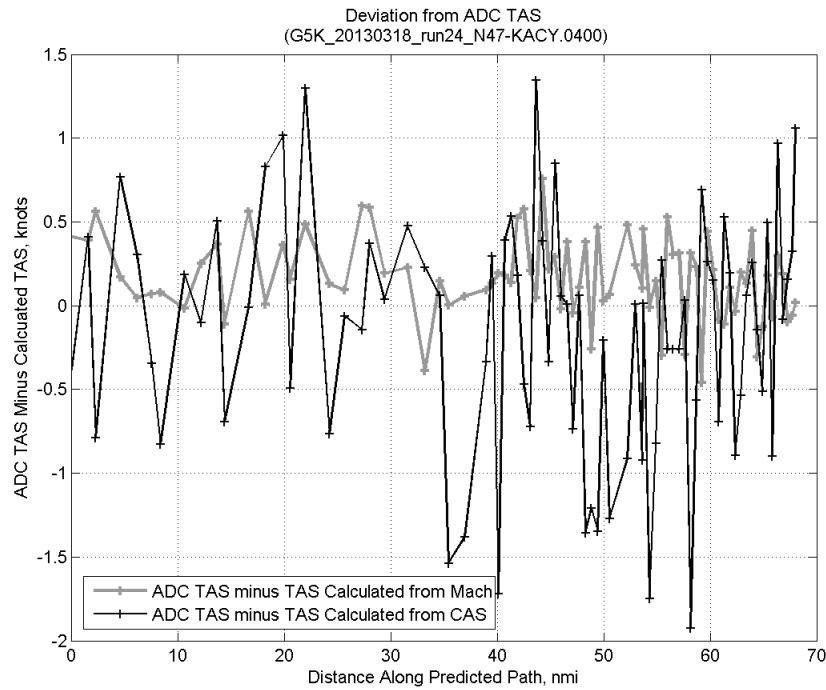


**Figure 396: Deviation from ADC flown TAS if calculating TAS using ADC flown CAS, Mach, atmospheric temperature, and atmospheric pressure for run 24.**

#### C.15.D. Speed Conformance

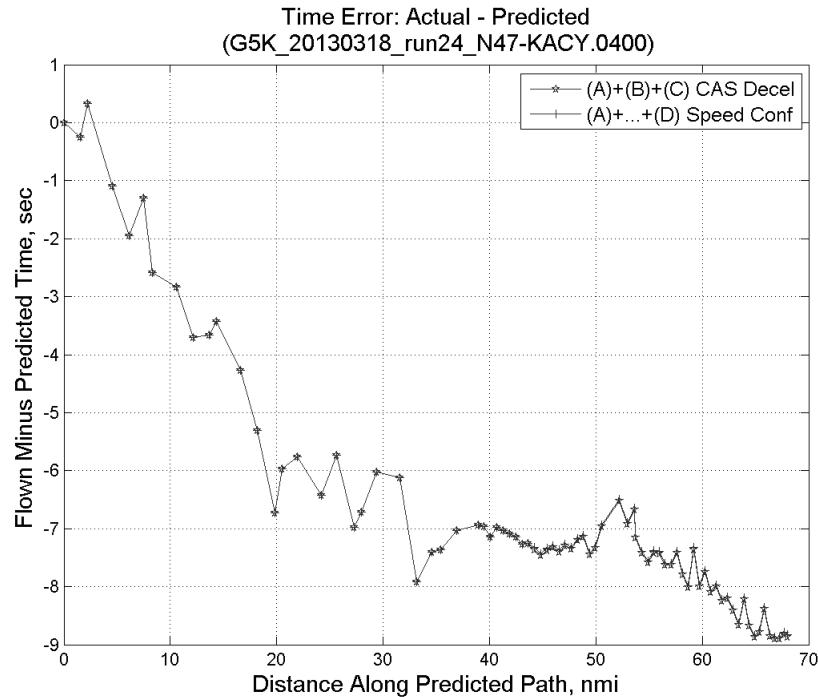


**Figure 397: Time error for run 24 before ((A)+(B)+(C) CAS Decel) and after ((A)+...+(D) Speed Conf) removing speed conformance error source.**

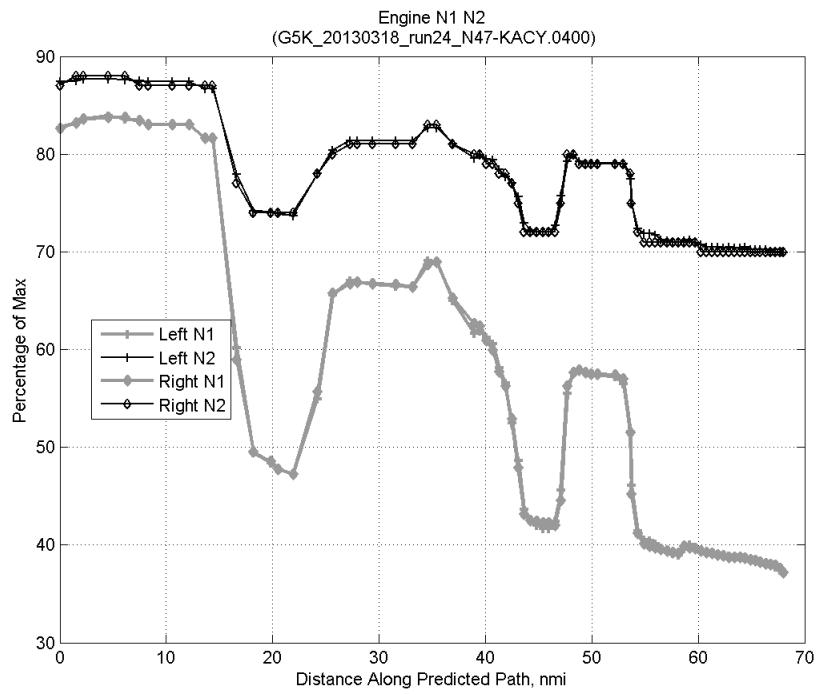


**Figure 398: Flown engine N1 and N2 for run 24.**

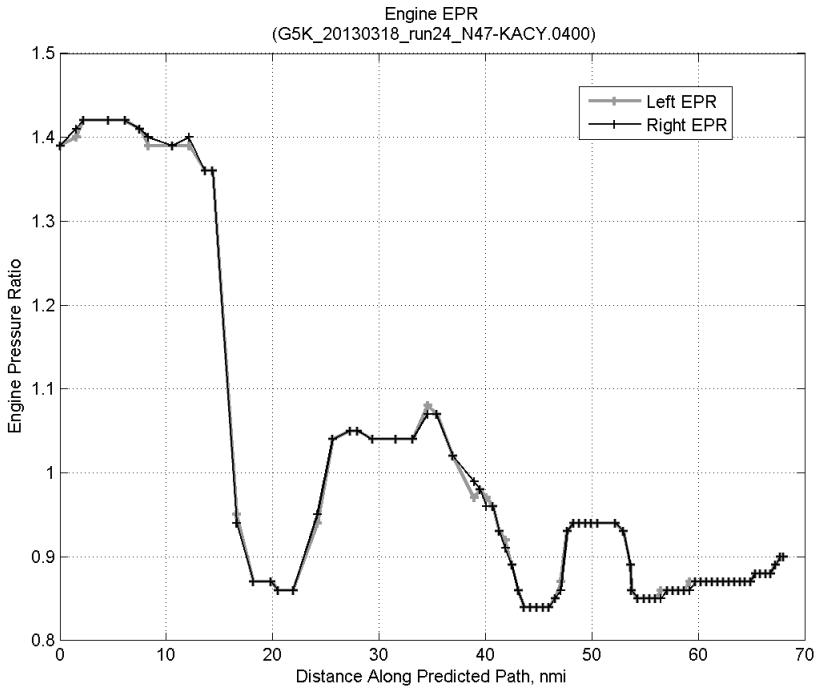


**Figure 399: Flown engine EPR for run 24.**

### C.15.E. Target Mach

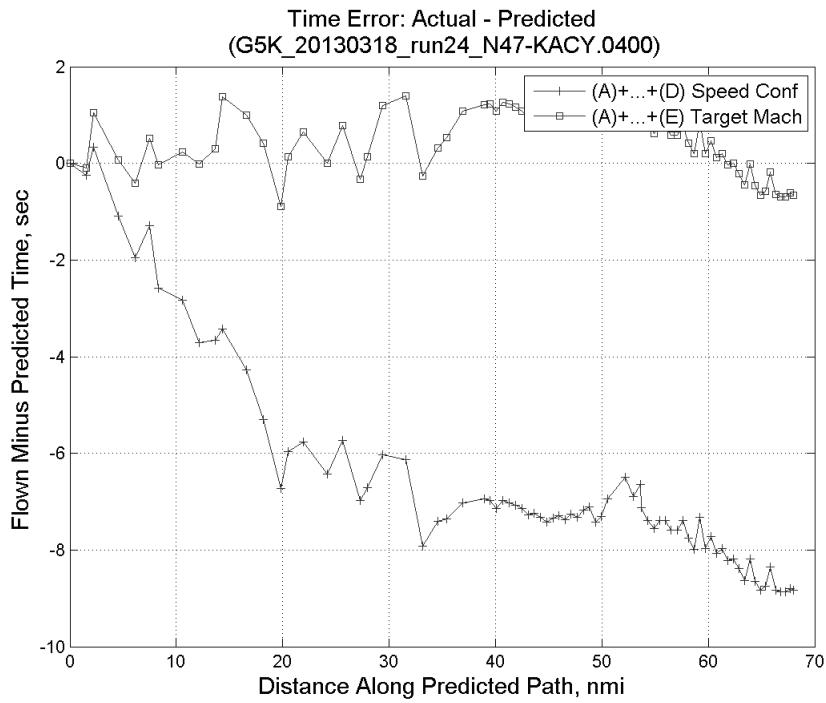


**Figure 400:** Time error for run 24 before ((A)+...+(D) Speed Conf) and after ((A)+...+(E) Target Mach) removing target Mach error source.

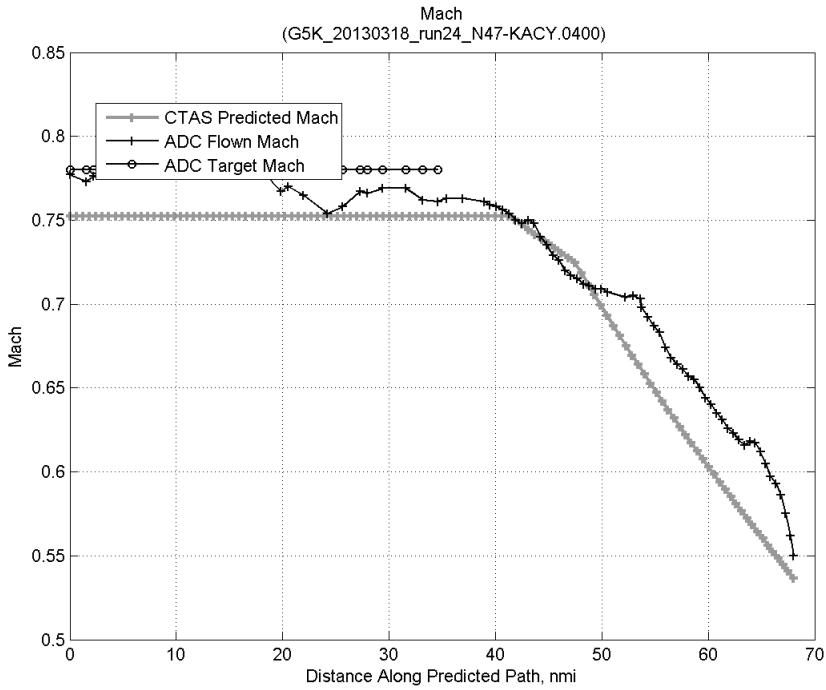


**Figure 401:** CTAS predicted and ADC flown Mach for run 24. Mach being targeted (ADC) shown with circle markers.

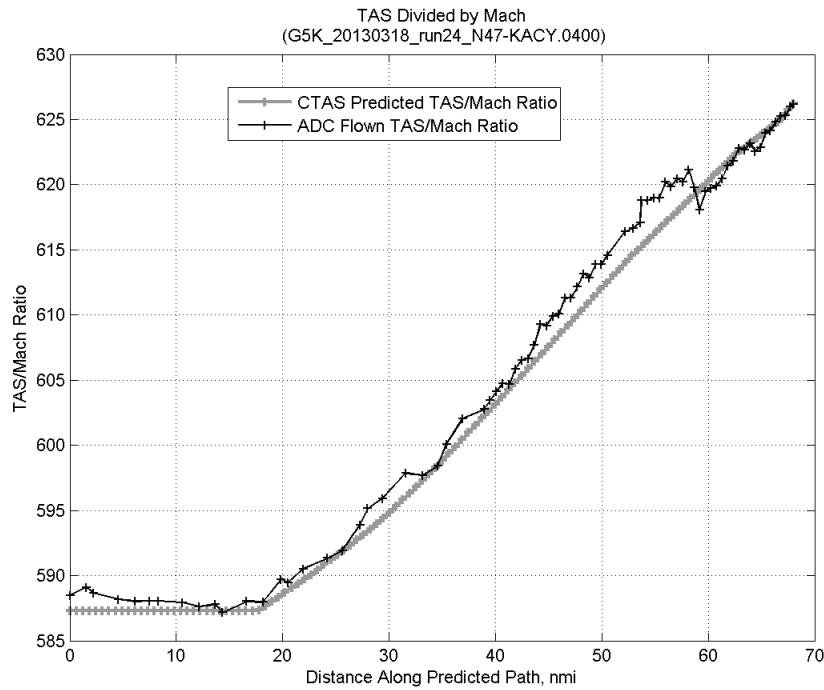


**Figure 402: CTAS predicted and ADC flown TAS/Mach ratio for run 24.**

#### C.15.F. Atmosphere/Altitude

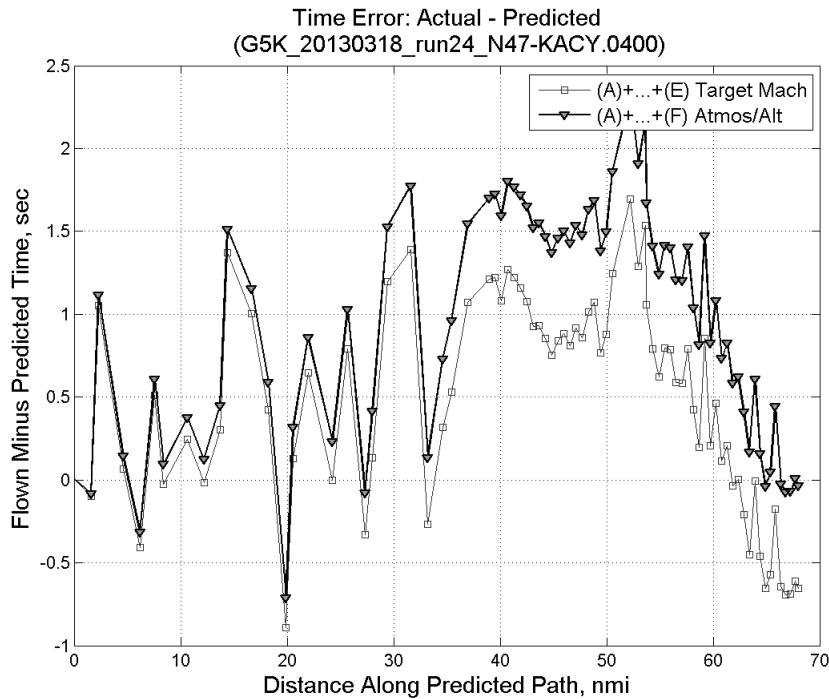


**Figure 403: Time error for run 24 before ((A)+...+(E) Target Mach) and after ((A)+...+(F) Atmos/Alt) removing atmosphere/altitude error source.**

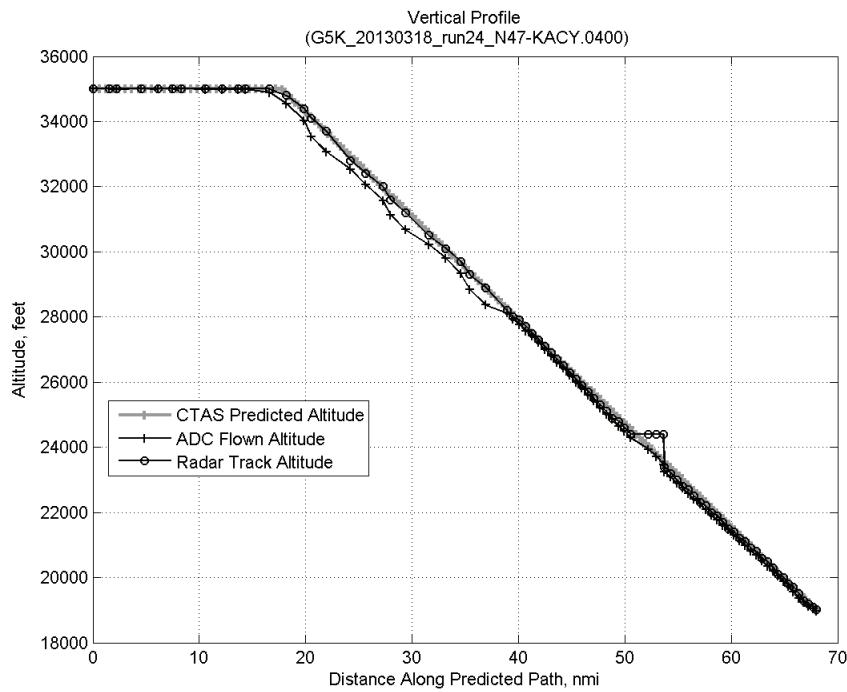


**Figure 404: Flown (ADC) and predicted (CTAS) vertical profile for run 24.**

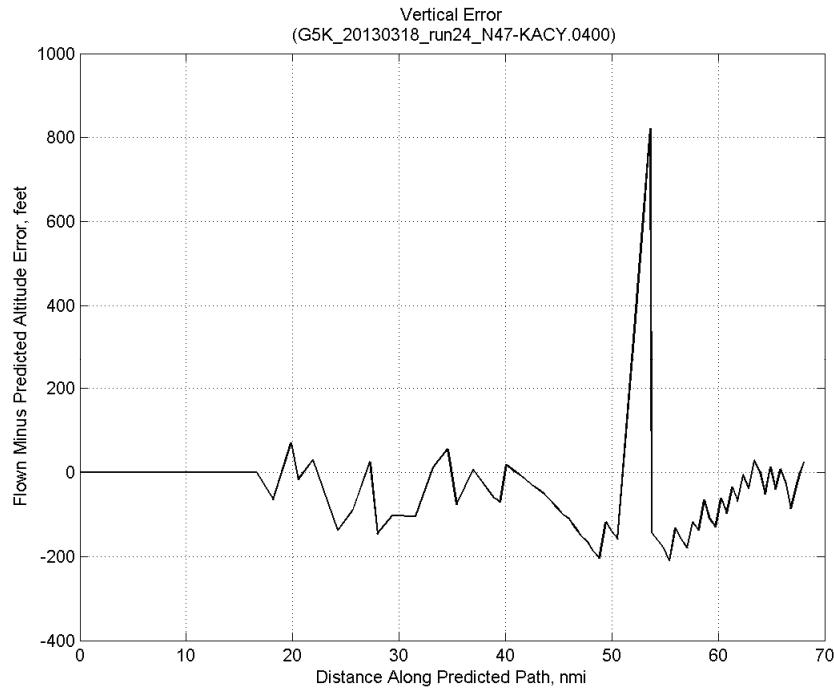


**Figure 405: Vertical error (flown minus predicted altitude) for run 24. Positive values indicate aircraft flew higher than predicted by CTAS.**

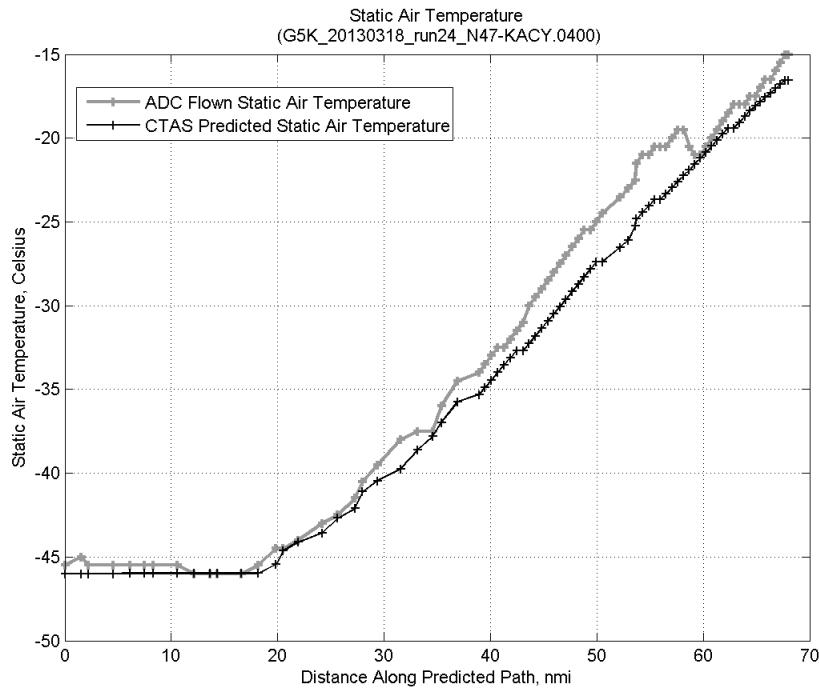


**Figure 406: Flown (ADC) and predicted (CTAS) static air temperature for run 24.**

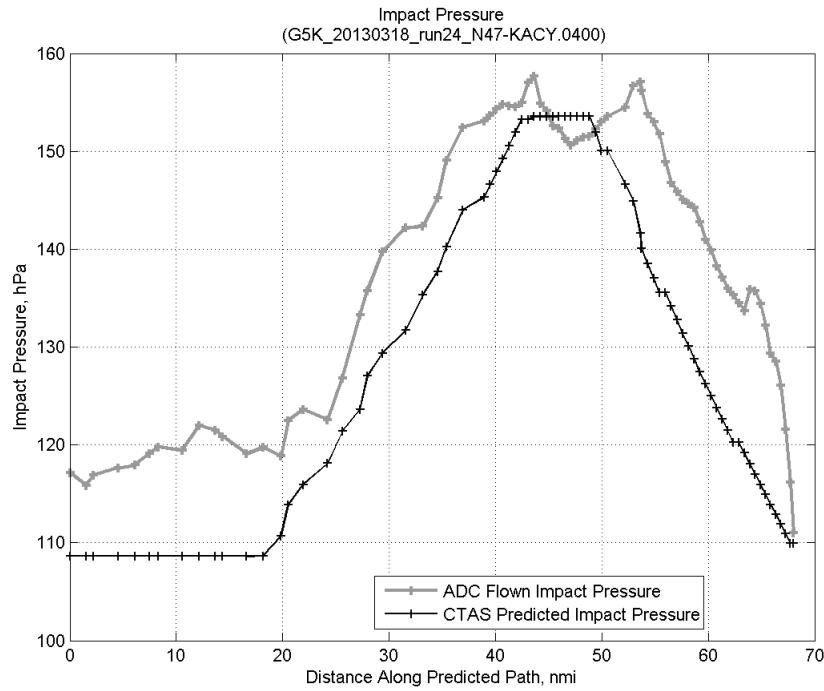


**Figure 407: Flown (ADC) and predicted (CTAS) impact pressure for run 24.**

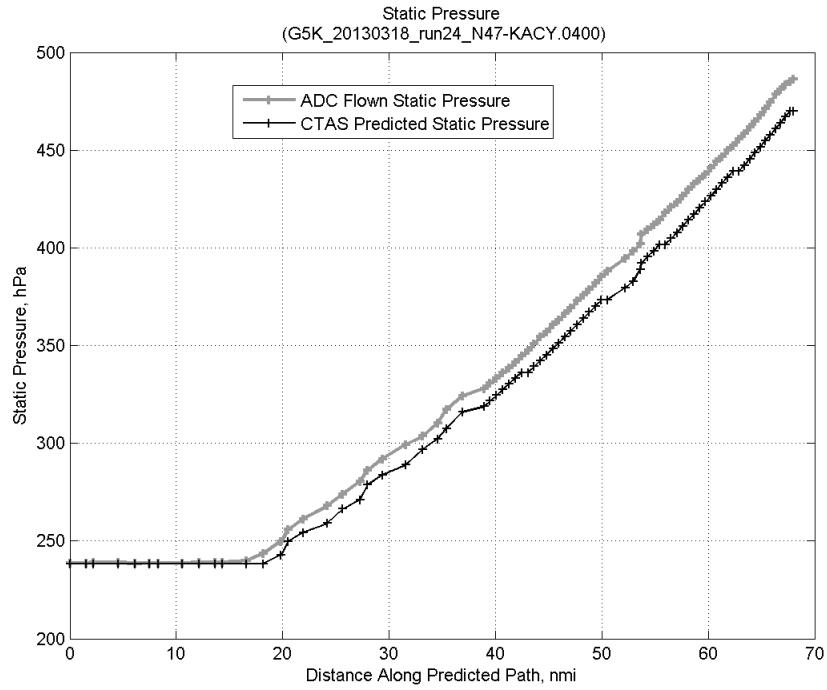


**Figure 408: Flown (ADC) and predicted (CTAS) static pressure for run 24.**

### C.15.G. Path Distance

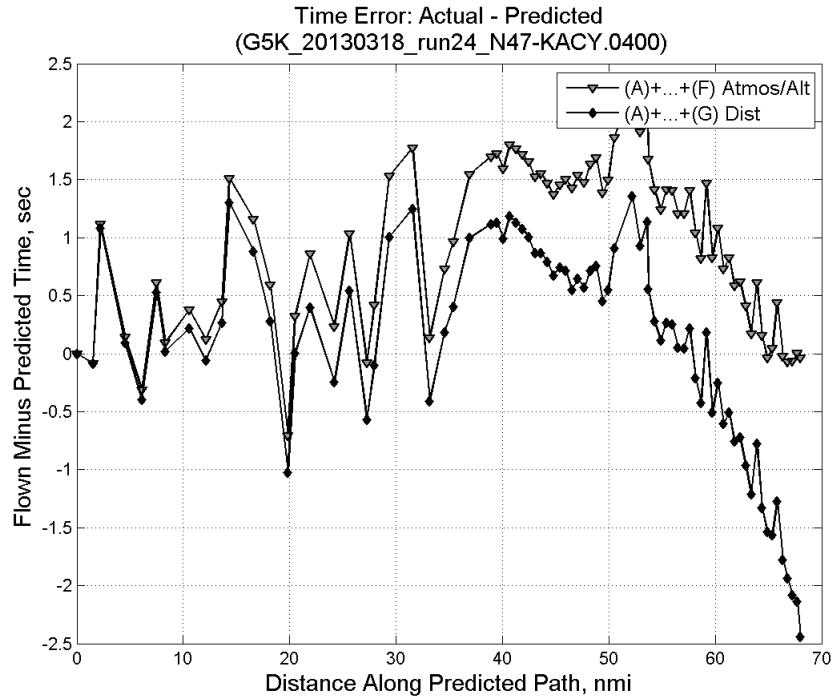


**Figure 409: Time error for run 24 before ((A)+...+(F) Atmos/Alt) and after ((A)+...+(G) Dist) removing path distance error source.**

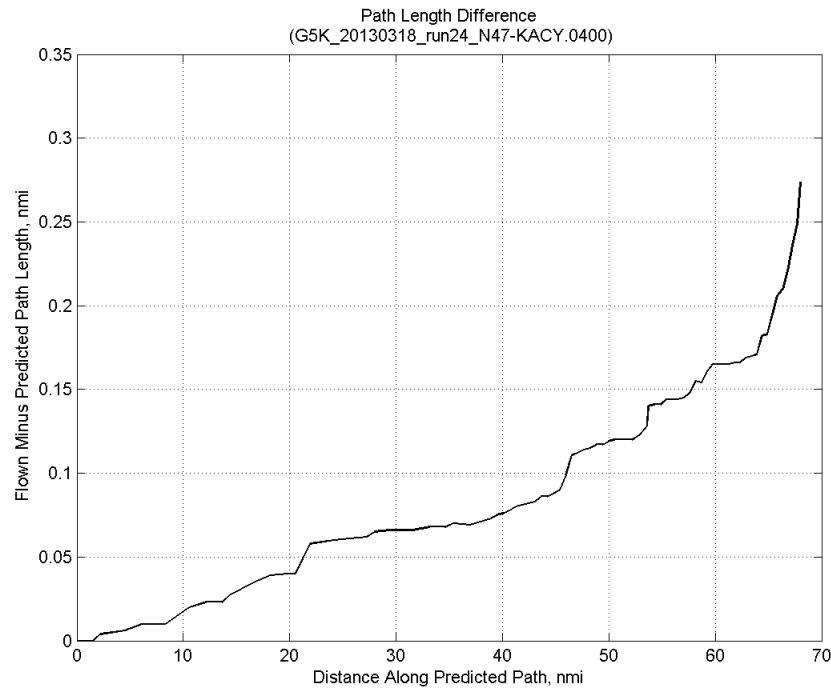


**Figure 410: ADC flown minus CTAS predicted path length for run 24. Positive values indicate aircraft followed a longer path than predicted by CTAS.**

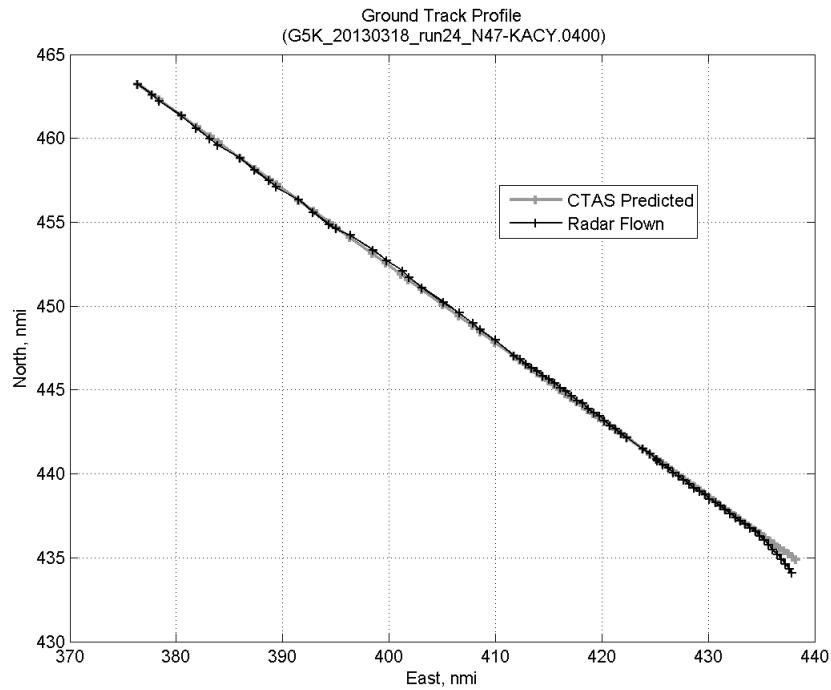


**Figure 411: CTAS predicted and radar flown ground track profile for run 24.**

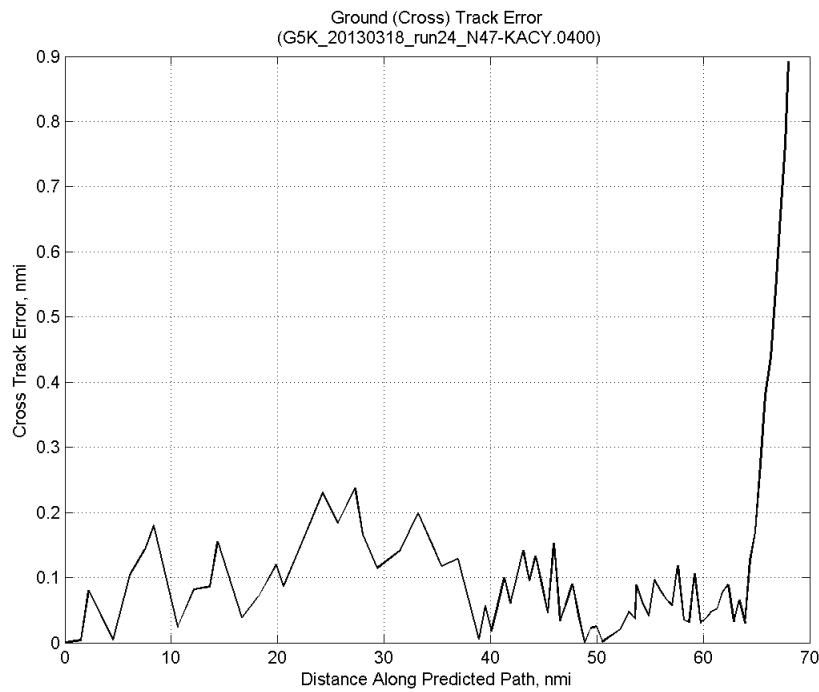


**Figure 412: Ground (cross) track error for run 24.**

### C.16. Run 25

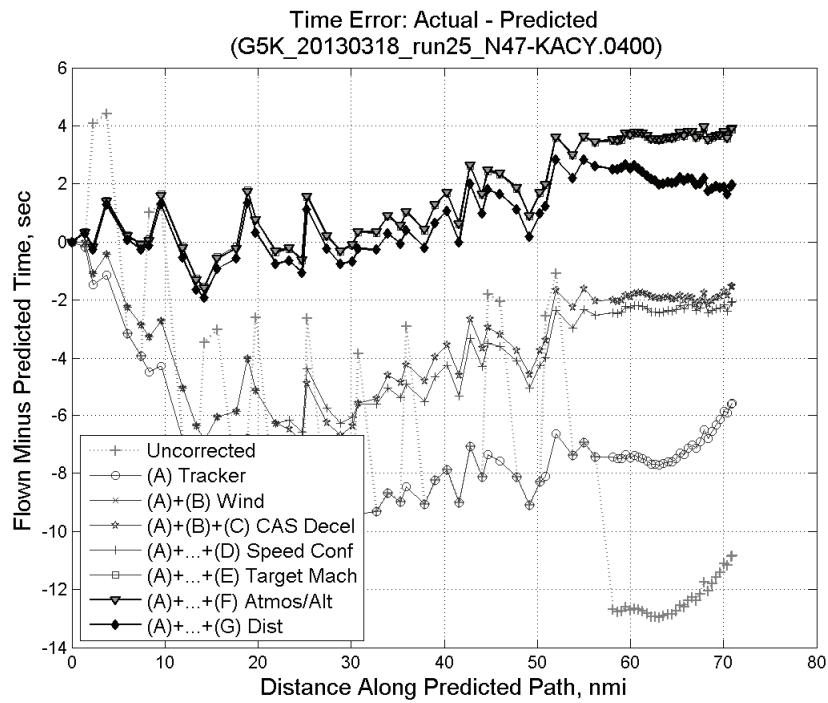


**Figure 413: Time error for run 25 showing incremental effect of removing each error source.**

#### C.16.A. Tracker Jumps

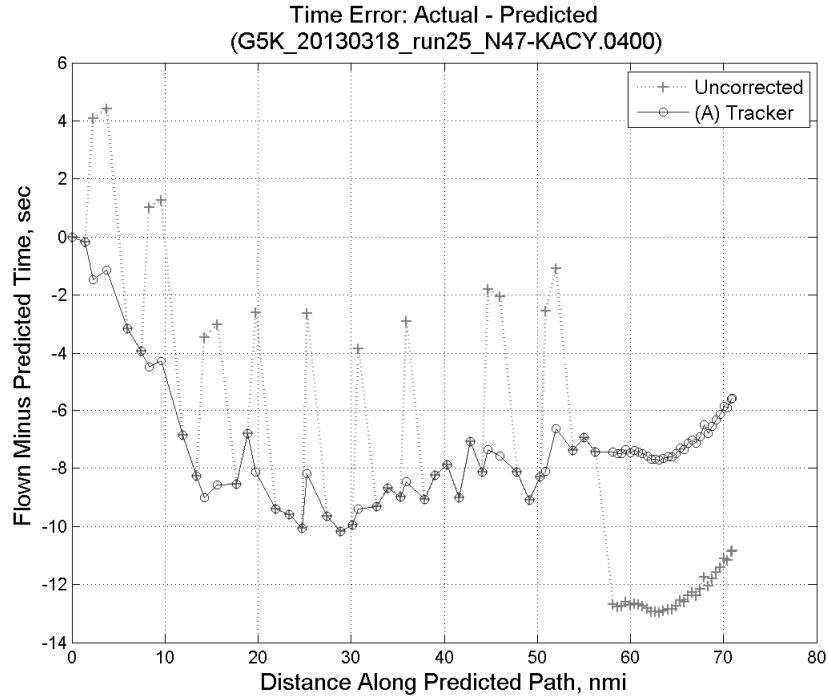


**Figure 414: Time error for run 25 before (Uncorrected) and after ((A) Tracker) removing tracker jump error source.**

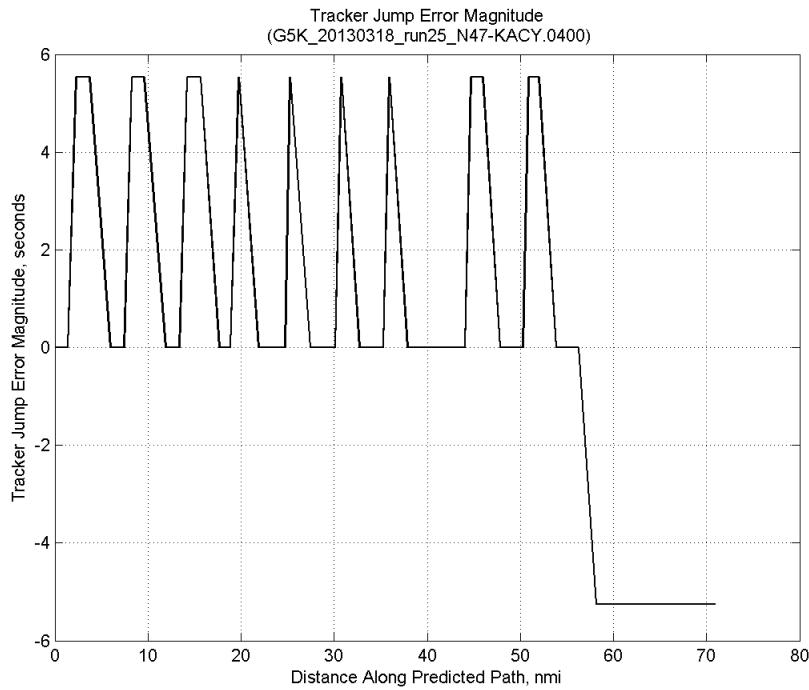


**Figure 415: Effect of tracker jump error source on time error for run 25.**

### C.16.B. Wind

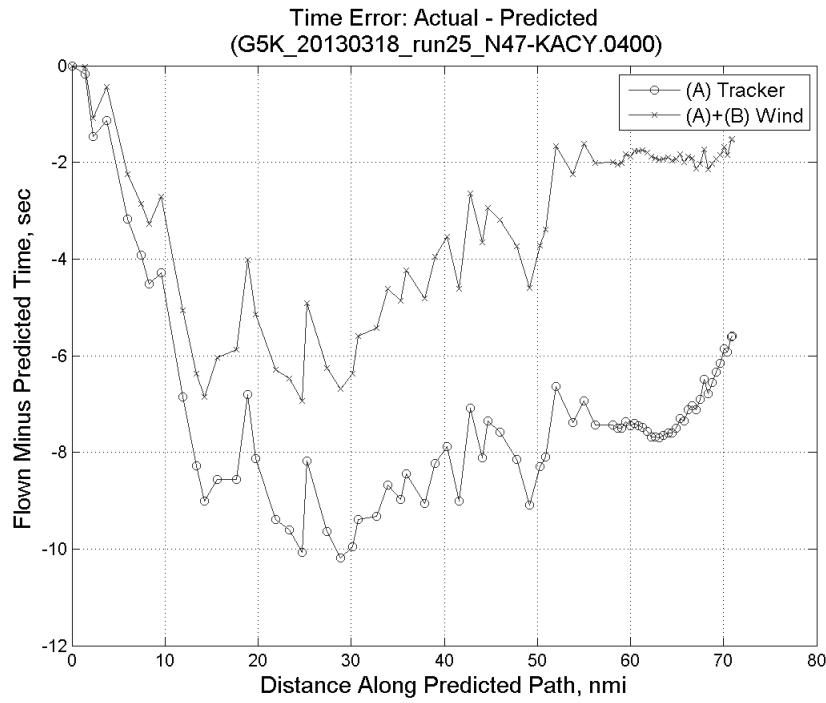


**Figure 416: Time error for run 25 before ((A) Tracker) and after ((A)+(B) Wind) removing wind error source.**

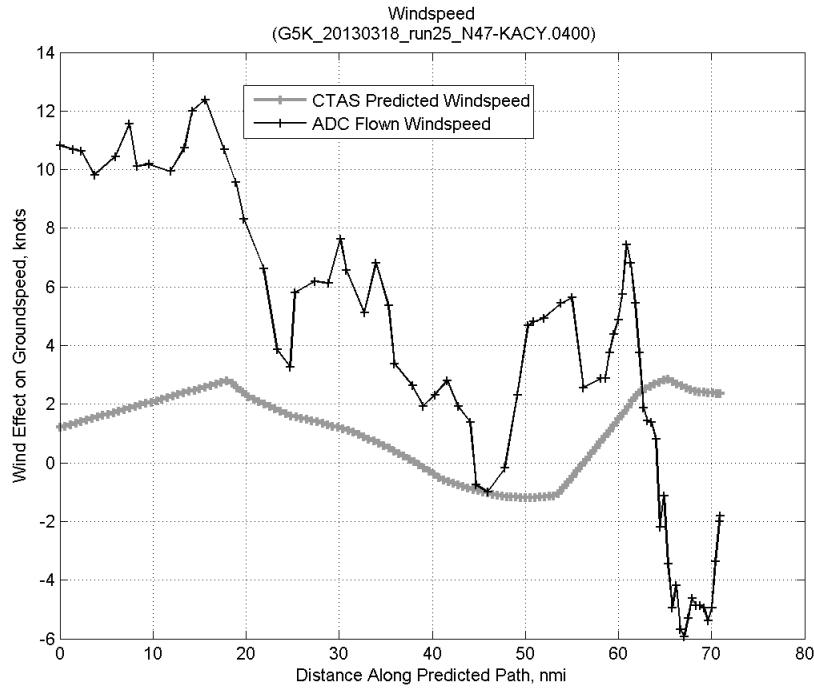


**Figure 417: CTAS predicted and ADC flown wind effect on ground speed for run 25. Negative values indicate a headwind.**

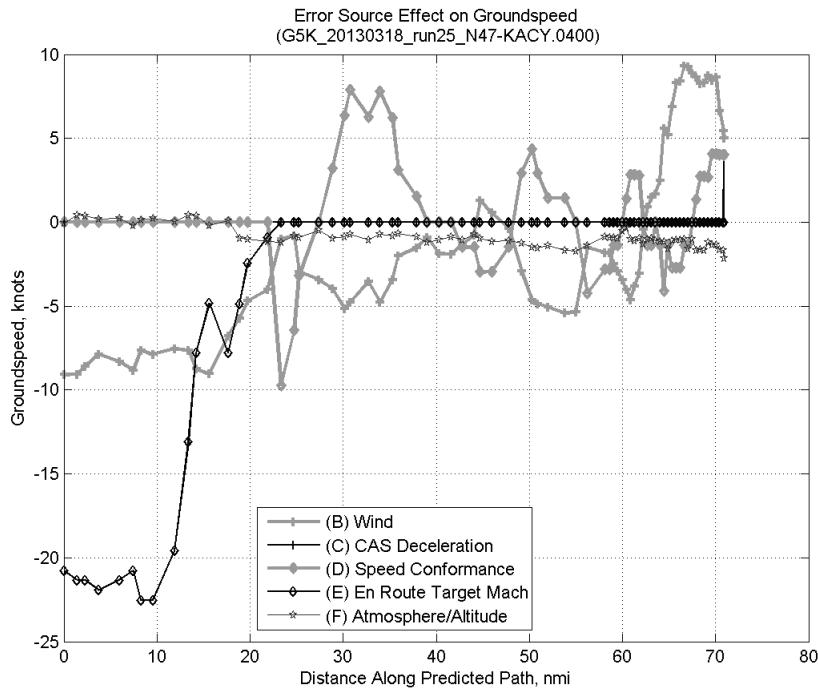


**Figure 418: Error sources (flown minus predicted) converted to a ground speed effect for run 25. Positive values indicate the flown ground speed was faster than the CTAS prediction.**

### C.16.C. CAS Deceleration

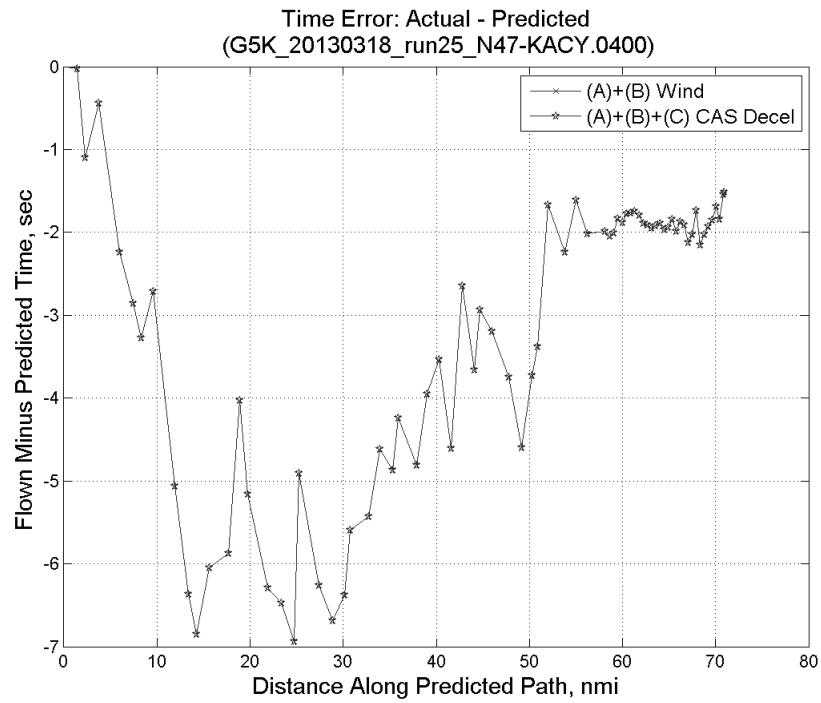


**Figure 419:** Time error for run 25 before ((A)+(B) Wind) and after ((A)+(B)+(C) CAS Decel) removing CAS deceleration error source.

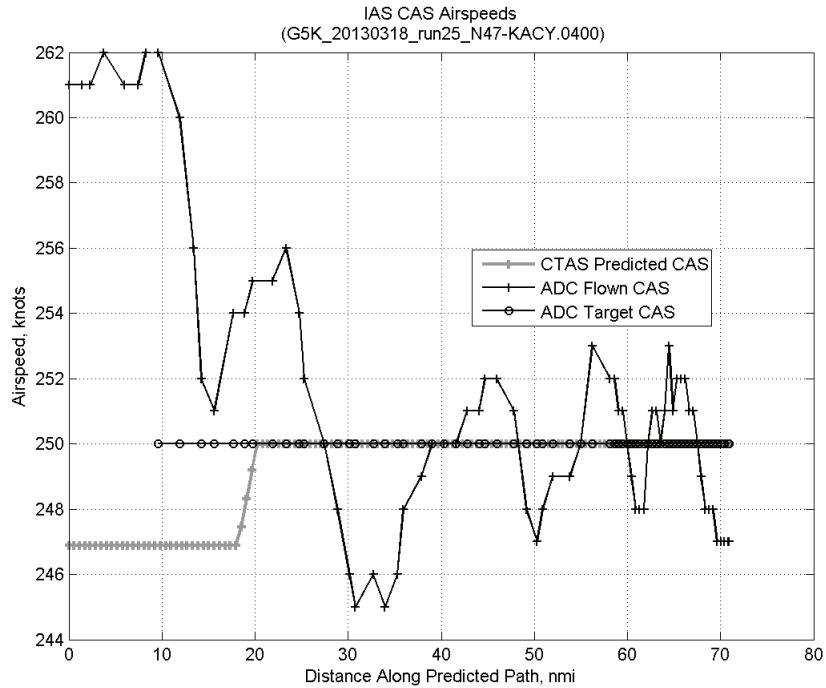


**Figure 420:** CTAS predicted and ADC flown CAS for run 25. CAS that is being targeted is shown with circle markers.

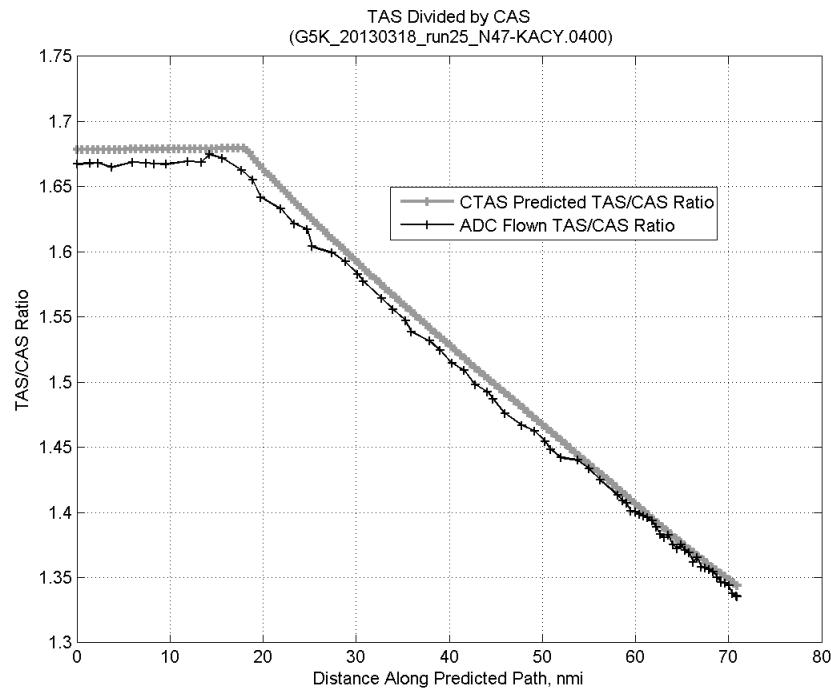


**Figure 421: CTAS predicted and ADC flown TAS/CAS ratio for run 25.**

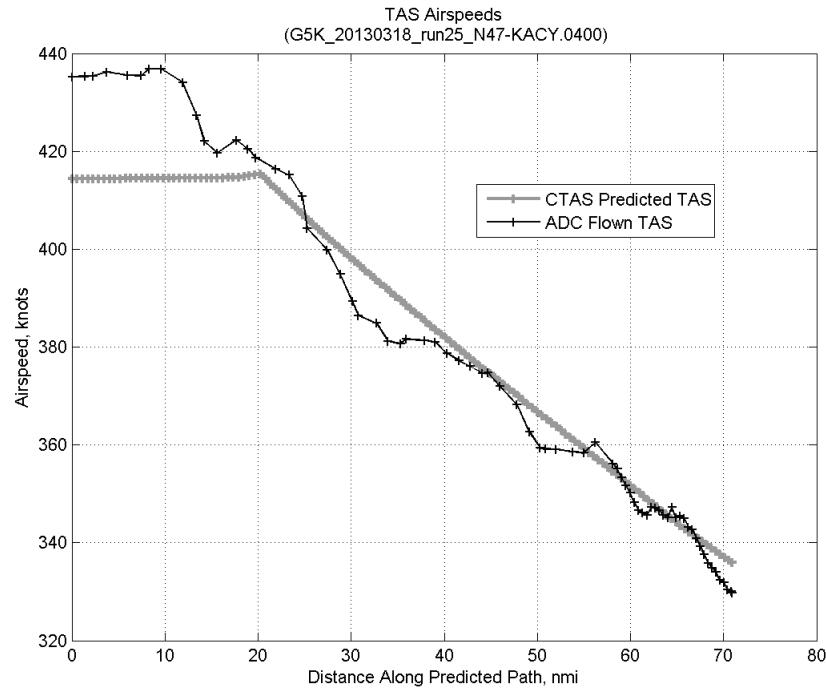


**Figure 422: CTAS predicted and ADC flown TAS for run 25.**

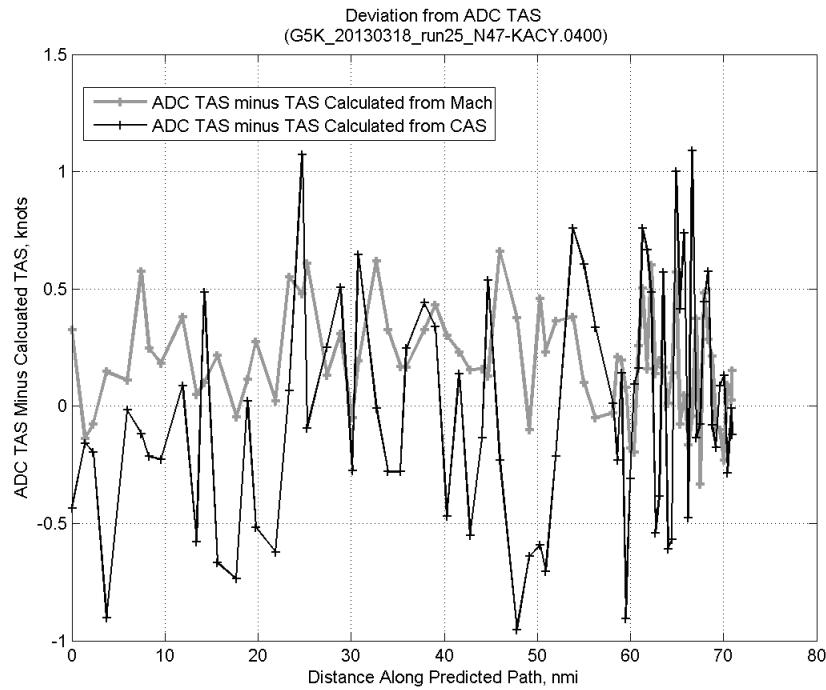


**Figure 423: Deviation from ADC flown TAS if calculating TAS using ADC flown CAS, Mach, atmospheric temperature, and atmospheric pressure for run 25.**

#### C.16.D. Speed Conformance

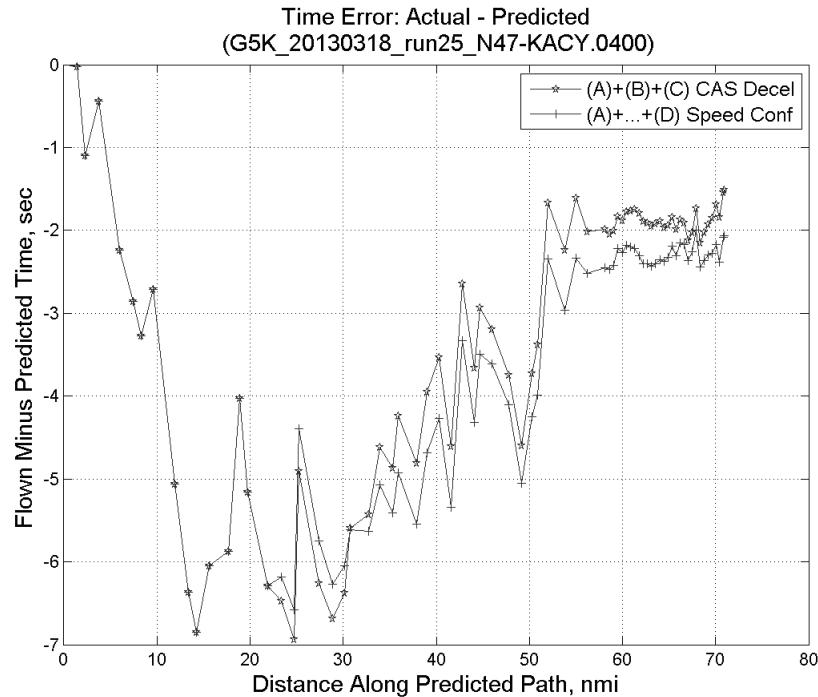


**Figure 424: Time error for run 25 before ((A)+(B)+(C) CAS Decel) and after ((A)+...+(D) Speed Conf) removing speed conformance error source.**

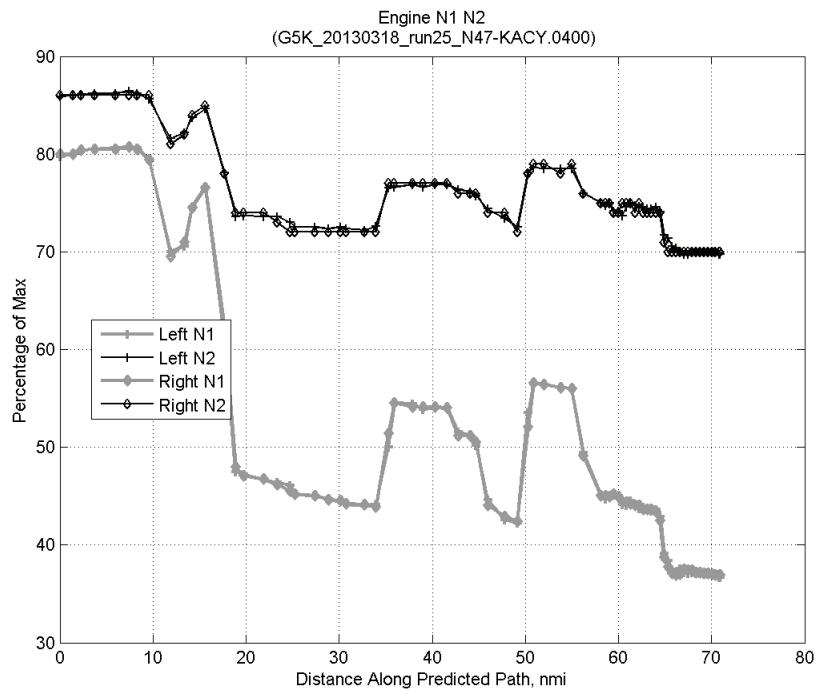


**Figure 425: Flown engine N1 and N2 for run 25.**

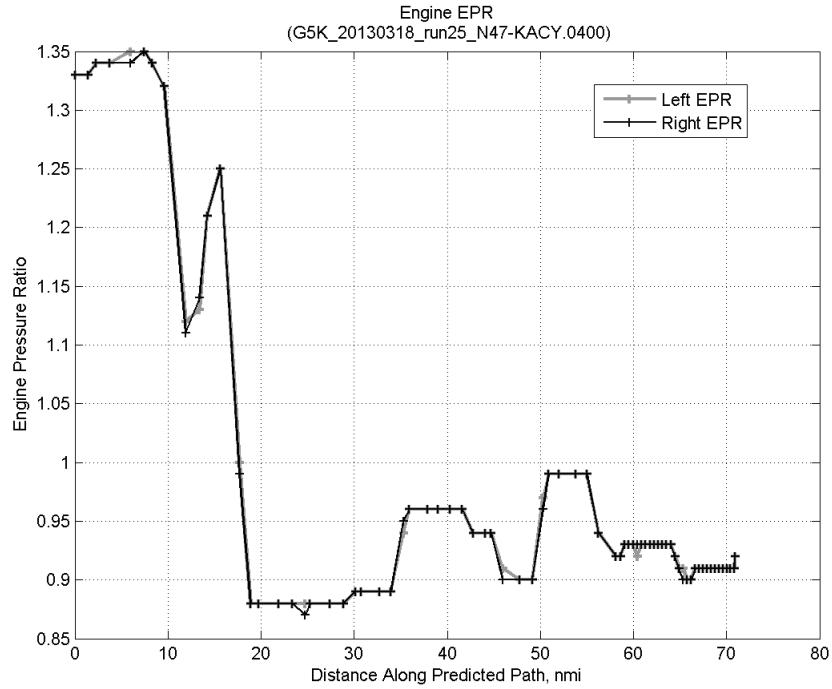


**Figure 426: Flown engine EPR for run 25.**

### C.16.E. Target Mach

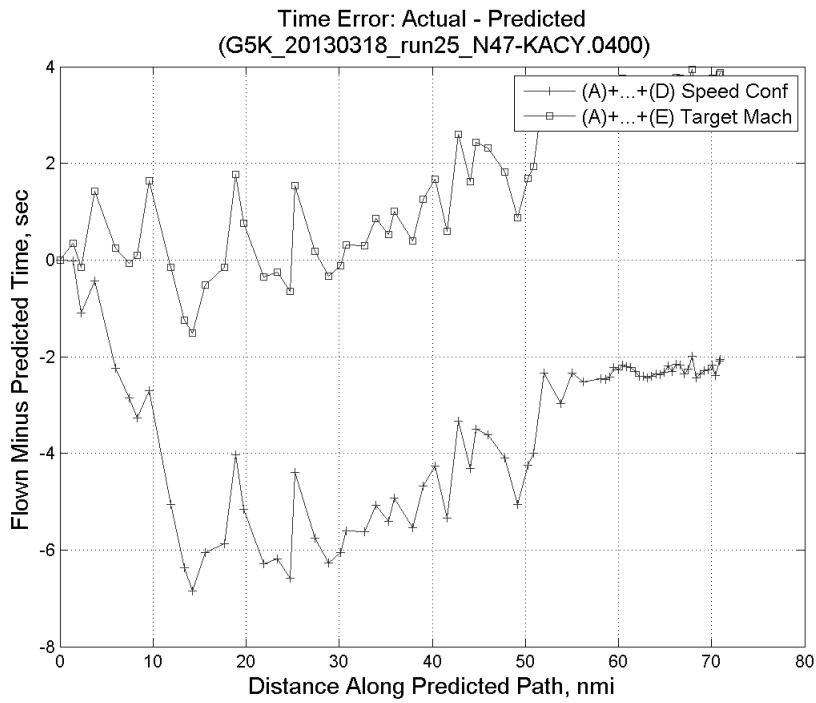


**Figure 427:** Time error for run 25 before ((A)+...+(D) Speed Conf) and after ((A)+...+(E) Target Mach) removing target Mach error source.

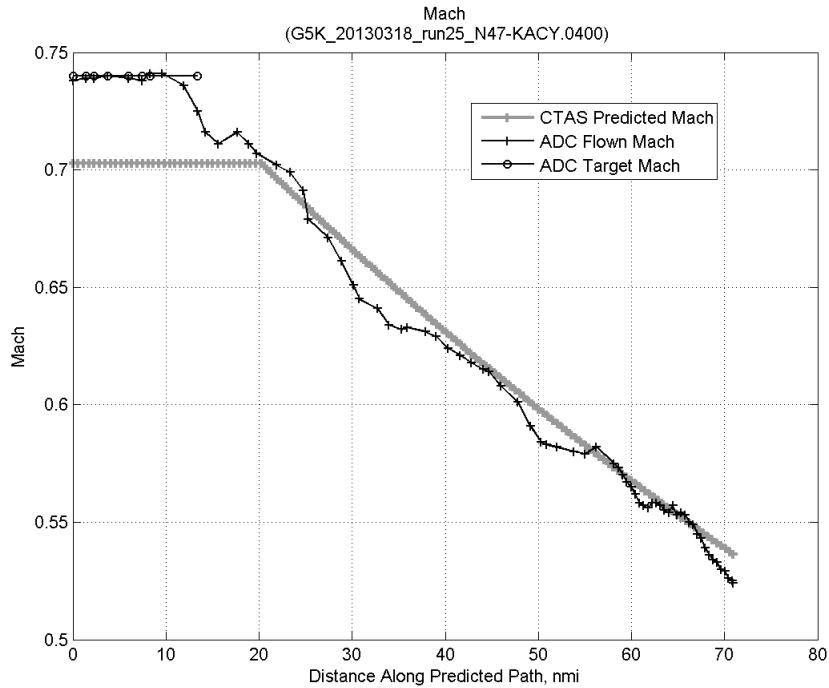


**Figure 428:** CTAS predicted and ADC flown Mach for run 25. Mach being targeted (ADC) shown with circle markers.

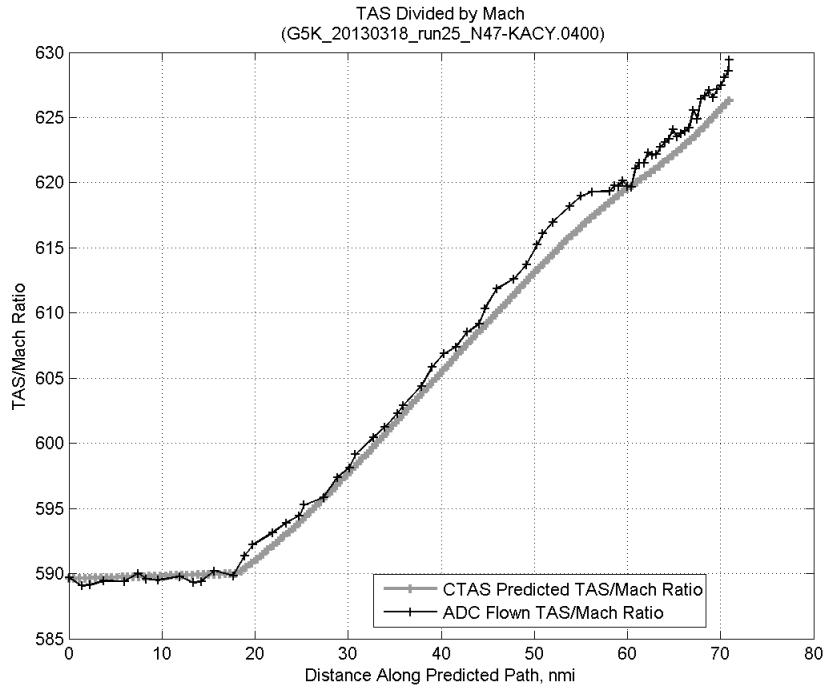


**Figure 429: CTAS predicted and ADC flown TAS/Mach ratio for run 25.**

#### C.16.F. Atmosphere/Altitude

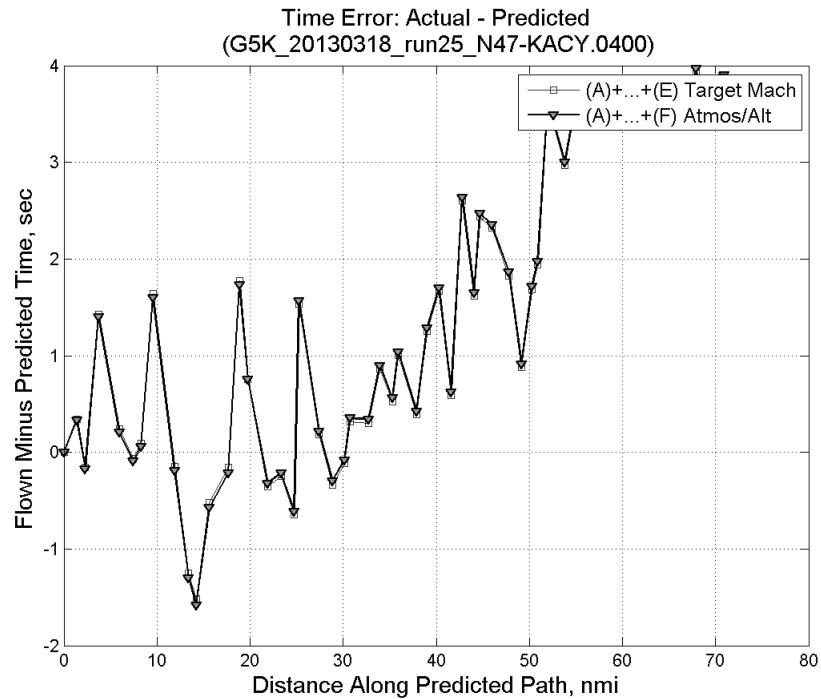


**Figure 430: Time error for run 25 before ((A)+...+(E) Target Mach) and after ((A)+...+(F) Atmos/Alt) removing atmosphere/altitude error source.**

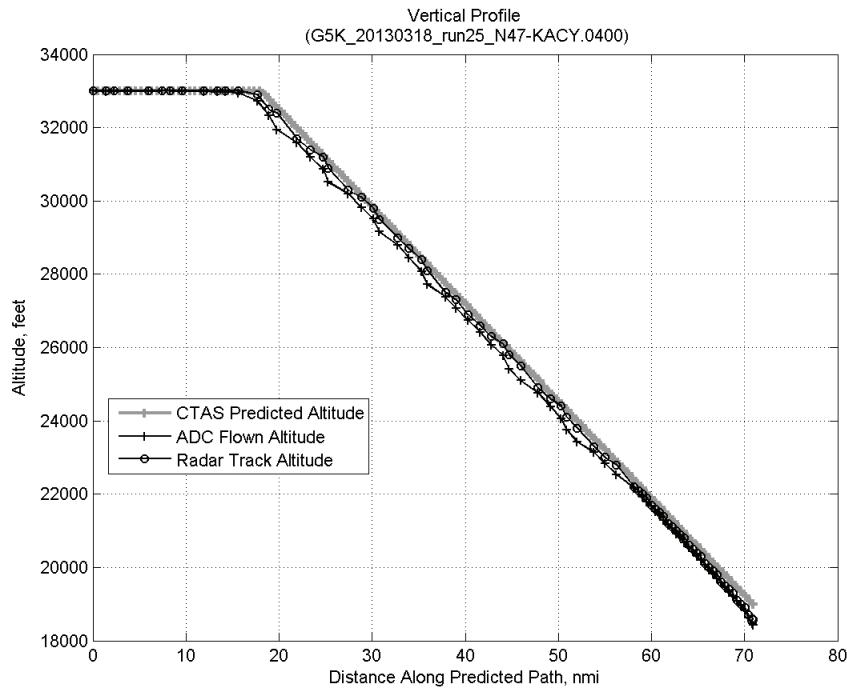


**Figure 431: Flown (ADC) and predicted (CTAS) vertical profile for run 25.**

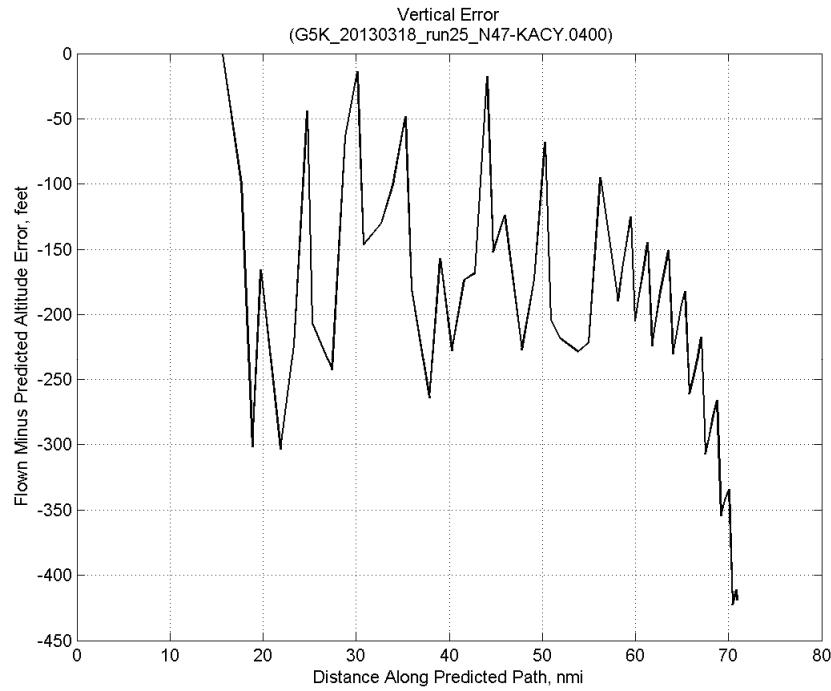


**Figure 432: Vertical error (flown minus predicted altitude) for run 25. Positive values indicate aircraft flew higher than predicted by CTAS.**

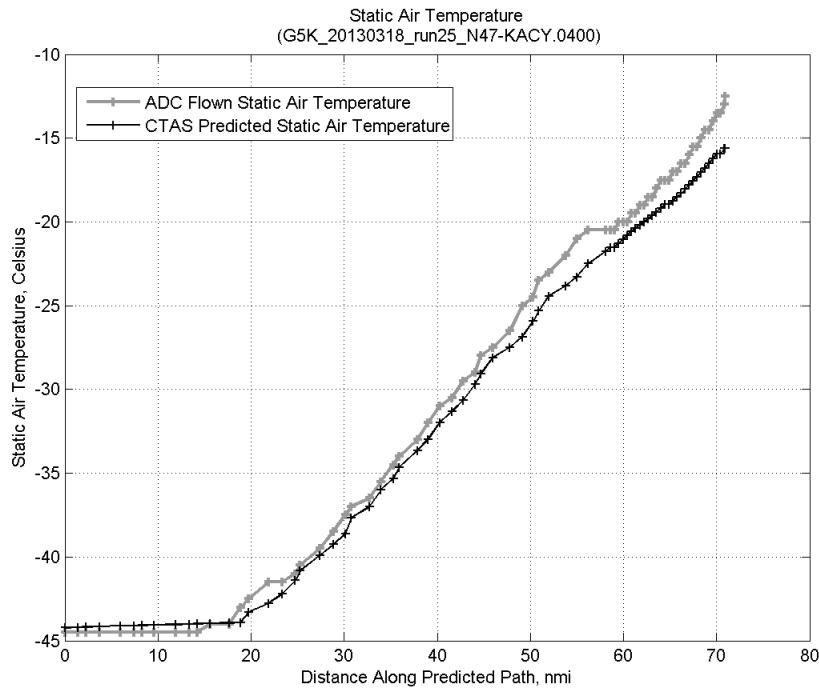


**Figure 433: Flown (ADC) and predicted (CTAS) static air temperature for run 25.**

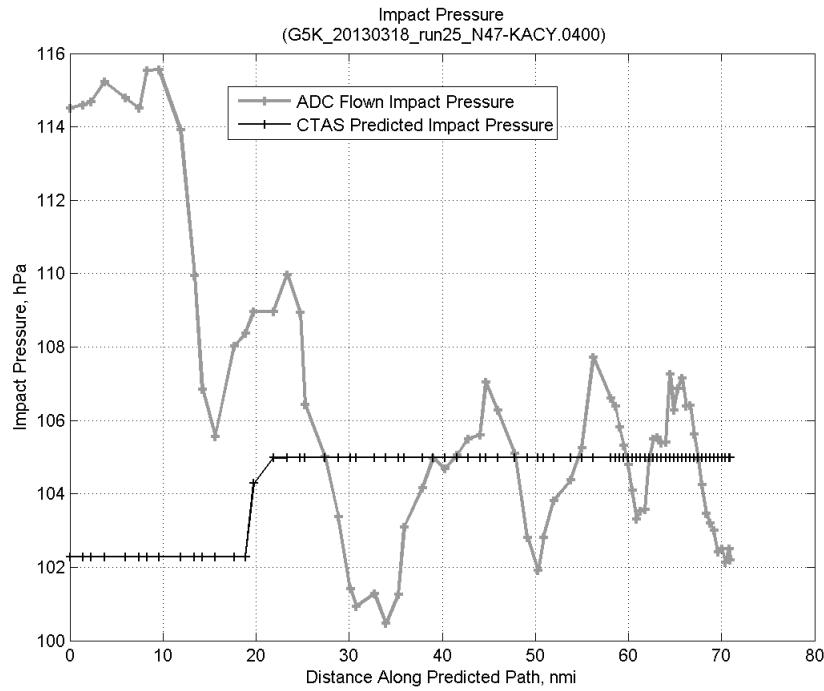


**Figure 434: Flown (ADC) and predicted (CTAS) impact pressure for run 25.**

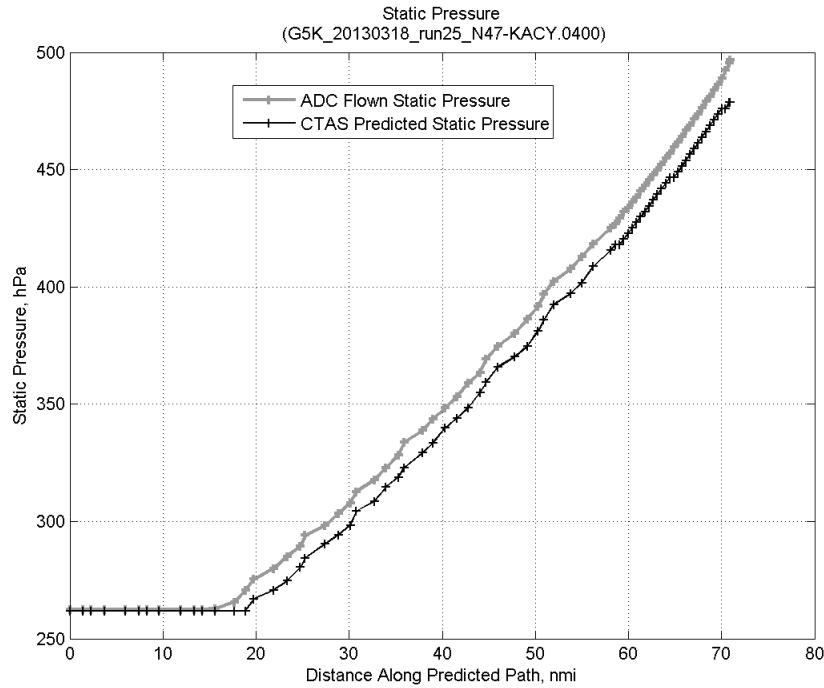


**Figure 435: Flown (ADC) and predicted (CTAS) static pressure for run 25.**

#### C.16.G. Path Distance

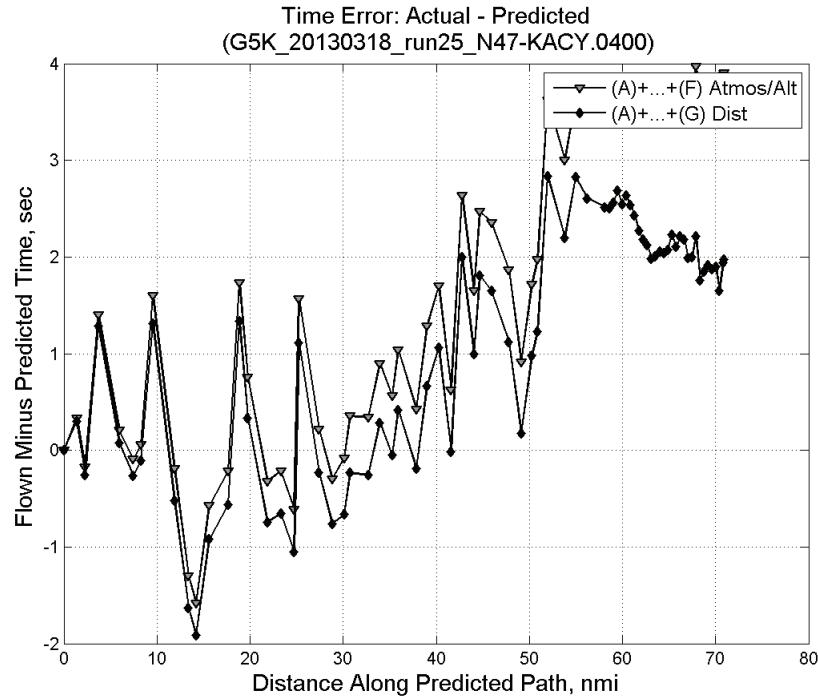


**Figure 436: Time error for run 25 before ((A)+...+(F) Atmos/Alt) and after ((A)+...+(G) Dist) removing path distance error source.**

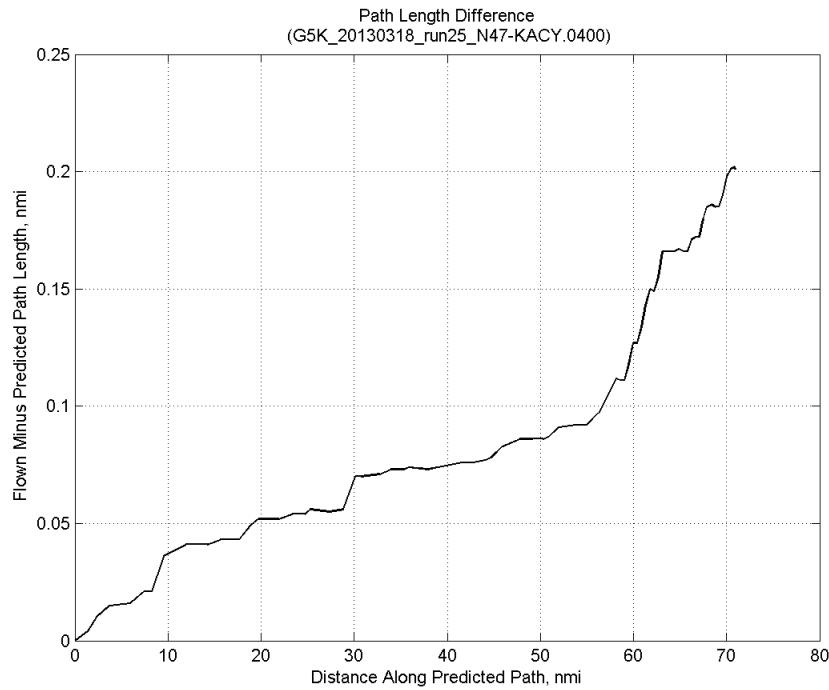


**Figure 437: ADC flown minus CTAS predicted path length for run 25. Positive values indicate aircraft followed a longer path than predicted by CTAS.**

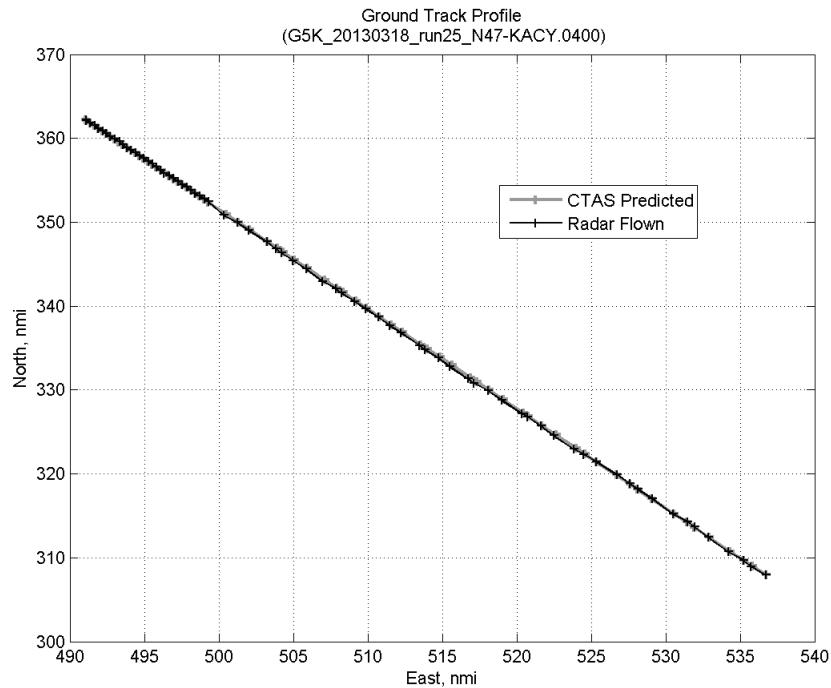


**Figure 438: CTAS predicted and radar flown ground track profile for run 25.**

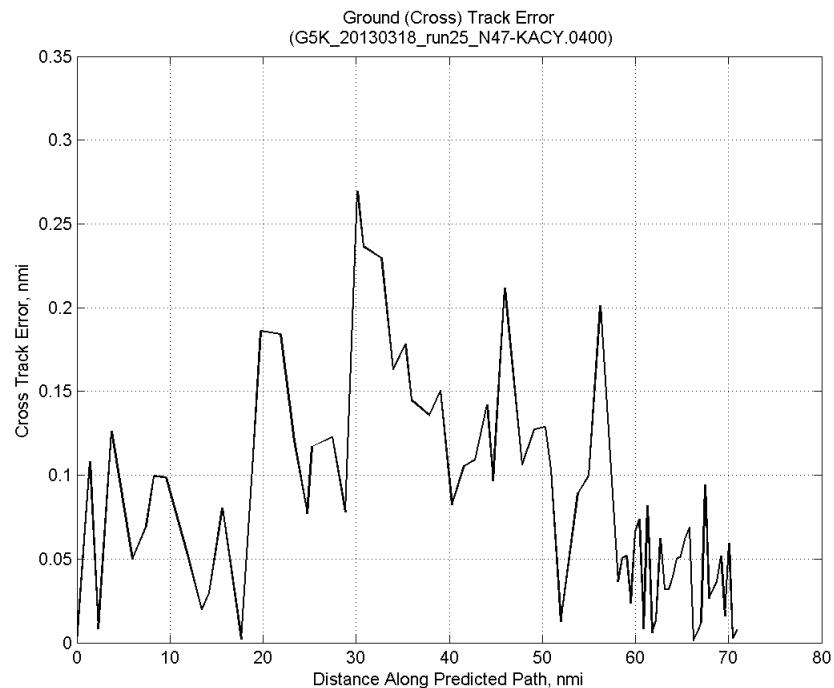


**Figure 439: Ground (cross) track error for run 25.**

### C.17. Run 26

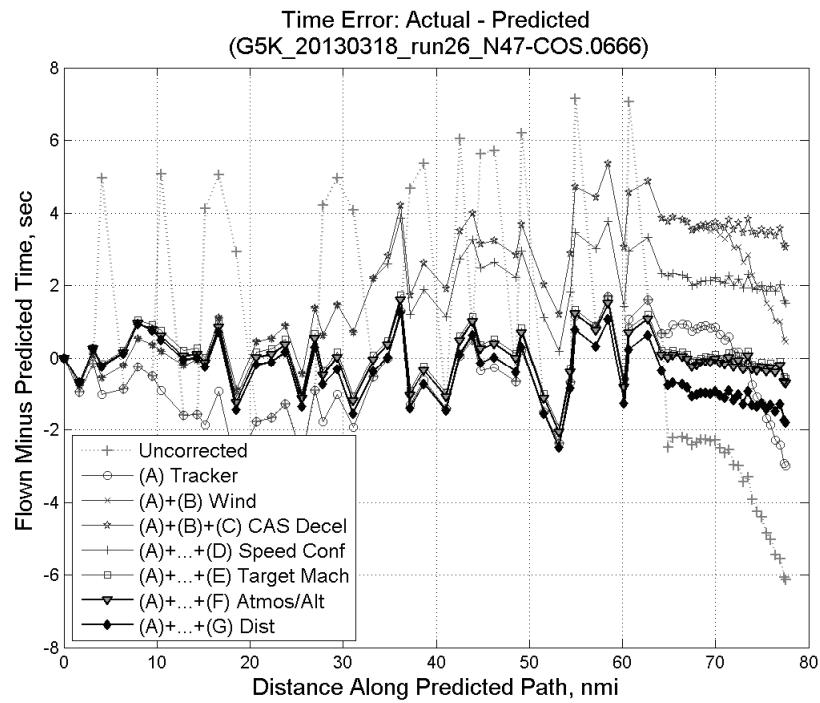


**Figure 440:** Time error for run 26 showing incremental effect of removing each error source.

#### C.17.A. Tracker Jumps

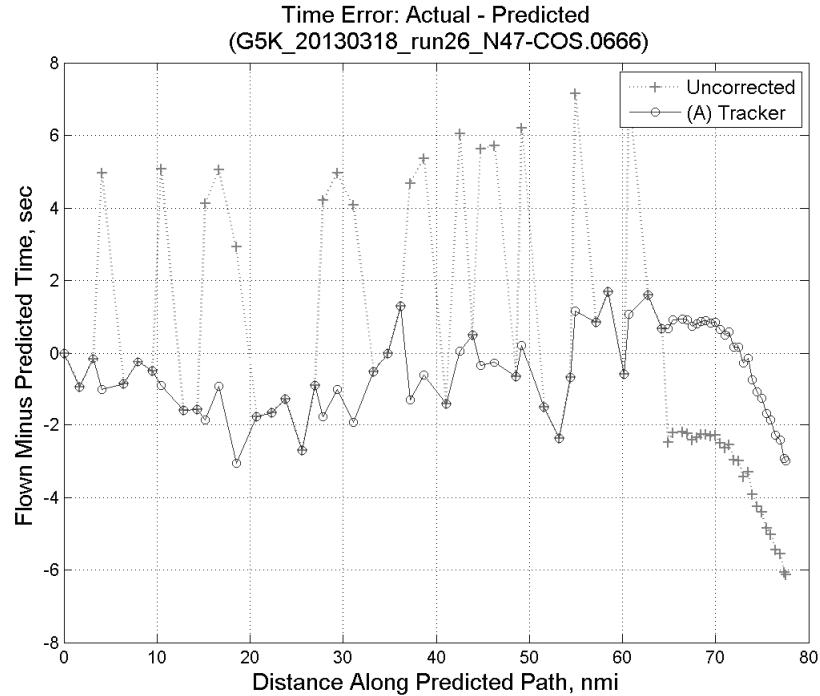


**Figure 441:** Time error for run 26 before (Uncorrected) and after ((A) Tracker) removing tracker jump error source.

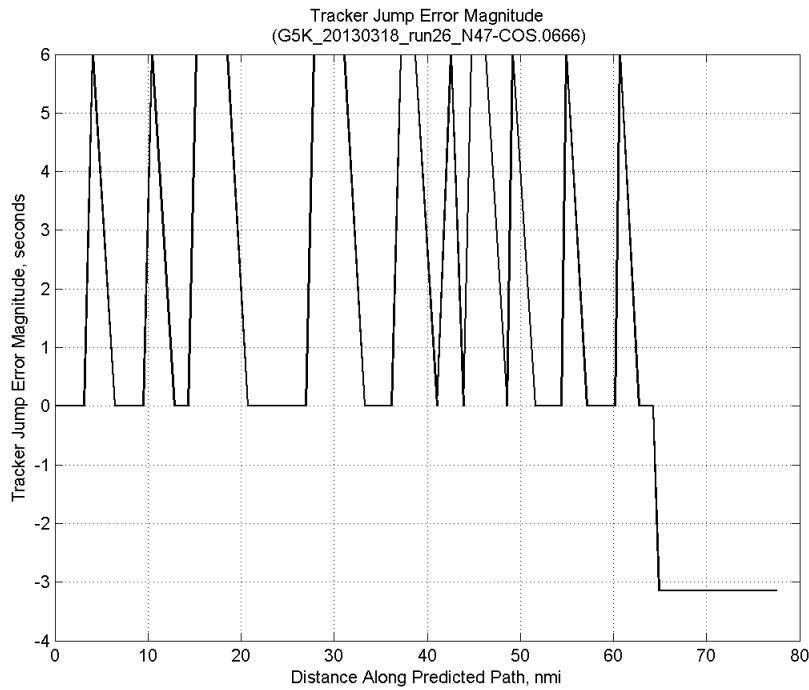


**Figure 442: Effect of tracker jump error source on time error for run 26.**

### C.17.B. Wind

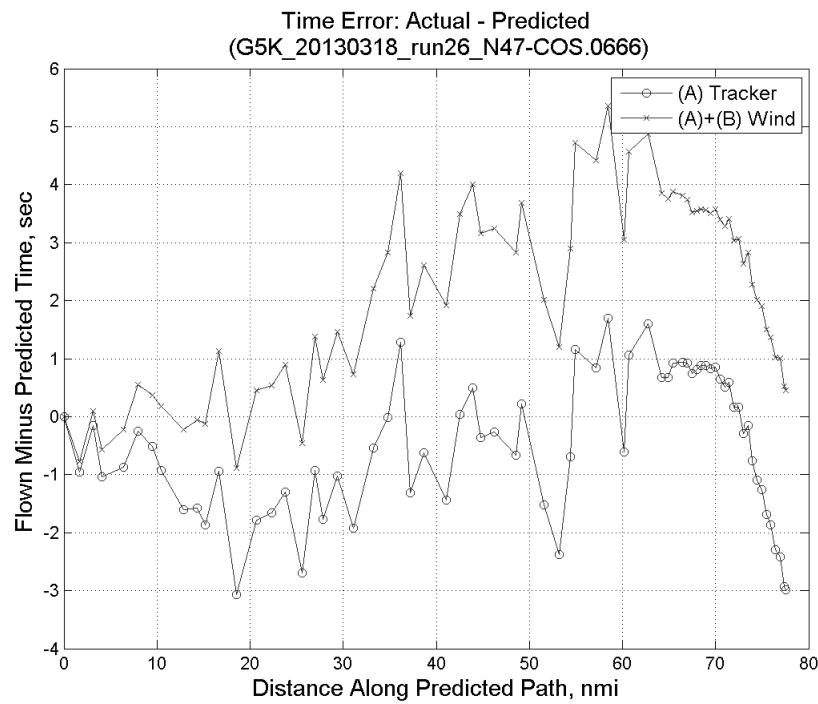


**Figure 443: Time error for run 26 before ((A) Tracker) and after ((A)+(B) Wind) removing wind error source.**

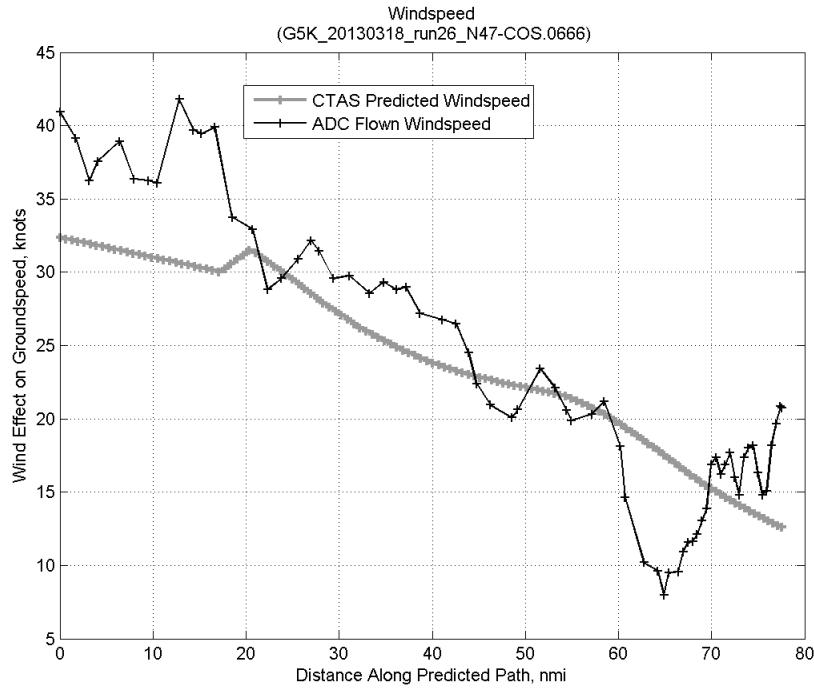


**Figure 444: CTAS predicted and ADC flown wind effect on ground speed for run 26. Negative values indicate a headwind.**

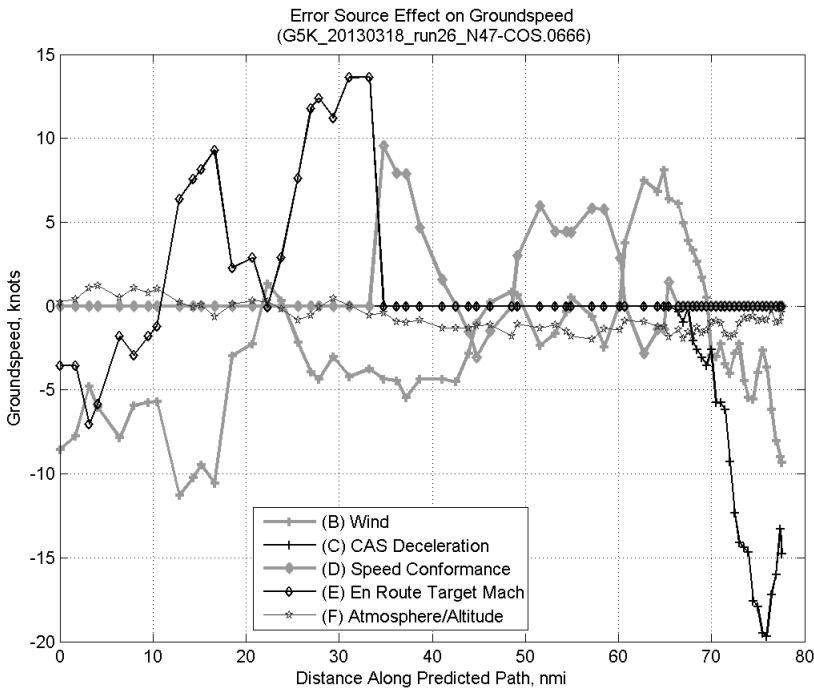


**Figure 445: Error sources (flown minus predicted) converted to a ground speed effect for run 26. Positive values indicate the flown ground speed was faster than the CTAS prediction.**

### C.17.C. CAS Deceleration

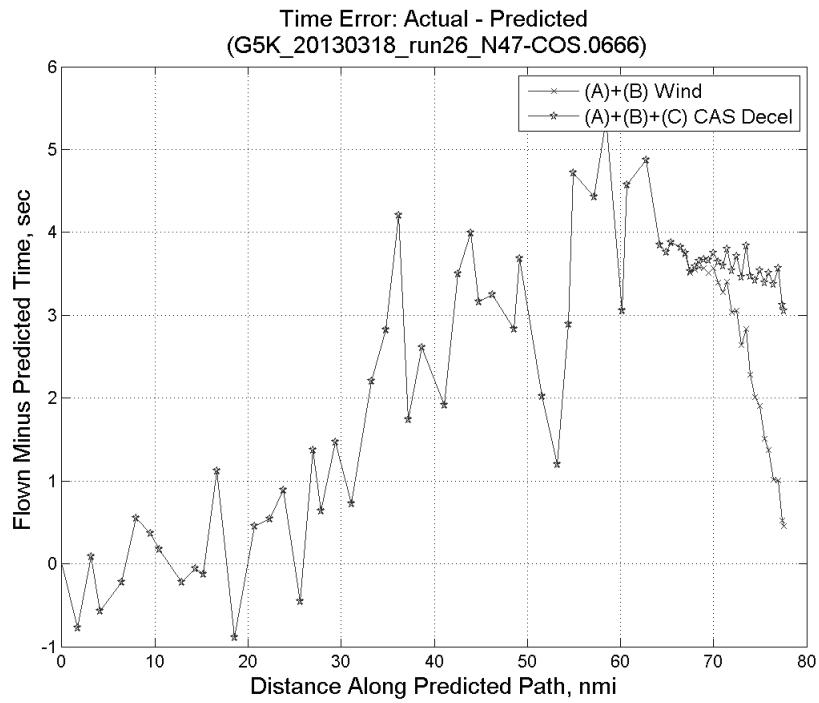


**Figure 446:** Time error for run 26 before ((A)+(B) Wind) and after ((A)+(B)+(C) CAS Decel) removing CAS deceleration error source.

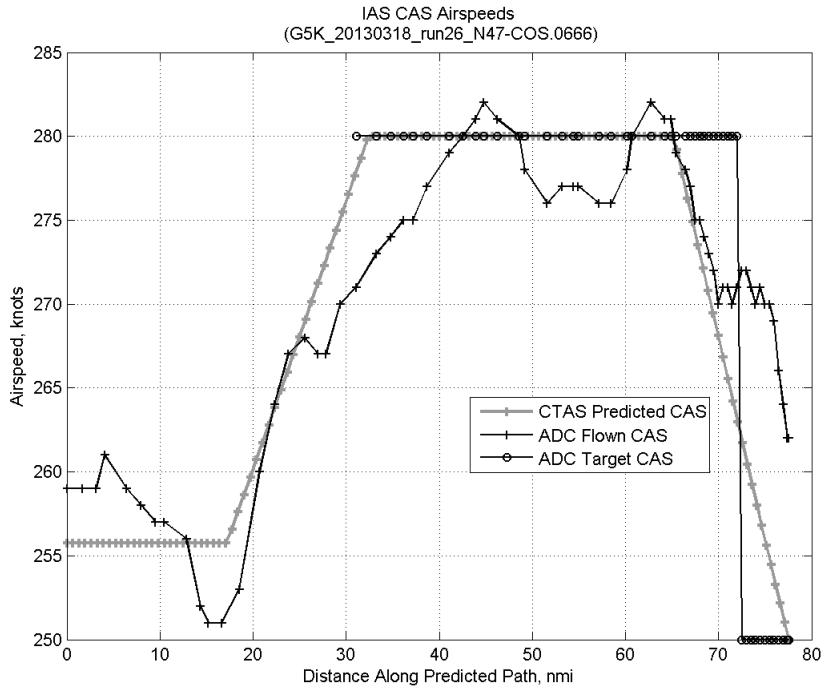


**Figure 447:** CTAS predicted and ADC flown CAS for run 26. CAS that is being targeted is shown with circle markers.

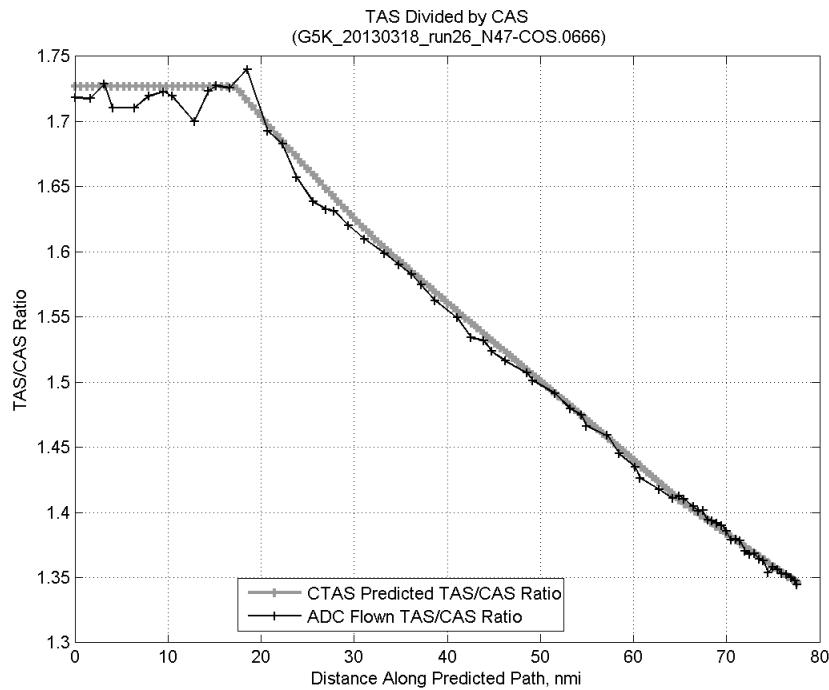


**Figure 448: CTAS predicted and ADC flown TAS/CAS ratio for run 26.**

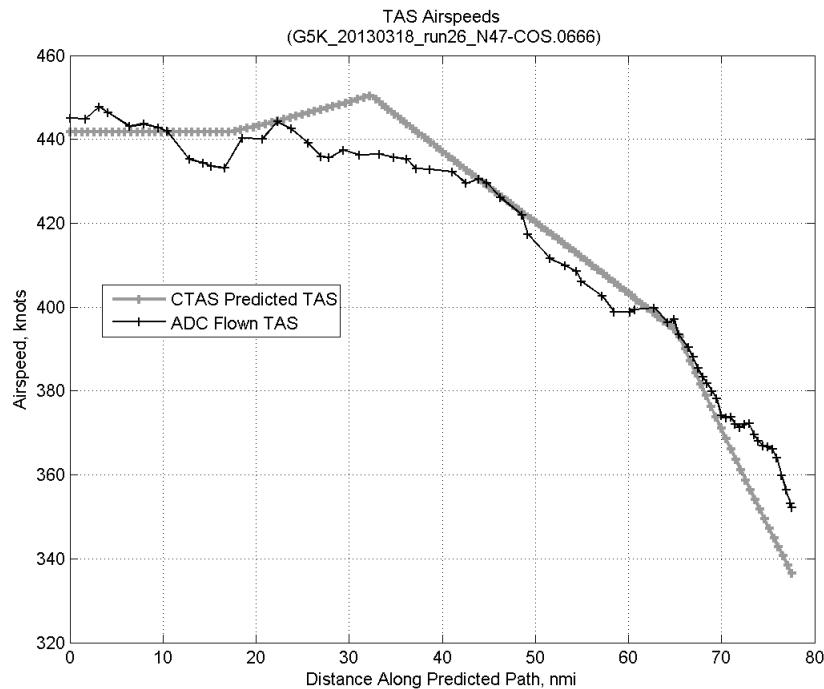


**Figure 449: CTAS predicted and ADC flown TAS for run 26.**

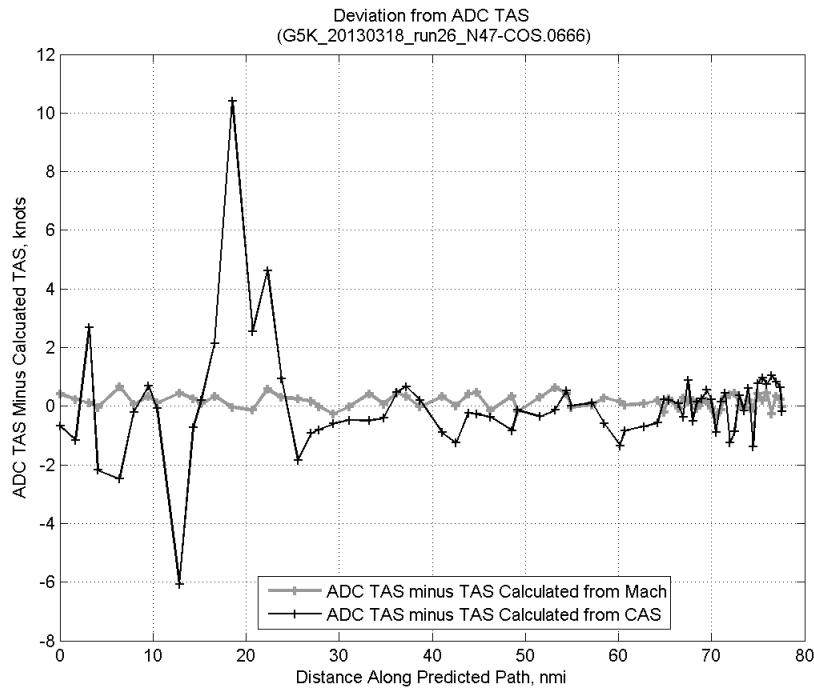


**Figure 450:** Deviation from ADC flown TAS if calculating TAS using ADC flown CAS, Mach, atmospheric temperature, and atmospheric pressure for run 26.

#### C.17.D. Speed Conformance

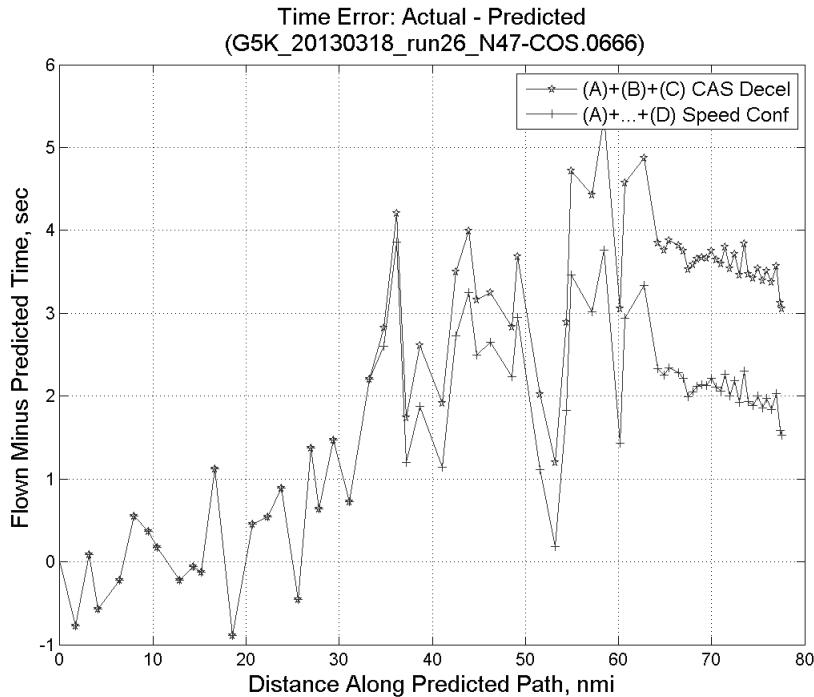


**Figure 451:** Time error for run 26 before ((A)+(B)+(C) CAS Decel) and after ((A)+...+(D) Speed Conf) removing speed conformance error source.

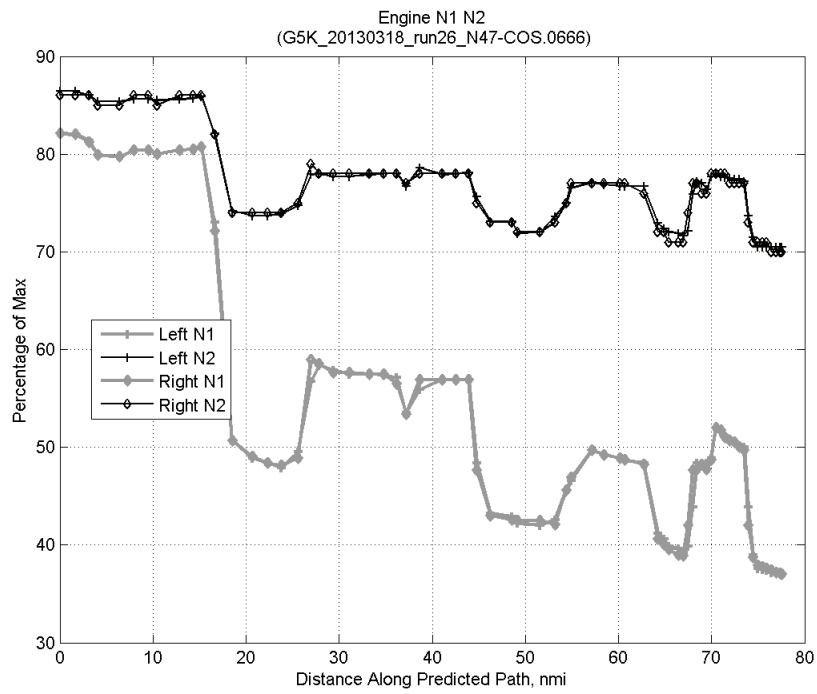


**Figure 452: Flown engine N1 and N2 for run 26.**

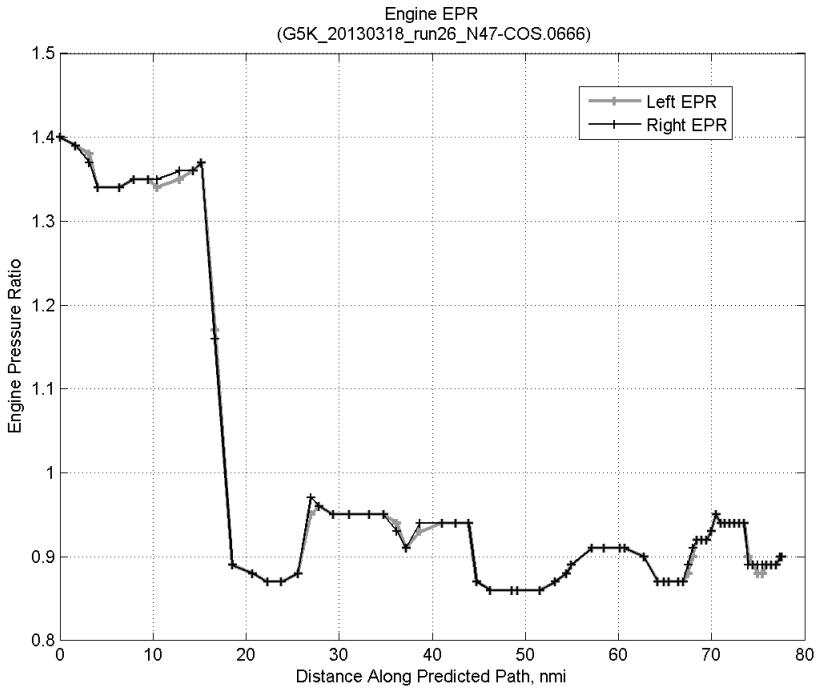


**Figure 453: Flown engine EPR for run 26.**

### C.17.E. Target Mach

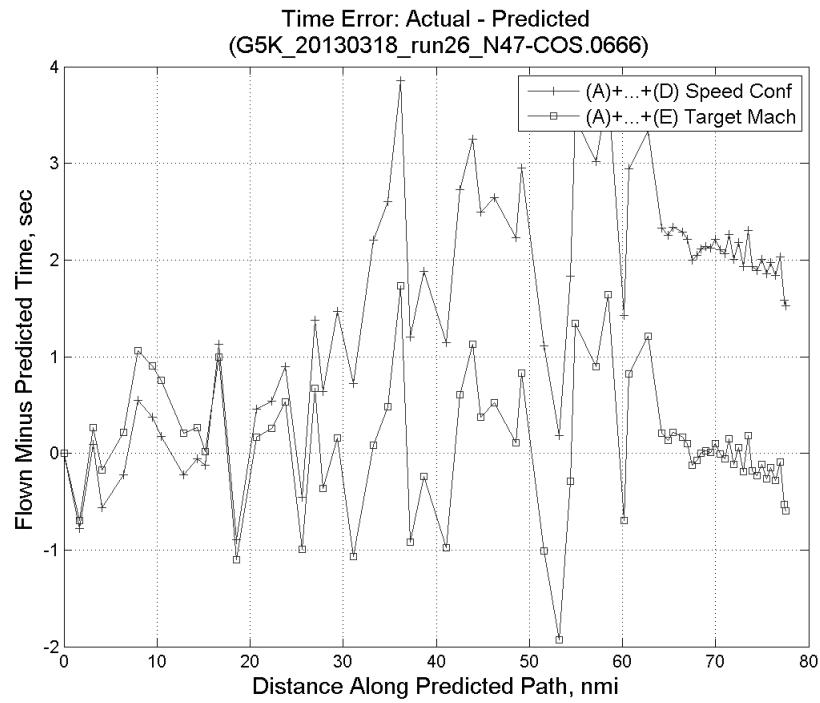


**Figure 454:** Time error for run 26 before ((A)+...+(D) Speed Conf) and after ((A)+...+(E) Target Mach) removing target Mach error source.

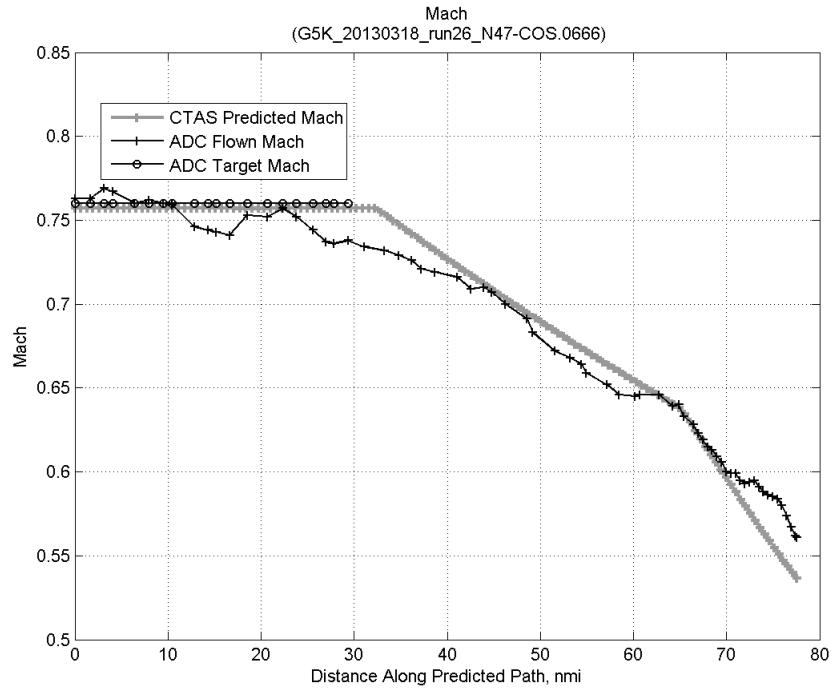


**Figure 455:** CTAS predicted and ADC flown Mach for run 26. Mach being targeted (ADC) shown with circle markers.

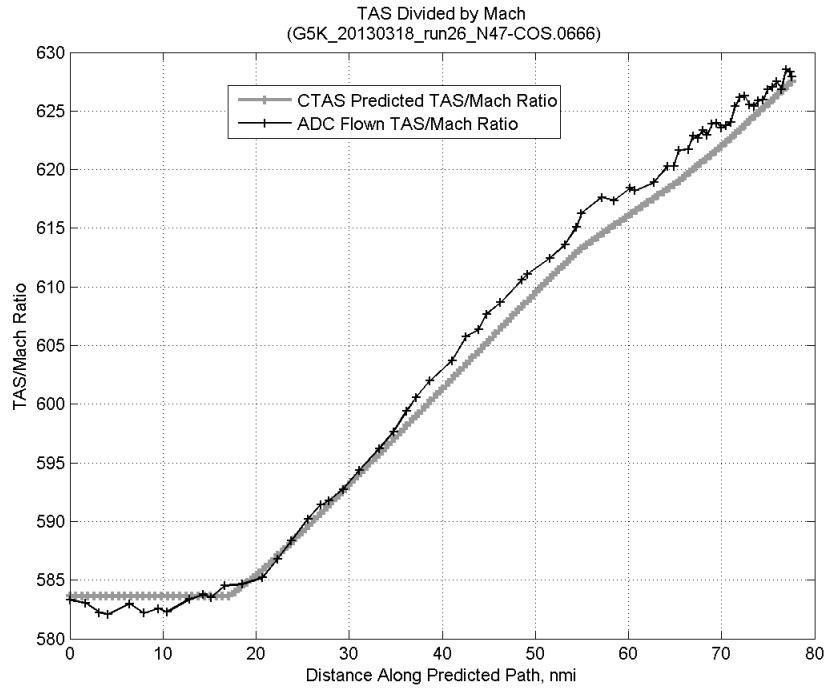


**Figure 456: CTAS predicted and ADC flown TAS/Mach ratio for run 26.**

#### C.17.F. Atmosphere/Altitude

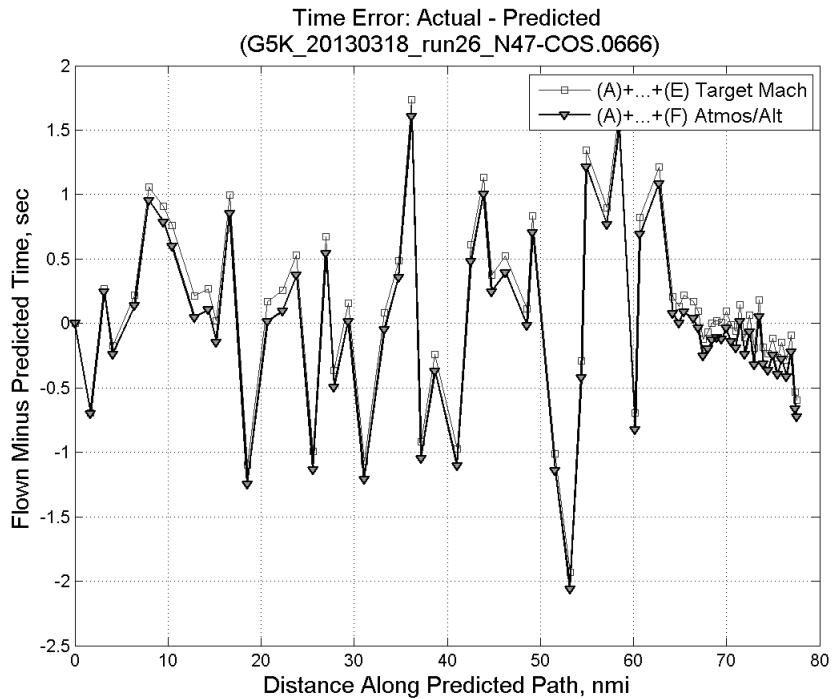


**Figure 457: Time error for run 26 before ((A)+...+(E) Target Mach) and after ((A)+...+(F) Atmos/Alt) removing atmosphere/altitude error source.**

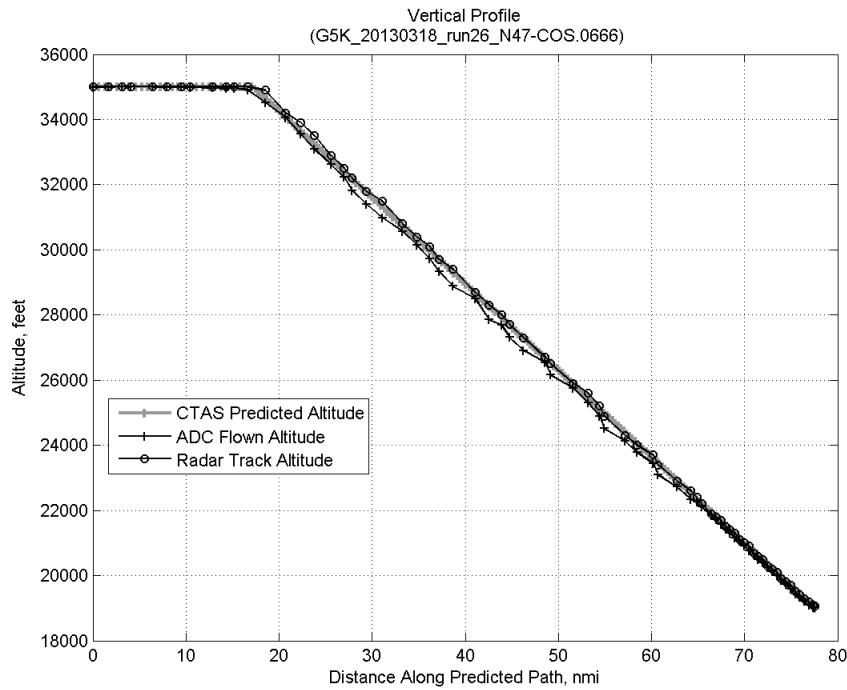


**Figure 458: Flown (ADC) and predicted (CTAS) vertical profile for run 26.**

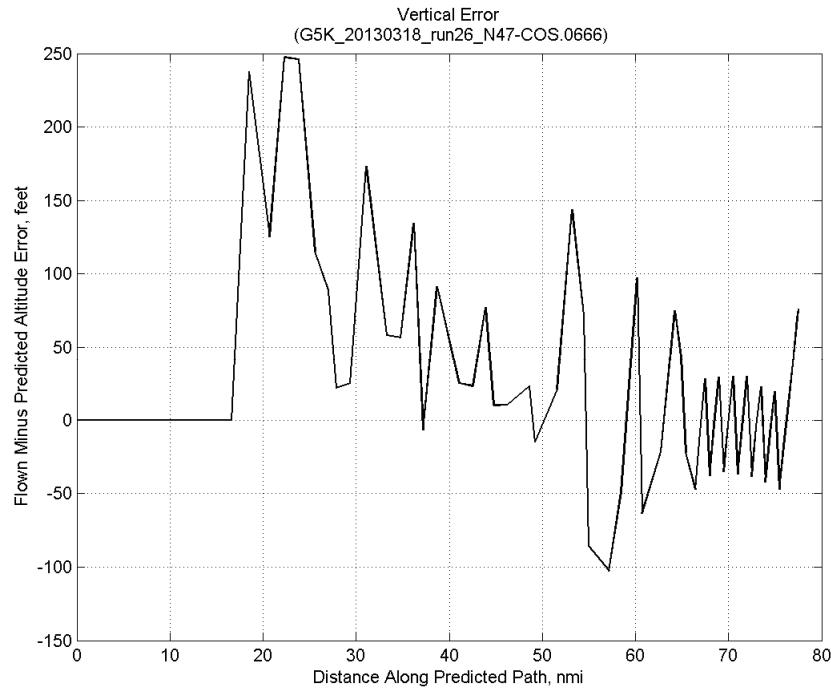


**Figure 459: Vertical error (flown minus predicted altitude) for run 26. Positive values indicate aircraft flew higher than predicted by CTAS.**

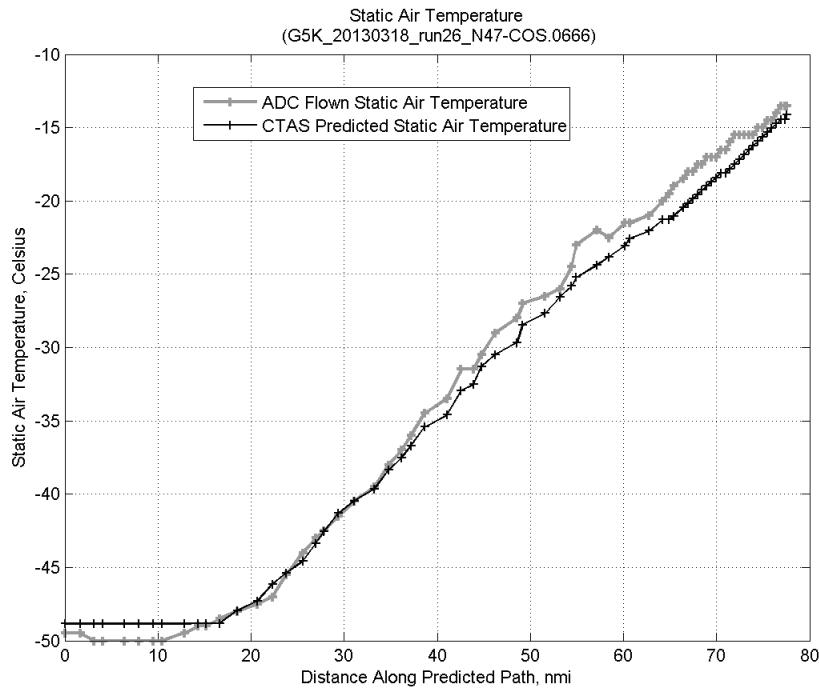


**Figure 460:** Flown (ADC) and predicted (CTAS) static air temperature for run 26.

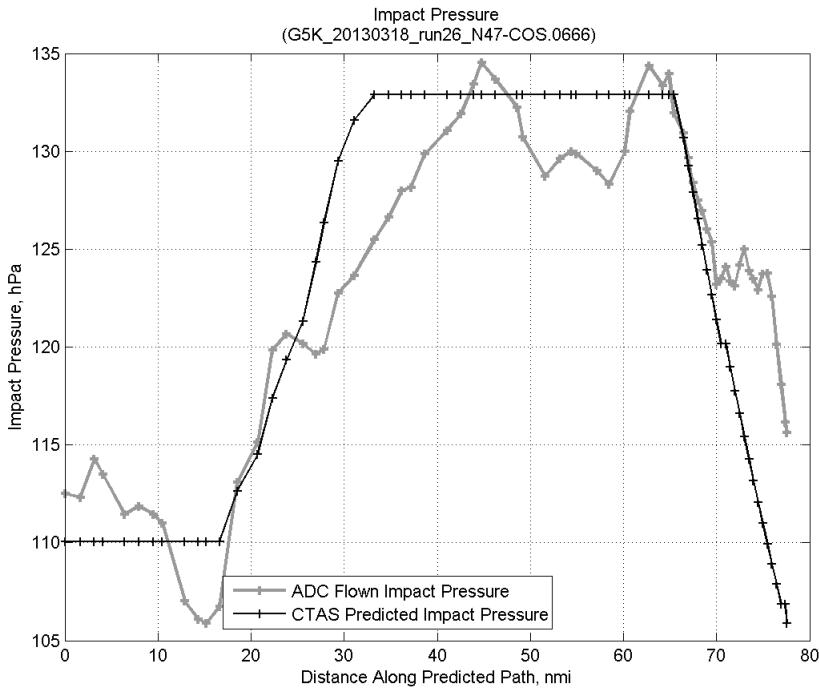


**Figure 461:** Flown (ADC) and predicted (CTAS) impact pressure for run 26.

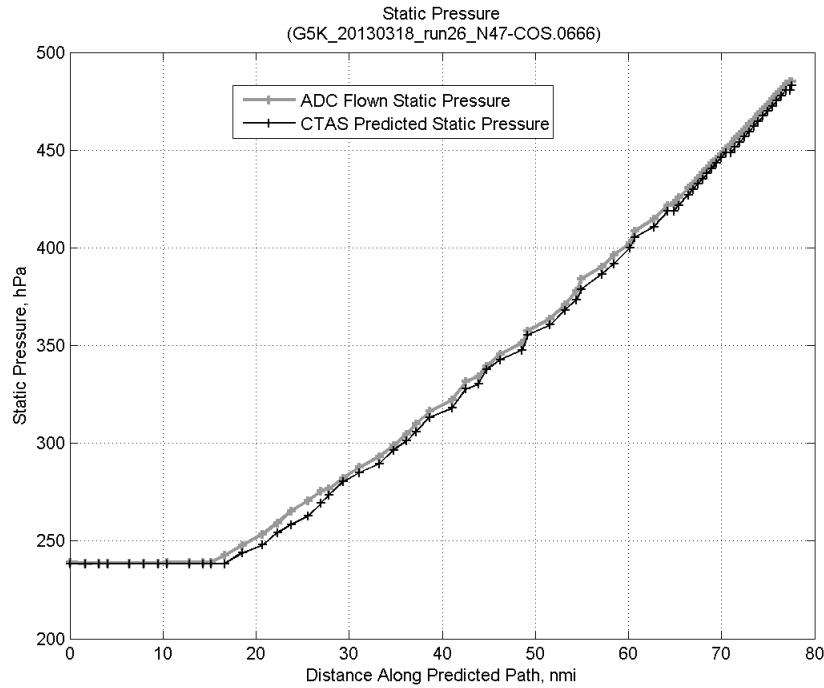


**Figure 462: Flown (ADC) and predicted (CTAS) static pressure for run 26.**

#### C.17.G. Path Distance

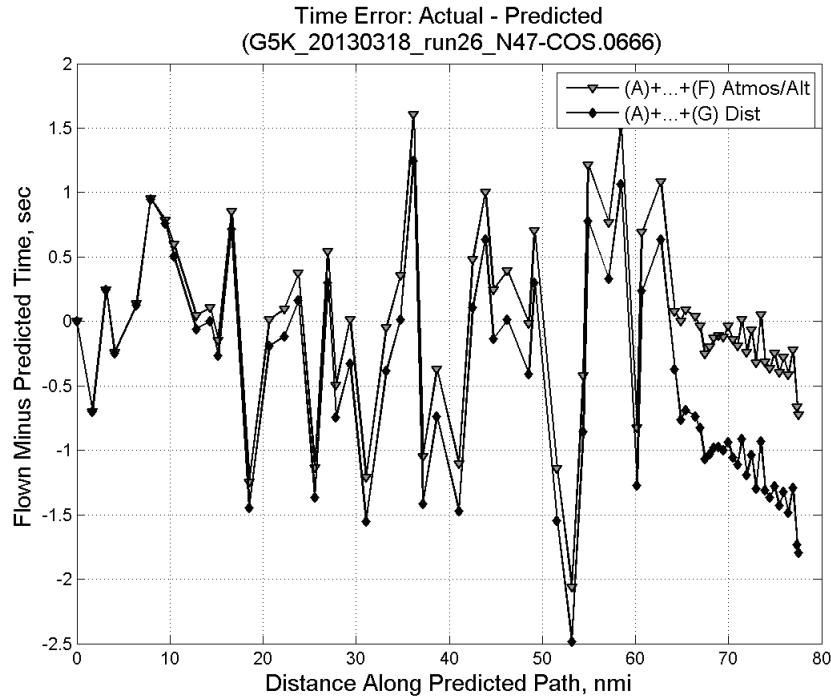


**Figure 463: Time error for run 26 before ((A)+...+(F) Atmos/Alt) and after ((A)+...+(G) Dist) removing path distance error source.**

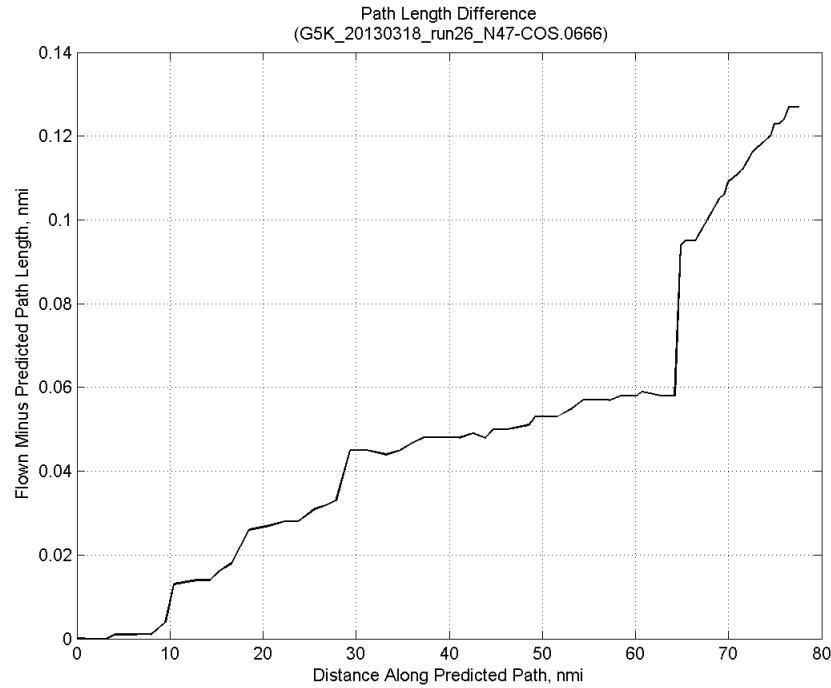


**Figure 464: ADC flown minus CTAS predicted path length for run 26. Positive values indicate aircraft followed a longer path than predicted by CTAS.**

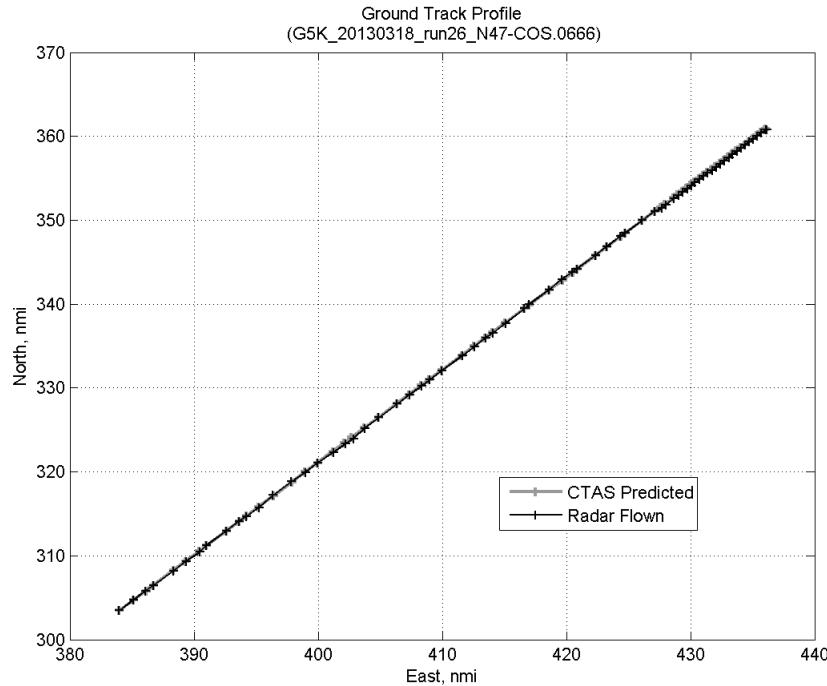


**Figure 465: CTAS predicted and radar flown ground track profile for run 26.**

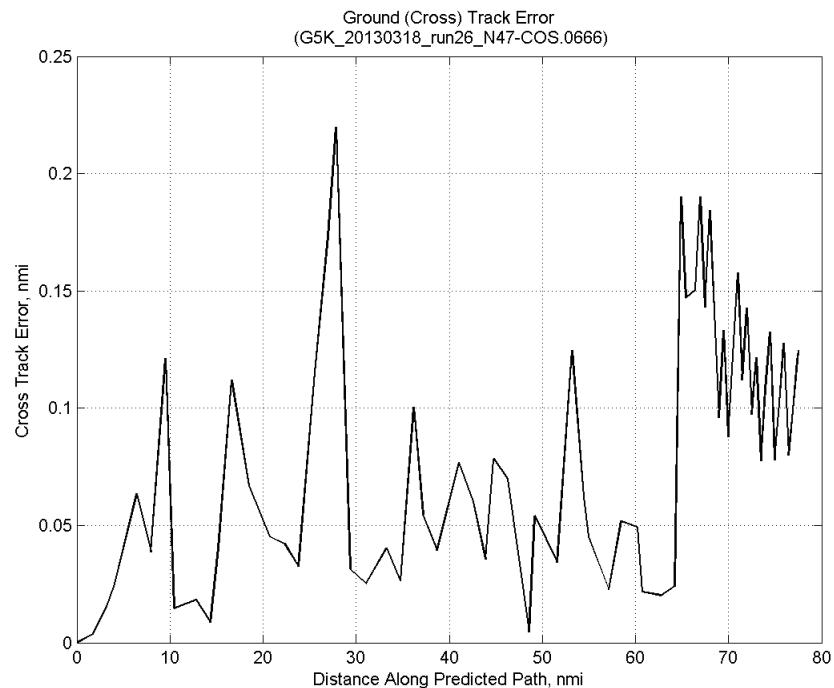


**Figure 466: Ground (cross) track error for run 26.**

### C.18. Run 28

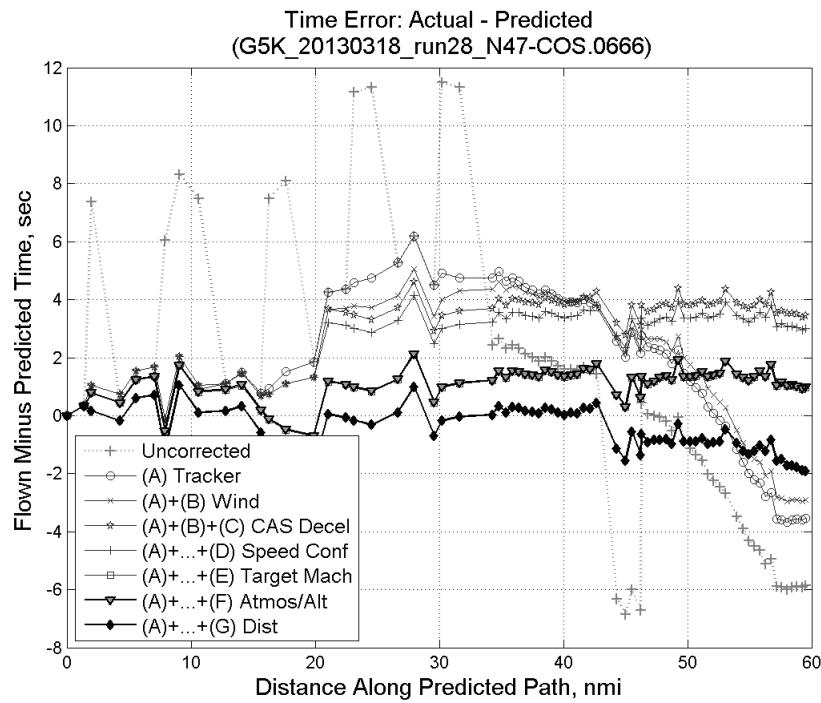


**Figure 467:** Time error for run 28 showing incremental effect of removing each error source.

#### C.18.A. Tracker Jumps

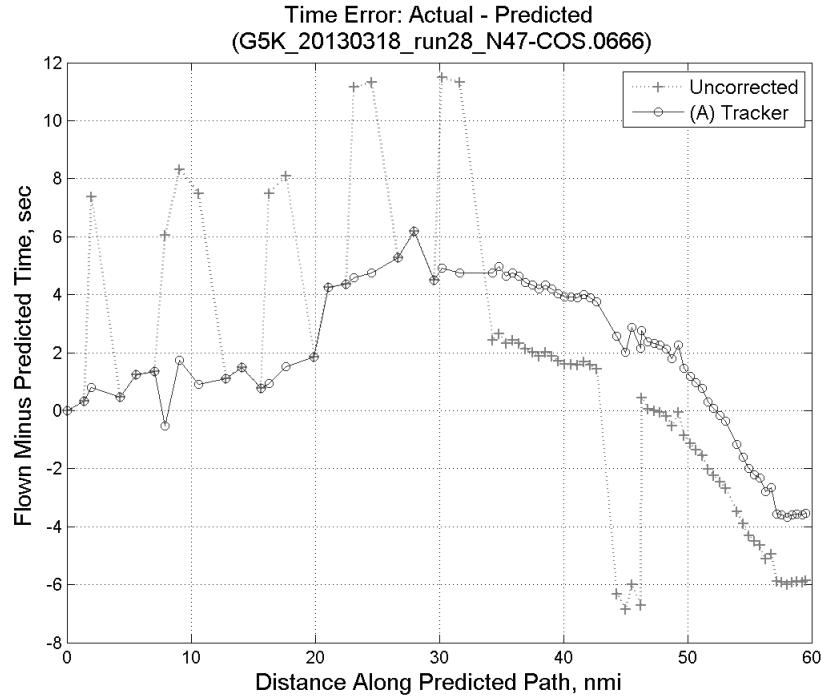


**Figure 468:** Time error for run 28 before (Uncorrected) and after ((A) Tracker) removing tracker jump error source.

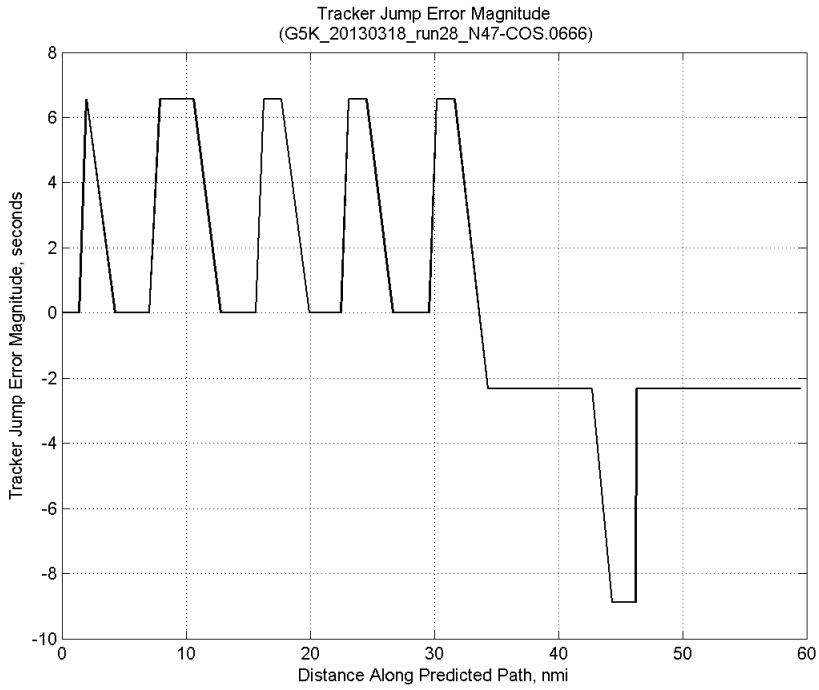


**Figure 469: Effect of tracker jump error source on time error for run 28.**

### C.18.B. Wind

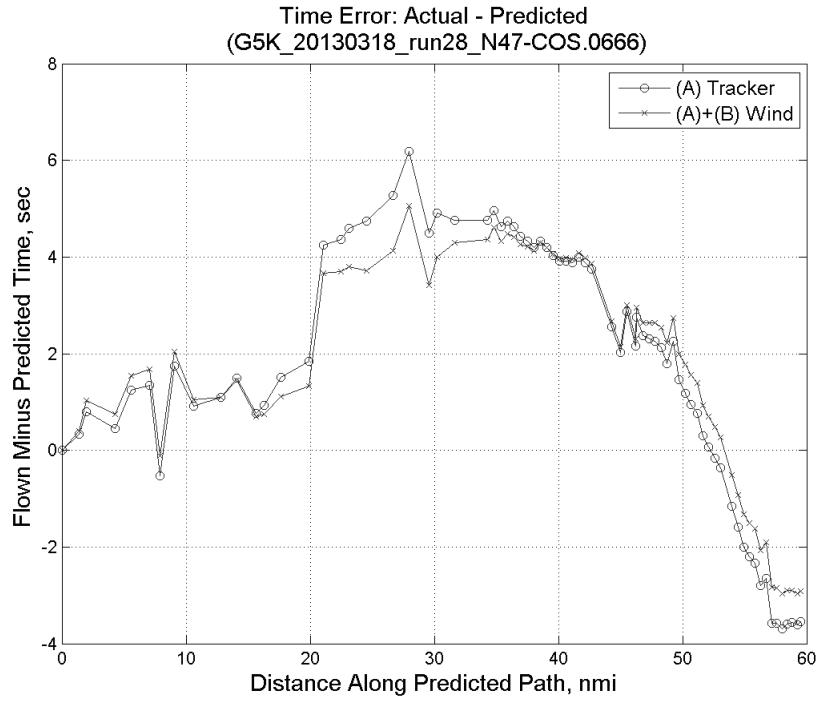


**Figure 470: Time error for run 28 before ((A) Tracker) and after ((A)+(B) Wind) removing wind error source.**

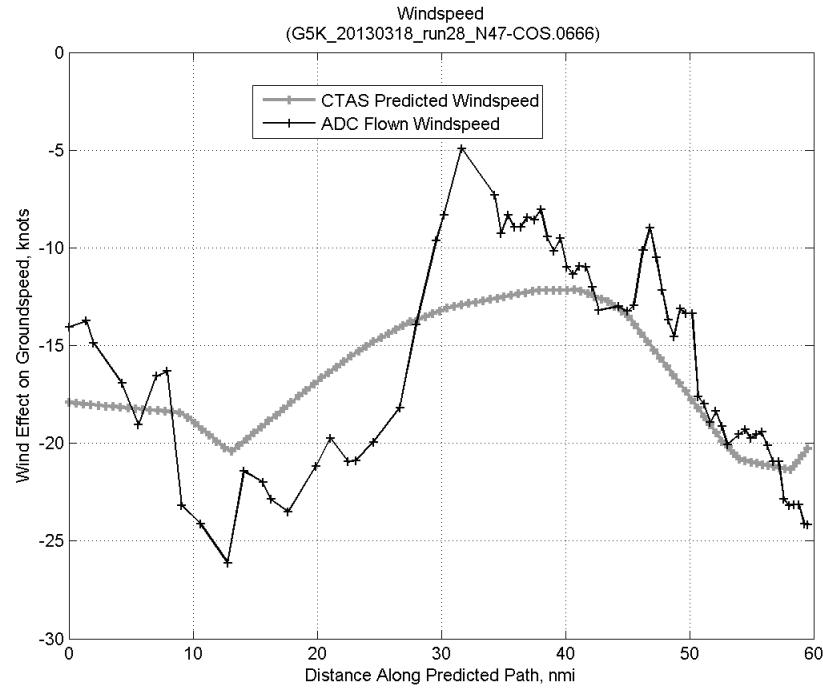


**Figure 471: CTAS predicted and ADC flown wind effect on ground speed for run 28. Negative values indicate a headwind.**

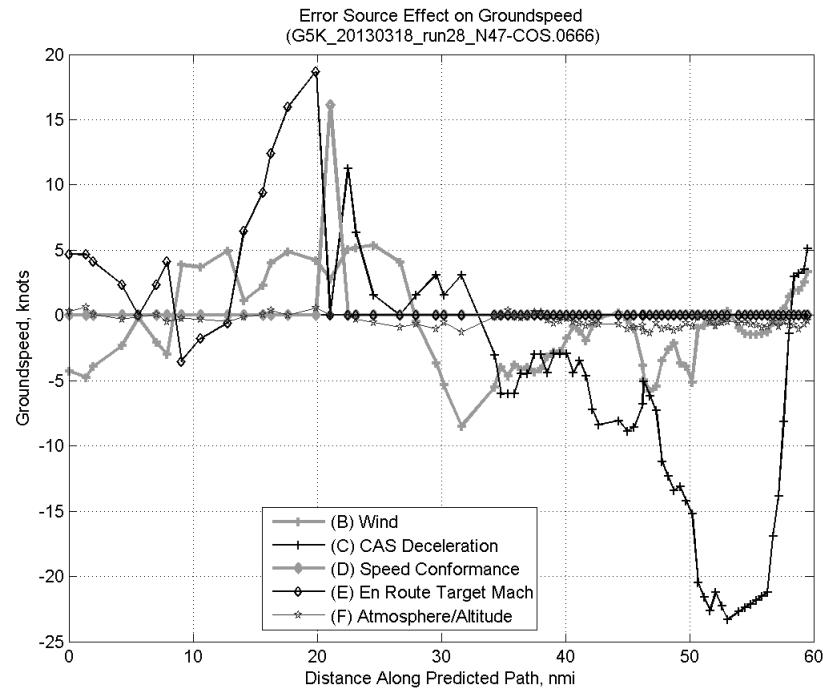


**Figure 472: Error sources (flown minus predicted) converted to a ground speed effect for run 28. Positive values indicate the flown ground speed was faster than the CTAS prediction.**

### C.18.C. CAS Deceleration

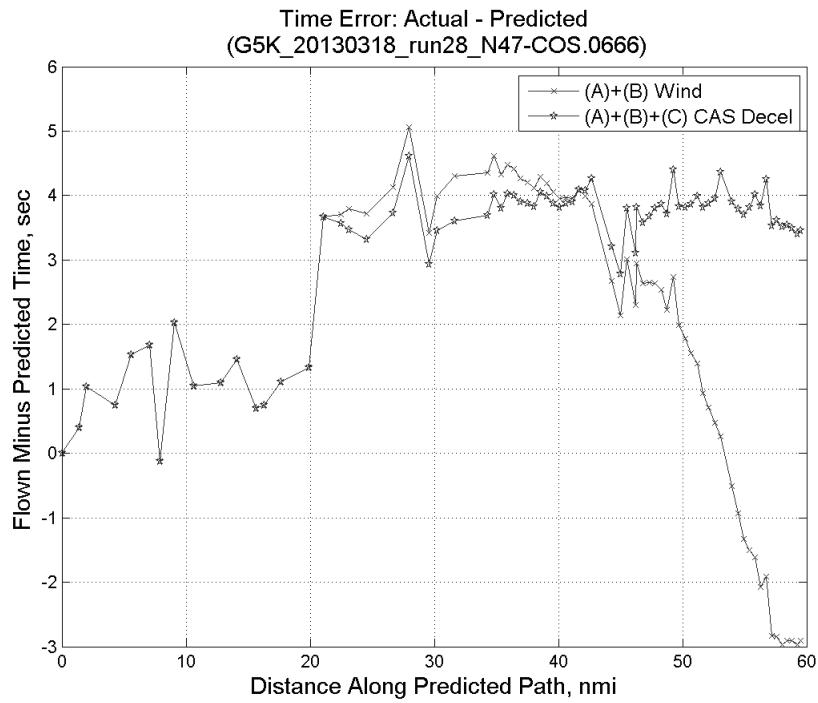


**Figure 473:** Time error for run 28 before ((A)+(B) Wind) and after ((A)+(B)+(C) CAS Decel) removing CAS deceleration error source.

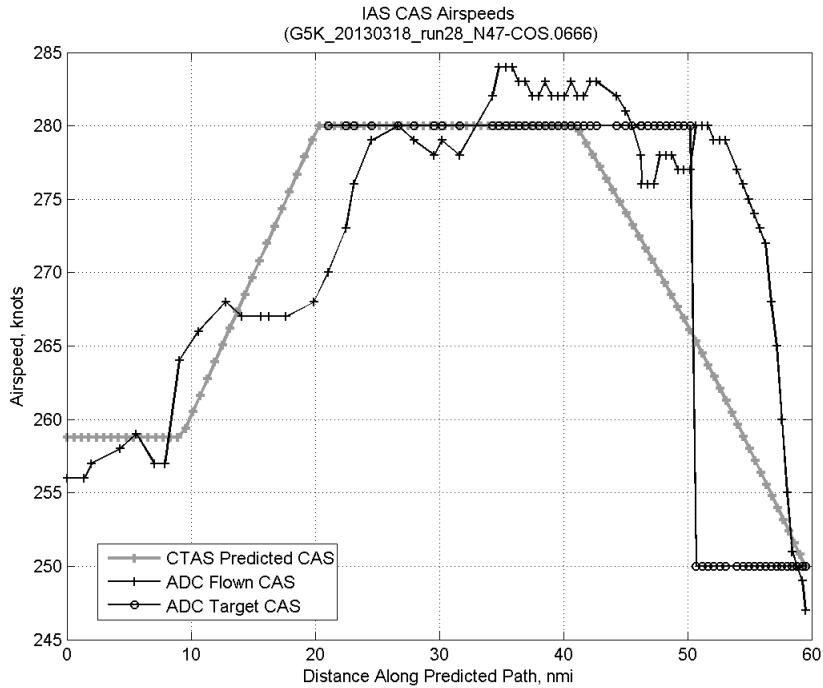


**Figure 474:** CTAS predicted and ADC flown CAS for run 28. CAS that is being targeted is shown with circle markers.

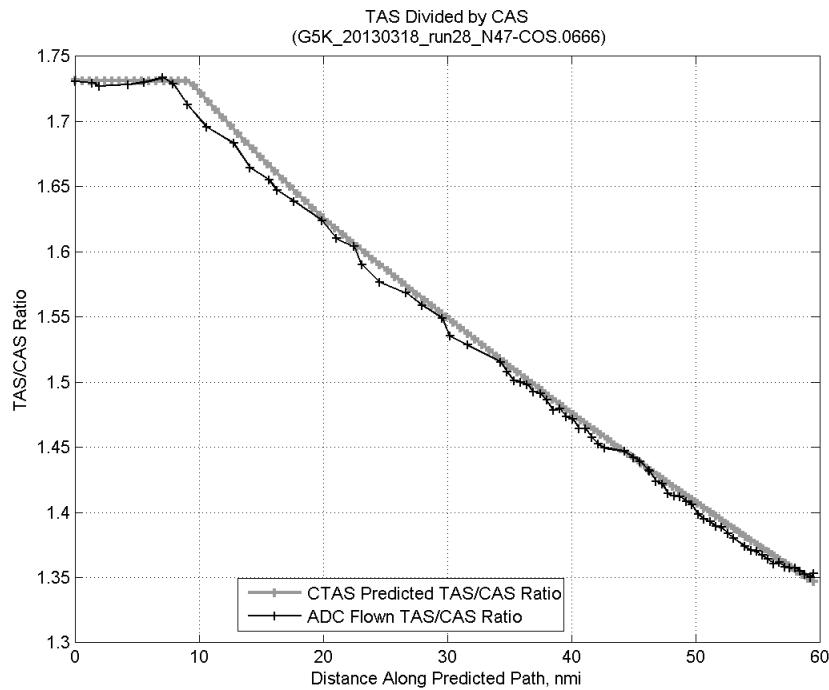


**Figure 475: CTAS predicted and ADC flown TAS/CAS ratio for run 28.**

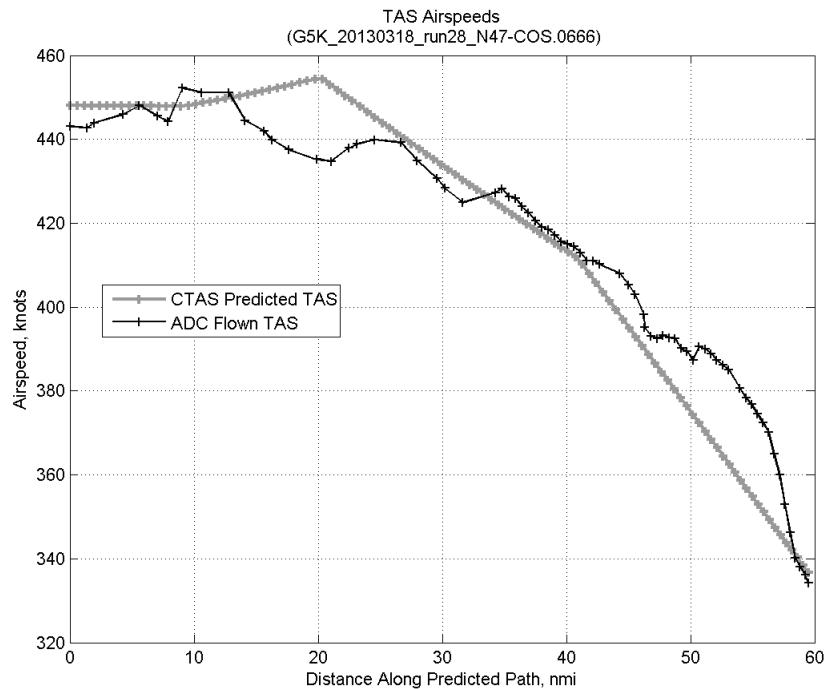


**Figure 476: CTAS predicted and ADC flown TAS for run 28.**

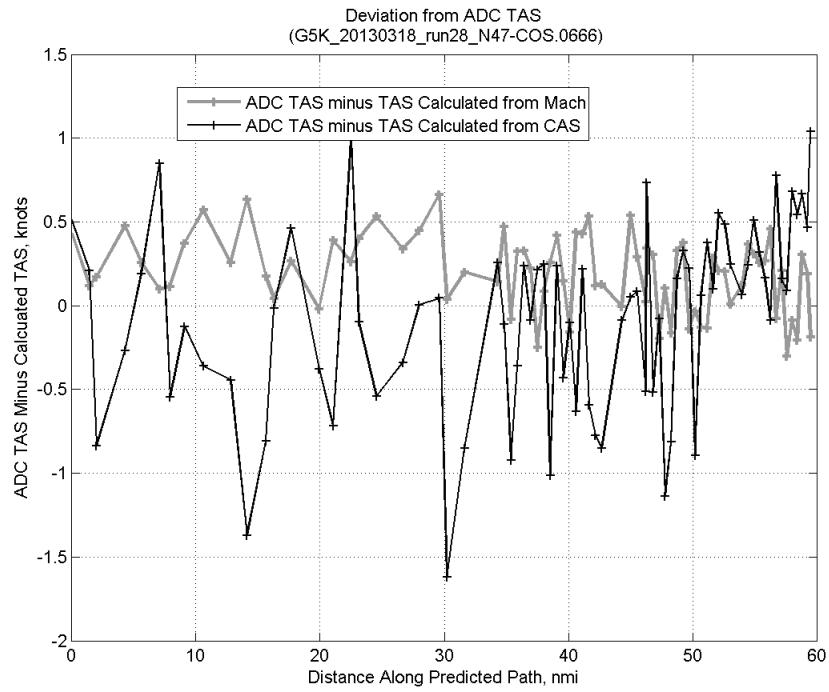


**Figure 477: Deviation from ADC flown TAS if calculating TAS using ADC flown CAS, Mach, atmospheric temperature, and atmospheric pressure for run 28.**

#### C.18.D. Speed Conformance

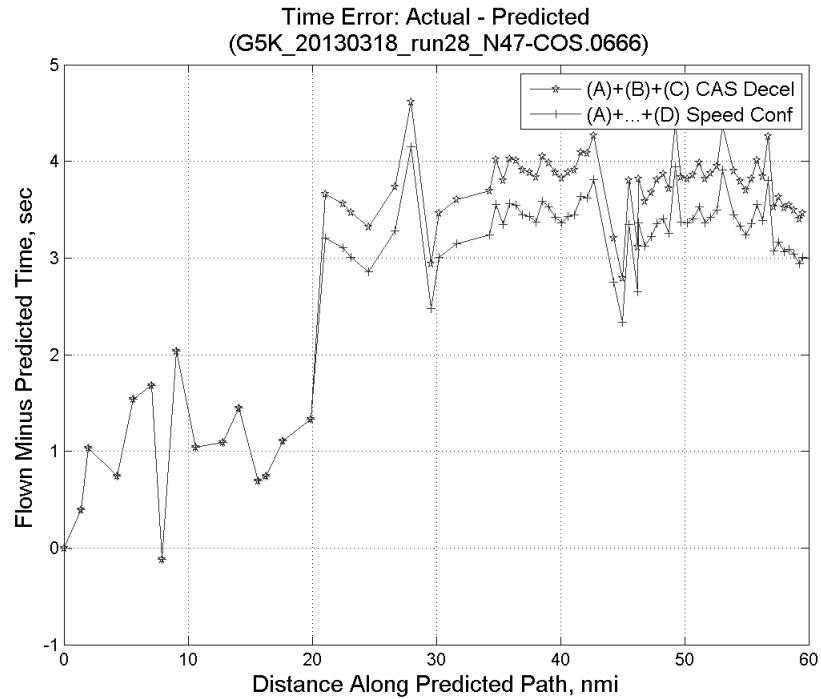


**Figure 478: Time error for run 28 before ((A)+(B)+(C) CAS Decel) and after ((A)+...+(D) Speed Conf) removing speed conformance error source.**

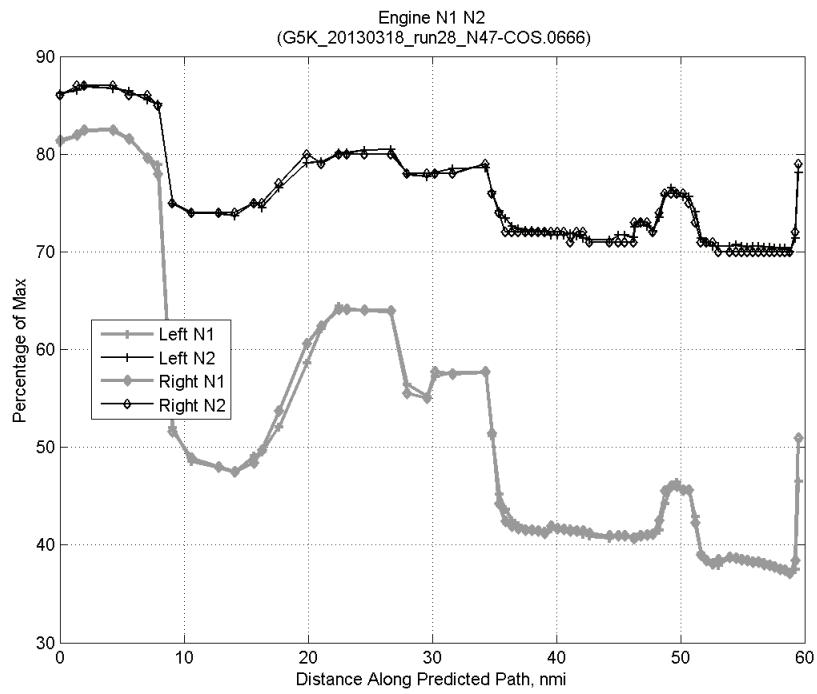


**Figure 479: Flown engine N1 and N2 for run 28.**

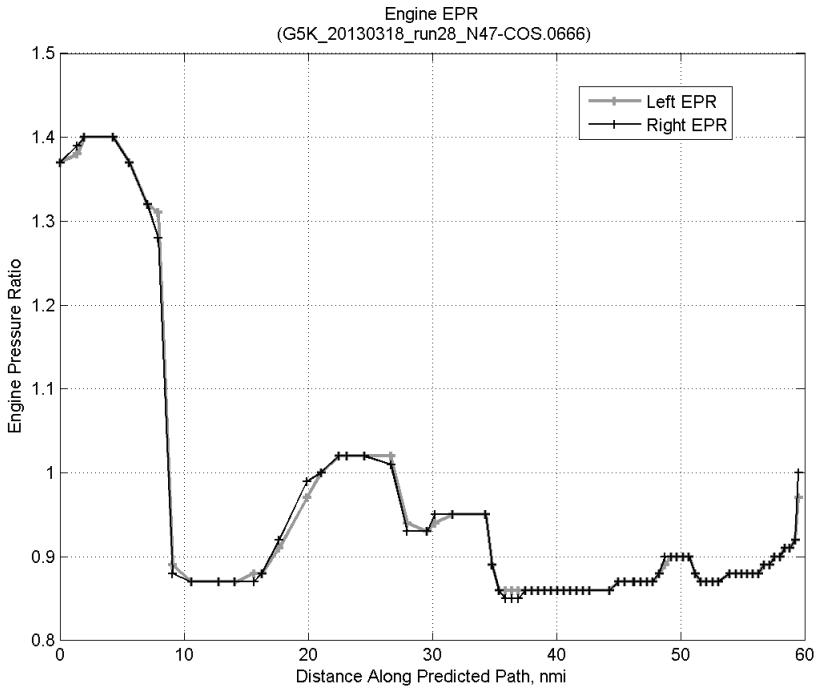


**Figure 480: Flown engine EPR for run 28.**

### C.18.E. Target Mach

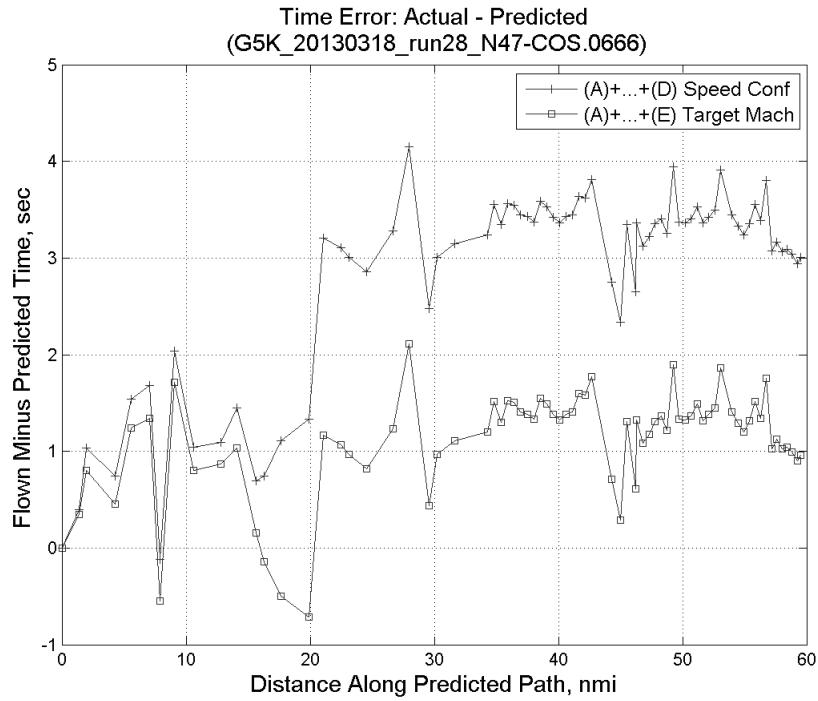


**Figure 481:** Time error for run 28 before ((A)+...+(D) Speed Conf) and after ((A)+...+(E) Target Mach) removing target Mach error source.

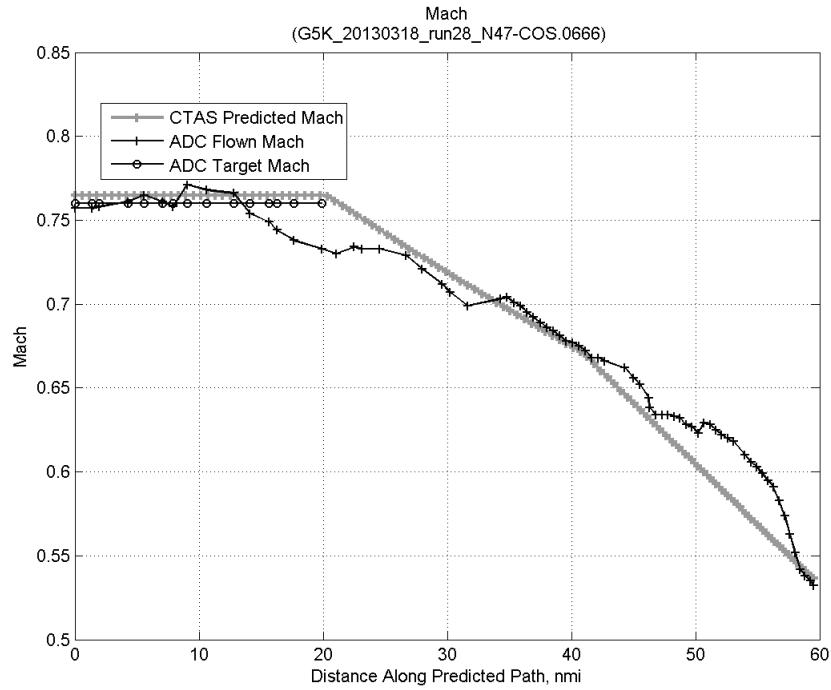


**Figure 482:** CTAS predicted and ADC flown Mach for run 28. Mach being targeted (ADC) shown with circle markers.

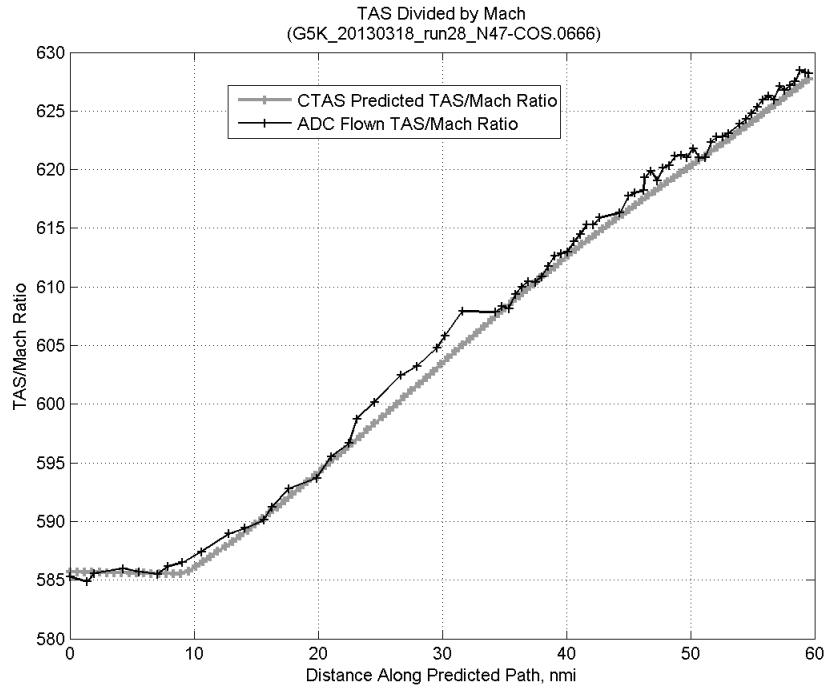


**Figure 483: CTAS predicted and ADC flown TAS/Mach ratio for run 28.**

#### C.18.F. Atmosphere/Altitude

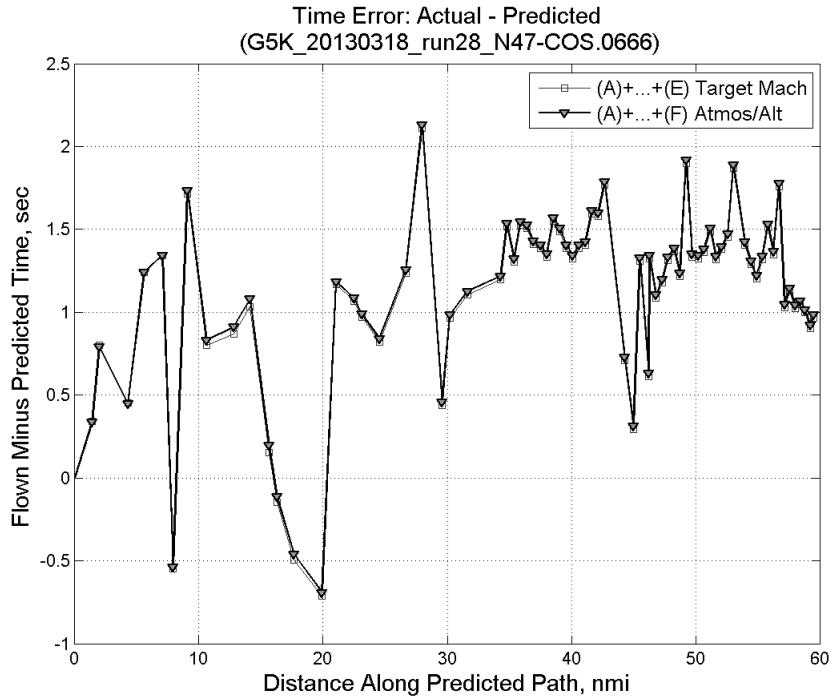


**Figure 484: Time error for run 28 before ((A)+...+(E) Target Mach) and after ((A)+...+(F) Atmos/Alt) removing atmosphere/altitude error source.**

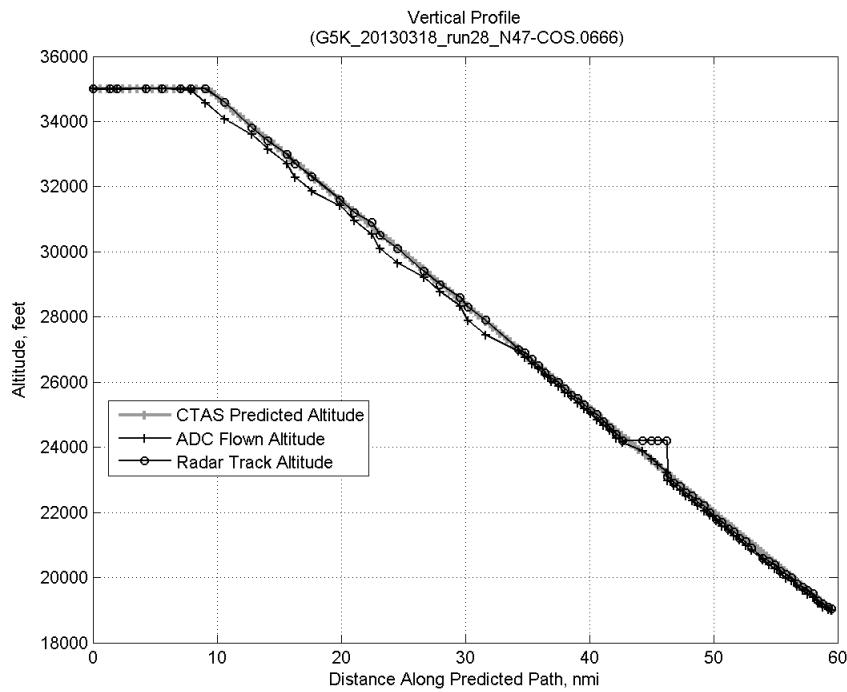


**Figure 485: Flown (ADC) and predicted (CTAS) vertical profile for run 28.**

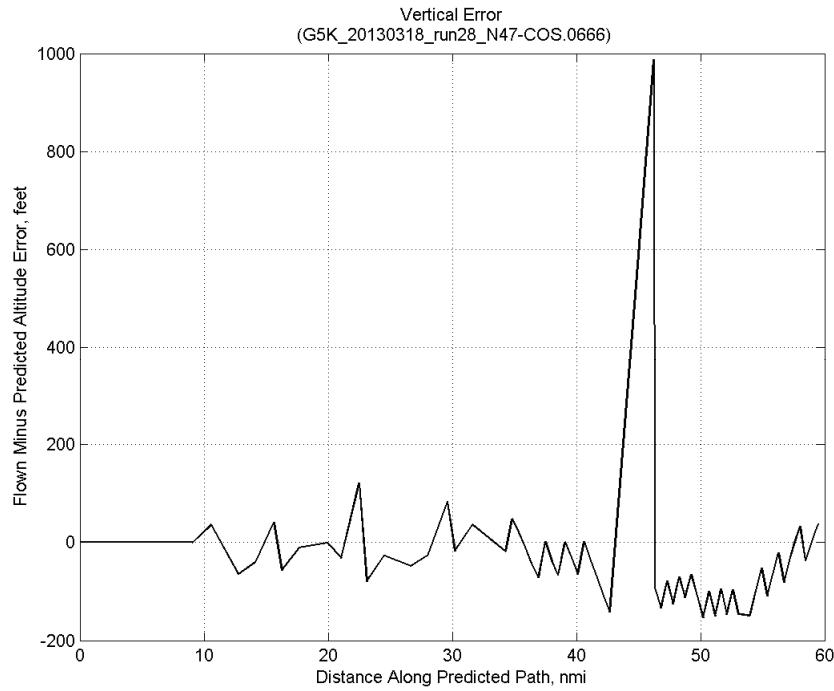


**Figure 486: Vertical error (flown minus predicted altitude) for run 28. Positive values indicate aircraft flew higher than predicted by CTAS.**

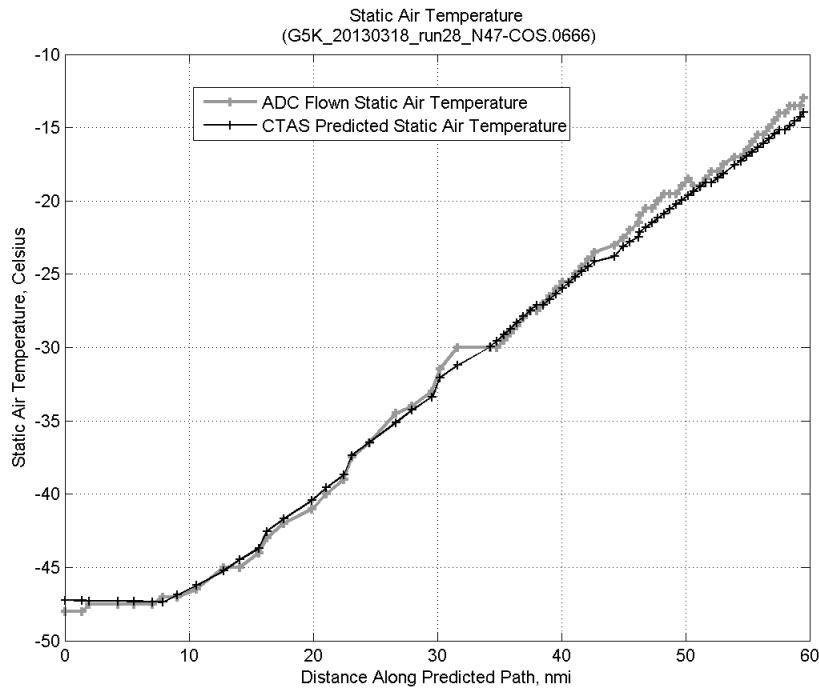


**Figure 487:** Flown (ADC) and predicted (CTAS) static air temperature for run 28.

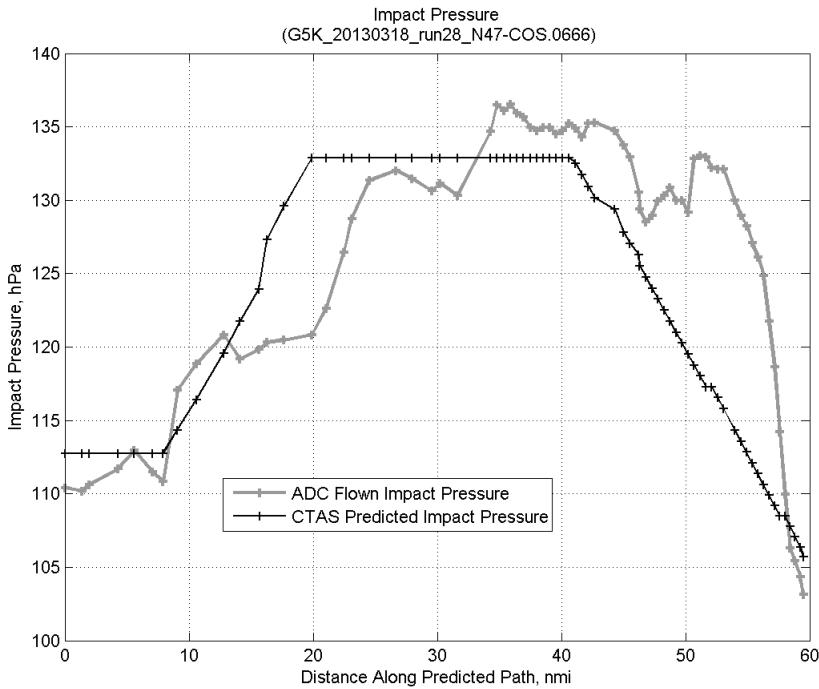


**Figure 488:** Flown (ADC) and predicted (CTAS) impact pressure for run 28.

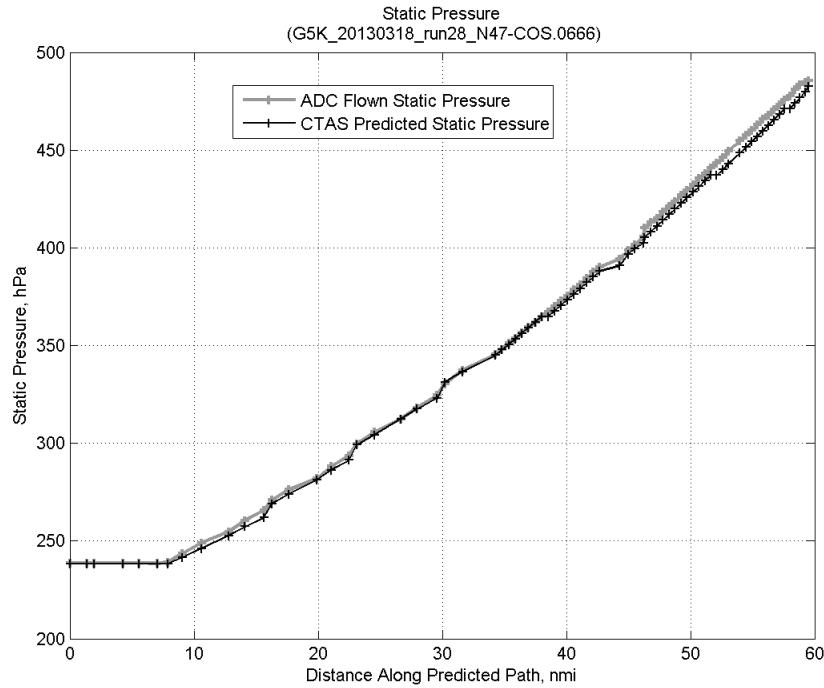


**Figure 489: Flown (ADC) and predicted (CTAS) static pressure for run 28.**

#### C.18.G. Path Distance

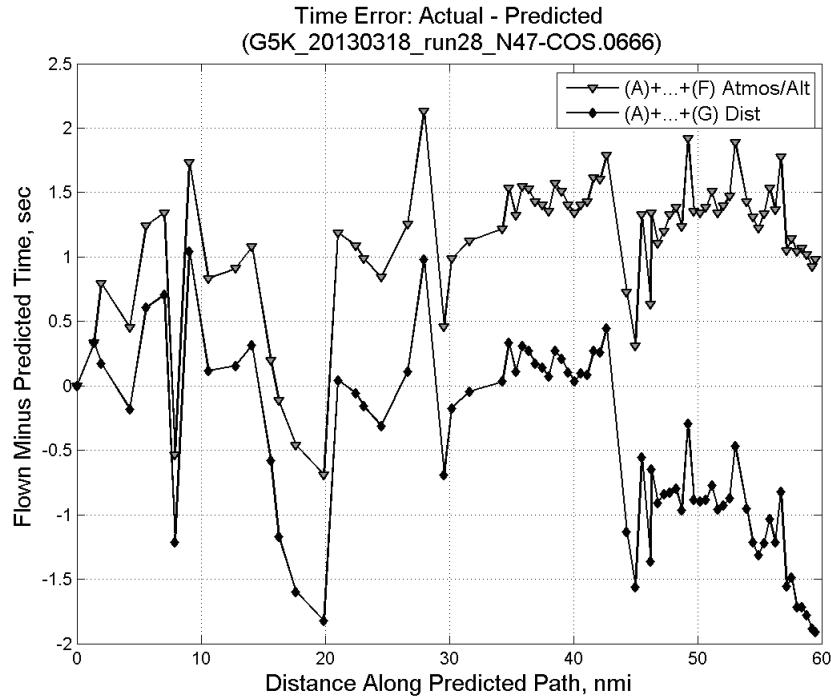


**Figure 490: Time error for run 28 before ((A)+...+(F) Atmos/Alt) and after ((A)+...+(G) Dist) removing path distance error source.**

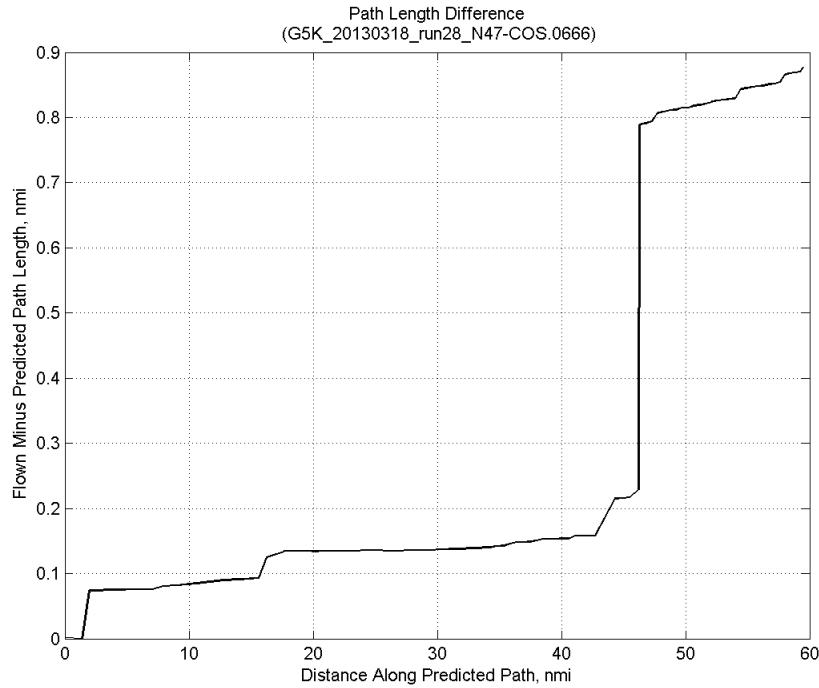


**Figure 491: ADC flown minus CTAS predicted path length for run 28. Positive values indicate aircraft followed a longer path than predicted by CTAS.**

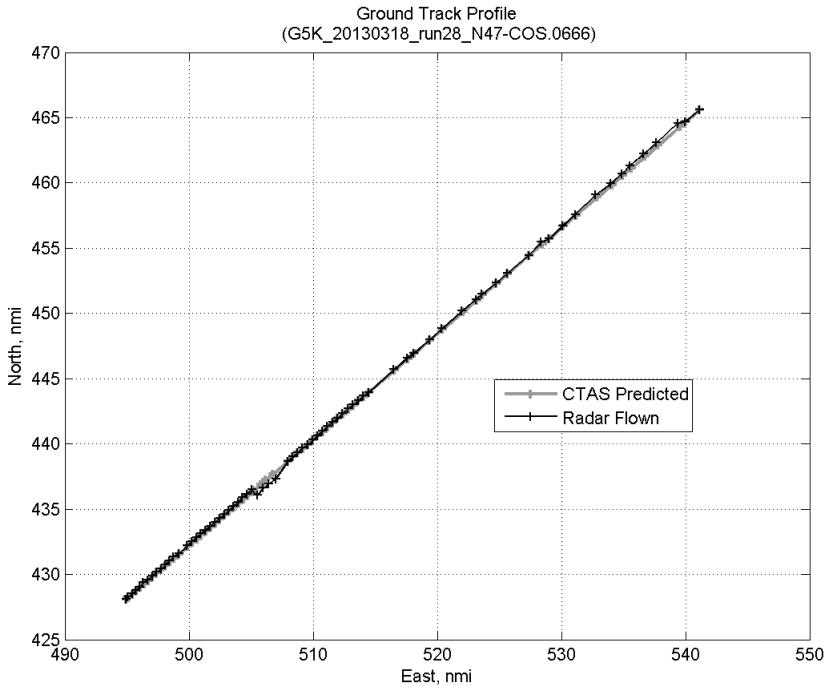


**Figure 492: CTAS predicted and radar flown ground track profile for run 28.**

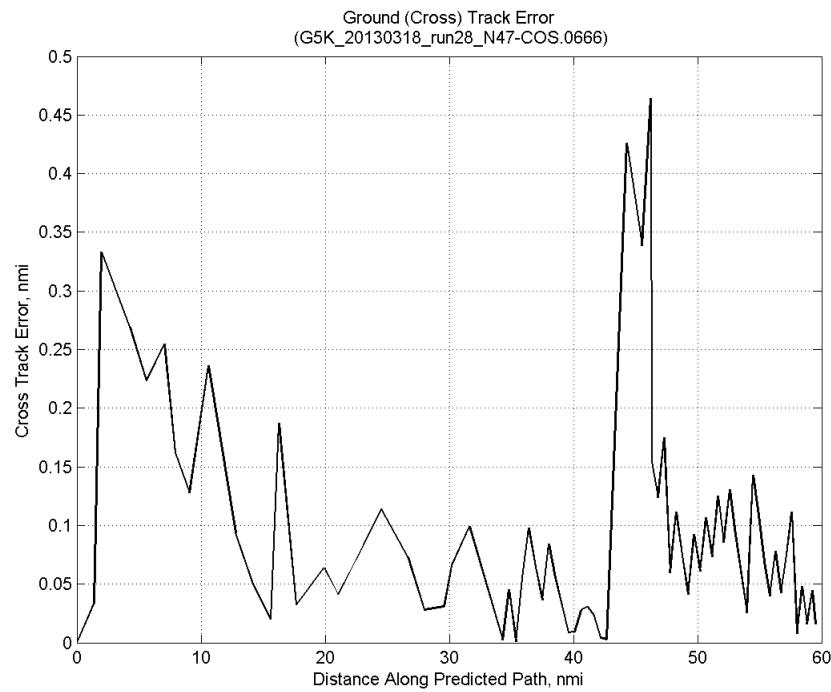


**Figure 493: Ground (cross) track error for run 28.**

### C.19. Run 29

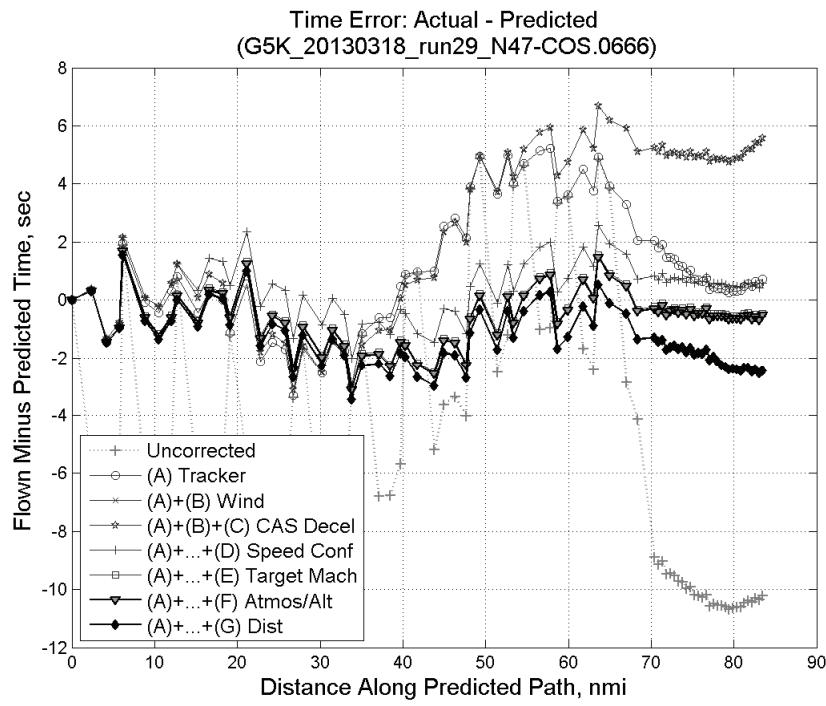


**Figure 494:** Time error for run 29 showing incremental effect of removing each error source.

#### C.19.A. Tracker Jumps

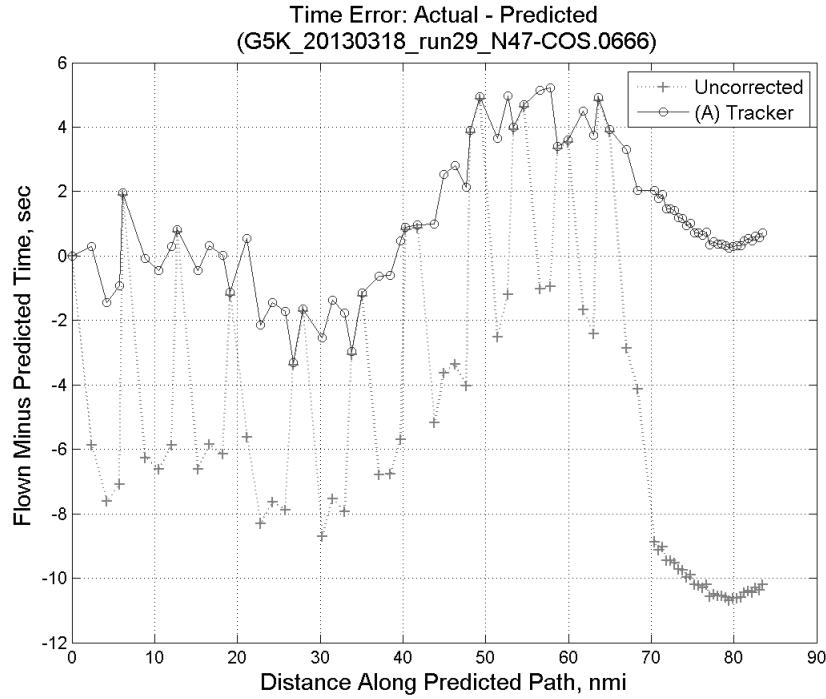


**Figure 495:** Time error for run 29 before (Uncorrected) and after ((A) Tracker) removing tracker jump error source.

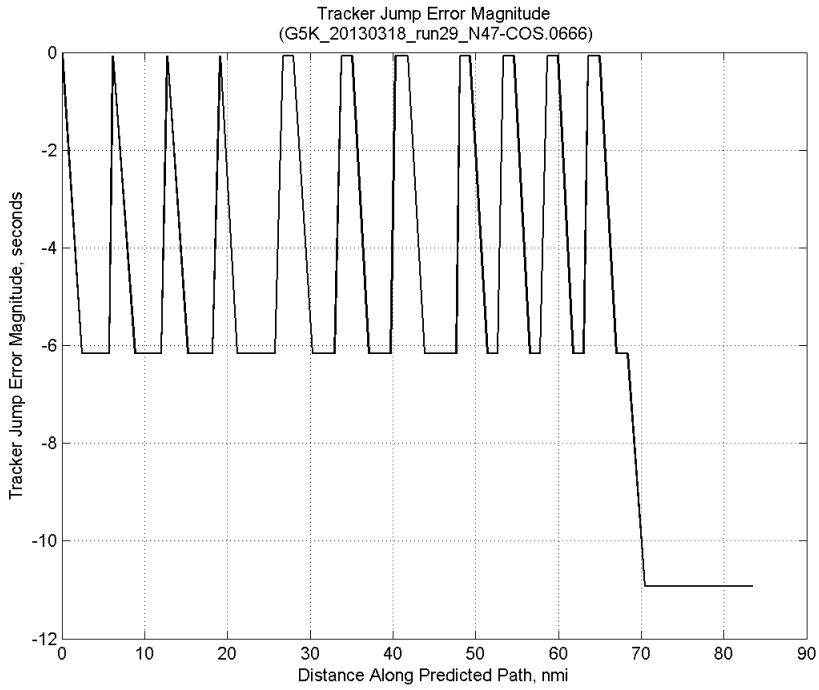


**Figure 496: Effect of tracker jump error source on time error for run 29.**

### C.19.B. Wind

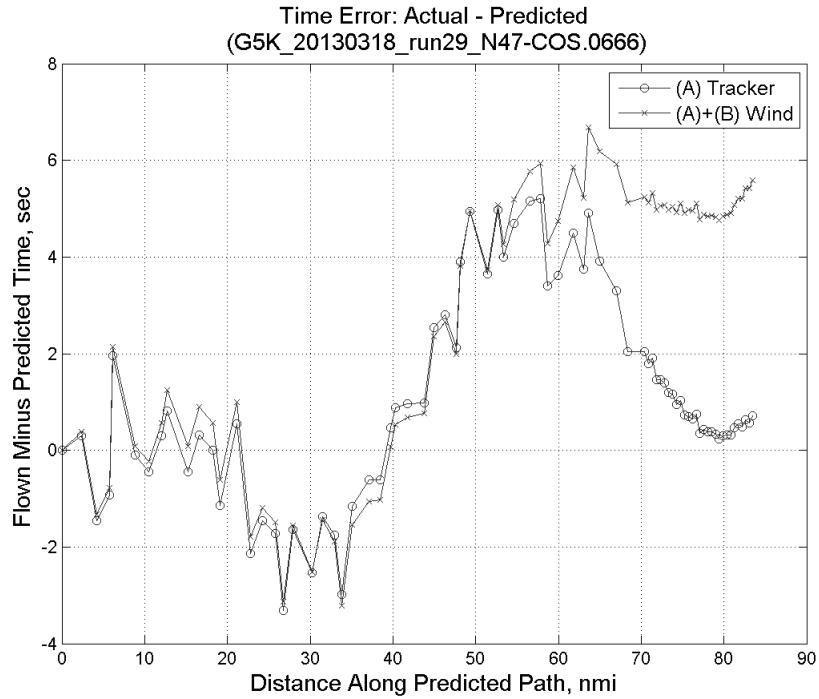


**Figure 497: Time error for run 29 before ((A) Tracker) and after ((A)+(B) Wind) removing wind error source.**

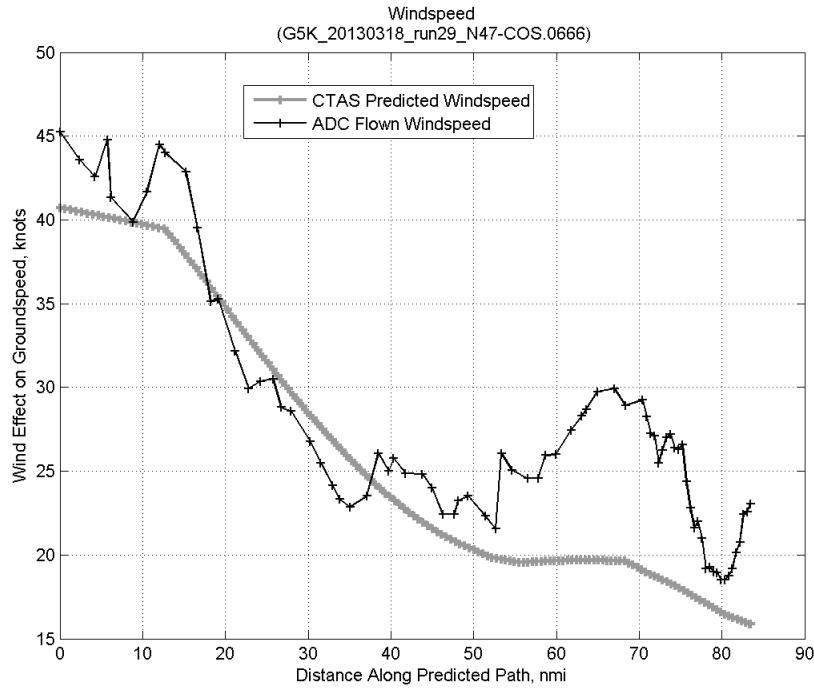


**Figure 498: CTAS predicted and ADC flown wind effect on ground speed for run 29. Negative values indicate a headwind.**

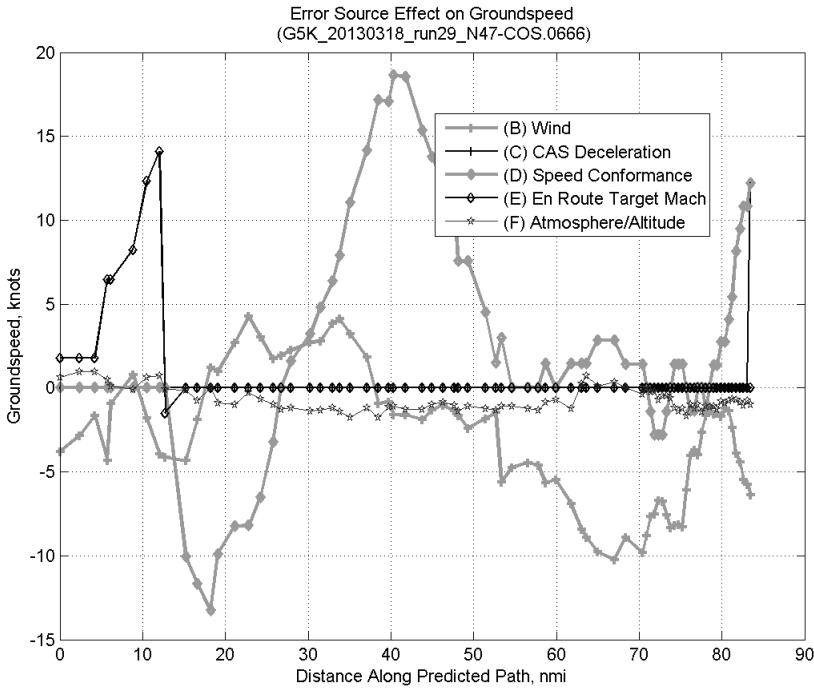


**Figure 499: Error sources (flown minus predicted) converted to a ground speed effect for run 29. Positive values indicate the flown ground speed was faster than the CTAS prediction.**

### C.19.C. CAS Deceleration

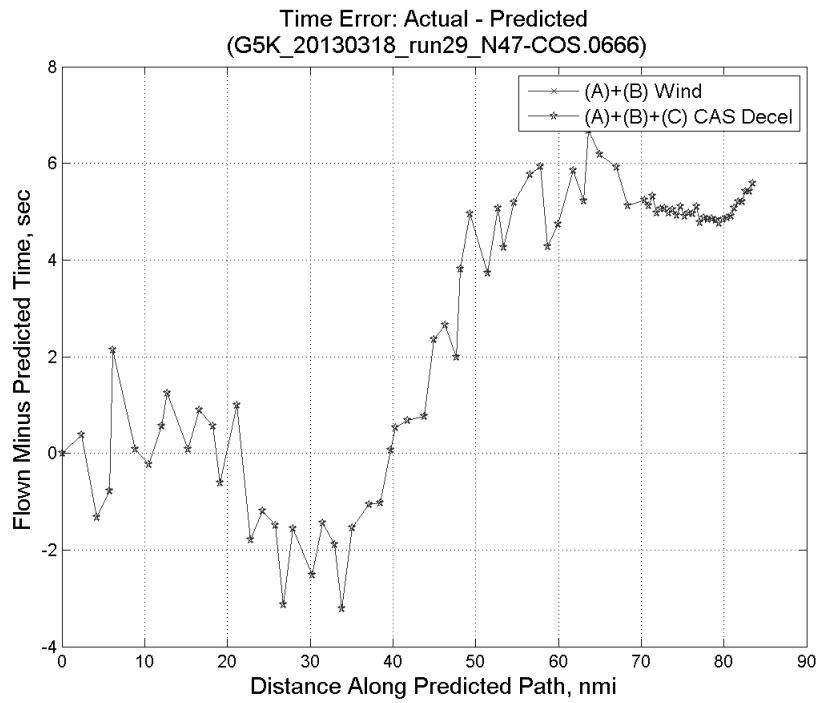


**Figure 500:** Time error for run 29 before ((A)+(B) Wind) and after ((A)+(B)+(C) CAS Decel) removing CAS deceleration error source.

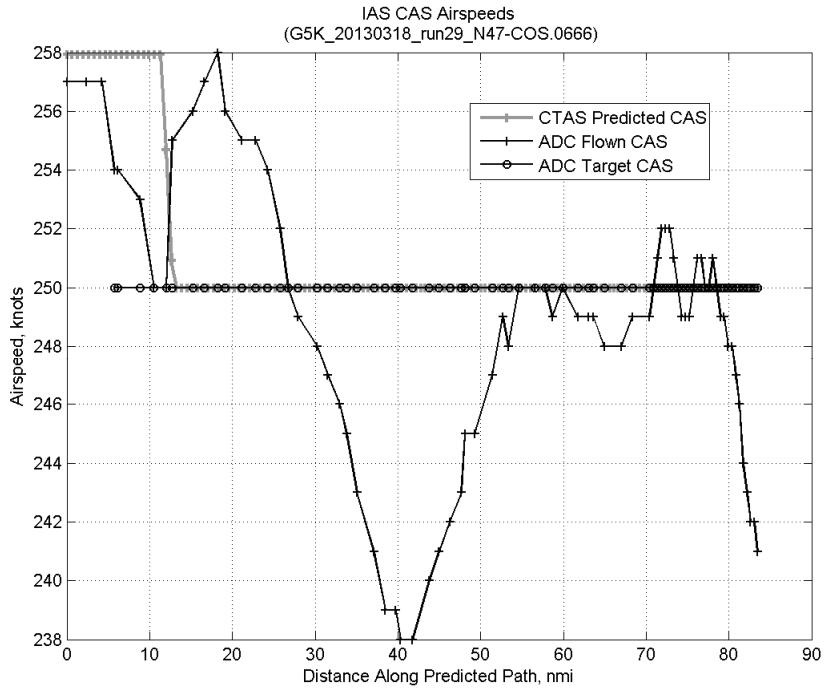


**Figure 501:** CTAS predicted and ADC flown CAS for run 29. CAS that is being targeted is shown with circle markers.

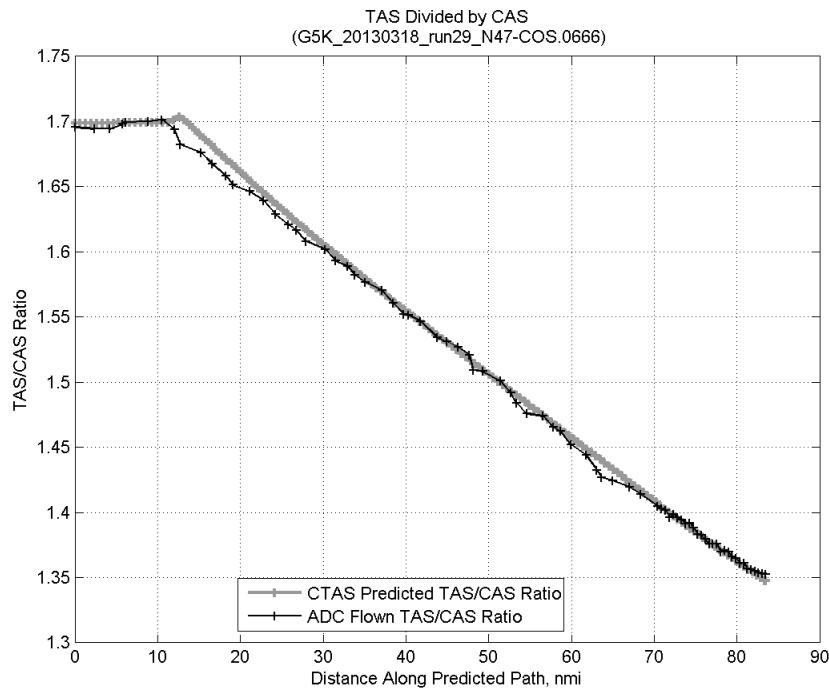


**Figure 502: CTAS predicted and ADC flown TAS/CAS ratio for run 29.**

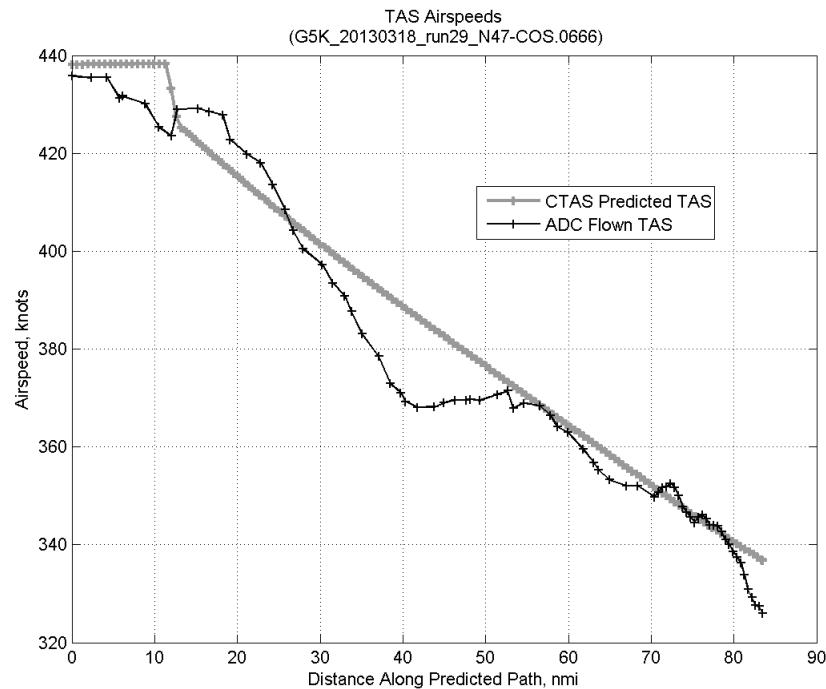


**Figure 503: CTAS predicted and ADC flown TAS for run 29.**

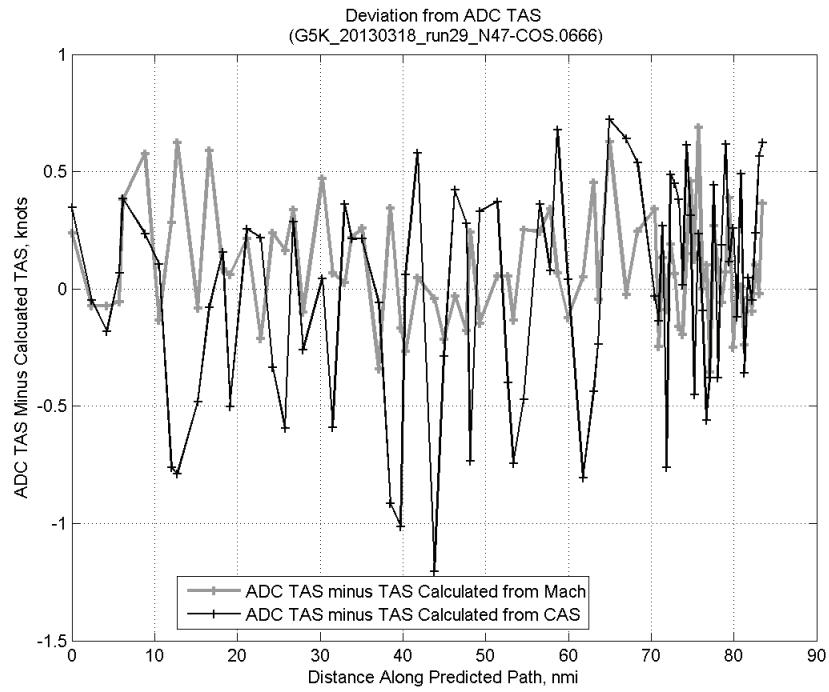


**Figure 504:** Deviation from ADC flown TAS if calculating TAS using ADC flown CAS, Mach, atmospheric temperature, and atmospheric pressure for run 29.

#### C.19.D. Speed Conformance

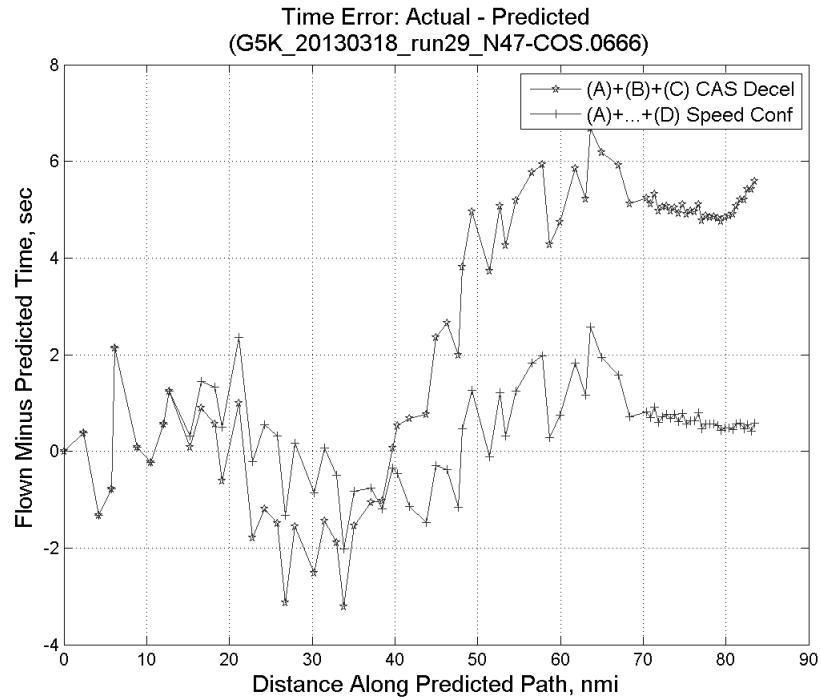


**Figure 505:** Time error for run 29 before ((A)+(B)+(C) CAS Decel) and after ((A)+...+(D) Speed Conf) removing speed conformance error source.

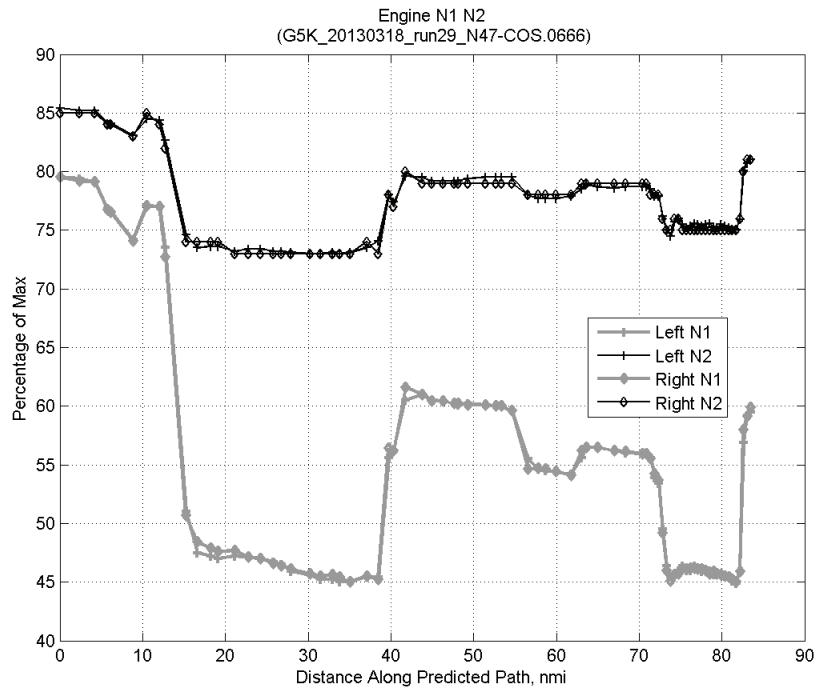


**Figure 506: Flown engine N1 and N2 for run 29.**

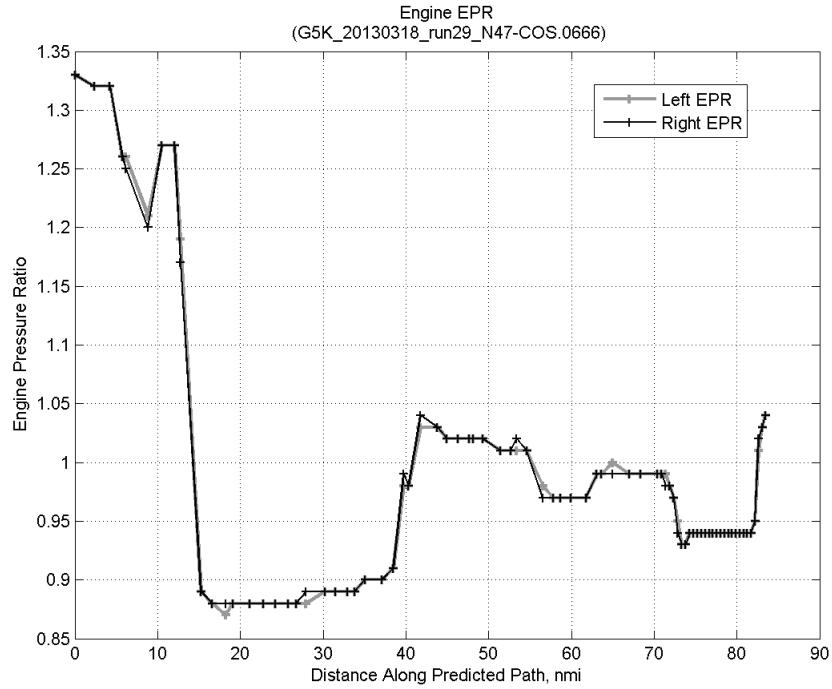


**Figure 507: Flown engine EPR for run 29.**

### C.19.E. Target Mach

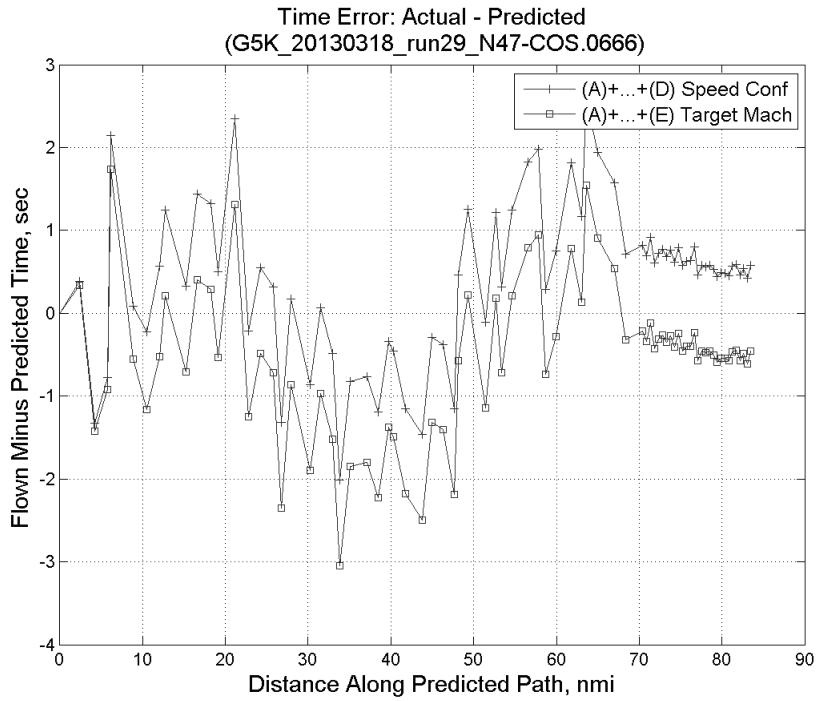


**Figure 508:** Time error for run 29 before ((A)+...+(D) Speed Conf) and after ((A)+...+(E) Target Mach) removing target Mach error source.

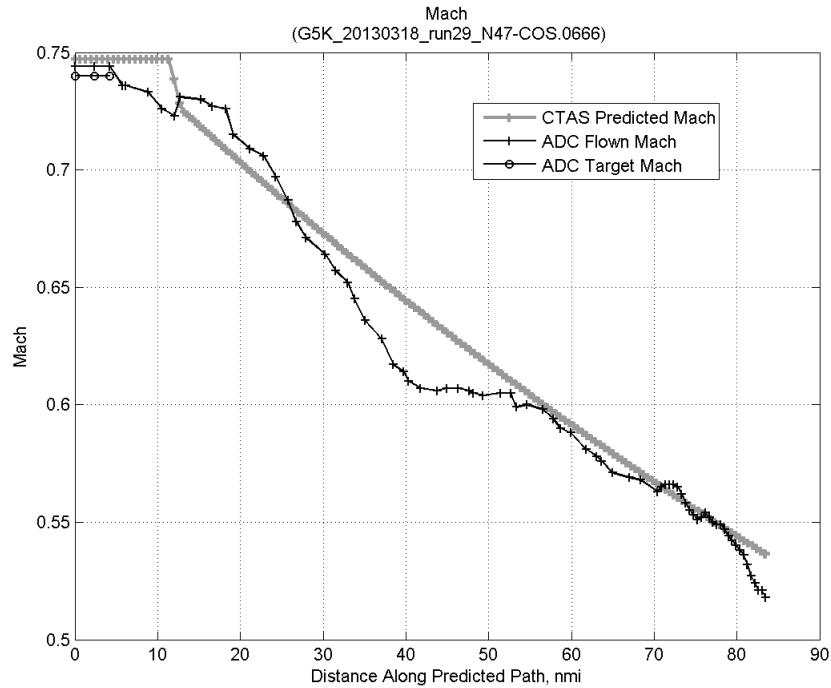


**Figure 509:** CTAS predicted and ADC flown Mach for run 29. Mach being targeted (ADC) shown with circle markers.

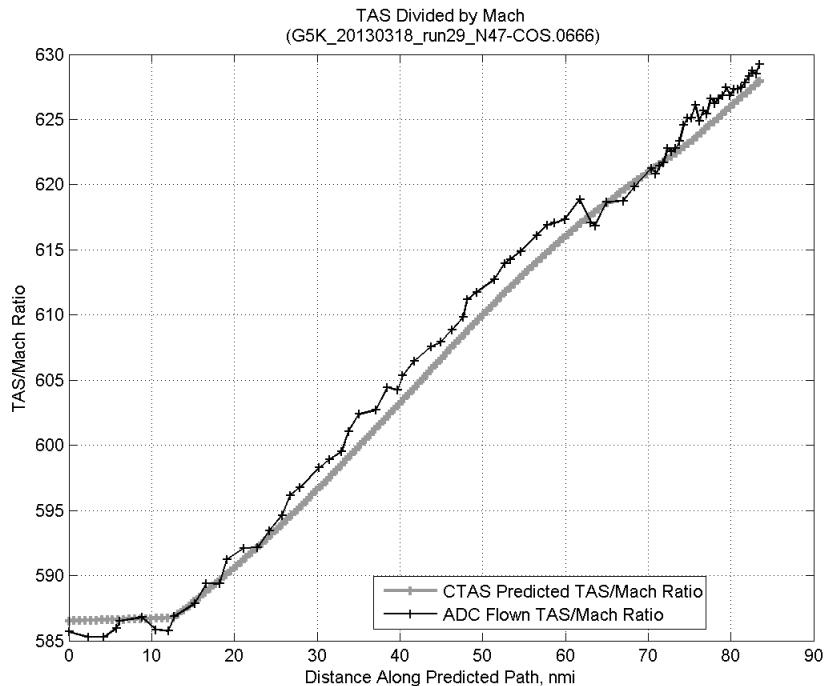


**Figure 510: CTAS predicted and ADC flown TAS/Mach ratio for run 29.**

#### C.19.F. Atmosphere/Altitude

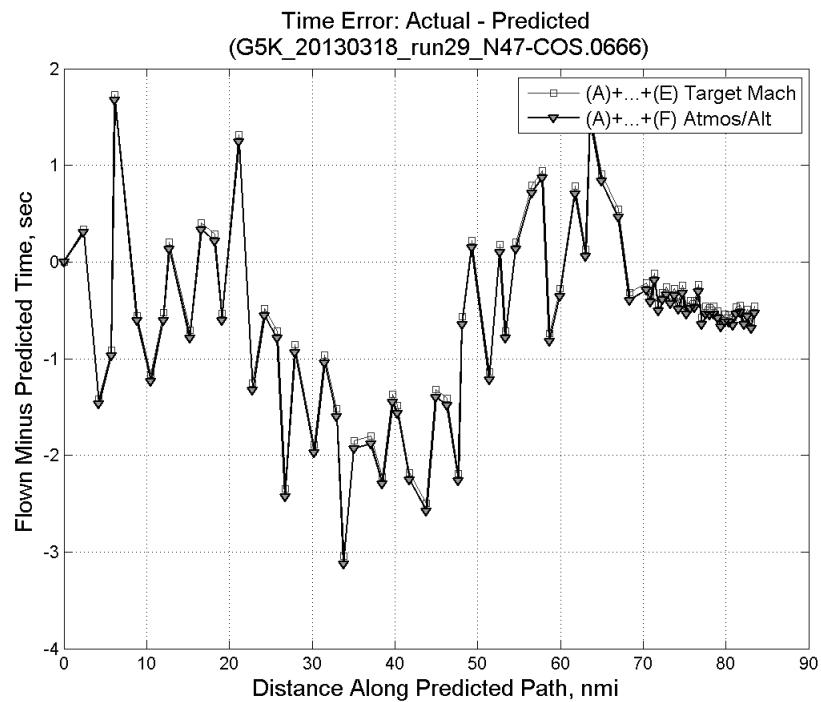


**Figure 511: Time error for run 29 before ((A)+...+(E) Target Mach) and after ((A)+...+(F) Atmos/Alt) removing atmosphere/altitude error source.**

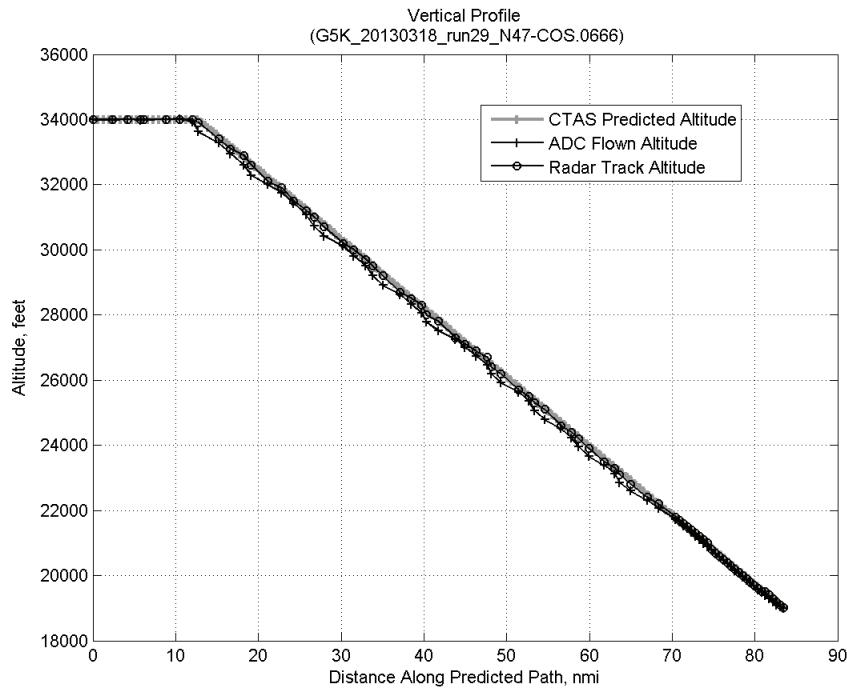


**Figure 512: Flown (ADC) and predicted (CTAS) vertical profile for run 29.**

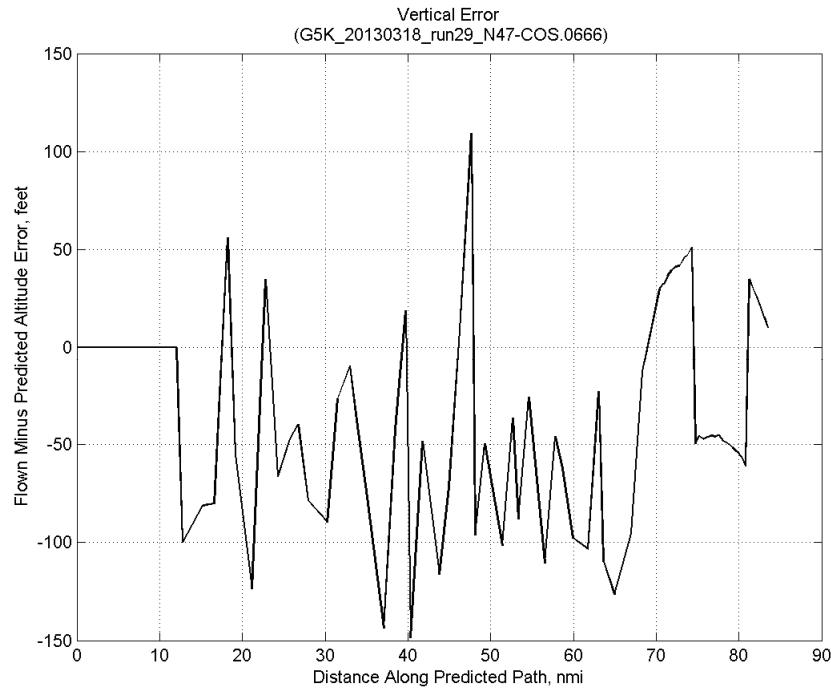


**Figure 513: Vertical error (flown minus predicted altitude) for run 29. Positive values indicate aircraft flew higher than predicted by CTAS.**

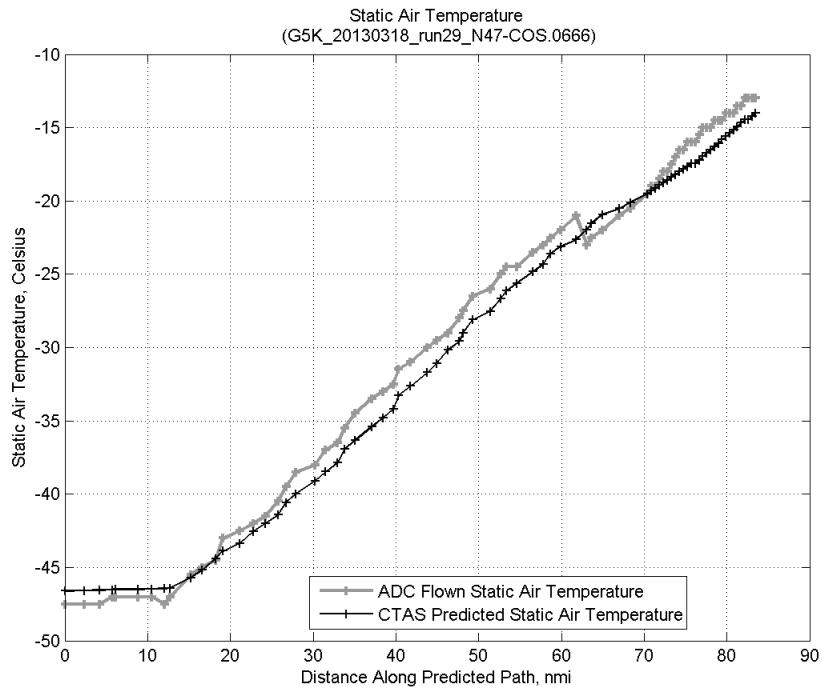


**Figure 514:** Flown (ADC) and predicted (CTAS) static air temperature for run 29.

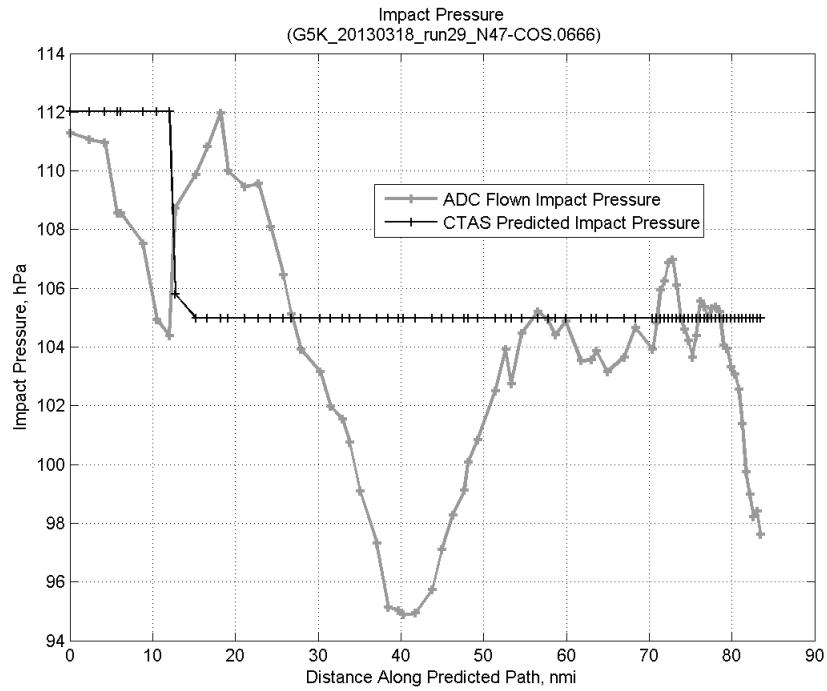


**Figure 515:** Flown (ADC) and predicted (CTAS) impact pressure for run 29.

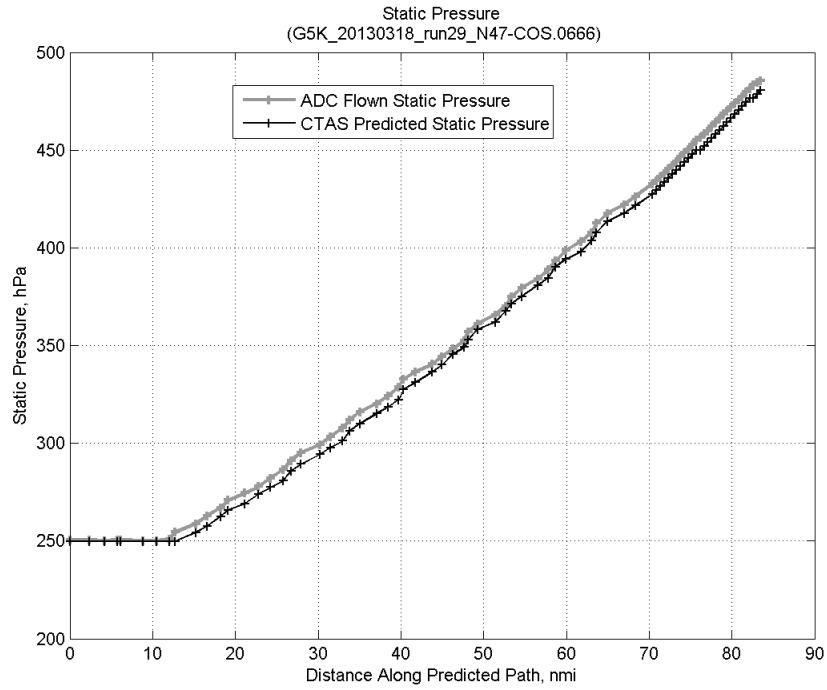


**Figure 516: Flown (ADC) and predicted (CTAS) static pressure for run 29.**

#### C.19.G. Path Distance

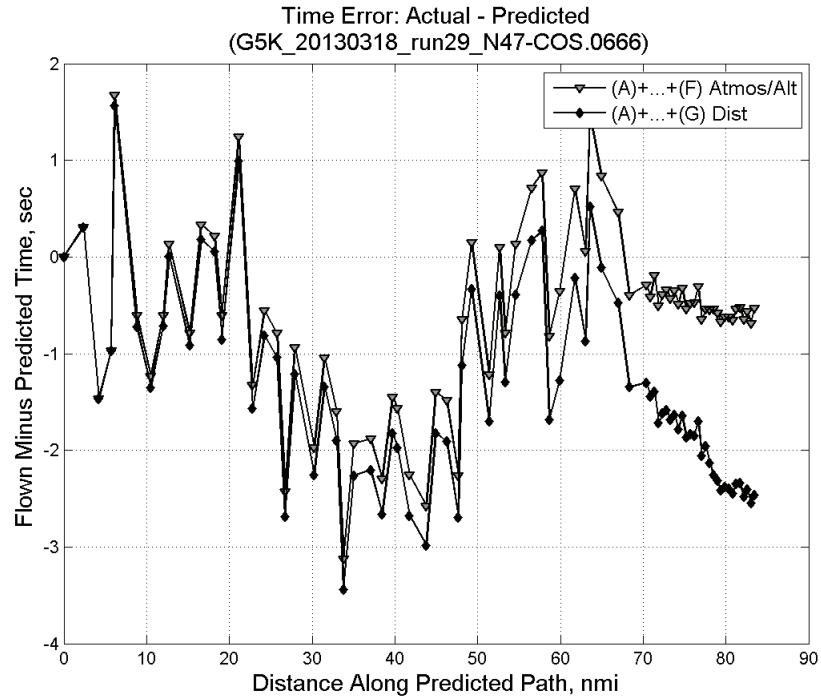


**Figure 517: Time error for run 29 before ((A)+...+(F) Atmos/Alt) and after ((A)+...+(G) Dist) removing path distance error source.**

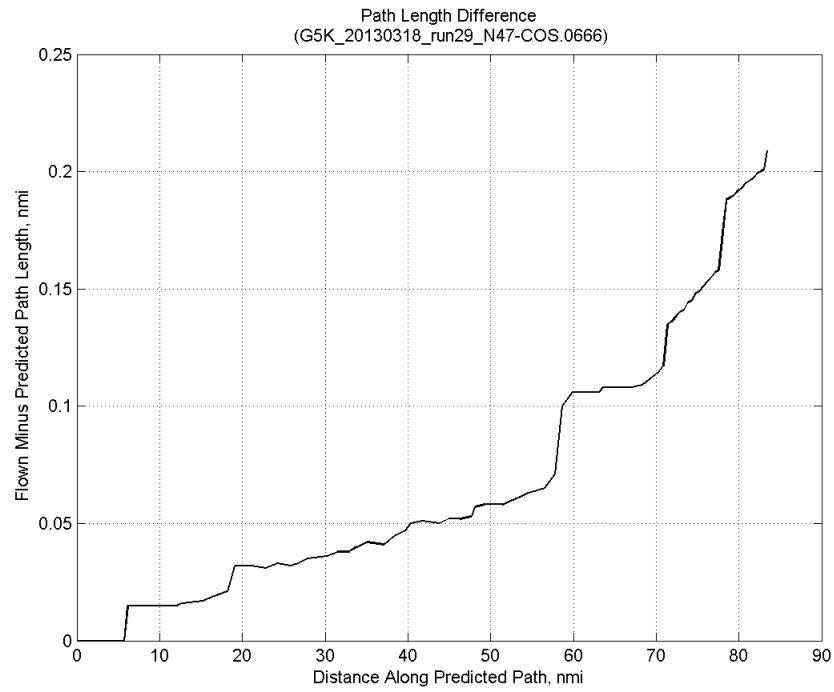


**Figure 518: ADC flown minus CTAS predicted path length for run 29. Positive values indicate aircraft followed a longer path than predicted by CTAS.**

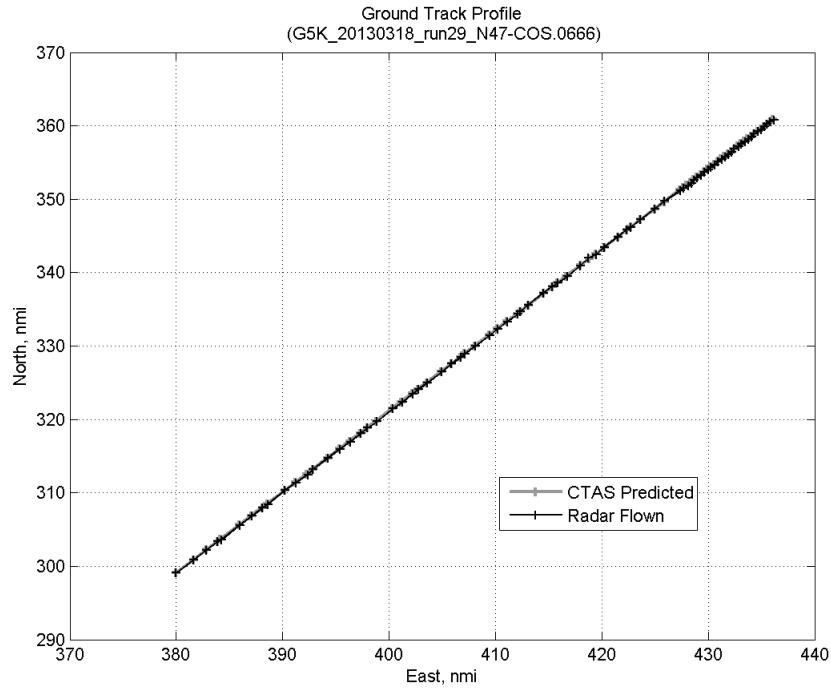


**Figure 519: CTAS predicted and radar flown ground track profile for run 29.**

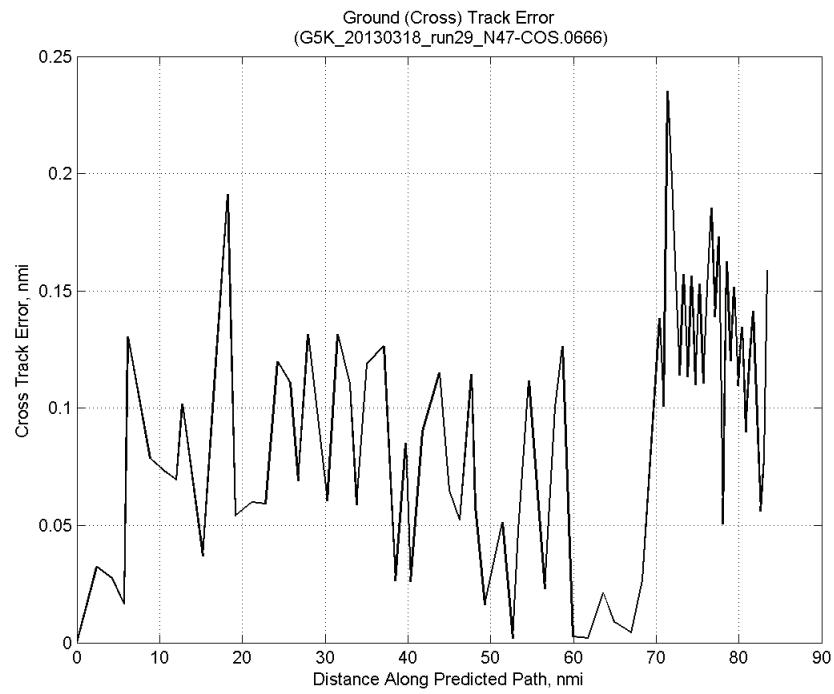


**Figure 520: Ground (cross) track error for run 29.**

## C.20. Run 30

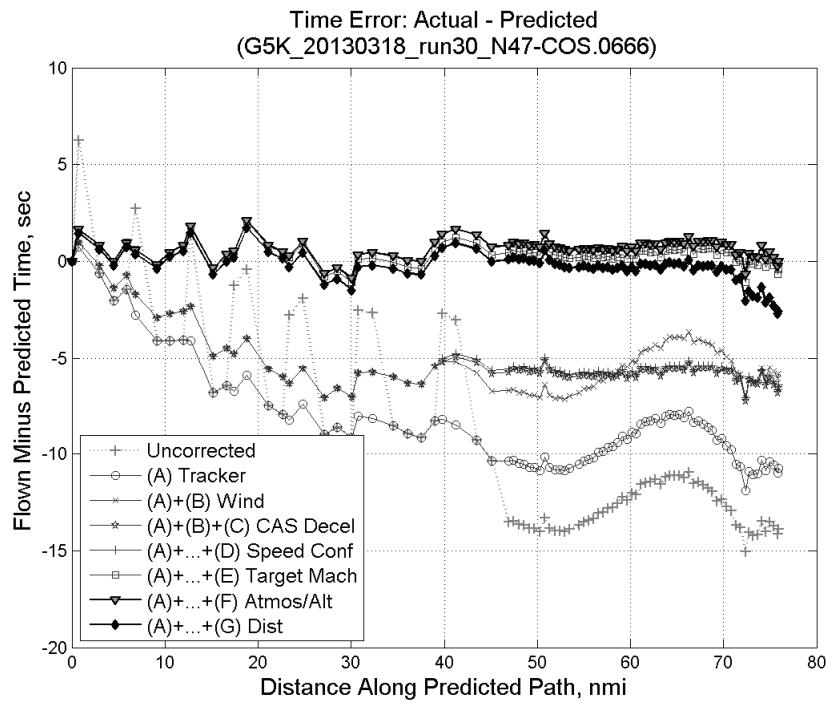


**Figure 521: Time error for run 30 showing incremental effect of removing each error source.**

### C.20.A. Tracker Jumps

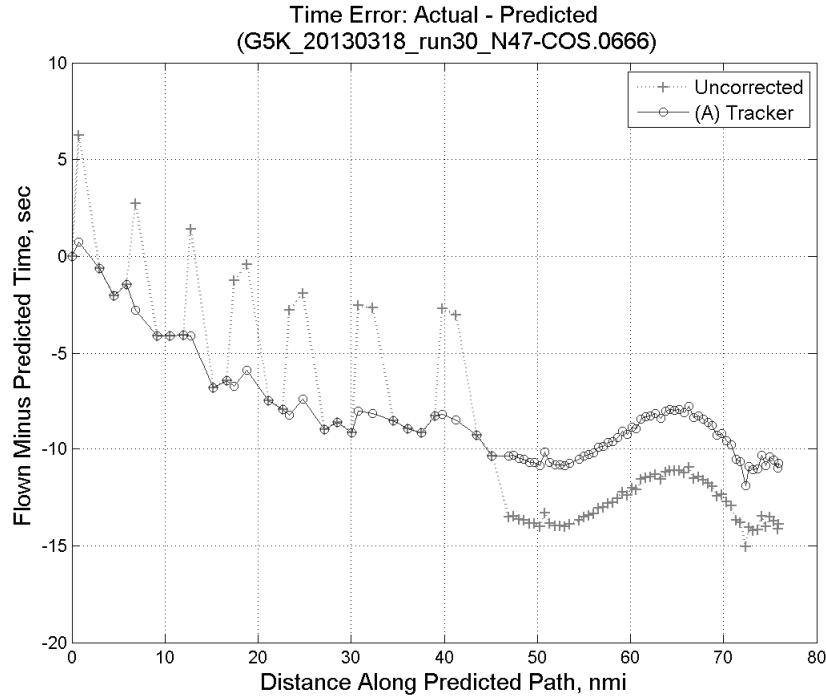


**Figure 522: Time error for run 30 before (Uncorrected) and after ((A) Tracker) removing tracker jump error source.**

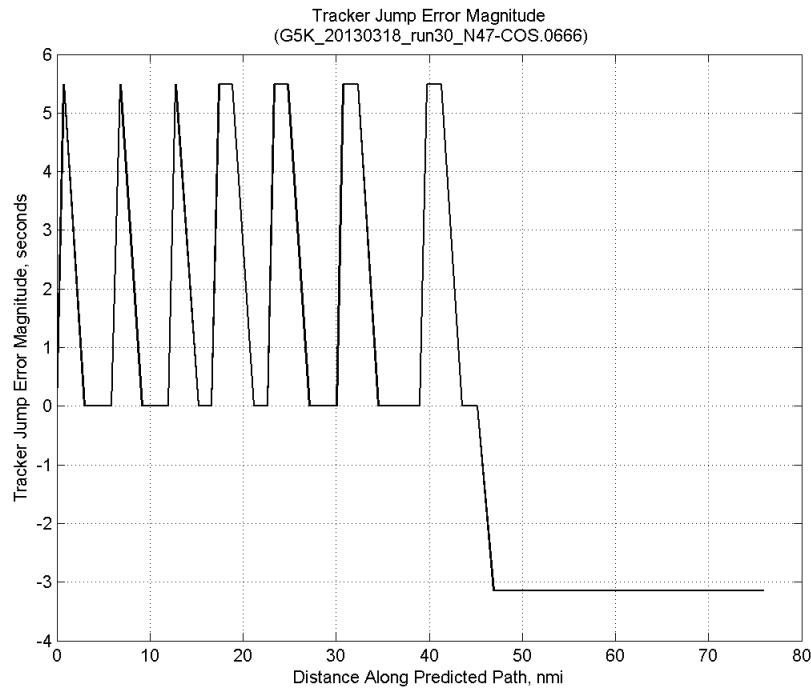


**Figure 523: Effect of tracker jump error source on time error for run 30.**

### C.20.B. Wind

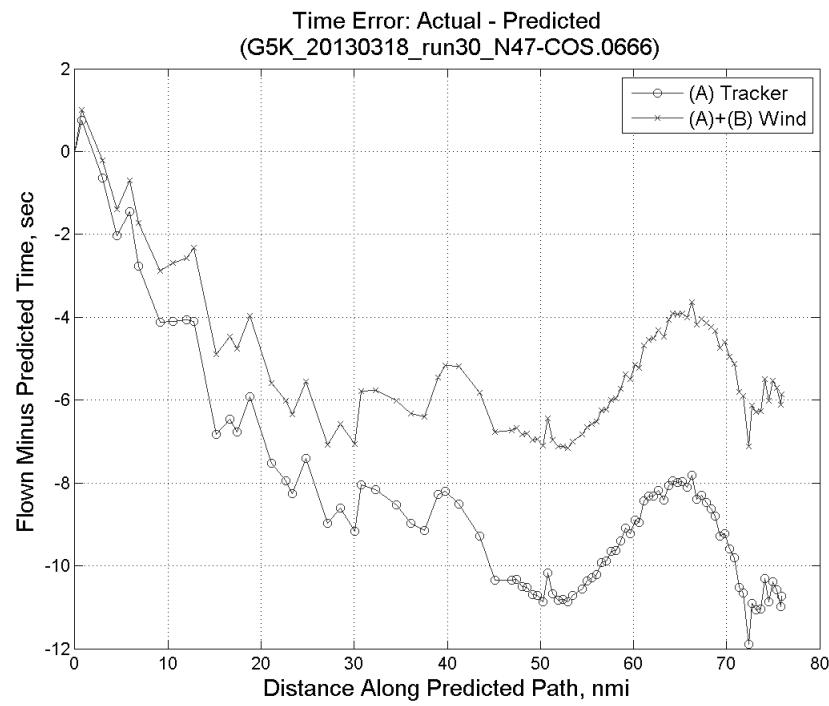


**Figure 524: Time error for run 30 before ((A) Tracker) and after ((A)+(B) Wind) removing wind error source.**

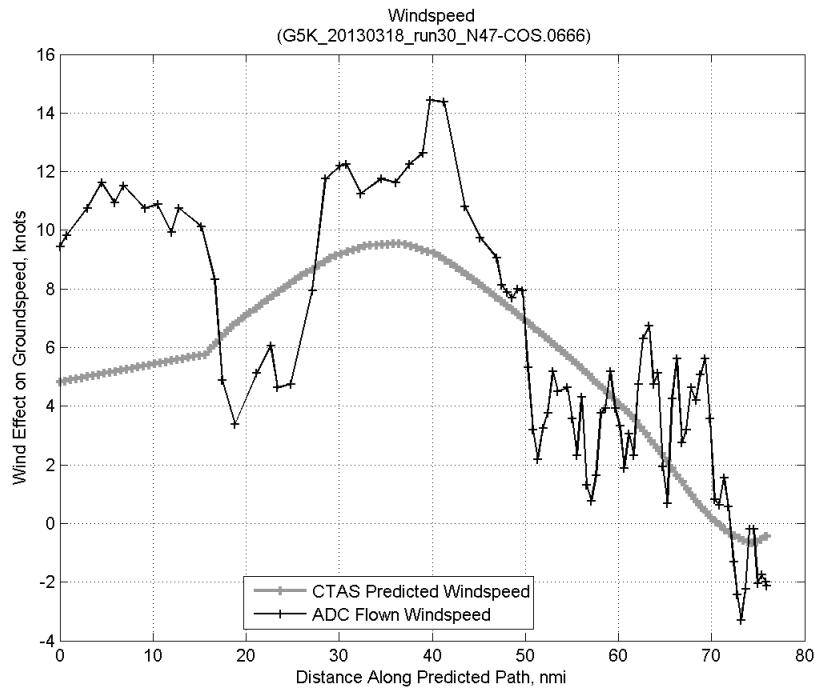


**Figure 525: CTAS predicted and ADC flown wind effect on ground speed for run 30. Negative values indicate a headwind.**

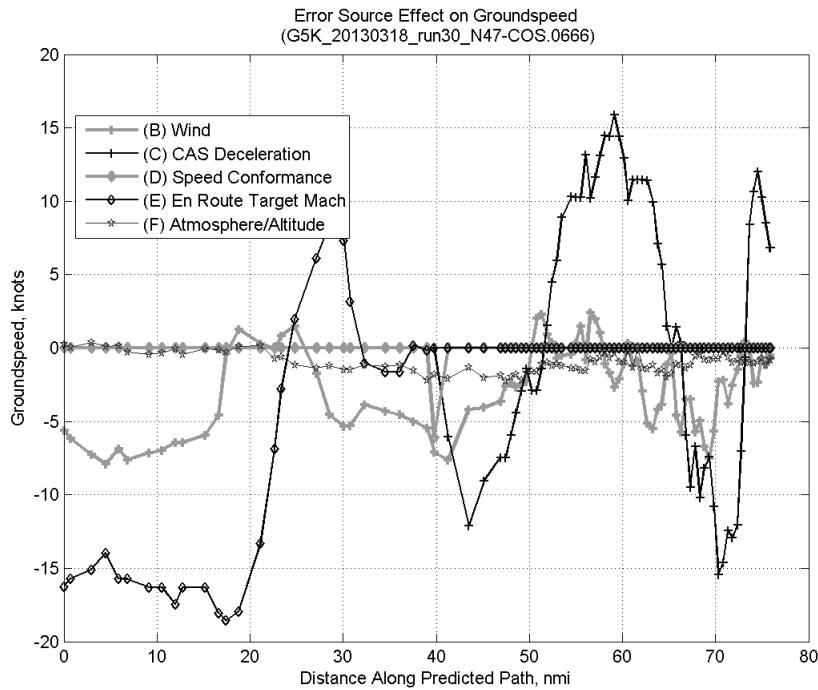


**Figure 526: Error sources (flown minus predicted) converted to a ground speed effect for run 30. Positive values indicate the flown ground speed was faster than the CTAS prediction.**

### C.20.C. CAS Deceleration

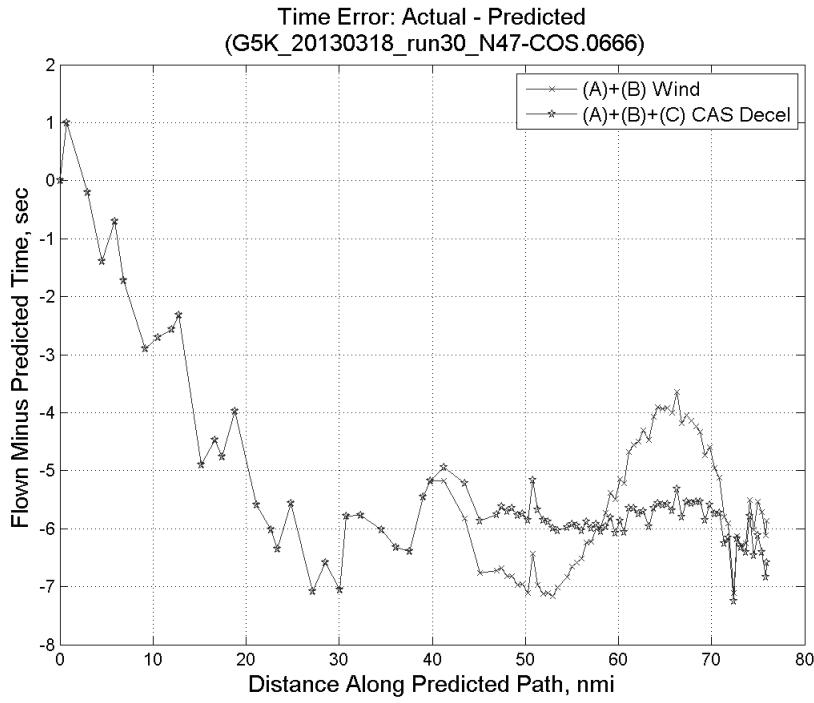


**Figure 527:** Time error for run 30 before ((A)+(B) Wind) and after ((A)+(B)+(C) CAS Decel) removing CAS deceleration error source.

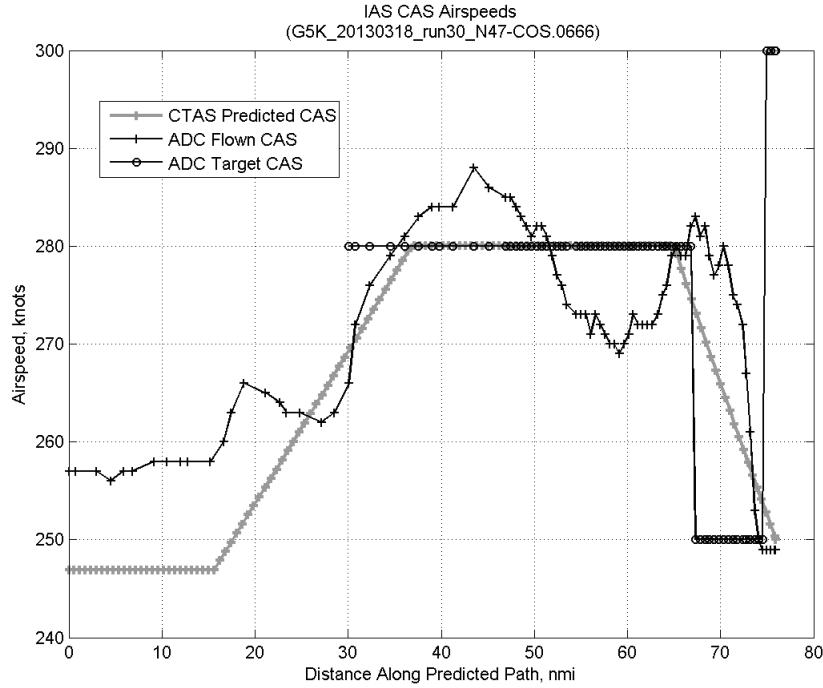


**Figure 528:** CTAS predicted and ADC flown CAS for run 30. CAS that is being targeted is shown with circle markers.

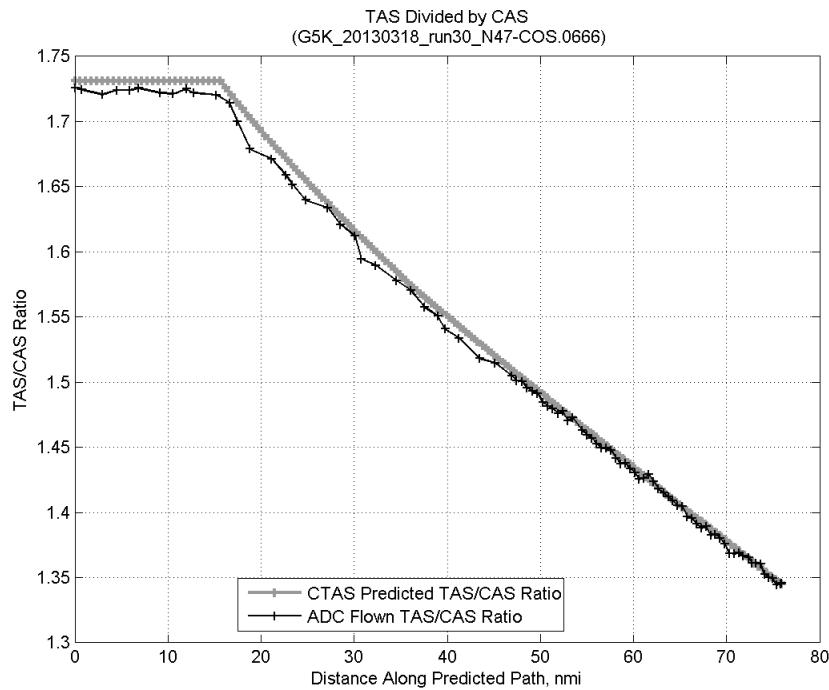


**Figure 529: CTAS predicted and ADC flown TAS/CAS ratio for run 30.**

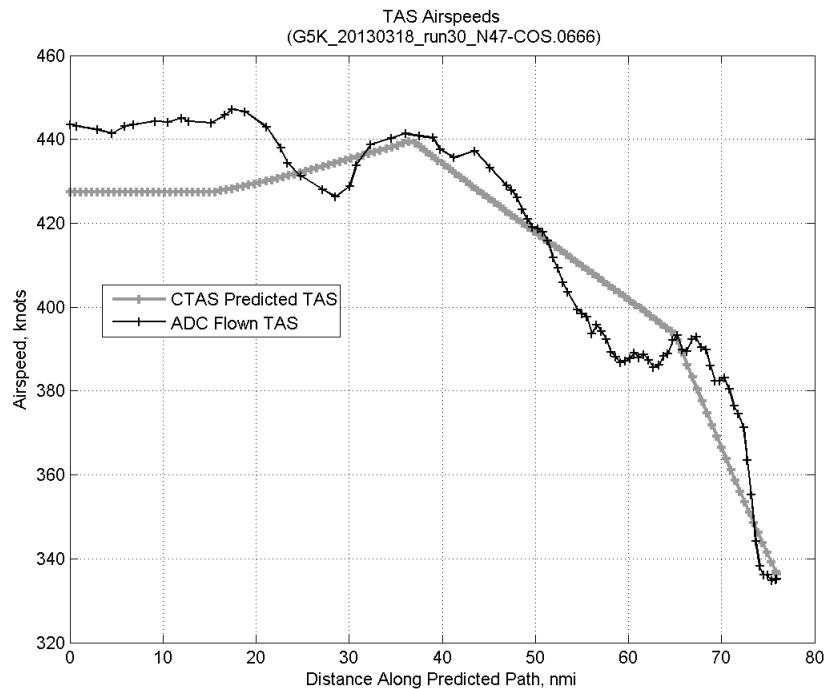


**Figure 530: CTAS predicted and ADC flown TAS for run 30.**

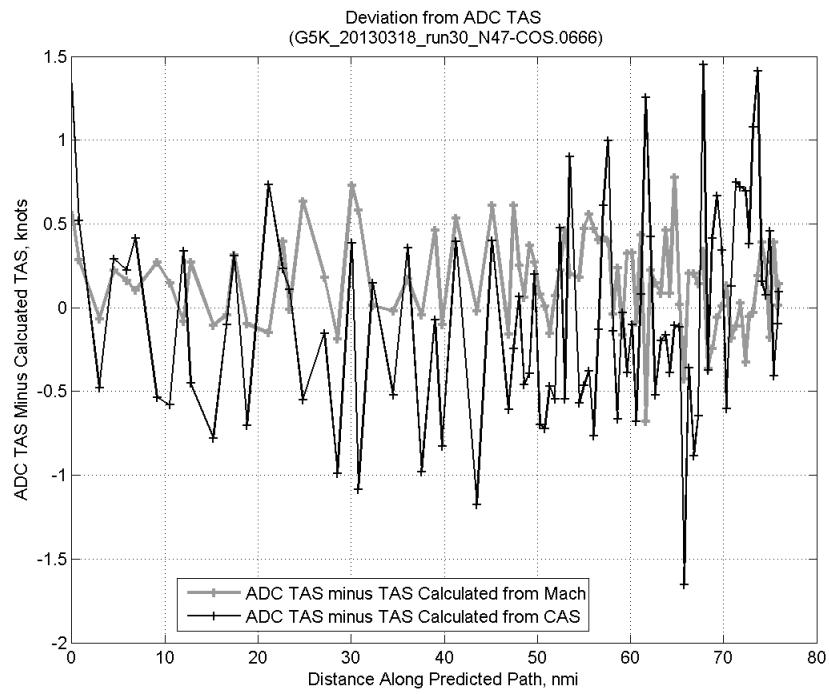


**Figure 531:** Deviation from ADC flown TAS if calculating TAS using ADC flown CAS, Mach, atmospheric temperature, and atmospheric pressure for run 30.

#### C.20.D. Speed Conformance

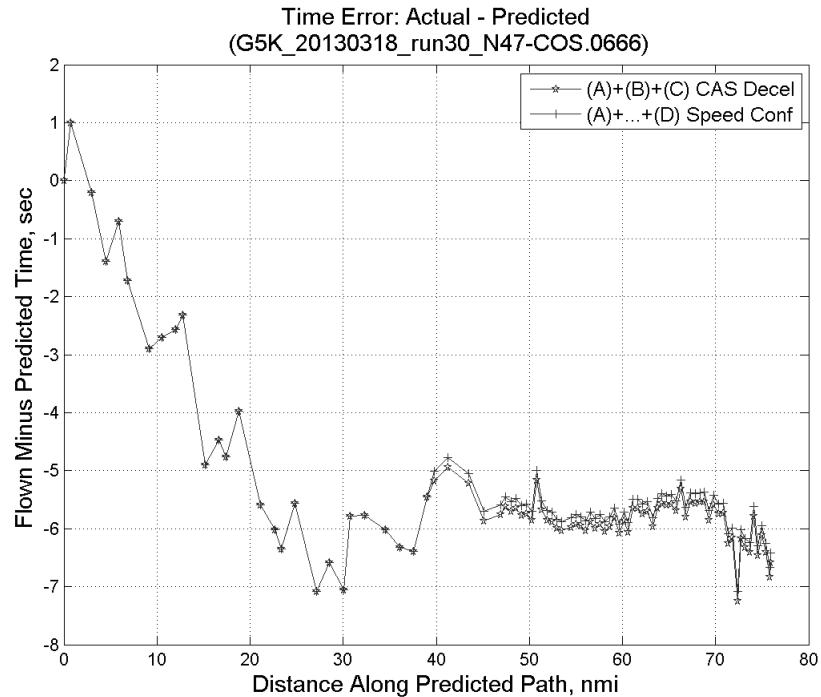


**Figure 532:** Time error for run 30 before  $((A)+(B)+(C) \text{ CAS Decel})$  and after  $((A)+\dots+(D) \text{ Speed Conf})$  removing speed conformance error source.

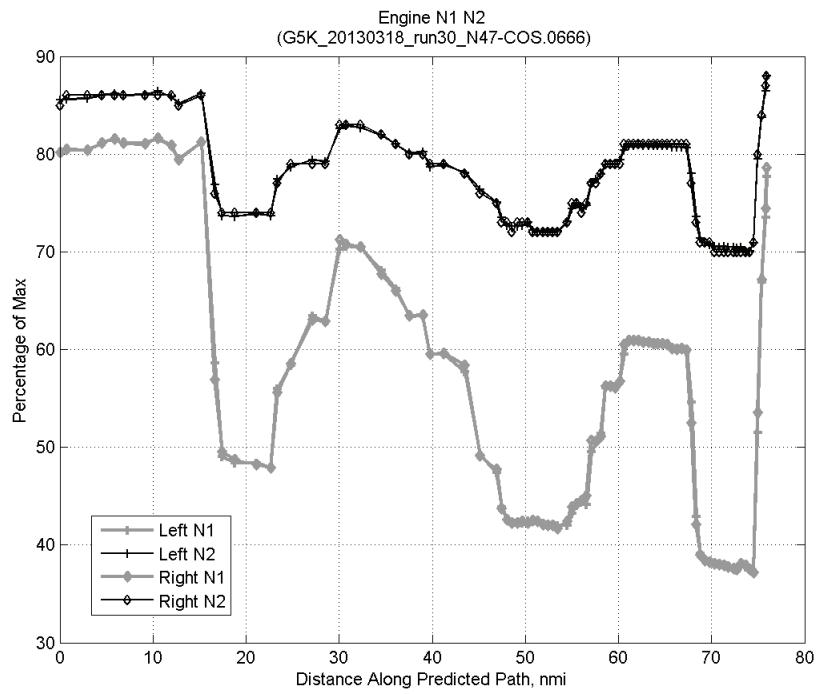


**Figure 533: Flown engine N1 and N2 for run 30.**

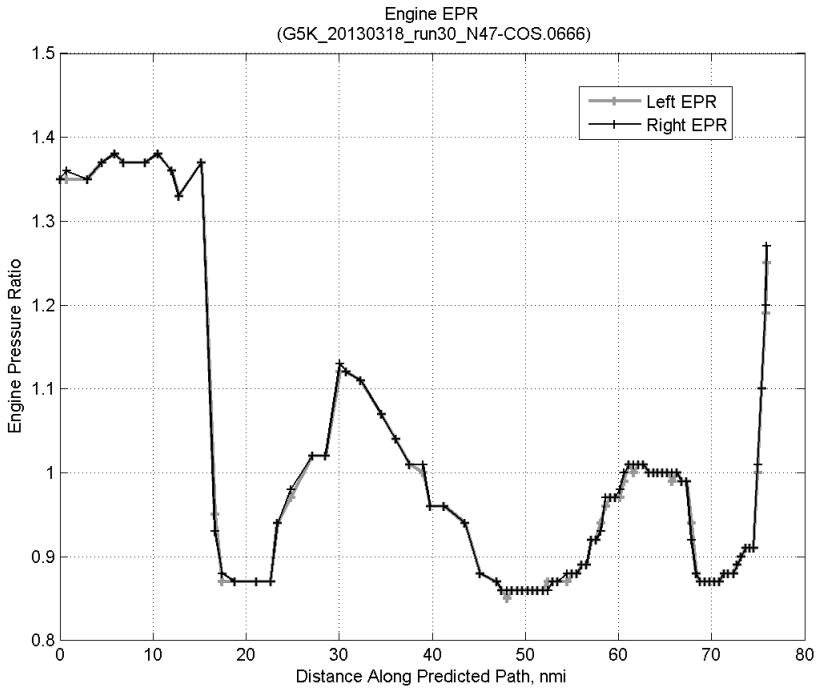


**Figure 534: Flown engine EPR for run 30.**

### C.20.E. Target Mach

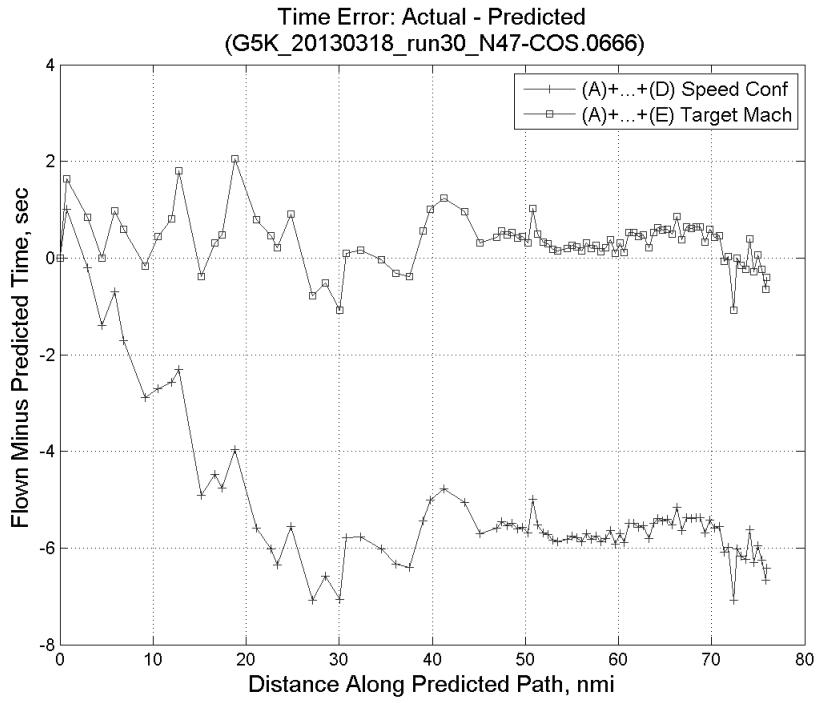


**Figure 535:** Time error for run 30 before ((A)+...+(D) Speed Conf) and after ((A)+...+(E) Target Mach) removing target Mach error source.

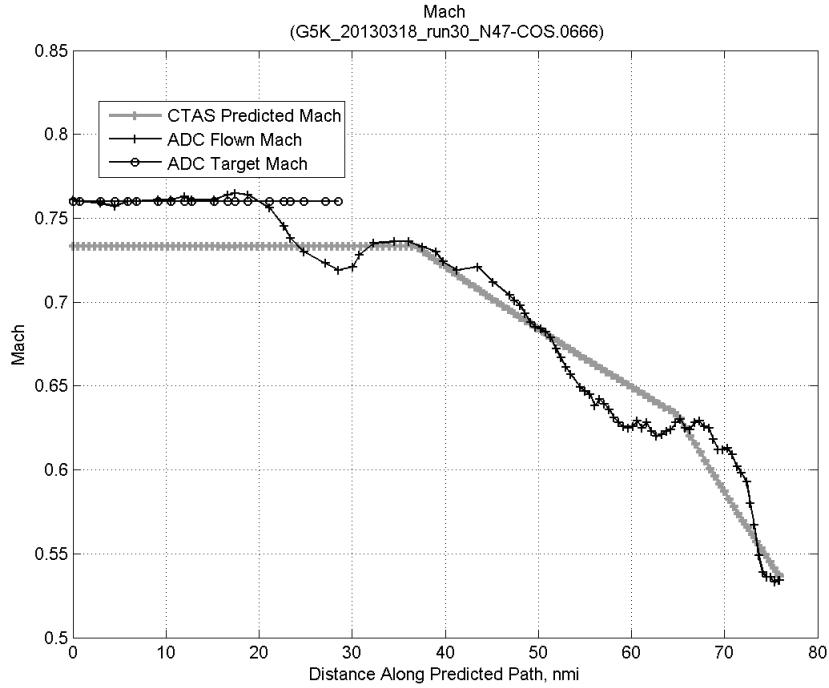


**Figure 536:** CTAS predicted and ADC flown Mach for run 30. Mach being targeted (ADC) shown with circle markers.

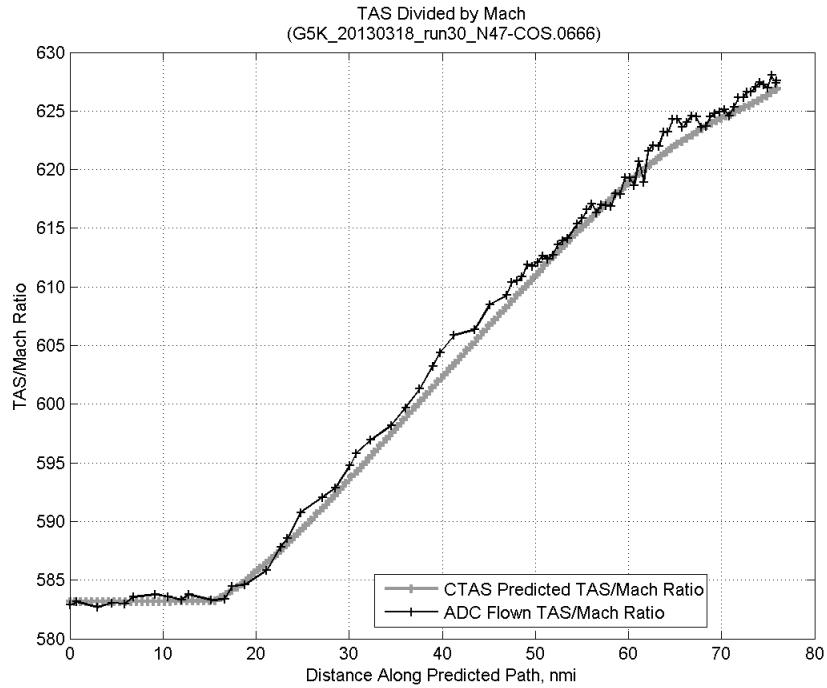


**Figure 537: CTAS predicted and ADC flown TAS/Mach ratio for run 30.**

#### C.20.F. Atmosphere/Altitude

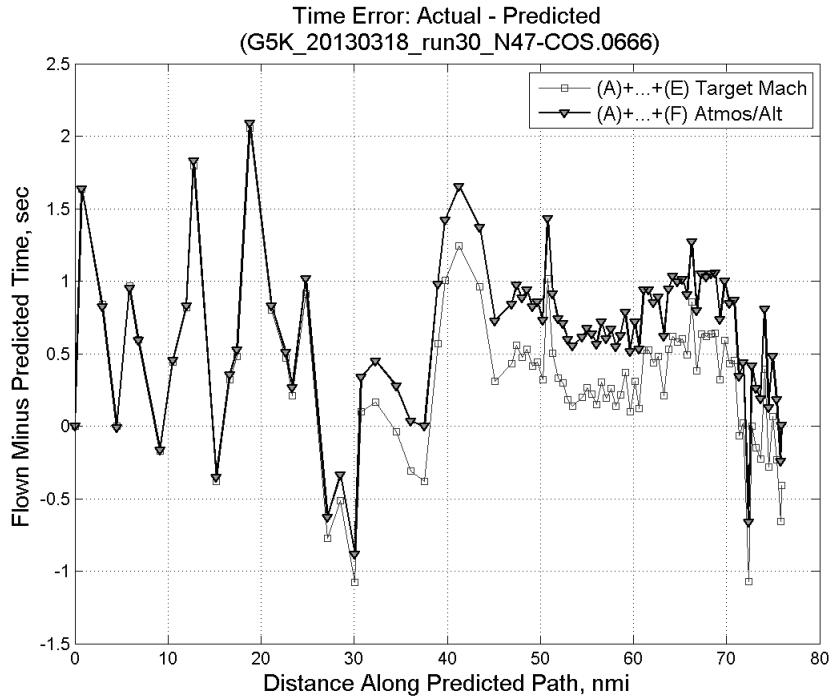


**Figure 538: Time error for run 30 before ((A)+...+(E) Target Mach) and after ((A)+...+(F) Atmos/Alt) removing atmosphere/altitude error source.**

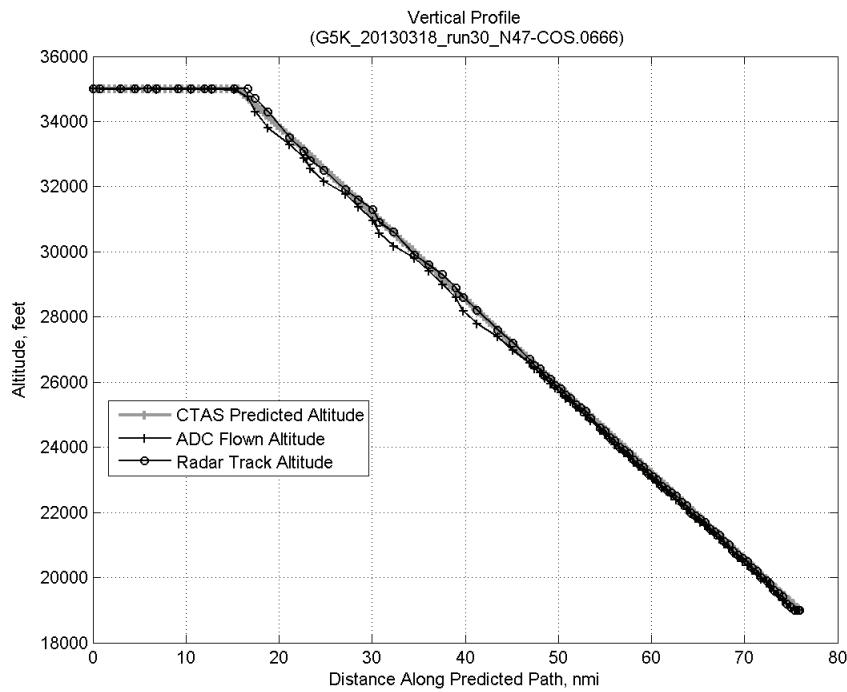


**Figure 539: Flown (ADC) and predicted (CTAS) vertical profile for run 30.**

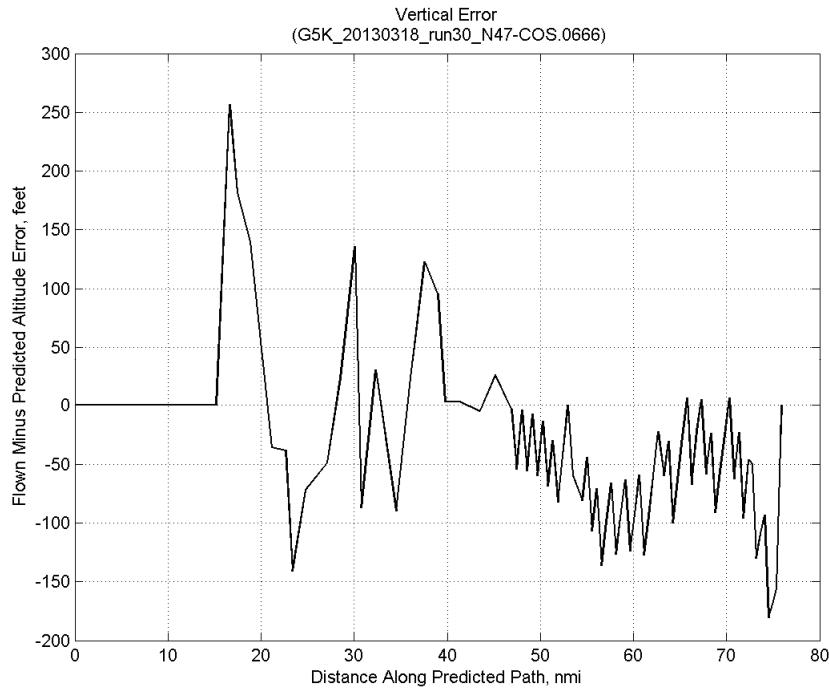


**Figure 540: Vertical error (flown minus predicted altitude) for run 30. Positive values indicate aircraft flew higher than predicted by CTAS.**

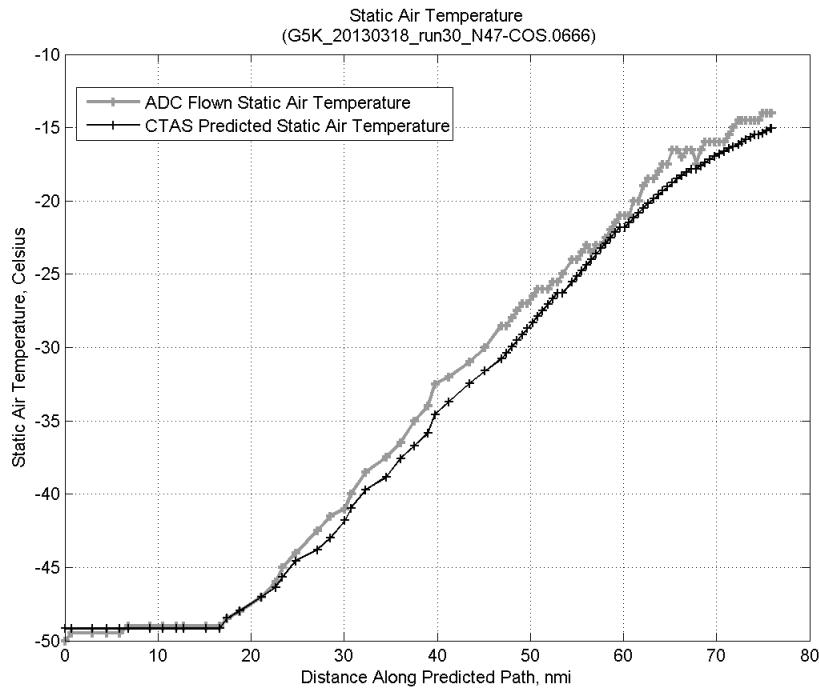


**Figure 541: Flown (ADC) and predicted (CTAS) static air temperature for run 30.**

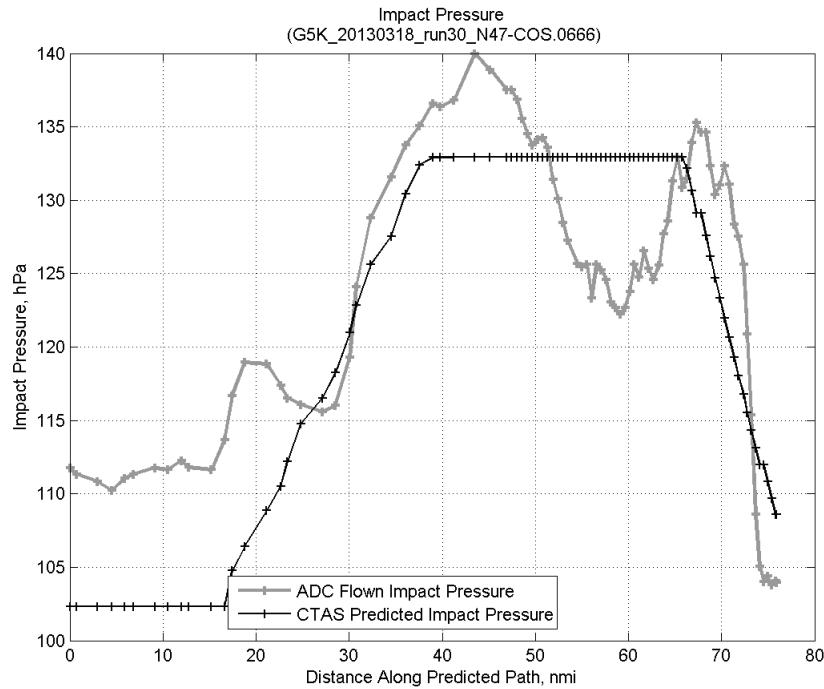


**Figure 542: Flown (ADC) and predicted (CTAS) impact pressure for run 30.**

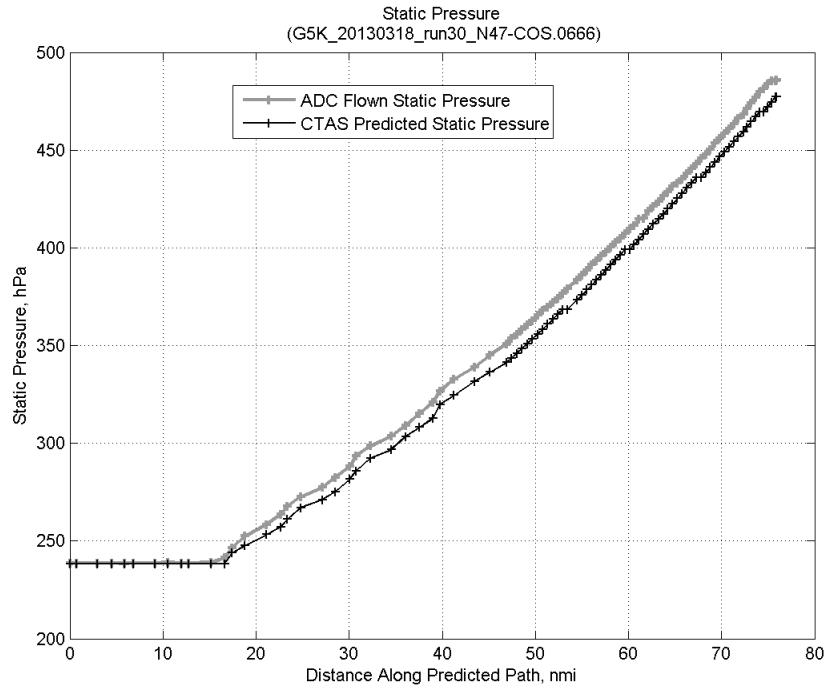


**Figure 543: Flown (ADC) and predicted (CTAS) static pressure for run 30.**

#### C.20.G. Path Distance

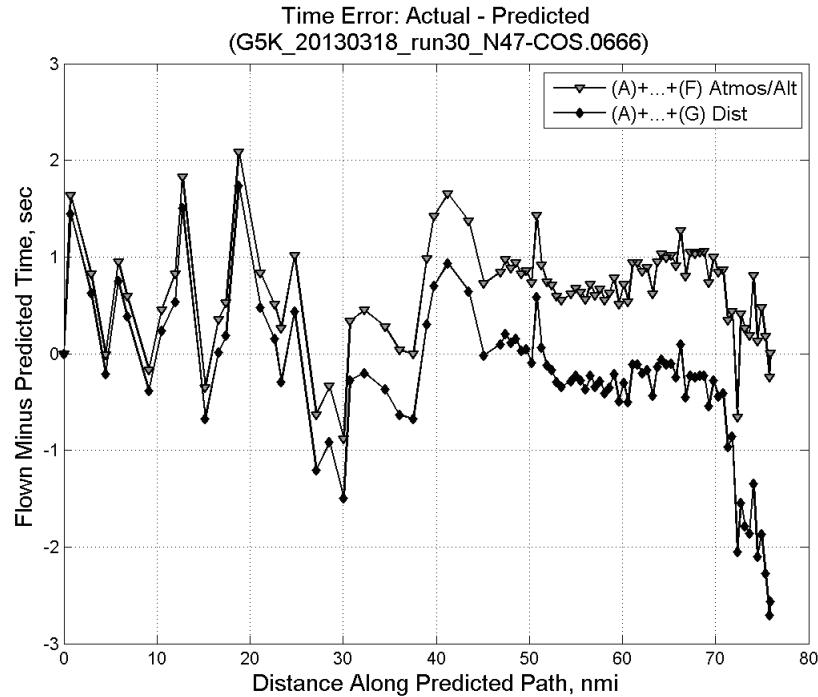


**Figure 544: Time error for run 30 before ((A)+...+(F) Atmos/Alt) and after ((A)+...+(G) Dist) removing path distance error source.**

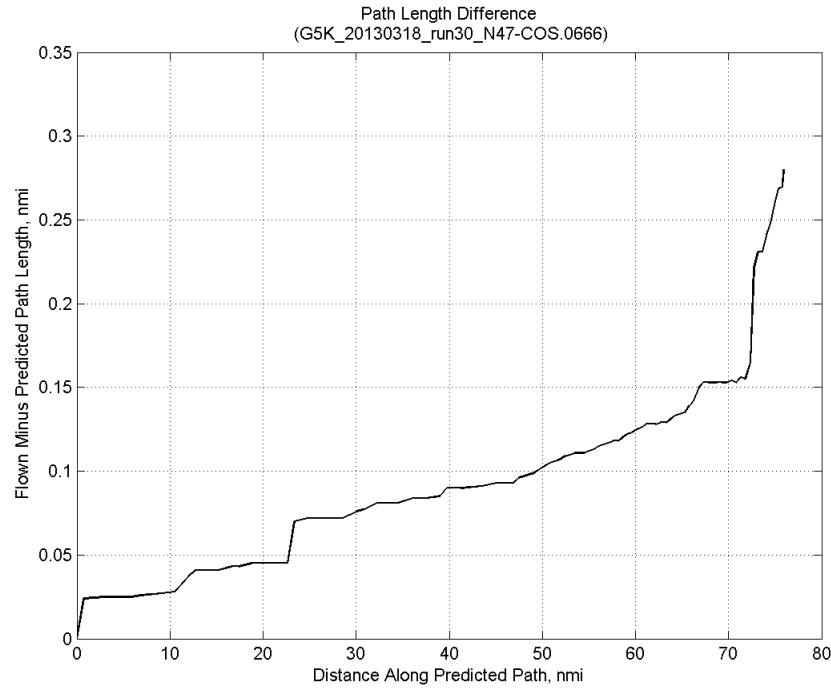


**Figure 545: ADC flown minus CTAS predicted path length for run 30. Positive values indicate aircraft followed a longer path than predicted by CTAS.**

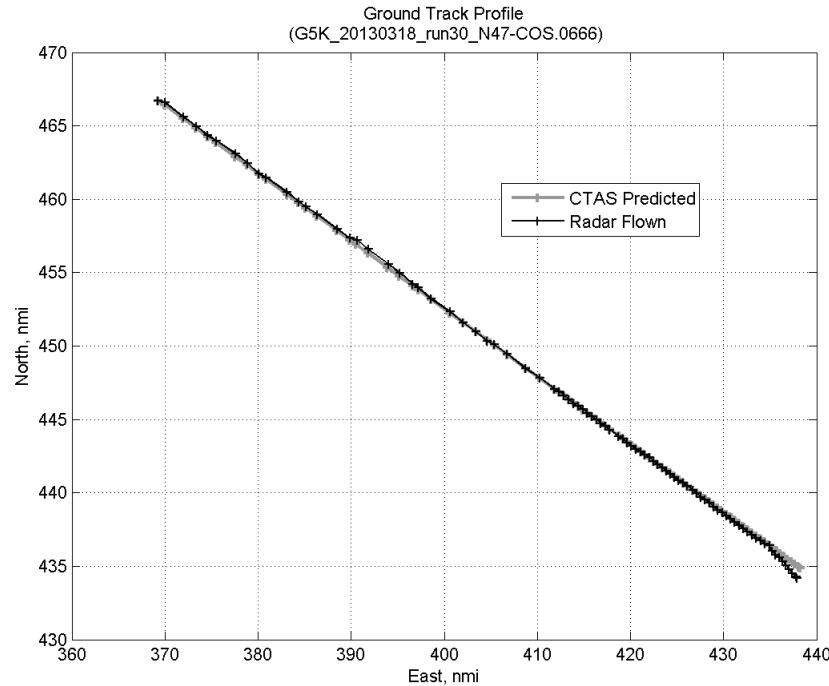


**Figure 546: CTAS predicted and radar flown ground track profile for run 30.**

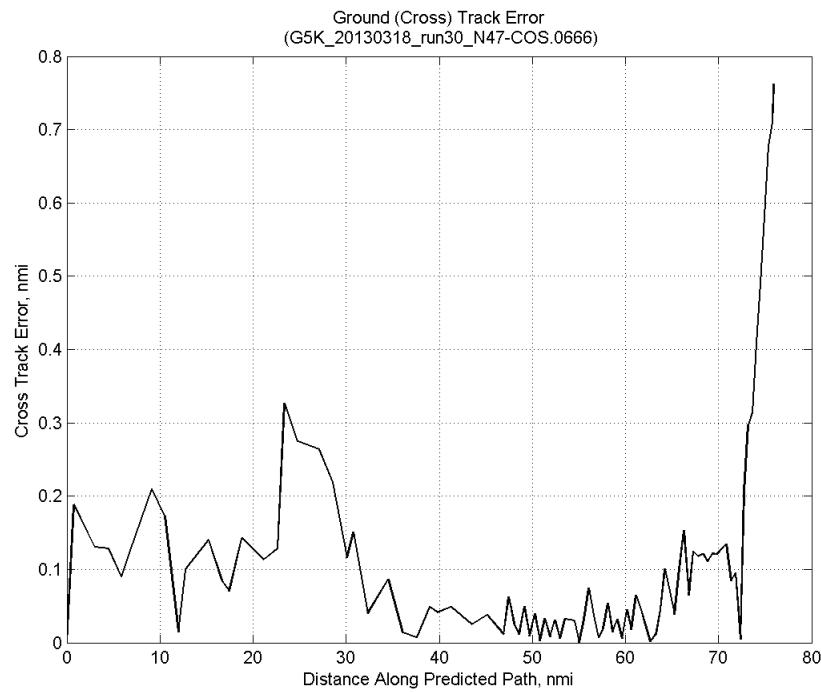


**Figure 547: Ground (cross) track error for run 30.**

## C.21. Run 31

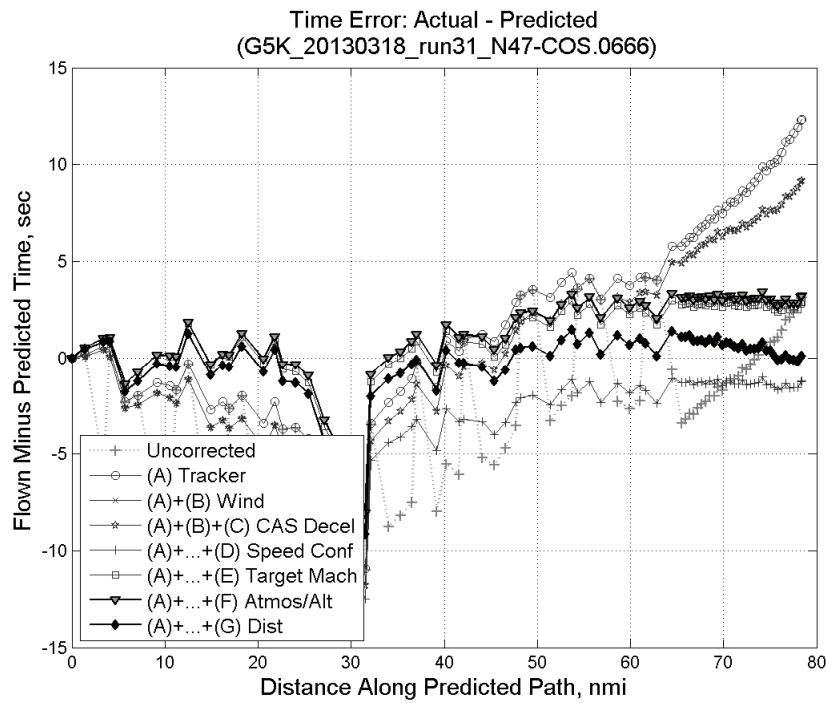


**Figure 548:** Time error for run 31 showing incremental effect of removing each error source.

### C.21.A. Tracker Jumps

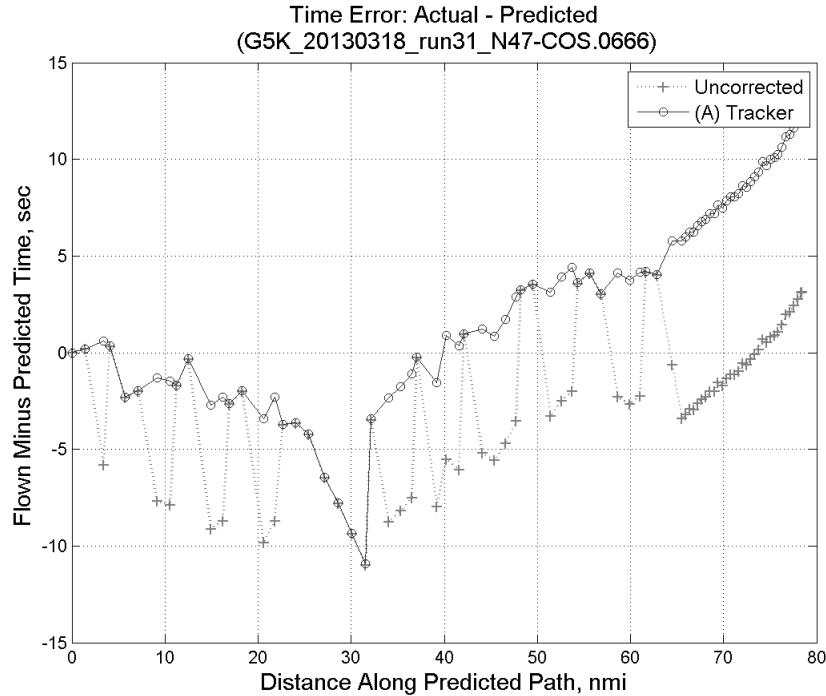


**Figure 549:** Time error for run 31 before (Uncorrected) and after ((A) Tracker) removing tracker jump error source.

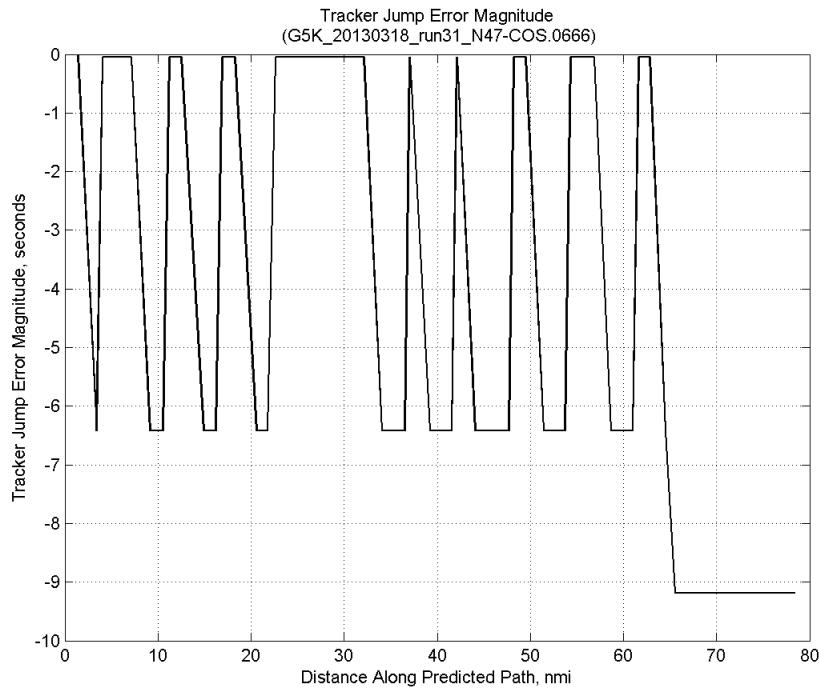


**Figure 550: Effect of tracker jump error source on time error for run 31.**

### C.21.B. Wind

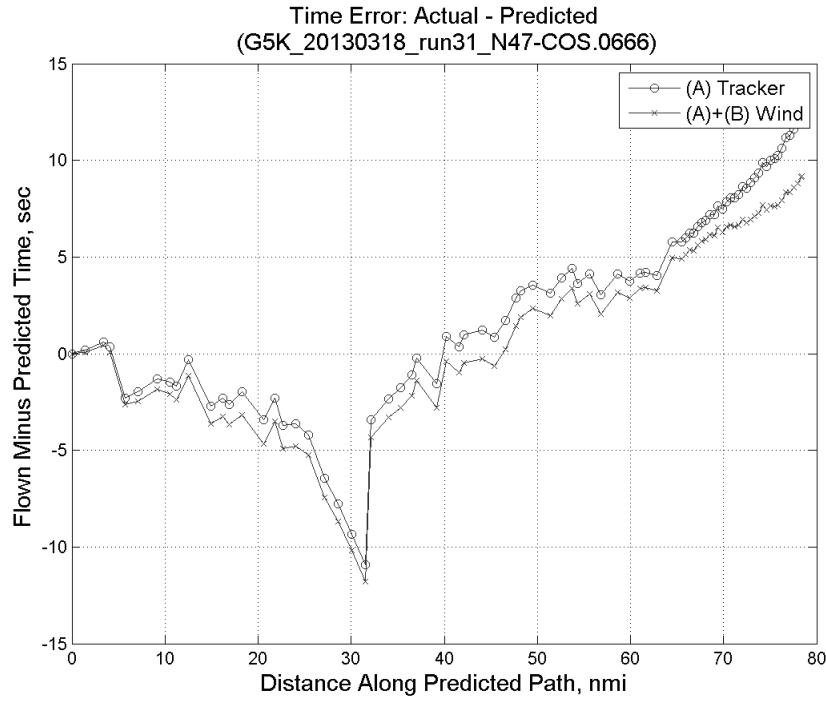


**Figure 551: Time error for run 31 before ((A) Tracker) and after ((A)+(B) Wind) removing wind error source.**

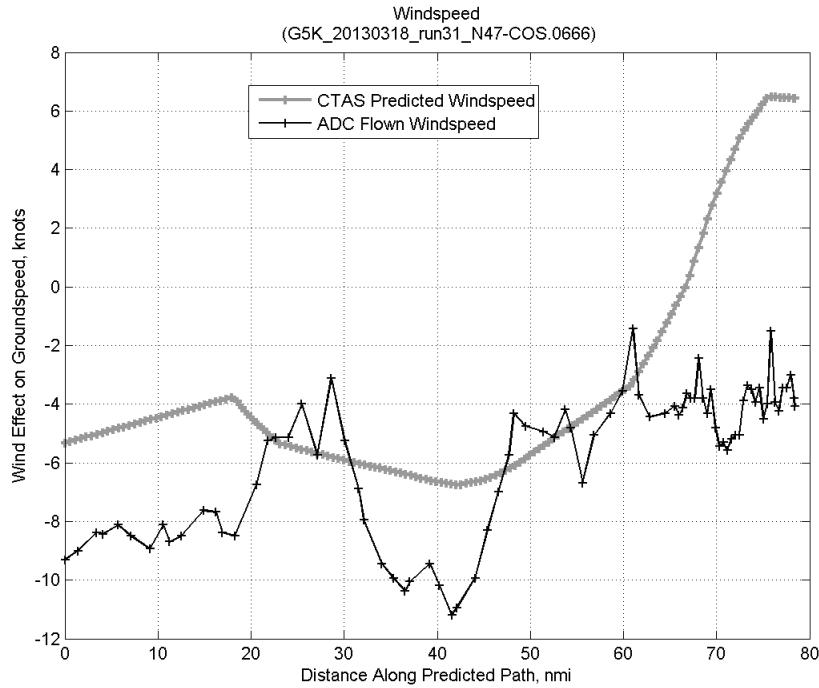


**Figure 552: CTAS predicted and ADC flown wind effect on ground speed for run 31. Negative values indicate a headwind.**

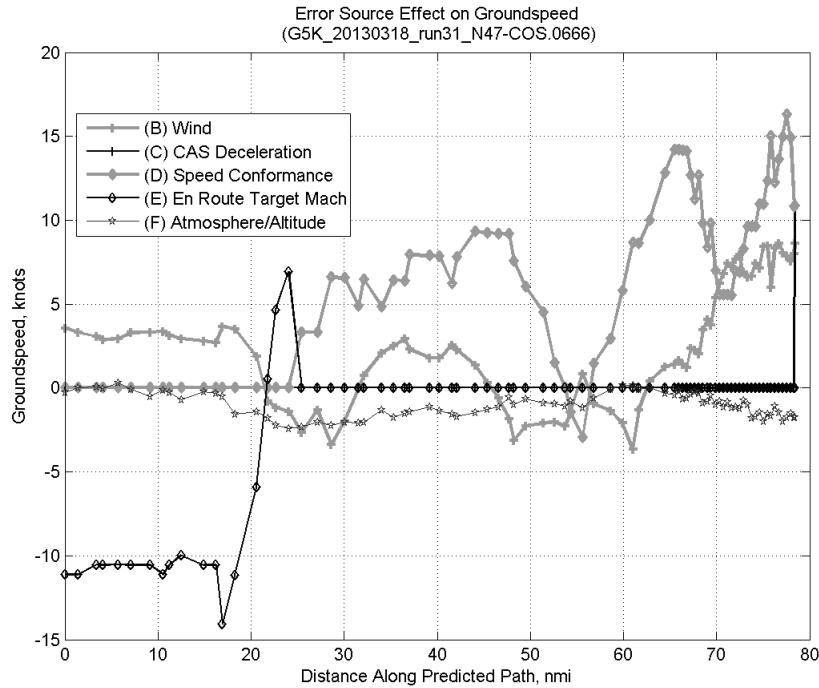


**Figure 553: Error sources (flown minus predicted) converted to a ground speed effect for run 31. Positive values indicate the flown ground speed was faster than the CTAS prediction.**

### C.21.C. CAS Deceleration

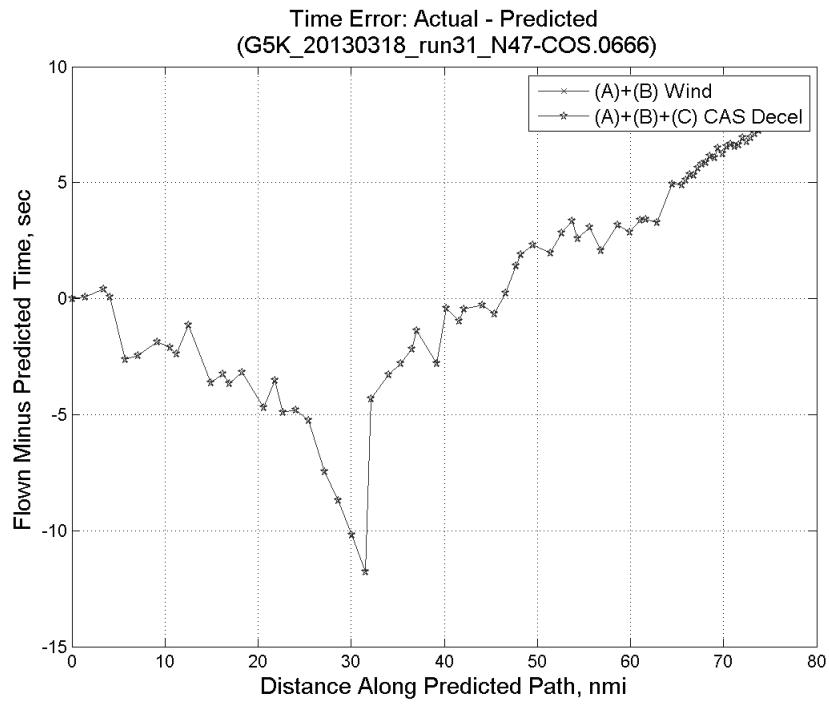


**Figure 554:** Time error for run 31 before ((A)+(B) Wind) and after ((A)+(B)+(C) CAS Decel) removing CAS deceleration error source.

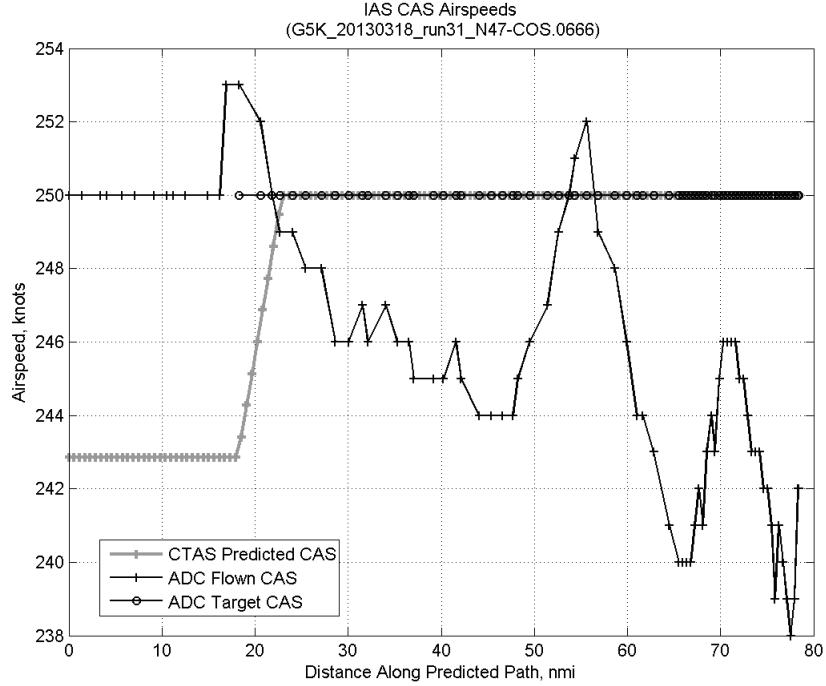


**Figure 555:** CTAS predicted and ADC flown CAS for run 31. CAS that is being targeted is shown with circle markers.

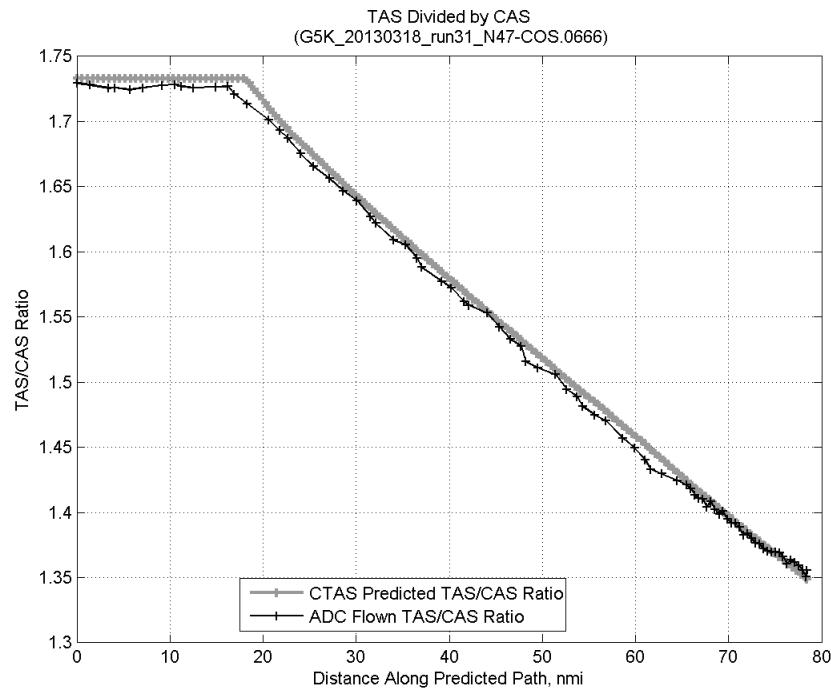


**Figure 556: CTAS predicted and ADC flown TAS/CAS ratio for run 31.**

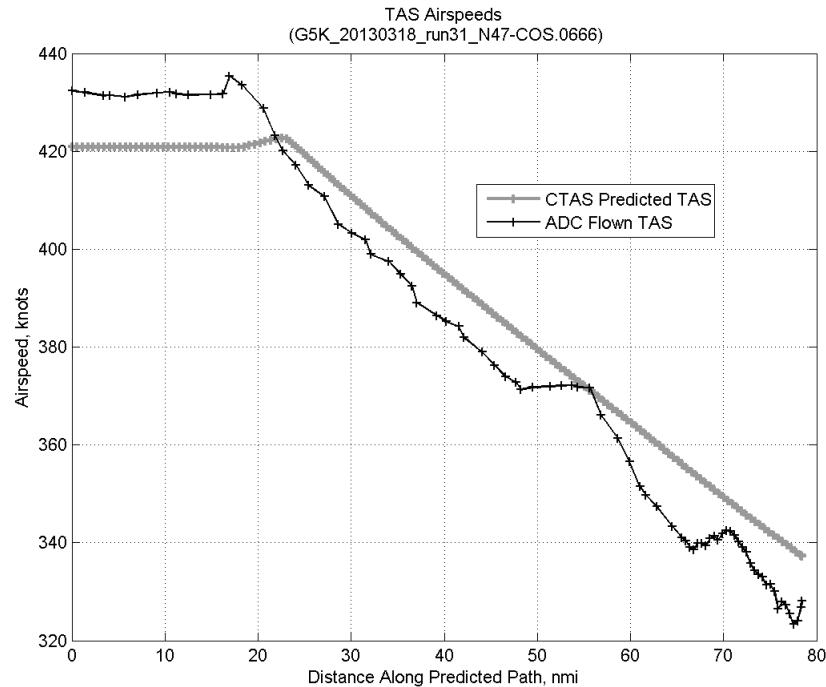


**Figure 557: CTAS predicted and ADC flown TAS for run 31.**

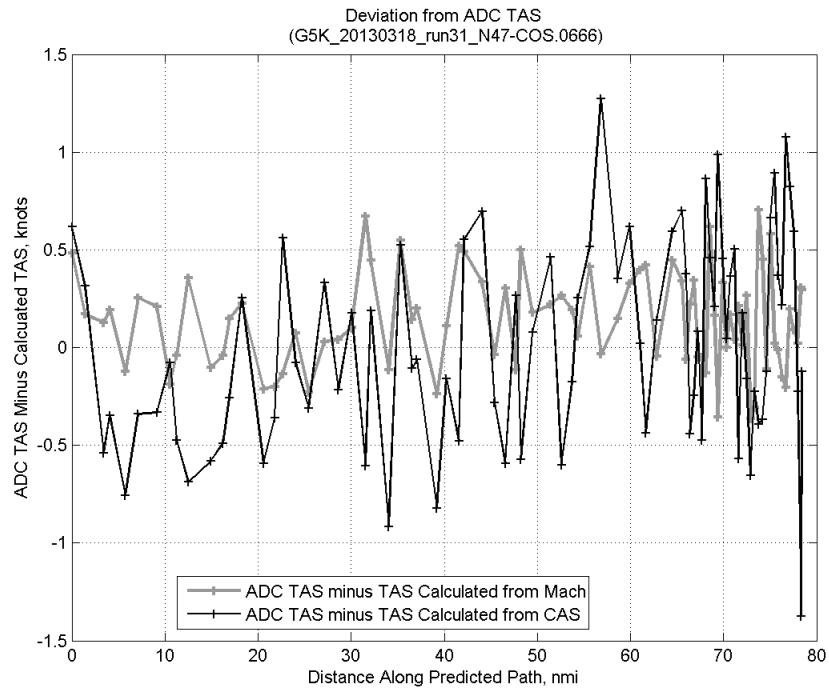


**Figure 558:** Deviation from ADC flown TAS if calculating TAS using ADC flown CAS, Mach, atmospheric temperature, and atmospheric pressure for run 31.

#### C.21.D. Speed Conformance

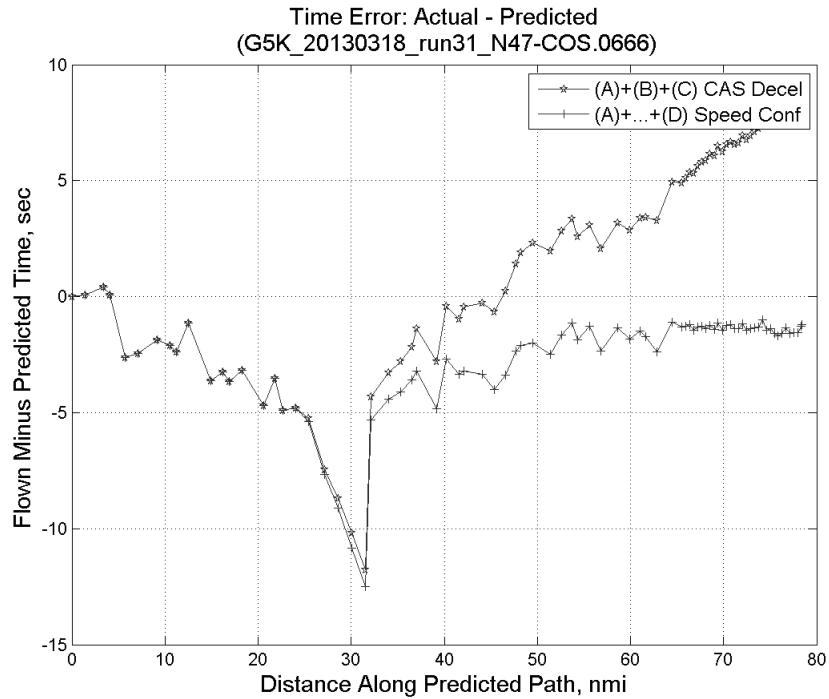


**Figure 559:** Time error for run 31 before ((A)+(B)+(C) CAS Decel) and after ((A)+...+(D) Speed Conf) removing speed conformance error source.

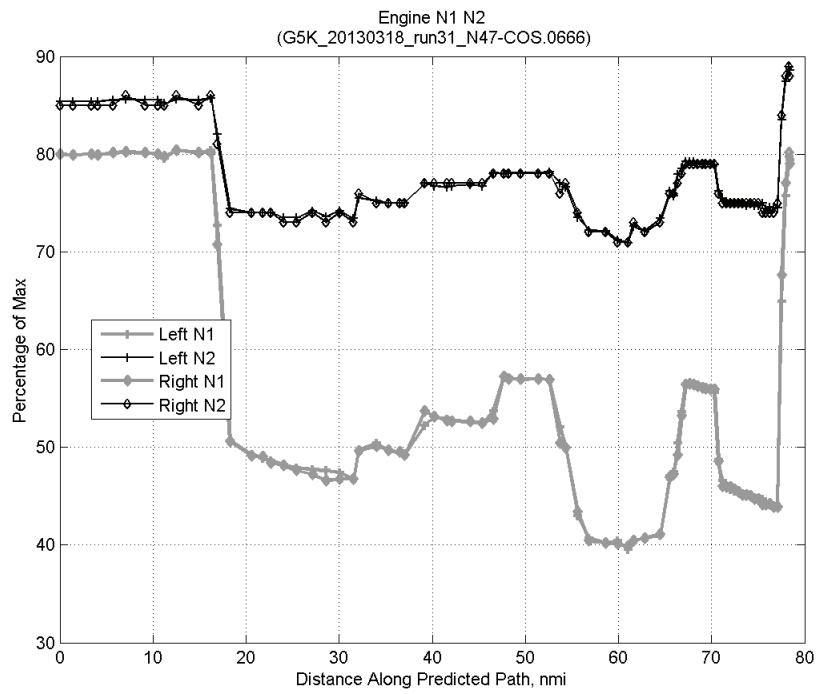


**Figure 560: Flown engine N1 and N2 for run 31.**

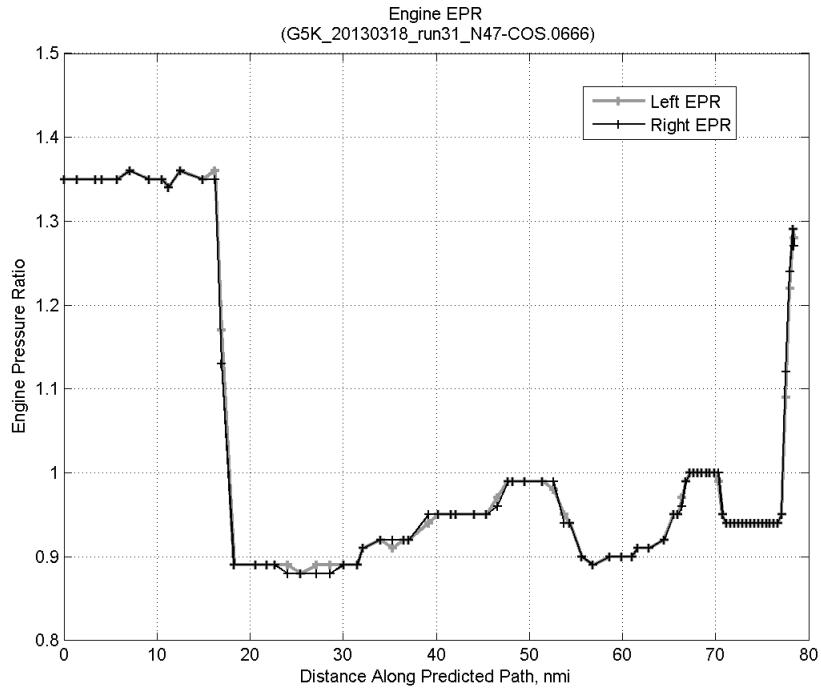


**Figure 561: Flown engine EPR for run 31.**

### C.21.E. Target Mach

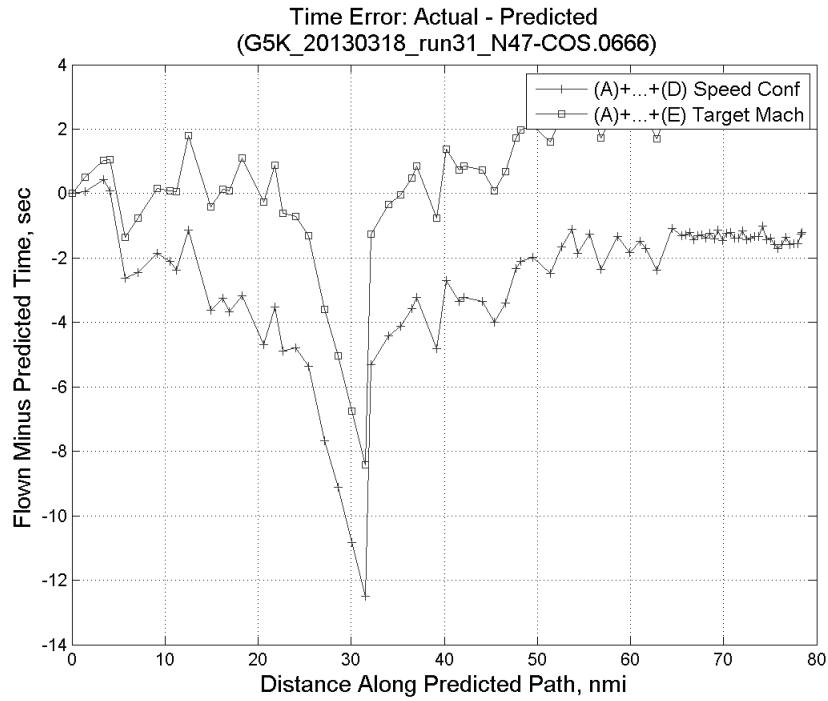


**Figure 562:** Time error for run 31 before ((A)+...+(D) Speed Conf) and after ((A)+...+(E) Target Mach) removing target Mach error source.

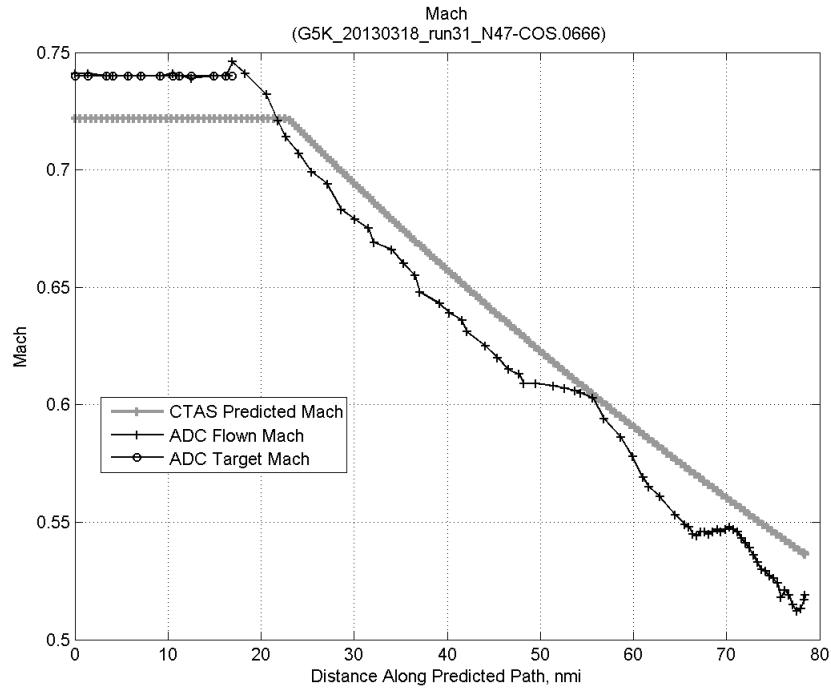


**Figure 563:** CTAS predicted and ADC flown Mach for run 31. Mach being targeted (ADC) shown with circle markers.

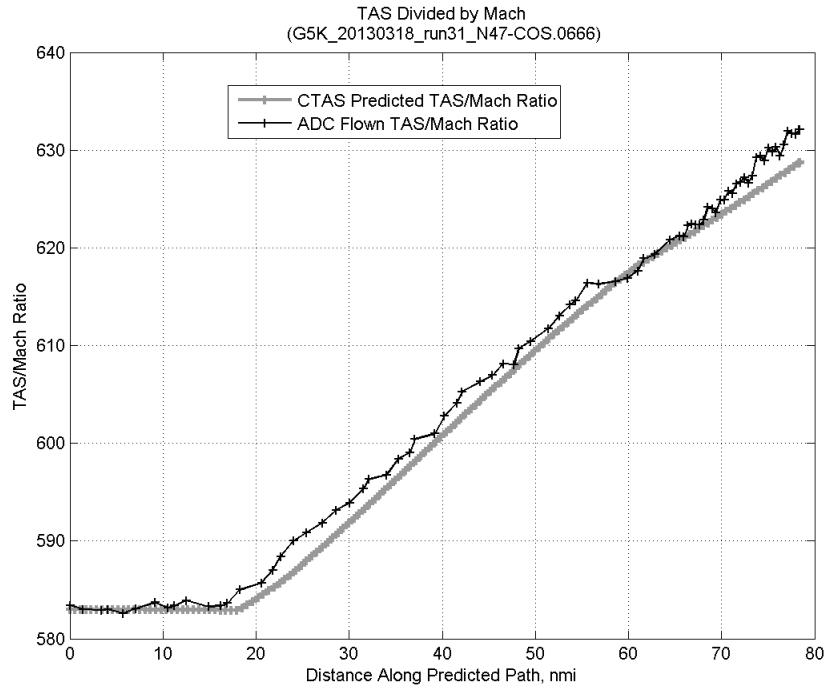


**Figure 564:** CTAS predicted and ADC flown TAS/Mach ratio for run 31.

#### C.21.F. Atmosphere/Altitude

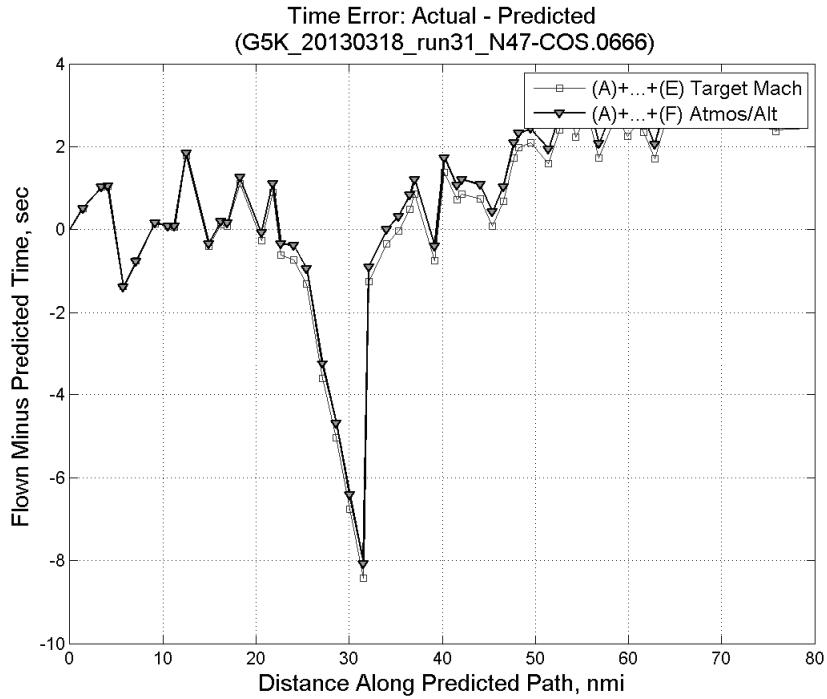


**Figure 565:** Time error for run 31 before ((A)+...+(E) Target Mach) and after ((A)+...+(F) Atmos/Alt) removing atmosphere/altitude error source.

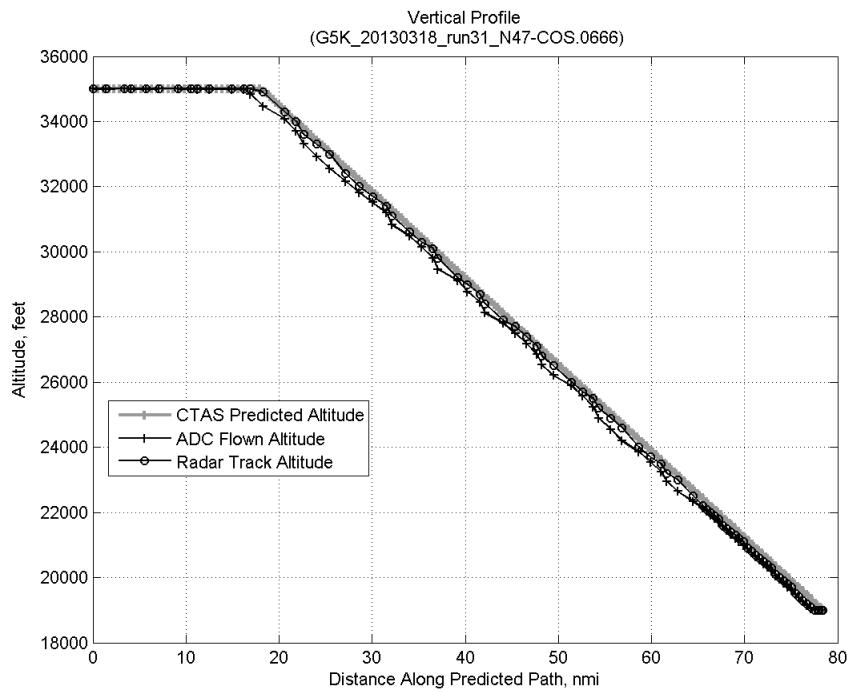


**Figure 566: Flown (ADC) and predicted (CTAS) vertical profile for run 31.**

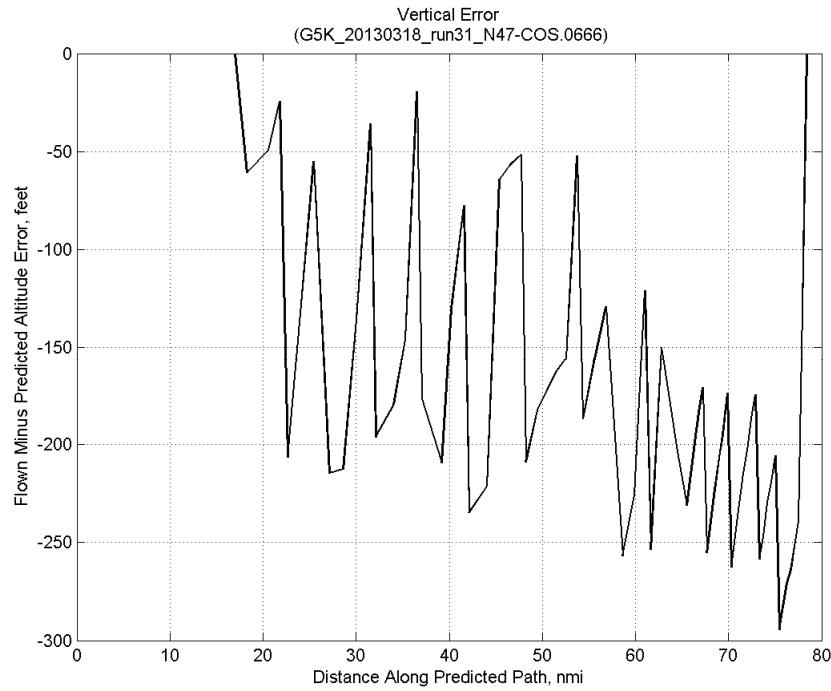


**Figure 567: Vertical error (flown minus predicted altitude) for run 31. Positive values indicate aircraft flew higher than predicted by CTAS.**

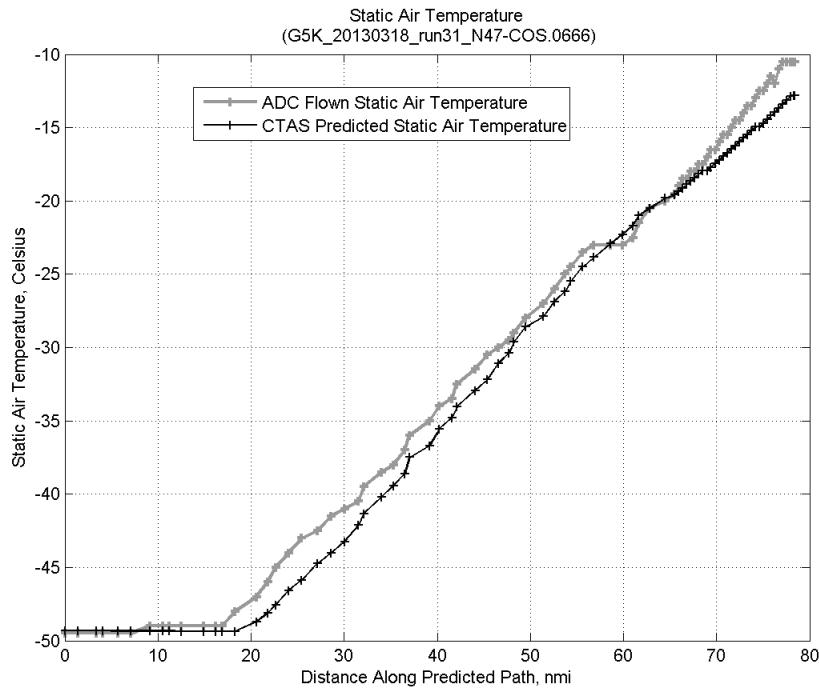


**Figure 568: Flown (ADC) and predicted (CTAS) static air temperature for run 31.**

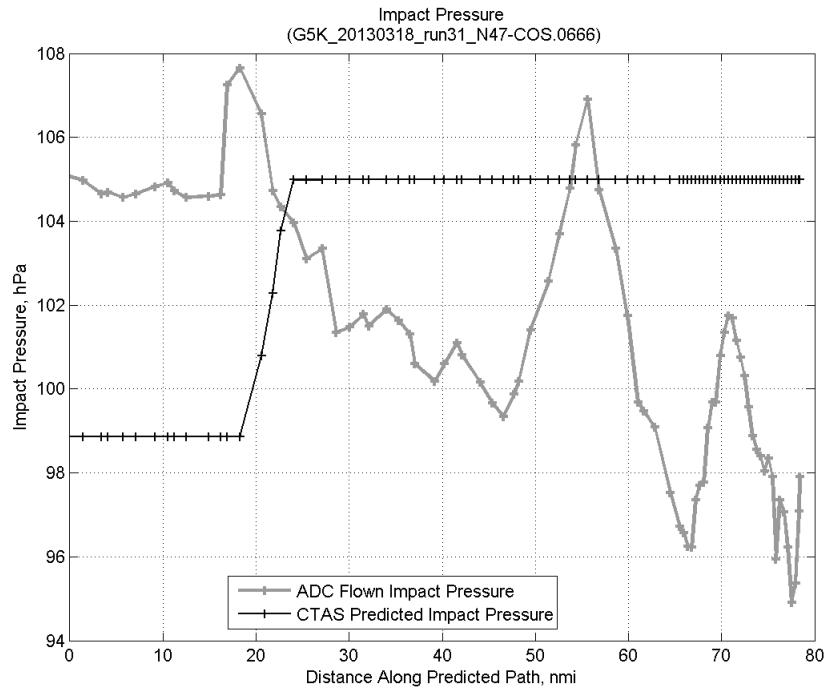


**Figure 569: Flown (ADC) and predicted (CTAS) impact pressure for run 31.**

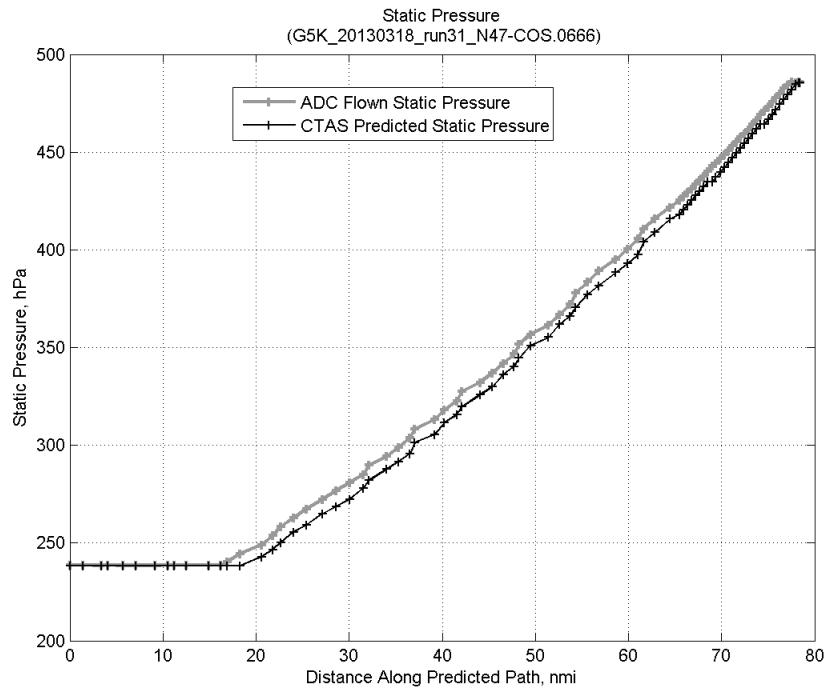


**Figure 570: Flown (ADC) and predicted (CTAS) static pressure for run 31.**

#### C.21.G. Path Distance

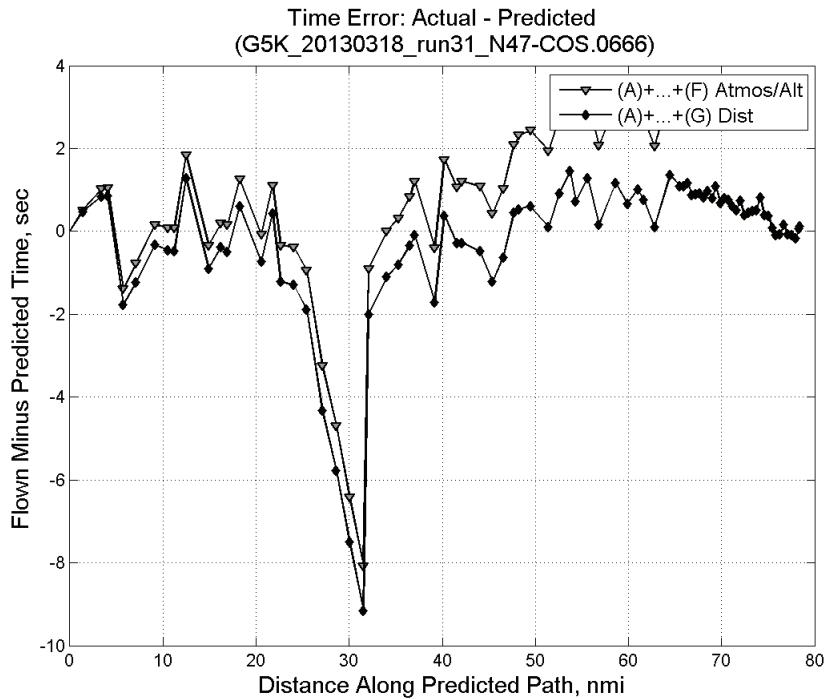


**Figure 571: Time error for run 31 before ((A)+...+(F) Atmos/Alt) and after ((A)+...+(G) Dist) removing path distance error source.**

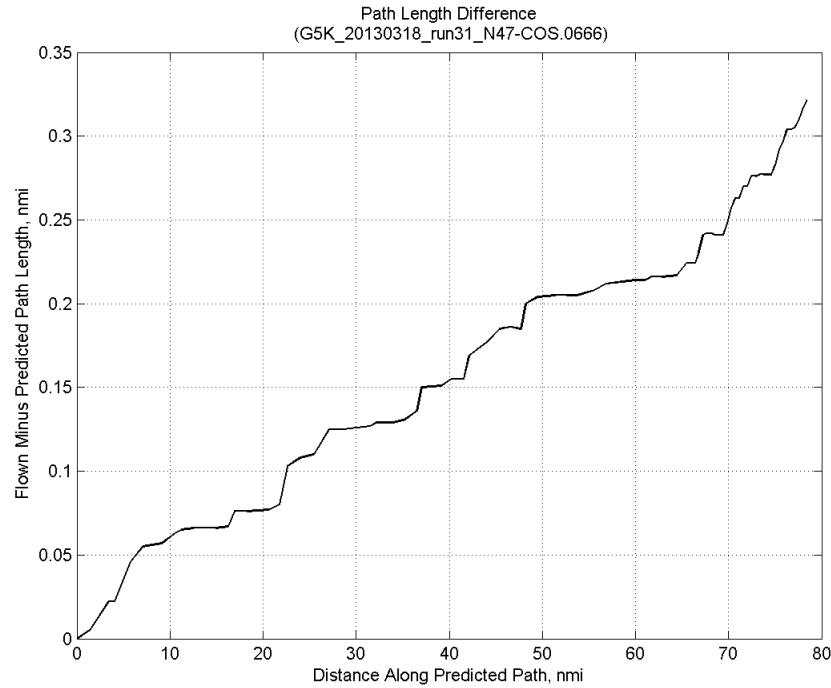


**Figure 572: ADC flown minus CTAS predicted path length for run 31. Positive values indicate aircraft followed a longer path than predicted by CTAS.**

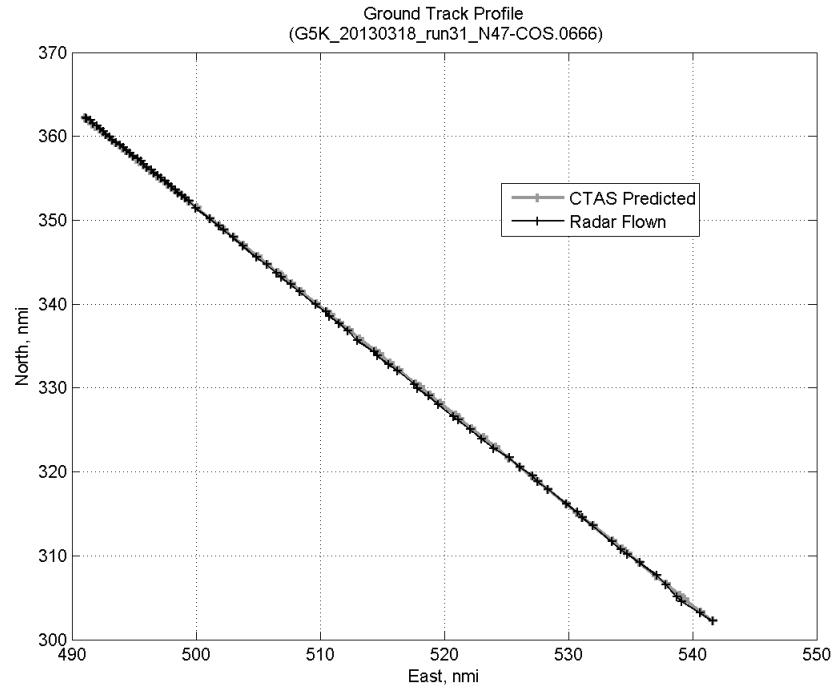


**Figure 573: CTAS predicted and radar flown ground track profile for run 31.**

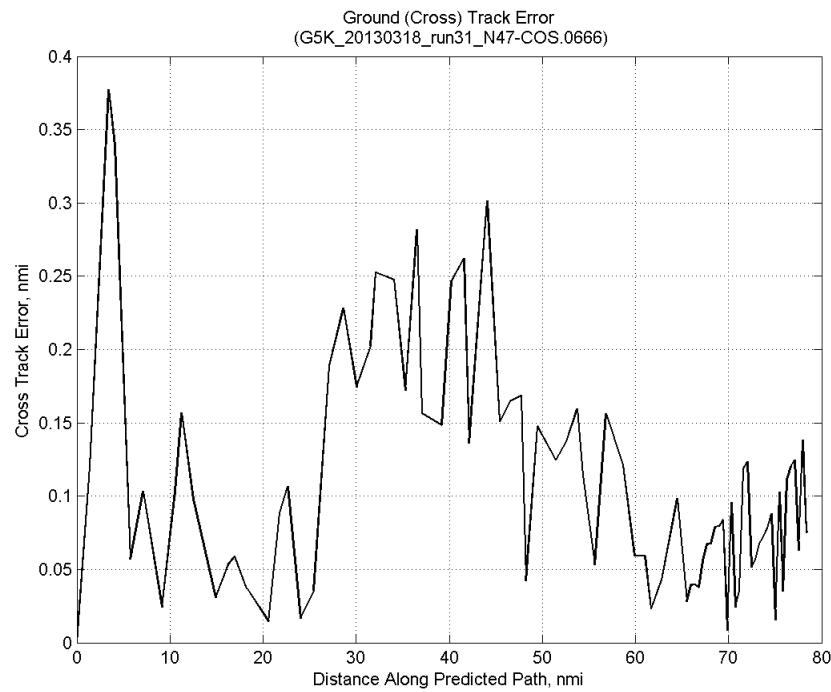


**Figure 574: Ground (cross) track error for run 31.**

## C.22. Run 32

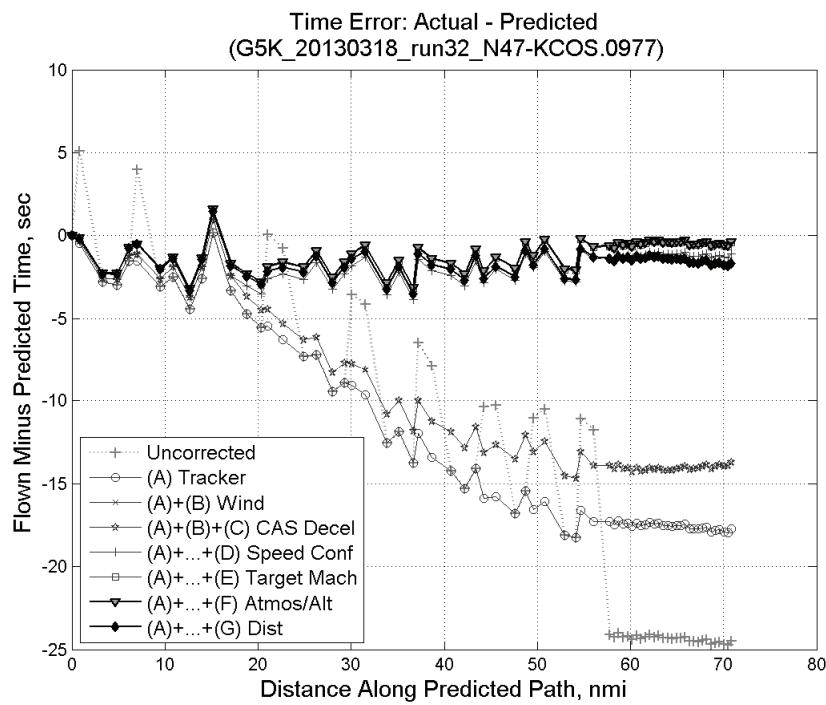


**Figure 575: Time error for run 32 showing incremental effect of removing each error source.**

### C.22.A. Tracker Jumps

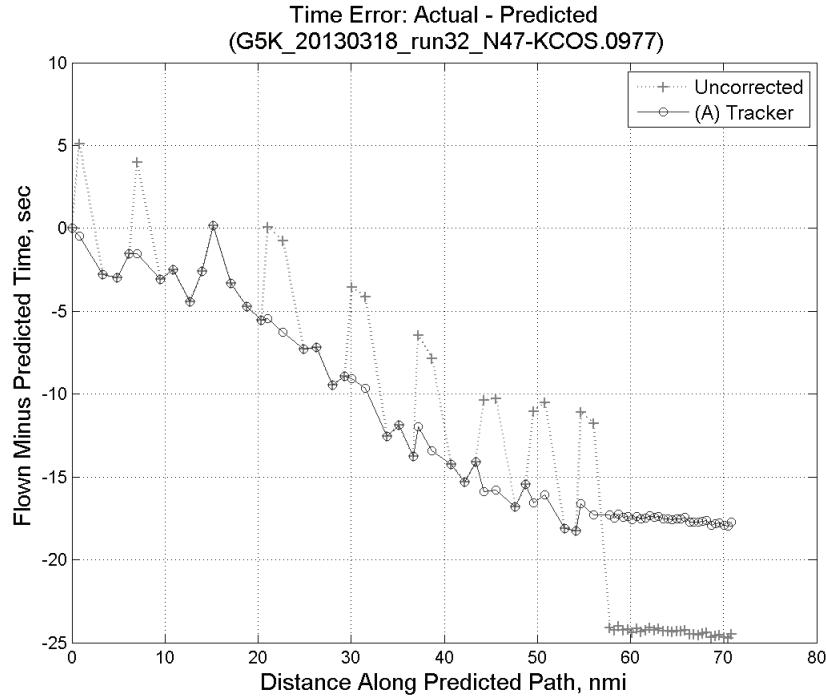


**Figure 576: Time error for run 32 before (Uncorrected) and after ((A) Tracker) removing tracker jump error source.**

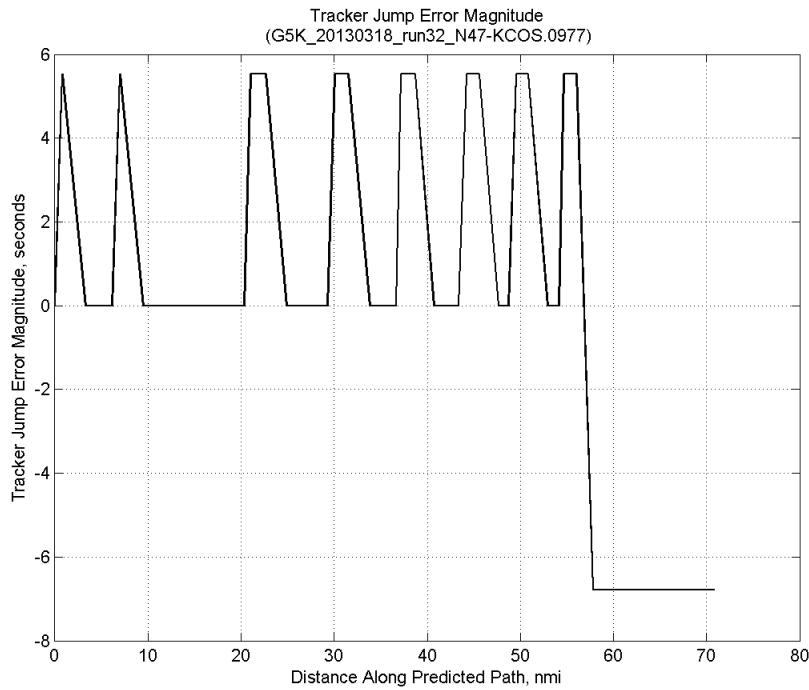


**Figure 577: Effect of tracker jump error source on time error for run 32.**

### C.22.B. Wind

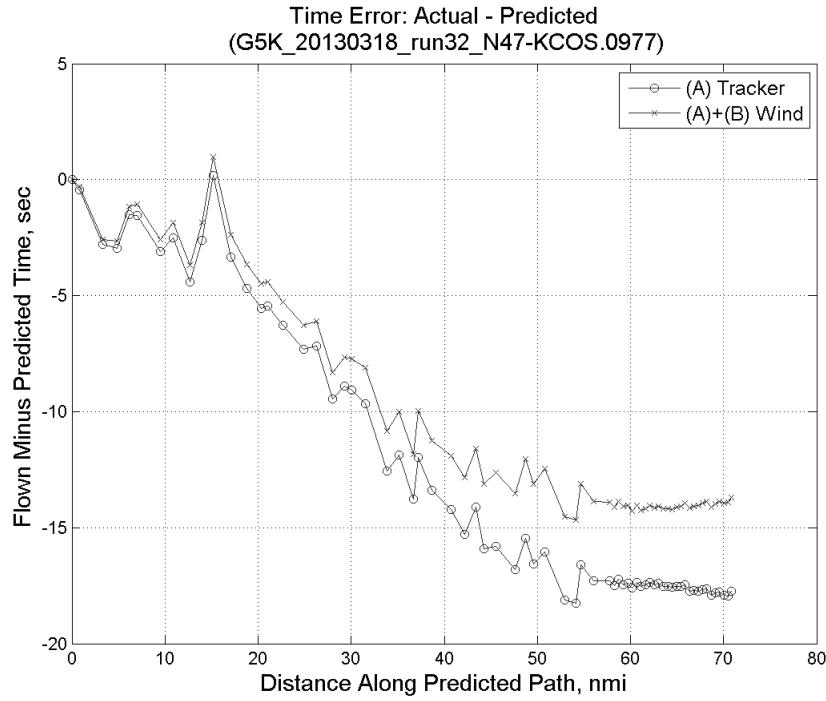


**Figure 578: Time error for run 32 before ((A) Tracker) and after ((A)+(B) Wind) removing wind error source.**

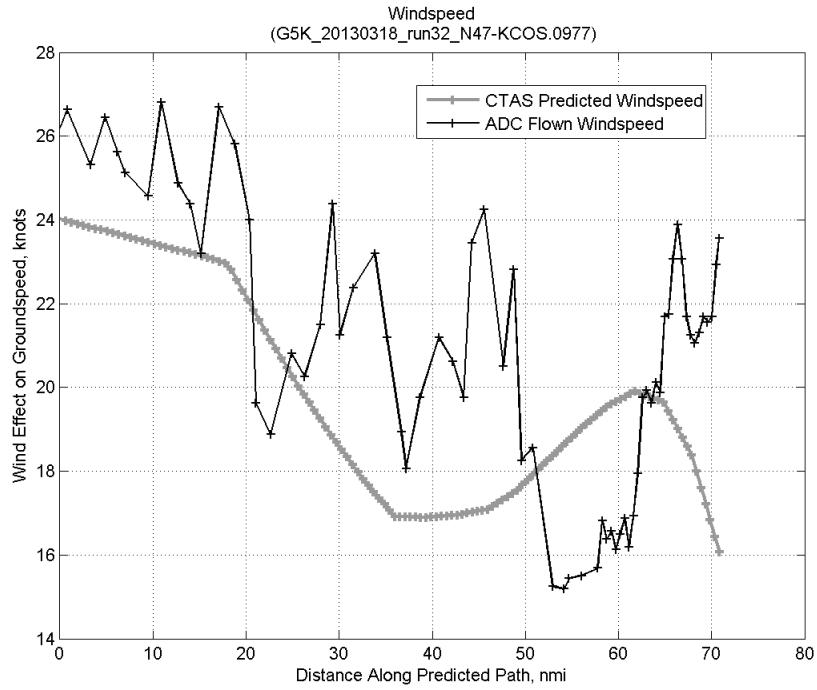


**Figure 579: CTAS predicted and ADC flown wind effect on ground speed for run 32. Negative values indicate a headwind.**

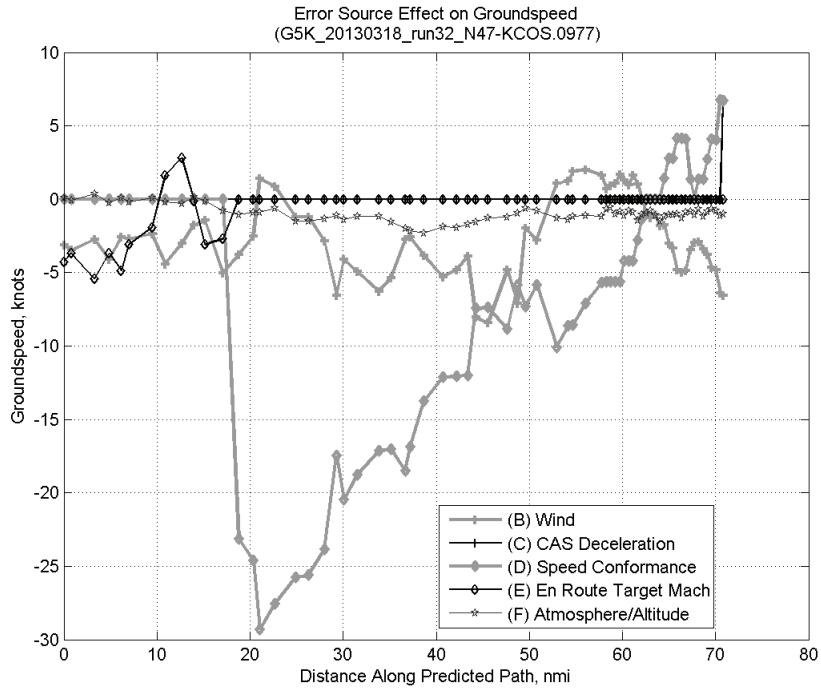


**Figure 580: Error sources (flown minus predicted) converted to a ground speed effect for run 32. Positive values indicate the flown ground speed was faster than the CTAS prediction.**

### C.22.C. CAS Deceleration

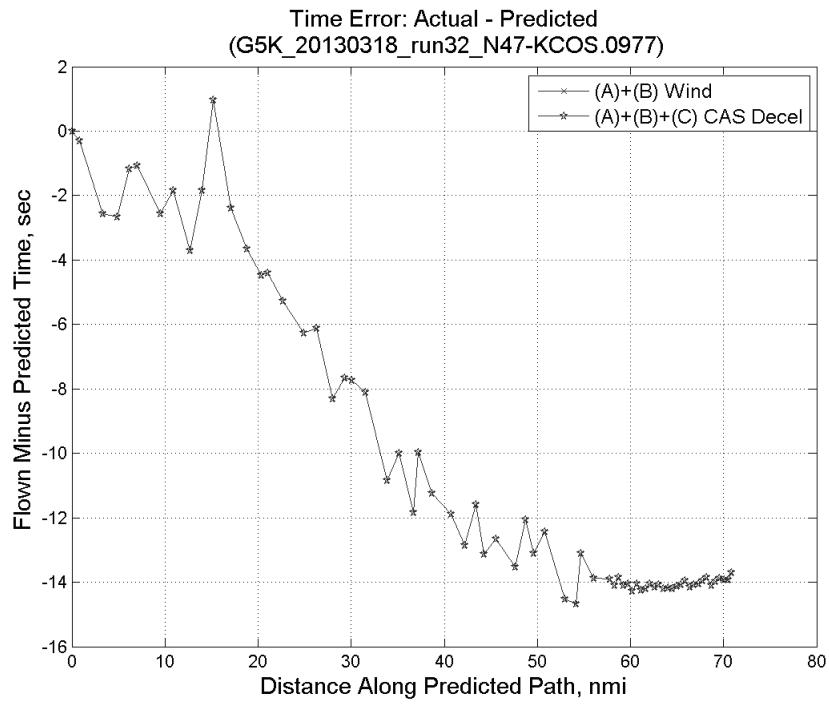


**Figure 581:** Time error for run 32 before ((A)+(B) Wind) and after ((A)+(B)+(C) CAS Decel) removing CAS deceleration error source.

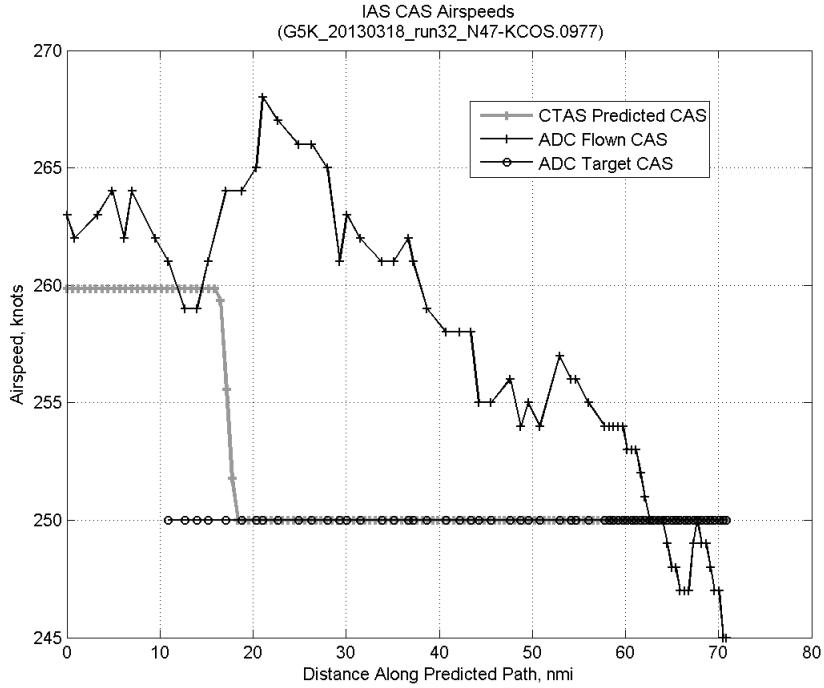


**Figure 582:** CTAS predicted and ADC flown CAS for run 32. CAS that is being targeted is shown with circle markers.

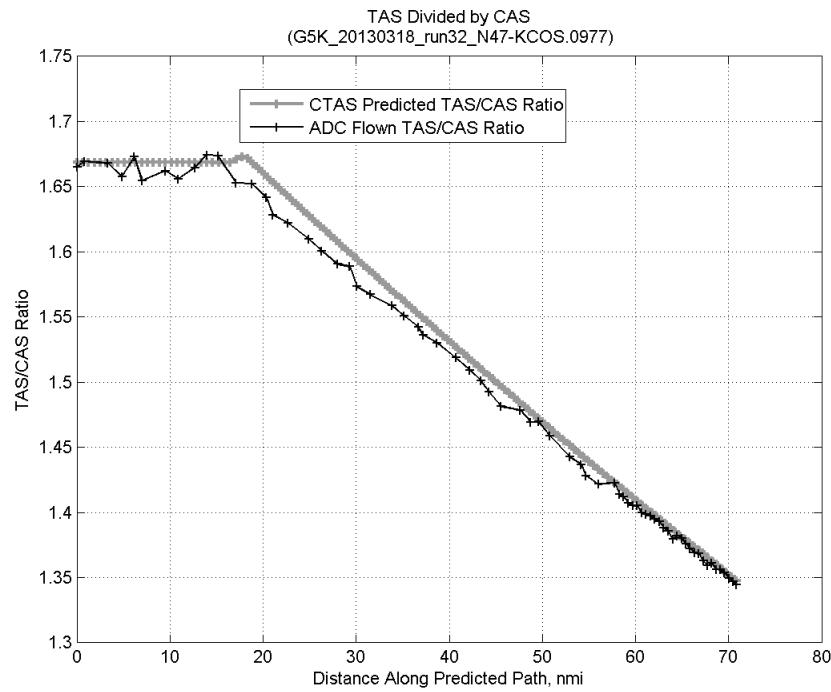


**Figure 583: CTAS predicted and ADC flown TAS/CAS ratio for run 32.**

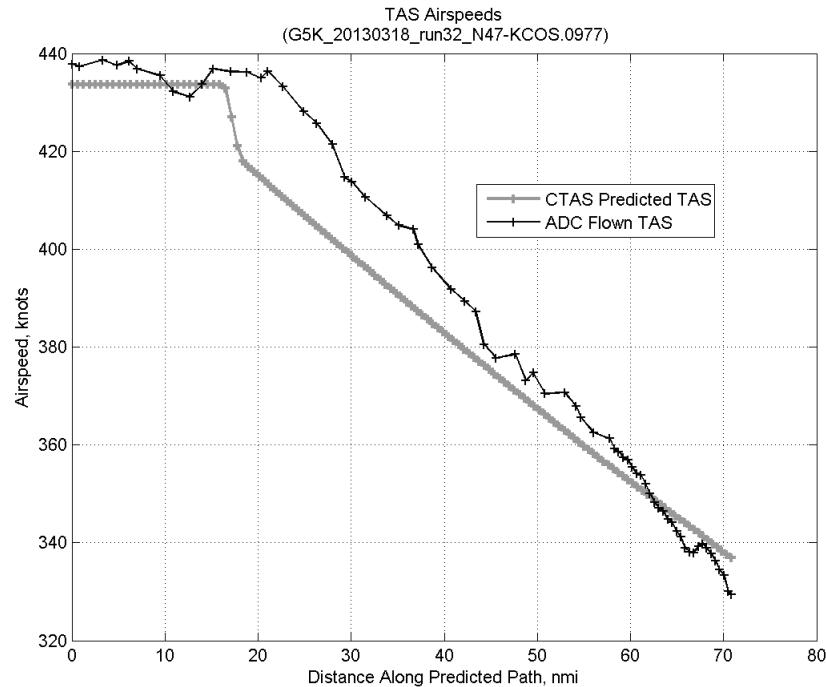


**Figure 584: CTAS predicted and ADC flown TAS for run 32.**

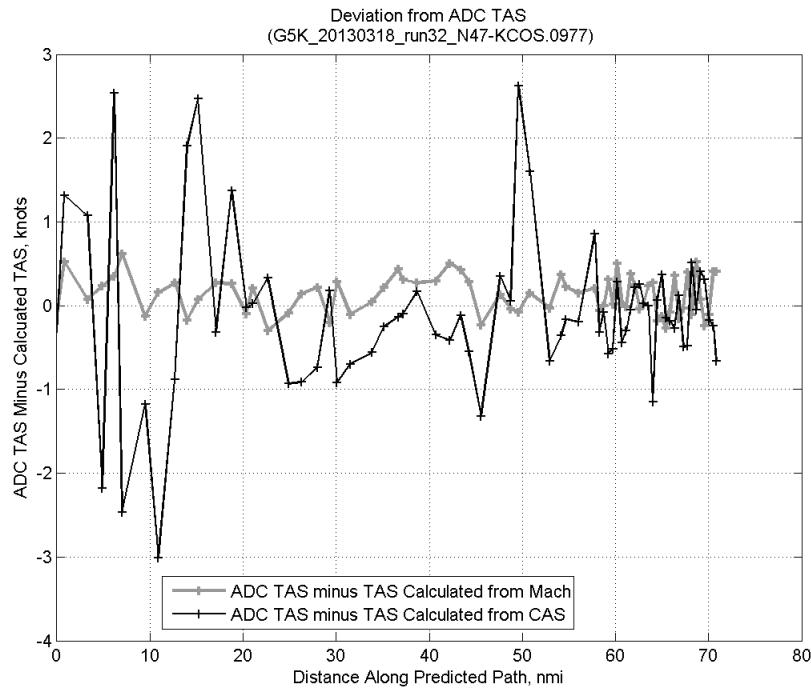


**Figure 585:** Deviation from ADC flown TAS if calculating TAS using ADC flown CAS, Mach, atmospheric temperature, and atmospheric pressure for run 32.

#### C.22.D. Speed Conformance

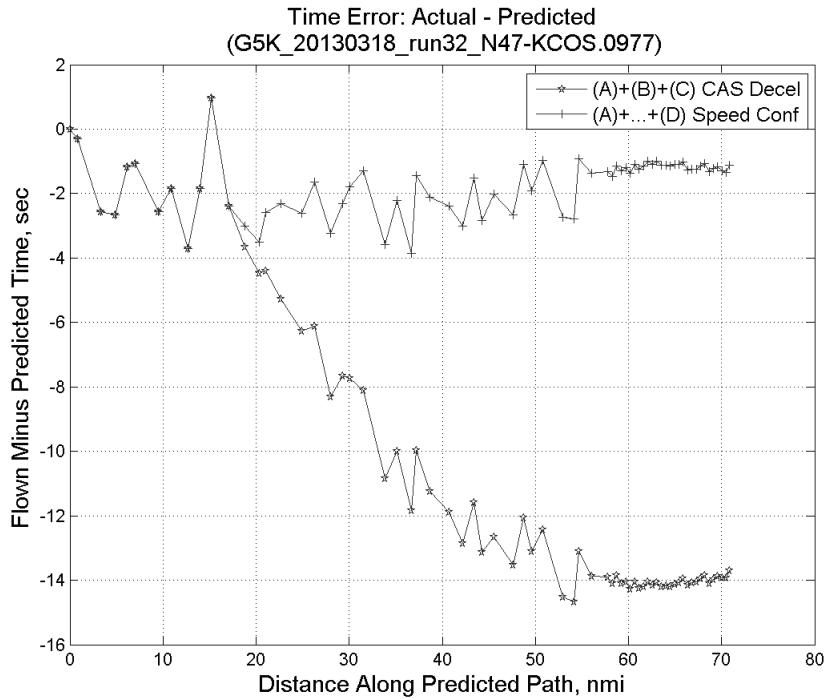


**Figure 586:** Time error for run 32 before  $((A)+(B)+(C) \text{ CAS Decel})$  and after  $((A)+\dots+(D) \text{ Speed Conf})$  removing speed conformance error source.

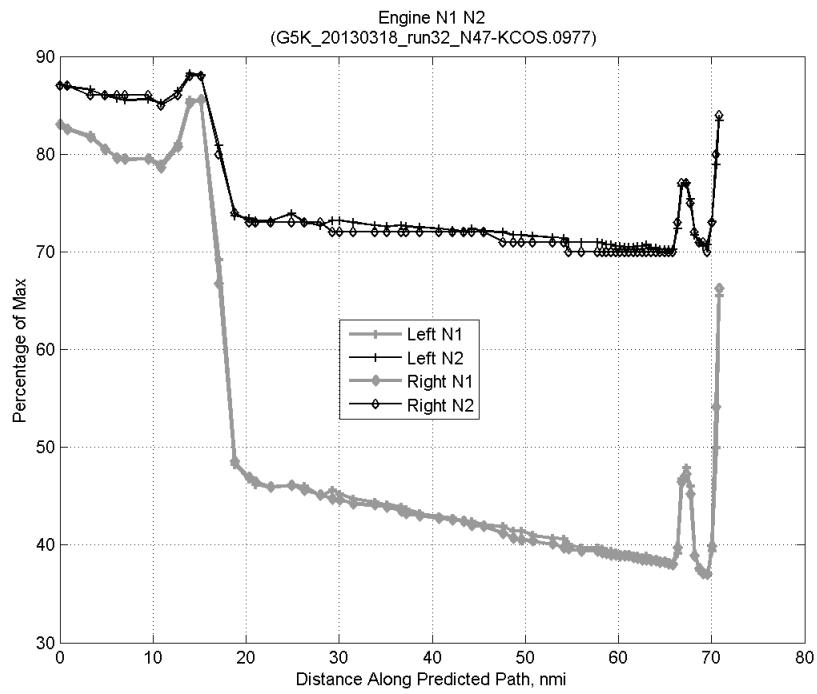


**Figure 587: Flown engine N1 and N2 for run 32.**

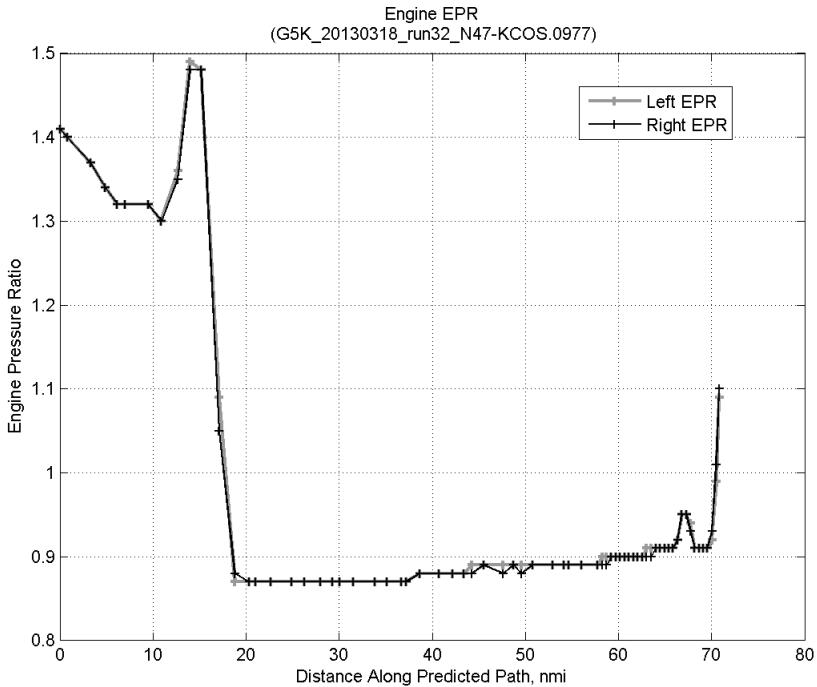


**Figure 588: Flown engine EPR for run 32.**

### C.22.E. Target Mach

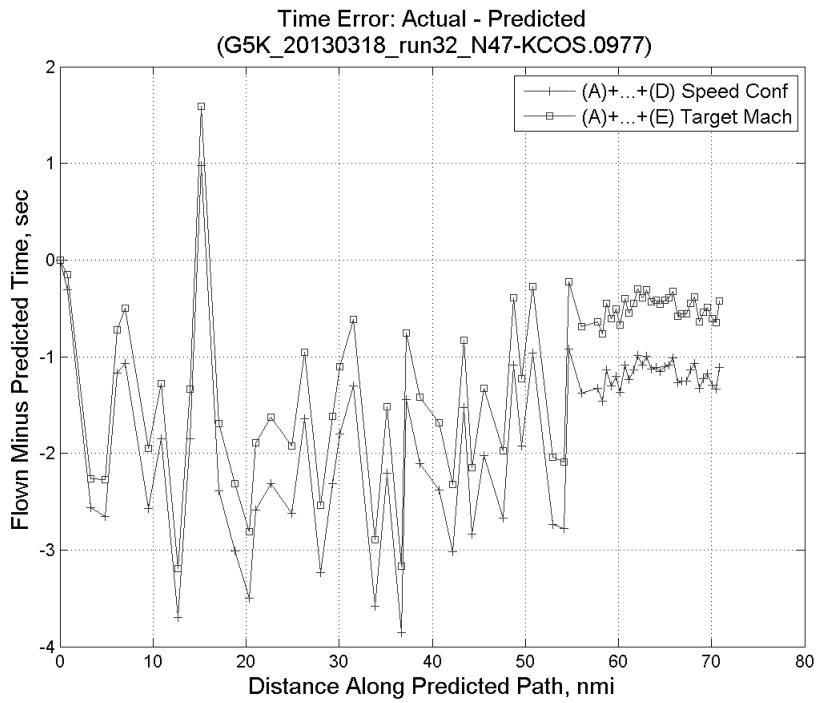


**Figure 589:** Time error for run 32 before ((A)+...+(D) Speed Conf) and after ((A)+...+(E) Target Mach) removing target Mach error source.

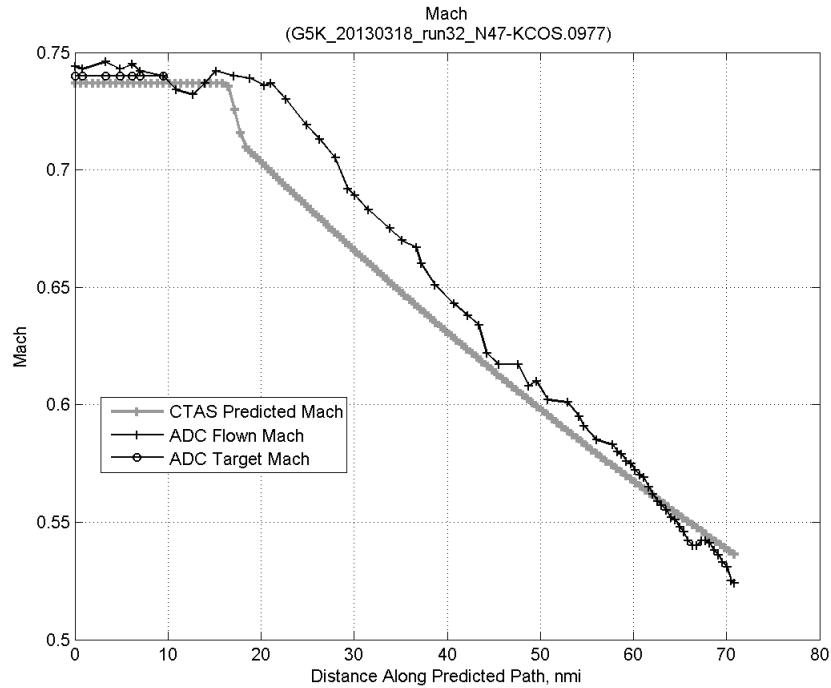


**Figure 590:** CTAS predicted and ADC flown Mach for run 32. Mach being targeted (ADC) shown with circle markers.

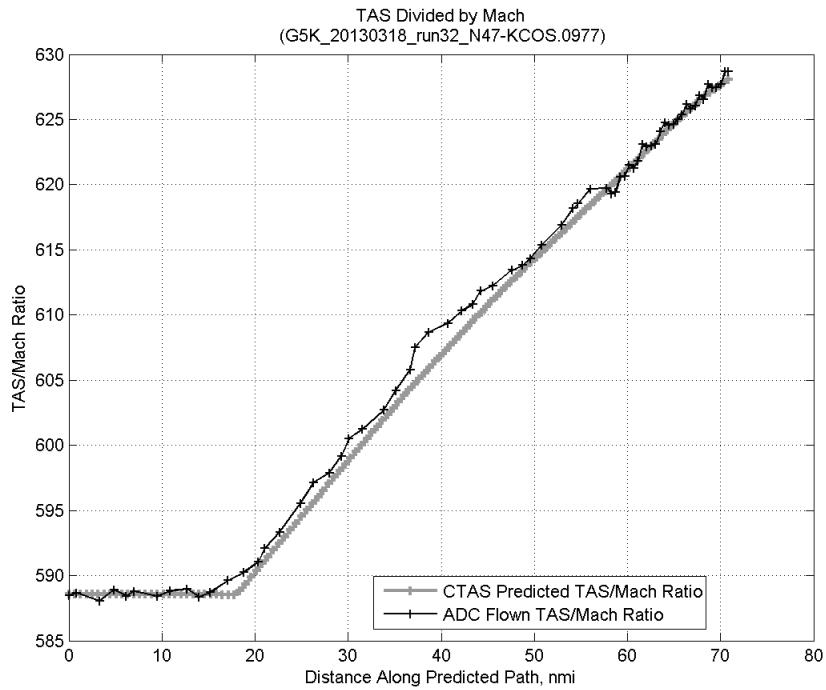


**Figure 591: CTAS predicted and ADC flown TAS/Mach ratio for run 32.**

#### C.22.F. Atmosphere/Altitude

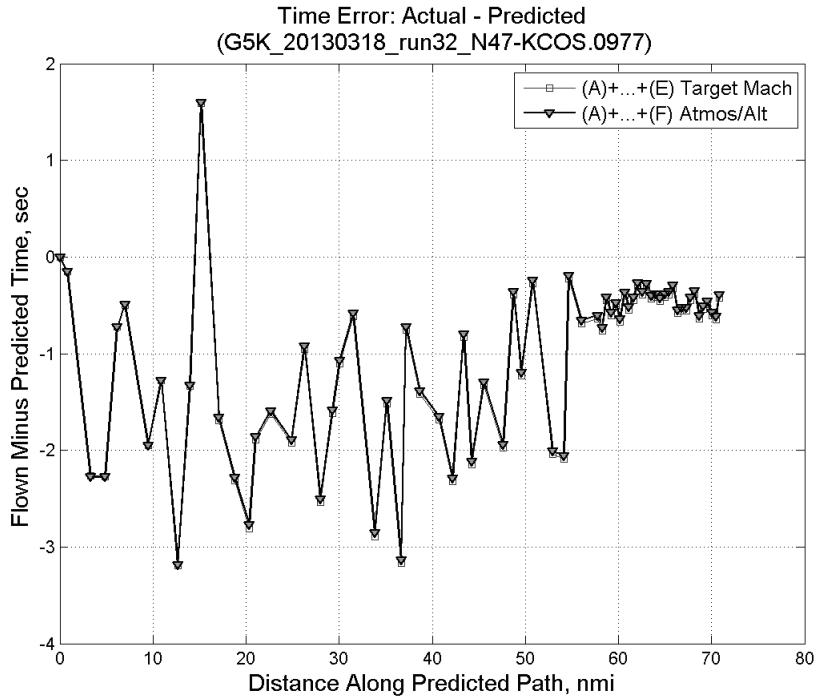


**Figure 592: Time error for run 32 before ((A)+...+(E) Target Mach) and after ((A)+...+(F) Atmos/Alt) removing atmosphere/altitude error source.**

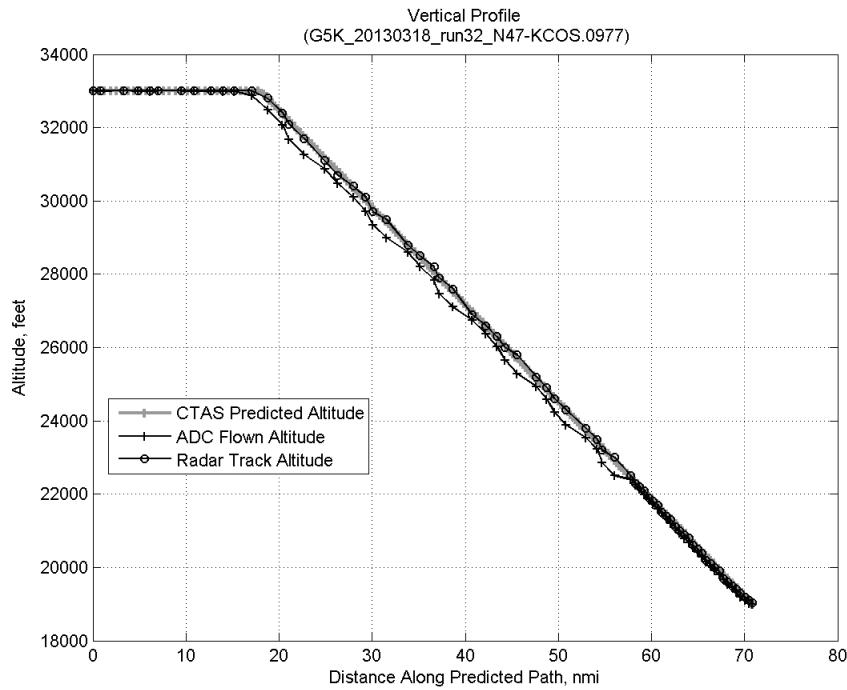


**Figure 593:** Flown (ADC) and predicted (CTAS) vertical profile for run 32.

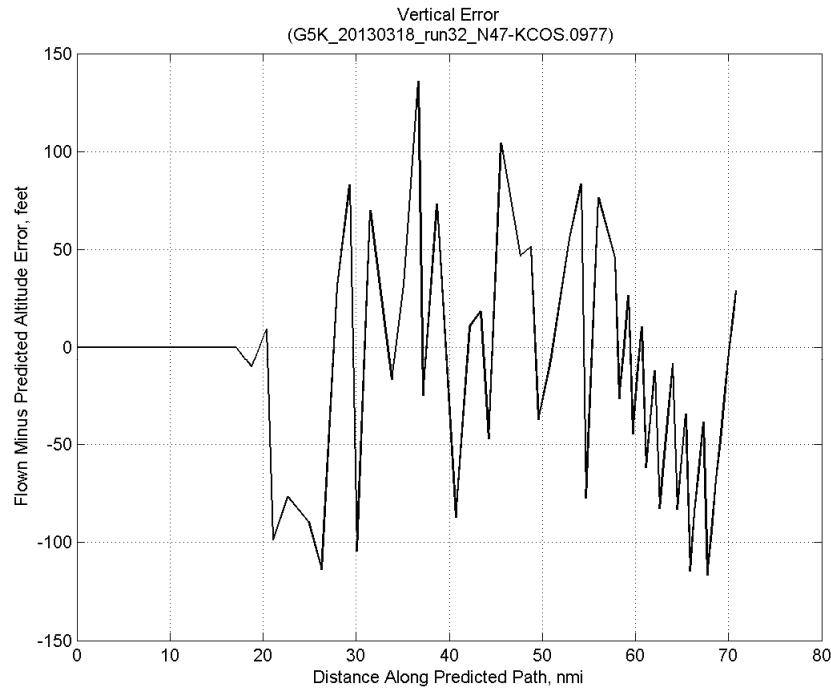


**Figure 594:** Vertical error (flown minus predicted altitude) for run 32. Positive values indicate aircraft flew higher than predicted by CTAS.

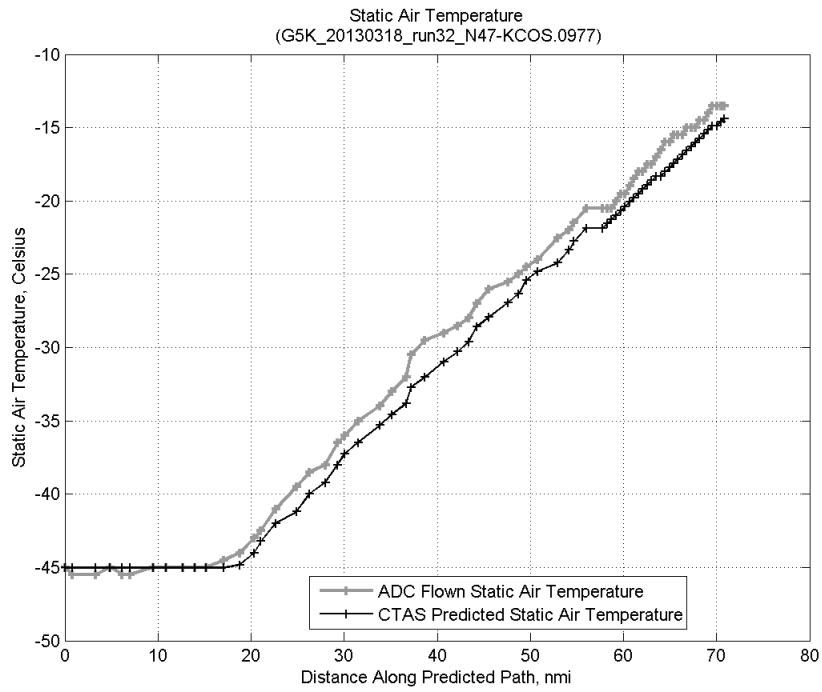


**Figure 595:** Flown (ADC) and predicted (CTAS) static air temperature for run 32.

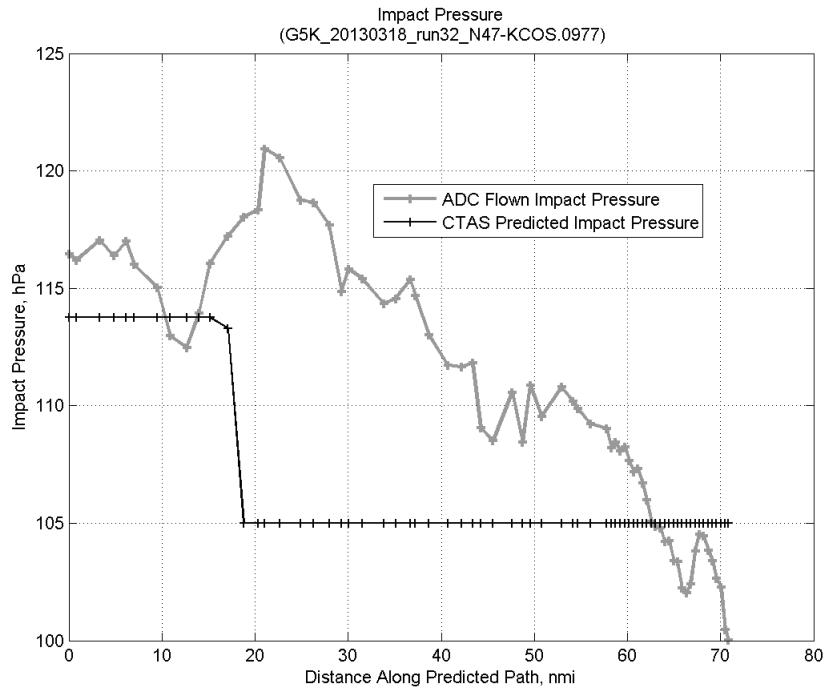


**Figure 596:** Flown (ADC) and predicted (CTAS) impact pressure for run 32.

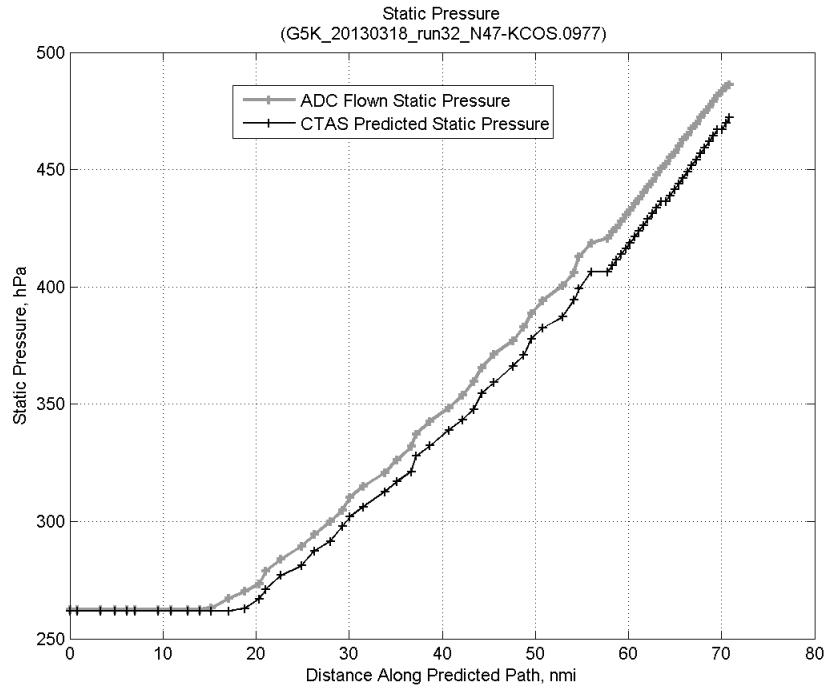


**Figure 597: Flown (ADC) and predicted (CTAS) static pressure for run 32.**

#### C.22.G. Path Distance

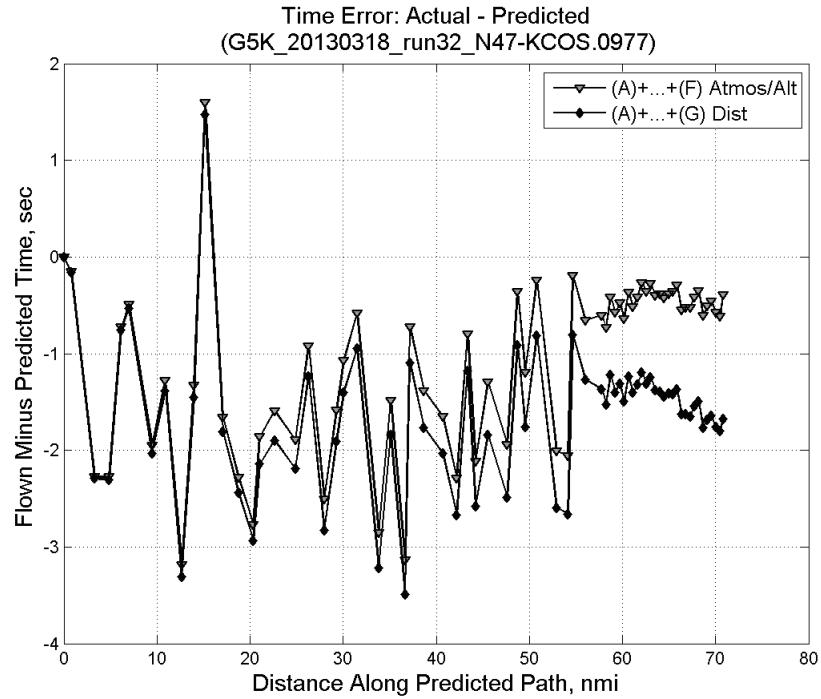


**Figure 598: Time error for run 32 before ((A)+...+(F) Atmos/Alt) and after ((A)+...+(G) Dist) removing path distance error source.**

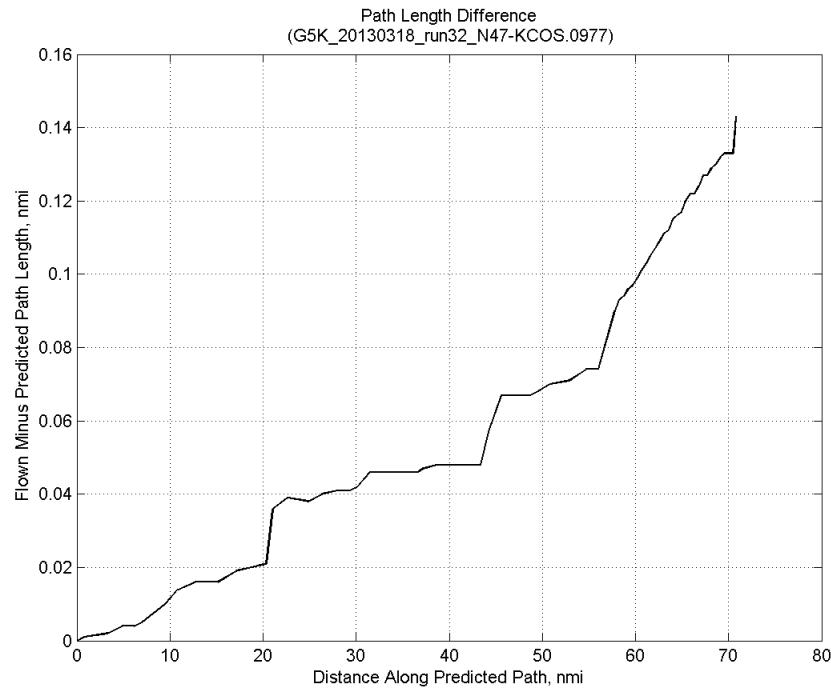


**Figure 599: ADC flown minus CTAS predicted path length for run 32. Positive values indicate aircraft followed a longer path than predicted by CTAS.**

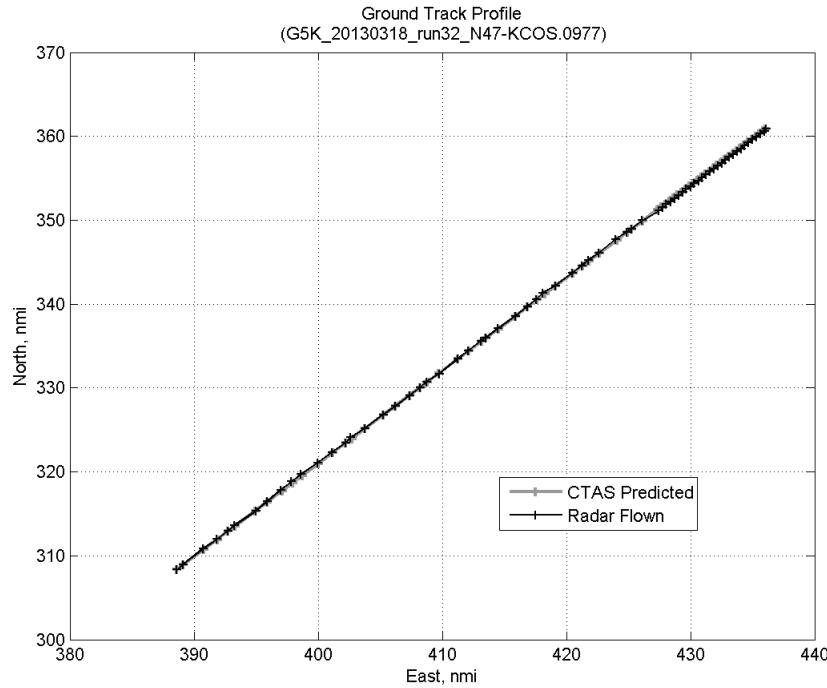


**Figure 600: CTAS predicted and radar flown ground track profile for run 32.**

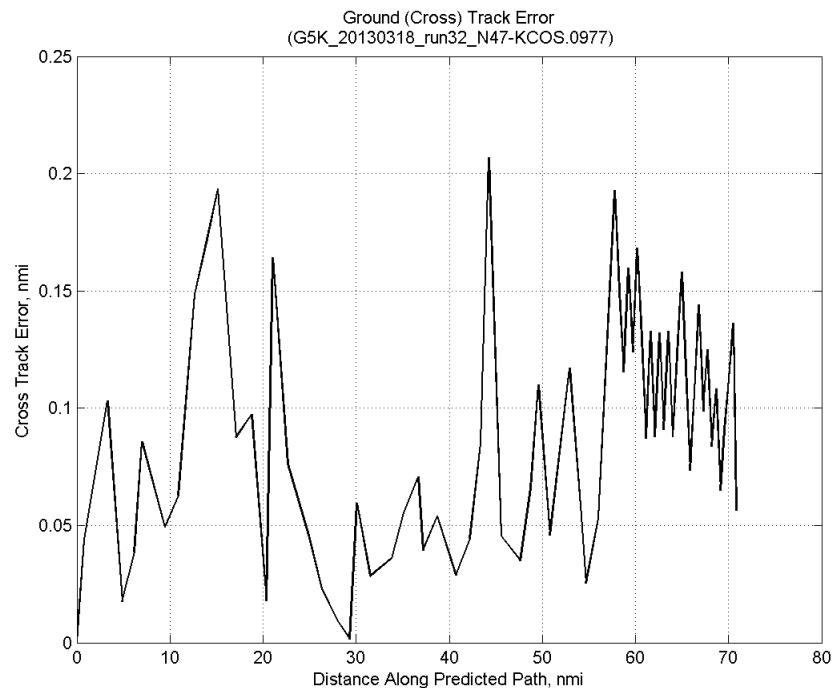


**Figure 601: Ground (cross) track error for run 32.**

### C.23. Run 34

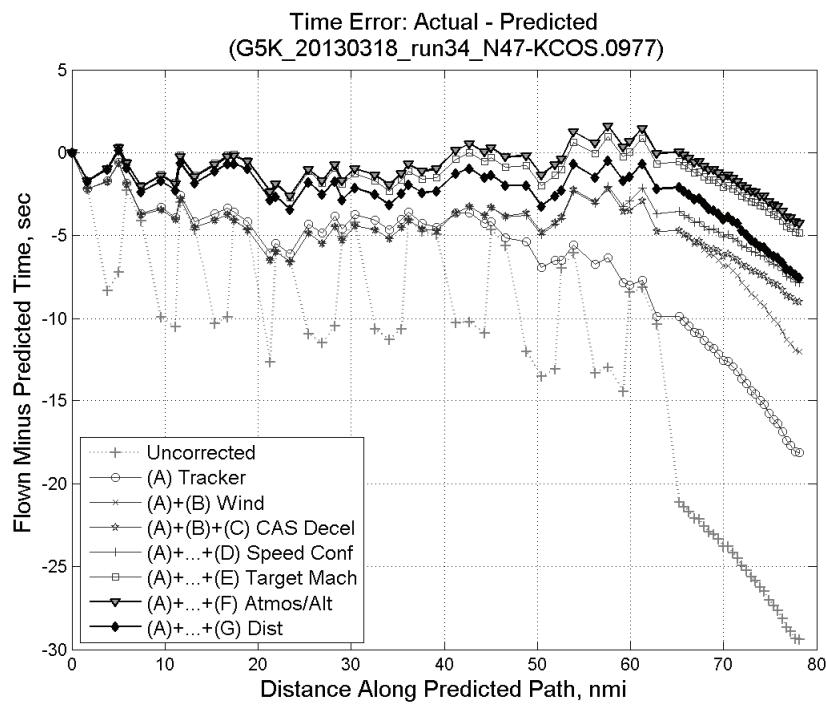


**Figure 602:** Time error for run 34 showing incremental effect of removing each error source.

#### C.23.A. Tracker Jumps

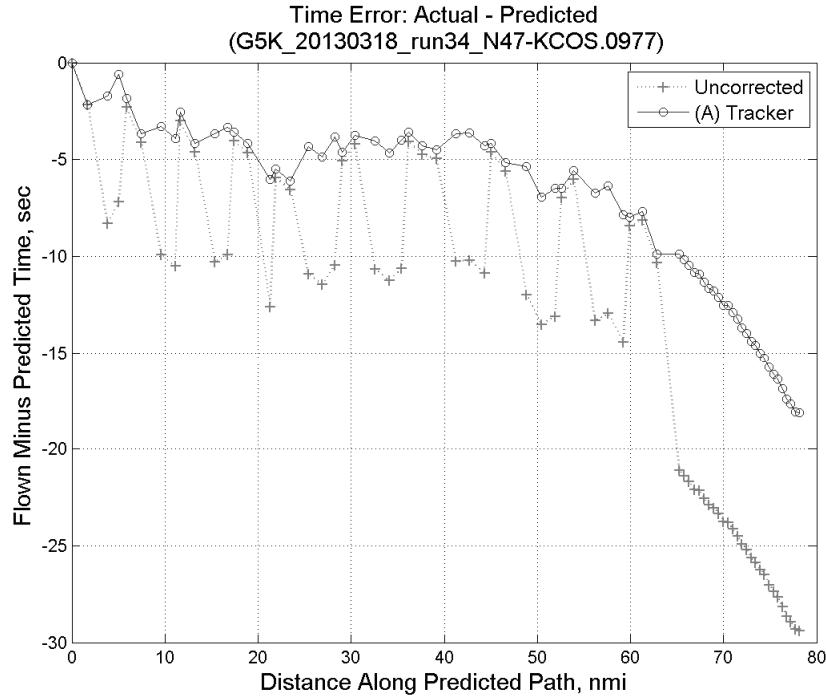


**Figure 603:** Time error for run 34 before (Uncorrected) and after ((A) Tracker) removing tracker jump error source.

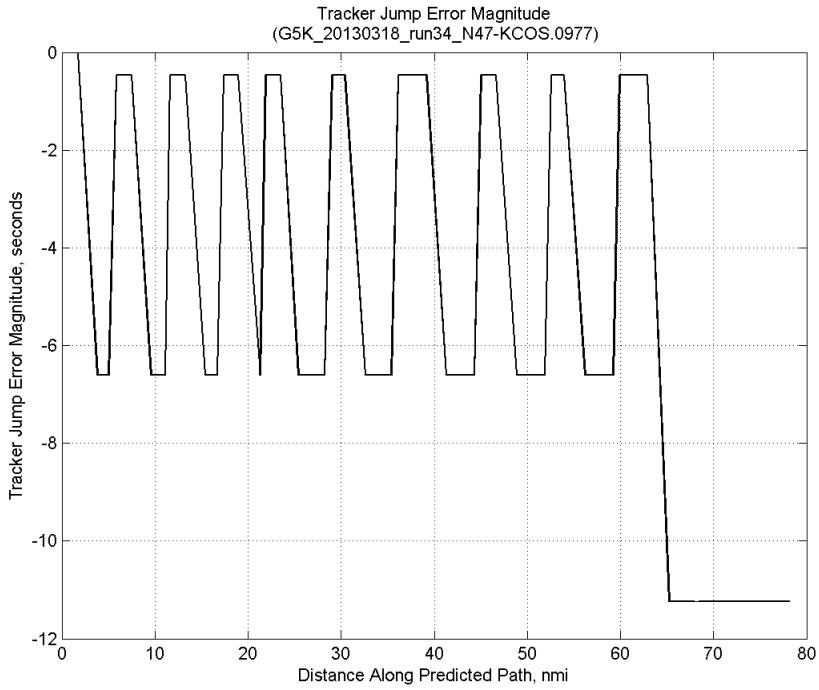


**Figure 604: Effect of tracker jump error source on time error for run 34.**

### C.23.B. Wind

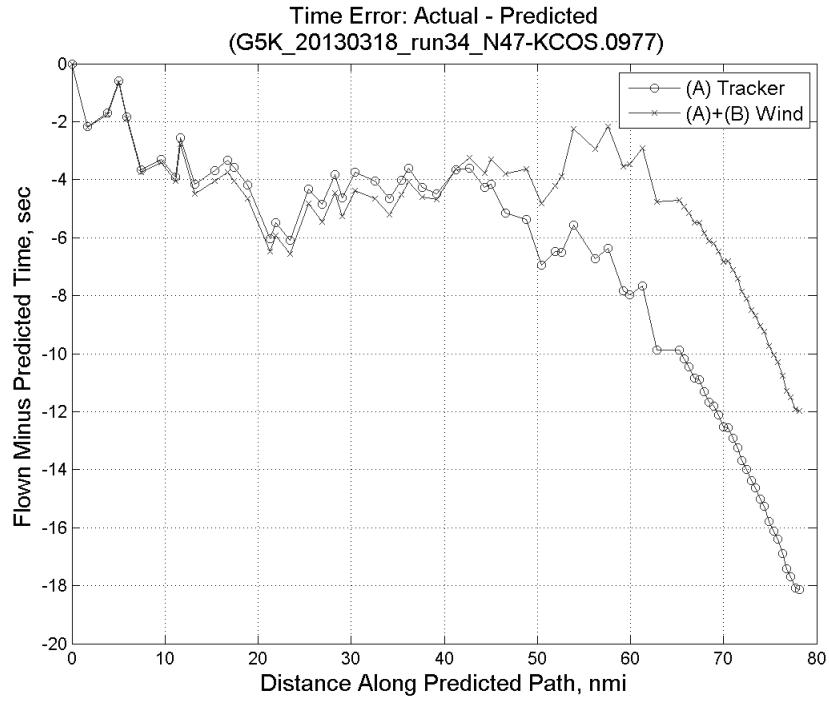


**Figure 605: Time error for run 34 before ((A) Tracker) and after ((A)+(B) Wind) removing wind error source.**

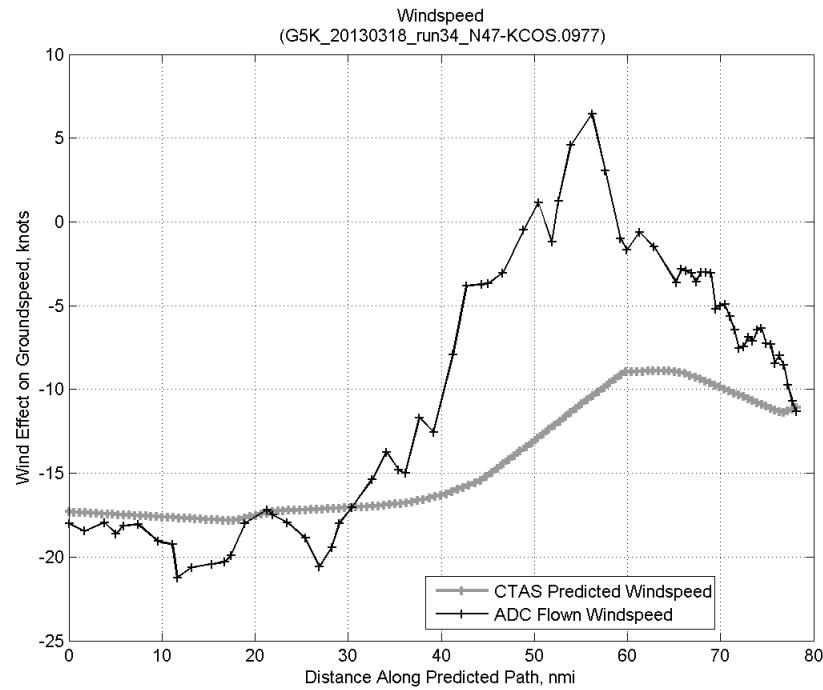


**Figure 606: CTAS predicted and ADC flown wind effect on ground speed for run 34. Negative values indicate a headwind.**

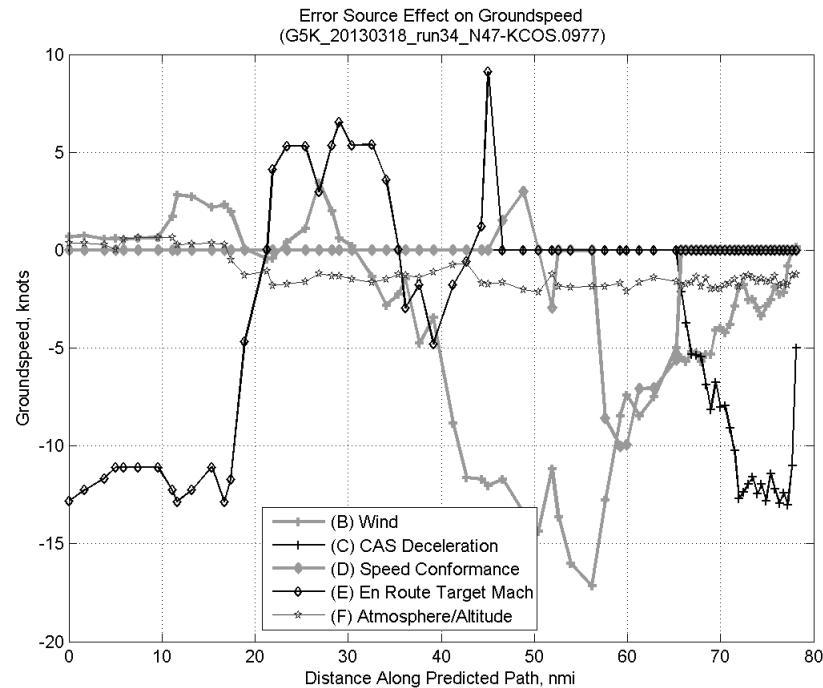


**Figure 607: Error sources (flown minus predicted) converted to a ground speed effect for run 34. Positive values indicate the flown ground speed was faster than the CTAS prediction.**

### C.23.C. CAS Deceleration

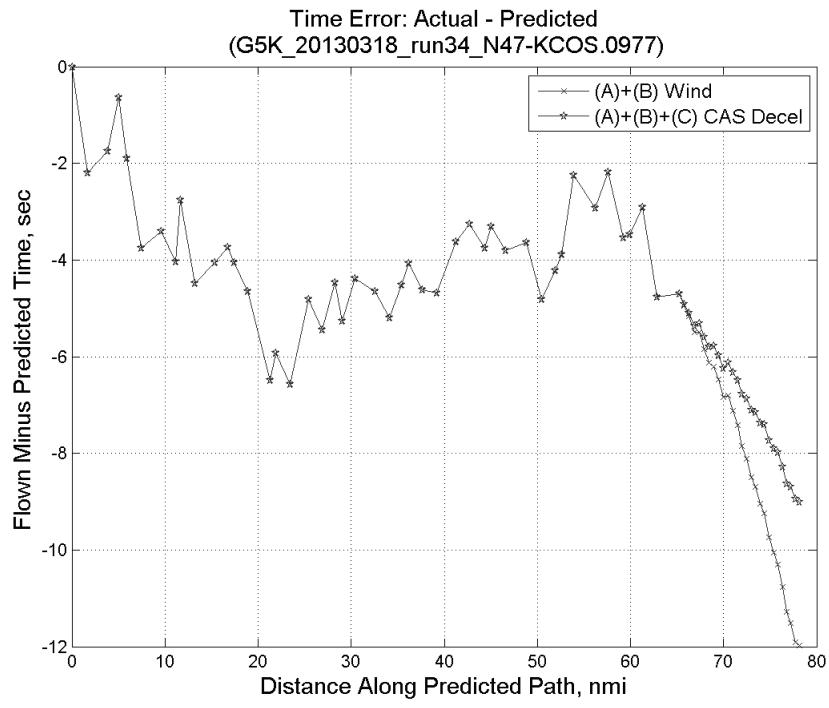


**Figure 608:** Time error for run 34 before ((A)+(B) Wind) and after ((A)+(B)+(C) CAS Decel) removing CAS deceleration error source.

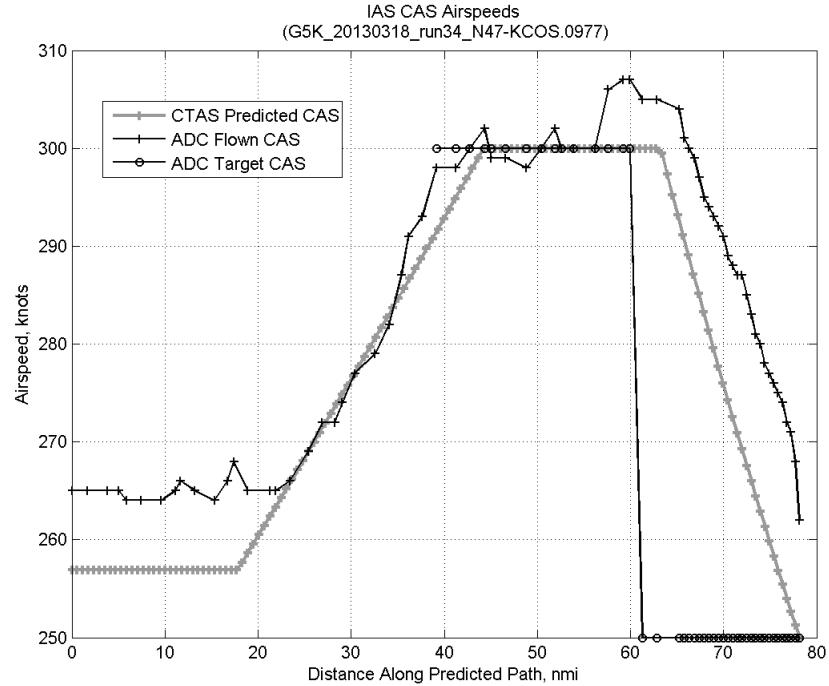


**Figure 609:** CTAS predicted and ADC flown CAS for run 34. CAS that is being targeted is shown with circle markers.

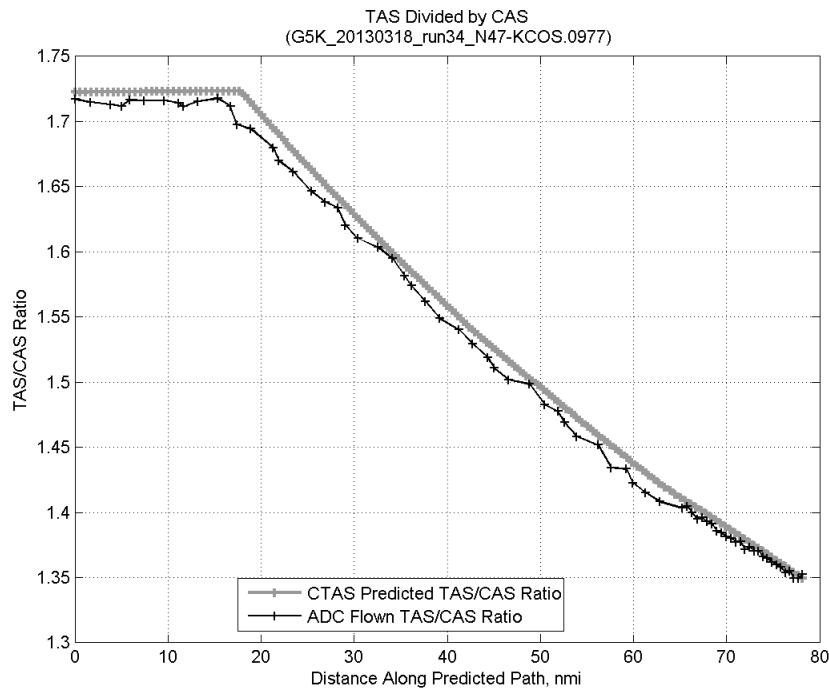


**Figure 610: CTAS predicted and ADC flown TAS/CAS ratio for run 34.**

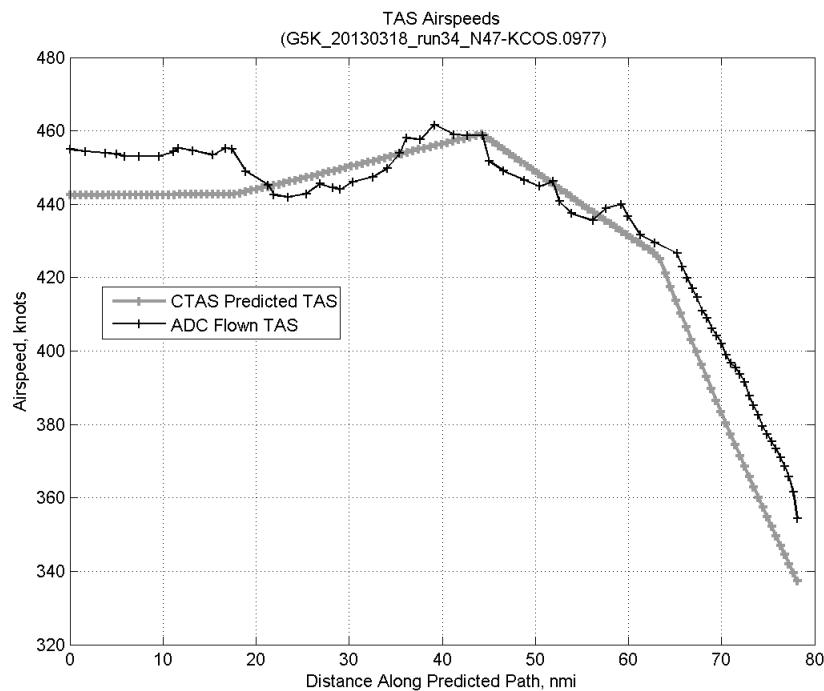


**Figure 611: CTAS predicted and ADC flown TAS for run 34.**

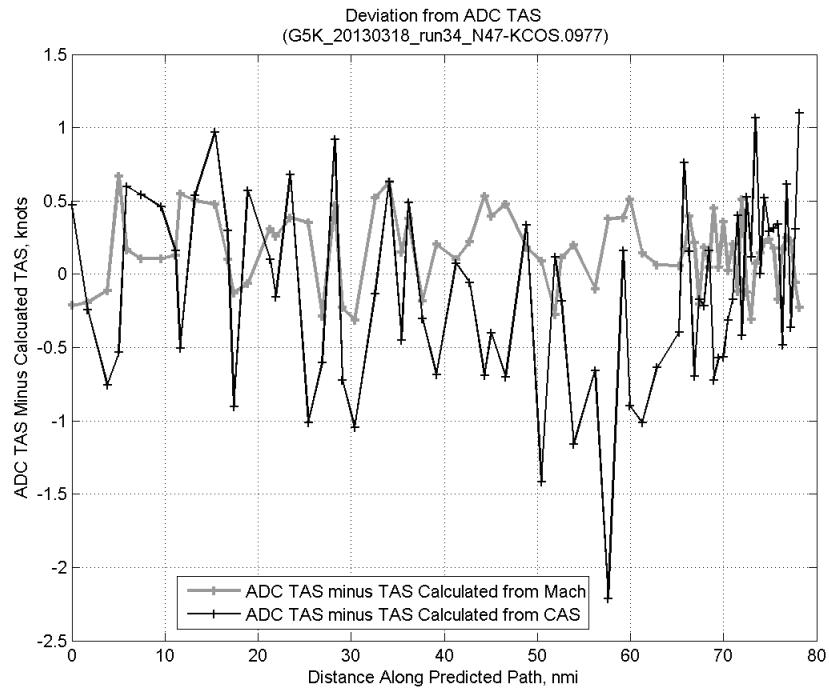


**Figure 612: Deviation from ADC flown TAS if calculating TAS using ADC flown CAS, Mach, atmospheric temperature, and atmospheric pressure for run 34.**

#### C.23.D. Speed Conformance

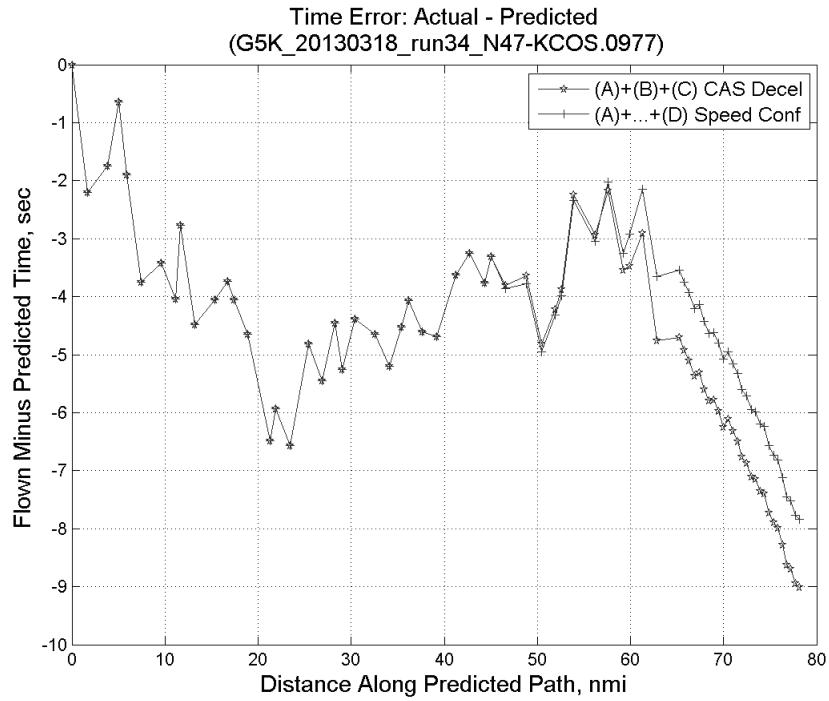


**Figure 613: Time error for run 34 before ((A)+(B)+(C) CAS Decel) and after ((A)+...+(D) Speed Conf) removing speed conformance error source.**

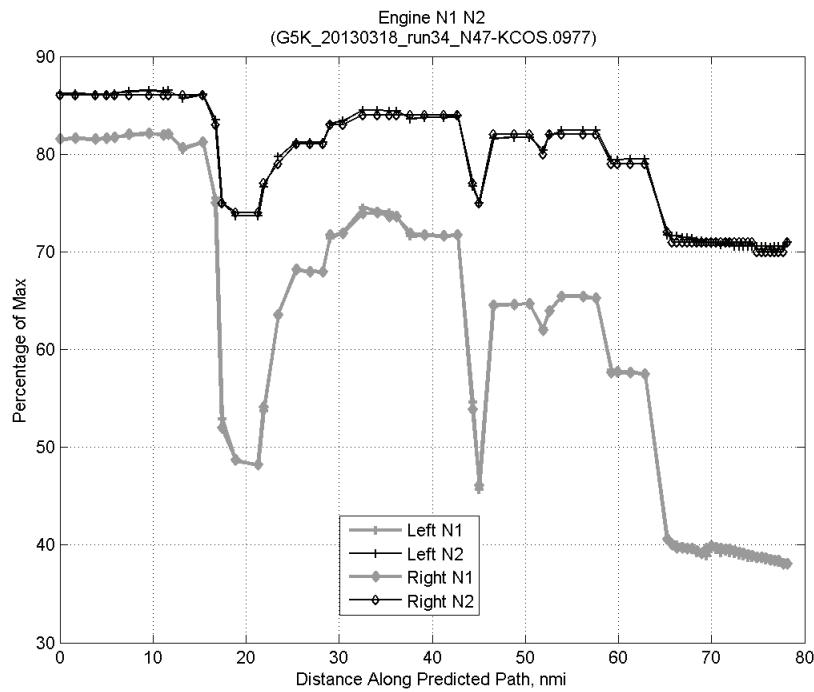


**Figure 614: Flown engine N1 and N2 for run 34.**

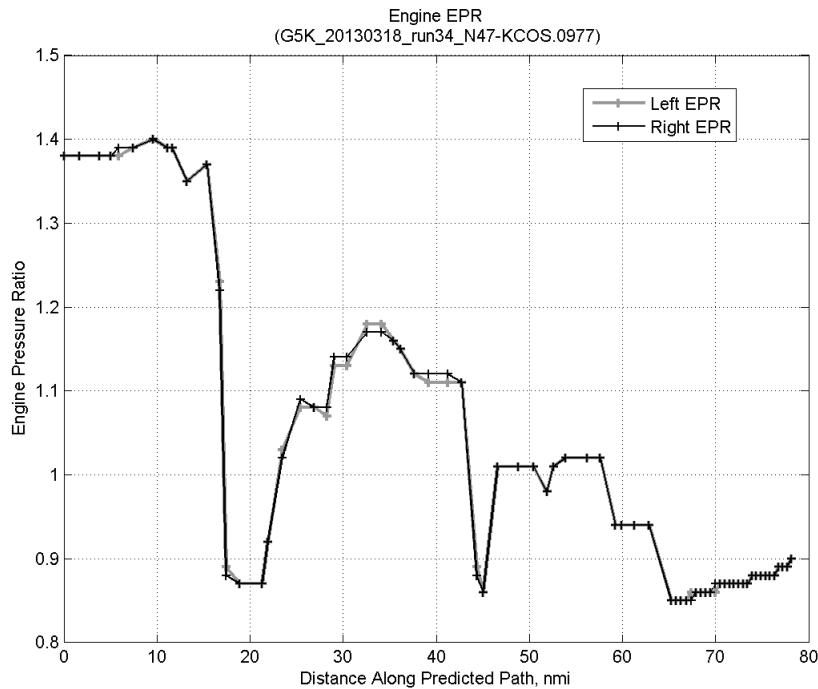


**Figure 615: Flown engine EPR for run 34.**

### C.23.E. Target Mach

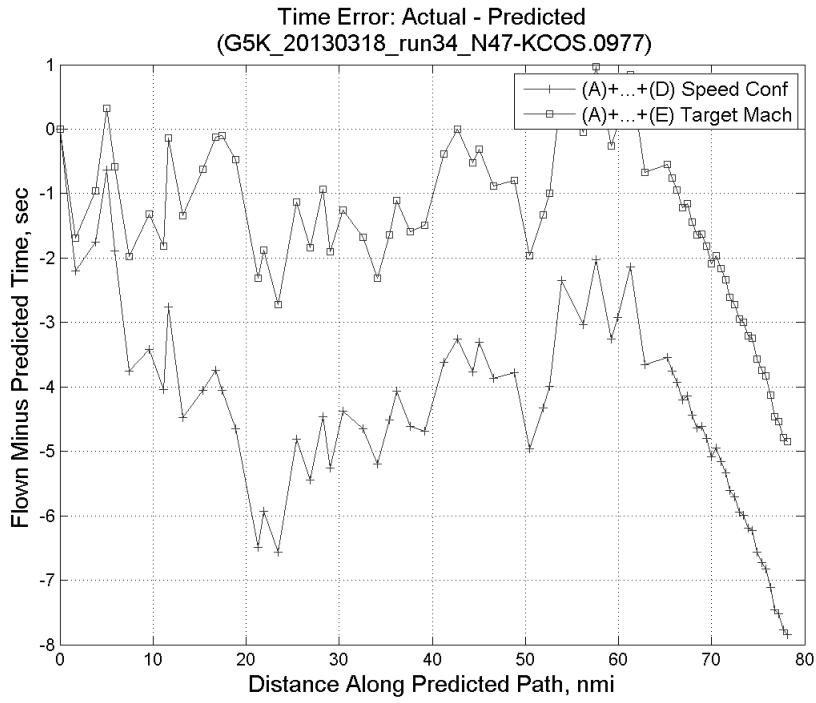


**Figure 616:** Time error for run 34 before ((A)+...+(D) Speed Conf) and after ((A)+...+(E) Target Mach) removing target Mach error source.

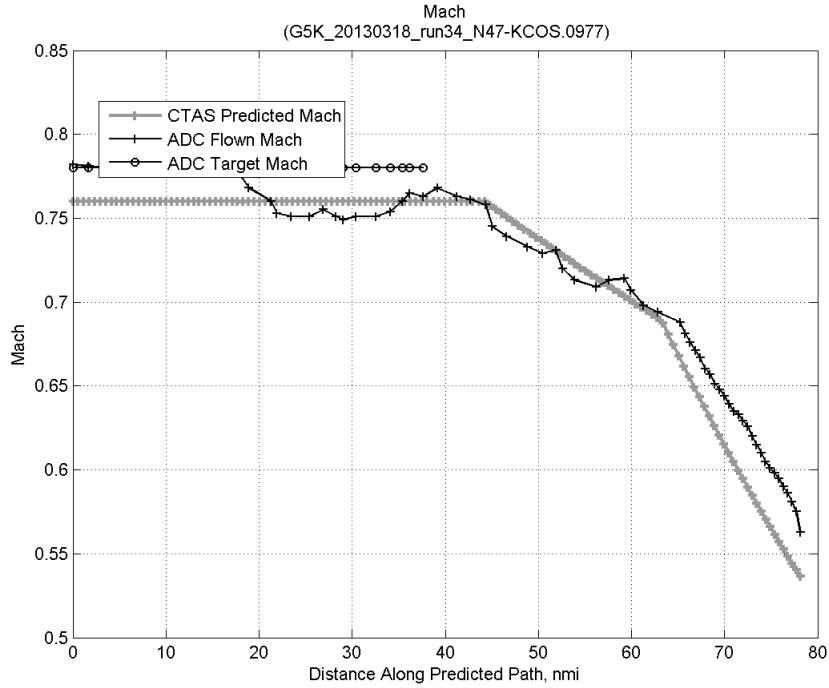


**Figure 617:** CTAS predicted and ADC flown Mach for run 34. Mach being targeted (ADC) shown with circle markers.

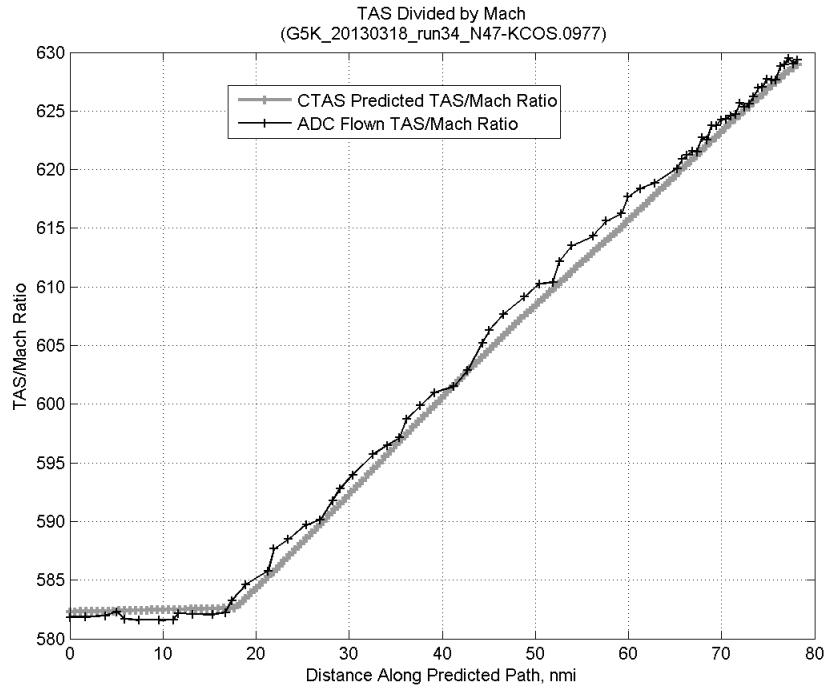


**Figure 618: CTAS predicted and ADC flown TAS/Mach ratio for run 34.**

#### C.23.F. Atmosphere/Altitude

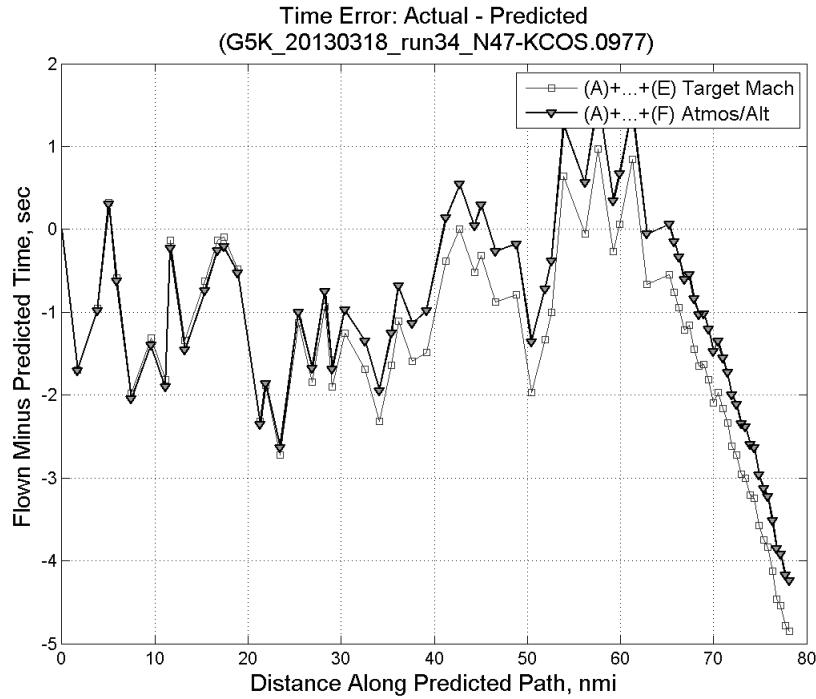


**Figure 619: Time error for run 34 before ((A)+...+(E) Target Mach) and after ((A)+...+(F) Atmos/Alt) removing atmosphere/altitude error source.**

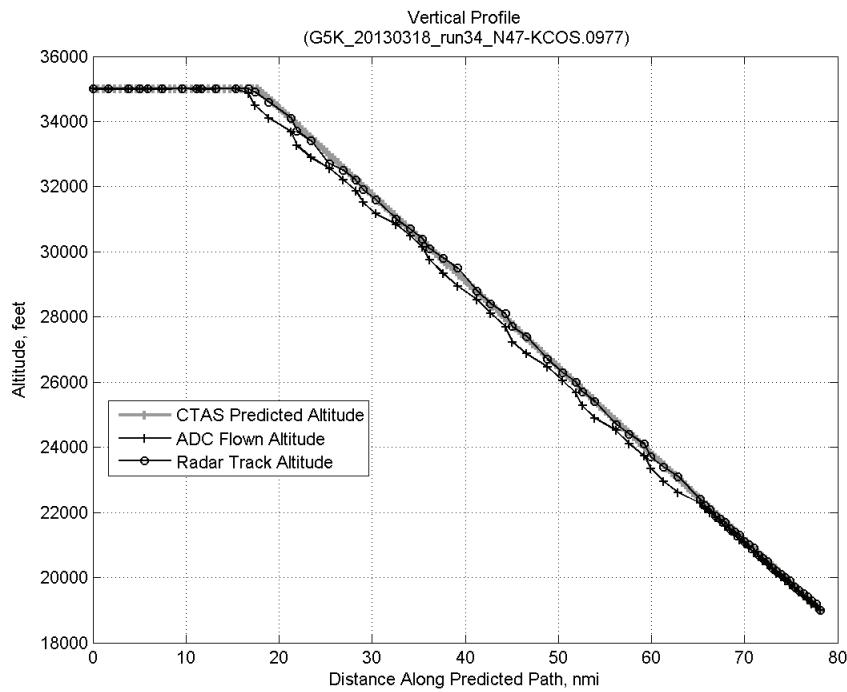


**Figure 620: Flown (ADC) and predicted (CTAS) vertical profile for run 34.**

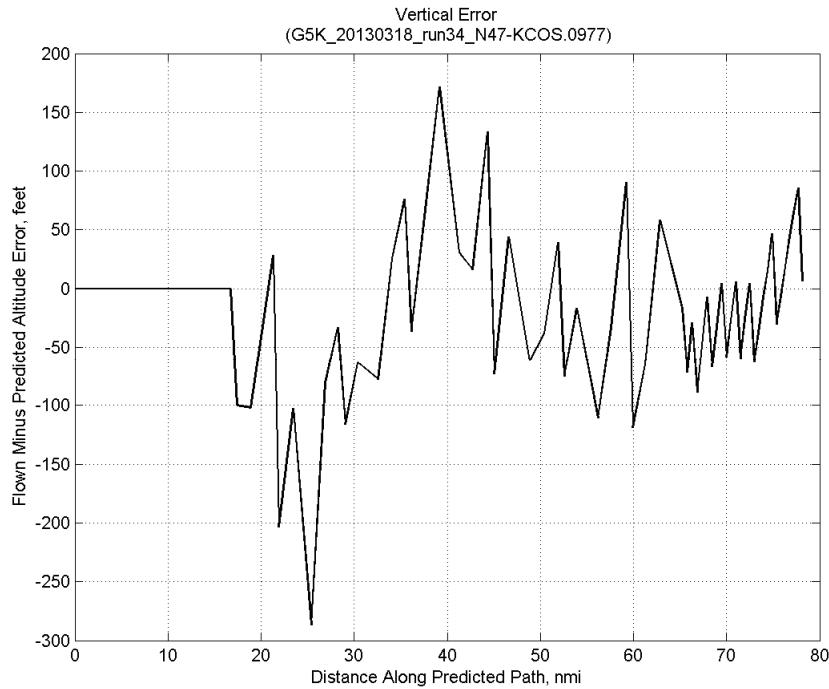


**Figure 621: Vertical error (flown minus predicted altitude) for run 34. Positive values indicate aircraft flew higher than predicted by CTAS.**

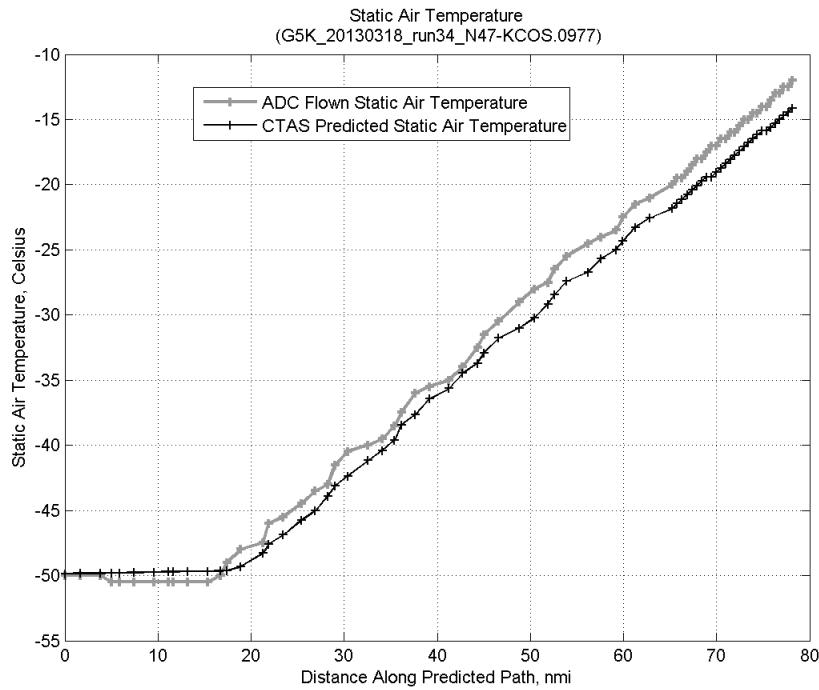


**Figure 622: Flown (ADC) and predicted (CTAS) static air temperature for run 34.**

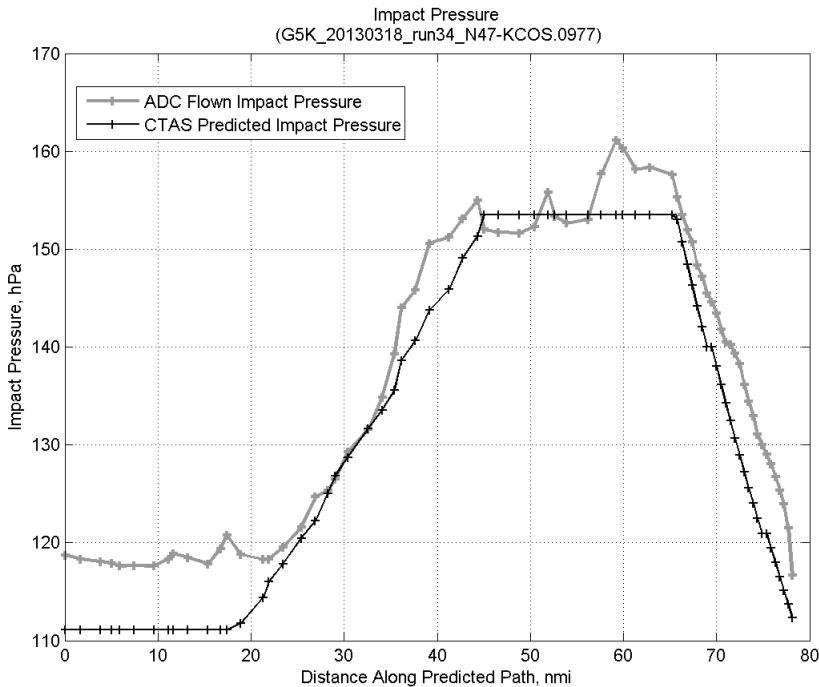


**Figure 623: Flown (ADC) and predicted (CTAS) impact pressure for run 34.**

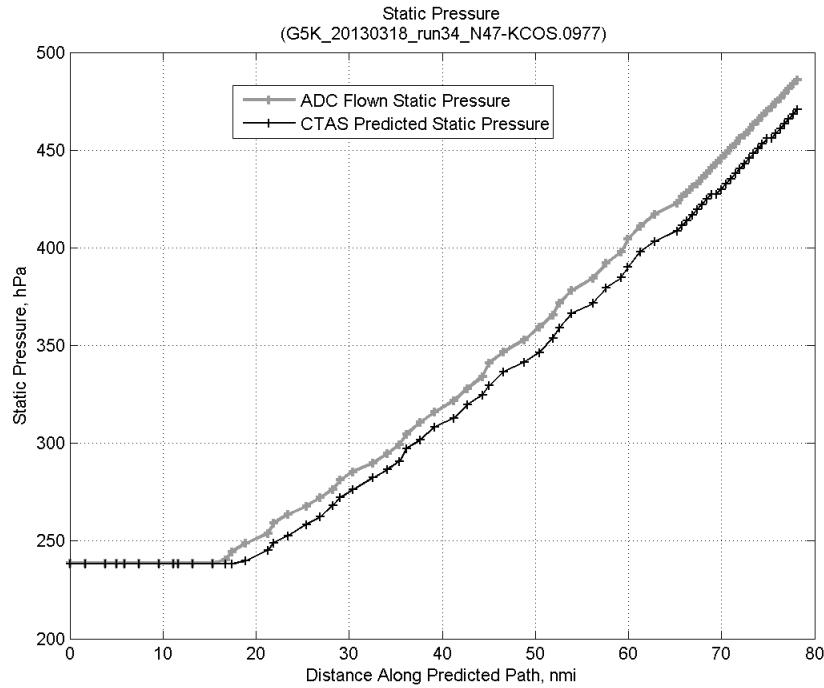


**Figure 624: Flown (ADC) and predicted (CTAS) static pressure for run 34.**

### C.23.G. Path Distance

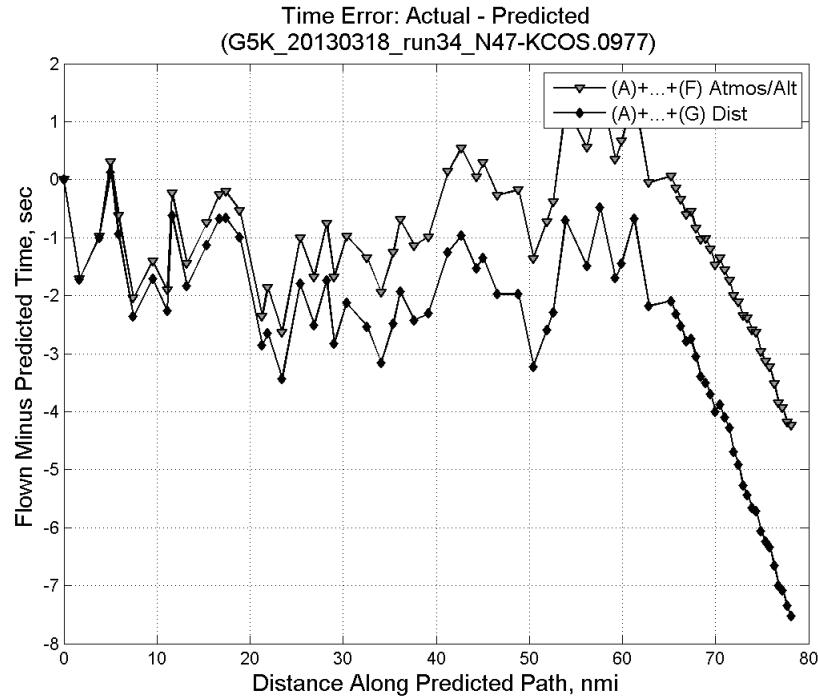


**Figure 625: Time error for run 34 before ((A)+...+(F) Atmos/Alt) and after ((A)+...+(G) Dist) removing path distance error source.**

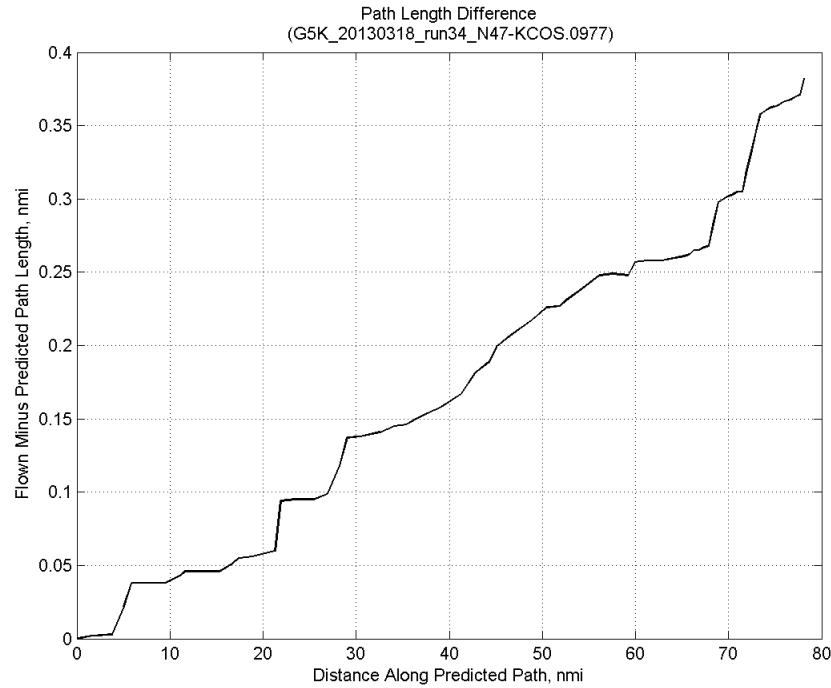


**Figure 626: ADC flown minus CTAS predicted path length for run 34. Positive values indicate aircraft followed a longer path than predicted by CTAS.**

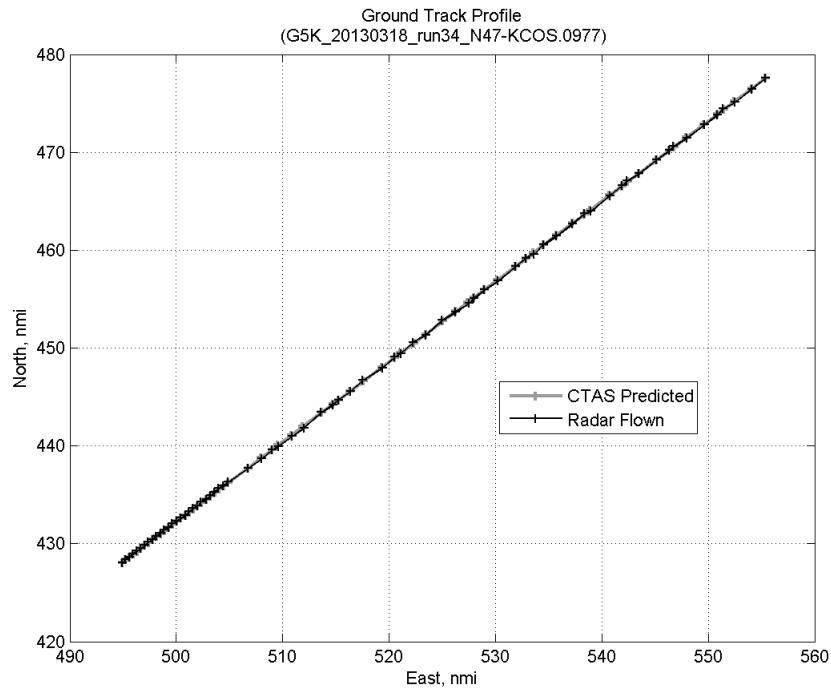


**Figure 627: CTAS predicted and radar flown ground track profile for run 34.**

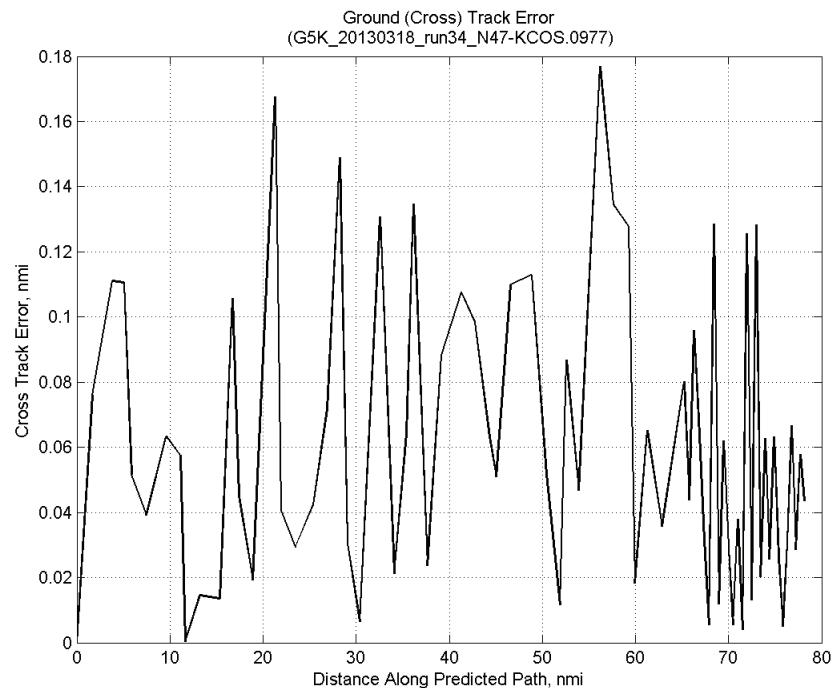


**Figure 628: Ground (cross) track error for run 34.**

## C.24. Run 35

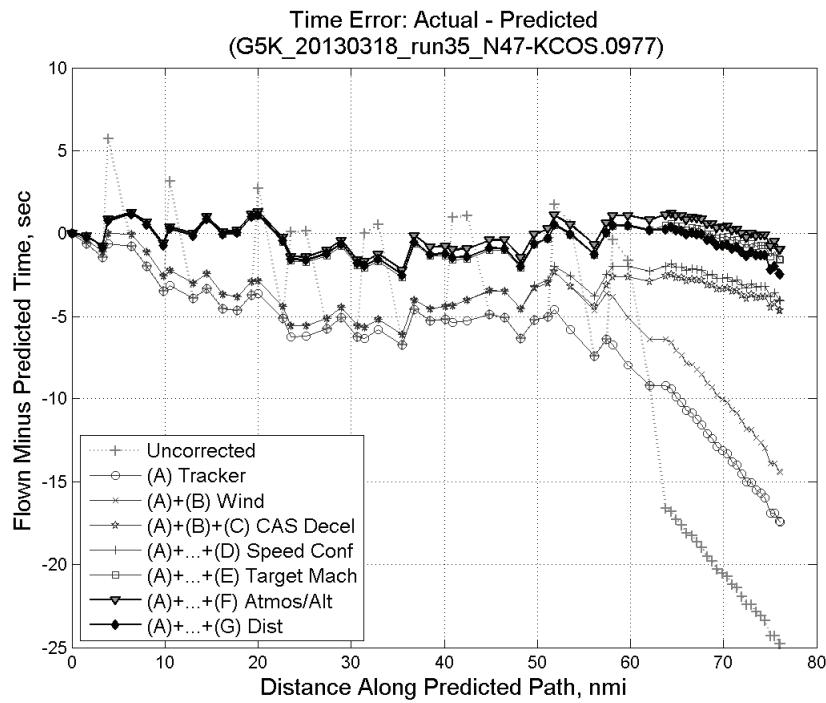


**Figure 629:** Time error for run 35 showing incremental effect of removing each error source.

### C.24.A. Tracker Jumps

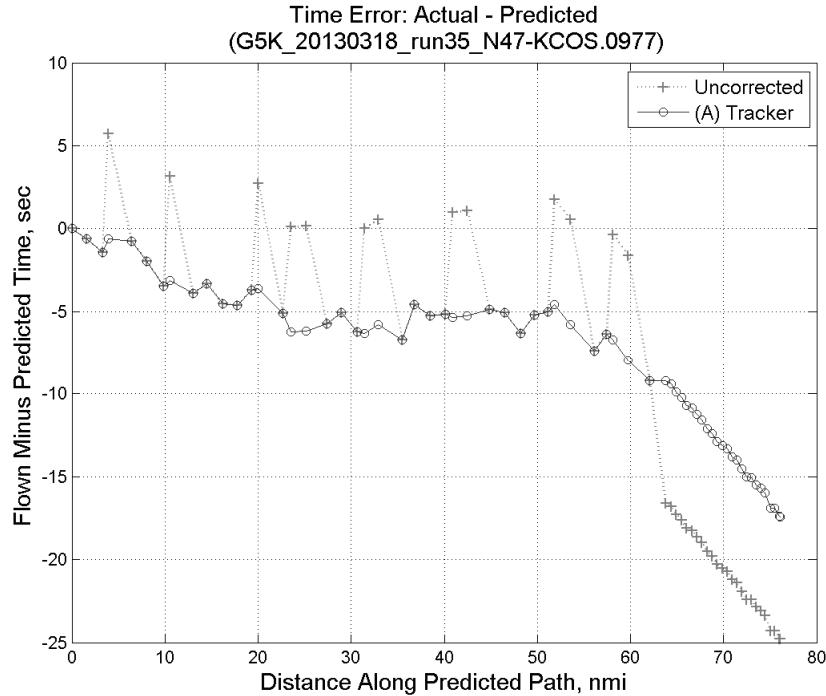


**Figure 630:** Time error for run 35 before (Uncorrected) and after ((A) Tracker) removing tracker jump error source.

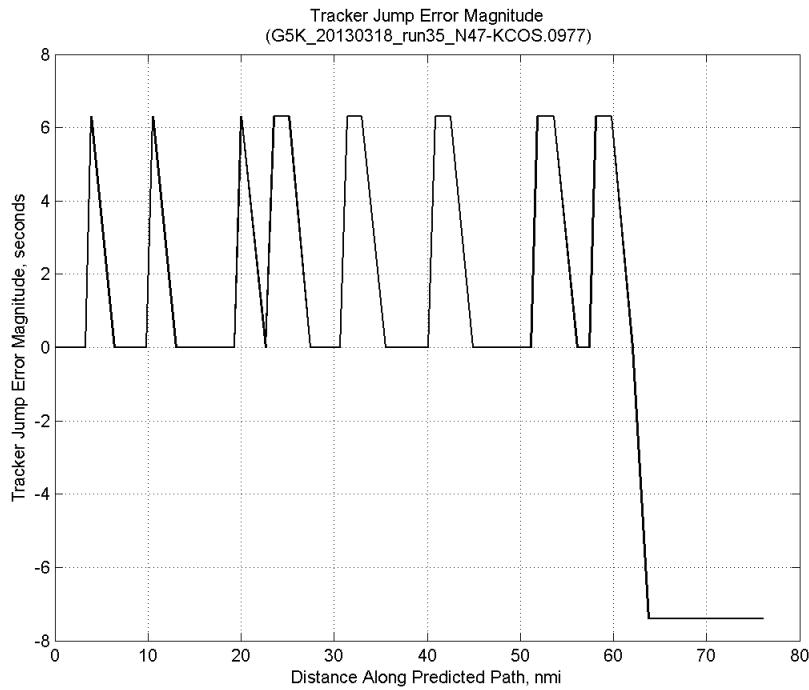


**Figure 631: Effect of tracker jump error source on time error for run 35.**

#### C.24.B. Wind

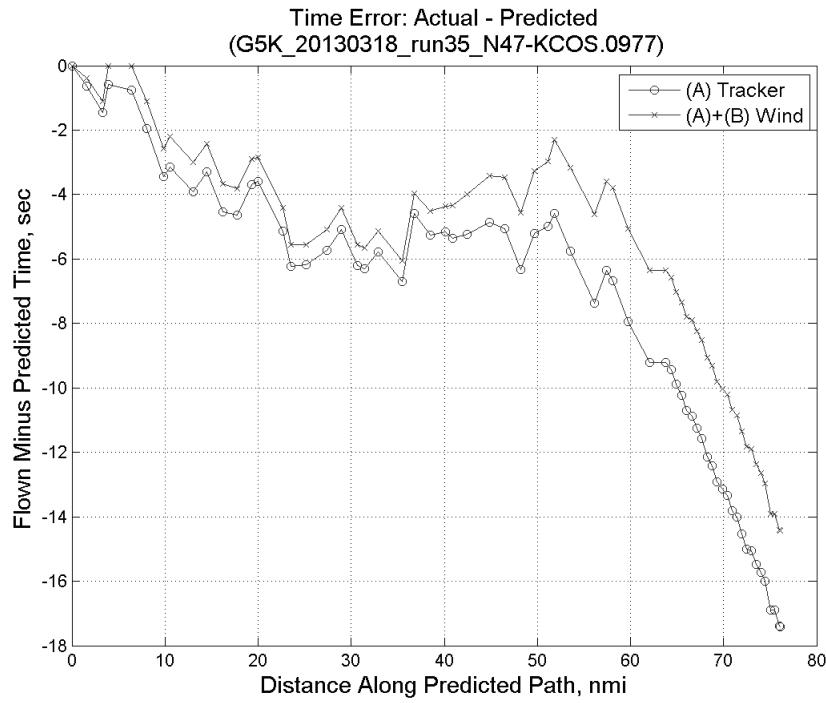


**Figure 632: Time error for run 35 before ((A) Tracker) and after ((A)+(B) Wind) removing wind error source.**

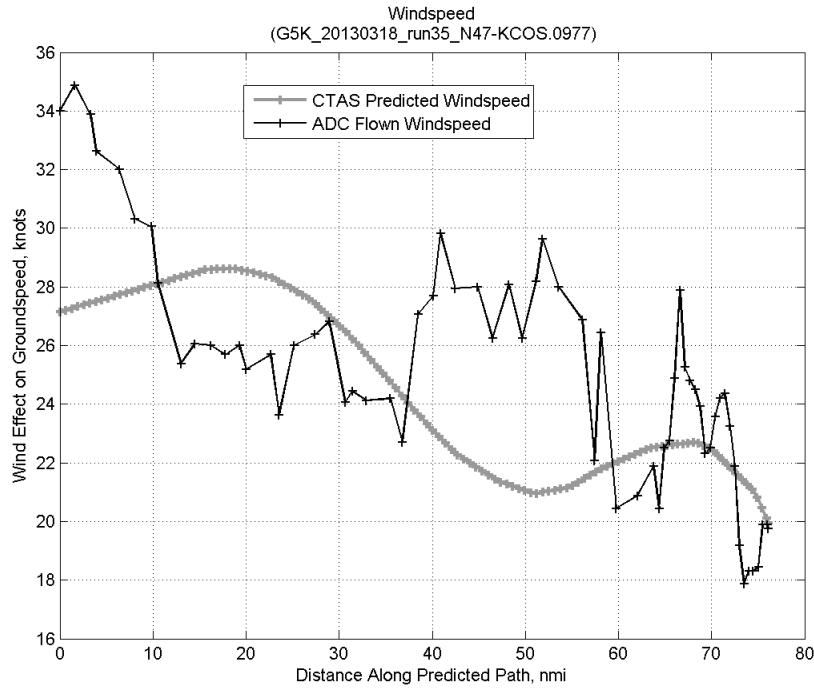


**Figure 633: CTAS predicted and ADC flown wind effect on ground speed for run 35. Negative values indicate a headwind.**

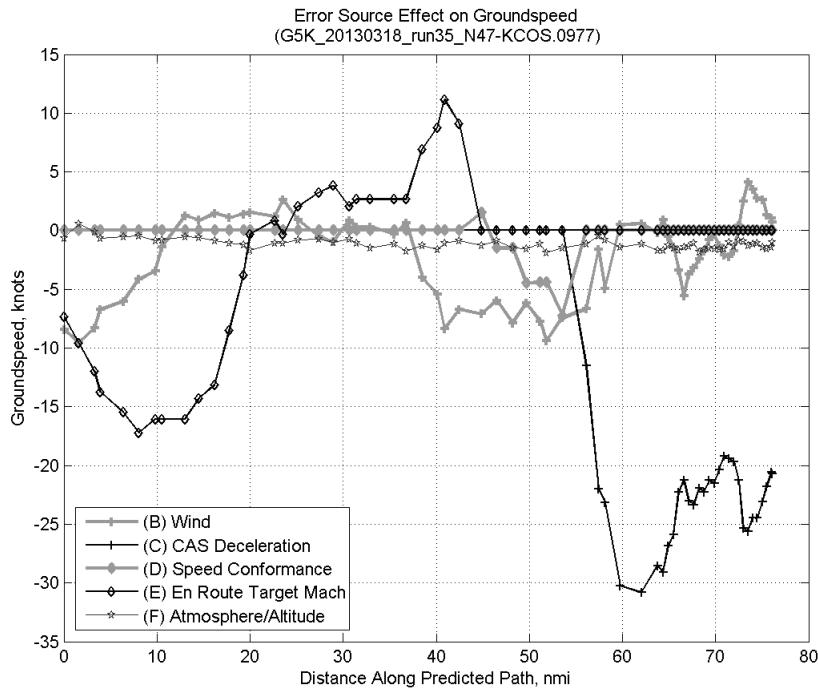


**Figure 634: Error sources (flown minus predicted) converted to a ground speed effect for run 35. Positive values indicate the flown ground speed was faster than the CTAS prediction.**

### C.24.C. CAS Deceleration

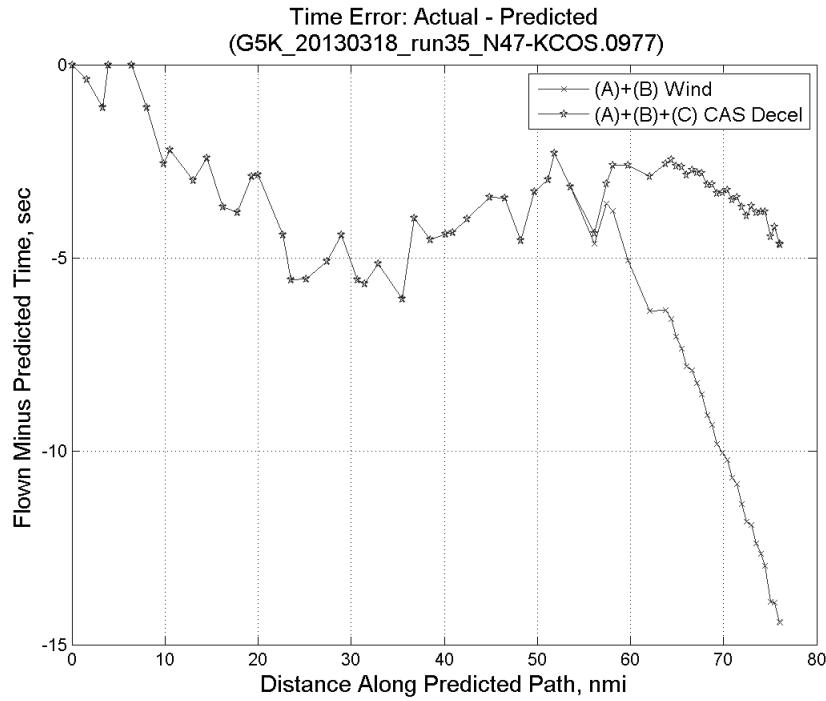


**Figure 635:** Time error for run 35 before ((A)+(B) Wind) and after ((A)+(B)+(C) CAS Decel) removing CAS deceleration error source.

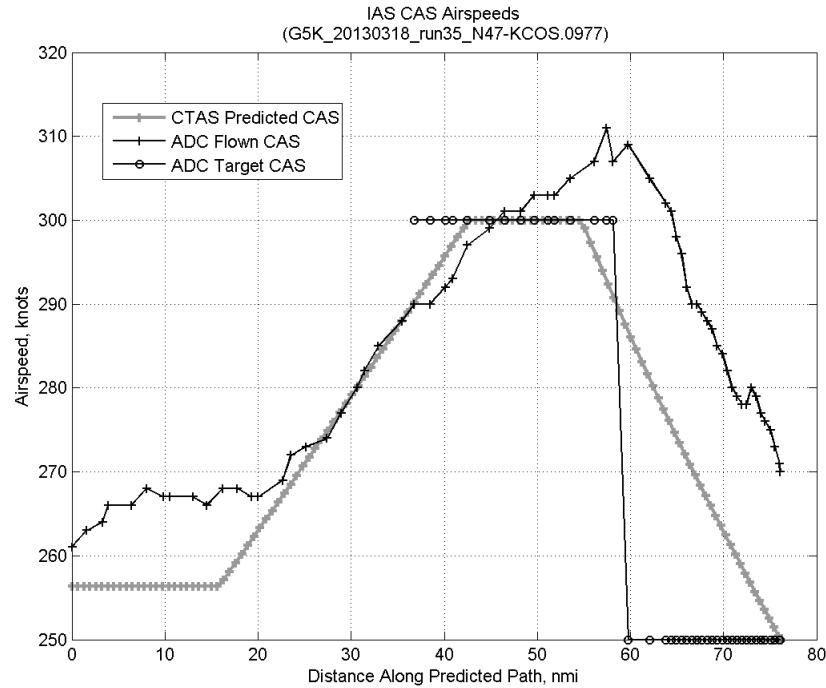


**Figure 636:** CTAS predicted and ADC flown CAS for run 35. CAS that is being targeted is shown with circle markers.

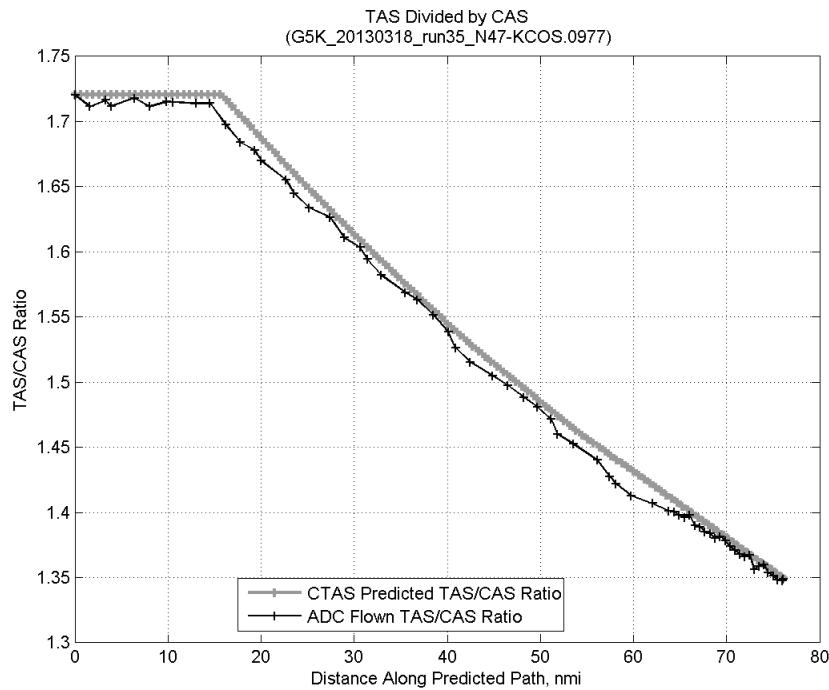


**Figure 637: CTAS predicted and ADC flown TAS/CAS ratio for run 35.**

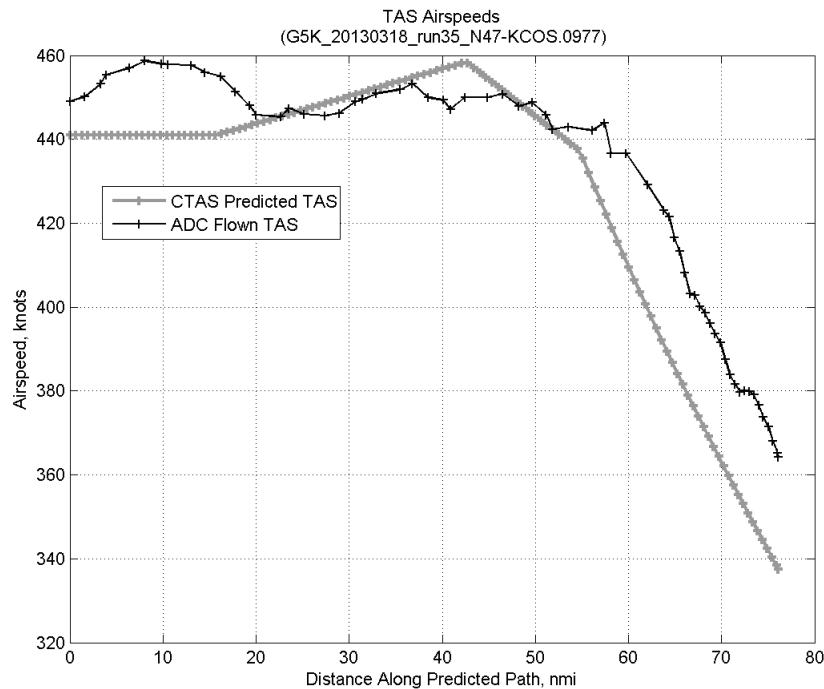


**Figure 638: CTAS predicted and ADC flown TAS for run 35.**

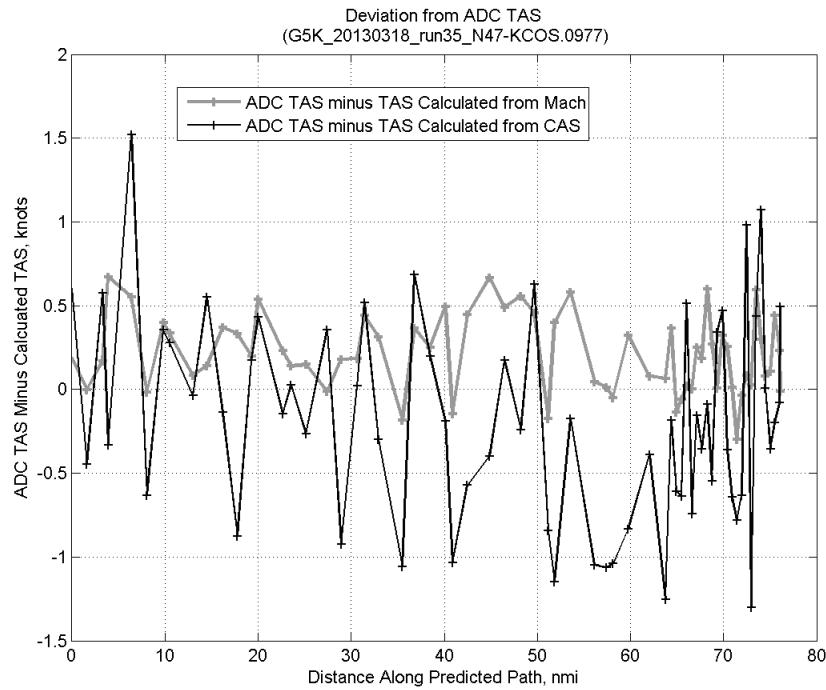


**Figure 639:** Deviation from ADC flown TAS if calculating TAS using ADC flown CAS, Mach, atmospheric temperature, and atmospheric pressure for run 35.

#### C.24.D. Speed Conformance

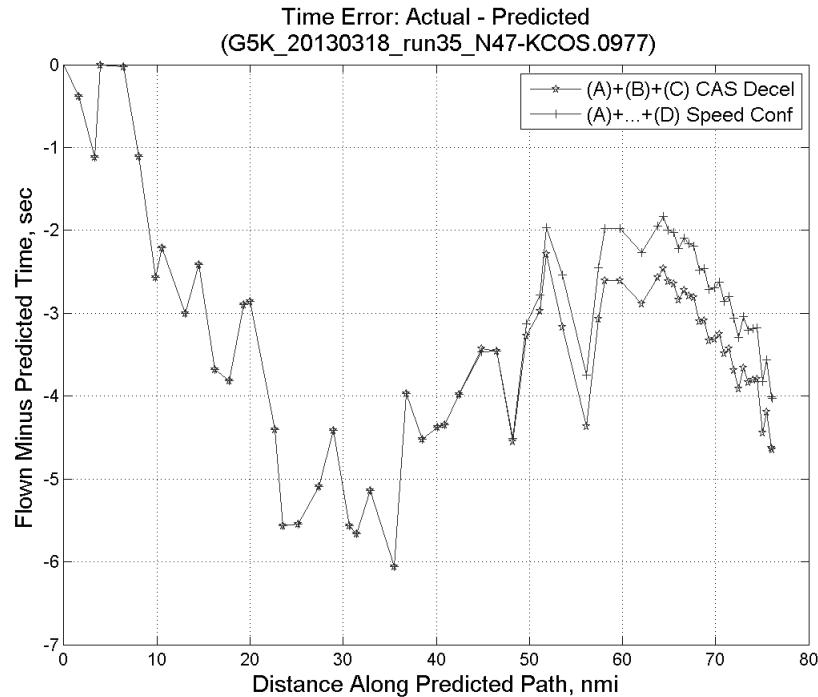


**Figure 640:** Time error for run 35 before  $((A)+(B)+(C) \text{ CAS Decel})$  and after  $((A)+\dots+(D) \text{ Speed Conf})$  removing speed conformance error source.

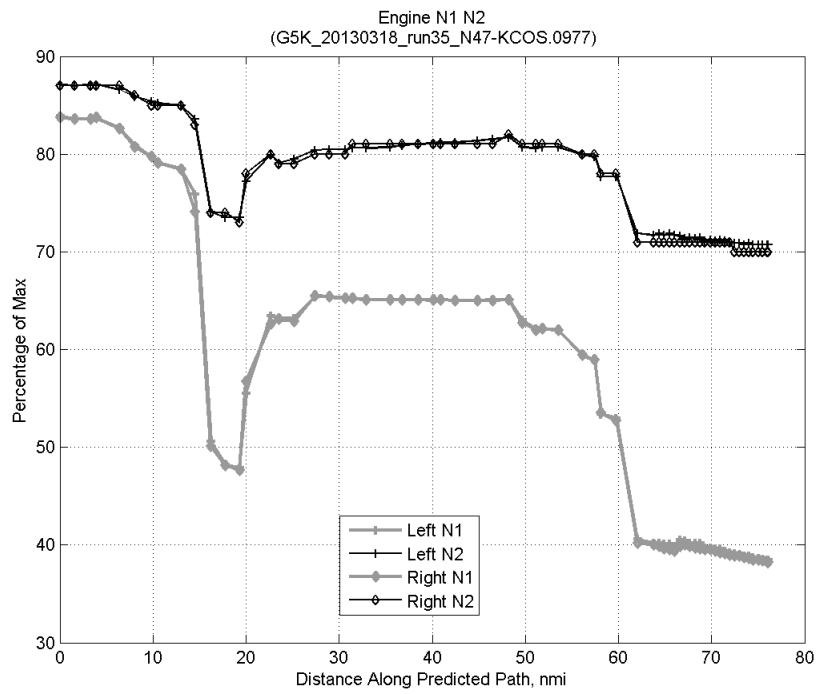


**Figure 641: Flown engine N1 and N2 for run 35.**

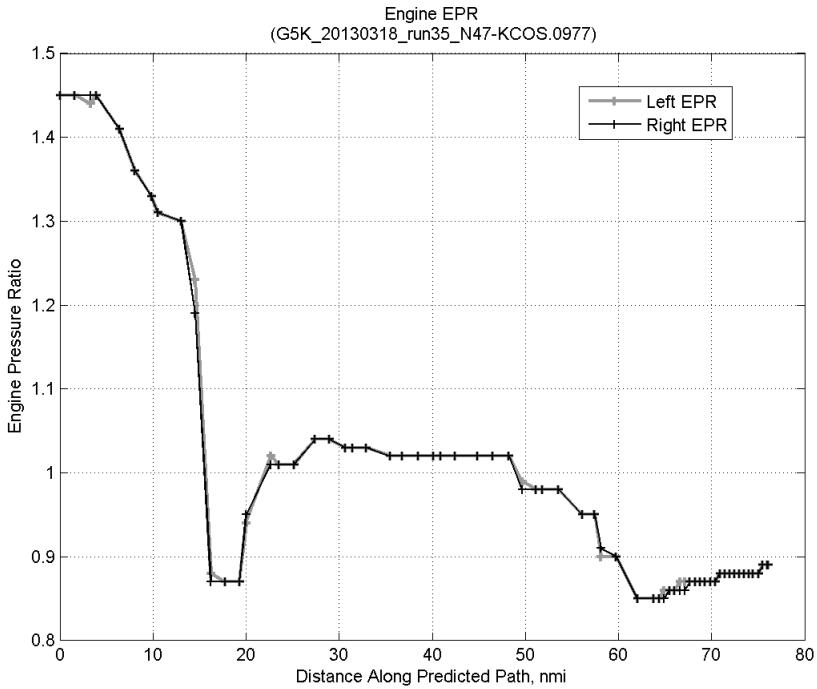


**Figure 642: Flown engine EPR for run 35.**

### C.24.E. Target Mach

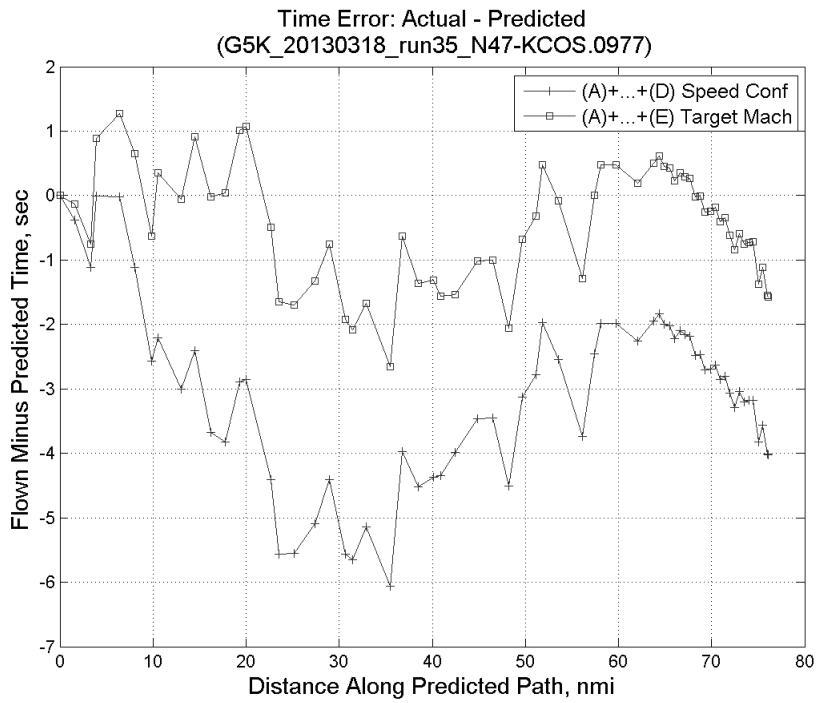


**Figure 643:** Time error for run 35 before ((A)+...+(D) Speed Conf) and after ((A)+...+(E) Target Mach) removing target Mach error source.

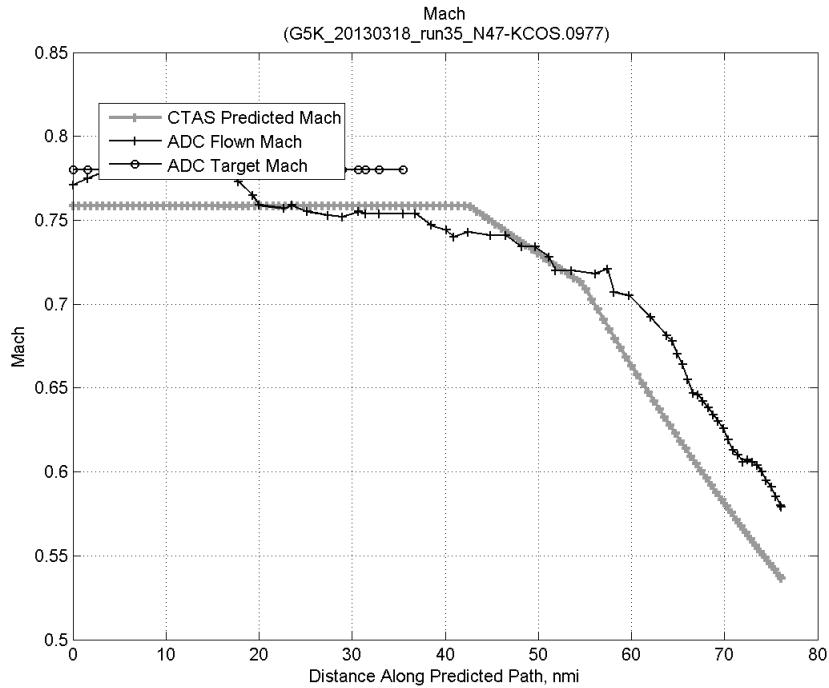


**Figure 644:** CTAS predicted and ADC flown Mach for run 35. Mach being targeted (ADC) shown with circle markers.

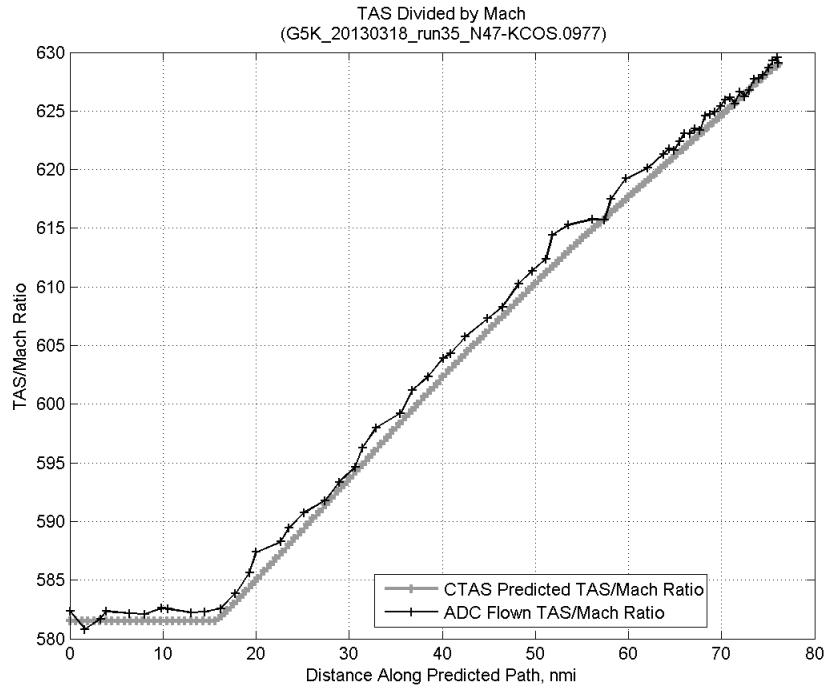


**Figure 645:** CTAS predicted and ADC flown TAS/Mach ratio for run 35.

#### C.24.F. Atmosphere/Altitude

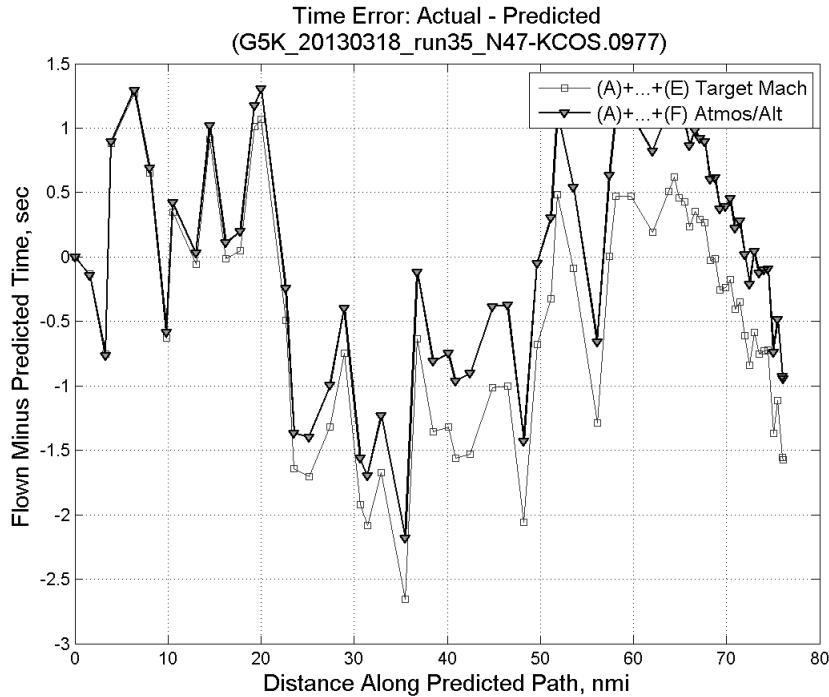


**Figure 646:** Time error for run 35 before ((A)+...+(E) Target Mach) and after ((A)+...+(F) Atmos/Alt) removing atmosphere/altitude error source.

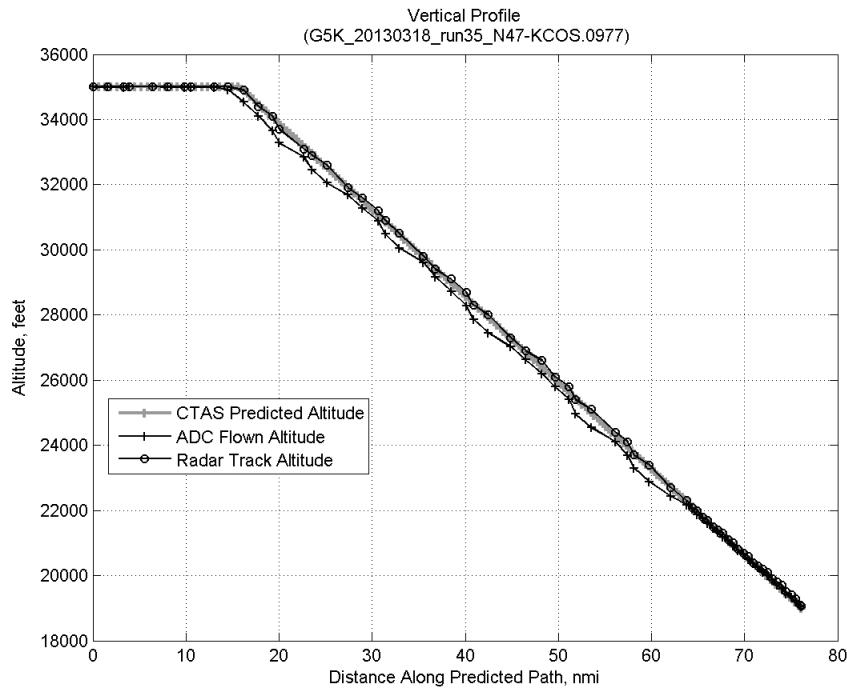


**Figure 647: Flown (ADC) and predicted (CTAS) vertical profile for run 35.**

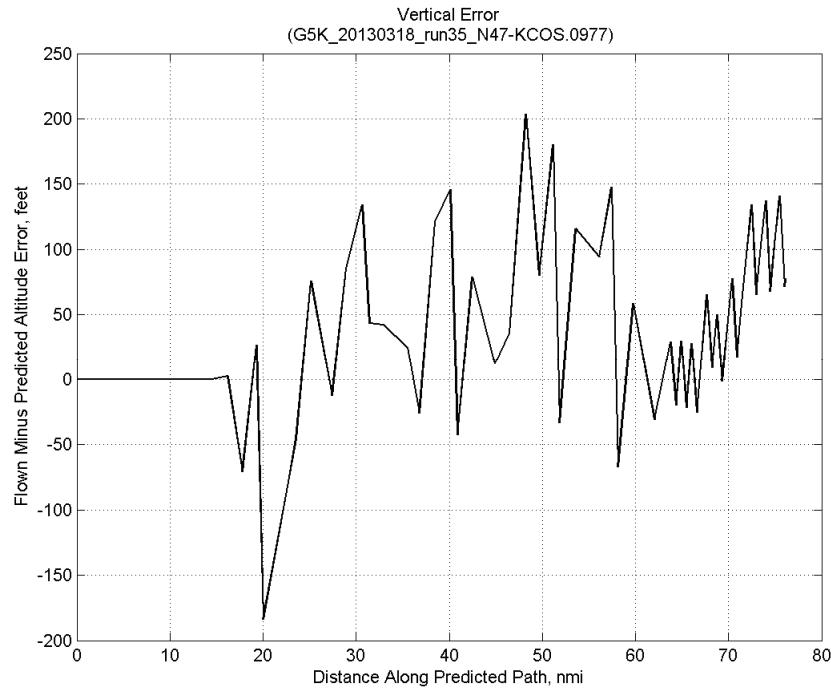


**Figure 648: Vertical error (flown minus predicted altitude) for run 35. Positive values indicate aircraft flew higher than predicted by CTAS.**

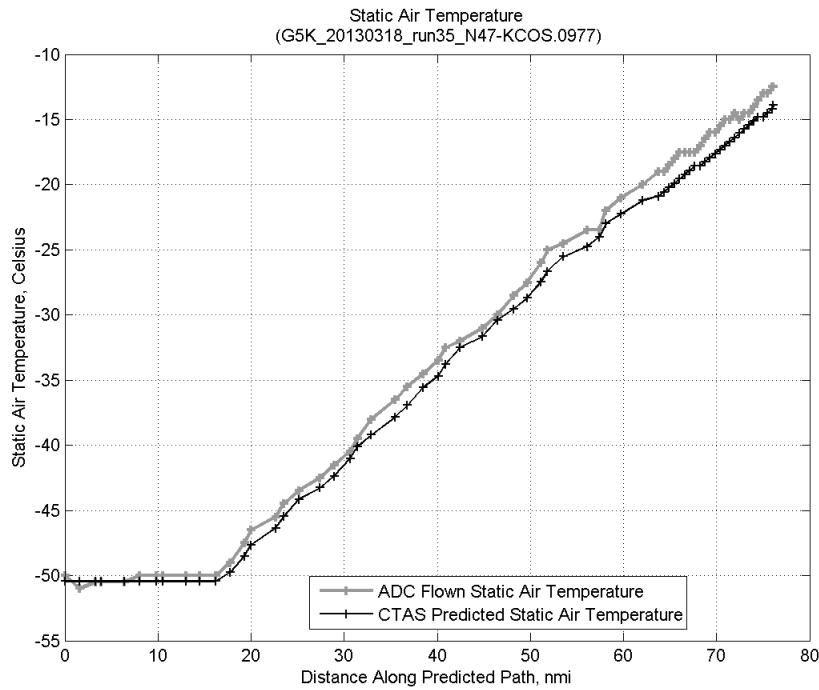


**Figure 649: Flown (ADC) and predicted (CTAS) static air temperature for run 35.**

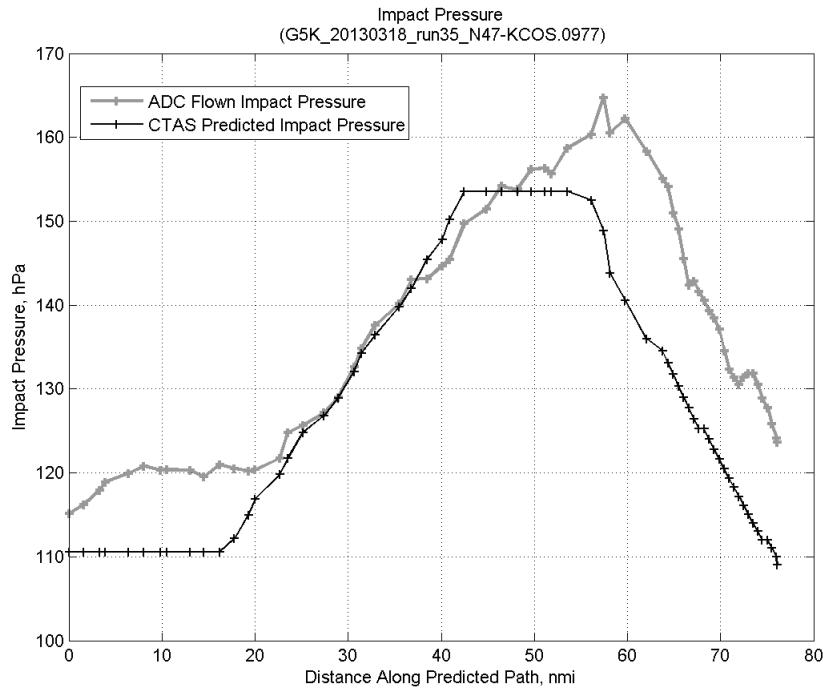


**Figure 650: Flown (ADC) and predicted (CTAS) impact pressure for run 35.**

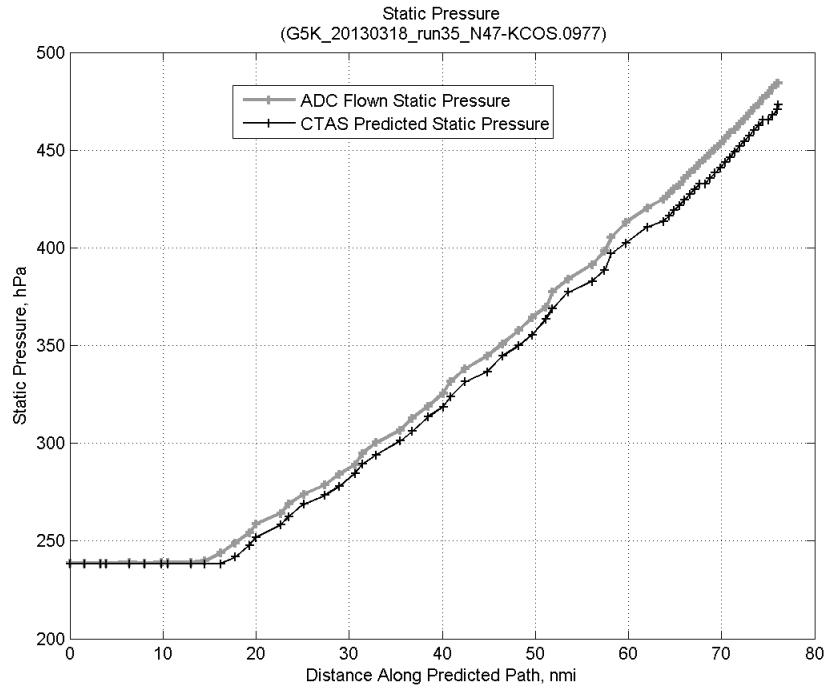


**Figure 651:** Flown (ADC) and predicted (CTAS) static pressure for run 35.

#### C.24.G. Path Distance

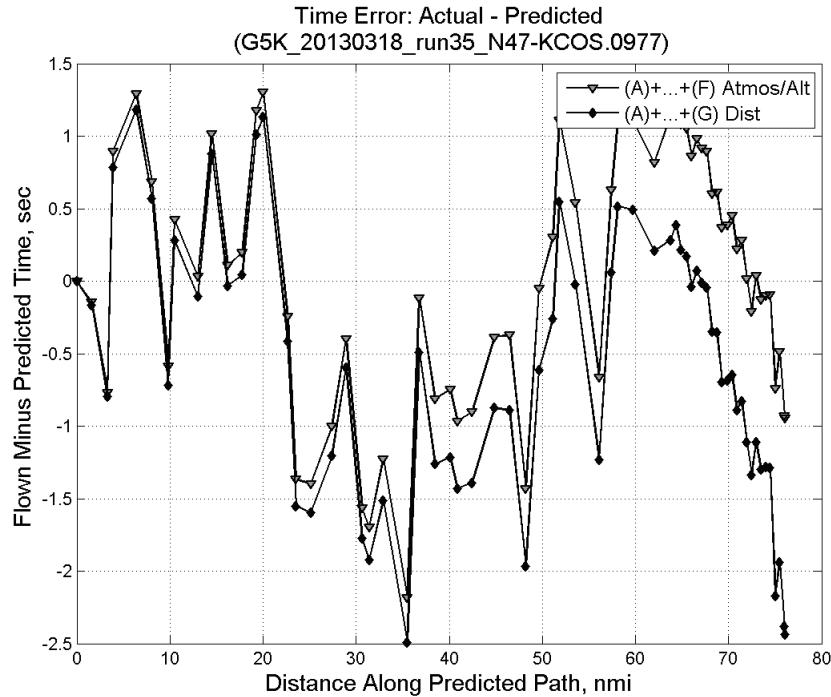


**Figure 652:** Time error for run 35 before ((A)+...+(F) Atmos/Alt) and after ((A)+...+(G) Dist) removing path distance error source.

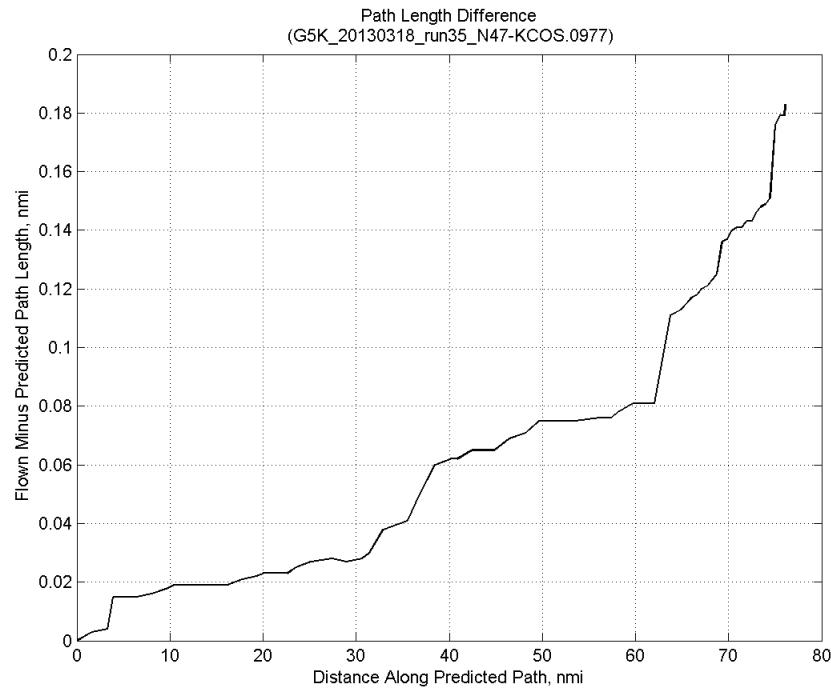


**Figure 653: ADC flown minus CTAS predicted path length for run 35. Positive values indicate aircraft followed a longer path than predicted by CTAS.**

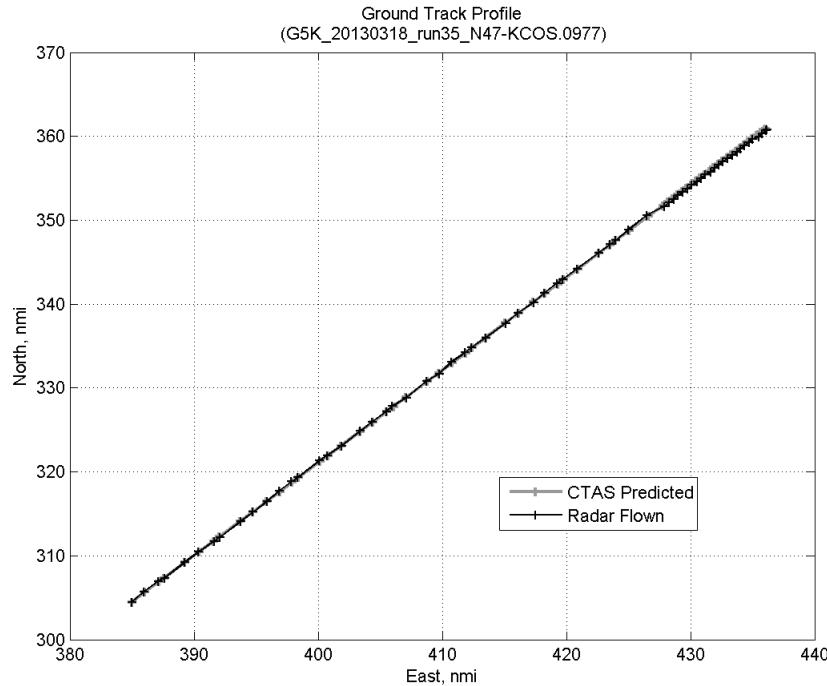


**Figure 654: CTAS predicted and radar flown ground track profile for run 35.**

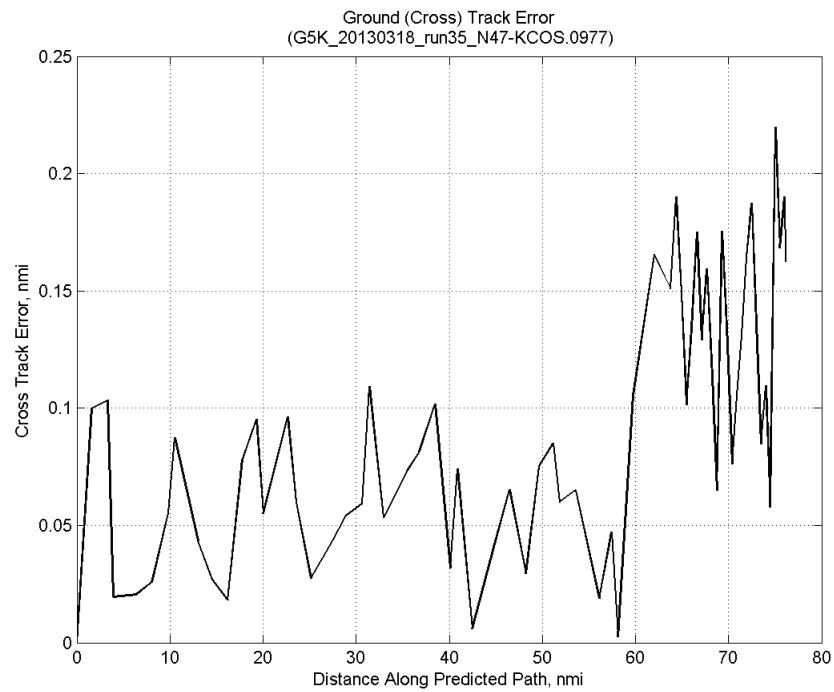


**Figure 655: Ground (cross) track error for run 35.**

### C.25. Run 36

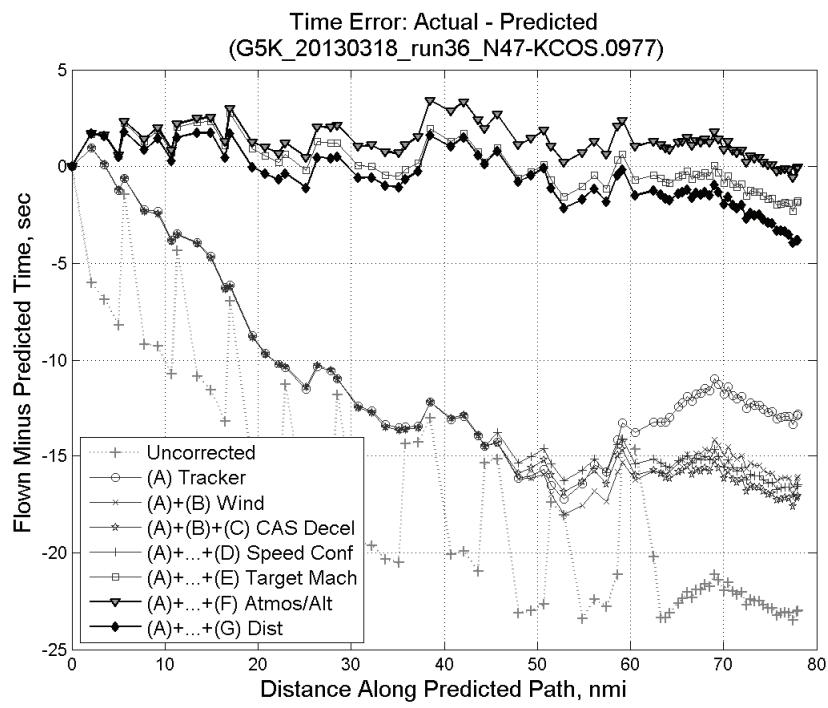


**Figure 656: Time error for run 36 showing incremental effect of removing each error source.**

#### C.25.A. Tracker Jumps

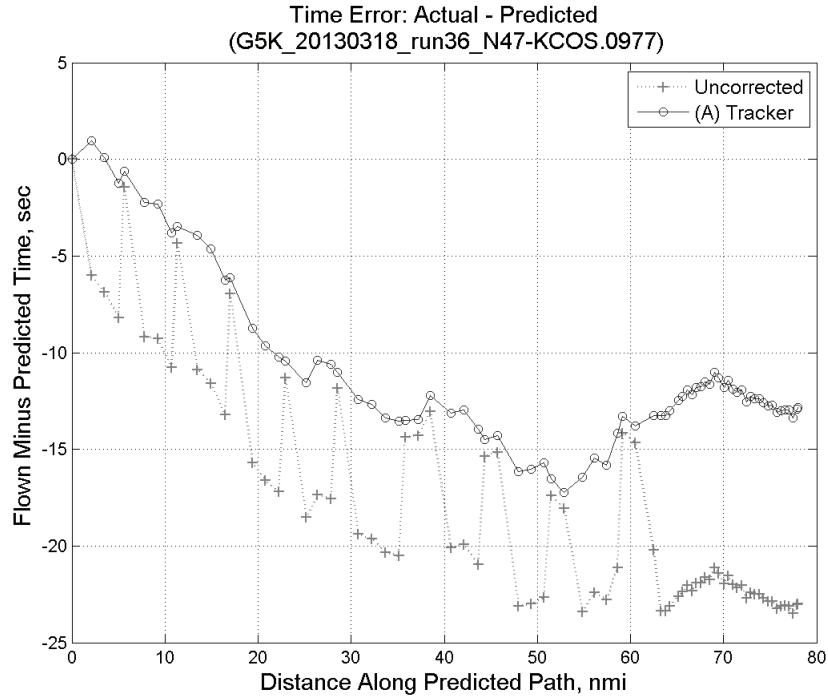


**Figure 657: Time error for run 36 before (Uncorrected) and after ((A) Tracker) removing tracker jump error source.**

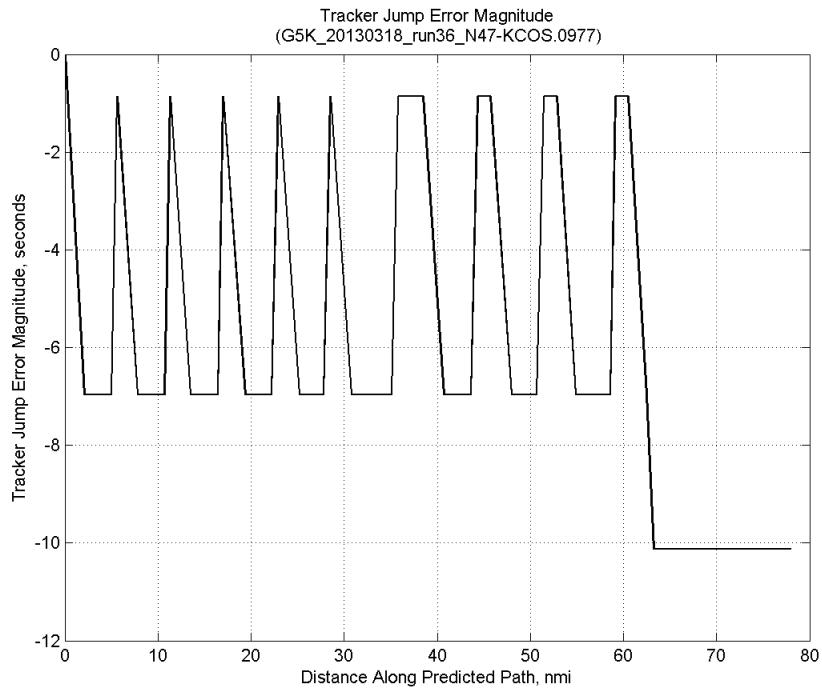


**Figure 658: Effect of tracker jump error source on time error for run 36.**

### C.25.B. Wind

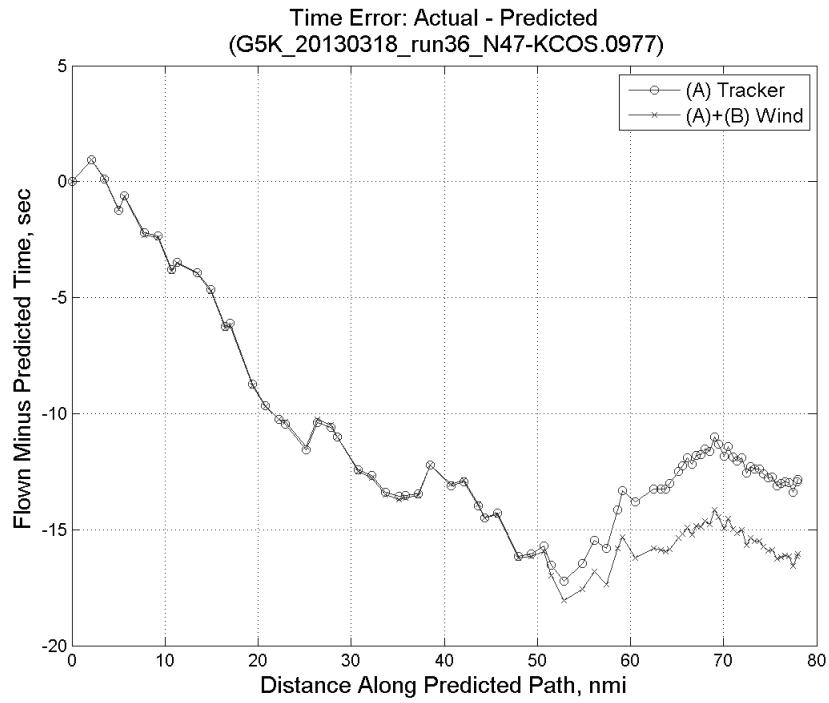


**Figure 659: Time error for run 36 before ((A) Tracker) and after ((A)+(B) Wind) removing wind error source.**

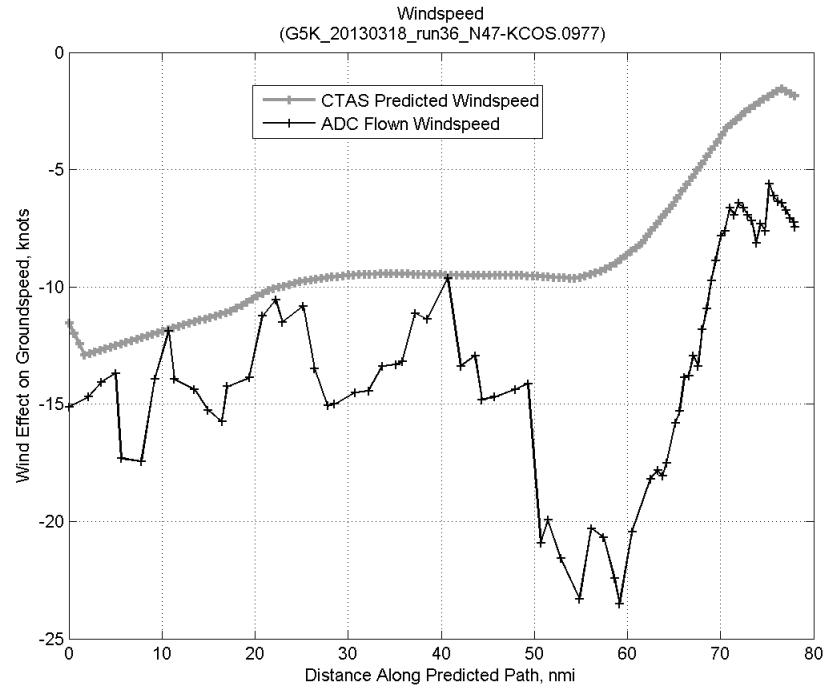


**Figure 660: CTAS predicted and ADC flown wind effect on ground speed for run 36. Negative values indicate a headwind.**

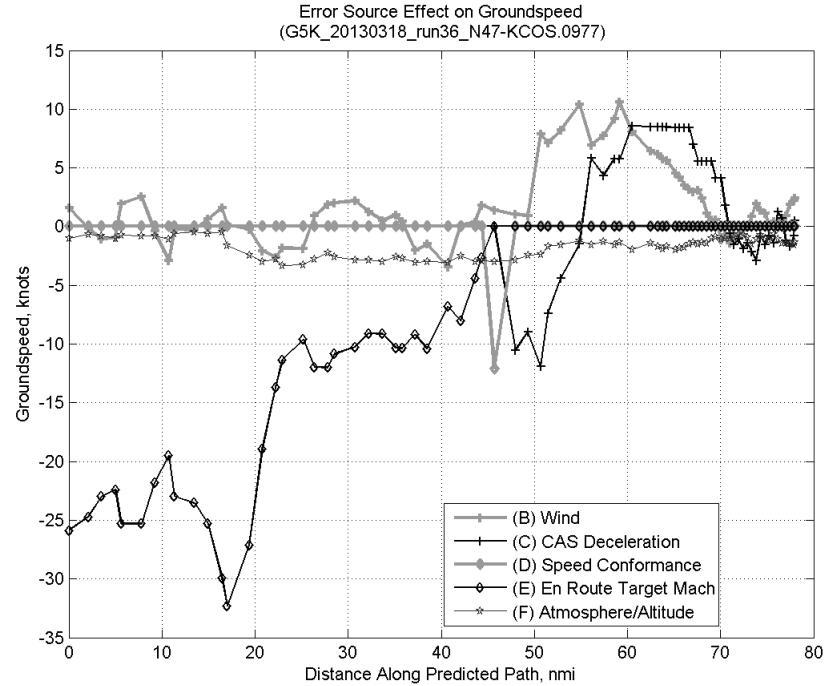


**Figure 661: Error sources (flown minus predicted) converted to a ground speed effect for run 36. Positive values indicate the flown ground speed was faster than the CTAS prediction.**

### C.25.C. CAS Deceleration

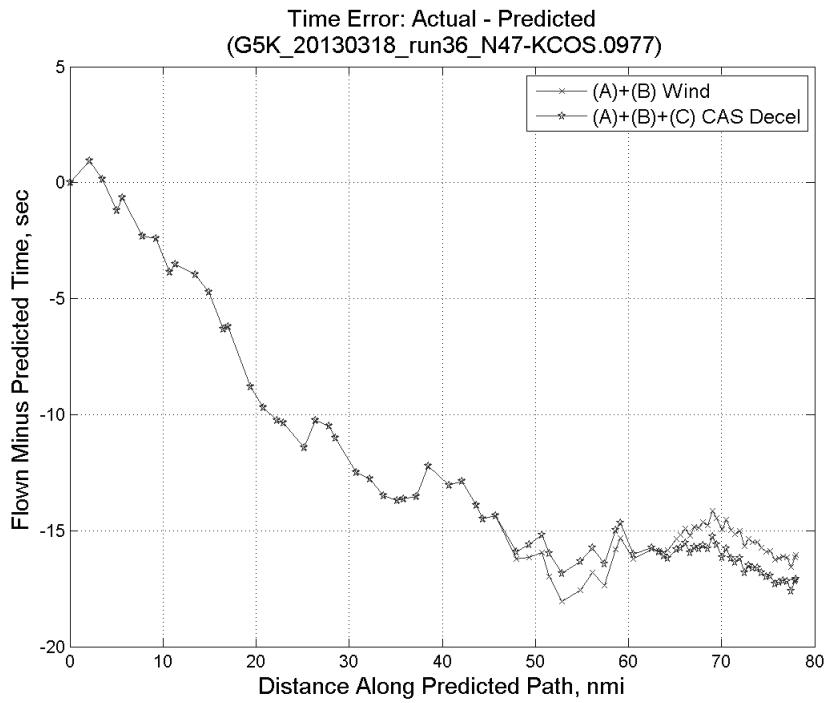


**Figure 662: Time error for run 36 before ((A)+(B) Wind) and after ((A)+(B)+(C) CAS Decel) removing CAS deceleration error source.**

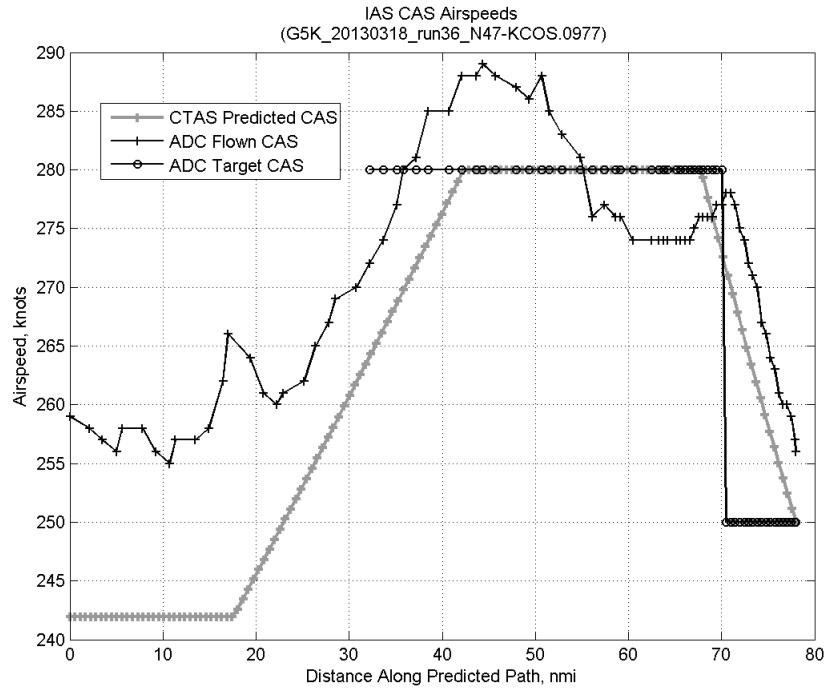


**Figure 663: CTAS predicted and ADC flown CAS for run 36. CAS that is being targeted is shown with circle markers.**

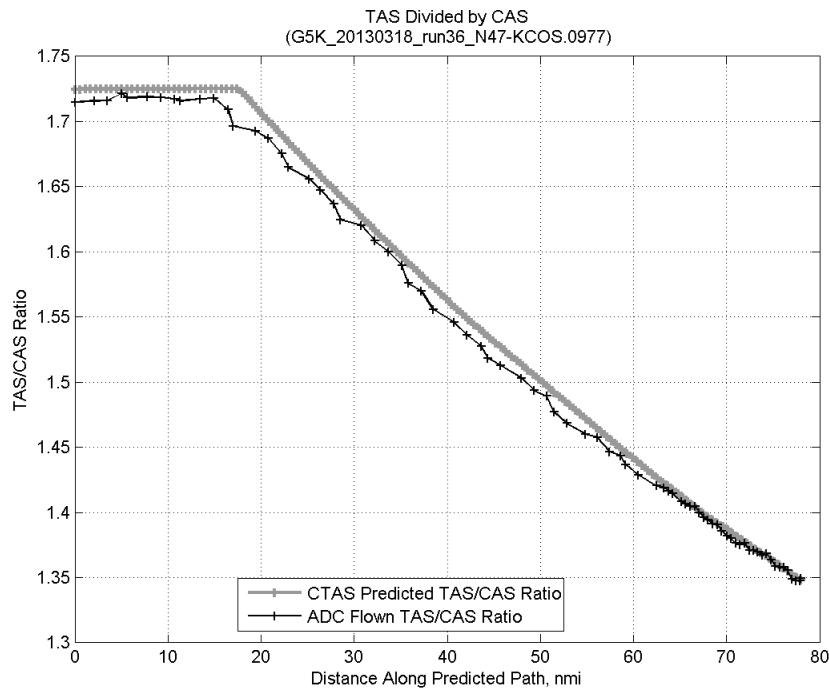


**Figure 664: CTAS predicted and ADC flown TAS/CAS ratio for run 36.**

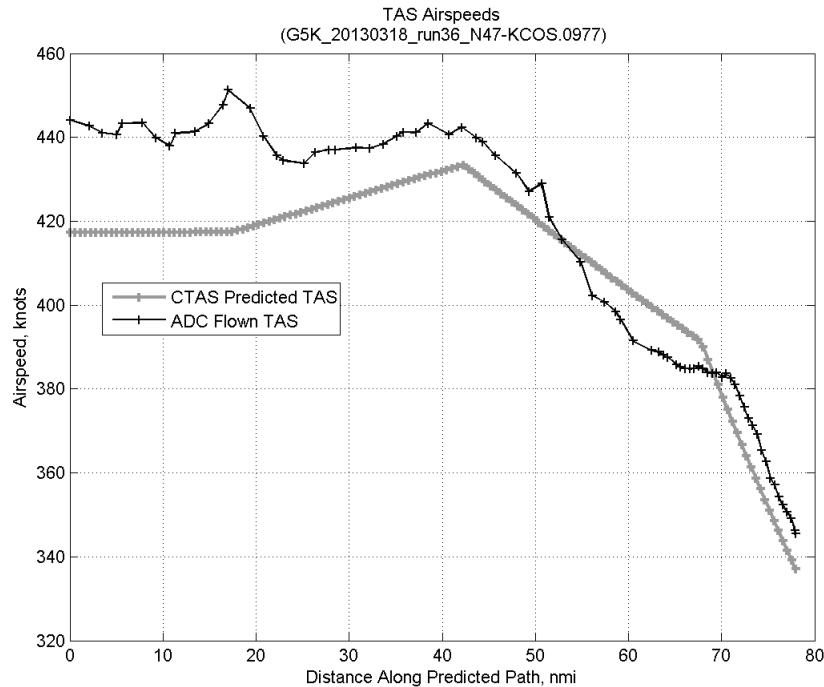


**Figure 665: CTAS predicted and ADC flown TAS for run 36.**

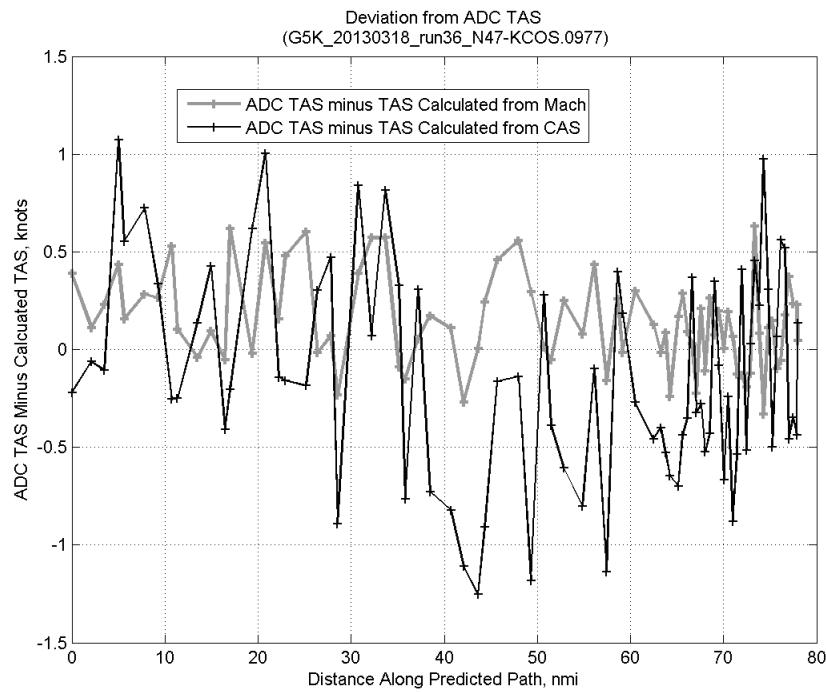


**Figure 666: Deviation from ADC flown TAS if calculating TAS using ADC flown CAS, Mach, atmospheric temperature, and atmospheric pressure for run 36.**

#### C.25.D. Speed Conformance

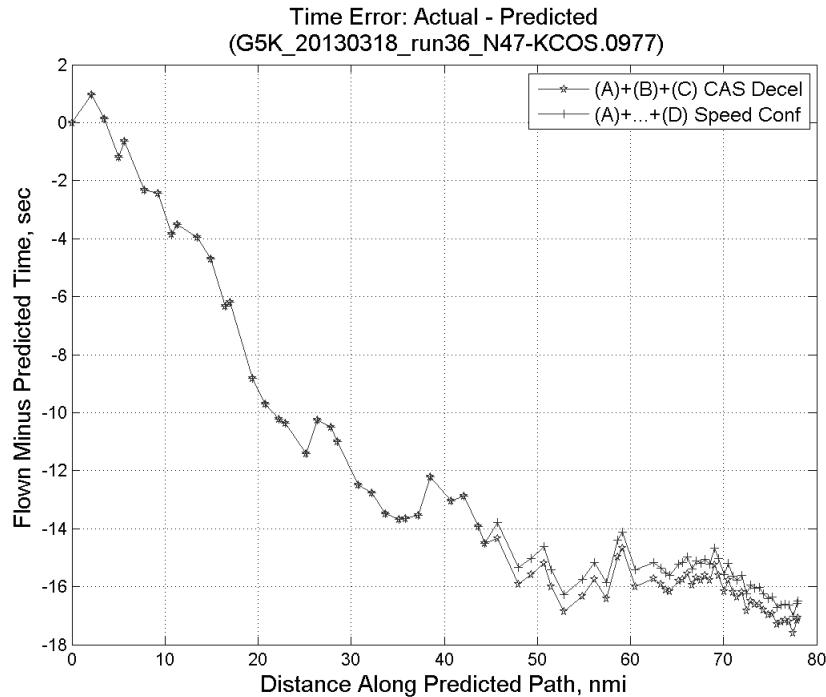


**Figure 667: Time error for run 36 before ((A)+(B)+(C) CAS Decel) and after ((A)+...+(D) Speed Conf) removing speed conformance error source.**

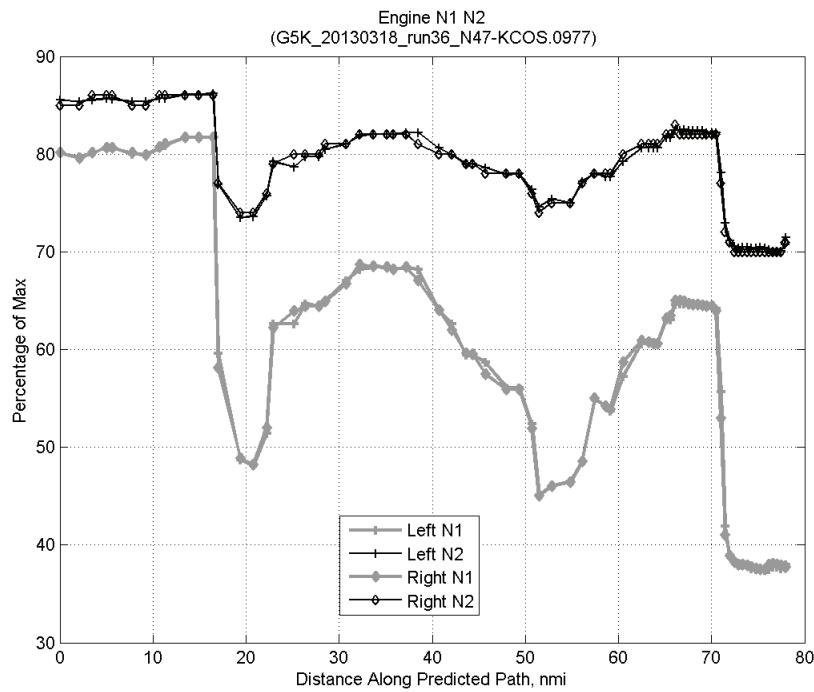


**Figure 668: Flown engine N1 and N2 for run 36.**

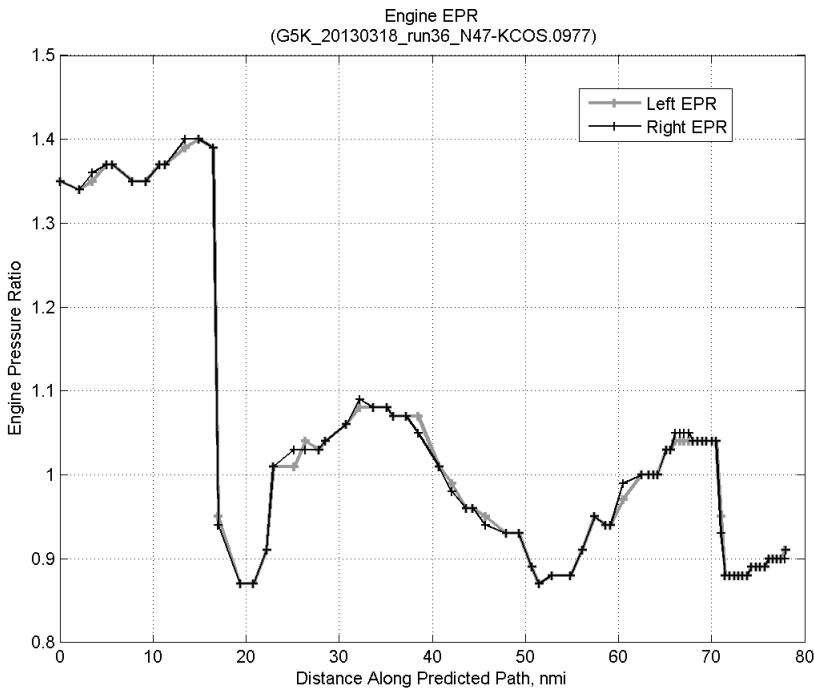


**Figure 669: Flown engine EPR for run 36.**

### C.25.E. Target Mach

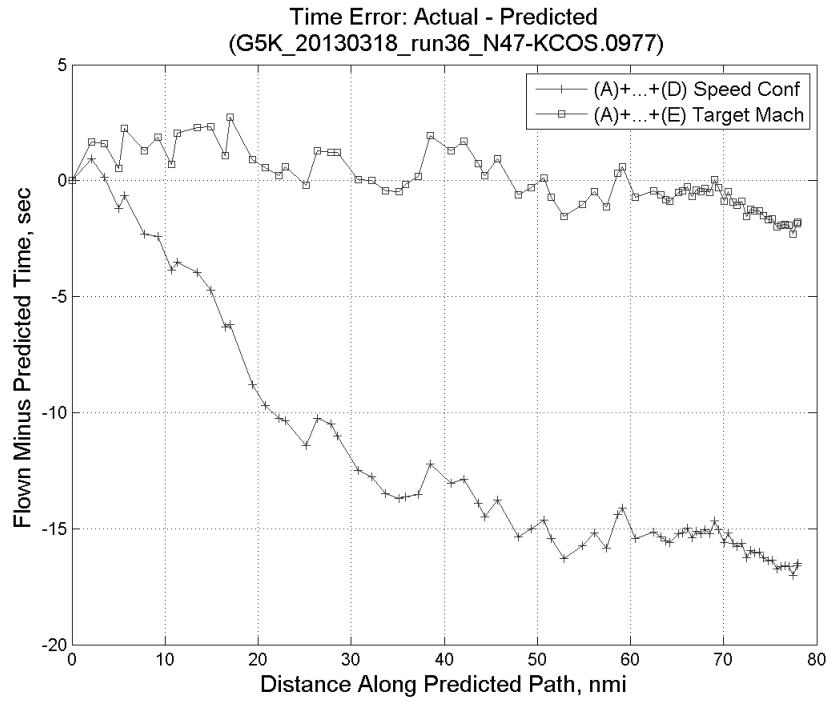


**Figure 670:** Time error for run 36 before ((A)+...+(D) Speed Conf) and after ((A)+...+(E) Target Mach) removing target Mach error source.

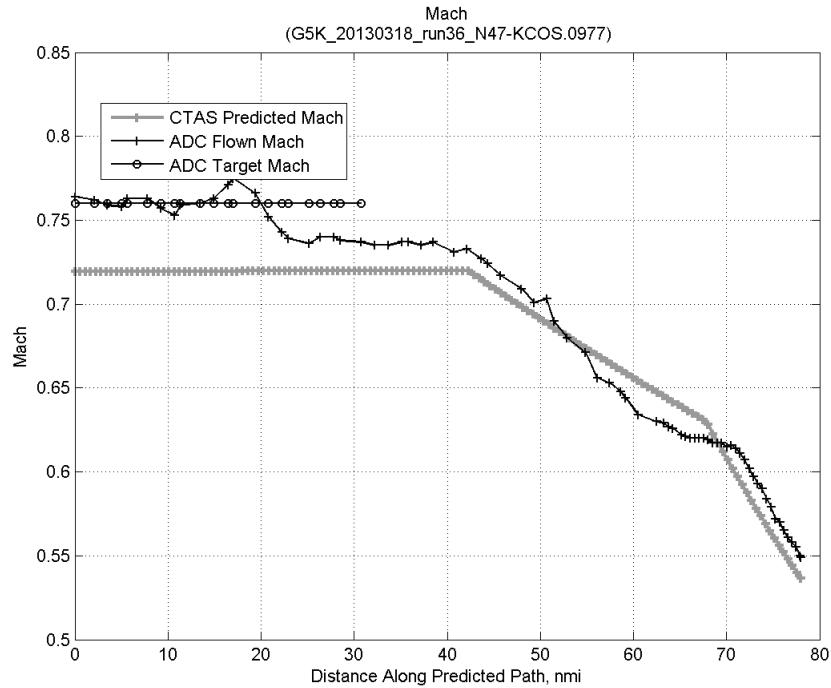


**Figure 671:** CTAS predicted and ADC flown Mach for run 36. Mach being targeted (ADC) shown with circle markers.

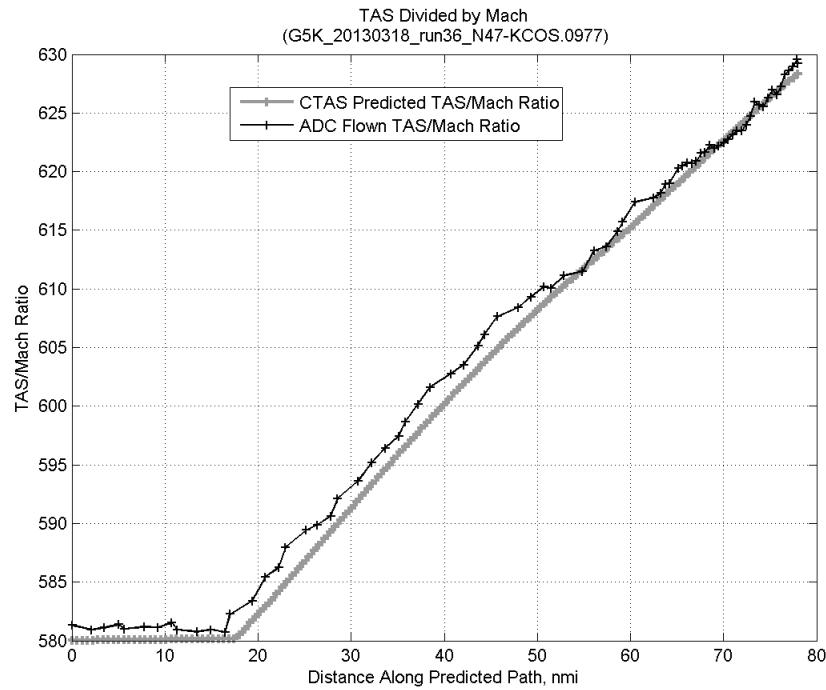


**Figure 672: CTAS predicted and ADC flown TAS/Mach ratio for run 36.**

#### C.25.F. Atmosphere/Altitude

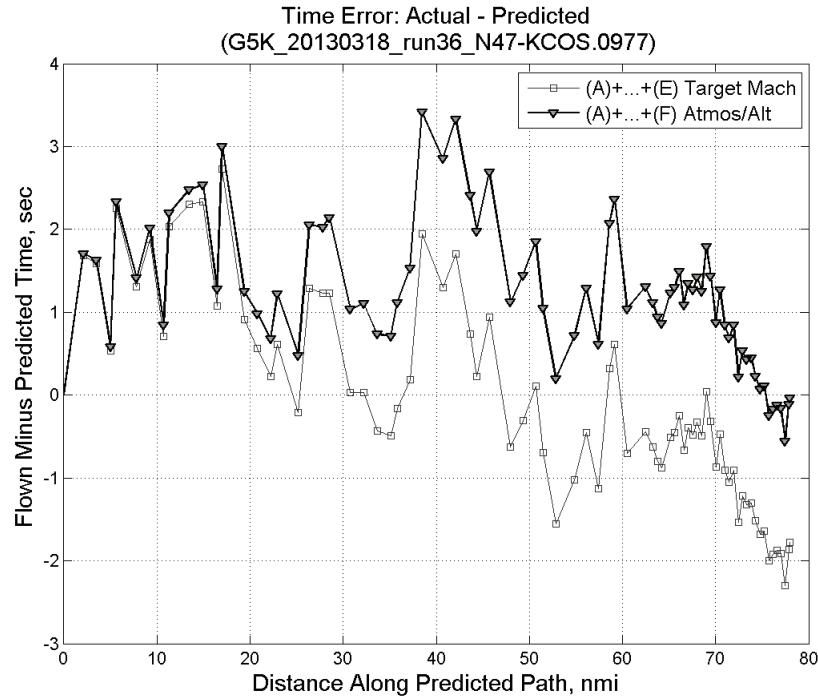


**Figure 673: Time error for run 36 before ((A)+...+(E) Target Mach) and after ((A)+...+(F) Atmos/Alt) removing atmosphere/altitude error source.**

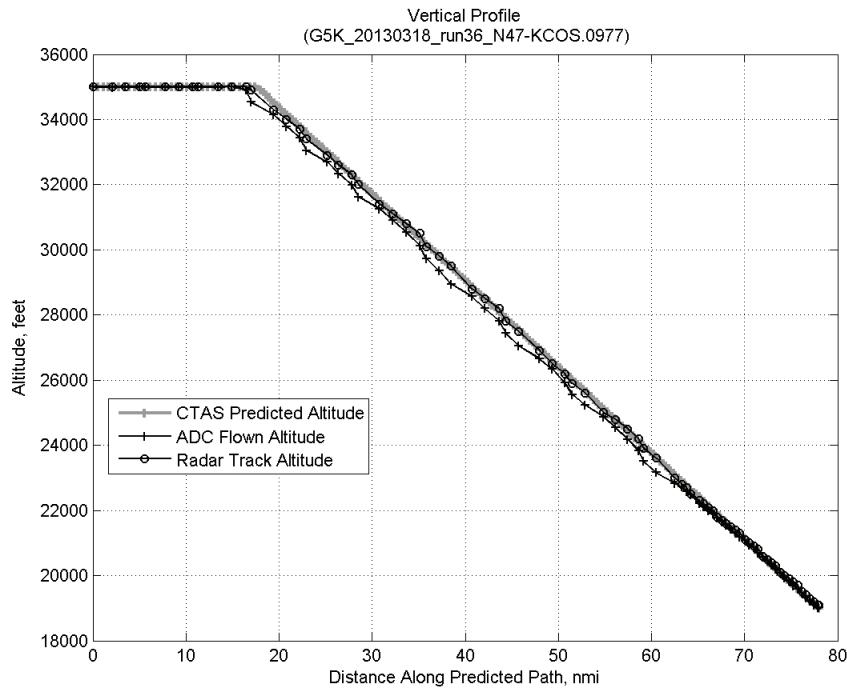


**Figure 674: Flown (ADC) and predicted (CTAS) vertical profile for run 36.**

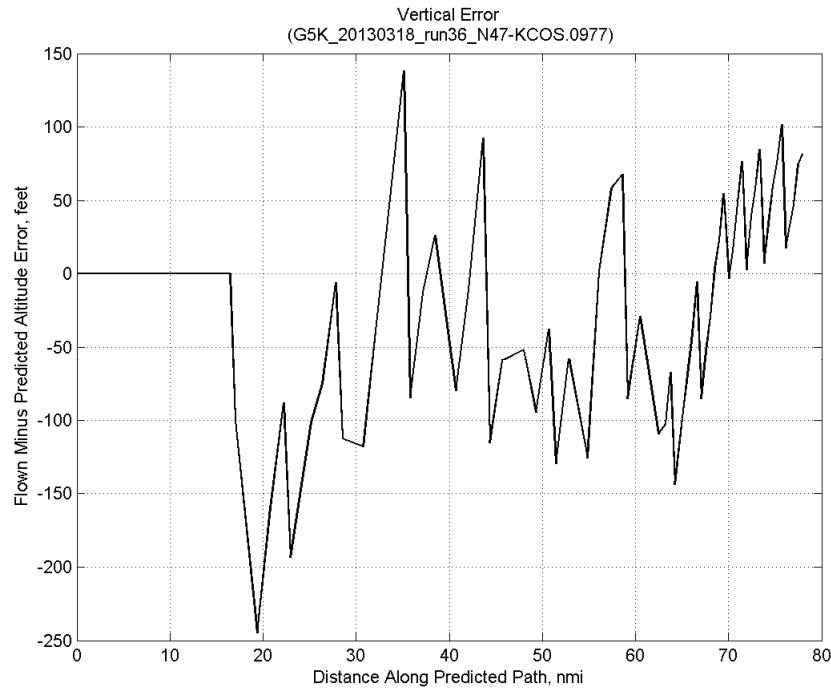


**Figure 675: Vertical error (flown minus predicted altitude) for run 36. Positive values indicate aircraft flew higher than predicted by CTAS.**

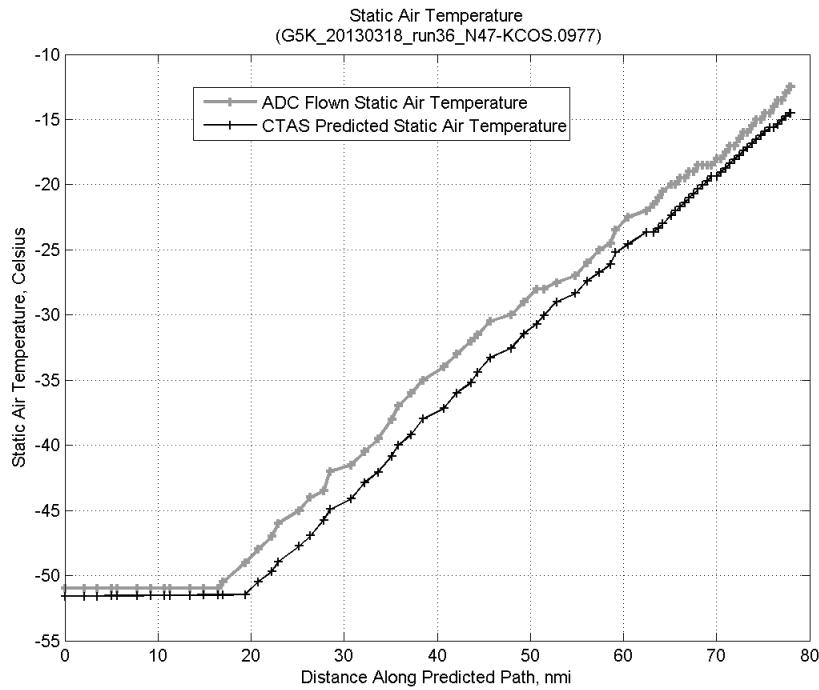


**Figure 676: Flown (ADC) and predicted (CTAS) static air temperature for run 36.**

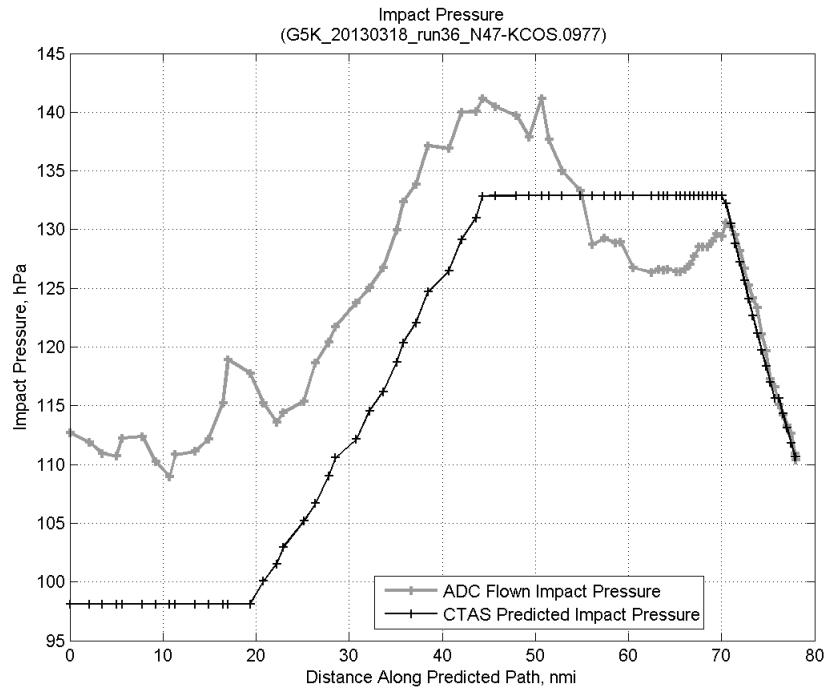


**Figure 677: Flown (ADC) and predicted (CTAS) impact pressure for run 36.**

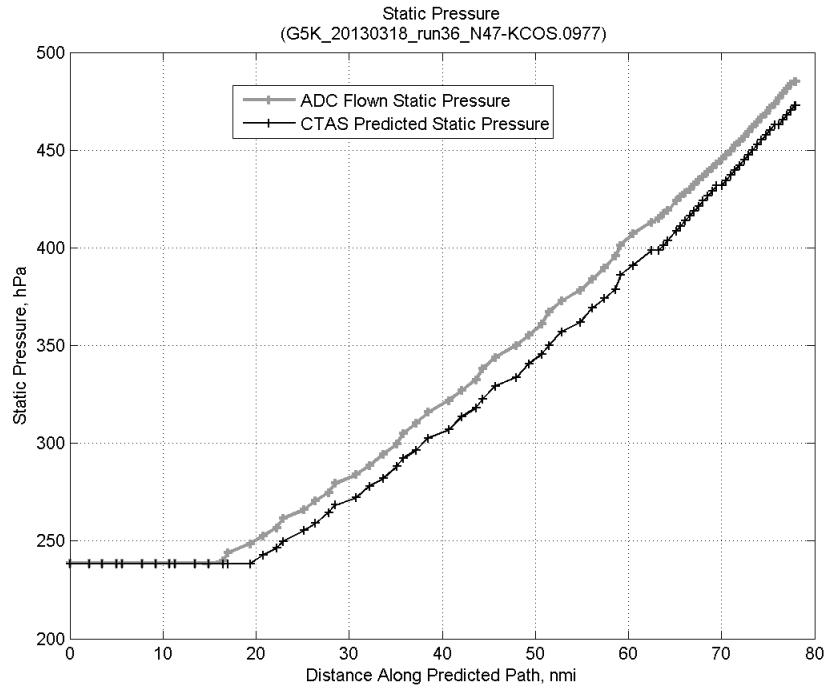


**Figure 678: Flown (ADC) and predicted (CTAS) static pressure for run 36.**

### C.25.G. Path Distance

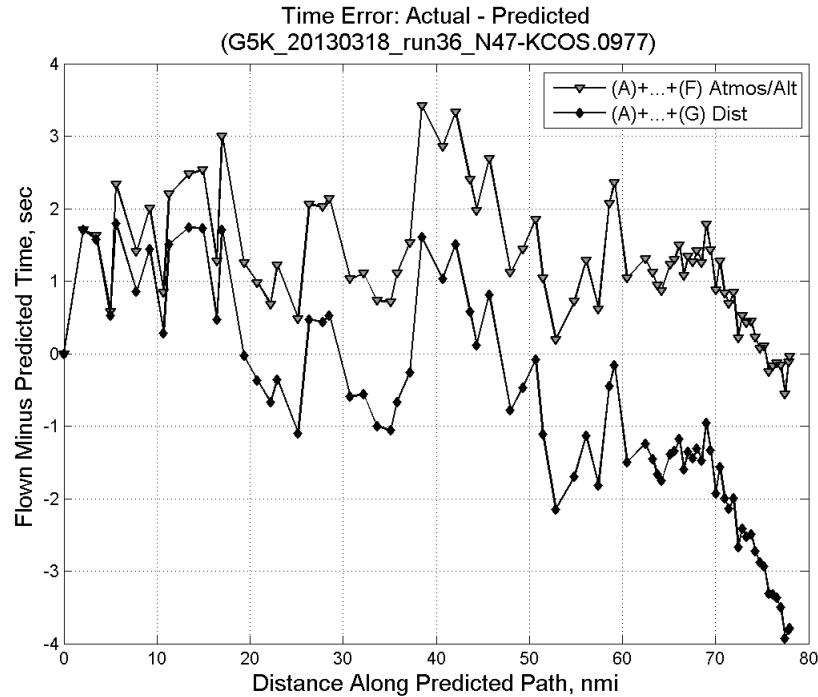


**Figure 679: Time error for run 36 before ((A)+...+(F) Atmos/Alt) and after ((A)+...+(G) Dist) removing path distance error source.**

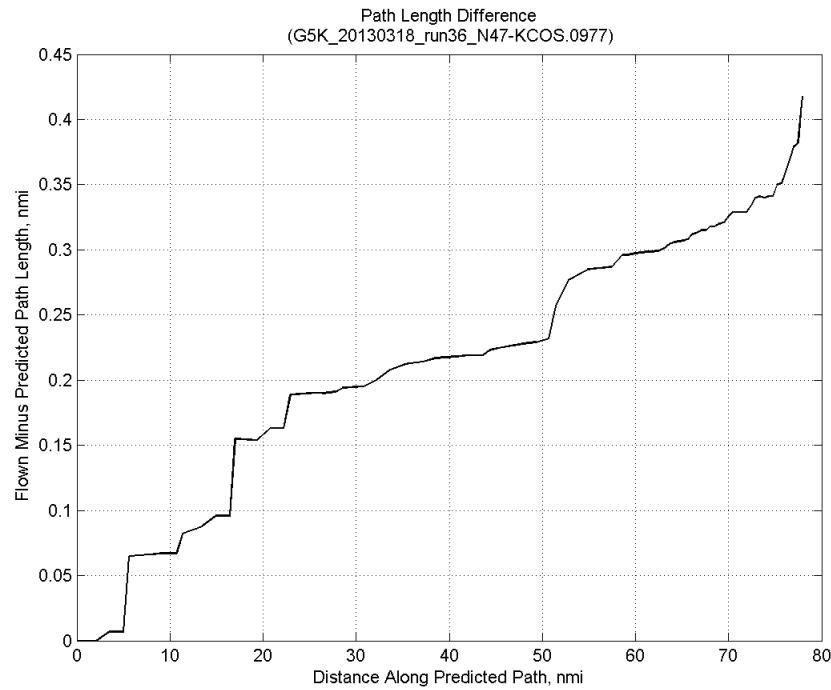


**Figure 680: ADC flown minus CTAS predicted path length for run 36. Positive values indicate aircraft followed a longer path than predicted by CTAS.**

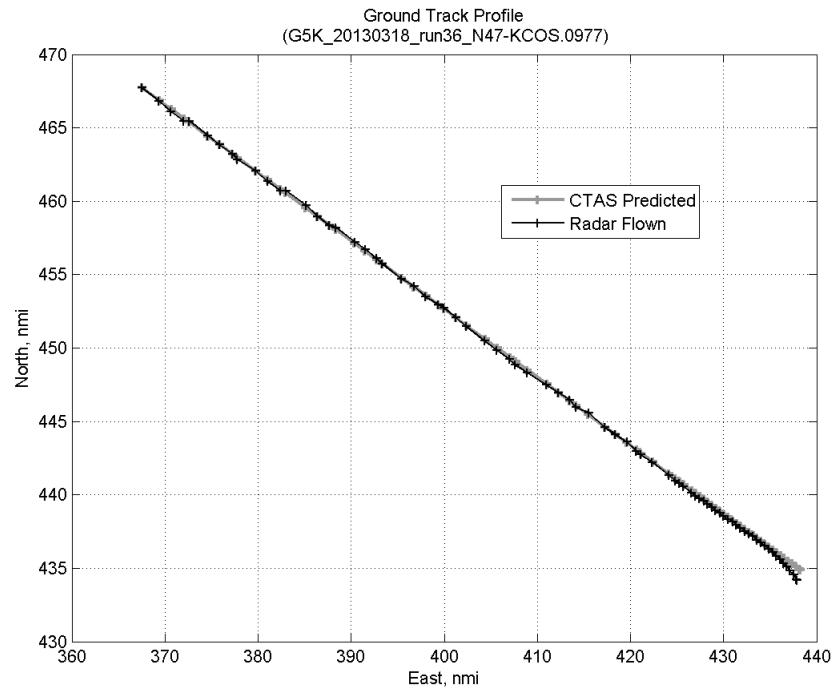


**Figure 681: CTAS predicted and radar flown ground track profile for run 36.**

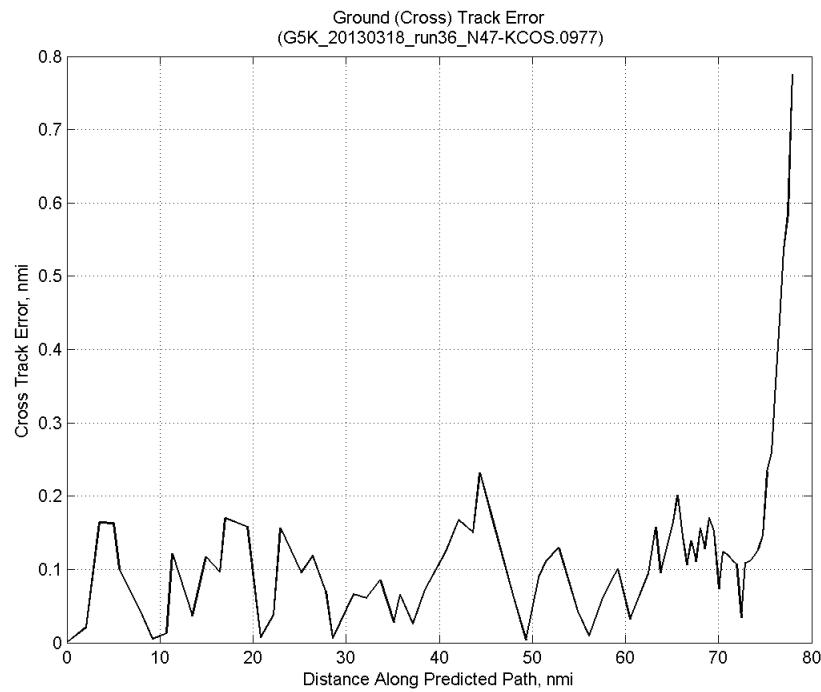


**Figure 682: Ground (cross) track error for run 36.**

## C.26. Run 37

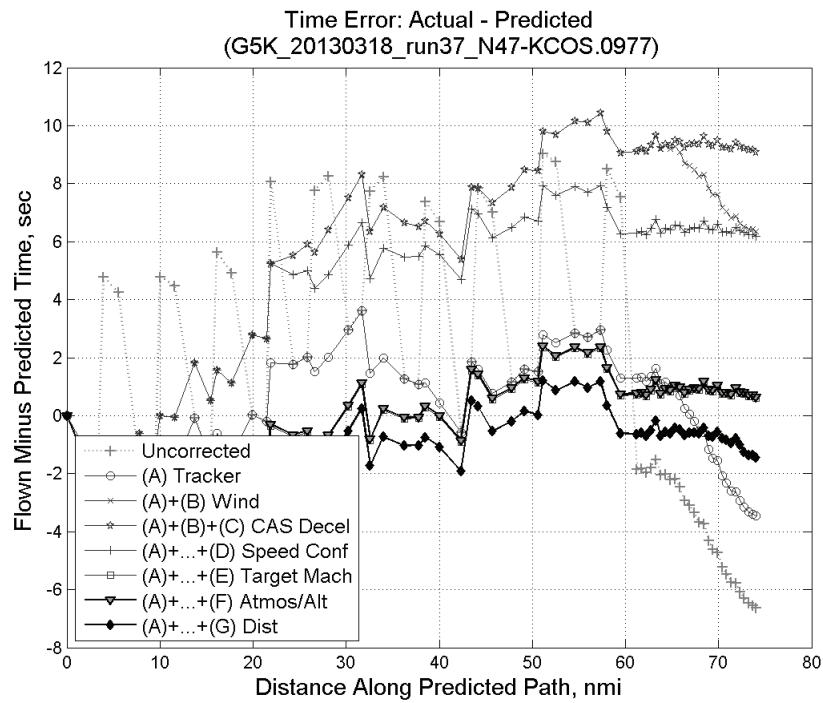


**Figure 683:** Time error for run 37 showing incremental effect of removing each error source.

### C.26.A. Tracker Jumps

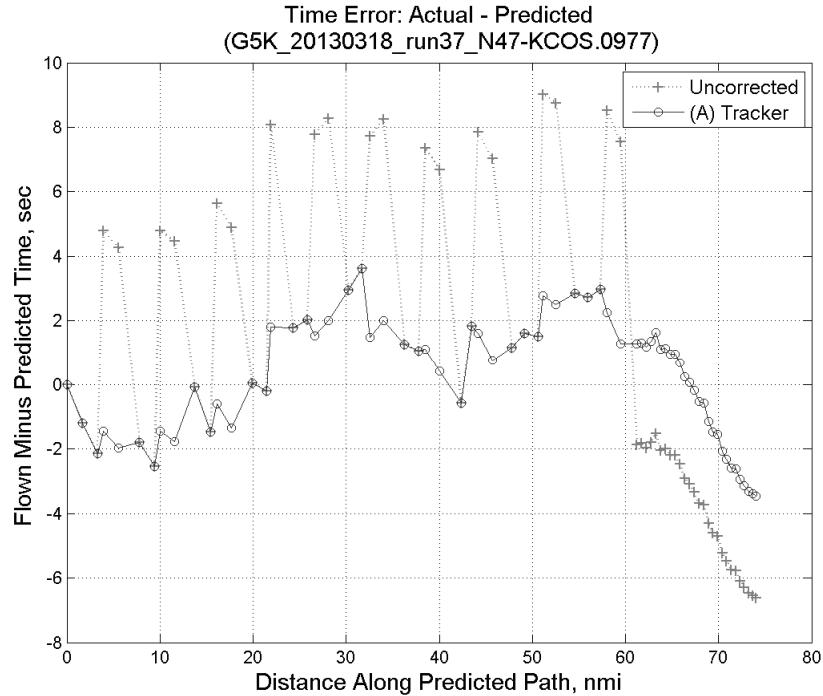


**Figure 684:** Time error for run 37 before (Uncorrected) and after ((A) Tracker) removing tracker jump error source.

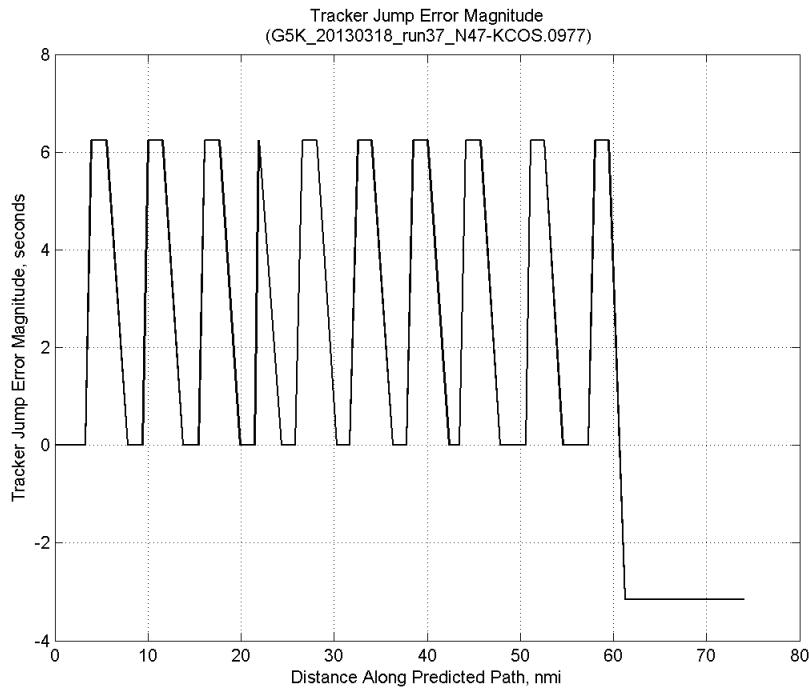


**Figure 685: Effect of tracker jump error source on time error for run 37.**

### C.26.B. Wind

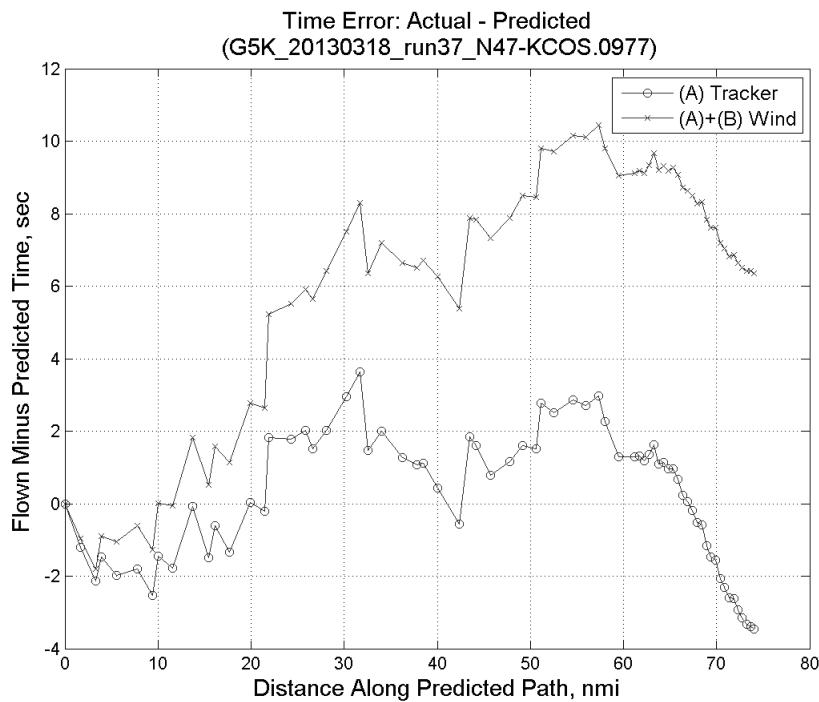


**Figure 686: Time error for run 37 before ((A) Tracker) and after ((A)+(B) Wind) removing wind error source.**

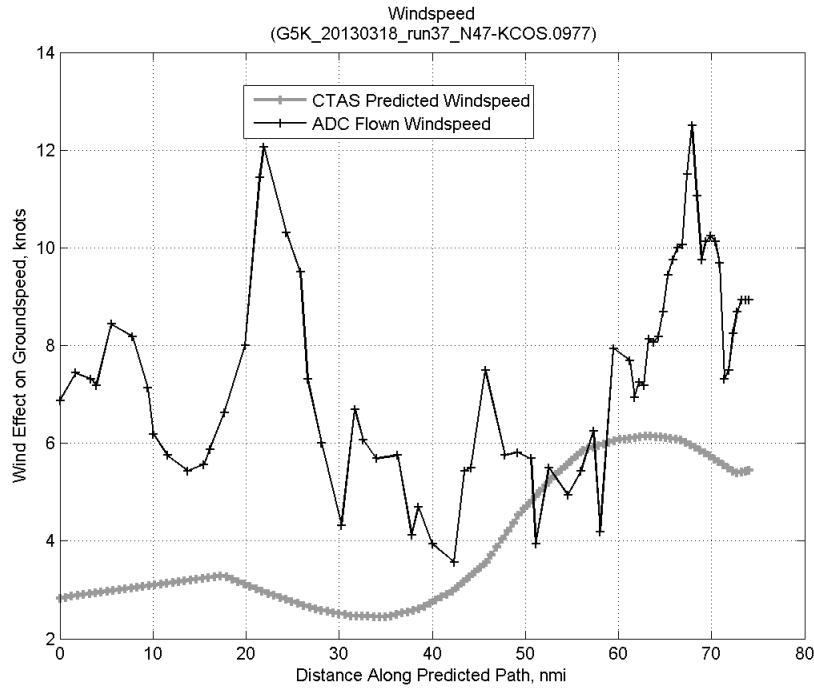


**Figure 687: CTAS predicted and ADC flown wind effect on ground speed for run 37. Negative values indicate a headwind.**

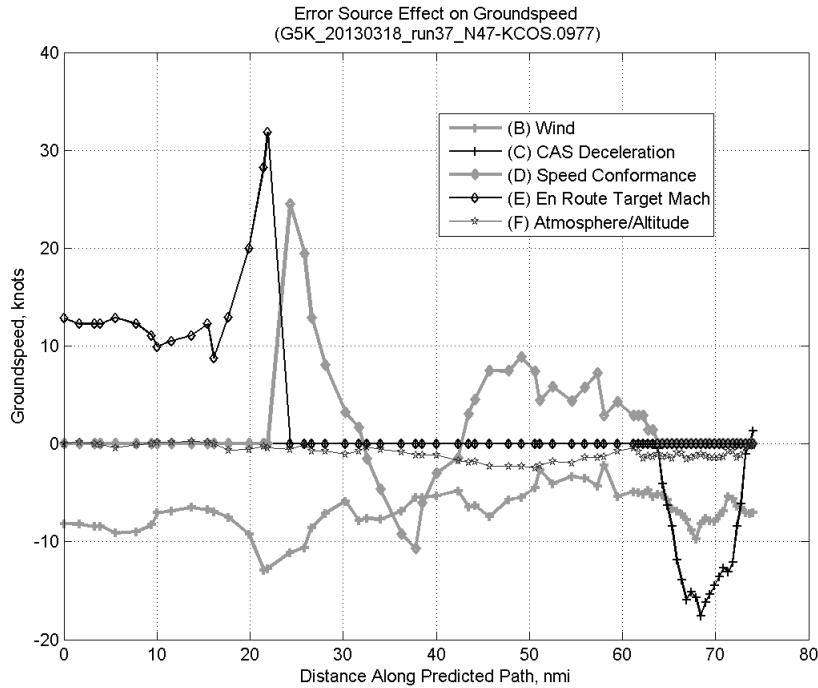


**Figure 688: Error sources (flown minus predicted) converted to a ground speed effect for run 37. Positive values indicate the flown ground speed was faster than the CTAS prediction.**

### C.26.C. CAS Deceleration

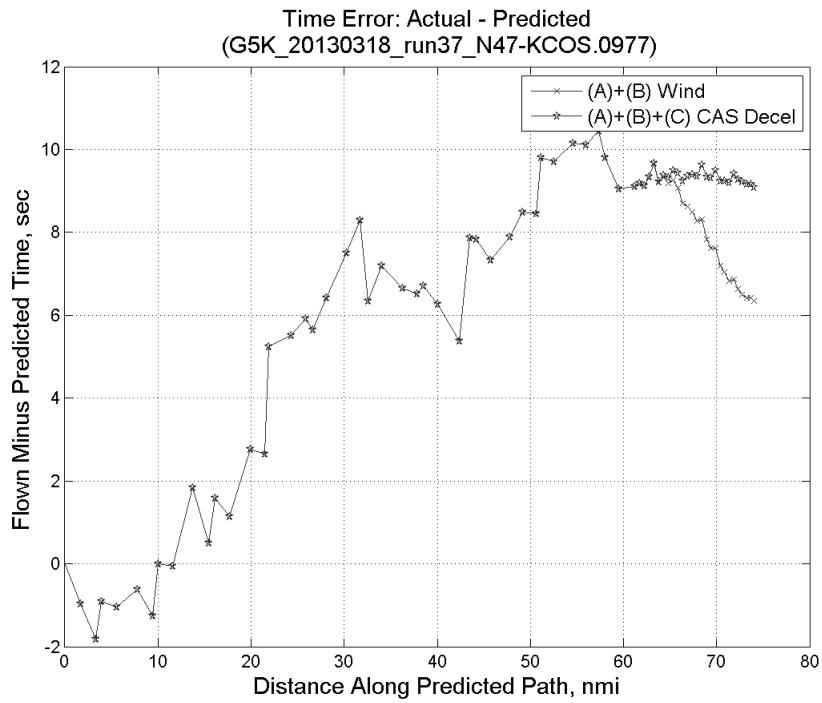


**Figure 689:** Time error for run 37 before ((A)+(B) Wind) and after ((A)+(B)+(C) CAS Decel) removing CAS deceleration error source.

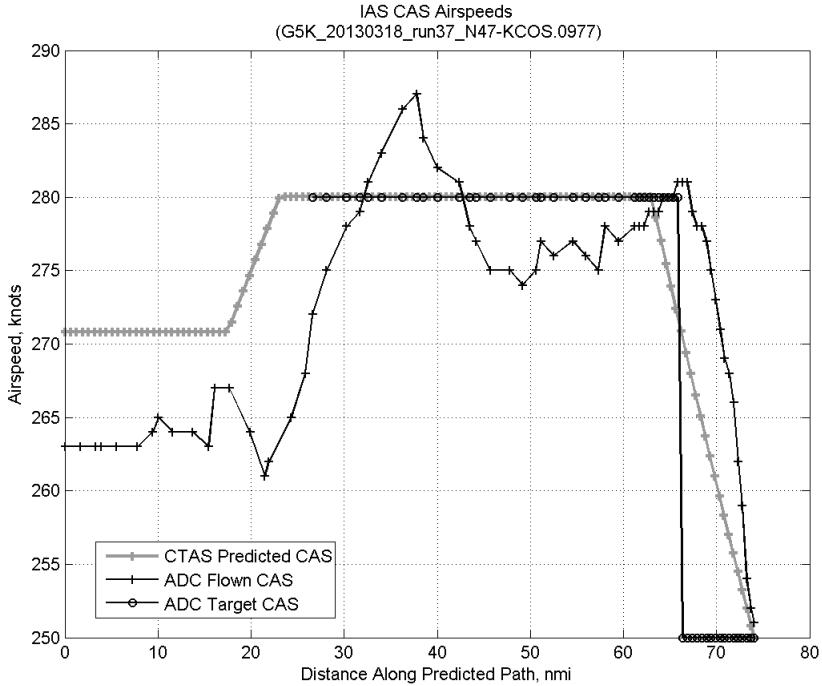


**Figure 690:** CTAS predicted and ADC flown CAS for run 37. CAS that is being targeted is shown with circle markers.

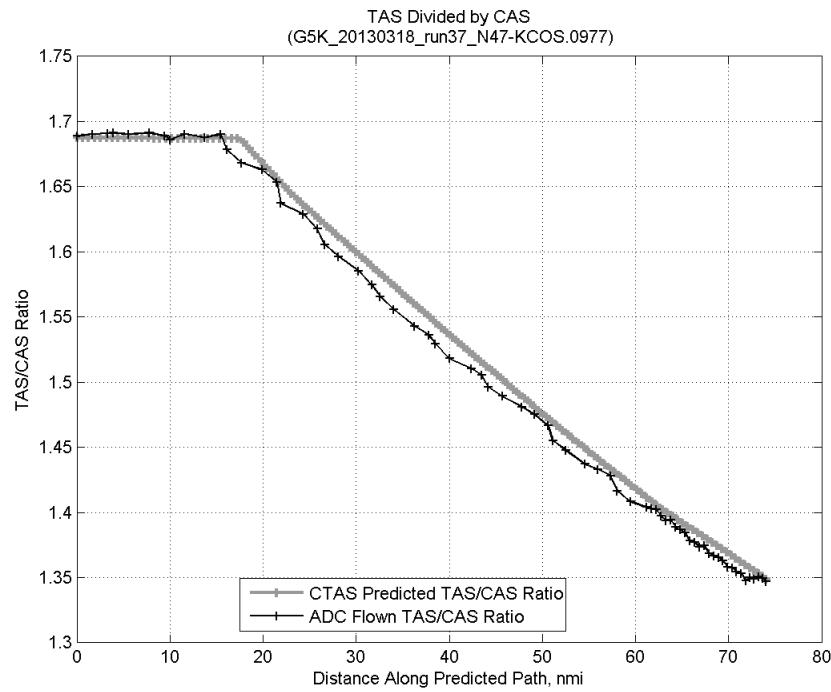


**Figure 691: CTAS predicted and ADC flown TAS/CAS ratio for run 37.**

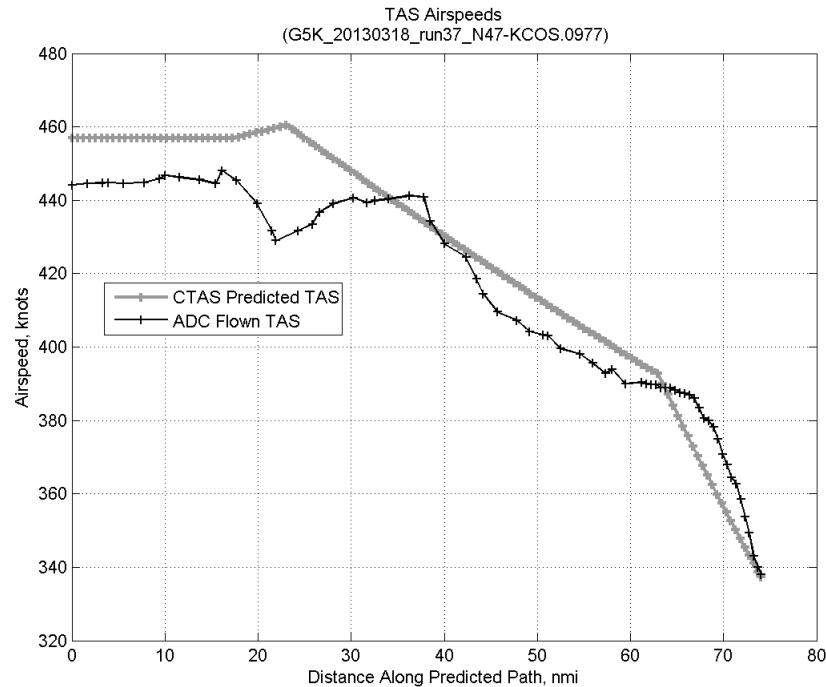


**Figure 692: CTAS predicted and ADC flown TAS for run 37.**

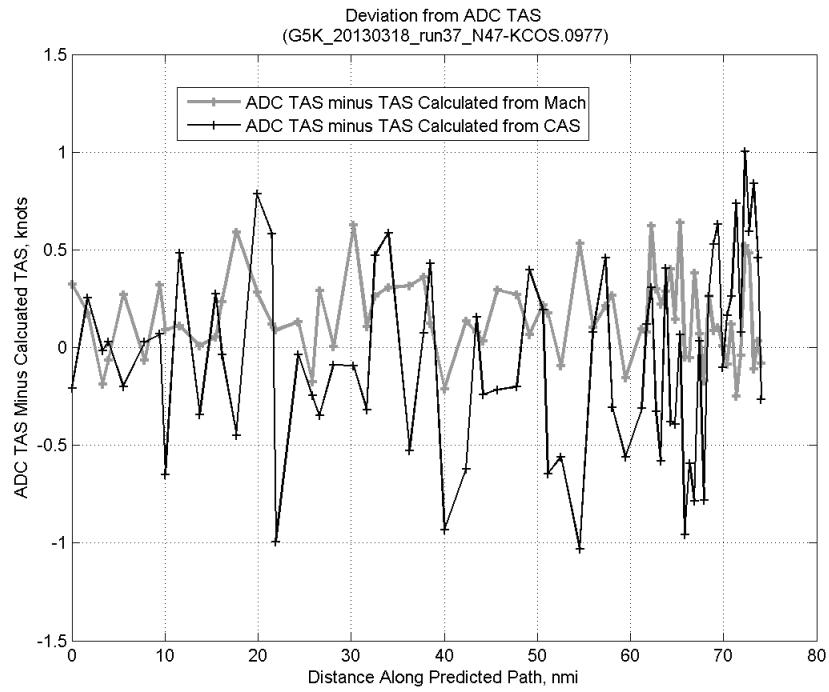


**Figure 693: Deviation from ADC flown TAS if calculating TAS using ADC flown CAS, Mach, atmospheric temperature, and atmospheric pressure for run 37.**

#### C.26.D. Speed Conformance

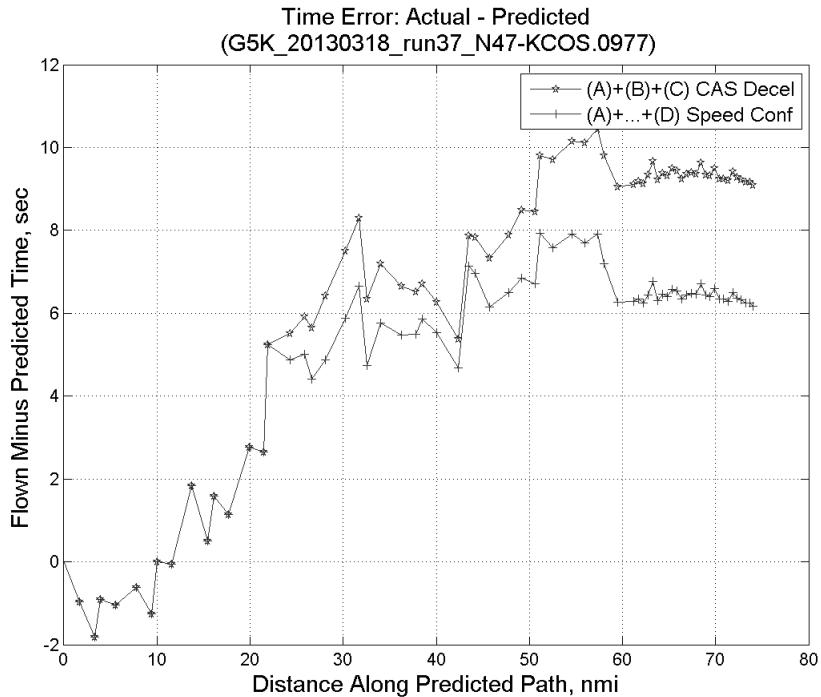


**Figure 694: Time error for run 37 before ((A)+(B)+(C) CAS Decel) and after ((A)+...+(D) Speed Conf) removing speed conformance error source.**

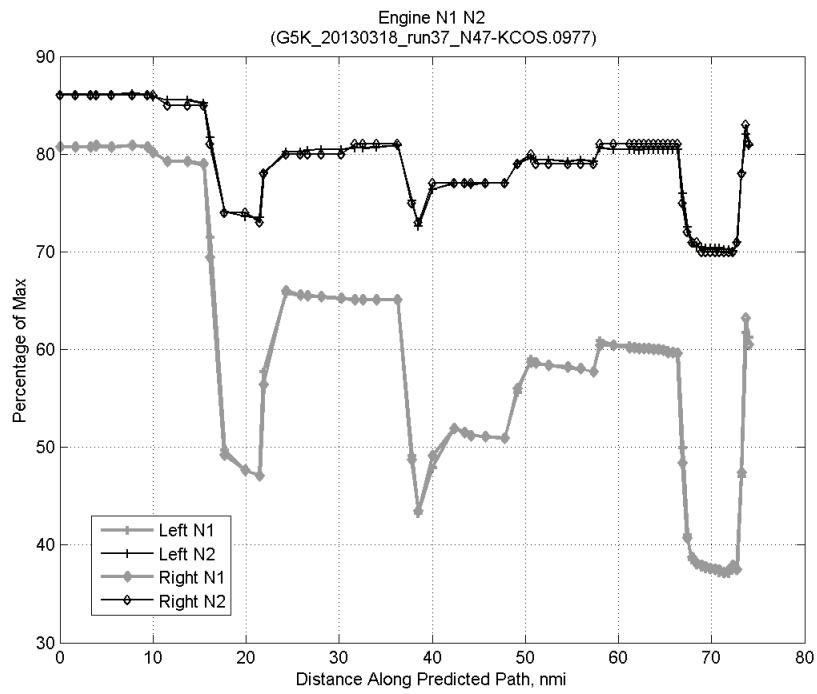


**Figure 695: Flown engine N1 and N2 for run 37.**

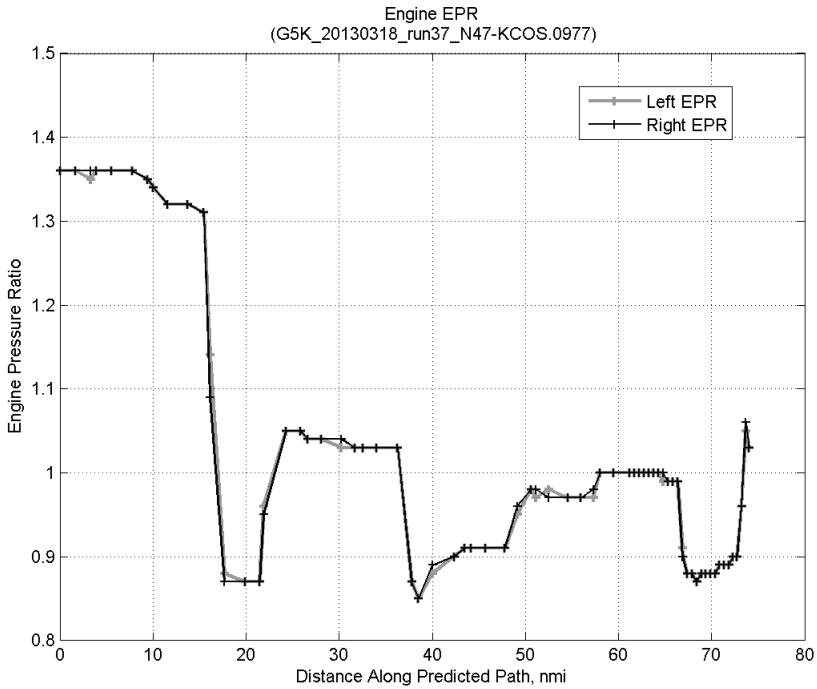


**Figure 696: Flown engine EPR for run 37.**

### C.26.E. Target Mach

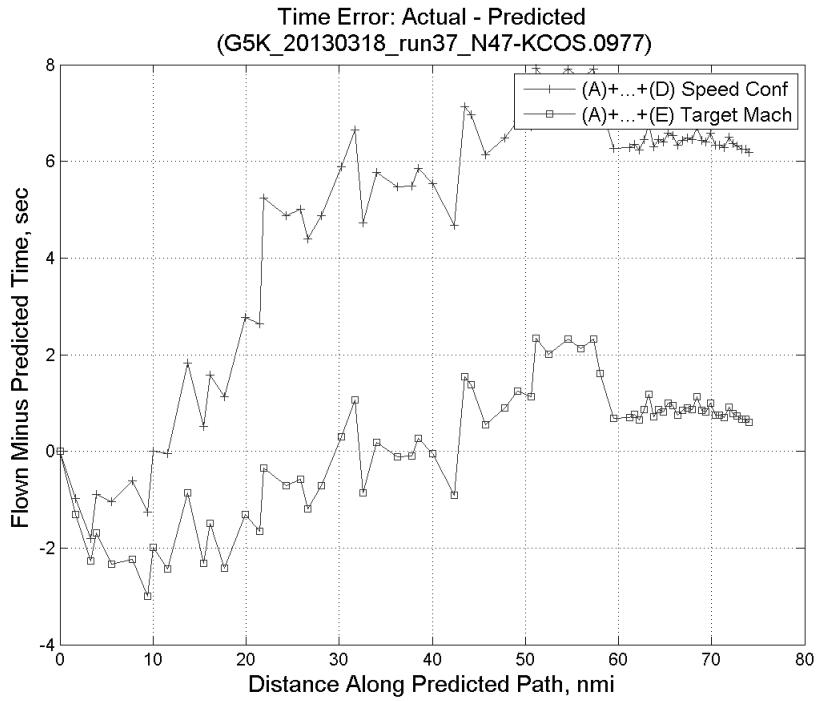


**Figure 697:** Time error for run 37 before ((A)+...+(D) Speed Conf) and after ((A)+...+(E) Target Mach) removing target Mach error source.

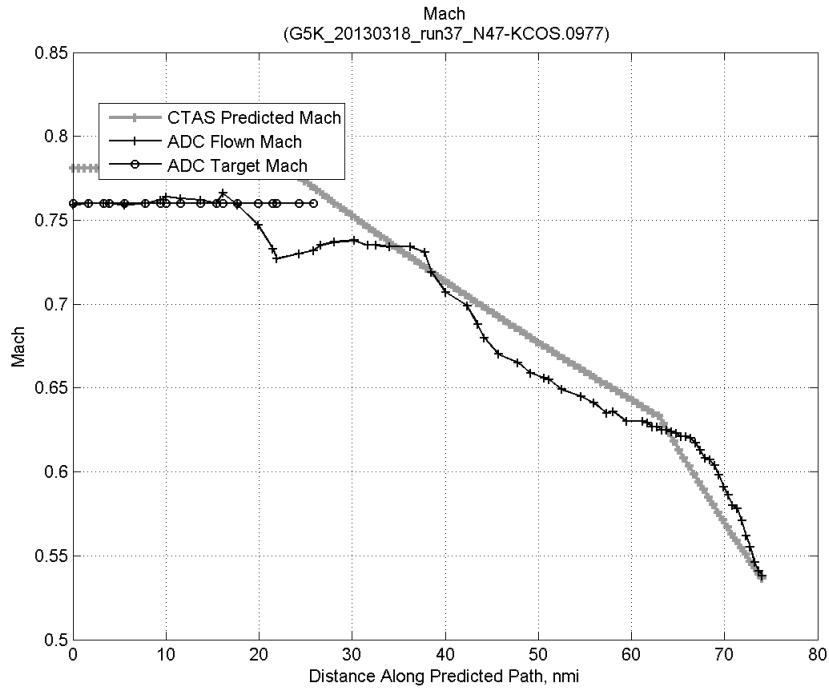


**Figure 698:** CTAS predicted and ADC flown Mach for run 37. Mach being targeted (ADC) shown with circle markers.

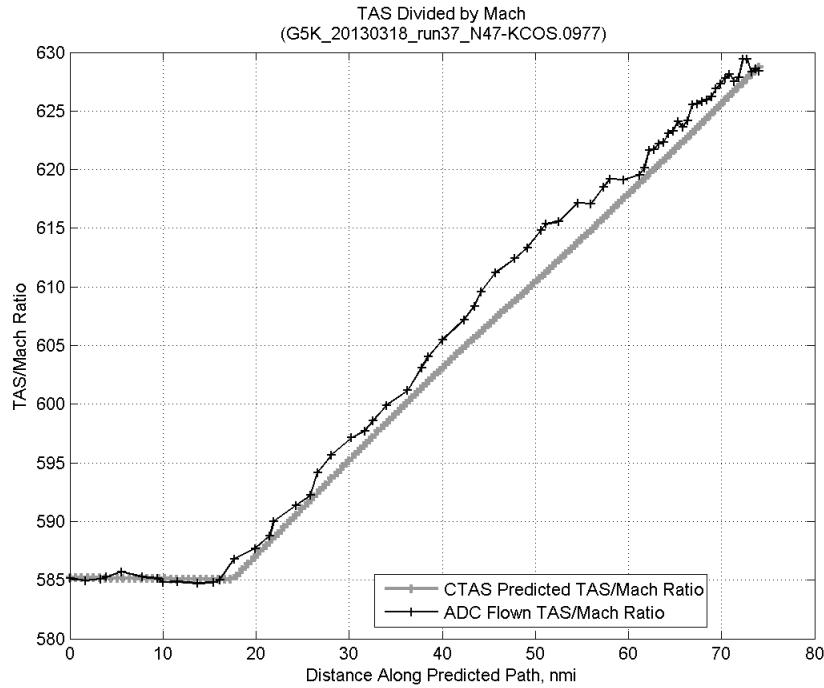


**Figure 699: CTAS predicted and ADC flown TAS/Mach ratio for run 37.**

#### C.26.F. Atmosphere/Altitude

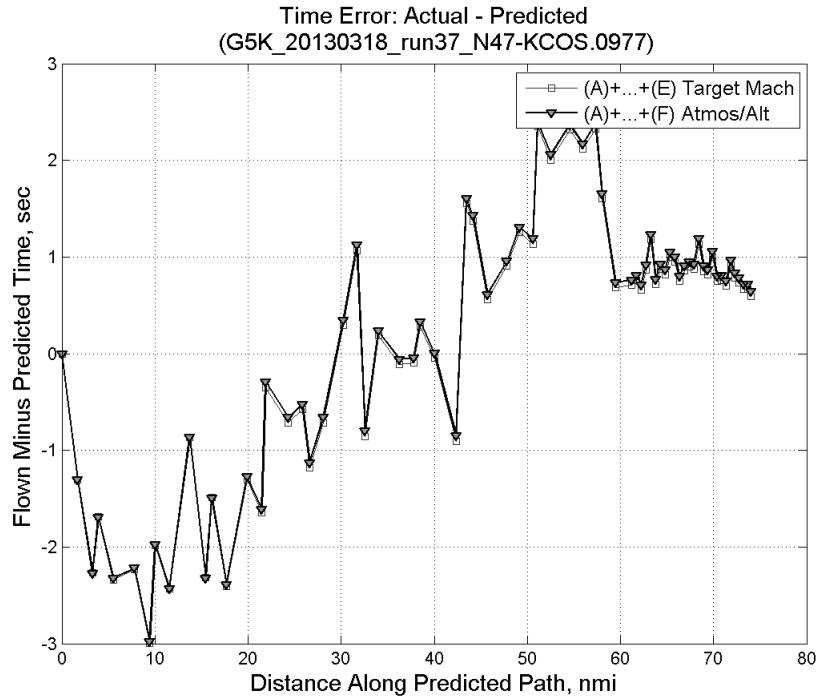


**Figure 700: Time error for run 37 before ((A)+...+(E) Target Mach) and after ((A)+...+(F) Atmos/Alt) removing atmosphere/altitude error source.**

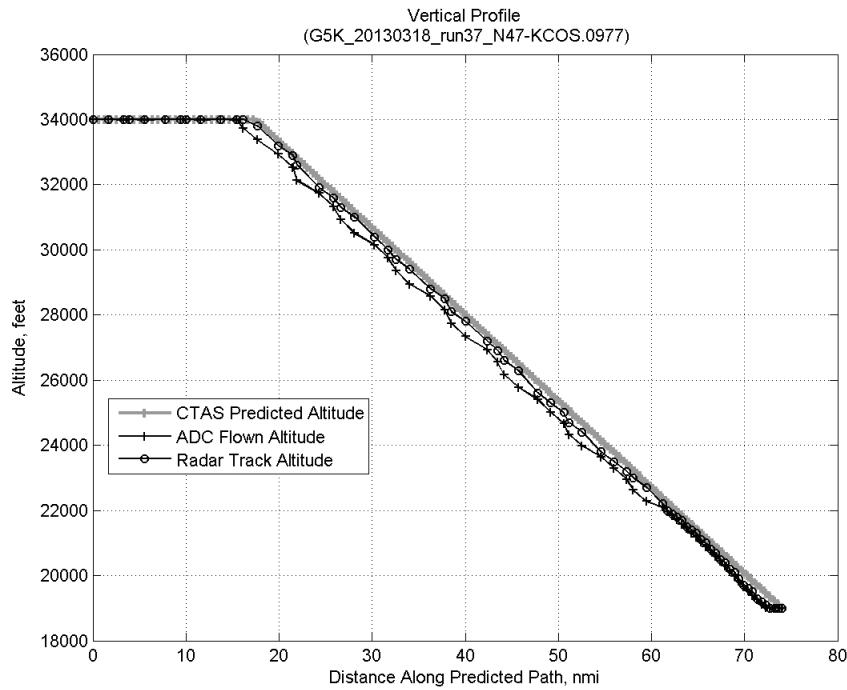


**Figure 701: Flown (ADC) and predicted (CTAS) vertical profile for run 37.**

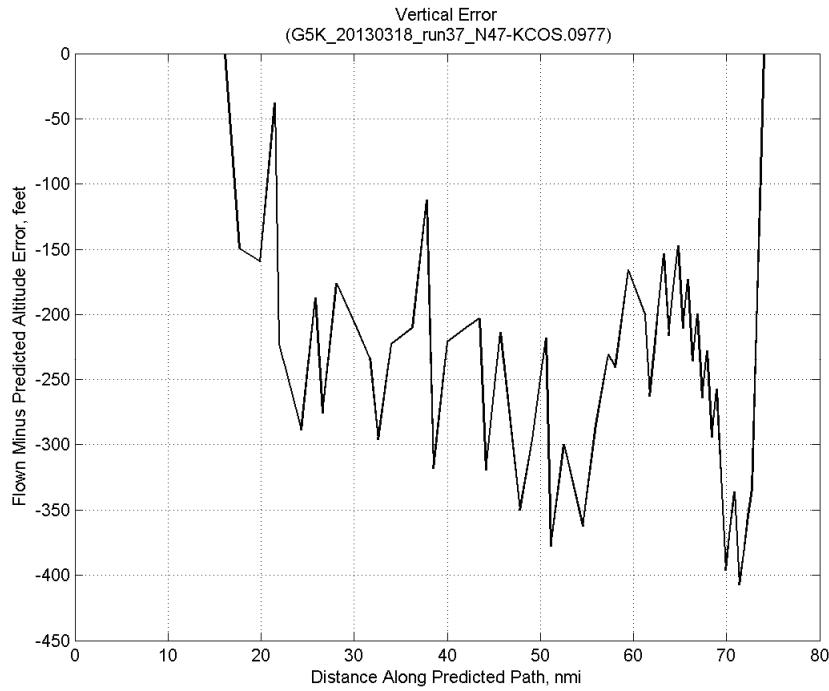


**Figure 702: Vertical error (flown minus predicted altitude) for run 37. Positive values indicate aircraft flew higher than predicted by CTAS.**

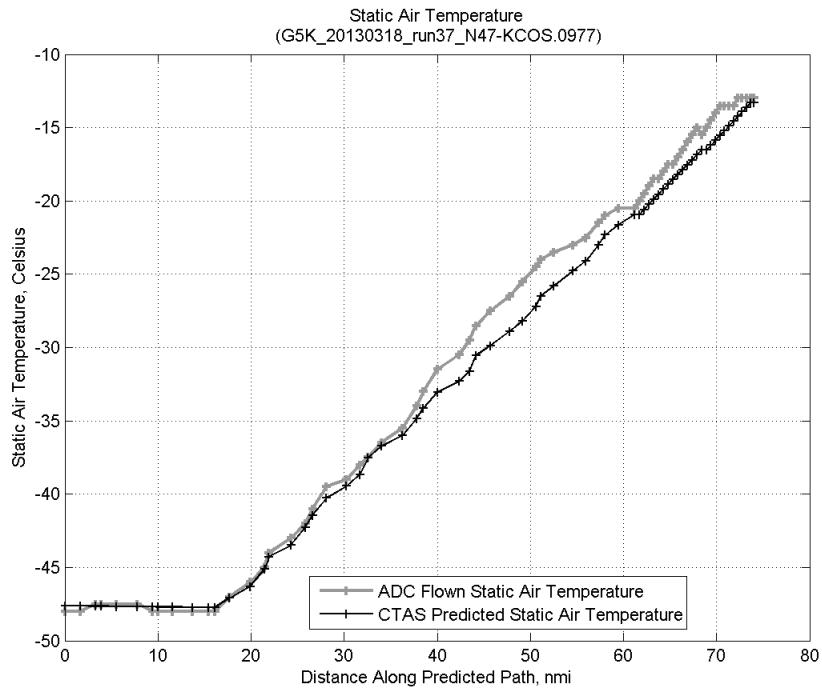


**Figure 703: Flown (ADC) and predicted (CTAS) static air temperature for run 37.**

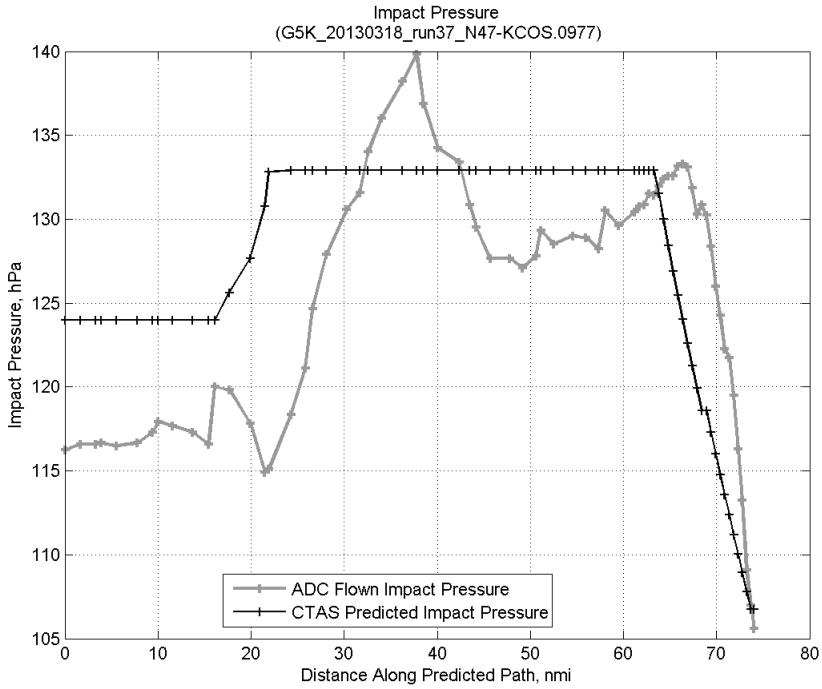


**Figure 704: Flown (ADC) and predicted (CTAS) impact pressure for run 37.**

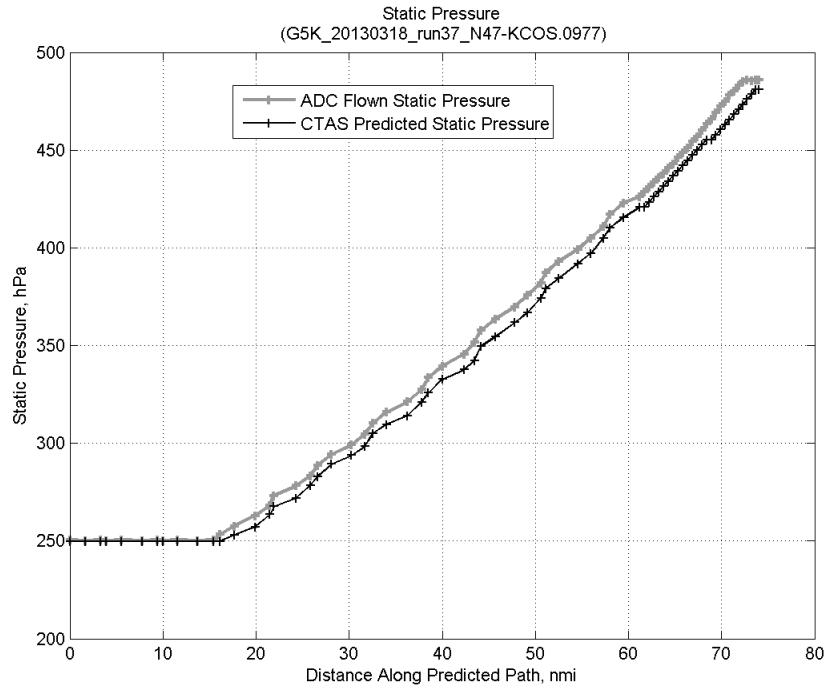


**Figure 705: Flown (ADC) and predicted (CTAS) static pressure for run 37.**

#### C.26.G. Path Distance

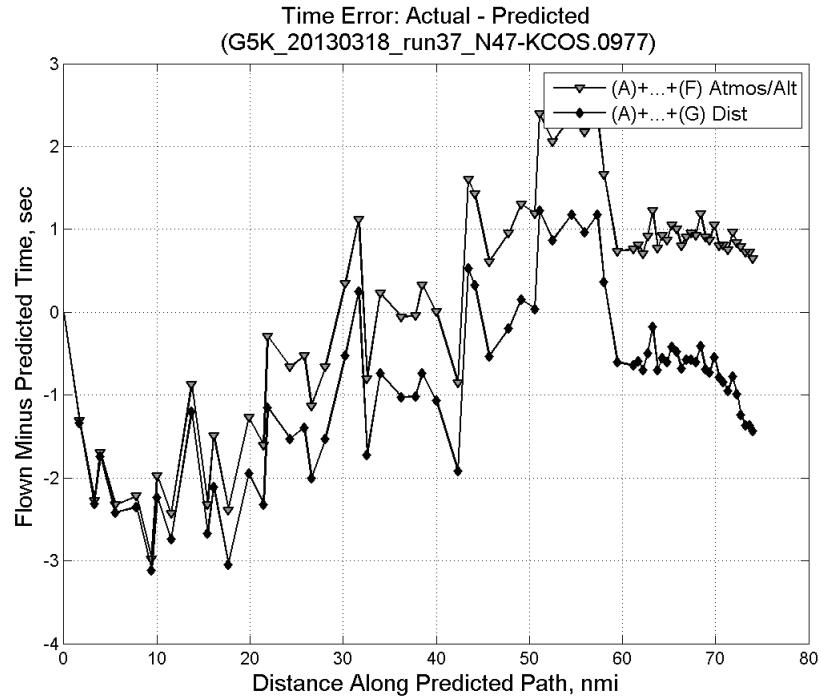


**Figure 706: Time error for run 37 before ((A)+...+(F) Atmos/Alt) and after ((A)+...+(G) Dist) removing path distance error source.**

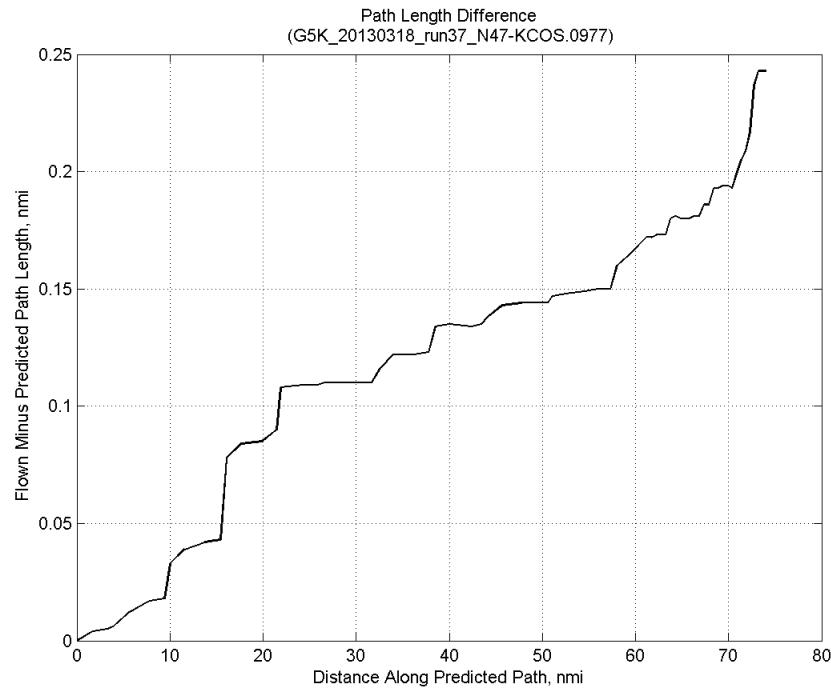


**Figure 707: ADC flown minus CTAS predicted path length for run 37. Positive values indicate aircraft followed a longer path than predicted by CTAS.**

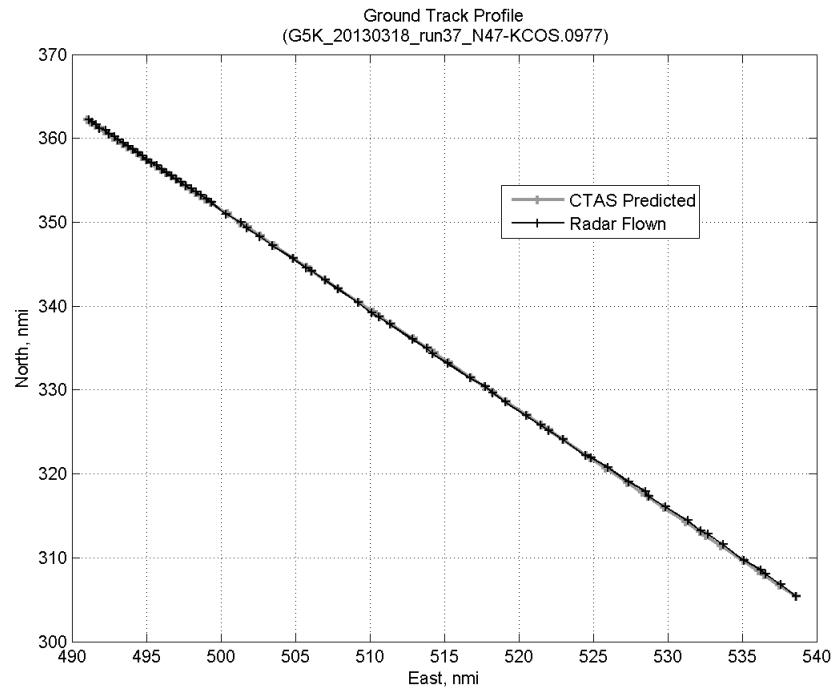


**Figure 708: CTAS predicted and radar flown ground track profile for run 37.**

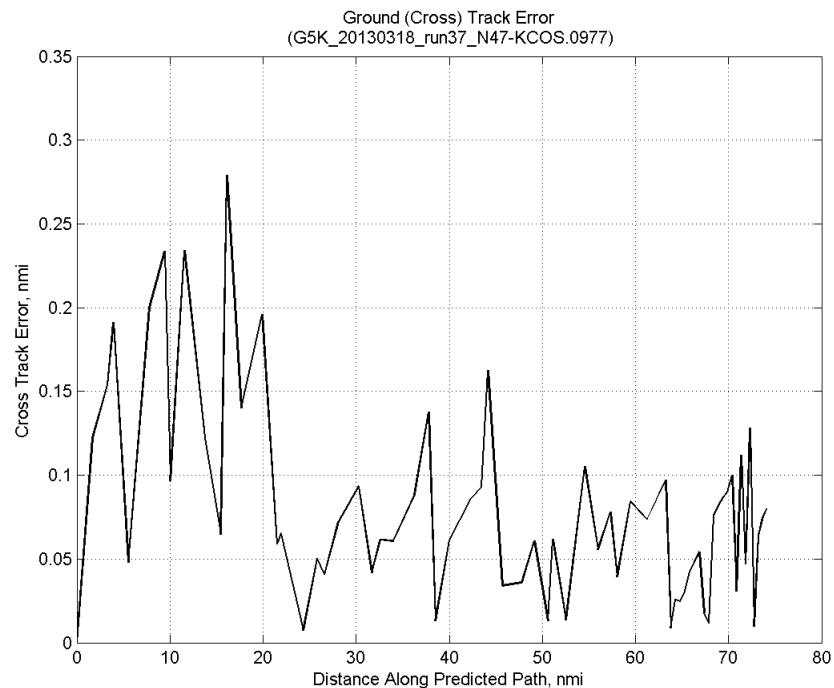


**Figure 709: Ground (cross) track error for run 37.**

### C.27. Run 38

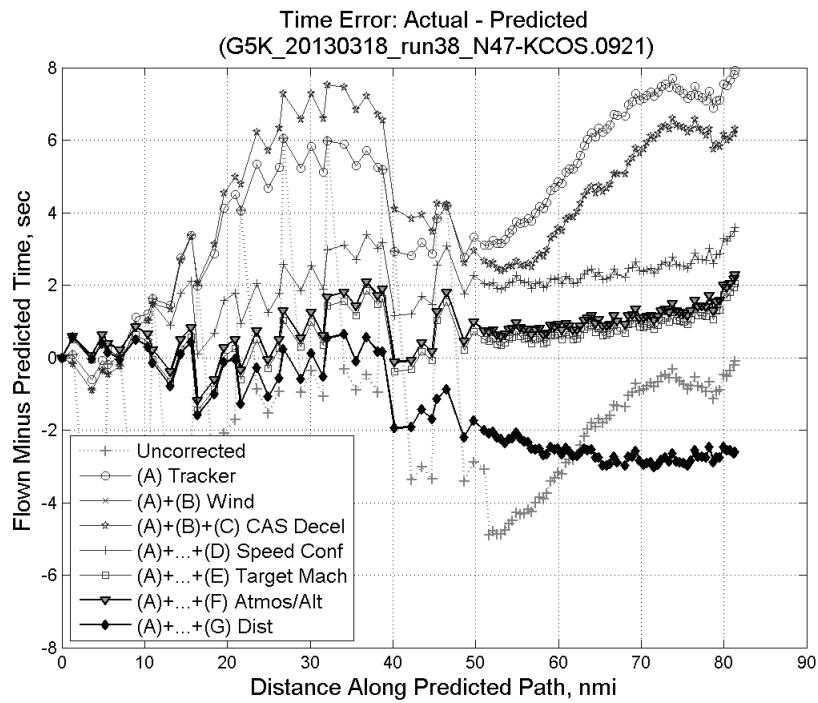


**Figure 710: Time error for run 38 showing incremental effect of removing each error source.**

#### C.27.A. Tracker Jumps

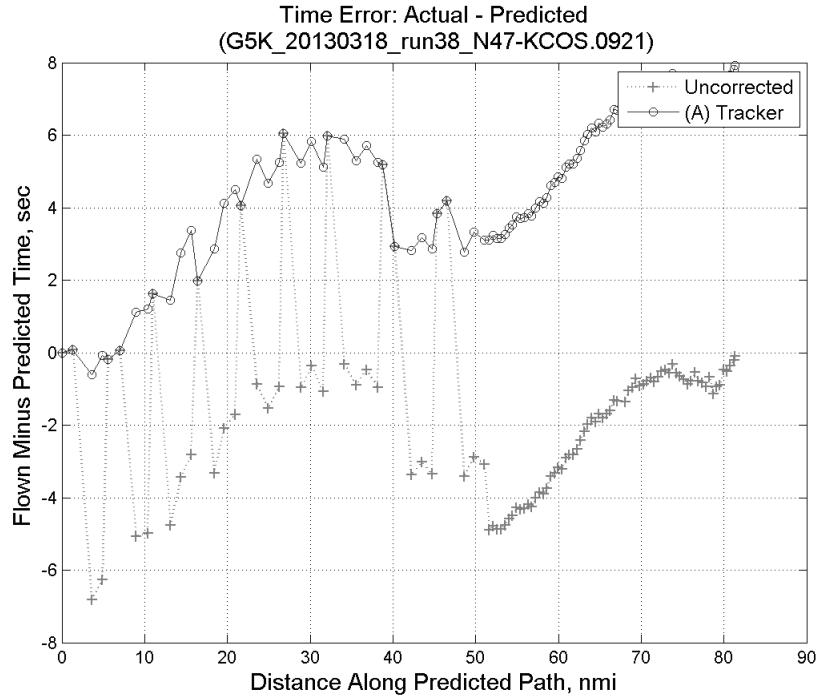


**Figure 711: Time error for run 38 before (Uncorrected) and after ((A) Tracker) removing tracker jump error source.**

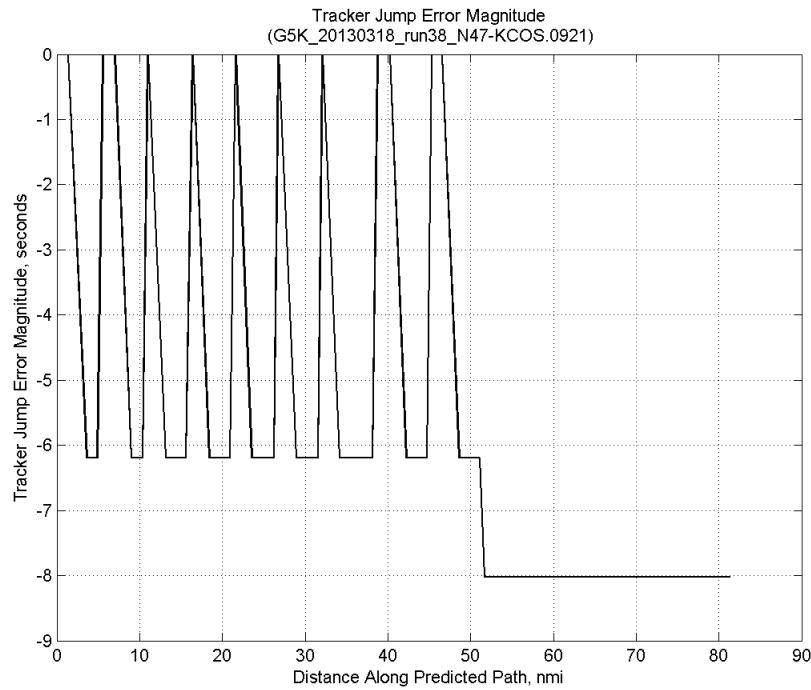


**Figure 712: Effect of tracker jump error source on time error for run 38.**

### C.27.B. Wind

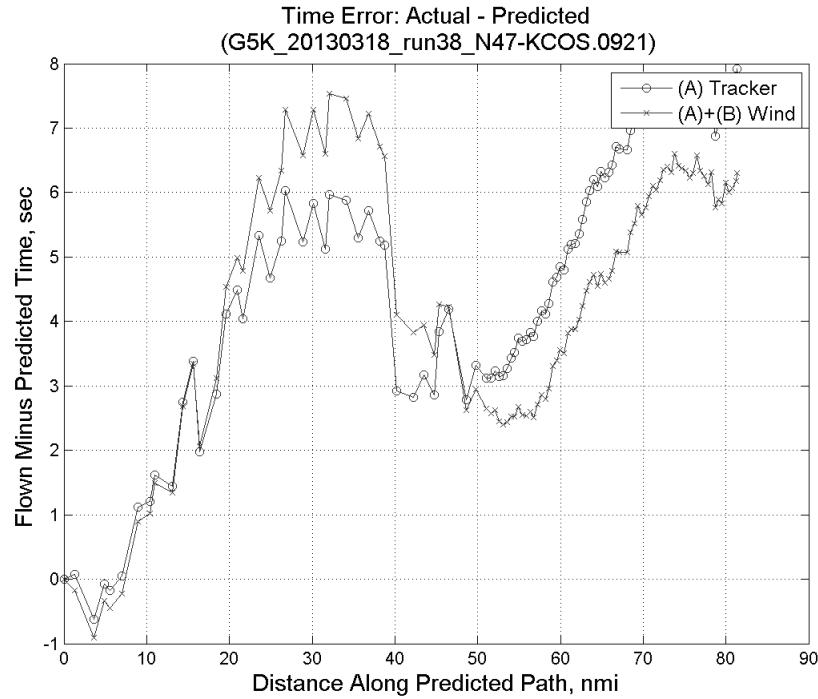


**Figure 713: Time error for run 38 before ((A) Tracker) and after ((A)+(B) Wind) removing wind error source.**

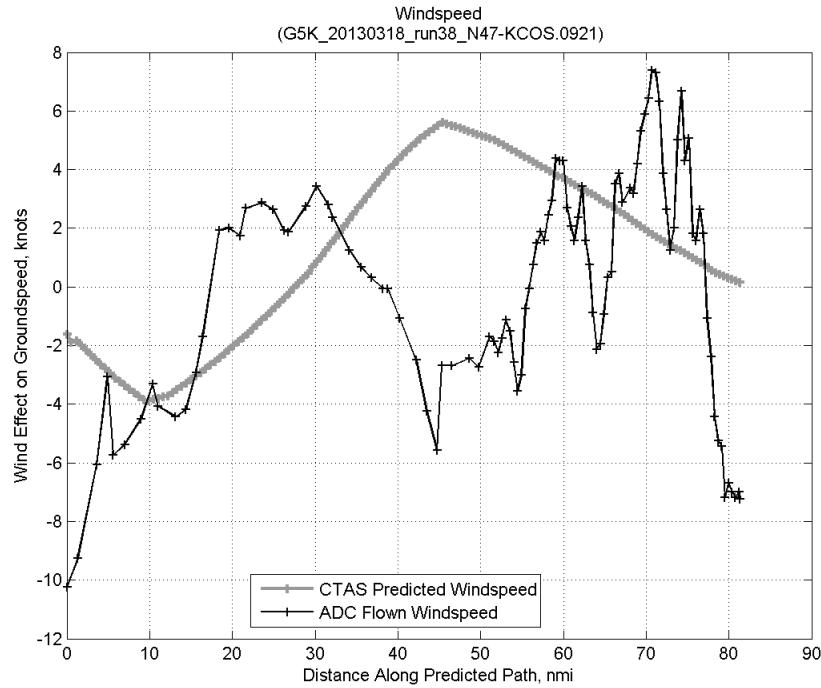


**Figure 714: CTAS predicted and ADC flown wind effect on ground speed for run 38. Negative values indicate a headwind.**

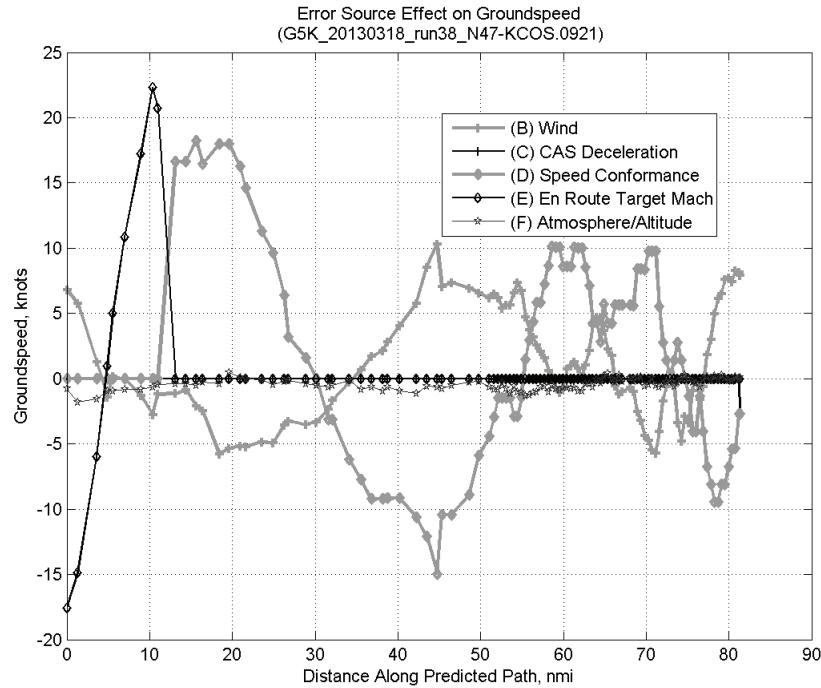


**Figure 715: Error sources (flown minus predicted) converted to a ground speed effect for run 38. Positive values indicate the flown ground speed was faster than the CTAS prediction.**

### C.27.C. CAS Deceleration

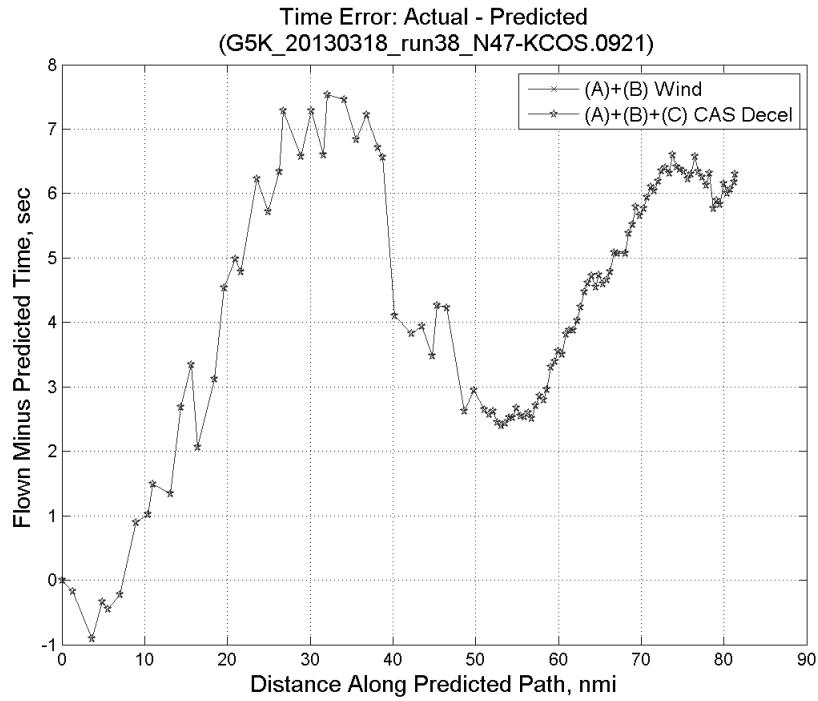


**Figure 716:** Time error for run 38 before ((A)+(B) Wind) and after ((A)+(B)+(C) CAS Decel) removing CAS deceleration error source.

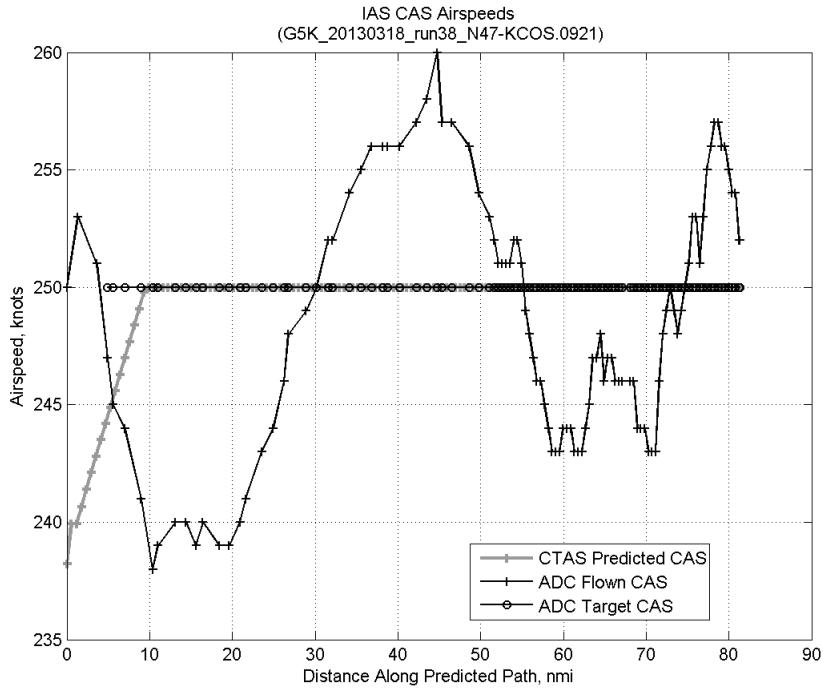


**Figure 717:** CTAS predicted and ADC flown CAS for run 38. CAS that is being targeted is shown with circle markers.

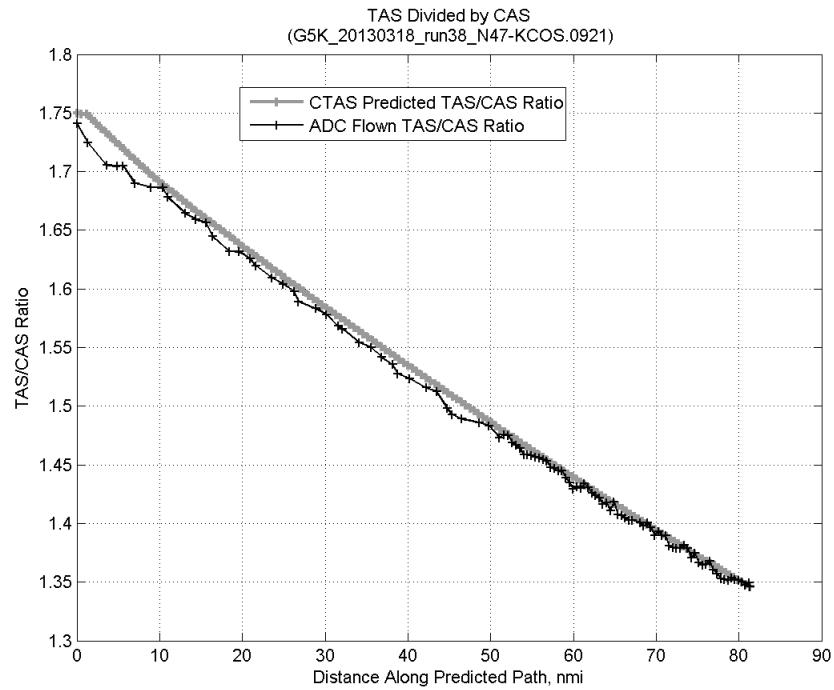


**Figure 718: CTAS predicted and ADC flown TAS/CAS ratio for run 38.**

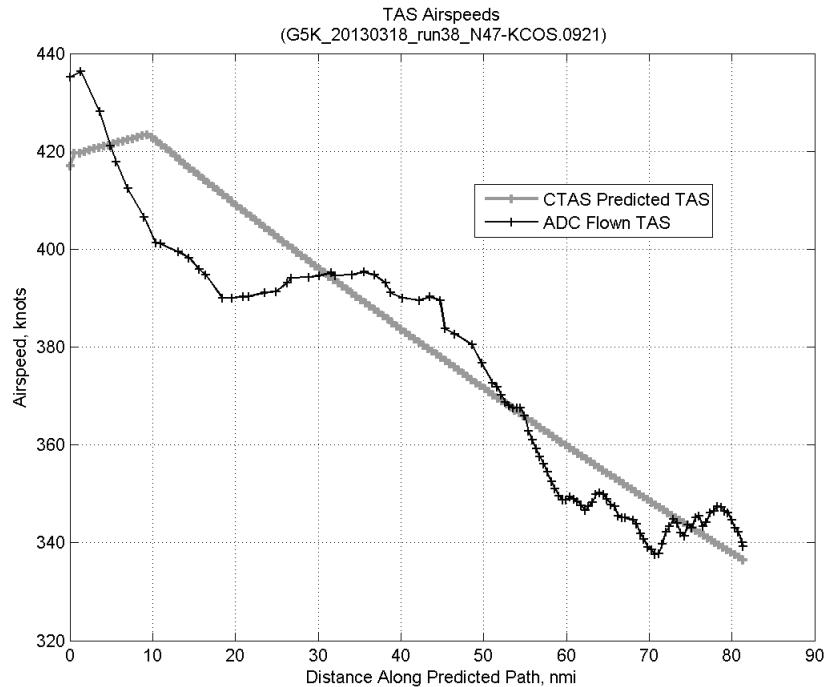


**Figure 719: CTAS predicted and ADC flown TAS for run 38.**

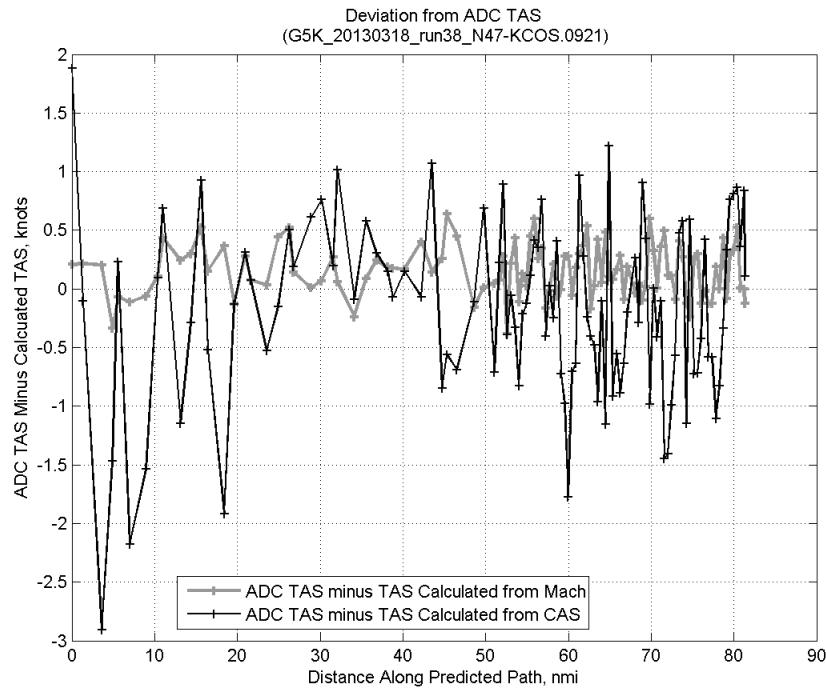


**Figure 720:** Deviation from ADC flown TAS if calculating TAS using ADC flown CAS, Mach, atmospheric temperature, and atmospheric pressure for run 38.

#### C.27.D. Speed Conformance

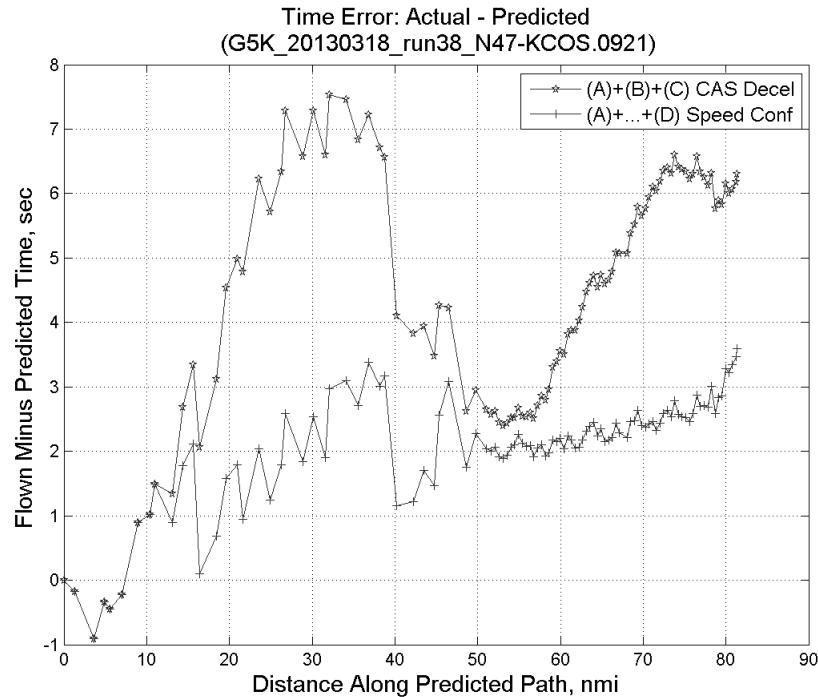


**Figure 721:** Time error for run 38 before  $((A)+(B)+(C) \text{ CAS Decel})$  and after  $((A)+\dots+(D) \text{ Speed Conf})$  removing speed conformance error source.

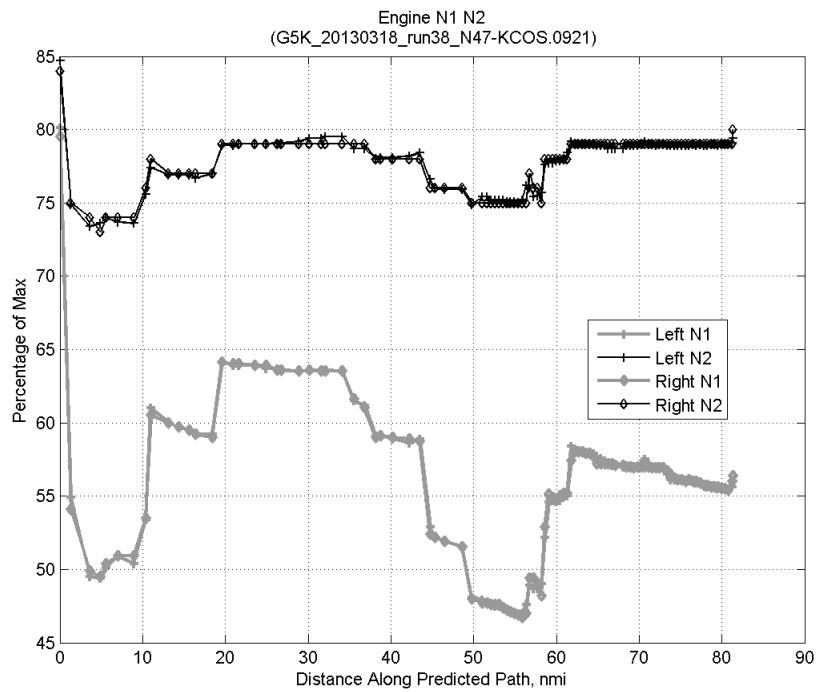


**Figure 722: Flown engine N1 and N2 for run 38.**

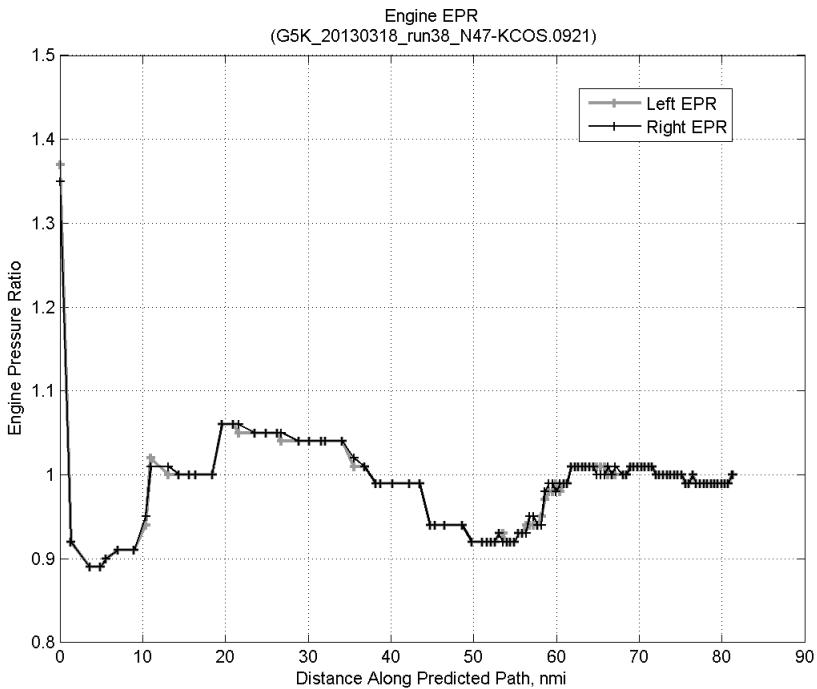


**Figure 723: Flown engine EPR for run 38.**

### C.27.E. Target Mach

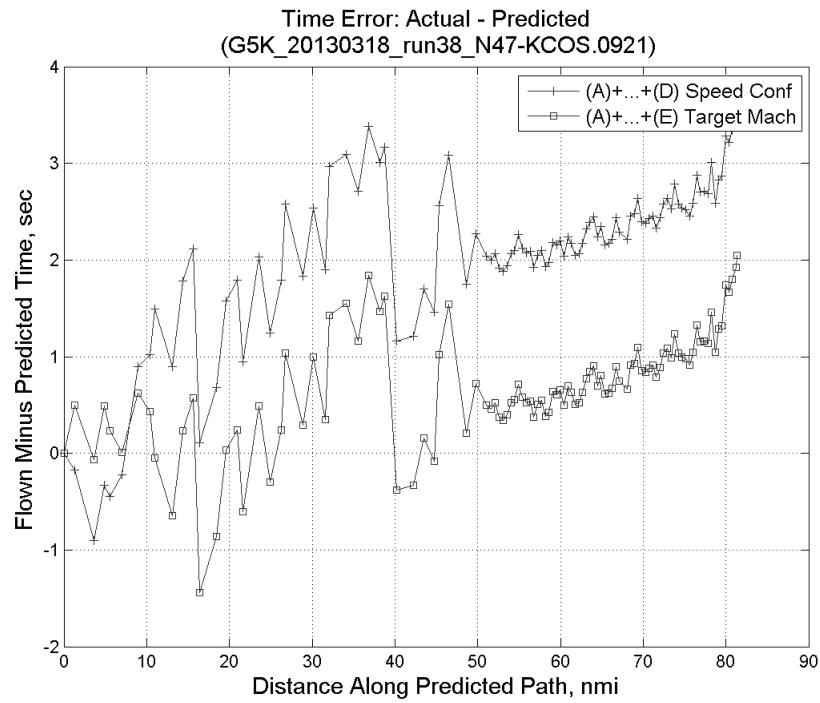


**Figure 724:** Time error for run 38 before ((A)+...+(D) Speed Conf) and after ((A)+...+(E) Target Mach) removing target Mach error source.

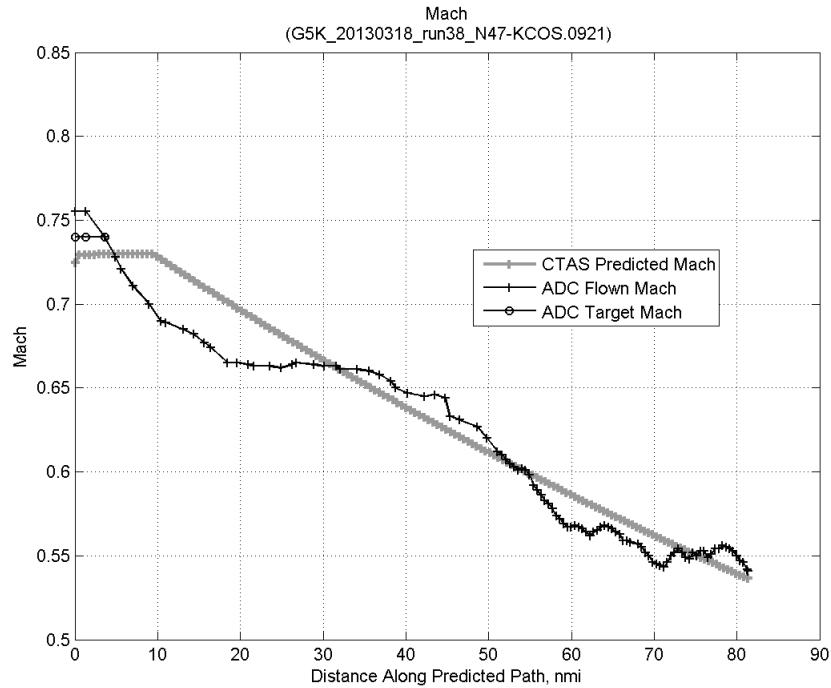


**Figure 725:** CTAS predicted and ADC flown Mach for run 38. Mach being targeted (ADC) shown with circle markers.

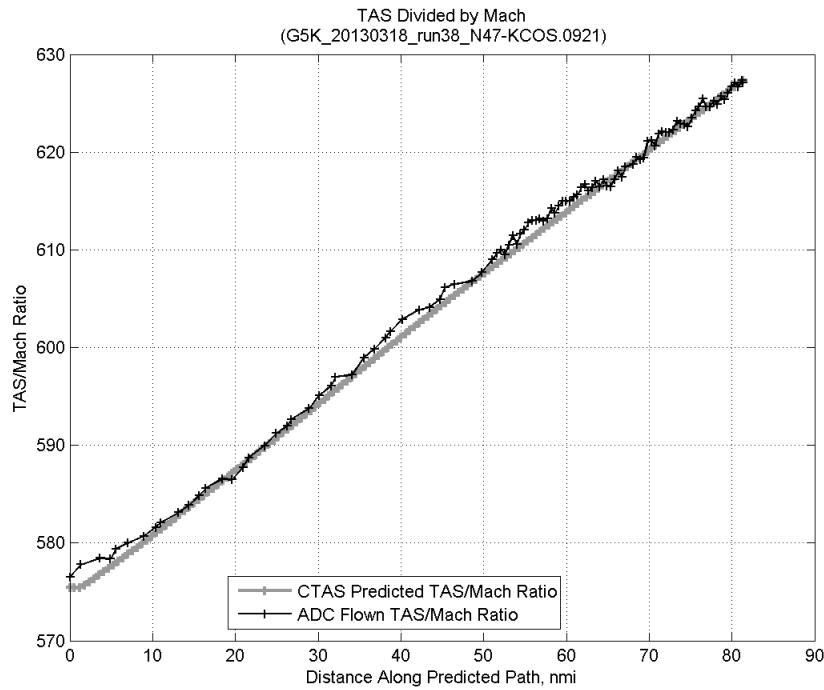


**Figure 726:** CTAS predicted and ADC flown TAS/Mach ratio for run 38.

#### C.27.F. Atmosphere/Altitude

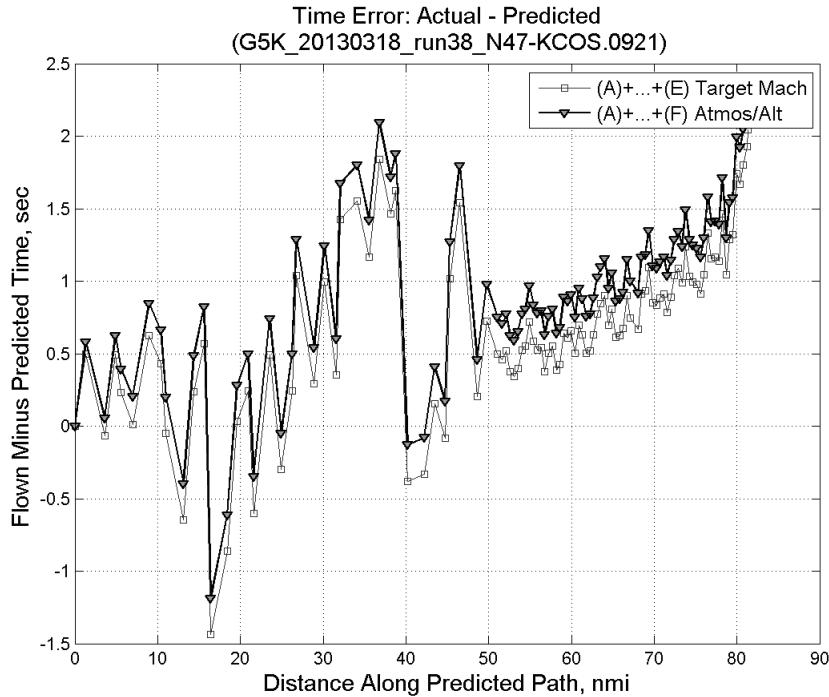


**Figure 727:** Time error for run 38 before ((A)+...+(E) Target Mach) and after ((A)+...+(F) Atmos/Alt) removing atmosphere/altitude error source.

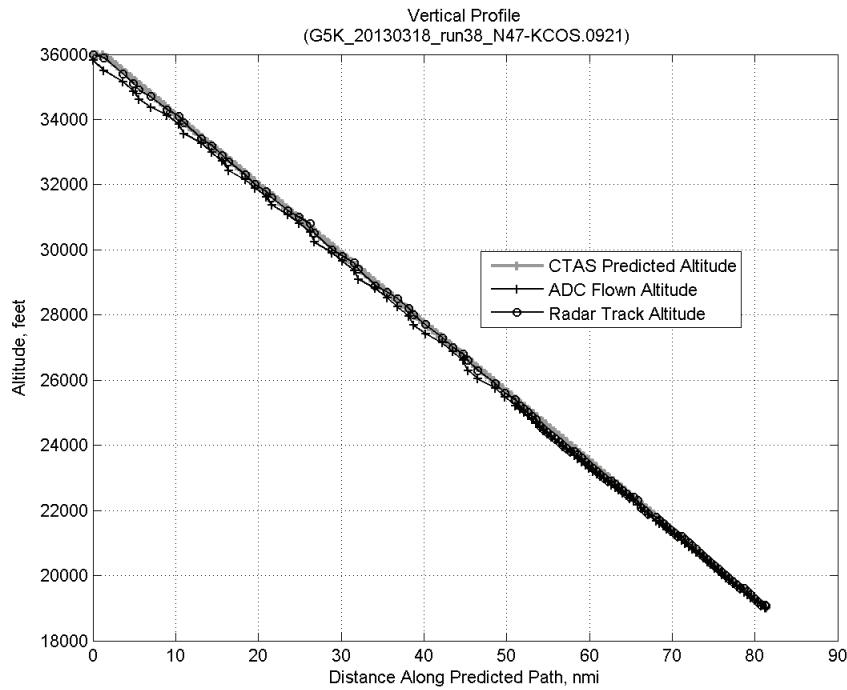


**Figure 728: Flown (ADC) and predicted (CTAS) vertical profile for run 38.**

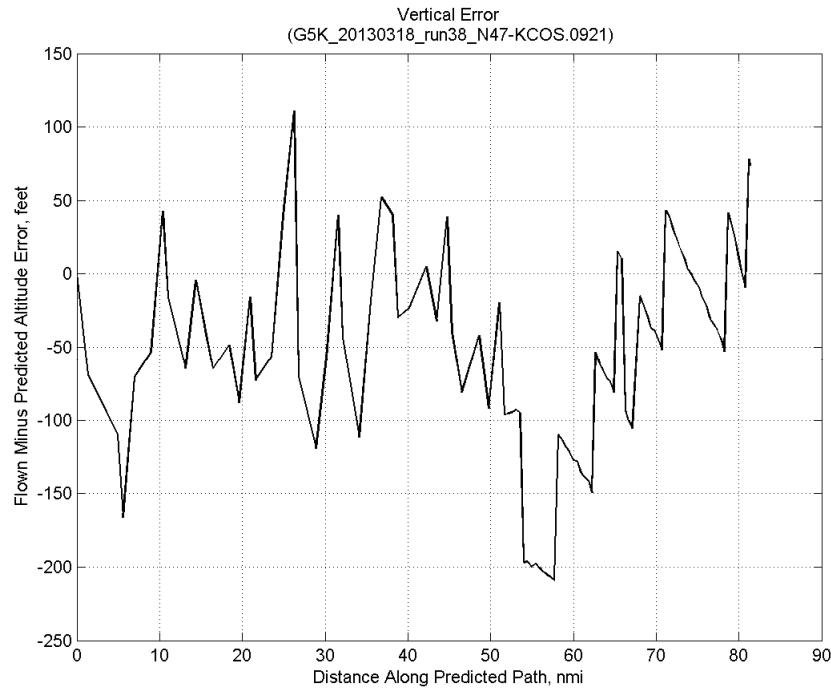


**Figure 729: Vertical error (flown minus predicted altitude) for run 38. Positive values indicate aircraft flew higher than predicted by CTAS.**

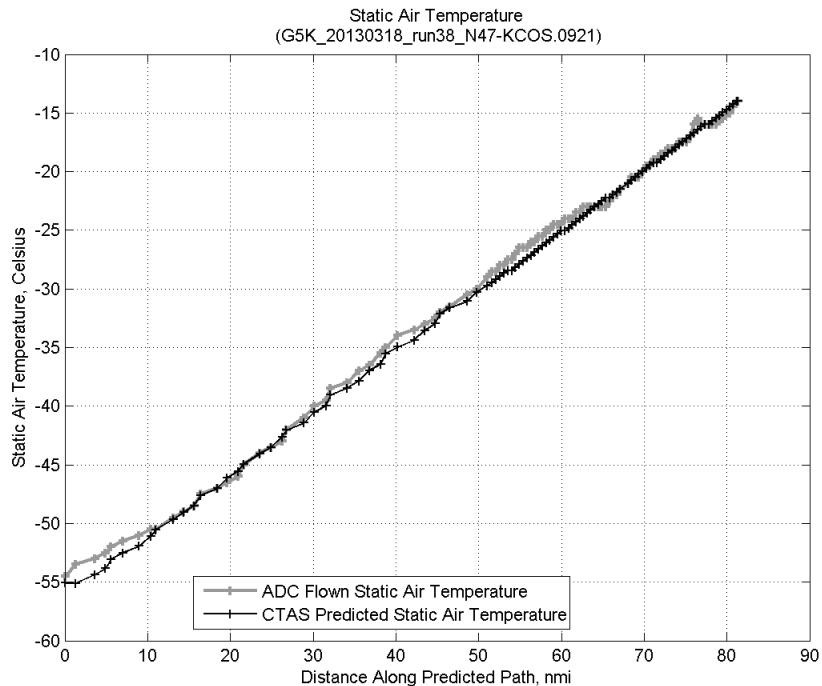


**Figure 730: Flown (ADC) and predicted (CTAS) static air temperature for run 38.**

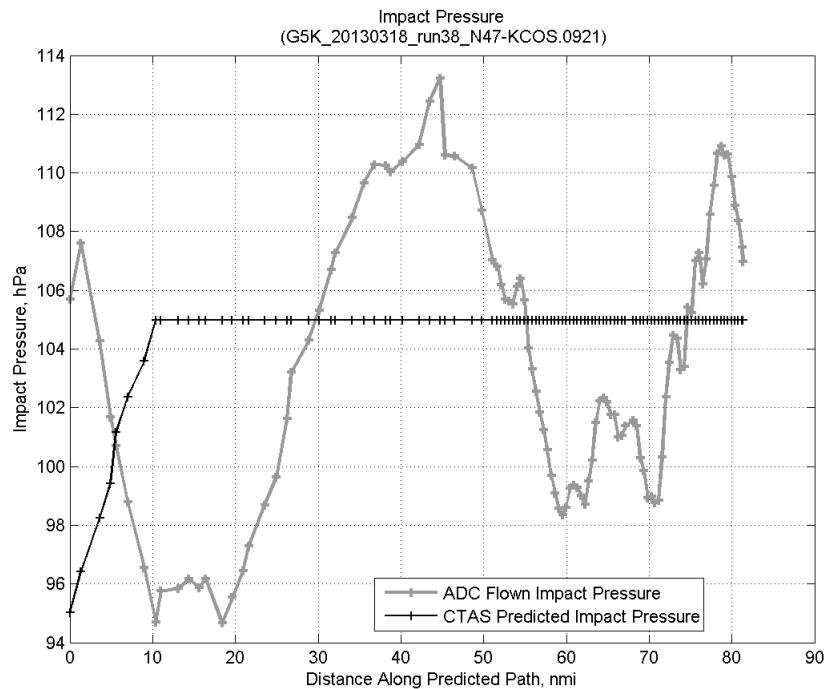


**Figure 731: Flown (ADC) and predicted (CTAS) impact pressure for run 38.**

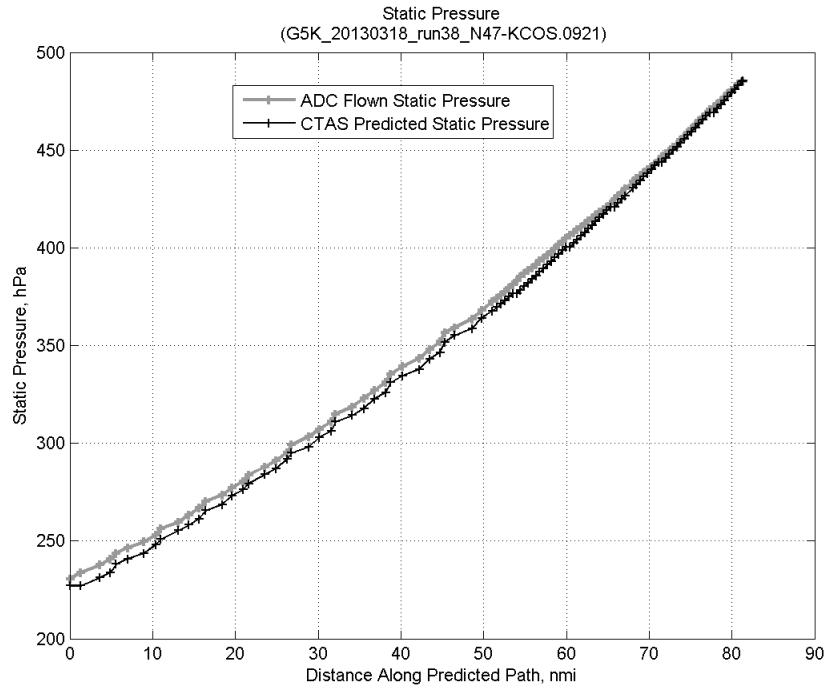


**Figure 732: Flown (ADC) and predicted (CTAS) static pressure for run 38.**

#### C.27.G. Path Distance

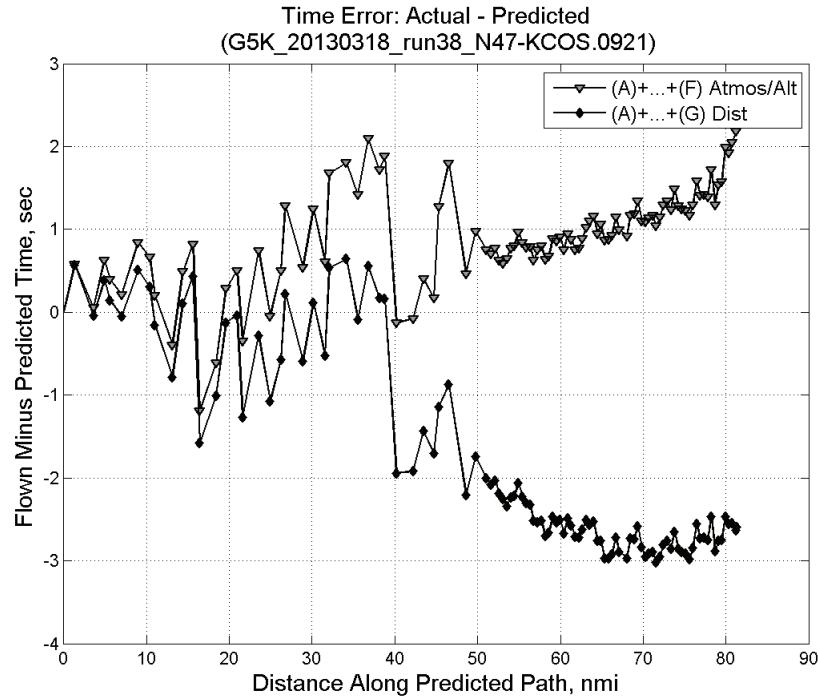


**Figure 733: Time error for run 38 before ((A)+...+(F) Atmos/Alt) and after ((A)+...+(G) Dist) removing path distance error source.**

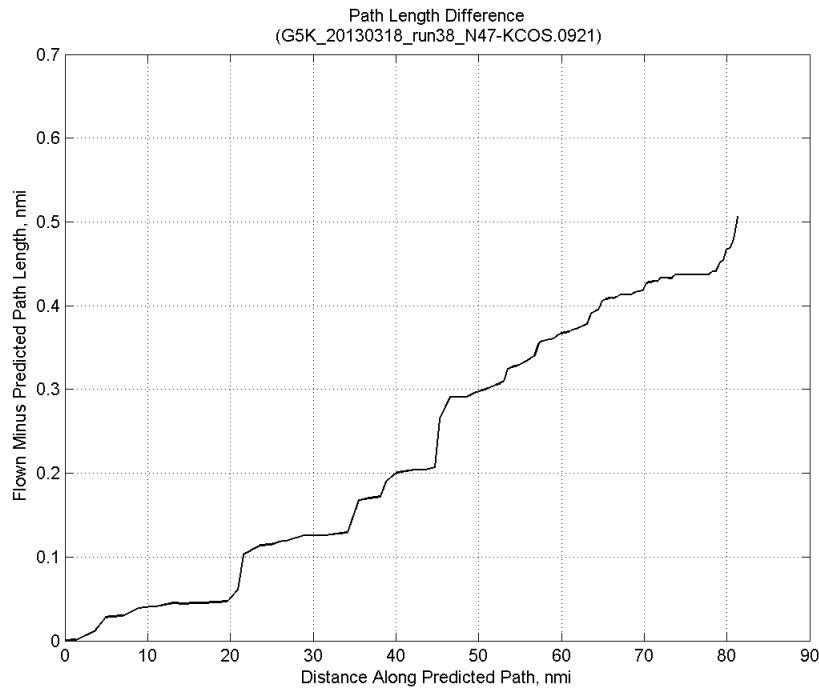


**Figure 734: ADC flown minus CTAS predicted path length for run 38. Positive values indicate aircraft followed a longer path than predicted by CTAS.**

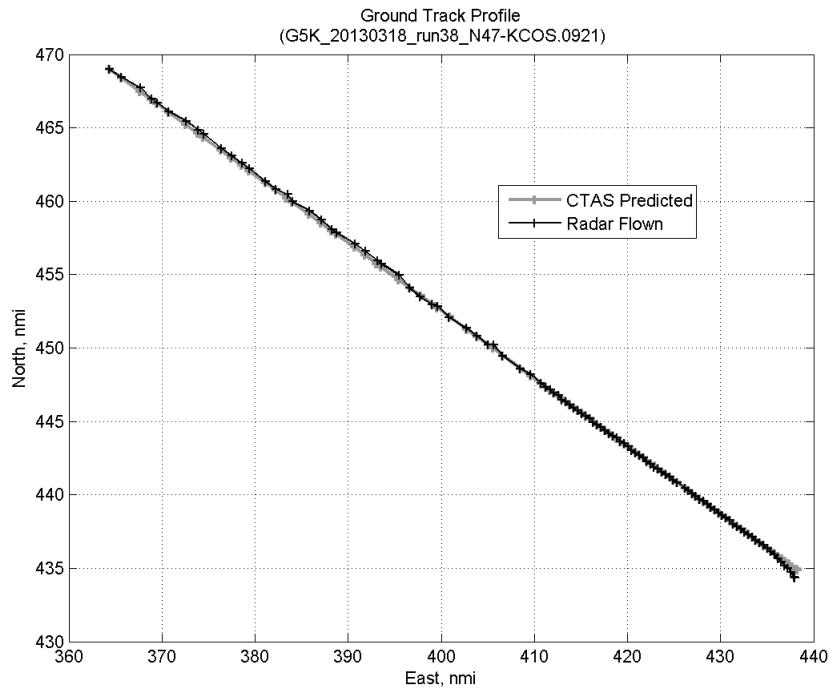


**Figure 735: CTAS predicted and radar flown ground track profile for run 38.**

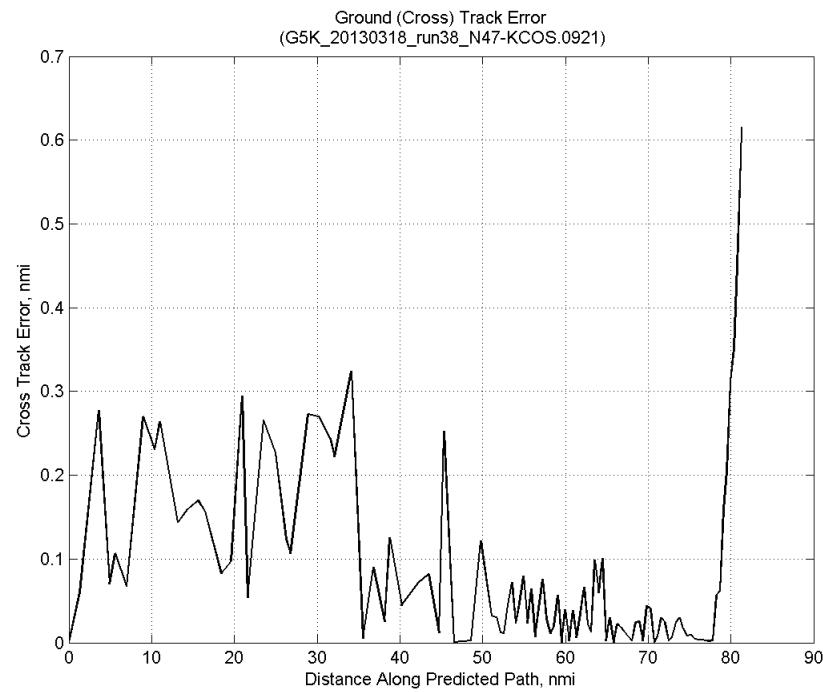


**Figure 736: Ground (cross) track error for run 38.**

### C.28. Run 39

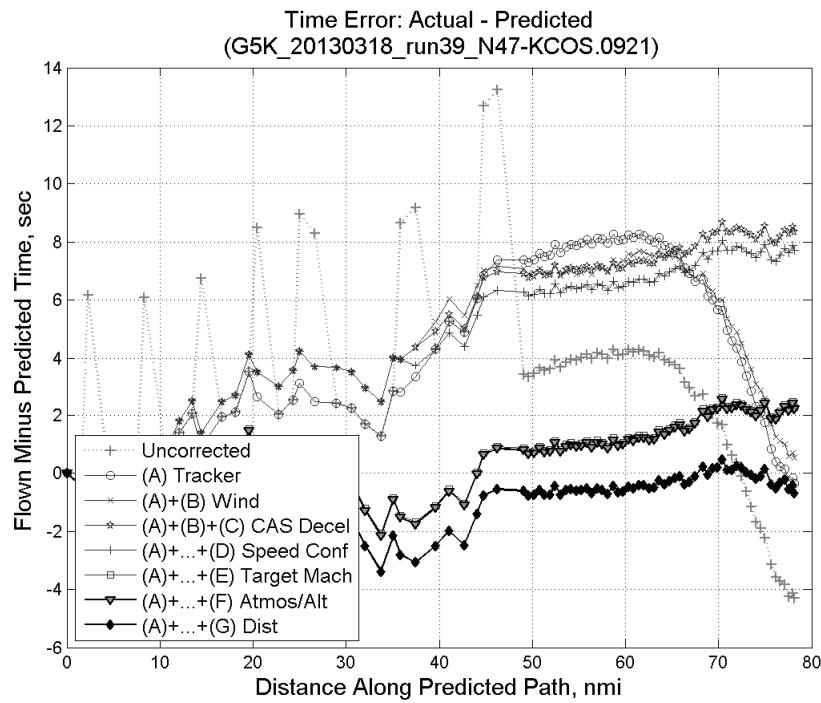


**Figure 737: Time error for run 39 showing incremental effect of removing each error source.**

#### C.28.A. Tracker Jumps

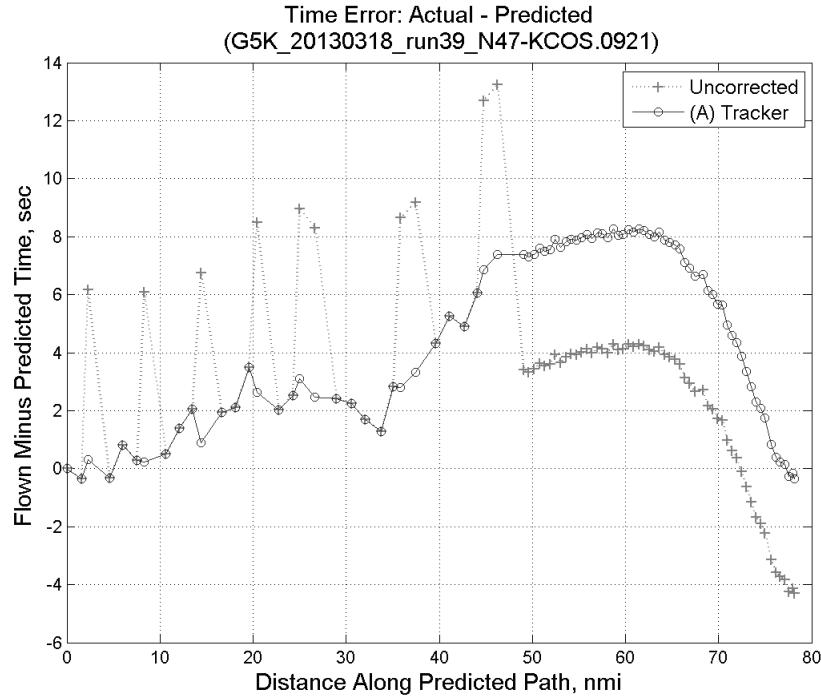


**Figure 738: Time error for run 39 before (Uncorrected) and after ((A) Tracker) removing tracker jump error source.**

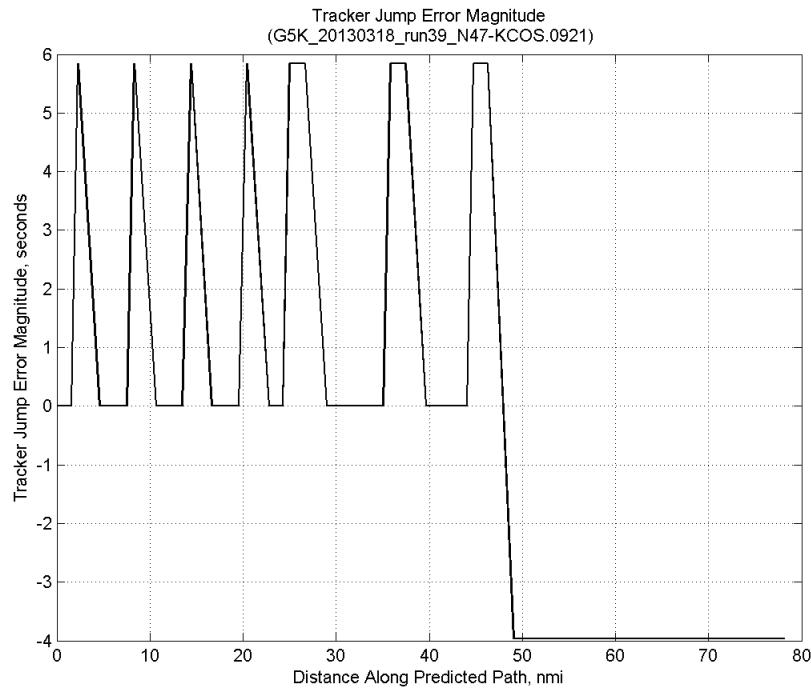


**Figure 739: Effect of tracker jump error source on time error for run 39.**

### C.28.B. Wind

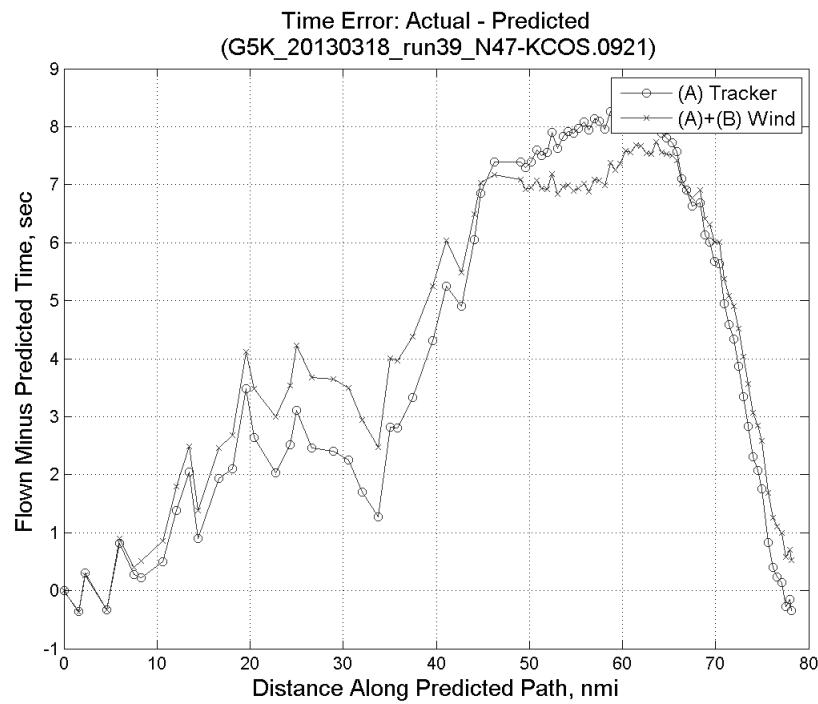


**Figure 740: Time error for run 39 before ((A) Tracker) and after ((A)+(B) Wind) removing wind error source.**

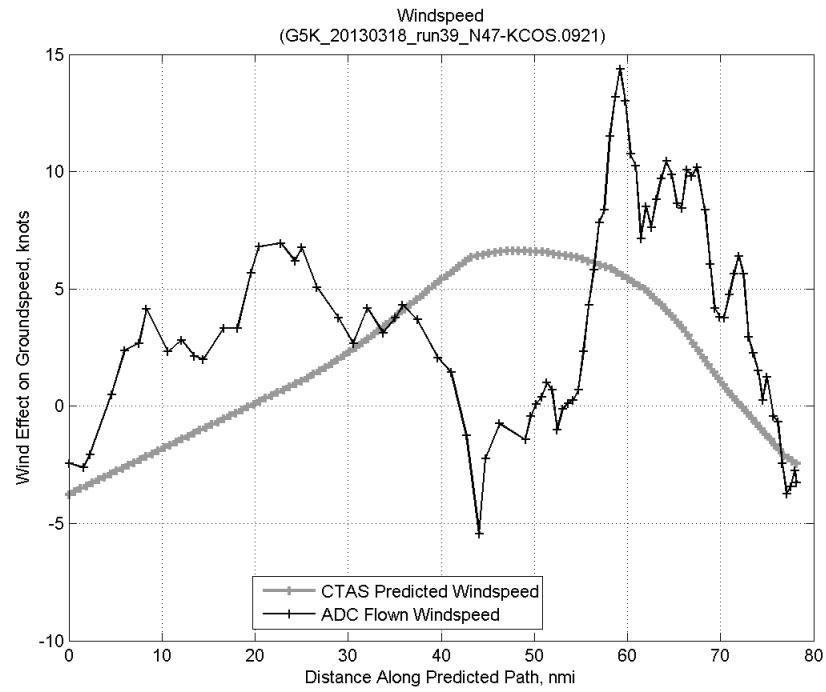


**Figure 741: CTAS predicted and ADC flown wind effect on ground speed for run 39. Negative values indicate a headwind.**

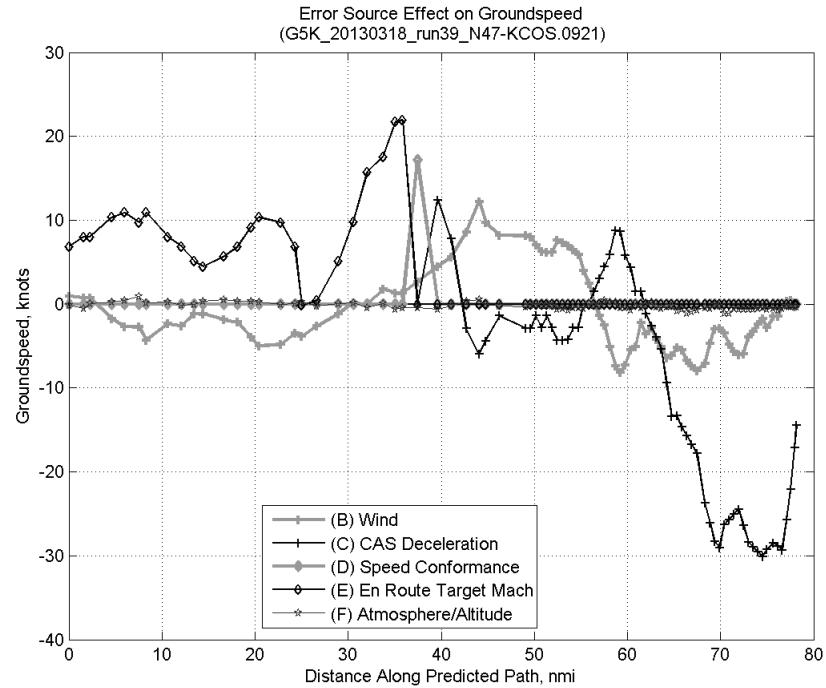


**Figure 742: Error sources (flown minus predicted) converted to a ground speed effect for run 39. Positive values indicate the flown ground speed was faster than the CTAS prediction.**

### C.28.C. CAS Deceleration

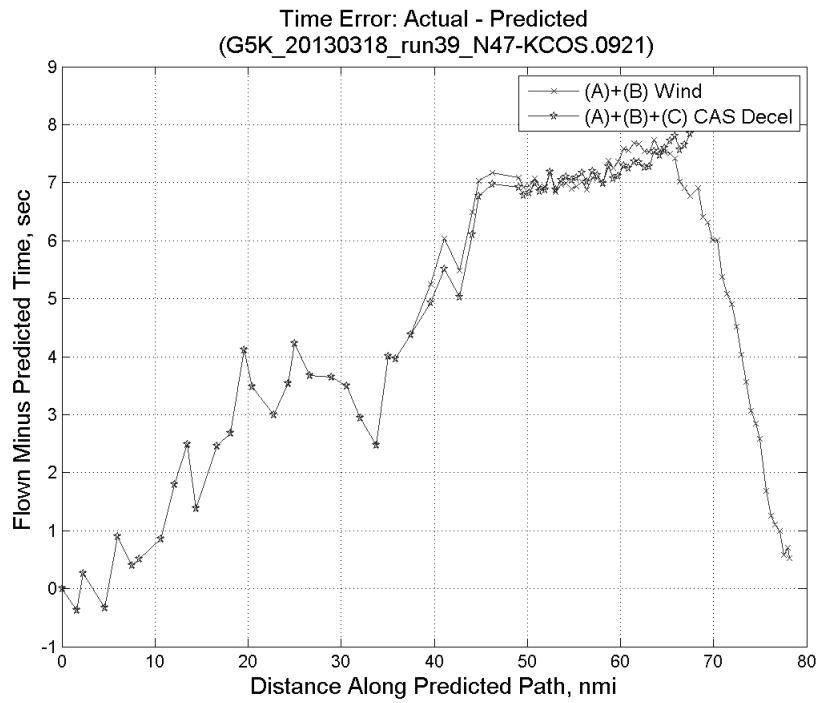


**Figure 743:** Time error for run 39 before ((A)+(B) Wind) and after ((A)+(B)+(C) CAS Decel) removing CAS deceleration error source.

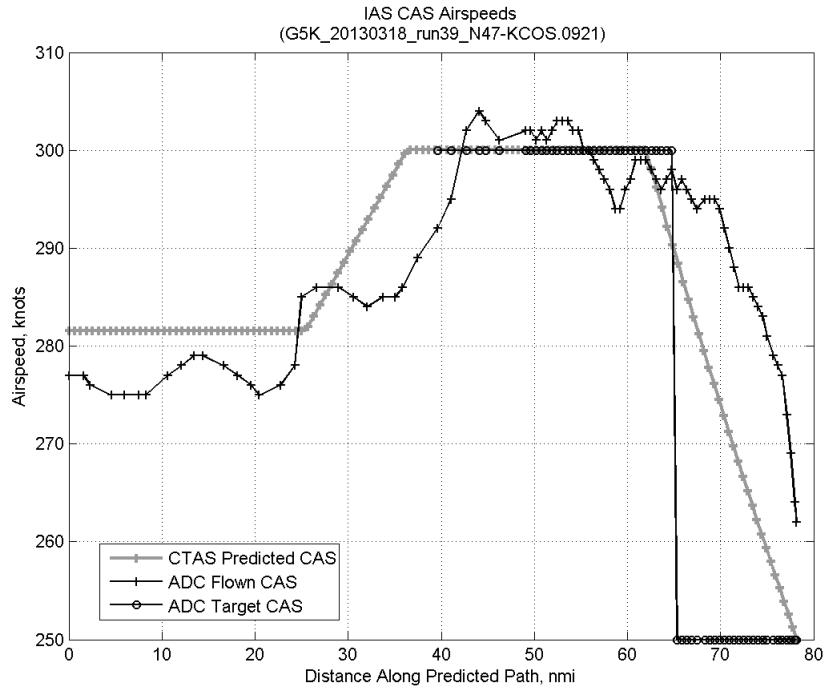


**Figure 744:** CTAS predicted and ADC flown CAS for run 39. CAS that is being targeted is shown with circle markers.

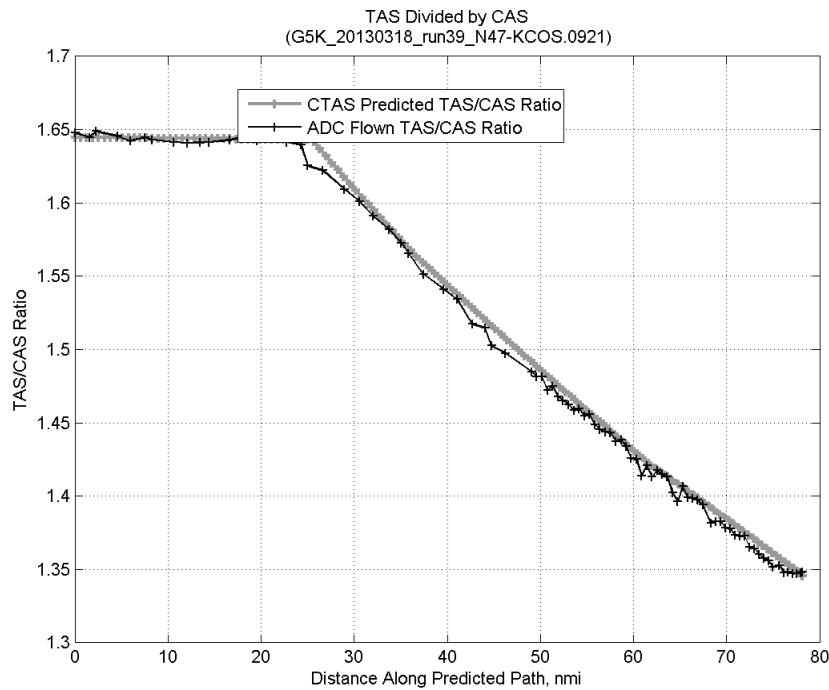


**Figure 745: CTAS predicted and ADC flown TAS/CAS ratio for run 39.**

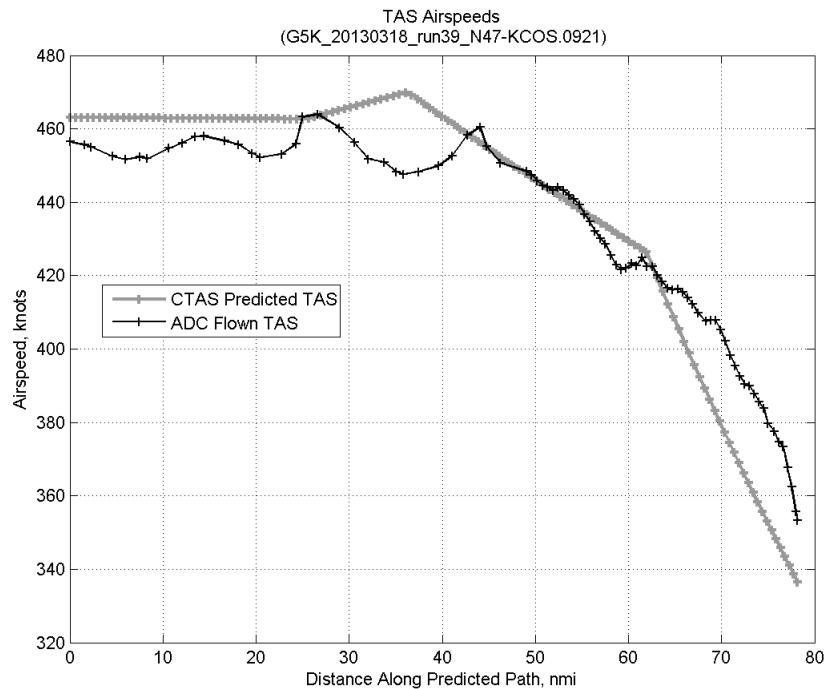


**Figure 746: CTAS predicted and ADC flown TAS for run 39.**

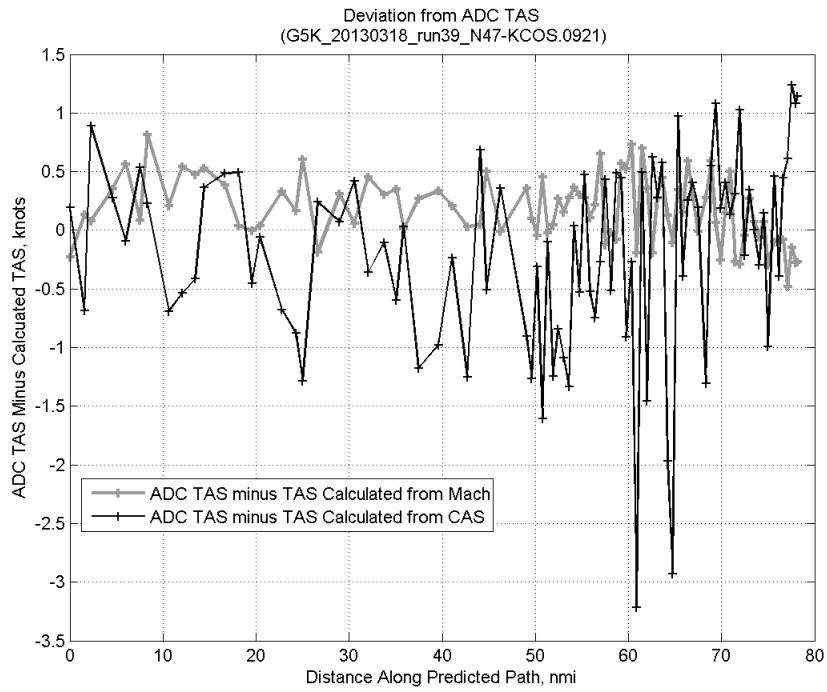


**Figure 747: Deviation from ADC flown TAS if calculating TAS using ADC flown CAS, Mach, atmospheric temperature, and atmospheric pressure for run 39.**

#### C.28.D. Speed Conformance

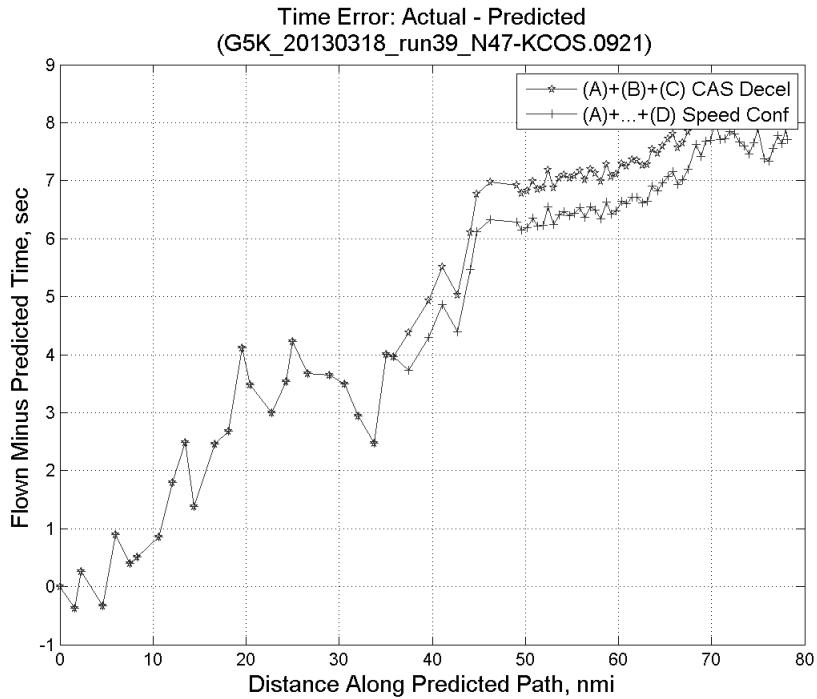


**Figure 748: Time error for run 39 before ((A)+(B)+(C) CAS Decel) and after ((A)+...+(D) Speed Conf) removing speed conformance error source.**

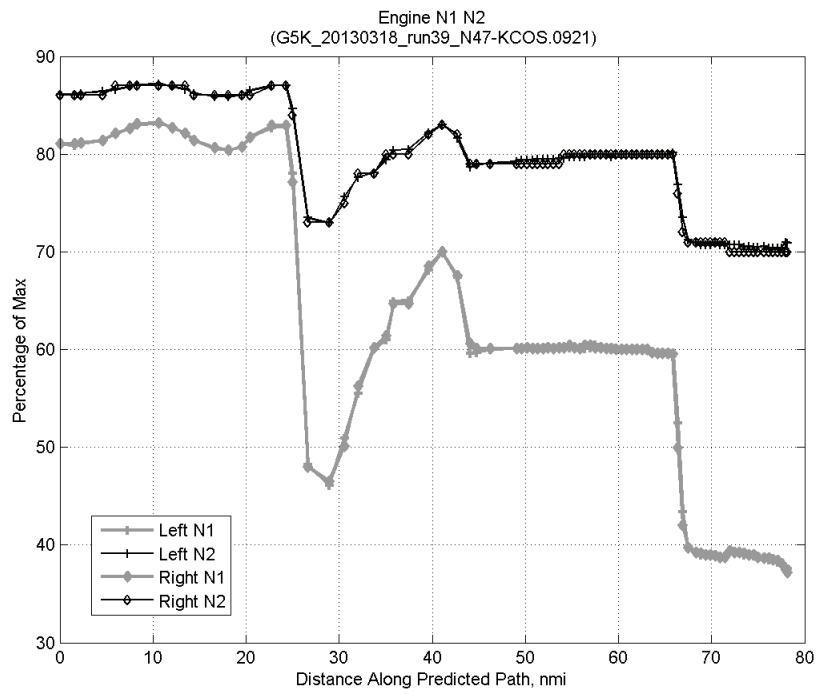


**Figure 749: Flown engine N1 and N2 for run 39.**

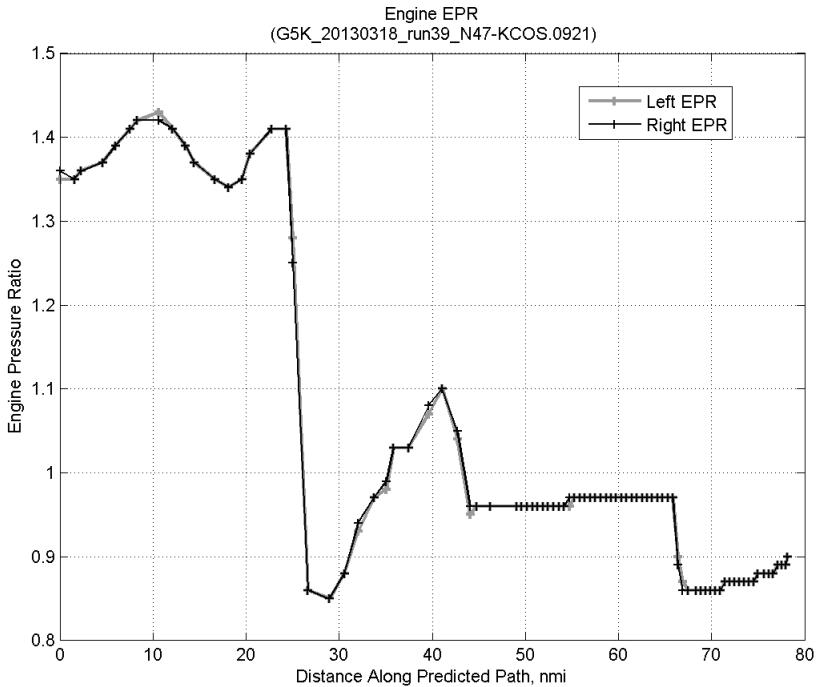


**Figure 750: Flown engine EPR for run 39.**

### C.28.E. Target Mach

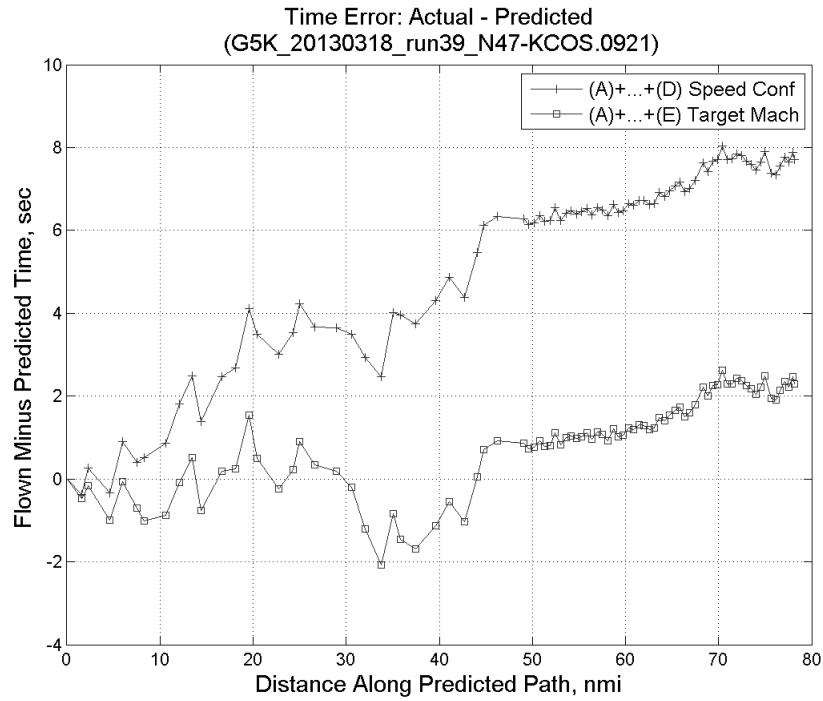


**Figure 751:** Time error for run 39 before ((A)+...+(D) Speed Conf) and after ((A)+...+(E) Target Mach) removing target Mach error source.

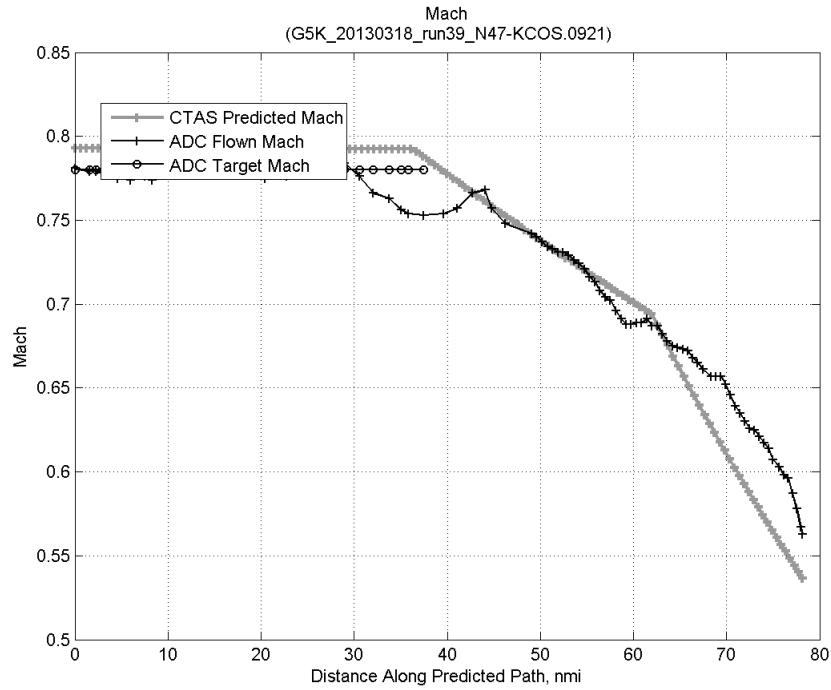


**Figure 752:** CTAS predicted and ADC flown Mach for run 39. Mach being targeted (ADC) shown with circle markers.

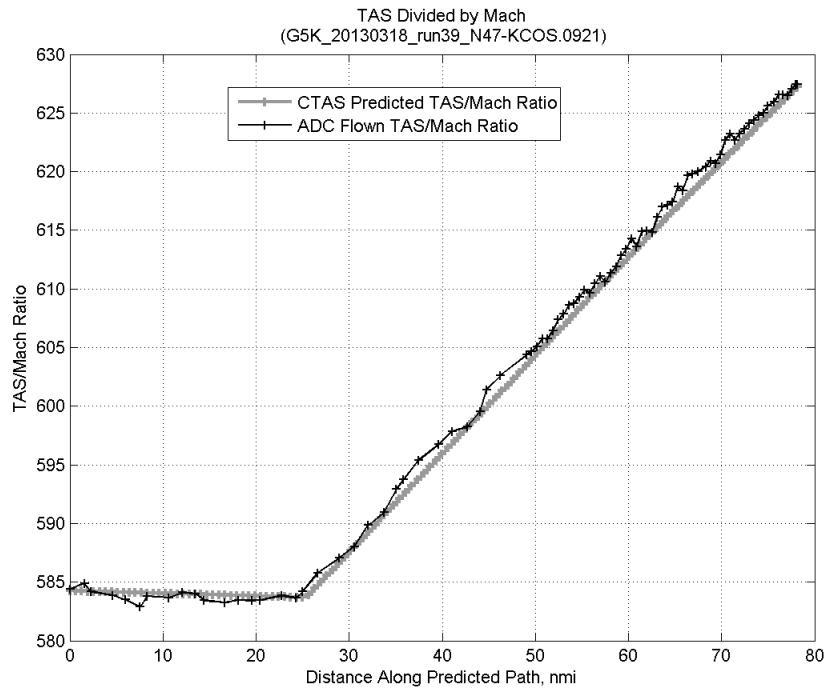


**Figure 753: CTAS predicted and ADC flown TAS/Mach ratio for run 39.**

#### C.28.F. Atmosphere/Altitude

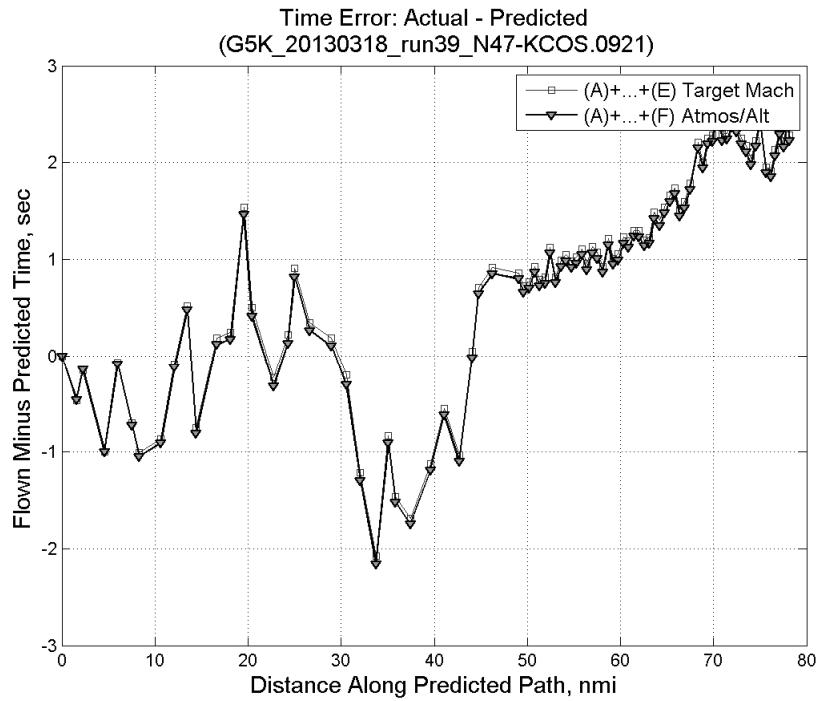


**Figure 754: Time error for run 39 before ((A)+...+(E) Target Mach) and after ((A)+...+(F) Atmos/Alt) removing atmosphere/altitude error source.**

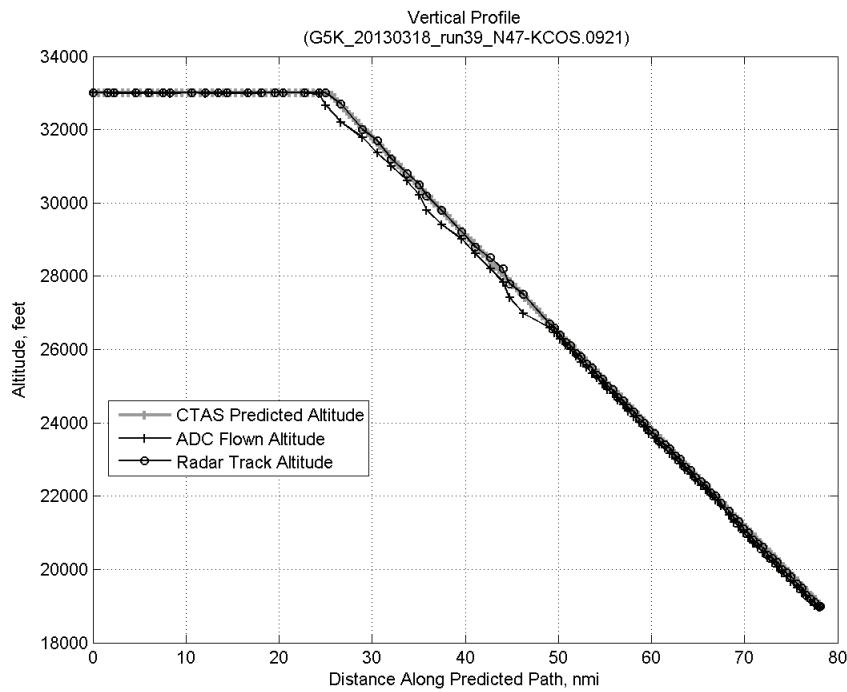


**Figure 755:** Flown (ADC) and predicted (CTAS) vertical profile for run 39.

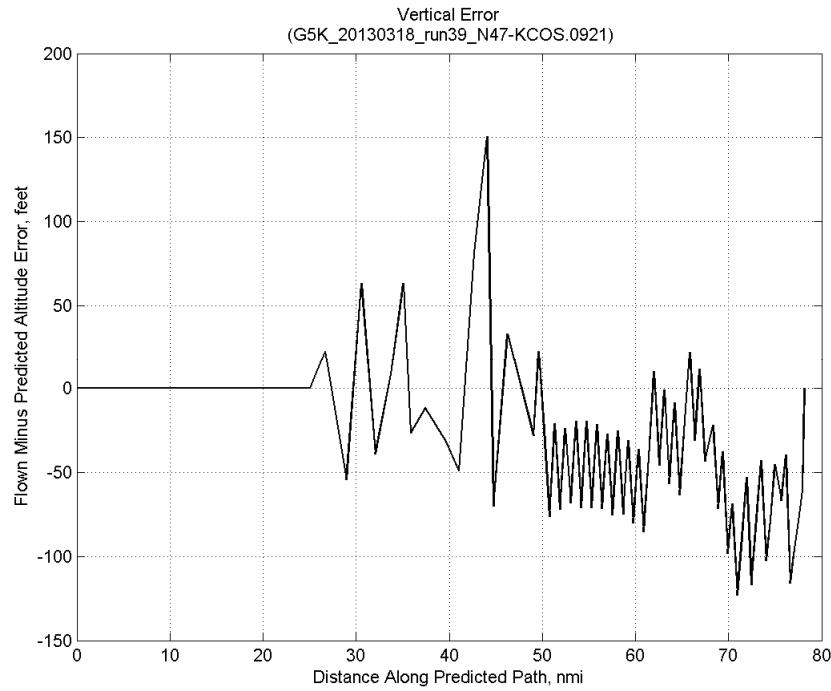


**Figure 756:** Vertical error (flown minus predicted altitude) for run 39. Positive values indicate aircraft flew higher than predicted by CTAS.

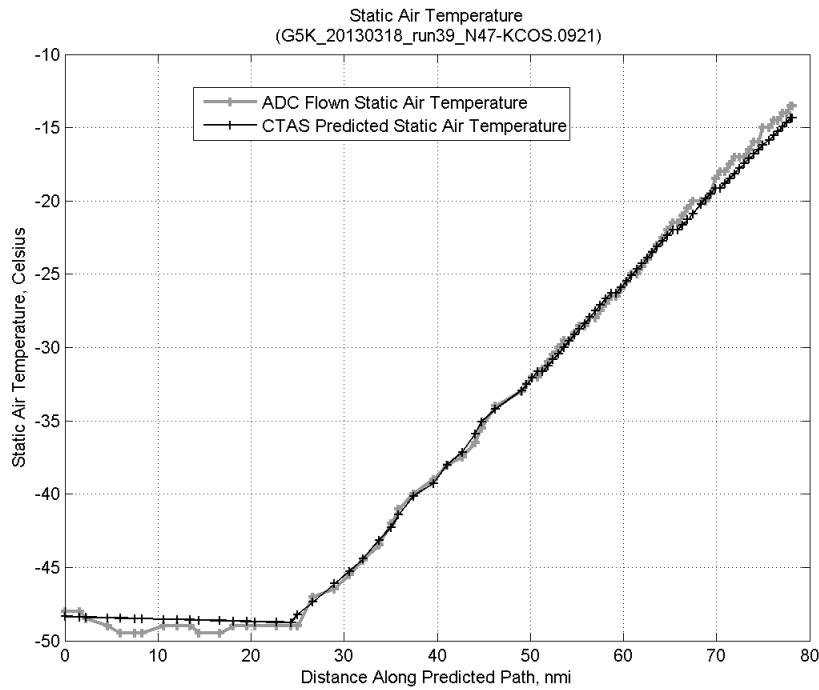


**Figure 757: Flown (ADC) and predicted (CTAS) static air temperature for run 39.**

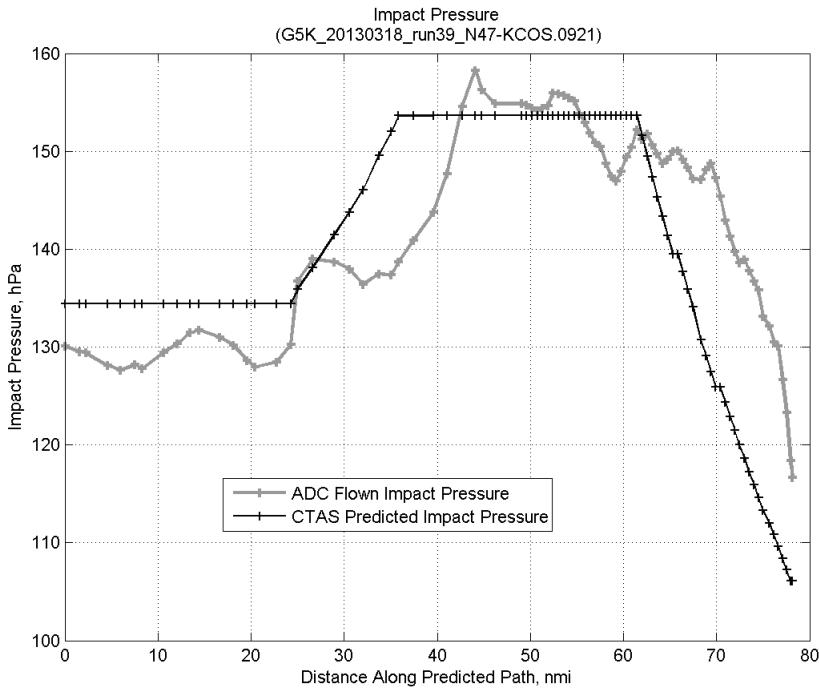


**Figure 758: Flown (ADC) and predicted (CTAS) impact pressure for run 39.**

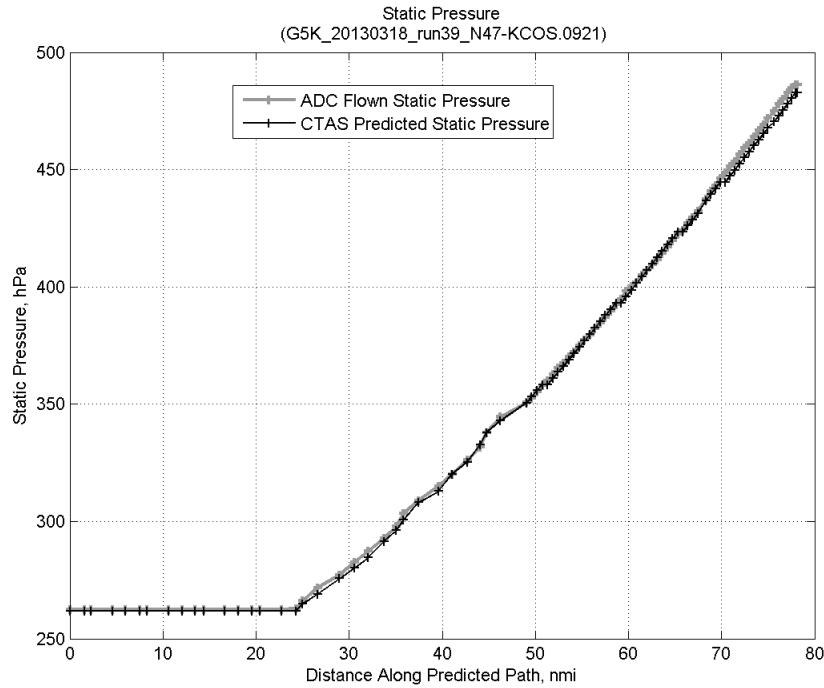


**Figure 759: Flown (ADC) and predicted (CTAS) static pressure for run 39.**

#### C.28.G. Path Distance

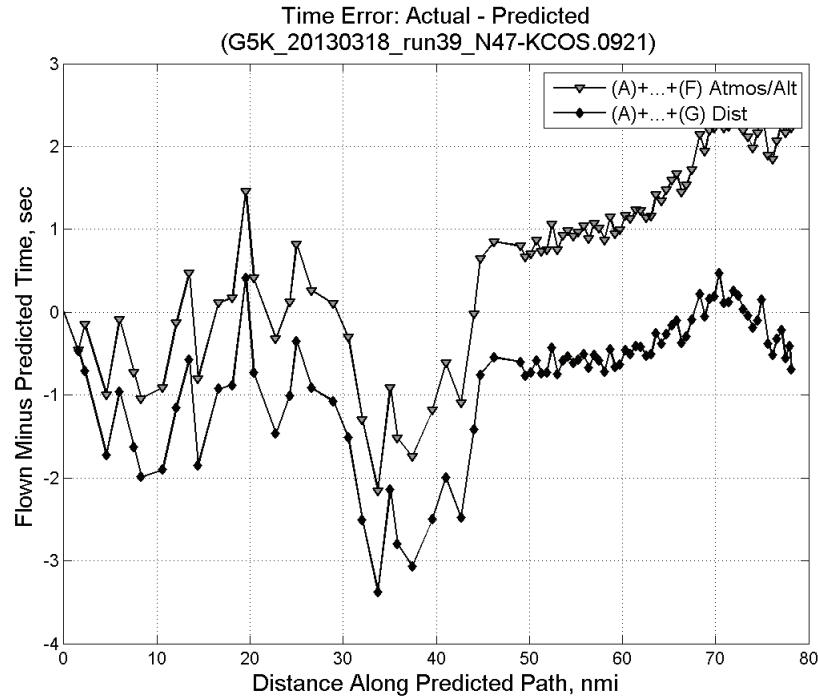


**Figure 760: Time error for run 39 before ((A)+...+(F) Atmos/Alt) and after ((A)+...+(G) Dist) removing path distance error source.**

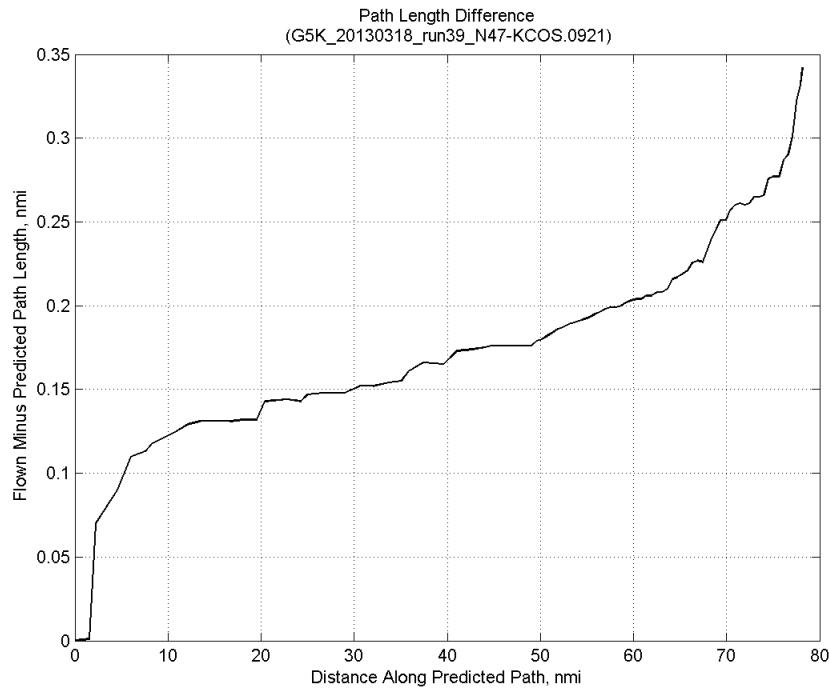


**Figure 761: ADC flown minus CTAS predicted path length for run 39. Positive values indicate aircraft followed a longer path than predicted by CTAS.**

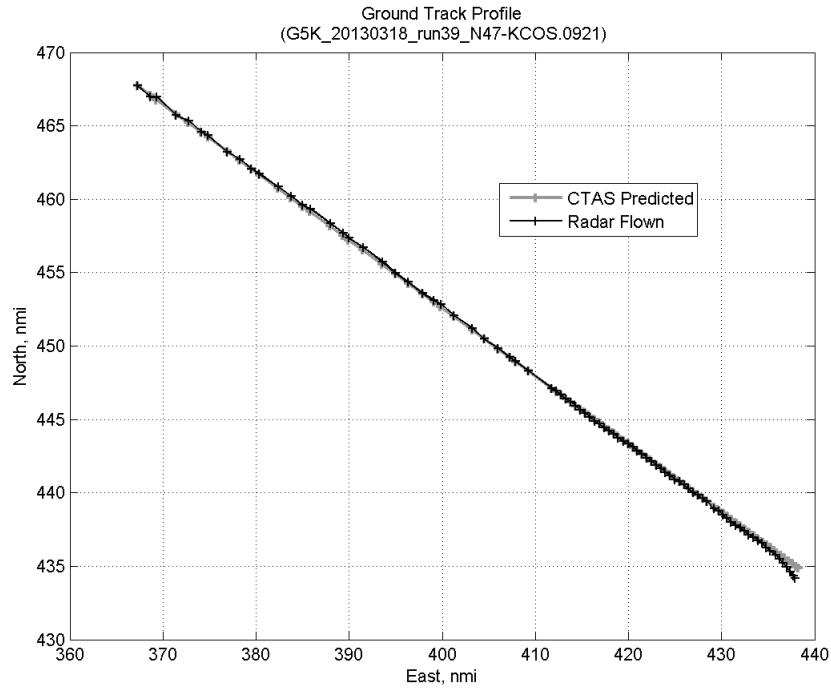


**Figure 762: CTAS predicted and radar flown ground track profile for run 39.**

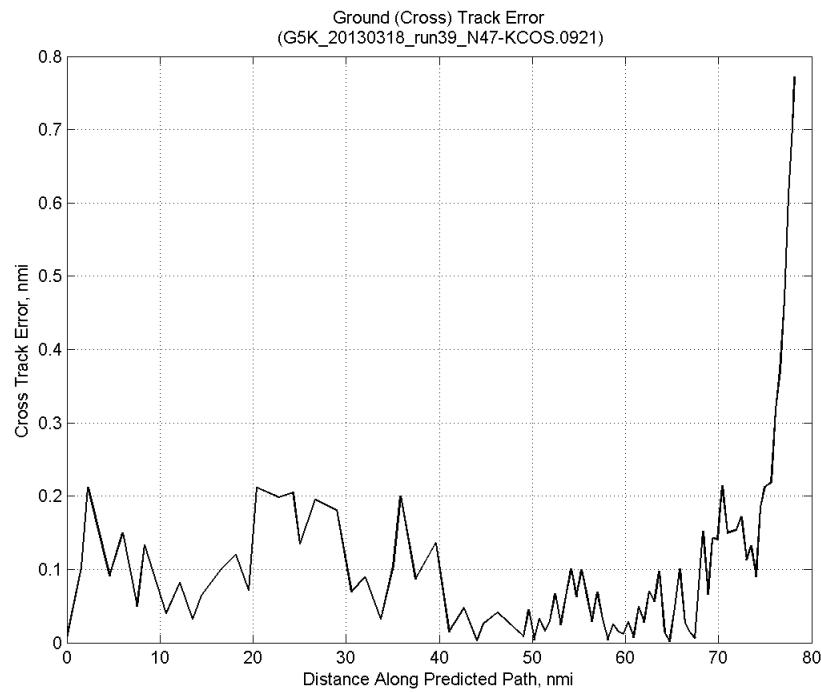


**Figure 763: Ground (cross) track error for run 39.**

### C.29. Run 41

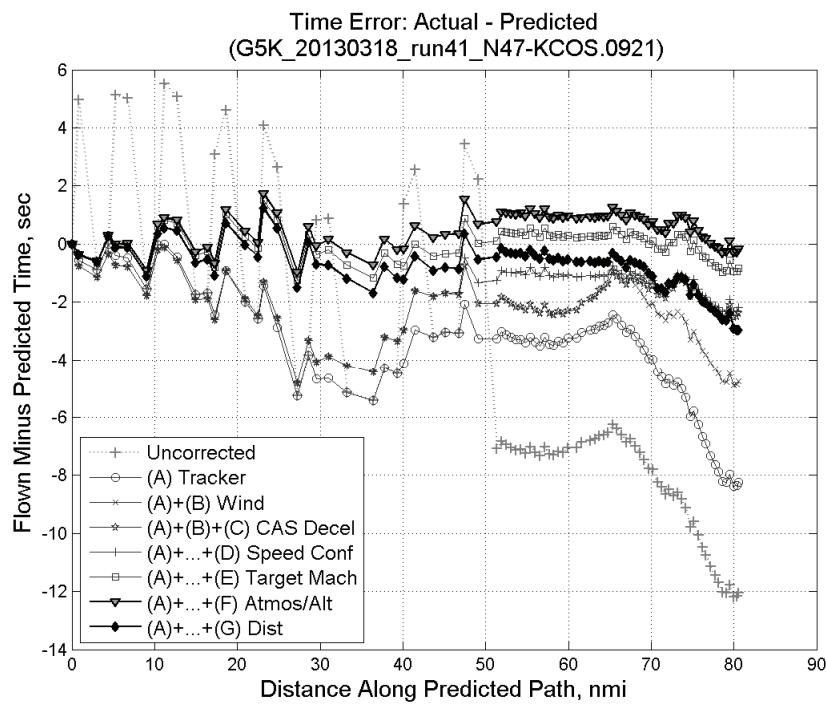


**Figure 764:** Time error for run 41 showing incremental effect of removing each error source.

### C.29.A. Tracker Jumps

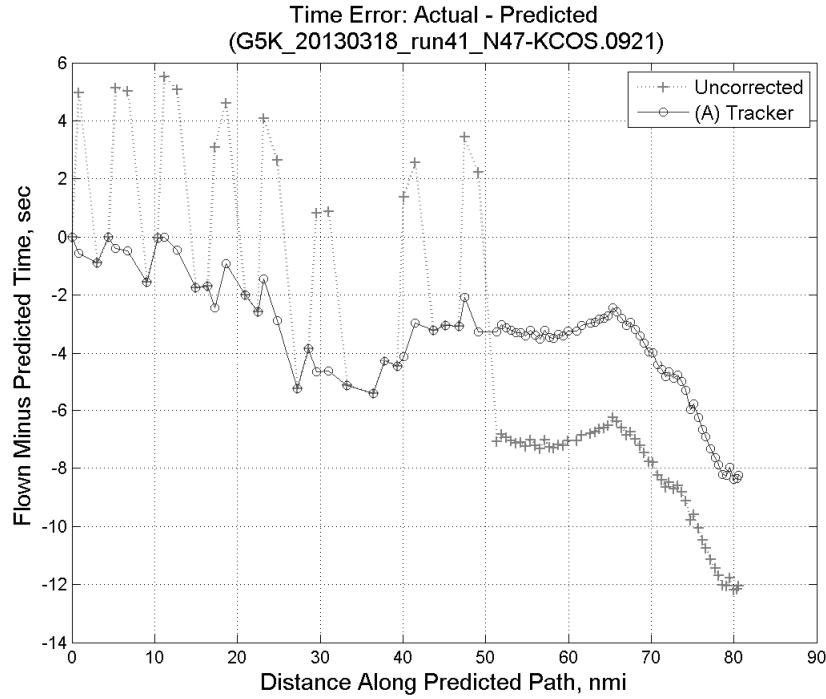


**Figure 765:** Time error for run 41 before (Uncorrected) and after ((A) Tracker) removing tracker jump error source.

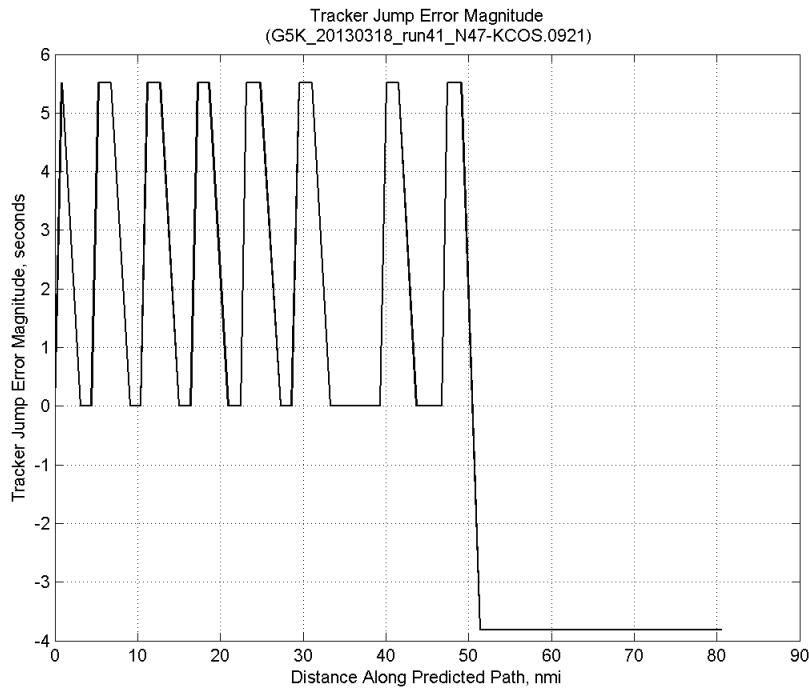


**Figure 766: Effect of tracker jump error source on time error for run 41.**

### C.29.B. Wind

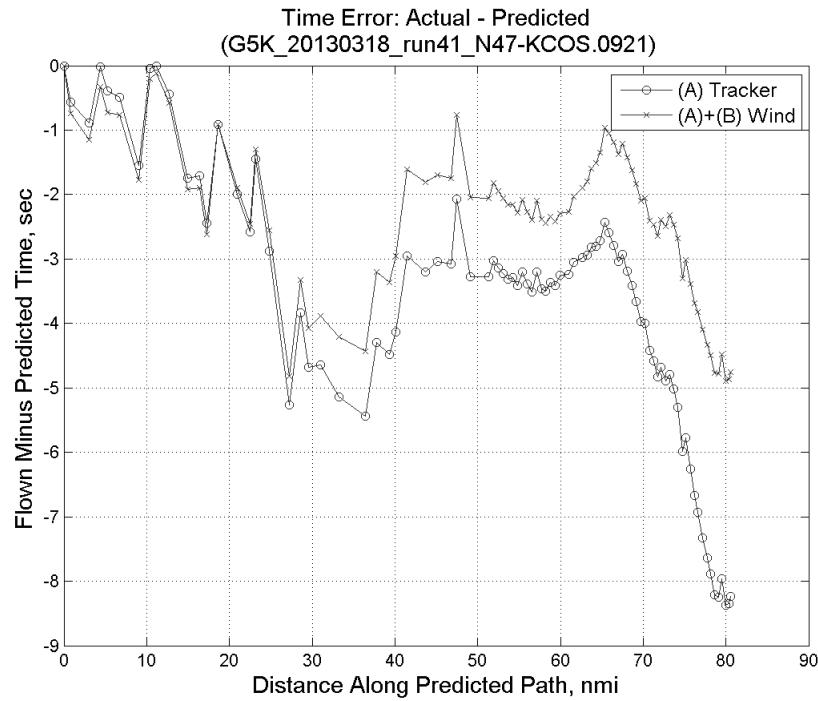


**Figure 767: Time error for run 41 before ((A) Tracker) and after ((A)+(B) Wind) removing wind error source.**

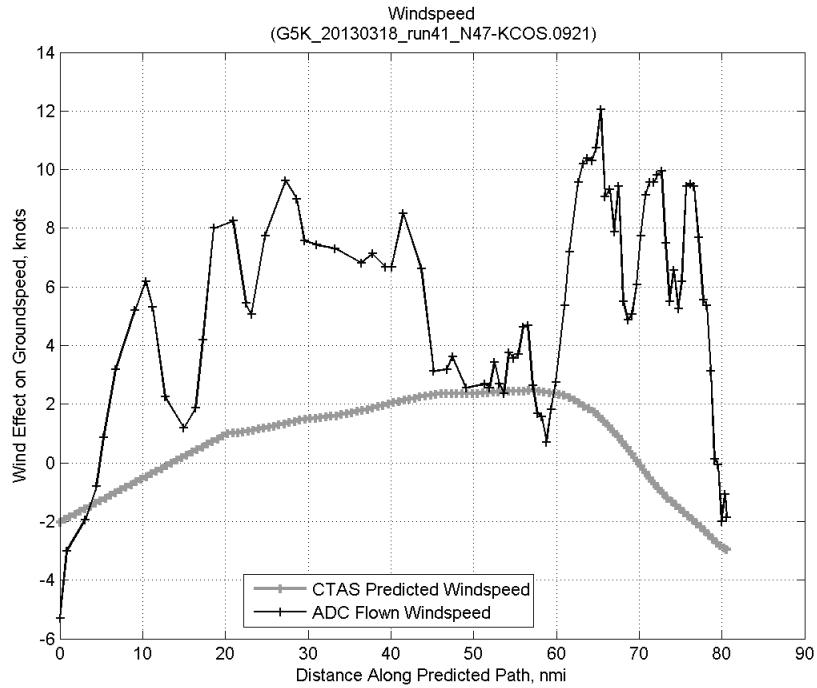


**Figure 768: CTAS predicted and ADC flown wind effect on ground speed for run 41. Negative values indicate a headwind.**

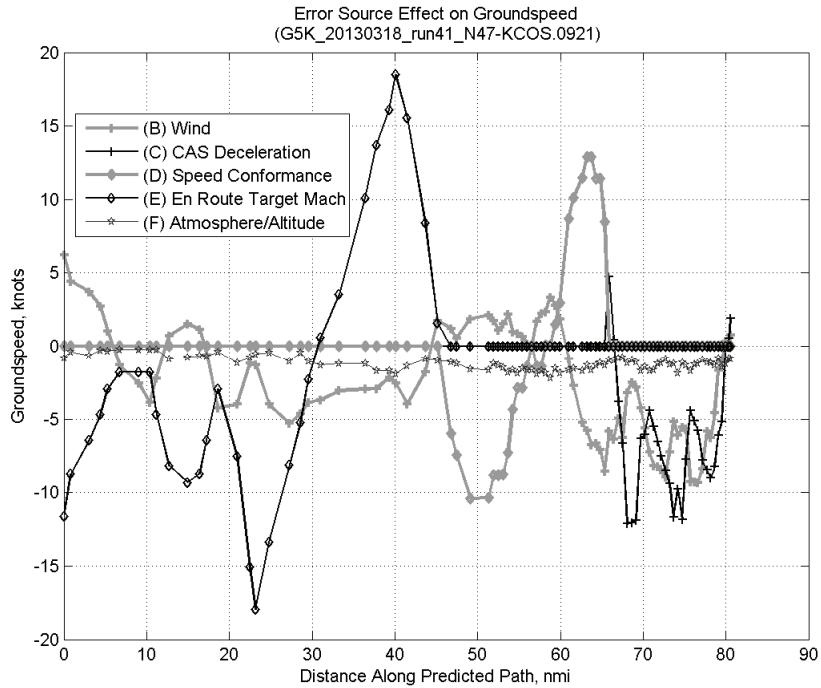


**Figure 769: Error sources (flown minus predicted) converted to a ground speed effect for run 41. Positive values indicate the flown ground speed was faster than the CTAS prediction.**

### C.29.C. CAS Deceleration

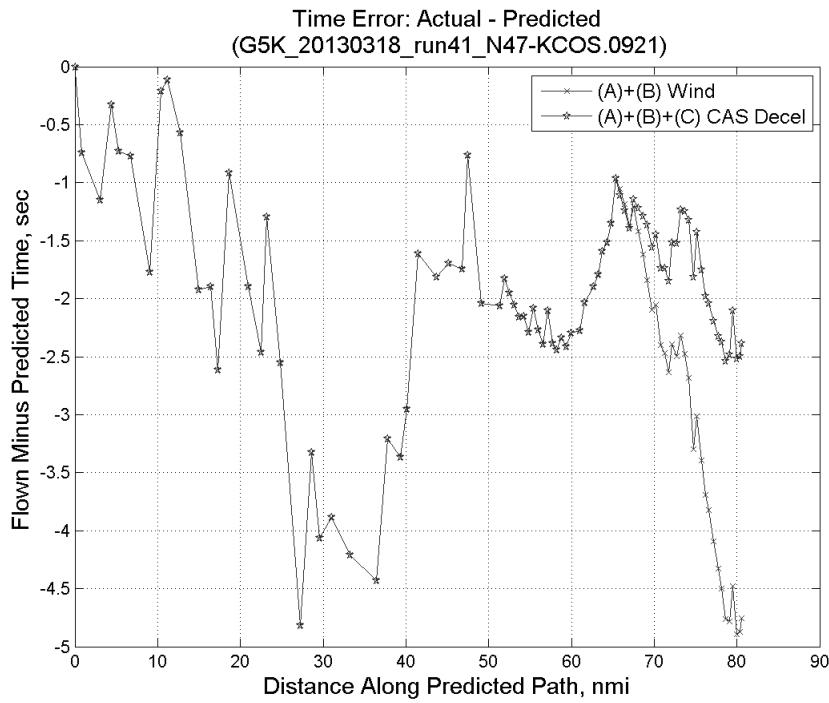


**Figure 770:** Time error for run 41 before ((A)+(B) Wind) and after ((A)+(B)+(C) CAS Decel) removing CAS deceleration error source.

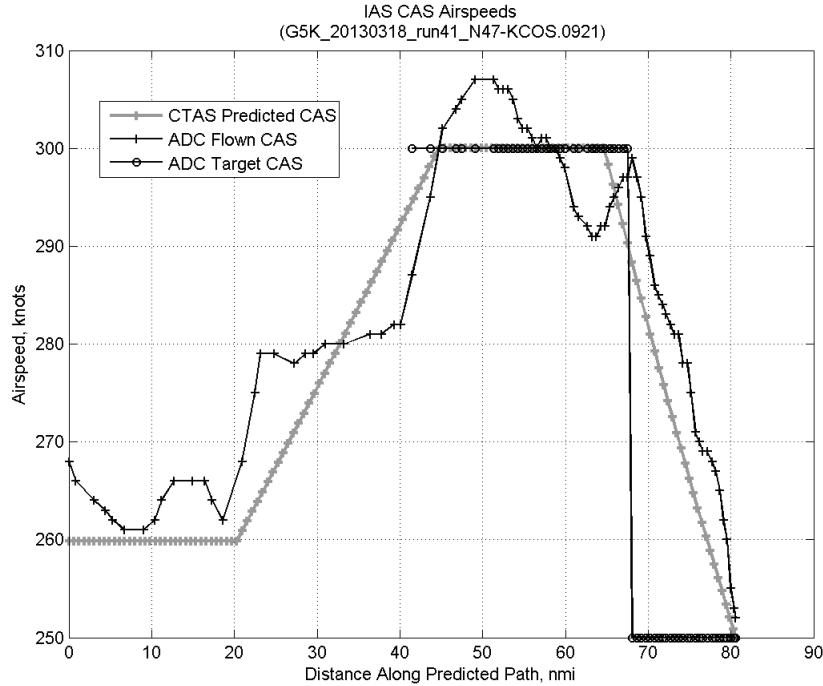


**Figure 771:** CTAS predicted and ADC flown CAS for run 41. CAS that is being targeted is shown with circle markers.

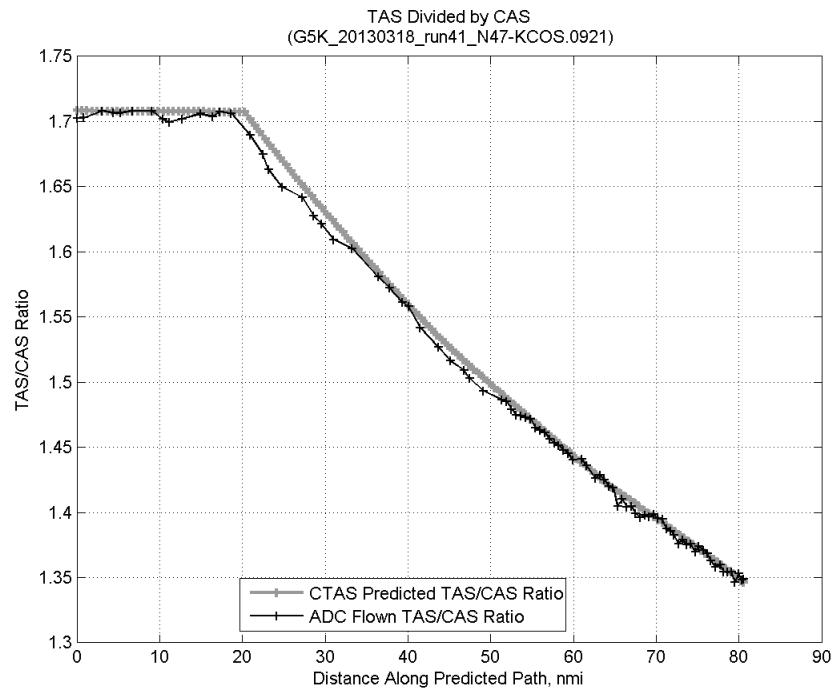


**Figure 772: CTAS predicted and ADC flown TAS/CAS ratio for run 41.**

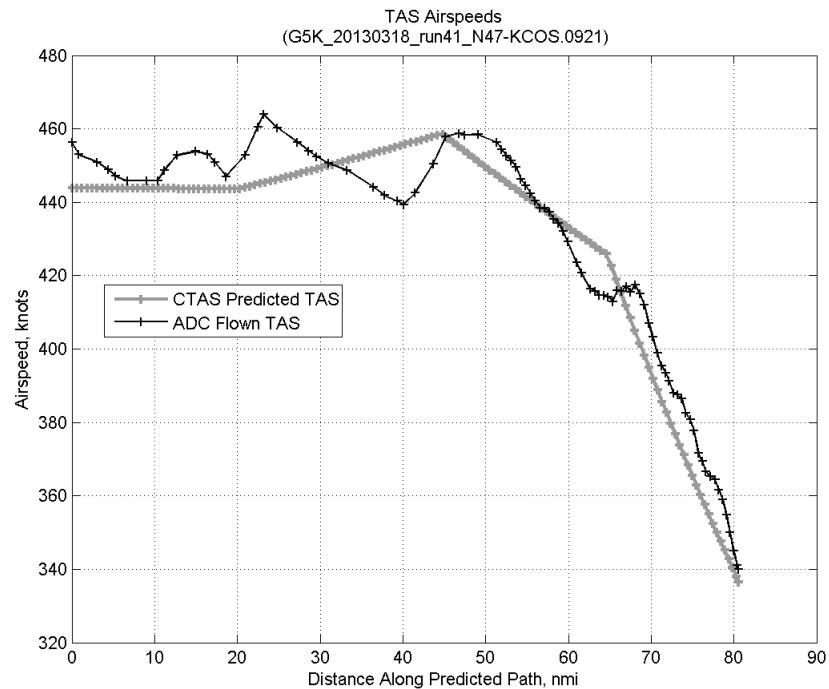


**Figure 773: CTAS predicted and ADC flown TAS for run 41.**

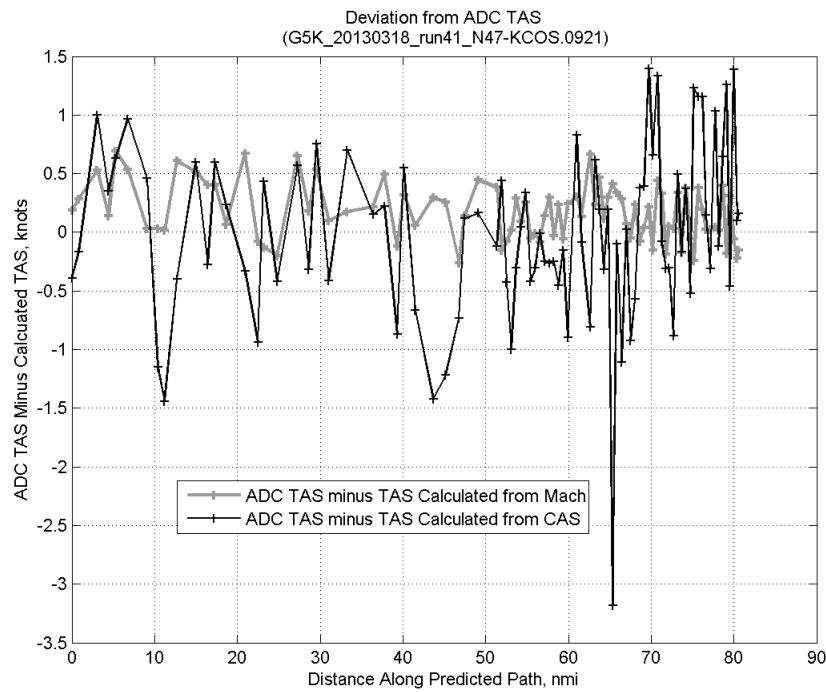


**Figure 774: Deviation from ADC flown TAS if calculating TAS using ADC flown CAS, Mach, atmospheric temperature, and atmospheric pressure for run 41.**

#### C.29.D. Speed Conformance

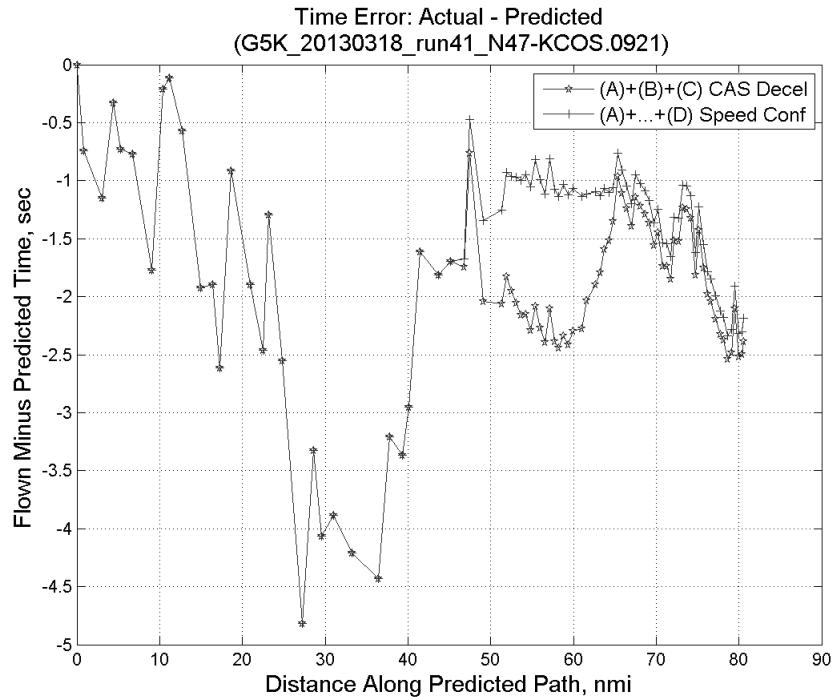


**Figure 775: Time error for run 41 before ((A)+(B)+(C) CAS Decel) and after ((A)+...+(D) Speed Conf) removing speed conformance error source.**

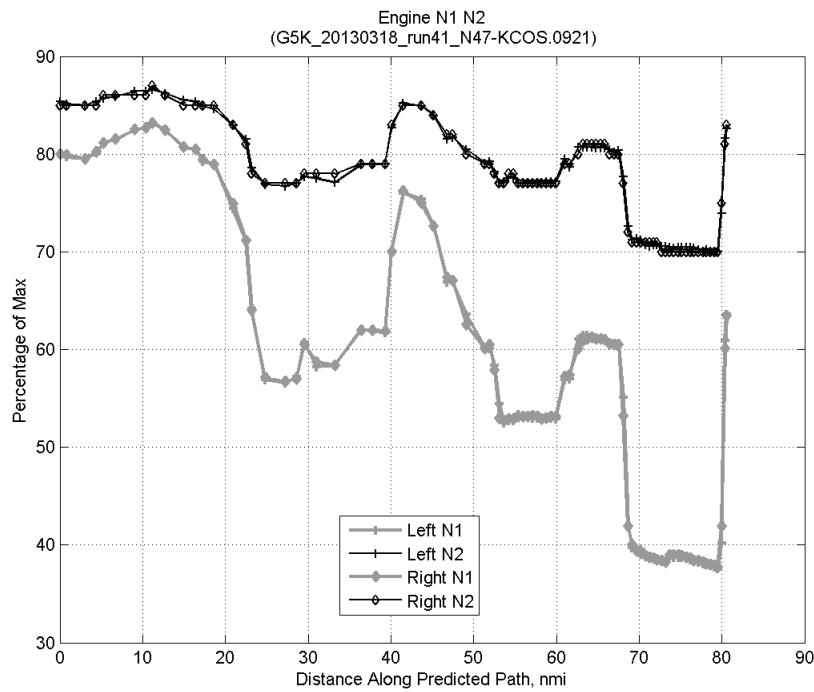


**Figure 776: Flown engine N1 and N2 for run 41.**

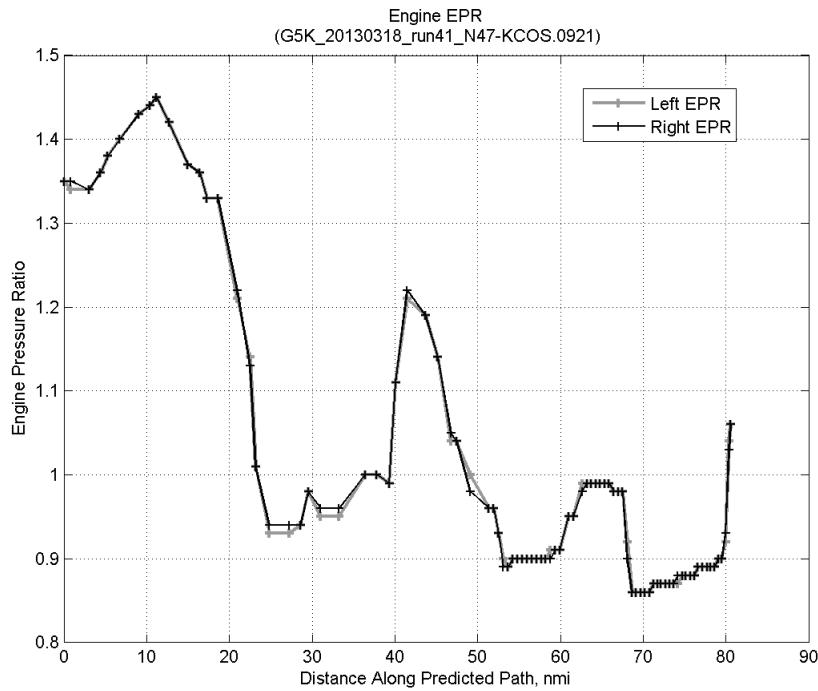


**Figure 777: Flown engine EPR for run 41.**

### C.29.E. Target Mach

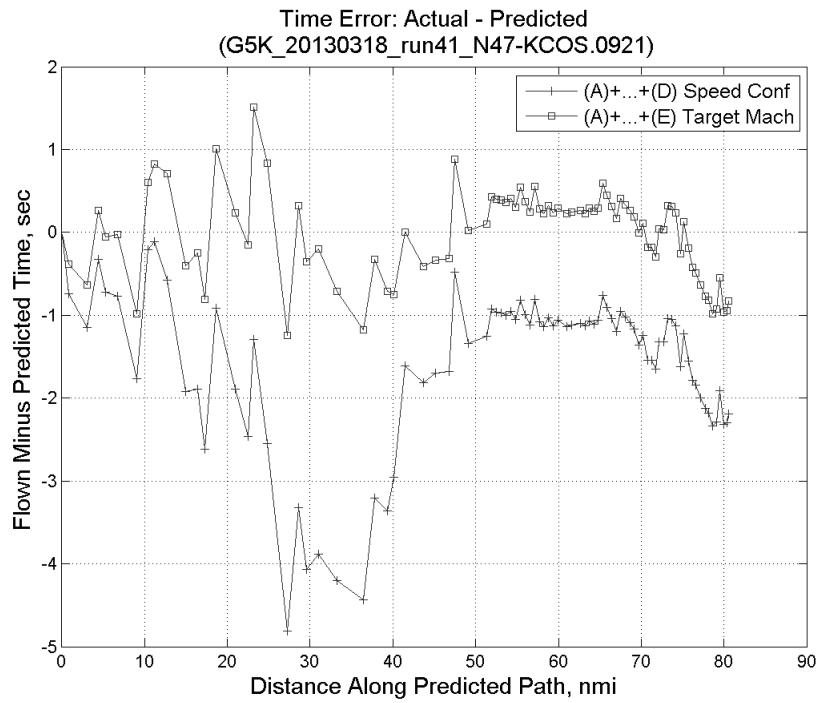


**Figure 778:** Time error for run 41 before ((A)+...+(D) Speed Conf) and after ((A)+...+(E) Target Mach) removing target Mach error source.

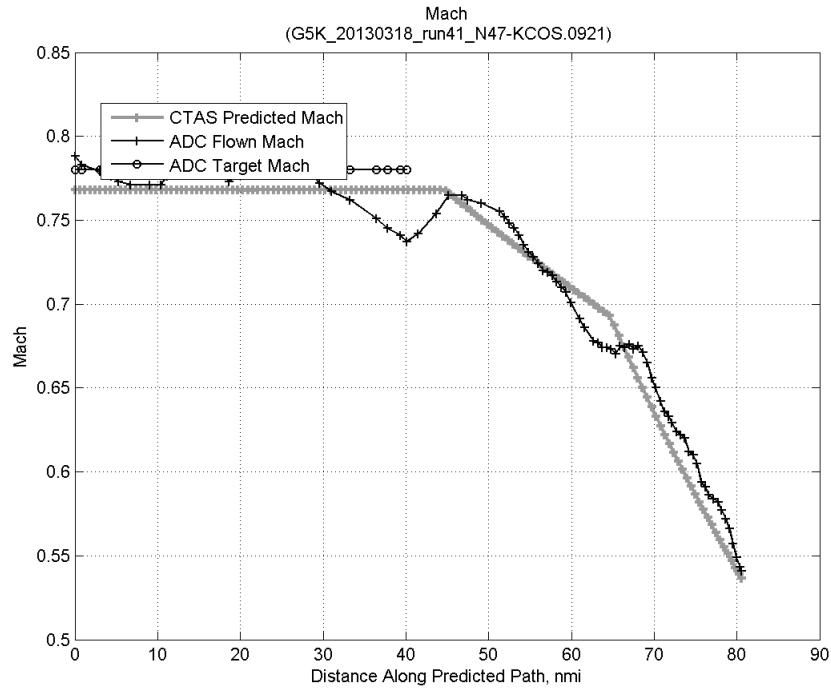


**Figure 779:** CTAS predicted and ADC flown Mach for run 41. Mach being targeted (ADC) shown with circle markers.

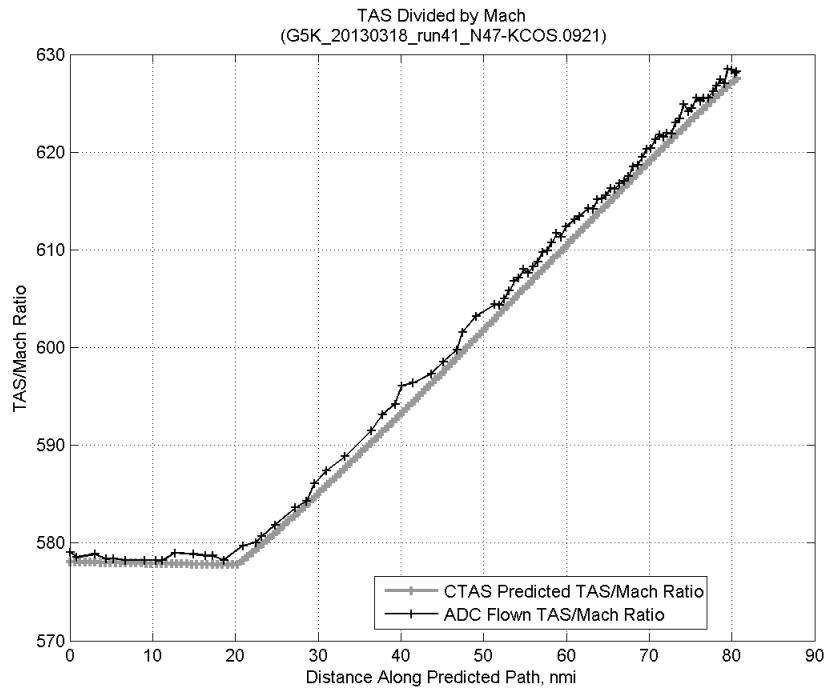


**Figure 780: CTAS predicted and ADC flown TAS/Mach ratio for run 41.**

#### C.29.F. Atmosphere/Altitude

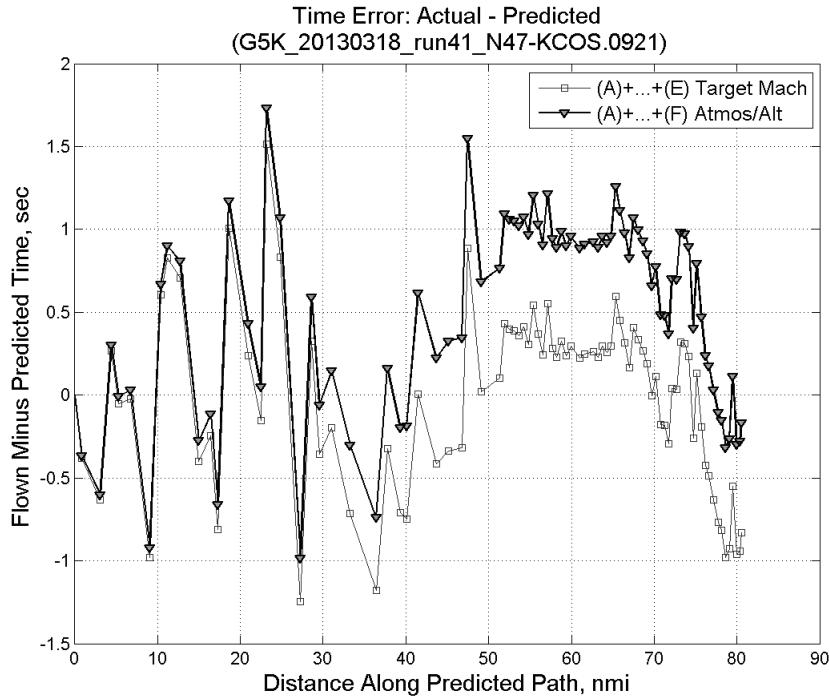


**Figure 781: Time error for run 41 before ((A)+...+(E) Target Mach) and after ((A)+...+(F) Atmos/Alt) removing atmosphere/altitude error source.**

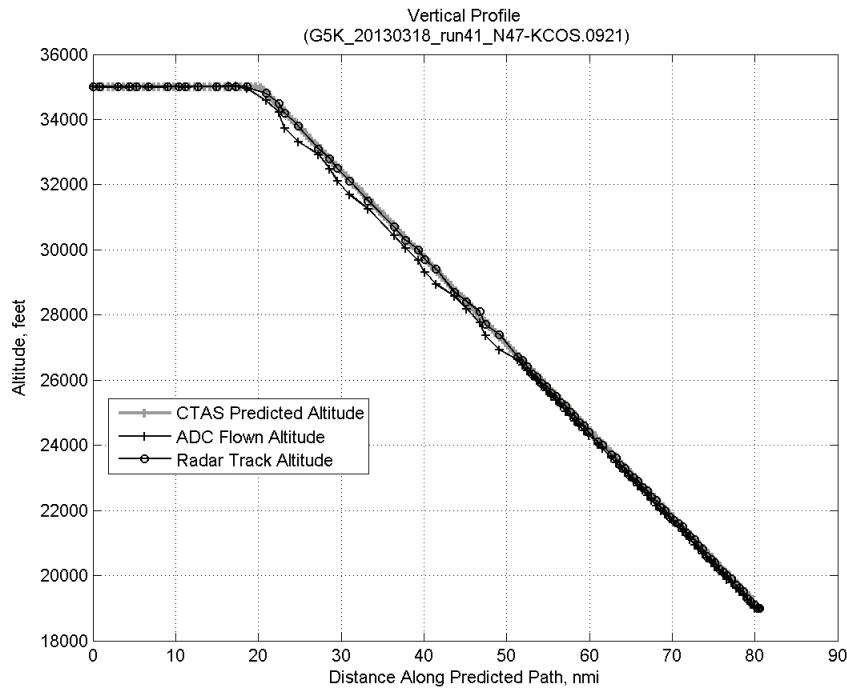


**Figure 782: Flown (ADC) and predicted (CTAS) vertical profile for run 41.**

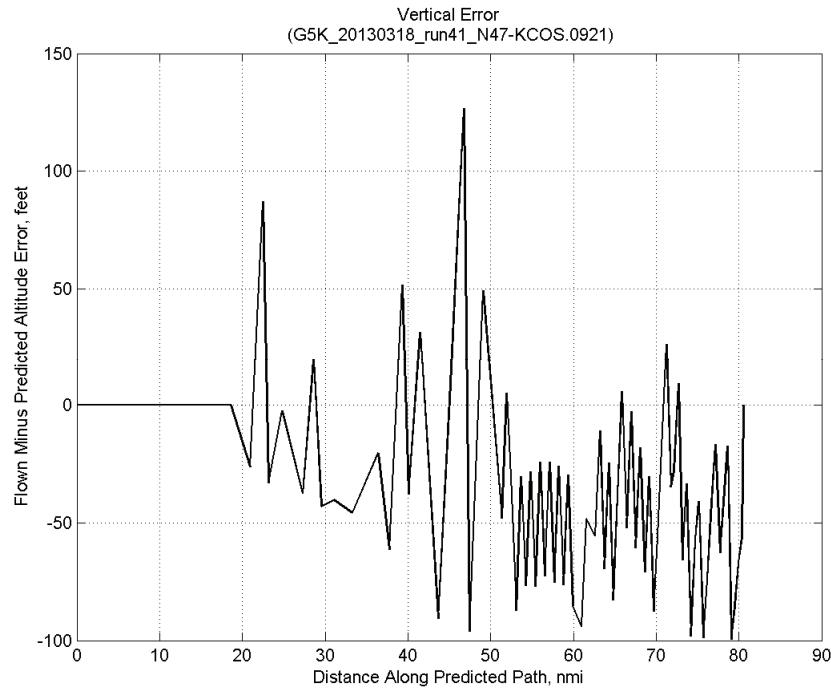


**Figure 783: Vertical error (flown minus predicted altitude) for run 41. Positive values indicate aircraft flew higher than predicted by CTAS.**

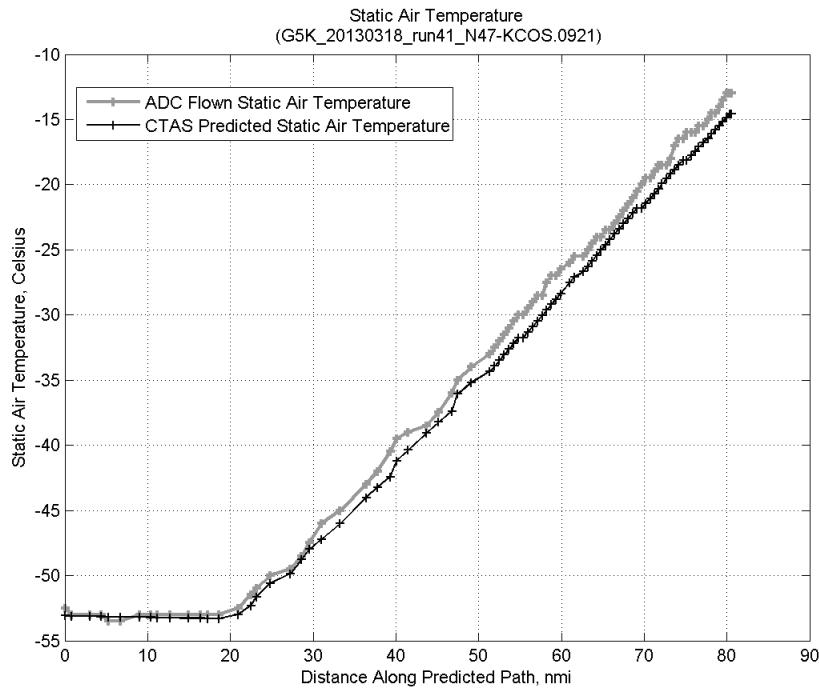


**Figure 784: Flown (ADC) and predicted (CTAS) static air temperature for run 41.**

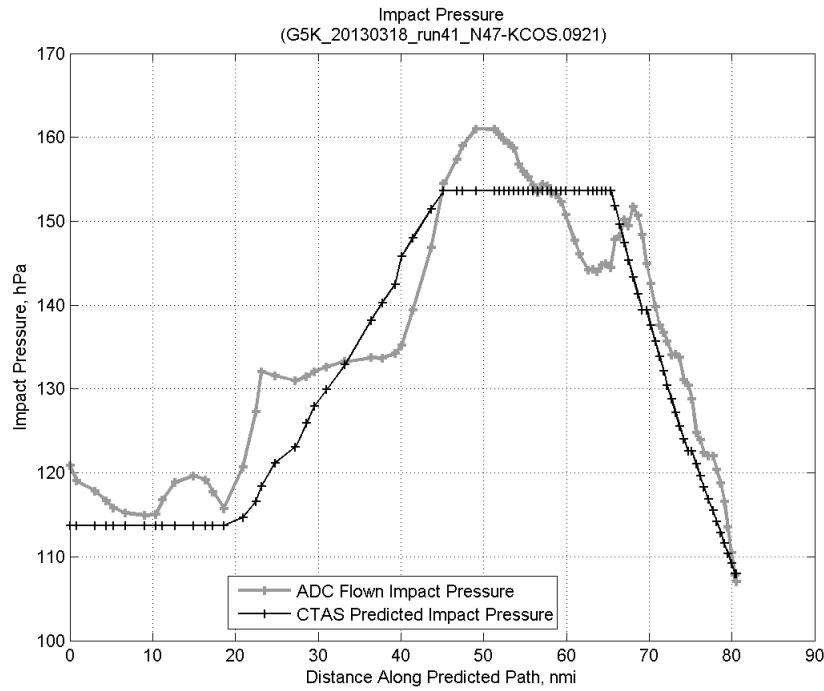


**Figure 785: Flown (ADC) and predicted (CTAS) impact pressure for run 41.**

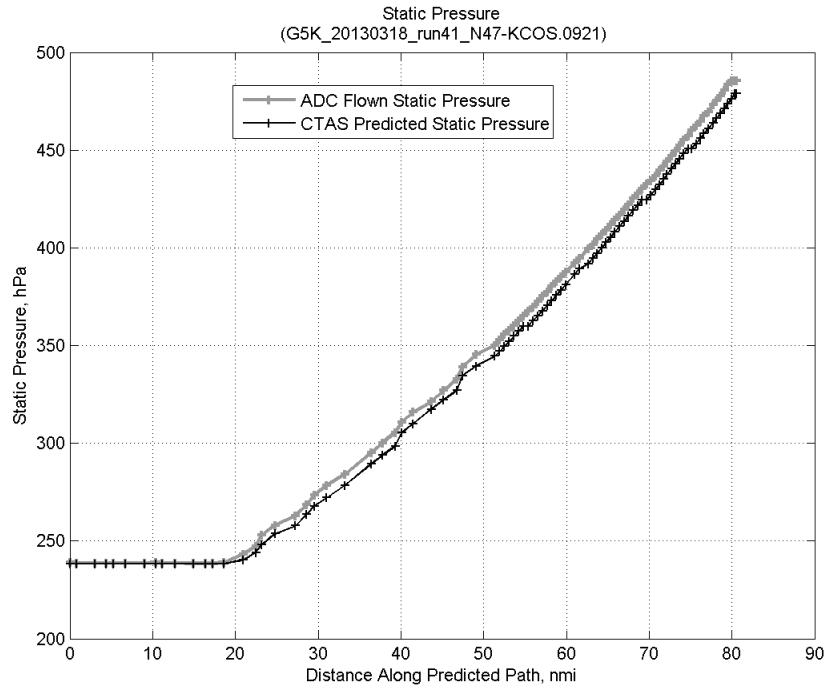


**Figure 786: Flown (ADC) and predicted (CTAS) static pressure for run 41.**

### C.29.G. Path Distance

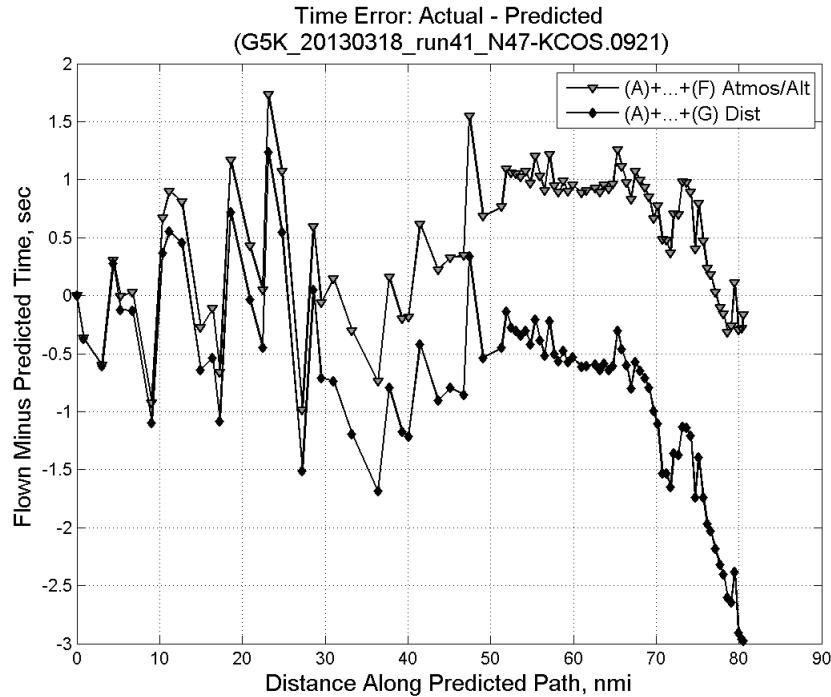


**Figure 787: Time error for run 41 before ((A)+...+(F) Atmos/Alt) and after ((A)+...+(G) Dist) removing path distance error source.**

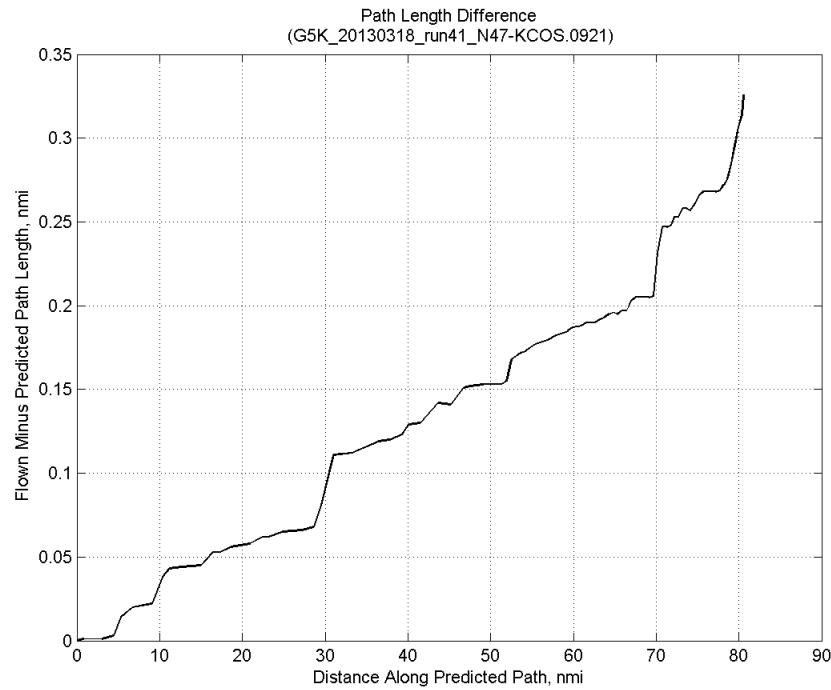


**Figure 788: ADC flown minus CTAS predicted path length for run 41. Positive values indicate aircraft followed a longer path than predicted by CTAS.**

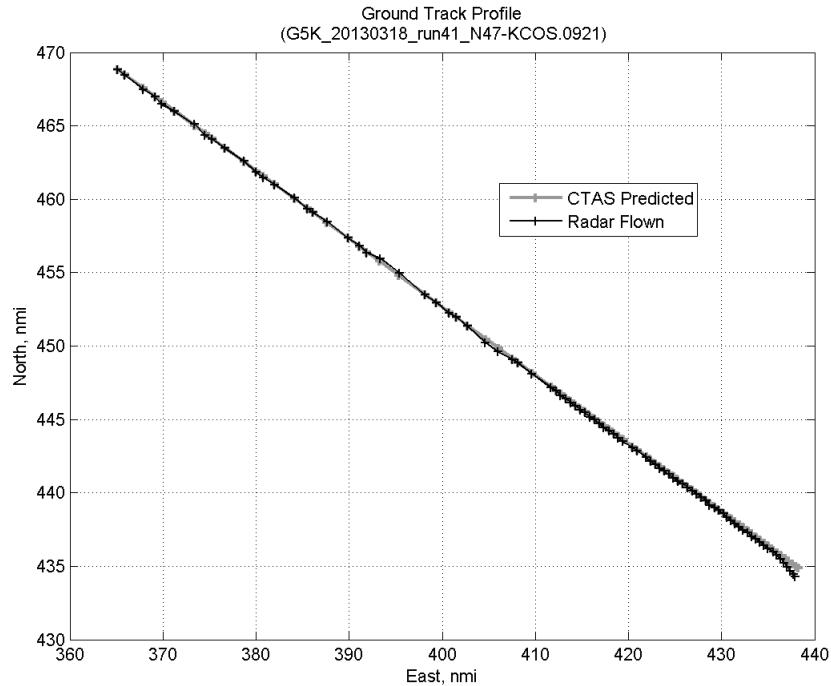


**Figure 789: CTAS predicted and radar flown ground track profile for run 41.**

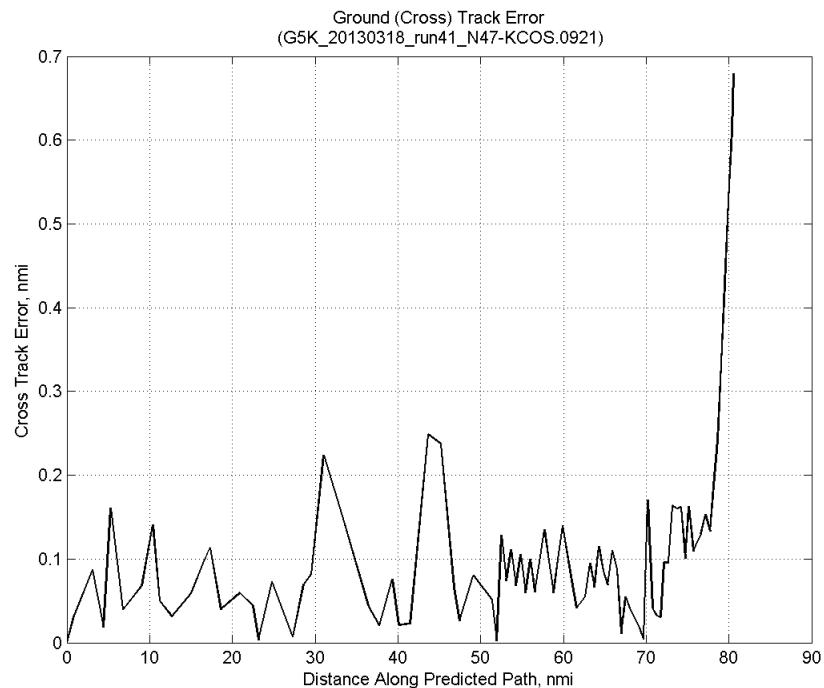


**Figure 790: Ground (cross) track error for run 41.**

### C.30. Run 42

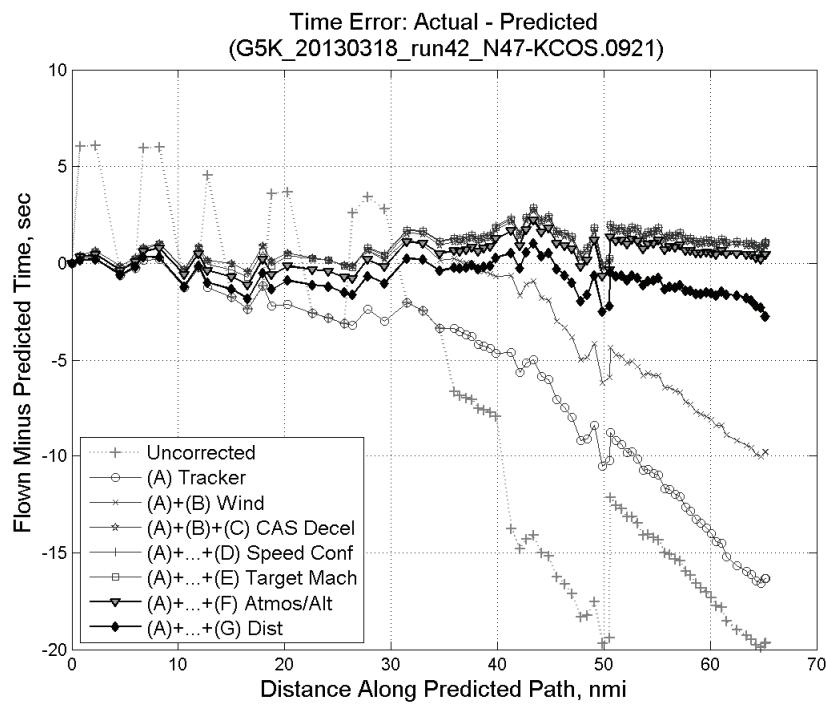


**Figure 791: Time error for run 42 showing incremental effect of removing each error source.**

#### C.30.A. Tracker Jumps

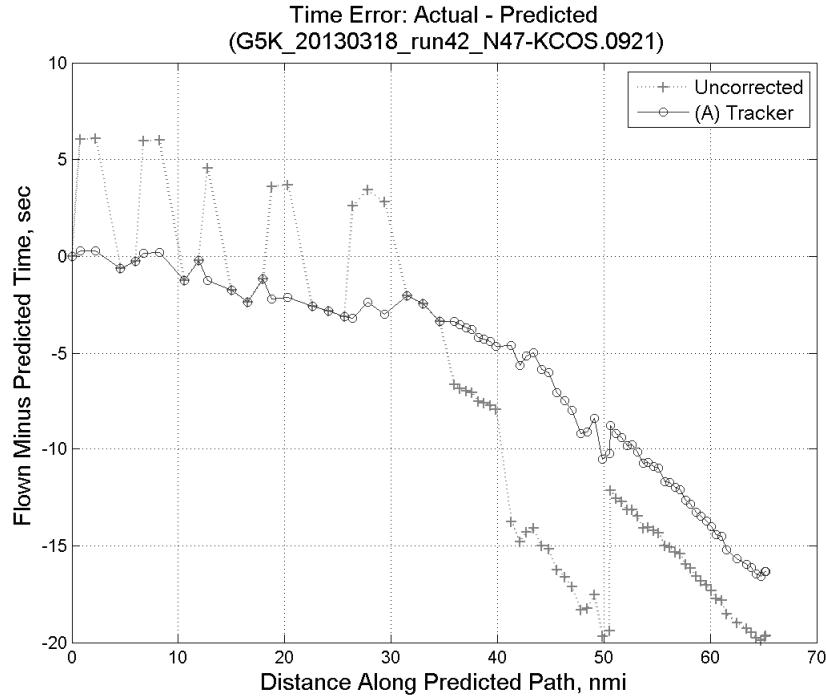


**Figure 792: Time error for run 42 before (Uncorrected) and after ((A) Tracker) removing tracker jump error source.**

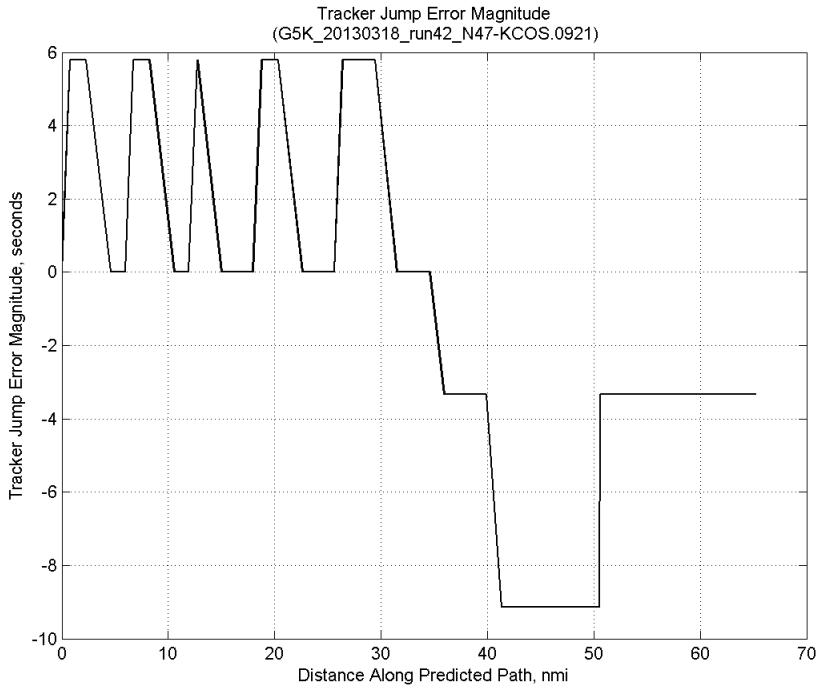


**Figure 793: Effect of tracker jump error source on time error for run 42.**

### C.30.B. Wind

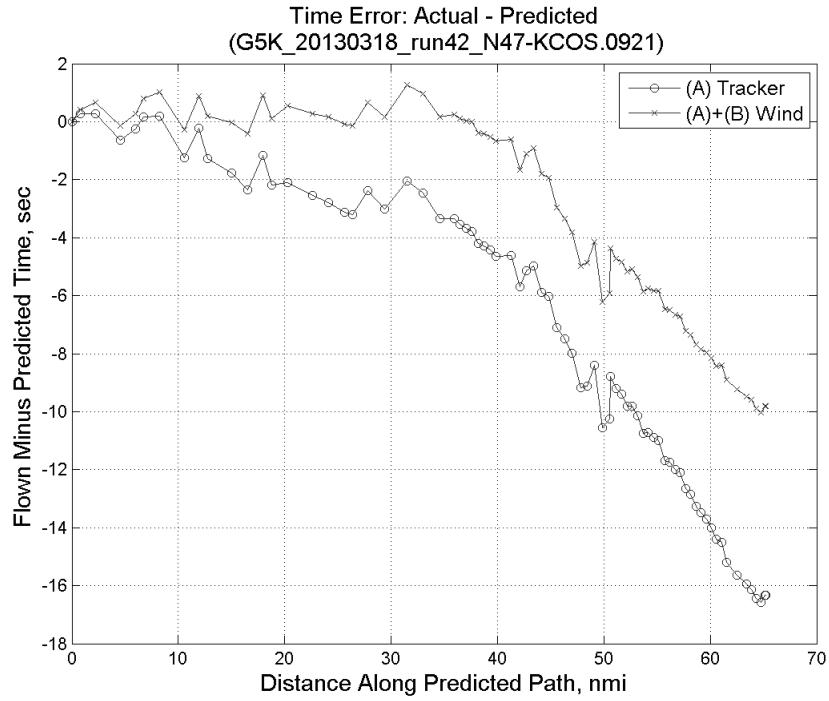


**Figure 794: Time error for run 42 before ((A) Tracker) and after ((A)+(B) Wind) removing wind error source.**

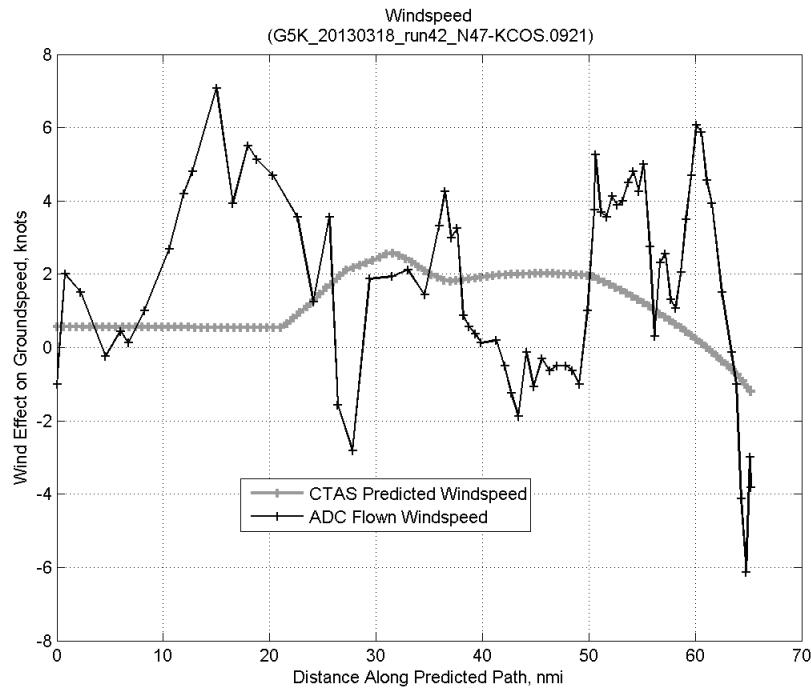


**Figure 795: CTAS predicted and ADC flown wind effect on ground speed for run 42. Negative values indicate a headwind.**

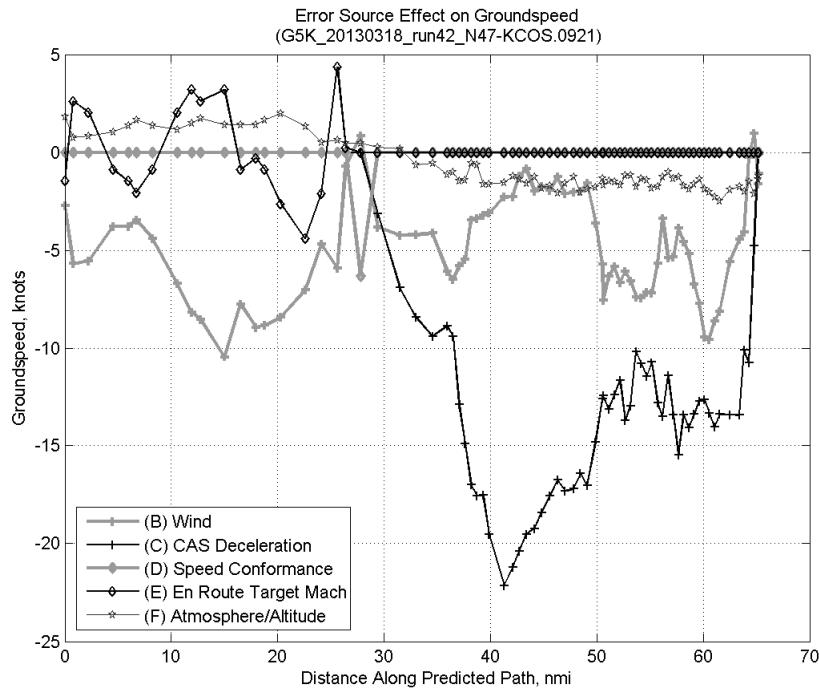


**Figure 796: Error sources (flown minus predicted) converted to a ground speed effect for run 42. Positive values indicate the flown ground speed was faster than the CTAS prediction.**

### C.30.C. CAS Deceleration

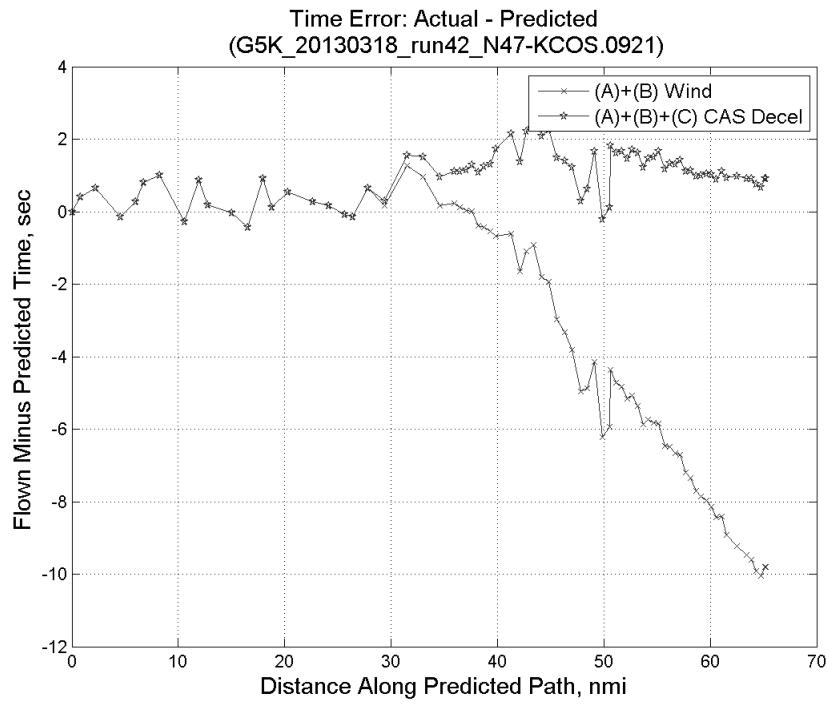


**Figure 797:** Time error for run 42 before ((A)+(B) Wind) and after ((A)+(B)+(C) CAS Decel) removing CAS deceleration error source.

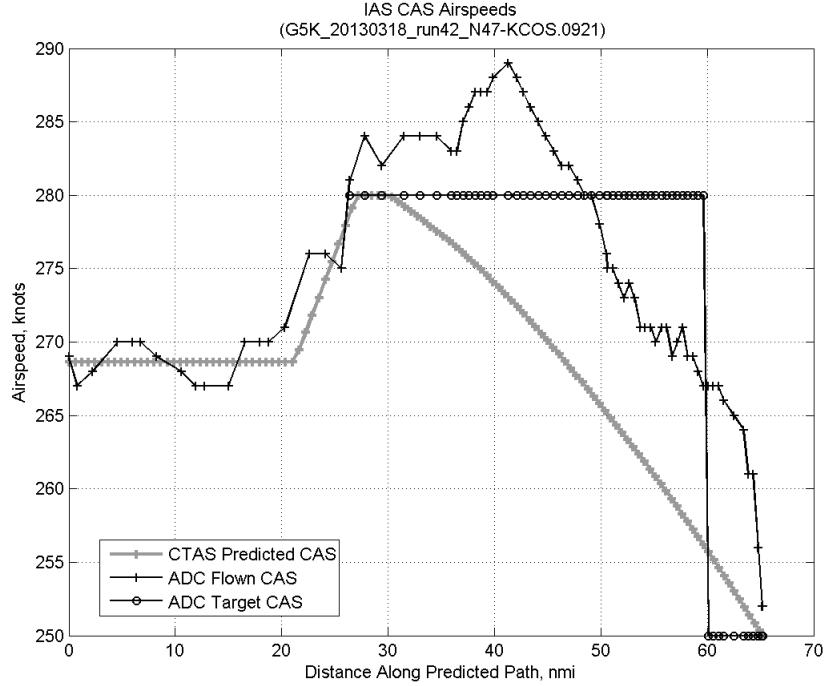


**Figure 798:** CTAS predicted and ADC flown CAS for run 42. CAS that is being targeted is shown with circle markers.

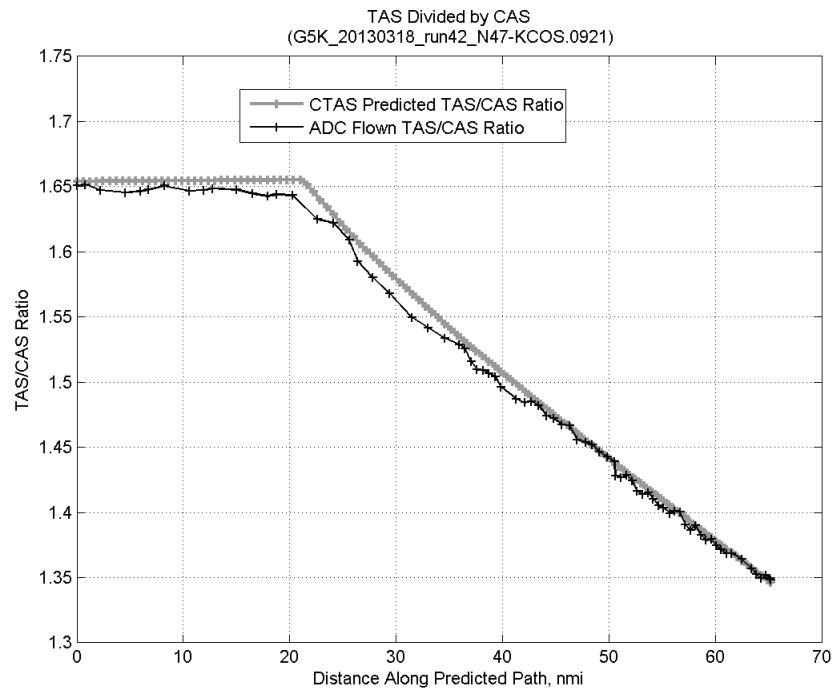


**Figure 799: CTAS predicted and ADC flown TAS/CAS ratio for run 42.**

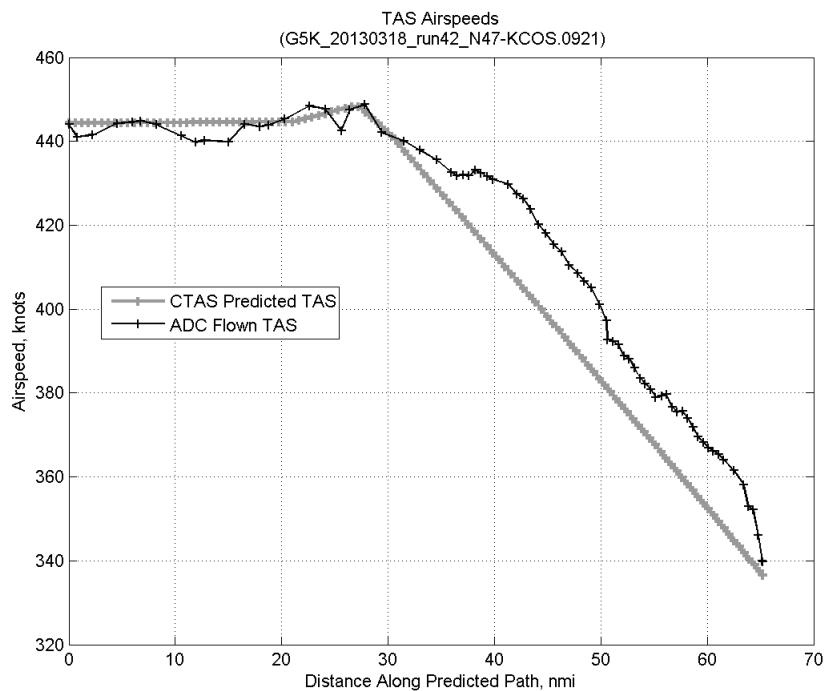


**Figure 800: CTAS predicted and ADC flown TAS for run 42.**

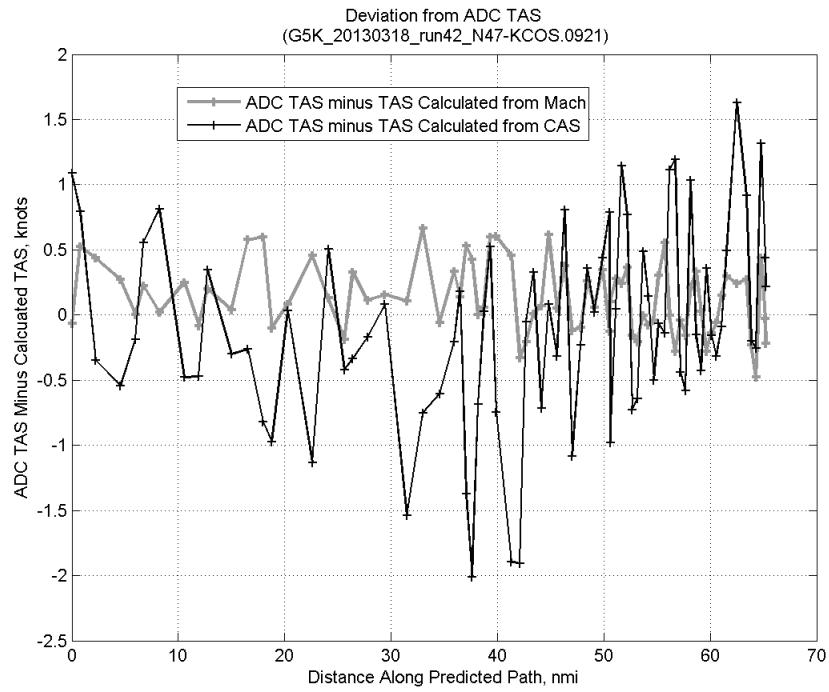


**Figure 801:** Deviation from ADC flown TAS if calculating TAS using ADC flown CAS, Mach, atmospheric temperature, and atmospheric pressure for run 42.

#### C.30.D. Speed Conformance

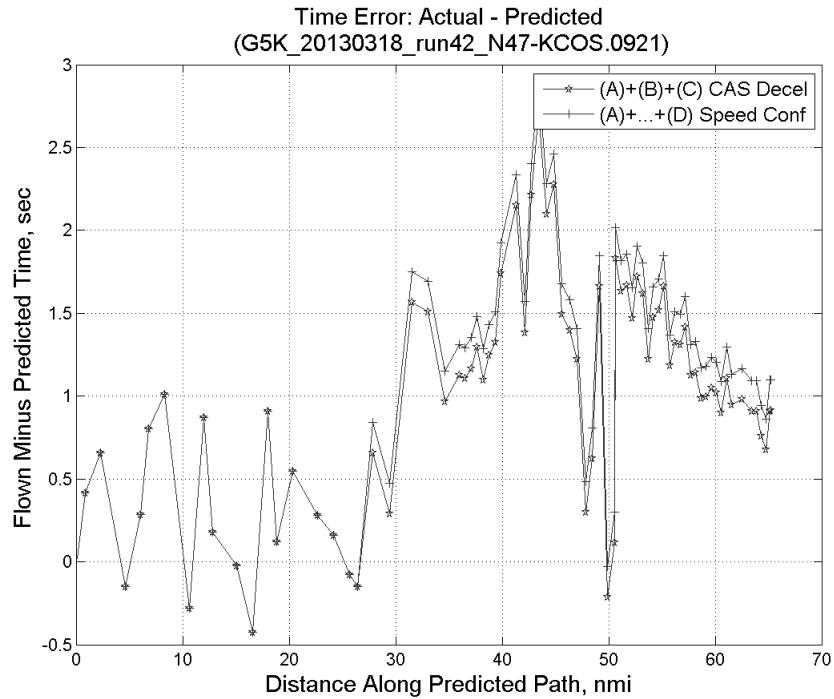


**Figure 802:** Time error for run 42 before  $((A)+(B)+(C) \text{ CAS Decel})$  and after  $((A)+\dots+(D) \text{ Speed Conf})$  removing speed conformance error source.

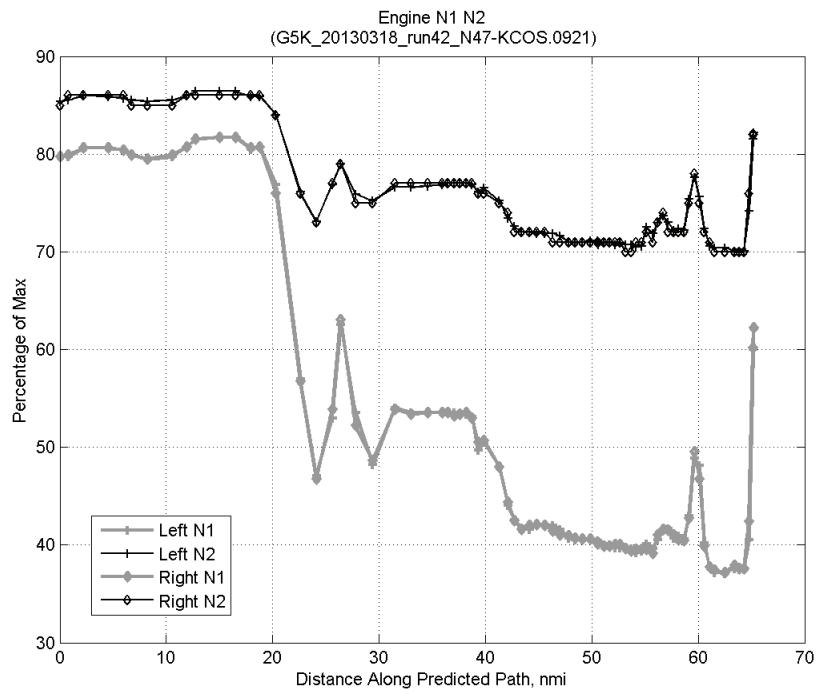


**Figure 803: Flown engine N1 and N2 for run 42.**

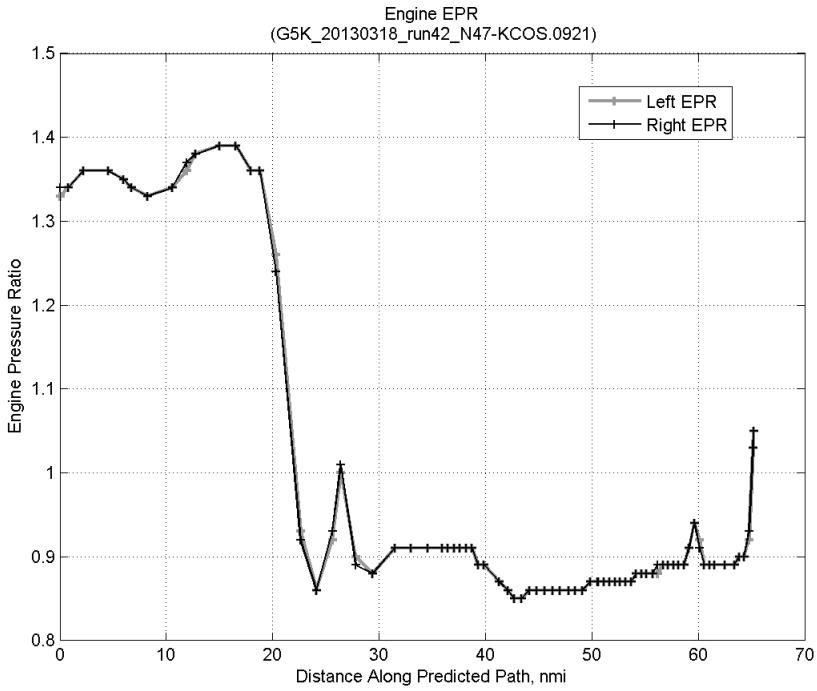


**Figure 804: Flown engine EPR for run 42.**

### C.30.E. Target Mach

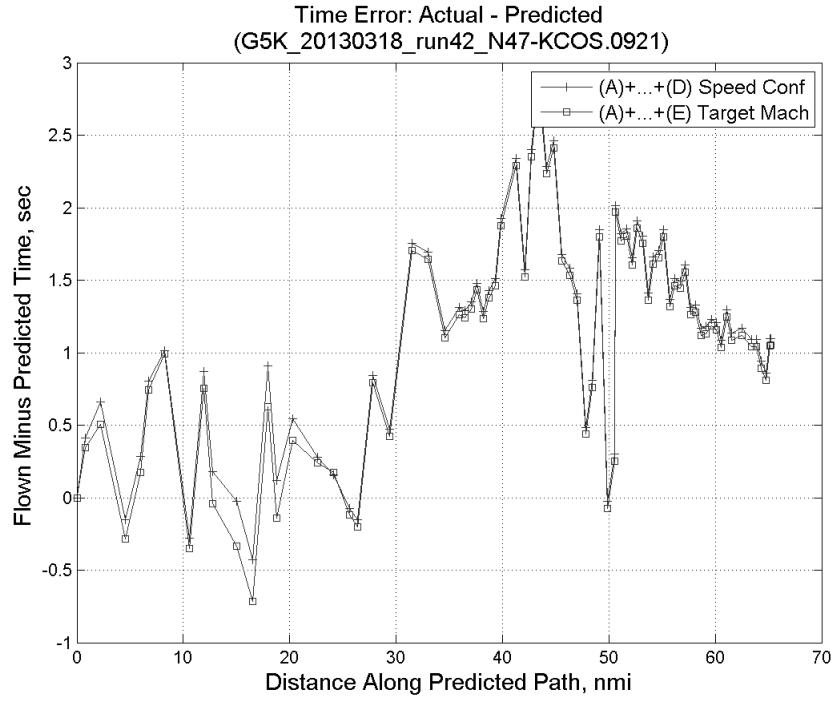


**Figure 805:** Time error for run 42 before ((A)+...+(D) Speed Conf) and after ((A)+...+(E) Target Mach) removing target Mach error source.

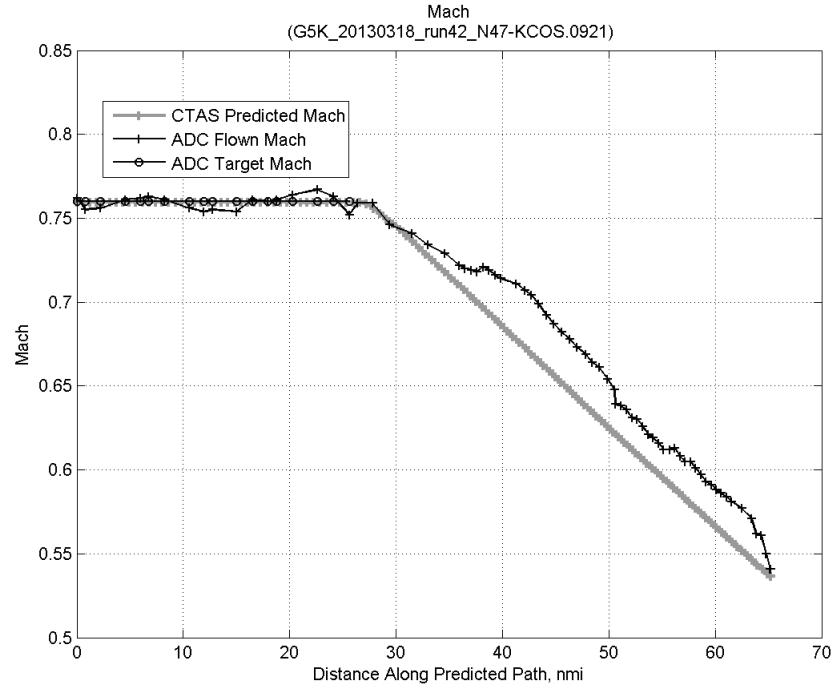


**Figure 806:** CTAS predicted and ADC flown Mach for run 42. Mach being targeted (ADC) shown with circle markers.

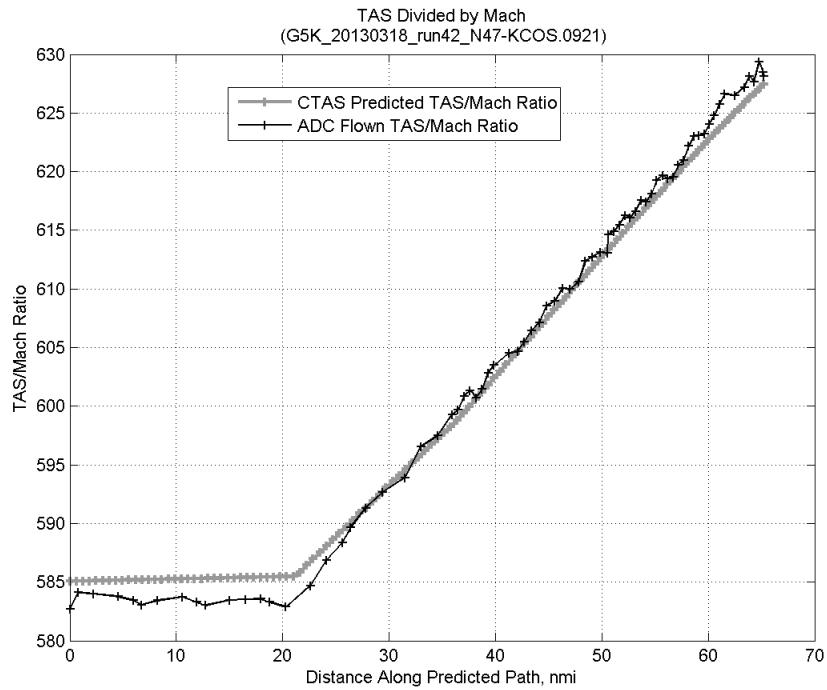


**Figure 807: CTAS predicted and ADC flown TAS/Mach ratio for run 42.**

### C.30.F. Atmosphere/Altitude

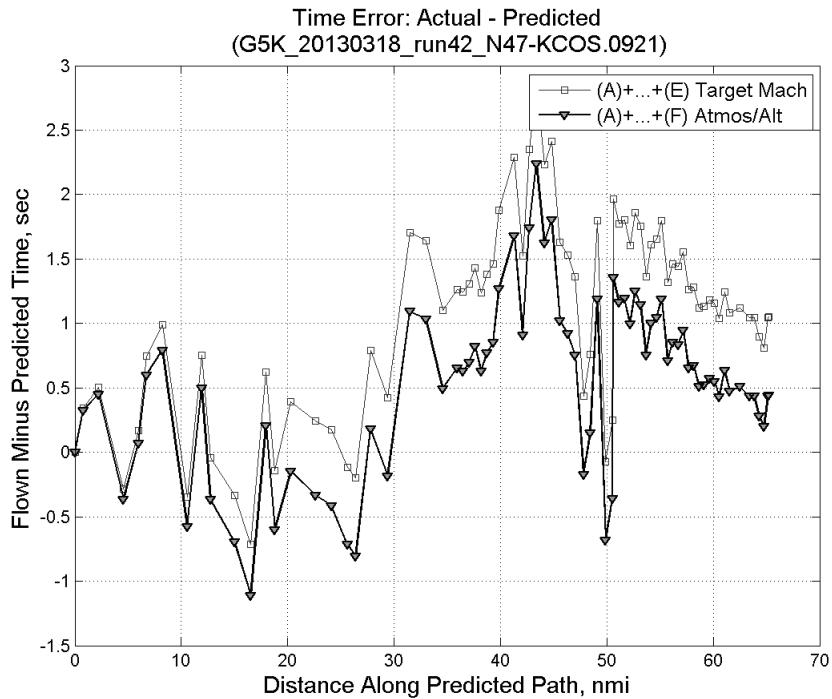


**Figure 808: Time error for run 42 before ((A)+...+(E) Target Mach) and after ((A)+...+(F) Atmos/Alt) removing atmosphere/altitude error source.**

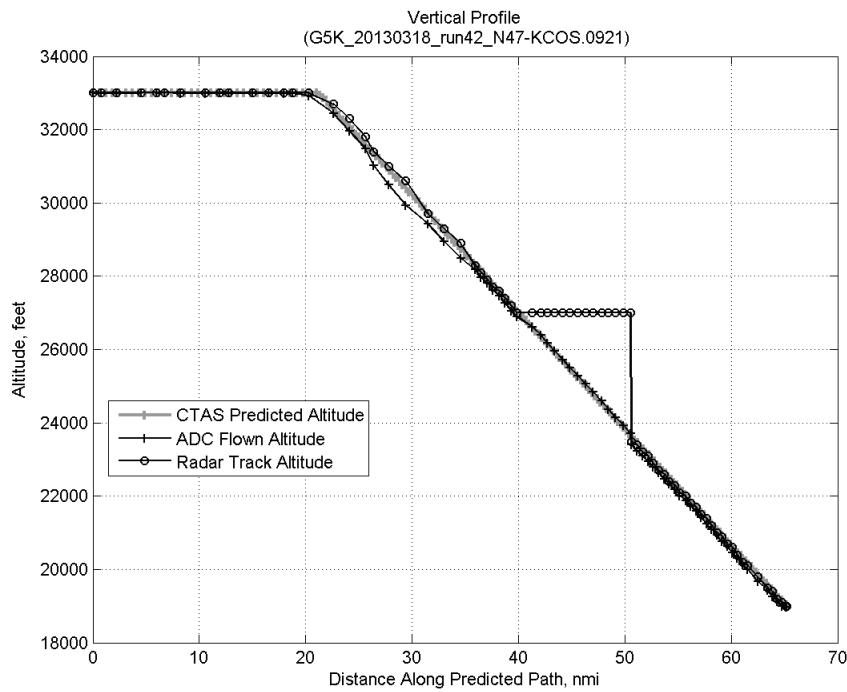


**Figure 809: Flown (ADC) and predicted (CTAS) vertical profile for run 42.**

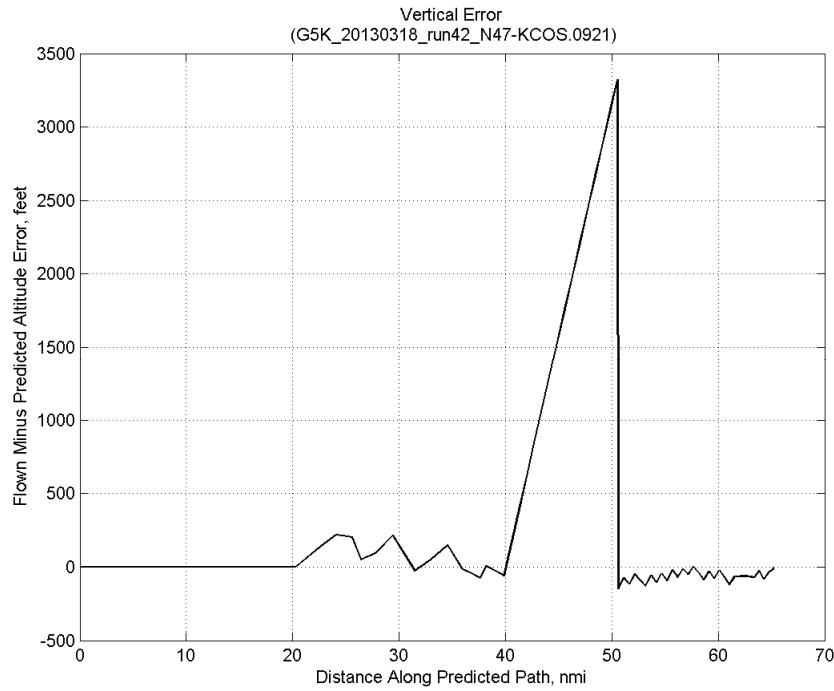


**Figure 810: Vertical error (flown minus predicted altitude) for run 42. Positive values indicate aircraft flew higher than predicted by CTAS.**

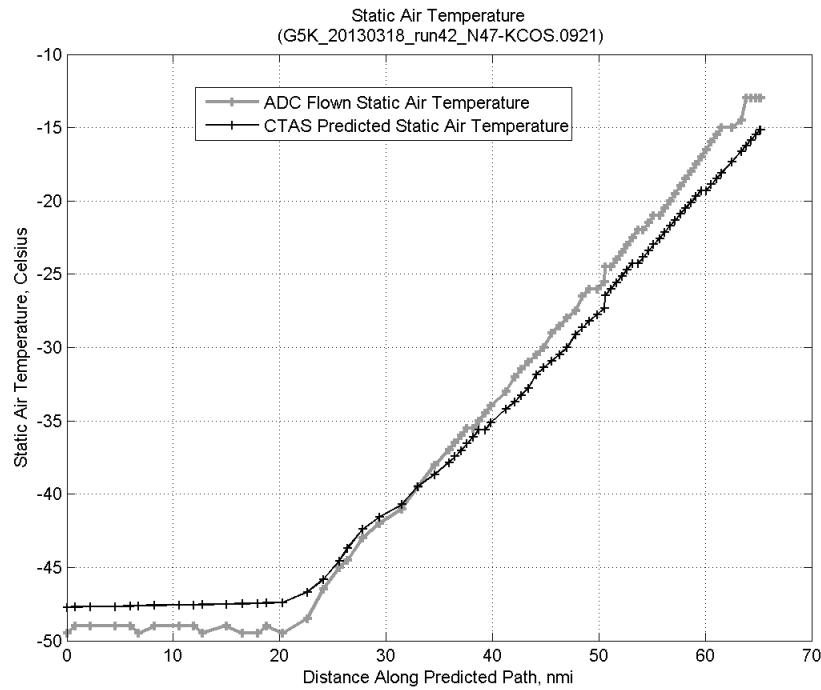


**Figure 811: Flown (ADC) and predicted (CTAS) static air temperature for run 42.**

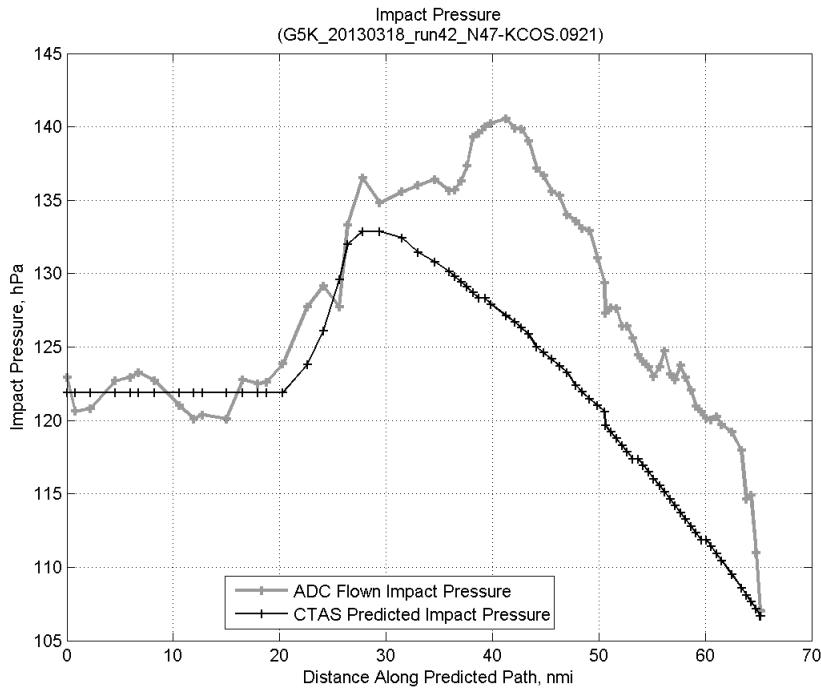


**Figure 812: Flown (ADC) and predicted (CTAS) impact pressure for run 42.**

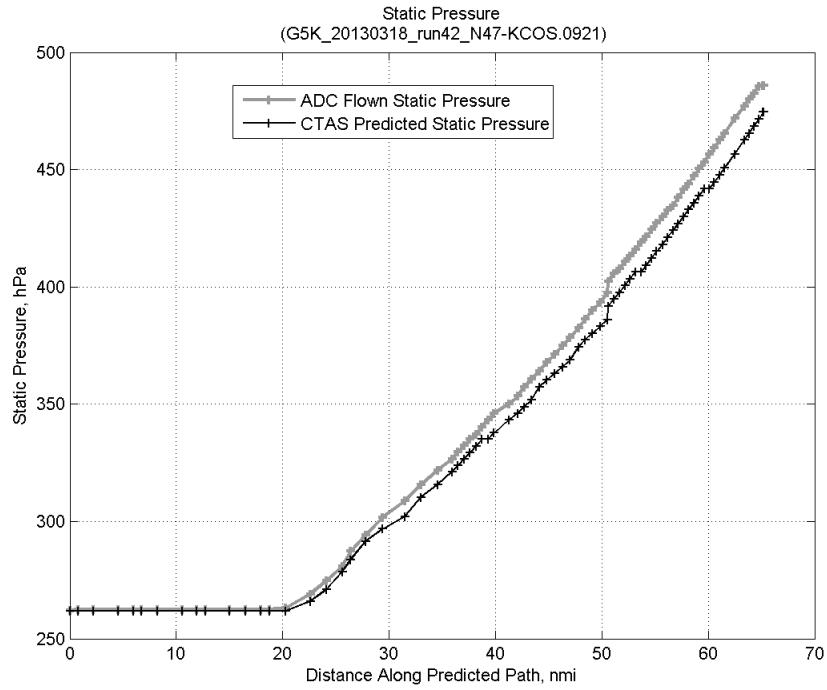


**Figure 813: Flown (ADC) and predicted (CTAS) static pressure for run 42.**

### C.30.G. Path Distance

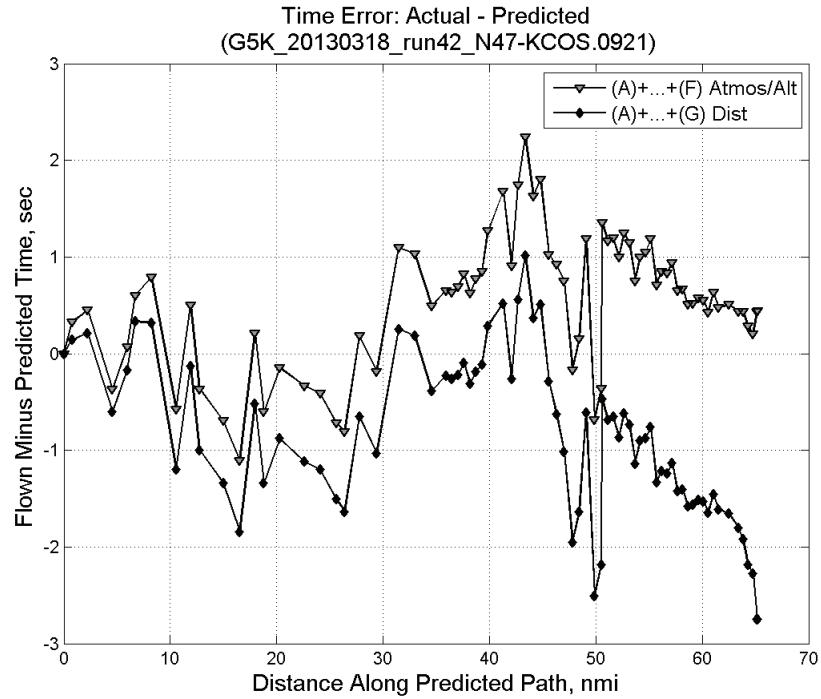


**Figure 814: Time error for run 42 before ((A)+...+(F) Atmos/Alt) and after ((A)+...+(G) Dist) removing path distance error source.**

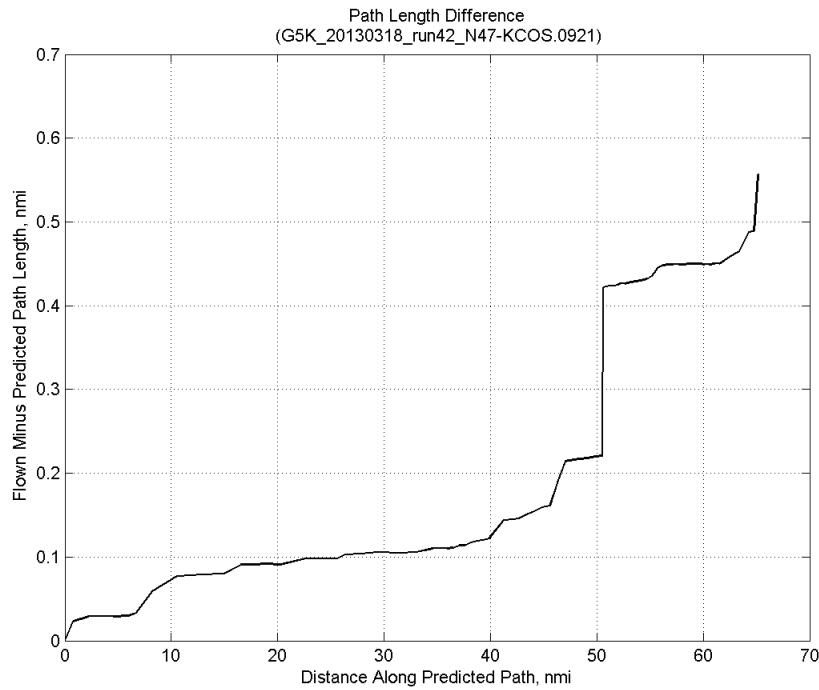


**Figure 815: ADC flown minus CTAS predicted path length for run 42. Positive values indicate aircraft followed a longer path than predicted by CTAS.**

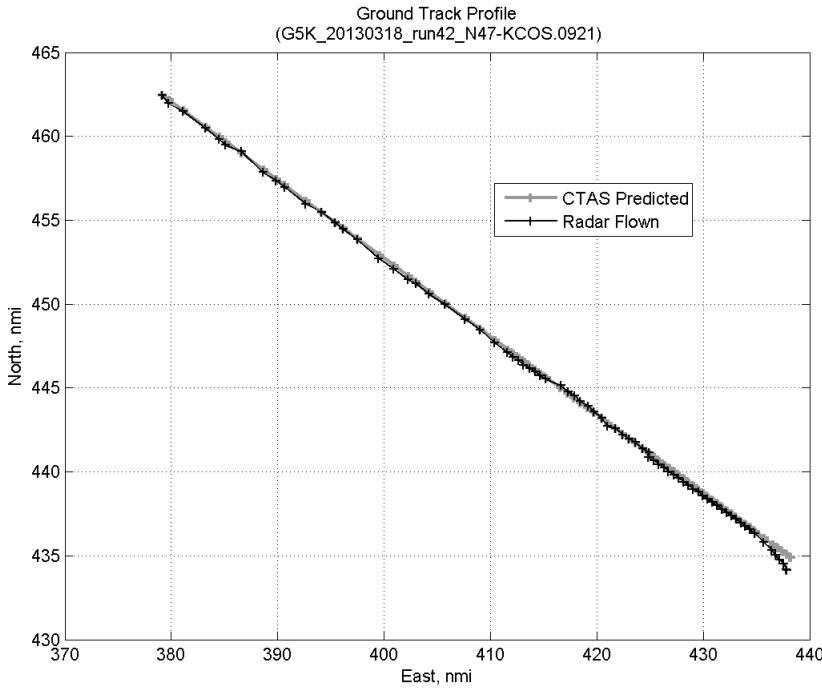


**Figure 816: CTAS predicted and radar flown ground track profile for run 42.**

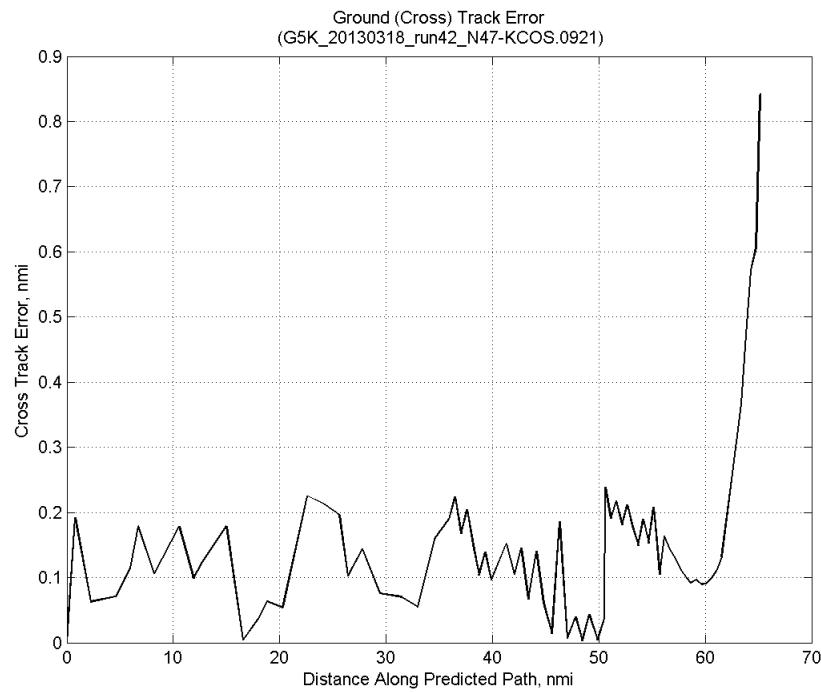


**Figure 817: Ground (cross) track error for run 42.**

### C.31. Run 43

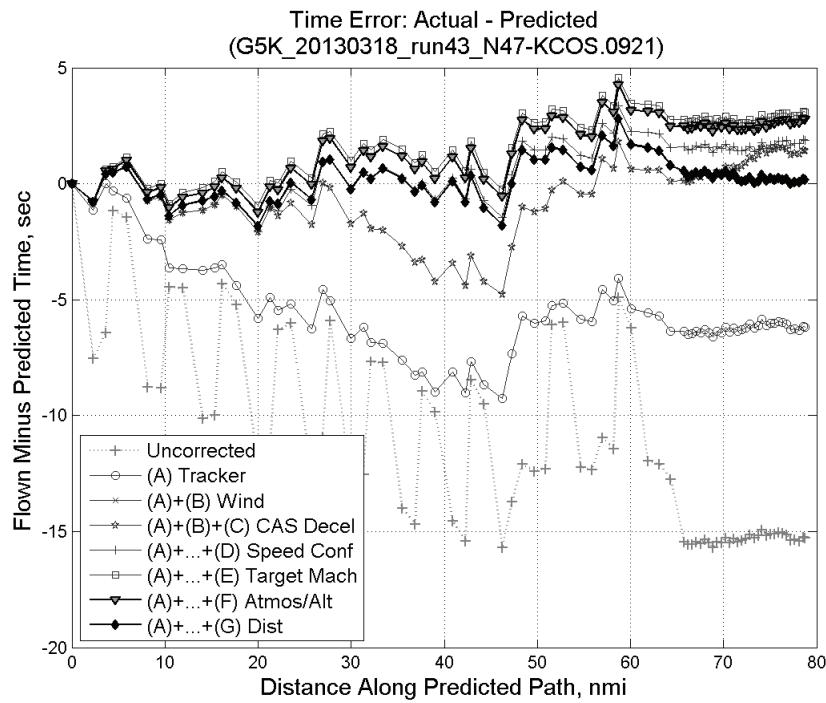


**Figure 818: Time error for run 43 showing incremental effect of removing each error source.**

#### C.31.A. Tracker Jumps

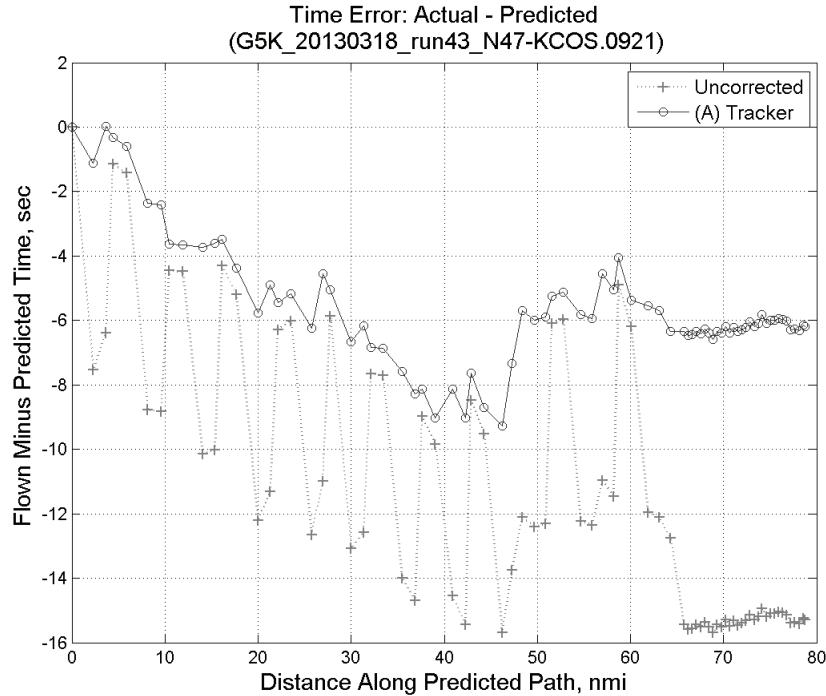


**Figure 819: Time error for run 43 before (Uncorrected) and after ((A) Tracker) removing tracker jump error source.**

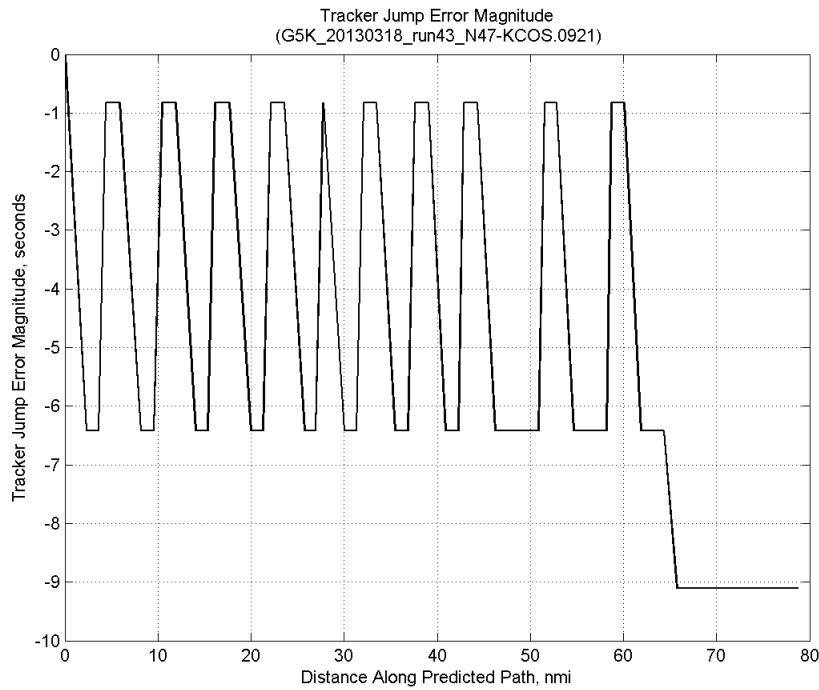


**Figure 820: Effect of tracker jump error source on time error for run 43.**

### C.31.B. Wind

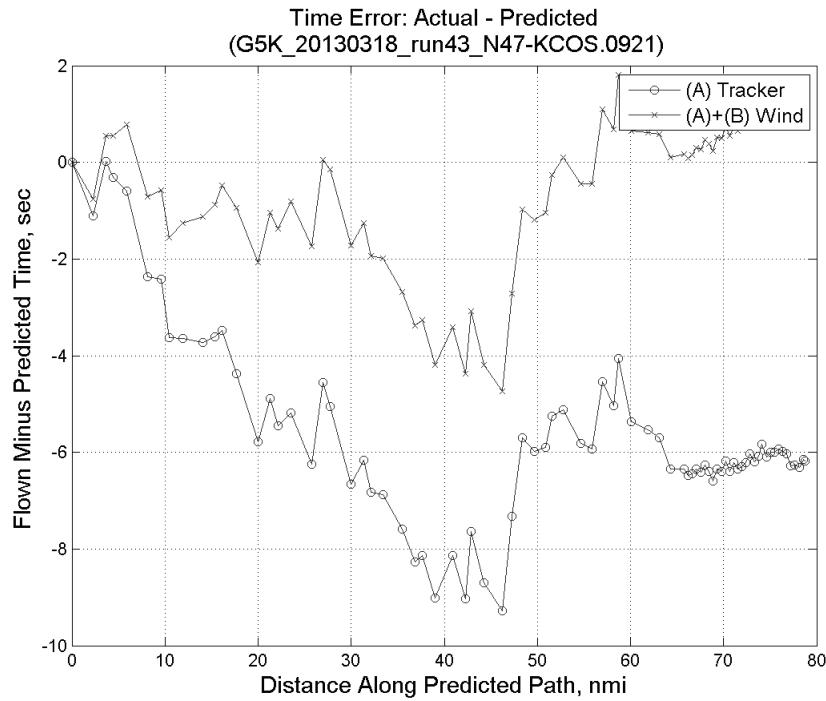


**Figure 821: Time error for run 43 before ((A) Tracker) and after ((A)+(B) Wind) removing wind error source.**

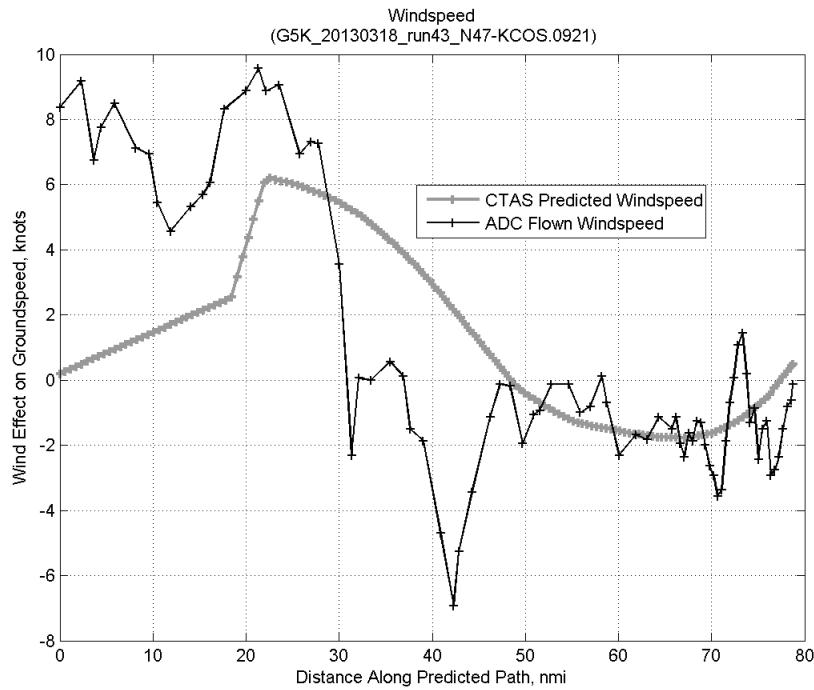


**Figure 822: CTAS predicted and ADC flown wind effect on ground speed for run 43. Negative values indicate a headwind.**

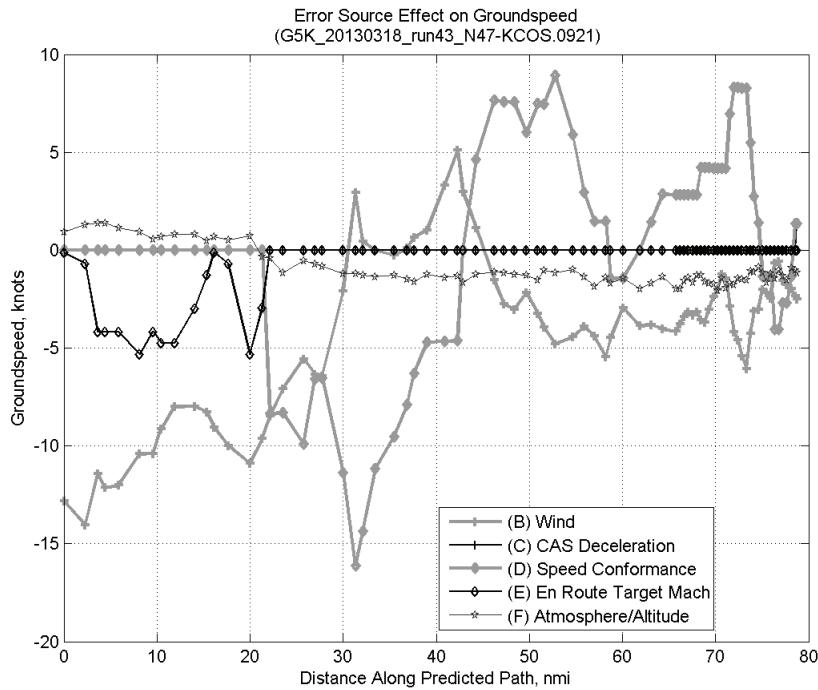


**Figure 823: Error sources (flown minus predicted) converted to a ground speed effect for run 43. Positive values indicate the flown ground speed was faster than the CTAS prediction.**

### C.31.C. CAS Deceleration

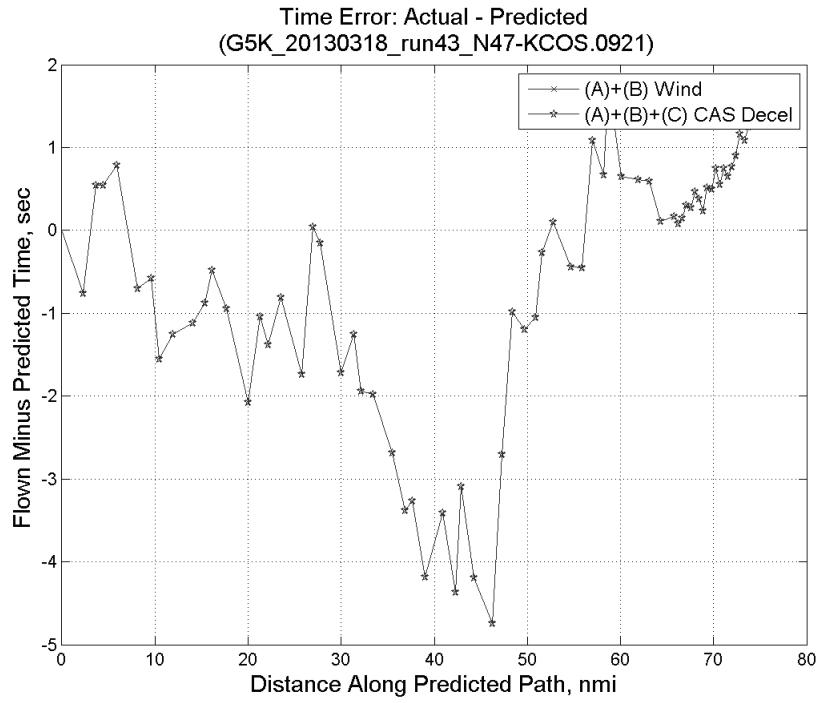


**Figure 824:** Time error for run 43 before ((A)+(B) Wind) and after ((A)+(B)+(C) CAS Decel) removing CAS deceleration error source.

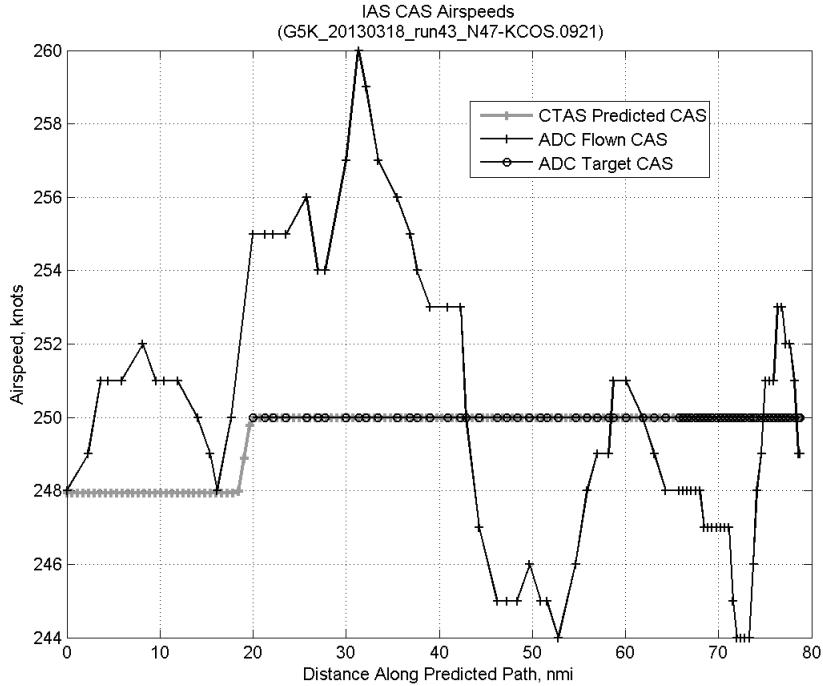


**Figure 825:** CTAS predicted and ADC flown CAS for run 43. CAS that is being targeted is shown with circle markers.

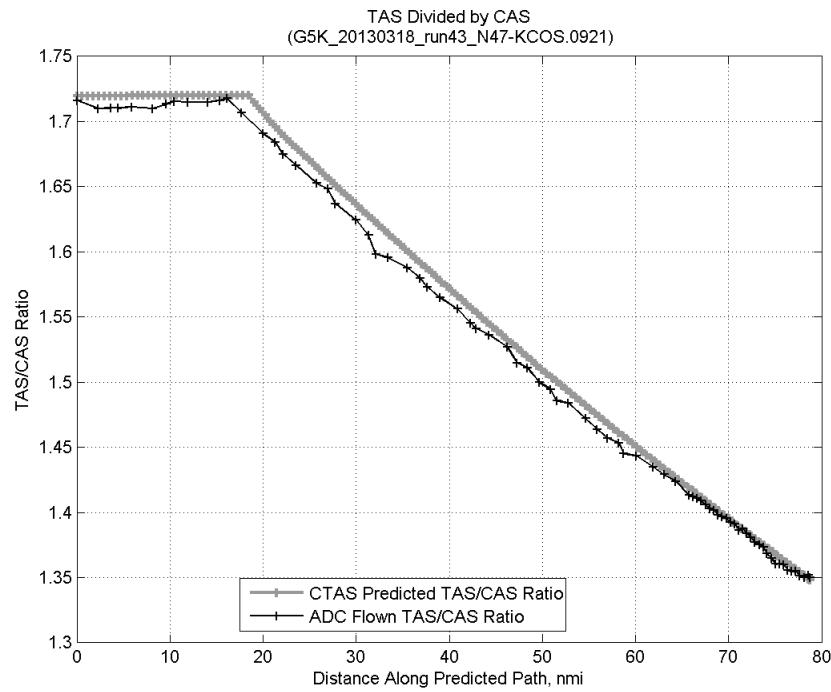


**Figure 826: CTAS predicted and ADC flown TAS/CAS ratio for run 43.**

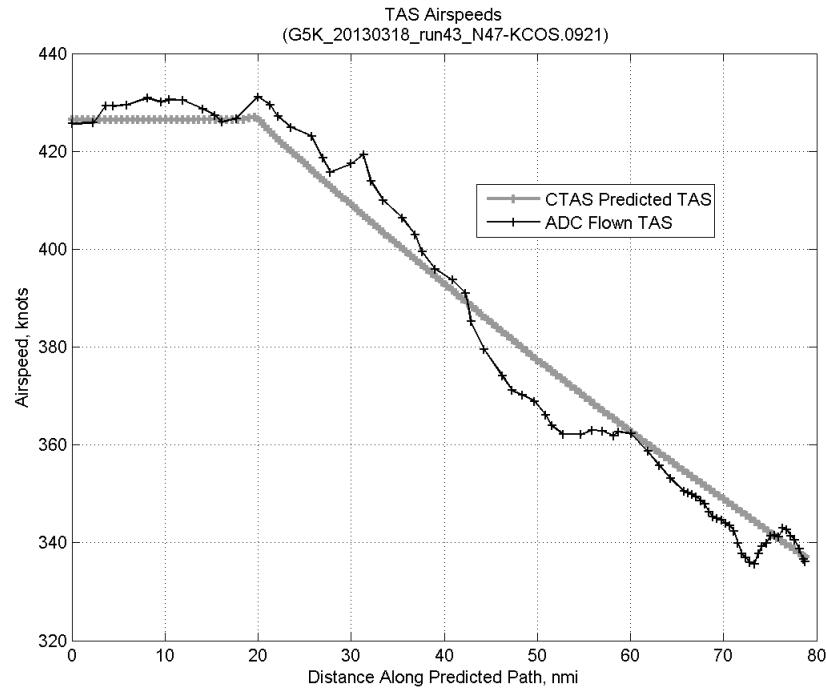


**Figure 827: CTAS predicted and ADC flown TAS for run 43.**

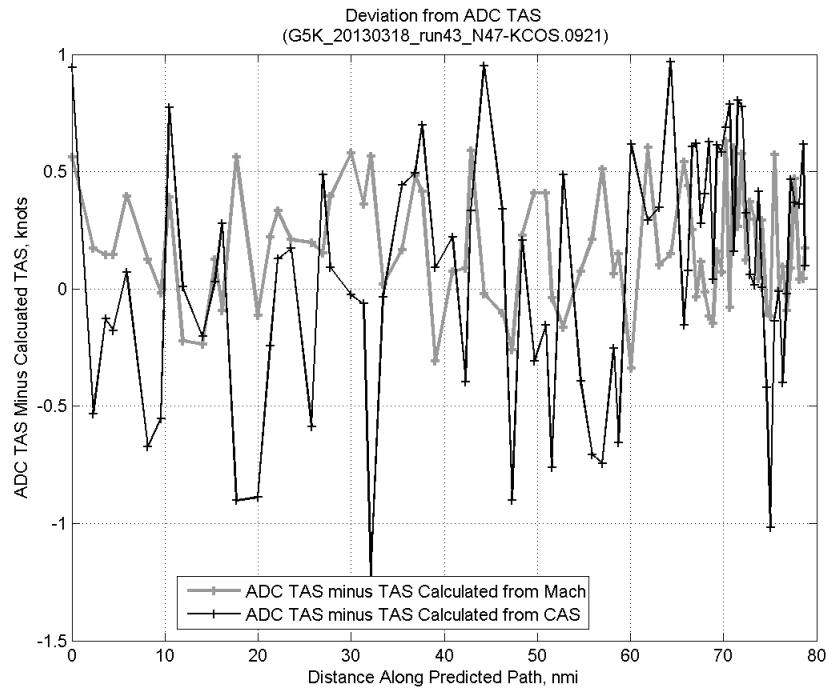


**Figure 828:** Deviation from ADC flown TAS if calculating TAS using ADC flown CAS, Mach, atmospheric temperature, and atmospheric pressure for run 43.

### C.31.D. Speed Conformance

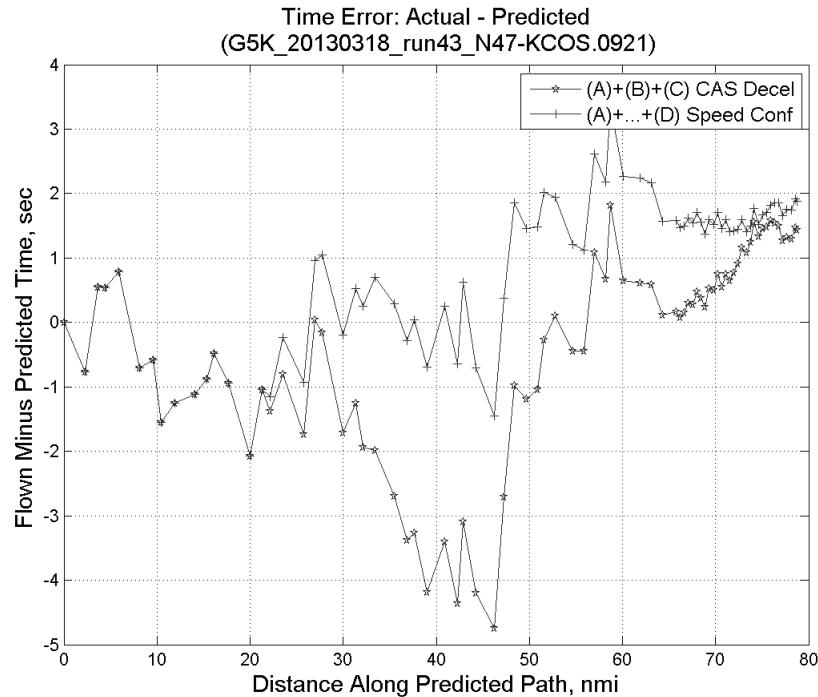


**Figure 829:** Time error for run 43 before  $((A)+(B)+(C) \text{ CAS Decel})$  and after  $((A)+\dots+(D) \text{ Speed Conf})$  removing speed conformance error source.

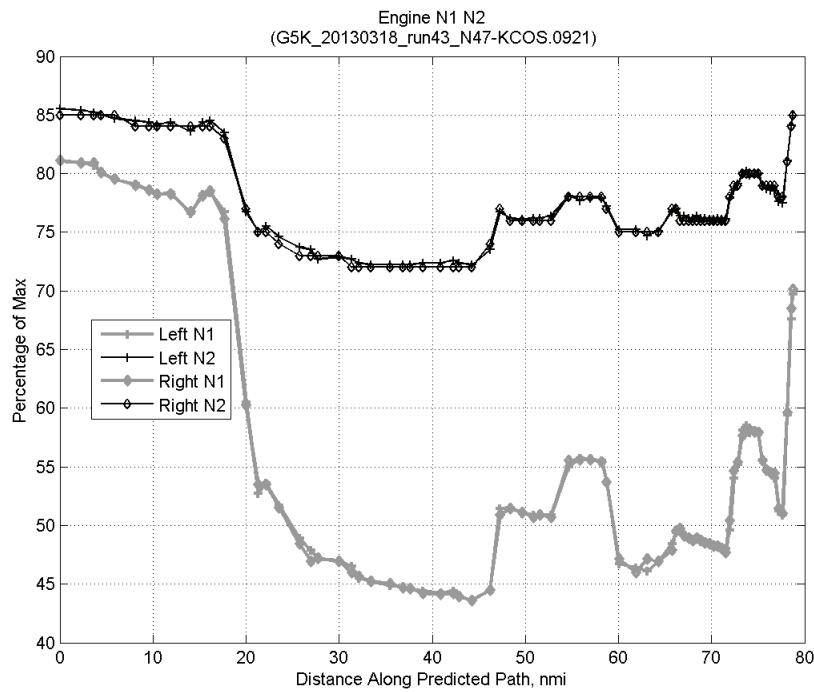


**Figure 830: Flown engine N1 and N2 for run 43.**

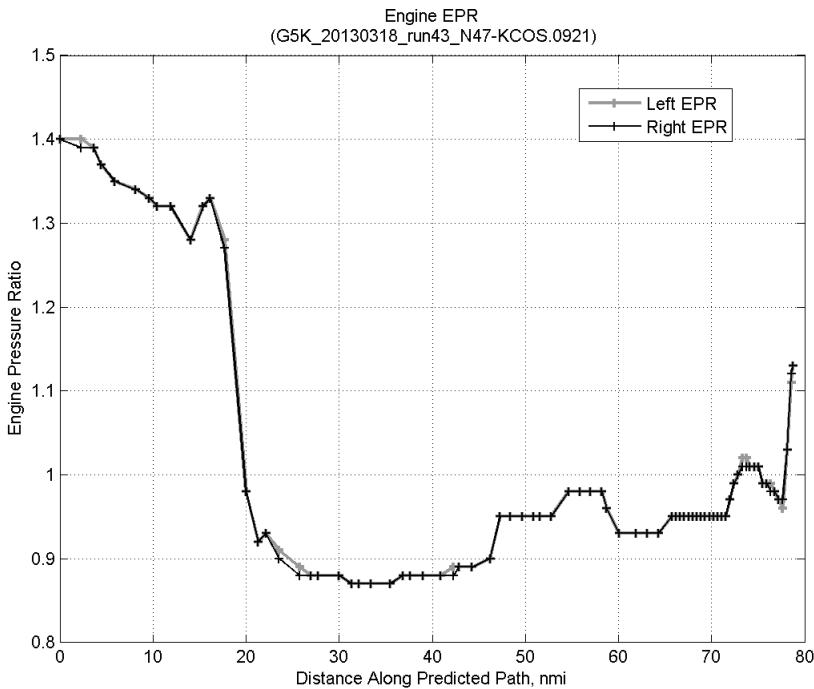


**Figure 831: Flown engine EPR for run 43.**

### C.31.E. Target Mach

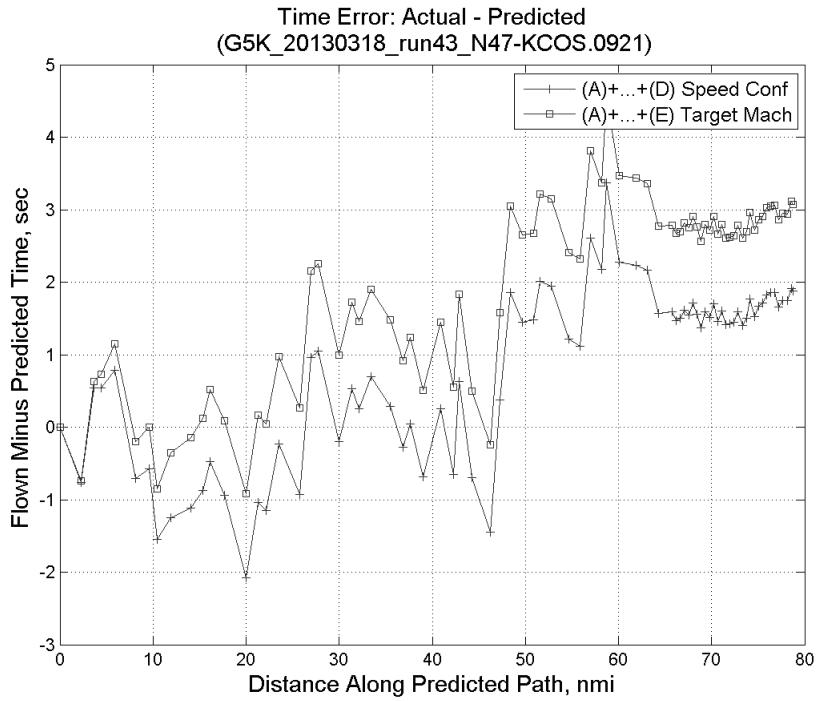


**Figure 832:** Time error for run 43 before ((A)+...+(D) Speed Conf) and after ((A)+...+(E) Target Mach) removing target Mach error source.

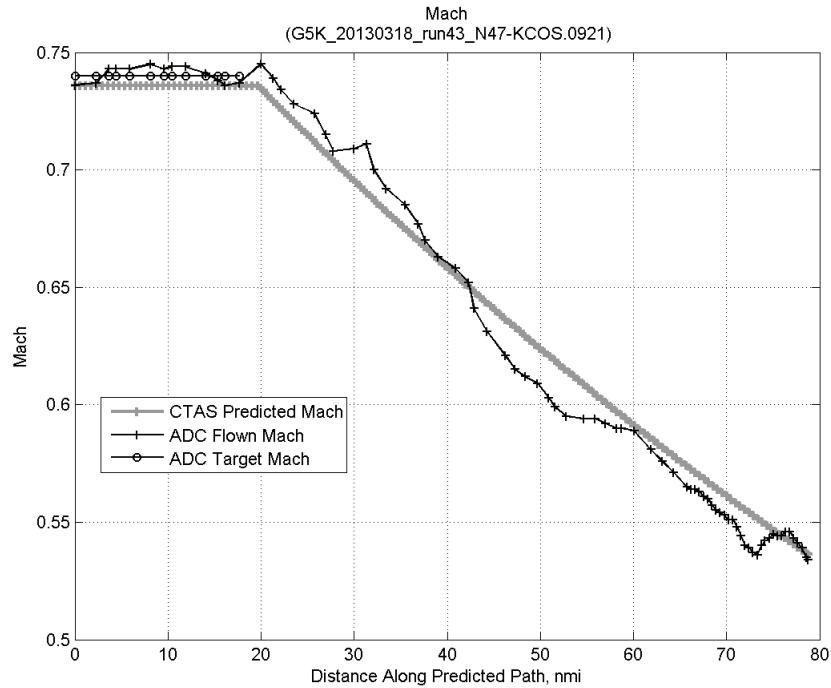


**Figure 833:** CTAS predicted and ADC flown Mach for run 43. Mach being targeted (ADC) shown with circle markers.

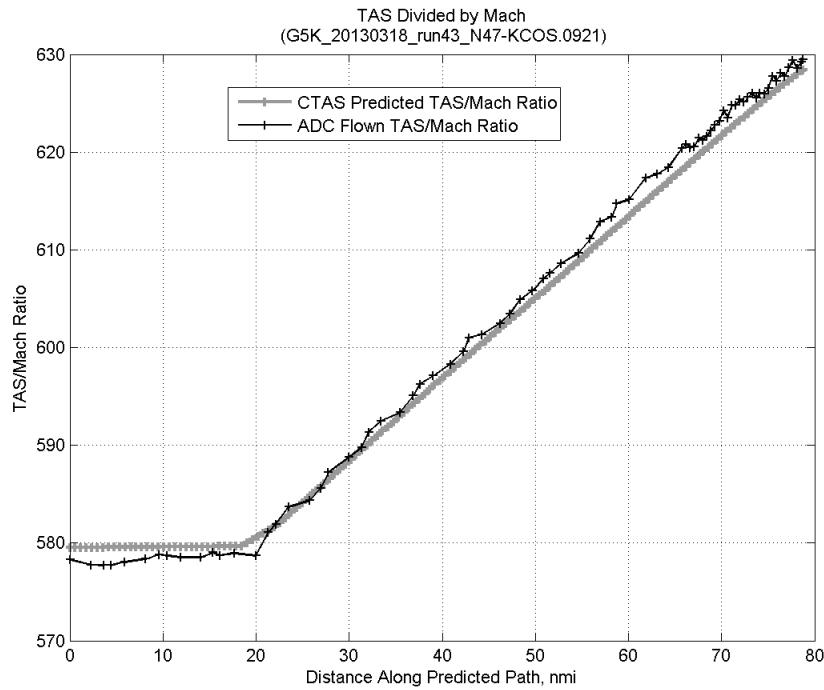


**Figure 834: CTAS predicted and ADC flown TAS/Mach ratio for run 43.**

### C.31.F. Atmosphere/Altitude

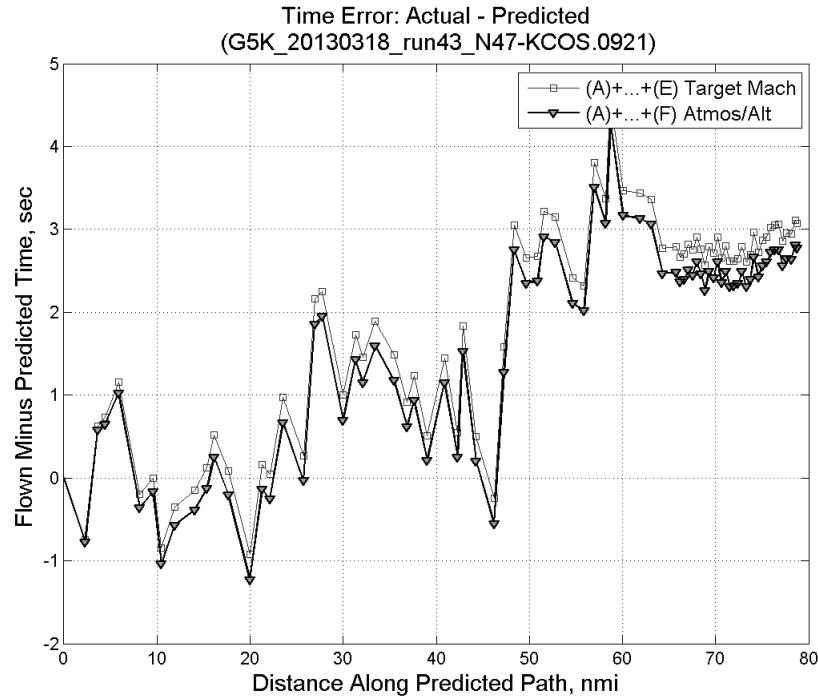


**Figure 835: Time error for run 43 before ((A)+...+(E) Target Mach) and after ((A)+...+(F) Atmos/Alt) removing atmosphere/altitude error source.**

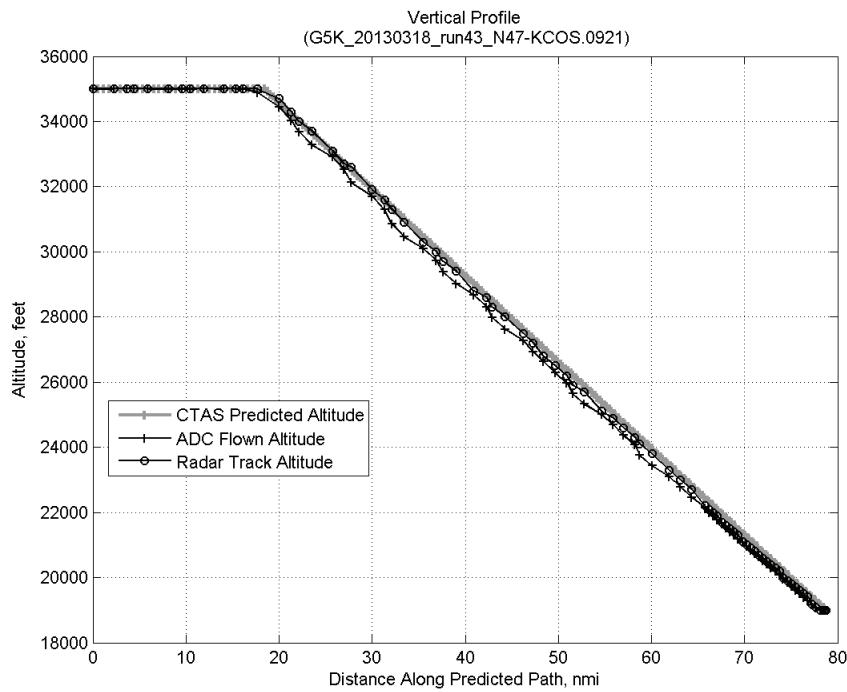


**Figure 836: Flown (ADC) and predicted (CTAS) vertical profile for run 43.**

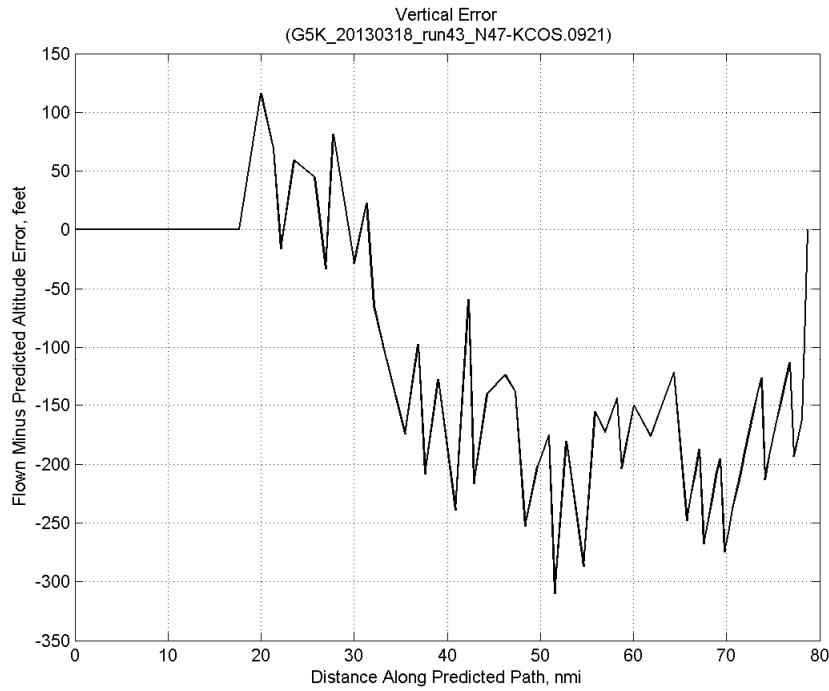


**Figure 837: Vertical error (flown minus predicted altitude) for run 43. Positive values indicate aircraft flew higher than predicted by CTAS.**

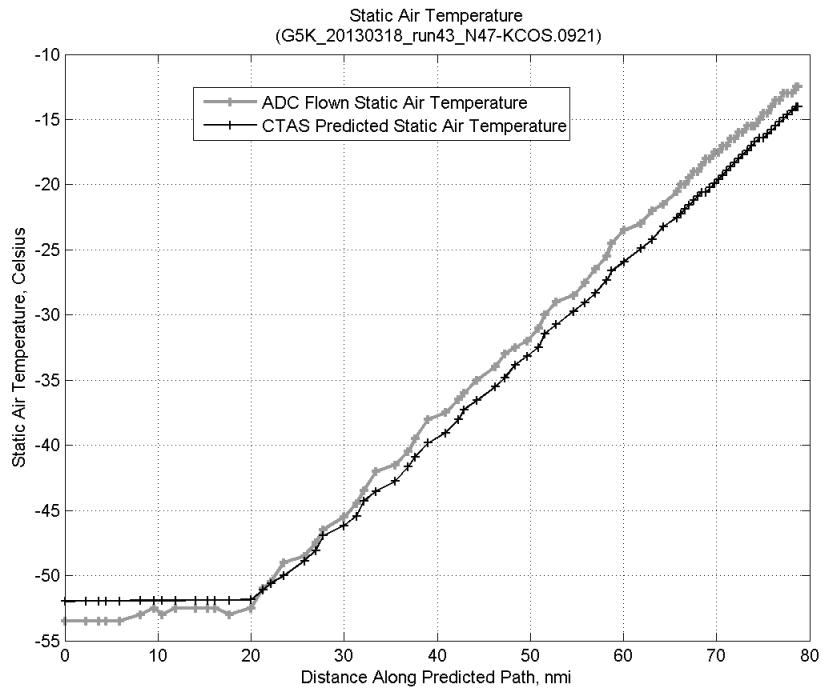


**Figure 838: Flown (ADC) and predicted (CTAS) static air temperature for run 43.**

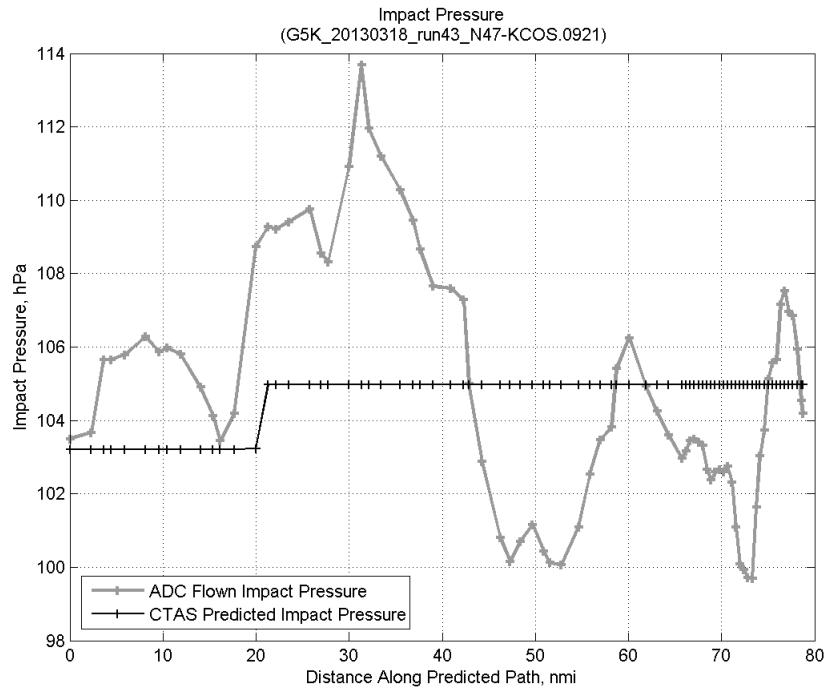


**Figure 839: Flown (ADC) and predicted (CTAS) impact pressure for run 43.**

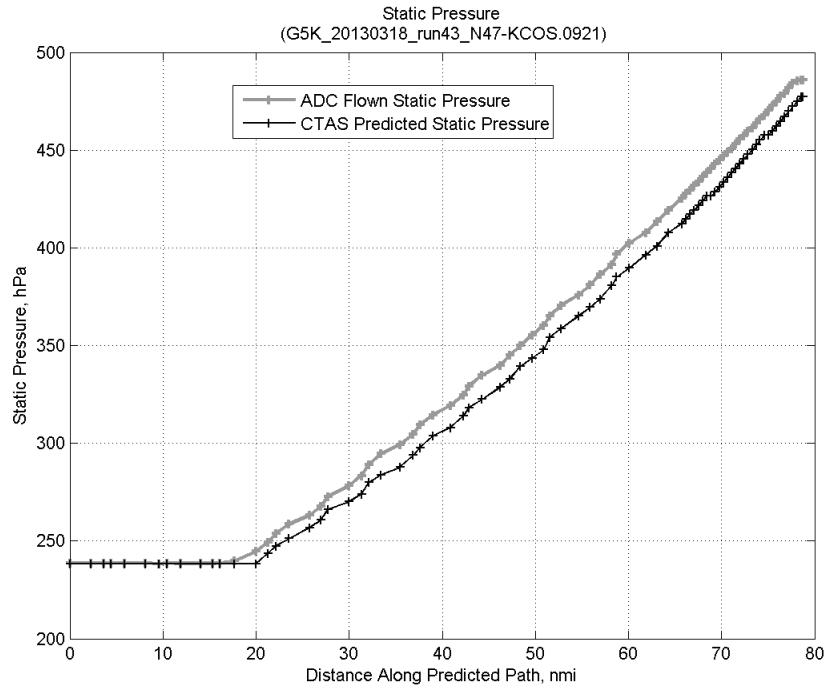


**Figure 840: Flown (ADC) and predicted (CTAS) static pressure for run 43.**

### C.31.G. Path Distance

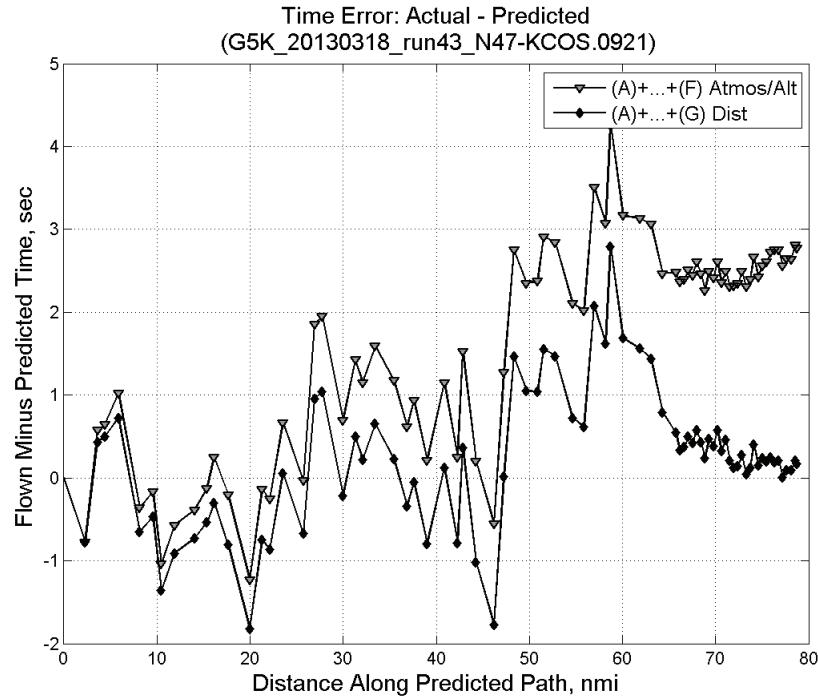


**Figure 841: Time error for run 43 before ((A)+...+(F) Atmos/Alt) and after ((A)+...+(G) Dist) removing path distance error source.**

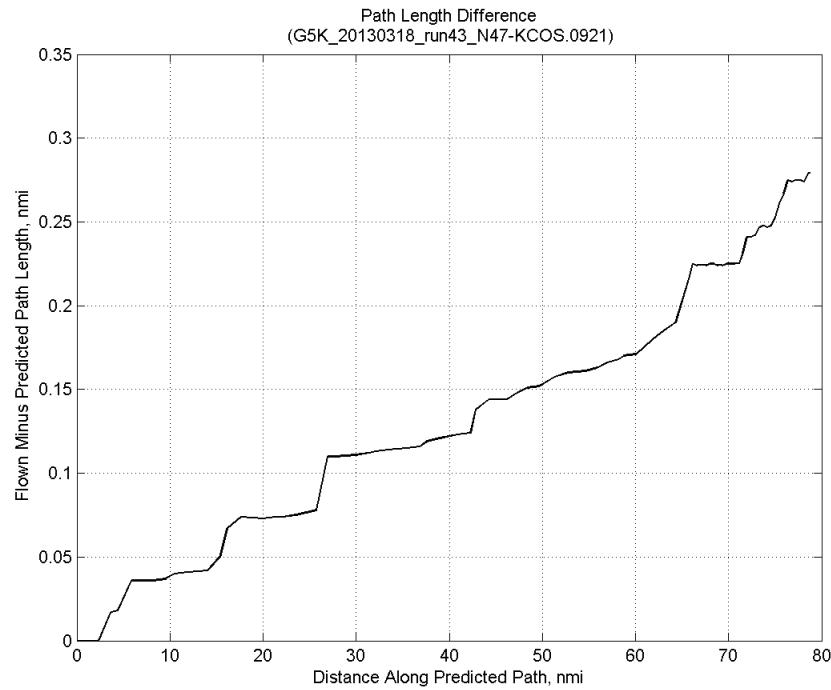


**Figure 842: ADC flown minus CTAS predicted path length for run 43. Positive values indicate aircraft followed a longer path than predicted by CTAS.**

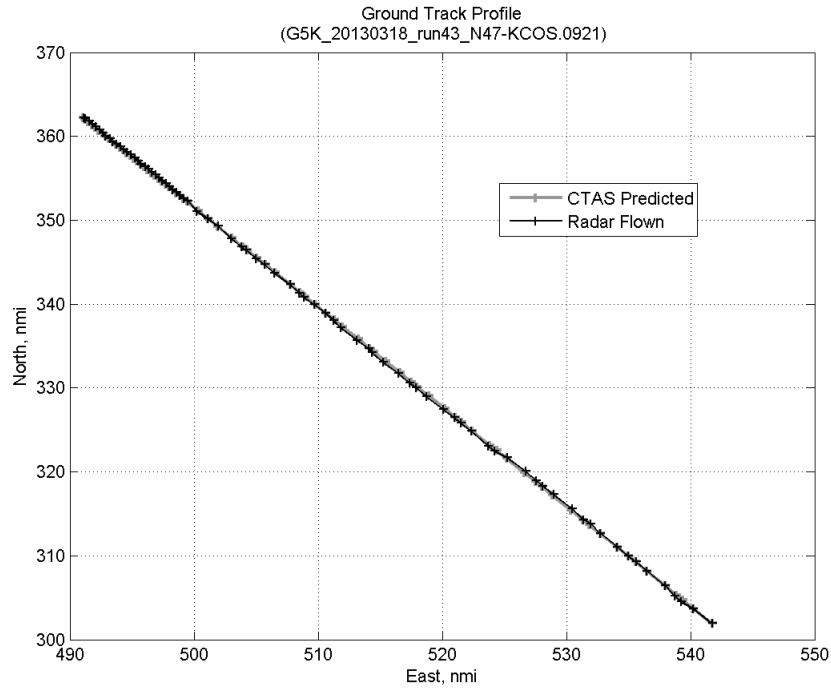


**Figure 843: CTAS predicted and radar flown ground track profile for run 43.**

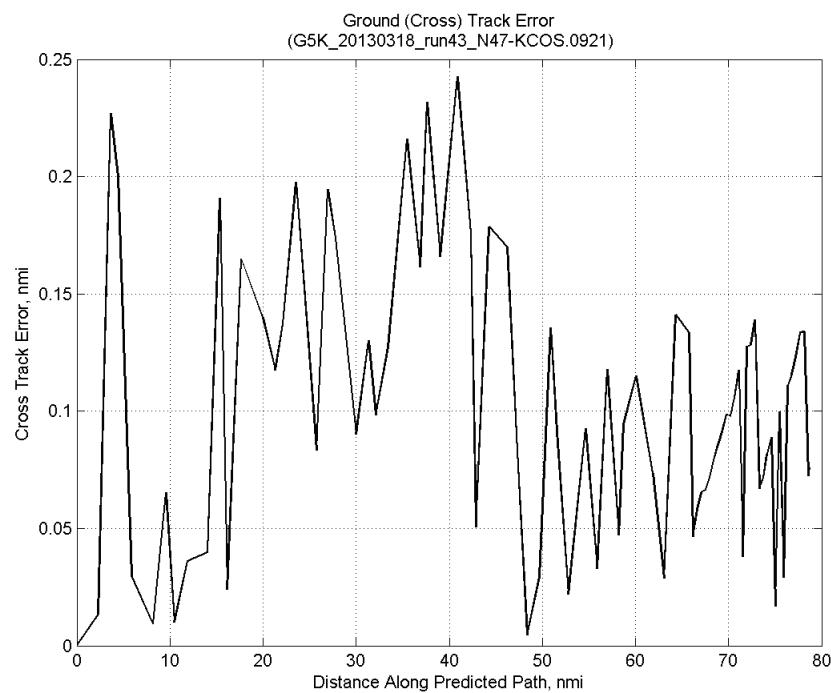


**Figure 844: Ground (cross) track error for run 43.**

### C.32. Run 44

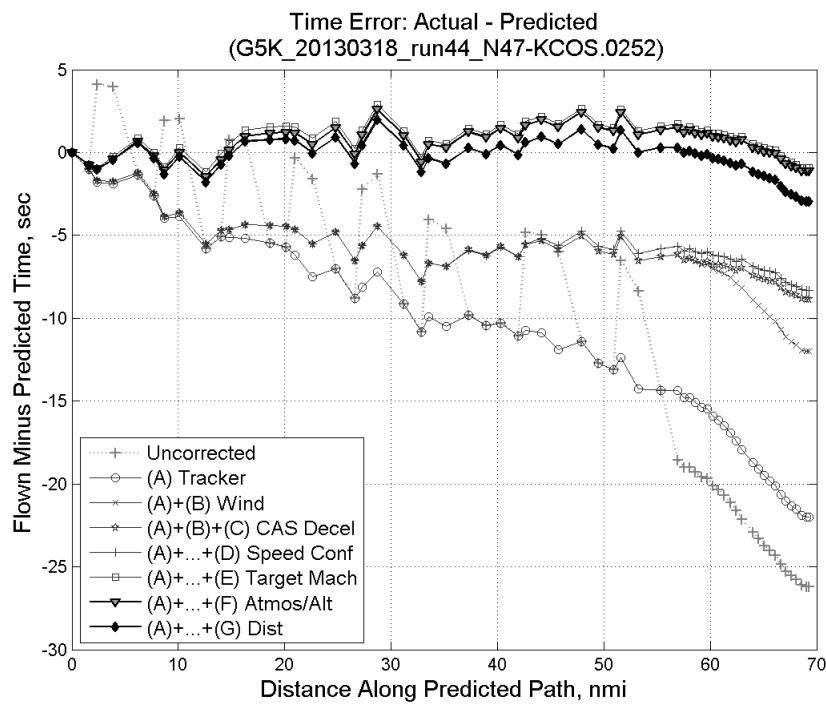


**Figure 845:** Time error for run 44 showing incremental effect of removing each error source.

#### C.32.A. Tracker Jumps

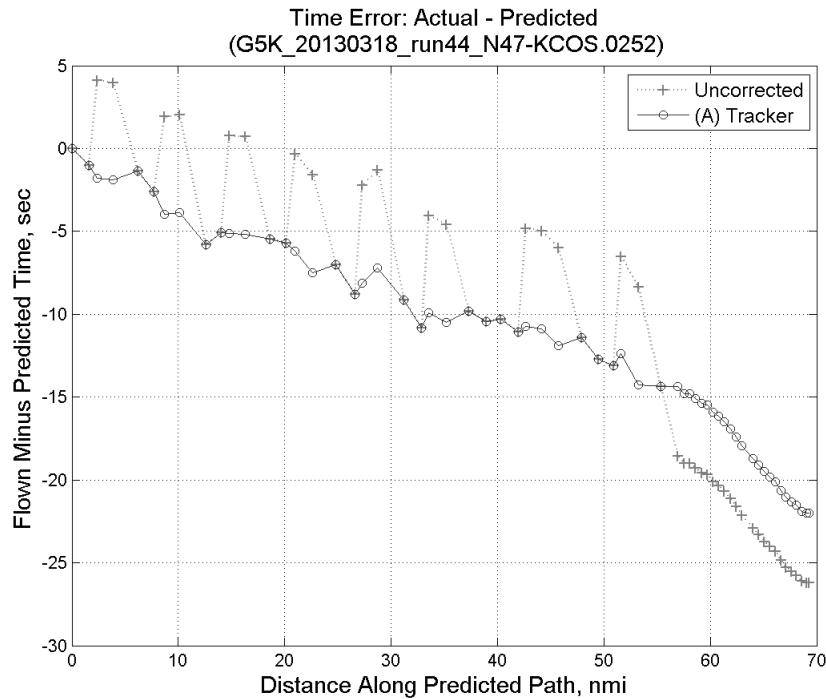


**Figure 846:** Time error for run 44 before (Uncorrected) and after ((A) Tracker) removing tracker jump error source.

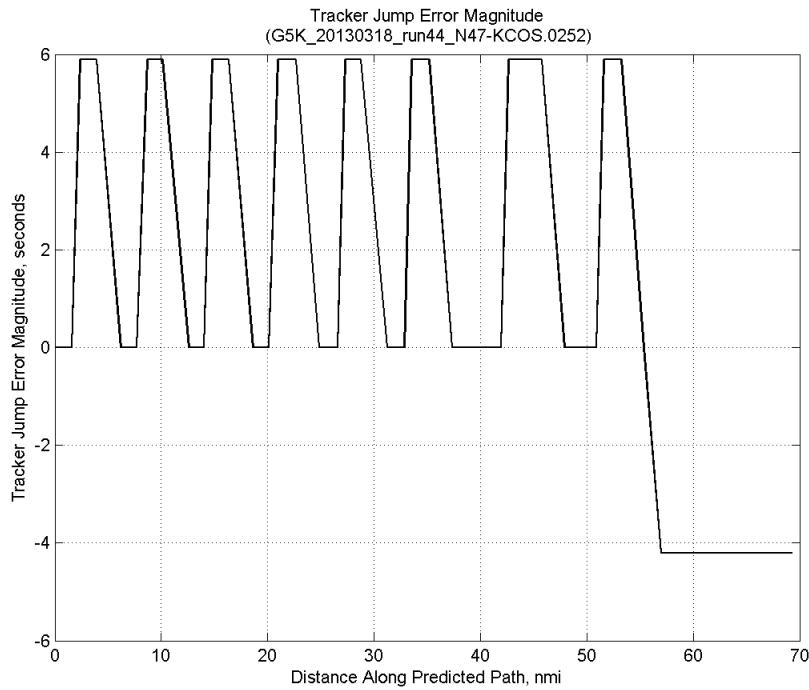


**Figure 847: Effect of tracker jump error source on time error for run 44.**

### C.32.B. Wind

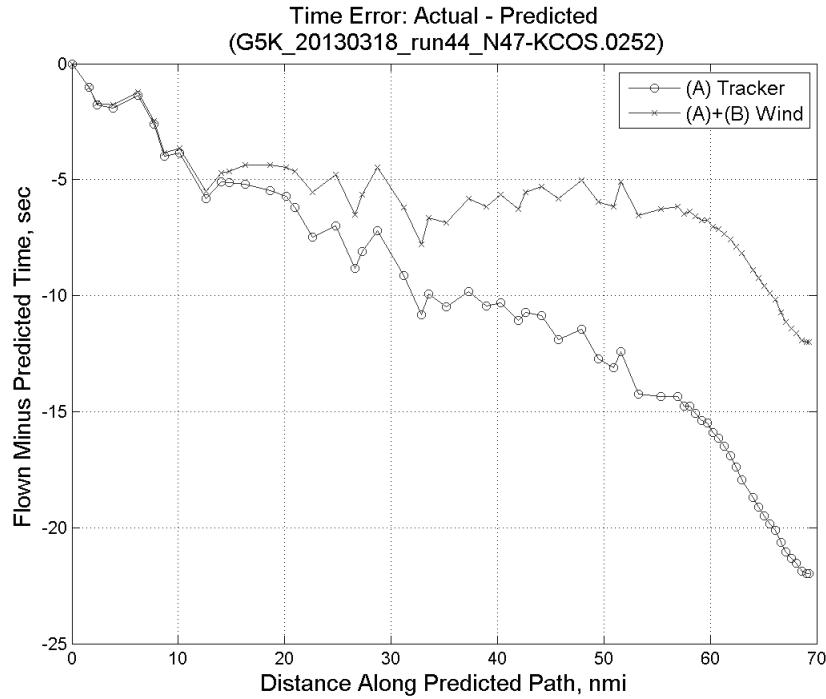


**Figure 848: Time error for run 44 before ((A) Tracker) and after ((A)+(B) Wind) removing wind error source.**

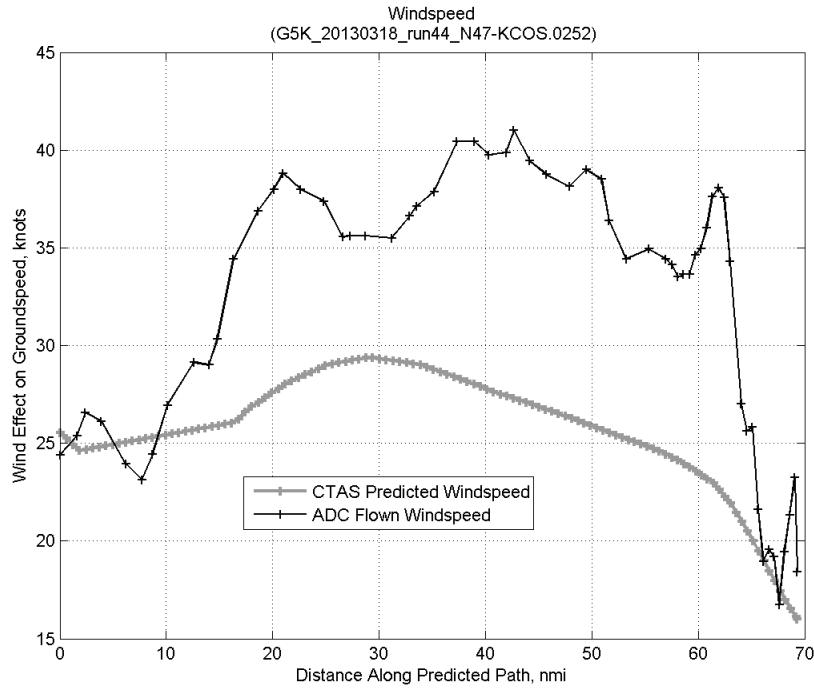


**Figure 849: CTAS predicted and ADC flown wind effect on ground speed for run 44. Negative values indicate a headwind.**

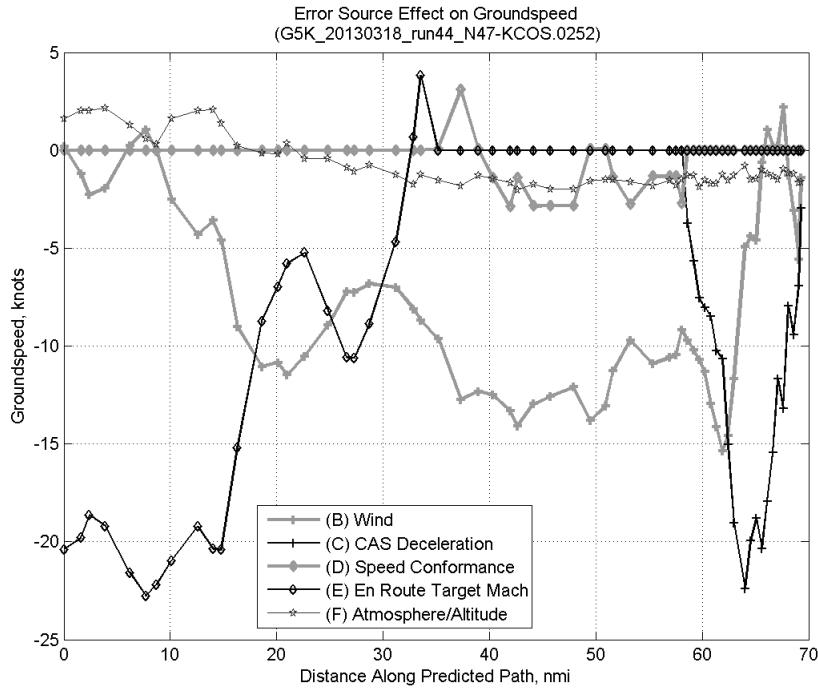


**Figure 850: Error sources (flown minus predicted) converted to a ground speed effect for run 44. Positive values indicate the flown ground speed was faster than the CTAS prediction.**

### C.32.C. CAS Deceleration

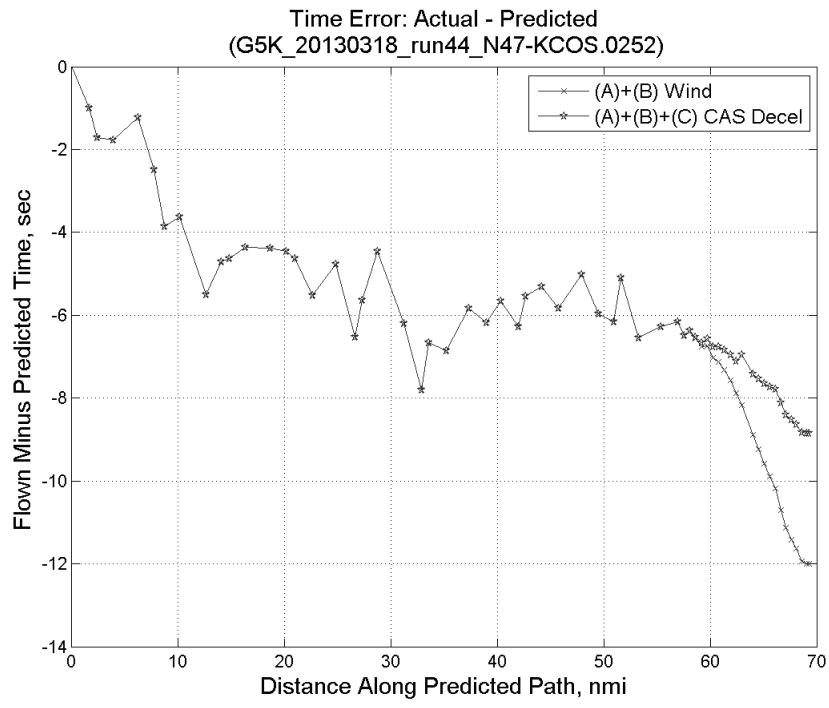


**Figure 851:** Time error for run 44 before ((A)+(B) Wind) and after ((A)+(B)+(C) CAS Decel) removing CAS deceleration error source.

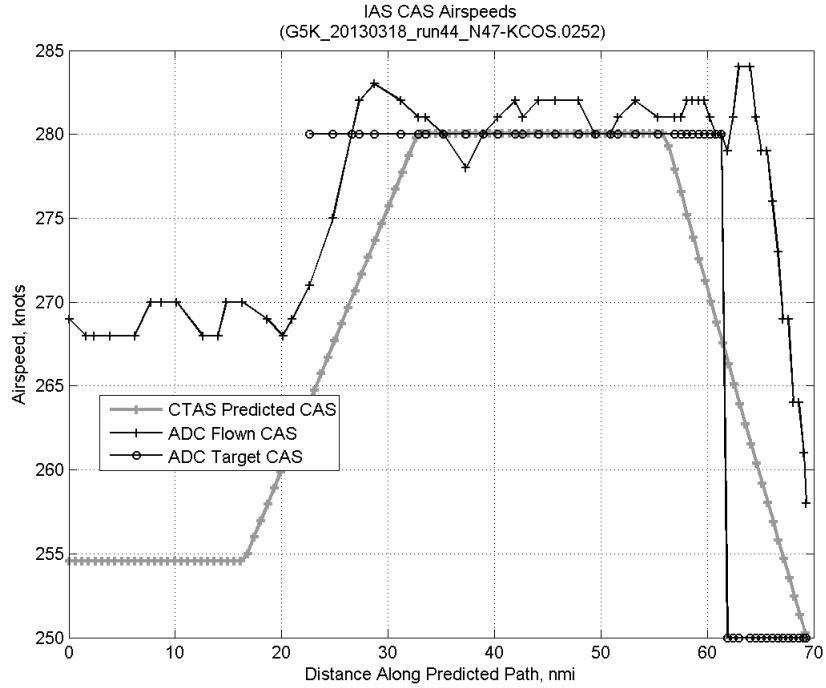


**Figure 852:** CTAS predicted and ADC flown CAS for run 44. CAS that is being targeted is shown with circle markers.

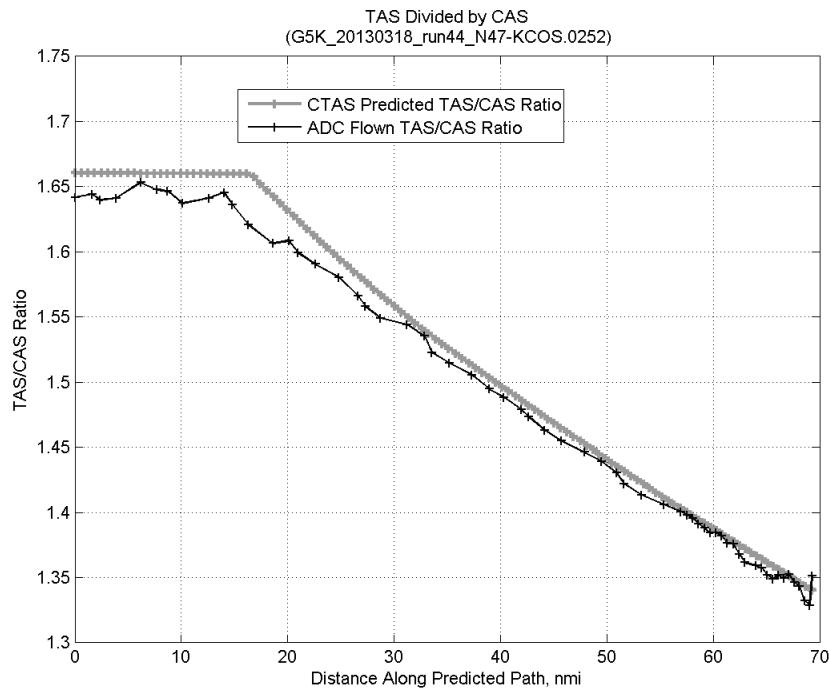


**Figure 853: CTAS predicted and ADC flown TAS/CAS ratio for run 44.**

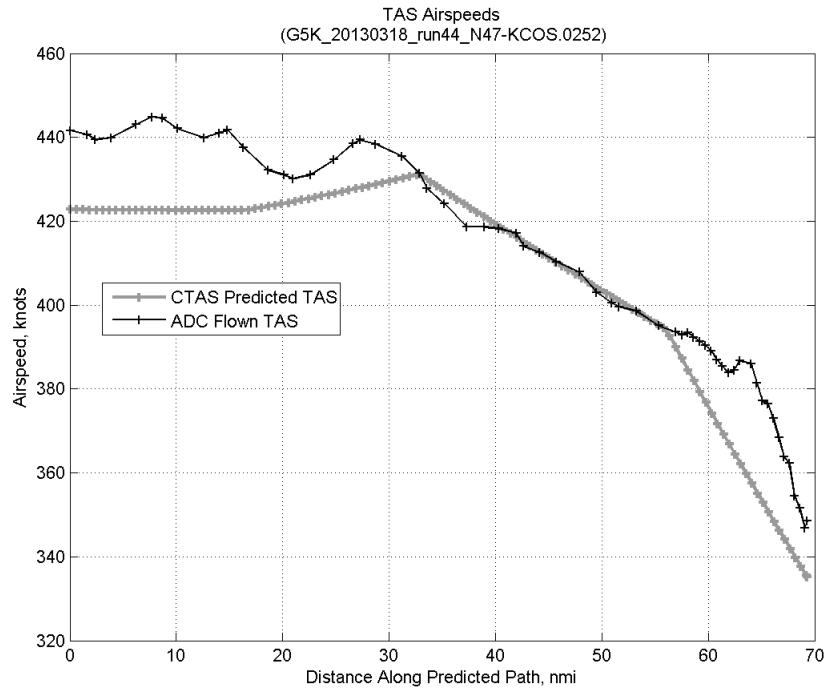


**Figure 854: CTAS predicted and ADC flown TAS for run 44.**

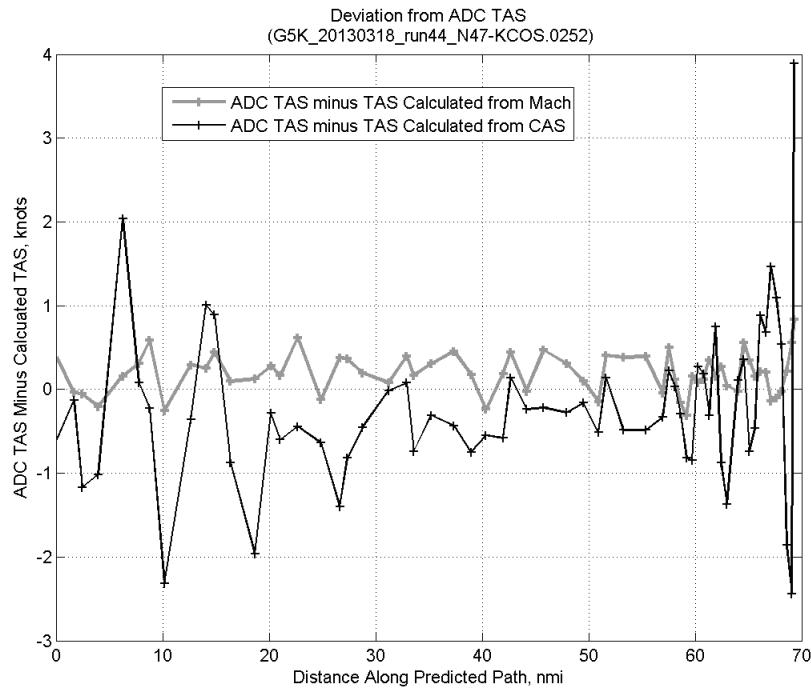


**Figure 855:** Deviation from ADC flown TAS if calculating TAS using ADC flown CAS, Mach, atmospheric temperature, and atmospheric pressure for run 44.

### C.32.D. Speed Conformance

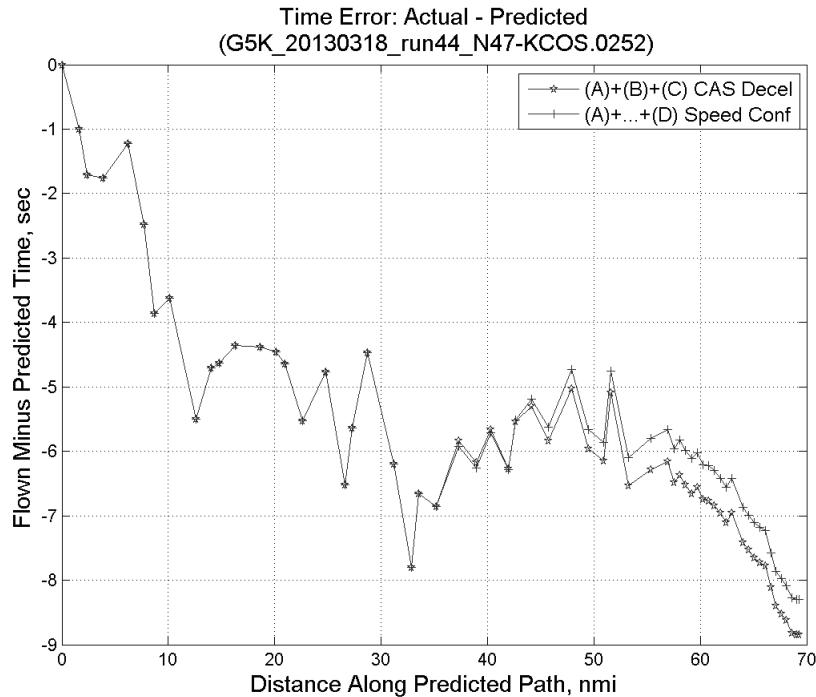


**Figure 856:** Time error for run 44 before ((A)+(B)+(C) CAS Decel) and after ((A)+...+(D) Speed Conf) removing speed conformance error source.

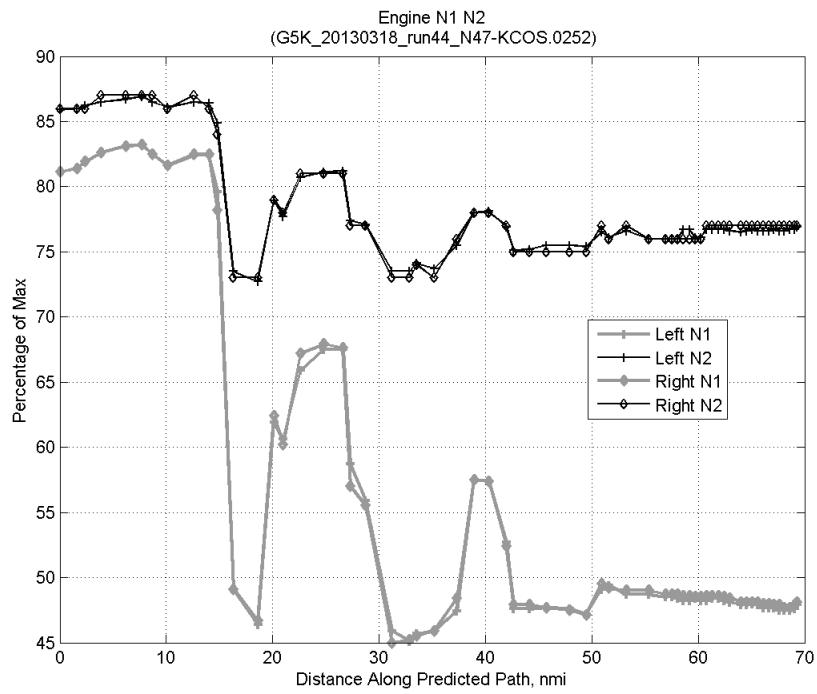


**Figure 857: Flown engine N1 and N2 for run 44.**

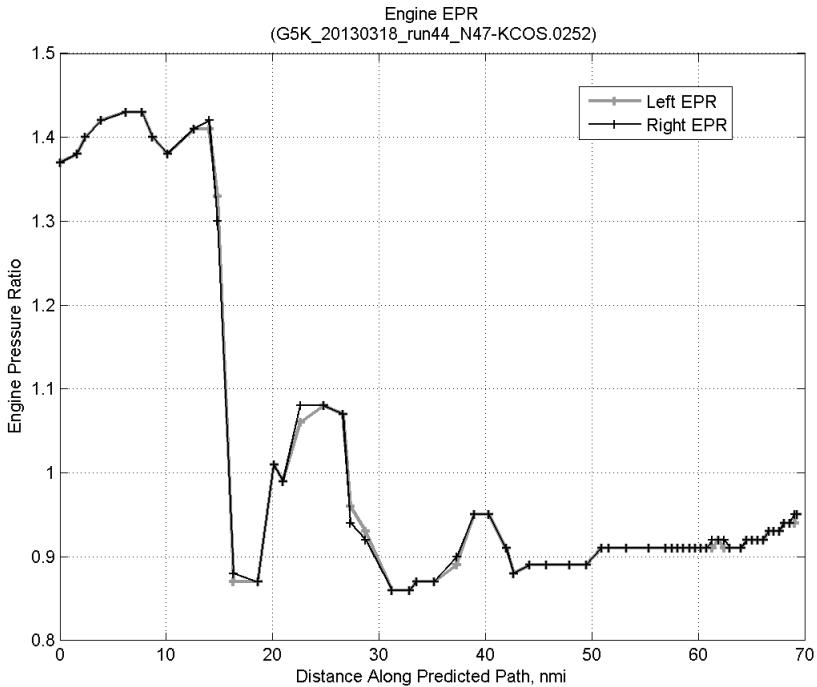


**Figure 858: Flown engine EPR for run 44.**

### C.32.E. Target Mach

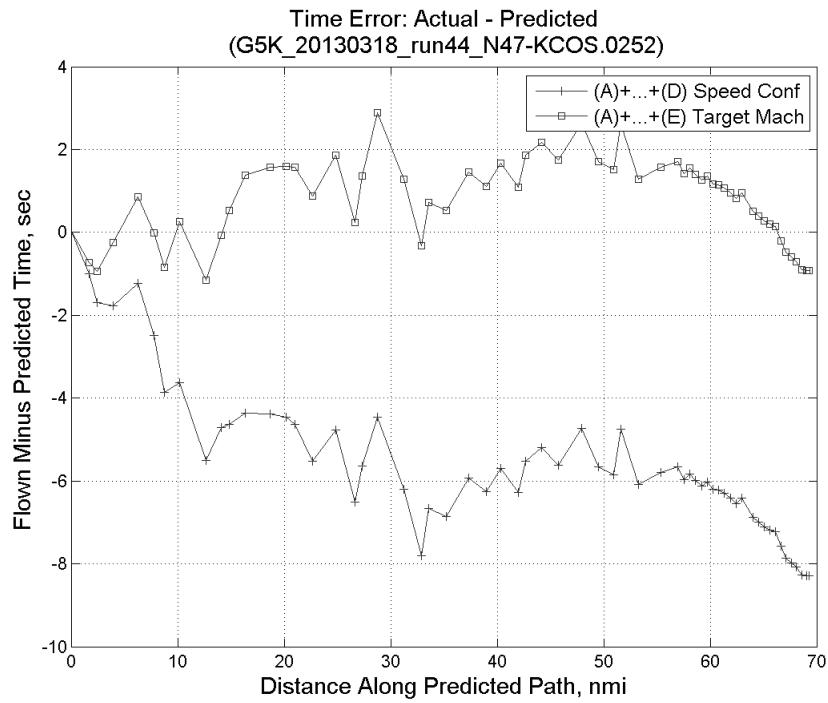


**Figure 859:** Time error for run 44 before ((A)+...+(D) Speed Conf) and after ((A)+...+(E) Target Mach) removing target Mach error source.

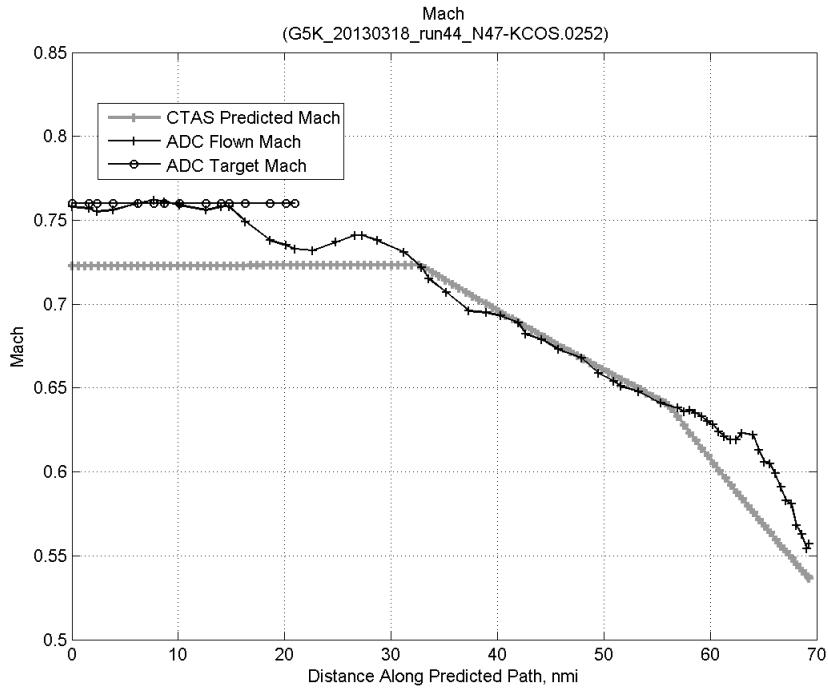


**Figure 860:** CTAS predicted and ADC flown Mach for run 44. Mach being targeted (ADC) shown with circle markers.

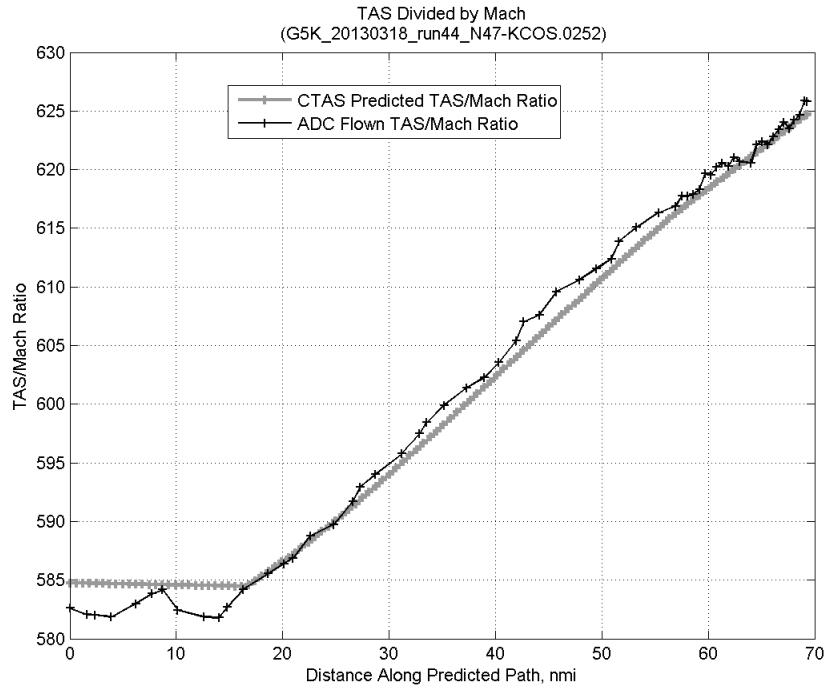


**Figure 861:** CTAS predicted and ADC flown TAS/Mach ratio for run 44.

### C.32.F. Atmosphere/Altitude

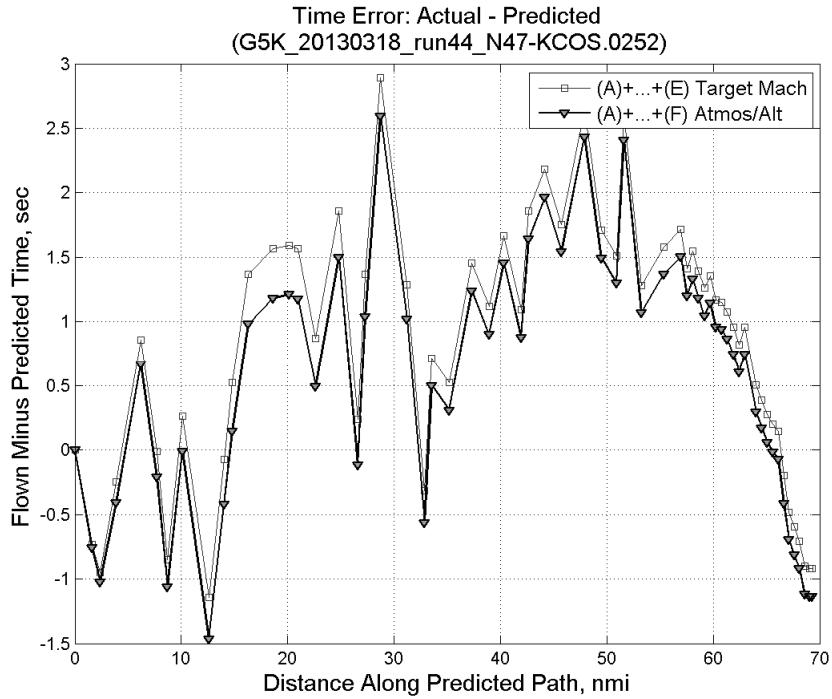


**Figure 862:** Time error for run 44 before ((A)+...+(E) Target Mach) and after ((A)+...+(F) Atmos/Alt) removing atmosphere/altitude error source.

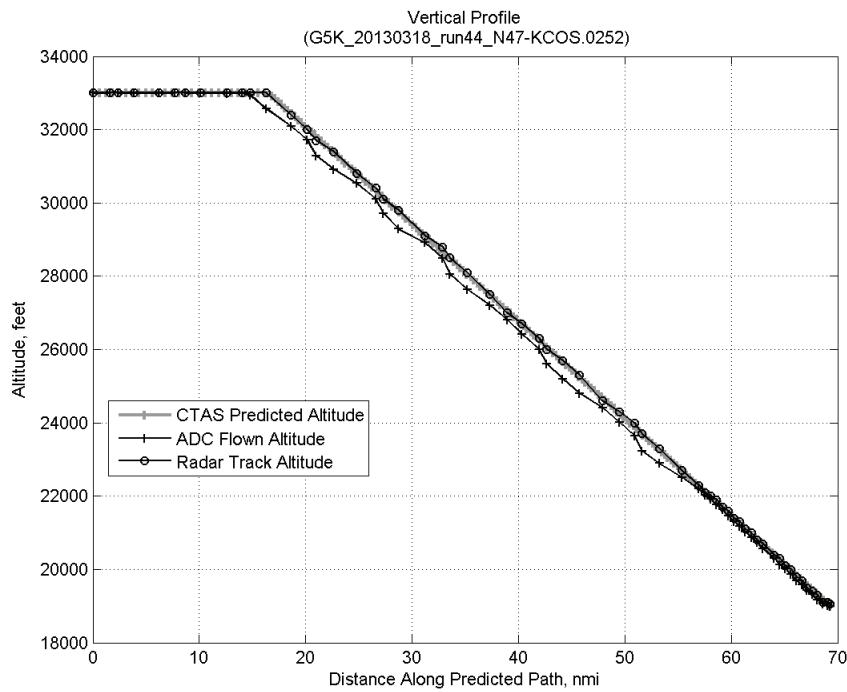


**Figure 863: Flown (ADC) and predicted (CTAS) vertical profile for run 44.**

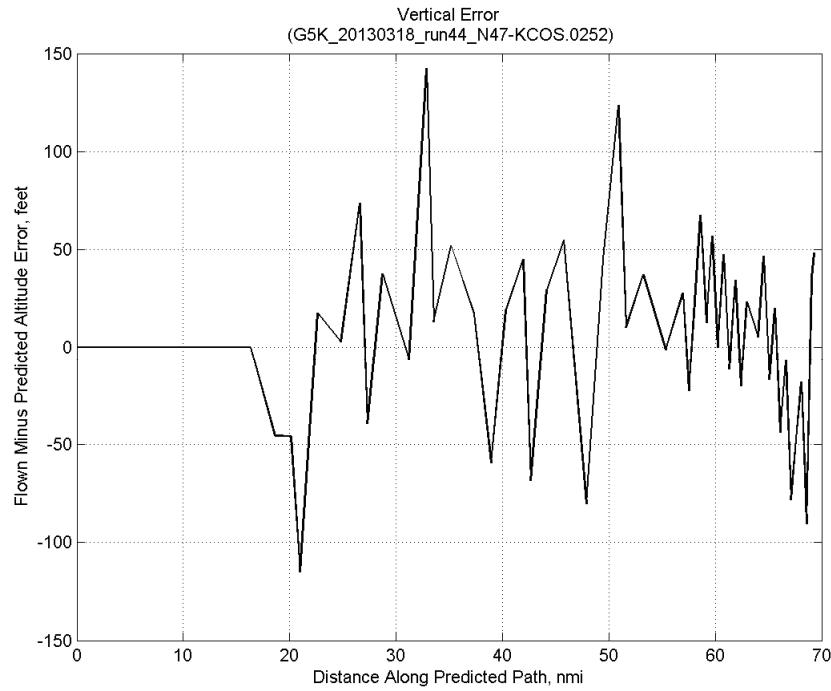


**Figure 864: Vertical error (flown minus predicted altitude) for run 44. Positive values indicate aircraft flew higher than predicted by CTAS.**

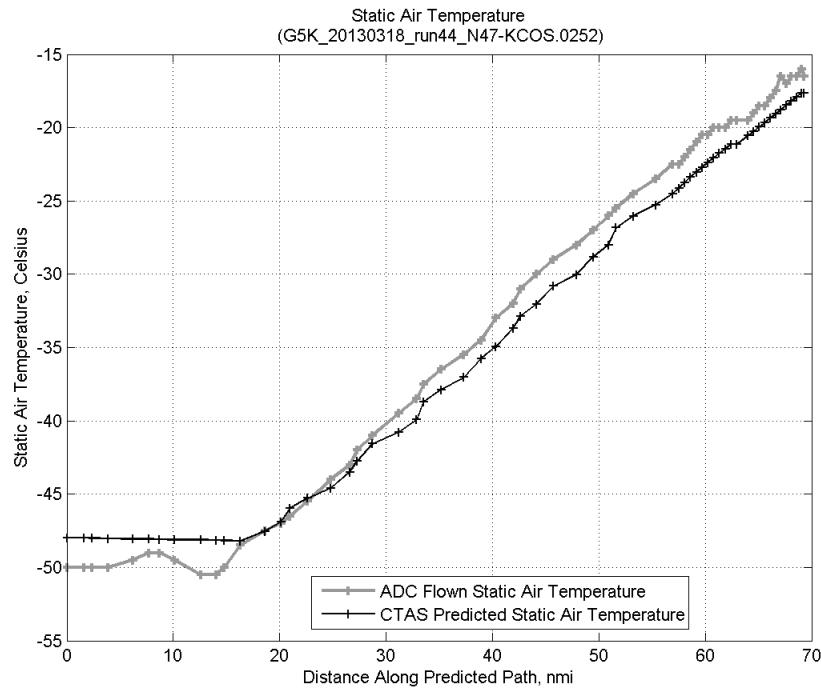


**Figure 865: Flown (ADC) and predicted (CTAS) static air temperature for run 44.**

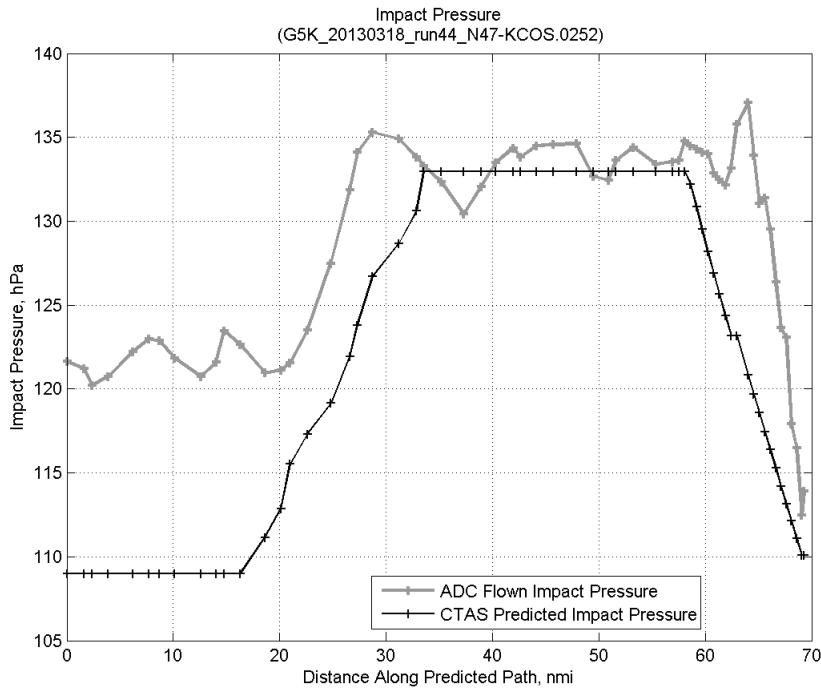


**Figure 866: Flown (ADC) and predicted (CTAS) impact pressure for run 44.**

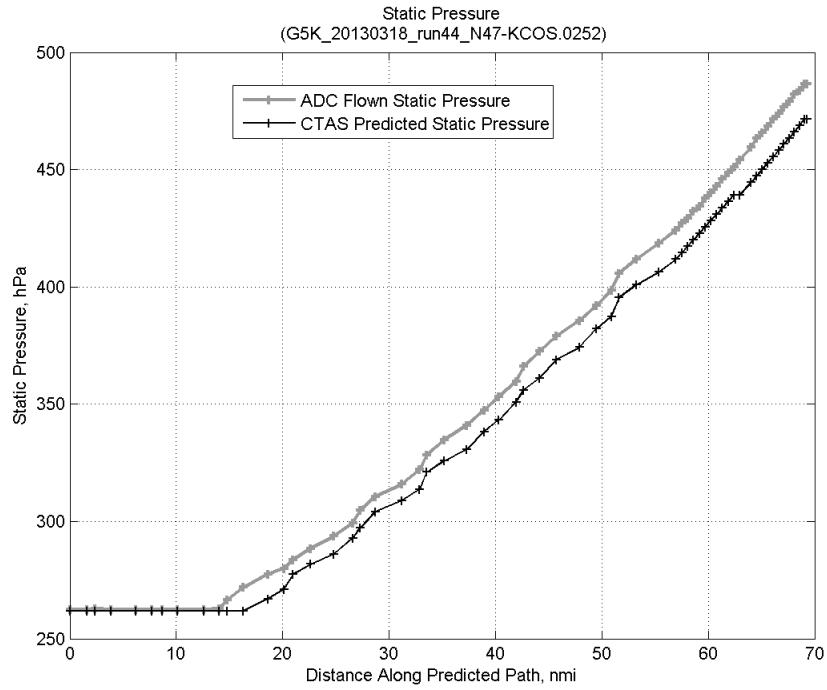


**Figure 867: Flown (ADC) and predicted (CTAS) static pressure for run 44.**

### C.32.G. Path Distance

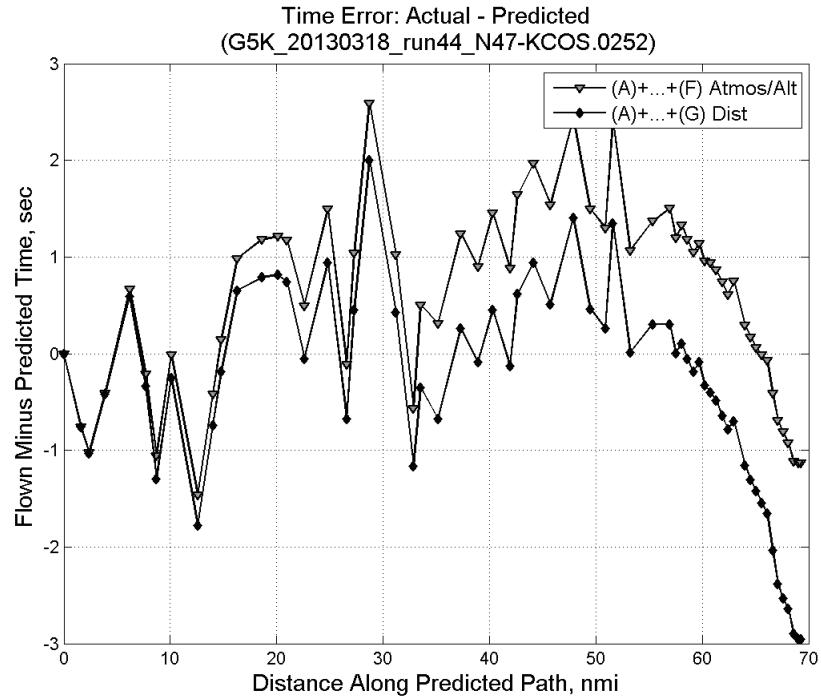


**Figure 868: Time error for run 44 before ((A)+...+(F) Atmos/Alt) and after ((A)+...+(G) Dist) removing path distance error source.**

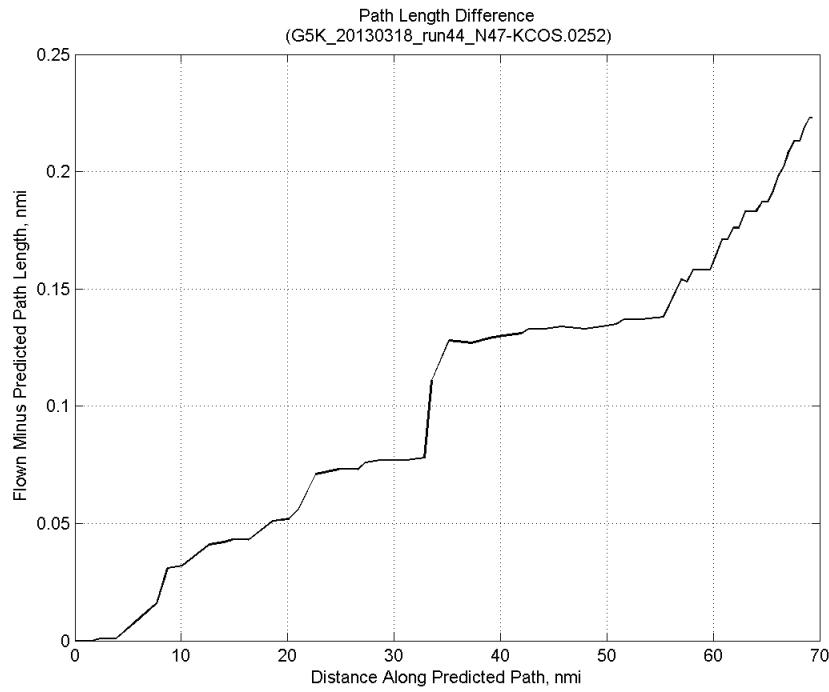


**Figure 869: ADC flown minus CTAS predicted path length for run 44. Positive values indicate aircraft followed a longer path than predicted by CTAS.**

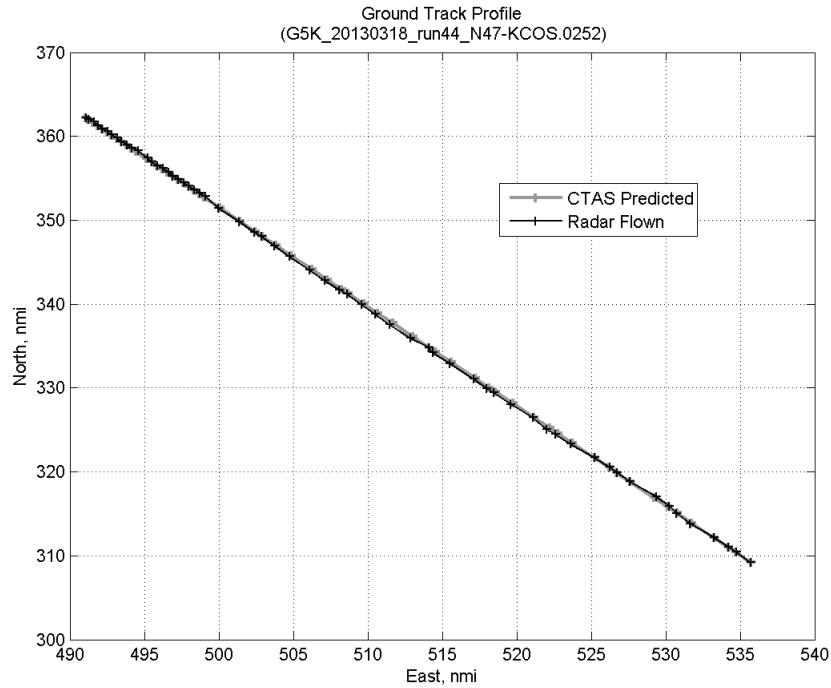


**Figure 870: CTAS predicted and radar flown ground track profile for run 44.**

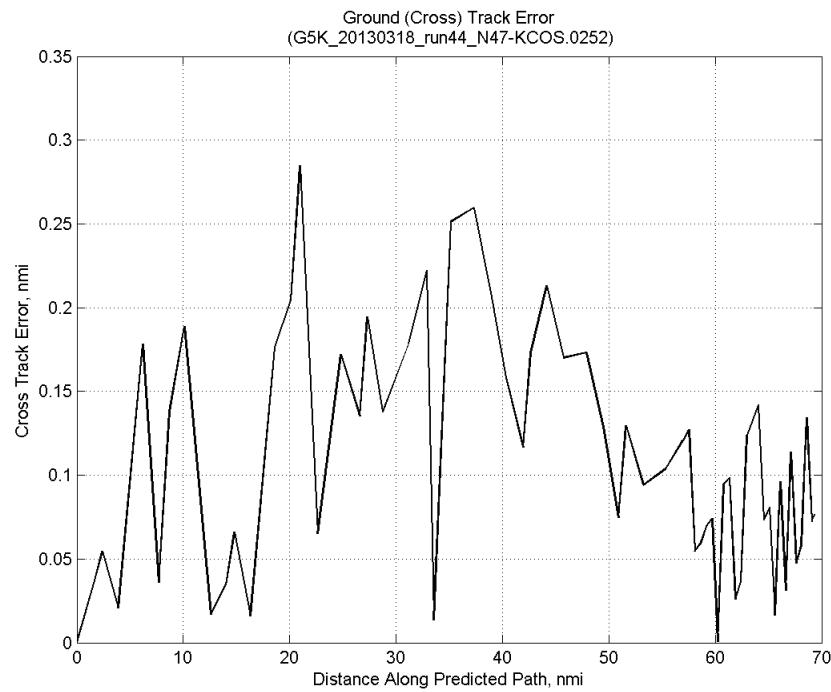


**Figure 871: Ground (cross) track error for run 44.**

## **Appendix D: Run-by-Run Results for Path-Stretch Runs**

This appendix includes plots for the runs with path-stretch clearances. A description of these plots is included at the beginning of Appendix C.

## D.1. Run 6

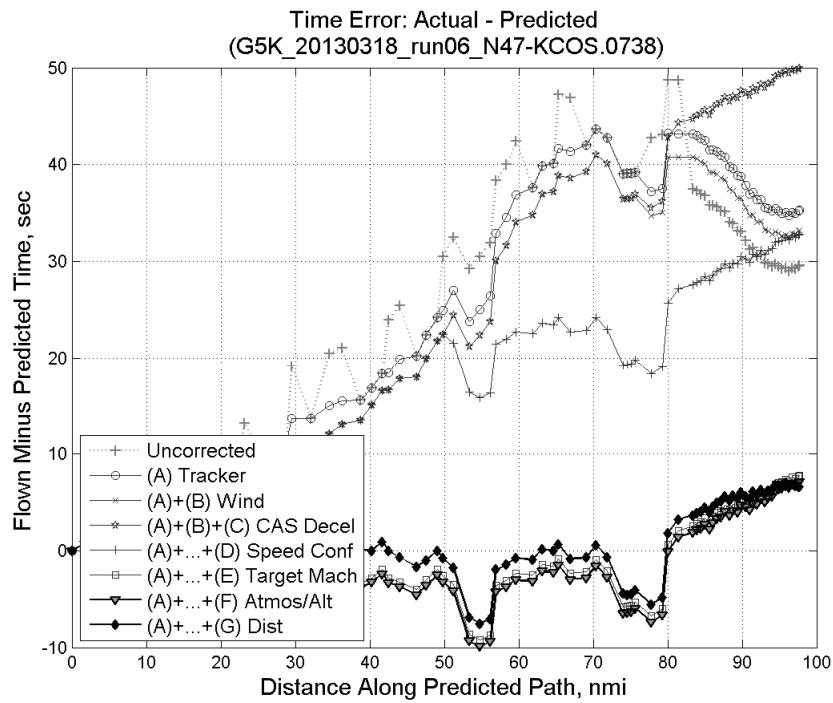


**Figure 872:** Time error for run 6 showing incremental effect of removing each error source.

### D.1.A. Tracker Jumps

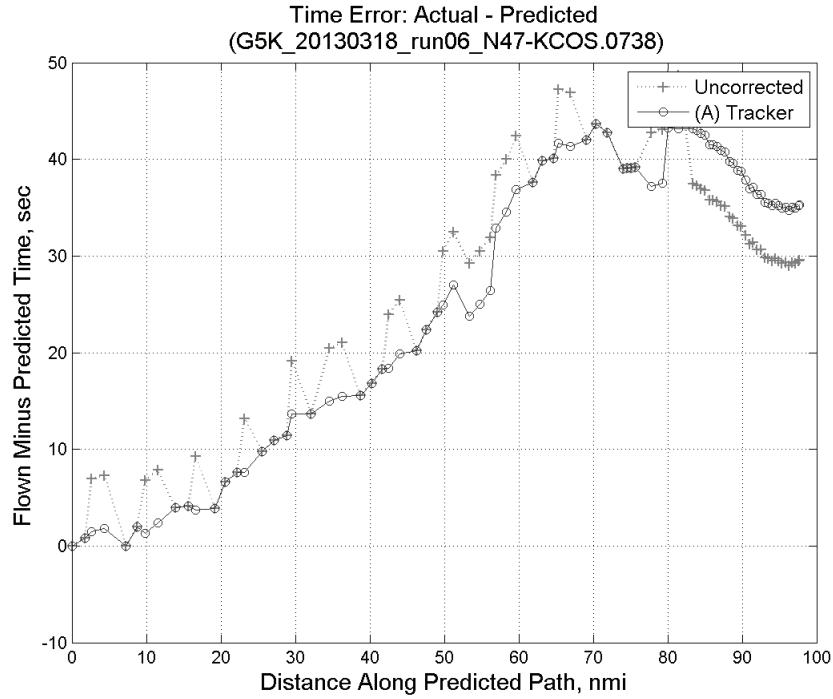


**Figure 873:** Time error for run 6 before (Uncorrected) and after ((A) Tracker) removing tracker jump error source.

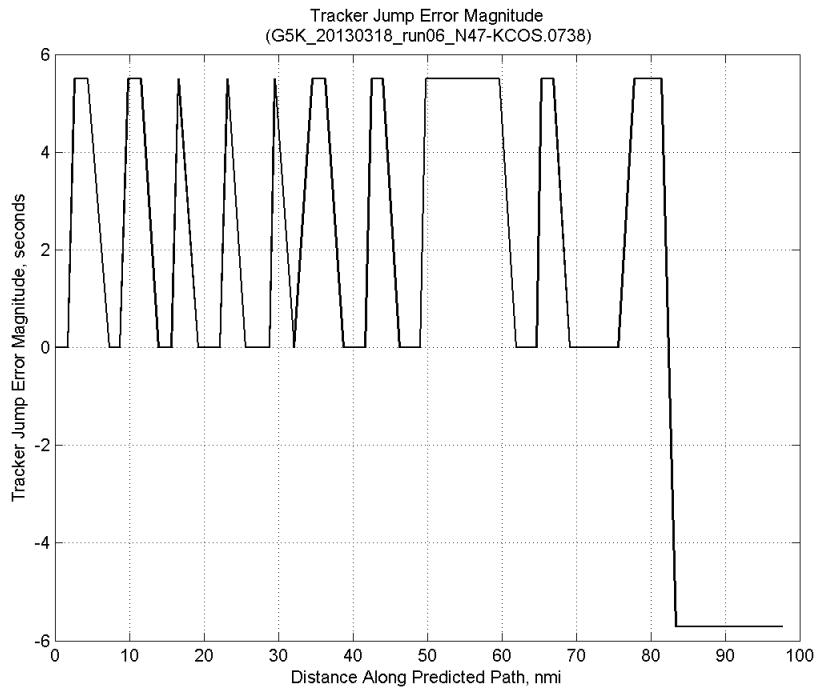


**Figure 874: Effect of tracker jump error source on time error for run 6.**

#### D.1.B. Wind

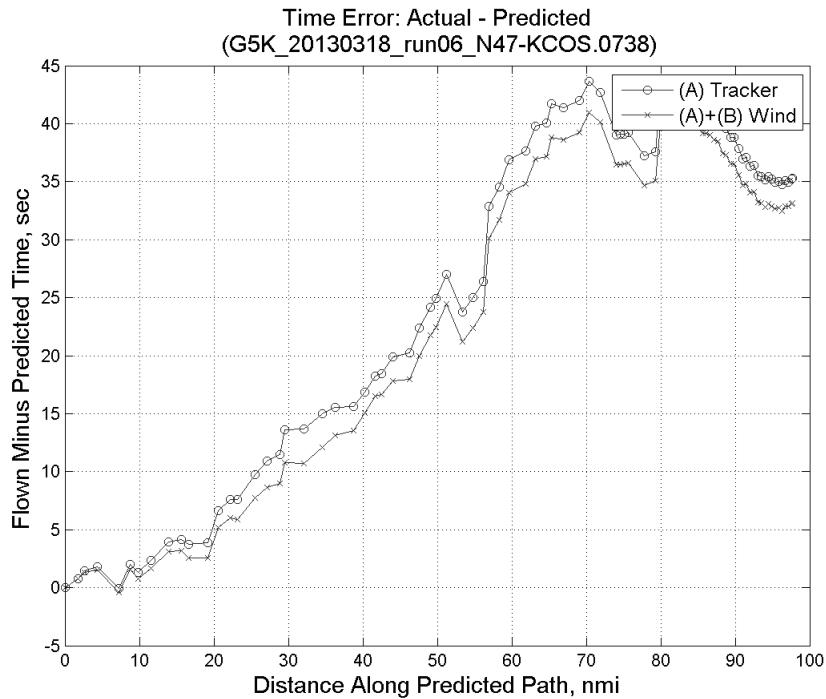


**Figure 875: Time error for run 6 before ((A) Tracker) and after ((A)+(B) Wind) removing wind error source.**

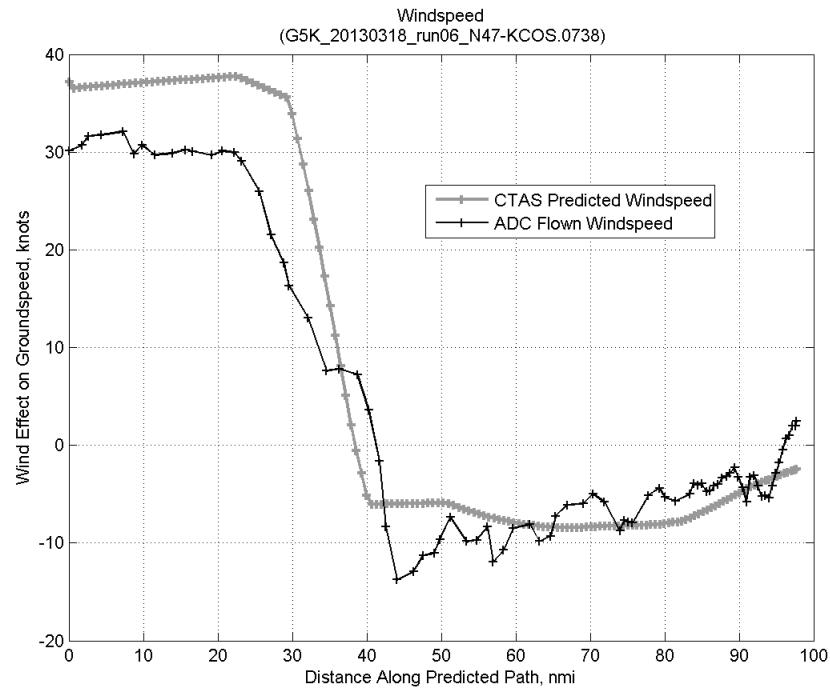


**Figure 876: CTAS predicted and ADC flown wind effect on ground speed for run 6. Negative values indicate a headwind.**

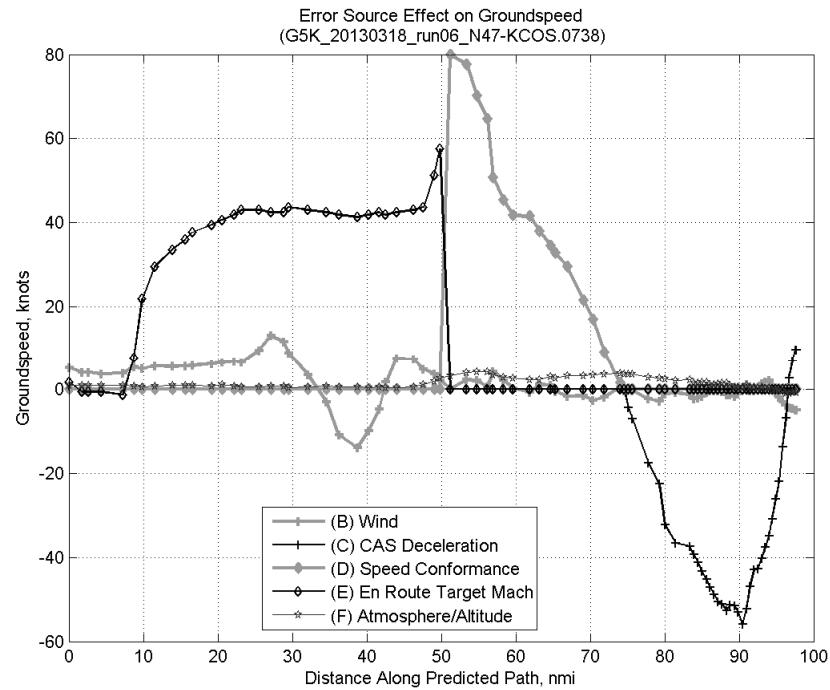


**Figure 877: Error sources (flown minus predicted) converted to a ground speed effect for run 6. Positive values indicate the flown ground speed was faster than the CTAS prediction.**

### D.1.C. CAS Deceleration

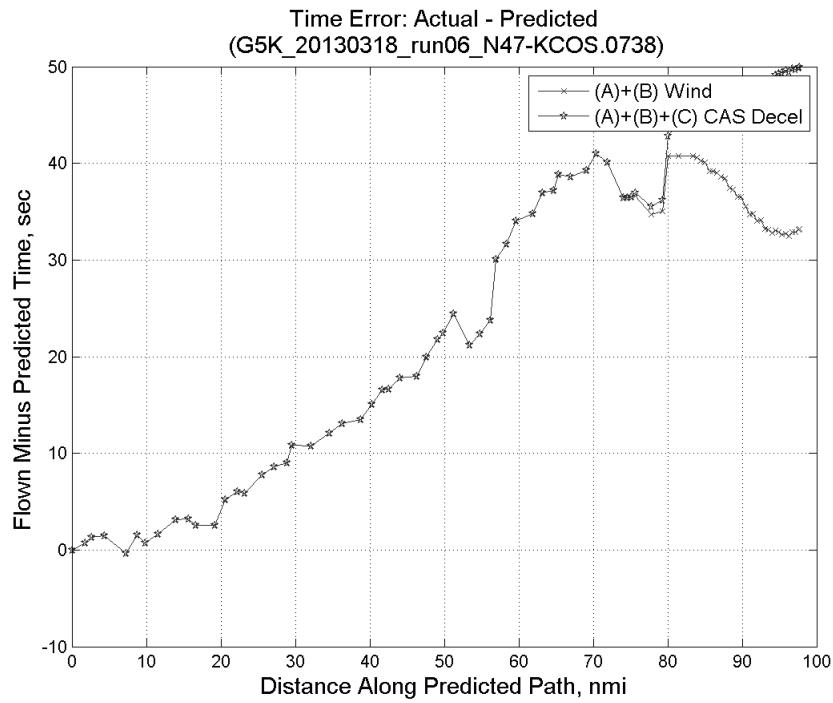


**Figure 878:** Time error for run 6 before ((A)+(B) Wind) and after ((A)+(B)+(C) CAS Decel) removing CAS deceleration error source.

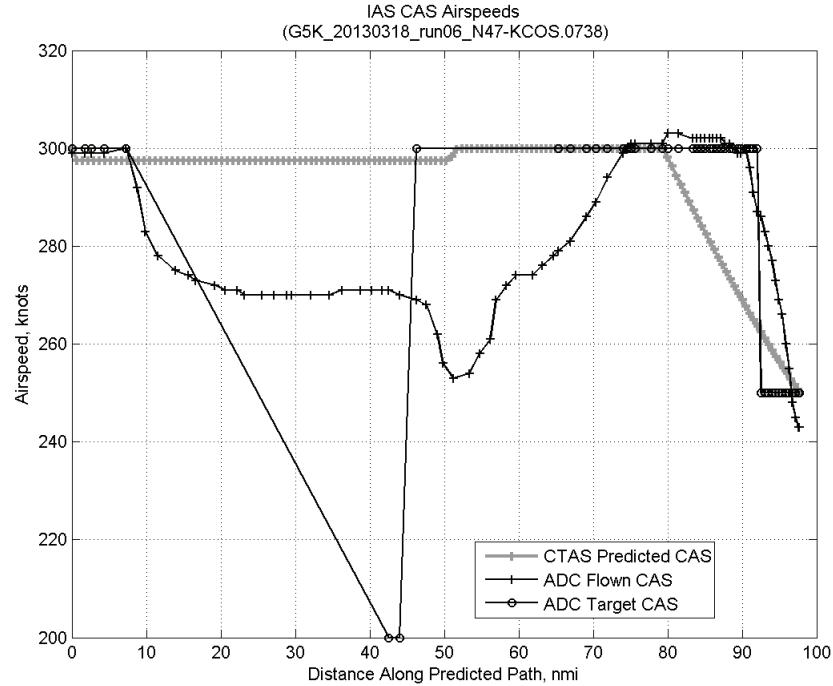


**Figure 879:** CTAS predicted and ADC flown CAS for run 6. CAS that is being targeted is shown with circle markers.

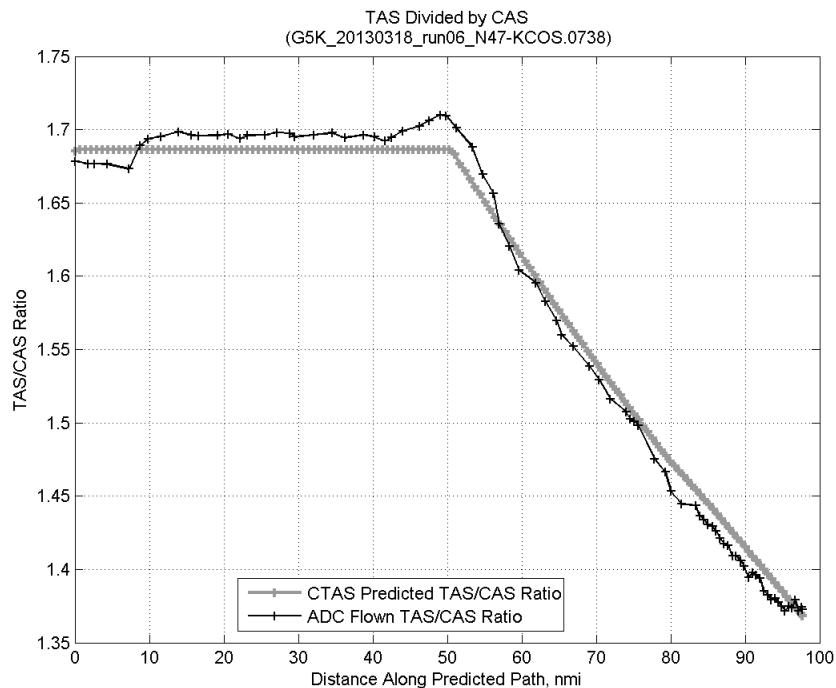


**Figure 880: CTAS predicted and ADC flown TAS/CAS ratio for run 6.**

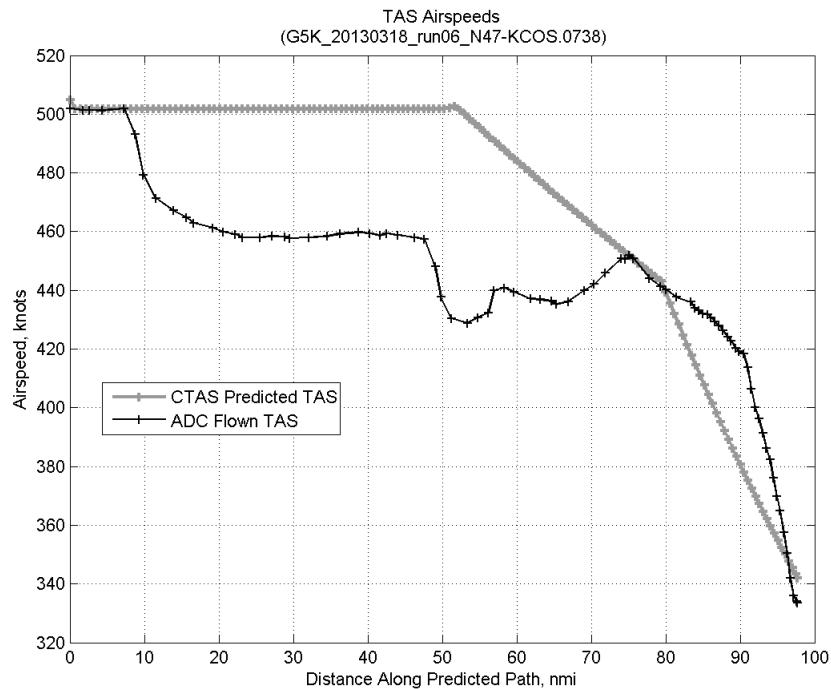


**Figure 881: CTAS predicted and ADC flown TAS for run 6.**

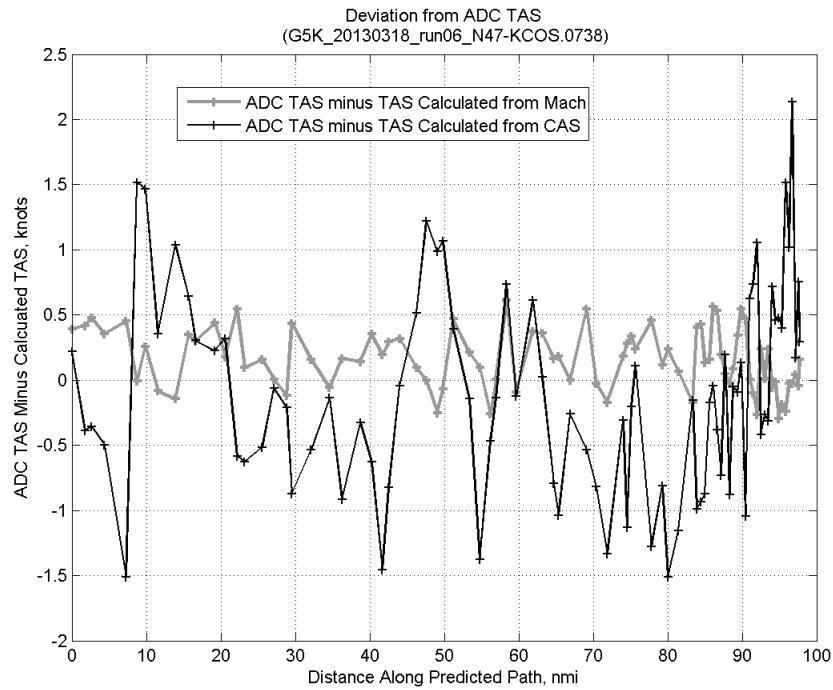


**Figure 882:** Deviation from ADC flown TAS if calculating TAS using ADC flown CAS, Mach, atmospheric temperature, and atmospheric pressure for run 6.

#### D.1.D. Speed Conformance

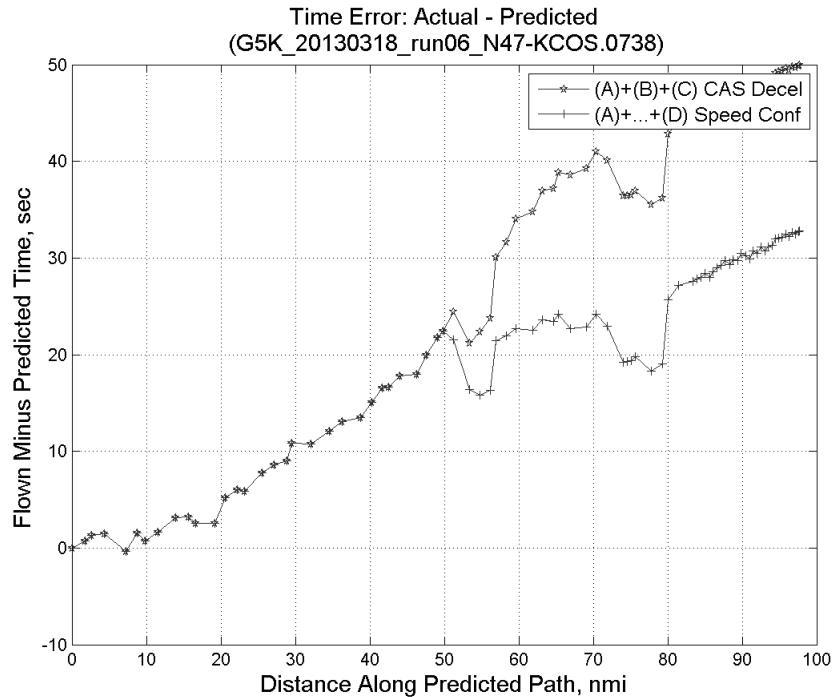


**Figure 883:** Time error for run 6 before ((A)+(B)+(C) CAS Decel) and after ((A)+...+(D) Speed Conf) removing speed conformance error source.

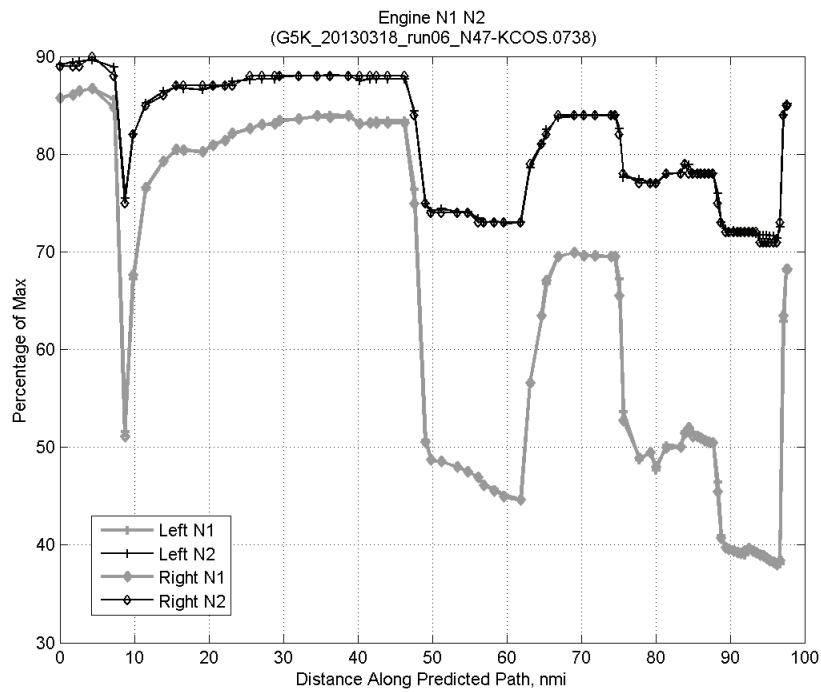


**Figure 884: Flown engine N1 and N2 for run 6.**

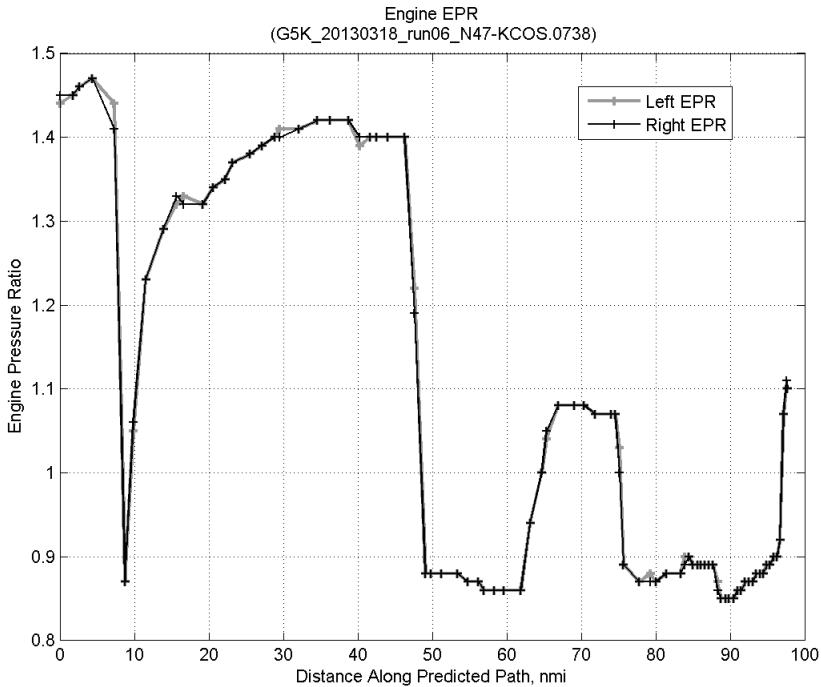


**Figure 885: Flown engine EPR for run 6.**

### D.1.E. Target Mach

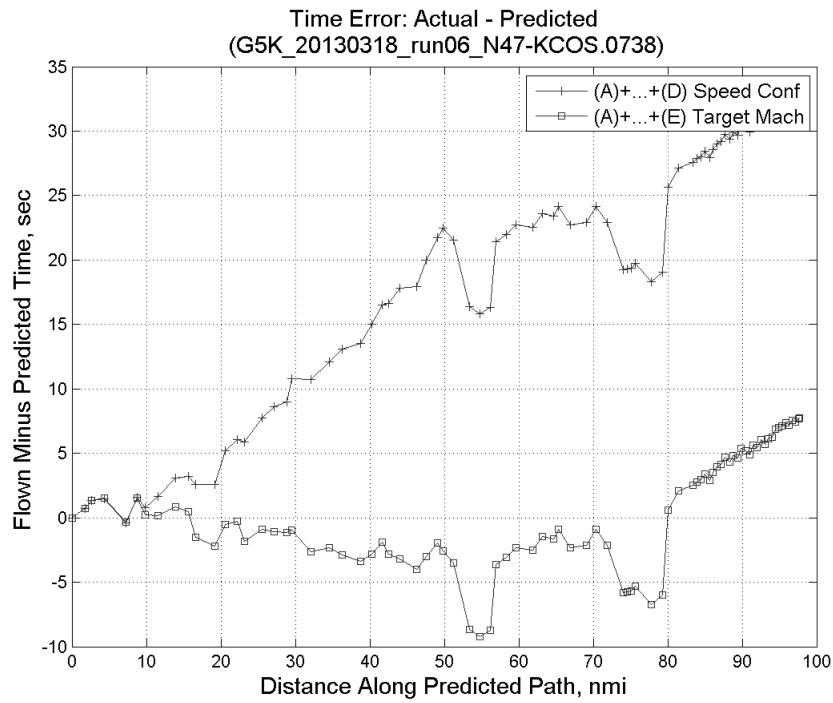


**Figure 886:** Time error for run 6 before ((A)+...+(D) Speed Conf) and after ((A)+...+(E) Target Mach) removing target Mach error source.

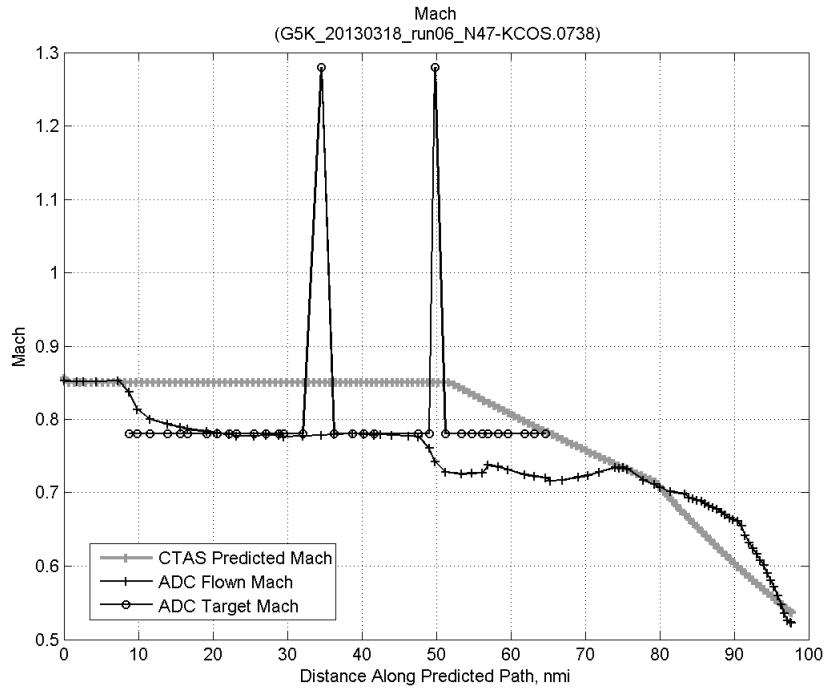


**Figure 887:** CTAS predicted and ADC flown Mach for run 6. Mach being targeted (ADC) shown with circle markers.

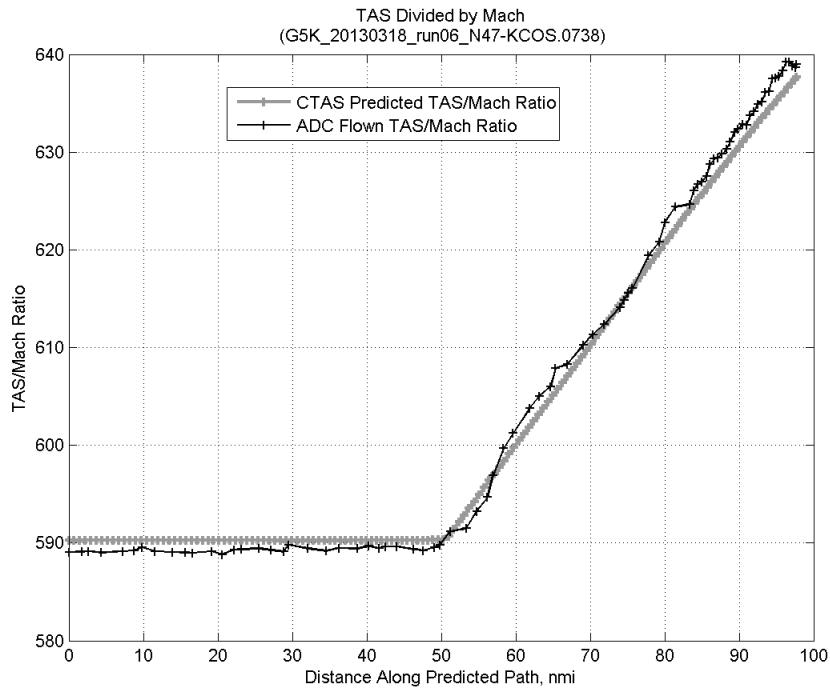


**Figure 888: CTAS predicted and ADC flown TAS/Mach ratio for run 6.**

#### D.1.F. Atmosphere/Altitude

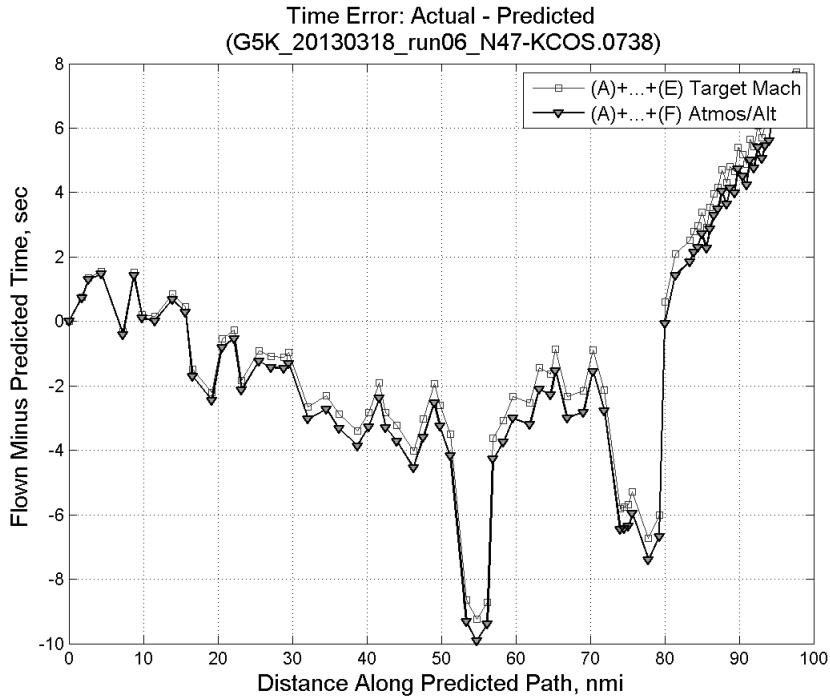


**Figure 889: Time error for run 6 before ((A)+...+(E) Target Mach) and after ((A)+...+(F) Atmos/Alt) removing atmosphere/altitude error source.**

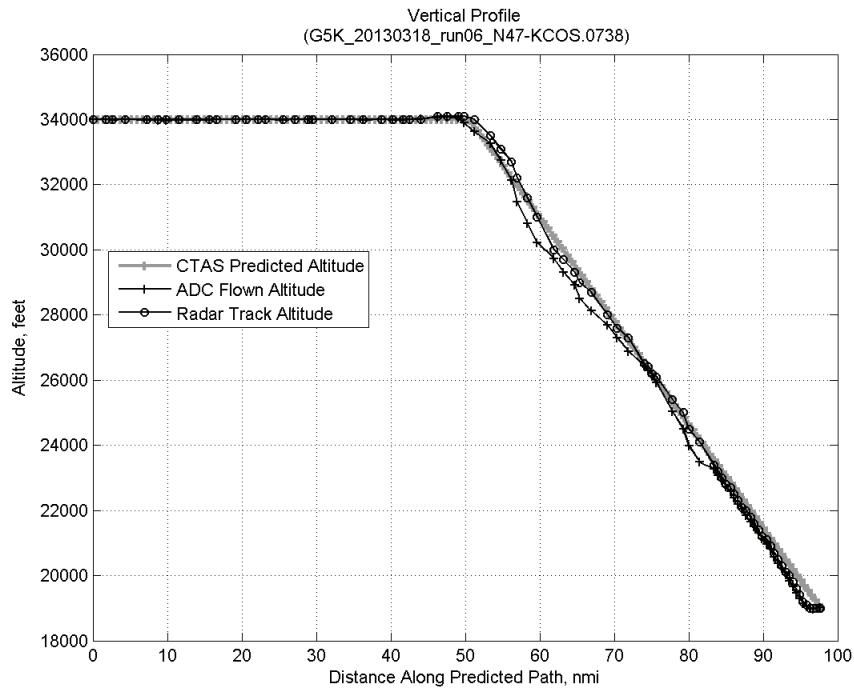


**Figure 890: Flown (ADC) and predicted (CTAS) vertical profile for run 6.**

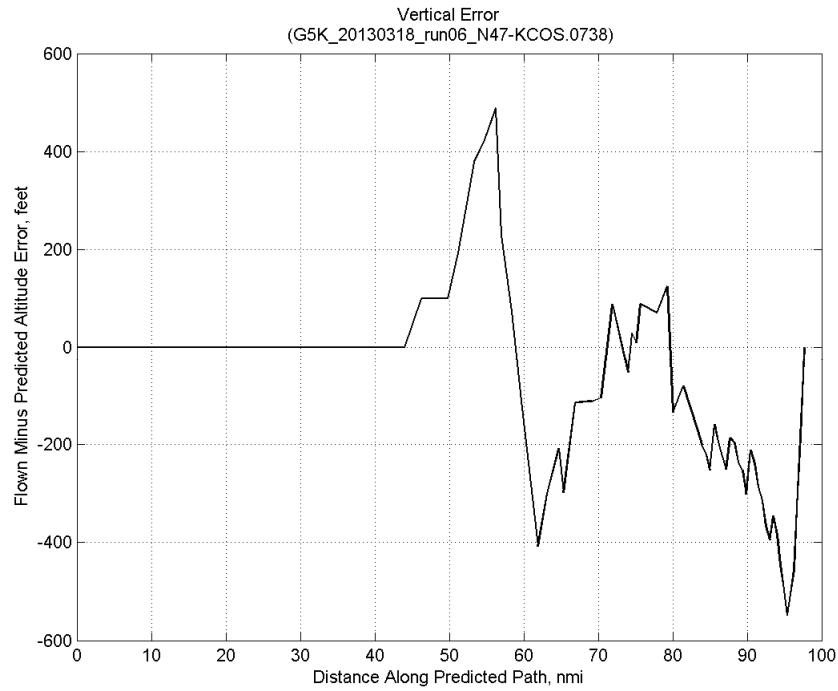


**Figure 891: Vertical error (flown minus predicted altitude) for run 6. Positive values indicate aircraft flew higher than predicted by CTAS.**

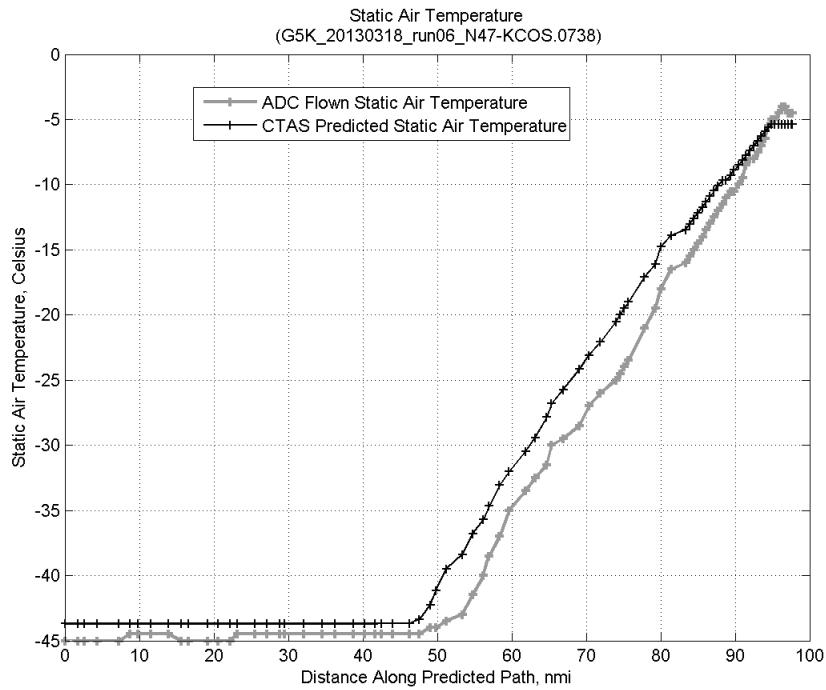


**Figure 892: Flown (ADC) and predicted (CTAS) static air temperature for run 6.**

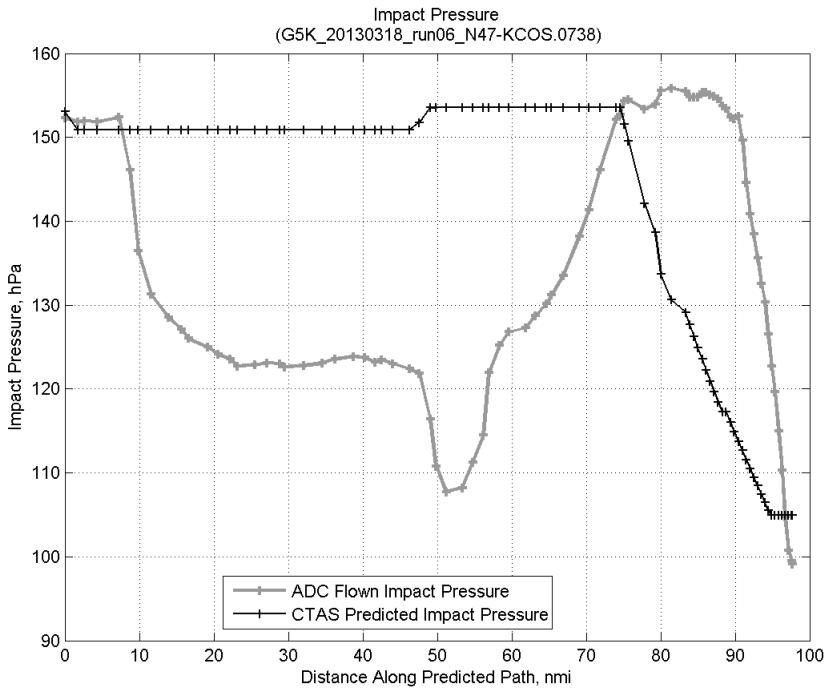


**Figure 893: Flown (ADC) and predicted (CTAS) impact pressure for run 6.**

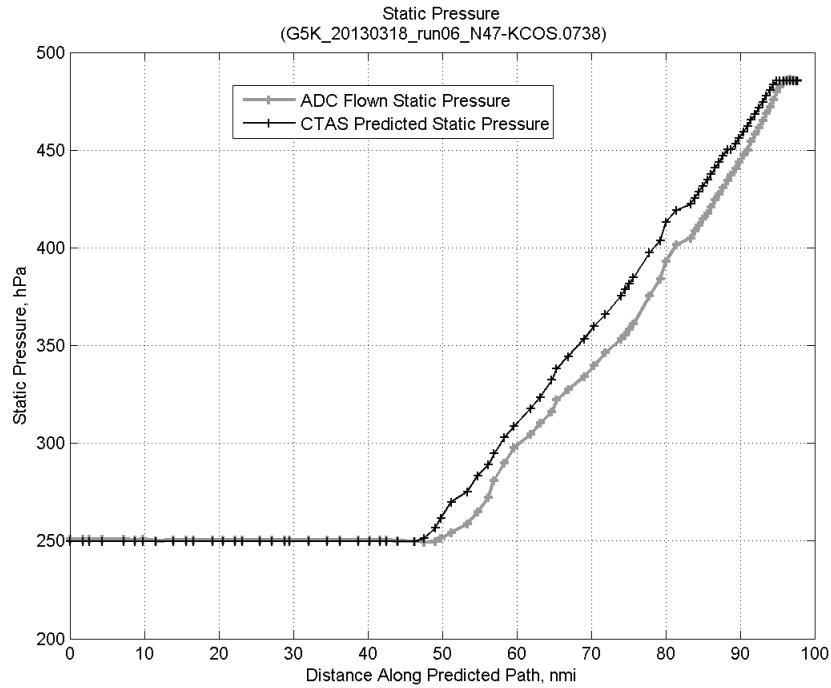


**Figure 894: Flown (ADC) and predicted (CTAS) static pressure for run 6.**

#### D.1.G. Path Distance

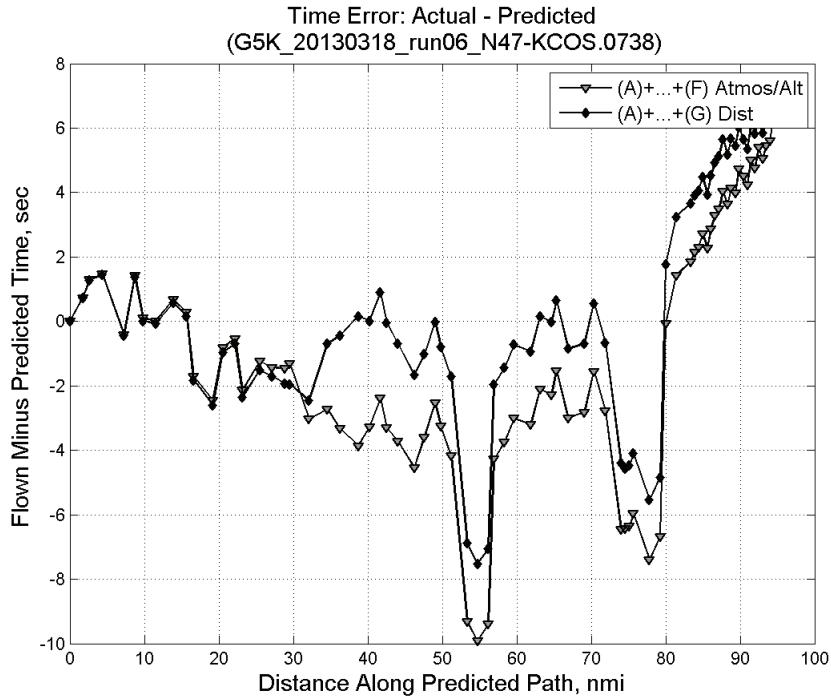


**Figure 895: Time error for run 6 before ((A)+...+(F) Atmos/Alt) and after ((A)+...+(G) Dist) removing path distance error source.**

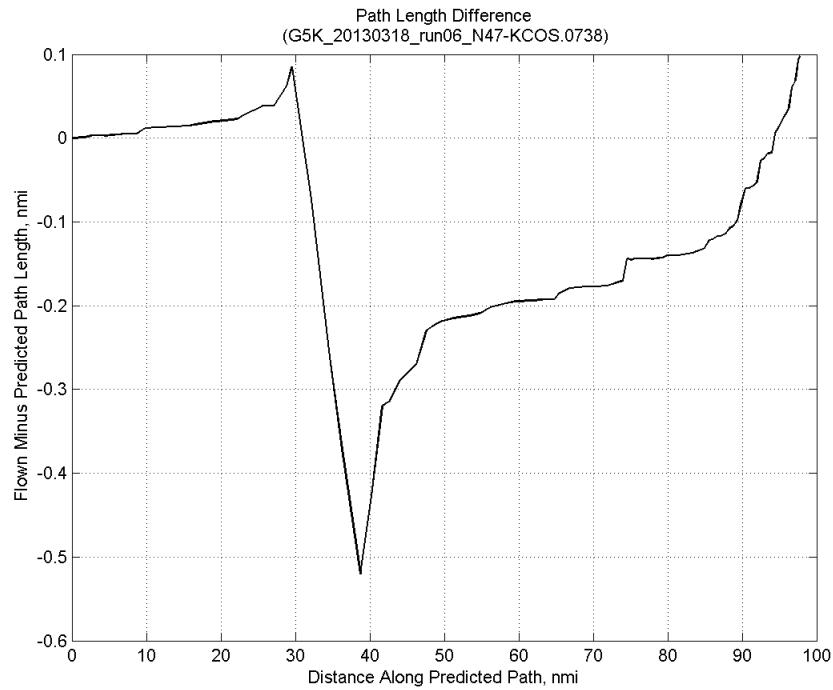


**Figure 896: ADC flown minus CTAS predicted path length for run 6. Positive values indicate aircraft followed a longer path than predicted by CTAS.**

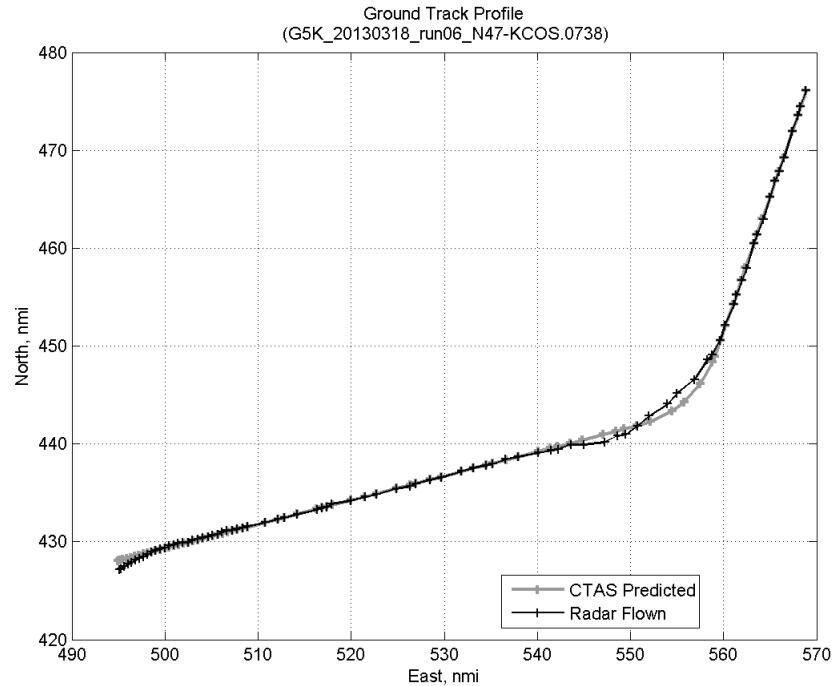


**Figure 897: CTAS predicted and radar flown ground track profile for run 6.**

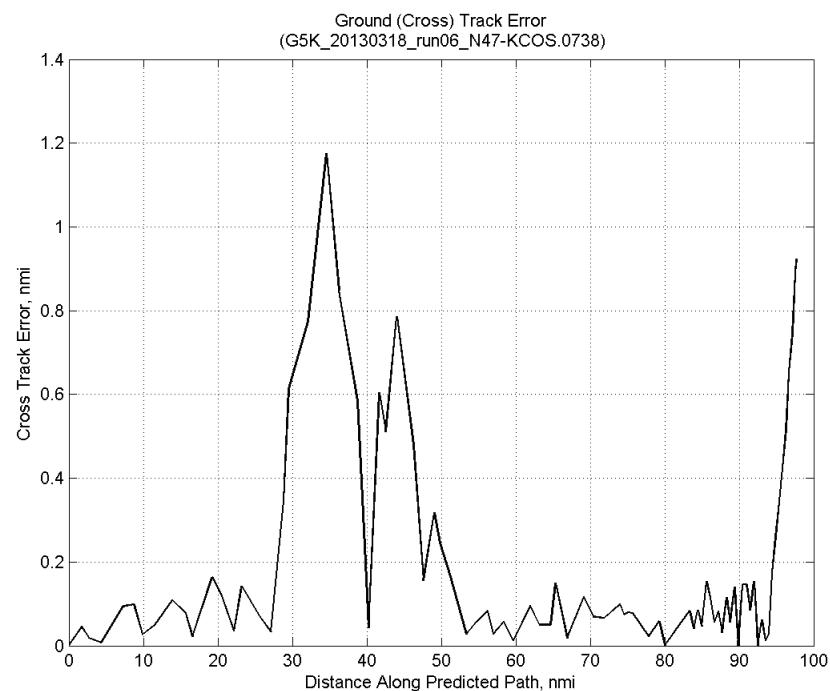


**Figure 898: Ground (cross) track error for run 6.**

## D.2. Run 8

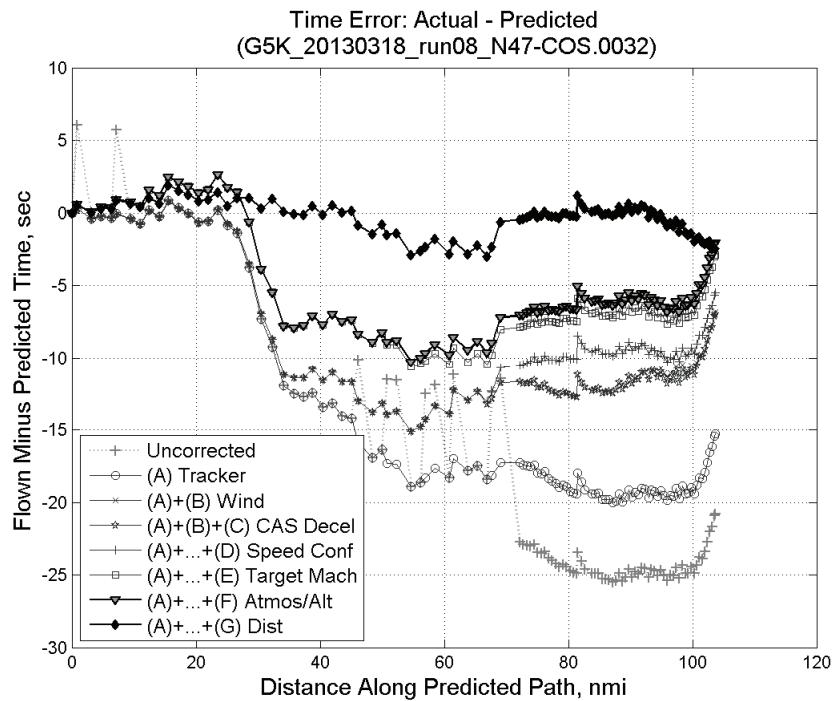


**Figure 899:** Time error for run 8 showing incremental effect of removing each error source.

### D.2.A. Tracker Jumps

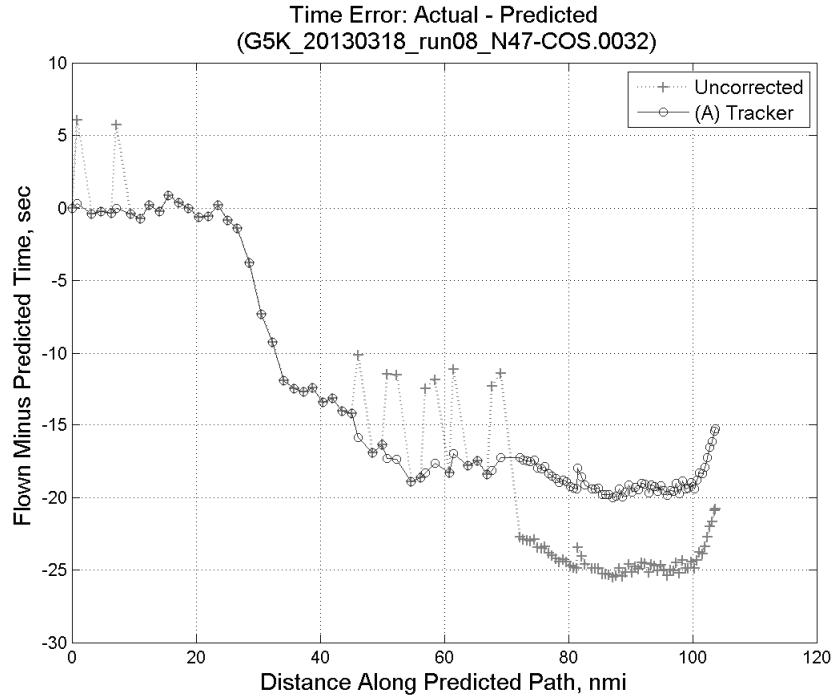


**Figure 900:** Time error for run 8 before (Uncorrected) and after ((A) Tracker) removing tracker jump error source.

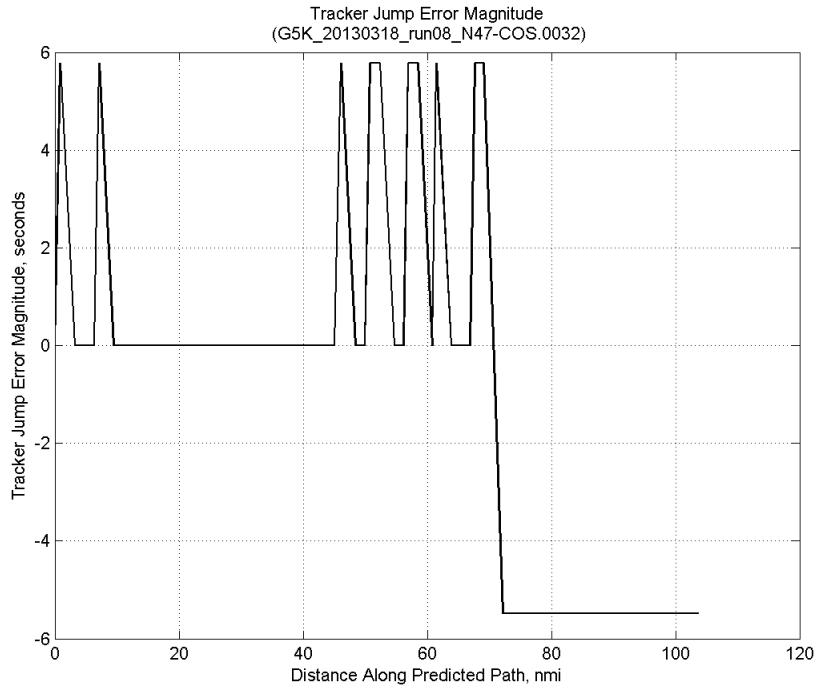


**Figure 901: Effect of tracker jump error source on time error for run 8.**

#### D.2.B. Wind

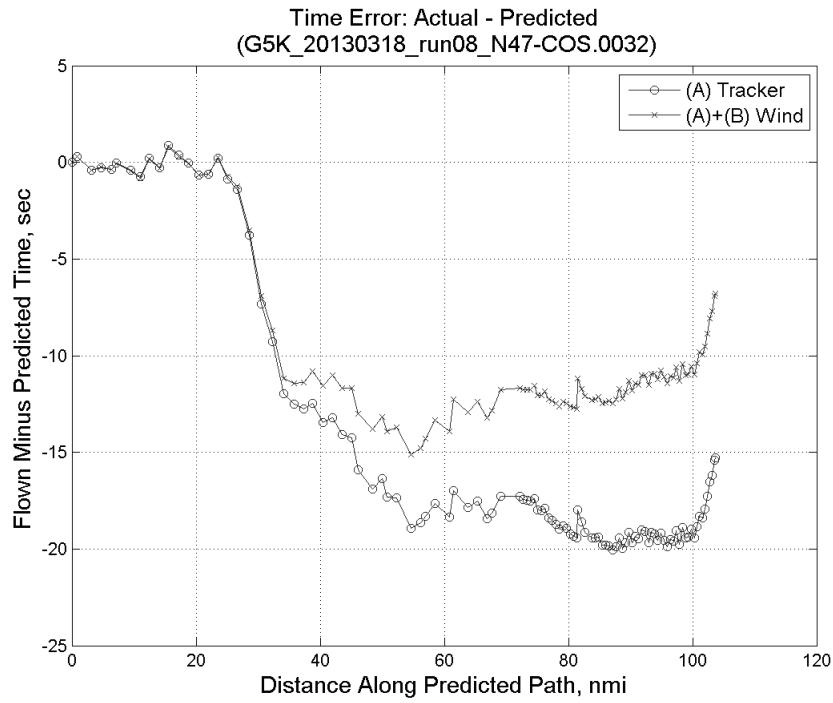


**Figure 902: Time error for run 8 before ((A) Tracker) and after ((A)+(B) Wind) removing wind error source.**

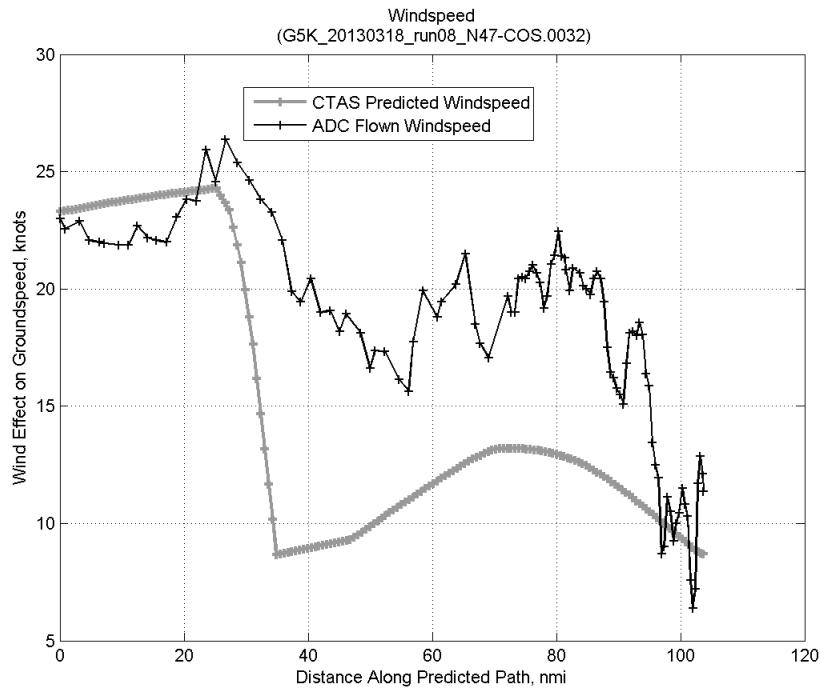


**Figure 903: CTAS predicted and ADC flown wind effect on ground speed for run 8. Negative values indicate a headwind.**

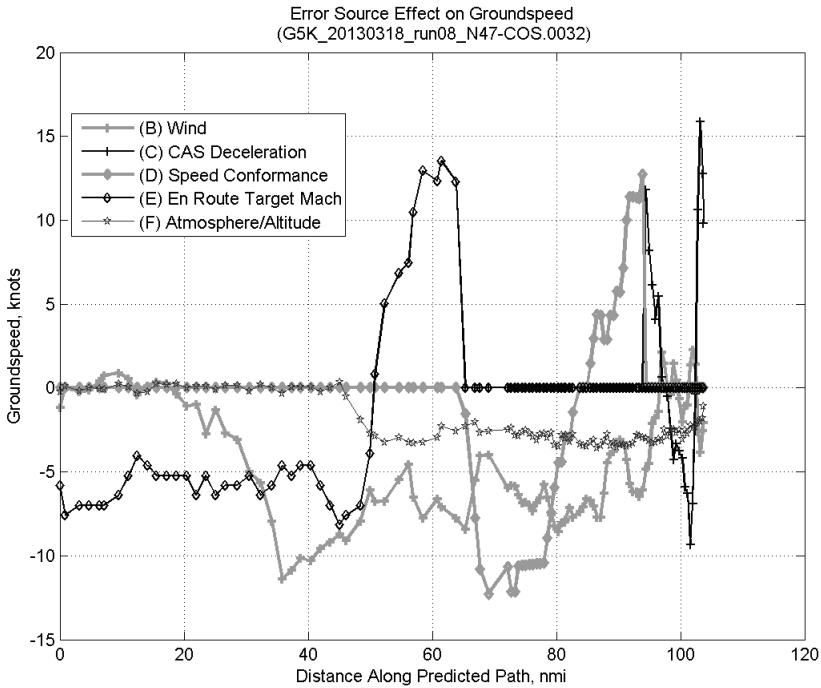


**Figure 904: Error sources (flown minus predicted) converted to a ground speed effect for run 8. Positive values indicate the flown ground speed was faster than the CTAS prediction.**

### D.2.C. CAS Deceleration

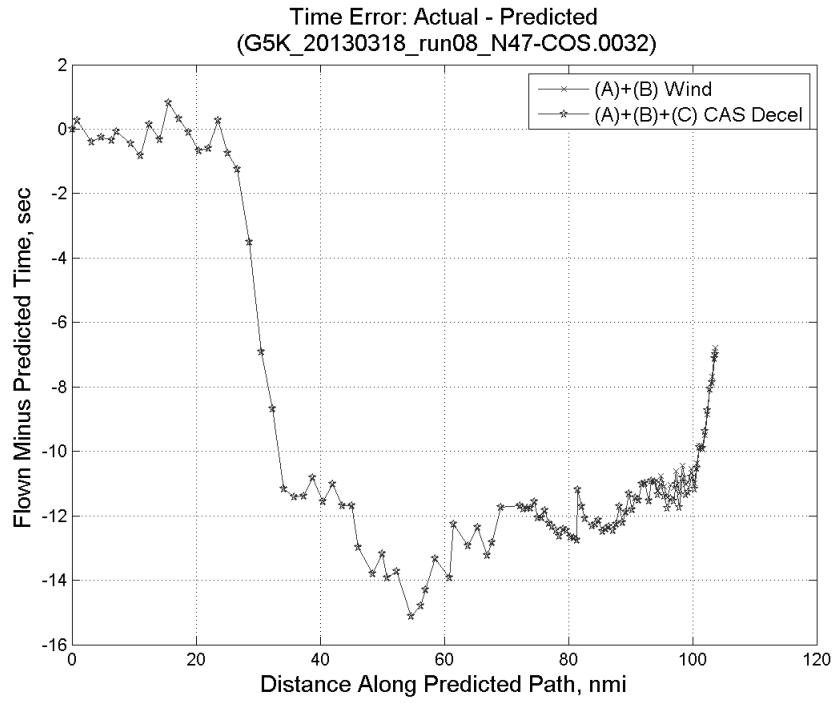


**Figure 905:** Time error for run 8 before ((A)+(B) Wind) and after ((A)+(B)+(C) CAS Decel) removing CAS deceleration error source.

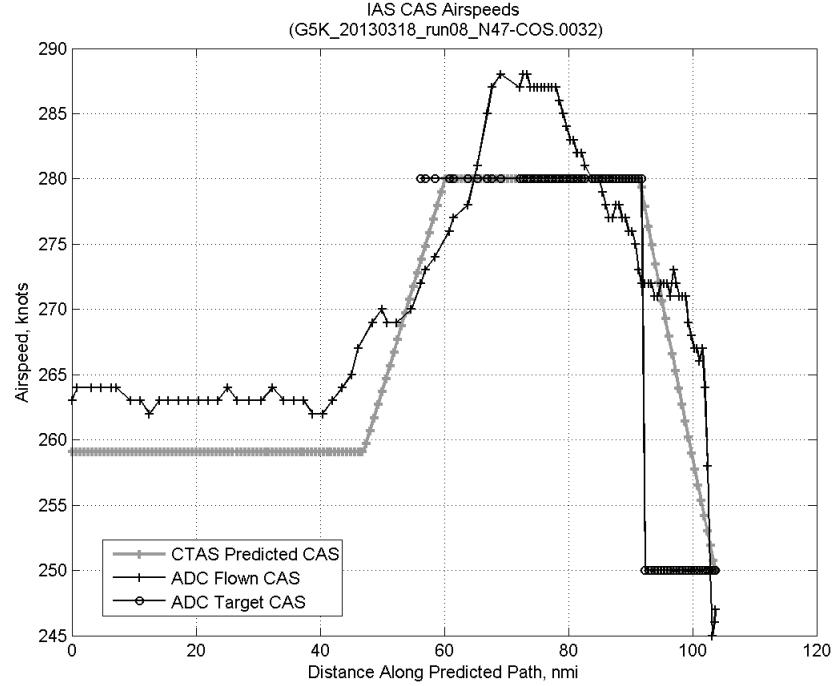


**Figure 906:** CTAS predicted and ADC flown CAS for run 8. CAS that is being targeted is shown with circle markers.

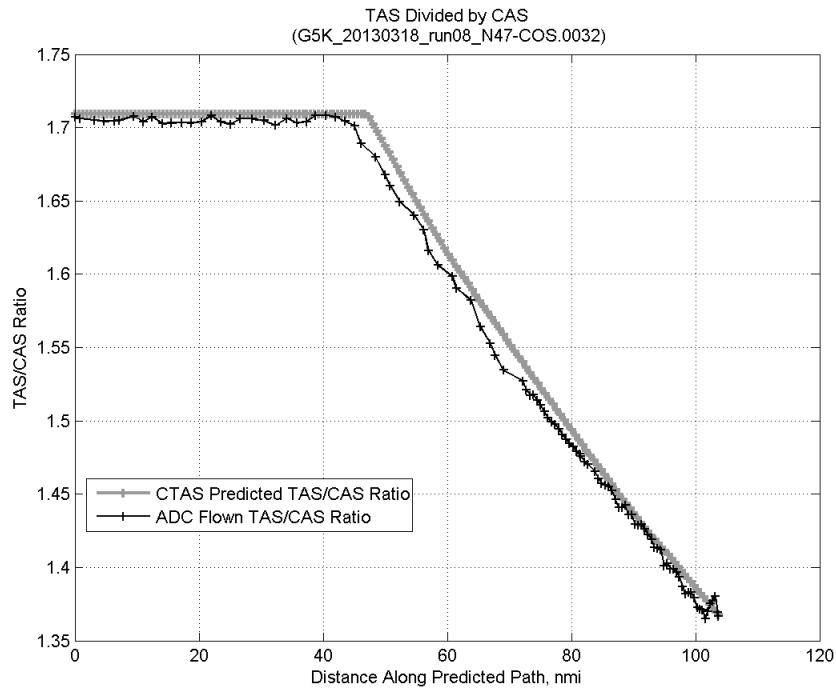


**Figure 907: CTAS predicted and ADC flown TAS/CAS ratio for run 8.**

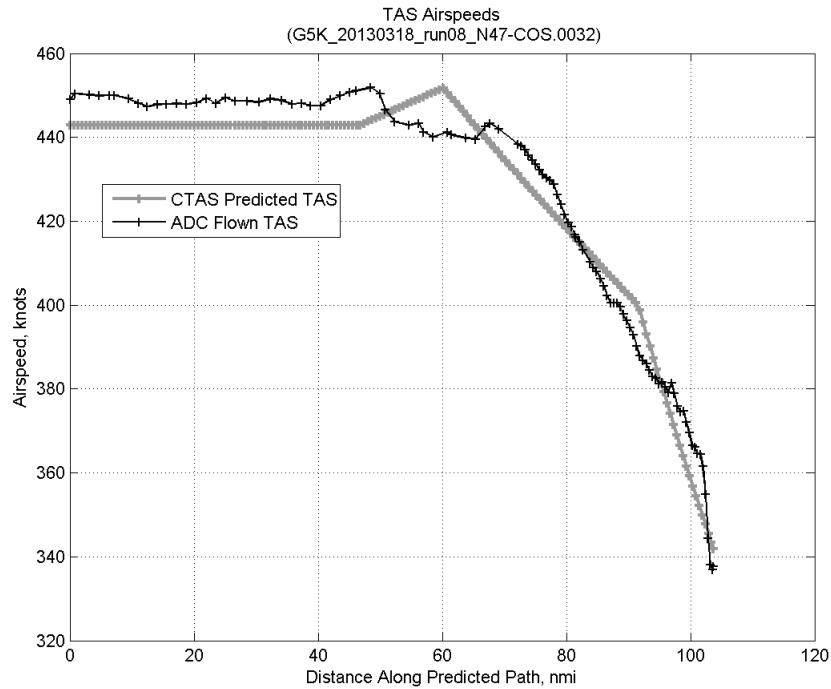


**Figure 908: CTAS predicted and ADC flown TAS for run 8.**

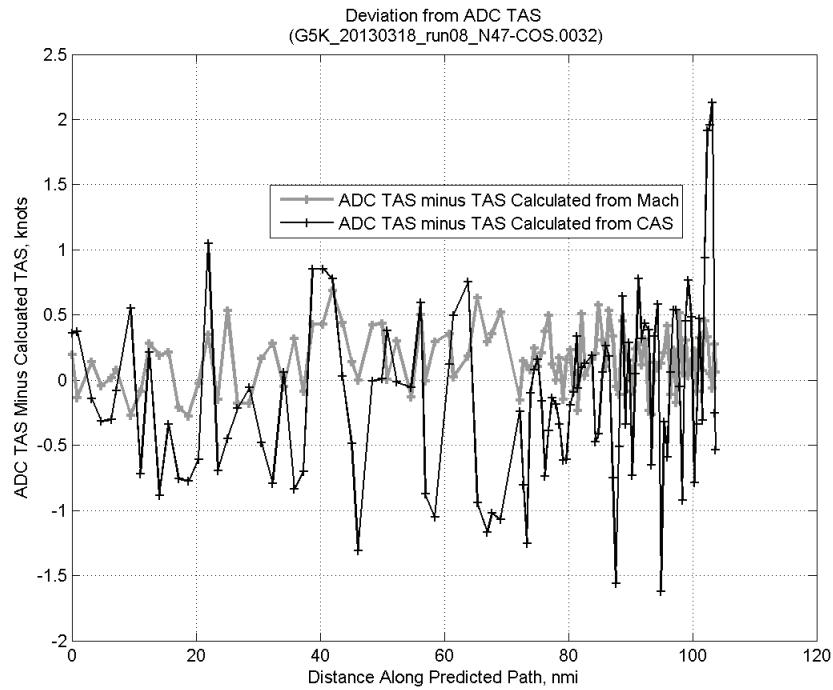


**Figure 909: Deviation from ADC flown TAS if calculating TAS using ADC flown CAS, Mach, atmospheric temperature, and atmospheric pressure for run 8.**

#### D.2.D. Speed Conformance

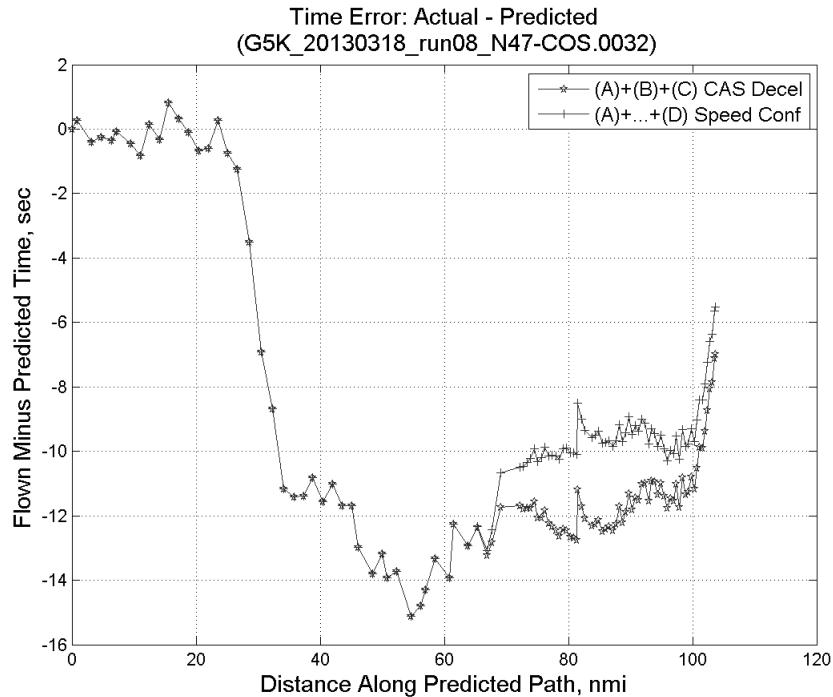


**Figure 910: Time error for run 8 before ((A)+(B)+(C) CAS Decel) and after ((A)+...+(D) Speed Conf) removing speed conformance error source.**

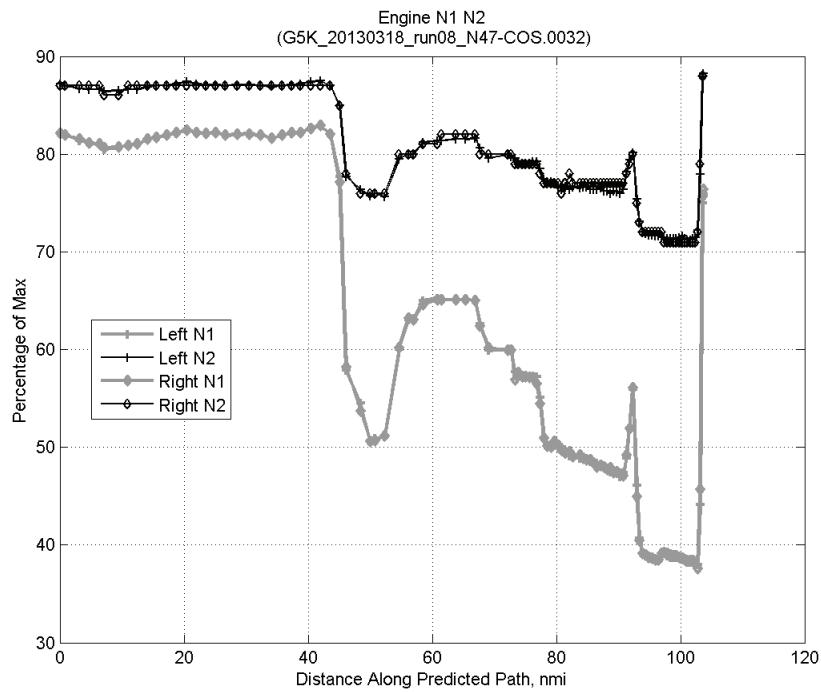


**Figure 911: Flown engine N1 and N2 for run 8.**

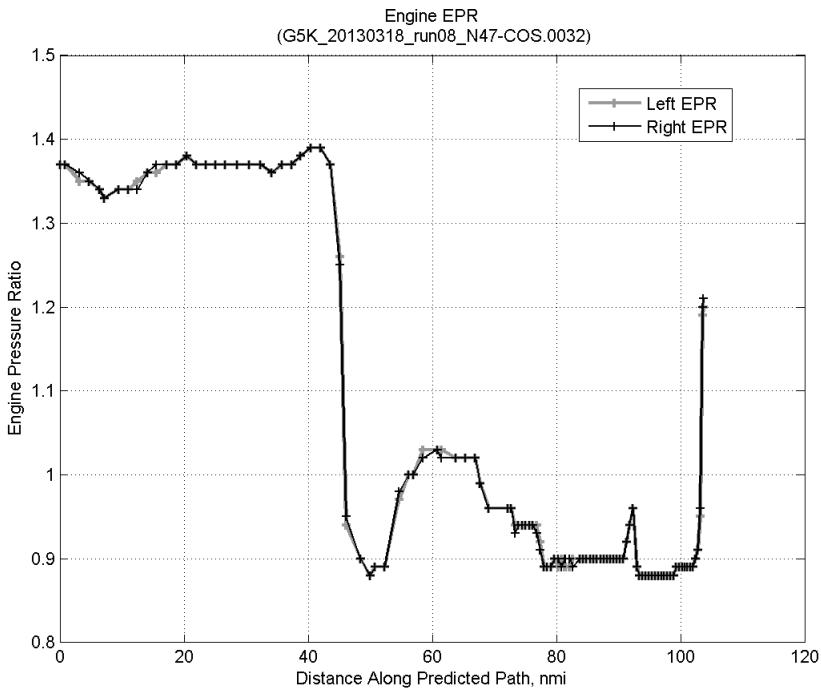


**Figure 912: Flown engine EPR for run 8.**

### D.2.E. Target Mach

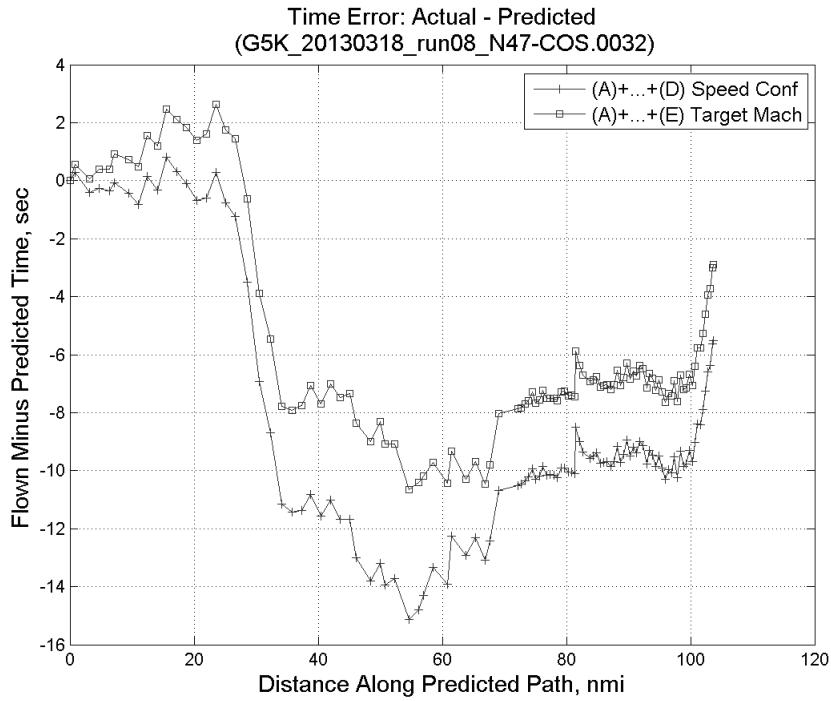


**Figure 913:** Time error for run 8 before ((A)+...+(D) Speed Conf) and after ((A)+...+(E) Target Mach) removing target Mach error source.

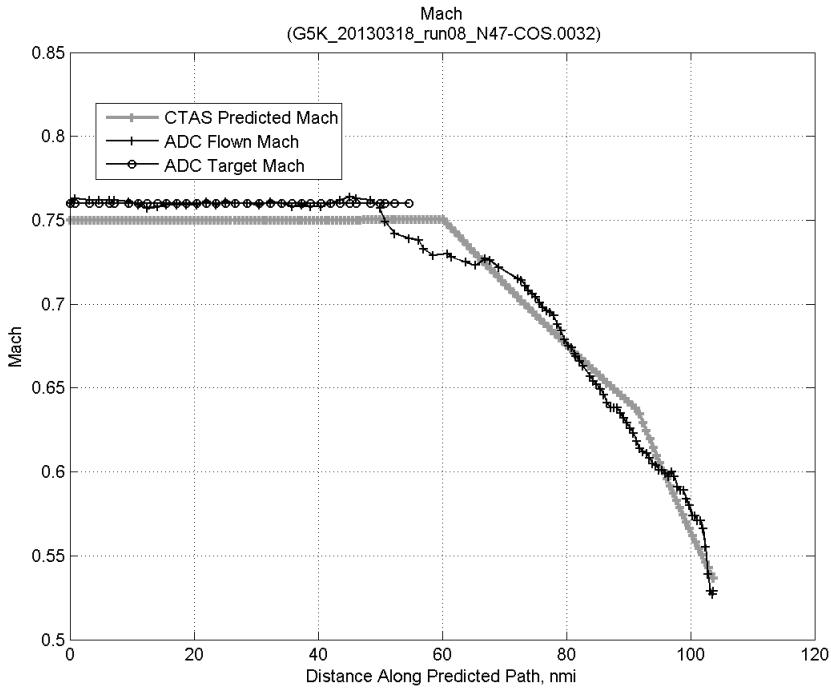


**Figure 914:** CTAS predicted and ADC flown Mach for run 8. Mach being targeted (ADC) shown with circle markers.

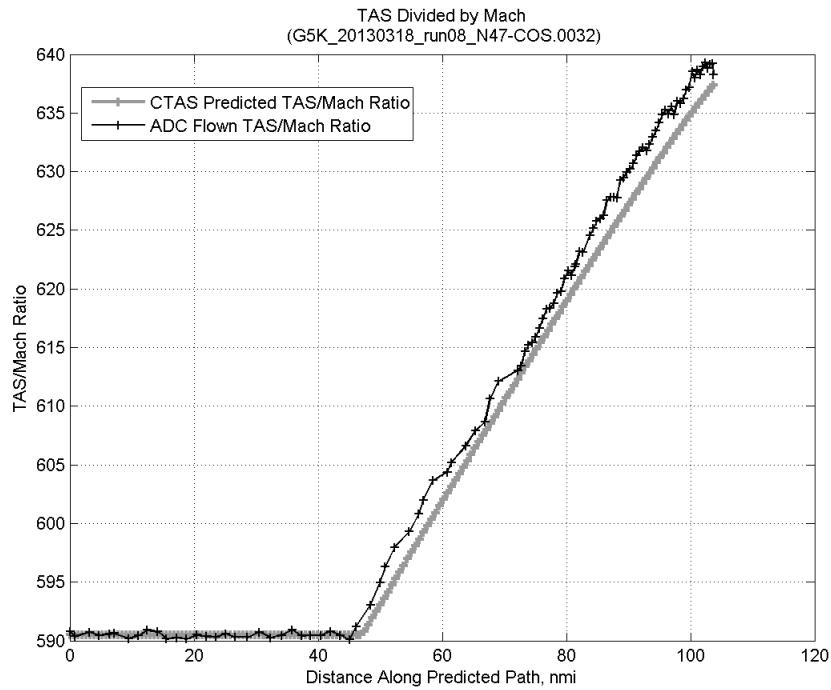


**Figure 915: CTAS predicted and ADC flown TAS/Mach ratio for run 8.**

#### D.2.F. Atmosphere/Altitude

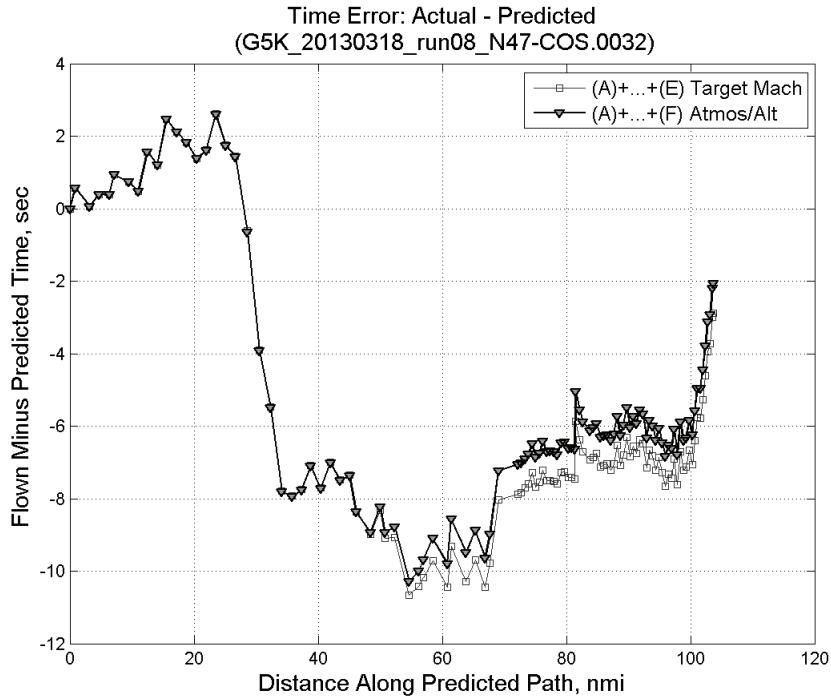


**Figure 916: Time error for run 8 before ((A)+...+(E) Target Mach) and after ((A)+...+(F) Atmos/Alt) removing atmosphere/altitude error source.**

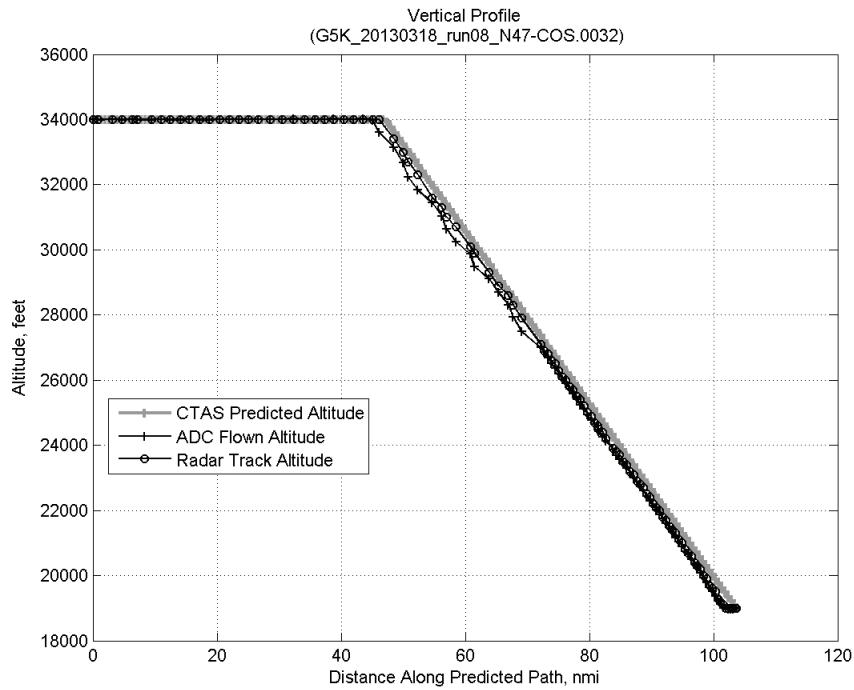


**Figure 917: Flown (ADC) and predicted (CTAS) vertical profile for run 8.**

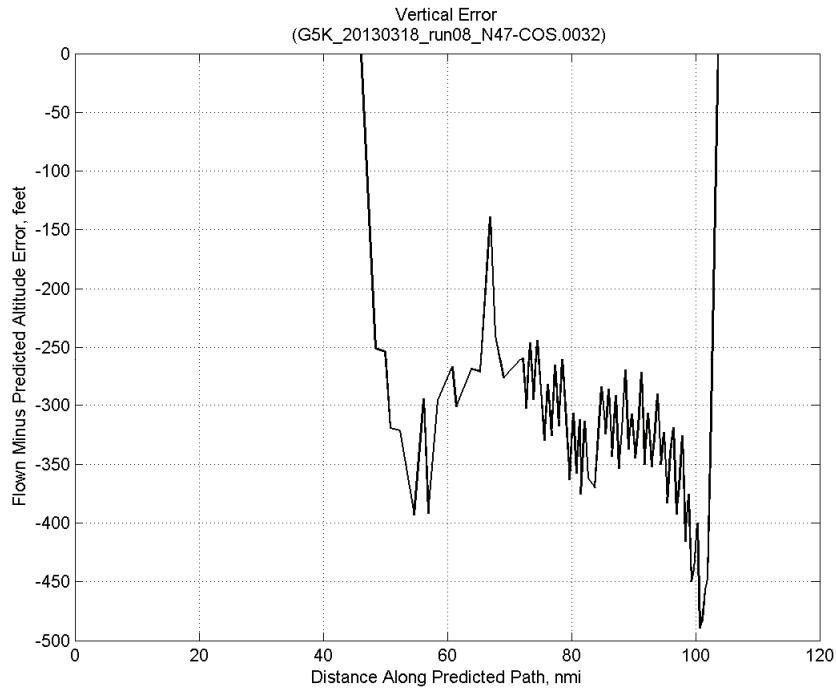


**Figure 918: Vertical error (flown minus predicted altitude) for run 8. Positive values indicate aircraft flew higher than predicted by CTAS.**

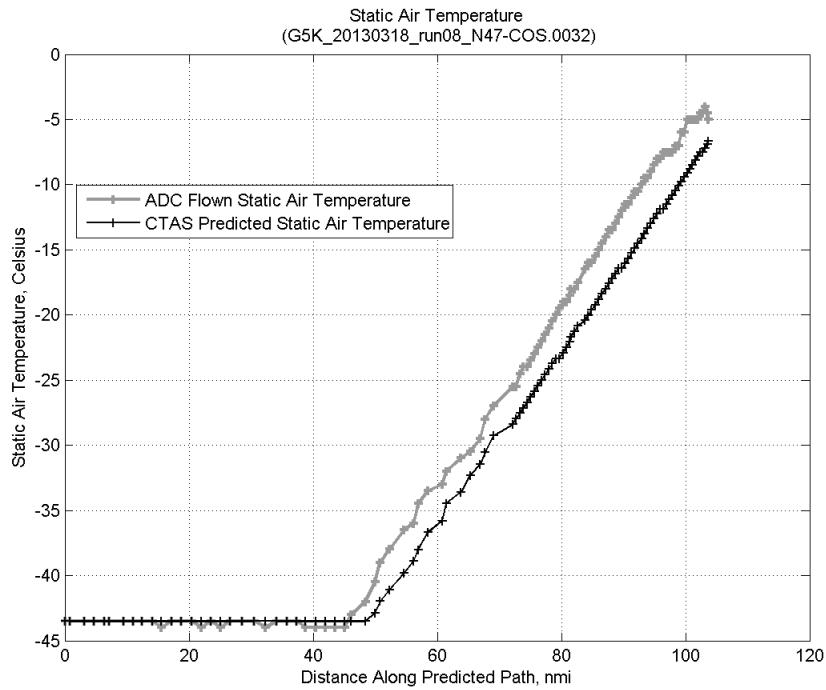


**Figure 919: Flown (ADC) and predicted (CTAS) static air temperature for run 8.**

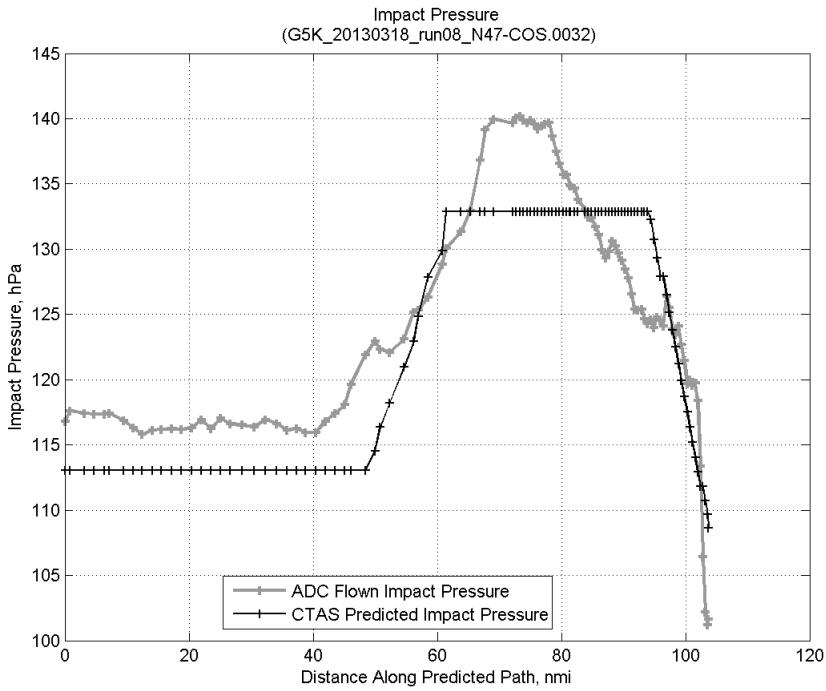


**Figure 920: Flown (ADC) and predicted (CTAS) impact pressure for run 8.**

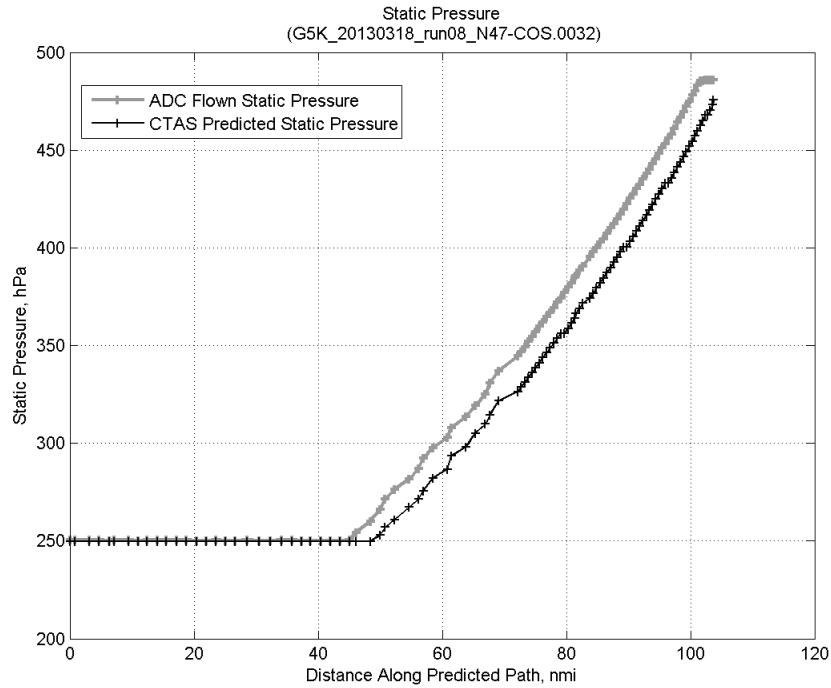


**Figure 921: Flown (ADC) and predicted (CTAS) static pressure for run 8.**

#### D.2.G. Path Distance

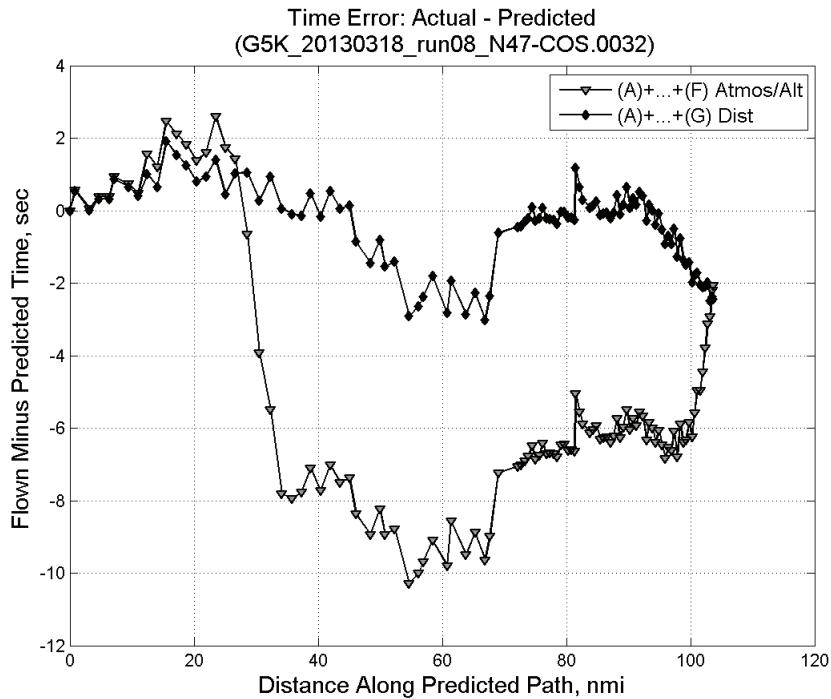


**Figure 922: Time error for run 8 before ((A)+...+(F) Atmos/Alt) and after ((A)+...+(G) Dist) removing path distance error source.**

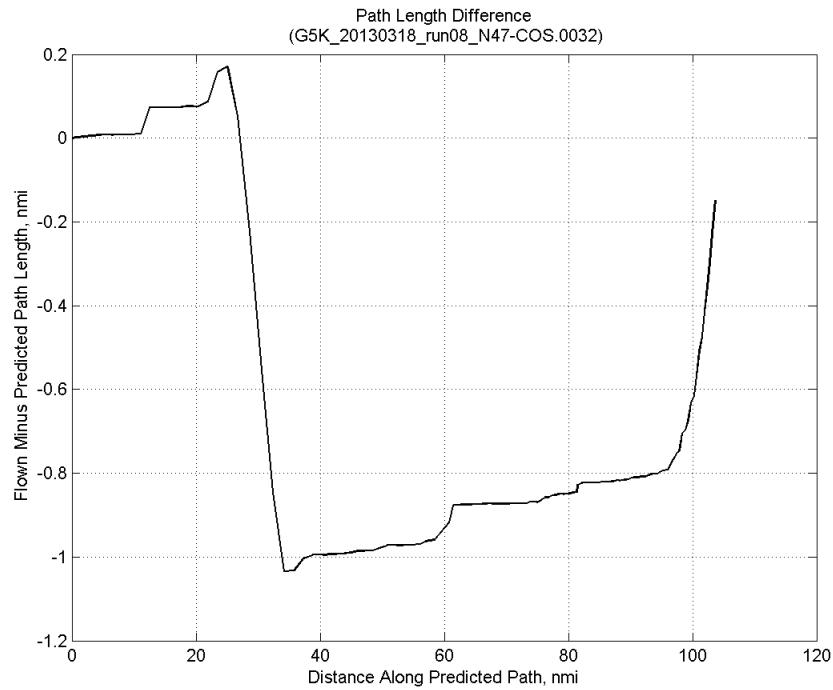


**Figure 923: ADC flown minus CTAS predicted path length for run 8. Positive values indicate aircraft followed a longer path than predicted by CTAS.**

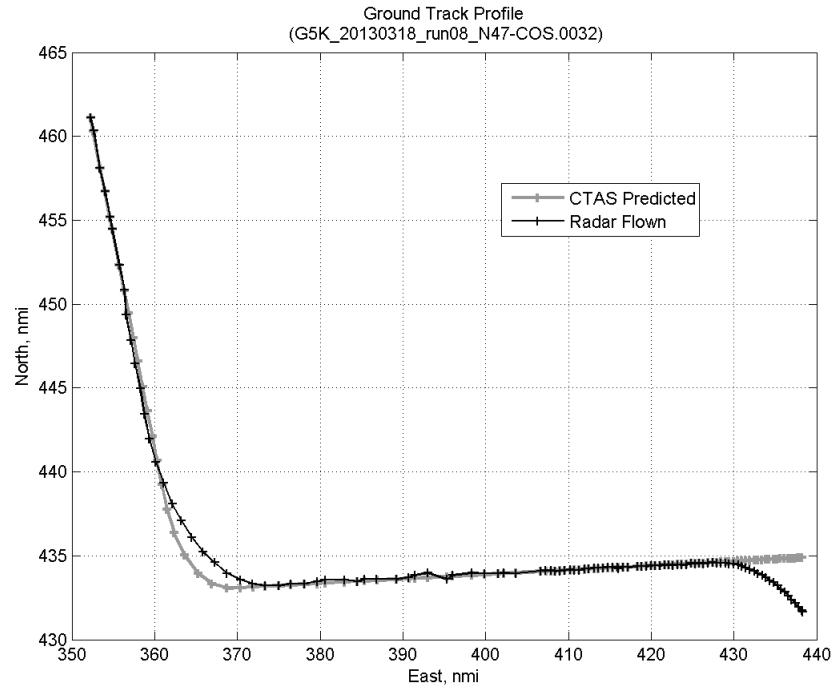


**Figure 924: CTAS predicted and radar flown ground track profile for run 8.**

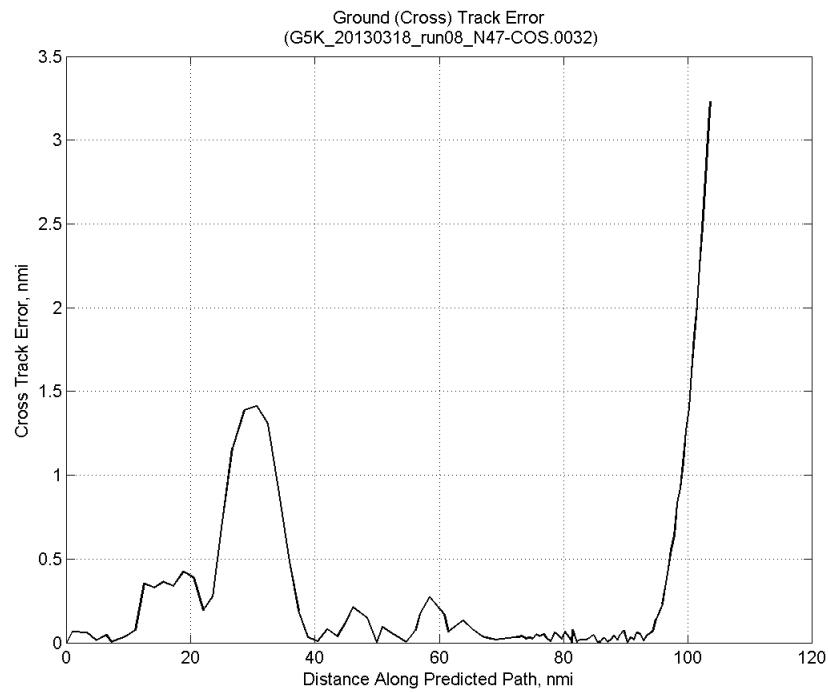


**Figure 925: Ground (cross) track error for run 8.**

### D.3. Run 13

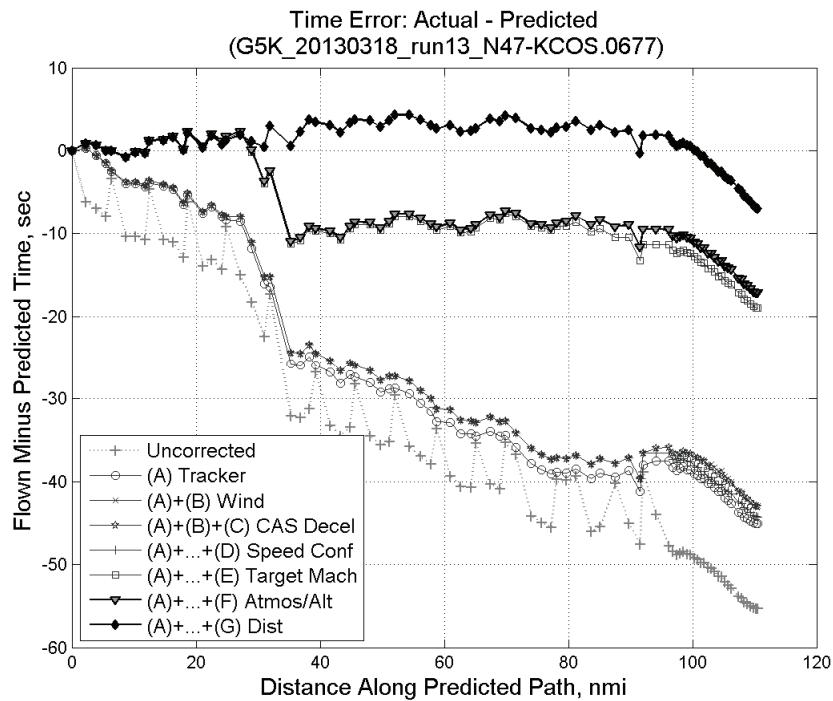


**Figure 926: Time error for run 13 showing incremental effect of removing each error source.**

#### D.3.A. Tracker Jumps

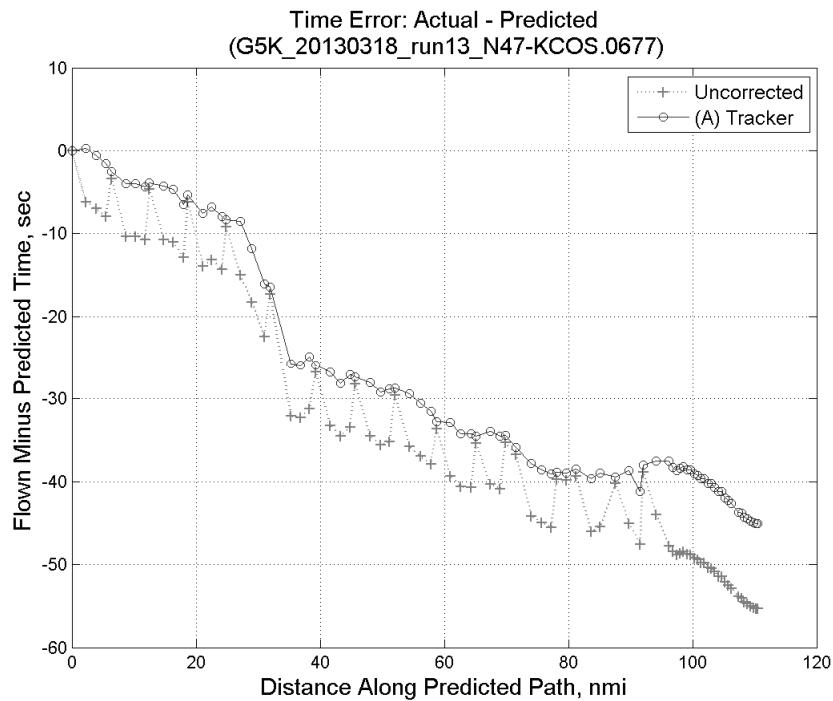


**Figure 927: Time error for run 13 before (Uncorrected) and after ((A) Tracker) removing tracker jump error source.**

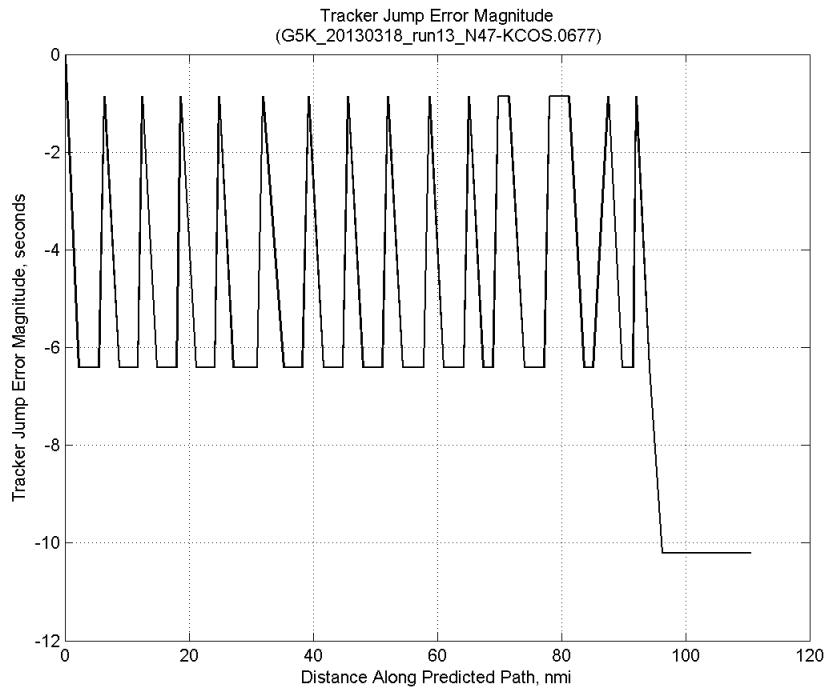


**Figure 928: Effect of tracker jump error source on time error for run 13.**

### D.3.B. Wind

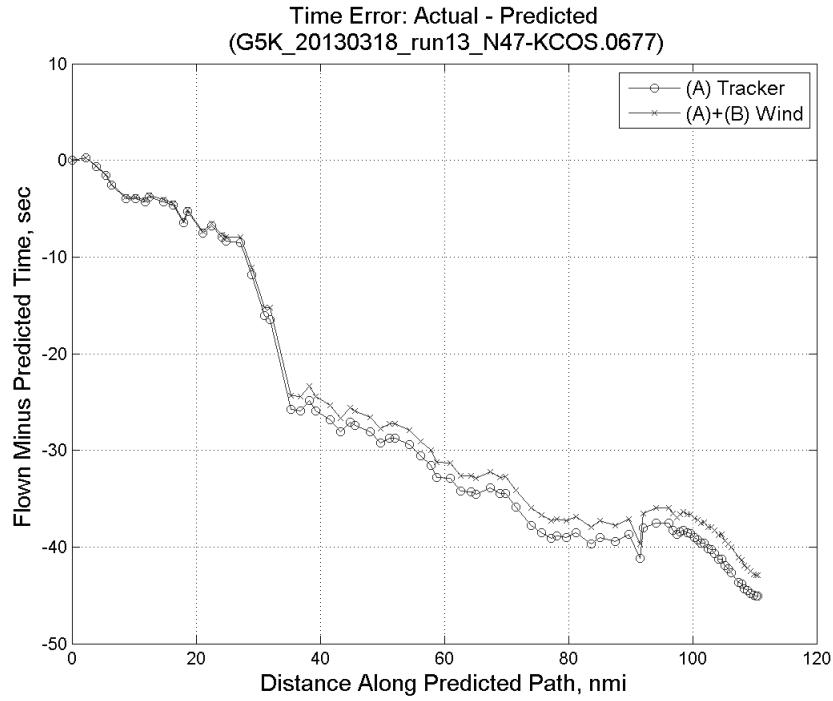


**Figure 929: Time error for run 13 before ((A) Tracker) and after ((A)+(B) Wind) removing wind error source.**

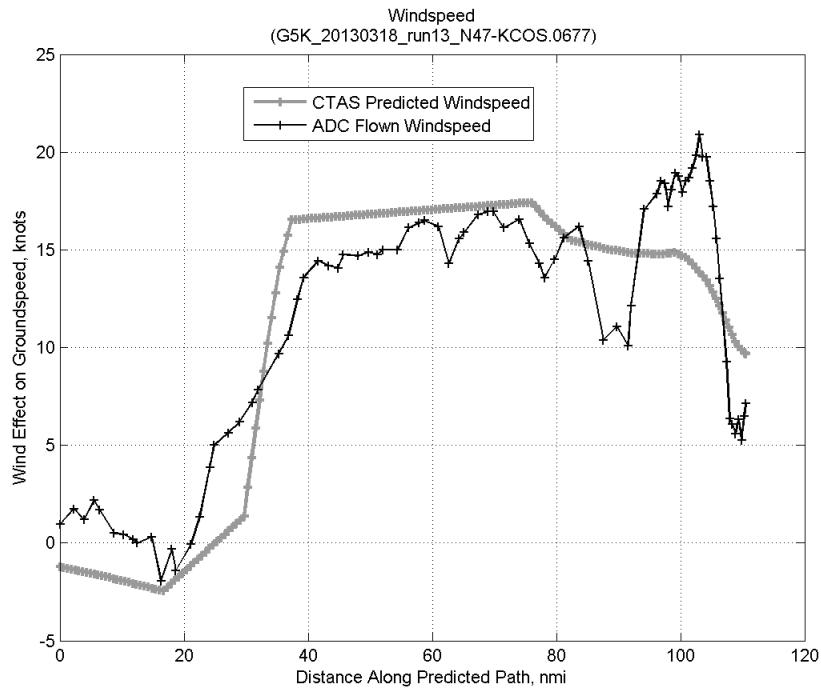


**Figure 930: CTAS predicted and ADC flown wind effect on ground speed for run 13. Negative values indicate a headwind.**

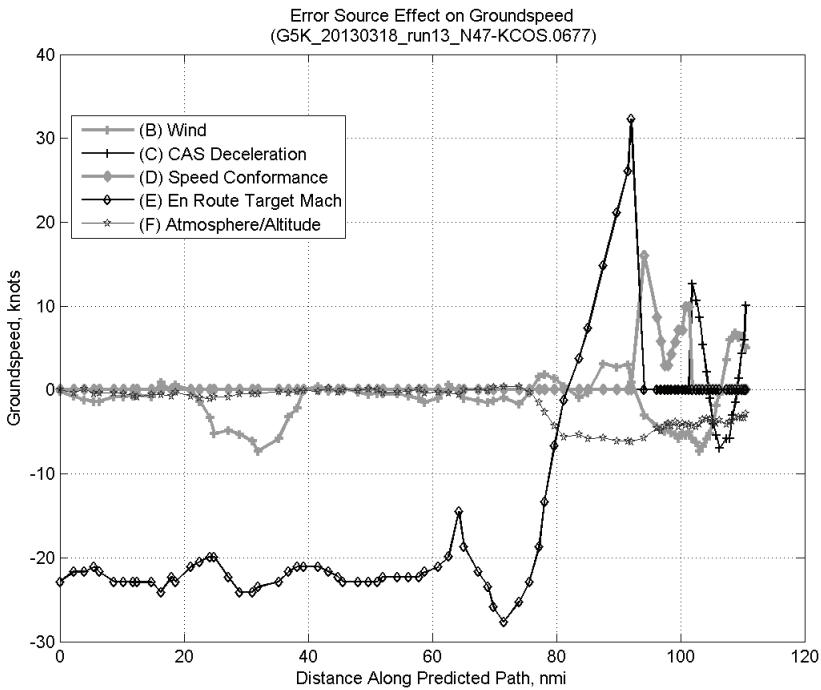


**Figure 931: Error sources (flown minus predicted) converted to a ground speed effect for run 13. Positive values indicate the flown ground speed was faster than the CTAS prediction.**

### D.3.C. CAS Deceleration

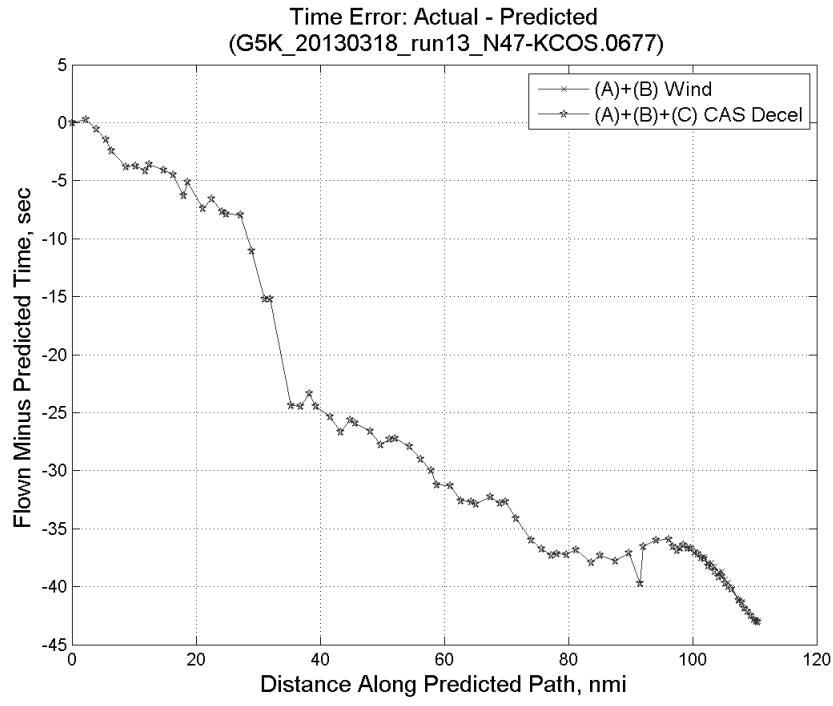


**Figure 932:** Time error for run 13 before ((A)+(B) Wind) and after ((A)+(B)+(C) CAS Decel) removing CAS deceleration error source.

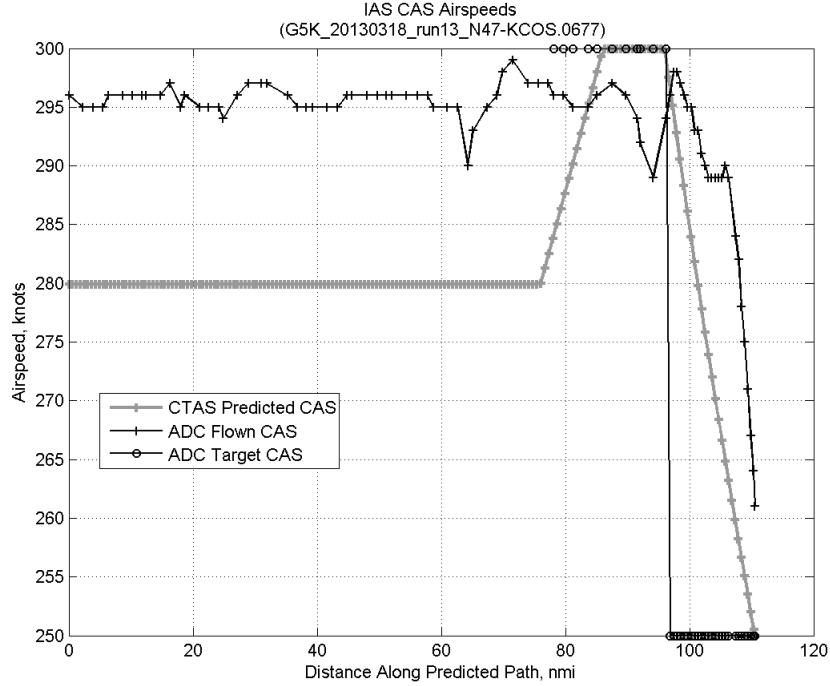


**Figure 933:** CTAS predicted and ADC flown CAS for run 13. CAS that is being targeted is shown with circle markers.

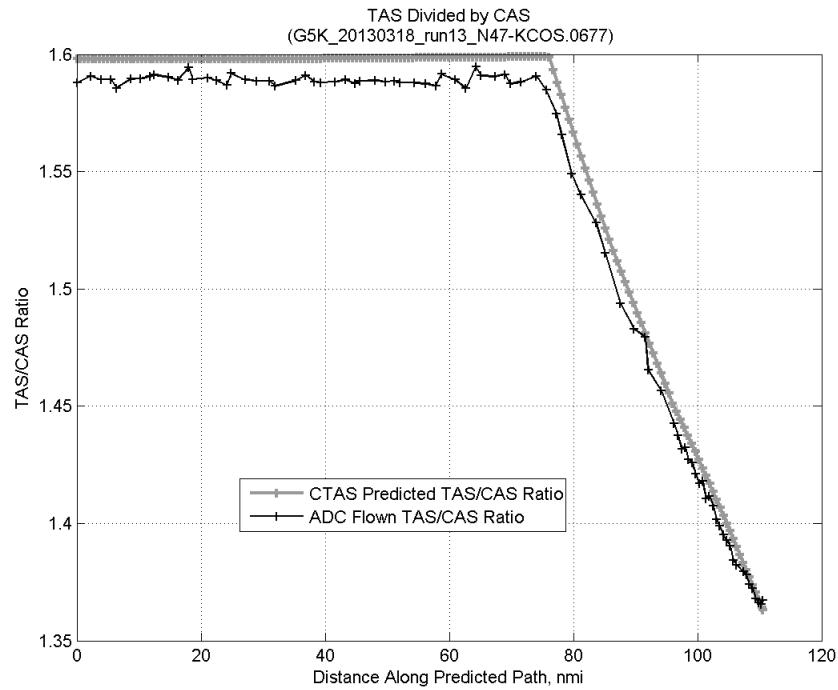


**Figure 934: CTAS predicted and ADC flown TAS/CAS ratio for run 13.**

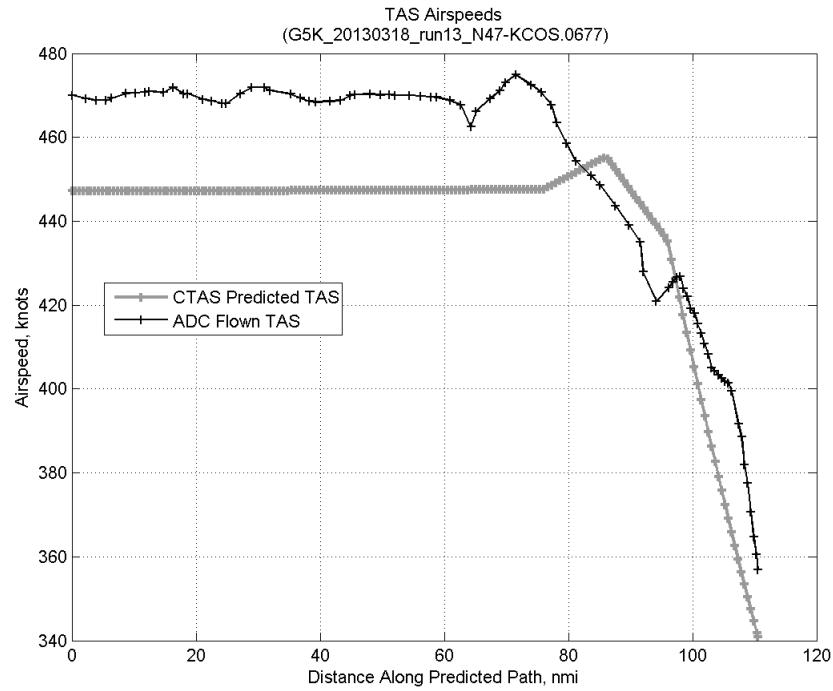


**Figure 935: CTAS predicted and ADC flown TAS for run 13.**

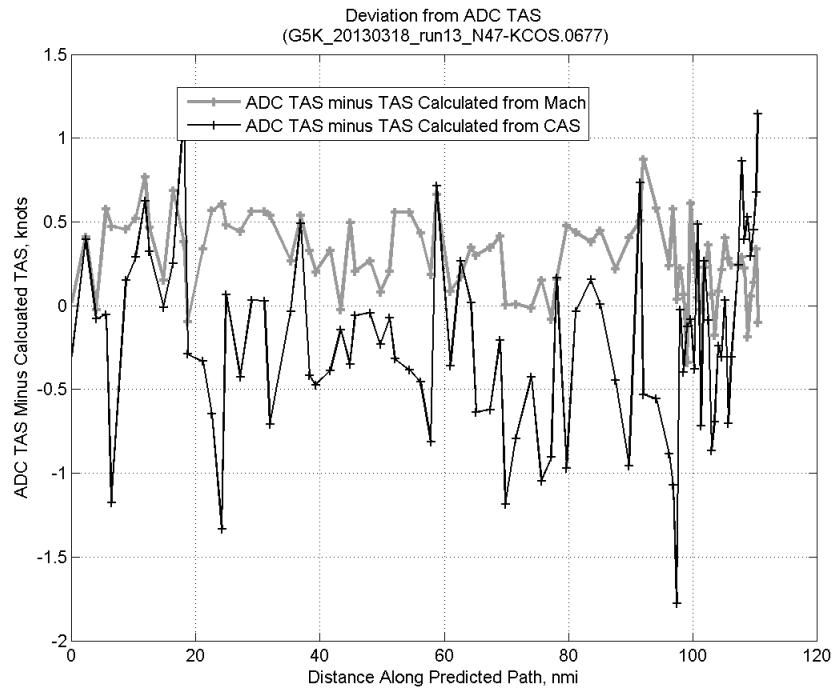


**Figure 936: Deviation from ADC flown TAS if calculating TAS using ADC flown CAS, Mach, atmospheric temperature, and atmospheric pressure for run 13.**

#### D.3.D. Speed Conformance

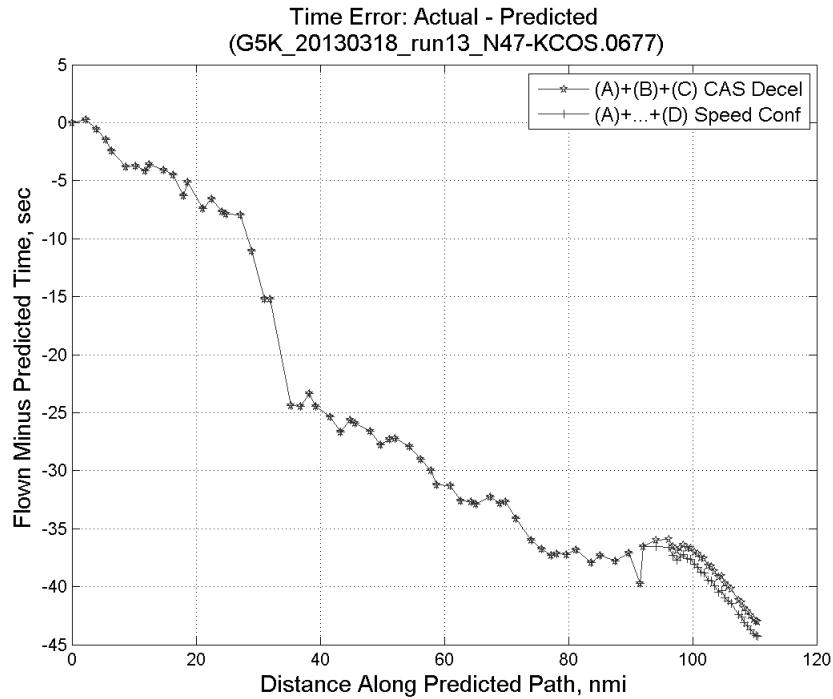


**Figure 937: Time error for run 13 before ((A)+(B)+(C) CAS Decel) and after ((A)+...+(D) Speed Conf) removing speed conformance error source.**

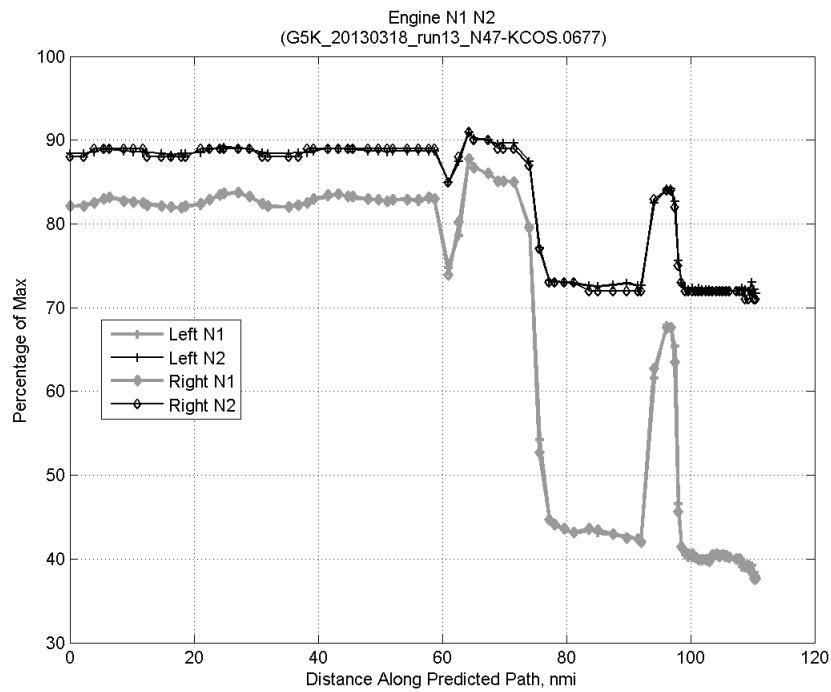


**Figure 938: Flown engine N1 and N2 for run 13.**

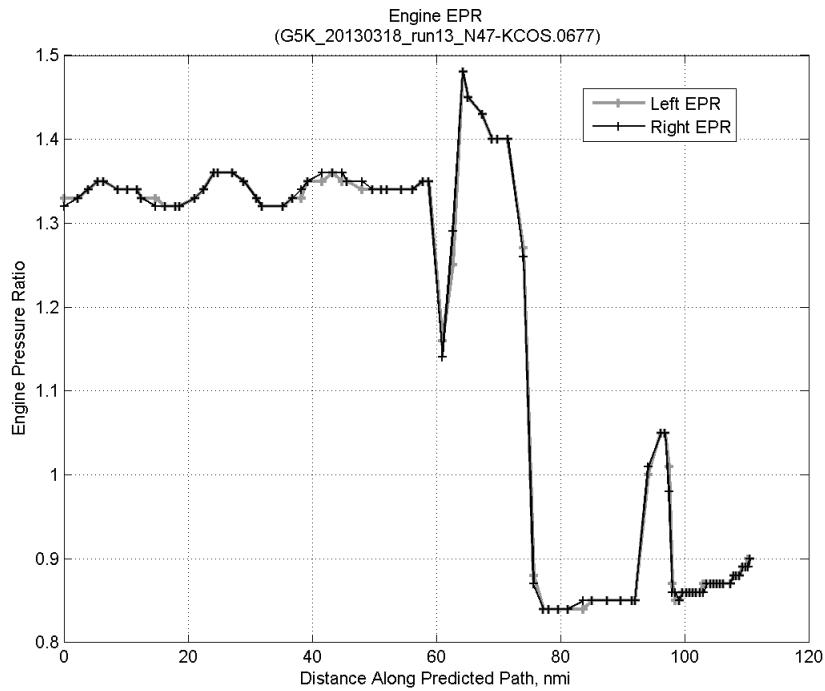


**Figure 939: Flown engine EPR for run 13.**

### D.3.E. Target Mach

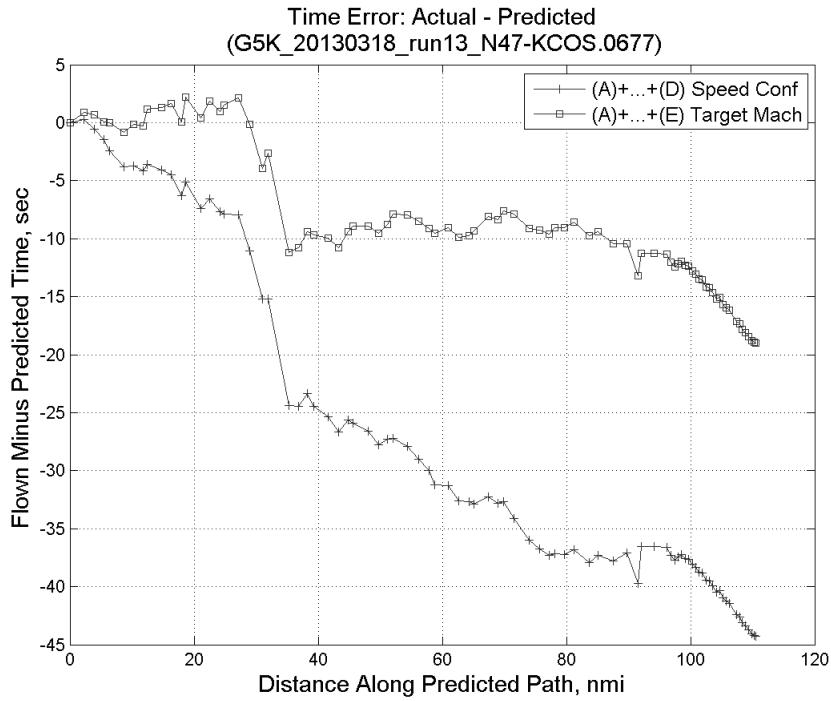


**Figure 940:** Time error for run 13 before ((A)+...+(D) Speed Conf) and after ((A)+...+(E) Target Mach) removing target Mach error source.

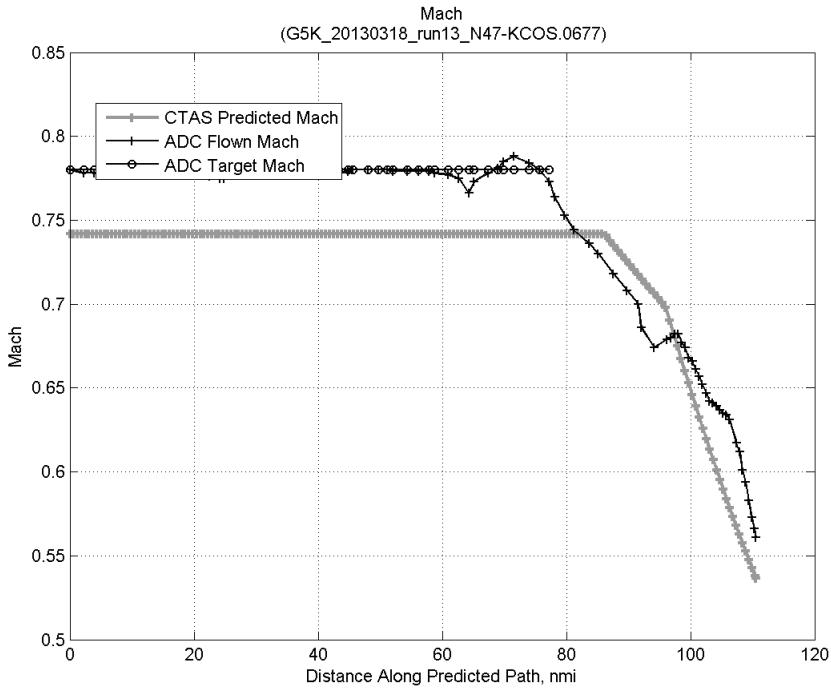


**Figure 941:** CTAS predicted and ADC flown Mach for run 13. Mach being targeted (ADC) shown with circle markers.

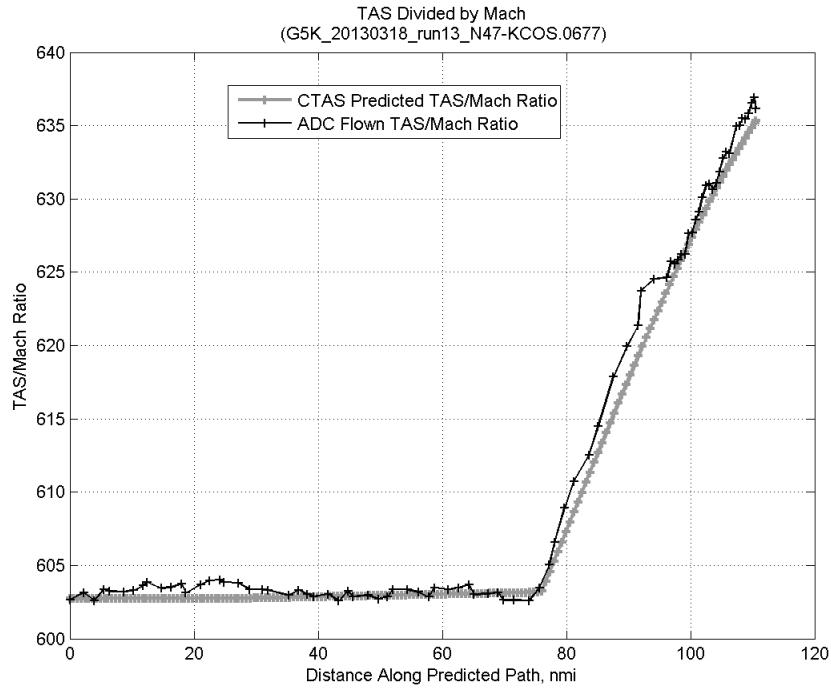


**Figure 942: CTAS predicted and ADC flown TAS/Mach ratio for run 13.**

#### D.3.F. Atmosphere/Altitude

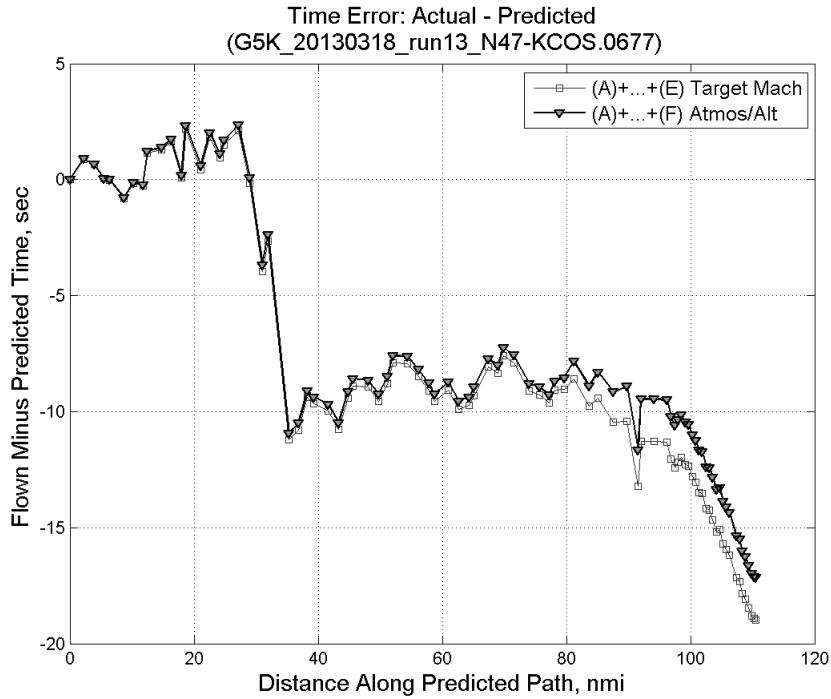


**Figure 943: Time error for run 13 before ((A)+...+(E) Target Mach) and after ((A)+...+(F) Atmos/Alt) removing atmosphere/altitude error source.**

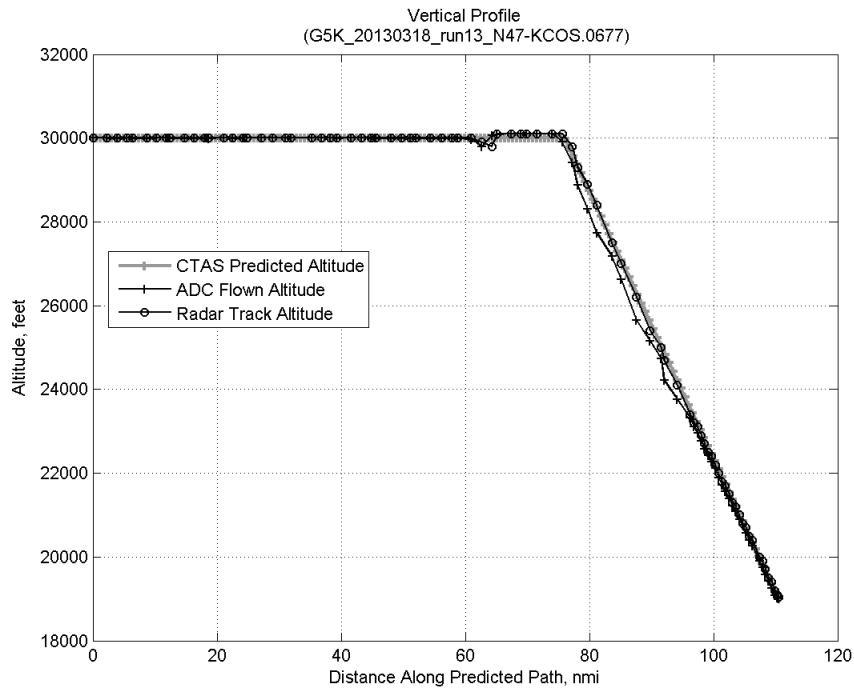


**Figure 944:** Flown (ADC) and predicted (CTAS) vertical profile for run 13.

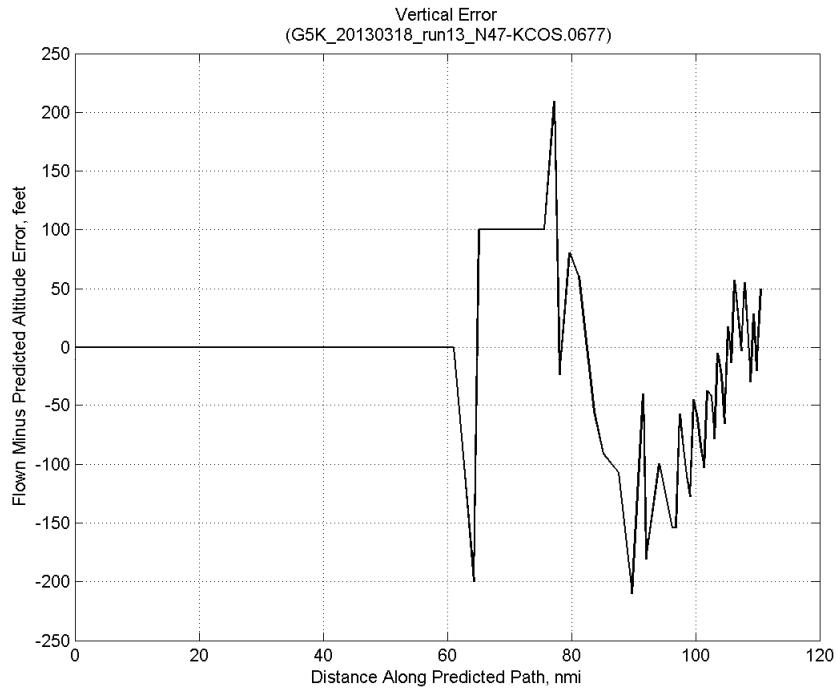


**Figure 945:** Vertical error (flown minus predicted altitude) for run 13. Positive values indicate aircraft flew higher than predicted by CTAS.

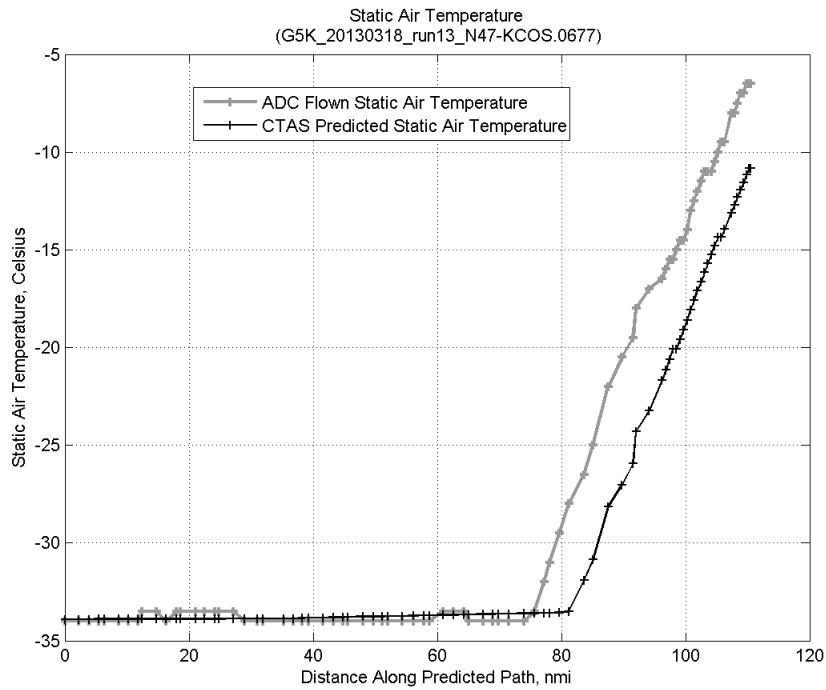


**Figure 946: Flown (ADC) and predicted (CTAS) static air temperature for run 13.**

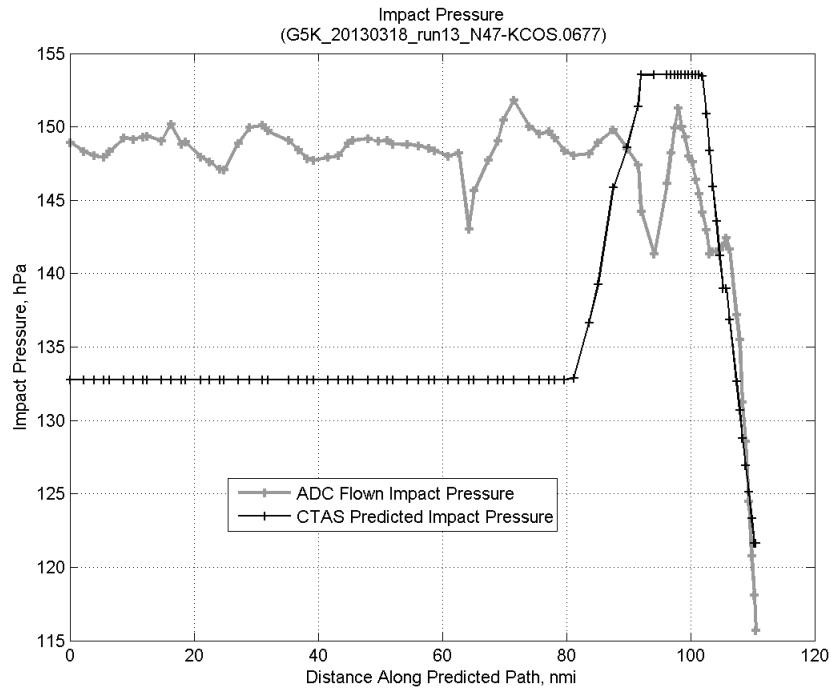


**Figure 947: Flown (ADC) and predicted (CTAS) impact pressure for run 13.**

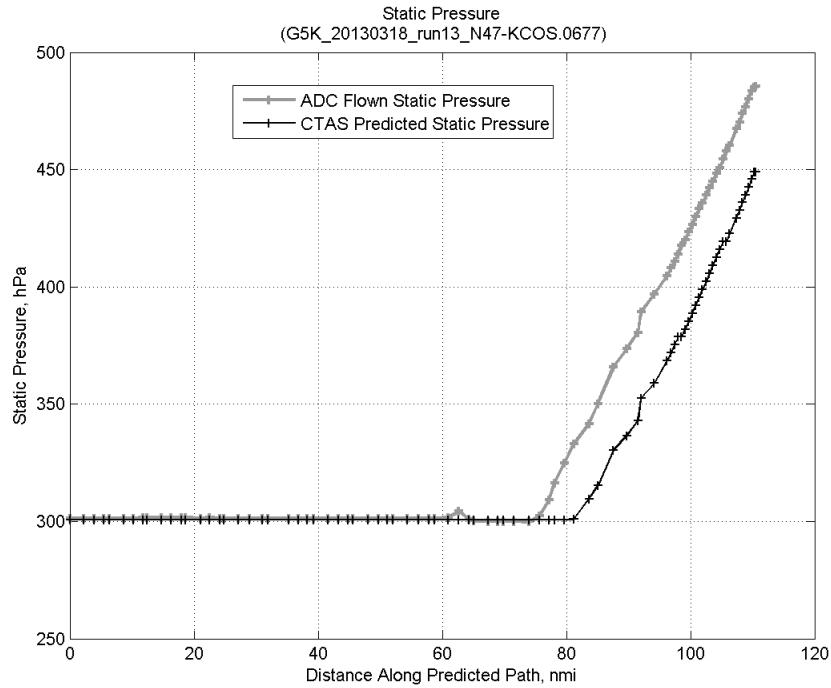


**Figure 948: Flown (ADC) and predicted (CTAS) static pressure for run 13.**

### D.3.G. Path Distance

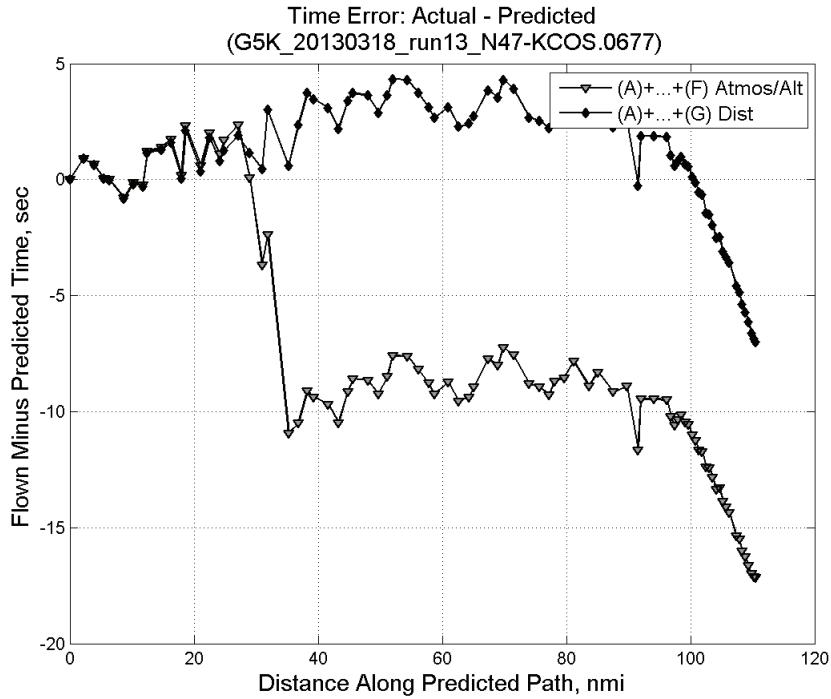


**Figure 949: Time error for run 13 before ((A)+...+(F) Atmos/Alt) and after ((A)+...+(G) Dist) removing path distance error source.**

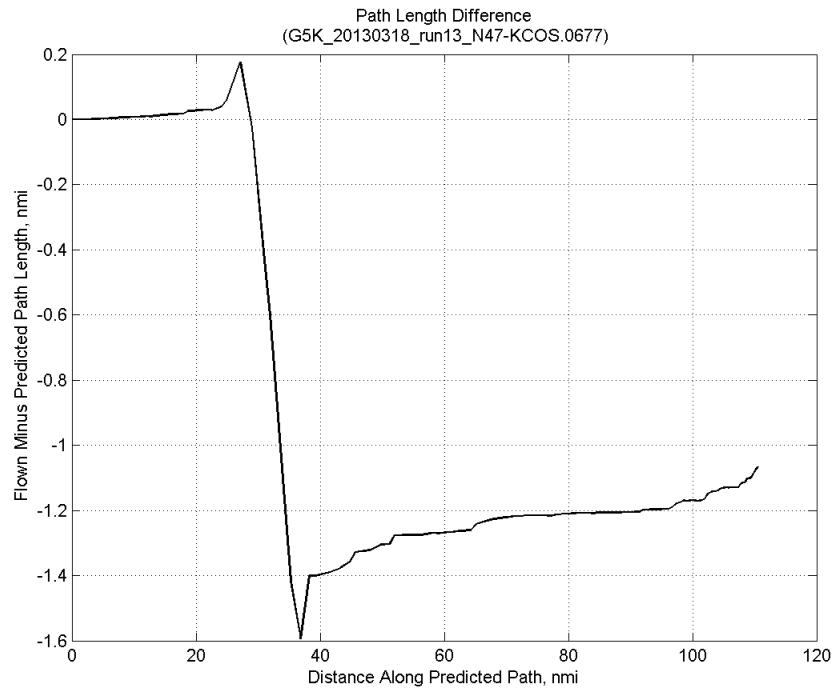


**Figure 950: ADC flown minus CTAS predicted path length for run 13. Positive values indicate aircraft followed a longer path than predicted by CTAS.**

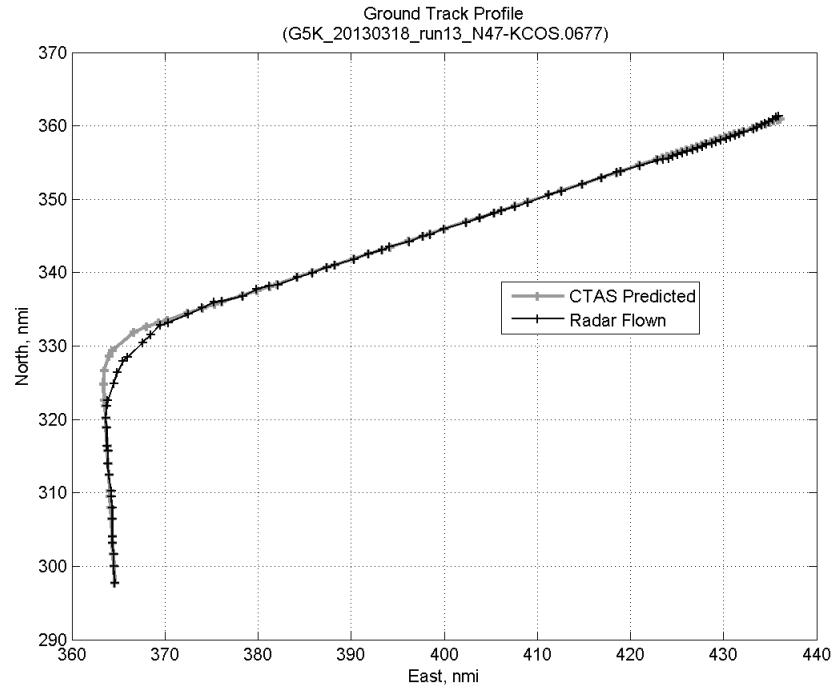


**Figure 951: CTAS predicted and radar flown ground track profile for run 13.**

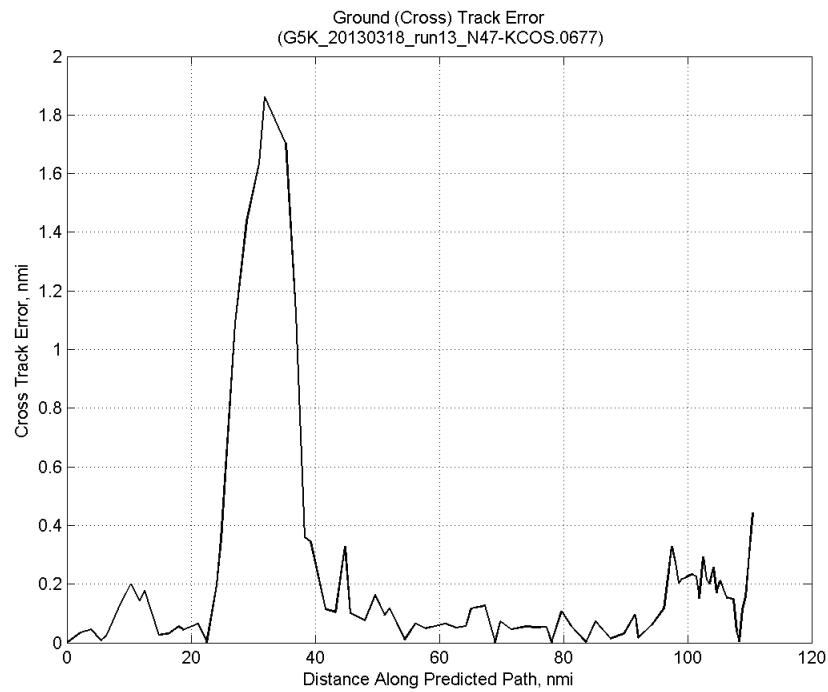


**Figure 952: Ground (cross) track error for run 13.**

#### D.4. Run 15

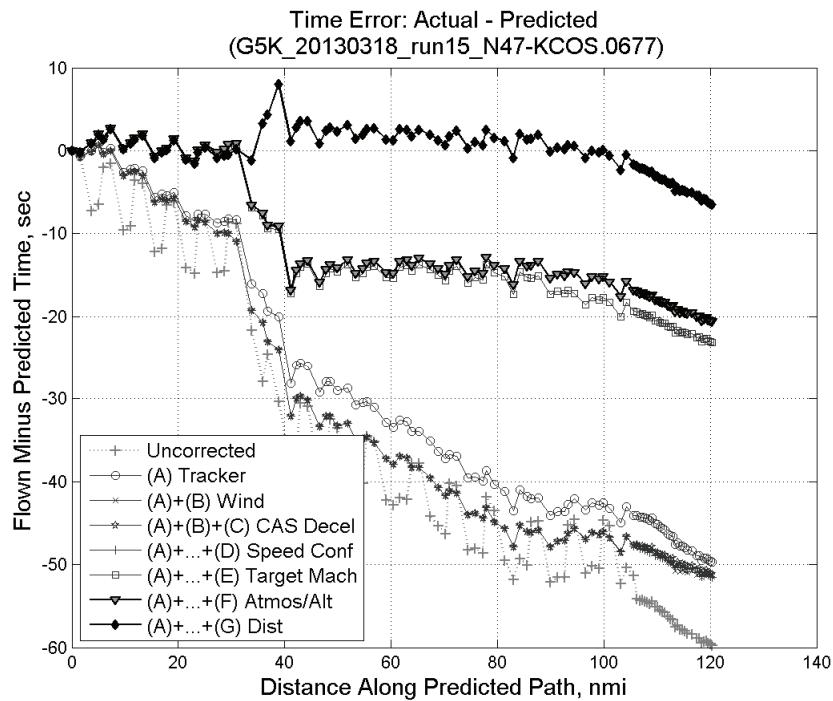


**Figure 953:** Time error for run 15 showing incremental effect of removing each error source.

#### D.4.A. Tracker Jumps

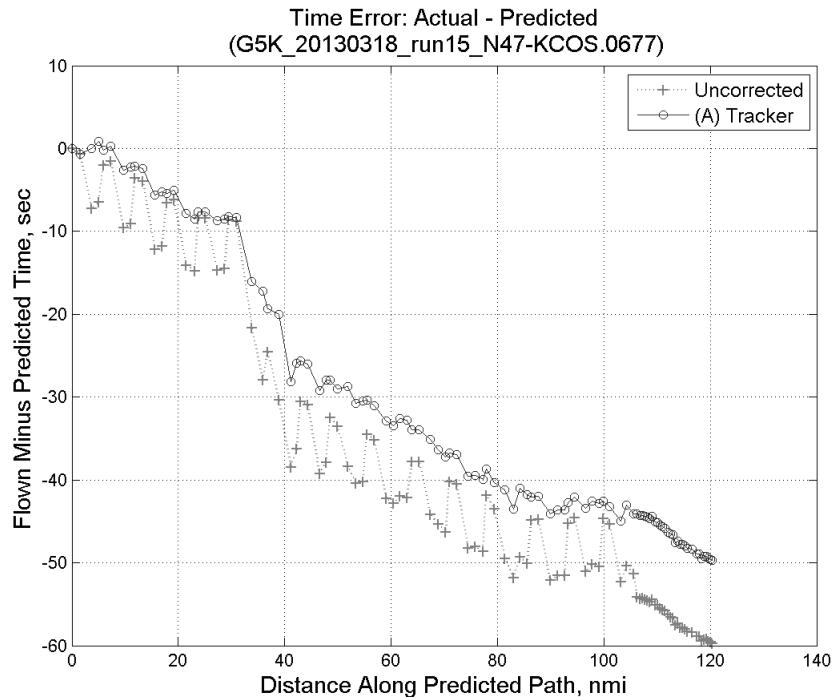


**Figure 954:** Time error for run 15 before (Uncorrected) and after ((A) Tracker) removing tracker jump error source.

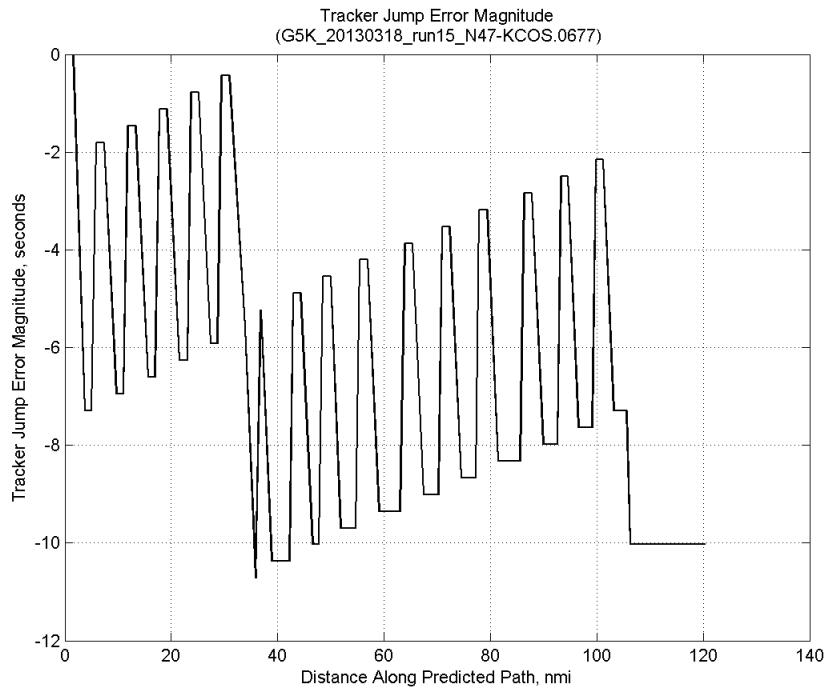


**Figure 955: Effect of tracker jump error source on time error for run 15.**

#### D.4.B. Wind

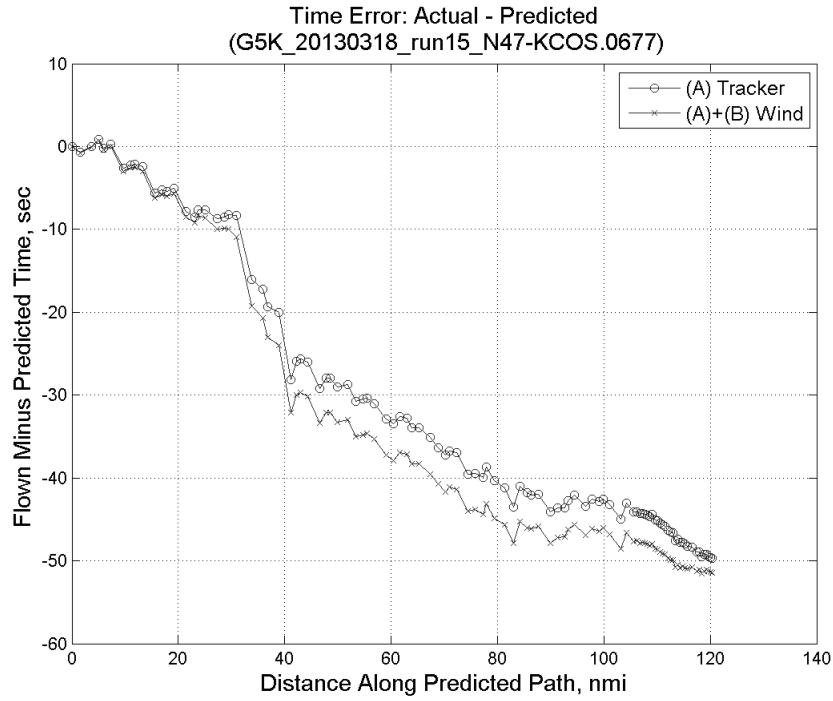


**Figure 956: Time error for run 15 before ((A) Tracker) and after ((A)+(B) Wind) removing wind error source.**

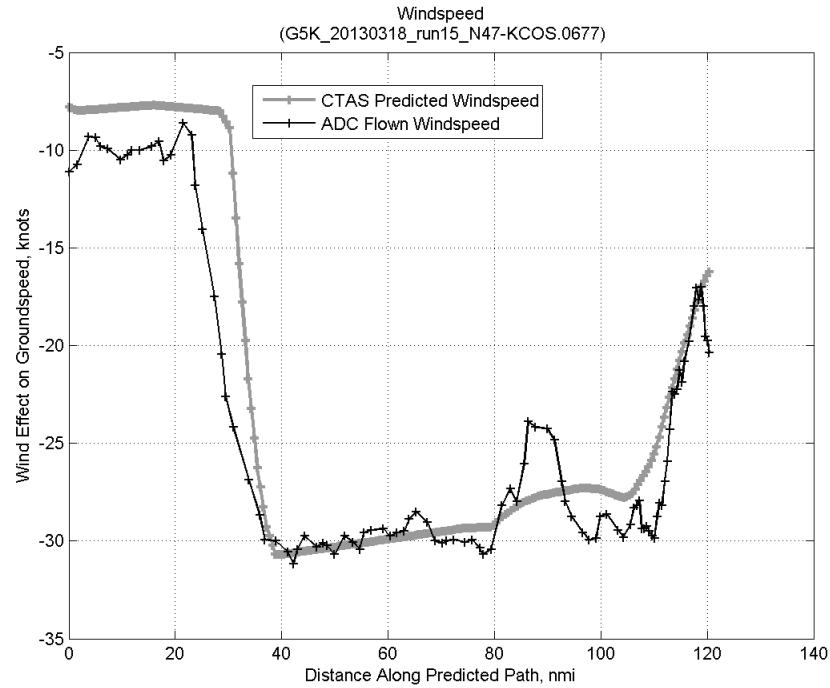


**Figure 957: CTAS predicted and ADC flown wind effect on ground speed for run 15. Negative values indicate a headwind.**

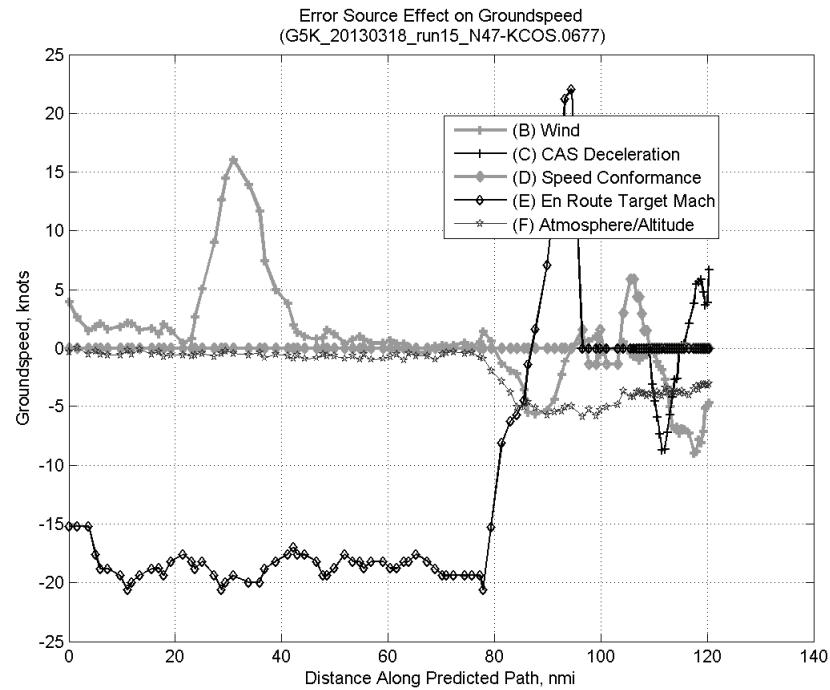


**Figure 958: Error sources (flown minus predicted) converted to a ground speed effect for run 15. Positive values indicate the flown ground speed was faster than the CTAS prediction.**

#### D.4.C. CAS Deceleration

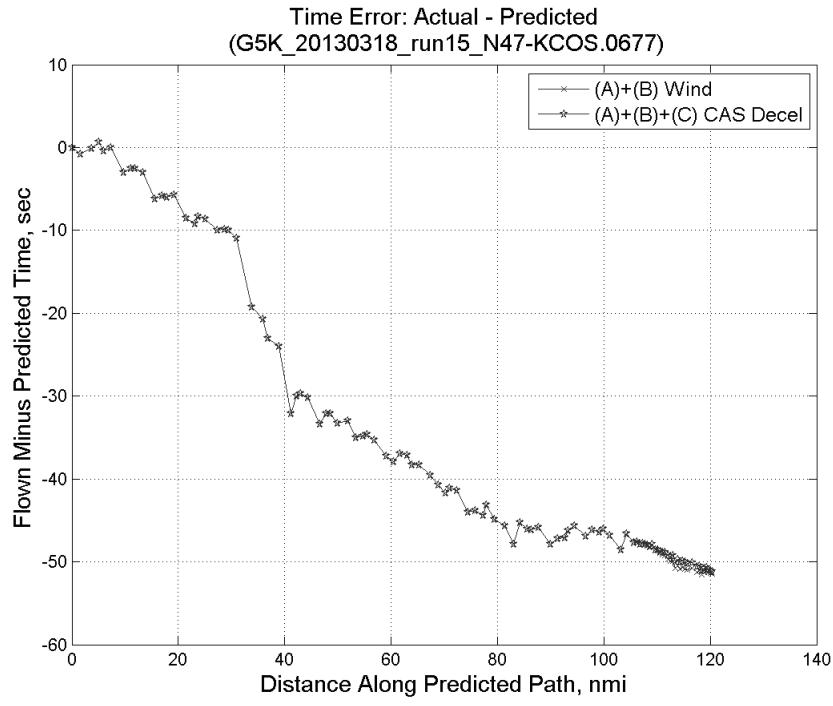


**Figure 959: Time error for run 15 before ((A)+(B) Wind) and after ((A)+(B)+(C) CAS Decel) removing CAS deceleration error source.**

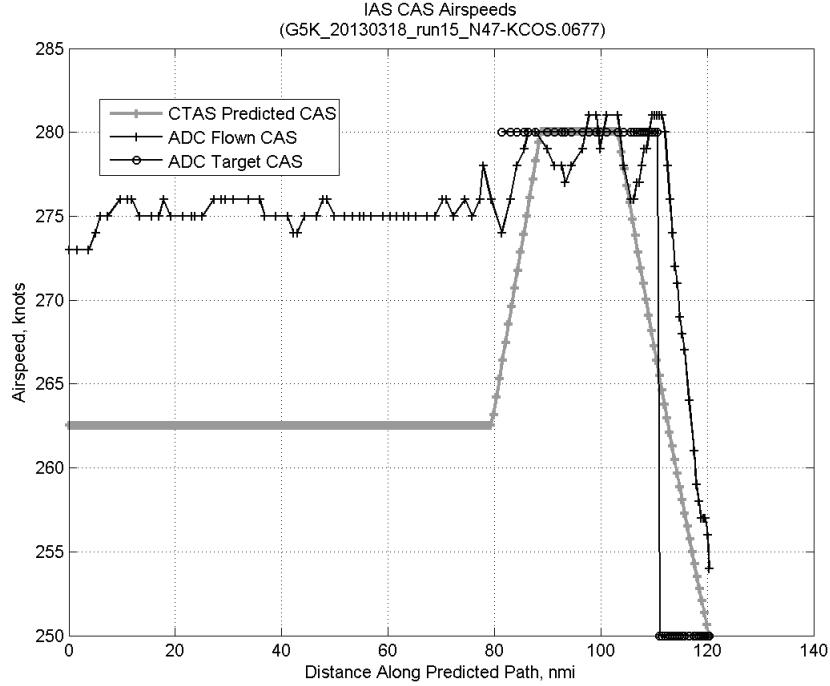


**Figure 960: CTAS predicted and ADC flown CAS for run 15. CAS that is being targeted is shown with circle markers.**

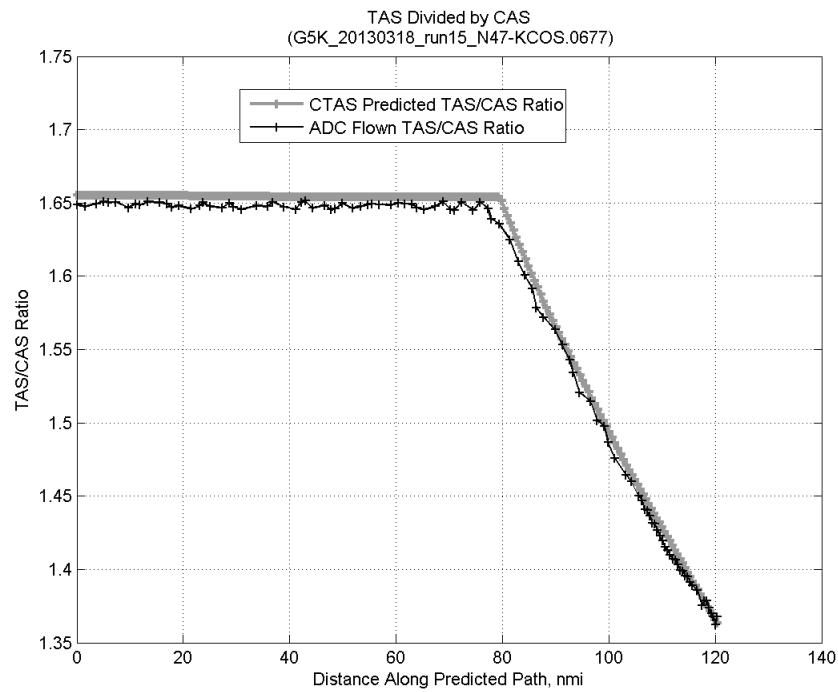


**Figure 961: CTAS predicted and ADC flown TAS/CAS ratio for run 15.**

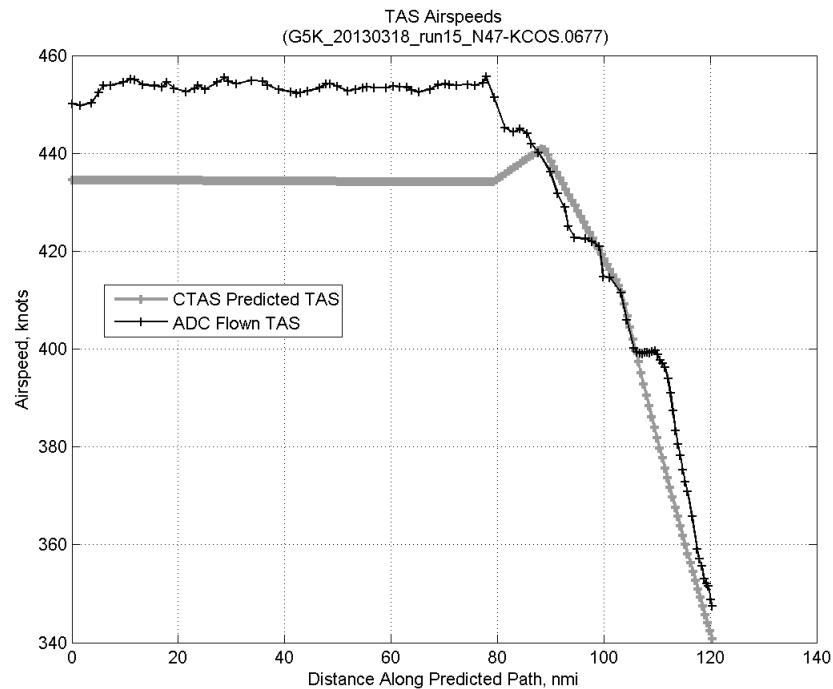


**Figure 962: CTAS predicted and ADC flown TAS for run 15.**

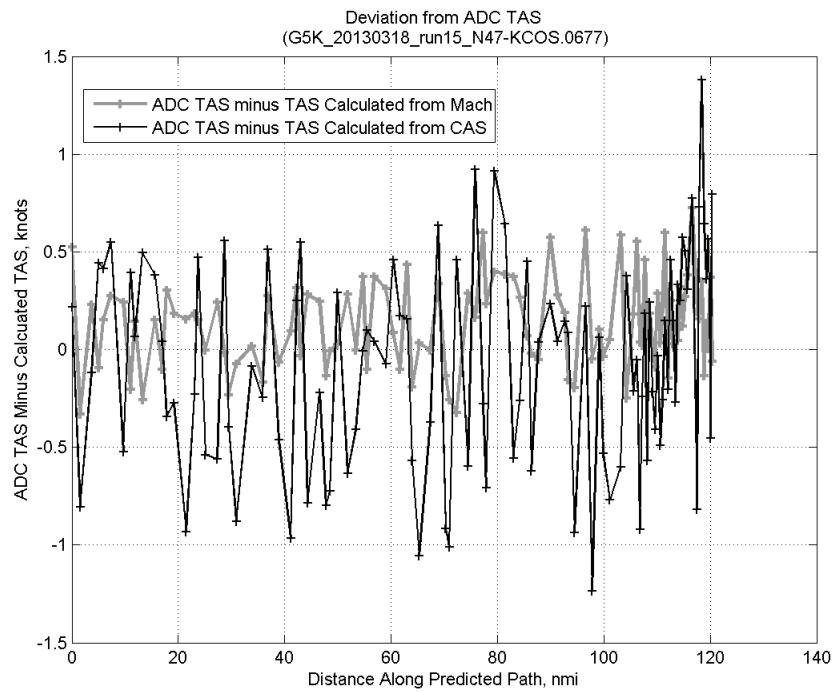


**Figure 963:** Deviation from ADC flown TAS if calculating TAS using ADC flown CAS, Mach, atmospheric temperature, and atmospheric pressure for run 15.

#### D.4.D. Speed Conformance

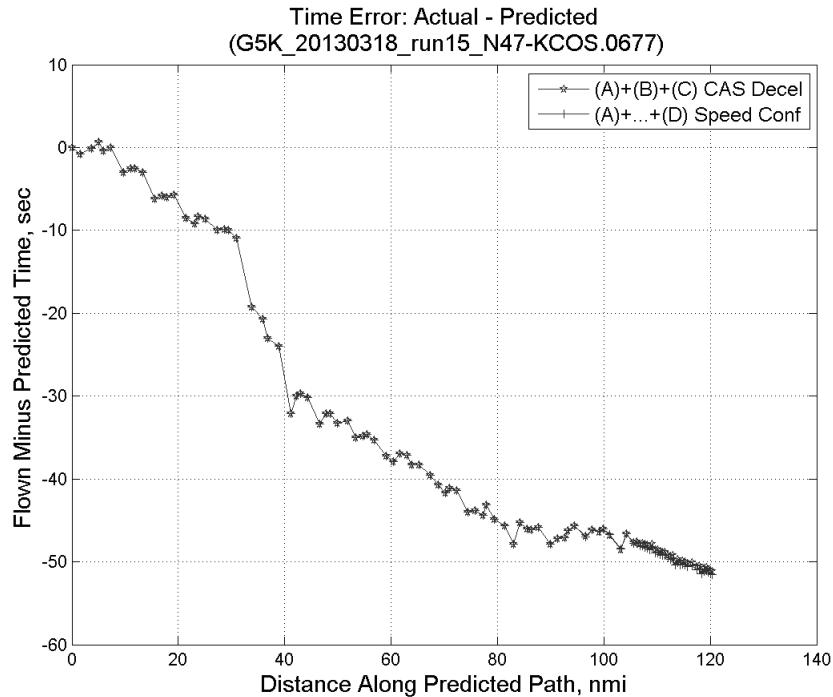


**Figure 964:** Time error for run 15 before  $((A)+(B)+(C) \text{ CAS Decel})$  and after  $((A)+\dots+(D) \text{ Speed Conf})$  removing speed conformance error source.

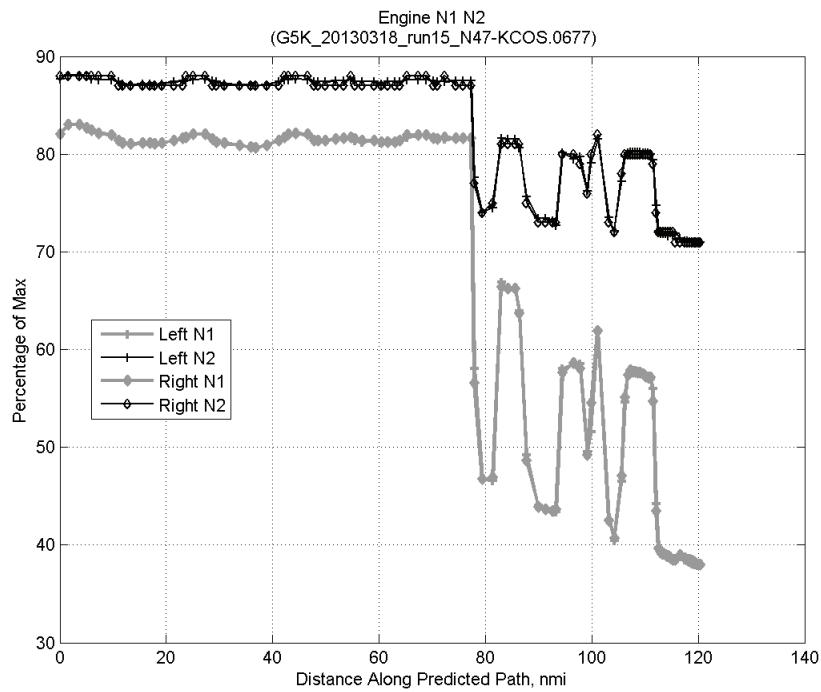


**Figure 965: Flown engine N1 and N2 for run 15.**

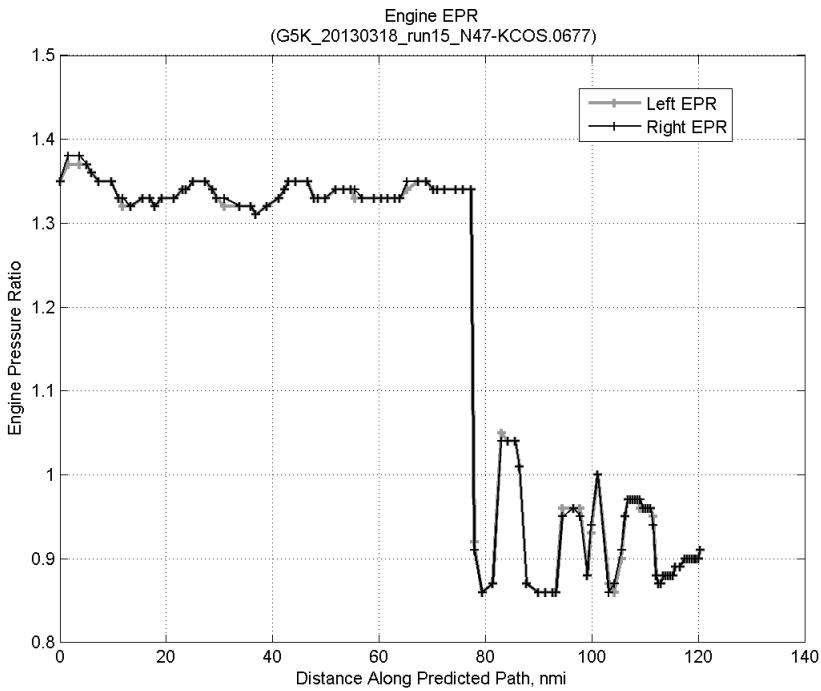


**Figure 966: Flown engine EPR for run 15.**

#### D.4.E. Target Mach

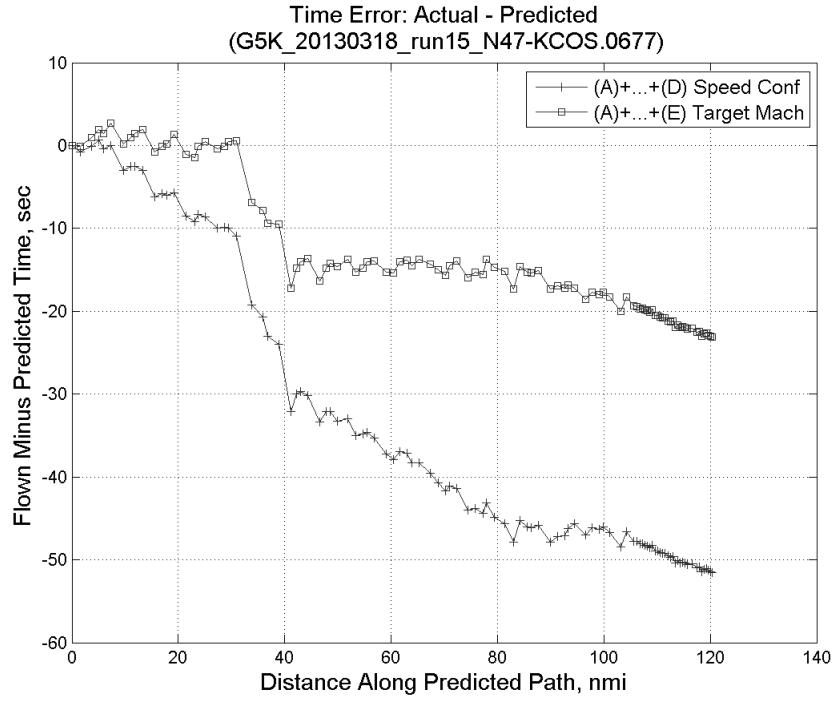


**Figure 967:** Time error for run 15 before ((A)+...+(D) Speed Conf) and after ((A)+...+(E) Target Mach) removing target Mach error source.

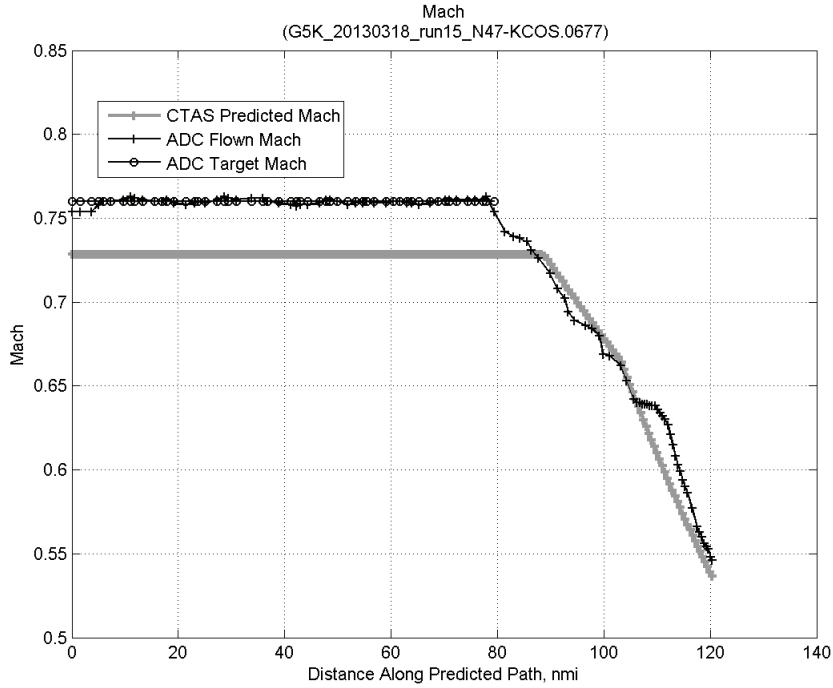


**Figure 968:** CTAS predicted and ADC flown Mach for run 15. Mach being targeted (ADC) shown with circle markers.

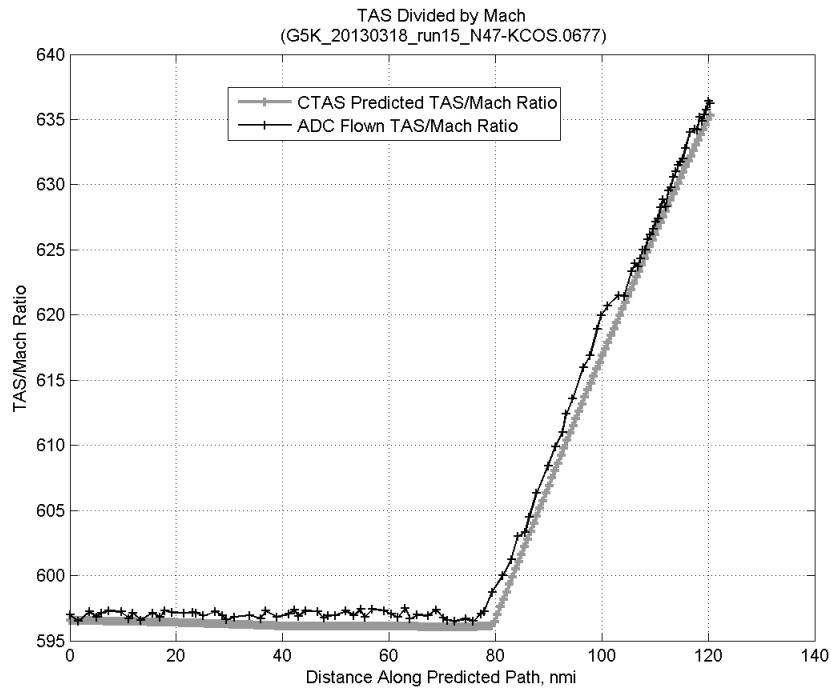


**Figure 969:** CTAS predicted and ADC flown TAS/Mach ratio for run 15.

#### D.4.F. Atmosphere/Altitude

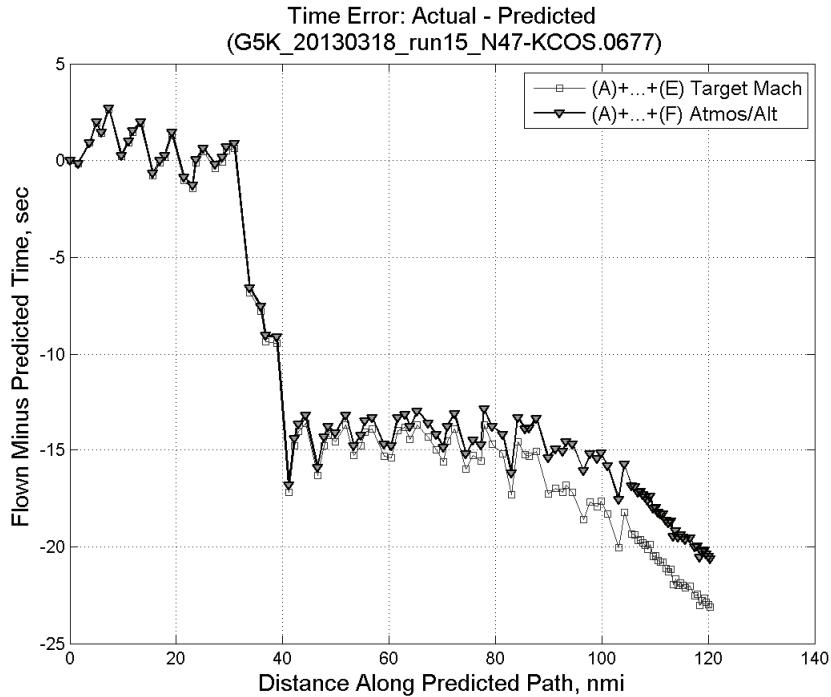


**Figure 970:** Time error for run 15 before ((A)+...+(E) Target Mach) and after ((A)+...+(F) Atmos/Alt) removing atmosphere/altitude error source.

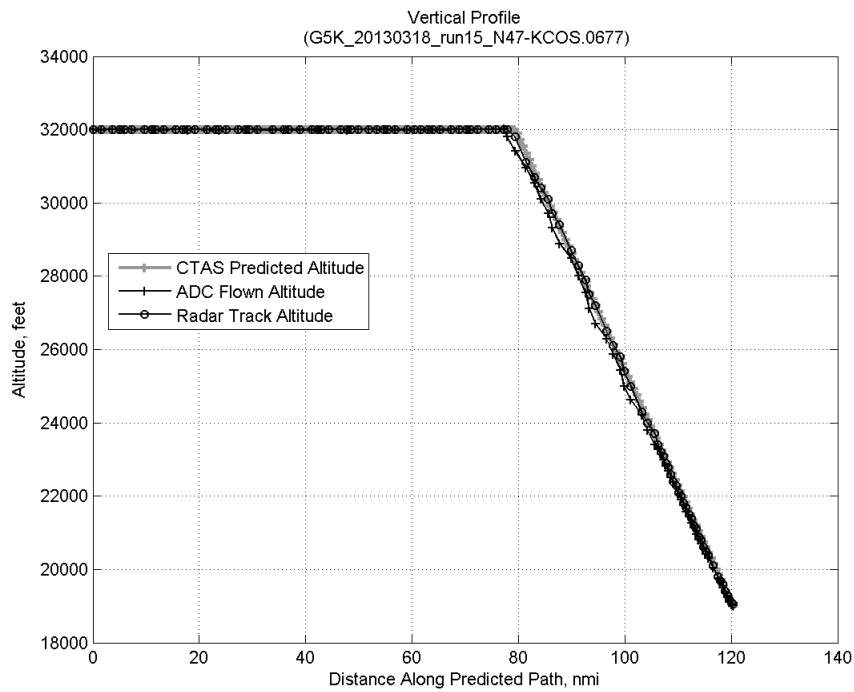


**Figure 971: Flown (ADC) and predicted (CTAS) vertical profile for run 15.**

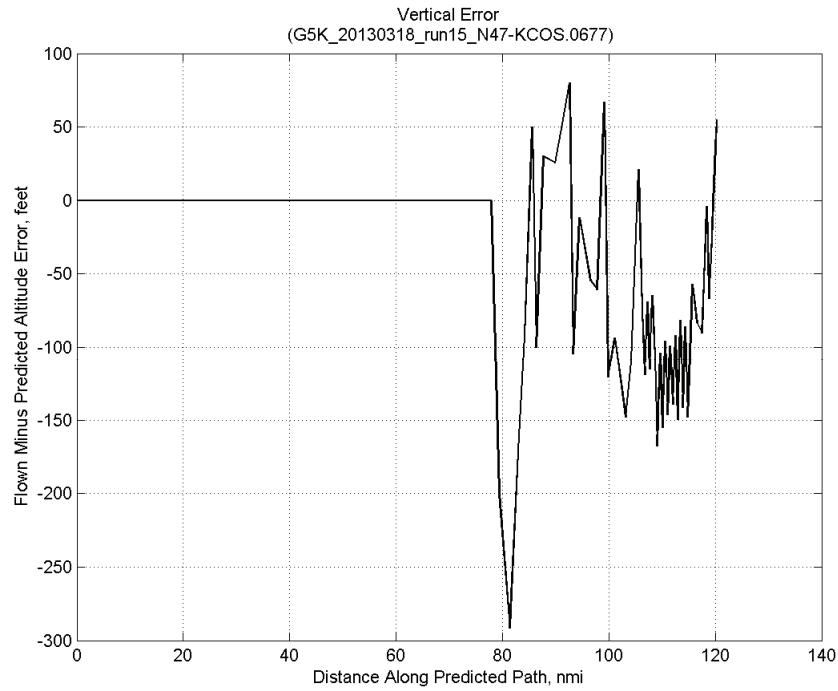


**Figure 972: Vertical error (flown minus predicted altitude) for run 15. Positive values indicate aircraft flew higher than predicted by CTAS.**

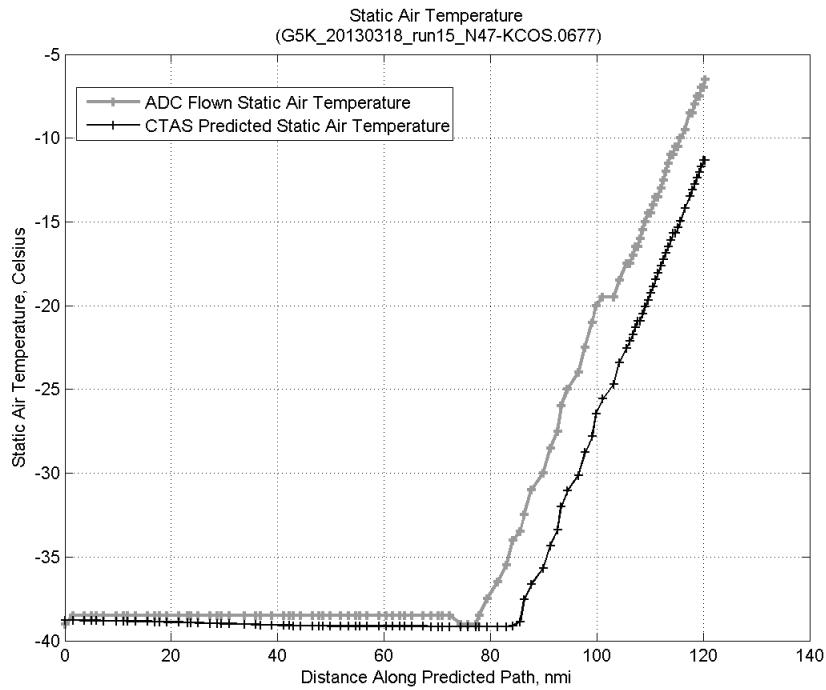


**Figure 973: Flown (ADC) and predicted (CTAS) static air temperature for run 15.**

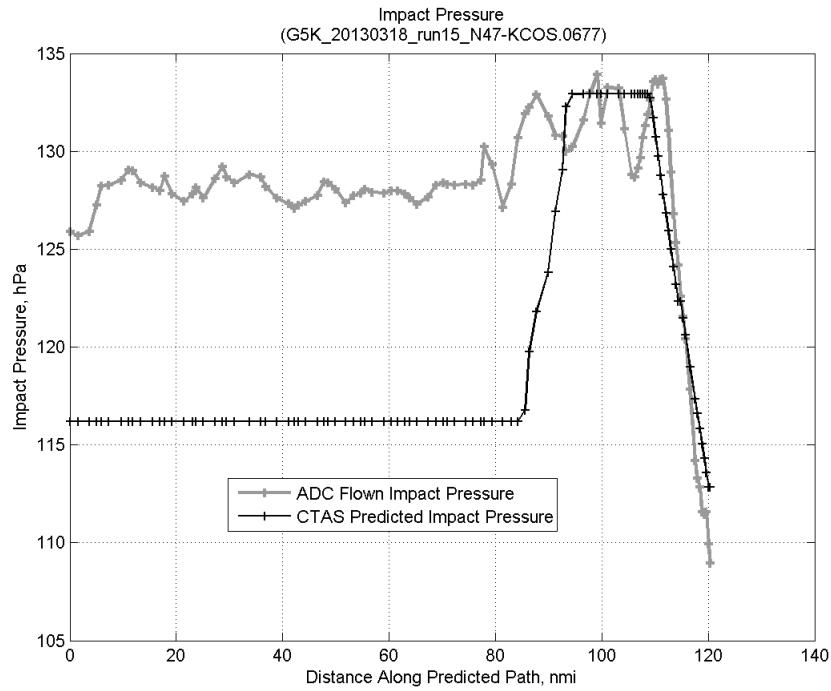


**Figure 974: Flown (ADC) and predicted (CTAS) impact pressure for run 15.**

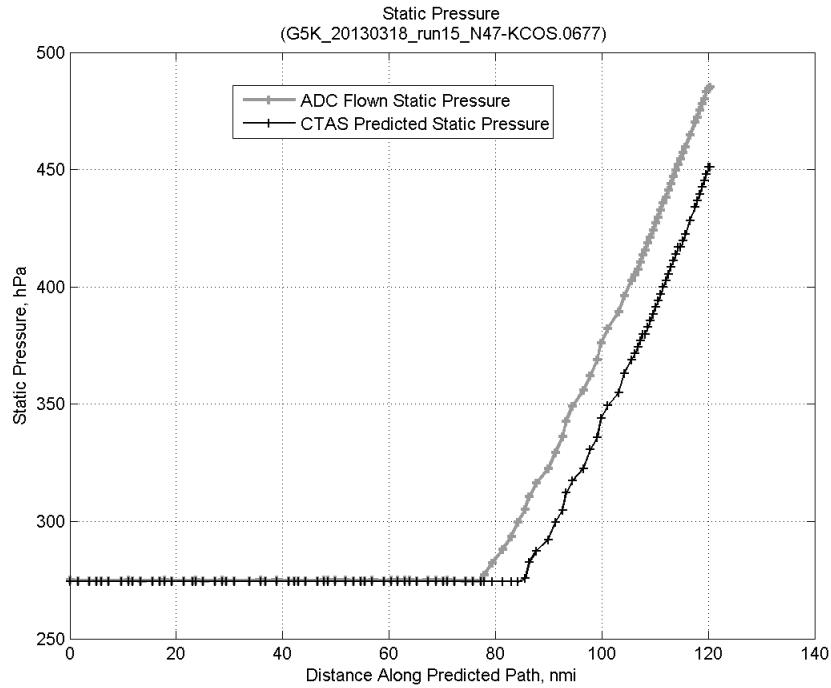


**Figure 975: Flown (ADC) and predicted (CTAS) static pressure for run 15.**

#### D.4.G. Path Distance

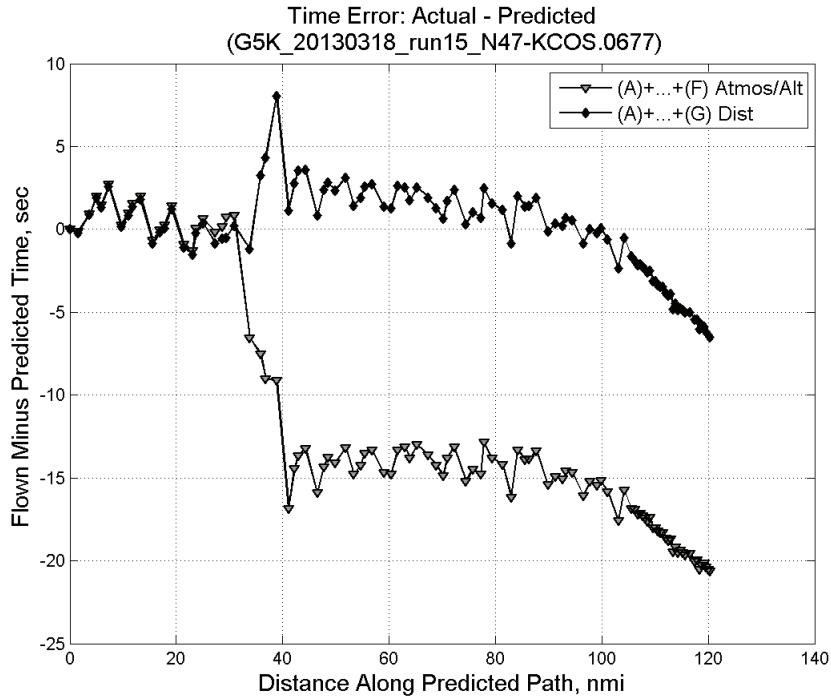


**Figure 976: Time error for run 15 before ((A)+...+(F) Atmos/Alt) and after ((A)+...+(G) Dist) removing path distance error source.**

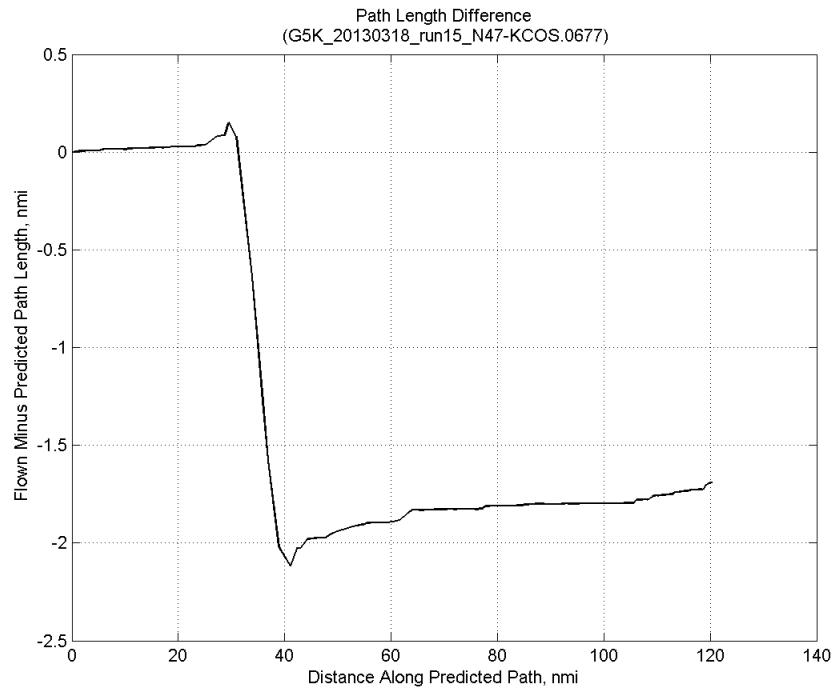


**Figure 977: ADC flown minus CTAS predicted path length for run 15. Positive values indicate aircraft followed a longer path than predicted by CTAS.**

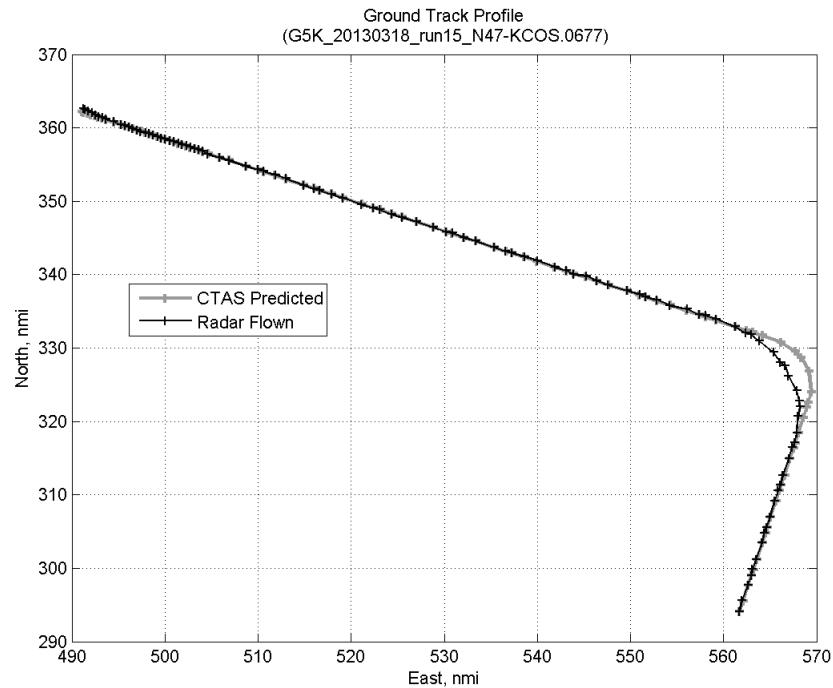


**Figure 978: CTAS predicted and radar flown ground track profile for run 15.**

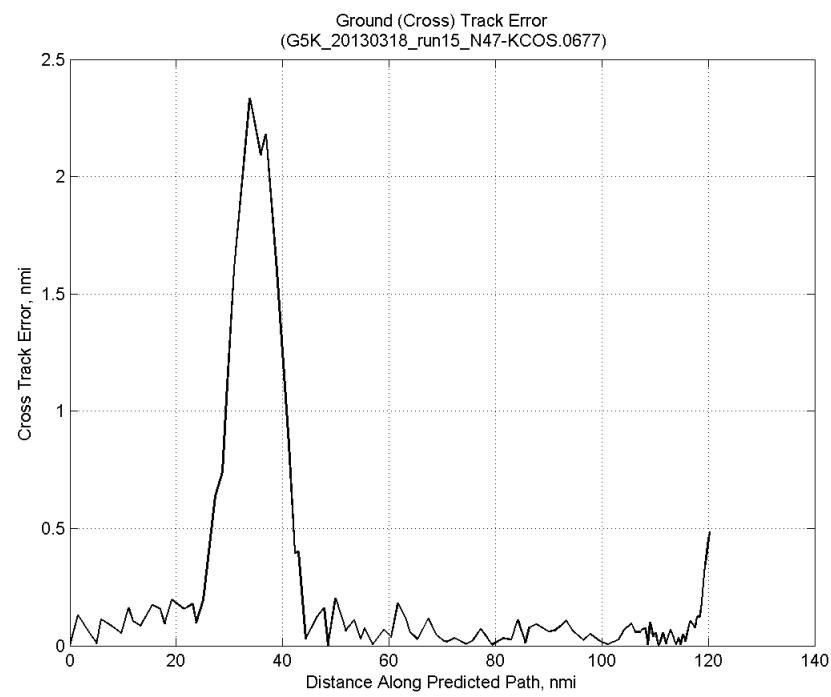


**Figure 979: Ground (cross) track error for run 15.**

## D.5. Run 17

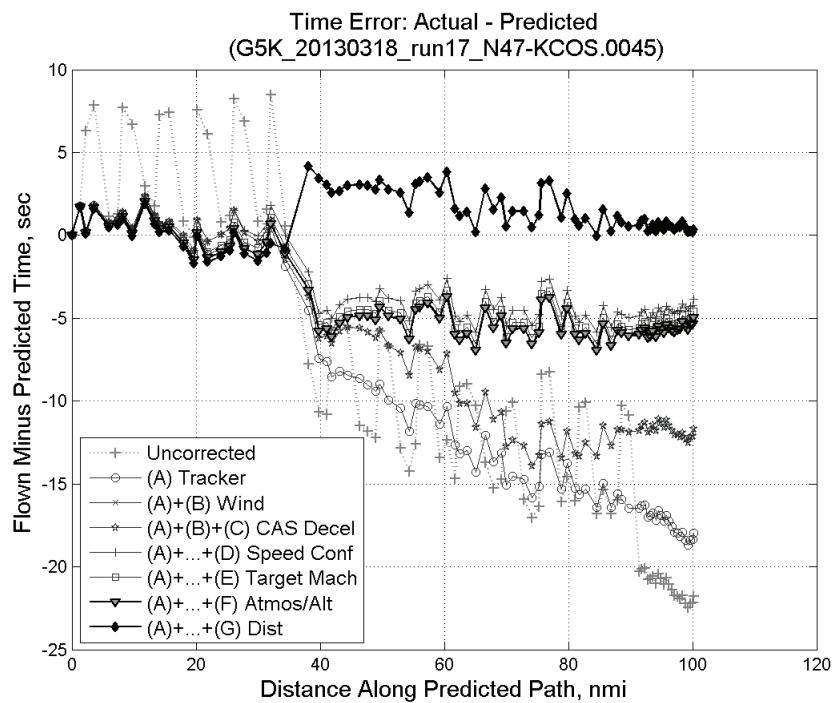


**Figure 980:** Time error for run 17 showing incremental effect of removing each error source.

### D.5.A. Tracker Jumps

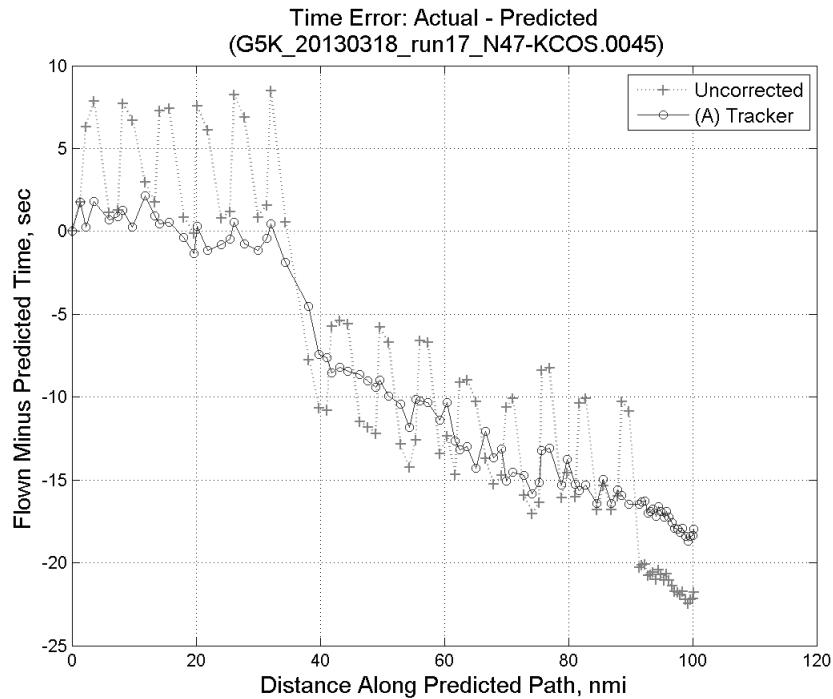


**Figure 981:** Time error for run 17 before (Uncorrected) and after ((A) Tracker) removing tracker jump error source.

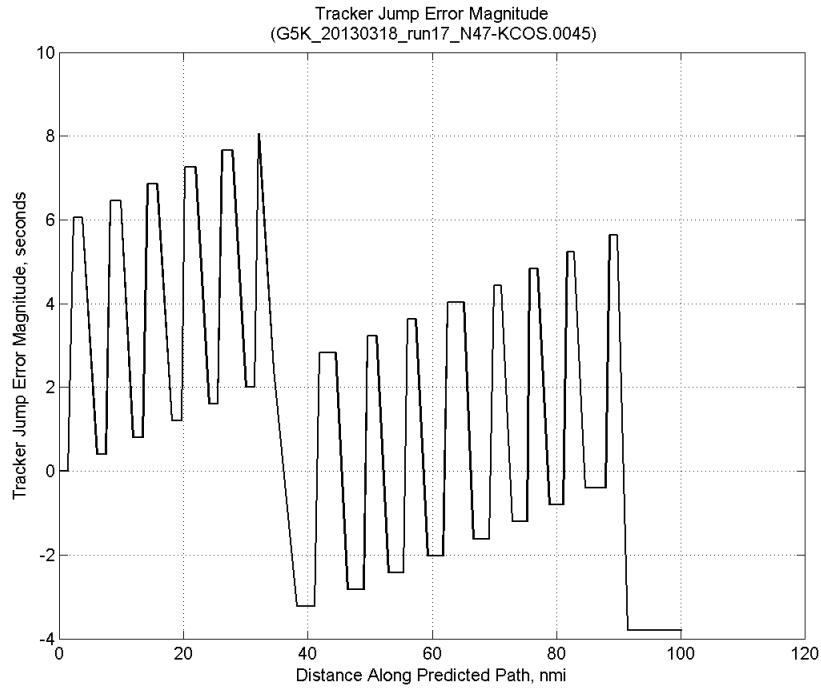


**Figure 982: Effect of tracker jump error source on time error for run 17.**

#### D.5.B. Wind

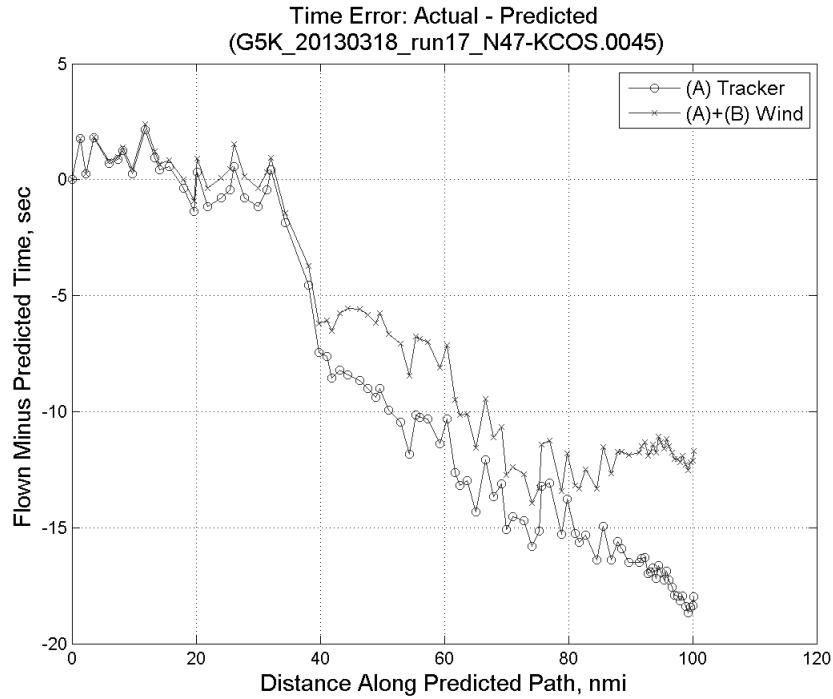


**Figure 983: Time error for run 17 before ((A) Tracker) and after ((A)+(B) Wind) removing wind error source.**

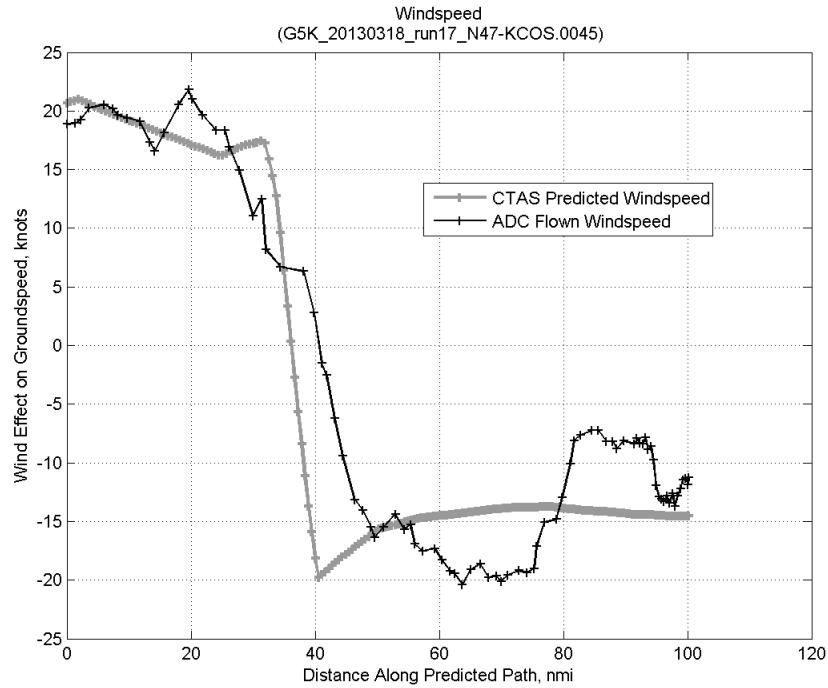


**Figure 984: CTAS predicted and ADC flown wind effect on ground speed for run 17. Negative values indicate a headwind.**

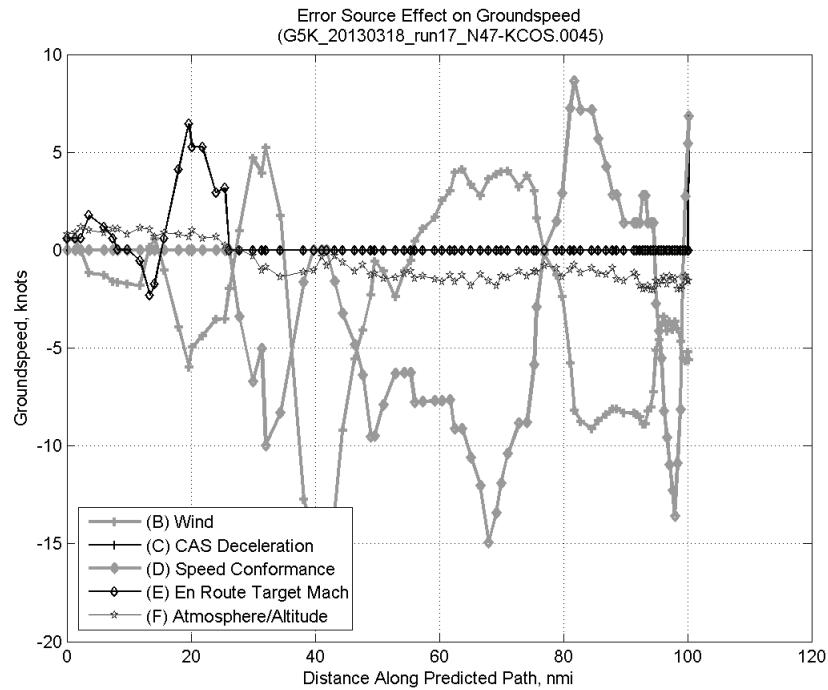


**Figure 985: Error sources (flown minus predicted) converted to a ground speed effect for run 17. Positive values indicate the flown ground speed was faster than the CTAS prediction.**

### D.5.C. CAS Deceleration

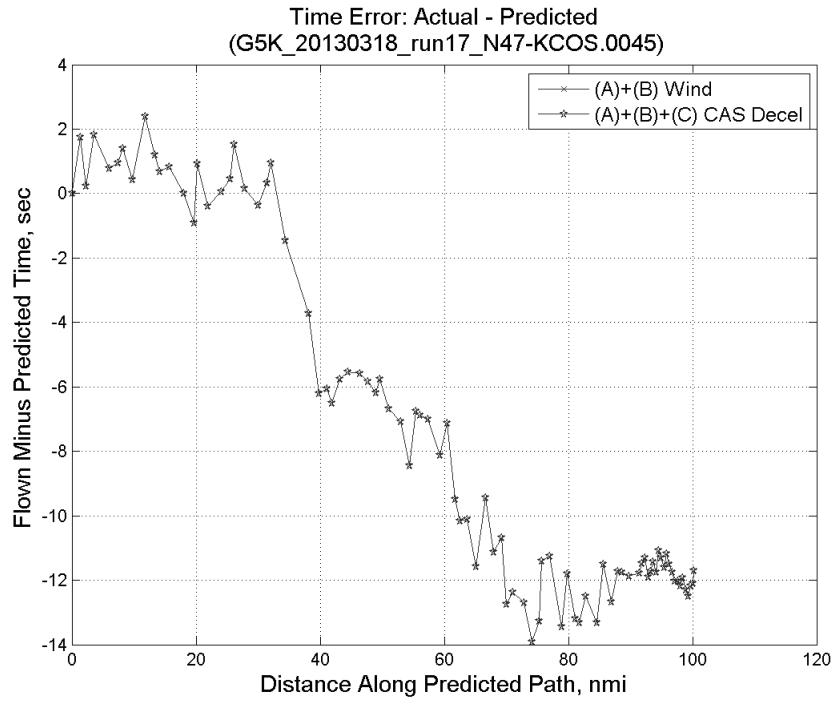


**Figure 986:** Time error for run 17 before ((A)+(B) Wind) and after ((A)+(B)+(C) CAS Decel) removing CAS deceleration error source.

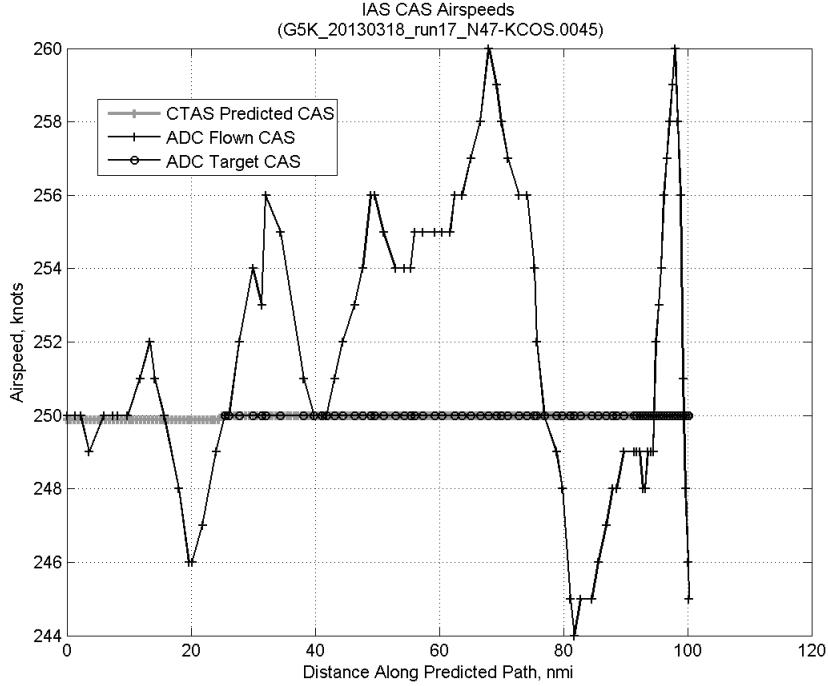


**Figure 987:** CTAS predicted and ADC flown CAS for run 17. CAS that is being targeted is shown with circle markers.

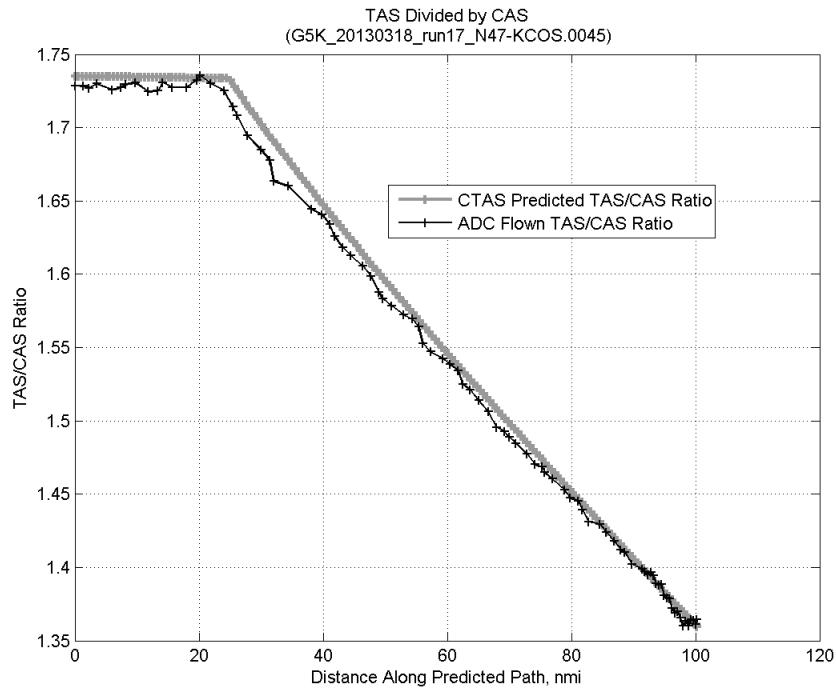


**Figure 988:** CTAS predicted and ADC flown TAS/CAS ratio for run 17.

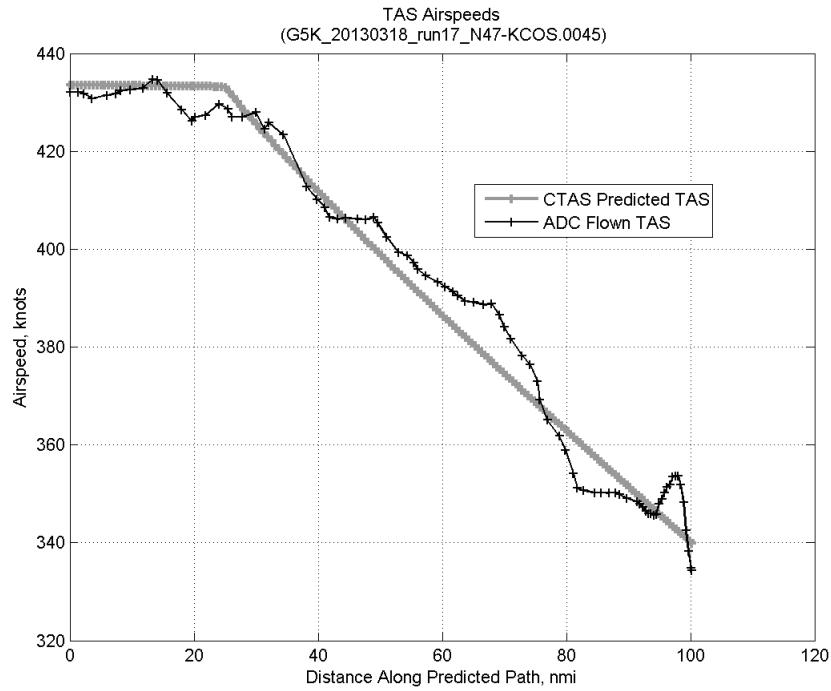


**Figure 989:** CTAS predicted and ADC flown TAS for run 17.

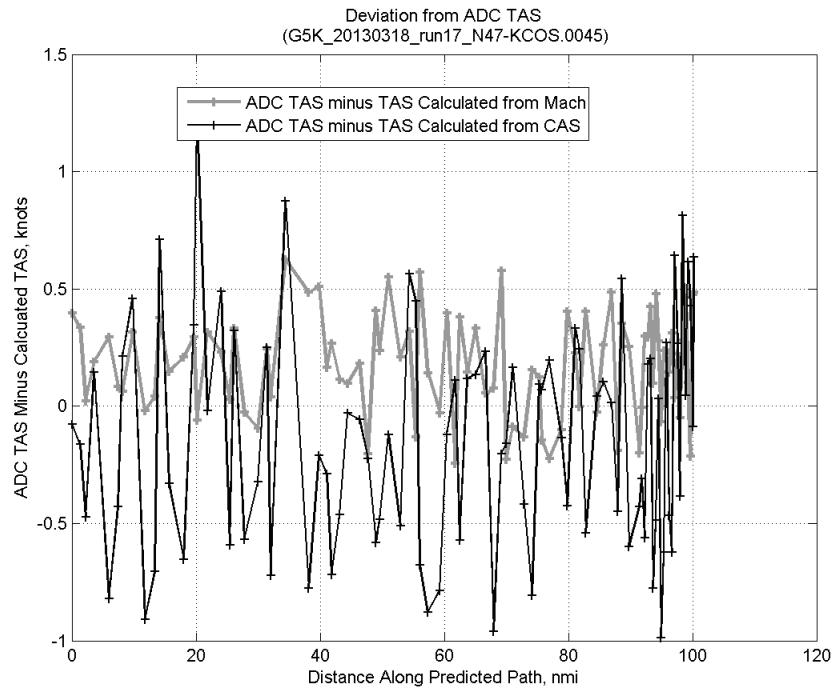


**Figure 990: Deviation from ADC flown TAS if calculating TAS using ADC flown CAS, Mach, atmospheric temperature, and atmospheric pressure for run 17.**

#### D.5.D. Speed Conformance

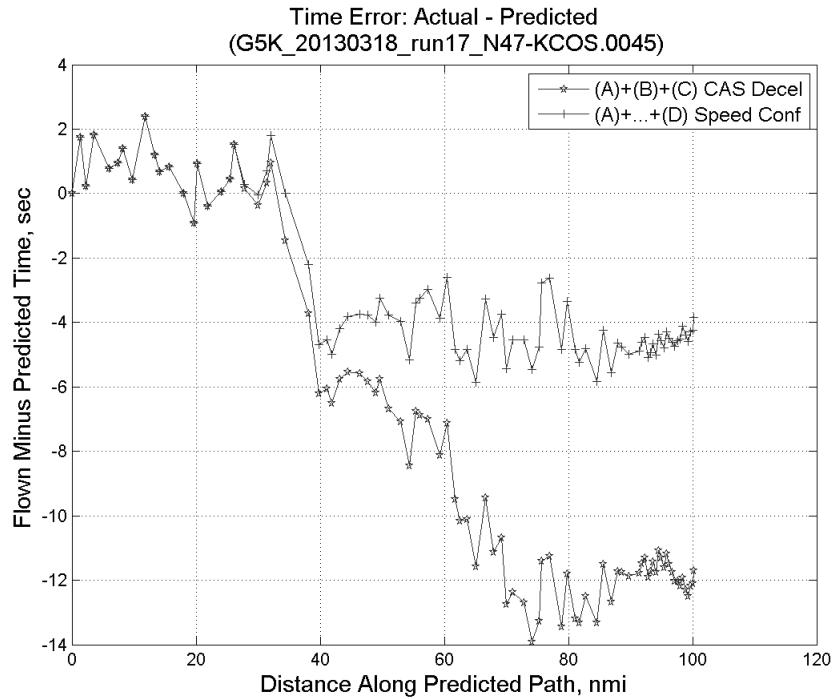


**Figure 991: Time error for run 17 before ((A)+(B)+(C) CAS Decel) and after ((A)+...+(D) Speed Conf) removing speed conformance error source.**

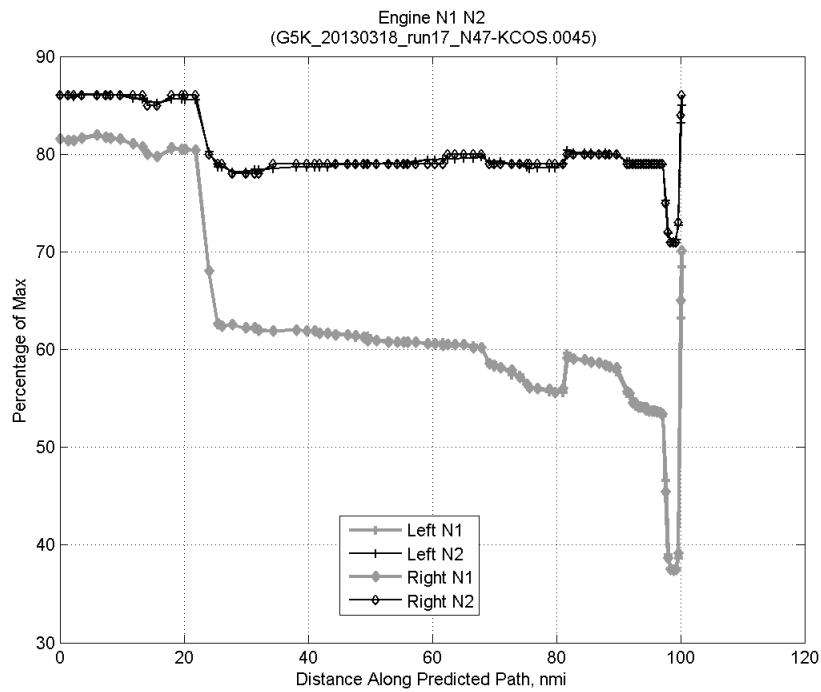


**Figure 992: Flown engine N1 and N2 for run 17.**

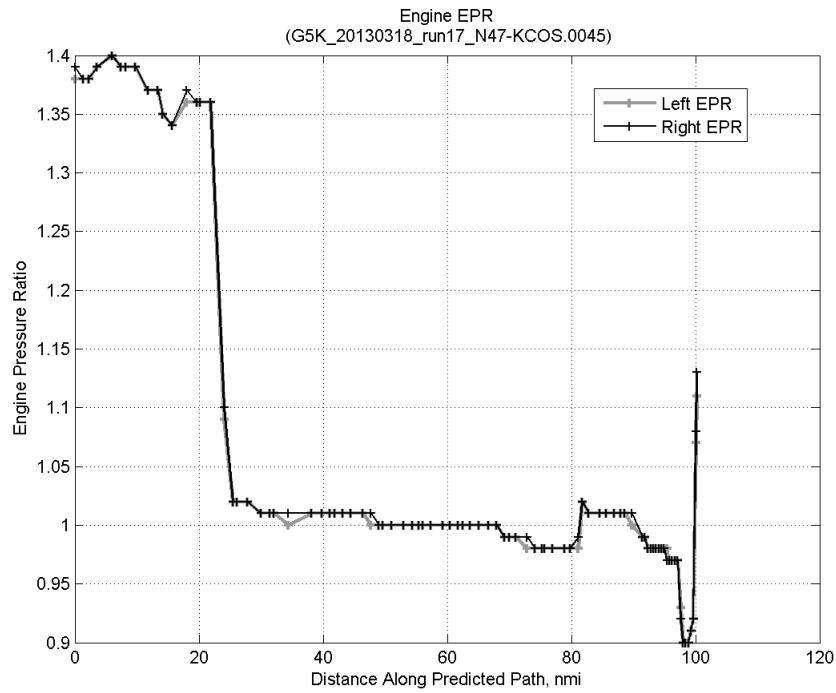


**Figure 993: Flown engine EPR for run 17.**

### D.5.E. Target Mach

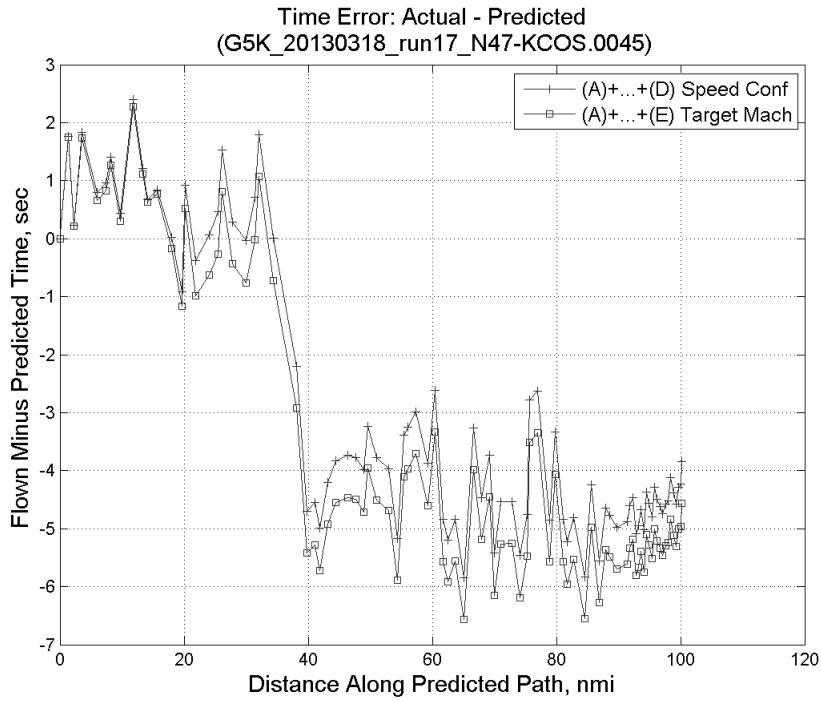


**Figure 994:** Time error for run 17 before ((A)+...+(D) Speed Conf) and after ((A)+...+(E) Target Mach) removing target Mach error source.

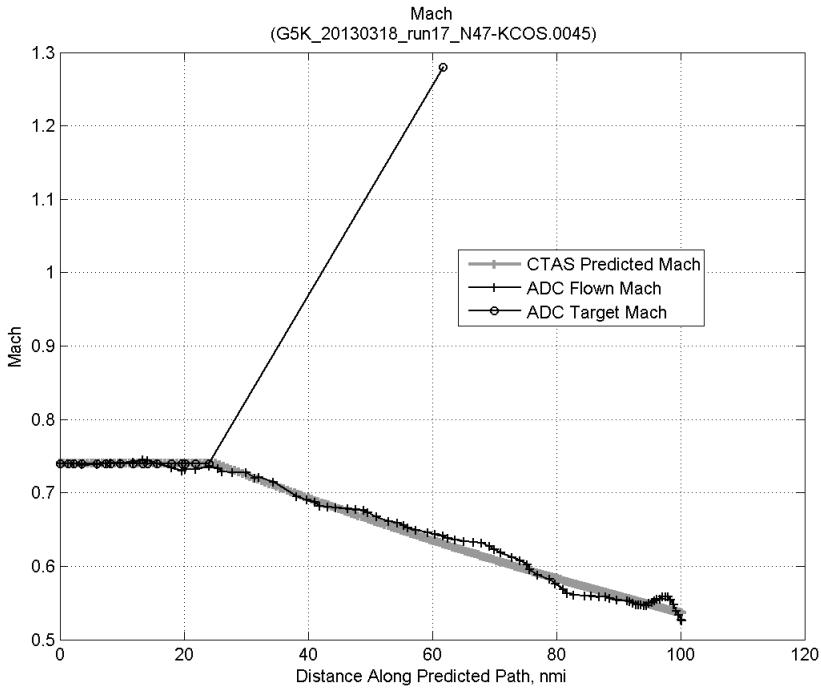


**Figure 995:** CTAS predicted and ADC flown Mach for run 17. Mach being targeted (ADC) shown with circle markers.

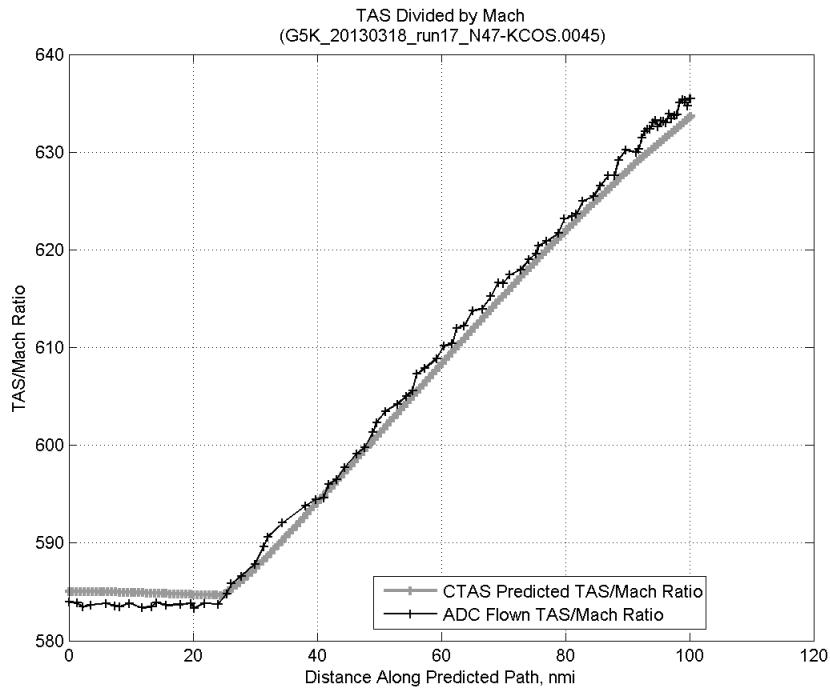


**Figure 996: CTAS predicted and ADC flown TAS/Mach ratio for run 17.**

#### D.5.F. Atmosphere/Altitude

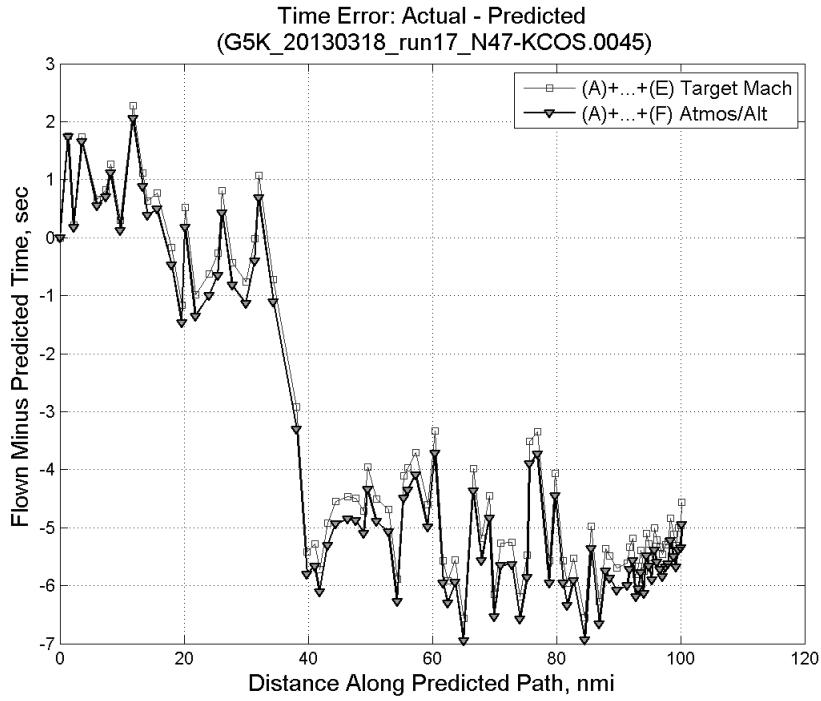


**Figure 997: Time error for run 17 before ((A)+...+(E) Target Mach) and after ((A)+...+(F) Atmos/Alt) removing atmosphere/altitude error source.**

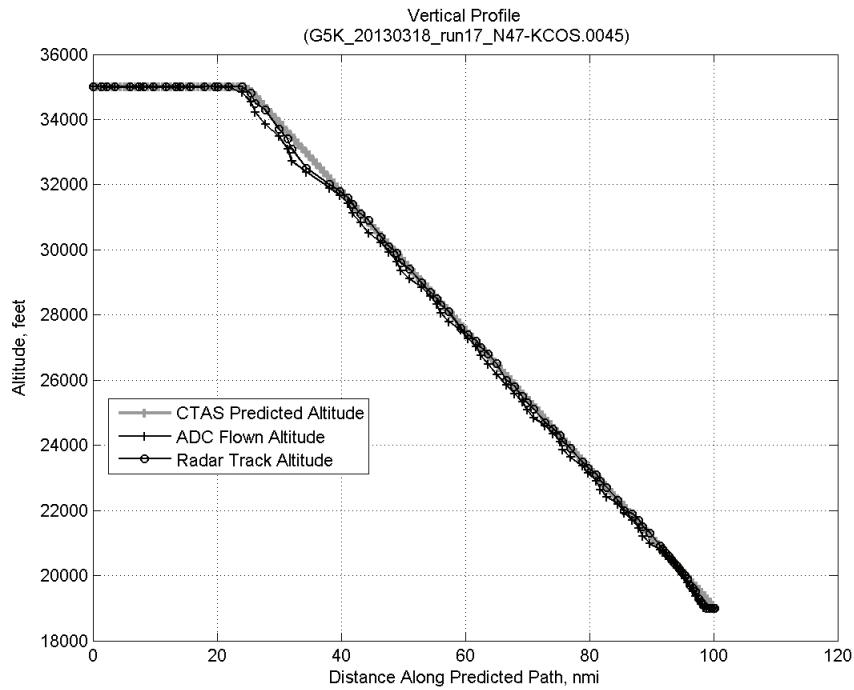


**Figure 998: Flown (ADC) and predicted (CTAS) vertical profile for run 17.**

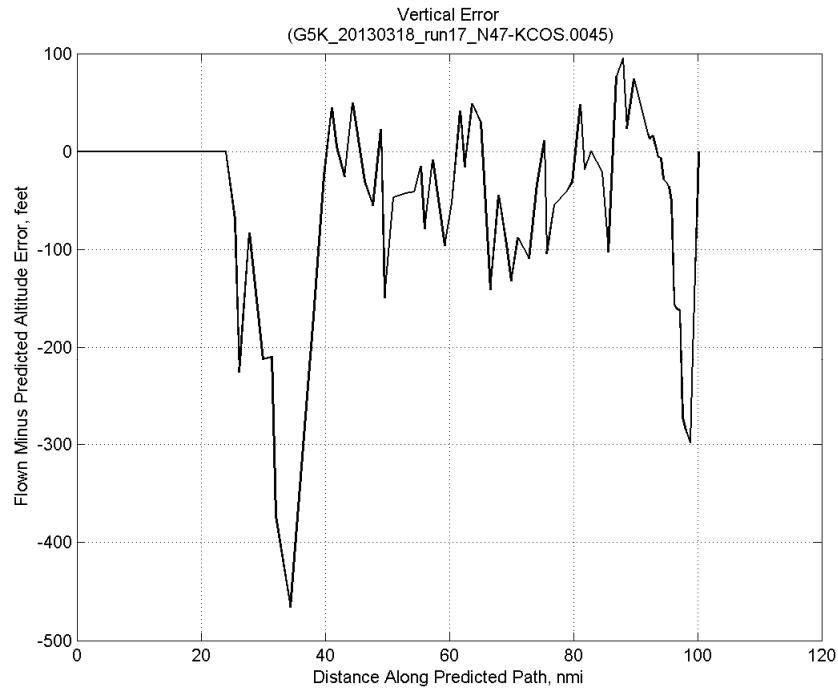


**Figure 999: Vertical error (flown minus predicted altitude) for run 17. Positive values indicate aircraft flew higher than predicted by CTAS.**

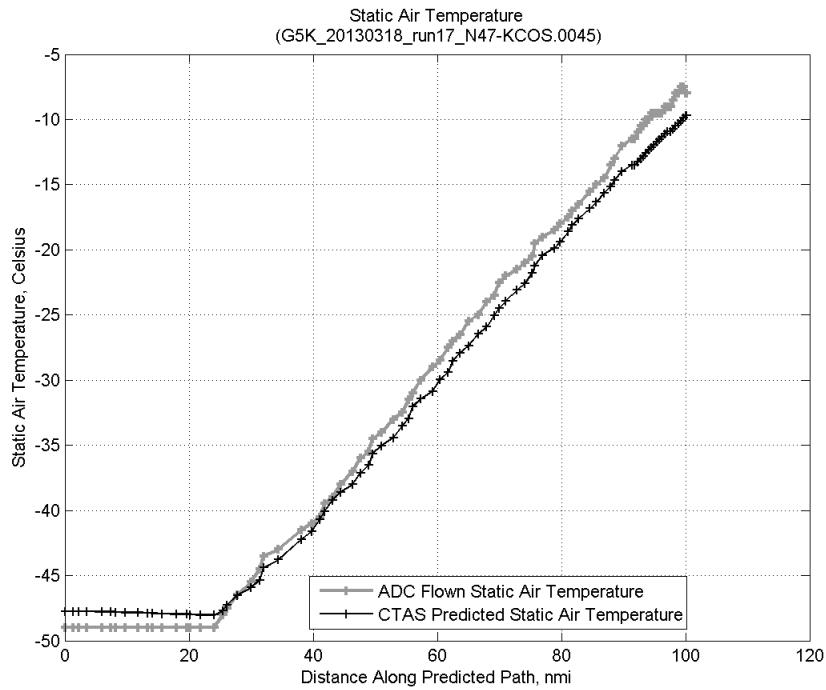


**Figure 1000: Flown (ADC) and predicted (CTAS) static air temperature for run 17.**

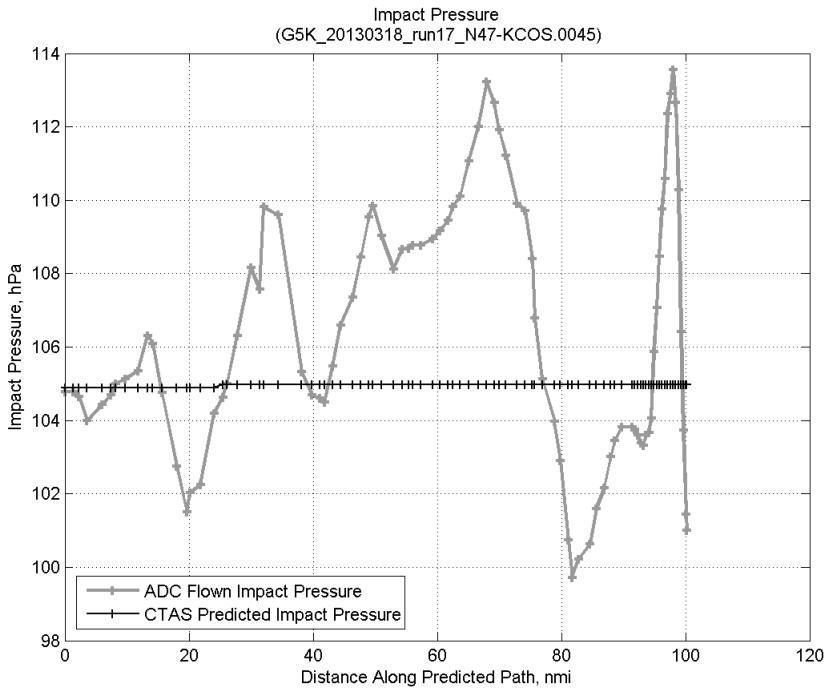


**Figure 1001: Flown (ADC) and predicted (CTAS) impact pressure for run 17.**

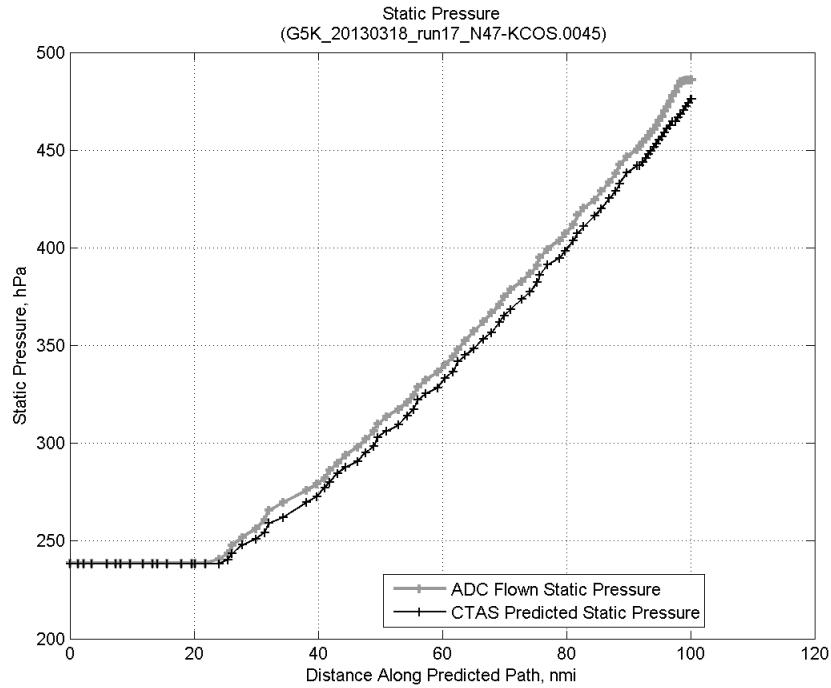


**Figure 1002: Flown (ADC) and predicted (CTAS) static pressure for run 17.**

#### D.5.G. Path Distance

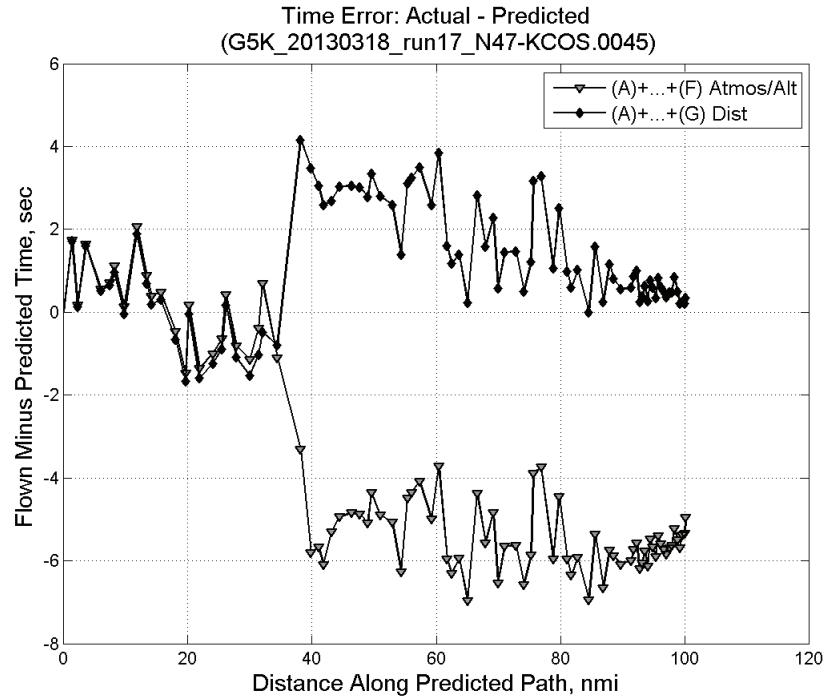


**Figure 1003: Time error for run 17 before ((A)+...+(F) Atmos/Alt) and after ((A)+...+(G) Dist) removing path distance error source.**

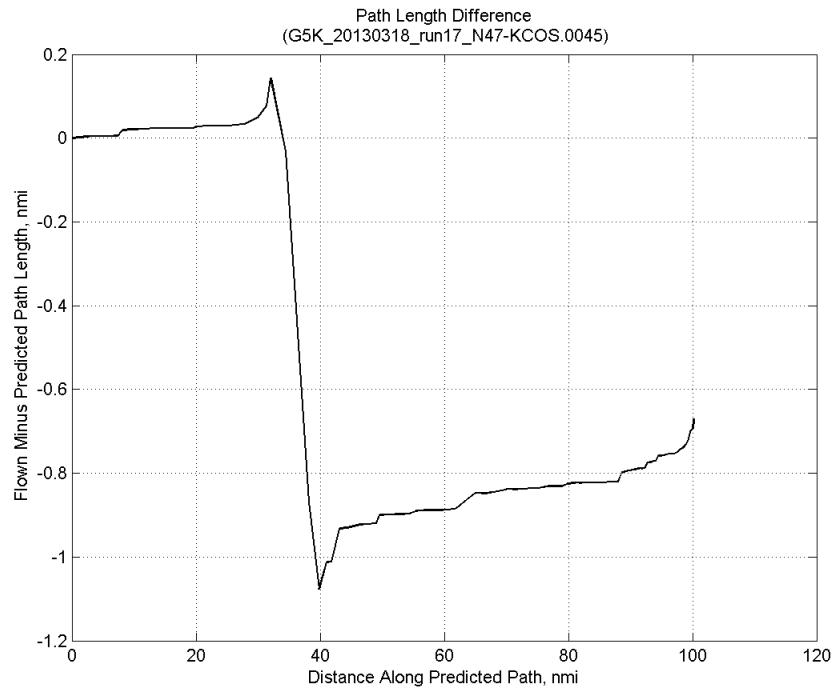


**Figure 1004: ADC flown minus CTAS predicted path length for run 17. Positive values indicate aircraft followed a longer path than predicted by CTAS.**

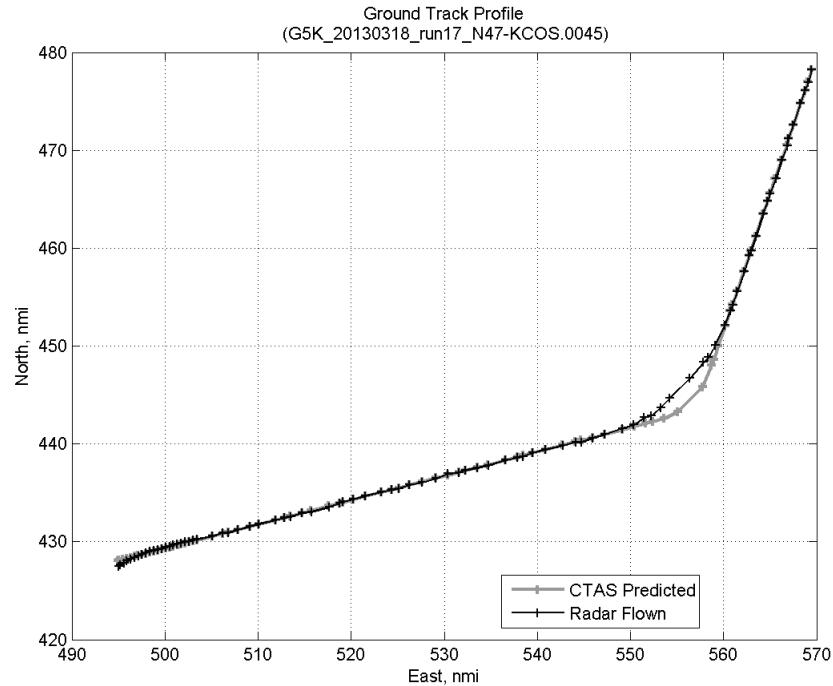


**Figure 1005: CTAS predicted and radar flown ground track profile for run 17.**

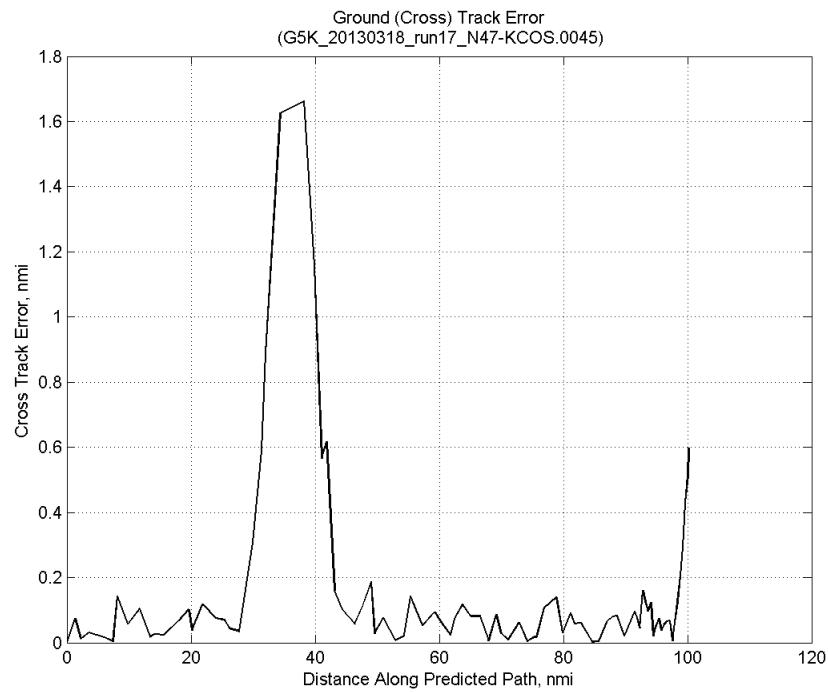


**Figure 1006: Ground (cross) track error for run 17.**

## D.6. Run 20

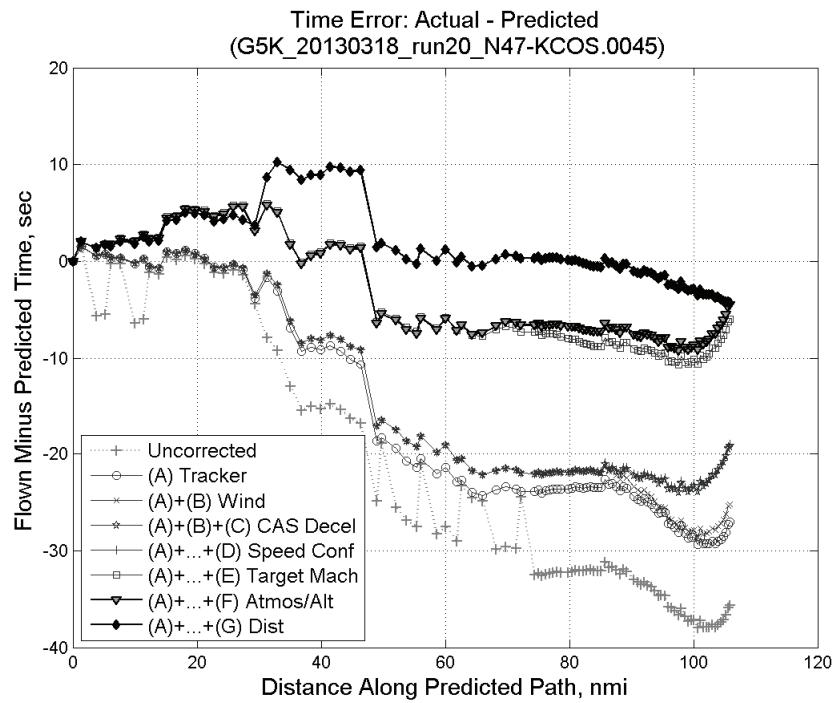


**Figure 1007:** Time error for run 20 showing incremental effect of removing each error source.

### D.6.A. Tracker Jumps

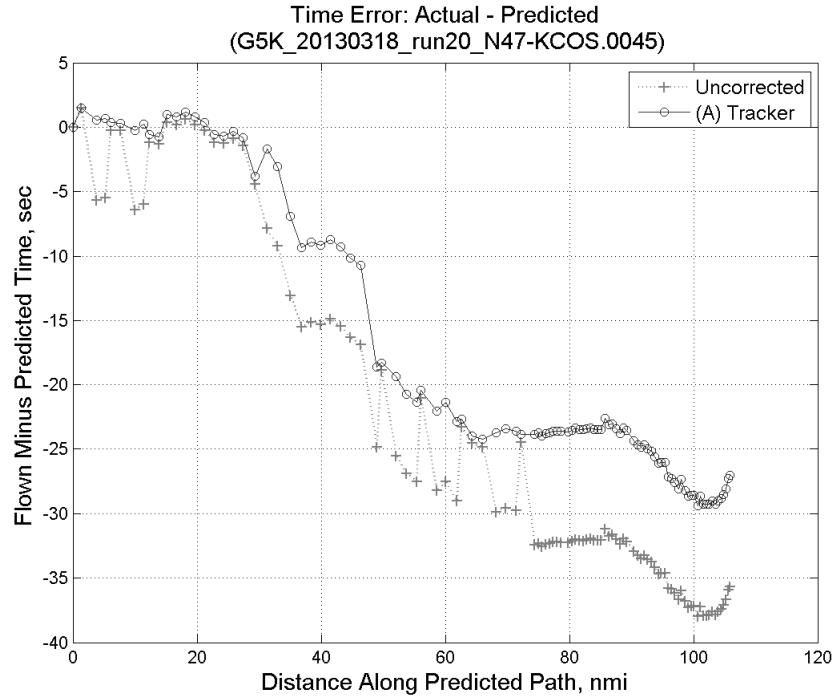


**Figure 1008:** Time error for run 20 before (Uncorrected) and after ((A) Tracker) removing tracker jump error source.

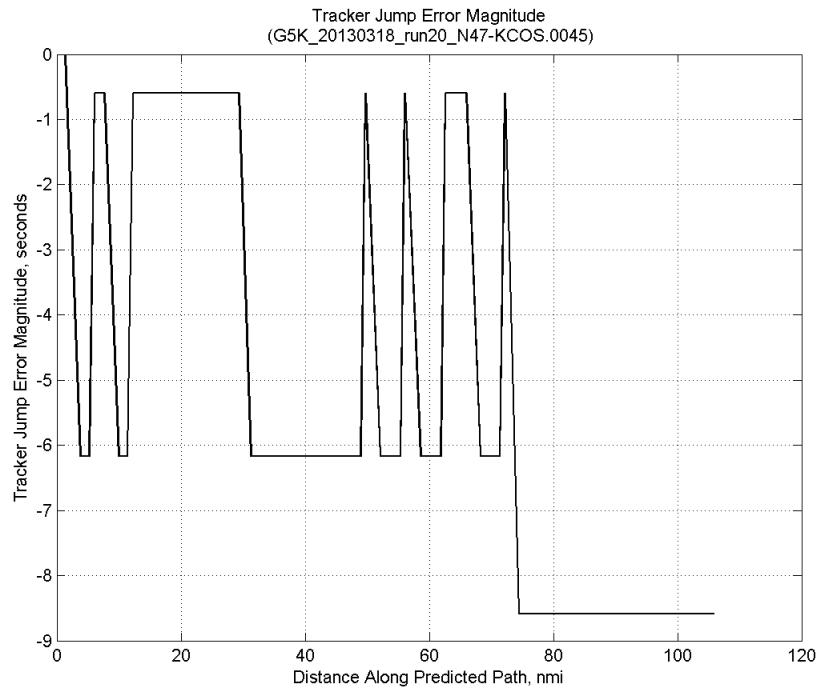


**Figure 1009: Effect of tracker jump error source on time error for run 20.**

#### D.6.B. Wind

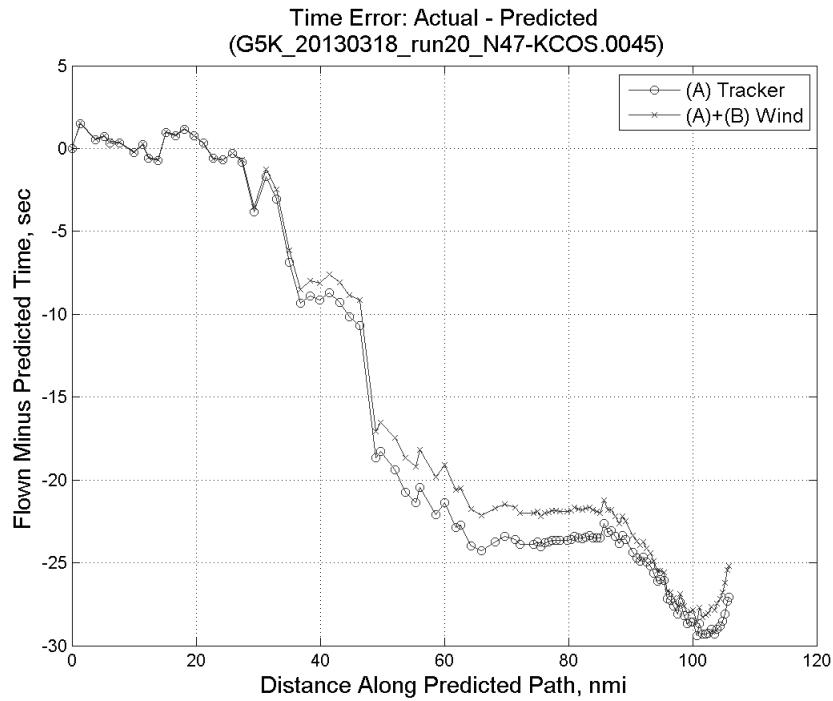


**Figure 1010: Time error for run 20 before ((A) Tracker) and after ((A)+(B) Wind) removing wind error source.**

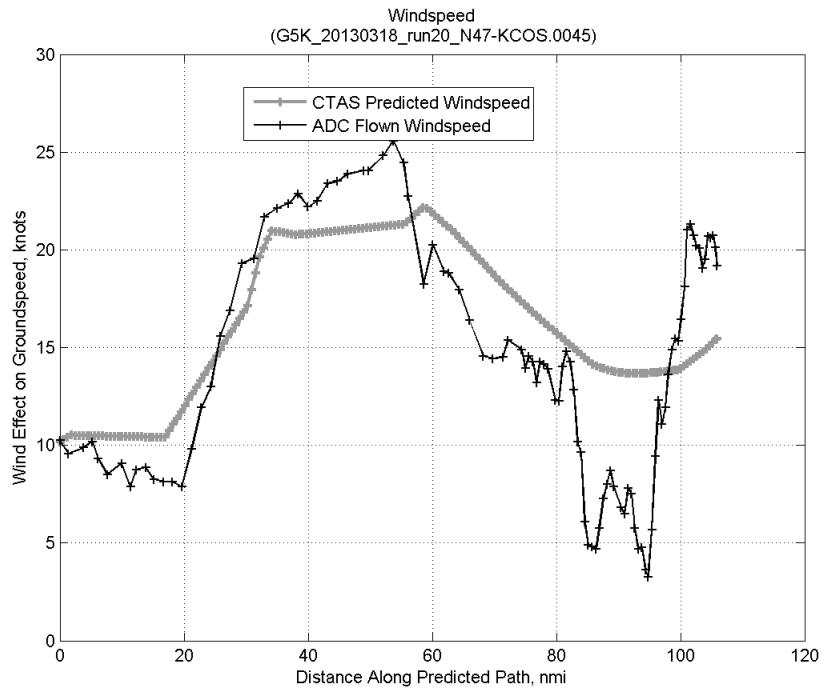


**Figure 1011: CTAS predicted and ADC flown wind effect on ground speed for run 20. Negative values indicate a headwind.**

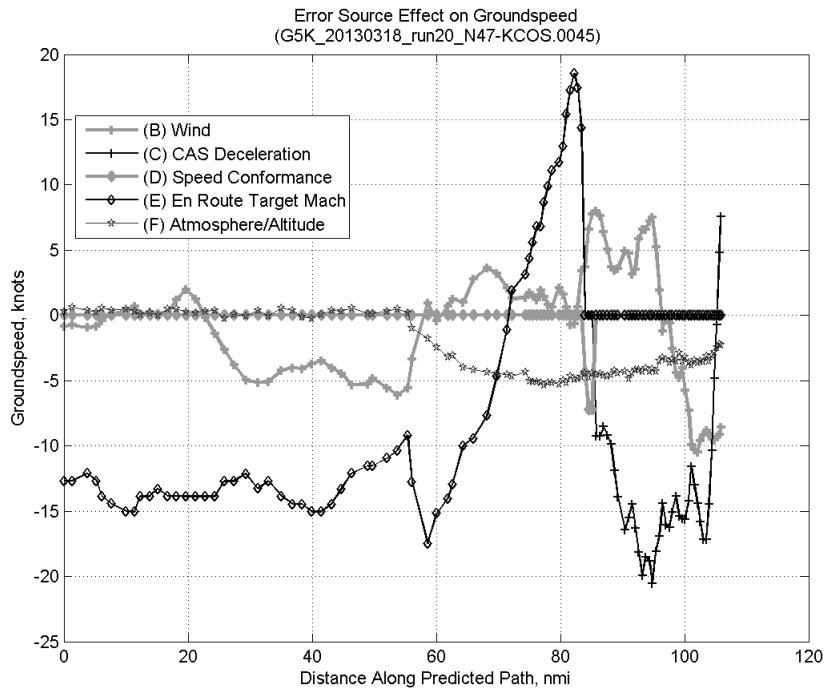


**Figure 1012: Error sources (flown minus predicted) converted to a ground speed effect for run 20. Positive values indicate the flown ground speed was faster than the CTAS prediction.**

### D.6.C. CAS Deceleration

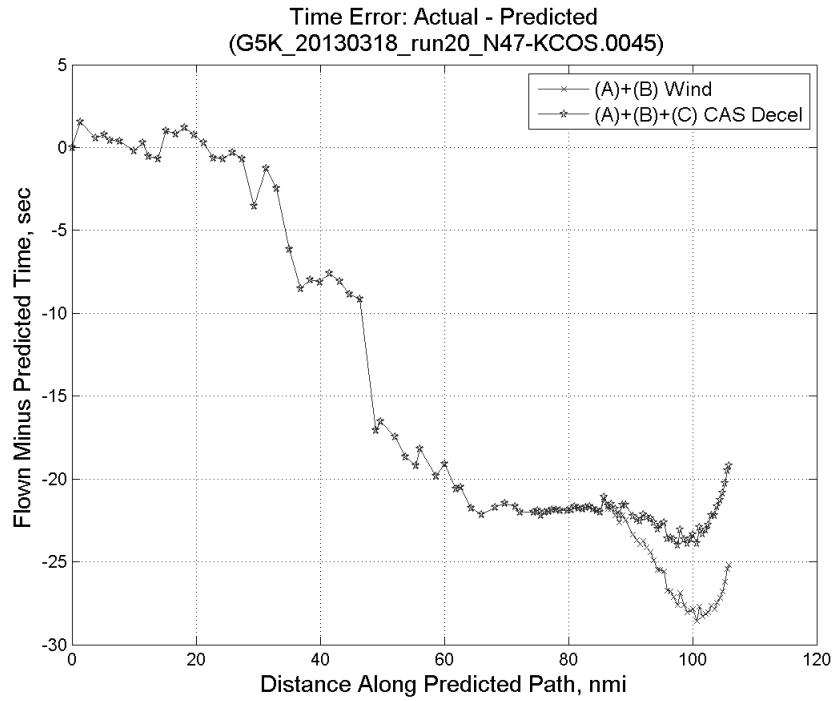


**Figure 1013:** Time error for run 20 before ((A)+(B) Wind) and after ((A)+(B)+(C) CAS Decel) removing CAS deceleration error source.

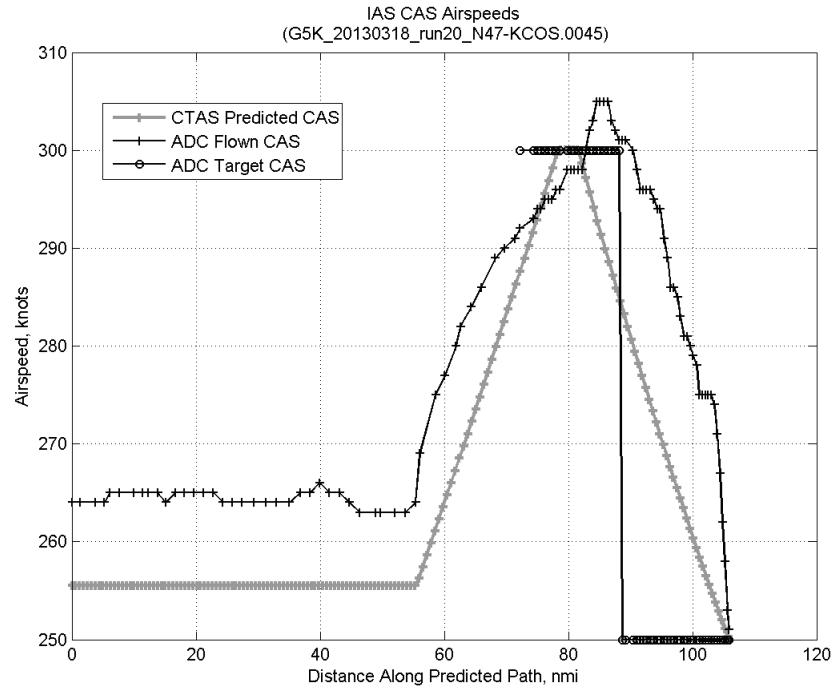


**Figure 1014:** CTAS predicted and ADC flown CAS for run 20. CAS that is being targeted is shown with circle markers.

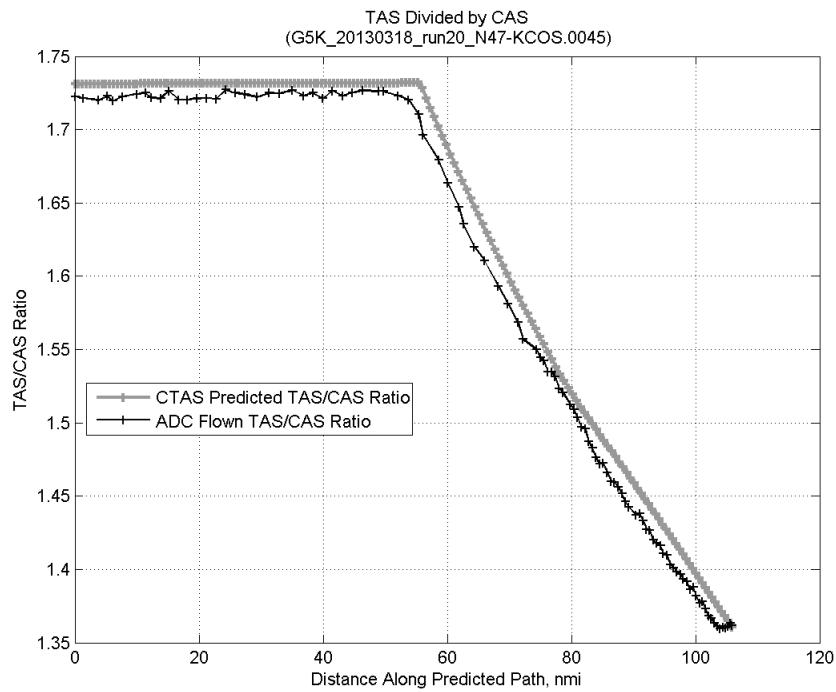


**Figure 1015: CTAS predicted and ADC flown TAS/CAS ratio for run 20.**

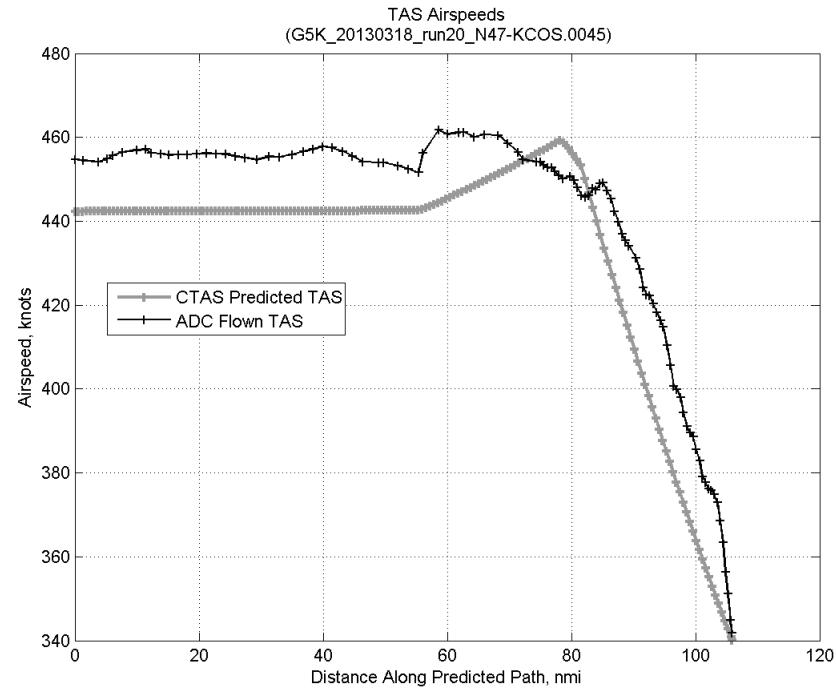


**Figure 1016: CTAS predicted and ADC flown TAS for run 20.**

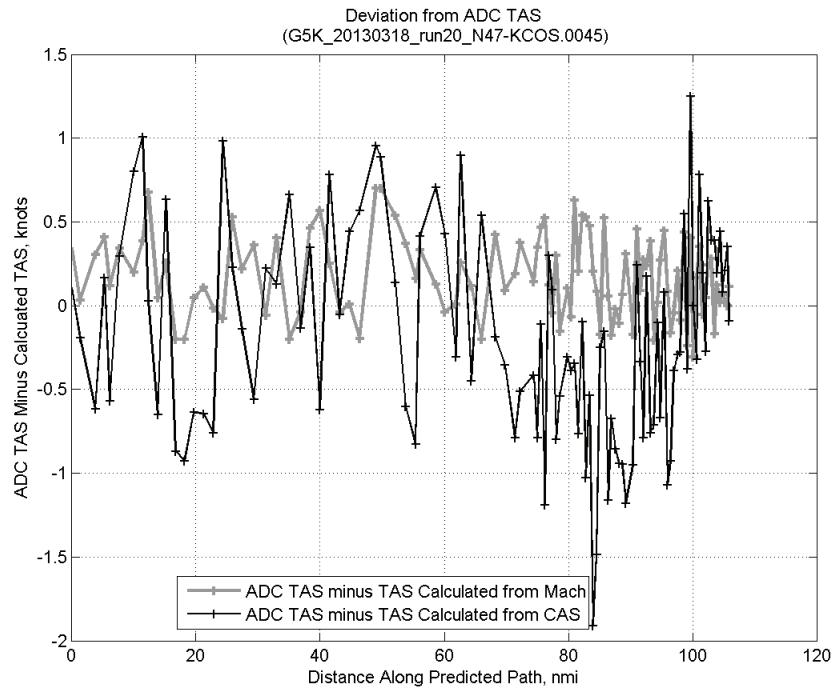


**Figure 1017:** Deviation from ADC flown TAS if calculating TAS using ADC flown CAS, Mach, atmospheric temperature, and atmospheric pressure for run 20.

#### D.6.D. Speed Conformance

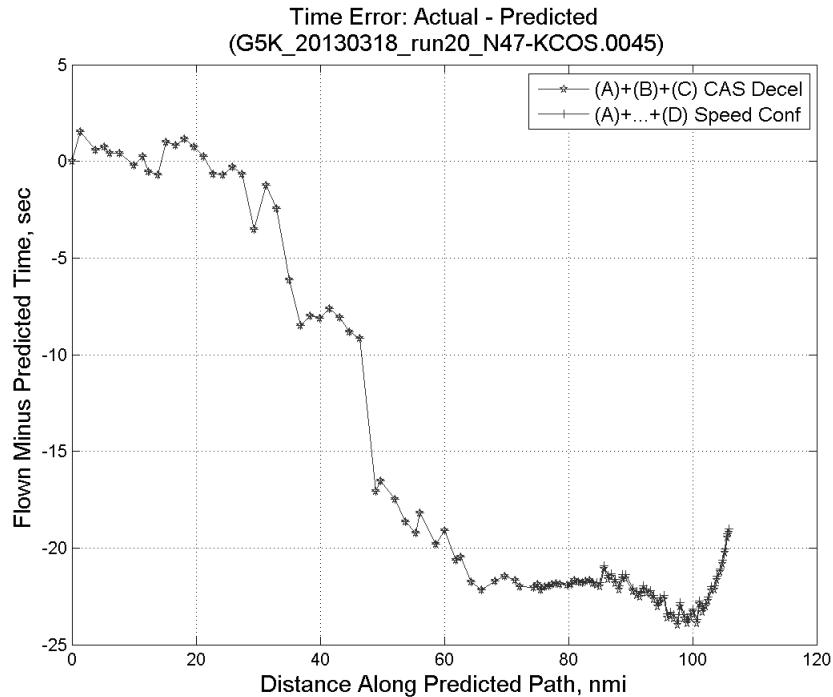


**Figure 1018:** Time error for run 20 before ((A)+(B)+(C) CAS Decel) and after ((A)+...+(D) Speed Conf) removing speed conformance error source.

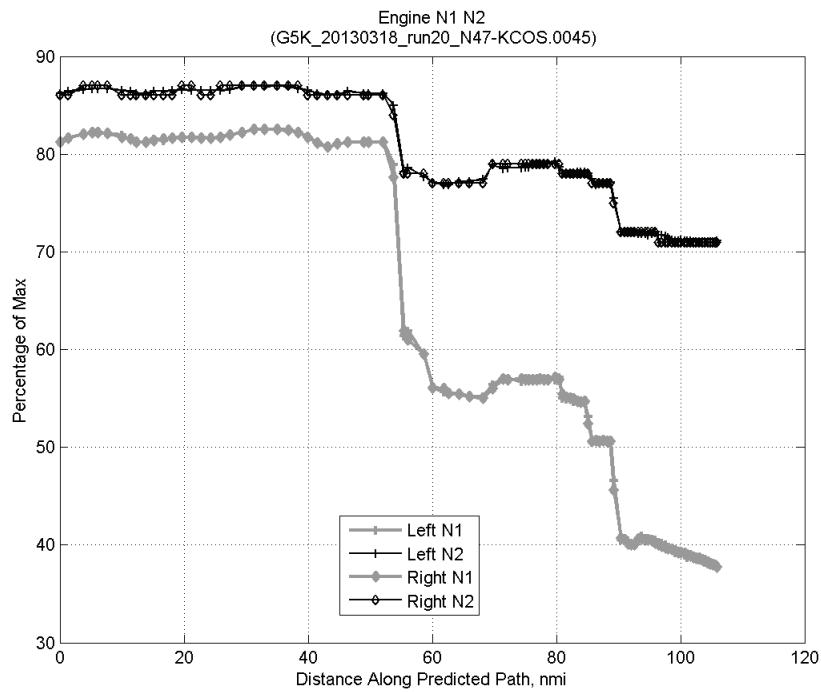


**Figure 1019: Flown engine N1 and N2 for run 20.**

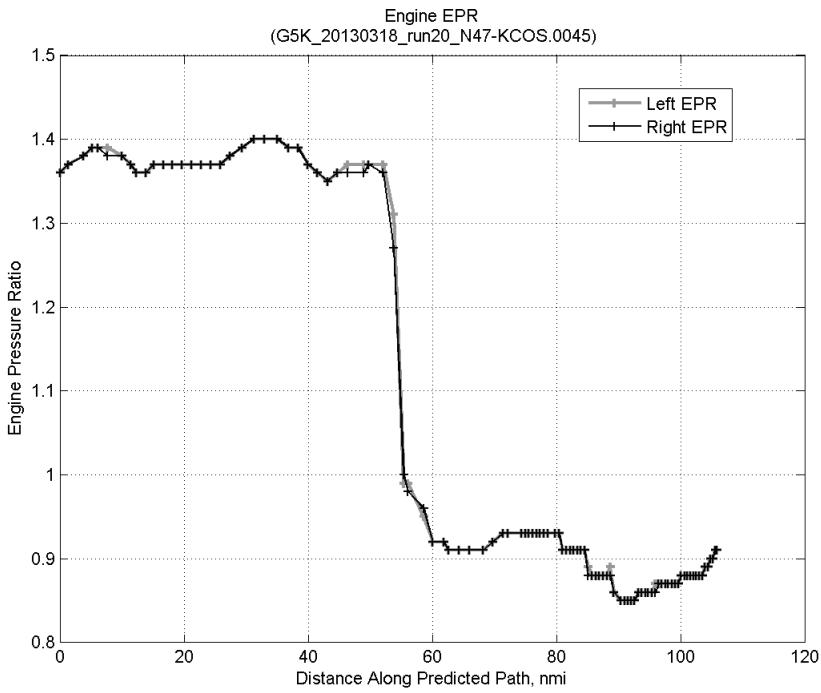


**Figure 1020: Flown engine EPR for run 20.**

### D.6.E. Target Mach

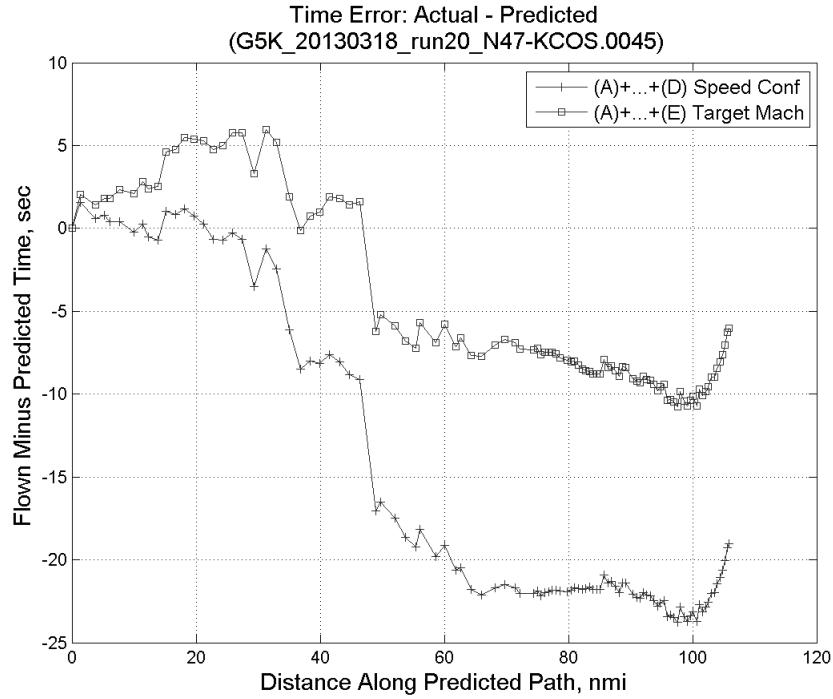


**Figure 1021:** Time error for run 20 before ((A)+...+(D) Speed Conf) and after ((A)+...+(E) Target Mach) removing target Mach error source.

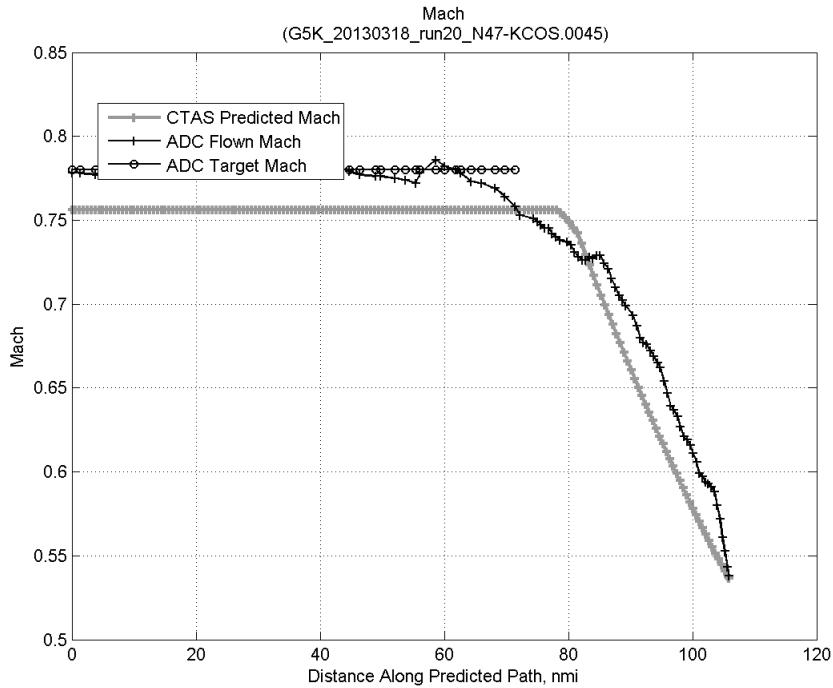


**Figure 1022:** CTAS predicted and ADC flown Mach for run 20. Mach being targeted (ADC) shown with circle markers.

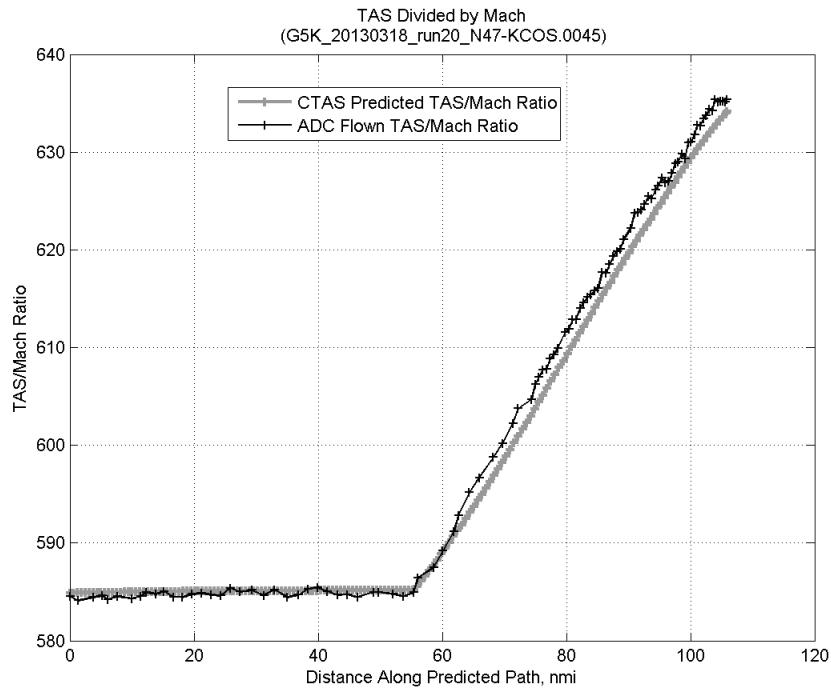


**Figure 1023: CTAS predicted and ADC flown TAS/Mach ratio for run 20.**

#### D.6.F. Atmosphere/Altitude

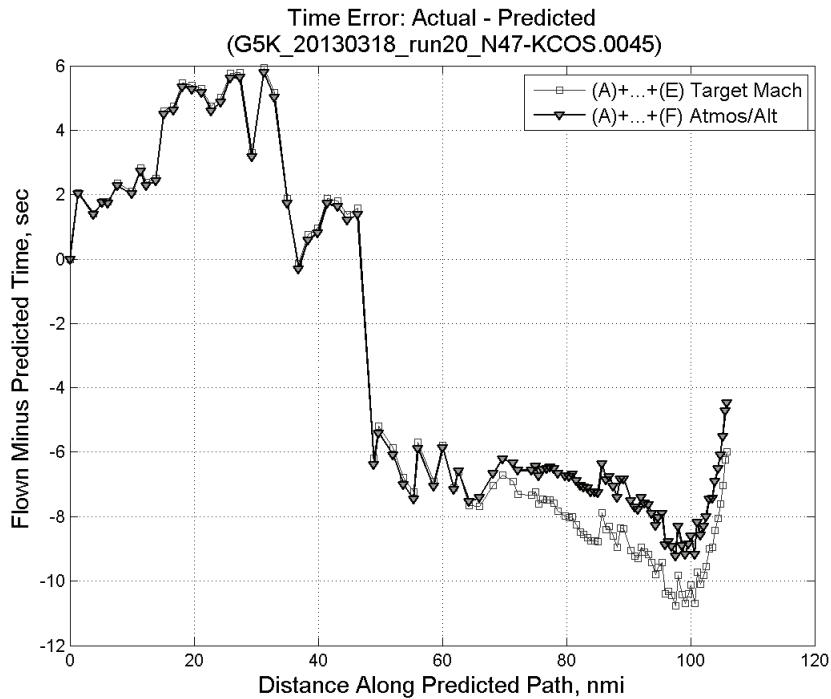


**Figure 1024: Time error for run 20 before ((A)+...+(E) Target Mach) and after ((A)+...+(F) Atmos/Alt) removing atmosphere/altitude error source.**

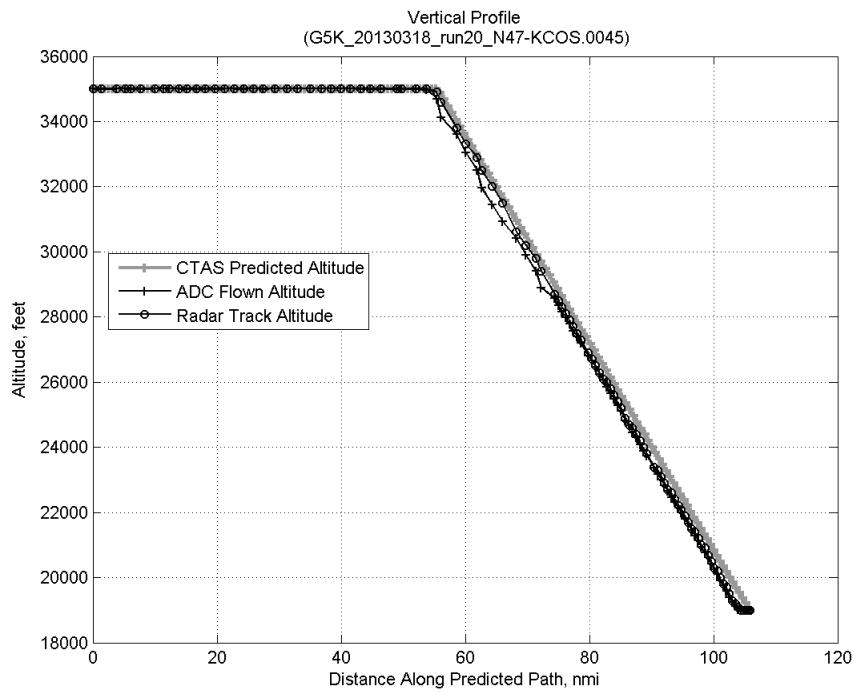


**Figure 1025: Flown (ADC) and predicted (CTAS) vertical profile for run 20.**

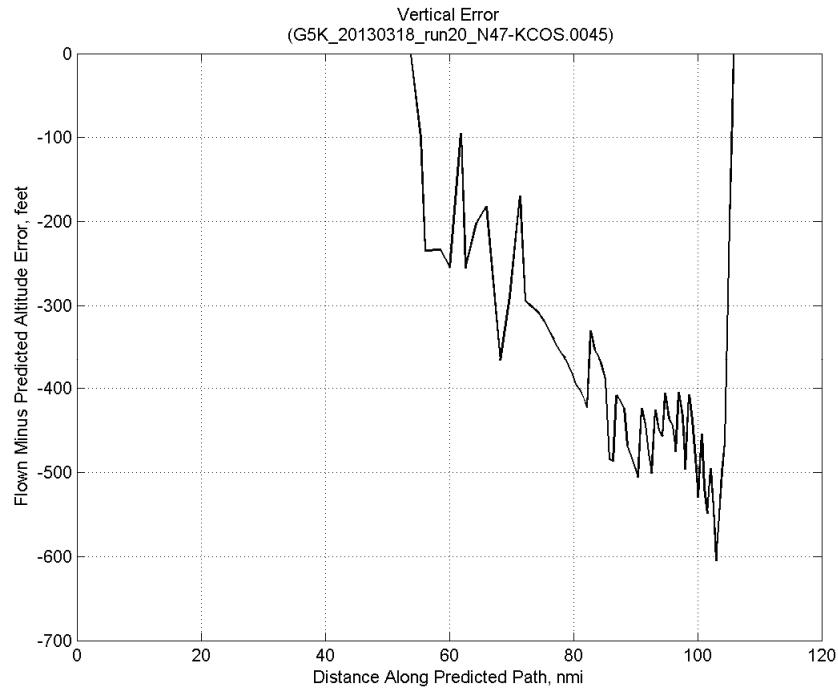


**Figure 1026: Vertical error (flown minus predicted altitude) for run 20. Positive values indicate aircraft flew higher than predicted by CTAS.**

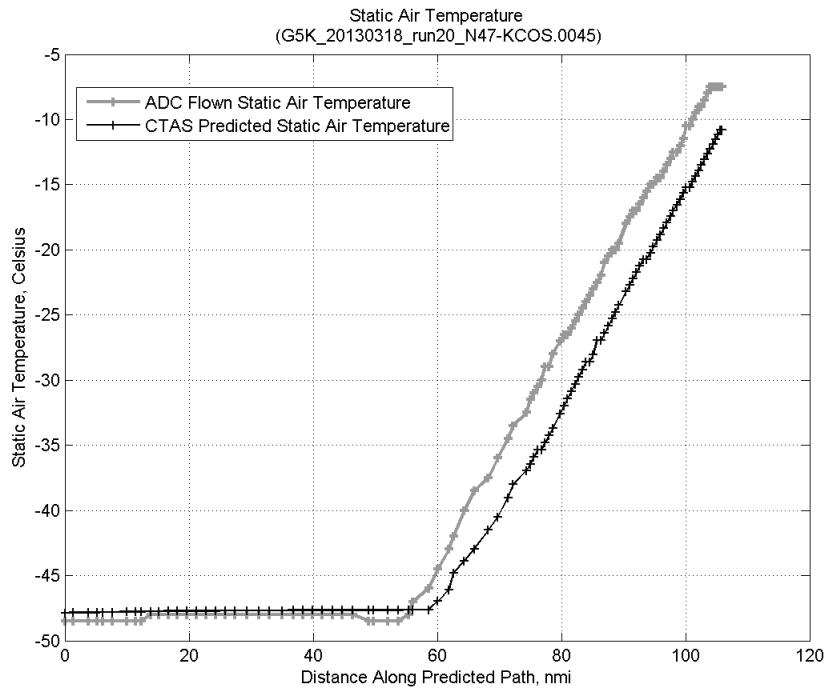


**Figure 1027: Flown (ADC) and predicted (CTAS) static air temperature for run 20.**

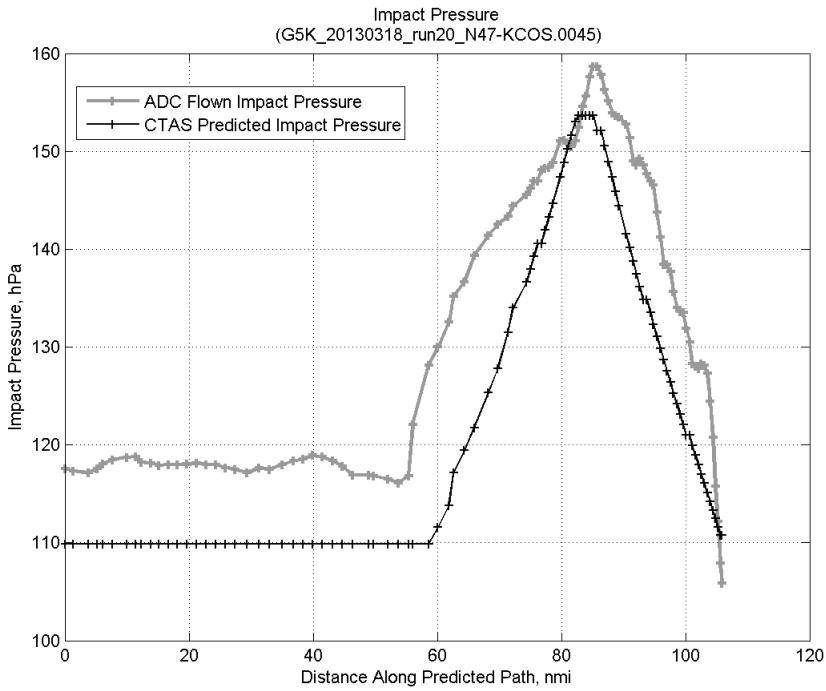


**Figure 1028: Flown (ADC) and predicted (CTAS) impact pressure for run 20.**

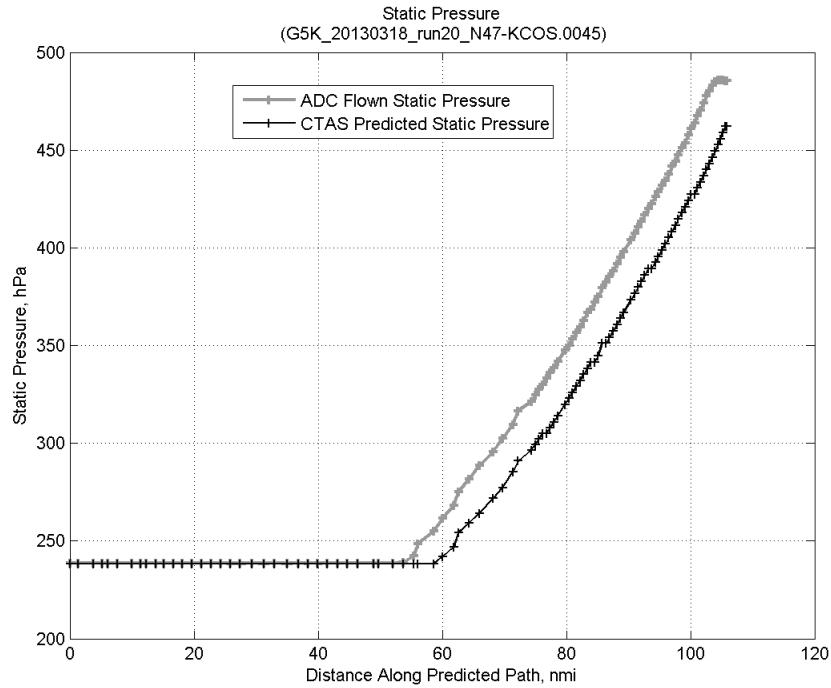


**Figure 1029: Flown (ADC) and predicted (CTAS) static pressure for run 20.**

#### D.6.G. Path Distance

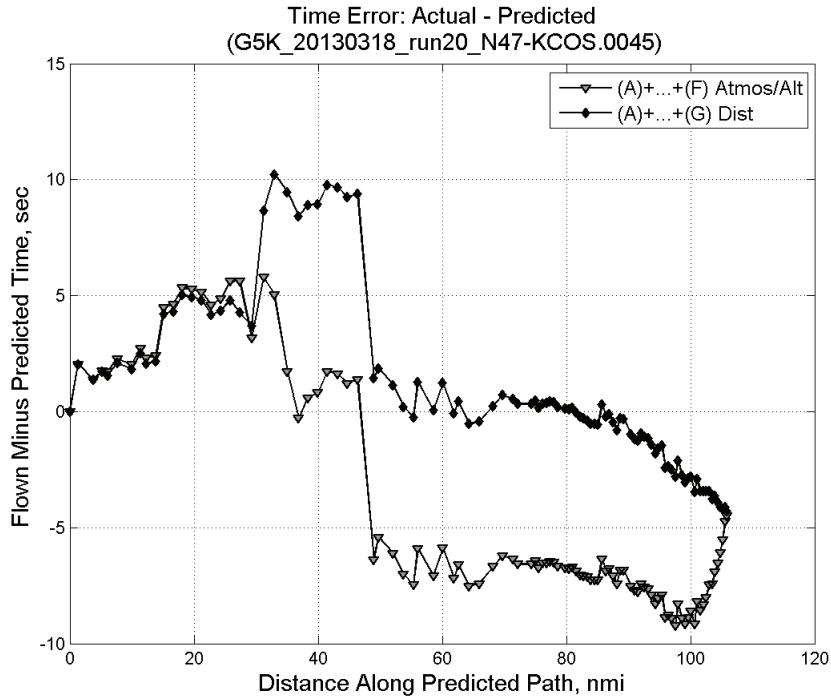


**Figure 1030: Time error for run 20 before ((A)+...+(F) Atmos/Alt) and after ((A)+...+(G) Dist) removing path distance error source.**

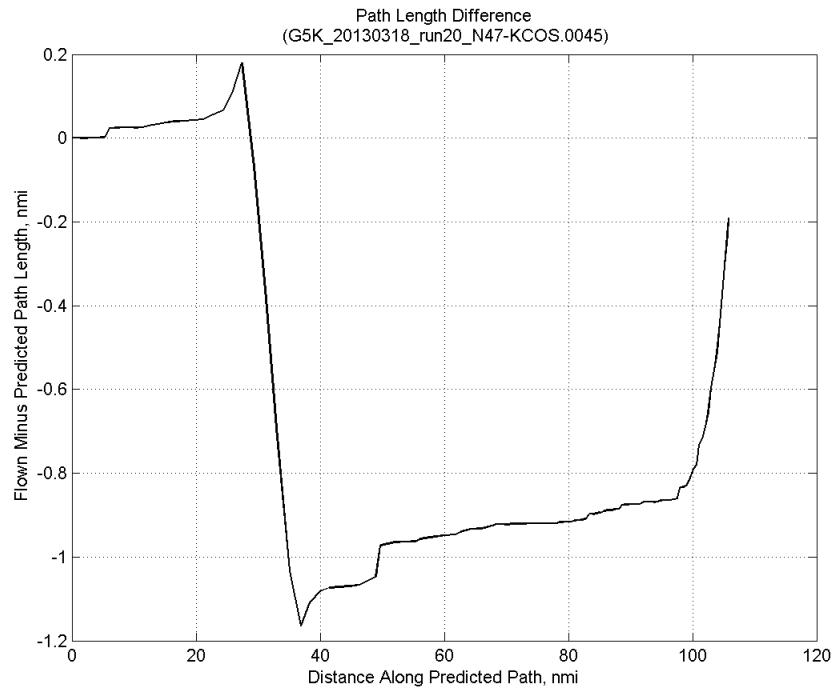


**Figure 1031: ADC flown minus CTAS predicted path length for run 20. Positive values indicate aircraft followed a longer path than predicted by CTAS.**

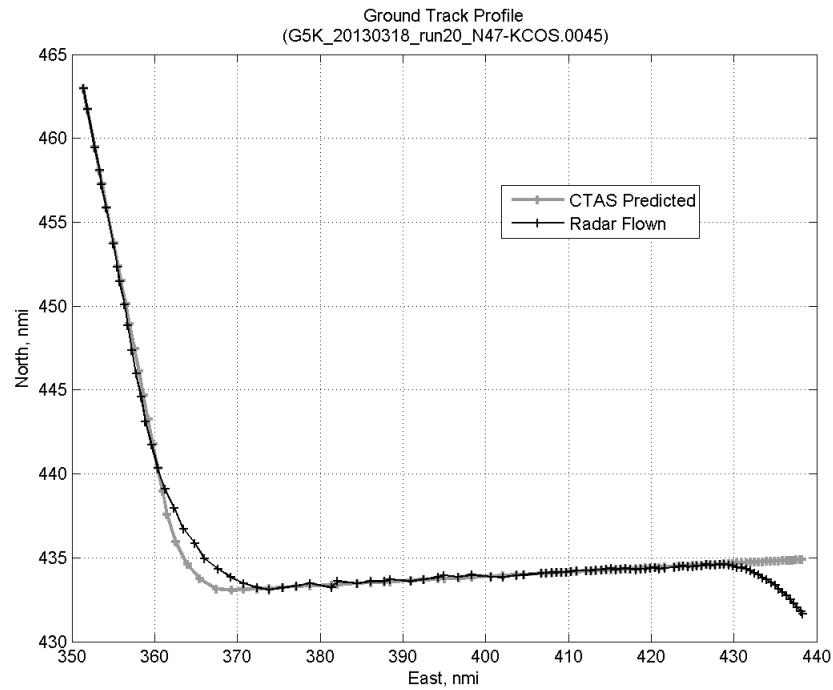


**Figure 1032: CTAS predicted and radar flown ground track profile for run 20.**

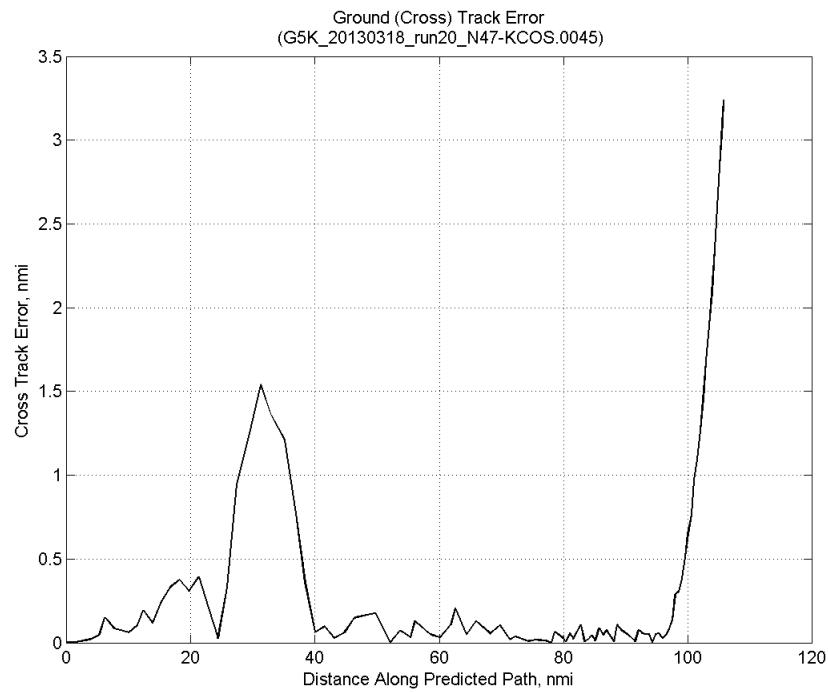


**Figure 1033: Ground (cross) track error for run 20.**

## D.7. Run 27

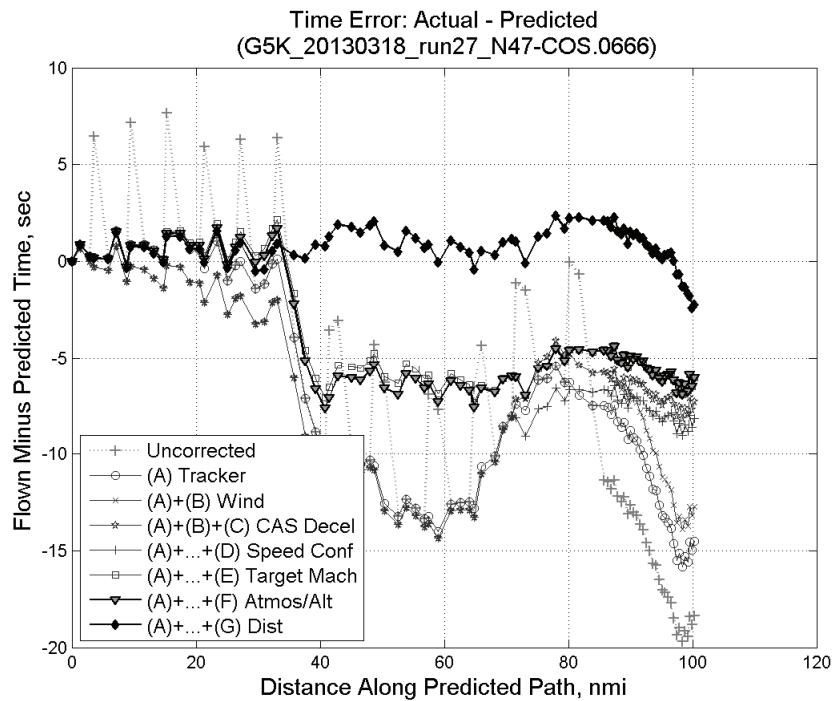


**Figure 1034:** Time error for run 27 showing incremental effect of removing each error source.

### D.7.A. Tracker Jumps

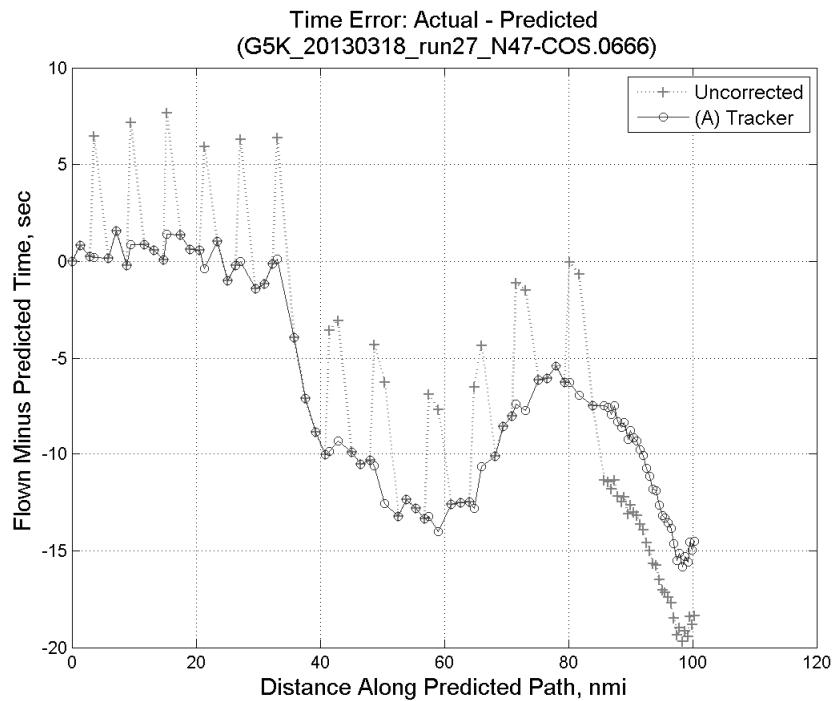


**Figure 1035:** Time error for run 27 before (Uncorrected) and after ((A) Tracker) removing tracker jump error source.

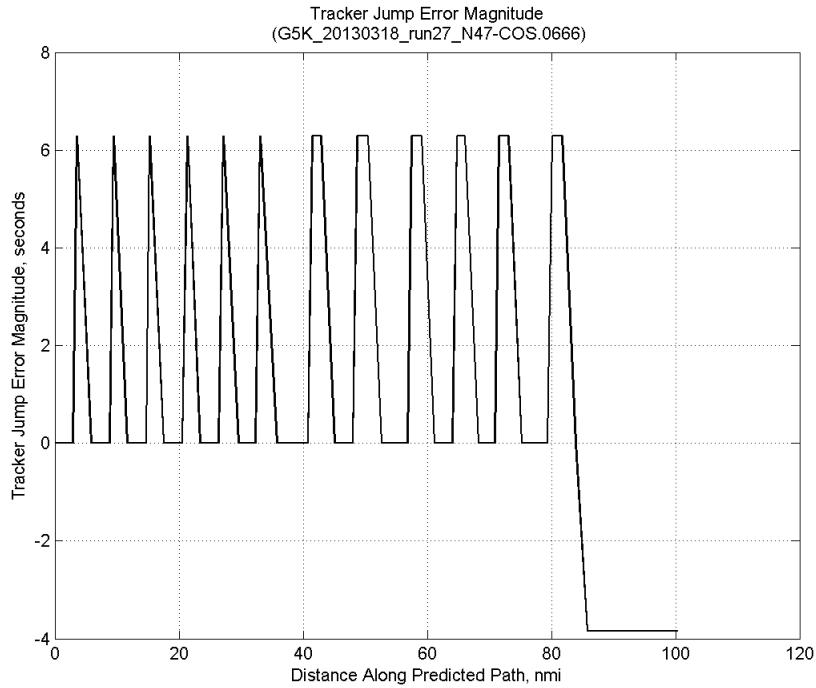


**Figure 1036: Effect of tracker jump error source on time error for run 27.**

#### D.7.B. Wind

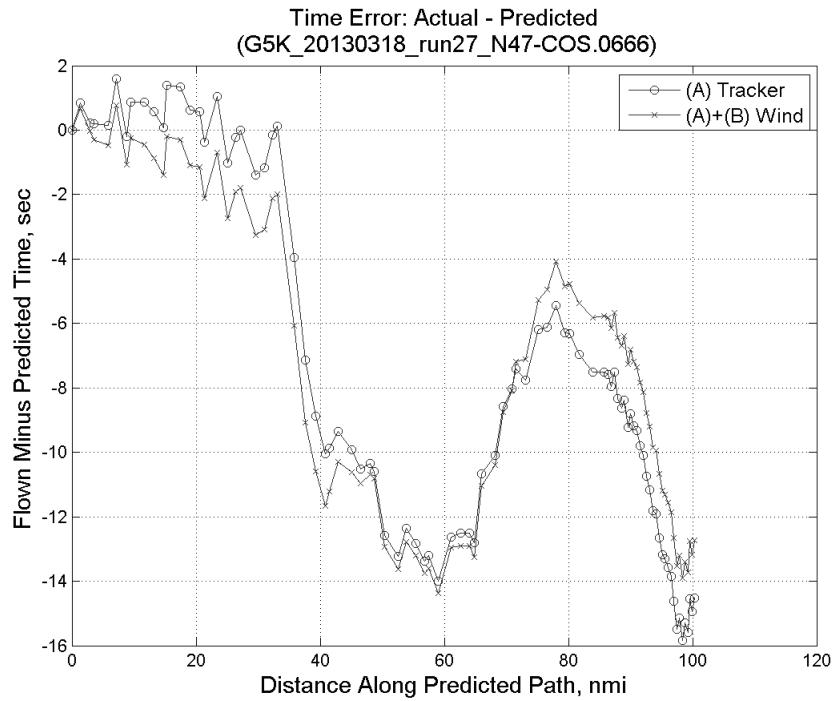


**Figure 1037: Time error for run 27 before ((A) Tracker) and after ((A)+(B) Wind) removing wind error source.**

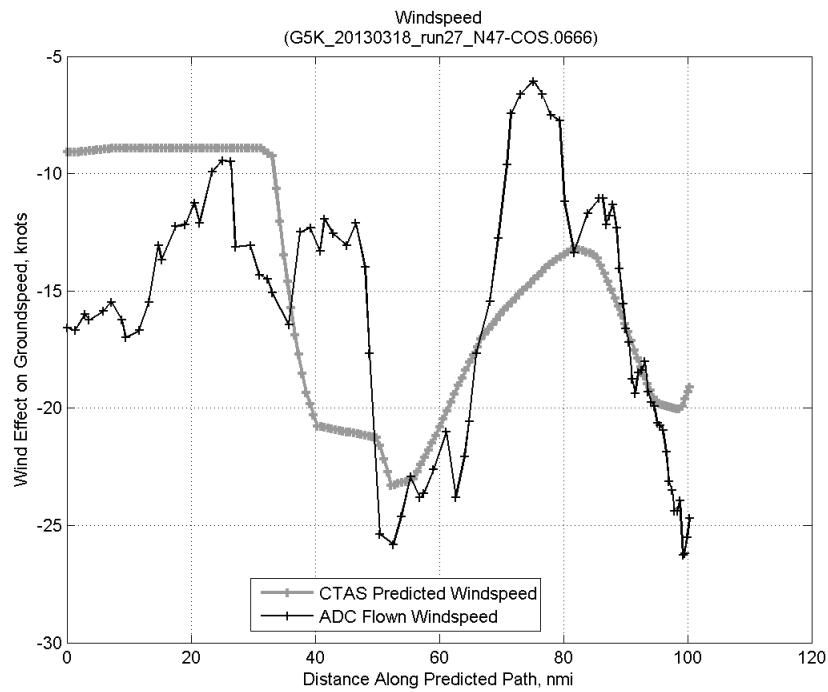


**Figure 1038: CTAS predicted and ADC flown wind effect on ground speed for run 27. Negative values indicate a headwind.**

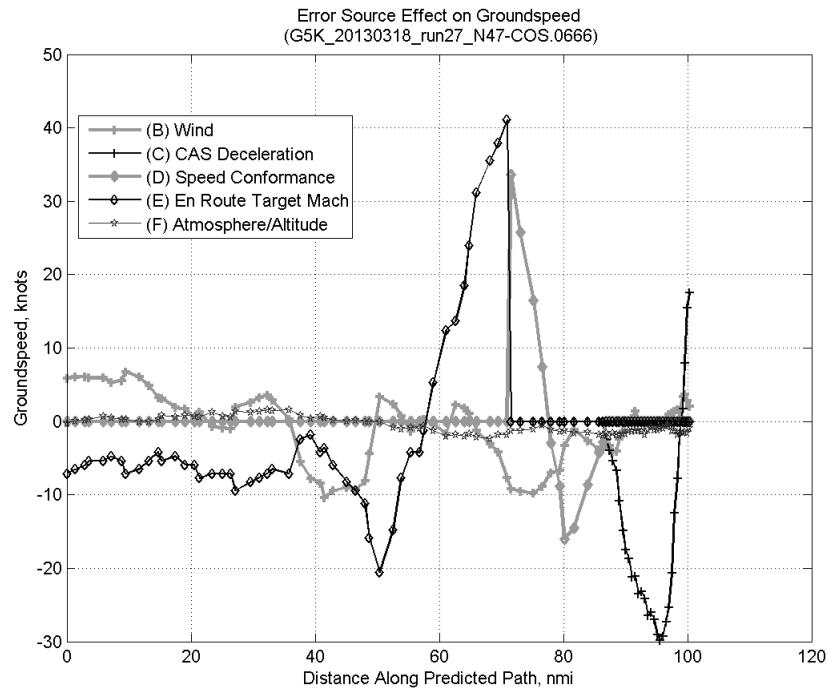


**Figure 1039: Error sources (flown minus predicted) converted to a ground speed effect for run 27. Positive values indicate the flown ground speed was faster than the CTAS prediction.**

### D.7.C. CAS Deceleration

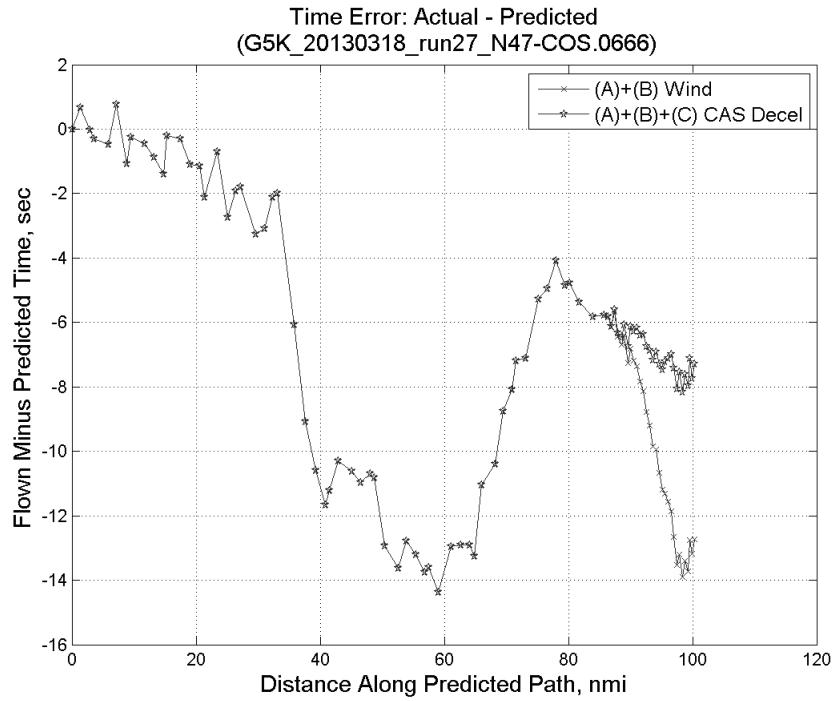


**Figure 1040:** Time error for run 27 before ((A)+(B) Wind) and after ((A)+(B)+(C) CAS Decel) removing CAS deceleration error source.

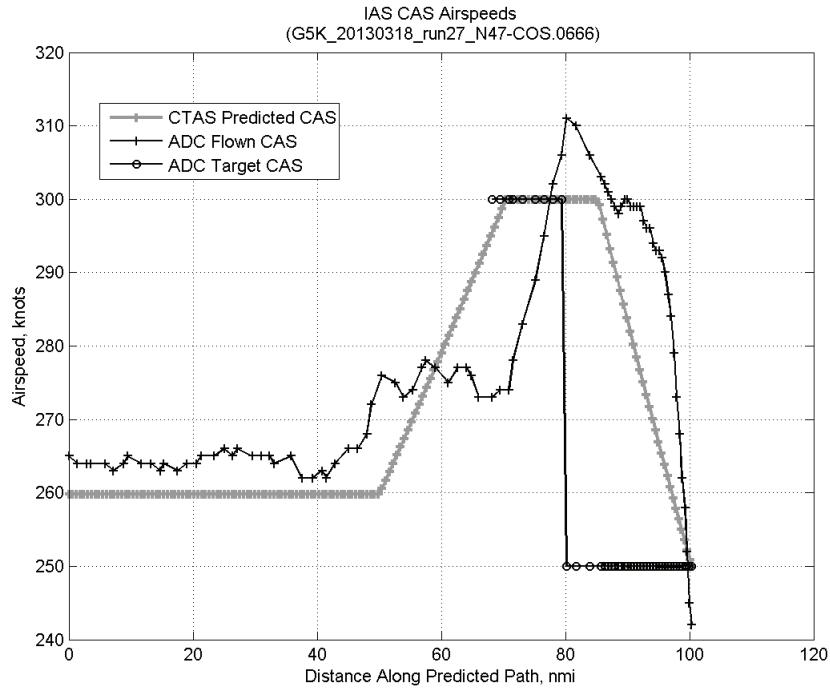


**Figure 1041:** CTAS predicted and ADC flown CAS for run 27. CAS that is being targeted is shown with circle markers.

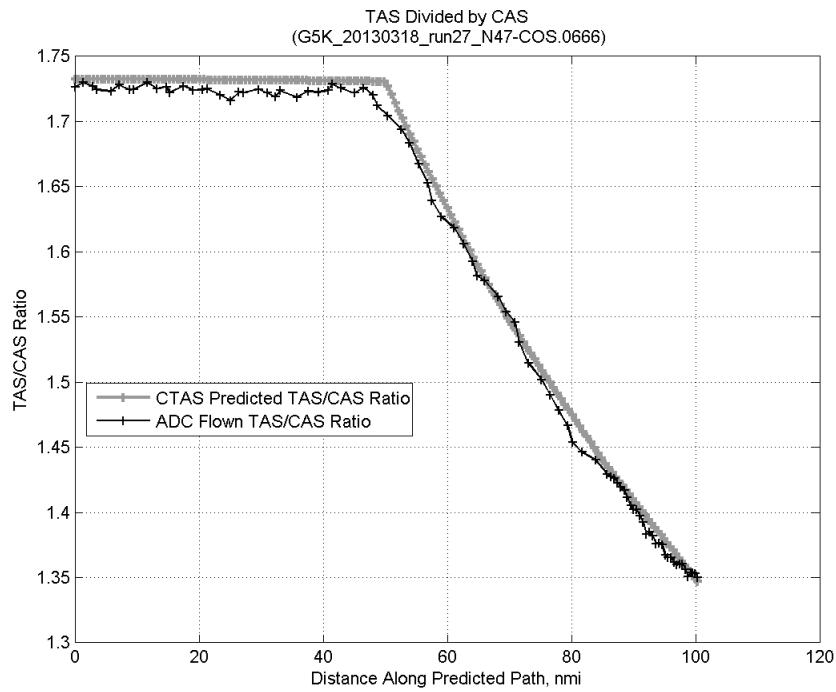


**Figure 1042: CTAS predicted and ADC flown TAS/CAS ratio for run 27.**

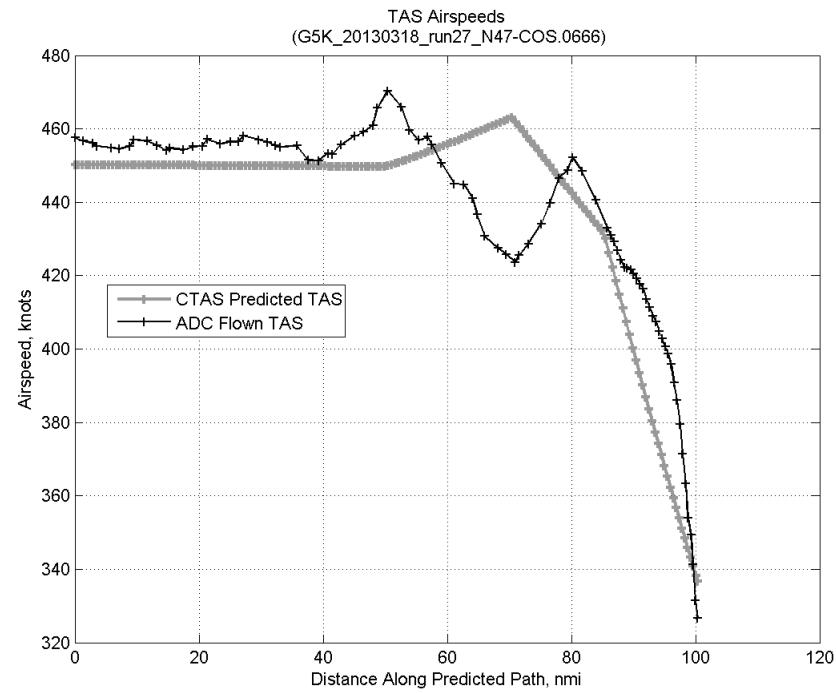


**Figure 1043: CTAS predicted and ADC flown TAS for run 27.**

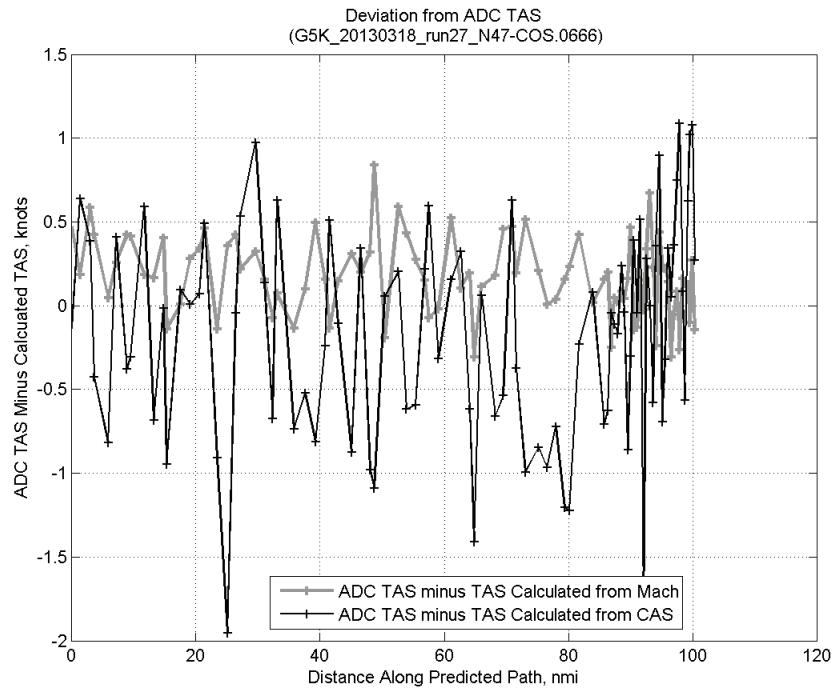


**Figure 1044:** Deviation from ADC flown TAS if calculating TAS using ADC flown CAS, Mach, atmospheric temperature, and atmospheric pressure for run 27.

#### D.7.D. Speed Conformance

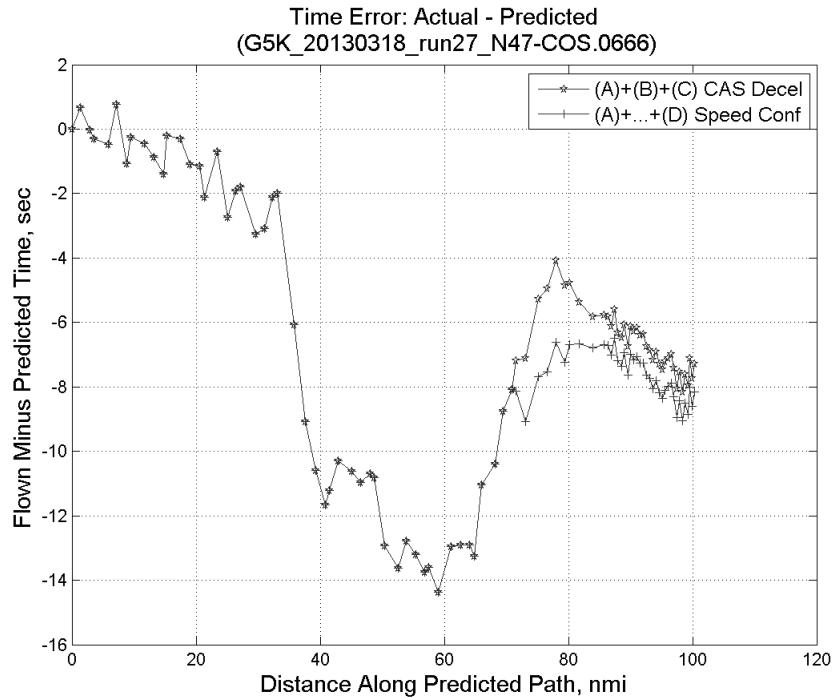


**Figure 1045:** Time error for run 27 before ((A)+(B)+(C) CAS Decel) and after ((A)+...+(D) Speed Conf) removing speed conformance error source.

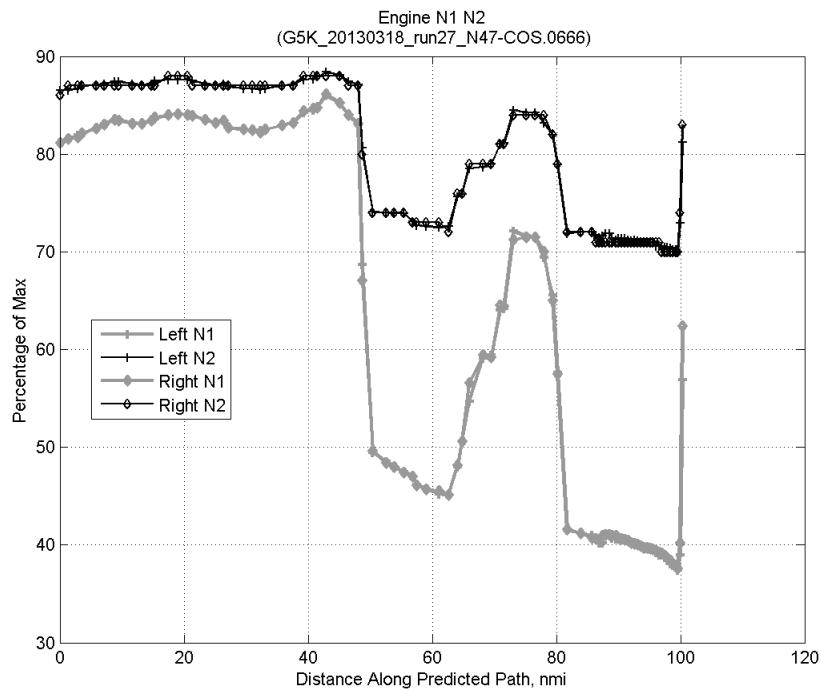


**Figure 1046: Flown engine N1 and N2 for run 27.**

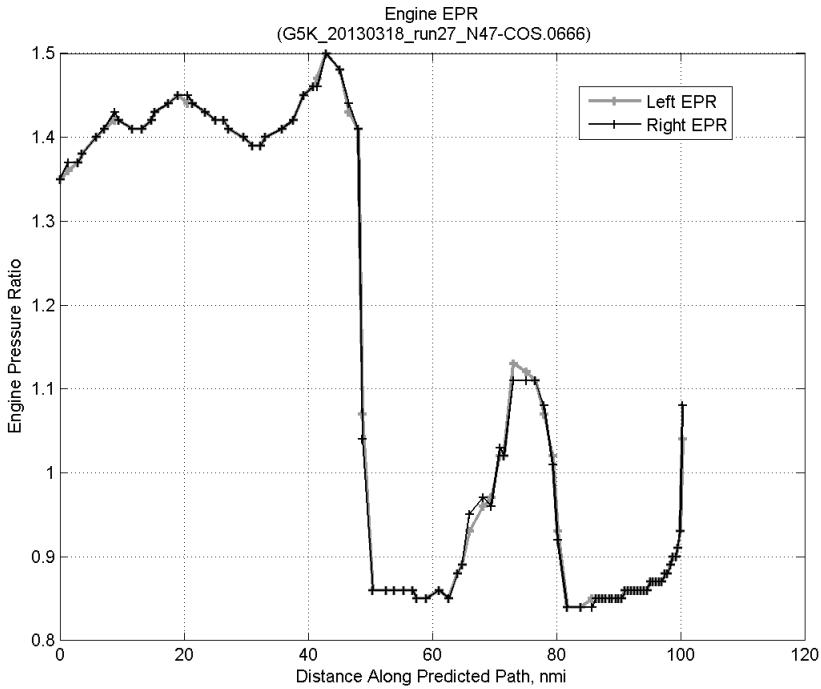


**Figure 1047: Flown engine EPR for run 27.**

### D.7.E. Target Mach

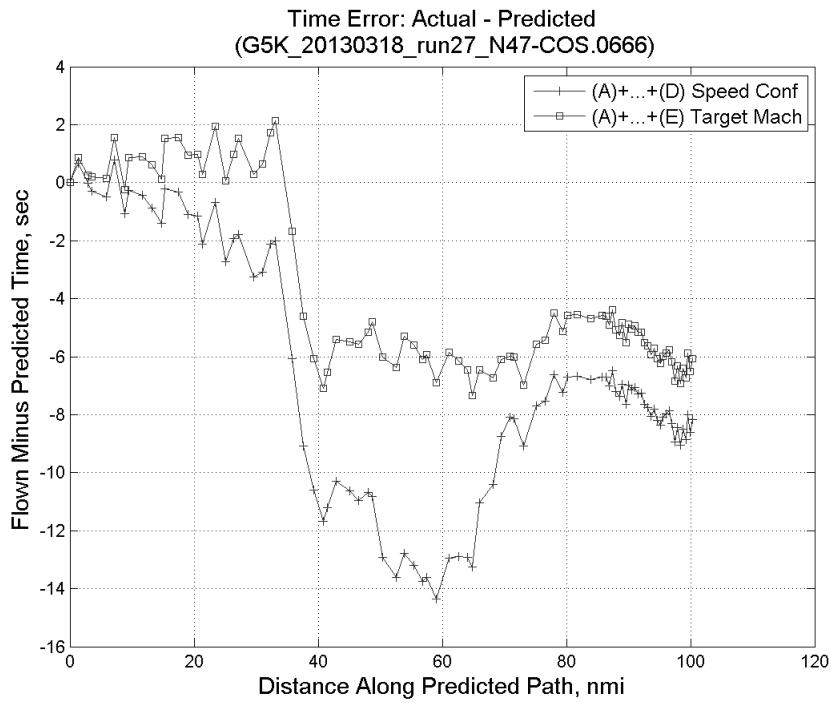


**Figure 1048: Time error for run 27 before ((A)+...+(D) Speed Conf) and after ((A)+...+(E) Target Mach) removing target Mach error source.**

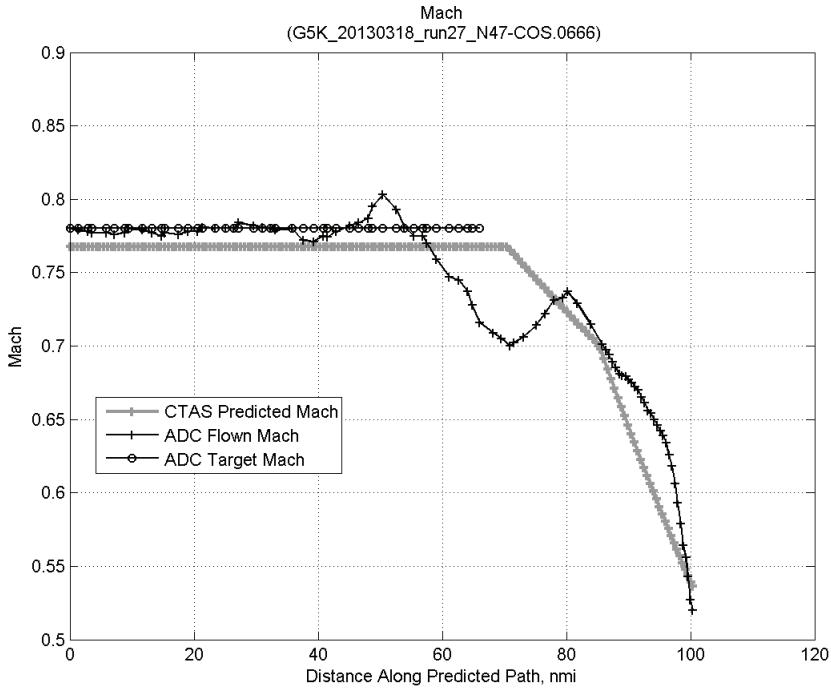


**Figure 1049: CTAS predicted and ADC flown Mach for run 27. Mach being targeted (ADC) shown with circle markers.**

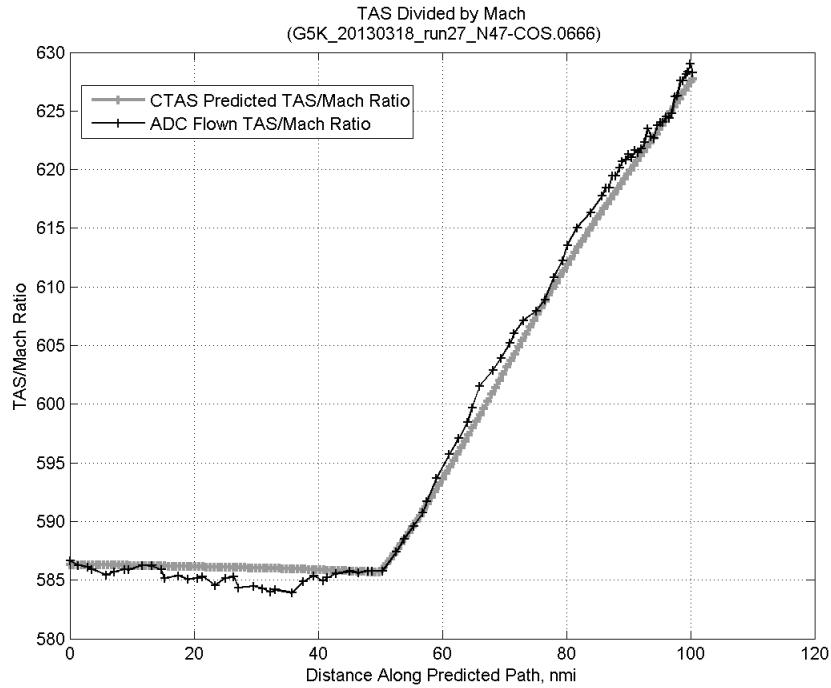


**Figure 1050: CTAS predicted and ADC flown TAS/Mach ratio for run 27.**

#### D.7.F. Atmosphere/Altitude

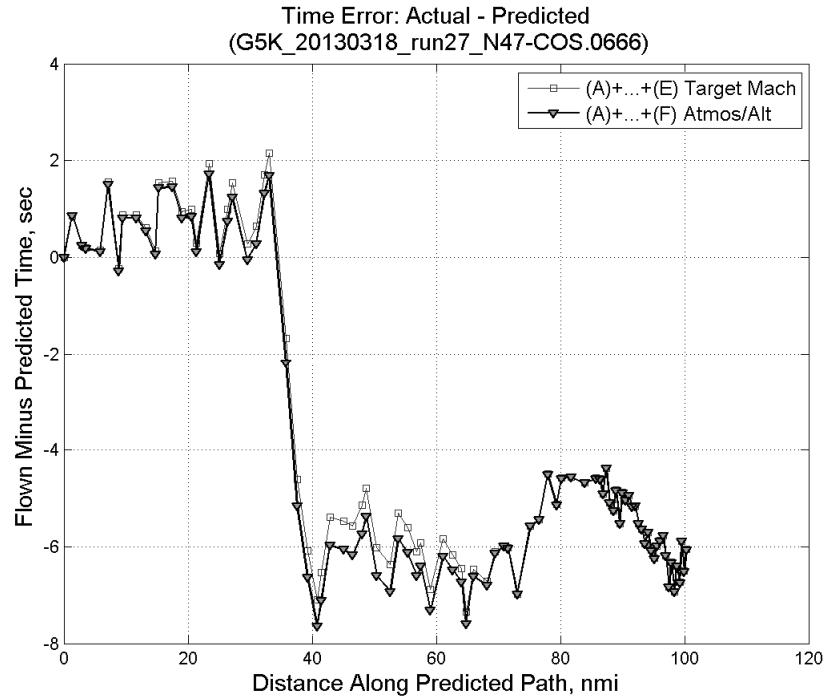


**Figure 1051: Time error for run 27 before ((A)+...+(E) Target Mach) and after ((A)+...+(F) Atmos/Alt) removing atmosphere/altitude error source.**

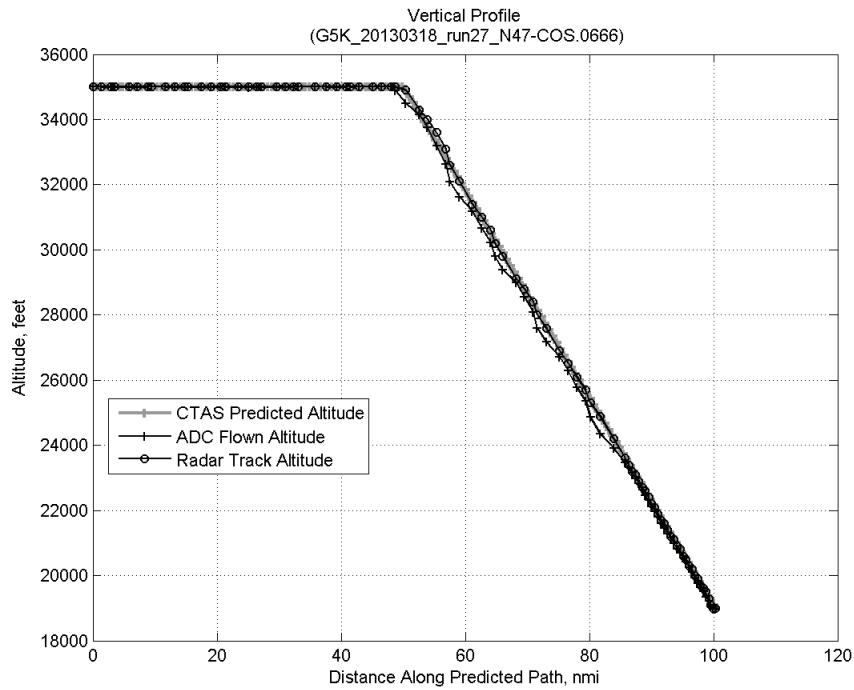


**Figure 1052: Flown (ADC) and predicted (CTAS) vertical profile for run 27.**

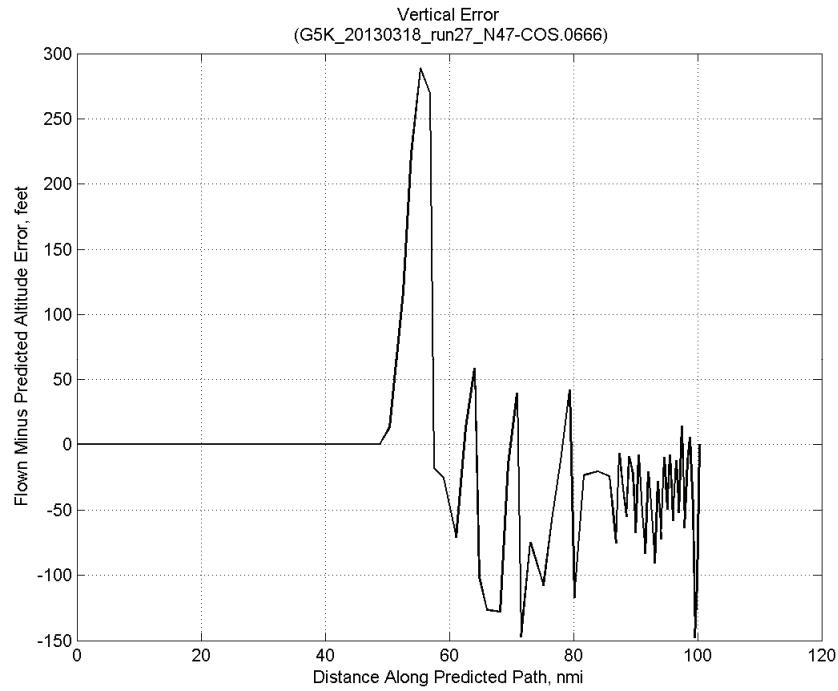


**Figure 1053: Vertical error (flown minus predicted altitude) for run 27. Positive values indicate aircraft flew higher than predicted by CTAS.**

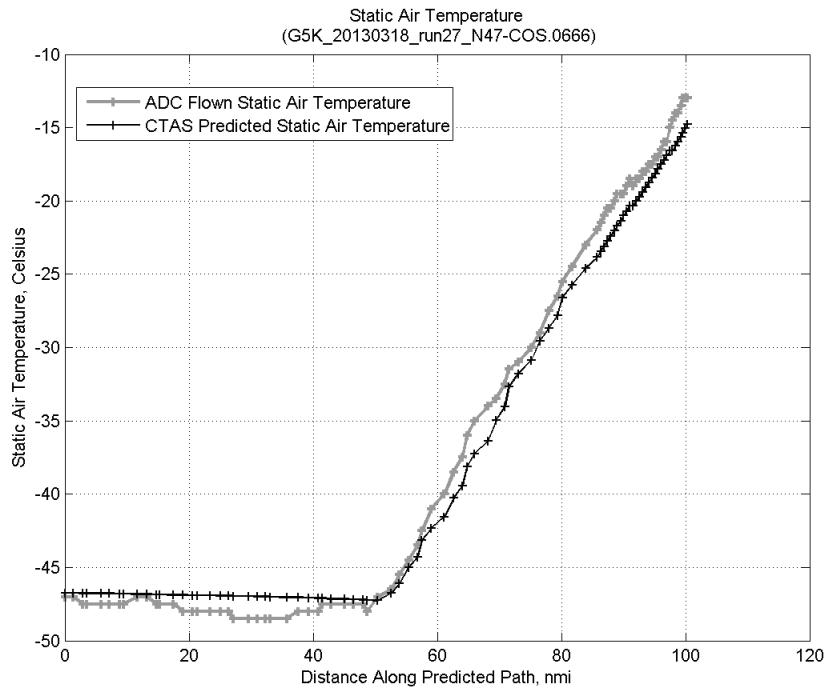


**Figure 1054: Flown (ADC) and predicted (CTAS) static air temperature for run 27.**

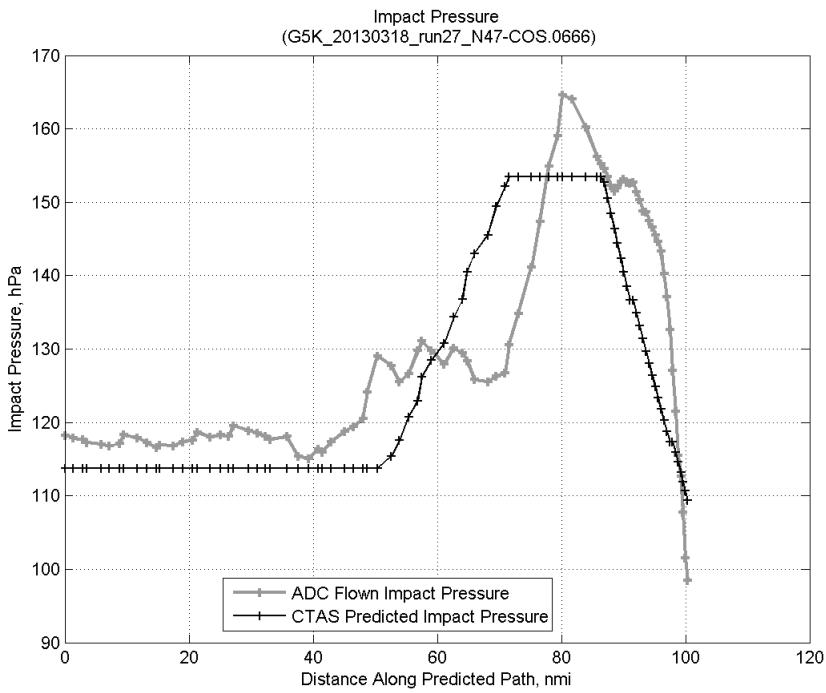


**Figure 1055: Flown (ADC) and predicted (CTAS) impact pressure for run 27.**

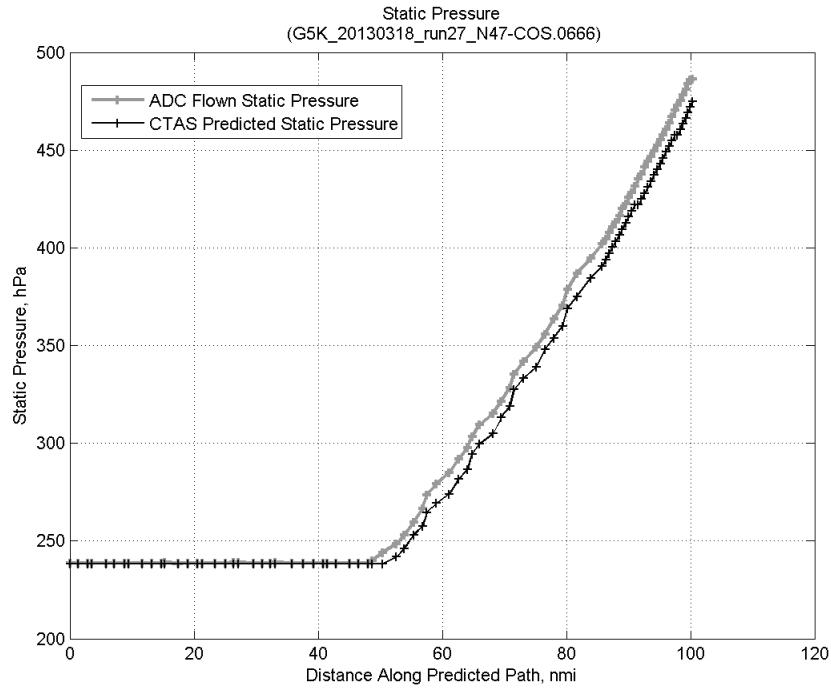


**Figure 1056: Flown (ADC) and predicted (CTAS) static pressure for run 27.**

#### D.7.G. Path Distance

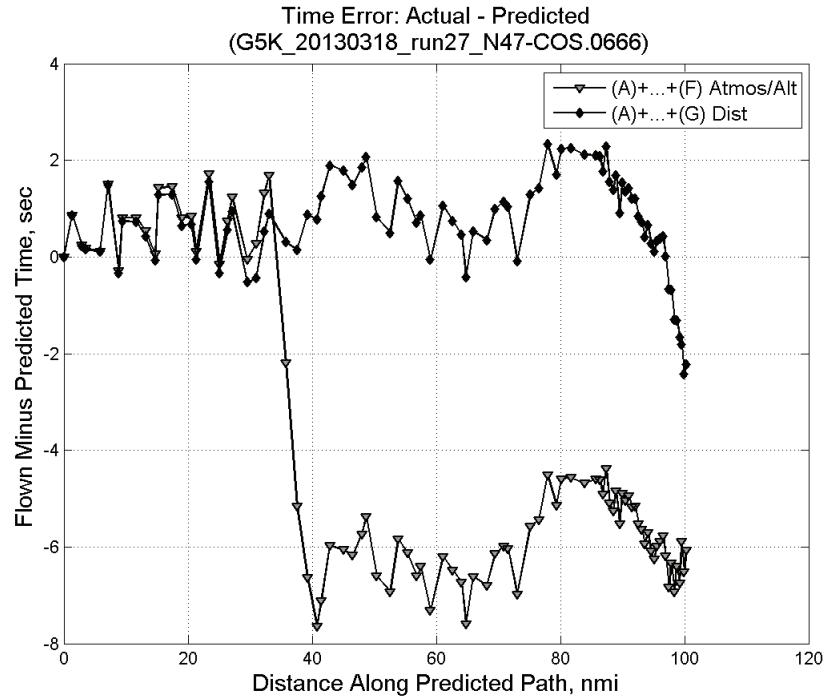


**Figure 1057: Time error for run 27 before ((A)+...+(F) Atmos/Alt) and after ((A)+...+(G) Dist) removing path distance error source.**

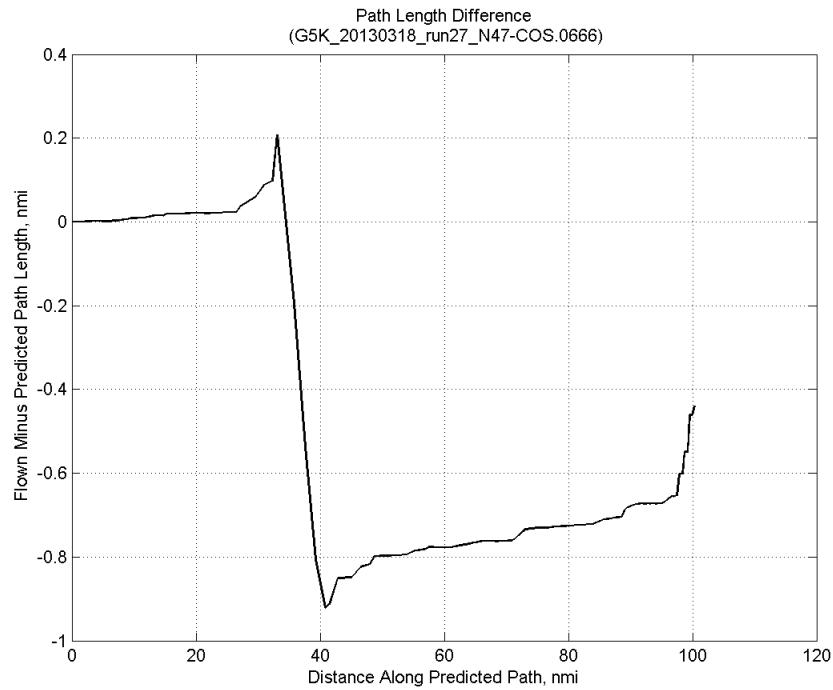


**Figure 1058: ADC flown minus CTAS predicted path length for run 27. Positive values indicate aircraft followed a longer path than predicted by CTAS.**

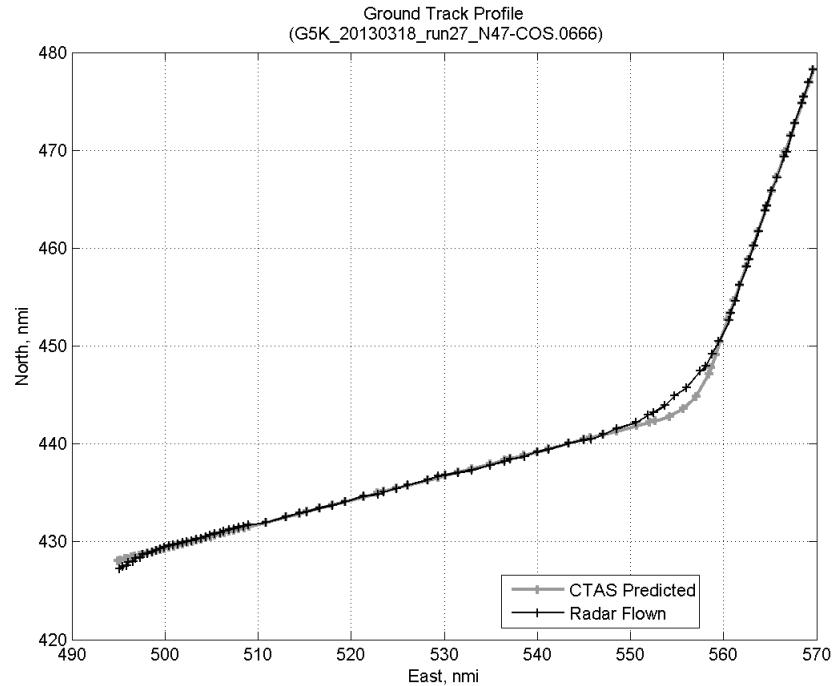


**Figure 1059: CTAS predicted and radar flown ground track profile for run 27.**

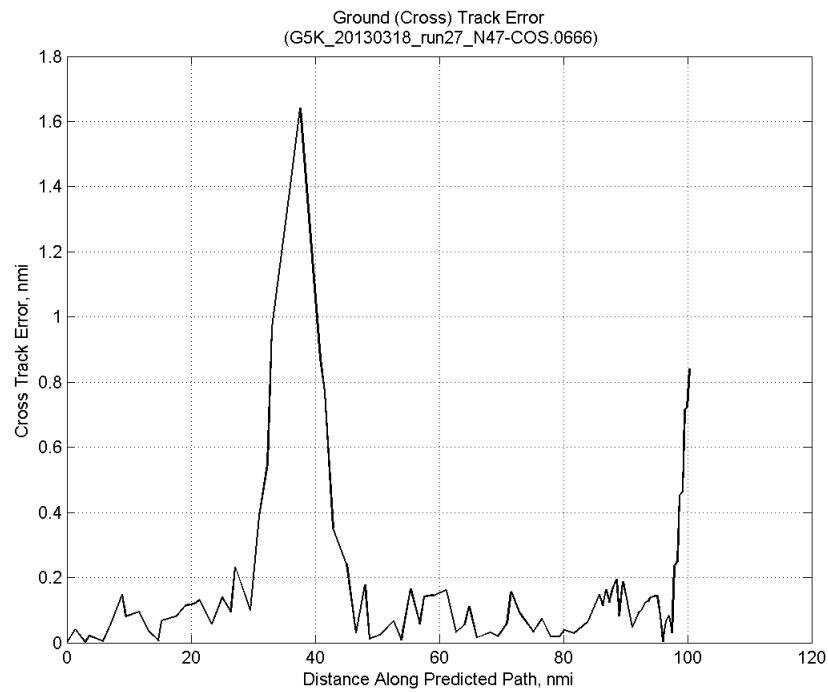


**Figure 1060: Ground (cross) track error for run 27.**

## D.8. Run 33

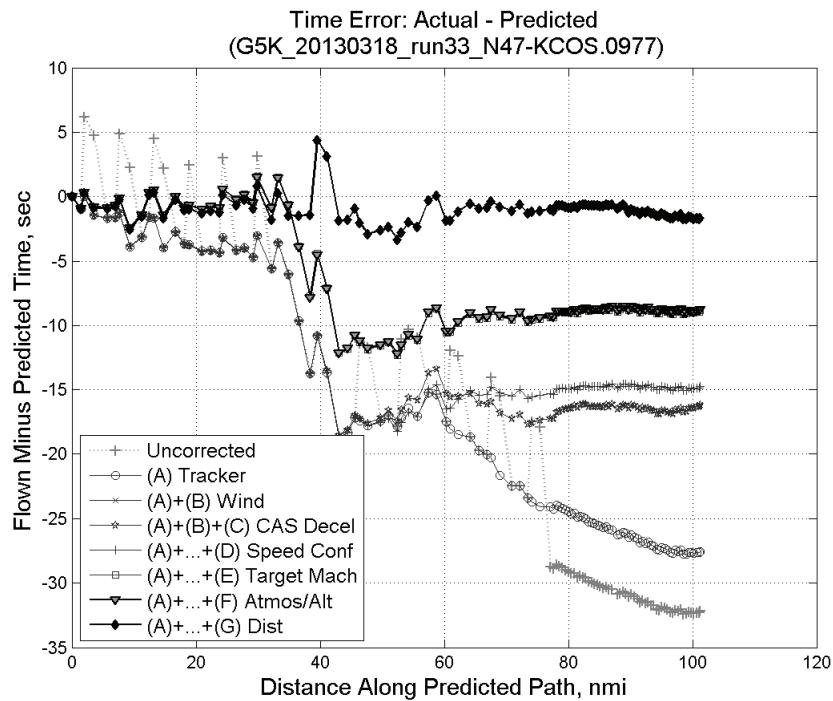


Figure 1061: Time error for run 33 showing incremental effect of removing each error source.

### D.8.A. Tracker Jumps

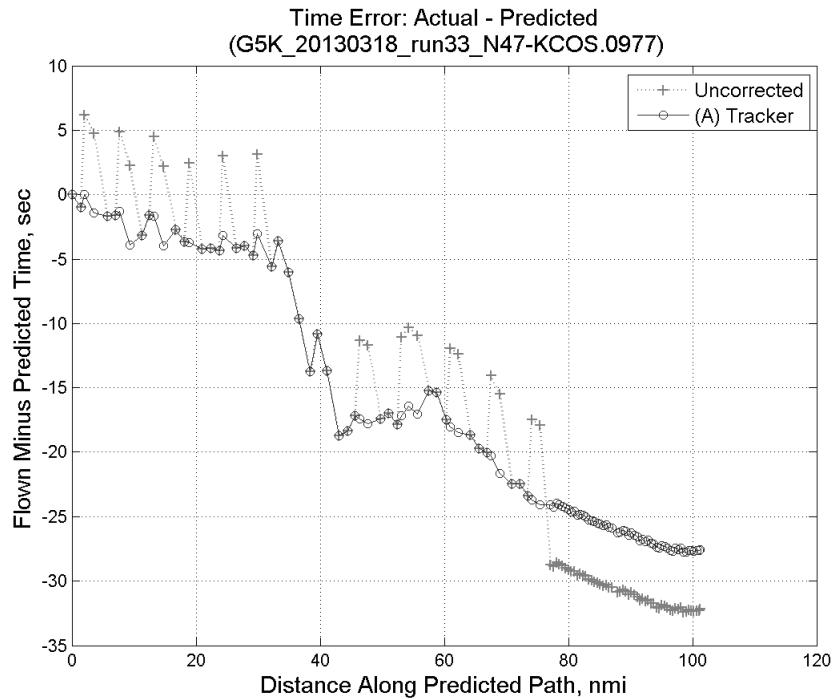
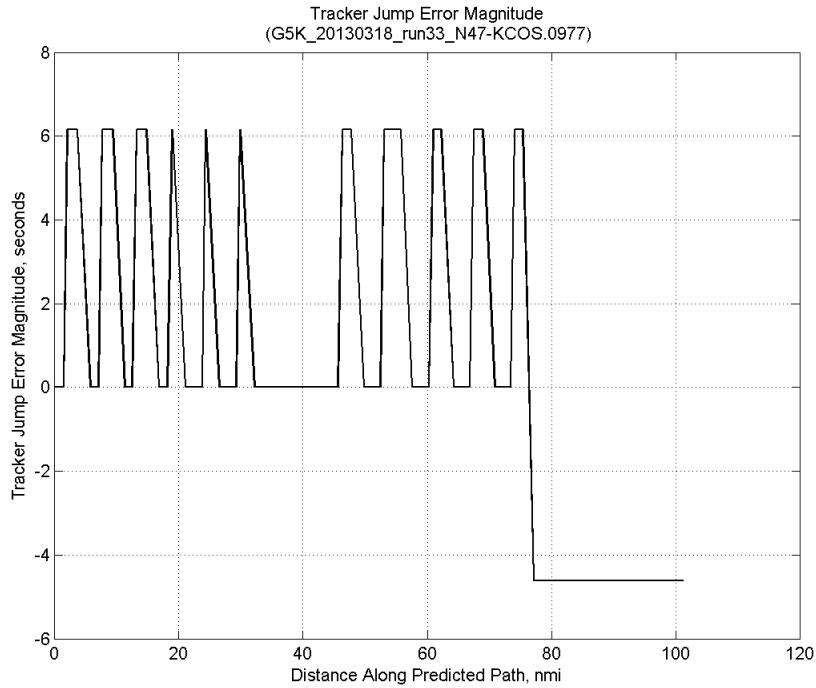
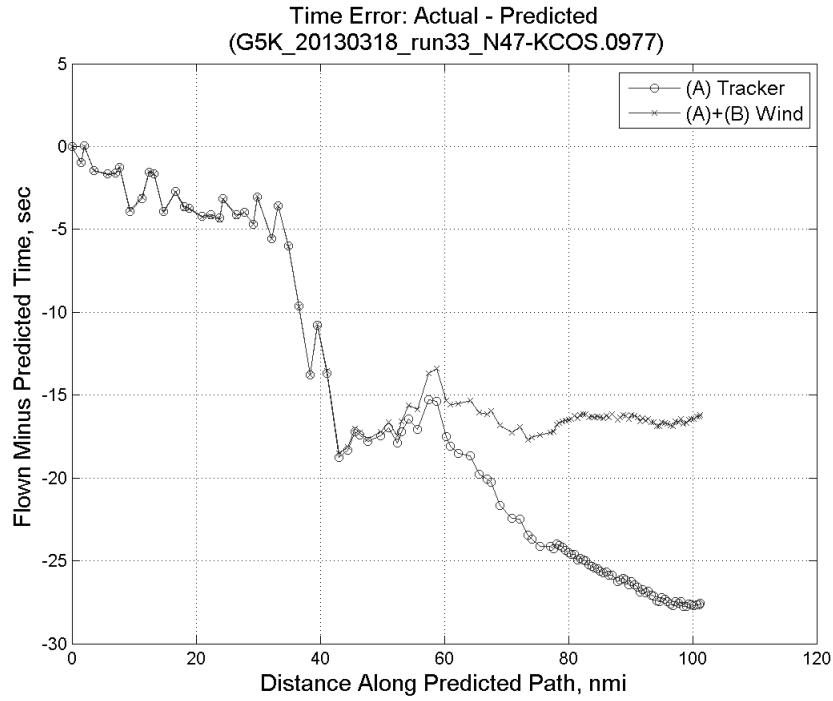


Figure 1062: Time error for run 33 before (Uncorrected) and after ((A) Tracker) removing tracker jump error source.



**Figure 1063: Effect of tracker jump error source on time error for run 33.**

#### D.8.B. Wind



**Figure 1064: Time error for run 33 before ((A) Tracker) and after ((A)+(B) Wind) removing wind error source.**

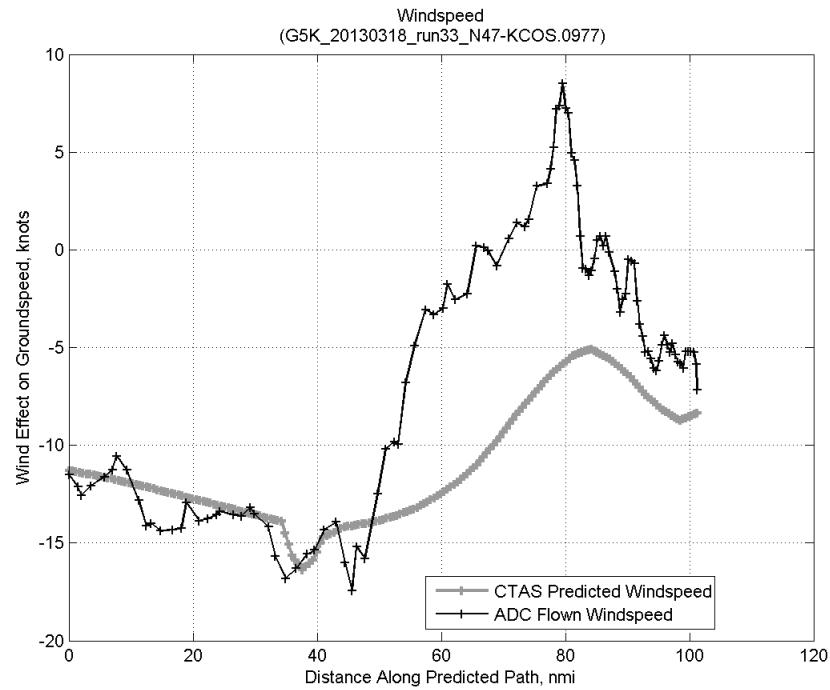


**Figure 1065: CTAS predicted and ADC flown wind effect on ground speed for run 33. Negative values indicate a headwind.**

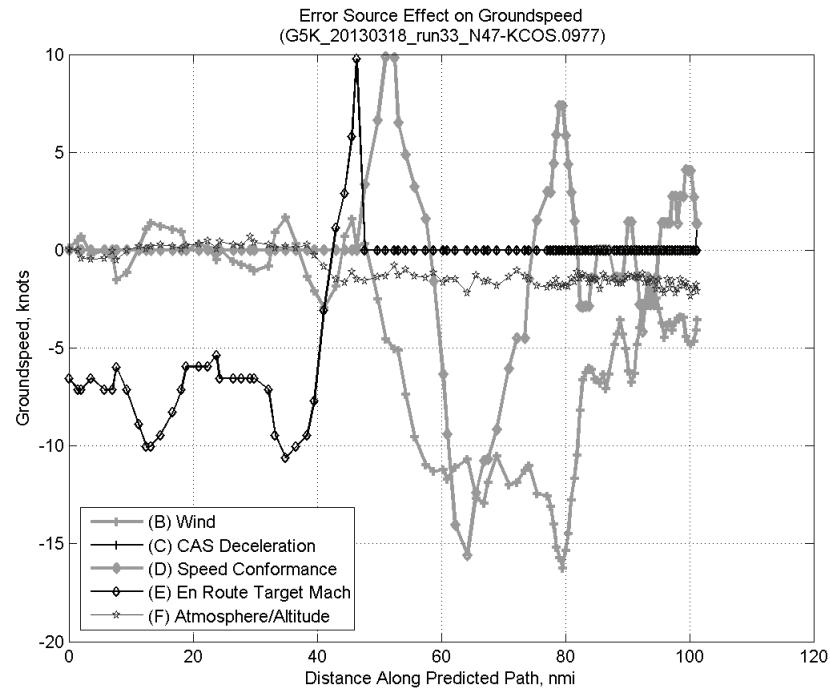


**Figure 1066: Error sources (flown minus predicted) converted to a ground speed effect for run 33. Positive values indicate the flown ground speed was faster than the CTAS prediction.**

### D.8.C. CAS Deceleration

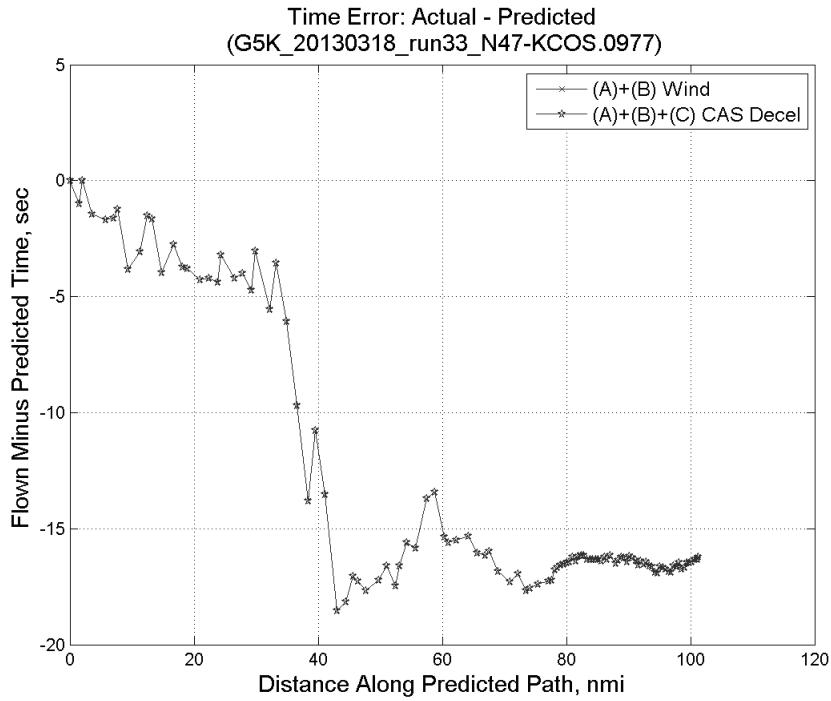


**Figure 1067:** Time error for run 33 before ((A)+(B) Wind) and after ((A)+(B)+(C) CAS Decel) removing CAS deceleration error source.

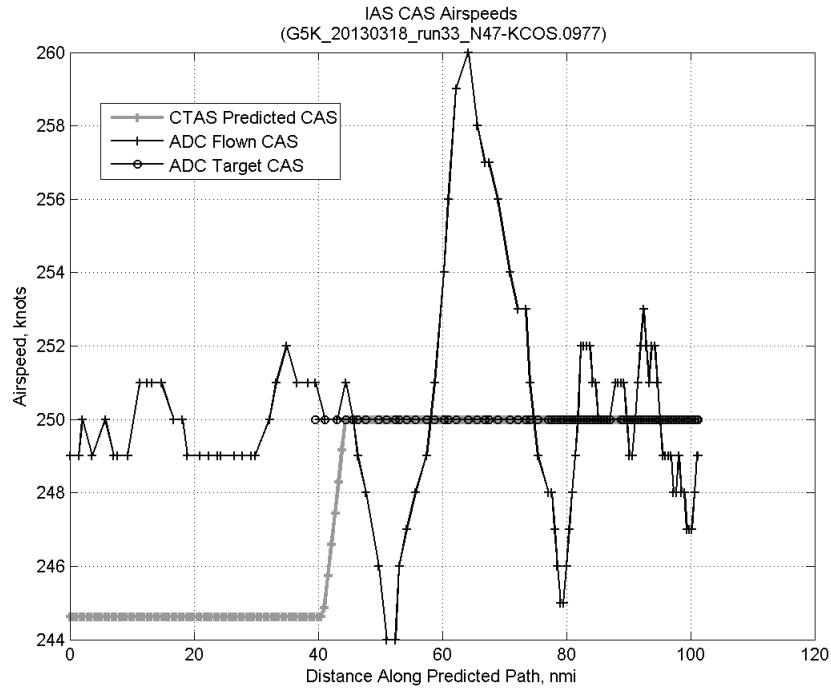


**Figure 1068:** CTAS predicted and ADC flown CAS for run 33. CAS that is being targeted is shown with circle markers.

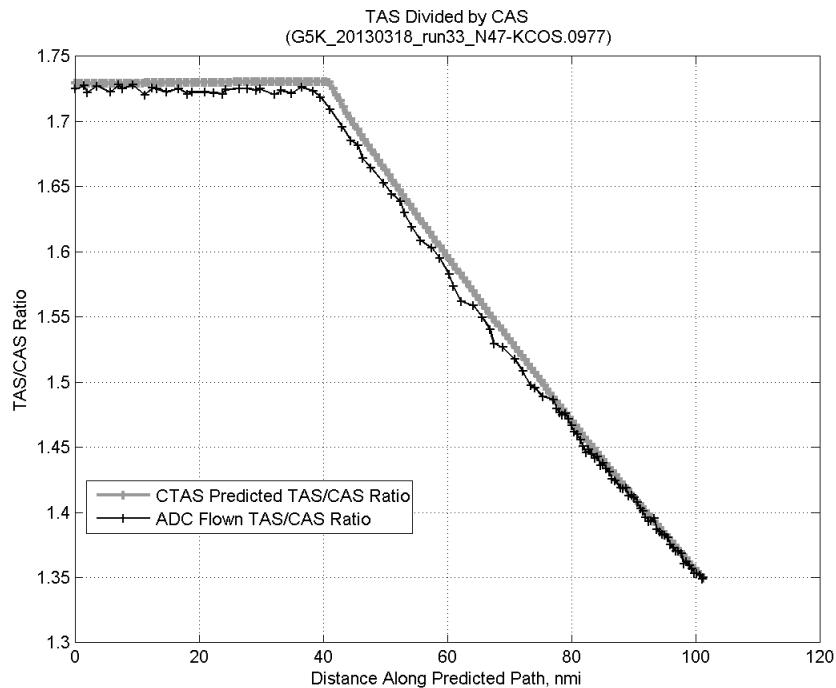


**Figure 1069: CTAS predicted and ADC flown TAS/CAS ratio for run 33.**

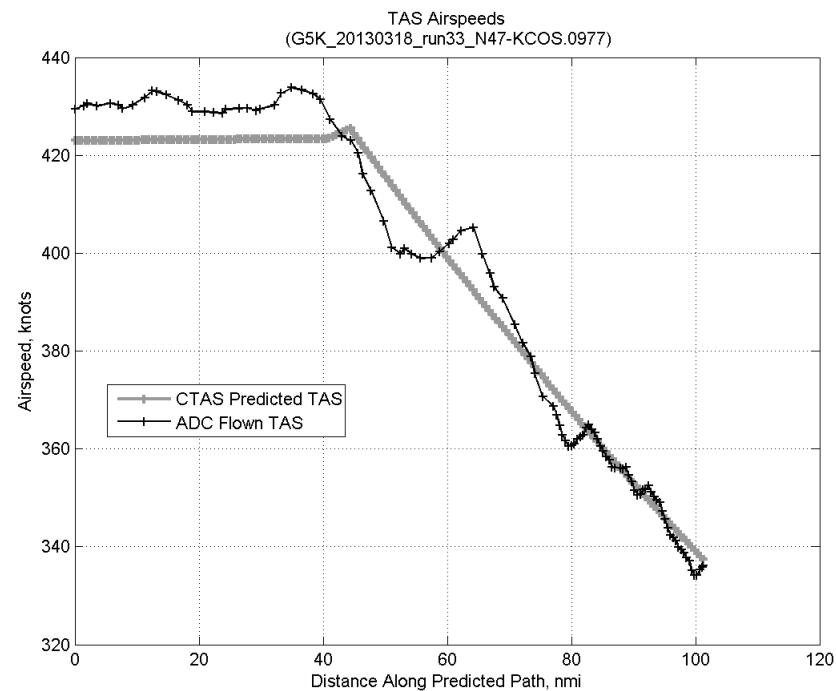


**Figure 1070: CTAS predicted and ADC flown TAS for run 33.**

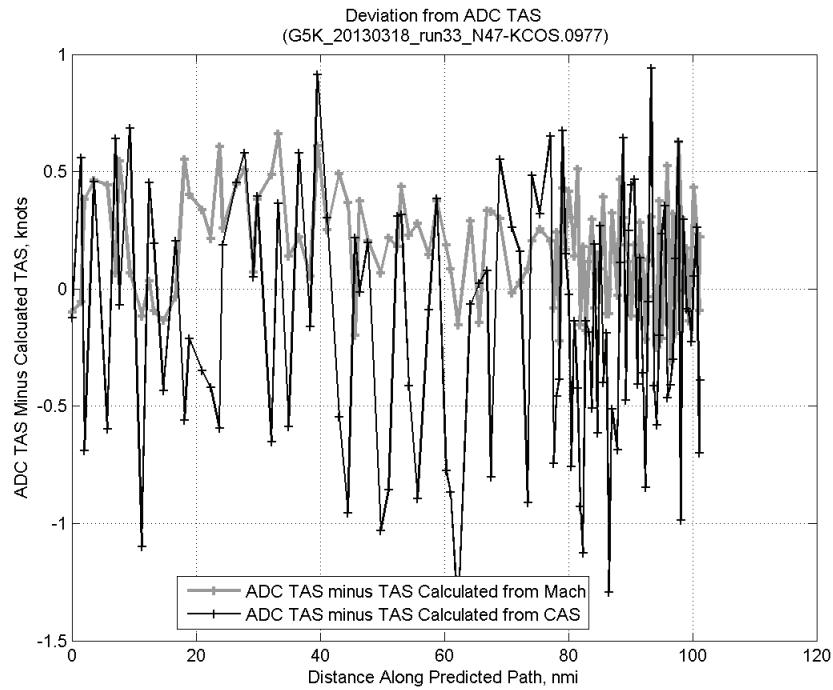


**Figure 1071:** Deviation from ADC flown TAS if calculating TAS using ADC flown CAS, Mach, atmospheric temperature, and atmospheric pressure for run 33.

#### D.8.D. Speed Conformance

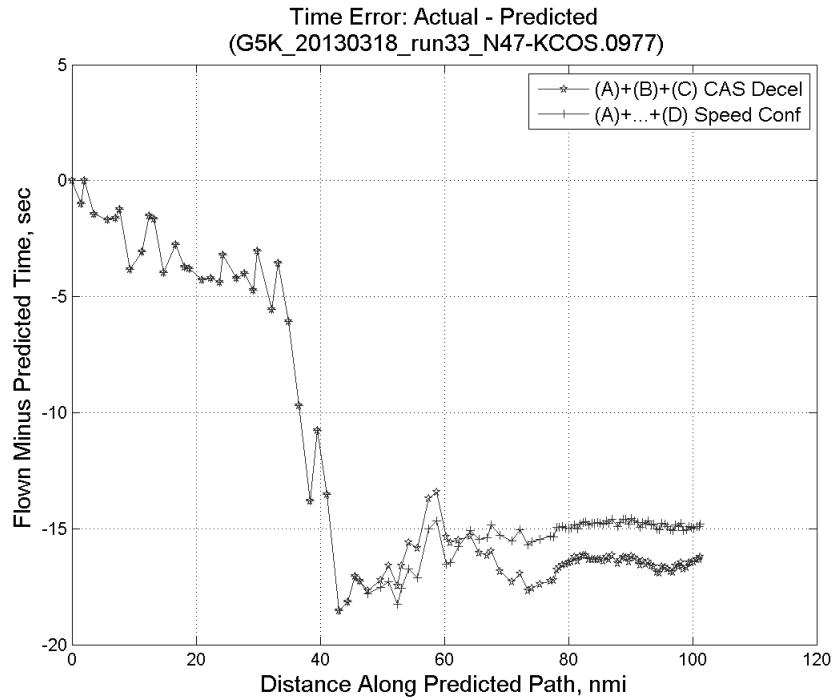


**Figure 1072:** Time error for run 33 before ((A)+(B)+(C) CAS Decel) and after ((A)+...+(D) Speed Conf) removing speed conformance error source.

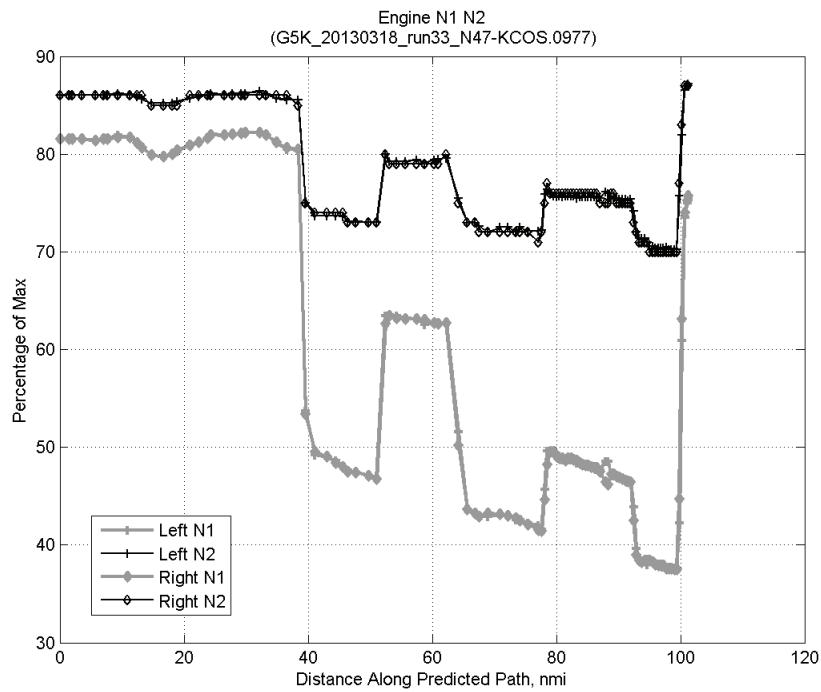


**Figure 1073: Flown engine N1 and N2 for run 33.**

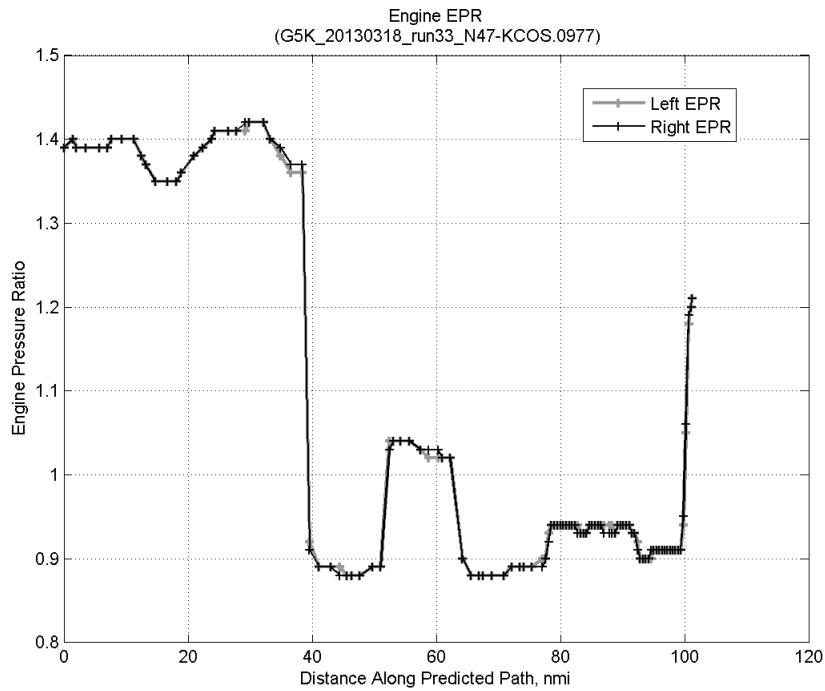


**Figure 1074: Flown engine EPR for run 33.**

### D.8.E. Target Mach

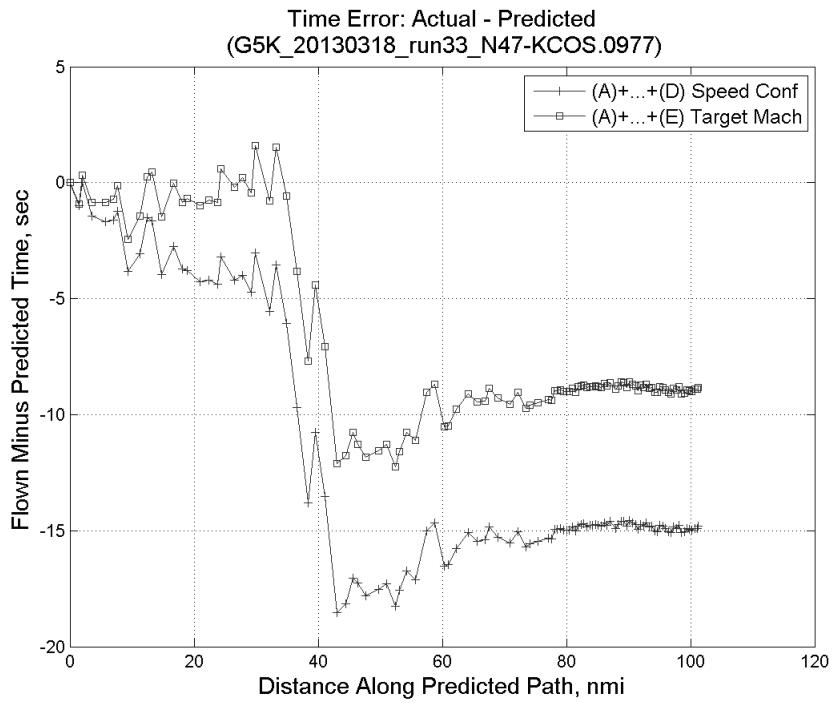


**Figure 1075:** Time error for run 33 before ((A)+...+(D) Speed Conf) and after ((A)+...+(E) Target Mach) removing target Mach error source.

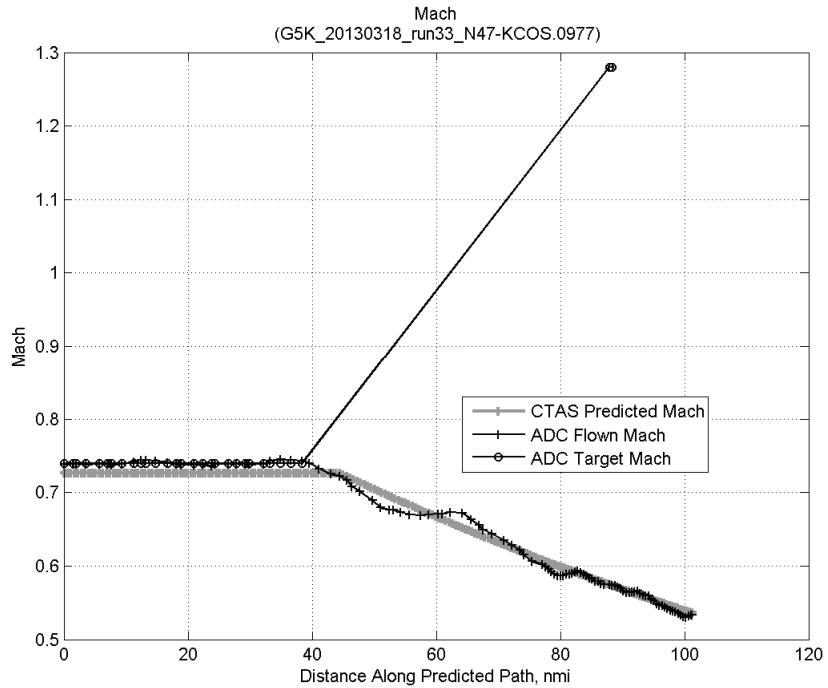


**Figure 1076:** CTAS predicted and ADC flown Mach for run 33. Mach being targeted (ADC) shown with circle markers.

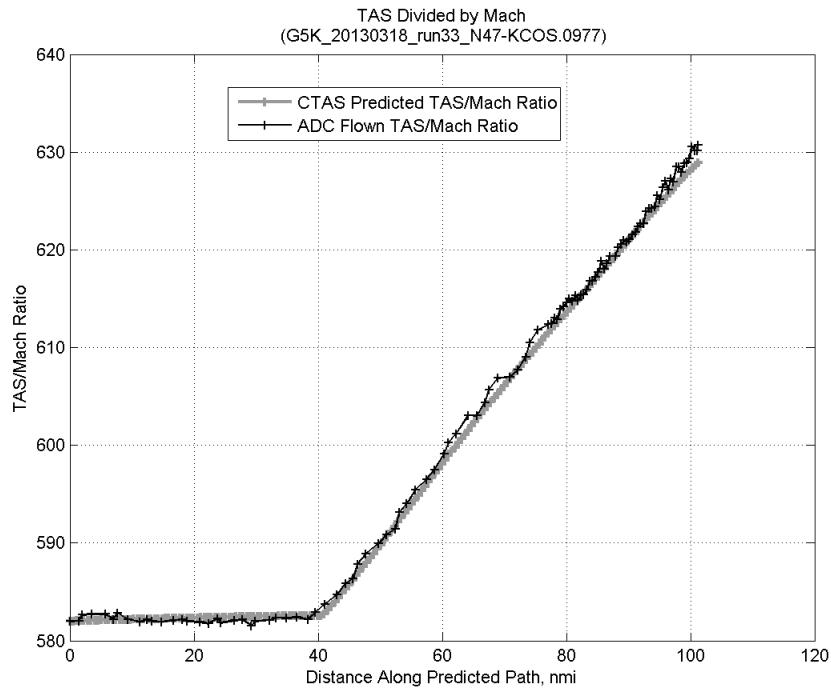


**Figure 1077: CTAS predicted and ADC flown TAS/Mach ratio for run 33.**

#### D.8.F. Atmosphere/Altitude

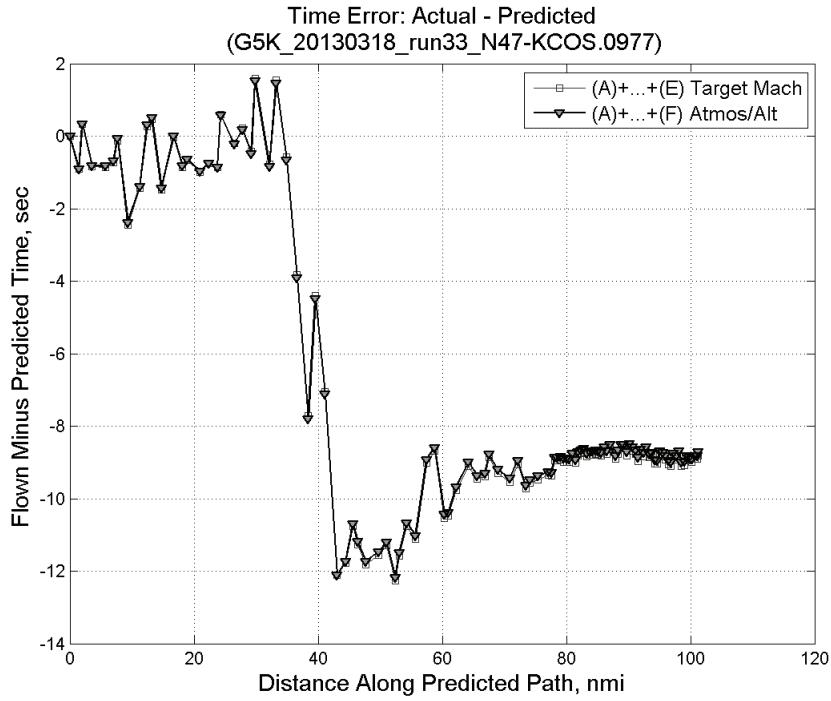


**Figure 1078: Time error for run 33 before ((A)+...+(E) Target Mach) and after ((A)+...+(F) Atmos/Alt) removing atmosphere/altitude error source.**

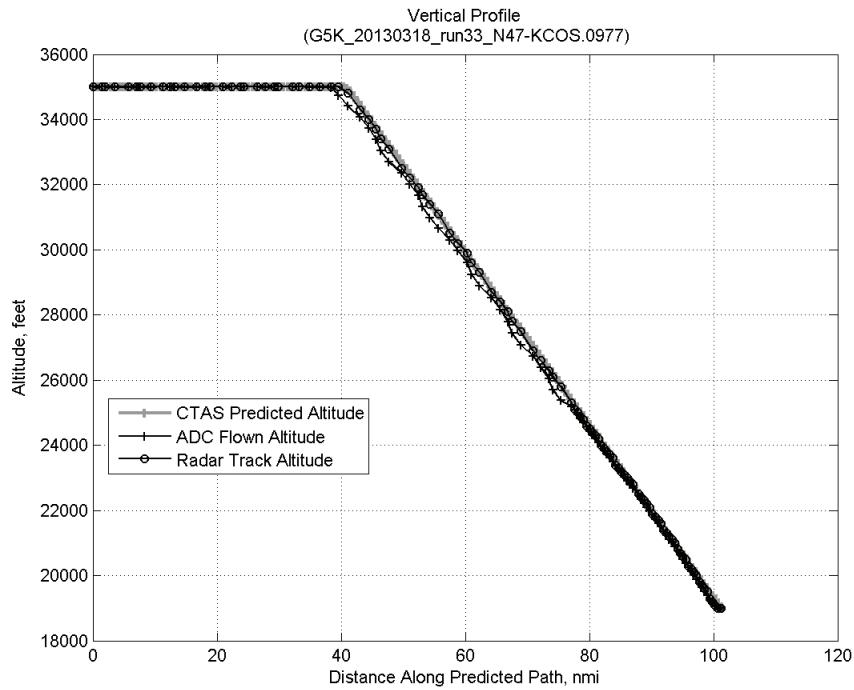


**Figure 1079: Flown (ADC) and predicted (CTAS) vertical profile for run 33.**

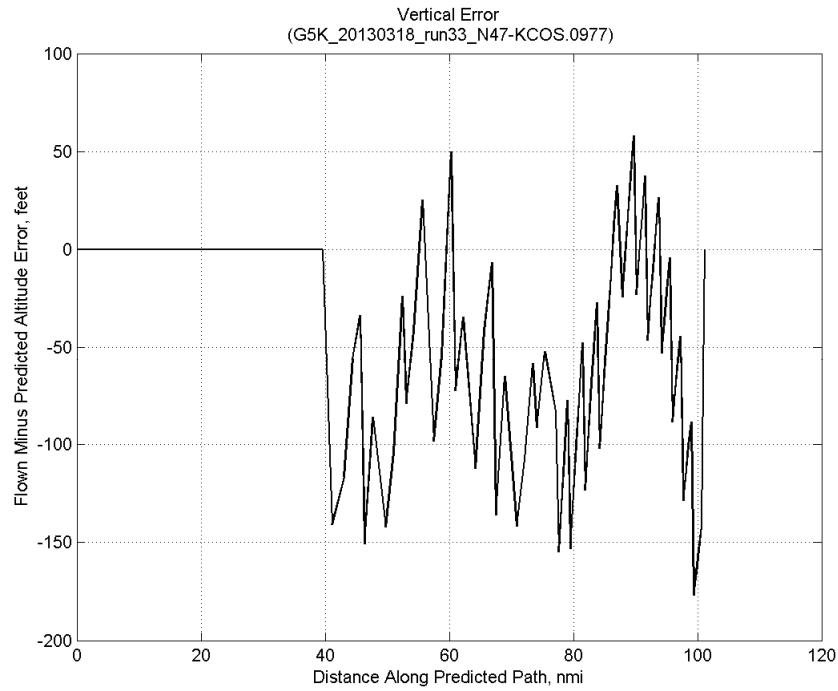


**Figure 1080: Vertical error (flown minus predicted altitude) for run 33. Positive values indicate aircraft flew higher than predicted by CTAS.**

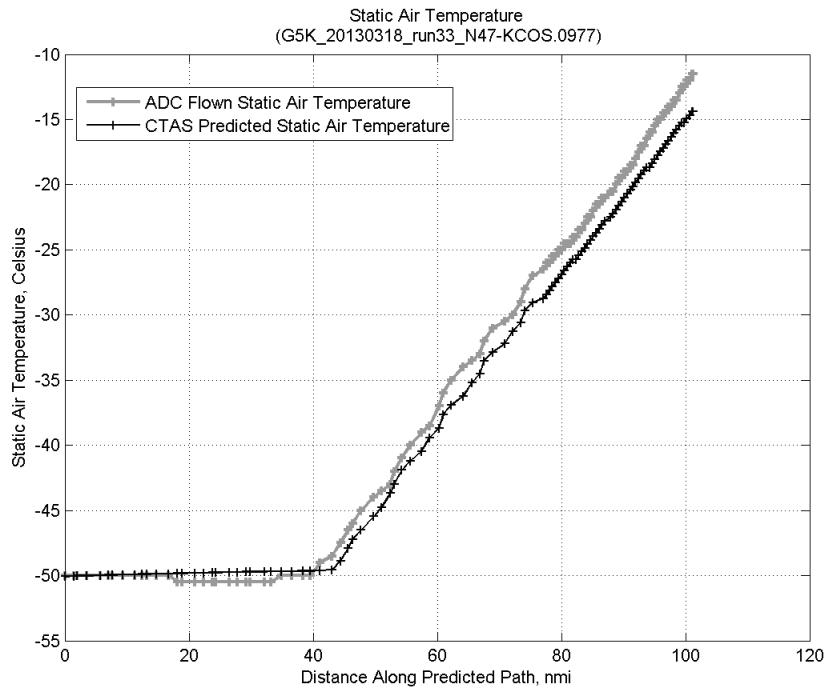


**Figure 1081: Flown (ADC) and predicted (CTAS) static air temperature for run 33.**

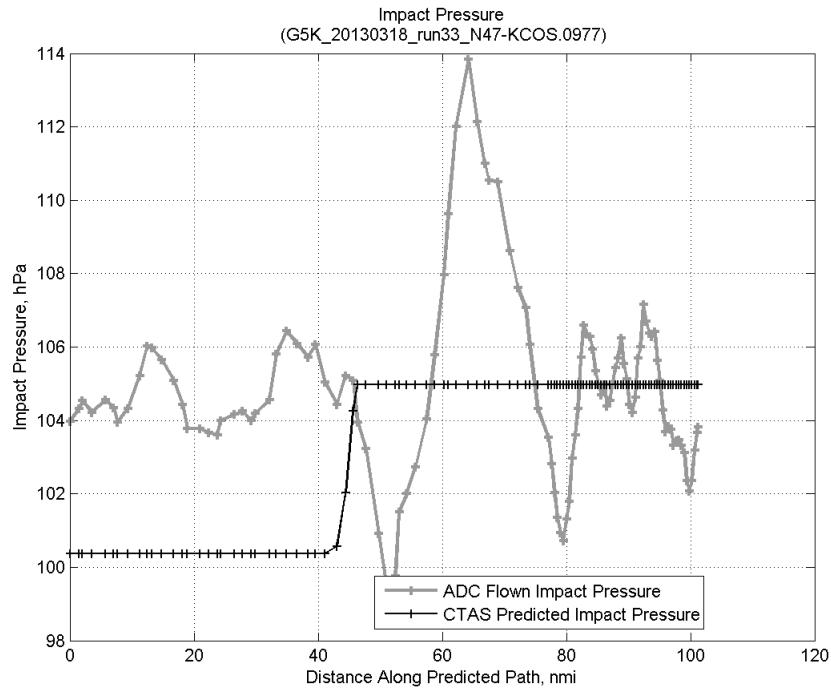


**Figure 1082: Flown (ADC) and predicted (CTAS) impact pressure for run 33.**

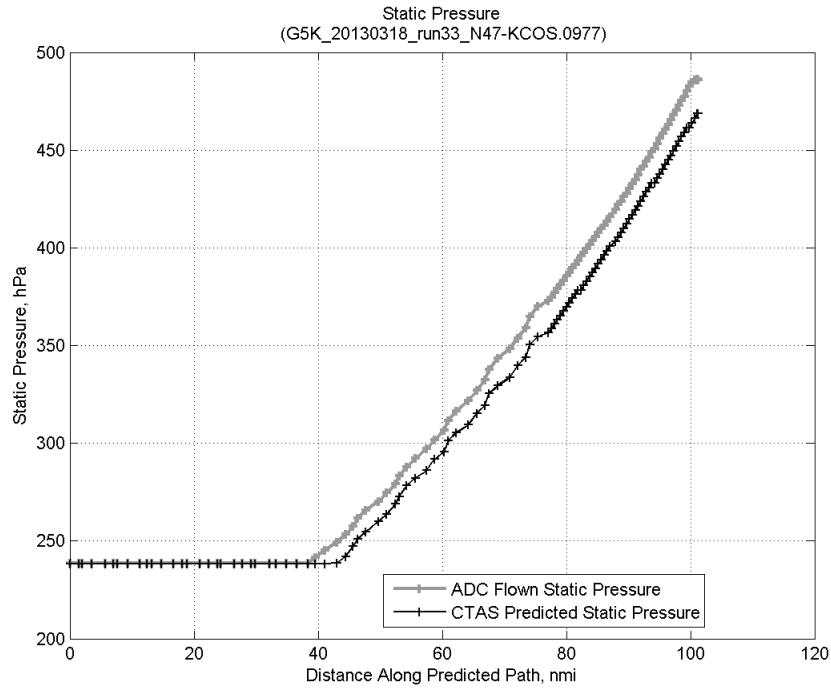


**Figure 1083: Flown (ADC) and predicted (CTAS) static pressure for run 33.**

#### D.8.G. Path Distance

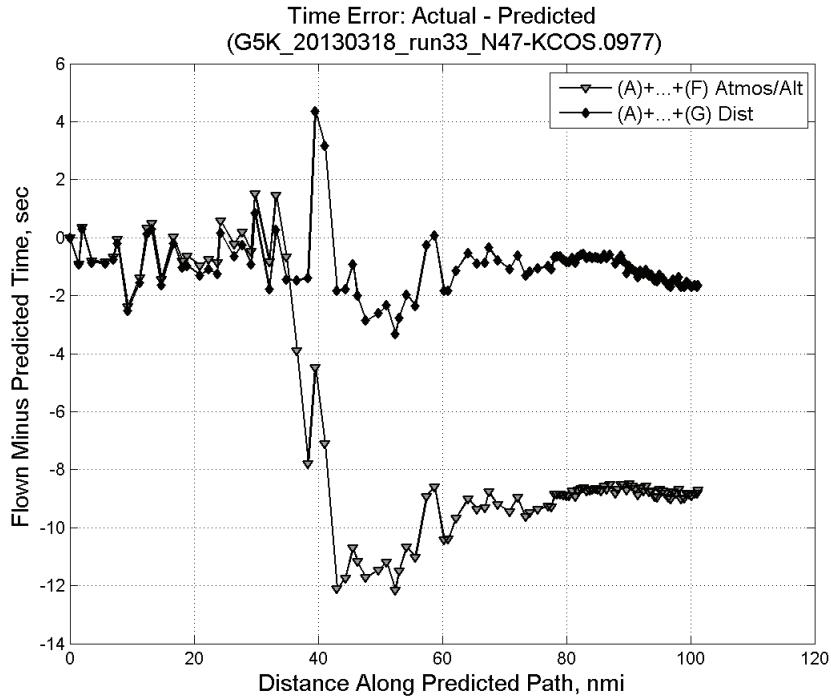


**Figure 1084: Time error for run 33 before ((A)+...+(F) Atmos/Alt) and after ((A)+...+(G) Dist) removing path distance error source.**

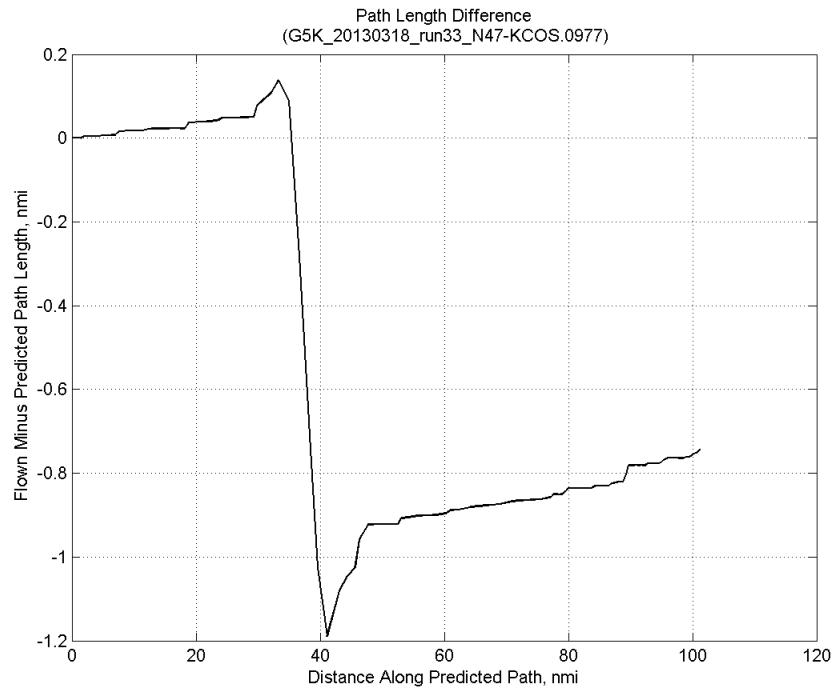


**Figure 1085: ADC flown minus CTAS predicted path length for run 33. Positive values indicate aircraft followed a longer path than predicted by CTAS.**

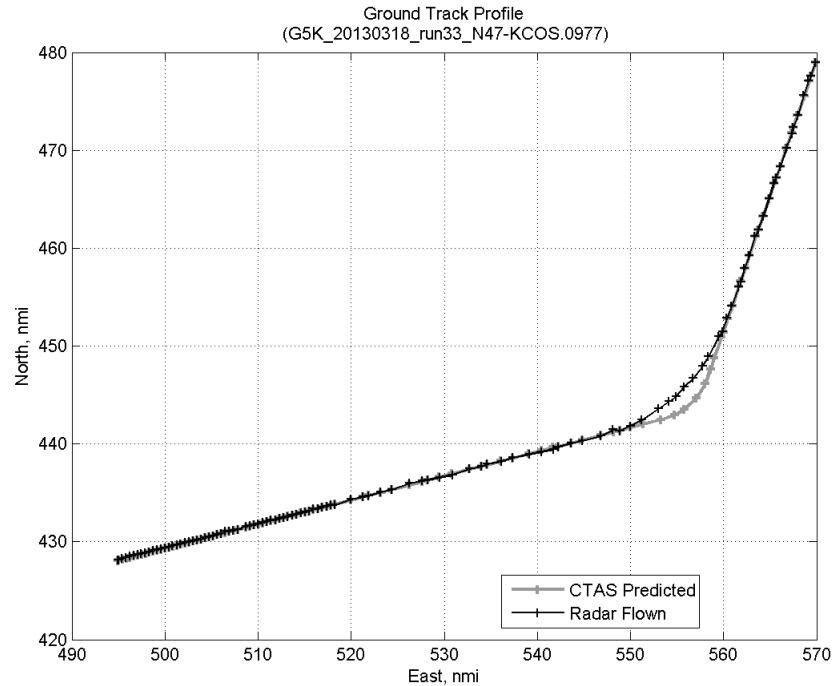


**Figure 1086: CTAS predicted and radar flown ground track profile for run 33.**

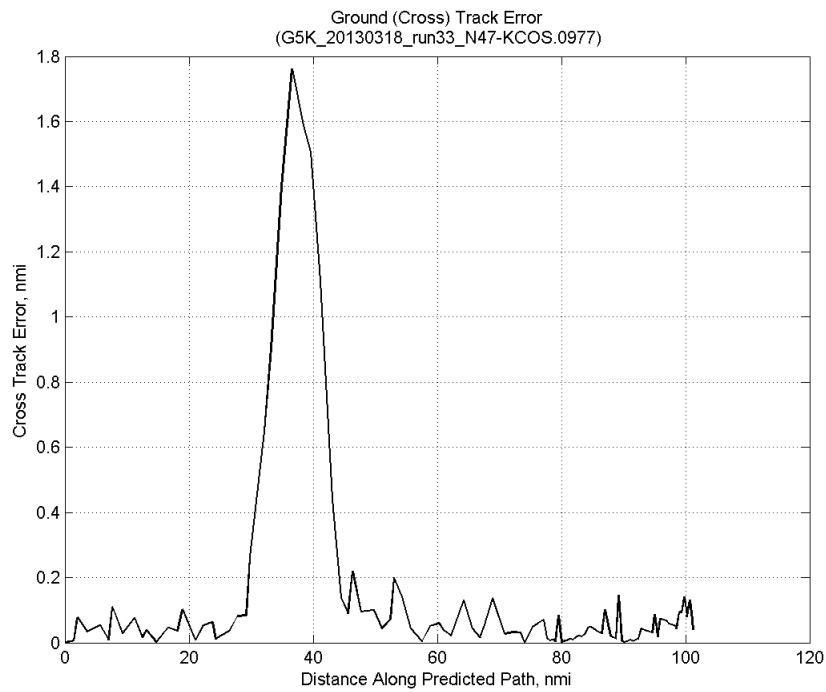


**Figure 1087: Ground (cross) track error for run 33.**

## D.9. Run 40

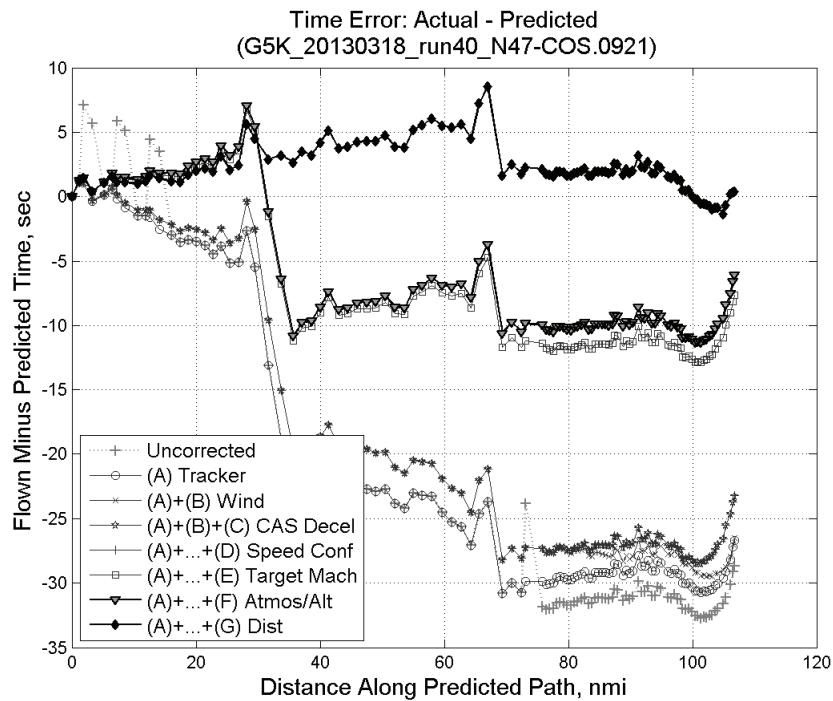


**Figure 1088:** Time error for run 40 showing incremental effect of removing each error source.

### D.9.A. Tracker Jumps

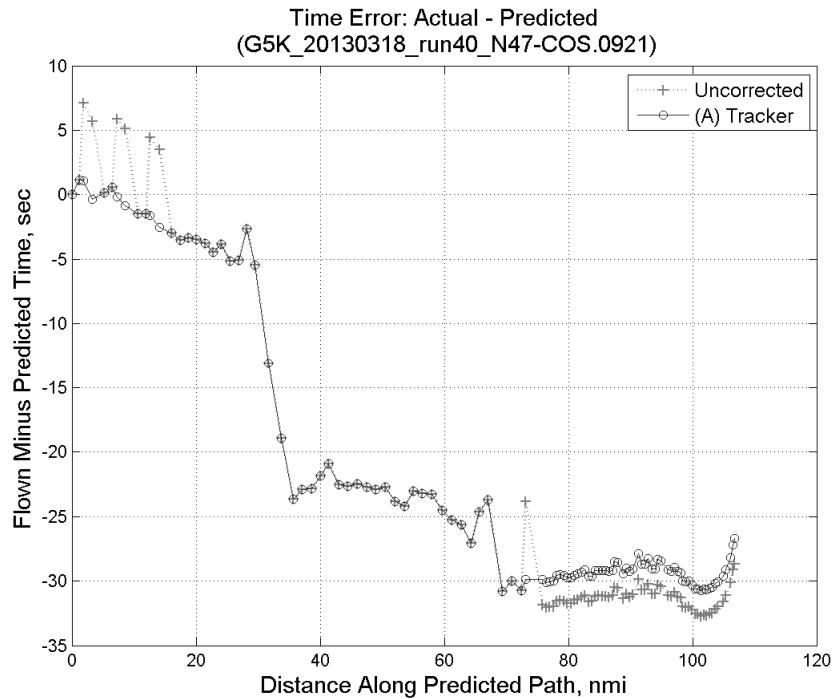


**Figure 1089:** Time error for run 40 before (Uncorrected) and after ((A) Tracker) removing tracker jump error source.

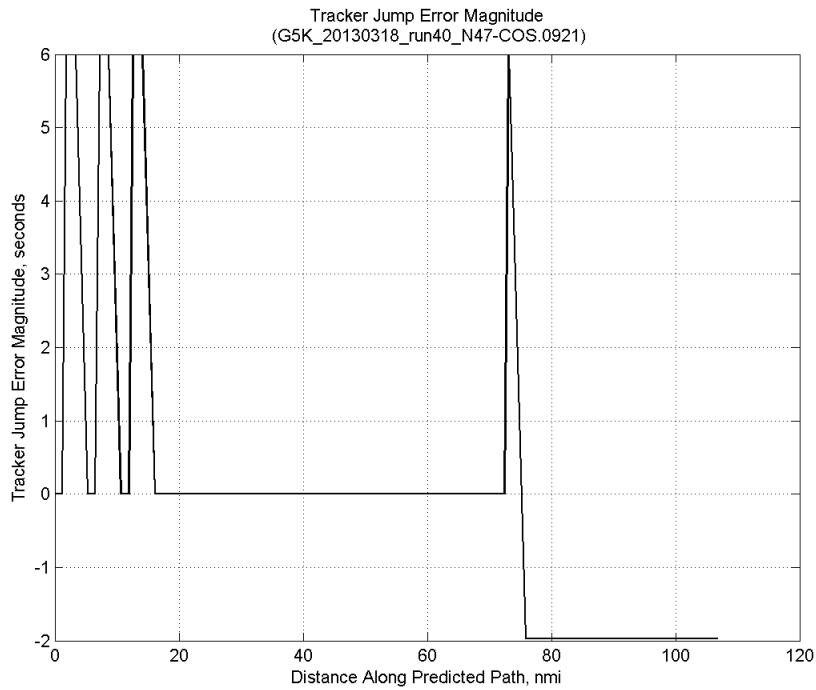


**Figure 1090: Effect of tracker jump error source on time error for run 40.**

#### D.9.B. Wind

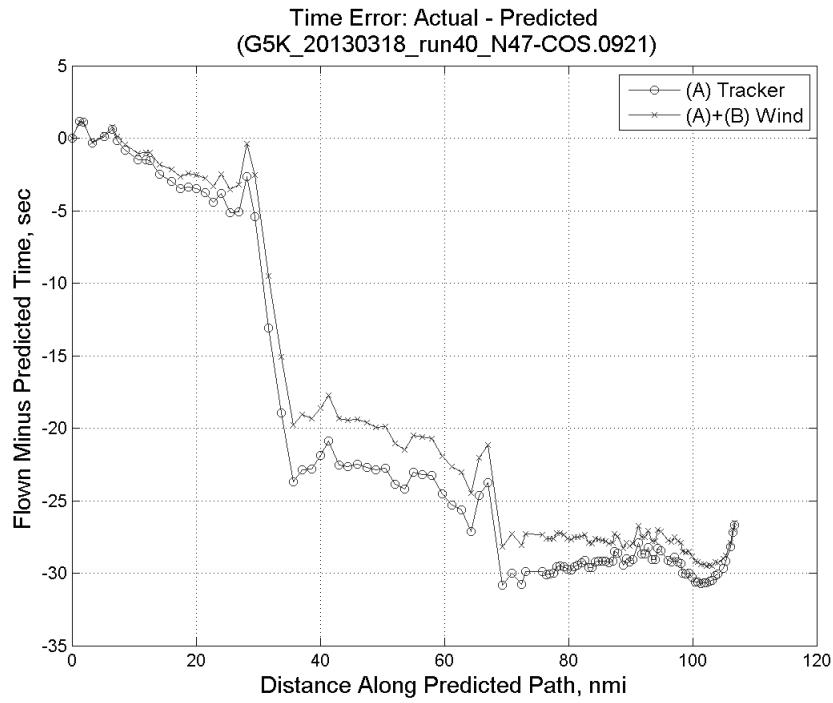


**Figure 1091: Time error for run 40 before ((A) Tracker) and after ((A)+(B) Wind) removing wind error source.**

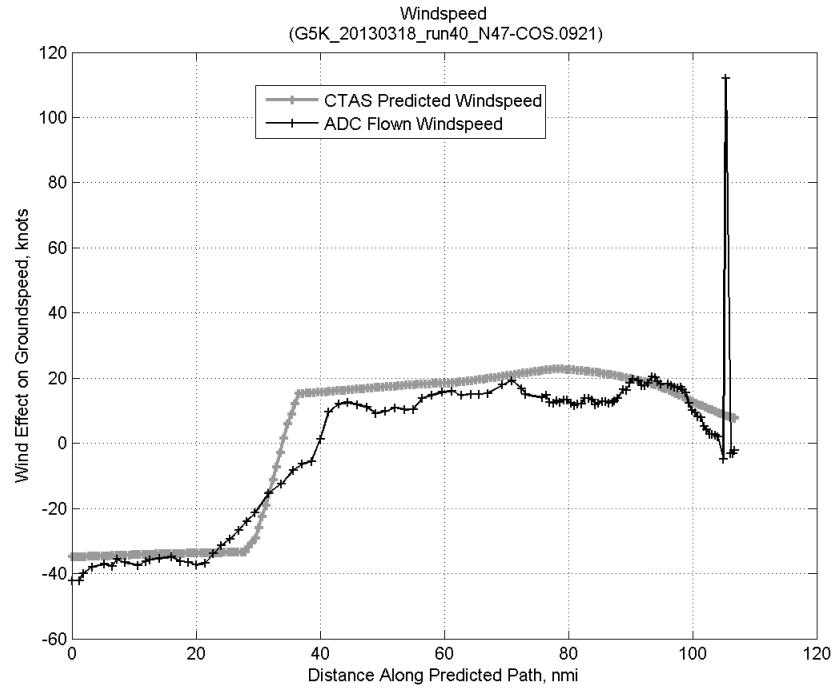


**Figure 1092: CTAS predicted and ADC flown wind effect on ground speed for run 40. Negative values indicate a headwind.**

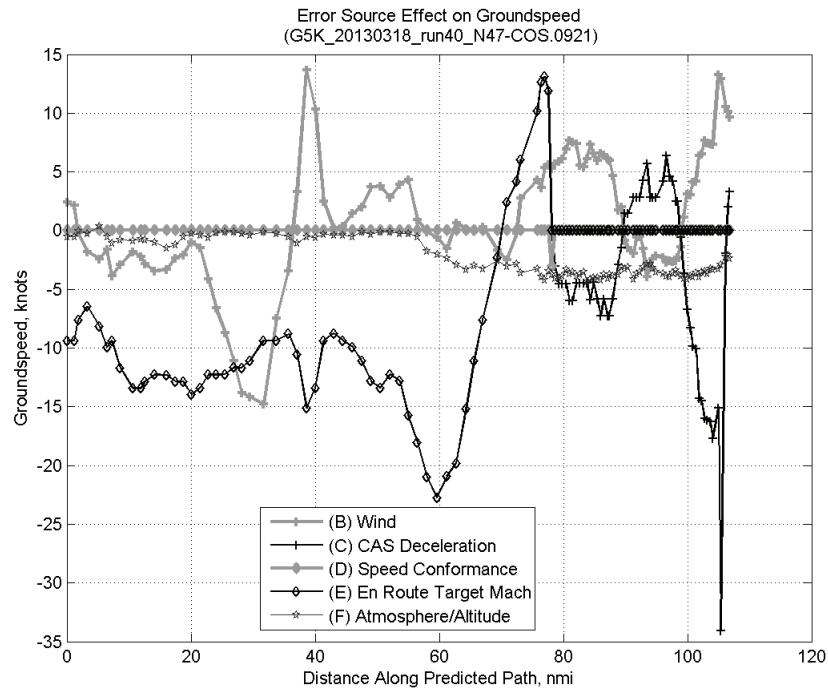


**Figure 1093: Error sources (flown minus predicted) converted to a ground speed effect for run 40. Positive values indicate the flown ground speed was faster than the CTAS prediction.**

### D.9.C. CAS Deceleration

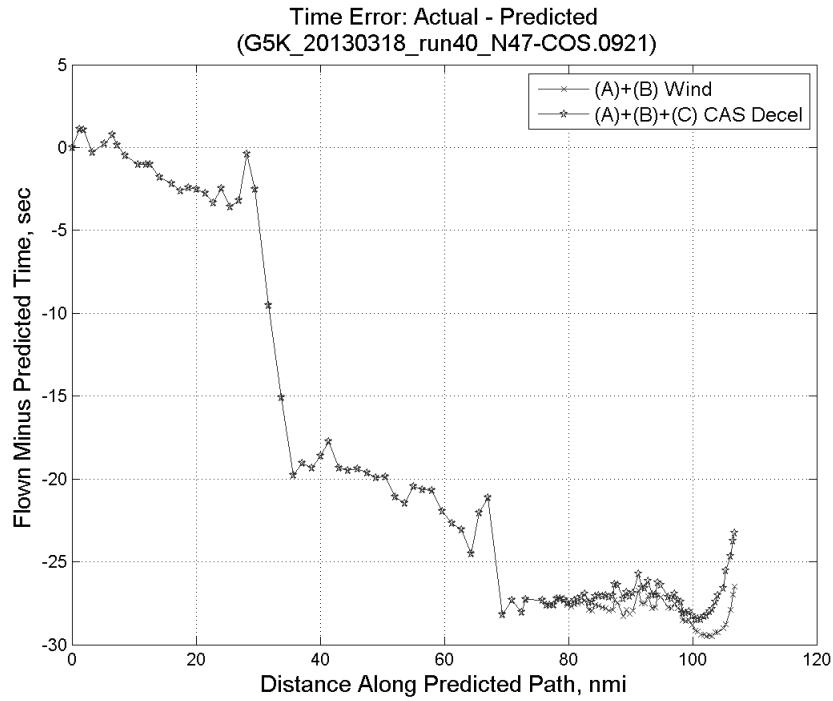


**Figure 1094:** Time error for run 40 before ((A)+(B) Wind) and after ((A)+(B)+(C) CAS Decel) removing CAS deceleration error source.

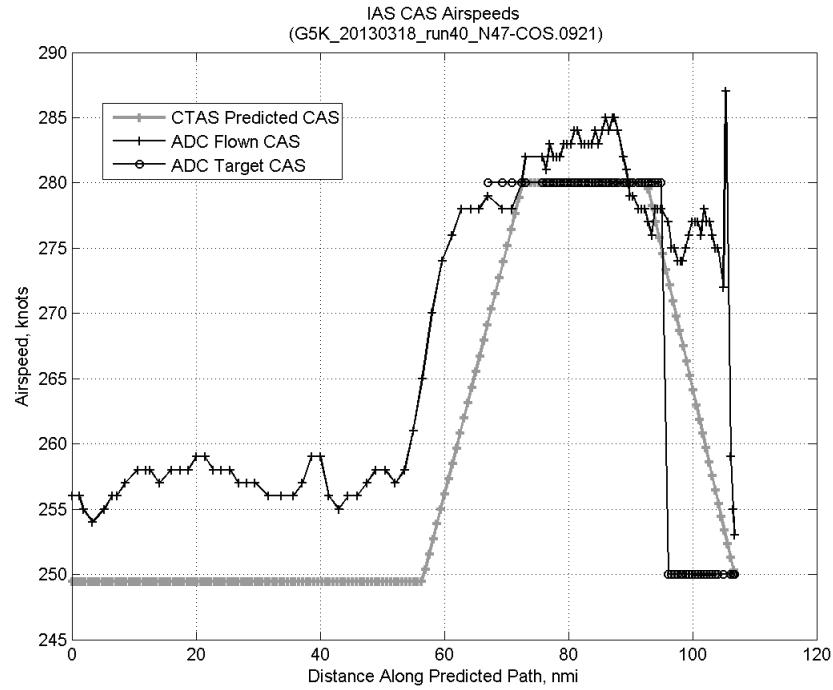


**Figure 1095:** CTAS predicted and ADC flown CAS for run 40. CAS that is being targeted is shown with circle markers.

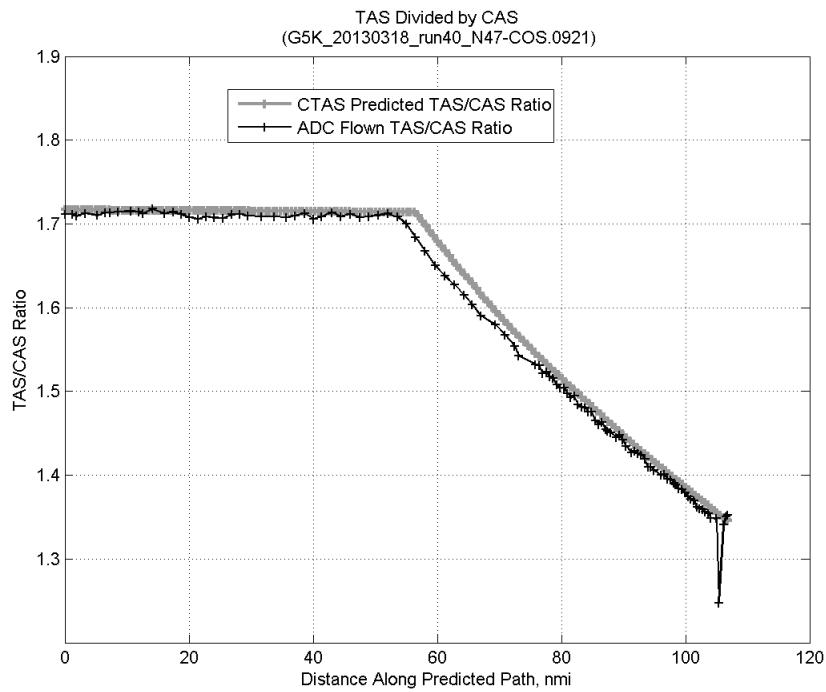


**Figure 1096:** CTAS predicted and ADC flown TAS/CAS ratio for run 40.

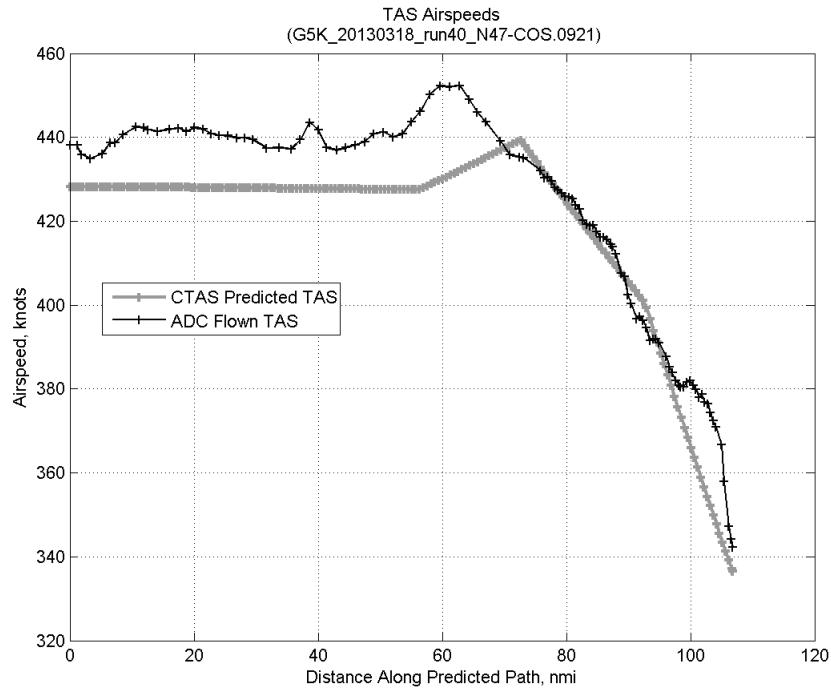


**Figure 1097:** CTAS predicted and ADC flown TAS for run 40.

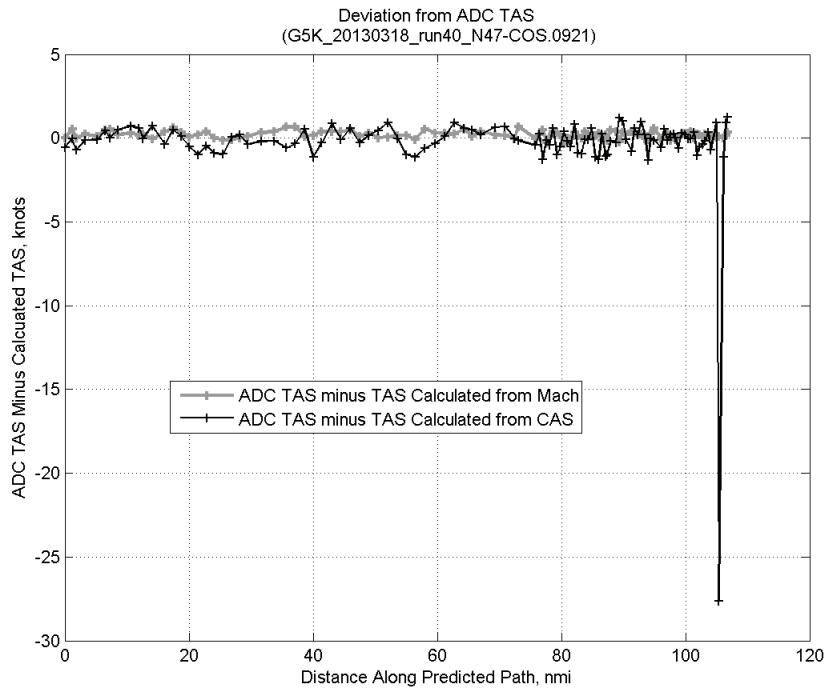


**Figure 1098: Deviation from ADC flown TAS if calculating TAS using ADC flown CAS, Mach, atmospheric temperature, and atmospheric pressure for run 40.**

#### D.9.D. Speed Conformance

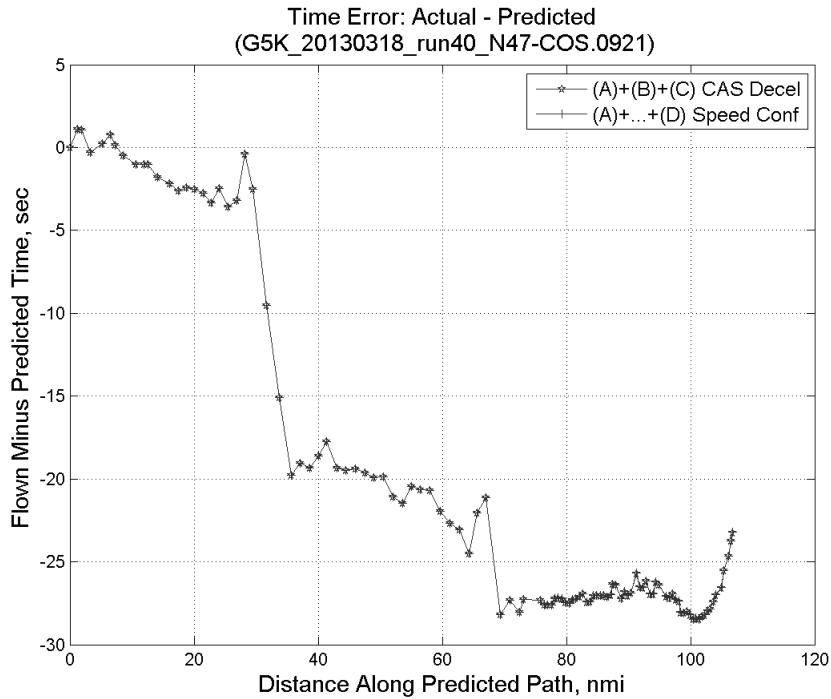


**Figure 1099: Time error for run 40 before ((A)+(B)+(C) CAS Decel) and after ((A)+...+(D) Speed Conf) removing speed conformance error source.**

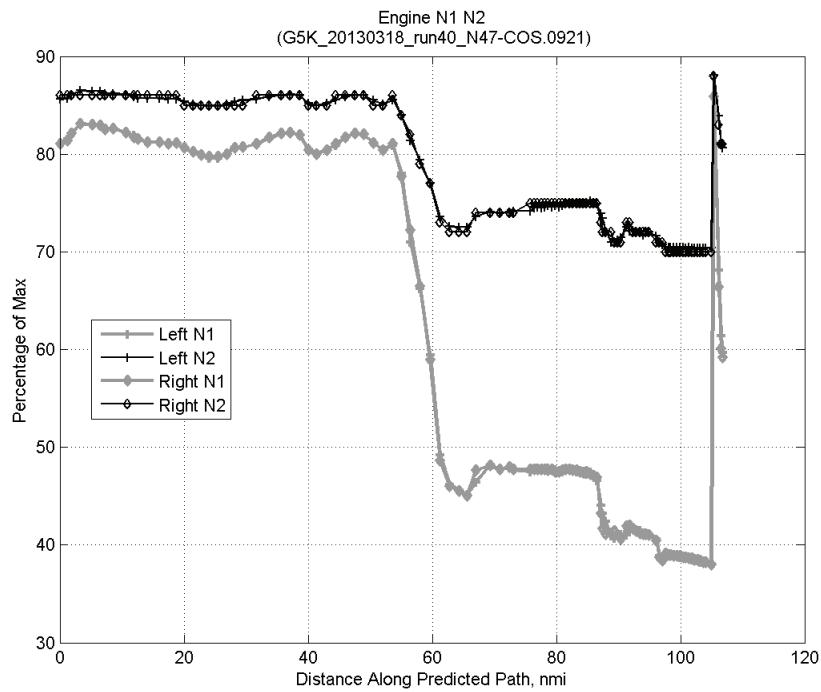


**Figure 1100: Flown engine N1 and N2 for run 40.**

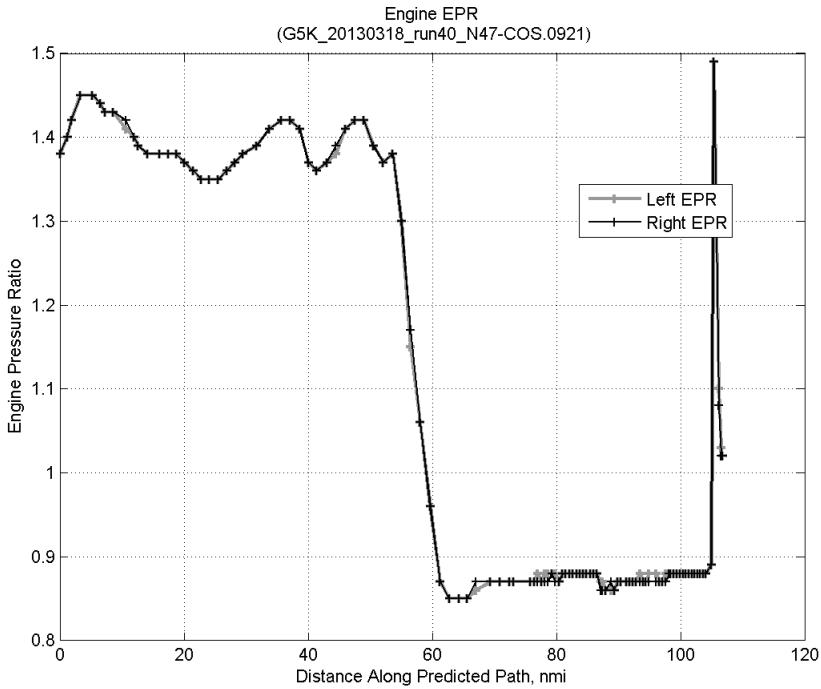


**Figure 1101: Flown engine EPR for run 40.**

### D.9.E. Target Mach

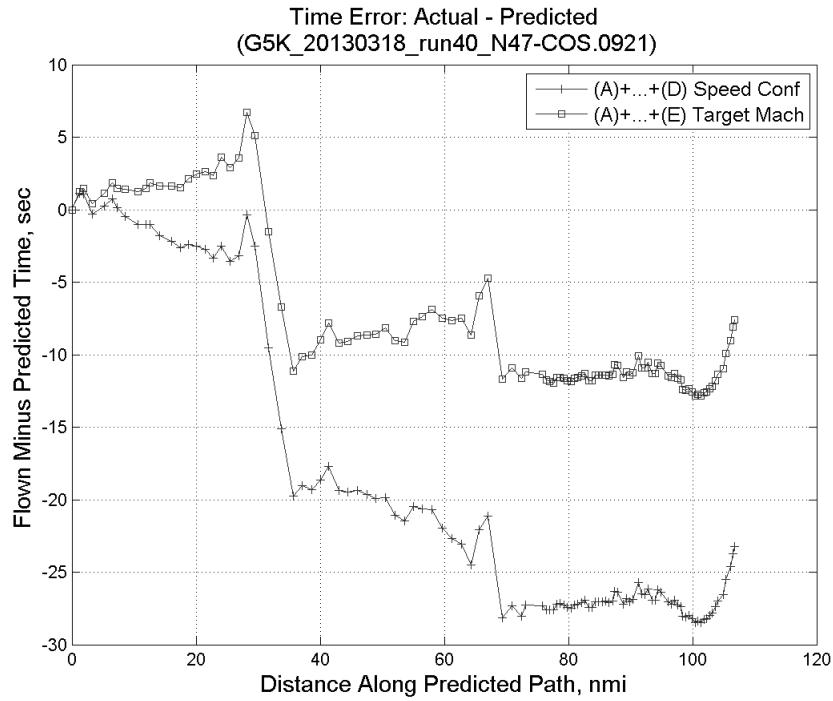


**Figure 1102:** Time error for run 40 before ((A)+...+(D) Speed Conf) and after ((A)+...+(E) Target Mach) removing target Mach error source.

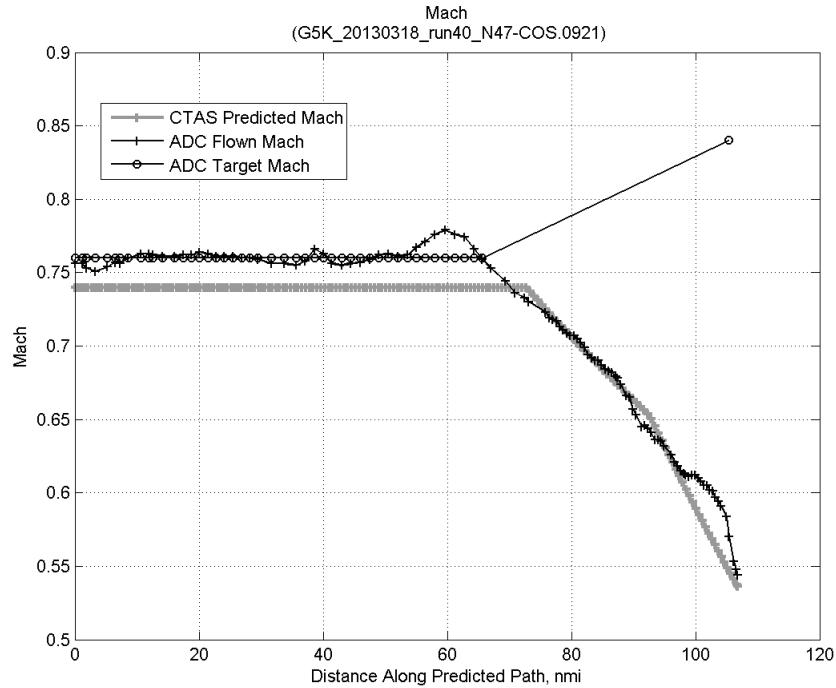


**Figure 1103:** CTAS predicted and ADC flown Mach for run 40. Mach being targeted (ADC) shown with circle markers.

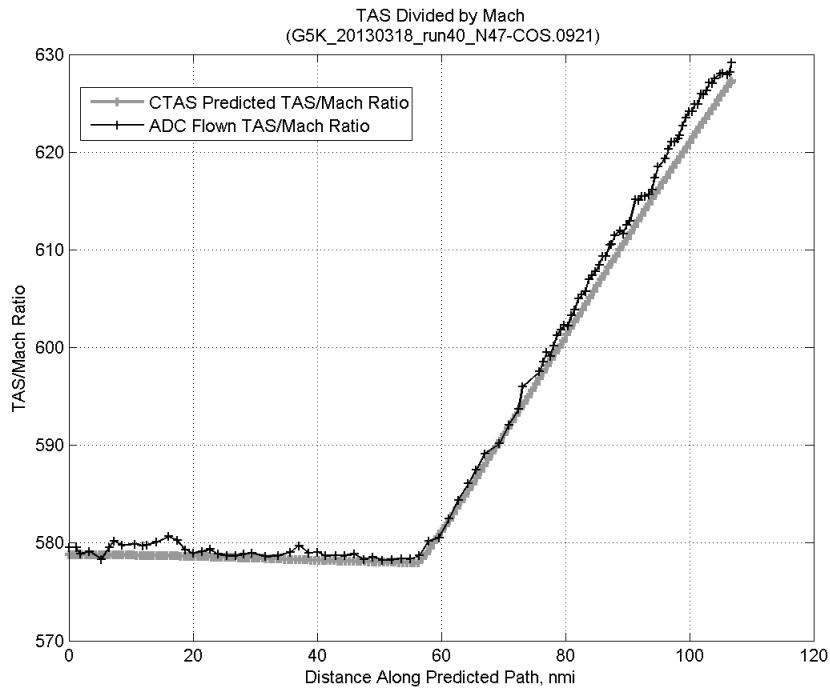


**Figure 1104: CTAS predicted and ADC flown TAS/Mach ratio for run 40.**

#### D.9.F. Atmosphere/Altitude

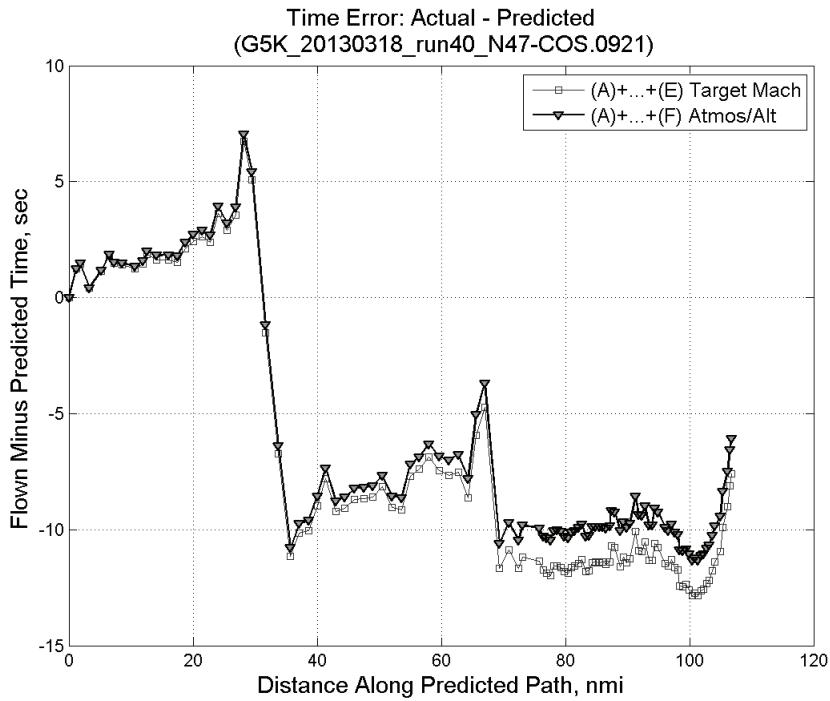


**Figure 1105: Time error for run 40 before ((A)+...+(E) Target Mach) and after ((A)+...+(F) Atmos/Alt) removing atmosphere/altitude error source.**

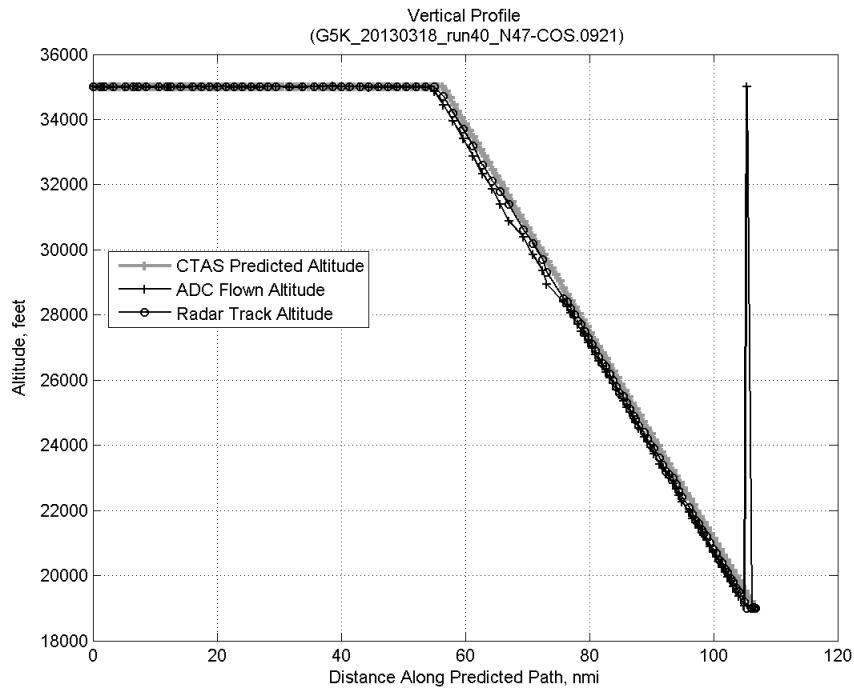


**Figure 1106: Flown (ADC) and predicted (CTAS) vertical profile for run 40.**

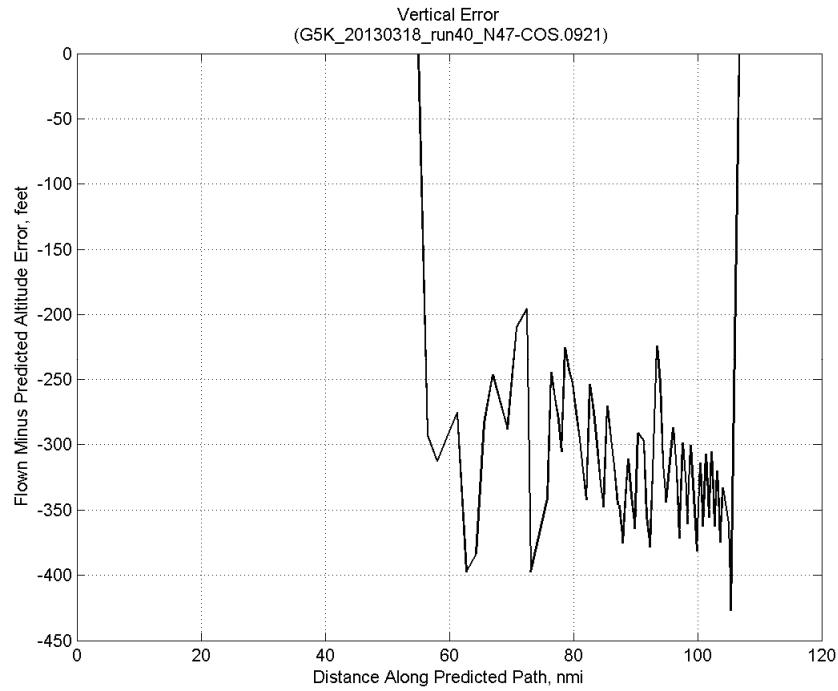


**Figure 1107: Vertical error (flown minus predicted altitude) for run 40. Positive values indicate aircraft flew higher than predicted by CTAS.**

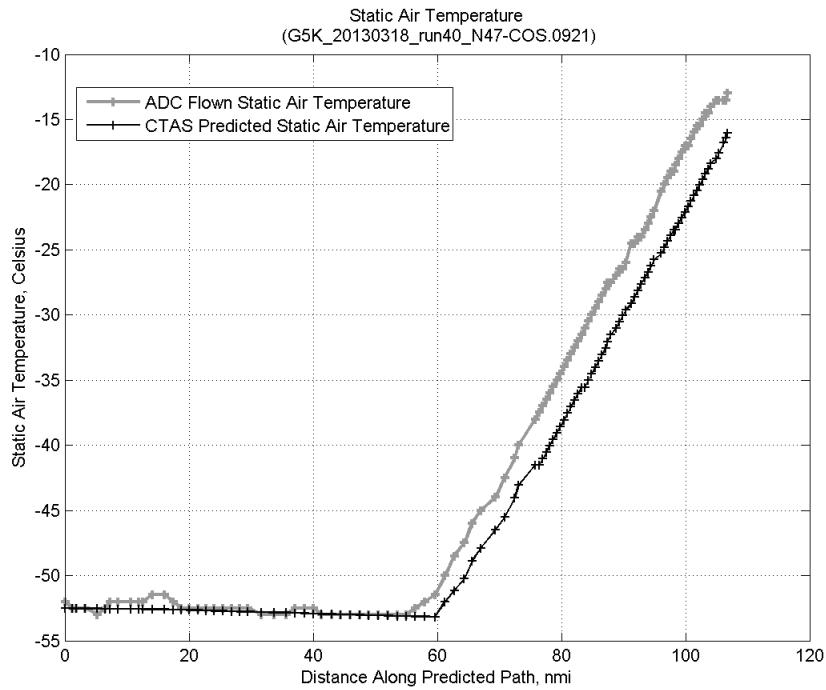


**Figure 1108: Flown (ADC) and predicted (CTAS) static air temperature for run 40.**

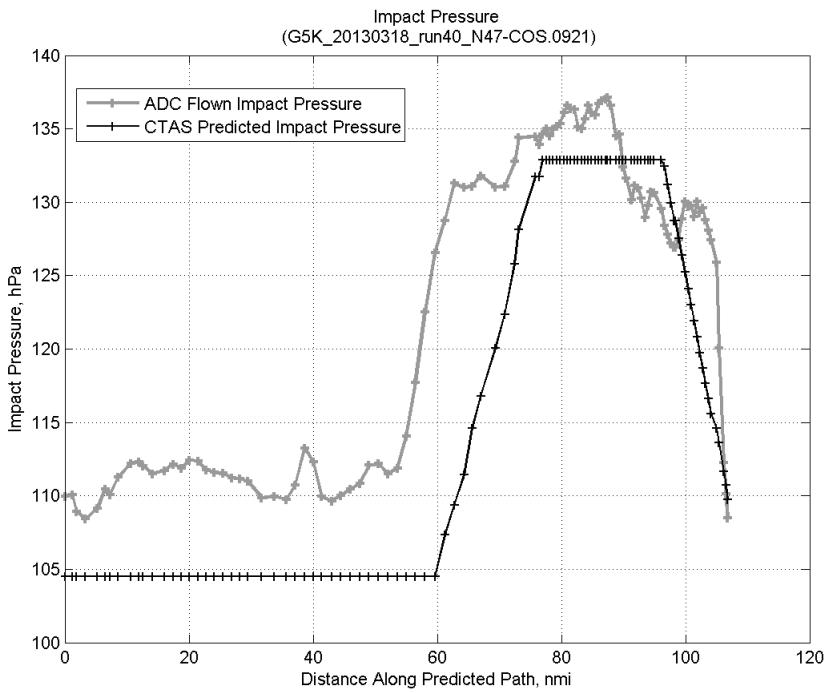


**Figure 1109: Flown (ADC) and predicted (CTAS) impact pressure for run 40.**

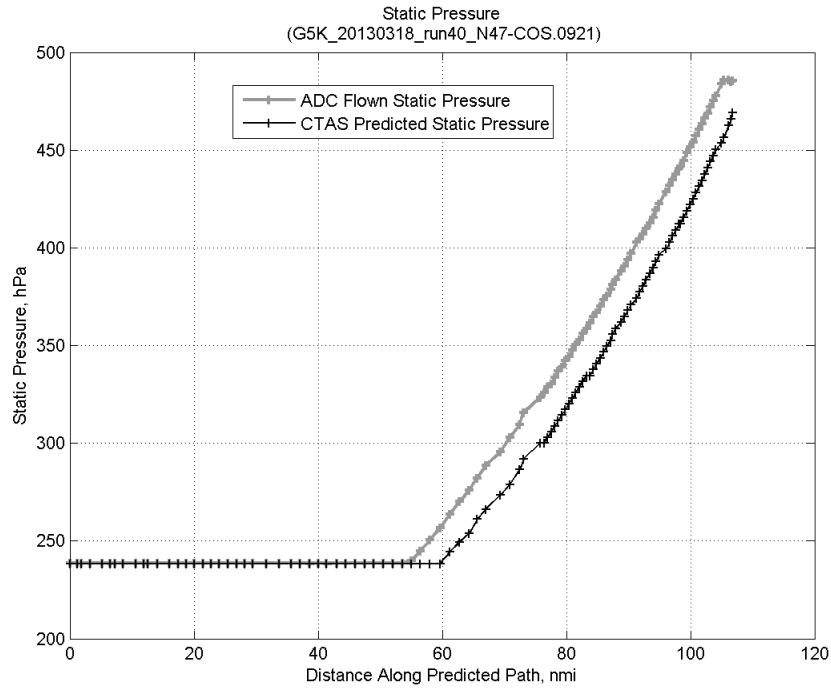


**Figure 1110: Flown (ADC) and predicted (CTAS) static pressure for run 40.**

#### D.9.G. Path Distance

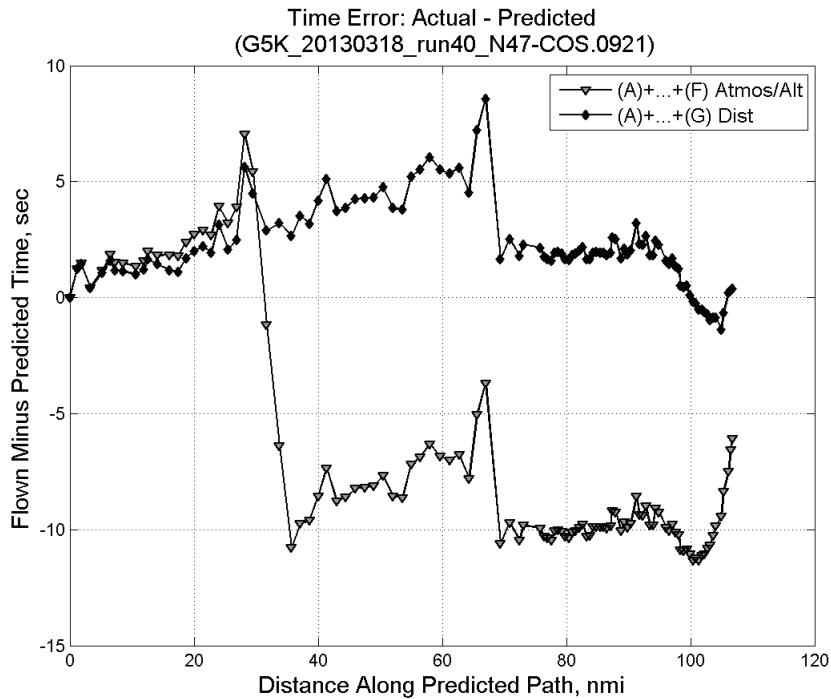


**Figure 1111: Time error for run 40 before ((A)+...+(F) Atmos/Alt) and after ((A)+...+(G) Dist) removing path distance error source.**

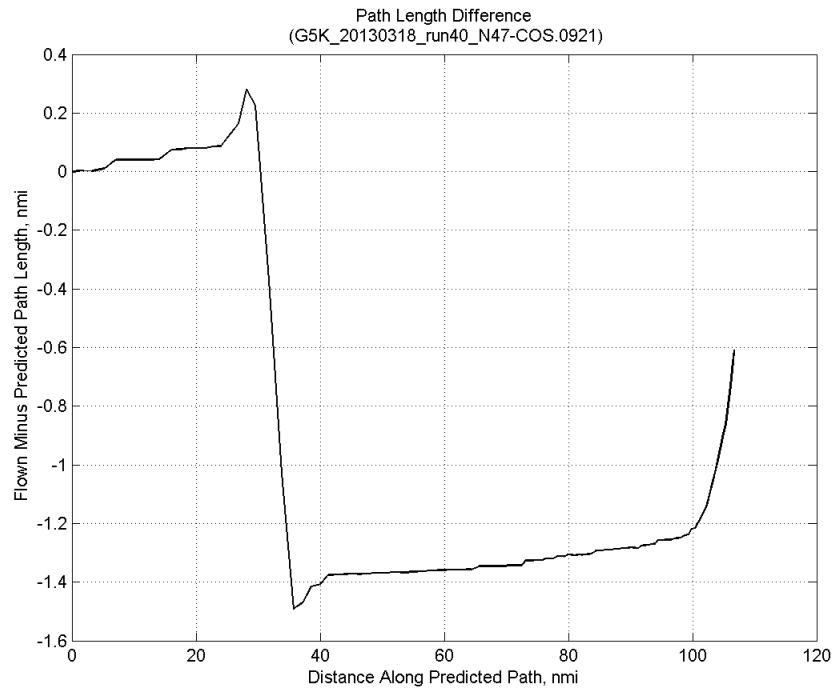


**Figure 1112: ADC flown minus CTAS predicted path length for run 40. Positive values indicate aircraft followed a longer path than predicted by CTAS.**

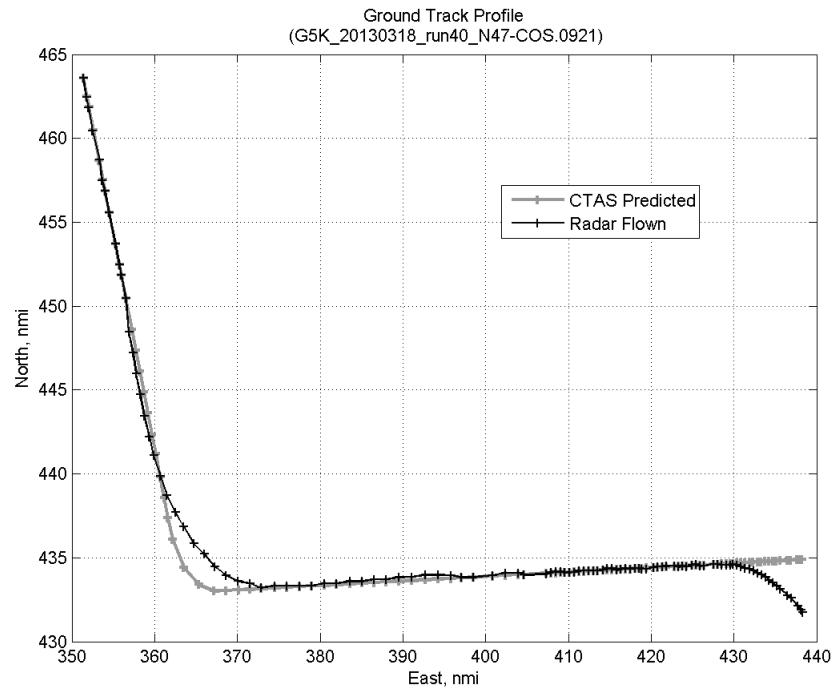


**Figure 1113: CTAS predicted and radar flown ground track profile for run 40.**

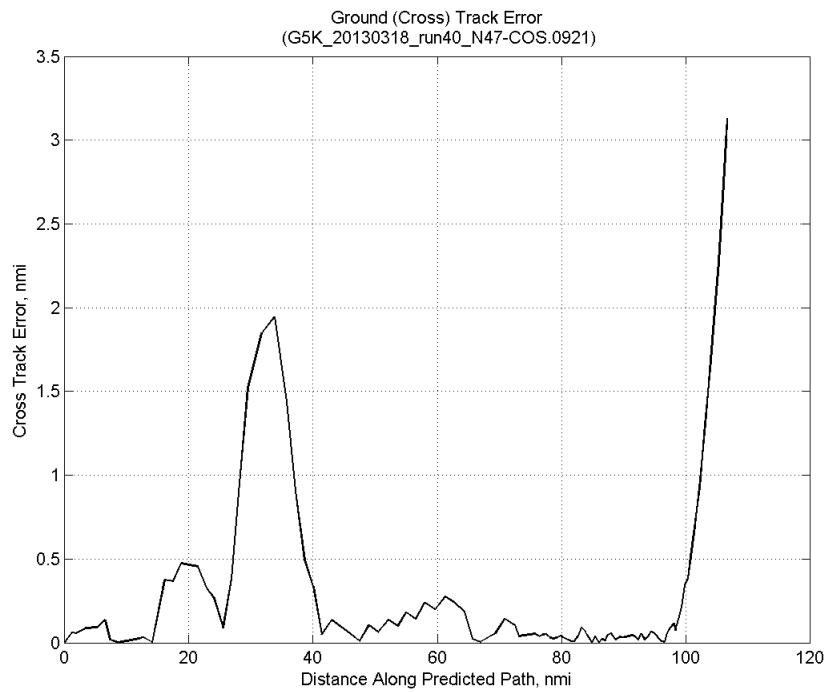


**Figure 1114: Ground (cross) track error for run 40.**



## Appendix E: Mean and Standard Deviation of Error Source Effect at Five Locations From Top of Descent to Meter Fix

The mean ( $\mu$ ) and standard deviation ( $\sigma$ ) of the effect of the seven error sources at six locations between top of descent and the meter fix inclusive are shown in Table 24 for both direct runs (labeled as the “D” rows) and path-stretch runs (label as the “PS” rows).

**Table 24. Mean ( $\mu$ ) and standard deviation ( $\sigma$ ) of error sources at locations along predicted trajectory for both direct runs (D) and path-stretch runs (PS).**

Error Source	D or PS	TOD		IA-4K		IA-6K		FA+4K		FA+2K		MF	
		$\mu$	$\sigma$										
A. Tracker Jumps	D	1.66	3.01	-0.67	4.04	-1.43	4.32	-2.51	5.79	-5.82	4.18	-6.08	3.67
	PS	0.38	4.92	-0.03	4.77	-2.36	4.56	-5.69	3.35	-6.03	2.93	-6.03	2.93
B. Wind	D	-1.36	1.49	-2.07	2.05	-2.34	2.28	-3.30	2.83	-3.75	3.02	-4.02	3.39
	PS	-0.39	2.60	-0.91	2.73	-1.34	3.00	-2.12	4.16	-2.73	4.46	-3.10	4.55
C. CAS Deceleration	D	0.00	0.00	-0.01	0.15	-0.11	0.49	-1.43	2.24	-2.88	3.79	-4.99	5.22
	PS	0.00	0.00	0.00	0.00	0.00	0.00	-0.94	1.84	-2.35	4.35	-3.50	5.57
D. Speed Conformance	D	-0.02	0.12	-0.22	1.66	-0.10	2.19	-0.16	2.91	0.01	3.19	0.10	3.36
	PS	0.32	0.97	1.45	4.52	1.39	5.72	0.73	6.81	1.03	6.53	0.97	6.67
E. Target Mach	D	-1.64	4.27	-1.26	5.50	-1.14	5.72	-1.12	5.74	-1.12	5.74	-1.12	5.74
	PS	-8.34	16.18	-8.70	16.46	-7.76	16.02	-7.48	15.94	-7.48	15.94	-7.48	15.94
F. Atmosphere/ Altitude	D	0.02	0.19	-0.25	0.37	-0.41	0.44	-0.90	0.56	-1.08	0.60	-1.29	0.63
	PS	0.03	0.55	-0.45	1.05	-0.78	1.34	-1.49	1.86	-1.87	2.09	-2.27	2.27
G. Path Distance	D	0.46	0.29	0.74	0.34	0.91	0.37	1.41	0.64	1.72	0.70	2.32	0.88
	PS	-8.21	4.87	-8.74	3.78	-8.62	3.80	-8.20	3.88	-7.79	3.92	-5.16	4.99
Total	D	-0.77	5.80	-3.92	6.70	-4.59	8.17	-7.50	8.87	-12.51	8.72	-15.65	9.88
	PS	-15.07	23.85	-16.97	26.33	-18.67	27.08	-23.89	26.49	-26.71	25.64	-26.99	25.78
Residual	D	0.11	1.27	-0.19	1.49	0.04	1.59	0.50	2.07	0.40	1.99	-0.57	2.49
	PS	1.12	2.34	0.41	1.77	0.80	1.49	1.31	1.45	0.50	2.21	-0.43	3.41